Electronic Poster

Probing the Myocardial Tissue Composition

Exhibition Hall — Monday 8:15 - 9:15

3095 Computer 1

Reducing magnetization-transfer-induced T1 estimation error in myocardial T1 mapping for the MOLLI sequence: simulation, phantom and in vivo studies

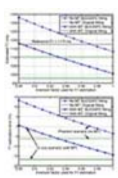

Jiaxin Shao[1], Dapeng Liu[1], Kyung Hyun Sung[1], Kim-Lien Nguyen[2], and Peng Hu[1]

[1]Radiology, University of California, Los Angeles, CA, United States, [2]Division of Cardiology, University of California, Los Angeles, CA, United States

The modified Look-Locker inversion-recovery (MOLLI) sequence is a widely used myocardial T1 mapping technique for tissue characterization. It is known that the MOLLI sequence underestimates myocardial T1 values (>10%) due to magnetization transfer (MT) effects and short myocardial tissue T2 values. In this work, we demonstrate that in vivo reduction of the inversion factor is predominantly responsible for the MT effect that reduces MOLLI T1 values. Thus, using an alternative T1 estimation algorithm with a measured inversion factor for the MOLLI sequence can reduce the MT effect on T1 estimation error.

3096 Computer 2

Ultrafast Cardiac Balanced Inversion Recovery with Interleaved Acquisition (UF-CABIRIA) for improved simultaneous T1 and T2 quantification of the heart at 3T.

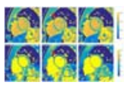

Francesco Santini[1,2], Grzegorz Bauman[1,2], and Oliver Bieri[1,2]

[1]Division of Radiological Physics, University of Basel Hospital, Basel, Switzerland, [2]Department of Biomedical Engineering, University of Basel, Basel, Switzerland

CABIRIA is a method for the simultaneous quantification of T1 and T2 values of the myocardium. As other T1-quantification sequences, it relies on a bSSFP readout, and it is thus susceptible to off-resonance effects. In this work, we show an improvement over the CABIRIA method that reduces the TR and therefore increases the robustness towards field inhomogeneities. This method can potentially be extended to other quantification techniques.

3097 Computer 3

Quantitative Tissue Characterization by Magnetization Transfer-Weighted Cardiac MRI Detects Fibrosis Progression without Gadolinium in Patients with End Stage Renal Disease

Tori A Stromp[1,2], Rebecca M Kidney[2], Tyler J Spear[2], Kristin N Andres[3], Joshua C Kaine[3], Steve W Leung[4], and Moriel H Vandsburger[1,2,5,6]

[1]Physiology, University of Kentucky, Lexington, KY, United States, [2]Cardiovascular Research Center, University of Kentucky, KY, United States, [3]College of Medicine, University of Kentucky, KY, United States, [4]Gill Heart Institute, University of Kentucky, KY, United States, [5]Biomedical Engineering, University of Kentucky, KY, United States, [6]Bioengineering, University of California Berkeley, Berkeley, United States

Long term hemodialysis treatment for end stage renal disease (ESRD) is associated with a time dependent increase in cardiac death. The inability to use late gadolinium enhancement (LGE) cardiac MRI (CMR) in patients with renal dysfunction impedes the noninvasive monitoring of fibrosis progression and appropriate treatment selection in the population. We used magnetization transfer (MT) weighted CMR to monitor the progression of ventricular fibrosis over 1 year in patients with ESRD. While no major changes in hypertrophy or contractility were apparent, pervasive increases in myocardial signal was measured by MT-weighted CMR, consistent with reduced MT and progressive fibrosis development.

3098 Computer 4

Improved Detection of Right Ventricular Myocardial Infarction Using 3D Navigator-Gated Free Breathing Delayed Enhancement Cardiac Magnetic Resonance

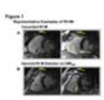

Jiwon Kim[1], Tara Shah[1], Neil Mehta[2], Jonathan Weinsaft[1], Pascal Spincemaille[3], Yi Wang[3], and Thanh Nguyen[3]

[1]Department of Cardiology, Weill Cornell Medical College, New York, NY, United States, [2]Department of Medicine, Weill Cornell Medical College, New York, NY, United States, [3]Department of Radiology, Weill Cornell Medical College, New York, NY, United States

Right ventricular myocardial infarction (RV-MI) is a serious consequence of coronary artery disease that adversely affects outcomes. Conventional CMR employs 2D breath-held imaging (CMR_{BH}) to detect RV-MI, an approach that may sacrifice spatial resolution to enable patient breath-holds, and is thus suboptimal for imaging the RV. This study compared 3D navigator-gated free breathing CMR (CMR_{NAV}) to CMR_{BH} for detection of RV-MI in 75 post-MI patients. Results demonstrated a 2-fold increase in detection rate of RV-MI by CMR_{NAV}, accompanied by higher spatial resolution in 30% less scan time.

3099 Computer 5

Simultaneous Imaging of Myocardial Fat and Scar using Dark Blood Late Gadolinium Enhancement

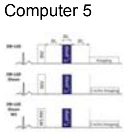

Maryam Nezafat[1,2], Ahmed S Fahmy[2], Gifty Addae[2], and René M. Botnar[1]

[1]Division of Imaging Sciences and Biomedical Engineering, King's College London, London, United Kingdom, [2]Department of Medicine, Beth Israel Deaconess Medical Centre and Harvard Medical School, Boston, MA, United States

Dark-Blood Late Gadolinium Enhancement (DB-LGE) sequence has been recently introduced to suppress the blood signal in order to enhance the contrast between blood and scar. However, it is difficult to distinguish scar from fat as both appear bright in DB-LGE images. In this study, we present a DB-LGE sequence that allows quantification of scar and fat volume in the heart in a single imaging sequence. Numerical simulation, phantom and in-vivo scans were performed to evaluate the proposed sequence.

3100

3D high resolution imaging of human hearts for visualization of the cardiac structure

Computer 6

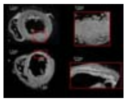

Julie Magat[1], Valéry Ozenne[1], Fanny Vaillant[1], David Benoist[1], Marion Constantin[1], Virginie Dubes[1], Stephen Gilbert[2], Mark L Trew[3], Jérôme Naulin[1], Louis Labrousse[4], Mélèze Hocini[4], Michel Haissaguerre[4], Olivier Bernus[1], and Bruno Quesson[1]

[1]IHU LIRYC/U1045, Université de Bordeaux, Pessac, France, [2]Mathematical Cell Physiology, Max Delbrück Center for Molecular Medicine, berlin, Germany, [3]Auckland Bioengineering Institute, University of Auckland, Auckland, New Zealand, [4]IHU LIRYC/U1045, CHU Bordeaux, Pessac, France

The motivation of this study is to develop high resolution 3D MR imaging of human hearts to characterize the cardiac structure non-invasively. For this purpose, T1-weighted images and diffusion MRI in 3D from intact and infarcted hearts were acquired and analyzed to compare myocyte and myolaminar orientations in healthy and pathological regions.

3101 Computer 7

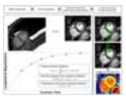

Improving precision of myocardial T_1 mapping with 3-parameter fit model using tissue characteristic-based denoising

Jihye Jang[1,2], Shiro Nakamori[1], and Reza Nezafat[1]

[1]Department of Medicine, Beth Israel Deaconess Medical Center and Harvard Medical School, Boston, MA, United States, [2]Department of Computer Science, Technical University of Munich, Munich, Germany

For the reconstruction of pixel-wise T_1 maps, 3-parameter fit model is highly accurate, but is sensitive to noise. Therefore, it is desirable to develop a robust method to reduce sensitivity to noise when 3-parameter fit model is used. In this work, we propose a robust denoising method based on tissue characteristics to improve precision of myocardial T_1 mapping. In phantom and in-vivo studies, denoising filtering provided similar T_1 measurements with significantly improved precision. This technique will make 3-parameter fit model more favorable by reducing sensitivity to noise and will allow for more accurate and precise myocardial T_1 mapping.

3102 Computer 8

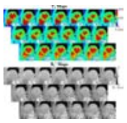

Cine T1 Mapping: Look-Locker inversion recovery for phase resolved T1-Mapping with B1+ Correction At 3T

Sebastian Weingärtner[1,2,3], Chetan Shenoy[4], Lothar R. Schad[3], and Mehmet Akçakaya[1,2]

[1]Electrical and Computer Engineering, University of Minnesota, Minneapolis, MN, United States, [2]Center for Magnetic Resonance Research, University of Minnesota, Minneapolis, MN, United States, [3]Computer Assisted Clinical Medicine, Heidelberg University, Mannheim, Germany, [4]Department of Cardiology, University of Minnesota, Minneapolis, MN, United States

Conventionally, evaluation of myocardial T_1-times is limited to a single snapshot of the cardiac cycle, leaving much of the dependence between functional and tissue characterization unstudied. Here, we propose an ECG-triggered steady-state Look-Locker technique that allows for functional, cardiac phase-resolved native T_1-mapping. Integratedly acquired phase-resolved B_1^+-maps are used for T_1-time correction. High accuracy and good consistency of the T_1-times across cardiac phases is shown in phantom scans. In-vivo T_1-times show slight underestimation and similar precision compared to saturation-recovery T_1-mapping. High visual image quality at all cardiac phases is obtained at temporal resolutions up to 40ms in a single breath-hold.

3103 Computer 9

Active Shape Models Based Motion Correction for Myocardial T_1 Mapping

Hossam El-Rewaidy[1], Shiro Nakamori[1], Gifty Addae[1], Warren Manning[1], and Reza Nezafat[1]

[1]Cardiovascular Division, Department of Medicine, Beth Israel Deaconess Medical Center, Harvard Medical School, Boston, MA, United States

A new framework based on Active Shape Models (ASM) is introduced to correct the motion artifacts induced by respiratory and cardiac motion in myocardial T_1 mapping. This framework includes three main steps: training ASM model to capture intensity variations of T_1 images at different inversion times, segmentation of T_1 weighted images using the trained model, and estimating and applying the registration parameters to correct for motion between images.

3104 Computer 10

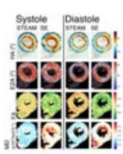

A comparison of STEAM and spin echo diffusion tensor CMR in hypertrophic cardiomyopathy patients

Zohya Khalique[1], Andrew Scott[1], Pedro Ferreira[1], Margarita Gorodezky[1], Ricardo Wage[1], Sonia Nielles-Vallespin[2], David Firmin[1], and Dudley Pennell[1]

[1]NIHR Cardiovascular Biomedical Research Unit, Royal Brompton Hospital, LONDON, United Kingdom, [2]National Heart Lung and Blood Institute, NIH, Bethesda, MD, United States

Diffusion tensor (DT) cardiovascular magnetic resonance (CMR) can provide myocardial microstructural information using either motion compensated spin echo (SE) or stimulated echo acquisition mode (STEAM) sequences. Here we present the first DT-CMR data from a cohort of hypertrophic cardiomyopathy patients using SE, and compare parameters obtained from SE and STEAM sequences at 3T in two phases of the cardiac cycle. We demonstrate that whilst reliability measures, diffusivity, and anisotropy differ between the sequences, both approaches are able to detect the sheetlet microstructure that is integral to wall thickening during cardiac contraction and shown to be aberrant in this condition.

3105 Computer 11

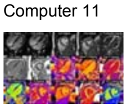

Identifying tissue changes of “normal-appearing” myocardium in pediatric myocarditis patients using quantitative T1 and T2 mapping techniques

Haipeng Wang[1], Bin Zhao[2], Cuiyan Wang[1], Tianyi Qian[3], Guangbin Wang[2], Jing An[4], Fei Gao[2], Andreas Greiser[5], and Junyu Zhao[6]

[1]Shandong Medical Imaging Research Institute, Ji'nan, People's Republic of China, [2]Shandong Medical Imaging Research Institute, [3]Siemens Healthcare, MR Collaborations NE Asia, Beijing, People's Republic of China, [4]Siemens SSMR, APPL, [5]Siemens Healthcare, Application Development, Erlangen, Germany, [6]Shandong Provincial Qianfoshan Hospital

This study aimed to identify diffuse myocardial tissue changes in pediatric myocarditis patients by applying T1 and T2 mapping techniques. The correlations between T1 and T2 values and cardiac function were assessed. Abnormal post-contrast T1 values and extracellular volume (ECV) of “normal appearing” myocardium in pediatric myocarditis patients were found and were correlated with left ventricular cardiac function and stroke volume (SV) in children with chronic myocarditis.

3106 Computer 12

The Effect of Mixing Time on Diffusion Spectrum Imaging of the Ex-vivo Porcine Heart

Claudia Zanella[1], Christian T Stoeck[1], Constantin von Deuster[1], and Sebastian Kozerke[1]

[1]Institute for Biomedical Engineering / University and ETH Zurich, Zurich, Switzerland

Higher order diffusion imaging has revealed new insights into myocardial microstructure. At the b-values required for diffusion kurtosis or diffusion spectrum imaging, translation into human in-vivo application requires Stimulated Echo Acquisition Mode imaging (STEAM) at prolonged mixing-times. In this study the effect of mixing time on diffusion parameters is investigated covering the range of current spin-echo and STEAM aproaches. Results show that fractional anisotropy increases and mean diffusivity decreases with mixing-time. Diffusional kurtosis was found to decrease with mixing-time by varying amounts along fiber, sheet and sheet-normal direction which needs to be considered when comparing spin-echo imaging with STEAM acquisitions.

3107 Computer 13

Whole-heart T1 mapping using a 2D fat image navigator with 100% scan efficiency

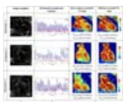

Giovanna Nordio[1], Gastao Cruz[1], Claudia Prieto[1], Torben Schneider[1,2], Rene M. Botnar[1], and Markus Henningsson[1]

[1]Division of Imaging Sciences and Biomedical Engineering, King’s College London, London, United Kingdom, London, United Kingdom, [2]Philips Healthcare, Guildford Surrey, United Kingdom

In this study a whole-heart saturation-recovery T1-mapping technique in combination with a fat image navigator (fat-iNAV) is proposed. Myocardial fat is imaged by the fat-iNAV to estimate respiratory motion. Each of the T1-weighted images are subsequently motion corrected prior to reconstruction of the T1 map. Fat-iNAV motion correction let to an improvement in myocardial borders delineation and accuracy of the myocardial T1 values, while there was a general underestimation of myocardial T1 in the non-motion corrected T1 maps (1115.4±110ms vs 998.6±101ms). Further work will investigate non-rigid motion correction and undersampled reconstruction for T1 mapping.

3108 Computer 14

Accelerating High-Resolution Whole-Heart 3D T2 Mapping

Dan Zhu[1], Haiyan Ding[2], Henry Halperin[3], and Daniel A. Herzka[1]

[1]Department of Biomedical Engineering, Johns Hopkins University School of Medicine, Baltimore, MD, United States, [2]Department of Biomedical Engineering, Tsinghua University, Beijing, People's Republic of China, [3]Department of Medicine, Johns Hopkins University School of Medicine, Baltimore, MD, United States

In this work, we aim to determine an optimal strategy for accelerating high-resolution 3D myocardial T2 mapping. We quantitatively evaluate the performance of diverse methods involving different subsampling patterns and different reconstruction strategies relative to volume-by-volume SENSE reconstruction. Reconstructions which address all volumes as a single reconstruction problem (i.e. joint-sparsity SENSE or model-based SENSE) outperform volume-by-volume approaches, and variable density sampling outperforms equal spacing or CAIPIRIHNA undersampling. The T2 values observed in parametric maps proved to be more sensitive to data corruption than images themselves, limiting the degree of data reduction tolerable.

3109 Computer 15

In-vivo comparison of STEAM EPI and STEAM spiral diffusion-weighted sequences

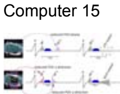

Margarita Gorodezky[1,2], Andrew D Scott[1,2], Pedro F Ferreira[1], Sonia Nielles-Vallespin[3], Zohya Khalique[1], Dudley J Pennell[1], and David N Firmin[1,2]

[1]Cardiovascular Biomedical Research Unit, The Royal Brompton Hospital, London, United Kingdom, [2]National Heart and Lung Institute, Imperial College, London, United Kingdom, [3]National Heart, Lung and Blood Institute, National Institutes of Health, Bethesda, MD, United States

A cardiac DTI STEAM spiral sequence with a novel asymmetric zonal excitation and a reduced FOV was implemented and compared to an established STEAM EPI sequence. 10 volunteers were scanned in systole and diastole and standard cDTI parameters were compared for both sequences. The spiral trajectory is both efficient and motion robust and its centre-out nature allows a shorter echo time and, therefore an increase in image SNR over EPI. The spiral trajectory is also able to take full advantage of the two-dimensional reduced in-plane field-of-view (FOV) made possible by the 3 RF pulses used in the STEAM sequence.

3110 Computer 16

Biopsy-based calibration of T2* magnetic resonance for estimation of liver iron concentration

Antonella Meloni[1], Filippo Leto[2], Daniele De Marchi[1], Vincenzo Positano[1], Laura Pistoia[1], Aurelio Maggio[2], and Alessia Pepe[1]

[1]Fondazione G. Monasterio CNR-Regione Toscana, Pisa, Italy, [2]Ospedale "V. Cervello", Palermo, Italy

An excellent linear agreement between R2* values and cardiac iron measured with emission spectroscopy was found. The results further validate the current clinical practice of monitoring cardiac iron in vivo by CMR.

3111 Computer 17

Myocardial Motion Velocity in Patients with Cirrhotic Cardiomyopathy

Ting-Hsu Chen[1], Ming-Ting Wu[2], Mao-Yuan Su[3], and Hsu-Hsia Peng[1]

[1]National Tsing Hua University, Hsinchu, Taiwan, [2]Department of Radiology, Kaohsiung Veterans General Hospital, Kaohsiung, Taiwan, [3]Department of Medical Imaging, National Taiwan University Hospital, Taipei

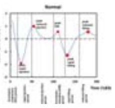

In this study, we employed MR tissue phase mapping (TPM) to evaluate three-directional left ventricular velocity. The purpose of this study is to establish quantitative indices to comprehend the characteristics of myocardial motion in patients with cirrhotic cardiomyopathy. Compared with normal subjects, patients displayed lower systolic Vz and prolonged systolic TTPz. Lower systolic Vphi was also demonstrated in patient group. In conclusion, to analyze myocardial velocity and TTP can potentially provide helpful information for realizing the myocardial compensatory mechanism in patients with cirrhotic cardiomyopathy.

3112 Computer 18

Dependence of the Precision of Myocardial Late Gadolinium Enhancement Quantification on Inversion Time Selection Simulated Using Synthetic Inversion Recovery MR Imaging

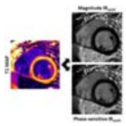

Akos Varga-Szemes[1], Rob J van der Geest[2], U. Joseph Schoepf[1], Carlo N De Cecco[1], Taylor M Duguay[1], and Pal Suranyi[1]

[1]Department of Radiology and Radiological Science, Medical University of South Carolina, Charleston, SC, United States, [2]Leiden University Medical Center, Leiden, Netherlands

Clinical late gadolinium enhancement (LGE) imaging of the myocardium requires inversion time (TI) optimization for adequate image quality. As the optimal TI (TI_0) depends on various factors, its influence on the precision of myocardial LGE quantification is of interest. In this study we aimed to prospectively investigate how the precision of LGE quantification varies in the clinically relevant TI range in 53 patients using T1-mapping-based synthetic inversion recovery (IR_{synth}) approach. We concluded that phase-sensitive IR_{synth} images provide precise quantification independent of TI, while magnitude IR_{synth}-based quantification is precise at TI_0 or longer TIs, but showing decreased precision below TI_0.

3113 Computer 19

Precision and sensitivity of radial MOLLI sequence for fast myocardial T1 mapping

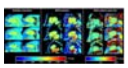

Benjamin Marty[1,2], Bertrand Coppa[1,2], and Pierre G Carlier[1,2]

[1]NMR Laboratory, Institute of Myology, Paris, France, [2]NMR Laboratory, CEA, DRF, I²BM, MIRCen, Paris, France

Quantitative cardiac NMR imaging, and more particularly T1 mapping has become a most important modality to characterize myocardial tissue. In this work, we evaluated the precision and sensitivity of a fast radial MOLLI sequence by comparison with conventional MOLLI on 14 subjects presenting different heart rates, BMI and cardiac conditions. This sequence demonstrated the same precision on T1 estimates than conventional MOLLI, and was not influenced by heart rate variations. It might represent a good candidate for ultra-fast acquisition of myocardial T1 maps.

3114 Computer 20

Temporal Diffusion Spectroscopy in the Heart with Oscillating Gradients

Irvin Teh[1], Jürgen E. Schneider[1], Hannah J. Whittington[1], Tim B. Dyrby[2,3], and Henrik Lundell[2]

[1]Division of Cardiovascular Medicine, Radcliffe Department of Medicine, University of Oxford, Oxford, United Kingdom, [2]Danish Research Centre for Magnetic Resonance, Centre for Functional and Diagnostic Imaging and Research, Copenhagen University Hospital Hvidovre, Denmark, [3]Department of Applied Mathematics and Computer Science, Technical University of Denmark, Denmark

Conventional pulsed gradient spin echo, with its longer diffusion time, is poorly sensitive to diffusion at short length scales. Oscillating gradient spin echo enables assessment of diffusion at sub-cellular length scales, providing information about cell size and the intracellular environment. We observed that time dependence of diffusion in the myocardium was more pronounced along the 2nd and 3rd eigenvectors compared to the 1st eigenvector of the diffusion tensor. This is consistent with known anisotropic cardiomyocyte geometry. Furthermore, the measured diffusion at high frequencies still exhibited strong anisotropy that may reflect anisotropy of intracellular organelles such as actin-myosin filaments.

3115 Computer 21

Cardiac CEST MRI with Dual-Echo Readout for B0 Correction: A Preliminary Reproducibility Study for Assessment of Metabolic Activity in the Heart

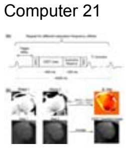

Zhengwei Zhou[1,2], Xiaoming Bi[3], and Debiao Li[1,2]

[1]Biomedical Imaging Research Institute, Cedars-Sinai Medical Center, Los Angeles, CA, United States, [2]Department of Bioengineering, University of California, Los Angeles, Los Angeles, CA, United States, [3]MR R&D, Siemens Healthcare, Los Angeles, CA, United States

Previous studies have shown that cardiac CEST technique can detect myocardial metabolic abnormalities in chronic myocardial infarction. However, this navigator-gated technique is still sensitive to B_0 field variations caused by respiratory motion within the acceptance window.

In this work, we developed a cardiac CEST dual-echo technique which not only acquires CEST-weighted image, but also enables acquisition of B_0 map for each saturation frequency offset. The reproducibility of this technique was also assessed.

3116 Computer 22

Dynamic Nitroxide-Enhanced MRI Detects Oxidative Stress in the Hearts of Mice Subject to Angiotensin II Infusion

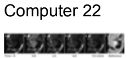

Sophia Xinyuan Cui[1], Rene J. Roy[2], Brent A. French[1,2], and Frederick H. Epstein[1,2]

[1]Biomedical Engineering, University of Virginia, Charlottesville, VA, United States, [2]Radiology, University of Virginia, Charlottesville, VA, United States

Oxidative stress contributes importantly to the pathophysiology of many types of cardiovascular disease. Nitroxides are relatively stable free radicals that have been used as redox-sensitive MRI contrast agents in preclinical studies to assess tumor redox status. We implemented a dynamic nitroxide-enhanced MRI method to test the hypothesis that MRI can detect cardiac oxidative stress in vivo. Imaging was performed in untreated controls and mice infused with angiotensin II for 7 days. The MRI signal decay rate in the heart was significantly higher in the angiotensin II group, indicating that these methods detect cardiac oxidative stress due to angiotensin II infusion.

Electronic Poster

Vascular Imaging: Lumen, Vessel Wall & Function

Exhibition Hall Monday 8:15 - 9:15

3117 Computer 25

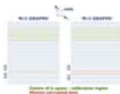

Estimation of motion-corrupted data using parallel imaging for carotid artery vessel wall imaging

Robert Frost[1,2,3], Luca Biasiolli[4], Linqing Li[5], Aaron T. Hess[4], and Peter Jezzard[3]

[1]Athinoula A. Martinos Center for Biomedical Imaging, Massachusetts General Hospital, Charlestown, MA, United States, [2]Department of Radiology, Harvard Medical School, Boston, MA, United States, [3]FMRIB Centre, Nuffield Department of Clinical Neurosciences, University of Oxford, Oxford, United Kingdom, [4]Oxford Centre for Clinical Magnetic Resonance Research, Division of Cardiovascular Medicine, University of Oxford, Oxford, United Kingdom, [5]Section on Magnetic Resonance Spectroscopy, National Institute of Mental Health, Bethesda, MD, United States

Carotid artery imaging is hampered by motion artefacts, including those caused by occasional swallowing motion. In this work, we extend previous work on intelligent reacquisition to estimate and replace motion-corrupted data. 'Bad' phase-encode lines were synthesized from surrounding 'good' lines using parallel imaging techniques. Estimation and replacement of corrupted data reduced background ghosting levels in comparison to the previous reacquisition approach. A small number of reacquisitions was maintained to ensure good quality data at the centre of k-space because these are essential for image quality and for calibration of the parallel imaging-based estimation.

3118 Computer 26

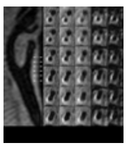

Three-dimensional black-blood multi-contrast protocol for carotid imaging using compressed sensing: a repeatability study

Jianmin Yuan[1], Ammara Usman[1], Scott A. Reid[2], Kevin F. King[3], Andrew J. Patterson[4], Jonathan H. Gillard[1], and Martin J. Graves[1,4]

[1]Department of Radiology, University of Cambridge, Cambridge, United Kingdom, [2]GE Healthcare, Amersham, United Kingdom, [3]GE Healthcare, Waukesha, Wisconsin, United States, [4]Department of Radiology, Cambridge University Hospitals NHS Foundation Trust, Cambridge, United Kingdom

Multi-contrast black-blood MRI protocol has demonstrated the ability to assess carotid plaque vulnerability. Current limitation for its wide application is the long scanning time. The purpose of this work is to evaluate the repeatability of a compressed sensing (CS) accelerated multi-contrast protocol at 3T.

3119 Computer 27

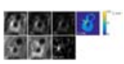

3D black blood T2 mapping of the carotid artery wall with compressed sensing and data-driven parallel imaging

Jianmin Yuan[1], Ammara Usman[1], Scott A. Reid[2], Kevin F. King[3], Andrew J. Patterson[4], Jonathan H. Gillard[1], and Martin J. Graves[1,4]

[1]Department of Radiology, University of Cambridge, Cambridge, United Kingdom, [2]GE Healthcare, Amersham, United Kingdom, [3]GE Healthcare, Waukesha, Wisconsin, USA, [4]Department of Radiology, Cambridge University Hospitals NHS Foundation Trust, Cambridge, United Kingdom

Quantitative MRI has many advantages over traditional contrast weighted methods, which may be more suitable for multi-centre studies across different MRI systems. This study describes the development of a 3D black blood T_2 mapping sequence with the combination of compressed sensing and data-driven parallel imaging. Phantom and volunteer experiments were performed to optimise the parameters and patients with atherosclerotic carotid artery disease were scanned using the optimised sequence.

3120 Computer 28

Whole-brain vessel wall imaging within 5 minutes using compressed sensing accelerated IR-SPACE

Zhaoyang Fan[1], Xiaoming Bi[2], Marcel Maya[3], Qi Yang[1,4], Shlee Song[5], Nestor Gonzalez[6], Schlick Konrad[5], Esther Raithel[7], Christoph Forman[7], Gerhard Laub[2], and Debiao Li[1]

[1]Biomedical Imaging Research Institute, Cedars-Sinai Medical Center, Los Angeles, CA, United States, [2]Siemens Healthcare, Los Angeles, CA, United States, [3]Imaging, Cedars-Sinai Medical Center, Los Angeles, CA, United States, [4]Xuanwu Hospital, Beijing, People's Republic of China, [5]Neurology, Cedars-Sinai Medical Center, Los Angeles, CA, United States, [6]Neurosurgery, Cedars-Sinai Medical Center, Los Angeles, CA, United States, [7]Siemens Healthcare, Erlangen, Germany

Inversion-recovery (IR) prepared SPACE was recently proposed as a whole-brain intracranial vessel wall imaging technique. This work aimed to investigate the feasibility of accelerating the scan from 8 min to <5 min using compressed sensing (CS). A prototype CS IR-SPACE sequence was implemented on a 3T system. Wavelet sparse regularization (λ) and iteration (Iter) were optimized for the scenario of sampling 15% of k-space data based on a volunteer study. Image quality was visually comparable between CS IR-SPACE and regular IR-SPACE scans. In addition, CS IR-SPACE and IR-SPACE showed comparable lesion delineation quality in patients despite markedly different scan times.

3121 Computer 29

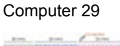

Endothelial permeability in the aortic root of atherosclerotic mice: quantification using 3 dimensional, black blood, self-gated T1 mapping

Alison Pruzan[1], Arthi Sridhar[1], Gustav Strijkers[1,2], Zahi A. Fayad[1], and Claudia Calcagno[1]

[1]Translational and Molecular Imaging Institute, Icahn School of Medicine at Mount Sinai, New York, NY, United States, [2]Academic Medical Center, Amsterdam, Netherlands

Atherosclerotic plaques prone to rupture are characterized by endothelial dysfunction and increased endothelial permeability. The aortic root is a vascular territory where permeable atherosclerotic plaques form consistently and reliably. However, morphological and quantitative parametric imaging of the mouse aortic root is very challenging, due to the small dimensions, rapid blood flow through the valves, and high heart rate. Here we demonstrate feasibility of pre and post-contrast T1 mapping of the mouse aortic root using a 3 dimensional, self-gated fast low angle shot (FLASH) sequence with black blood imaging for improved vessel wall delineation. Future studies will entail further development of this technique for the more accurate quantification of endothelial permeability and fractional blood volume in the mouse aortic root.

3122 Computer 30

Quantitative Multi-Contrast Atherosclerosis Characterization (qMATCH): Comprehensive Quantitative Evaluation of Atherosclerosis in a Single-Scan

Yibin Xie[1], Anthony Christodoulou[1], Nan Wang[1,2], and Debiao Li[1]

[1]Biomedical Imaging Research Institute, Cedars-Sinai Medical Center, Los Angeles, CA, United States, [2]Department of Bioengineering, University of California, Los Angeles, Los Angeles, CA, United States

Although MRI is an attractive imaging modality for the evaluation of carotid atherosclerosis thanks to its versatility and noninvasiveness, its current clinical usage is still limited. Major drawbacks of conventional protocols include long scan time and observer variability due to the qualitative nature of the images. In this work we proposed a fast, 3D, quantitative, multi-contrast MRI technique, qMATCH, for a comprehensive evaluation of carotid atherosclerosis in less than 8 minutes. Preliminary results from phantom and in vivo studies demonstrated excellent image quality and reliable quantification of tissue relaxation times.

3123 Computer 31

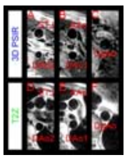

Aortic Vessel Wall Imaging Using 3D Phase Sensitive Inversion Recovery in Children and Young Adults

Animesh Tandon[1,2], Tarique Hussain[1,2], Andrew Tran[3], René M Botnar[4], Gerald F Greil[1,2], and Markus Henningsson[4]

[1]Pediatrics, Radiology, BME, University of Texas Southwestern Medical Center, Dallas, TX, United States, [2]Pediatric Cardiology, Children's Medical Center Dallas, Dallas, TX, United States, [3]Pediatrics, University of Texas Southwestern Medical Center, Dallas, TX, United States, [4]Biomedical Engineering, King's College, London, London, United Kingdom

Currently, T2-weighted TSE black blood zoom imaging (T2Z) is used to visualize atherosclerosis, but volumetric, high isotropic resolution datasets would be preferable. We compared aortic luminal sharpness (ALS) of a novel 3D bSSFP phase-sensitive inversion recovery black blood sequence (3DPSIR) to T2Z in 10 children and young adults with familial hypercholesterolemia at 5 aortic locations. 3DPSIR sequence duration was 7.0 minutes compared to 11.4 minutes for T2Z with no significant difference in ALS overall. 3DPSIR high resolution volumetric datasets will enable rapid, detailed 3D vessel wall imaging in children and young adults, allowing improved exploration of vascular health.

3124 Computer 32

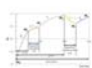

Quantitative T1 and T2* carotid atherosclerotic plaque imaging using 3D multi-echo phase-sensitive inversion recovery sequence: a feasibility study

Yasuhiro Fujiwara[1], Hirotoshi Maruyama[2], Kanako Toyomaru[3], Yuri Nishizaka[3], Kazuma Yamasaki[3], and Masahiro Fukamatsu[4]

[1]Department of Medical Imaging, Faculty of Life Sciences, Kumamoto University, Kumamoto, Japan, [2]Radiological Center, National Hospital Organization Kumamoto Saisyunsou Hospital, Kumamoto, Japan, [3]Graduate School of Health Sciences, Kumamoto University, Kumamoto, Japan, [4]Radiological Center, National Hospital Organization Kumamoto Medical Center, Kumamoto, Japan

A quantitative evaluation of plaques is required in MR plaque imaging. The purpose of this study was to determine whether the 3D multi-echo Phase-Sensitive Inversion Recovery sequence can improve the T1 intra-plaque hemorrhage (IPH)-to-muscle contrast while simultaneously providing accurate T1 and T2* values for an IPH. This sequence may have potential to improve plaque MR imaging and make it possible to obtain detailed information about the components of carotid atherosclerotic plaques.

3125 Computer 33

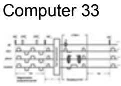

Quantitative Evaluation of RECS-3D MERGE MR Imaging for Carotid Plaque Assessment

Bo Li[1,2], Hao Li[3], Guofu Huang[1], Xia Qian[1], Wei Wang[1], and Li Dong[4]

[1]Center Laboratory, The First Hospital of Nanchang City, Nanchang, People's Republic of China, [2]Department of Radiology, The Third Affiliated Hospital of Nanchang University, Nanchang, People's Republic of China, [3]Department of Radiology, University of Cambridge, Cambridge, United Kingdom, [4]Department of Radiology, Beijing Anzhen Hospital, Beijing, People's Republic of China

We sought to quantitatively investigate the performances on blood suppression efficiency, wall-lumen CNR and plaque burden measurements for the RECS-3D MERGE sequence in carotid vessel wall MR imaging.

Twelve patients with carotid artery stenosis were recruited in this study. Lumen SNR and wall-lumen CNR were calculated and plaque burden measurements (i.e., lumen area, wall area, mean wall thickness and maximum wall thickness) were measured.

The RECS-3D MERGE was quantitatively demonstrated to have the ability to provide the comparable blood suppression, black-blood image quality and the highly correlated morphometry with the current plaque imaging protocol. The RECS-3D MERGE could be a promising tool for plaque burden measurement in a short scan time.

3126 Computer 34

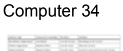

Evaluation of Four Injection Strategies for High Spatial Resolution Gadobenate Dimeglumine-Enhanced MR Angiography

Gregory J Wilson[1] and Jeffrey H Maki[1]

[1]Radiology, University of Washington, Seattle, WA, United States

Four injection profiles were evaluated in 40 subjects (10 each). The profiles were designed to provide a signal intensity plateau for a 20 second contrast-enhanced MR angiography scan, using gadobenate dimeglumine. The injection profiles were: 1) standard, non-diluted, 1.6 mL/sec; 2) diluted, 1.6 mL/sec; 3) diluted, bi-phasic, and 4) diluted, patient-tailored. All subjects received a total dose of 0.1 mmol/kg, divided between a test bolus and a full bolus. The "diluted" protocols included dilution of the total dose to 40 mL with normal saline. Signal intensity profiles were measured and analyzed for width of plateau (FW80M) and peak signal intensity.

3127 Computer 35

3D segmentation of the Pulmonary Arteries on Magnetic Resonance Angiography

Christopher S Johns[1], Alberto Biancardi[1,2], Guilhem J Collier[1], David A Capener[1], Andy J Swift[1,2], and Jim M Wild[1]

[1]Academic Radiology, The University of Sheffield, Sheffield, United Kingdom, [2]Insigneo, Institute of In-Silico Medicine, Sheffield, United Kingdom

Contrast enhanced magnetic resonance angiography (MRA) is in common use in the assessment of pulmonary hypertension. We present a novel method for segmentation of the pulmonary arteries allowing rapid assessment of the proximal pulmonary arteries down to the 4th generation. Whilst the strongest correlation with mean pulmonary artery pressure was with the right main pulmonary artery, the torsion of the 4th generation pulmonary arteries was also associated with increasing mean pulmonary artery pressure. We hope quantitative vessel segmentation will improve our understanding of the impact of proximal pulmonary arterial remodelling in pulmonary hypertension.

3128 Computer 36

The value of 3T contrast-enhanced whole-heart Coronary MRA in a integrated assessment of Cardiac Magnetic Resonance Protocol for Detection of suspected or known Coronary Artery Disease

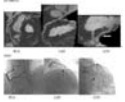

lijun zhang [1], Yi He[1], Zhan ming Fan[1], and Debiao Li[2]

[1]Radiology Department, Beijing Anzhen Hospital, Capital Medical University, Beijing, People's Republic of China, [2]Cedars-Sinai Medical Center, Biomedical Imaging Research Institute,University of California, Los Angeles, United States

We try to evaluate the additive diagnostic value of a 3T whole-heart CE-MRCA integration into a CMR-MPI/LGE protocol for the detection of coronary artery disease A total of 38 subjects were examined by CMR (including CMR-MPI, MRCA, and LGE)[j1] and x-ray invasive coronary angiography (ICA). Diagnostic performances of MRCA, CMR-MPI/LGE, and MRCA+CMR-MPI/LGE integration were determined having XA as standard for coronary artery disease. In per-vessel analysis, integrated protocol (AUC=0.84) performed better than the isolated CMR-MPI/LGE (AUC=0.63). In this suspected or known coronary artery disease population, integration of CE-MRCA significantly improved per-vessel diagnostic accuracy of a comprehensive 3T CMR-MPI/LGE protocol.

3129 Computer 37

A novel method for performing percutaneous transluminal renal angioplasty with the guide of non-contrast magnetic resonance angiography overlaid on fluoroscopy images

Yoshiaki Morita[1], Tetsuya Fukuda[1], Yoshiaki Watanabe[1], Tatsuya Nishii[1], Atsushi Kono[1], and Naoaki Yamada[1]

[1]Department of Radiology, National Cerebral and Cardiovascular Center, Suita, Osaka, Japan

Herein, we present a new method for the performance of percutaneous transluminal renal angioplasty (PTRA) guided by non-contrast magnetic resonance angiography (NATIVE True FISP) overlaid on intra-procedural fluoroscopy images. This novel overlay system led to sufficient visualization as the overlaid vasculature on the live fluoroscopic image, and enabled the safe completion of PTRA with fewer angiographic procedures, thus requiring lower volumes of iodinated contrast material and shorter fluoroscopic times.

3130 Computer 38

Velocity-selective unenhanced peripheral MR angiography: Initial clinical testing compared with digital subtraction angiography

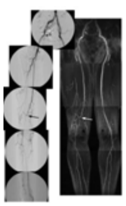

Taehoon Shin[1], Rajiv G Menon[2], Devin Watson[3], Rajabrata Sarkar[3], Sanjay Rajagopalan[4], and Robert Crawford[3]

[1]Diagnostic Radiology and Nuclear Medicine, University of Maryland, Baltimore, MD, United States, [2]New York University, New York, NY, United States, [3]Vascular Surgery, University of Maryland, Baltimore, MD, United States, [4]Cardiovascular Medicine, Case Western Reserve, Cleveland, OH, United States

We performed initial clinical testing of velocity-selective magnetization-prepared MR angiography (VS-MRA) in 31 patients with peripheral arterial disease with digital subtraction angiography (DSA) serving as the reference standard. The image quality score of VS-MRA was 2.8±0.6 in the scale of 0-3 (0: non-diagnostic, 3: excellent). The sensitivity and specificity for detecting significant stenosis were 90.1 % and 96.2%, respectively on a per-segment basis (n=286), and were 92.7% and 92.0 %, respectively on a per-region basis (n=105). The Fleiss-Cohen κ value for the agreement between VS-MRA and DSA was 0.91 on a per-segment basis and 0.88 on a per-region basis.

3131 Computer 39

Super-Resolution Intracranial Quiescent-Interval Slice-Selective Magnetic Resonance Angiography

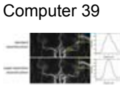

Ioannis Koktzoglou[1,2], Shivraman Giri[3], Jianing Pang[3], Jeremy D Collins[4], and Robert R Edelman[1,4]

[1]Radiology, NorthShore University HealthSystem, Evanston, IL, United States, [2]Radiology, University of Chicago Pritzker School of Medicine, Chicago, IL, United States, [3]Siemens Healthineers, Chicago, IL, United States, [4]Radiology, Northwestern University Feinberg School of Medicine, Chicago, IL, United States

We evaluated whether super-resolution reconstruction could be used to improve the vascular detail of quiescent-interval slice-selective (QISS) MRA of the intracranial circulation. Results suggest that super-resolution reconstruction can substantially improve intracranial arterial delineation without the signal-to-noise ratio penalty of directly acquiring thin-slice images.

3132 Computer 40

Simultaneous Bright and Black Blood Whole Heart Phase Sensitive Inversion Recovery (PSIR) for Non Contrast Enhanced Coronary Lumen and Plaque Characterization

Giulia Ginami[1], Radhouene Neji[2], Rene Botnar[1], and Claudia Prieto[1]

[1]Division of Imaging Sciences and Biomedical Engineering, King's College London, London, United Kingdom, [2]MR Research Collaborations, Siemens Healthcare Limited, Frimley, United Kingdom

This study introduces a 3D whole-heart sequence with image-based navigation for non-contrast enhanced coronary lumen and coronary thrombus/haemorrhage characterization. The sequence is based on a phase sensitive inversion recovery (PSIR)-like approach enabling the acquisition of two bright-blood datasets for visualization of the coronary lumen and estimation of motion parameters. Furthermore, a third, fully co-registered dark-blood dataset for thrombus/haemorrhage characterization is obtained from the PSIR reconstruction. With the proposed approach the coronary lumen is visualized with improved SNR/CNR and vessel sharpness when compared to a conventional T2 prepared coronary MRA acquisition. In addition, effective blood signal suppression and feasibility for thrombus visualization is shown with the PSIR reconstructed black-blood dataset.

3133 Computer 41

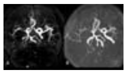

Evaluating Circle of Willis using Simultaneous Non-Contrast Angiography and intraPlaque Hemorrhage (SNAP)

Yalun Chen[1], Ling Tang[2], Le He[2], Xihai Zhao[2], Zhensen Chen[2], and Huijun Chen[3]

[1]Chongqing Medical University, Chongqing, People's Republic of China, [2]Department of Biomedical Engineering, School of Medicine, Tsinghua University, [3]Departement of Biomedical Engineering, School of medicine, Tsinghua University, Beijing, People's Republic of China

The purpose of this study is to evaluate the ability of SNAP to evaluate the CoW by comparing with an established non-contrast MRA technique, time of flight (TOF).We found SNAP have good agreement with TOF and similar intra-reader reproducibility in CoW evaluation. However, the agreement between TOF and SNAP and the reproducibility of each technique is moderate in the anterior communicating artery identification. Thus, SNAP shows great promise for imaging both intracranial artery and vessel wall with a single scan.

3134 Computer 42

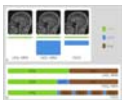

Flow enhanced (FEED) Arterial Spin Labeling Angiography with segmented Zero Echo Time Readout

Jianxun Qu[1], Bing Wu[1], and Zhenyu Zhou[1]

[1]MR Research China, GE Healthcare, Beijing, People's Republic of China

ASL based MRA with continuous labeling has the optimal label efficiency. To achieve data acquisition efficiency, a long readout train is frequently used after labeling. Flow void might appear due to the lack of tagged blood entering the imaging volume during readout. A method named hybrid ASL address this problem with additional pulsed inversion. Yet, blood inverted by pulsed ASL still experiences considerable T1 decay during readout. We propose a method termed flow enhanced ASL (FEED). Interleaved labeling modules along with segmented readout was employed. As the results show, FEED could increase the signal level without prolonging scan time.

3135 Computer 43

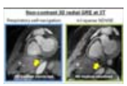

Free-breathing non-contrast 3D radial respiratory motion-resolved versus motion-corrected whole-heart coronary MRA at 3T

Jessica AM Bastiaansen[1], Lorenzo di Sopra[1], Jérôme Yerly[1,2], Davide Piccini[3], Ruud B van □eeswijk[1], and Matthias Stuber[1,2]

[1]Department of Radiology, Hospital Lausanne (CHUV) and University of Lausanne (UNIL), Lausanne, Switzerland, [2]Center for Biomedical Imaging, Lausanne, Switzerland, [3]Advanced Clinical Imaging Technology, Siemens Healthcare AG, Lausanne, Switzerland

Coronary MRA performed using respiratory self-navigation techniques that apply retrospective motion-correction suffer from artifacts originating from static anatomical structures surrounding the heart. This becomes even more complicated at 3T due to insufficient fat suppression. Here we implemented free-breathing self-navigated 3D coronary MRA at 3T. Instead of using a motion model, we resolved the motion using 4D k-t sparse SENSE. Resulting images were then quantitatively compared with those reconstructed from the same datasets but using a 1D motion correction. We demonstrate that non-contrast whole-heart coronary MRA can be performed at 3T and that 4D motion-resolved reconstruction effectively minimizes adverse effects of respiratory-motion.

3136 Computer 44

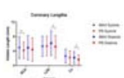

Dual-Phase Whole-Heart Imaging Using Image Navigation in Congenital Heart Disease

Danielle M. Moye[1,2], Tarique Hussain[1,2], Rene M. Botnar[3], Animesh Tandon[1,2], Gerald F. Greil[1,2], Adrian K. Dyer[1,2], and Markus Henningsson[3]

[1]Pediatric Cardiology, UT Southwestern Medical Center Dallas, Dallas, TX, United States, [2]Pediatric Cardiology, Children's Health, Children's Medical Center Dallas, Dallas, TX, United States, [3]Division of Imaging Sciences, King's College London

Dual phase whole heart imaging allows accurate depiction of cardiac segmental anatomy for congenital heart disease. We applied image-based navigation (iNAV) to improve its clinical utility. Qualitative and quantitative image quality scoring showed that iNAV gave equivalent image quality compared to the standard respiratory navigator. However, the distal coronary arteries were better visualized and the sequence duration was shorter. Using dual-phase iNAV, complete segmental anatomy was delineated in 27/30 patients (90%). The use of iNAV dual phase 3D SSFP whole heart acquisition allows complete morphological diagnosis for congenital heart disease with high image quality with more clinically acceptable time constraints.

3137 Computer 45

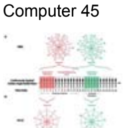

Improved Golden-Angle Stack-of-Stars Non-Contrast Enhanced 4D Dynamic MR Angiography using Parallel Imaging and Compressed Sensing

Ziwu Zhou[1], Fei Han[1], Songlin Yu[2], Dandan Yu[2], Stanislas Rapacchi[1], Danny J.J. Wang[3], Lirong Yan[3], and Peng Hu[1]

[1]Radiological Sciences, University of California, Los Angeles, Los Angeles, CA, United States, [2]Neurology, University of California, Los Angeles, Los Angeles, CA, United States, [3]Neurology, University of Southern California, Los Angeles, CA, United States

In this study, we investigated the feasibility of accelerating a recently proposed arterial spin labeling (ASL) based, time-resolved non-contrast enhanced dynamic MR angiography (NCE-dMRA) technique using parallel imaging and compressed sensing. By taking advantage of the inherent and unique “subtraction sparsity” in ASL type acquisition, we combined a recently developed CS technique, which uses a magnitude subtraction to enhance sparsity in MRA data, with the ESPIRiT method for SENSE type PI reconstruction. Proposed method was compared with the previously used KWIC reconstruction to demonstrate its advantage in reducing temporal blurring caused by view-sharing.

3138 Computer 46

Single-Shot Coronary QISS MRA in Children using Radial k-Space Sampling and Compressed Sensing

Daming Shen[1], Robert R. Edelman[2], Joshua D Robinson[3], Hassan Haji-Valizadeh[1], Shivraman Giri[4], Ioannis Koktzoglou[2], Cynthia K. Rigsby[3], and Daniel Kim[3]

[1]Biomedical Engineering, Northwestern University, Chicago, IL, United States, [2]Department of Radiology, NorthShore University HealthSystem, Evanston, IL, United States, [3]Department of Radiology, Northwestern University, Chicago, IL, United States, [4]Cardiovascular MR R&D, Siemens Healthineers, Chicago, IL, United States

Coronary MRA is complex to set up (e.g., navigator gating to track respiratory motion), typically takes 5-10 min to complete, and often produces inconsistent results. Quiescent-Interval Slice-Selective (QISS) MRA is a promising method for rapid coronary imaging. We sought to develop a single-shot (real-time) coronary QISS MRA using compressed sensing.

3139 Computer 47

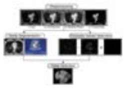

Automated Coronary Artery Ostia Detection in Magnetic Resonance Angiography

Bernhard Stimpel[1], Christoph Forman[2], Jens Wetzl[1,3], Michaela Schmidt[2], Andreas Maier[1,3], and Mathias Unberath[1,3]

[1]Pattern Recognition Lab, Department of Computer Science, Friedrich-Alexander-Universität Erlangen-Nürnberg, Erlangen, Germany, [2]Magnetic Resonance, Siemens Healthcare GmbH, Erlangen, Germany, [3]Erlangen Graduate School in Advanced Optical Technologies (SAOT), Friedrich-Alexander-Universität Erlangen-Nürnberg, Erlangen, Germany

Anomalies of the coronary ostia can have severe consequences. To provide a screening solution, automated ostia detection based on single breath-hold coronary MRA scans is presented. The aorta is segmented in the data sets to serve as an orientation point and vesselness enhancing filters are applied. Searching the aorta surface for high vessel responses by a ray-tracing procedure yields information about the position of the coronary ostia. The proposed approach was successfully validated in 10 volunteers with an average deviation of 7.6 ± 1.0° in angular and 1.2 ± 0.58 mm in superior-inferior direction.

3140 Computer 48

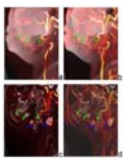

Using Non-Contrast-Enhanced Magnetic Resonance Angiography (MRA) in Evaluating Preoperative Facial Artery of Vacularized Submental Lymph Node Flap: Compared to Conventional Contrast-Enhanced MRA

Ming-Chen Wu[1], Ming-Yi Hsu[1], Ren-Fu Shie[1], Yui-Ping Fan[1], Hsiao-Ching Yu[1], Chien-Yuan Eddy Lin[2,3], and Sung-Yu Chu[1]

[1]Department of Medical Imaging and Intervention, Chang Gung Memorial Hospital, Taoyuan, Taiwan, [2]GE Healthcare, Taiwan, [3]GE Healthcare MR Research China, Beijing, People's Republic of China

The aim of this study was to determine whether the recently developed non-contrast-enhanced Inhance 3D velocity magnetic resonance angiography (Inhance 3D MRA) technique is capable of evaluating the course of facial artery (branch artery) in preoperative evaluation of vacularized submental lymph node flap. The result shows that Inhance 3D MRA is a promising method for assessing facial artery course without concerning the contrast media (CM) travel time and the venous contamination.

Electronic Poster

Cardiac Function

Exhibition Hall Monday 8:15 - 9:15

3141 Computer 49

Age-stratified normal left atrial deformation assessed by novel longitudinal strain parameters on a 3T MR scanner

Shuang Leng[1], Xiaodan Zhao[1], Angela Su-Mei Koh[1,2], Ru San Tan[1,2], and Liang Zhong[1,2]

[1]National Heart Centre Singapore, Singapore, Singapore, [2]Duke-NUS Medical School Singapore, Singapore, Singapore

The aim of this study was to examine the age-related normal left atrial (LA) longitudinal deformation by a novel and fast assessable strain parameter with standard cardiac magnetic resonance (CMR) imaging. A total of 60 heathy subjects (30 males, age between 20 and 80 years) were categorized by age into young, middle-aged, and elderly adults. The LA longitudinal strain and strain rate measurements corresponding to reservoir and conduit phases were negatively related to age, while no significant age-dependency was observed for LA contraction strain and strain rate values. These strain parameters can be used to evaluate LA deformation and functionality.

3142 Computer 50

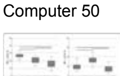

Right ventricular deformation by CMR feature tracking in patients with volume-overload and pressure-overload congenital heart diseases

Shuang Leng[1], Xiaodan Zhao[1], Wen Ruan[1], Ru San Tan[1,2], Ju Le Tan[1,2], and Liang Zhong[1,2]

[1]National Heart Centre Singapore, Singapore, Singapore, [2]Duke-NUS Medical School Singapore, Singapore, Singapore

Two major patterns of right ventricular (RV) overload are volume overload and pressure overload. This study aimed to investigate the differences of RV myocardial deformation associated with volume and pressure overload congenital heart diseases. Cardiac magnetic resonance feature tracking was applied to RV 4-chamber and short axis view in a subject group comprising 23 patients with repaired tetralogy of Fallot (rTOF), 23 patients with pulmonary hypertension (PH), and 23 age- and gender-matched normal controls. Results indicated that PH patients had most diminished RV longitudinal and circumferential strain. Patients with rTOF had reduced RV longitudinal strain but higher circumferential strain.

3143 Computer 51

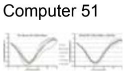

Accelerated Cardiac Cine “Watermark” MRI provides Cardiac Function via Magnitude Cine and 2D Myocardial Strain via Spatially Modulated Phase

Ronald J Beyers[1], Davis M Vigneault[2,3,4], Nouha Salibi[1,5], David A Bluemke[4], and Thomas S Denney[1]

[1]MRI Research Center, Auburn University, Auburn, AL, United States, [2]Department of Engineering Science, University of Oxford, Oxford, United Kingdom, [3]Sackler School of Graduate Biomedical Sciences, School of Medicine, Boston, MA, United States, [4]Radiology and Imaging Sciences, National Institutes of Health, Bethesda, MD, United States, [5]MR R&D, Siemens Healthcare, Malvern, PA

We developed a parallel imaging accelerated Cine Watermark (CWM) sequence to provide normal cine magnitude images plus phase image-only multi-directional spatial encoding for quantitative cine strain -- while requiring no extra operator effort. Spatial cosine modulation post-processed by complex image sum/differencing produced separate normal magnitude cine and unique phase-only spatial modulation for strain calculation. *In vivo* human scans demonstrated good magnitude cine and phase-only quantified displacement. Cardiac strains were tracked by a novel non-linear least squares method combining quadratic b-spline contours, nearest neighbor optimized phase tracking, and physically-motivated regularizers. Cardiac left ventricular, short-axis, circumferential strain results agreed with previous literature.

3144 Computer 52

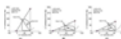

Left ventricular-arterial coupling and mechanical efficiency assessed by pressure-volume loop in pulmonary artery hypertension patients

Xiaodan Zhao[1], Fei Xu[2], Xiaoke Shang[3,4], Yang Dong[2], Wen Ruan[1], Gangcheng Zhang[5], Ru San Tan[1,6], Ju Le Tan[1,6], Yucheng Chen[2], and Liang Zhong[1,6]

[1]National Heart Centre Singapore, Singapore, Singapore, [2]West China Medical Centre of Sichuan University, People's Republic of China, [3]Wuhan Union Hospital, Tongji Medical College, Huazhong University of Science and Technology, Wuhan, People's Republic of China, [4]Department of Cardiology, Second Clinical College of Wuhan University, WuHan, People's Republic of China, [5]WuHan Asia Heart Hospital, People's Republic of China, [6]Duke-NUS Medical School Singapore, Singapore, Singapore

Left ventricular end-systolic elastance (Ees), arterial elastance (Ea) and ventricular arterial coupling (VAC) (ratio of Ea/Ees) has been considered “gold” standard to assess ventricular contractility and performance. Ventricular arterial uncoupling due to impaired Ees or augmented Ea impaired ventricular mechanical efficiency (ME) and cardiac output. Ventricular contractility and arterial loading and the degree of their mismatching have yet been studied in pulmonary hypertension (PH). A total of 42 PH subjects who underwent both cardiac magnetic resonance (CMR) and right heart catheterization (RHC) were categorized into three groups – preserved LV ejection fraction (LVEF > 50%) and VAC < 0.8 (group 1); preserved LVEF and VAC > 0.8 (group 2); reduced LVEF (< 50%) (group 3). The results showed that VAC was correlated negatively with ME, which indicated arterial-ventricular uncoupling impaired mechanical efficiency. Importantly, the group 2 with ventricular arterial uncoupling had impaired mechanical efficiency despite its preserved ejection fraction.

3145 Computer 53

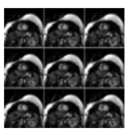

Cardiac function relation to preload variation based on free breathing motion

Teodora Chitiboi[1], Rebecca Ramb[1], Eve Piekarski[2], Li Feng[1], Anja Hennemuth[3], and Leon Axel[1]

[1]Radiology, New York University School of Medicine, New York, NY, United States, [2]Nuclear Medicine Ward, Pitié Salpétrière Hospital, Paris, Paris, France, [3]Fraunhofer MEVIS, Germany

Free-breathing cardiac cine MRI provides novel information on cardiac dynamics. In this work, we investigate the relation between cardiac function and left-ventricular preload variations induced by respiratory motion, in normal subjects and patients. We used the left-ventricular diameter perpendicular to the septum as a measure of preload and the relative change in diameter between end-systole and end-diastole as a measure of functional response. There was a significantly larger change in diameter during the respiratory cycle for normal subjects compared to patients. We also found a significant correlation between preload and cardiac function for normal subjects, which was reduced for patients.

3146 Computer 55

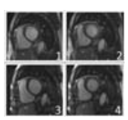

Quantitative Evaluation of Ultra-fast Real Time Imaging Compared to Cine at 1.5 T and Demonstration of Clinical Value in Atrial Fibrillation

Aaron T Hess[1], Betty Raman[1], Joana Leal[1], Adam Lewandowski[2], Jane Francis[1], Masliza Mahmod[1], Dirk Voit[3], Markus Untenberger[3], Jens Frahm[3], Stefan Neubauer[1], and Matthew David Robson[1]

[1]OCMR, Oxford University, Oxford, United Kingdom, [2]RDM, Oxford University, Oxford, United Kingdom, [3]Biomedizinishe NMR Forschungs GmbH, Max-Plank-Institut fur biophysikalische Chemie, Gottingen, Germany

Ultra-fast real time imaging allows cine imaging of the whole heart without gating or breath-holding in around 1 minute. Here clinical cardiac metrics are evaluated and compared with those from a standard clinical acquisition in normal volunteers. We find agreement adequate for clinical use. The real time approach is evaluated in a case of atrial fibrillation and found to provide a more robust evaluation of cardiac parameters in a shorter acquisition time.

3147 Computer 56

UNFOLDed spiral SPiRIT TPM enables high spatio-temporal resolution analysis of cardiac function

Marius Menza[1], Moritz Braig[1], Bend Jung[2], Daniela Föll[3], Jürgen Hennig[1], and Axel Joachim Krafft[1]

[1]Dept. of Radiology, Medical Physics, Medical Center – University of Freiburg, Freiburg, Germany, [2]Institute of Diagnostic, Interventional and Pediatric Radiology, University Hospital Bern, Bern, Switzerland, [3]Cardiology and Angiology, University Heart Center, Freiburg, Germany

A detailed TPM analysis of cardiac function necessitates high spatio-temporal resolution which leads to prolonged scan durations. These scan times are typically too long for data acquisition within a single breath hold. Respiratory navigator-gating can compensate breathing-related motion, but causes an additional increase in measurement time and images with residual motion artifacts. The aim of this study was to combine UNFOLD with variable density spiral SPiRIT TPM to achieve an additional scan time reduction by a factor of 2 and an effective undersampling factor of 6. UNFOLDed SPiRIT TPM demonstrates good results and enables scan times within very short breath holding.

3148 Computer 57

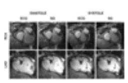

MOTION-RESOLVED 5D IMAGING OF THE HEART: TIME TO GET RID OF THE ECG?

Lorenzo Di Sopra[1], Davide Piccini[1,2], Simone Coppo[3], Jessica A.M. Bastiaansen[1], Matthias Stuber[1,4], and Jérôme Yerly[1,4]

[1]Department of Radiology, University Hospital (CHUV) and University of Lausanne (UNIL), Lausanne, Switzerland, [2]Advanced Clinical Imaging Technology, Siemens Healthcare AG, Lausanne, Switzerland, [3]Department of Radiology, Case Western Reserve University, Cleveland, OH, [4]Center for Biomedical Imaging (CIBM), Lausanne, Switzerland

The performance of motion-resolved whole-heart MR imaging strongly depends on the quality of cardiac- and respiratory-gating signals. While navigators or self-navigation can be used to account for respiratory motion, ECG is a mainstay for synchronizing data acquisition with the cardiac cycle. We tested whether physiological motion information, directly extracted from k-space-center, can replace respiratory navigators and ECG signals. The proposed solution was applied in 9 healthy volunteers and results were compared to those obtained with the ECG-signal. Correlation between R-wave time-stamps from the ECG and the cardiac self-gating signal was excellent, while image quality and coronary artery conspicuity remained unchanged.

3149

Computer 58

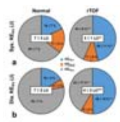

Does Right Ventricular Myocardial Kinetic Energy Correlate With Pressure Overload in Repaired Tetralogy of Fallot Patients?

Meng-Chu Chang[1], Ming-Ting Wu[2], Ken-Pen Weng[3], Mao-Yuan Su[4], Marius Menza[5], Hung-Chieh Huang[2], and Hsu-Hsia Peng[1]

[1]Department of Biomedical Engineering and Environmental Sciences, National Tsing Hua University, Hsinchu, Taiwan, [2]Department of Radiology, Kaohsiung Veterans General Hospital, Kaohsiung, Taiwan, [3]Department of Pediatrics, Kaohsiung Veterans General Hospital, Kaohsiung, Taiwan, [4]Department of Medical Imaging, National Taiwan University Hospital, Taipei, Taiwan, [5]Medical Physics, Department of Radiology, University Hospital Freiburg, Freiburg, Germany

The association of right ventricular (RV) myocardium adapted to pressure overload of repaired tetralogy of Fallot (rTOF) patient is still unclear. We evaluated three-directional myocardial kinetic energy (KE) and correlated it with RV-related pressure. The recruited rTOF patients presented decreased peak KE_{RV} both in systole and diastole. However, patient group exhibited increased percentage of radial KE_{RV}, accompanying with highly positive correlation with RV systolic pressure. In conclusion, the investigation of the correlation between myocardial kinetic energy and RV pressure overload may helpful to comprehend compensatory mechanism and myocardial remodeling in patients with rTOF.

3150

Computer 59

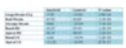

Myocardial Strain Imaging with Feature Tracking MRI in Patients with Cardiac Amyloidosis: Comparison with Normal Control Subjects

James Glockner[1]

[1]Radiology, Mayo Clinic, Rochester, MN, United States

Feature tracking (FT) myocardial strain analysis was performed in 87 patients with biopsy proven cardiac amyloidosis and in 64 control subjects using long and short axis ECG-triggered b-SSFP images and commercial software. Radial, circumferential, and longitudinal peak systolic strain values were all significantly different between amyloid patients and control subjects, suggesting that this technique is feasible in assessing patients with suspected cardiac amyloidosis.

3151

Computer 60

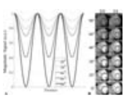

Feature-Tracking Regional Myocardial Strain: Effects of Tag Strength and Flip Angle

Eric Schrauben[1], Andreas Greiser[2], Brett Cowan[3], and Alistair Young[3]

[1]Physiology & Experimental Medicine, University of Toronto, Toronto, ON, Canada, [2]Siemens Healthcare, Erlangen, Germany, [3]Anatomy and Medical Imaging, University of Auckland, Auckland, New Zealand

Using feature-tracking combined with variable tag strength and flip angle, myocardial strain is measured and compared against traditional tagging MRI in healthy volunteers .

3152

Computer 61

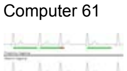

Free-Breathing Self-Navigated Isotropic 3-D CINE Imaging of the Whole Heart using Adaptive Triggering and Retrospective Gating

Jens Wetzl[1,2], Felix Lugauer[1], Randall Kroeker[3], Michaela Schmidt[3], Andreas Maier[1,2], and Christoph Forman[3]

[1]Pattern Recognition Lab, Department of Computer Science, Friedrich-Alexander-Universität Erlangen-Nürnberg, Erlangen, Germany, [2]Erlangen Graduate School in Advanced Optical Technologies (SAOT), Friedrich-Alexander-Universität Erlangen-Nürnberg, Erlangen, Germany, [3]Siemens Healthcare GmbH, Erlangen, Germany

We present a method for free-breathing whole-heart 3-D CINE imaging based on adaptive triggering and retrospective gating and compare it to a previously published method using prospective triggering. We show that our method is simultaneously robust to heart-rate variability during the scan and able to cover the entire cardiac cycle, which is not the case for prospective triggering. A validation in 6 volunteers shows reduced end-diastolic volume bias compared to a gold-standard 2-D reference for our method. Image reconstruction is integrated into the scanner system and takes less than 3 minutes.

3153

Computer 62

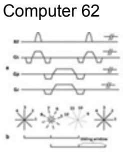

Real-time cardiac cine based on a radial bSSFP sequence and compressed sensing: initial experience on the evaluation of left ventricular function in patients

Xiaoyong Zhang[1,2], Zhongzhou Chen[2], Xiaohai Ma[3], Lei Zhao[3], Hui Chen[3], Caiyun Shi[2], Shi Su[2], Xin Liu[2], Bensheng Qiu[4], Zhaoyang Fan[5], and Guoxi Xie[2]

[1]Centers for Biomedical Engineering, University of Science and Technology of China, Hefei, People's Republic of China, [2]Shenzhen Institutes of Advanced Technology, Chinese Academy of Sciences, Shenzhen, People's Republic of China, [3]Beijing Anzhen Hospital, Capital Medical University, Beijing, People's Republic of China, [4]Centers for Biomedical Engineering, University of Science and Technology of China, Heifei, People's Republic of China, [5]Cedars-Sinai Medical Center, Los Angeles, CA, United States

Cardiac cine magnetic resonance imaging is a valuable technique for assessing cardiac function. However, conventional cardiac cine imaging is based on breath-holding and ECG-triggering, which has particularly difficulty to be used for the diagnosis of the patients with arrhythmia. In this work, a novel technique for real-time cardiac cine imaging was developed and used to evaluate the left ventricular (LV) function in patients with arrhythmia. Preliminary experiment results demonstrated that the proposed method can accurately evaluate patient's LV function without the use of ECG triggering and improve the image quality of the patients with arrhythmia.

3154 Computer 63

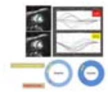

Global circumferential strain derived from feature tracking imaging can detect early subclinical myocardial disorders in patients with heart failure preserved ejection fraction: Comparison with tagged cine magnetic resonance imaging

Yoshiaki Morita[1], Naoaki Yamada[1], Makoto Amaki[2], Yoshiaki Watanabe[1], Tatsuya Nishii[1], Atsushi Kono[1], and Tetsuya Fukuda[1]

[1]Department of Radiology, National Cerebral and Cardiovascular Center, Suita, Osaka, Japan, [2]Division of Cardiology, National Cerebral and Cardiovascular Center, Suita, Osaka, Japan

The heart failure preserved ejection fraction (HFpEF) accounts for 40–50% of all causes of heart failure. For HFpEF, identification of strain disturbances where systolic function is seemingly preserved is a decisive step toward revealing hidden heart damage. Recently, the novel technique of feature tracking imaging (FTI) was introduced for myocardial strain measurement directly from conventional cine images. We demonstrated that FTI allows for detailed strain assessment with acceptable correlation with the tagging method. In particular, global circumferential strain, which cannot be detected by analysis using cine images, may possibly serve as a sensitive and early marker of cardiac dysfunction.

3155 Computer 64

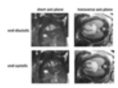

The utility of fetal MRI using real-time cine imaging for the functional assessment of congenital cardiovascular abnormality

Yoshiaki Morita[1], Mitsuhiro Tsuritani[2], Naoaki Yamada[1], Yoshiaki Watanabe[1], Tatsuya Nishii[1], Atsushi Kono[1], Jun Yoshimatsu[2], and Tetsuya Fukuda[1]

[1]Department of Radiology, National Cerebral and Cardiovascular Center, Suita, Osaka, Japan, [2]Department of Perinatology and Gynecology, National Cerebral and Cardiovascular Center, Suita, Osaka, Japan

Volumetric analysis of the fetal heart by ultrasound (US) in congenital heart disease is often difficult due to its complex anatomy and US-specific artifacts. We implemented the real-time cine sequence without ECG triggering and the post-processing technique (PhyZiodynamics), which enabled noise reduction and interpolation based on motion coherence. Fetal MRI using real-time cine imaging allowed for detailed functional assessment in both ventricles and showed acceptable levels of correlation with both the prenatal and postnatal US findings, suggesting that this technique is a promising diagnostic tool for functional assessment of congenital cardiovascular abnormalities.

3156 Computer 65

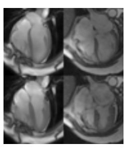

Four Chamber Endocardial Surface Reconstruction from Cardiac MRI Data

Xiaoxia Zhang[1,2], Steven Lloyd[3,4], Himanshu Gupta[3,4], James Davies[3], Nouha Salibi[1,5], Louis Dell'Italia[3,4], and Thomas Denney[1,2]

[1]Auburn University MRI Research Center, Auburn University, Auburn, AL, United States, [2]Electrical and Computer Engineering, Auburn University, Auburn, AL, United States, [3]Division of Cardiovascular Disease, University of Alabama at Birmingham, Birmingham, AL, United States, [4]Birmingham Veterans Affairs Medical Center, Birmingham, AL, United States, [5]MR R&D, Siemens Healthcare, Malvern, PA, United States

Shape analysis of cardiac chambers has important implications for cardiac diseases, most extensively studied in mitral regurgitation (MR). Here we present a novel algorithm for fitting surfaces to the endocardium of all four chambers through the entire cardiac cycle and demonstrate its use in patients with MR. This algorithm, which is based on standard CMR acquisitions, demonstrates improved visualization of the chambers and their function, which can help cardiologists and surgeons in treatment planning in conditions such as mitral regurgitation.

3157 Computer 66

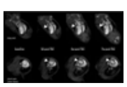

Regions of spared hypertrophy in pressure overloaded hearts promote severe systolic dysfunction as assessed by comprehensive cardiovascular magnetic resonance

Sebastian Maximilian Haberkorn[1,2], Joachim Schmitt[3], Christoph Jacoby[1], Jürgen Schrader[2,4], Malte Kelm[1,4], and Uli Flögel[2,4]

[1]Department of Cardiology, University Hospital Duesseldorf, Duesseldorf, Germany, [2]Department of Molecular Cardiology, Heinrich-Heine University Duesseldorf, Duesseldorf, Germany, [3]Heinrich-Heine University Duesseldorf, Department of Pharmacology and Clinical Pharmacology, Duesseldorf, Germany, [4]Cardiovascular Research Institute, Heinrich-Heine University Duesseldorf, Duesseldorf, Germany

Regional heterogeneity of contractile function was described in patients with left ventricular (LV) hypertrophy, suggesting a predominant impairment of areas with distinct hypertrophy. Heterogeneity of myocardial hypertrophy therefore may contribute to global and regional abnormalities of LV function. Here, we systematically investigated the spatial and temporal patterning of myocardial hypertrophy in response to experimental pressure overload by cardiovascular MRI. Surprisingly, we identified a specific basolateral LV segment that is frequently spared from the development of myocardial hypertrophy and promotes systolic dysfunction. Moreover, the initial LV geometry and the vascular topology seemed to limit the extent of adaptation to pressure overload.

3158 Computer 67

Healthy aging of the left ventricle in relationship to cardiovascular risk factors: The Multi-Ethnic Study of Atherosclerosis (MESA)

Chia-Ying Liu[1], Shenghan Lai[2], Nadine Kawel-Boehm[3], Harjit Chahal[4], Bharath Ambale-Venkatesh[4], Joao Lima[4], and David Bluemke[5]

[1]radiology and imaging sciences, national Institute of Health, bethesda, MD, United States, [2]Johns Hopkins School of Medicine, [3]3Kantonsspital Graubuenden, Clinic of Radiology, [4]Johns Hopkins Hospital, [5]Radiology and Imaging Sciences, National Institutes of Health

We used cardiovascular magnetic resonance imaging to measure the LV and aortic structure and function in the Multi-Ethnic Study of Atherosclerosis (MESA). The cohort was divided into groups with or without traditional risk factors. In multivariable analyses adjusting for age, sex and race, individuals with risk factors had significantly larger LV mass index (by 17%) and lower LV contractility (circumference strain, lower by 14%). LV structure and function are also better preserved in senescent hearts in the absence of traditional cardiovascular risk factors.

3159 Computer 68

MRI Feature Tracking Strain Provides Incremental Prognostic Information Over Serum Biomarkers in AL Amyloidosis

Jeffery E Illman[1], James F Glockner[1], Ian C Chang[2], Arvin E Arani[1], Shivaram Poigai Arunachalam[1], Kiaran P McGee[1], Martha E Grogan[2], Angela E Dispenzieri[3], and Philip A Araoz[1]

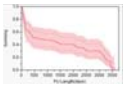

[1]Radiology, Mayo Clinic, Rochester, MN, United States, [2]Cardiovascular Medicine, Mayo Clinic, Rochester, MN, United States, [3]Department of Medicine, Division of Hematology, Mayo Clinic, Rochester, MN, United States

The association of MRI feature tracking (FT) strain with all-cause mortality was retrospectively performed on 76 patients with new diagnosis of AL amyloid. Mean follow-up was 4 years. MRI FT radial, circumferential, and longitudinal strain were each associated with all-cause mortality in univariate analysis. In separate multivariate models with serum biomarker stage, radial, circumferential, and longitudinal strain each remained prognostic. This study shows the incremental prognostic value of MRI FT strain in AL amyloidosis.

3160 Computer 69

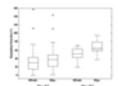

The impact of heterogeneity on regurgitation classification for pulmonary artery after repaired Tetralogy of Fallot

Pei-Hsin Wu[1], Hsiao-Wen Chung[2], Ming-Ting Wu[3], and Cheng-Wen Ko[4]

[1]Radiology, Brigham and Women's Hospital, Harvard Medical School, Boston, MA, United States, [2]Institute of Biomedical Electronics and Bioinformatics, National Taiwan University, Taipei, Taiwan, [3]Radiology, Kaohsiung Veterans General Hospital, Kaohsiung, Taiwan, [4]Computer Science and Engineering, National Sun Yat-Sen University, Kaohsiung, Taiwan

The degree of pulmonary regurgitation has been a determinant for re-intervention for patients with repaired TOF. However, in practice, the accurate assessment of regurgitation may be interfered by the simultaneous existence of forward flow and backward flow in any single cardiac phase, which may mislead clinical decision making. In this study, we investigated the impact of heterogeneity in blood flow profiles on guiding management and the classification of regurgitation. Preliminary results suggest that pixel-wise reexamination may be required for reclassification, especially for patients with marginal moderate regurgitant fraction value.

3161 Computer 70

Feasibility Study: 2-D Self-Navigation using Compressed Sensing Reconstruction for Respiratory Gating in Free-breathing 3-D CINE Imaging

Ivo Prochaska[1], Jens Wetzl[1,2], Christoph Forman[3], Armin Nagel[4], and Andreas Maier[1,2]

[1]Pattern Recognition Lab, Department of Computer Science, Friedrich-Alexander-Universität Erlangen-Nürnberg, Erlangen, Germany, [2]Erlangen Graduate School in Advanced Optical Technologies (SAOT), Friedrich-Alexander-Universität Erlangen-Nürnberg, Erlangen, Germany, [3]Siemens Healthcare GmbH, Magnetic Resonance, Erlangen, Germany, [4]Universitätsklinikum Erlangen, Erlangen, Germany

We investigate the feasibility of using 2-D self-navigation for respiratory gating for free-breathing whole-heart 3-D CINE imaging, where respiration-induced cardiac motion may be more easily detected than in commonly used 1-D self-navigation methods. We compare self-navigation images, derived gating signals and resulting 3-D CINE images of the 1-D and 2-D methods and find that respiratory motion can be well visualized with the 2-D method; both methods show a good overlap of gating signals and little difference in resulting image quality. 2-D self-gating may thus be considered a promising alternative to 1-D self-navigation as it allows easier detection of respiratory motion.

3162 Computer 71

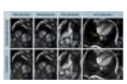

Accelerated 2D Cine MRI Featuring Compressed Sensing and ECG-triggered Retro-gating

Christoph Forman[1], Randall Kroeker[1], and Michaela Schmidt[1]

[1]Siemens Healthcare GmbH, Erlangen, Germany

We present the combination of ECG-triggered retrospective gating and compressed sensing for segmented 2D Cine imaging at high spatiotemporal resolution. This enables capturing the complete cardiac cycle in segmented acquisitions, while significantly reducing the total acquisition time with compressed sensing and auto-calibration. The method was evaluated in 8 healthy volunteers and ventricular function parameters were compared to reference 2D Cine acquisitions featuring ECG-triggered retro-gating. Both methods resulted in comparable image quality and equivalent quantitative values for ventricular function parameters.

3163 Computer 72

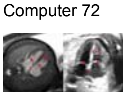

Identification and Measurement of Anatomical Landmarks Using Fetal Cardiac Cine MRI in Comparison with the Clinical Gold Standard Echocardiography

Jerome Yerly[1,2], Jerome Chaptinel[1], Yvan Mivelaz[3], Milan Prsa[3], Leonor Alamo[1], Yvan Vial [4], Gregoire Berchier[1], Jean-Baptiste Ledoux[1,2], Chantal Rohner[1,2], and Matthias Stuber[1,2]

[1]Department of Radiology, University Hospital (CHUV) and University of Lausanne (UNIL), Lausanne, Switzerland, [2]Center for Biomedical Imaging (CIBM), Lausanne, Switzerland, [3]Department of Pediatrics, University Hospital (CHUV) and University of Lausanne (UNIL), Lausanne, Switzerland, [4]Department of Gynecology-Obstetrics, University Hospital (CHUV) and University of Lausanne (UNIL), Lausanne, Switzerland

The recent development of a self-gated framework to reconstruct cardiac cine MR images without the need for an external ECG signal has opened the door to prenatal cardiac examination with MRI. This study investigates the potential of this technique for fetal cardiac MRI and compares its performance with the clinical gold standard echocardiography. Standard views from clinical fetal echocardiographic examinations were acquired with both imaging modalities and two experienced readers independently compared them qualitatively and quantitatively. The results showed good agreement between the two modalities and validate the use of MRI for prenatal evaluation of the heart.

Electronic Poster

Body: Diffusion

Exhibition Hall — Monday 8:15 - 9:15

3164 Computer 73

Contribution of DKI and IVIM to liver T1rho imaging in the prediction of hepatitis B virus-related liver fibrosis

shuangshuang xie[1], qing li[1], zhizheng zhuo[2], yu zhang[2], yue cheng[1], and wen shen[1]

[1]Tianjin First Center Hospital, Tianjin, People's Republic of China, [2]Philips healthcare, Beijing, People's Republic of China

This study evaluated the individual T1rho and combined performances of T1rho, IVIM and DKI in predicting HBV related liver fibrosis. Twenty-two patients with HBV related liver fibrosis and twenty healthy control subjects were underwent whole-liver T1rho MR imaging, IVIM and DKI. The T1rho, D, D*, f , MD and MK values were compared between the two groups, and then the single and combined diagnostic efficiency of T1rho, IVIM and DKI was analyzed. Our results showed liver T1rho and MK increased and D, f, MD decreased in normal control group, and liver T1rho and MD had significantly difference between the two groups. T1rho had a moderate diagnostic efficiency, IVIM and DKI had a mild diagnostic efficiency to detect fibrosis. While, the combination of T1rho, IVIM and DKI improved the diagnostic efficiency significantly and had a good diagnostic efficiency to detect fibrosis. We conclude T1rho can be used to predicting liver fibrosis effectively, and IVIM and DKI can effectively complement existing T1rho MR imaging in predicting of liver fibrosis.

3165 Computer 74

Role of diffusion-weighted imaging in distinguishing thoracoabdominal neuroblastic tumors of various histological types and differentiation grades

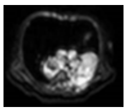

Yang Wen[1], Yun Peng[1], Xiaomin Duan[1], and Nan Zhang[2]

[1]Department of Radiology, Beijing Children's Hospital, Beijing, People's Republic of China, [2]Department of Pathology, Beijing Children's Hospital, Beijing, People's Republic of China

Purpose: To evaluate whether DWI allow discrimination of thoracoabdominal neuroblastic tumors of various histological types and differentiation grades. **Materials and Methods:** The DWI scans of the thoracoabdominal neuroblastic tumors in twenty-five children were retrospectively evaluated. DWI was performed with 2 b values of 0 and 800s/mm2 on a 3.0T MR scanner. **Results:** In the 25 cases, ganglioneuroma (GN) was in 3 cases, ganglioneuroblastoma (GNB) -Intermixed in 4, GNB-Nodular in 3 and neuroblastoma (NB) in 15. The ADC values of the NBs were significantly lower than those of GNs/GNBs (P < .001). The ADC of GNB-Nodular/NB was significantly less than that of GN/GNB-Intermixed (p<0.0001). In GNB-Nodular and NB, the tumors with poorly differentiated and undifferentiated lesions (n=12) had significantly smaller ADC than those with differentiated composition (n=6) (P=.0012). **Conclusion:** ADC of DWI is highly valuable for discriminating thoracoabdominal neuroblastic tumors of different histological types and subtypes.

3166 Computer 75

Focus or Spread? An Investigation of the Effects of b-Value Acquisition Strategies on the Stability and Bias of Prostate Diffusion Imaging Results

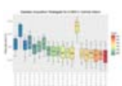

Xiaodong Zhong[1,2], Phil Young[3], Peter Kollasch[4], Venkata Chebrolu[4], and Brian M. Dale[5]

[1]MR R&D Collaborations, Siemens Healthcare, Atlanta, GA, United States, [2]Department of Radiology and Imaging Sciences, Emory University, Atlanta, GA, United States, [3]Department of Radiology, Mayo Clinic, Rochester, MN, United States, [4]MR R&D Collaborations, Siemens Healthcare, Rochester, MN, United States, [5]MR R&D Collaborations, Siemens Healthcare, Cary, NC, United States

In order to investigate the effects of b-value acquisition strategies on the stability and bias of the prostate DWI results, including calculated b-value images and ADC, a framework was developed. Using the DWI data from 8 prostate patients, this study revealed that acquiring many averages at a few b-values increases bias compared to acquiring few averages at many b-values, particularly when large numbers of averages have been removed. The framework and strategies proposed in this work may provide a useful tool to design b-value acquisition protocols to achieve the stability of prostate DWI results in clinic.

3167 Computer 76

The IASLC/ ITMIG Thymic Epithelial Tumor Staging: Comparison of Staging Capability among Whole-Body PET/MRI, MRI including DWI, PET/CT and Conventional Radiological Examination

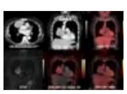

Yoshiharu Ohno[1,2], Yuji Kishida[3], Sinichiro Seki[1,2], Kota Aoyagi[4], Masao Yui[4], Yoshimori Kassai[5], Wakiko Tani[6], Noriyuki Negi[6], Katsusuke Kyotani[6], and Takeshi Yoshikawa[1,2]

[1]Division of Functional and Diagnostic Imaging Research, Department of Radiology, Kobe University Graduate School of Medicine, Kobe, Japan, [2]Advanced Biomedical Imaging Research Center, Kobe University Graduate School of Medicine, Kobe, Japan, [3]Division of Radiology, Department of Radiology, Kobe University Graduate School of Medicine, Kobe, Japan, [4]Center for Medical Research and Development, Toshiba Medical Systems Corporation, Otawara, Japan, [5]MR Clinical Solution department, Toshiba Medical Systems Corporation, Otawara, Japan, [6]Center for Radiology and Radiation Oncology, Kobe University Hospital, Kobe, Japan

Accurate stage assessment is essential for choosing the appropriate treatment strategy for thymic epithelial tumor patients. Recently, the International Association for the Study of Lung Cancer (IASLC) and International Thymic Malignancies Interest Group (ITMIG) proposed a new IASLC/ITMIG thymic epithelial tumor stage classification system. The purpose of this study was to compare the diagnostic capability for the IASLC/ ITMIG thymic epithelial tumor staging among whole-body FDG-PET/MRI, MRI, FDG-PET/CT and conventional radiological examinations based on guidelines.

3168 Computer 77

Motion Correction of Multi-b-value Diffusion-Weighted Images in the Kidney by Pyramidal Lucas-Kanade Registration

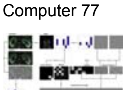

Jun Lv[1], Wenjian Huang[1], Jue Zhang[1,2], Xiaoying Wang[1,3], and Jing Fang[1,2]

[1]Academy for Advanced Interdisciplinary Studies, Peking University, Beijing, People's Republic of China, [2]College of Engineering, Peking University, Beijing, People's Republic of China, [3]Department of Radiology, Peking University First Hospital, Beijing, People's Republic of China

Intravoxel incoherent motion diffusion weighted imaging (IVIM-DWI) is a novel functional MRI technique which has been demonstrated with excellent diagnostic capability. Respiratory motion artifacts are the main source of error in the acquisition and quantification of parameters for multi-b-value DWI. This work develops a reliable approach to compensate for misalignments between multi-b-value images during free-breathing based on pyramidal Lucas-Kanade registration. Preliminary results show that our proposed approach can well correct motion-related artifacts misalignment. In addition, visual quality of the ADC, f, D and D* maps indicate that contours of kidney look better defined after registration.

3169 Computer 78

Intravoxel Incoherent Motion Analysis for Perfusion Using Portal Vein Embolization Pig Model

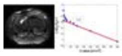

Jia Ning[1], Tilman Schubert[2,3], Huijun Chen[1], Chun Yuan[1,4], and Scott B Reeder[3,5,6,7,8]

[1]Center for Biomedical Imaging Research, Department of Biomedical Engineering, School of Medicine, Tsinghua University, Beijing, People's Republic of China, [2]Clinic for Radiology and Nuclear Medicine, Basel University Hospital, Basel, Switzerland, [3]Department of Radiology, University of Wisconsin-Madison, Madison, WI, United States, [4]Department of Radiology, University of Washington, Seattle, WA, United States, [5]Department of Medical Physics, University of Wisconsin-Madison, Madison, WI, United States, [6]Department of Biomedical Engineering, University of Wisconsin-Madison, Madison, WI, United States, [7]Department of Medicine, University of Wisconsin-Madison, Madison, WI, United States, [8]Department of Emergency Medicine, University of Wisconsin-Madison, Madison, WI, United States

Portal vein embolization (PVE) is often performed before liver tumor resection, to induce hypertrophy of the anticipated liver remnant and reduce the complications after partial liver resection. The perfusion changes of the embolized and non-embolized liver segments are of great interest. Intravoxel incoherent motion (IVIM) is a component of the diffusion weighted signal model that allows for separating estimation of perfusion. Estimation of IVIM from diffusion weighted imaging which may provide a unique way to measure the perfusion of liver tissue. This study aimed to test the intra-observer repeatability of IVIM and parameters change after PVE used a pig model.

3170 Computer 79

Free-breathing 3D Body Diffusion Imaging at 3T Using M1-compensated Diffusion Preparation and Stack-of-Stars Readout

Xiaoming Bi[1], Christopher Nguyen[2], Zhaoyang Fan[2], Yutaka Natsuaki[1], Rola Saouaf[2], Debiao Li[2], and Gerhard Laub[1]

[1]Siemens Healthcare, Los Angeles, CA, United States, [2]Cedars-Sinai Medical Center, Los Angeles, CA, United States

Diffusion-weighted (DW) MRI enables qualitative and quantitative assessment of tissue diffusivity. Body diffusion imaging at 3T using conventional single-shot EPI sequence is challenged by respiratory and cardiac motions of subject, limited spatial resolution, and image distortion and ghosting. In this work, a new 3D imaging technique incorporating M1-compensated diffusion preparation and motion-robust stack-of-stars data acquisition was developed. Preliminary volunteer studies demonstrated its feasibility for free-breathing body diffusion imaging at 3T. From one patient underwent MR-PET scan, reduced ADC and increased FDG uptake was observed in the same focal lesion.

3171 Computer 80

A cardiac stationary phase based ECG trigger (CaspECG) of intravoxel incoherent motion diffusion MR in left liver lobe.

Zhiming Xiang[1], Zhu Ai[2], Jianke Liang[2], Guijin Li[3], Xiaolei Zhu[4], Xu Yan[5], Changhong Liang[6], Suzanne Palmer[7], and ChiShing Zee[7]

[1]Department of Radiology, Panyu Center Hospital of Guangzhou, 8 Fuyu Dong Road, Panyu District Guangzhou, P.R. China 510080, Guangzhou, People's Republic of China, [2]Panyu Center Hospital of Guangzhou, 8 Fuyu Dong Road, Panyu District Guangzhou, P.R. China 510080, Guangzhou, People's Republic of China, [3]Siemens Healthcare, Application NE Asia, Guangzhou, China, Guangzhou, People's Republic of China, [4]Siemens Healthcare, MR Scientific Marketing NE Asia, Guangzhou, China, Guangzhou, People's Republic of China, [5]Siemens Healthcare, MR Collaboration NE Asia, Shanghai, China, Shanghai, People's Republic of China, [6]Department of Radiology, Guangdong General Hospital, 106 Zhongshan Er Road, Guangzhou, P.R. China 510080, Guangzhou, People's Republic of China, [7]Department of Radiology, Keck School of Medicine, University of Southern California, Los Angeles, California, USA, Los Angeles, CA, United States

Intravoxel incoherent motion (IVIM) Diffusion weighted imaging (DWI) showed high clinical value in liver disease evaluation. However, it suffers from signal loss and motion artifacts due to cardiac and respiratory movement, especially in the left lobe. To improve robustness and reproducibility of parameter estimation for IVIM DWI, a novel DWI acqusition technique was introduced, which uses ECG trigger with delay time optimized by the periods of cardiac relative stationary phase. The results showed that the proposed acquisition method improves SNR of DWI data, and the repeatability and stability of IVIM-DWI derived parameters.

3172 Computer 81

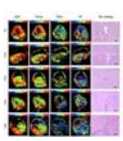

Intravoxel incoherent motion diffusion-weighted imaging of hepatic warm ischemia-reperfusion injury in a rabbit model

Qian Ji[1], Zhi-qiang Chu[2], Pan-li Zuo[3], and Wen Shen[1]

[1]Radiology, Tianjin First Central Hospital, Tianjin, People's Republic of China, [2]Transplantation, Tianjin First Central Hospital, Tianjin, People's Republic of China, [3]MR Collaborations NE Asia, Siemens Healthcare, Beijing, People's Republic of China

Hepatic warm ischemia-reperfusion injury (WIRI) is clinically relevant in liver operation. We undertook this study to determine the feasibility of using IVIM for the early diagnosing and grading of hepatic WIRI. Fifty different grades of hepatic WIRI models and control rabbits were examined using a 3T clinical MR scanner, which followed by biochemical and histopathological analysis. There were significant differences of IVIM parameters between different groups. IVIM parameters corresponded well with biochemical parameters. ROC analysis showed the AUC of PF was the largest. This indicated that IVIM is a noninvasive and valuable technique for assessing and grading of hepatic WIRI.

3173 Computer 82

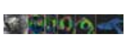

Elucidation of Male Urethral Sphincter Complex Using Diffusion Tensor Imaging (DTI) based Fiber-Tracking

Kyoko Sakamoto[1], Mahadevan Rajasekaran[1], Valmiki Bhargava[2], Vadim Malis[3], and Shantanu Sinha[4]

[1]VA Medical Center, San Diego, CA, United States, [2]VA Medical Center, [3]Physics, UC San Diego, San Diego, CA, United States, [4]Radiology, UC San Diego, San Diego, CA, United States

Urethral sphincters play an important role in urinary incontinence, a major clinical problem affecting the aging population. We elucidate the anatomy of the urethral sphincter muscles pertinent to urinary continence function using in vivo, non-invasive proton-density and diffusion tensor imaging and DTI-based fiber tracking in young adults. Muscle fiber tracking consistently revealed, perhaps for the first time, the existence of two sphincter like muscles, with one proximal near the bladder neck and the other more distal, supporting the two sphincter concept to constrict/close the urethral opening with important implications for the effect of prostatectomy on urethral closure function.

3174 Computer 83

Is voxel-wise ADC histogram repeatable?

Masamitsu Hatakenaka[1], Naomi Koyama[1], Koichi Onodera[1], Naoya Yama[1], Maki Onodera[1], Yoshifusa Kyuna[1], and Mitsuhiro Nakanishi[2]

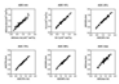

[1]Diagnostic Radiology, Sapporo Medical University, Sapporo, Japan, [2]Division of Radiology, Sapporo Medical University Hospital, Sapporo, Japan

Skewness and kurtosis of voxel-wise apparent diffusion coefficient show low repeatability. Radiologist should take this characteristic into account when interpreting DWI of the prostate.

3175 Computer 84

Segmentation of Bone Marrow of Pelvis in Multi-parametric MRI (T1-w/ADC-map) of Metastatic Breast Cancer Patients

Mahsa Rostamie[1], Anahita Fathi Kazerooni[1,2], and Hamidreza Saligheh Rad[1]

[1]Quantitative MR Imaging and Spectroscopy Group, Research Center for Molecular and Cellular Imaging, Tehran University of Medical Sciences, Tehran, Iran, [2]Department of Medical Physics and Biomedical Engineering, Tehran University of Medical Sciences, Tehran, Iran

To assess treatment response through quantitative analysis, in metastatic breast cancer patients, computer-aided segmentation of bone marrows is beneficial. We propose a semi-automatic segmentation method based on level-set and region growing techniques applied to T1-W images to facilitate extraction of apparent diffusion coefficient (ADC) features for the purpose of treatment response assessment from bone marrows of pelvic region. The results of applying the method on T1w/ADC-map of 10 patients shows a dice score of 81%, suggestive of high agreement of our proposed segmentation approach with expert’s opinion.

3176 Computer 85

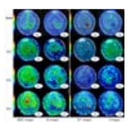

Early evaluation of liver fibrosis in radiation-induced liver fibrosis rat models using intra-voxel incoherent motion theory

Zhongping Zhang[1], Rong Ma[2], Dong Zhang[2], Changzheng Shi[2], and Liangping Luo[2]

[1]MR Research China, GE Healthcare, Beijing, People's Republic of China, [2]Medical Imaging Center, The First Affiliated Hospital of Jinan University, Guangzhou, People's Republic of China

This study found that IVIM-derived D could efficiently detect and differentiate the liver fibrosis in radiation-treaed rats at the early stage in vivo.

3177 Computer 86

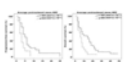

Prognostic value of the pretreatment apparent diffusion coefficient (ADC) for outcome prediction of chemorefractory colorectal liver metastases undergoing 90-Yttrium Radioembolization

Frederic Carsten Schmeel[1], Julian Alexander Luetkens[1], Frank Träber[1], Leonard Christopher Schmeel[1], Amir Sabet[2], Birgit Simon[1], Hans Heinz Schild[1], and Dariusch Reza Hadizadeh[1]

[1]Department of Radiology, University Hospital Bonn, Bonn, Germany, [2]Department of Nuclear Medicine, University Hopsital Saarland, Homburg/Saar, Germany

Imaging-based prediction of therapeutic response is highly desireable for further therapy decisions in patients with advanced malignancies. Therefore, we investigated whether pre-treatment values of the apparent diffusion coefficient (ADC) on diffusion-weighted MRI could predict the outcome of patients with liver-predominant metastatic colorectal cancer prior to 90-Yttrium microspheres radioembolization. Uni- and multivariate analyses were performed comparing various variables with potential impact on progression-free and overall survival. Our results reveal that pathologic pre-treatment ADC, alongside with established clinical parameters, is a strong and independent predicor of both progression-free and overall survival before RE treatment.

3178 Computer 87

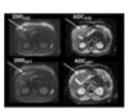

Clinical Robustness of Accelerated and Optimized Abdominal Diffusion Weighted Imaging

Jana Taron[1], Jakob Weiss[1], Petros Martirosian[2], Alto Stemmer[3], Konstantin Nikolaou[1], and Mike Notohamiprodjo[1]

[1]Department of of Diagnostic and Interventional Radiology, University Hospital of Tuebingen, Tuebingen, Germany, [2]Section on Experimental Radiology, Department of Diagnostic and Interventional Radiology, University Hospital of Tuebingen, Tuebingen, Germany, [3]Siemens Healthcare GmbH, Erlangen, Germany

We evaluated the robustness of an accelerated and optimized diffusion-weighted sequence using the simultaneous-multislice (SMS) technique for scan time reduction and a 3D Diagonal diffusion mode to optimize image quality in clinical routine. 152 patients received clinically indicated abdominal MRI including the optimized diffusion-weighted sequence (DWI_{OPT}). A subgroup of 41 patients additionally received a standard diffusion-weighted sequence (DWI_{STD}) as reference. Qualitative and quantitative image parameters were evaluated. In the interindividual comparison, DWI_{OPT} proved equal to superior to DWI_{STD} with comparable ADC-values. In the patients receiving DWI_{OPT} only, image quality maintained substantial proving constant and stable results in a large cohort.

3179 Computer 88

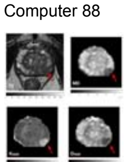

Mean Kurtosis discriminates between low- and high-risk prostate cancer better than Mean diffusivity does

Maria Giovanna Di Trani[1,2], Alessandra Caporale[2,3], Marco Nezzo[4], Roberto Miano[5], Alessandro Mauriello[6], Pierluigi Bove[7], Guglielmo Manenti[4], and Silvia Capuani[8]

[1]SAIMLAL Dept., Morphogenesis and Tissue Engineering, Sapienza University of Rome, Rome, Italy, [2]Physics Dept., CNR ISC UOS Roma Sapienza, Rome, Italy, [3]SAIMLAL Dept., Morpho-functional Sciences, Sapienza University of Rome, Rome, [4]Department of Diagnostic and Interventional Radiology, Molecular Imaging and Radiotherapy, PTV Foundation, “Tor Vergata” University of Rome, Rome, Italy, [5]Urology Unit, Department of Experimental Medicine and Surgery, [6]Anatomic Pathology, Department of Biomedicine and Prevention, PTV Foundation, “Tor Vergata” University of Rome, [7]Urology Unit, Department of Experimental Medicine and Surgery, PTV Foundation, “Tor Vergata” University of Rome, [8]CNR ISC UOS Roma Sapienza, Rome, Italy

This work was finalized to compare the diagnostic potential of Diffusion Tensor and Diffusion Kurtosis Imaging in discriminating between low- and high-risk prostate cancer (Pca). Maps of Mean Diffusivity (MD), apparent Kurtosis (K) and apparent diffusion coefficient (D) were obtained from DWIs of 24 patients with different tumour grade. K maps better highlight differences between periferal PCa, PCa and benign tissue. In particular K discriminates between low- and high-risk PCa with a higher statistical significance compared to that of MD. DKI can improve the accuracy of the current PCa diagnosis providing a useful tool for PCa detection and grading.

3180 Computer 89

Unbiased diffusional kurtosis measurements in the pelvis at low signal-to-noise ratio: A new approach for noise-level estimations

Olaf Dietrich[1], Martina Brandlhuber[1], Moritz J. Schneider[1], Marco Armbruster[1], Melvin D'Anastasi[1], and Maximilian F. Reiser[1]

[1]Institute for Clinical Radiology, Ludwig-Maximilians-University Hospital Munich, Munich, Germany

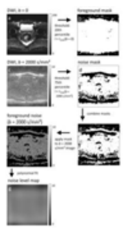

The purpose of this study was to propose a robust technique for the determination of unbiased kurtosis values in body applications; for this aim, a new strategy to pixelwise estimate the noise level in DKI acquisitions is described and its feasibility for pelvic DKI is demonstrated in prostate tissue.

The "naive" evaluation (without considering the image noise) resulted in significantly biased positive kurtosis values of urine of $K=0.42\,(\text{standard deviation: }0.06)$, indicating non-monoexponential signal decay caused by the influence of noise at higher b-values. This bias is almost completely removed ($K=-0.01\,(0.32)$) after including the pre-calculated noise-level map in the evaluation.

3181 Computer 90

Gradient First Moment Dependence of ADC in Liver Diffusion Weighting Imaging.

Kévin Moulin[1], Eric Aliotta[1,2], and Daniel B. Ennis[1,2]

[1]Department of Radiological Sciences, University of California, Los Angeles, CA, United States, [2]Biomedical Physics IDP, University of California, Los Angeles, CA, United States

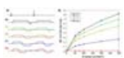

The effect of perfusion on Diffusion Weighting Imaging (DWI) and particularly the Apparent Diffusion Coefficient (ADC) at low ***b-value*** is a confounder in pathology assessment. In this study, in order to investigate the gradient first moment (***M1***) dependence of perfusion on the ADC, waveforms were generated using convex diffusion encoding (CODE) framework leading to a range of ***M1*** for a given ***b-value***. After comparing ADC calculated with different ***M1*** and different ***b-value***, we found that motion compensated waveform (***M1=0***) ensures independence of the ADC to perfusion even at low ***b-value***, which can improve SNR.

3182 Computer 91

Prognostic Value of Pretreatment Diffusion Weighted Magnetic Resonance Imaging based Texture in Concurrent Chemo-radiotherapy of Esophageal Squamous Cell Cancer

Zhenjiang Li[1], Chun Han[2], Hongsheng Li[1], Lan Wang[2], Jian Zhu[1], Weibo Chen[3], and Baosheng Li[1]

[1]Shandong Cancer Hospital to Shandong University, Shandong Academy of Medical Sciences, Jinan, People's Republic of China, [2]Department of Radiation Oncology, the Fourth Hospital of Hebei Medical University, Shijiazhuang, People's Republic of China, [3]Philips Healthcare, Shanghai, People's Republic of China

This study has important clinical significance. The pretreatment texture features combined with conventional prognostic factors may present a more accurate predictive tool for OS of ESCC patients. The parameters can be used to evaluate the prognosis of ESCC after CRT at an early time.

3183 Computer 92

Imaging non-enlarged abdominal lymph nodes and measuring their diffusion coefficient

Hannah Grace Williams[1,2], Caroline L Hoad[1,3], Luca Marciani[2], Gordon Moran[2], Giles Major[2], Robert Scott[3], and Penny A Gowland[1]

[1]Sir Peter Mansfield Imaging Centre, School of Physics and Astronomy, University of Nottingham, Nottingham, United Kingdom, [2]Nottingham Digestive Diseases Centre, University of Nottingham, Nottingham, United Kingdom, [3]NIHR Biomedical Research Unit in Gastrointestinal and Liver Diseases, Nottingham University Hospital, Nottingham, United Kingdom

Inflammatory conditions such as Crohn's disease cause changes in the lymphatics including enlargement and necrosis, and so improved measures of number, size and function of lymph nodes could provide novel markers of local inflammatory response. Being able to identify small nodes would allow the effect of inflammatory diseases and response to therapy to be monitored. DWIBS was used here to isolate the signal from small abdominal lymph nodes. The diffusion coefficient of the pelvic and abdominal lymph nodes and the cisterna chyli with IVIM effects eliminated, were 0.9±0.2, 1.4±0.3 and 1.7±0.6 x10^{-3} mm^2/s.

3184 Computer 93

Towards development of tools for quantitative body DWI

Raj Attariwala[1], Amy Chamber, Wayne Picker, and Mikko Maatta

[1]AIM Medical Imaging, Vancouver, BC, Canada

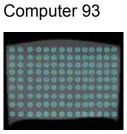

Body DWI is a technique that is potentially quantifiable, and numerous clinical publications have demonstrated tissue variability of the ADC parameter. The variability of machine hardware and acquisition parameters impacts the signal from which ADC is calculated. To address the needs of standardization of machines, a body diffusion phantom and analysis software is being developed. Preliminary results are presented here.

3185 Computer 94

High Resolution Diffusion Weighted Imaging of the Liver using Readout Segmented EPI on 3T

Yishi Wang[1], Zhe Zhang[1], Xiaodong Ma[1], Ha-Kyu Jeong[2], Chun Yuan[1,3], and Hua Guo[1]

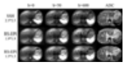

[1]Center for Biomedical Imaging Research, Department of Biomedical Engineering, School of Medicine, Tsinghua University, Beijing, People's Republic of China, [2]BIU Clinical Science MR, Philips Korea, Seoul, Korea, Republic of, [3]Vascular Imaging Laboratory, Department of Radiology, University of Washington, Seattle, WA, United States

Readout segmented EPI (RS-EPI) can be used for high-resolution diffusion weighted imaging but there are still limited reports on its application to liver DWI. In this study, we reported to use RS-EPI for high resolution DWI of the liver.

3186 Computer 95

Training an Artificial Neural Network by Diffusion-Weighted MRI Data to Differentiate Between Prostate Cancer With High and With Low Gleason Score

Sebastiano Barbieri[1] and Harriet C Thoeny[1]

[1]Department of Diagnostic, Interventional and Pediatric Radiology, Inselspital, University of Bern, Bern, Switzerland

We prospectively assess the feasibility of using DW-MRI data to train an artificial neural network which distinguishes between prostate cancer lesions with high (≥7) and with low (=6) Gleason scores in 84 patients. The accuracy of the artificial neural network is compared with the accuracy of classification based on apparent diffusion coefficient (ADC) values.

3187 Computer 96

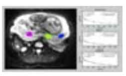

Diffusion and perfusion parameters extracted by bi-exponential model are markers of healthy human placenta development.

Michele Guerreri[1,2], Silvia Capuani[2], Amanda Antonelli[3], and Lucia Manganaro[3]

[1]SAIMLAL Dept., Morphogenesis & Tissue Engineering, Sapienza University of Rome, Rome, Italy, [2]Physics Dept., CNR ISC UOS Roma Sapienza, Rome, Italy, [3]Radiology Dept., Department of Radiology, Sapienza University of Rome, Rome, Italy

The purpose was to investigate the potential of bi-exponential model of diffusion-weighted (DW) signal decay to quantify diffusion and perfusion in healthy human placentas. The relation between diffusion and perfusion parameters with microstructural changes occurring during placenta development was also investigated. 26 pregnant women underwent DW examination. Apparent diffusion coefficient D, pseudo-perfusion fraction f and pseudo-diffusion coefficient D* were obtained in specific placental regions. The Pearson correlations between D, D*,f and clinical data (Gestational Age, Body-Mass Index and basal Glycaemia) were evaluated. D and f show to be good indicators of placenta morphological changes due to Gestational Age.

Electronic Poster

Liver

Exhibition Hall — Monday 8:15 - 9:15

3188 Computer 97

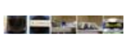

Hepatic MR Elastography (MRE) System Longitudinal Quality Assurance (QA) Protocol

Jun Chen[1], Phillip J Rossman[1], Kevin J Glaser[1], and Richard L Ehman[1]

[1]Radiology, Mayo Clinic, Rochester, MN, United States

A suitable quality assurance (QA) phantom and image acquisition and processing procedures were developed for confirming the proper function and longitudinal stability of these MRE systems. The goals of this educational poster are to demonstrate the QA phantom, the longitudinal testing protocol, and the utility of detecting a problem caused by discontinuous motion.

3189 Computer 98

Radiologic-Pathologic Correlation and MR Analysis of Hepatocellular Adenoma Subtypes.

Daniel Kehler[1], George Yang[2], Christine Zwart[1], Marcela Salomao[3], and Alvin Silva[1]

[1]Radiology, Mayo Clinic Arizona, Scottsdale, AZ, United States, [2]University of Pennsylvania, PA, United States, [3]Pathology, Mayo Clinic Arizona, Scottsdale, AZ, United States

Hepatocellular adenomas (HCA) present as four genetic subtypes that vary greatly in their clinical behavior and MR appearance. Inflammatory HCA has the highest propensity for hemorrhage, is characterized by hyperintense T2 signal, and displays arterial hyper-enhancement that persists on portal venous and delayed phases. HNF1-alpha mutated HCA portends a good prognosis, and is characterized by diffuse intracellular lipid. Beta-catenin HCA is less common and difficult to diagnose on imaging, though arguably the most important because of its high likelihood for malignant transformation. Unclassified HCA is not well understood in terms of imaging or clinical significance.

3190 Computer 99

MRI Technique and Interpretation in the Evaluation of Hepatic Steatosis

Zachary Borden[1] and Scott Reeder[2]

[1]Department of Radiology, University of Wisconsin-Madison, Madison, WI, United States, [2]Department of Radiology, University of Wisconsin-Madison, WI, United States

Hepatic steatosis is a common affliction with important prognostic implications. Conventionally, liver biopsy has been required for the diagnosis of steatosis although this may result in inadequate spatial sampling and significant associated complications. The non-interventional imaging methods of ultrasound and computed tomography may be used but are limited in accuracy. MRI offers an ideal method to globally and accurately interrogate for liver fat. Multiple MRI techniques including spectroscopy, in-phase/out-phase, conventional fat suppression, complex and magnitude-based CSE-MRI methods have been used in the evaluation of hepatic steatosis. These techniques possess unique advantages and disadvantages which must be understood to optimize patient care.

3191 Computer 100

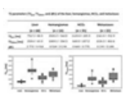

Feasibility of measuring the T1 relaxation times before and after Gd-EOB-DTPA administration for characterization of liver tumors

Yoshihiko Fukukura[1], Takashi Iwanaga[2], Yuichi Kumagae[1], Hiroto Hakamada[1], Koji Takumi[1], Kiyohisa Kamimura[1], Masanoari Nakajo[1], Hiroshi Imai[3], and Takashi Yoshiura[1]

[1]Radiology, Kagoshima University Graduate School of Medical and Dental Sciences, Kagoshima, Japan, [2]Radiological Technology, Kagoshima University Hospital, Kagoshima, Japan, [3]Siemens Healthcare K.K., Tokyo, Japan

This study focused on the potential of T1 relaxation times measurement before and 20 min after Gd-EOB-DTPA administration to characterize liver tumors. T1 relaxation before Gd-EOB-DTPA administration showed the highest area under the receiver operating characteristic (ROC) curve for distinguishing hemangiomas and HCCs. T1 relaxation times 20 min after Gd-EOB-DTPA administration showed the highest the area under the ROC curve for differentiating HCCs from metastases. ΔR1 was considered to be useful for differentiation between hemangiomas and metastases because of the highest the area under the ROC curve.

3192 Computer 101

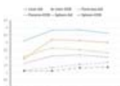

Dynamic contrast enhanced 3D T1WI at upper abdomen using combination of parallel imaging and compressed sensing on a wide-bore 3T unit: Comparison of effects with Gd-DTPA and Gd-EOB-DTPA

Motoyuki Katayama[1], Takayuki Masui[1], Kei Tsukamoto[1], Mitsuteru Tsuchiya[1], Yuki Hayashi[1], Masako Sasaki[1], Takahiro Yamada[1], Yuji Iwadate[2], Naoyuki Takei[2], Kang Wang[3], Kevin King[4], and Harumi Sakahara[5]

[1]Radiology, Seirei Hamamatsu General Hospital, Hamamatsu, Japan, [2]Global MR Applications and Workflow, GE Healthcare Japan, Hino, Japan, [3]Global MR Applications and Workflow, GE Healthcare, Madison, WI, United States, [4]Global MR Applications and Workflow, GE Healthcare, Waukesha, WI, United States, [5]Radiology, Hamamatsu University School of Medicine, Hamamatsu, Japan

Consecutive four phases of dynamic contrast enhanced 3D T1WI in the upper abdomen could be obtained during one breath-hold in combined use of parallel imaging and compressed sensing at wide-bore 3T system. The imaging protocols with Gd-DTPA and Gd-EOB-DTPA provided good image quality. Although image contrasts with Gd-EOB-DTPA might be inferior to those with Gd-DTPA, patterns of time intensity curves with study with dynamic contrast of each protocol were similar to each other.

3193 Computer 102

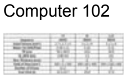

T2* measurements in liver at 1.5, 3 and 7T

E. Doran[1], S. J. Bawden[1], P. M. Glover[1], A. M. Peters[1], S. T. Francis[1], R. Bowtell[1], and P. A. Gowland[1]

[1]Sir Peter Mansfield Imaging Centre, School of Physics and Astronomy, University of Nottingham, Nottingham, United Kingdom

Whole body 7T MRI has the potential to improve monitoring of chronic liver disease by building on advances made in parallel transmit technology. This abstract outlays the measurement of T2* in the liver at 7T and compares with measurements on the same subjects at 3 and 1.5T. Acceptable values were obtained across all field strengths and T2* maps of the liver were obtained from analysis of multi-gradient echo imaging sequences. This work forms the start of a normative 7T data set that will provide vital information for developing other 7T MR liver sequences.

3194 Computer 103

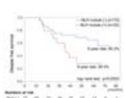

Gadoxetic acid-enhanced MRI findings as a risk of multicentric recurrence of hepatocellular carcinoma after hepatectomy

Masaki Matsuda[1], Shintaro Ichikawa[1], Utaroh Motosugi[1], Masanori Matsuda[2], and Hiroshi Onishi[1]

[1]Radiology, University of Yamanashi, Chuoh-shi, Japan, [2]First surgery, University of Yamanashi, Chuoh-shi, Japan

Nodules of non-hypervascular and low signal intensity during hepatobiliary phase (NLH nodules) detected by gadoxetic acid-enhanced magnetic resonance imaging (EOB-MRI), also known as hypovascular hypointense nodules, is important MR features that indicate the hepatocellular carcinoma (HCC) development in the future. The presence of NLH nodules is known as at high risk of HCC development in the liver. Hence, we hypothesized that NLH nodules can be also a risk of recurrence after surgical resection of HCCs. We evaluated the prognostic value of NLH nodules in patients with HCC. Presence of NLH nodules is at high risk of multicentric recurrence after hepatectomy.

3195 Computer 104

IDEAL-IQ MR Imaging at 3 T for the Quantification of Fat: A Phantom Study

Masatoshi Hori[1], Nicoline F. Post[1,2], Hiromitsu Onishi[1], Hiroyuki Tarewaki[3], Aliou A. Dia[1], Takashi Ota[1], Paul E. Sijens[2], and Noriyuki Tomiyama[1]

[1]Diagnostic and Interventional Radiology, Osaka University Graduate School of Medicine, Suita, Japan, [2]University of Groningen, Groningen, Netherlands, [3]Radiology, Osaka University Hospital, Suita, Japan

The purpose of this study was to evaluate the accuracy of fat quantification and the effects of iron on the measurement in IDEAL-IQ MR imaging at 3 Tesla by comparing the results of MRS using a fat-water-iron phantom. A gel phantom comprised of twenty-eight vials containing various proportions of fat and iron was constructed. Fat fraction and R_2* value were measured by IDEAL-IQ and MRS on a 3-T scanner. This study showed that IDEAL-IQ yielded an accurate quantification of fat content with a smaller degree of error due to susceptibility effects of iron compared to MRS at 3 Tesla.

3196 Computer 105

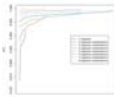

Accurate hepatic MRI proton density fat fraction assessment can be achieved with four regions-of-interest

Cheng William Hong[1], Tanya Wolfson[2], Ethan Z Sy[1], Alexandra Schlein[1], Soudabeh Fazeli Dehkordy[1], Adrija Mamidipalli[1], Scott B Reeder[3], Rohit Loomba[4], and Claude B Sirlin[1]

[1]Liver Imaging Group, Department of Radiology, University of California, San Diego, San Diego, CA, United States, [2]Computational and Applied Statistics Laboratory, University of California, San Diego, San Diego, CA, United States, [3]Departments of Radiology, Medical Physics, Biomedical Engineering, Medicine, and Emergency Medicine, University of Wisconsin, Madison, Madison, WI, United States, [4]NAFLD Research Center, Division of Gastroenterology, Department of Medicine, University of California, San Diego, San Diego, CA, United States

A common approach to estimating a composite proton density fat fraction (PDFF) on MRI-PDFF maps is to draw a region-of-interest (ROI) in each of the nine Couinaud segments. This is laborious and technically challenging, however. In this secondary analysis of 398 patients, we demonstrate that 4-ROI sampling strategies that sample 2 ROIs in each hepatic lobe achieve close agreement with the 9-ROI composite. With further validation, a simple 4-ROI sampling strategy may become the new standard for measuring PDFF in clinical trials.

3197 Computer 106

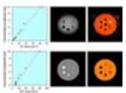

Quantitative Estimation of Liver Function using Gadoxetic Acid-Enhanced MR Imaging: in Vitro and in Vivo Comparison between R1 and R2* Relaxometry

Keitaro Sofue[1,2], Masakatsu Tsurusaki[3], Takamichi Murakami[3], Katsusuke Kyotani[4], Yu Ueda[5], Tomoyuki Okuaki[6], Satoru Takahashi[1], Mustafa R. Bashir[7,8], and Kazuro Sugimura[1]

[1]Radiology, Kobe University Graduate School of Medicine, Kobe, Japan, [2]Center for Endovascular Therapy, Kobe University Hospital, Kobe, Japan, [3]Radiology, Kinki University Faculty of Medicine, [4]Division of Radiology, Kobe University Hospital, Kobe, Japan, [5]Philips Electronics Japan, [6]Philips Healthcare, [7]Radiology, Duke University Medical Center, Durham, NC, United States, [8]Center for Advanced Magnetic Resonance Development, Duke University Medical Center

R2* relaxometry that is simultaneously obtained on proton density fat fraction map in gadxetic acid-enhanced MRI can quantitatively estimate liver function. PDFF sequence can potentially quantify steatosis, iron overload, and liver function simultaneously.

3198 Computer 107

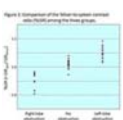

Estimation of Lobar Liver Function using Gadoxetic Acid-Enhanced MR Imaging: Comparison with 99mTc-GSA SPECT Imaging

Keitaro Sofue[1,2], Masakatsu Tsurusaki[3], Takamichi Murakami[3], Kazuhiro Kitajima[4], Utaru Tanaka[1], Masato Yamaguchi[1,2], Koji Sugimoto[1,2], Satoru Takahashi[1], and Kazuro Sugimura[1]

[1]Radiology, Kobe University Graduate School of Medicine, Kobe, Japan, [2]Center for Endovascular Therapy, Kobe University Hospital, [3]Radiology, Kinki University Faculty of Medicine, [4]Nuclear Medicine and PET Center, Hyogo College of Medicine

Hepatobiliary phase image on gadoxetic acid-enhanced magnetic resonance (MR) imaging has been described as a way to quantify liver function and potential to estimate regional liver function. The purpose of this study was to investigate whether gadoxetic acid-enhanced MR imaging can estimate lobar liver function by comparing with ^{99m}Tc-GSA SPECT imaging.

The results of this study showed that hepatic lobar function significantly differs according to the presence of biliary obstruction. Combined volumetric and functional assessment calculated by hepatobiliary phase images on gadoxetic acid-enhanced MR images can estimate lobar liver function.

3199 Computer 108

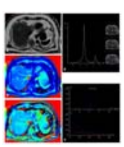

Water-fat separated T1 mapping in the liver and correlation to hepatic fat fraction

Claudia Fellner[1], Philipp Wiggermann[1], Dominik Nickel[2], Niklas Verloh[1], Stephan Kannengießer[2], Christian Stroszczynski[1], and Michael Haimerl[1]

[1]Institute of Radiology, University Hospital Regensburg, Regensburg, Germany, [2]MR Application Predevelopment, Siemens Healthcare, Erlangen, Germany

Fat signal fraction (FF) and R2* mapping as well as MRS of the liver were performed in 201 patients. Results for FF from imaging and MRS were compared to a newly defined parameter T1_FF. T1_FF was calculated from a variable flip angle 3D GRE technique with 2 echo times. Based on the Dixon method, T1 maps from in-phase and from water signal were calculated and T1_FF was deduced. T1_FF correlated well with FF and might be used as a novel estimation of fat fraction. Relevant discrepancies were seen in cases with high R2*.

3200 Computer 109

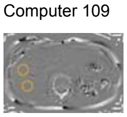

Quantitative Assessment of Liver Fibrosis using MR-Phase Information

Motohira Mio[1], Tetsuya Yoneda[2], Kazuki Tani[1], Tatsuo Toyofuku[1], Toshihiro Maeda[1], and Syoichi Morimoto[3]

[1]Department of Radiology, Fukuoka University Chikushi Hospital, Fukuoka, Japan, [2]Department of Medical Physics in Advanced Biomedical Sciences, Faculty of Life Sciences, Kumamoto University, Kumamoto, Japan, [3]Department of Radiology, Fukuoka University Hospital, Fukuoka, Japan

The aim of this study was to evaluate a potential of MR-phase information for a quantification of liver fibrosis. We measured phase value of the liver and examined the correlation between that value and the stage of fibrosis. Additionally, we also evaluate the correlations among phase value and the serum biomarkers of fibrosis and cirrhosis. The phase value showed high statistical correlation to stages of fibrosis, and to be linearly proportional to the following biomarkers; PLT, APRI, FIB-4 index. In conclusion, MR-phase information may is to be a noninvasive quantitative tool for liver fibrosis and its progression.

3201 Computer 110

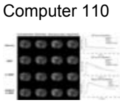

Weighted k-t SPIRiT with Golden Angle Radial Sampling for Dynamic Contrast-Enhanced Liver Imaging

Junyu Wang[1,2], Fuyixue Wang[2], Yajie Wang[2], Jia Ning[2], Zijing Dong[2], Kui Ying[3], and Huijun Chen[2]

[1]Department of Biomedical Engineering, Beijing Jiaotong University, Beijing, People's Republic of China, [2]Center for Biomedical Imaging Research, Department of Biomedical Engineering, School of Medicine, Tsinghua University, Beijing, People's Republic of China, [3]Key Laboratory of Particle and Radiation Imaging, Ministry of Education, Medical Engineering and Institute, Department of Engineering Physics, Tsinghua University, Beijing, People's Republic of China

Acquiring high spatial-temporal resolution images is important for dynamic contrast-enhanced (DCE) imaging. In this work, we proposed a weighted k-t SPIRiT method and tested it in both simulation and in-vivo liver imaging studies based on motion-insensitive golden angle radial stack-of-stars sampling. In this study, feasibility of the weighted k-t SPIRiT has been validated. The results showed that, weighted k-t SPIRiT can improve the image quality compared with SPIRiT, while preserve highly accurate temporal information.

3202 Computer 111

Assessment of early stage of liver fibrosis using MRI T1rho

Qing Li[1], Shuangshuang Xie[2], Zhizheng Zhuo[3], Yue Cheng[2], and Wen Shen[2]

[1]Tianjin First Center Hospital, Tianjin, People's Republic of China, [2]Tianjin First Center Hospital, People's Republic of China, [3]Philips healthcare, Beijing, People's Republic of China

This study assessed the potential of MR T1rho for early liver fibrosis. Ten normal contrast (N), twelve patients with liver fibrosis stage F1 and seven with F2 took the MR T1rho scan. With the stage of liver fibrosis raising, T1rho value increased. And T1rho value of N vs. F1, N vs. F2 and N vs. F1-2 showed significant difference. And the AUC of N vs. F1, N vs. F2 and N vs. F1-2 were 0.858, 0.810, and 0.838. We conclude that MR T1rho has potential to diagnose the early stage of liver fibrosis.

3203 Computer 112

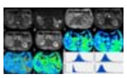

Use of intravoxel incoherent motion (IVIM) derived texture parameters in prediction of microvascular invasion of hepatocellular carcinoma (HCC) in patients with hepatitis B virus infection

Qungang Shan[1], Jingbiao Chen[1], Ronghua Yan[1], Yao Zhang[1], Hao Yang[1], Xin Li[2], Zhongping Zhang[3], Yunhong Shu[4], Churong Lin, Tianhui Zhang[1], Bingjun He[1], Zhuang Kang[1], Xi Long[1], and Jin Wang[1]

[1]Department of Radiology, the Third Affiliated Hospital, Sun Yat-sen University (SYSU), Guangzhou, People's Republic of China, [2]GE Healthcare MR Research China, Guangzhou, People's Republic of China, [3]MR Research China,GE Healthcare, Beijing, [4]Mayo Clinic

Hepatocellular carcinoma (HCC) is the most common primary malignancy of the liver worldwide. Microvascular invasion (MVI) is a significant predictor of prognosis and preoperative prediction of MVI is useful for deciding treatment strategy. We assessed the value of ADC and IVIM texture parameters in predicting the MVI of HBV-related HCCs by whole tumor analysis. Our results showed that ADC and IVIM derived texture parameters were useful for the prediction of MVI of HCCs. Texture analysis of ADC and IVIM is a promising method for predicting MVI of HBV-related HCC.

3204 Computer 113

magna cum laude

Liver R2 Quantification at 3 Tesla in Patients with Iron Overload - Interim Validation Result

Ali Pirasteh[1], Qing Yuan[1], Changqing Wang[2], Diego Hernando[2], Scott B Reeder[3], Ivan Pedrosa[4], and Takeshi Yokoo[1]

[1]Radiology, University of Texas Southwestern Medical Center, Dallas, TX, United States, [2]Radiology, Medical Physics, University of Wisconsin, Madison, WI, United States, [3]Radiology, Medical Physics, Biomedical Engineering, Medicine, Emergency Medicine, University of Wisconsin, Madison, WI, United States, [4]Radiology, Advanced Imaging Research Center, University of Texas Southwestern Medical Center, TX, United States

Determination of liver iron concentration (LIC) by R2-relaxometry has been extensively validated at 1.5T but feasibility of translating this technology to 3T remains uncertain. The purpose of this study was to assess the feasibility of a R2 quantification at 3T against the standard 1.5T R2 in subjects with known or suspected iron overload. In 13 subjects enrolled thus far, we found that liver R2 at 3T linearly correlated with R2 at 1.5T over observed LIC range of 0.3-32.3 mg iron/g liver. We conclude that noninvasive liver LIC determination may be feasible by R2-relaxometry at 3T.

3205 Computer 114

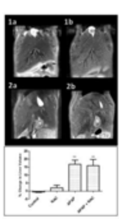

Assessment of magnetic resonance imaging markers in the event of drug induced liver toxicity

Abigail Kaur Chahil [1], Dan Antoine [1], Atul Minhas[2], Thomas Leather [2], Anja Kipar[3], Kevin Park[1], and Harish Poptani[2]

[1]Molecular and Clinical Pharmacology, University of Liverpool, Liverpool, United Kingdom, [2]Centre for Pre-Clinical Imaging, University of Liverpool, Liverpool, United Kingdom, [3]Institute for Veterinary Pathology, University of Zurich, Zurich, Switzerland

Challenges faced in diagnosis and treatment of drug induced liver injury (DILI) have formed the aim of this project to quantify non-invasive MRI and MRS markers to aide research into future therapeutics of DILI. Using an acetaminophen overdose model, we have managed to quantify 4 different MRI biomarkers: liver volume, T2 mapping, ADC and water/fat ratio. Significant changes were observed with an increase in liver volume and T2 relaxation and water/fat ratio, with a decrease in diffusion coefficient. Some degree of normalization in T2 and ADC values was noted after NAC treatment indicating that MRI and MRS can play an important role in the diagnosis of DILI.

3206 Computer 115

Quantitative characterization of disease progression in a mouse model of non-alcoholic steatohepatitis using molecular MR and non-contrast MR imaging

Philip Alan Waghorn[1], Diego Ferreira[1], Chloe Jones[1], Nicholas Rotile[1], Iris Chen[1], Chuantao Tu[1], Bryan Fuchs[2], and Peter Caravan[1]

[1]A.A. Martinos Center for Biomedical Imaging, Charlestown, MA, United States, [2]Division of Surgery, Massachusetts General Hospital, Boston, MA, United States

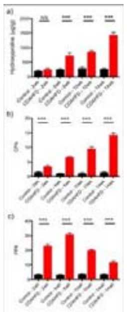

To deliver a non-invasive quantitative measure of patients with nonalcoholic fatty liver disease (NAFLD) who are likely to develop a fibrotic pathology, we characterized the natural history of a nonalcoholic steatohepatitis (NASH) mouse model using MRI. Characterization included fat quantification and MR relaxometry measurements by imaging at 4 time points and comparing with histology and biochemical markers. Fibrogenesis was assessed using the novel Gd-based MR probe, Gd-Hyd which was previously shown to detect fibrogenesis in a mouse CCl4 model of liver fibrosis

---

3207 Computer 116

Using MRI to assess alterations in liver blood flow and oxygenation in response to physiological stress tests: meal challenge, hypercapnia and hyperoxia.

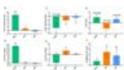

Eleanor F Cox[1,2], Naveenthan Palaniyappan[2], Richard Dury[1], Robert Scott[2], Guruprasad P Aithal[2], I Neil Guha[2], and Susan T Francis[1,2]

[1]Sir Peter Mansfield Imaging Centre, University of Nottingham, Nottingham, United Kingdom, [2]NIHR Nottingham Digestive Diseases Biomedical Research Unit, Nottingham University Hospitals Trust and the University of Nottingham, Nottingham, United Kingdom

Assessment of the capacity for dynamic changes in liver blood flow and oxygenation may provide a mechanism to improve the stratification of chronic liver injury. Here we assess dynamic hepatic blood flow and liver T_2* alterations in response to postprandial hyperaemia following a meal, and hypercapnia and hyperoxia gas challenges. We show significant changes in blood flow and T_2* in response to these challenges, and highlight that both the mode and FWHM of the T_2* distribution should be assessed. However, such stress tests can only be applied in participants with higher baseline T_2* for any change to be evident.

3208 Computer 117

MR ARTS-GROWL: A Non-Iterative Motion-Resistant Technique for High Spatiotemporal Liver DCE Imaging

Zhifeng Chen[1], Liyi Kang[1], Zhongbiao Xu[2], Chenguang Zhao[3], Feng Huang[4], Feng Liu[5], and Ling Xia[1,6]

[1]Department of Biomedical Engineering, Zhejiang University, Hangzhou, People's Republic of China, [2]School of Biomedical Engineering, Guangdong Provincial Key Laborary of Medical Image Processing, Southern Medical University, Guangzhou, People's Republic of China, [3]Philips Healthcare (Suzhou) Co. Ltd., Suzhou, People's Republic of China, [4]Neusoft Medical, Shanghai, China, [5]School of Information Technology and Electrical Engineering, The University of Queensland, Brisbane, Australia, [6]State Key Lab of CAD&CG, Zhejiang University, Hangzhou, People's Republic of China

Motion, mainly caused by respiration, is an unavoidable problem in abdomen MR imaging, which often leads to image blurring and edge ghosting. We propose to combine motion-sorted information with dynamic artificial sparsity approach for radial dynamic contrast-enhanced (DCE) MR imaging. The results demonstrate that better image quality including SNR and low image bluring and more diagnostic information can be generated compared to non-motion-resistant scheme incorporated method.

3209 Computer 118

Variable Density CAIPIRINHA for Highly Accelerated Volumetric Dynamic Contrast-Enhanced Imaging of Liver

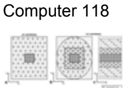

Fuyixue Wang[1,2], Zijing Dong[1], Feiyu Chen[3,4], Yuxin Hu[3,4], Jia Ning[1], Feng Huang[5], and Huijun Chen[1]

[1]Center for Biomedical Imaging Research, Department of Biomedical Engineering, School of Medicine, Tsinghua University, Beijing, People's Republic of China, [2]Harvard-MIT Health Sciences and Technology, MIT, Cambridge, MA, United States, [3]Department of Radiology, Stanford University, Stanford, CA, United States, [4]Department of Electrical Engineering, Stanford University, Stanford, CA, United States, [5]Neusoft Medical System, People's Republic of China

Dynamic Contrast-Enhanced (DCE) imaging is widely used in detection and characterization of many liver diseases. In clinical practice, breath holding is commonly used to overcome respiratory motion and get high quality images. However, long breath holds can be painful or unavailable for some patients. To address this problem, we present a variable density 2D CAIPIRINHA sampling technique with a novel reconstruction framework for highly accelerated volumetric DCE liver imaging. Simulation and in-vivo experiments were performed to evaluate the performance of the proposed method compared with other current techniques. The results show great improvement of image quality within shorter acquisition time.

3210 Computer 119

Factors related to the failure of MR elastography of the liver: multivariate analysis

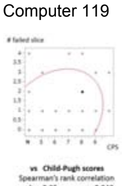

Kengo Yoshimitsu[1]

[1]Radiology, Fukuoka University, Fukuoka, Japan

Seventy consecutive patients with chronic liver diseases and whose R2* values of the liver exceeded 100 s^{-1} were retrospectively recruited, and factors related to MR elastography failure were analyzed. Iron accumulation which corresponds to R2* value over 200 s^{-1} and Child-Pugh score 10 are found to be the two independently significant factors that are related to the failure of MR elastography of the liver. For the assessment of the degree of liver fibrosis in those associated with these factors, other modality, such as ultrasonic elastography, may be considered.

3211 Computer 120

Diagnosis of Liver Cirrhosis Using Morphological Score with Magnetic Resonance Laparoscopy

Satoshi Funayama[1], Utaroh Motosugi[1], Shintaro Ichikawa[1], and Hiroshi Onishi[1]

[1]Department of Radiology, University of Yamanashi, Japan, Yamanashi, Japan

Liver biopsy is a gold standard for the diagnosis of liver cirrhosis. However, biopsy can be false negative because of small amount of tissue sampled. Laparoscopy has been also used as another gold standard for the diagnosis of cirrhosis by directly assessing the liver surface, which compensate for the limitation of biopsy. Laparoscopy like 3D image can be obtained by 3D reconstruction of gadoxetic acid-enhanced hepatobiliary phase images (MR laparoscopy). The two MR laparoscopy findings, i.e. the rib pitting of liver surface and the sharpness of edge, showed good performance for discriminating liver cirrhosis from non-cirrhosis.

Electronic Poster

Velocity & Flow

Exhibition Hall — Monday 9:15 - 10:15

3212 — Computer 49

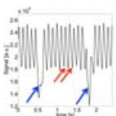

Fast self-gated 4D flow measurements in the murine aortic arch with retrospective radial sampling

Patrick Winter[1], Kristina Andelovic[2], Thomas Kampf[1,3], Peter Jakob[1,4], Wolfgang Bauer[2], and Volker Herold[1]

[1]Experimentelle Physik V, Universität Würzburg, Würzburg, Germany, [2]Medizinische Klinik und Poliklinik I des Universitätsklinikums Würzburg, Würzburg, Germany, [3]Universitätsklinikum Würzburg, Institut für Diagnostische und Interventionelle Radiologie, Würzburg, Germany, [4]Fraunhofer IIS, Fraunhofer EZRT, Magnetresonanz- und Röntgenbildgebung (MRB), Universität Würzburg, Würzburg, Germany

A self-navigated radial 4D-PC sequence is presented for accelerated ECG-free 4D flow measurements in the murine aortic arch. Self-navigation signals were extracted from the radial DC signal and used for retrospective motion synchronization. 3D-Cines with 30 frames were reconstructed with a spatial resolution of 100 µm. The volume flow was determined at 4 2D slices extracted from the 3D dataset and the 3D flow was visualized with streamlines. The results are in good accordance with results reported for ECG-triggered measurements. The new method yields high potential for preclinical studies of hemodynamics and can also be transferred to applications in humans.

3213 — Computer 50

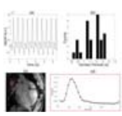

Fast self-navigated PC-MRI for human cardiac flow measurements using retrospective radial sampling

Patrick Winter[1], Kristina Andelovic[2], Peter Jakob[1,3], Wolfgang Bauer[2], and Volker Herold[1]

[1]Experimentelle Physik V, Universität Würzburg, Würzburg, Germany, [2]Medizinische Klinik und Poliklinik I des Universitätsklinikums Würzburg, Würzburg, [3]Fraunhofer IIS, Fraunhofer EZRT, Magnetresonanz- und Röntgenbildgebung (MRB)

A self-navigated radial PC-MRI sequence is presented for fast ECG-free 2D-Cine measurements with 3-dimensional flow encoding. The radial DC signal was used for retrospective self-navigation. Reconstructions were performed with an iterative CG-Sense algorithm. For each flow encoding step 2D-Cines with 30 frames, respectively, and a spatial resolution of 2.34 mm were reconstructed. The time-dependent volume flow through the pulmonary artery was quantified and the blood flow through the ventricles was visualized. The proposed method does not rely on ECG signals and is immune to distortions often observed with conventional triggering. It hence yields high potential for clinical applications.

3214 — Computer 51

magna cum laude

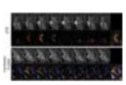

Cardiac 4D phase-contrast MRI at 9.4 T using self-gated ultra-short echo time (UTE) imaging

Martin Krämer[1], Abdallah G Motaal[2], Karl-Heinz Herrmann[1], Bettina Löffler[3], Jürgen R Reichenbach[1,4,5,6], Gustav J Strijkers[2,7], and Verena Hoerr[3]

[1]Medical Physics Group, Institute of Diagnostic and Interventional Radiology, Jena University Hospital - Friedrich Schiller University Jena, Jena, Germany, [2]Biomedical NMR, Department of Biomedical Engineering, Eindhoven University of Technology, Eindhoven, Netherlands, [3]Institute of Medical Microbiology, Jena University Hospital - Friedrich Schiller University Jena, Jena, Germany, [4]Michael Stifel Center for Data-driven and Simulation Science Jena, Friedrich Schiller University Jena, Jena, Germany, [5]Abbe School of Photonics, Friedrich Schiller University Jena, Jena, Germany, [6]Center of Medical Optics and Photonics, Friedrich Schiller University Jena, Jena, Germany, [7]Biomedical Engineering and Physics, Academic Medical Center, Netherlands

Time resolved 4D phase contrast (PC) MRI in mice is challenging and often susceptible to artifacts due to long scan times, ECG-gating and the rapid blood flow and cardiac motion of small rodents. To overcome several of these technical challenges we implemented a retrospectively self-gated 4D-PC radial UTE acquisition scheme and assessed its performance in healthy mice by comparing the results with those obtained with an ECG-triggered 4D-PC fast low angle shot (FLASH) sequence.

3215 — Computer 52

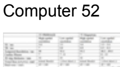

Effect of field strength and spatial resolution on quantifying intracranial hemodynamics with PEAK-GRAPPA accelerated Dual-Venc 4D flow MRI

Susanne Schnell[1], Maria Aristova[1], Can Wu[1,2], Pierre-Francois Van de Moortele[3], Bharathi Dasan Jagadeesan[4], Kamil Ugurbil[3], Michael Markl[1,5], and Sebastian Schmitter[3,6]

[1]Radiology, Northwestern University, Chicago, IL, United States, [2]Philips Healthcare, Gainesville, FL, United States, [3]Center for Magnetic Resonance in Medicine, University of Minnesota, Minneapolis, MN, United States, [4]University of Minnesota, Minneapolis, MN, United States, [5]Biomedical Engineering, Northwestern University, Evanston, IL, United States, [6]Physikalisch-Technische Bundesanstalt, Braunschweig and Berlin, Germany

Dual-*venc* 4D flow MRI was applied in 5 healthy volunteers at two different field strengths of 3T and 7T and at two different isotropic spatial image resolutions, approximately $(1.2mm)^3$ and $(0.8mm)^3$. The aim of this study was to systematically investigate the effect of field strength as well as the impact of resolution for intracranial 4D flow MRI with respect to image quality (vessel sharpness and depiction of small intracranial vessels) and quantification of intracranial flow parameters (net flow, peak velocity).

3216 — Computer 53

An MRI Phantom Study to Assess the Effects of Localized Stiffness on Aortic Hemodynamics

Khalil Rachid[1] and Dima Rodriguez[1]

[1]Laboratoire d'Imagerie par Résonance Magnétique Médicale et Multi-Modalités (IR4M), Univ. Paris-Sud, CNRS, Université Paris-Saclay, Orsay, France

Cardiovascular complications have been highly associated with arterial stiffness which results from aging and/or vascular disease. Reduced arterial elasticity, particularly at the aorta level, increases the left ventricle load. In this work, we studied the effects of localized stiffness on an aortic phantom with respect to its severity and position relative to an upstream proximal site. As expected, our results showed that the aortic hemodynamics were altered: the pulse pressure was increased, and the flow rate decreased. Moreover, the local proximal compliance was reduced as the stiffness was brought closer to the heart. However, the pulse wave velocity remained unchanged suggesting that global stiffness measuring approaches might not detect regional wall alterations

---

3217 Computer 54

Interobserver reproducibility of blood flow measurements with an abdominal 4D flow MRI sequence with spiral sampling and compressed sensing

Octavia Bane[1], Steven Peti[2], Mathilde Wagner[1,3], Stefanie Hectors[1], Hadrien A Dyvorne[1,4], and Bachir Taouli[1,2]

[1]Translational and Molecular Imaging Institute, Icahn School of Medicine at Mount Sinai, New York, NY, United States, [2]Department of Radiology, Icahn School of Medicine at Mount Sinai, New York, NY, United States, [3]Radiology, Groupe Hospitalier Pitié Salpêtrière, Paris, France, [4]4Catalyzer, Guilford, CT, United States

Our study evaluated the interobserver reproducibility of flow quantification in abdominal vessels using a novel 4D flow phase-contrast (PC) MRI sequence. The effect of liver fibrosis on blood flow metrics was also examined in 20 patients. Time-averaged vessel cross-section area, through-plane velocity and volume flow measured in 14 abdominal vessels in a subset of 10 patients were found to have acceptable interobserver agreement (Cohen's kappa 0.762). A significant increase in the hepatic artery velocity and flow, splenic vein area and flow, middle hepatic vein velocity and flow, and right hepatic vein velocity was observed in patients with advanced fibrosis/cirrhosis.

3218 Computer 55

Comparison of SENSE, GRAPPA, SPIRiT and ESPIRiT for accelerated 4D flow MRI Imaging

Xiaole Wang[1], Aiqi Sun[1], Jianwen Luo[1], and Rui Li[1]

[1]Center for Biomedical Imaging Research, Department of Biomedical Engineering, School of Medicine, Tsinghua University, Beijing, People's Republic of China

Parallel imaging is a promising method to shorten the scanning time of 4D flow MRI. We applied SENSE, GRAPPA, SPIRiT and ESPIRiT in 4D flow imaging on six healthy volunteers and compared the accuracy of four algorithm. We found that ESPIRiT and SPIRiT showed the better velocity maps than SENSE and Grappa. The temporal fidelity of ESPIRIT can be the best among four methods, while SENSE and GRAPPA resulted in overestimates of peak flow. In conclusion, we validate the accuracy of four widely-used parallel imaging methods for the reconstruction of velocity map in 4D flow MR Imaging.

3219 Computer 56

UNFOLDed Spiral SPiRIT Phase Contrast Velocity Mapping for Scan Time Reduction of Coronary Blood Flow Measurements

Axel Joachim Krafft[1], Simon Reiss[1], Jürgen Hennig[1], and Marius Menza[1]

[1]Radiology – Medical Physics, Medical Center – University of Freiburg, Freiburg, Germany

Coronary flow measurements can provide important information, e.g. to assess coronary stenosis, but remain challenging due to the need for high spatio-temporal resolution in the presence of heart and respiratory motion. Progress has been made by using spiral acquisitions enabling data acquisition within a breath hold. We combined spiral SPiRIT flow measurements with UNFOLD, a technique that allows for further data undersampling and scan time shortening (here by a factor of 2), to achieve coronary flow measurements with a spatio-temporal resolution of $1\times1\times8mm^3$/<15.5msec. The combined UNFOLD-spiral approach was implemented into different spiral sampling patterns and evaluated in healthy volunteers.

3220 Computer 57

Respiratory changes in pulmonary flow distribution in Fontan circulation using "5-D" flow MRI

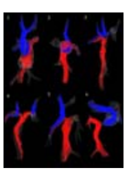

David Rutkowski[1,2], Christopher J. François[2], and Alejandro Roldán-Alzate[1,2,3]

[1]Mechanical Engineering, UW Madison, Madison, WI, United States, [2]Radiology, UW Madison, Madison, WI, United States, [3]Biomedical Engineering, UW Madison, Madison, WI, United States

The purpose of this study was to evaluate the respiratory effects on particle trace distribution from the vena cava to the pulmonary arteries in single ventricle patients with TCPC. Six patients were imaged using PC-VIPR and a scheme that allows for double gating to the ECG and respiratory cycles, providing flow data for separate respiratory phases. Results displayed a non-equal flow distribution to the pulmonary arteries from the vena cava and a significant difference in pulmonary flow distribution between inspiration and expiration. This may indicate the importance accounting for respiratory cycle variations when interpreting clinical TCPC results.

3221 Computer 58

Bootstrapped Estimates of Velocity Uncertainty for 4D Flow PC-MRI

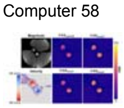

Michael Loecher[1] and Daniel B. Ennis[1]

[1]Department of Radiological Sciences, University of California, Los Angeles, CA, United States

We implement and analyze a bootstrapping method to estimate VNR measurements with a limited number of 4D Flow acquisitions. Bootstrapped estimates were created from sets of 2 acquisitions and sets of 5 acquisitions. The VNR maps were compared to a ground truth VNR measurement generated from 50 acquisitions in a flow phantom. The method was also demonstrated *in vivo* to generate VNR maps of the carotid arteries.

3222 Computer 59

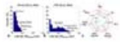

Evaluate right ventricle-pulmonary artery interaction in patients with repaired tetralogy of Fallot by 4D flow-derived kinetic energy

Meng-Chu Chang[1], Ming-Ting Wu[2], Ken-Pen Weng[3], Mao-Yuan Su[4], Marius Menza[5], Hung-Chieh Huang[2], and Hsu-Hsia Peng[1]

[1]National Tsing Hua University, Hsinchu, Taiwan, [2]Department of Radiology, Kaohsiung Veterans General Hospital, Kaohsiung, Taiwan, [3]Department of Pediatrics, Kaohsiung Veterans General Hospital, Kaohsiung, Taiwan, [4]Department of Medical Imaging, National Taiwan University Hospital, Taipei, Taiwan, [5]Medical Physics, Department of Radiology, University Hospital Freiburg, Freiburg, Germany

We quantified the kinetic energy (KE) of intraventricular RV flow ($KE_{RV,flow}$), PA forward flow (KE_{PA}) and PA retrograde flow ($KE_{PA,regur}$). The purpose is to establish 4D flow-derived KE-related indices for better understanding of the RV-PA interaction. We observed the interaction between RV and PA by assessing the correlation between diastolic $KE_{PA,regur}$ and late diastolic $KE_{RV,flow}$ as well as between systolic KE_{PA} and RV mean pressure. In conclusion, we verified that altered hemodynamic conditions of RV interacted with severe PR, which may lead to RV overloading pathology and adverse outcome in rTOF patients.

3223 Computer 60

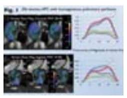

Energy-loss in Fontan Circulation Develops Heterogeneous Pulmonary Perfusion: Hybrid Analysis of 2D Vortex Flow Map and 4D Flow MRI

Michinobu Nagao[1], Umiko Ishizaki[1], Yumi Shiina[2], Kenji Fukushima[1], Yuka Matsuo[1], Tatsunori Takahashi[3], Kei Inai[2], In-Sam Park[3], Yasuhiro Goto[4], Yamato Shimomiya[5], Yuzo Yamasaki[6], Ichiro Sakamoto[7], Kenichiro Yamamura[8], Atsushi Takemura[9], Masami Yoneyama[9], and Shuji Sakai[1]

[1]Diagnostic Imaging & Nuclear Medicine, Tokyo Women's Medical University, Tokyo, Japan, [2]Clinical Reserch for ACHD, Tokyo Women's Medical University, [3]Pediatric Cardiology, Tokyo Women's Medical University, [4]Radiological service, Tokyo Women's Medical University, [5]Clinical Application Development Marketing Division, Ziosoft Inc, [6]Clinical Radiology, Kyushu University, [7]Cardiovascular Medicine, Kyushu University, [8]Pediatrics, Kyushu University, [9]Philips Electronics Japan

Patients with Fontan-operation, single-ventricle heart frequent have systematic collaterals that increase pulmonary blood flow. The competitive flow elevates pulmonary artery pressure, a process leading to erosion of flow energy. We developed a novel post-processing of 2D cine MRI named for "vortex flow map" to evaluate the energy-loss in Fontan-circuit. Vortex flow map shows energy-loss as small magnitude of vortex flow (MVF) and reveals the relation to heterogeneous pulmonary perfusion. In total cavopulmonary conversion, 4D flow can visualize energy-loss caused by a meandering extra-cardiac conduit and the conflict flow, leading to reduce unilateral lung perfusion.

3224 Computer 61

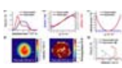

Accurate Flow MRI: the importance of velocity distribution asymmetry

Antoine Vallatos[1], Haitham F. I. Al-Mubarak[1], James M. Mullin[1], and William M. Holmes[1]

[1]Glasgow Experimental MRI Centre, Institute of Neuroscience and Psychology, University of Glasgow, Glasgow, United Kingdom

This work proposes a theoretical and experimental investigation into the unexplored effect of asymmetric distribution of intra-voxel velocities on the accuracy of Flow MRI. Our experimental results show that asymmetric velocity distributions can compromise the linearity of measured phase against applied gradient, leading to important velocimetry errors. A theoretical expression of the observed phase measurement errors is introduced, relating them to velocity distribution properties such as variance, skewness and kurtosis. This enables to explain previously reported velocimetry errors and propose solutions so as to increase the accuracy of velocity measurements.

3225 Computer 62

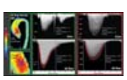

Comparison of Doppler Echocardiography Mean Transvalvular Aortic Pressure Gradient to 4D Flow MRI

Michael James Rose[1], Kelly Jarvis[2,3], Susanne Schnell[2], James D Thomas[4], Joshua D Robinson[1,5,6], Cynthia K Rigsby[1,2], Michael Markl[2,3], and Alex J Barker[2]

[1]Medical Imaging, Ann & Robert H. Lurie Children's Hospital of Chicago, Chicago, IL, United States, [2]Department of Radiology, Feinberg School of Medicine, Northwestern University, [3]Department of Biomedical Engineering, McCormick School of Engineering, Northwestern University, [4]Division of Cardiology, Feinberg School of Medicine, Northwestern University, [5]Division of Pediatric Cardiology, Ann & Robert H. Lurie Children's Hospital of Chicago, Chicago, IL, United States, [6]Department of Pediatrics, Feinberg School of Medicine, Northwestern University

Mean and peak pressure gradients are an important measure of aortic stenosis severity. In this study, we present a novel method for measuring mean pressure gradients using 4D flow MRI. 4D flow MRI peak and mean pressure gradients were measured in 23 pediatric BAV patients and compared to Doppler echocardiography (echo). There was no significant difference between 4D flow MRI and echo in peak or mean pressure gradients. 4D flow MRI mean pressure gradients correlated better with echo than peak pressure gradients ($R2= 0.78$ vs. $R2=0.27$), suggesting 4D flow to be better suited for measuring mean pressure gradients.

3226 Computer 63

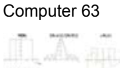

On Partial Fourier Acquisition in 4D Flow MRI of Mean Velocities and Turbulent Kinetic Energy

Jonas Walheim[1] and Sebastian Kozerke[1]

[1]ETH Zurich, Zurich, Switzerland

Scan time reduction with partial Fourier was investigated for 4D flow MRI of mean velocity and turbulent kinetic energy. It was shown analytically, that PF leads to a loss in resolution for phase images. According to experiments with in-vivo data, the precondition of slowly varying phases is not met for PF reconstructions of 4D flow MRI, making homodyne reconstruction and POCS fail. Therefore, it is concluded, that PF cannot recover missing k-space samples in 4D flow MRI and does not offer a benefit over symmetric k-space sampling with the same number of phase encodes.

3227 Computer 64

Comparison of 4D Flow MRI and Tomographic Particle Image Velocimetry

Rafael Medero[1] and Alejandro Roldán-Alzate[2]

[1]Mechanical Engineering, University of Wisconsin-Madison, Madison, WI, United States, [2]Mechanical Engineering and Radiology Department, University of Wisconsin-Madison

4D flow MRI has shown promising results, assessing hemodynamics in different vascular territories. In order to keep expanding its clinical use, reliable validation of 4D flow MRI is needed for improvement of its accuracy and precision while reducing scan time. The purpose of this study was to compare velocity measurements through an in vitro carotid artery bifurcation model using 4D Flow MRI and particle image velocimetry. PIV system provides great insight into the velocity field within the model, using an excellent acquisition quality.

3228 Computer 65

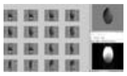

Combining Phase Information from Phased Array Coils without Phase Unwrapping in Phase Contrast Imaging

Yi Wang[1,2], Xingxian Shou[1], Hai Luo[2], Xiang Zhou[2], Bin Wang[2], and Leping Zha[1,2]

[1]Alltech Medical Systems America, Solon, OH, United States, [2]Alltech Medical Systems, Chengdu, People's Republic of China

In phase contrast flow quantitation, high spatial/temporal resolution and parallel imaging often entail the high density multiple phased array receive coils. To overcome ambiguities in coil signal combination introduced by motion, phase wrapping, image noise, and the unknown phase-offset among the coils, we used the k-space complex division of the same coil element signals from both flow compensated (FC) and flow encoded (FE) scans to eliminate the coil sensitivity phase associated with that coil element and then add all phase difference of each elements in complex domain to avoid phase unwrapping for a fast and accurate flow velocity mapping.

3229 Computer 66

Computational Fluid Dynamics of Pulmonary Circulation Before and After Induced Pulmonary Hypertension: 2D Flow versus 4D Flow MRI-Based Boundary Conditions

Sylvana García-Rodríguez[1], James Leschke[2], Alejandro Roldán-Alzate[1,3], and Christopher J. François[1]

[1]Department of Radiology, University of Wisconsin - Madison, Madison, WI, United States, [2]Rocky Vista University, CO, United States, [3]Department of Mechanical Engineering, University of Wisconsin - Madison, Madison, WI, United States

Acute pulmonary hypertension was induced in dogs by micro embolization. RHC was performed, as well as 4D flow MRI pre and post-embolization. MRI data was used to develop a CFD model of the proximal pulmonary circulation while comparing two inlet boundary conditions: velocity definition as defined from 2D flow MRI and from 4D flow MRI, which takes into account the directionality of the velocity. WSS tended to decrease post-embolization. Pressure gradient distribution shows that during peak systole, a constant normal inlet condition might be sufficient for CFD simulation; however, differences might be present during diastole.

3230 Computer 67

Improving visualization of cardiac QFlow by acquiring bSSFP cine images within the same breath hold

Matthew Lanier[1], Ryan Moore[2], Michael Taylor[2], Charles Dumoulin[1], and Hui Wang[3]

[1]Radiology, Cincinnati Children's Hospital Medical Center, Cincinnati, OH, United States, [2]Cardiology, Cincinnati Children's Hospital Medical Center, Cincinnati, OH, United States, [3]Philips, Cincinnati, OH, United States

In this study, we propose a method to acquire QFlow and bSSFP cine images in a single breath-hold that eliminates the need to have these scans acquired separately; thereby overcoming the need for inter-breath hold cross-registration. The approach provides improved registration of flow fields with high-resolution anatomic cine imaging.

3231 Computer 68

Improved blood flow velocity measurement in superficial perforating arteries of the white matter at 7 tesla MRI

Lennart J. Geurts[1], Geert Jan Biessels[2], and Jaco J. M. Zwanenburg[1]

[1]Radiology, UMC Utrecht, Utrecht, Netherlands, [2]Brain Center Rudolf Magnus, UMC Utrecht, Utrecht, Netherlands

7T 2D Qflow is capable of measuring blood flow velocity in the superficial perforating arteries. These arteries run though the semi oval center of the white matter in the brain and have diameters smaller than 200 µm. Due to the small diameters, partial volume effects of perforators with surrounding tissue cause velocity underestimation. With simulations and experiments we show that tilt optimized nonsaturated excitation (TONE) significantly increases SNR and decreases velocity underestimation in superficial perforating arteries.

3232 Computer 69

Blood flow velocity and pulsatility measurement of lenticulostriate arteries with 3T 2D Qflow MRI

Lennart J. Geurts[1], Jeroen Hendrikse[1], and Jaco J. M. Zwanenburg[1]

[1]Radiology, UMC Utrecht, Utrecht, Netherlands

The lenticulostriate arteries are involved in small vessel disease and their blood flow velocity and pulsatility has been measured with 7T 2D Qflow. To make this measurement more widely available we aimed to translate it to 3T by increasing blood SNR with a contrast agent. In this study we show that the 2D Qflow acquisition can measure blood flow velocity and its pulsatility in lenticulostriate arteries at 3T, even without the use of a contrast agent.

3233 Computer 70

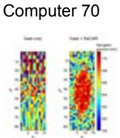

Respiratory Controlled Adaptive K-space Reordering (ReCAR) Improves 4D Flow Image Quality

Ning Jin[1], Andreas Greiser[2], Kelvin Chow[3], Susanne Schnell[4], Alex J Barker[4], and Michael Markl[4,5]

[1]Siemens Healthcare, Columbus, OH, United States, [2]Application Development, Siemens Healthcare, Erlangen, Germany, [3]Siemens Healthcare, Chicago, IL, United States, [4]Department of Radiology, Feinberg School of Medicine, Northwestern University, Chicago, IL, United States, [5]Department of Biomedical Engineering, Northwestern University, Chicago, IL

4D flow normally uses respiratory gating to mitigate breathing artifacts for thoracic and abdominal applications. Respiratory Controlled Adaptive *k*-space Reordering (ReCAR) employs k-space reordering based on the current respiratory position. It has been reported to increase respiratory gating efficiency for 4D flow applications. The purpose of this study was to systematically compare the image quality of 4D flow data acquired with and without adaptive k-space reordering.

3234 Computer 71

Respiratory self-gated golden-angle spiral 4D flow MRI

Rene Bastkowski[1], Kilian Weiss[1,2], David Maintz[1], and Daniel Giese[1]

[1]Radiology, University Hospital of Cologne, Cologne, Germany, [2]Healthcare, Philips GmbH, Hamburg, Germany

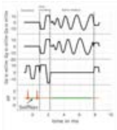

A spiral self-gated 4D Flow sequence is presented that operates at a predictable scan time. The respiratory self-navigation signal is extracted from the FID during the fat saturation pulse. The sequence allows to reconstruct 4D flow data in multiple respiratory states. This technique potentially allows to analyze respiratory dependent flow.

3235 Computer 72

The importance of correcting for through-plane heart motion in the assessment of aortic regurgitation using PC-MRI as estimated by feature tracking cine-MRI

Frida Svensson[1,2], Alexander Johansson[3], Åse Johnsson[2,3], and Kerstin Magdalena Lagerstrand[1,2]

[1]Dept. of Medical Physics and Techniques, Sahlgrenska University Hospital, Gothenburg, Sweden, Sahlgrenska University Hospital, Gothenburg, Sweden, [2]Institute of Clinical Sciences, Sahlgrenska Academy, University of Gothenburg, Gothenburg, Sweden, [3]Dept of Radiology, Sahlgrenska University Hospital, Gothenburg, Sweden, Sahlgrenska University Hospital

Phase contrast measurements are prone to velocity offsets due to through-plane motion of the heart. Here we examine the impact of these velocity offsets on the assessment of aortic regurgitation using a promising method for quantification of the through-plane heart motion. Without correction for through-plane heart motion, the phase contrast measurements significantly underestimated the severity of the regurgitation and the underestimation varied highly between individuals. This calls for development of reliable and robust methods, such as the proposed tracking method, for individual correction of through-plane heart motion in the phase contrast measurements.

Electronic Poster

Myocardial Ischemia Imaging

Exhibition Hall Monday 9:15 - 10:15

3236 Computer 1

Coronary flow velocity reserve by 3T-MRI fast velocity-encoded cine can detect patients with high-risk coronary artery disease

Masanao Naya[1], Yasuka Kikuchi, Noriko Oyama-Manabe, Masahiko Obara, Tadao Aikawa, Osamu Manabe, Hiroyuki Sugimori, and Nagara Tamaki

[1]Hokkaido University Graduate School of Medicine, Sapporo, Japan

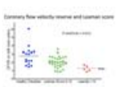

Low coronary flow velocity reserve (CFVR) on left main coronary trunk can predict downstream coronary organic stenosis and myocardial scar, suggesting that CFVR derived by flow velocity by MRI is a simple and reliable index to detect patients with high-risk coronary artery disease.

3237 Computer 2

Cardiac ASL using Single-Shot EPI at 3T

Ahsan Javed[1] and Krishna Nayak[1]

[1]Electrical Engineering, University of Southern California, Los Angeles, CA, United States

Arterial spin labeling (ASL) is a non-contrast method for measuring tissue perfusion, and can be applied to the measurement of myocardial blood flow and myocardial perfusion reserve. Current cardiac ASL methods predominantly use balanced steady state free precession (bSSFP) imaging. In this work, we revisit one of the original cardiac ASL imaging schemes, single-shot EPI (Poncelet et al., MRM 1999), and experimentally demonstrate its potential advantages and its current limitations at 3T.

3238 Computer 3

Quantitative dynamic MRI in the phase domain: Characterization of coronary arterial morphology using a simple Fourier method to accurately estimate bolus arrival times in DCE-MRI perfusion imaging

Karl P Kunze[1], Teresa Vitadello[2], Christoph Rischpler[1], Markus Schwaiger[1], and Stephan G Nekolla[1]

[1]Nuclear Medicine, TU Munich, Munich, Germany, [2]Cardiology, TU Munich, Munich, Germany

This abstract proposes a simple method to extract the bolus arrival time (BAT) from myocardial DCE-MRI perfusion data using a low-frequency phase reconstruction of the deconvolution of arterial input functions with myocardial tissue curves. A simulation study is performed to test the proposed technique with respect to accuracy, robustness and superiority to existing approaches. A clinical PET/MRI example and a control group are examined to show the robustness of BAT estimation even without post-processing steps like surface coil intensity correction or saturation correction. The interpretation of the BAT as a surrogate for coronary path lengths is supported by coronary angiography.

3239 Computer 4

Validation of the Intravoxel Incoherent Motion Model in the Healthy Human Heart using Black-Blood Preparation

Georg Spinner[1], Constantin von Deuster[1], Christian Torben Stoeck[1], and Sebastian Kozerke[1]

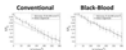

[1]Institute for Biomedical Engineering, ETH Zürich, Zürich, Switzerland

In vivo cardiac Intravoxel Incoherent Motion Imaging (IVIM) offers the potential to estimate myocardial perfusion without the need for contrast agents. The IVIM parameter estimates, however, suffer from low signal-to-noise ratio, patient motion and are depending on imaging settings as well as on diffusion gradient shapes. In the present work, further evidence is presented that estimation of perfusion using a second-order motion compensated diffusion weighted sequence in the in vivo human heart is possible.

3240 Computer 5

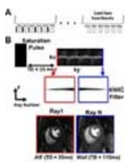

Accelerated Cardiac Perfusion MRI with Radial k-space Sampling, Compressed Sensing, and KWIC filtering to Enable Qualitative and Quantitative Analyses of Perfusion.

Nivedita K. Naresh[1], Hassan H. Valizadeh[2], KyungPyo Hong[1], Amir A. Rahsepar[1], Daniele Procissi[1], Jeremy D. Collins[1], James C Carr[1,3,4], Daniel C. Lee[1,4], and Daniel Kim[1]

[1]Radiology, Northwestern University, Chicago, IL, United States, [2]Biomedical Engineering, Northwestern University, Chicago, IL, United States, [3]McCormick School of Engineering, Northwestern University, Chicago, IL, United States, [4]Medicine, Northwestern University, Chicago, IL, United States

First-pass cardiac perfusion MRI is widely used as an important diagnostic tool for cardiovascular disease and extensive efforts are focused on improving spatial coverage, minimizing dark rim artifacts and quantifying absolute myocardial blood flow. In this study, we used a combination of radial k-space sampling, compressed sensing, and KWIC filtering to address these issues. Compared to the conventional perfusion technique, the accelerated method improved spatial coverage, minimized dark rim artifact and enabled quantification of myocardial blood flow.

3241 Computer 6

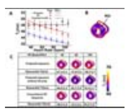

Heart-Rate Independent T2 Mapping for Overcoming Loss of BOLD Sensitivity in Conventional Cardiac T2 MRI Acquired Under Vasodilator Stress

Hsin-Jung yang[1], Damini Dey[1], Jane Sykes[2], John Butler[2], Xiaoming Bi[3], Behzad Sharif[1], Ivan Cokic[1], Sotirios Tsaftaris[4], Debiao Li[1], Piotr Slomka[1], Frank Prato[2], and Rohan Dharmakumar[1]

[1]Cedars Sinai Medical Center, Los Angeles, CA, United States, [2]Lawson Health Research Institute, [3]Siemens Healthcare, [4]IMT School for Advanced Studies Lucca

Despite the advances to date, myocardial BOLD MRI continues to be plagued by imaging confounders, which limit its reliability. We hypothesized that (a) the loss in BOLD sensitivity is dependent on the magnitude of the change in heart rate (HR) between rest and vasodilator stress; and (b) HR-insensitive T2 maps can enable BOLD changes to be accurately captured. We tested our hypothesis by examining the BOLD response to a HR-insensitive T2 mapping approach and conventional T2 mapping. Our results show that reliability of T2-based myocardial BOLD MRI could be markedly improved through heart-rate-insensitive T2 acquisitions.

3242 Computer 7

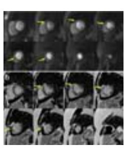

Spiral simultaneous multi-slice first-pass myocardial perfusion imaging

Yang Yang[1], Matthew Van Houten[2], Patrick Norton[3], Klaus Hagspiel[3], Christopher Kramer[1,3], John Mugler[2,3], and Michael Salerno[1,2,3]

[1]Medicine, University of Virginia, Charlottesville, VA, United States, [2]Biomedical Engineering, University of Virginia, Charlottesville, VA, United States, [3]Radiology, University of Virginia, Charlottesville, VA, United States

First-pass contrast-enhanced myocardial perfusion imaging is an important tool to assess patients with coronary artery disease, but current techniques are still limited by spatial-temporal resolution and ventricular coverage. Simultaneous multi-slice (SMS) utilizes multi-band (MB) RF pulses which can greatly improve sampling efficiency. We develop an SMS-spiral perfusion pulse sequence by modulating the phase of excitation RF pulses of multiple slices with a Hadamard matrix to achieve significant signal cancellation and an incoherent aliasing pattern. The pulse sequence is evaluated in 23 patients with MB factors of 2, 3 and 4 resulting in high image quality.

3243 Computer 8

Quantitative 3D myocardial perfusion at systole and diastole with a dual echo arterial input function

Jason K Mendes[1], Ganesh Adluru[1], Devavrat Likhite[1], Apoorva Pedgaonkar[1], Merlin J Fair[2,3], Peter D Gatehouse[2,3], Brent Wilson[4], and Edward V DiBella[1]

[1]Radiology and Imaging Sciences, University of Utah, Salt Lake City, UT, United States, [2]Cardiovascular Magnetic Resonance Unit, Royal Brompton Hospital, London, United Kingdom, [3]National Heart & Lung Institute, Imperial College London, London, United Kingdom, [4]Cardiology, University of Utah, UT, United States

Quantitative 3D myocardial perfusion is a clinically realistic goal and this work further develops and combines several innovative sequence designs to achieve this goal. These developments include an optimized 3D stack of stars readout (150ms per beat), acquisition and T2* correction of an arterial input function, tailored saturation pulse design and potential whole heart coverage at both systole and diastole at heart rates up to 109 bpm. Implementation and quantitative perfusion results are shown for healthy volunteers and a patient with known coronary disease.

3244 Computer 9

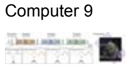

10-fold Spatial-Only Acceleration For High-Resolution Myocardial Perfusion Using Multi-Band Imaging and Multi-Band Outer Volume Suppression

Sebastian Weingärtner[1,2,3], Steen Moeller[2], Chetan Shenoy[4], and Mehmet Akçakaya[1,2]

[1]Electrical and Computer Engineering, University of Minnesota, Minneapolis, MN, United States, [2]Center for Magnetic Resonance Research, University of Minnesota, Minneapolis, MN, United States, [3]Computer Assisted Clinical Medicine, Heidelberg University, Mannheim, Germany, [4]Department of Cardiology, University of Minnesota, Minneapolis, MN, United States

Myocardial perfusion imaging is clinically established for the detection of myocardial ischemia and requires rapid imaging to monitor the uptake of a contrast-agent in the heart. Spatial resolution or coverage is commonly increased by exploiting temporal correlations, at the risk of inducing temporal blurring. Here, we investigate the use of simulteaneous multi-slice imaging for high spatial-only acceleration. Outer-volume-suppression using multi-band saturation-slabs (MB-OVS) were used to facilitate high multi-band factors. Phantom results, show through signal suppression outside region-of-interest with MB-OVS. In-vivo results show robust image quality throughout the contrast uptake and washout with 9-slice LV coverage at a temporal resolution <550ms.

3245 Computer 10

Estimating extraction fraction and blood flow by combining first-pass myocardial perfusion and T1 mapping results

Devavrat Likhite[1], Promporn Suksaranjit[2], Ganesh Adluru[1], Chris McGann[2], Brent Wilson[2], and Edward DiBella[1]

[1]Department of Radiology and Imaging sciences, University of Utah, Salt Lake City, UT, United States, [2]Division of Cardiovascular Medicine, University of Utah, Salt Lake City, UT, United States

Dynamic contrast enhanced MRI is maturing as a tool in contemporary cardiovascular medicine. However, there are challenging areas that have not been fully understood, such as modeling extraction of the contrast agent from the vasculature to the extravascular space. We present a technique that exploits information overlap between two different cardiac MRI techniques, namely, DCE-MRI and T1 mapping, in order to estimate extraction and flow. Our study shows that extraction fraction and myocardial blood flow can be estimated by fixing extracellular volume (ECV) to values obtained from T1 mapping.

3246 Computer 11

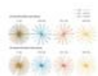

Optimized 2D radial CAIPIRINHA for cardiac perfusion MRI

Ye Tian[1,2], Ganesh Adluru[2], Jason Mendes[2], and Edward DiBella[2]

[1]Physics and Astronomy, University of Utah, Salt Lake City, UT, United States, [2]Radiology and Imaging Sciences, University of Utah, Salt Lake City, UT, United States

We propose an optimized offset golden angle trajectory of 3-slice radial CAIPI for more uniform distribution of phase modulated rays. Both computer simulation and phantom scan demonstrate that our proposed method has less artifact. Simulation studies show a 41% reduction in aliasing energy when compared to conventional golden angle trajectory. As well, optimization with an asymmetric echo readout resulted in a reduction of acquisition time by 15% with little sacrifice of image quality. These two methods can benefit simultaneous multi-slice perfusion acquisitions.

3247 Computer 12

Analysis of Coronary Contrast Agent Transport in Bolus Based Quantitative Myocardial Perfusion MRI Measurements with Computational Fluid Dynamics (CFD) Simulations in High Performance Computing (HPC) Environments

Johannes Martens[1], Sabine Panzer[1], Jeroen van den Wijngaard[2], Maria Siebes[2], and Laura Maria Schreiber[1]

[1]Comprehensive Heart Failure Center, University Hospital Wuerzburg, Wuerzburg, Germany, [2]Dept. of Biomedical Engineering & Physics, Academic Medical Center, Amsterdam, Netherlands

Aim of the project is the execution of computationally extremely challenging CFD simulations of blood flow and contrast agent (CA) transport in coronary arteries on HPC clusters. Therefore scalability testing is performed to assess the suitability of applied software codes in HPC environments. Cardiovascular 3D-models are extracted from high-resolution cryomicrotome imaging data and meshed with computational grids. Navier-Stokes-equations for blood flow and the advection-diffusion-equation for CA transport are solved to obtain CA bolus dispersion in the epicardial vessels. We find indications of asymptotically decreasing dispersion effects with increasing vessel generation.

3248 Computer 13

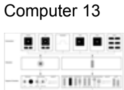

An analysis of radial sequence parameters in myocardial first-pass perfusion for optimised imaging

Merlin J Fair[1,2], Peter D Gatehouse[1,2], Edward VR DiBella[3], and David N Firmin[1,2]

[1]CBRU, Royal Brompton Hospital, London, United Kingdom, [2]NHLI, Imperial College London, London, United Kingdom, [3]UCAIR, University of Utah, UT, United States

A simulation framework is devised to analyse sequence parameters in radial first-pass perfusion for optimised imaging. A model containing left-ventricular myocardium, bloodpool and defect was radially sampled in 2D and 3D under multiple sequence parameters variations, tested with differing imaging environments. Automatic measures of sharpness, signal variation and CNR were made on the N=1016 simulation reconstructed images and results of interest are presented.

3249 Computer 14

Quantitative MRI measurement of the interplay between myocardial function, perfusion, structure and metabolism during acute and chronic remodeling in a porcine model of myocardial infarction

Smita Sampath[1], Sarayu Annamalai Parimal[2], Wei Huang[3], Ibrahim Mazlan[4,5], Grace Croft[4,5], Teresa Totman[4,5], Yvonne Wei Zheng Tay[6], Elaine Manigbas[6], Miko May Lee Chang[7], Anqi Qiu[7], Michael Klimas[8], Jeffrey L Evelhoch[8], Dominique PV de Kleijn[4,5], and Chih-Liang Chin[1]

[1]Translational Biomarkers, Merck Sharp & Dohme, Singapore, Singapore, [2]Translational Biomarkers, Merck Sharp & Dohme, Singapore, [3]Advanced Imaging Research Center, Oregon Health and Science University, Portland, OR, United States, [4]Cardiovascular Research Institute, National University Heart Center, Singapore, [5]Department of Surgery, Yong Loo Lin School of Medicine, National University of Singapore, Singapore, [6]Comparative Medicine Imaging Facility, Center for Life Sciences, National University of Singapore, Singapore, [7]Department of Biomedical Engineering, National University of Singapore, Singapore, [8]Translational Biomarkers, Merck & Co., Inc., West Point, PA, United States

We present a comprehensive characterization of LV structure, function, perfusion and metabolism in a porcine animal model with myocardial infarction with view to develop a translational platform for future testing of safety and efficacy of novel heart failure therapeutics. Dynamic contrast enhanced MRI and tagging MRI are employed to obtain non-invasive quantitative magnetic resonance imaging (MRI) biomarkers for characterization. Results demonstrate an acute decrease in function and perfusion in the infarct region and functional compensation in the remote region with associated increased metabolic activity. Chronic remodeling is associated with decreased metabolic activity in the infarct region along with increased fibrosis.

3250 Computer 15

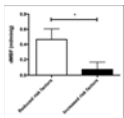

Exenatide decreases ectopic fat accumulation but have no impact on myocardial function and perfusion in patients with obesity and type 2 diabetes

Ines Imane Abdesselam[1], Anne Dutour[2], Alexis Jacquier[3], Frank Kober[4], Patricia Ancel[5], Oliver Rider[6], Monique Bernard[4], and Benedicte Gaborit[2]

[1]Aix-Marseille University, CRMBM, NORT, Marseille, France, [2]Aix-Marseille University, NORT, AP-HM, [3]Aix-Marseille University, CRMBM, AP-HM, [4]Aix-Marseille University, CRMBM, [5]Aix-Marseille University, NORT, [6]University of Oxford, OCMR

The objective of the study is to assess the impact of Exenatide on endothelial reactivity, and change in ectopic fat and cardiac function. This study included 44 patients (mean 52 years) randomized to Exenatide or reference treatment. Magnetic resonance imaging was used to assess ectopic fat accumulation, coronary vasoreactivity and cardiac function. 16-weeks of Exenatide treatement resulted in a significant improvement in glycemic control and a significant reduction of both epicardial fat and hepatic steatosis. However, we found no effect of Exenatide on myocardial function. In addition, one-week of exenatide treatment had only a modest effect on vascular reactivity, albeit non-significant.

3251 Computer 16

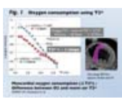

BOLD Effect of Oxygen-Inhalation T2-star MRI Surrogates Systemic and Myocardial Oxygen Consumption in Heart Failure and Myocardial Infarction

Michinobu Nagao[1], Kenji Fukushima[1], Umiko Ishizaki[1], Yuka Matsuo[1], Yuzo Yamasaki[2], Tetsuya Matoba[3], Tomomi Ide[3], Atsushi Takemura[4], Mitsuru Momose[1], and Shuji Sakai[1]

[1]Diagnostic Imaging & Nuclear Medicine, Tokyo Women's Medical University, Tokyo, Japan, [2]Clinical Radiology, Kyushu University, [3]Cardiovascular Medicine, Kyushu University, [4]Philips Electronics Japan

Measurement of oxygen consumption (OC) has been less than satisfactory in patients with heart failure. This has necessitated the invasive techniques to measure the total oxygen demand with cardiopulmonary exercise (CPX). The present study proposes a novel method to quantify OC using BOLD effect of oxygen-inhalation T2* MRI. Difference between oxygen-T2* and room-air-T2* (ΔT2*) was identified as an estimate of OC. ΔT2* was significantly correlated with systematic and myocardial OC expressed as the results of CPX and myocardial fatty acid scintigraphy. Our method allows assessing non-invasively OC in vivo. ΔT2* could be used as an imaging biomarker for heart failure.

3252 Computer 17

Analytically-derived Parameter Scouting for Dark-Blood Late Gadolinium Enhancement (DB-LGE) Imaging

Ahmed S Fahmy[1], Tamer A Basha[1], and Reza Nezafat[1]

[1]Cardiology, BIDMC-Harvard, Boston, MA, United States

In Dark Blood Late Gadolinium Enhanced (DB-LGE) imaging, simultaneous signal nulling of the healthy myocardium and the blood and thus yields superior contrast-to-noise ratio of the scared tissues. The method employs a T_2-preparation pulse applied after the inversion recovery pulse to rapidly damp the myocardium magnetization relative to the blood. Accurate timing of the inversion pulse, T_2-preparation pulse, and echo acquisition is essential for the success of the technique. In this work, we present a simple method for accurately estimating these parameters through fast low-resolution scouting scans played prior to DB-LGE scans.

3253 Computer 18

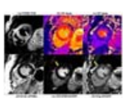

Myocardial Edema Imaging using Single-shot T2STIR Prepared bSSFP

Yanjie Zhu[1], Dan Yang[2], Yucheng Chen[2], Dong Liang[1], Xin Liu[1], and Yiu-Cho Chung[1]

[1]Paul C. Lauterbur Research Centre for Biomedical Imaging, Shenzhen Institutes of Advanced Technology,Chinese Academy of Sciences, Shenzhen, People's Republic of China, [2]Department of Cardiology, West China Hospital, Chengdu, People's Republic of China

STIR-TSE is useful in imaging myocardial edema. However, it is sensitivity to cardiac motion, resulting in myocardial inhomogeneity. T2p-bSSFP overcomes this issue, but averaging is commonly used to improve its contrast. We propose a novel single-shot imaging technique that generates "STIR like" contrast and improves contrast between edema and normal myocardium compared to T2p-bSSFP. The performance of the new sequence (T2STIR-bSSFP) was evaluated by phantom study and in patients with acute myocardial infraction. The results show that the average CNR of T2STIR-bSSFP between edema and myocardium was 1.9 times better than T2p-bSSFP.

3254 Computer 19

Ungated free-breathing late gadolinium enhancement imaging with a radial simultaneous multi-slice acquisition

Ganesh Adluru[1], Jason Mendes[1], Brent Wilson[2], and Edward DiBella[1]

[1]Radiology and Imaging Sciences, University of Utah, Salt lake city, UT, United States, [2]Cardiology, University of Utah, Salt Lake City, UT, United States

Late Gadolinium Enhancement imaging is the gold standard for identifying infarcted myocardium. Existing data acquisition methods rely on good ECG-gating signal and breathholding to acquire images in quiescent diastolic cardiac phase. However, in patients with arrhythmias and when imaging at higher field strengths, R-R interval is inconsistent and a good ECG signal can be challenging. This can lead to increased acquisition time and inconsistent recovery of longitudinal magnetization affecting signal-to-noise ratio and optimal myocardial nulling. Here we propose an ungated free-breathing scheme that acquires multiple slices at the same time with consistent nulling of healthy myocardium at systole and diastole.

3255 Computer 20

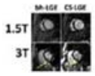

High Resolution, Single-shot LGE MRI with Compressed Sensing and Radial k-space Sampling

Hassan Haji-Valizadeh[1], Jeremy D. Collins [2], Daniel C. Lee[2,3], James C. Carr[2], and Daniel Kim[2]

[1]Biomedical Engineering, Northwestern University, Chicago, IL, United States, [2]Radiology, Northwestern university, Chicago, IL, United States, [3]Division of Cardiology, Internal Medicine, Northwestern University, Chicago, IL, United States

We sought to develop a high resolution single-shot LGE pulse sequence using Radial Compressed Sensing. We then evaluated in patients the performance of our acquisition scheme with respect to segmented clinical LGE.

3256 Computer 21

magna cum laude

Quantitative Inversion Time Prescription for Late Gadolinium Enhancement Using T1-based Synthetic Inversion Recovery Imaging – Eliminating the Subjective Estimation of Inversion Time

Akos Varga-Szemes[1], Rob J van der Geest[2], Carlo N De Cecco[1], Taylor M Duguay[1], U. Joseph Schoepf[1], and Pal Suranyi[1]

[1]Department of Radiology and Radiological Science, Medical University of South Carolina, Charleston, SC, United States, [2]Department of Radiology, Leiden University Medical Center, Leiden, Netherlands

Conventional Look-Locker (LL)-based inversion time (TI) estimation prior to late gadolinium enhancement (LGE) imaging has multiple limitations, including: the long breath-hold, the collected images are in different cardiac phases, and the subjective TI estimation. In this study we aimed to develop a quantitative T1 mapping-based synthetic inversion recovery (IR_{synth}) approach allowing for the quantitative determination of the optimal TI for LGE imaging. We showed in 40 patients that the IR_{synth} method provides better quality of myocardial signal nulling, retrospective TI selection, higher TI resolution, no need for further LL correction or TI adjustment, and less operator dependence.

3257 Computer 22

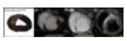

Validation of Contrast Enhanced Cine Steady-State Free Precession and T2-Weigthed CMR for Assessment of Ischemic Myocardial Area-At-Risk

Esben Søvsø Szocska Hansen[1,2], Steen Fjord Pedersen[3], Steen Bønløkke Pedersen[4], Hans Erik Stilling Bøtker[5], and Won Yong Kim[5]

[1]The MR Research Centre, Aarhus University, 8200, Denmark, [2]Danish Diabetes Academy, Odense, Denmark, [3]Department of Cardiothoracic and Vascular Surgery T, Aarhus University Hospital, 8200, Denmark, [4]Department of Endocrinology and Internal Medicine, Aarhus University Hospital THG, Denmark, [5]Department of Cardiology, Aarhus University Hospital, 8200, Denmark

Measuring myocardial salvage is important to evaluate the possible cardioprotective effects of adjunctive cardioprotective intervention in patients with myocardial infarction undergoing primary percutaneous intervention. Contrast-enhanced steady-state free precession magnetic resonance imaging (CE-CINE) has recently been used to quantify AAR and validated against myocardial perfusion SPECT. In this study we sought to determine how well T2-STIR and CE-CINE depicts AAR in an experimental porcine model of myocardial ischemia-reperfusion injury using histopathology as the reference for infarct size and AAR.

3258 Computer 23

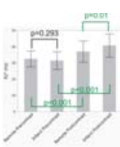

Effects of a Gadolinium Based Contrast Agent on the Myocardial R2* Relaxation Rate in Patients with Chronic Myocardial Infarction

James W Goldfarb[1], Nathaniel Reichek[1], Jie J Cao[1], and Dana C Peters[2]

[1]St Francis Hospital, Roslyn, NY, United States, [2]Yale University, New Haven, CT, United States

In this proof-of-concept study, we studied the effects of a contrast agent on R2*/T2* relaxation in dense myocardial fibrosis. A significant change in myocardial R2* was found after contrast and an R2* difference existed after contrast agent administration between fibrosis and remote myocardium. On average, viable myocardial R2* increased by 4.5 Hz while infarcted increased by 9.3 Hz at 1.5T with a clinical contrast agent.

Electronic Poster

New Methods

Exhibition Hall — Monday 9:15 - 10:15

3259 Computer 25

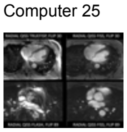

QISS FISS (Quiescent-Interval Slice-Selective Fast Interrupted Steady-State): A Best-of-Both-Worlds Solution to Nonenhanced MR Angiography at 3 Tesla

Robert R. Edelman[1,2], Shivraman Giri[3], and Ioannis Koktzoglou[4,5]

[1]Radiology, NorthShore University HealthSystem, Evanston, IL, United States, [2]Radiology, Northwestern University, Chicago, IL, United States, [3]Siemens HealthCare, [4]Radiology, NorthShore University HealthSystem, [5]Radiology, University of Chicago

QISS is a robust method for nonenhanced MRA that conventionally uses a TrueFISP readout. At 3 Tesla, use of TrueFISP is challenging due to high RF power deposition and sensitivity to off-resonance artifacts. In order to overcome these limitations, we implemented a QISS technique that incorporates a new type of readout that is a hybrid of TrueFISP and FLASH pulse sequences, which we call "Fast Interrupted Steady-State" (FISS). A pilot study was conducted to evaluate the potential benefits of QISS FISS at 3 Tesla for evaluation of the peripheral arteries and great vessels of the chest.

3260 Computer 26

Characterizing the Cardiac Phase Dependence of Motion Compensated CODE cDTI

Eric Aliotta[1,2], Kevin Moulin[1], Patrick Magrath[1,3], and Daniel B. Ennis[1,2,3]

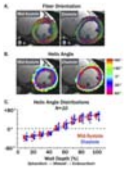

[1]Department of Radiological Sciences, University of California, Los Angeles, CA, United States, [2]Biomedical Physics IDP, University of California, Los Angeles, CA, United States, [3]Department of Bioengineering, University of California, Los Angeles, CA, United States

First and second order motion compensated convex optimized diffusion encoding (CODE-M_1M_2) enables robust, high resolution cardiac diffusion tensor imaging (cDTI). However, timing of the diffusion encoding relative to the cardiac cycle still requires careful evaluation to achieve precise and accurate measurements. In this study, CODE-M_1M_2 cDTI was acquired in healthy volunteers at both mid-systole and diastole to identify differences in fiber orientation, fiber cone of uncertainty (CoU), mean diffusivity (MD) and fractional anisotropy (FA). While fiber orientations were equivalent, lower CoU, lower MD, and higher FA were observed in mid-systole than in diastasis indicating improved performance.

3261 Computer 27

Insights from comprehensive fetal cardiovascular MRI assessment using 3D motion-correction and metric-optimised gated phase contrast in cases of suspected coarctation of the aorta

David F A Lloyd[1,2], Joshua F P van Amerom[1], Maria Murgasova[1], Bernard Kainz[3], Kuberan Pushparajah[2], John Simpson[2], Mary Rutherford[1], Jo V Hajnal[1], and Reza Razavi[1,2]

[1]Division of Imaging Sciences and Biomedical Engineering, King's College London, London, United Kingdom, [2]Department of Paediatric and Fetal Cardiology, Evelina London Children's Hospital, London, United Kingdom, [3]Department of Computing (BioMedIA), Imperial College London

The antenatal diagnosis of coarctation of the aorta can be life saving; however, it is notoriously difficult to predict using ultrasound alone. We present 16 fetal cases with suspected coarctation of the aorta between 30-36 weeks, assessed using a combination of novel prenatal MRI techniques: three-dimensional motion corrected slice-volume registration and metric-optimised gated phase contrast flow measurements. Detailed 3D analysis revealed significant correlation between the size and position of the aortic isthmus and the need for neonatal surgical repair. Retrograde flow at the aortic isthmus and the angle of its insertion relative to the arterial duct may also be important variables. The comprehensive physiological data generated by combining novel fetal MRI techniques may offer powerful insights into traditionally challenging antenatal diagnoses.

3262 Computer 28

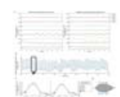

Contact-free Cardiac Motion Estimation using the Scatter of a Parallel Transmit Coil at 7T MRI

Sven H.F. Jaeschke[1], Caitlin O'Brien[2], Aaron T. Hess[1], and Matthew D. Robson[1]

[1]Oxford Centre for Clinical Magnetic Resonance Research, University of Oxford, Oxford, United Kingdom, [2]Oxford Centre for Functional MRI of the Brain, University of Oxford, United Kingdom

Cardiovascular MRI at ultra-high field strength is a growing field of research and as such there is a need for reliable, accurate, and user-independent triggering and gating. We propose a novel approach that uses directional couplers from the SAR monitoring system and an 8-channel pTx coil to measure the reflection coefficients simultaneously to determine cardiac motion with an independent component analysis and Gaussian shaped RF-monitoring pulses. This approach has the potential to improve cardiac imaging at ultra-high field CMR by providing robust triggering in periods of breath-hold and free-breathing, additional gating information and an optimised workflow with no additional set-up.

3263 Computer 29

Fetal cardiac volume reconstruction from motion-corrected multi-slice dynamic MRI

Joshua FP van Amerom[1], David A Lloyd[1], Maria Kuklisova Murgasova[1], Anthony N Price[1], Shaihan J Malik[1], Paul Aljabar[2], Joanna M Allsop[2], Ana Gomes[2], Mary A Rutherford[1,2], Kuberan Pushparajah[1,3], Reza Razavi[1,3], and Joseph V Hajnal[1]

[1]Division of Imaging Sciences and Biomedical Engineering, King's College London, London, United Kingdom, [2]Centre for the Developing Brain, King's College London, London, United Kingdom, [3]Department of Congenital Heart Disease, King's College LondonEvelina London Children's Hospital, London, United Kingdom

Motion is a significant challenge in fetal cardiac MRI. Multi-slice 2D dynamic MR data was used to reconstruct high-temporal resolution real-time images to be combined in time as 2D cine images and then in space as volumes with full coverage of the heart. Retrospective, image-based post-processing (motion correction, outlier rejection) was used to improve image quality in the presence of intra- and inter-slice motion. Reconstructed multi-slice cine images depict the complex anatomy of the fetal heart across the cardiac cycle and preliminary volume reconstructions allow multiple views to be visualised.

3264 Computer 30

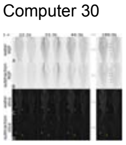

Time-Resolved Contrast-Enhanced MR Angiography with Single-Echo Dixon Background Suppression

Eric G. Stinson[1], Joshua D. Trzasko[1], Norbert G. Campeau[1], John Huston III[1], Phillip M. Young[1], and Stephen J. Riederer[1]

[1]Radiology, Mayo Clinic, Rochester, MN, United States

Contrast-enhanced MR angiography (CE-MRA) typically relies on a time-subtraction technique to suppress the background signal and emphasize the contrast-enhanced blood signal. However, Dixon-based background suppression has been reported to reduce motion sensitivity and improve signal-to-noise ratio in CE-MRA studies. Dual-echo Dixon techniques suffer a time penalty from acquiring an image at a second echo time, but single-echo Dixon techniques require an image at only one echo time and can reduce the time penalty. Here, time-resolved 3D single-echo Dixon CE-MRA at 3.0T with image update times of under 5 seconds is reported with results in the calves, hands, and brain.

3265 Computer 31

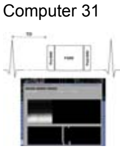

Free-breathing navigator 3D Cardiac Quantitative Susceptibility Mapping (QSM): initial experience at 1.5T and 3T.

Yan Wen[1,2], Thanh Nguyen[2], Pascal Spincemaille[2], Jiwon Kim[3], Jonathan W. Weinsaft[3], and Yi Wang[1,2]

[1]Meinig School of Biomedical Engineering, Cornell University, New York, NY, United States, [2]Radiology, Weill Cornell Medicine, New York, NY, United States, [3]Medicine, Weill Cornell Medicine, New York, NY, United States

To improve signal-to-noise ratio (SNR) in cardiac QSM (cQSM), we introduce here 3D acquisition that is more SNR efficient than previous 2D acquisition. Respiratory motion artifacts during the long 3D acquisition are compensated using navigator gating. We also investigated potential SNR gain at 3T over previous 1.5T. Our initial results seem to suggest possible issues at 3T that prevent the realization of potential cQSM improvement at from 1.5T to 3T in terms of SNR and contrast.

3266 Computer 32

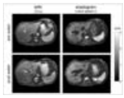

Tomoelastography of the abdominal aorta and inferior vena cava in different hydration states

Thomas Elgeti[1], Jing Guo[1], Heiko Tzschätzsch[1], Florian Dittmann[1], Eric Barnhill[1], Jürgen Braun[1], and Ingolf Sack[1]

[1]*Charité - Universitätsmedizin Berlin, Berlin, Germany*

Tomoelastography was recently introduced for high-resolution stiffness mapping in abdominal organs. The method is based on multifrequency MR elastography and noise-robust reconstruction of shear wave speed maps. This study demonstrates the feasibility of tomoelastography for measurement of the mechanical properties of the abdominal aorta (AA) and inferior vena cava (IVC) in healthy volunteers. AA was measured stiffer than IVC with increasing disparity after drinking one liter of water. Our results demonstrate the sensitivity of MRE-measured effective stiffness values in AA and IVC to physiological alteration of the hydration state and offer a new perspective for MRE of abdominal vessels.

3267 Computer 33

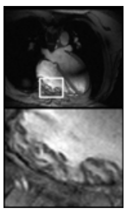

Contact- free diaphragm navigation using the scatter of a parallel transmit coil at 7T

Aaron Timothy Hess[1] and Matthew D Robson[1]

[1]*Oxford Centre for Clinical Magnetic Resonance Research (OCMR), University of Oxford, Oxford, United Kingdom*

A method is presented to measure respiratory motion in mm units based on the scatter of a parallel transmit coil. The respiratory changes in scatter are observed by the local SAR monitor and converted into a respiratory measure through a calibration phase. The newly described measure was compared to the diaphragm position measured in MR images. The standard deviation of the difference between the two was 1.1±0.4 mm across six volunteers. The method was implemented into a free breathing cardiac cine which showed no respiratory artefact when used to gate.

3268 Computer 34

Interleaved ^{31}P-MR spectroscopy and cine ^{1}H-MR imaging of the human heart at 3 Tesla

Madeleine Daemen[1,2], Aart J. Nederveen[1], Jeroen A.L. Jeneson[1,3], Gustav J. Strijkers[4], and Adrianus J. Bakermans[1]

[1]*Department of Radiology, Academic Medical Center, Amsterdam, Netherlands,* [2]*Biomedical NMR, Department of Biomedical Engineering, Eindhoven University of Technology, Eindhoven, Netherlands,* [3]*Neuroimaging Center, University Medical Center Groningen, Groningen, Netherlands,* [4]*Department of Biomedical Engineering and Physics, Academic Medical Center, Amsterdam, Netherlands*

Changes in the myocardial energy homeostasis have been linked to decreases in cardiac pumping performance. Current MR practice requires two consecutive recordings of ^{31}P-MRS and ^{1}H-MRI to assess both aspects of heart physiology, with consequently long scan times, considerable patient burden, and potentially a mismatch between data from separate sessions. By efficiently interleaving 3D ISIS acquisitions for localized ^{31}P-MRS with short-axis cine ^{1}H-MR imaging, both myocardial energy status as well as left-ventricular ejection fraction could be quantified from MR data that were acquired essentially simultaneously.

3269 Computer 35

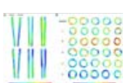

Computational modeling of arterial wall strain in a rabbit model of atherosclerosis using an elastin-specific MR contrast agent

Andrew Comerford[1], Rene Botnar[1], and Alkystis Phinikaridou[1]

[1]*Imaging Sciences & Biomedical Engineering, King's College London, London, United Kingdom*

Vulnerable plaque rupture is a major cause of common clinical events such as heart attacks and strokes. Plaques form in the arterial wall due to atherosclerosis, however not all plaques that do develop are at risk from rupture. Risk stratification is a major clinical need. This study combines elastin-specific MR contrast agent and CINE MR data from a rabbit model of atherosclerosis with finite element modeling. This combination allows the biomechanics of the arterial wall to be compared with morphological and biological indicators. Wall strains were shown to vary depending on the wall thickness and elastin content.

3270 Computer 36

Dynamic PET/MR Imaging of Glucose Utilization and Contractile Function Under Hypoxic Stress

Gregory Barton[1], Kara Goss[2], Niti Aggarwal[3], Marlowe Eldridge[1], and Alan McMillan[4]

[1]*Department of Pediatrics, University of Wisconsin-Madison, Madison, WI, United States,* [2]*Department of Medicine, University of Wisconsin-Madison, Madison, WI, United States,* [3]*Departments of Medicine & Radiology, University of Wisconsin-Madison, Madison, WI, United States,* [4]*Department of Radiology, University of Wisconsin-Madison, Madison, WI, United States*

The purpose of this study was to establish a methodology that could be used to study the dynamic relationship between cardiac contractile function and metabolism in a serial rest-stress model using dynamic cardiac PET/MR. To assess dynamic changes in cardiac glucose metabolism we evaluated the use of a continuous infusion of ^{18}F-FDG. We found that increases in cardiac contractility were coupled with an increase in glucose utilization in the myocardium under hypoxic stress conditions. These results demonstrate the feasibility of performing simultaneous measures of contractile function and metabolism in the heart.

3271 Computer 37

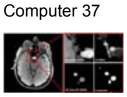

Statistical paradigm for composite MR Angiography generated from multi-contrast MRI

Dahan Kim[1,2], Patrick Turski[2,3], Oliver Wieben[2,3,4], and Kevin M Johnson[2,3]

[1]Department of Physics, University of Wisconsin - Madison, Madison, WI, United States, [2]Department of Medical Physics, University of Wisconsin - Madison, Madison, WI, United States, [3]Department of Radiology, University of Wisconsin - Madison, Madison, WI, United States, [4]Department of Biomedical Engineering, University of Wisconsin - Madison, Madison, WI, United States

We present an innovative paradigm to overcome artifacts of individual MR angiography techniques by utilizing complimentary information existing across multi-contrast MR images. This technique applies Bayesian statistics to extract vessel likelihoods from each image type and generates a single 'composite' angiogram. Composite angiograms are computed utilizing black blood (BB), contrast enhanced MRA (CE-MRA), and phase contrast MRA (PC-MRA) images acquired in subjects with known neurovascular disease. The composite angiogram is demonstrated to improve vessel lumen depiction overcoming artifacts in individual source images from background enhancement, air cavities, and flow in CE-MRA, BB, and PC-MRA, respectively.

3272 Computer 38

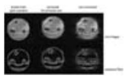

Novel Ultrasound Real-time Feedback Slice Tracking with Spatially Resolved MR-compatible Ultrasound for Cardio-vascular MRI

Lindsey A Crowe[1], Francesco Santini[2,3], Gibran Manasseh[1], Matthieu Destrade[1,4], Iris Friedli[1], Oliver Bieri[2,3], Rares Salomir[1], and Jean-Paul Vallée[1]

[1]Department of Radiology, Geneva University Hospitals, Geneva, Switzerland, [2]Department of Radiology, Division of Radiological Physics, University of Basel Hospital, Basel, Switzerland, [3]Department of Biomedical Engineering, University of Basel, Basel, Switzerland, [4]HEI, école d'Yncréa Hauts-de-France, France

Spatially resolved MR-compatible ultrasound was used to detect a respiratory-mimicking motion for prospective correction of cine MR data acquisitions. A scaling factor relating the motion between the two modalities was derived in real-time and was chosen to compare motion-corrected MR images to a static phantom 'breath-hold' and an uncorrected cine image series.

3273 Computer 39

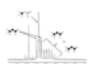

The impact of kinetic isotope effects in using deuterated glucose for metabolic experiments

Alexander Funk[1], Brian Anderson[1], Xiaodong Wen[1], Chalermchai Khemtong[1], Dean Sherry[1,2], and Craig Malloy[1]

[1]Advanced Imaging Research Center, UT Southwestern Medical Center, Dallas, TX, United States, [2]University of Texas at Dallas

Deuteration of ^{13}C-enriched glucose has been used to prolong T_1 of hyperpolarized ^{13}C with the objective of monitoring glucose metabolism to lactate. However, the effect of deuteration on the flux in glycolysis in vivo has not been investigated extensively. Deuterated glucose was studied in perfused hearts and extracts were analyzed for a deuterium kinetic isotope effect using ^{1}H, ^{13}C and ^{2}H NMR spectroscopy. Unexpectedly, there was extensive exchange of methyl deuterons in lactate with aqueous medium. Perdeuteration slows metabolism of glucose to lactate.

3274 Computer 40

Improving Shear Wave Signal-to-Noise Ratio in 3D High Frequency Cardiac Magnetic Resonance Elastography with Subjects in Prone Position

Shivaram Poigai Arunachalam[1], Arvin Arani[1], Ian Chang[2], Yi Sui[1], Phillip Rossman[1], Kevin Glaser[1], Joshua Trzasko[1], Kiaran McGee[1], Armando Manduca[3], Richard Ehman[1], and Philip Araoz[1]

[1]Radiology, Mayo Clinic, Rochester, MN, United States, [2]Cardiovascular Diseases, Mayo Clinic, Rochester, MN, United States, [3]Biomedical Engineering and Physiology, Mayo Clinic, Rochester, MN, United States

Myocardial stiffness is a novel biomarker for diagnosing a variety of cardiac diseases. Our recent work demonstrated the feasibility of measuring in-vivo myocardial stiffness using 3D high frequency cardiac MR elastography (MRE) in normal volunteers using octahedral signal-to-noise ratio (OSS-SNR) as a shear wave quality metric. The purpose of this work is to determine whether scanning subjects in prone position can improve the OSS-SNR compared to supine position. 47 healthy volunteers were enrolled and OSS-SNR in prone position (mean: 1.98) was significantly higher ($p < 0.01$) than the OSS-SNR in supine position (mean: 1.52) with comparable mean stiffness.

3275 Computer 41

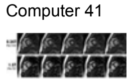

Feasibility of Cardiac bSSFP Cine MRI at 0.35T: A Comparison with 1.5T

Shams Rashid[1], Fei Han[2], Yu Gao[2], Yingli Yang[3], and Peng Hu[2,4]

[1]Radiological Sciences, UCLA, Los Angeles, CA, United States, [2]Radiological Sciences, University of California, Los Angeles, Los Angeles, CA, United States, [3]Radiation Oncology, University of California, Los Angeles, Los Angeles, CA, United States, [4]Biomedical Physics Graduate Program, University of California, Los Angeles, Los Angeles, CA, United States

In this study, we demonstrate the feasibility of cardiac cine MRI at 0.35T using bSSFP and compared the results with bSSFP at 1.5T.

3276 Computer 42

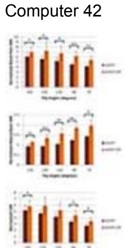

Cardiac Cine MRI with bSSFP-EPI at 0.35T

Shams Rashid[1], Fei Han[1], Yu Gao[1], Yingli Yang[2], and Peng Hu[1,3]

[1]Radiological Sciences, University of California, Los Angeles, Los Angeles, CA, United States, [2]Radiation Oncology, University of California, Los Angeles, Los Angeles, CA, United States, [3]Biomedical Physics Graduate Program, University of California, Los Angeles, Los Angeles, CA, United States

We have developed a bSSFP-EPI cine sequence and implemented it on a 0.35T MR system. The bSSFP-EPI cine sequence has reduced acquisition duration compared to conventional bSSFP cine.

3277 Computer 43

Optimized 2D-PACE for aorta blood flow gating and its application in T1W morphological cMRI

Fang Dong[1], Kun Zhou[1], and Shi Cheng[1]

[1]*Siemens Shenzhen Magnetic Resonance Ltd., ShenZhen, People's Republic of China*

Electrocardiogram gating is commonly used in clinical cardiac MRI. However, it takes time to attach ECG electrodes and gating signals can be easily affected. In this abstract, the 2D-PACE technique is optimized for blood flow monitoring to explore its potential as an alternative to ECG gating. A new protocol triggered by 2D-PACE for T1W cardiac morphology was also proposed. Our results showed that the optimized 2D-PACE was robust for blood flow peak detection. And combining with our new protocol, it provided comparable image quality to those from ECG gated conventional protocol, which showed a great potential for cardiac triggering.

3278 Computer 44

Post-Contrast Black-blood HASTE: Initial Results with Ferumoxytol

Takegawa Yoshida[1,2], Eun-ah Park[1,2], Peng Hu[1,2], Kim-Lien Nguyen[1,3], and J. Paul Finn[1,2]

[1]*Diagnostic Cardiovascular Imaging Laboratory, David Geffen School of Medicine at UCLA, Los Angeles, CA, United States,* [2]*Department of Radiological Sciences, David Geffen School of Medicine at UCLA,* [3]*Division of Cardiology, David Geffen School of Medicine at UCLA and VA Greater Los Angeles Healthcare System*

Black blood imaging is helpful in cardiovascular evaluation, but is challenging due to its dependence on through-plane blood flow. We explored ferumoxytol-enhanced black-blood Half-Fourier Acquisition Single-shot Turbo Spin-echo (HASTE) imaging for cardiovascular morphologic evaluation and compared its effectiveness with pre-contrast double inversion (DIR) HASTE. Post-ferumoxytol HASTE showed complete and homogeneous blood suppression and better qualitative image scores (all, $p<0.001$) for all cardiovascular regions. The technique holds promise for confident definition of thrombus or plaque, independently of blood flow.

3279 Computer 45

4D Ferumoxytol Enhanced MUSIC: Value-Based MRI in Neonates and Infants with Congenital Heart Disease

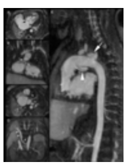

Kim-Lien Nguyen[1,2], Fei Han[1,3], Ziwu Zhou[1,3], Daniel Z Brunengraber[1,3], Ihab Ayad[4], Daniel S Levi[5], Gary M Satou[5], Brian L Reemtsen[6], Peng Hu[1,3], and J. Paul Finn[1,3]

[1]*Diagnostic Cardiovascular Imaging Laboratory, David Geffen School of Medicine at UCLA, Los Angeles, CA, United States,* [2]*Division of Cardiology, David Geffen School of Medicine at UCLA and VA Greater Los Angeles Healthcare System,* [3]*Department of Radiological Sciences, David Geffen School of Medicine at UCLA, Los Angeles, CA, United States,* [4]*Department of Anesthesiology, David Geffen School of Medicine at UCLA,* [5]*Division of Pediatric Cardiology, David Geffen School of Medicine at UCLA,* [6]*Department of Cardiothoracic Surgery, David Geffen School of Medicine at UCLA*

Conventional cardiovascular magnetic resonance imaging (MRI) in congenital heart disease (CHD) enables dynamic morphologic and vascular assessment. However, current techniques require multi-slice cine imaging and angiography with supplemental phase-contrast. We demonstrate that 4D multiphase steady state imaging with contrast (MUSIC) can provide high-resolution dynamic images of all relevant cardiovascular anatomy without breath-holding or operator input in a cohort of neonates and infants with CHD. Further, 4D MUSIC has high clinical impact on the care of small children.

3280 Computer 46

Ferumoxytol Enhanced Cardiac Cine MRI in Patients with Implanted Cardiac Devices

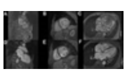

Kim-Lien Nguyen[1,2], Takegawa Yoshida[1,3], Peng Hu[1,3], and J. Paul Finn[1,3]

[1]*Diagnostic Cardiovascular Imaging Laboratory, David Geffen School of Medicine at UCLA, Los Angeles, CA, United States,* [2]*Division of Cardiology, David Geffen School of Medicine at UCLA and VA Greater Los Angeles Healthcare System,* [3]*Department of Radiological Sciences, David Geffen School of Medicine at UCLA, Los Angeles, CA, United States*

With an aging population, more patients are receiving implantable cardiac devices (ICDs) annually. Many will need one or more cardiac MRI exams over the course of their lifetime. ICDs can cause artifacts and obscure evaluation of intra-cardiac morphology. While researchers have dealt with artifacts during late gadolinium enhancement imaging by using wideband inversion recovery, off resonance artifacts preclude reliable SSFP cine and SGE cine is degraded by blood saturation. We explored the use of ferumoxytol to mitigate device-related artifacts and flow limiting artifacts during cine MRI in patients with ICDs.

3281 Computer 47

Vascular Access Mapping with Ferumoxytol MRA for TAVR Planning in Patients with Renal Impairment: A Step Closer Towards Patient-Specific Care

Kim-Lien Nguyen[1,2], Takegawa Yoshida[1,3], Adam N Plotnick[1,3], John M Moriarty[1,3], Peng Hu[1,3], and J. Paul Finn[1,3]

[1]*Diagnostic Cardiovascular Imaging Laboratory, David Geffen School of Medicine at UCLA, Los Angeles, CA, United States,* [2]*Division of Cardiology, David Geffen School of Medicine at UCLA and VA Greater Los Angeles Healthcare System,* [3]*Department of Radiological Sciences, David Geffen School of Medicine at UCLA*

Transcatheter aortic valve replacement (TAVR) has transformed the treatment of critical aortic stenosis, particularly for those patients whose surgical operative risks are high. However, pre-TAVR vascular mapping with CT requires 40-120 mls of iodinated contrast, which in older patients with renal impairment increases the risk of acute renal injury that portends poor prognosis. We demonstrated that ferumoxytol MRA can provide reliable vascular mapping in patients with renal impairment undergoing TAVR evaluation, without exposure to iodinated or gadolinium contrast agents.

3282 Computer 48

Transpedal MR-lymphangiography - A new imaging tool for pre-interventional planning of lymphatic interventions in patients with chylous effusions

Claus Christian Pieper[1] and Hans Heinz Schild[1]

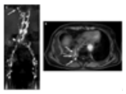

[1]Radiology, University Hospital Bonn, Bonn, Germany

Lymphatic interventions are increasingly performed for the treatment of chylous leakages. Pre-interventional evaluation of the central lymphatic system is important for adequate patient selection and planning of the interventional technique. We describe a new transpedal approach for MR-lymphangiography (tMRL) to evaluate the anatomy of central lymphatics including anatomical variations, as well as for detection of leakages and analysis of a potential interventional access site. Our results demonstrate that central lymphatic anatomy can be readily evaluated using tMRL in the majority of patients scheduled for lymphatic interventions. It is a well-tolerated, valuable diagnostic tool in the pre-interventional work-up of lymphatic interventions.

Electronic Poster

Genitourinary

Exhibition Hall — Monday 9:15 - 10:15

3283 Computer 73

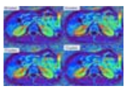

Impact of temporal resolution on quantitative renal perfusion MRI: Assessment using a single contrast injection and a continuous golden-angle radial sampling technique with iterative reconstruction.

Johannes Budjan[1], Philipp Riffel[2], Melissa M Ong[2], Robert Grimm[3], Kai Tobias Block[4], Frank G Zöllner[5], Stefan O Schoenberg[2], Ulrike I Attenberger[2], and Daniel Hausmann[2]

[1]Department of Clinical Radiology and Nuclear Medicine, University Medical Center Mannheim, Medical Faculty Mannheim, Mannheim, Germany, [2]Department of Clinical Radiology and Nuclear Medicine, University Medical Center Mannheim, Medical Faculty Mannheim, Heidelberg University, [3]Siemens Healthcare GmbH, Erlangen, Germany, [4]Center for Advanced Imaging Innovation and Research (CAI2R), Department of Radiology, New York University School of Medicine, New York, NY, United States, [5]Computer Assisted Clinical Medicine, Medical Faculty Mannheim, Heidelberg University, Mannheim, Germany

To evaluate the impact of temporal resolution on quantitative renal perfusion MRI, an intra-individual comparison of retrospectively reconstructed datasets with 4 different temporal resolutions (1.5s to 10.1s) was performed in 22 patients. This was achieved using a continuously acquired sequence that uses a combination of radial sampling, sparse imaging, iterative reconstruction, parallel imaging, and a single contrast injection. No statistically significant differences in renal plasma flow were found between the groups. This suggests that the effect of temporal resolution plays a subordinated role in quantitative renal perfusion MRI.

3284 Computer 74

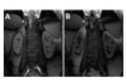

Optimization of inversion-time sampling for precise estimation of renal perfusion with ASL

Christopher C. Conlin[1] and Jeff L. Zhang[1]

[1]Department of Radiology and Imaging Sciences, University of Utah, Salt Lake City, UT, United States

This study outlines an approach for selecting optimal TIs at which to sample renal ASL data. We present an error-propagation factor for a model of the ASL signal and propose to optimize TI sampling through minimization of this factor. Using FAIR ASL data from 7 human subjects, we show that renal perfusion estimates obtained with optimal TI sampling are more accurate and precise than estimates obtained with uniform TI sampling, particularly when ASL data is acquired at only a few TIs.

3285 Computer 75

MR renography shows that serum-clearance methods overestimate GFR in patients with ascites

Christopher C. Conlin[1], Jeff L. Zhang[1], Kristi Carlston[1], Daniel Kim[2], Kathryn A. Morton[1], and Vivian S. Lee[1]

[1]Department of Radiology and Imaging Sciences, University of Utah, Salt Lake City, UT, United States, [2]Department of Radiology, Northwestern University, Chicago, IL, United States

In this study, the impact of ascites on clearance-based GFR estimation was examined by comparing GFR estimates from ^{99m}Tc-DTPA clearance and MR renography in cirrhosis patients with varying degrees of ascites. ^{99m}Tc-DTPA clearance significantly overestimated GFR relative to MR renography in patients with moderate-to-severe ascites, likely because of extra-renal clearance of tracer into abdominal ascites fluid. Conversely, MR renography was unaffected by the presence of ascites because it tracked uptake and excretion of tracer specifically by the kidneys. This ascites-insensitivity makes MR renography a promising technique for GFR assessment in cirrhosis patients, a population with a high incidence of ascites.

3286 Computer 76

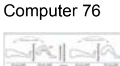

Influence of hip position on oxygenation and perfusion of renal allografts using BOLD, DWI and ASL MRI

Maryam Seif[1,2], Laila Mani[3], Florence Nikles[1], Chris Boesch[1], Gaelle Diserens[1], Bruno Vogt[3], and Peter Vermathen[1]

[1]Depts. Radiology and Clinical Research, University Bern, Bern, Switzerland, [2]Spinal cord injury Center, Balgrist University Hospital, University of Zurich, Zurich, Switzerland, [3]Dept. Nephrology, Hypertension and Clinical Pharmacology, Hospital University of Bern, Bern, Switzerland

Functional kinking due to tethering of iliac arteries by adjacent fibrotic tissue may occur in kidney graft recipients when sitting, and in turn lead to repetitive graft hypoperfusion. The aim was to investigate if perfusion and oxygenation were changed in transplanted kidneys during leg flexion (>90°) compared to the straight-leg position by employing fMRI (DWI, BOLD, ASL). Contradicting our hypothesis, perfusion increased in flexed leg compared to straight-leg position. Furthermore, furosemide had a significantly lower impact on R2*-values in flexed than in straight leg position. In conclusion, results demonstrated an acute impact of strong leg flexion on functional renal parameters.

3287 Computer 77

Reproducibilty of Multiparametric Assessment of Chronic Kidney Disease

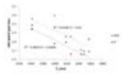

Charlotte Elizabeth Buchanan[1], Huda Mahmoud[2], Eleanor F Cox[1], Benjamin Prestwich[1], Nicholas M Selby[2], Maarten W Taal[2], and Susan T Francis[1]

[1]Sir Peter Mansfield Imaging Centre, University of Nottingham, Nottingham, United Kingdom, [2]Centre for Kidney Research and Innovation, University of Nottingham, Nottingham, United Kingdom

Chronic kidney disease (CKD) is a heterogeneous disease, with previous studies showing conflicting changes in MR parameters. Here, we use multi-parametric MRI of DWI, T_1 and T_2* mapping and ASL to assess haemodynamic and structural changes in Stage 3 and 4 CKD patients and examine the reproducibility of these measures. A significant reduction in renal cortex ADC and perfusion was found between CKD patients and healthy volunteers. In contrast, renal cortex and medulla T_1 values increased in CKD, with a reduction in corticomedullary differentiation. MR measures in CKD patients were found to be highly reproducible between scan sessions.

3288 Computer 78 Multiparametric Assessment of Acute Kidney Injury

Charlotte Elizabeth Buchanan[1], Huda Mahmoud[2], Eleanor F Cox[1], Benjamin Prestwich[1], Maarten W Taal[2], Nicholas M Selby[2], and Susan T Francis[1]

[1]Sir Peter Mansfield Imaging Centre, University of Nottingham, Nottingham, United Kingdom, [2]Centre for Kidney Research and Innovation, University of Nottingham, Nottingham, United Kingdom

Acute Kidney Injury (AKI) is a sudden reduction in kidney function, with causes and degree of renal recovery varying widely between individuals. MRI provides a method to assess changes associated with AKI. Here, we use multi-parametric MRI to monitor renal changes in AKI at time of injury and recovery. At peak AKI an increase was seen in renal volumes and T_2* values while cortical ADC and perfusion was lower during the AKI phase. T_1 maps showed an increase at time of AKI with a reduction in corticomedullary differentiation. At 3 months post AKI, T_1 remained higher than HVs.

3289 Computer 79 Reliable estimation of kidney filtration rate with DCE-MRI using motion-robust high spatiotemporal resolution Radial VIBE

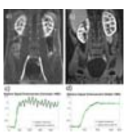

Sila Kurugol[1], Onur Afacan[2], Deborah R Stein[3], Michael A Ferguson[3], Richard S Lee[4], Reid Nichols[2], Ravi T Seethamraju[5], Jeanne S Chow[2], and Simon K Warfield[6]

[1]Radiology, Boston Children's Hospital and Harvard Medical School, Bosotn, MA, United States, [2]Radiology, Boston Children's Hospital and Harvard Medical School, Boston, MA, United States, [3]Pediatrics, Boston Children's Hospital and Harvard Medical School, Boston, MA, United States, [4]Surgery, Boston Children's Hospital and Harvard Medical School, Boston, MA, United States, [5]Siemens Healthcare, [6]Boston Children's Hospital and Harvard Medical School, Boston, MA, United States

Chronic kidney disease poses a significant health burden, and patients benefit from early detection of kidney function. Serum-creatinine based estimation is insensitive to early changes and nuclear medicine studies expose patients to radiation. In this work, we evaluated a novel technique, motion-robust high spatiotemporal resolution Dynamic Radial VIBE (DRV) with compressed sensing, to reconstruct high-quality dynamic image series, and to precisely estimate filtration rate per kidney and per voxel. Our results suggest that, compared to conventional Cartesian VIBE, DRV reconstructs higher quality motion-robust images and results in improved the goodness-of-fit to the tracer kinetic model, reducing RMSE and increasing the precision of filtration rate parameter.

3290 Computer 80 Multiparametric MRI of renal transplant: preliminary results and repeatability study in patients with stable renal function.

Octavia Bane[1], Sonja Gordic[1], Stefanie Hectors[1], Paul Kennedy [1], Mathilde Wagner[1,2], Jeff Lei Zhang[3], Rafael Khaim[4], Fadi Salem[5], Vinay Nair[4], Madhav Menon[4], Sara Lewis[1], and Bachir Taouli[1]

[1]Translational and Molecular Imaging Institute, Icahn School of Medicine at Mount Sinai, New York, NY, United States, [2]Radiology, Groupe Hospitalier Pitié Salpêtrière, Paris, France, [3]Radiology, University of Utah, Salt Lake City, UT, United States, [4]Recanati Miller Transplantation Institute, Icahn School of Medicine at Mount Sinai, New York, NY, United States, [5]Pathology, Icahn School of Medicine at Mount Sinai, New York, NY, United States

Intrinsic conditions leading to renal graft dysfunction have so far been difficult to diagnose non-invasively because of the overlap in symptoms and laboratory metrics. MRI provides an accurate assessment of the morphology of the transplanted kidney, as well as of vascular or obstructive renal disorders. The long-term goal of our study is to validate functional MRI as a “virtual biopsy” by developing a multiparametric MRI protocol using advanced quantitative MRI sequences in renal transplant patients. We report initial results and test-retest repeatability of quantitative mpMRI parameters of diffusion, perfusion and hypoxia in renal allografts.

3291 Computer 81 Treating male infertility: Can spectroscopy supplant biopsy in the search for sperm?

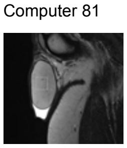

Pippa Storey[1], Oded Gonen[1], Andrew B. Rosenkrantz[1], Kiranpreet K. Khurana[2,3], Tiejun Zhao[4], Rajesh Bhatta[1], and Joseph P. Alukal[2]

[1]Radiology Department, New York University School of Medicine, New York, NY, United States, [2]Urology Department, New York University School of Medicine, New York, NY, United States, [3]Urology Department, Case Western Reserve University, Cleveland, OH, United States, [4]Siemens Healthcare, New York, NY, United States

Many men who wish to start a family but lack sperm in their semen undergo surgical exploration of the testes in the hope of extracting sperm at source. However, there are currently no tests that can accurately predict whether sperm will be found. We performed proton spectroscopy at 3T in the testes of eight infertile patients and nine controls. Choline concentrations were significantly lower in patients (mean 1.4mM, range 0.8 – 1.9mM) than controls (mean 4.1mM, range 3.0 – 5.1mM), p<0.0001. This suggests that choline, which is a marker of membrane synthesis and cell proliferation, may be useful for detecting spermatogenesis noninvasively.

3292 Computer 82 Machine Learning to Identify Sarcomatoid De-Differentiation in Renal Cell Carcinoma by Multiparametric MRI

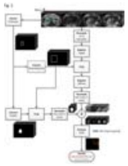

Nicolas Rognin[1], Daniel Jeong[2], Jasreman Dhillon[3], Michael Poch[4], and Natarajan Raghunand[1]

[1]Department of Cancer Imaging & Metabolism, Moffitt Cancer Center, Tampa, FL, United States, [2]Department of Diagnostic & Interventional Radiology, Moffitt Cancer Center, Tampa, FL, United States, [3]Department of Anatomic Pathology, Moffitt Cancer Center, Tampa, FL, United States, [4]Department of Genitourinary Oncology, Moffitt Cancer Center, Tampa, FL, United States

We developed a machine learning application to detect renal cell carcinoma (RCC) tumors with sarcomatoid de-differentiation, a rare form of aggressive cancer with poor prognosis. Proof-of-concept was demonstrated by analyzing multiparametric MRI volumetric data of 24 tumors, of which 11 were sarcomatoid RCC and 13 were non-sarcomatoid clear cell RCC. Our machine correctly classified 10 out of 11 sarcomatoid RCC cases (91% sensitivity) and 10 out of 13 clear cell RCC cases (77% specificity), with an overall classification accuracy of 20 out of 24 tumors (83%).

3293 Computer 83

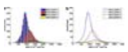

Apparent diffusion coefficient histogram shape analysis for monitoring early response in patients with advanced cervical cancers undergoing concurrent chemoradiotherapy

Zhengyang Zhou[1], Jian He[2], Weibo Chen[3], and Lijing Zhu[4]

[1]Department of Radiology, Drum Tower Hospital, School of Medicine, Nanjing University, Nanjing, People's Republic of China, [2]Department of Radiology, Drum Tower Hospital, School of Medicine, Nanjing University, [3]Philips Healthcare, Shanghai, People's Republic of China, [4]Department of Oncology, Drum Tower Hospital, School of Medicine, Nanjing University

Thirty-two patients with advanced cervical cancer underwent DWI before CCRT, at the end of 2nd and 4th week during CCRT and immediately after CCRT completion to explore whether ADC histogram shape could assess the treatment response. Whole lesion ADC histogram analysis generated several histogram shape including skewness, kurtosis, s-sDav, width, standard deviation, as well as first-order entropy and second-order entropies. Skewness and kurtosis both showed high early decline rate at the end of 2nd week of CCRT. All entropies kept decreasing since 2 weeks after CCRT. ADC histogram shape analysis held the potential in monitoring early tumor response during CCRT.

3294 Computer 84

Evaluation of renal allograft function after transplantation using diffusion kurtosis imaging

Wangxing Fu[1], Dandan Zheng[2], Jingliang Cheng[1], Yingyu Che[1], and Chunxiao Bu[1]

[1]MRI, The First Affiliated Hospital of ZhengZhou University, ZhengZhou, People's Republic of China, [2]MR Research China, GE Healthcare, Beijing, People's Republic of China

To evaluate the feasibility of DKI in assessment of renal allograft function after transplantation, 13 patients with renal allograft underwent DKI of kidneys，which were divided into two groups according to eGFR. Maps of fractional anisotropy FA, MK, Ka, Kr and MD were generated. There was significant differences in FA, MK, Ka, Kr values of both the cortex and medulla of kidney between two groups. There was significant correlation between eGFR and cortical FA, MK, Ka, Kr, medullary FA, Ka. DKI could be a useful tool in the evaluation of renal function in allograft after transplantation.

3295 Computer 85

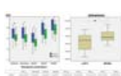

Whole-Tumor Quantitative Apparent Diffusion Coefficient Histogram and Texture Analysis to Differentiation of Minimal Fat Angiomyolipoma from Clear Cell Renal Cell Carcinoma

Anqin Li[1], Zhen Li[1], Haojie Li[1], and Daoyu Hu[1]

[1]Department of Radiology, Tongji Hospital, Tongji Medical College, Huazhong University of Science and Technology, Wuhan, People's Republic of China

The purpose of this study was to determine whether whole-tumor ADC histogram and texture analysis is helpful for distinguishing MFAML from ccRCC. The differences of ADC histogram and texture parameters between MFAML and ccRCC were compared using the independent-sample t test. There were significant differences on ADCmean, ADCmedian, ADC25%, ADC75%, ADC90% and skewness between MFAML and ccRCC. The ADC90% derived from the whole-tumor ADC histogram analysis showed the best diagnostic value in discriminating MFAML and ccRCC. Therefore, whole-tumor ADC histogram and texture parameters can be used as a quantitative tool to distinguish MFAML from ccRCC.

3296 Computer 86

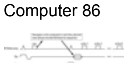

Free breathing prospectively navigated renal BOLD for improved SNR and T2* accuracy

Glen Morrell[1] and Vivian S. Lee[1]

[1]Radiology and Imaging Sciences, University of Utah, Salt Lake City, UT, United States

A prospectively gated free-breathing renal BOLD sequence was compared to conventional breath hold renal BOLD. The new sequence gives consistently better SNR than the conventional sequence. RMS error of T2* estimation was investigated as a measure of accuracy. The free-breathing renal BOLD sequence allows flexible tradeoff of imaging time with SNR and can improve the accuracy of renal BOLD T2* estimation.

3297 Computer 87

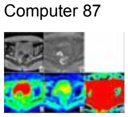

Prospective study of intravoxel incoherent motion (IVIM) MRI of bladder as a biomarker for prediction of bladder cancer aggressiveness

Miaomiao Zhang[1], Yan Chen[1], Xinying Cong[2], and Lizhi Xie[3]

[1]Department Of Imaging Diagnosis, National Cancer Center/Cancer Hospital, Chinese Academy of Medical Science and Peking Union Medical College, Beijing, People's Republic of China, [2]China Rehabilition Research Center, [3]GE Healthcare, MR Research China, Beijing China

Comparing the IVIM-MRI parameters with postoperative histopathological findings, we found significant correlations between quantitative parameters derived from IVIM-MRI and histological grade, as well as the depth of invasion. We concluded that IVIM-MRI quantitative parameter could be a promising imaging biomarker for prediction of bladder cancer aggressiveness.

3298 Computer 88

The Cortico-Medullary ADC Difference reduces inter-system variability in Renal Diffusion-Weighted Imaging

Iris Friedli[1], Lindsey A Crowe[1], Bénédicte MA Delattre[2], Thomas De Perrot[2], Pierre-Yves Martin[2], Sophie De Seigneux[2], and Jean-Paul Vallée[2]

[1]Radiology, University of Geneva, Geneva, Switzerland, [2]Geneva University Hospitals

Our goal was to determine if the cortico-medullary Apparent Diffusion Coefficient difference (ΔADC), that previously exhibited a strong correlation with renal fibrosis, is independent of MR system. Comparison of ADC (cortex, medulla and Δ) over Siemens (1.5T AERA, 3T PRISMA, 3T SKYRA) and Philips (1.5T INGENIA, 3T PET-MR) systems was carried out in eight volunteers. Significant ADC differences were measured for the cortex and medulla independently using PRISMA and AERA and, for cortex of AERA and INGENIA ($p<0.05$). ΔADC corrected inter-scanner variability with no significant differences across all MR systems ($p>0.05$).

3299 Computer 89

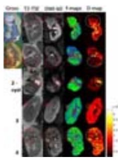

Kidney tumor characterization with diffusion-MRI: diffusion-tensor and tri-exponential modeling

Sophie van Baalen[1], Marino Asselman[2], Caroline Klazen[3], Martijn Froeling[4], Frank F.J. Simonis[1], Bart Vroling[1], and Bennie ten Haken[1]

[1]Faculty of Science and Technology, University of Twente, Enschede, Netherlands, [2]Urology, Medisch Spectrum Twente, Enschede, Netherlands, [3]Radiology, Medisch Spectrum Twente, Enschede, Netherlands, [4]Radiology, University Medical Center Utrecht, Utrecht, Netherlands

We present preliminary results of our study into the characterization of kidney tumors using diffusion derived parameters. We have acquired DTI and IVIM sequences and fitted the diffusion tensor and tri-exponential model to obtain parameters FA, MD, f_{fast}, $f_{intermediate}$ and D. Among the first four patients planned for nephrectomy for suspected kidney tumor we found three RCCs, one cyst and one hemangioma. f_{fast}, the fraction of the diffusion signal that reflects fast fluid motion, is lower in non-malignant lesions, whereas D is lower in the two cc-RCCs. The differences in parameter values between lesion types are reflected in parameter maps.

3300 Computer 90

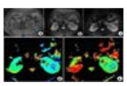

Diffusion Tensor Imaging (DTI) in the Differential Diagnosis of Clear Cell Renal Cell Carcinoma (ccRCC) and infiltrative Transitional Cell Carcinoma (TCC)

mingzhe Xu[1], ailian Liu, meiyu Sun, lihua Chen, and bing Wu[2]

[1]First Affiliated Hospital of Dalian Medical University, Dalian, People's Republic of China, [2]GE healthcare China, Beijing, People's Republic of China

It’s difficult to differentiate intrarenal transitional cell carcinoma from centrally located renal cell carcinoma by contrast enhanced CT when the tumor composition is complex. In this study, DTI were performed to investigate the utility of the apparent diffusion coefficient (ADC) and fractional anathtropy (FA) values for differential diagnosis of ccRCC and infiltrative TCC, thus assessing the sensitivity and specificity of ADC and FA values. The FA value from DTI, which reveals the different structure of tumors, provides an effectively non-invasive means to distinguish ccRCC from TCC because of its good sensitivity.

3301 Computer 91

Does PROPELLER acquisition improve bladder imaging by substantially reducing motion artifacts?

Huyen Thanh Nguyen[1], Zarine K Shah[1], Lai Wei[2], and Michael V Knopp[1]

[1]Wright Center of Innovation in Biomedical Imaging, Department of Radiology, The Ohio State University, Columbus, OH, United States, [2]Center for Biostatistics, The Ohio State University, Columbus, OH, United States

This study is to evaluate the clinical application of PROPELLER reconstruction technique to reduce breathing-induced motion artifacts in bladder imaging. High resolution T2W images were acquired with and without multivane (PROPELLER technique) in fourteen patient scans. Image quality was assessed by a radiologist in terms of motion artifacts and the visualization of tumor margins. Scores were given in the range of 1 to 4. The results showed that the application of multivane significantly improved both motion artifacts and tumor visualization (both $P<0.001$). In conclusion, PROPERLLER reconstruction is a robust technique to substantially reduce the artifacts caused by unavoidable breathing motion to provide the delineation of bladder tumors against surrounding tissues.

3302 Computer 92

Phosphorescence Lifetime Imaging to validate BOLD MRI Derived blood PO2

Jon Thacker[1], Anthony E. Felder[2], Pottumarthi V Prasad[1,3,4], and Mahnaz Shahidi[2]

[1]Northwestern University, Evanston, IL, United States, [2]University of Illinois at Chicago, [3]NorthShore University HealthSystem, [4]University of Chicago

BOLD MRI measurements are the only non-invasive method sensitive to renal oxygenation. In a previous study we showed that BOLD MRI measurements can be combined with a statistical model to estimate renal oxygenation in rat kidneys. In this study, we examine the use of phosphorescence lifetime imaging (PLI) as a potential method for refining the model. It is important to differentiate between blood and tissue PO2, which is a key benefit of PLI. We found that the PLI is sensitive to changes following LNAME. However, the absolute PO2 values were lower than those estimated by BOLD MRI and possible reasons are discussed.

3303 Computer 93

Detectability of oxygen saturation in renal blood using intravoxel incoherent motion (IVIM) imaging

Tatsuo Nagasaka[1], Hideki Ota[2], Hitoshi Nemoto[1], and Hajime Tamura[3]

[1]Radiology, Tohoku University Hospital, Sendai, Japan, [2]Diagnostic Radiology, Tohoku University Hospital, Sendai, Japan, [3]Graduate School of Medicine, Tohoku University, Sendai, Japan

IVIM imaging acquired with two echo times may provide transverse relaxation time of blood fraction, which can be converted to blood oxygen saturation.   We confirmed consistent increases in the renal blood oxygen saturation estimated by this method after an oral water load. IVIM imaging may become a non-invasive method to estimate blood oxygen saturation in kidneys.

3304 Computer 94

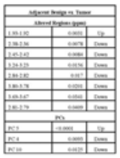

Adjacent Benign vs. Tumor		
Altered Regions (ppm)		
[illegible]	[illegible]	Up
[illegible]	[illegible]	Down
[illegible]	[illegible]	Down
[illegible]	[illegible]	Down
[illegible]	[illegible]	Down
[illegible]	[illegible]	Down
[illegible]	[illegible]	Down
[illegible]	[illegible]	Down
PCs		
[illegible]	[illegible]	Up
[illegible]	[illegible]	Down
[illegible]	[illegible]	Down

Metabolomic Analysis by HRMAS-MRS: Preliminary Study for Tumor Diagnosis

Francesco L Palmas[1,2], Sarah L Prophet[3], Lindsey L Vandergrift[3], Taylor L. Fuss[3], Shulin Wu[3], Chin-Lee Wu[3], Adam Feldman[3], and Leo L. Cheng[3]

[1]Pathology, Massachusetts General Hospital, Charlestown, MA, United States, [2]Chemical and Geological Sciences, University of Cagliari, Cagliari, Italy, [3]Massachusetts General Hospital, Charlestown, MA, United States

Kidney cancer is the third most common genitourinary malignancy in the US and leads to over 14,000 deaths and over 61,000 new cancer diagnoses per year. Since metabolic pathways affect the development of several malignancies, MRS was applied to highlight the existing alteration between adjacent benign and cancer tissues. Furthermore, comparison of fresh-frozen paired samples was performed to assess whether such strategy may interfere and deliver different results. This approach was able to discriminate according to pathological condition (benign-tumor) and showed no significant differences in fresh-frozen pairs.

3305 Computer 95

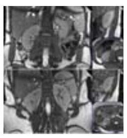

In-Vivo semi-LASER Renal Magnetic Resonance Spectroscopy (MRS): Pilot Study in Healthy Volunteers

Kartik Jhaveri[1] and Timothy DeVito[2]

[1]UHN, University of Toronto, Toronto, ON, Canada, [2]Siemens Healthcare Limited

MR Spectroscopy (MRS) can provide chemical composition of in vivo tissue non-invasively. Detection of signature chemical composition in tumors which are expected based on knowledge of histopathology could enable discrimination between tumor subtypes and grade by MRS. In this feasibility study we demonstrate ability to perform with success renal MRS in health volunteers mapping normal signature composition of renal tissue and provide a platform to expand the work to renal cancer tumor composition mapping and discrimination therewith based on metabolite content.

3306 Computer 96

Arterial Spin Labeling Imaging for Evaluation of Renal Changes in Remaining and Donated Kidneys Early after Living Renal Allograft Transplantation

Fan Mao[1], LiHua Chen[1], Tao Ren[1], ChengLong Wen[1], Zhen Wang[2], and Wen Shen[1]

[1]Department of Radiology, Tianjin First Center Hospital, TianJin, People's Republic of China, [2]Organ Tranplant Center, Tianjin First Center Hospital, TianJin, People's Republic of China

Arterial Spin Labeling (ASL) MRI is a noninvasive approach for assess renal function,which provides a quantitative measure of perfusion without the use of an exogenous contrast. Our study detected cortex perfusion changes in remaining and donated Kidneys. The result showed ASL can be used for detecting renal changes in remaining and donated kidneys early after living renal allograft transplantation.

Electronic Poster

Thoracic MRI-2

Exhibition Hall Monday 9:15 - 10:15

3307 Computer 97

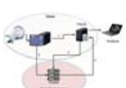

Respiratory motion-resolved MRI of the lung and liver for evaluation of cystic fibrosis

Alexander B. Hilario T.[1,2], Eduardo Baum[1,3], Alexandre Rosa Franco[1,3,4], Li Feng[5], Marilisa Baldissera[2], Ricardo Bernardi Soder[1], Bruno Hochhegger[1,4], Matteo Baldisserotto[1,2,3], and Ricardo Otazo[5]

[1]Brain Institute of Rio Grande do Sul (Brains) - PUCRS, Porto Alegre, RS, Brazil, [2]Graduate Program in Pediatrics and Child Health PUCRS, Porto Alegre, RS, Brazil, [3]Graduate Program in Electrical Engineering PUCRS, Porto Alegre, RS, Brazil, [4]Graduate Program in Medicine and Health Sciences PUCRS, Porto Alegre, RS, Brazil, [5]Center for Advanced Imaging Innovation and Research New York University School of Medicine, New York, NY, United States

Free-breathing MRI with reconstruction of respiratory phases using the XD-GRASP technique is demonstrated for evaluation of cystic fibrosis patients. A platform for automated data processing is developed for robust utilization in a clinical setting. XD-GRASP is validated in a cohort of 9 patients against the conventional technique.

3308 Computer 98

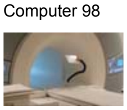

Optimized 3D ultrashort echo-time lung imaging of young children without sedation

Wingchi Edmund Kwok[1], Jacqueline Wameling[1], Mitchell Chess[1], Clement Ren[2], Gloria Pryhuber[1], and Jason C. Woods[3]

[1]University of Rochester, Rochester, NY, United States, [2]Indiana University, Indianapolis, IN, United States, [3]Cincinnati Children's Hospital Medical Center, Cincinnati, OH, United States

Our purpose was to develop an optimized study design for 3D ultrashort TE lung imaging of young children without sedation. Eight preterm born subjects all at age 4 were recruited. Siemens work-in-progress PETRA_D sequence was used with respiratory triggering. Repeated short scans were acquired to reduce motion artifacts. Various techniques, including video watching, practicing lying still at home and gift incentive, were employed to help achieve subject compliance. Five subjects were scanned successfully. The images revealed abnormalities including peribronchial thickening, pneumatocele and atelectasis. Our study design allows the monitoring of lung development and evaluation of lung diseases in young children.

3309 Computer 99

A preliminary study of in-vivo visualization of oxide oxide enhancement in focal inflammatory lesion of lung parenchyma using a 3D radial gradient-echo-based UTE sequence (CODE)

Soon Ho Yoon[1], Suh-Young Lee[2], Chanhee Lee[3], Jinil Park[3,4], Jin Mo Goo[1], and Jang-Yeon Park[3,4]

[1]Department of radiology, Seoul National University Hospital, Seoul National University College of Medicine, Seoul, Korea, Republic of, [2]Division of Pulmonary, Allergy, and Critical Care Medicine, Department of Internal Medicine, Kangdong Sacred Heart Hospital, Hallym University College of Medicine, Seoul, Korea, Republic of, [3]Center for Neuroscience Imaging Research, Institute for Basic Science (IBS), Suwon-si, Gyeonggi-do, Korea, Republic of, [4]Department of Biomedical Engineering, Sungkyunkwan University, Suwon-si, Gyeonggi-do, Korea, Republic of

Dual-echo ultrashort echo-time CODE pulmonary MRI preliminarily succeeded in generating a positive contrast of iron oxide in rabbits with granulomatous lung disease, by using clinically-usable superparamagnetic iron-oxide nanoparticles, ferumoxytol, which was hardly achievable via conventional T2* MR sequence. This new pulmonary MR imaging biomarker possibly gives a chance to differentiate a benign inflammatory lesion from malignancy.

3310 Computer 100

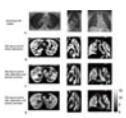

Repeatability of global percent enhancement and regional defect quantification in oxygen-enhanced 3D radial ultrashort echo time MRI

Wei Zha[1], Stanley J Kruger[1], Kevin M Johnson[1,2], Robert V Cadman[1], Andrew D Hahn[1], Scott K Nagle[1,2,3], and Sean B Fain[1,2,4]

[1]Medical Physics, University of Wisconsin-Madison, Madison, WI, United States, [2]Radiology, University of Wisconsin-Madison, Madison, WI, United States, [3]Pediatrics, University of Wisconsin-Madison, Madison, WI, United States, [4]Biomedical Engineering, University of Wisconsin-Madison, Madison, WI, United States

Oxygen-enhanced 3D radial UTE MRI (OE-MRI) shows promise as an alternative to hyperpolarized gas MRI for evaluation of ventilation abnormalities. Ten subjects (2 normal, 2 asthmatics and 6 cystic fibrosis) underwent OE-MRI for multiple scans (test/re-test) during visits separated ≤15 days apart. The intra-subject percent signal enhancement (PSE) maps from OE-MRI were compared for median whole-lung PSE, ventilation defect percent (VDP) and spatial agreement between defects. The results suggest good agreement on two global measures, Median PSE and VDP, with low-to-moderate spatial alignment on the inter-visit segmented defects. Improvement of spatial defect repeatability will be a goal of future work.

3311 Computer 101

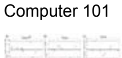

Repeatability of regional lung ventilation quantification using 19F fluorinated gas washout magnetic resonance imaging in free breathing

Marcel Gutberlet[1,2], Andreas Voskrebenzev[1,2], Agilo Kern[1,2], Till Kaireit[1,2], Jens Hohlfeld[2,3], Frank Wacker[1,2], and Jens Vogel-Claussen[1,2]

[1]Institute of Radiology, Hannover Medical School, Hannover, Germany, [2]Biomedical Research in Endstage and Obstructive Lung Disease Hannover (BREATH), Hannover, Germany, [3]Clinical Airway Research, Fraunhofer Institute for Toxicology and Experimental Medicine, Hannover, Germany

Since quantification of regional lung ventilation using ^{19}F fluorinated gas washout imaging in free breathing is feasible even in obstructed lungs, it may improve diagnosis, monitoring and therapy of obstructive lung diseases like asthma and COPD. However, for application in clinical studies the knowledge of the accuracy of this technique is important. Repeatability of the ^{19}F gas washout parameters washout time, number of breaths and fractional ventilation between to scans was assessed in eight healthy volunteers. Due to the excellent repeatability of the number of breaths and fractional ventilation, regional lung ventilation can be accurately quantified using ^{19}F gas washout MRI in free breathing.

3312 Computer 102

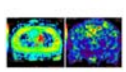

MR Elastography vs. Diffusion-weighted MRI in Characterization of Anterior Mediastinal Solid Tumours

Wei Tang[1], Ning Wu[1], and Yao Huang[1]

[1]Diagnostic Radiology, Cancer Hospital, Chinese Academy of Medical Sciences, Peking Union Medical College, Beijing, People's Republic of China

Anterior mediastinal solid tumours were routinely interpreted on CT and MR imaging. However, imaging features of these tumours could be non-specific; evidence suggestive of definitive diagnosis was needed and obtained with invasive procedure of biopsy for some cases. In the present study, we attempted to extent the application of MR elastography to the mediastinum in characterization of anterior mediastinal solid tumours, with the comparison to diffusion-weighted MRI. Thirty-four patients histologically-confirmed with thymic carcinoma in 10, thymoma in 10 and lymphoma in 14 were evaluated. It was found that stiffness value measured on elastogram was significantly higher in thymic carcinoma than that of thymoma and lymphoma. However, measurements of apparent diffusion coefficient (ADC) were not significantly different among three groups. It was demonstrated that MR elastography reflecting the mechanical properties of tumours can be used to characterize anterior mediastinal solid tumours, particularly in distinguishing thymic carcinoma from lymphoma.

3313 Computer 103

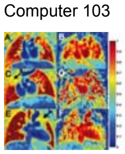

Mapping Vascular Behaviour in Lung Perfusion of two-year old children after Congenital Diaphragmatic Hernia Repair using Tissue Similarity Maps

Dimitrios Markellos[1], Meike Weis[2], Thomas Schaible[3], Stefan O Schoenberg[2], Lothar R Schad[1], and Frank G Zöllner[1]

[1]Computer Assisted Clinical Medicine, Heidelberg University, Mannheim, Germany, [2]Department of Radiology and Nuclear Medicine, Heidelberg University, Mannheim, Germany, [3]Department of Neonatology, University Medical Center Mannheim, Mannheim, Germany

Congenital Diaphragmatic Hernia (CDH) is associated with lung hypoplasia reflected in decreased pulmonary microcirculation and secondary pulmonary hypertension. Using tissue similarity maps (TSM), Haacke et al. demonstrated mapping vascular behaviour and calculating relative pulmonary blood volume (rPBV) maps in perfusion weighted imaging of the brain. In this study we have investigated the significance of the TSM technqiue for lung perfusion imaging in two-year old children after CDH repair.

3314 Computer 104

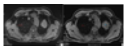

Diagnosing Lung Nodules on various MRI Imaging: comparison of T1-Weighted-3D VIBE-dixon sequence and T1-weighted 3D star vibe sequence

Chuangbo Yang[1], Nan Yu, Qi Yang, Shaoyu Yu, Youmin Guo, and Liya Ma

[1]The first affiliated hosptial of Shaanxi traditional chinese medical university, Xian Yang, People's Republic of China

T1-weighted 3D Star VIBE sequence obtaining scan under free breathing can provide high-resolution imaging. Therefore, our study was to assess the accuracy of various MRI sequences for the diagnosis of pulmonary nodules and to estimate the ability of MRI for display the morphology of pulmonary nodules. We concluded that T1-weighted 3D Star VIBE sequence allow for identification of patients with pulmonary nodules with high detection rate. It can also provide more information of nodules than routine T1-weighted 3D VIBE sequence dose.

3315 Computer 105

Exploring Lung Inflation Mechanisms with 3D 3He and 129Xe Whole Lung Morphometry Mapping

Ho-Fung Chan[1], Juan Parra-Robles[1,2], Guilhem J Collier[1], and Jim M Wild[1]

[1]Academic Unit of Radiology, University of Sheffield, Sheffield, United Kingdom, [2]Department of Bioengeering, Universidad Carlos III de Madrid, Madrid, Spain

Alveolar dimensions change with lung inflation, however, there is currently no consensus on whether this change is primarily due to expansion and if alveolar recruitment plays a role. Here, multiple b-value DW-MRI was used to investigate lung inflation mechanisms in-vivo, and 3D ^{3}He and ^{129}Xe whole lung morphometry (Lm_D) maps were acquired in five healthy volunteers at lung inflation states of FRC+1L and TLC. Decreases in the anterior to posterior gravitational gradient were observed between FRC+1L and TLC with both nuclei. Smaller than predicted Lm_D values at TLC suggests that both alveolar expansion and recruitment may occur during lung inflation.

3316 Computer 106

Analysis of Regional Lung Function Detected by Hyperpolarized Xenon-129 MRI in Subjects with Interstitial Lung Diseases

Kun Qing[1], Talissa A. Altes[2], John P. Mugler, III[1], Nicholas J. Tustison[1], Kai Ruppert[3], Jaime F. Mata[1], Yun Michael Shim[1], G.Wilson Miller[1], Iulian C. Ruset[4], F.William Hersman[4,5], and Borna Mehrad[1]

[1]University of Virginia, Charlottesville, VA, United States, [2]University of Missouri School of Medicine, Columbia, MO, United States, [3]University of Pennsylvania, Philadelphia, PA, United States, [4]Xemed, LLC, Durham, NH, United States, [5]University of New Hampshire, Durham, NH, United States

Previous study showed that hyperpolarized xenon-129 MRI is highly sensitive in detecting functional changes in lungs with interstitial lung diseases (ILD). The degree to which these changes vary regionally in the lung has not been determined, however. In this work, we compared abnormalities in lung function in different regions of the lung, and found significant differences in xenon-129 gas uptake between subjects with ILD and controls. These results support that xenon-129 MRI may provide unique information about lung physiology associated with lung fibrosis.

3317 Computer 107

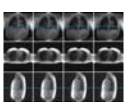

Self-gated ultra-short echo time lung MRI for quantitative ventilation assessment

Lenon Mendes Pereira[1], Tobias Wech[1], Andreas M. Weng[1], Andreas S. Kunz[1], Simon Veldhoen[1], Thorsten A. Bley[1], and Herbert Köstler[1]

[1]Department of Diagnostic and Interventional Radiology, University Hospital Wurzburg, Wurzburg, Germany

Self-gated Non-Contrast-enhanced Functional Lung MRI (SENCEFUL) is a technique based on a FLASH sequence that can assess ventilation and perfusion in free-breathing without the use of contrast agents. However, SENCEFUL suffers from the fast T_2-induced signal decay in the lung parenchyma and offers no real 3D coverage. Thus, this work presents the use of a 3D ultra-short echo time (UTE) sequence in SENCEFUL MRI for the generation of ventilation-weighted maps.

3318 Computer 108

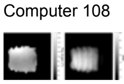

Steady-state Free Precession for Improved Signal to Noise in Lung Ventilation Imaging with ^{19}F Perfluoropropane at 1.5 T

Adam Maunder[1], Neil J Stewart[1], Madhwesha Rao[1], Fraser J. L. Robb[1,2], and Jim M Wild[1]

[1]Unit of Academic Radiology, University of Sheffield, Sheffield, United Kingdom, [2]GE Healthcare Inc., Aurora, OH, United States

Fluorinated gas MRI is a promising method for pulmonary ventilation imaging that does not require additional polarization equipment. To date, short echo time spoiled gradient echo sequences with long repetition times relative to T_1 have been employed for lung ventilation imaging in humans. Here, we present an optimization of steady state free precession sequences for imaging of C_3F_8 gas in lungs, and demonstrate that image signal-to-noise ratio may be improved by exploiting the short T_1, and relatively long T_2.

3319 Computer 109

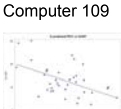

Hyperpolarized Helium-3 MRI Insights into Subtypes of Emphysema in Chronic Obstructive Pulmonary Disease (COPD)

Yanping Sun[1], Christian M. Lo Cascio[1], Pallavi P Balte[1], Jia Guo[2], Emilia A Hermann[1], Firas S. Ahmed[3], Belinda M. Dsouza[3], Robert M. Steiner[3], Jay S. Leb[3], Casandra Almonte[1], Paul JC Hughes[4], Stephen M. Dashnaw[3], James M. Wild[4], Martin R. Prince[3,5], Emlyn W. Hughes[6], Benjamin Smith[1], Eric Hoffman[7], and R. Graham Barr[1]

[1]Department of Medicine, Columbia University Medical Center, New York, NY, United States, [2]Taub Institute for Research on Alzheimer's Disease and the Aging Brain, Columbia University Medical Center, New York, NY, United States, [3]Department of Radiology, Columbia University Medical Center, New York, NY, United States, [4]Department of Infection, Immunity & Cardiovascular Disease, University of Sheffield, Sheffield, United Kingdom, [5]Department of Radiology, Weill Cornell Medical Center, [6]Department of Physics, Columbia University Medical Center, New York, NY, United States, [7]Department of Radiology, University of Iowa Carver College of Medicine, IA, United States

To examine the association of ventilation defects on 3He MRI with emphysema subtypes, participants (n=41) between 60 and 85 years of age with 10 or more packyears of smoking were studied. Ventilation defect percentage (VDP) was associated with percent emphysema (r =0.43; p=0.008) and, with borderline statistical significance, extent of visual emphysema (r=0.31; p=0.07). There was no relationship between VDP and extent of centrilobular (p=0.61) or panlobular (P=0.98) emphysema. VDP was associated with extent of paraseptal emphysema (PSE) (r=0.42; p=0.01). These findings suggest that small airways disease may be a component of PSE but not other subtypes of emphysema.

3320 Computer 110

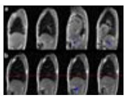

Temporally-resolved volumetric imaging (4DMRI) of the lungs

Zarko Celicanin[1,2], Alina Giger[2,3], Grzegorz Bauman[1,2], Philippe Cattin[2,3], and Oliver Bieri[1,2]

[1]Division of Radiological Physics; Department of Radiology, University of Basel Hospital, Basel, Switzerland, [2]Department of Biomedical Engineering, University of Basel, Basel, Switzerland, [3]Medical Image Analysis Center, University of Basel, Basel, Switzerland

Treatment planning relies on accurate organ motion modeling. Temporally-resolved volumetric imaging (4DMRI) of the lungs using a recently developed ultra fast steady state free precession sequence was attempted. No artifacts were present in the lungs, while image stacking was accurate with no significant image sorting issues.

3321 Computer 111

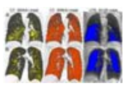

Ultra-Short Echo Time MRI Quantification of Airspace Enlargement in Bronchopulmonary Dysplasia and Alpha-1 Antitrypsin Deficiency: Parenchyma Destruction, Air trapping or Both?

Heather M Young[1], Dante PI Capaldi[1], Khadija Sheikh[1], David M McCormack[2], Cory M Yamashita[2], and Grace Parraga[1]

[1]Robarts Research Institute, London, ON, Canada, [2]Division of Respirology, The University of Western Ontario, London, ON, Canada

UTE MRI signal-intensity has not yet been evaluated in young patients with AATD and BPD, where there may be different mechanisms of parenchyma and airway destruction. There is the potential to demonstrate UTE MRI as a quantitative-measurement-tool for longitudinal and treatment-response evaluations in these vulnerable patients. We evaluated UTE MRI and CT using -950HU and -856HU radiodensity-thresholds, and a 'sliding-threshold' for the UTE image, identifying regions with low-signal-intensity for multiple threshold values. Regions of normalized UTE signal-intensity <29 suggest airspace enlargement, and demonstrate the potential utility of UTE MRI in quantifying this without ionizing-radiation in AATD and BPD subjects.

3322 Computer 112

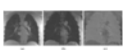

T2* Quantification of the Lung Using 3D Ultrashort Echo Time Cones Sequences

Amin Nazaran[1], Michael Carl[2], Yanchun Zhu[1], Yajun Ma[1], Eric Y. Chang[1,3], and Jiang Du[1]

[1]The University California, San Diego, San Diego, CA, United States, [2]2GE Healthcare, San Diego, San Diego, CA, United States, [3]Radiology Service, VA San Diego Healthcare System, San Diego, CA, United States

Imaging of the lungs without a contrast agent is a challenging task due to the low SNR. The main challenge stems from the air in the lungs, which causes low proton density and high magnetic susceptibility at interfaces with tissue. Ultra short echo time (UTE) techniques have the potential to acquire high signal-to-noise ratio (SNR) images due to their short achievable TEs, much less than 1ms. The lung imaging based on 3D radial UTE sequences were previously reported. In this work, we applied three-dimensional UTE with Cones trajectories (3D UTE-Cones) to quantify lungs' tissue.

3323 Computer 113

Self-gated Non–Contrast-Enhanced Functional Lung (SENCEFUL) MRI for Evaluation of Endoscopic Lung Volume Reduction in Patients with Lung Emphysema

Simon Veldhoen[1], Andreas Max Weng[1], Tobias Wech[1], Andreas Steven Kunz[1], Stephanie Sauer[1], Thorsten Alexander Bley[1], and Herbert Köstler[1]

[1]Department of Diagnostic and Interventional Radiology, University Hospital Würzburg, Würzburg, Germany

Purpose of the study was to assess the feasibility of SENCEFUL ventilation imaging for evaluation of therapy success after endoscopic lung volume reduction. Two patients with lung emphysema who underwent bronchial valve implantation were scanned before and after the procedure using SENCEFUL-MRI. Color-coded lung ventilation maps and quantitative ventilation values were pre- and postinterventionally compared. The first patient showed a ventilation defect corresponding to the location of the implanted valves with reduction of the quantitative ventilation. The second patient did not present such alterations and was later classified as non-responder to therapy. SENCEFUL-MRI detected clinically successful and non-successful outcomes correctly.

3324 Computer 114

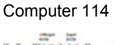

Single Breath CSSR-DWI: A New Method to Simultaneously and Quantitatively Assess the Changes of Respiratory Membrane and Pulmonary Microstructure in Human

Junshuai Xie[1], Huiting Zhang[1], Xiuchao Zhao[1], Haidong Li[1], Sa Xiao[1], Ke Wang[2], Hao Yang[2], Xianping Sun[1], Guangyao Wu[2], Chaohui Ye[1], and Xin Zhou[1]

[1]Key Laboratory of Magnetic Resonance in Biological Systems, State Key Laboratory of Magnetic Resonance and Atomic and Molecular Physics, National Center for Magnetic Resonance in Wuhan, Wuhan Institute of Physics and Mathematics, Chinese Academy of Sciences, Wuhan, People's Republic of China, [2]Department of Radiology, Zhongnan Hospital of Wuhan University, Wuhan, People's Republic of China

The blood-gas exchange function and the pulmonary microstructure are generally affected by the lung inflation levels. Here We developed a new method Single Breath CSSR-DWI to simultaneously quantify the respiratory membrane and the pulmonary microstructure via hyperpolarized ^{129}Xe in a single breath. A new parameter SVRd/g was defined from ADC and SVRd to characterize the '%-predicted dissolved SVR'. Human pulmonary functional and structure information were successfully obtained in a single breath via hyperpolarized ^{129}Xe. Compared to the healthy young subjects, SVRd/g of the asymptomatic aged subjects decreases while the size of the pulmonary microstructure increases.

3325 Computer 115

Quantify Pulmonary Gas-Exchange Function with Hyperpolarized 129Xe CEST MRI

Haidong Li[1], Zhiying Zhang[1], Xiuchao Zhao[1], Yeqing Han[1], Xianping Sun[1], Chaohui Ye[1], and Xin Zhou[1]

[1]Key Laboratory of Magnetic Resonance in Biological Systems, State Key Laboratory of Magnetic Resonance and Atomic and Molecular Physics, National Center for Magnetic Resonance in Wuhan, Wuhan Institute of Physics and Mathematics, Chinese Academy of Sciences, Wuhan, People's Republic of China

In this study, the pulmonary gas-exchange function was quantitatively evaluated globally and regionally by hyperpolarized 129Xe MRI using the method of chemical exchange saturation transfer (CEST). A new parameter, named as pulmonary gas consumption time constant (Toc), was proposed to characterize the gas exchange function. The parameter showed significant difference between the COPD and healthy rats, and we believe it will be a useful parameter in evaluating the pulmonary function.

3326 Computer 116

A spatial comparison of CT-based surrogates of ventilation with hyperpolarized Helium-3 & Xenon-129 MRI

Bilal Tahir[1,2], Paul Hughes[2], Helen Marshall[2], Neil Stewart[1], Felix Horn[2], Guilhem Collier[2], Graham Norquay[2], Kerry Hart[1], James Swinscoe[1], Matthew Hatton[1], Jim Wild[2], and Rob Ireland[1]

[1]Academic Unit of Clinical Oncology, University of Sheffield, Sheffield, United Kingdom, [2]Academic Radiology, University of Sheffield, Sheffield, United Kingdom

Synopsis: Image registration of lung CT images acquired at different inflation levels has been proposed as a surrogate method to map lung 'ventilation'. However, this technique requires validation against established ventilation modalities such as hyperpolarised gas MRI. Here, we develop an image acquisition and analysis strategy to facilitate direct spatial correlation of ventilation CT with both hyperpolarised ^{3}He & ^{129}Xe MRI and apply our method to a cohort of lung cancer patients.

3327 Computer 117

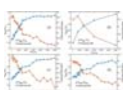

Evaluation of 129Xe-RBC signal dynamics and chemical shift in the cardiopulmonary circuit using hyperpolarized 129Xe NMR

Graham Norquay[1], Neil J Stewart[1], and Jim M Wild[1]

[1]Academic Unit of Radiology, University of Sheffield, Sheffield, United Kingdom

The signal dynamics of hyperpolarized ^{129}Xe in the pulmonary capillaries and veins was evaluated by employing multi-TR pulse sequences, with TR values ranging from 100-6000ms. The ratio of signal from ^{129}Xe dissolved in red blood cells (RBC) and tissue/plasma (TP) was found to increase for longer TRs whilst the ^{129}Xe-RBC chemical shift was observed to decrease with increasing TR. This observed chemical shift difference is unprecedented, and understanding the nature of the underlying mechanisms causing this shift is crucial for future in vivo experiments using ^{129}Xe-RBC chemical shift as a measure of blood oxygenation.

3328 Computer 118

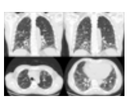

Assessment of acinar destruction in idiopathic pulmonary fibrosis with hyperpolarised 3He gas diffusion-weighted MRI: reproducibility of ADC metrics and correlation with physiological parameters of disease severity.

Nicholas D Weatherley[1], Ho-Fung Chan[1], Neil J Stewart[1], Laura C Saunders[1], Guilhem J Collier[1], Graham Norquay[1], Madhwesha Rao[1], Laurie Smith[1], Matthew Austin[2], Stephen A Renshaw[3], Stephen M Bianchi[2], and Jim M Wild[1]

[1]Academic Unit of Radiology, University of Sheffield, Sheffield, United Kingdom, [2]Academic Directorate of Respiratory Medicine, Sheffield Teaching Hospitals, Sheffield, United Kingdom, [3]Infection, Immunity and Cardiovascular Disease, University of Sheffield, Sheffield, United Kingdom

Outcome metrics from diffusion-weighted MRI (DW-MRI) were evaluated for reproducibility and clinical correlation in a cohort of patients with idiopathic pulmonary fibrosis (IPF). It was hypothesized that fibrotic lung tissue in IPF undergoes changes that increase the rate of intra-acinar Brownian diffusion.

Apparent diffusion coefficient (ADC) mean, median and histogram metrics are highly reproducible and correlate both quantitatively with regional fibrosis on CT and qualitatively with carbon monoxide transfer coefficient (KCO) from pulmonary function tests. DW-MRI imaging metrics may provide novel insights into microstructural disease severity in IPF and may prove to be a useful non-ionising imaging biomarker of disease.

3329 Computer 119

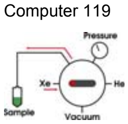

Hyperpolarized xenon by d-DNP using the clinical GE SpinLab polarizer system

Christian Østergaard Mariager[1], Steffen Ringgaard[1], Jan Henrik Ardenkjær-Larsen[2,3], and Christoffer Laustsen[1]

[1]Department of Clinical Medicine, The MR Research Centre, Aarhus University Hospital, Aarhus N, Denmark, [2]Department of Electrical Engineering, Center for Hyperpolarization in Magnetic Resonance, Technical University of Denmark, Kgs. Lyngby, Denmark, [3]GE Healthcare, Denmark

Hyperpolarized (HP) ^{129}Xe have been demonstrated as a useful probe for magnetic resonance (MR) lung imaging and show promise for in vivo perfusion imaging and brown adipose tissue characterization. Reports of large polarization enhancements for ^{129}Xe using dynamic nuclear polarization (DNP) have raised expectations that DNP can be an alternative to the standard spin exchange optical pumping (SEOP) method. We show that it is possible to produce HP ^{129}Xe gas using the clinical GE SpinLab polarizer, thus extending the practical use of the system beyond the primary purpose of hyperpolarizing liquid biomolecules.

3330 Computer 120

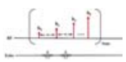

Combination of Variable and Constant Flip Angles for Hyperpolarized 129Xe Multi-b Diffusion MRI in a Single Breath-hold

Weiwei Ruan[1,2], Jianping Zhong[1], Ming Zhang[1], He Deng[1], Yeqing Han[1], Chaohui Ye[1], and Xin Zhou[1]

[1]Key Laboratory of Magnetic Resonance in Biological Systems, State Key Laboratory of Magnetic Resonance and Atomic and Molecular Physics, National Center for Magnetic Resonance in Wuhan, Wuhan Institute of Physics and Mathematics, Chinese Academy of Sciences, Wuhan, People's Republic of China, [2]University of Chinese Academy of Sciences, Beijing, People's Republic of China

To propose a novel flip angle scheme for hyperpolarized gas multi-b diffusion MRI. It combined the variable and constant flip angles and was named as the combination of variable and constant flip angle (CVCFA). Computer simulation was used to systematically compare the proposed flip angle scheme with the common-used flip angle schemes, including the interleaved constant flip angle (ICFA) and the variable flip angle (VFA) schemes. The CVCFA scheme was used for hyperpolarized xenon diffusion MRI to measure the pulmonary morphology in rats, noninvasively. The results showed the CVCFA was suited for the hyperpolarized gas multi-b diffusion MRI.

Electronic Poster

Diffusion: Acquisition

Exhibition Hall — Monday 13:45 - 14:45

3331 Computer 1

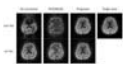

Multi-shot Diffusion Imaging using 1D Navigator Acquisition with Parallel Imaging and Iterative Reconstruction

Zhe Zhang[1], Xiaodong Ma[1], Erpeng Dai[1], and Hua Guo[1]

[1]Center for Biomedical Imaging Research, Department of Biomedical Engineering, School of Medicine, Tsinghua University, Beijing, People's Republic of China

Multi-shot EPI can achieve high resolution diffusion imaging but shot-to-shot phase variation correction is indispensable. Previous multi-shot EPI diffusion imaging methods can be categorized into two groups based on different phase navigation strategies: navigator acquired from a second echo and navigator calculated from image-echo itself using parallel imaging technique. These methods may suffer prolonged scan time or limitation from high reduction factor penalty. In this work, we proposed a new strategy for efficient navigating in multi-shot DWI using 1D navigator acquisition with parallel imaging and iterative reconstruction. Results show the proposed methods can effectively correct the motion-induced artifacts in diffusion imaging.

3332 Computer 2

Joint Non-local Means Reconstruction for Correction of Phase-Induced Errors in Diffusion Tensor Imaging

Sevgi Gokce Kafali[1,2], Tolga Cukur[1,2], and Emine Ulku Saritas[1,2]

[1]Electrical and Electronics Engineering, Bilkent University, Ankara, Turkey, [2]National Magnetic Resonance Research Center (UMRAM), Ankara, Turkey

Multiple acquisitions have to be averaged to achieve reasonable signal-to-noise ratio (SNR) in high-resolution diffusion tensor imaging (DTI). However, involuntary global/local motions during diffusion-sensitizing gradients create k-space shifts, and global/local phase differences between different acquisitions, complicating image reconstruction. In this work, we propose a phase-correcting joint non-local means reconstruction that effectively prevents phase cancellations and reduces noise. This technique jointly utilizes the images from different diffusion-encoding directions to preserve the fractional anisotropy (FA) map. Results are demonstrated for in vivo spinal cord DTI and on a simulated DTI dataset.

3333 Computer 3

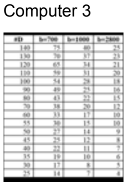

Accelerating Diffusion Kurtosis Imaging Using Model Based Denoising

Jonathan I Sperl[1], Tim Sprenger[1,2], Ek T Tan[3], Marion I Menzel[1], Christopher J Hardy[3], and Luca Marinelli[3]

[1]GE Global Research, Garching, Germany, [2]Technische Universität München, Munich, Germany, [3]GE Global Research, Niskayuna, NY, United States

Diffusion Kurtosis Imaging (DKI) suffers from high sensitivity to noise and therefore requires long scanning times (up to 150 diffusion weighted images, DWIs). This work proposes a model-based denoising technique to overcome this limitation: A generalized multi-shell spherical deconvolution model is formulated and DWIs are denoised by a projection into the space spanned the model. We demonstrate noise reduction for DKI metrics yielding improved image quality of kurtosis maps from as few as 30 DWIs. This corresponds to greater than four-fold reduction in scan time as compared to the widely used 140-DWI acquisitions.

3334 Computer 4

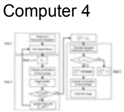

Improved Reconstruction for Simultaneous Multi-Slice (SMS) Accelerated Interleaved EPI DWI

Erpeng Dai[1], Xiaodong Ma[1], Zhe Zhang[1], Chun Yuan[1,2], and Hua Guo[1]

[1]Center for Biomedical Imaging Research, Department of Biomedical Engineering, School of Medicine, Tsinghua University, Beijing, People's Republic of China, [2]Vascular Imaging Laboratory, Department of Radiology, University of Washington, Seattle, WA, United States

Recently, simultaneous multi-slice (SMS) has been proved to be effective for accelerating single-shot EPI (ssh-EPI) based diffusion weighted imaging (DWI). More importantly, SMS can be combined with multi-shot interleaved EPI (iEPI) DWI to achieve high resolution and high throughput simultaneously. However, signal dropout problems may exist in the final DW images, especially at high SMS acceleration factors. The main reason is the prominent cerebrospinal fluid (CSF) pulsation, which may degrade the reconstruction performance. In this study, the reconstruction algorithm is augmented by using iteration and data rejection. In-vivo experiments have demonstrated that the augmented algorithm can effectively alleviate the signal dropout problems.

3335 Computer 5

The Effects of 2D Navigator Distortion and Noise Level on Interleaved EPI DWI Reconstruction: A Simulation Study

Erpeng Dai[1], Xiaodong Ma[1], Zhe Zhang[1], Chun Yuan[1,2], and Hua Guo[1]

[1]Center for Biomedical Imaging Research, Department of Biomedical Engineering, School of Medicine, Tsinghua University, Beijing, People's Republic of China, [2]Vascular Imaging Laboratory, Department of Radiology, University of Washington, Seattle, WA, United States

Interleaved EPI (iEPI) with a 2D navigator is an effective way to acquire high-resolution and less-distorted DWI. The inter-shot phase variations can be corrected with acquired 2D navigator. However, the performance is limited by the geometric distortion mismatch between the navigator-echo and image-echo. Parallel imaging can be used to reduce the navigator distortion, but can cause noise amplification. Previously, the effects of the navigator were studied with in vivo experiments, but the effects of distortion and noise were mixed together. In this study, the effects of navigator distortion and noise are studied individually with both DWI and DTI simulations.

3336 Computer 6

Improved Navigator-free Multi-shot DTI Reconstruction with Inter-image Correlation Constraint

Xiaodong Ma[1], Zhe Zhang[1], Erpeng Dai[1], Chun Yuan[1,2], and Hua Guo[1]

[1]Center for Biomedical Imaging Research, Department of Biomedical Engineering, School of Medicine, Tsinghua University, Beijing, China, Beijing, People's Republic of China, [2]Vascular Imaging Laboratory, Department of Radiology, University of Washington, Seattle, WA, United States

To improve the image quality for navigator-free multi-shot DTI reconstruction, the inter-image correlation constraint is introduced. Group sparsity and anisotropic sparsity are proposed as two specific implementations, using the POCS-ICE algorithm. Results show that both constraints can improve the image quality with increased SNR. In addition, anisotropy sparsity has less blurring and can better maintain the detailed structures.

3337 Computer 7

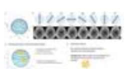

Rotating Single-shot Acquisition (RoSA) combined with parallel imaging for fast high-resolution diffusion imaging

Qiuting Wen[1], Brian Dale[2], Shivraman Giri[3], and Yu-Chien Wu[1]

[1]Radiology and Imaging Science, Indiana University, Indianapolis, IN, United States, [2]Siemens Medical Solutions, Inc. , Hanover, NH, United States, [3]Siemens Medical Solutions, Inc. , Morrisville, NC, United States

High-resolution diffusion-weighted MRI often relies on multi-shot acquisitions, which suffer from long acquisition time. Rotating single-shot acquisition (RoSA) was proposed to accelerate high-resolution diffusion MRI by taking advantage of the similarity between diffusion-weighted images. In RoSA only a strip of k-space (i.e., blade) per diffusion direction is acquired, and high-resolution image was achieved via composite reconstruction. In this work, we implemented RoSA with parallel imaging. We demonstrated that improved data quality and imaging speed was achieved in both simulation and in human data.

3338 Computer 8

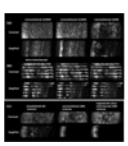

Diffusion imaging with intra volume interleaving of b values

Jana Hutter[1], Paddy J Slator[2], Anthony N Price[3], Ana Dos Santos Gomes[4], Laura McCabe[4], Maria Murgasova Kuklisova[5], Paul Aljabar[1], Mary Rutherford[4], and Joseph V Hajnal[3]

[1]Biomedical Engineering, King's College London, London, United Kingdom, [2]Centre for Medical Image Computing, University College London, London, United Kingdom, [3]Biomedical Engineering Department, King's College London, London, United Kingdom, [4]Centre for the Developing Brain, King's College London, London, United Kingdom, [5]Perinatal Imaging, King's College London, London, United Kingdom

Conventional diffusion MRI acquisitions acquire all slices per volume with the same diffusion weighting. This can have two drawbacks: Excessive heating of gradient hardware caused by multiple repeats of the same combination of large drive currents, and low signal at high b-values, which impairs motion correction based on image registration. For placental diffusion MRI, where large slice stack are needed for spatial coverage and anatomical structure can be lost after diffusion, both of these factors can be extreme. We propose intra-volume interleaving of different diffusion weightings, ordered to facilitate image registration for motion correction and minimise gradient heating.

3339 Computer 9

Randomizing simultaneously excited slice groups in SMS to reduce slice leakage artifacts in diffusion MRI

Daniel Olson[1], Andrew Nencka[2], Volkan Arpinar[2], and L. Tugan Muftuler[3]

[1]Biophysics, Medical College of Wisconsin, Milwaukee, WI, United States, [2]Radiology, Medical College of Wisconsin, Milwaukee, WI, United States, [3]Neurosurgery, Medical College of Wisconsin, Milwaukee, WI, United States

Simultaneous Multi-slice (SMS) techniques excite multiple slices simultaneously to accelerate MRI data acquisition. However, slice separation during image reconstruction is not exact and results in coupling between separated voxels. While this may not be critical for most anatomic imaging methods, small but consistent leakage of information from another slice in a DTI dataset will cause bias in diffusion parameter estimates. Here, we propose a randomized-slice pairing technique to alleviate this problem in diffusion MRI acquisitions.

3340 Computer 10

Optimal design of motion-compensated diffusion gradient waveforms

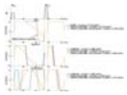

Óscar Peña-Nogales[1], Rodrigo de Luis-Garcia[1], Santiago Aja-Fernández[1], Yuxin Zhang[2,3], James H. Holmes[2], and Diego Hernando[2,3]

[1]Laboratorio de Procesado de Imagen, Universidad de Valladolid, Valladolid, Spain, [2]Radiology, University of Wisconsin-Madison, Madison, WI, United States, [3]Medical Physics, University of Wisconsin-Madison, Madison, WI, United States

Diffusion-Weighted MRI (DW-MRI) often suffers from motion-related artifacts in organs that experience physiological motion. Importantly, organ motion during the application of diffusion gradients results in signal losses, which complicate image interpretation and bias quantitative measures. Motion-compensated gradient designs have been proposed, however they typically result in substantially lower b-values or severe concomitant gradient effects. In this work, we develop an approach for design of first- and second-order motion-compensated gradient waveforms based on a b-value maximization formulation including concomitant gradient nulling, and we compare it to existing techniques. The proposed design provides optimized b-values with motion compensation and concomitant gradient nulling.

3341 Computer 11

Determination of the optimal set of b-values for ADC mapping under a Rician noise assumption

Óscar Peña-Nogales[1], Diego Hernando[2,3], Santiago Aja-Fernández[1], and Rodrigo de Luis-Garcia[1]

[1]Laboratorio de Procesado de Imagen, Universidad de Valladolid, Valladolid, Spain, [2]Radiology, University of Wisconsin-Madison, Madison, WI, United States, [3]Medical Physics, University of Wisconsin-Madison, Madison, WI, United States

Mapping of the apparent diffusion coefficient (ADC), estimated from a set of diffusion-weighted (DW) images acquired with different b-values, often suffers from low SNR, which can introduce large variance in ADC maps. Unfortunately, there is no consensus on the optimal b-values to maximize the noise performance of ADC map. In this work, we determine the optimal b-values to maximize the noise performance of ADC mapping by using a Cramér-Rao Lower Bound (CRLB) approach under realistic noise assumptions. The strong agreement between the CRLB-based analysis, Monte-Carlo simulations, and ADC phantom experiment, suggests the utility of this approach to optimize DW-MRI acquisitions.

3342 Computer 12

Towards Achieving the Optimal SNR Efficiency for 3D Multi-shot Diffusion-Weighted Echo-Planar Imaging

Xiaoxi Liu[1], Edward S. Hui[1,2], Cui Di[1], Nan-Kuei Chen[3,4], and Hing-Chiu Chang[1]

[1]Department of Diagnostic Radiology, The University of Hong Kong, Hong Kong, Hong Kong, [2]The State Key Laboratory of Brain and Cognitive Sciences, The University of Hong Kong, Hong Kong, Hong Kong, [3]Department of Biomedical Engineering, University of Arizona, Tucson, AZ, United States, [4]Brain Imaging and Analysis Center, Duke University Medical Center, Durham, NC, United States

Due to the assumption of 2D phase variations, the feasible maximum slab thickness is relatively thin (e.g. < 25 mm) for 3D multi-shot diffusion-weighted echo-planar imaging. We have thus proposed a new method in another study to correct for 3D inter-shot phase variations, thereby significantly increasing the feasible maximum slab thickness. In this study, we have demonstrated by simulations and experiments that slab thickness can be significantly increased to allow whole brain coverage with a TR that achieves optimal SNR efficiency.

3343 Computer 13

Field-map correction in read-out segmented echo planar imaging for reduced spatial distortion in prostate DWI – a phantom study

Robert Bergen[1,2] and Lawrence Ryner[1,2]

[1]Physics & Astronomy, University of Manitoba, Winnipeg, MB, Canada, [2]Medical Physics, CancerCare Manitoba, Winnipeg, MB, Canada

Diffusion-weighted magnetic resonance imaging (DWI) is routinely used in prostate cancer assessment, but suffers from image distortions primarily due to the tissue-air interface at the rectal cavity. Readout-segmented echo planar imaging (RESOLVE) improves image quality through segmented acquisition of k-space, increasing bandwidth in the phase direction. However, distortions of several millimeters may still exist in RESOLVE images. This study quantified distortions in a prostate phantom by varying the number of RESOLVE segments and using field mapping correction techniques. Field mapping correction decreased image distortion by 28% compared to the 7-segment RESOLVE scan.

3344 Computer 14

Simultaneous Multi-Slice Double Diffusion Encoding Imaging

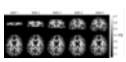

Grant Kaijuin Yang[1,2], Hua Wu[3], Qiyuan Tian[1,2], Adam Kerr[3], Robert Dougherty[3], and Jennifer McNab[2]

[1]Electrical Engineering, Stanford University, Stanford, CA, United States, [2]Radiology, Stanford University, Stanford, CA, United States, [3]Center for Cognitive and Neurobiological Imaging, Stanford University, CA, United States

Double diffusion encoding (DDE) sequences can measure microscopic diffusion anisotropy even in complex structures such as cortex or crossing fiber regions in white matter. However, DDE sequences require long TEs to accommodate the additional diffusion gradients, resulting in lower signal-to-noise ratio (SNR) and reduced slice coverage limiting its clinical feasibility. In this work, we implement a DDE sequence with simultaneous multi-slice (SMS) to improve the SNR efficiency and allow for full-brain DDE scans in a clinically feasible time.

3345 Computer 15

A measurement weighting scheme for optimal powder average estimation

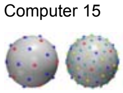

Filip Szczepankiewicz[1], Carl-Fredrik Westin[2,3], and Hans Knutsson[3,4]

[1]Medical Radiation Physics, Lund University, Lund, Sweden, [2]Brigham and Women's Hospital, Harvard Medical School, Boston, MA, United States, [3]Department of Biomedical Engineering, Linköping University, Linköping, Sweden, [4]Center for Medical Image Science and Visualization, Linköping University, Linköping, Sweden

The powder-averaged signal is used in several analysis techniques in diffusion MRI. Assuming uniformly distributed diffusion encoding directions, it is calculated simply as the arithmetic signal average. However, perfectly uniform sampling is generally unattainable.

We demonstrate how non-uniformity can be accounted for by using weighted signal averaging, and we describe how optimal weights can be calculated for existing diffusion encoding schemes to yield improved accuracy of the powder average estimate.

3346 Computer 16

Can eddy currents and concomitant fields be compensated at the same time in flow-compensated diffusion MRI?

Lars Mueller[1], Tristan Anselm Kuder[1], and Frederik Bernd Laun[1,2]

[1]Medical Physics in Radiology, German Cancer Research Center, Heidelberg, Germany, [2]Institute of Radiology, University Hospital Erlangen

The possibility to simultaneous compensate for flow, concomitant fields and eddy currents in diffusion weighted MRI were examined by means of numerical simulations. For this purpose, sequences with three to five gradient pulses and one or two refocusing pulses were examined. It is shown that it is possible to effectively minimize all three effects with different sequences. For short to intermediate echo times, it is beneficial to use only one refocusing pulse, while for long echo times two refocusing pulses can yield higher b-values. There is a trade-off between compensation of more effects and the achievable b-value.

3347 Computer 17

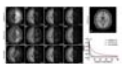

A new method for the image reconstruction of multi-shot navigator-free DWI

Zhangxuan Hu[1], Chun Yuan[1,2], and Hua Guo[1]

[1]Center for Biomedical Imaging Research, Department of Biomedical Engineering, School of Medicine, Tsinghua University, Beijing, People's Republic of China, [2]Department of Radiology, University of Washington, 1959 NE Pacific Street, SS-202, Seattle, WA 98195-7117, USA, WA, United States

Multi-shot techniques can help to achieve high spatial resolution in diffusion imaging. Due to the application of diffusion gradients, phase errors are induced by shot-to-shot motions, which need to be corrected during image reconstruction. Some phase correction approaches have been proposed, such as SENSE+CG, POCS-ICE, and PR-SENSE. Compressed sensing (CS) method has been used in image reconstruction and shows great insensitivity to noise, and can be effectively solved by the Alternating Direction Method of Multipliers (ADMM) algorithm. In this work, the ADMM method of CS reconstruction is used in multi-shot diffusion imaging and proved that it can provide higher reconstruction quality.

3348 Computer 18

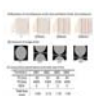

Simultaneous multi-slice (SMS) echo planar imaging (EPI); which combination of parameters is clinically most efficient?

Koji Sakai[1], Hiroshi Imai[2], Hiroyasu Ikeno[3], Jun Tazoe[1], Masashi Yasuike[1], Hitomi Nagano[1], Himanshu Bhat[4], and Kei Yamada[1]

[1]Kyoto Prefectural University of Medicine, Kyoto, Japan, [2]Siemens Japan K. K., [3]Kyoto Prefectural University of Medicine Hospital, [4]Siemens Medical Solutions USA

To find clinically feasible combinations of parameter for simultaneous multi-slice echo planar imaging (SMS-EPI) acquisition diffusion tensor imaging (DTI), we investigated the combinations of SMS factors and the amounts of inter-slice image shift to find which one can provide better signal-to-noise ratio (SNR) by two different head coils (20ch and 32ch), respectively. The SMS factors 2 and 3 with imaging shifts (>1/2) on 32ch judged clinically feasible and can be substituted on conventional DTI. The SMS factor 2 with imaging shifts 0, 1/2, 1/4 on 20ch head coil judged clinically feasible.

3349 Computer 19

To accelerate or not: An Investigation on the Impact of Fast Diffusion Imaging with High Angular Resolution on Diffusion Measures in Fiber Tracts

Chia-Ling Chang[1], Jr-Yuan George Chiou[2], Ming-Long Wu[1,3,4], Shang-Yueh Tsai[5], Stephan Ernst Maier[2,6], Bruno Madore[2], and Tzu-Cheng Chao[1,4]

[1]Department of Computer Science and Information Engineering, National Cheng Kung University, Tainan, Taiwan, [2]Department of Radiology, Brigham and Women's Hospital, Harvard Medical School, Boston, MA, United States, [3]Institute of Applied Computer Science, Harvard University, Cambridge, MA, United States, [4]Institute of Medical Informatics, National Cheng Kung University, Tainan, Taiwan, [5]Graduate Institute of Applied Physics, National Cheng Chi University, Taipei, Taiwan, [6]Department of Radiology, Sahlgrenska Academy, Gothenburg University

A novel technique, Fast Diffusion Imaging with High Angular Resolution, is proposed to achieve whole-brain HARDI scans for clinical applications with better geometrical fidelity and shorter scan time. The present study compares tractography results and diffusion properties of each analyzed fiber tract among four-fold segmented (multi-shot) HARDI scans with different acceleration rates and a clinically used sequence with two-fold SENSE. A fully sampled four-shot HARDI scan was used as the reference. The results suggest that the novel acceleration strategy permits a four-minute scan with fairly compatible results while the clinically used method takes ten minutes.

3350 Computer 20

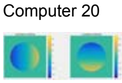

Applied Gradient Nonlinearity Correction for Quantitative Diffusion MRI

Baxter P Rogers[1], Allen T Newton[1], E Brian Welch[1], Jeffrey J Luci[2], Heidi A Edmonson[3], and Bennett A Landman[4]

[1]Vanderbilt University Medical Center, Nashville, TN, United States, [2]University of Texas at Austin, [3]Mayo Clinic, [4]Vanderbilt University

Accurate and reliable quantitative diffusion MRI depends on correcting for spatially varying errors in applied diffusion gradients due to nonlinearity of the gradient coil fields. We measured the temporal and inter-scanner variability of a phantom-based correction protocol on four different scanners. Estimated errors in diffusion gradient b-value and direction were significant, and differed between scanners. Scanner differences in temporal stability indicated the need for site-specific calibrations.

3351 Computer 21

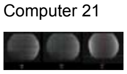

Correcting a slice distortion artifact in the multiband diffusion images

Jiancheng Zhuang[1]

[1]University of Southern California, Los Angeles, CA, United States

The diffusion weighted images acquired with the multiband sequence or the Lifespan protocols shows a type of slice distortion artifact. We find that this artifact is caused by the eddy currents, which can be induced by the diffusion gradient associated with either current DW image or the previous DW images. The artifact can be corrected by further tuning the compensation circuit in the MR hardware, or by a correction algorithm which includes the diffusion gradients from the current and previous DW images.

3352 Computer 22

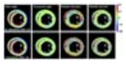

Evaluation of diffusion directions vs averages for accurate and reproducible cardiac DTI

Darryl McClymont[1], Irvin Teh[1], Hannah Whittington[1], and Jürgen Schneider[1]

[1]Cardiovascular Medicine, University of Oxford, Oxford, United Kingdom

Cardiac DTI is subject to long scan times and low SNR, which invariably leads to a trade-off between the number of averages and diffusion-encoding directions to acquire. However, the exact relationship between the diffusion tensor and these parameters is unclear. In this work we utilise DTI data from five high quality ex-vivo rat hearts, and vary the SNR between 2 and 97 and the number of directions between 7 and 61. Results show that the apparent diffusion coefficient is optimised for scan time when SNR is maximised and directions are minimised, whereas parametric angle measurements are time-optimised with more directions. At typical in-vivo settings, we estimate that fractional anisotropy is being overestimated by up to 20%, while the precision of sheetlet angles may be as poor as ±36 degrees.

3353 Computer 23

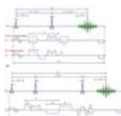

Eddy current artifact reduction in diffusion-weighted single-refocused spin-echo EPI

Manoj Shrestha[1], Pavel Hok[2], Ulrike Nöth[1], and Ralf Deichmann[1]

[1]Brain Imaging Center (BIC), Goethe University Frankfurt, Frankfurt am Main, Germany, [2]Palacky University Olomouc, University Hospital Olomouc, Czech Republic

Diffusion-weighted (DW) MRI with single-refocused spin-echo preparation suffers from eddy-current induced image distortions. In this study, a method for substantial reduction of eddy-current artifacts is proposed. Dummy scans comprising DW gradients prior to the acquisition of each multi-slice data volume yield a steady state of eddy-currents and thus comparable distortions across the volume which subsequently can be corrected via an advanced setting of the eddy-current correction FMRIB software library tool. In comparison to the commonly used twice-refocused spin-echo sequence for eddy-current compensation, the proposed method is less sensitive to radiofrequency inhomogeneities and offers higher signal-to-noise ratio due to shorter echo-time.

3354 Computer 24

Reducing Distortion in DWI Acquisitions of Prostate Scans

Roger C Grimm[1], Adam T Froemming[1], and Stephen J Riederer[1]

[1]Mayo Clinic, Rochester, MN, United States

Diffusion images obtained with spin echo – echo planar imaging (SE-EPI) can be acquired quickly and efficiently. In prostate applications areas of susceptibility can cause image distortion. The purpose of this work is to address these distortions with the use of multi-shot EPI techniques. A previously defined term, pseudo-gradient, is shown to be a useful analytical tool to explain and guide in the choice of acquisition parameters. Phantom and in-vivo results show the benefits of multi-shot scans to reduce distortions.

Electronic Poster

Diffusion: Analysis

Exhibition Hall Monday 13:45 - 14:45

3355 Computer 25

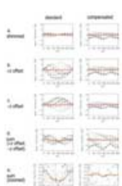

Evidence for Cross-Term Effects in Double Diffusion Encoding Experiments of Human Cortical Gray Matter

Marco Lawrenz[1,2] and Jürgen Finsterbusch[1,2]

[1]Department of Systems Neuroscience, University Medical Center Hamburg-Eppendorf, Hamburg, Germany, [2]Neuroimage Nord, University Medical Centers Hamburg-Kiel-Lübeck, Hamburg-Kiel-Lübeck, Germany

Double diffusion encoding (DDE) experiments with two weighting periods applied successively in the same acquisition are a promising tool to investigate microscopic tissue properties, e.g. the cell eccentricity and the related diffusion anisotropy on a microscopic scale. Recent experiments detected the signal pattern typical for microscopic diffusion anisotropy in human cortical gray matter in vivo but were hampered by an additional signal modulation that could be related to field inhomogeneities near the skull. In this study, cross-term-compensated DDE experiments are performed to investigate the effect of field inhomogeneities on the detection of the microscopic diffusion anisotropy.

3356 Computer 26

magna cum laude

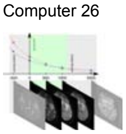

On the Potential of DWI with Extrapolated High and Negative b-Values for Contrast Enhancement and Image Segmentation

Marcel Gratz[1,2] and Harald H. Quick[1,2]

[1]Erwin L. Hahn Institute, University Duisburg-Essen, Essen, Germany, [2]High Field and Hybrid MR Imaging, University Hospital Essen, Essen, Germany

A method is presented that extends the concept of calculated DWI for the generation of high tissue contrast from trace-weighted data. Using the whole range of b-values including the physically inaccessible negative b-values, image segmentation, visual hinting and ROI generation can be provided for assistance of the clinical readers. 24 patient data sets involving different pathologies were used to test the feasibility and clinical potentials of the new approach. It was found that the extrapolation to negative b-values helps to extract fluid regions, whereas internal structures of lesions and noise masking may be obtained with high b-values.

3357 Computer 27

Assessing local brain morphology changes with diffusion tensor-driven tensor based morphometry (D-TBM): Application to a genetic model of dysgenesis

Elizabeth B Hutchinson[1,2,3], Neda Sadeghi[1,2], Okan Irfanoglu[1,2,3], Mary Whitman[4,5], Michelle Delisle[6], Elizabeth Engle[4,5,6,7,8], and Carlo Pierpaoli[1,2]

[1]Quantitative Medical Imaging Section, NIBIB, NIH, Bethesda, MD, United States, [2]SQITS/NICHD, NIH, Bethesda, MD, United States, [3]Henry M. Jackson Foundation, Bethesda, MD, United States, [4]Opthamology, Harvard Medical School, Boston, MA, United States, [5]Opthamology, Boston Children's Hospital, Boston, MA, United States, [6]Neurology, Boston Children's Hospital, Boston, MA, United States, [7]Neurology, Harvard Medical School, Boston, MA, United States, [8]Howard Hughes Medical Institute, Chevy Chase, MD, United States

Brain volume registration using diffusion tensor information faithfully matches anatomic features that are not accessible to structural registration algorithms such as white matter tracts. Thus, inspection of the deformation fields from DT-based registration using TBM (D-TBM) is advantageous for revealing local morphometric differences when compared with conventional TBM. In this study, D-TBM was used to evaluate morphometric differences and heterogeneity of abnormalities in a mouse model of dysgenesis.

3358 Computer 28

Stretched-exponential model DWI as a non-invasive biomarker in grading gliomas and predicting of EGFR status

Jingjing Jiang[1] and Wenzhen Zhu[1]

[1]Tongji hospital, Tongji medical college, Huazhong university of science and technology, Wuhan, People's Republic of China

Stretched-exponential diffusion weighted imaging (SEM-DWI) provided a more accurate estimate than conventional DWI in grading gliomas. Moreover, SEM-DWI derived α value could effectively differentiate EGFR negative and positive group and had a significantly negative correlation with EGFR expression . Therefore, it was concluded that SEM-DWI might be applied as an effective imaging biomarker in grading gliomas and predicting of EGFR status and thus in guiding individual treatment and targeted therapy.

3359 Computer 29

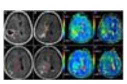

Comparing the value of MRI ultra-high-b-value DWI and standard DWI in grading cerebral astrocytomas and their association with aquaporin-4

Yan Tan[1], Hui Zhang[1], Xiaochun Wang[1], and Dandan Zheng[2]

[1]The First Hospital of Shanxi Medical University, TaiYuan, People's Republic of China, [2]GE Healthcare MR Research China, People's Republic of China

Ultral-High-b-value DWI (UHBV-DWI) was shown to improve the diagnostic performance of DWI in grading gliomas. We compare the value of MRI UHBV-DWI and conventional DWI for grading astrocytomas, and to analyze the correlation of respective parameters with aquaporin (AQP) expression. We found UHBV-ADC (0.810) showed a larger area under the curve (AUC) than that of ADC (0.713) ($P < 0.05$). The ADC value showed a negative correlation with AQP4 mRNA expression ($r = -0.357$; $P = 0.024$). UHBV-ADC value positively correlated with the AQP4 mRNA expression ($r = 0.646$; $P < 0.01$). So UHBV-DWI allowed for a more accurate grading of cerebral astrocytoma as compared to DWI. UHBV-ADC may be related with the AQP4 mRNA levels.

3360 Computer 30

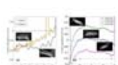

Characterization of B0 Shim-Induced Bias in Diffusion Weighting Gradients

Yuxi Pang[1], Dariya I Malyarenko[1], Michael Schar[2], Lisa J Wilmes[3], David Newitt[3], Michael A Jacobs[2], and Thomas L Chenevert[1]

[1]Department of Radiology, University of Michigan, Ann Arbor, MI, United States, [2]Department of Radiology and Radiological Science, The Johns Hopkins University School of Medicine, Baltimore, MD, United States, [3]Department of Radiology and Biomedical Imaging, University of California San Francisco, San Francisco, CA, United States

To eliminate technical variability in quantitative diffusion imaging applications, the systematic bias in diffusion weighting gradients should be corrected. The major source of this bias is the system-specific spatial gradient non-linearity (GNL) that can be rectified using gradient design information independent of the scanned object. This study characterizes the residual sources of nonuniform diffusion weighting introduced by imperfect object-dependent B0 shimming. Using controlled de-shim gradients, we show that an imperfect shim leads to systematic offsets of the otherwise symmetric GNL profile relative to the isocenter. The empiric strategies are proposed to mitigate the shim-induced errors in ADC measurements.

3361 Computer 31

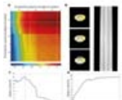

Does artifact correction in spinal cord DTI improve sensitivity at the group level?

Gergely David[1,2], Patrick Freund[1,3,4], and Siawoosh Mohammadi[2,4]

[1]Spinal Cord Injury Center, Balgrist University Hospital, Zurich, Zurich, Switzerland, [2]Department of Systems Neuroscience, University Medical Center Hamburg-Eppendorf, Hamburg, Germany, [3]Department of Neurophysics, Max Planck Institute for Human Cognitive and Brain Sciences, Leipzig, Germany, [4]Wellcome Trust Centre for Neuroimaging, UCL Institute of Neurology, London, United Kingdom

In this manuscript, we investigate how application of established post-processing methods (spatial registration and robust tensor fitting) and of a newly introduced outlier rejection technique referred to as reliability masking influence the statistical power of a clinical spinal cord DTI study. The assessment was performed using a previously published clinical dataset investigating microstructural correlates of spinal degeneration in cervical spondylotic myelopathy (CSM). We found that the established post-processing methods had almost no influence on the statistical power by which the microstructural differences is observed, whereas reliability masking increased the statistical power by more than 13%.

3362 Computer 32

Investigating microstructural signatures for low-grade gliomas using Linear Multi-scale Modeling of diffusion MRI data

Barbara D. Wichtmann[1,2], Aapo Nummenmaa[1], Qiuyun Fan[1], Thomas Witzel[1], Elizabeth R. Gerstner[3], Alexandra J. Golby[4,5], Sandro Santagata[6], Bruce R. Rosen[1], Lothar Schad[2], Lawrence L. Wald[1,7], and Susie Y. Huang[1,7]

[1]A. A. Martinos Center for Biomedical Imaging, Department of Radiology, Massachusetts General Hospital, Harvard Medical School, Charlestown, MA, United States, [2]Computer Assisted Clinical Medicine, Medical Faculty Mannheim, Heidelberg University, Mannheim, Germany, [3]Department of Neurology, Center for Neuro-Oncology, Massachusetts General Hospital, Harvard Medical School, Boston, MA, United States, [4]Department of Neurosurgery, Brigham and Women's Hospital, Harvard Medical School, Boston, MA, United States, [5]Department of Radiology, Brigham and Women's Hospital, Harvard Medical School, Boston, MA, United States, [6]Department of Pathology, Brigham and Women's Hospital, Harvard Medical School, Boston, MA, United States, [7]Harvard-MIT Division of Health Sciences and Technology, Massachusetts Institute of Technology, Cambridge, MA, United States

Linear Multi-scale Modeling (LMM) of diffusion MRI data is a recently developed DWI analysis technique for separating orientation distributions of restricted and hindered diffusion water compartments over a range of length scales, thereby allowing more detailed characterization of tissue microstructure. Here, we apply the LMM framework to characterize a low-grade oligodendroglioma prior to resection. We use the distinct microstructural signature of the tumor to delineate tumor extent and use results from pathology and numerical simulations to refine our understanding of the tumor microstructure.

3363 Computer 33

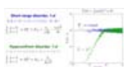

Revealing the nature of microstructural correlations along axons in human brain white matter with time-dependent diffusion

Hong-Hsi Lee[1], Els Fieremans[1], and Dmitry S. Novikov[1]

[1]Center for Biomedical Imaging, New York University, New York, NY, United States

We explore axial diffusivity dependence on both diffusion time and gradient pulse width in major white matter tracts. This allows us to differentiate between two possible arrangements of restrictions (e.g. beads) along fibers: (1) short-range disorder, or (2) "hyperuniform" disorder (arrangement qualitatively closer to periodic). Unexpectedly, model prediction for hyperuniform disorder is more consistent with our data than for short-range disorder. If conformed histologically in human or animal studies, this would mean that restrictions along axons are not "purely" randomly distributed but rather spatially correlated − perhaps, for optimizing physiological constraints.

3364 Computer 34

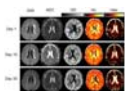

Longitudinal MR Imaging Study of Standard Diffusion-Weighted Imaging and NODDI in ischemic Stroke: Evolution of NODDI metrics and Correlation with Clinical Outcome

Min Tang[1], Wei Di, Xin Zhang, Jie Gao, Kaining Shi[2], Xiaohong Wu, and Xiaoling Zhang

[1]Shaanxi Provincial People`s Hospital, Xi'an, People's Republic of China, [2]Clinical science, Philips Healthcare China

To observe the microstructural longitudinal alterations in neural tissues after ischemic stroke and assess the correlation with clinical outcome and NODDI metrics. 18 subjects were enrolled. Intra-cellular volume fraction(Vic) and orientation dispersion index(OD) exhibited positive correlations with NIHSS scores of patients at day 30. The correlation of the susceptibility with the NODDI metrics and prognosis is higher than the ADC values with it. NODDI may provide a more promising and reliable methods for microstructural reorganization follow-up stroke than other measures previously used in studies of stroke recovery.

3365 Computer 35

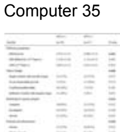

Comprehensive analysis of the predictors of microvessel invasion in hepatocellular carcinoma: Diffusion kurtosis imaging (DKI) combined with radiological and clinical factors.

wentao wang[1], LI Yang[1], Xixing HU[1], Robert Grimm[2], caixia Fu[3], XU Yan[4], mengsu zeng[1], and shengxiang rao[1]

[1]Radiology department, zhongshan Hospital, Shanghai, People's Republic of China, [2]MR Application Developmen, Siemens Healthcare, Erlangen, Germany, [3]Siemens Shenzhen Magnetic Resonance Ltd, shenzhen, People's Republic of China, [4]MR Collaboration NE Asia, Siemens Healthcare, shanghai, People's Republic of China

Diffusion Kurtosis Imaging (DKI) maps, preoperative radiological features and clinical-pathologic findings were calculated to assess their diagnostic accuracy for microvascular invasion (MVI) of hepatocellular carcinoma (HCC) in patients who were undergoing curative liver resection. Multivariate regression analysis was performed to identify independent predictive factors for MVI. The study shows that Mean Kurtosis (MK), non-smooth margin, peritumoral enhancement and incomplete radiological capsule suggest a high probability of microvessel invasion of HCC. Multivariate analysis confirmed that MK and capsule integrity show statistical significance correlation with MVI. In conclusion, MK and capsule appearance might be the predictors for MVI of primary hepatocellular carcinoma.

3366 Computer 36

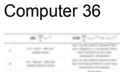

Influence of post-processing method on the repeatability of diffusion-weighted imaging parameters in healthy brain

Ashley M Stokes[1], Jack T Skinner[2], Laura C Bell[1], Adrienne N Dula[3], Thomas E Yankeelov[3], and C. Chad Quarles[1]

[1]Translational Bioimaging Group, Barrow Neurological Institute, Phoenix, AZ, United States, [2]Imaging Programs, National Comprehensive Cancer Network (NCCN), Philadelphia, PA, United States, [3]University of Texas - Austin

The purpose of this study is to investigate the influence of post-processing method on the reproducibility of brain diffusion metrics, including apparent diffusion coefficients (ADCs) and intra-voxel incoherent motion (IVIM) parameters, in healthy controls and to apply these results in a cohort of brain tumor patients undergoing treatment. ADC was highly reproducible for all methods. The IVIM diffusion and perfusion fraction showed the highest reproducibility using constrained fitting, while IVIM pseudo-diffusion showed limited reproducibility. By establishing limits of repeatability for ADC and IVIM metrics, these methods can be applied in neuropathology to determine significant changes related to treatment effects.

3367 Computer 37

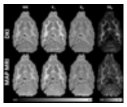

Higher-order statistics of 3D spin displacement probability distributions measured with MAP MRI

Alexandru Vlad Avram[1], Elizabeth Hutchinson[2], and Peter Basser[2]

[1]NIBIB, National Institutes of Health, Bethesda, MD, United States, [2]NICHD, National Institutes of Health, Bethesda, MD, United States

We compute the higher-order statistics of the 3D spin displacement probability distributions measured with mean apparent propagator (MAP) MRI and quantify microstructural tissue parameters such as the mean kurtosis (MK), axial kurtosis ($K_{\parallel}$), radial kurtosis ($K_{\perp}$) and kurtosis fractional anisotropy (FA_K). This extension of the family of MAP tissue parameters provides a direct link between the frameworks of MAP MRI and other advanced diffusion techniques facilitating interpretation of findings in clinical MAP MRI studies in the context of existing literature on advanced diffusion MRI applications.

3368 Computer 38

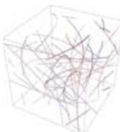

A New Fiber Orientation Distribution Function

Tom Dela Haije[1], Andrea Fuster[1], and Luc Florack[1]

[1]Department of Mathematics and Computer Science, Eindhoven University of Technology, Eindhoven, Netherlands

In this work we introduce the barrier orientation distribution function (ODF) as an alternative to the fiber ODF that can be computed with constrained spherical deconvolution. The barrier ODF is computed directly from the data, without the need to e.g. specify a single fiber response function.

3369 Computer 39

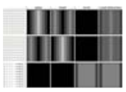

Exploring Local White Matter Geometric Structure in diffusion MRI Using Director Field Analysis

Jian Cheng[1] and Peter J. Basser[1]

[1]National Institutes of Health, Bethesda, MD, United States

In this abstract, inspired by microscopic theoretical treatment of phases in liquid crystals[1], we introduce a novel mathematical framework, called Director Field Analysis (DFA), to study local geometric structural information of white matter. DFA extracts some meaningful scalar indices related with the degree of orientational alignment, dispersion, and orientational distortion, from the Orientation Distribution Function (ODF) field reconstructed by Diffusion Tensor Imaging (DTI) or High Angular Resolution Diffusion Imaging (HARDI).

3370 Computer 40

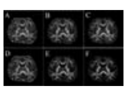

Shall we use denoising in the preprocessing of diffusion weighted imaging?

Maryam Afzali[1], Hu Cheng[1], and Sharlene Newman[1]

[1]Department of psychological and brain sciences, Indiana University, Bloomington, IN, United States

Many denoising techniques have been proposed in an attempt to remedy the low signal-to-noise ratio (SNR) of diffusion weighted images (DWI) [1-3], especially with high b values. It was shown that denoising might benefit DWI data processing such as fiber tracking [4]. However, denoising is not widely accepted as a mandatory step in the preprocessing of DWI data due to little well documented study about the effect of denoising. In this work, we tested if denoising can overcome the low SNR in tensor based diffusion analysis and fiber tracking.

3371 Computer 41

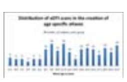

Diffusion - Tensor Based Morphometry (DTBM) of Normal Human Brain Development from Infancy to Adulthood

Amritha Nayak[1,2,3], Neda Sadeghi[2], M Okan Irfanoglu[1,2,3], and Carlo Pierpaoli[1,2]

[1]Quantitative Medical Imaging Section, National Institute of Biomedical imaging and Bioengineering, Bethesda, MD, United States, [2]Section for Quantitative Imaging and Tissue Sciences, Eunice Kennedy Shriver National Institute of Child Health and Human Development, Bethesda, MD, United States, [3]Henry . M. Jackson Foundation for the Advancement of Military Medicine, Bethesda, MD, United States

During postnatal brain development brain structures undergo large changes in size, shape, composition and microstructural appearance. Diffusion tensor imaging (DTI) is an MRI modality particularly informative on white matter. We perform tensor based morphometry (TBM) using deformation fields constructed using all scalar and directional information provided by diffusion tensor data (DTBM) to measure volumetric changes of brain structures from neonate to adulthood. Our results indicate that DTBM reveals interesting patterns in the developmental trajectories for different structures in the human brain. This information would be important to characterize deviation from normal developmental patterns due to developmental delay or other disorders.

3372 Computer 42

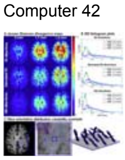

Impact of denoising in diffusion-weighted data on spherical deconvolution modelling

Marina Rakic[1], Luis Miguel Lacerda[1], Ahmad Beyh[2], Pedro Luque-Laguna[1], Rachel Barrett[2], Francisco De Santiago Requejo[1], Steven Williams[1], Gareth Barker[1], Fernando Zelaya[1], and Flavio Dell'Acqua[1,2]

[1]Dept. of Neuroimaging, King's College London, London, United Kingdom, [2]Dept. of Forensic and Neurodevelopmental Science, King's College London, London, United Kingdom

A well-known dilemma in DW-MRI acquisitions is to determine the extent to which signal-to-noise ratio (SNR) can be can be sacrificed in favour of higher spatial resolution on one hand, and in favour of shorter acquisition time on the other. In this study we quantify the reproducibility of spherical deconvolution results at 3 spatial resolutions with and without denoising, as it is still unclear how denoising methods6 affect the uncertainty in subsequent diffusion model fitting and whether it introduces or improves bias in modelled fibre direction.

3373 Computer 43

Density-Based Non-Rigid Registration of Diffusion-Weighted Images

Henrik Grønholt Jensen[1], Francois Lauze[1], Mads Nielsen[1], and Sune Darkner[1]

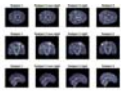

[1]Computer Science, University of Copenhagen, Copenhagen, Denmark

We present a non-rigid registration method for Diffusion-Weighted MRI which uses a density and scale space approach to estimate image similarity. It allows us to employ smooth intensity-invariant similarity measures, such as Mutual Information (MI), in contrast to the model-driven registrations. Using the inherent microstructure of High Angular Resolution Diffusion Imaging (HARDI) scans, we obtain a less regularized and more flexible registration that can be used on either raw diffusion signals or reconstructions of the fiber orientations. We show some promising results on Human Connectome Project (HCP) subjects and an artificial example.

3374 Computer 44

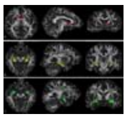

Microstructural alteration of amygdala-hippocampus-nucleus accumbens circuit in methamphetamine users : an in vivo diffusion tensor imaging study

Yadi Li[1], Haibo Dong[1], Feng Li[1], Gaoyan Wang[1], Nadan Zhao[1], Yong Zhang[2], and Wenhua Zhou[3]

[1]Radiology, Lihuili Hospital, Ningbo, People's Republic of China, [2]MR Research China, GE Healthcare, Shanghai, People's Republic of China, [3]Ningbo Addiction Research and Treatment Center, Ningbo, People's Republic of China

No previous in vivo studies have investigated drug-related changes of microstructural integrity of amygdala-hippocampus-nucleus accumbens circuit using diffusion tensor imaging. This study demonstrated reduced microstructural integrity of this circuit in methamphetamine users by applying automated and semi-automated segmentation techniques to acquire regions of interest. The microstructural impairment of hippocampal subiculum and basolateral amygdala might be implicated in the development of anxiety and psychosis. Enhanced anatomical connectivity between left BLA and bilateral NAc may underlie the relapse of MA intake and production of psychosis.

3375 Computer 45

Evaluating NODDI's a priori fixed parameters by combining NODDI and mcDESPOT

Samira Bouyagoub[1], Charlotte L. Clarke[1], Nicholas G. Dowell[1], Tobias C. Wood[2,3], Hui Zhang[4], and Mara Cercignani[1]

[1]Clinical Imaging Sciences Centre, Brighton and Sussex Medical School, Brighton, United Kingdom, [2]Neuroimaging, IoPPN, King's College London, London, United Kingdom, [3]Wellcome Trust Consortium for Neuroimmunology of Mood Disorders and Alzheimer's Disease, London, United Kingdom, [4]Centre for Medical Image Computing, University College London, London

NODDI is a popular diffusion MRI technique that estimates indices about tissue microstructure. However it makes a priori assumptions, particularly fixing intrinsic diffusivity (DI) to be the same throughout the brain. We aim to validate this assumption by combining NODDI with mcDESPOT, which enables an independent estimation of the CSF volume fraction. By doing this, we enable NODDI to estimate voxel-wise maps of DI as well as of the perpendicular diffusivity by removing the tortuosity constraint. Our estimated DI maps show that the assumed value is more suitable for white matter than gray matter and resulted in sharper contrast in neurite density maps but noisier orientation dispersion (ODI) maps. Removing the tortuosity assumption restored the ODI but degraded the quality of the neurite density map.

3376 Computer 46

A Novel Framework for Simulating the In-Vivo Diffusion MRI Signal in Solid Tumours, Based on High-Resolution Optical Imaging Data from Real-World Tumours.

Ben Hipwell[1], Tom Roberts[1], Paul Sweeney[2], Angela D'Esposito[1], Morium Ali[1], Eleftheria Panagiotaki[3], Mark Lythgoe[1], Daniel Alexander[3], Rebecca Shipley[2], and Simon Walker-Samuel[1]

[1]Centre for Advanced Biomedical Imaging, University College London, London, United Kingdom, [2]Mechanical Engineering, University College London, London, United Kingdom, [3]Centre for Medical Image Computing and Computer Science, University College London, London, United Kingdom

We report the development of a novel *in-silico* modelling framework for probing the *in-vivo* diffusion MRI signal in tumours, based on high-resolution (5-10µm) optical imaging data from complete tumours. Blood flow in tissue substrates was estimated using fluid dynamical modelling. We then simulated the MRI signal using a Monte Carlo approach, and fitted the VERDICT model. VERDICT has previously been proposed as a method to noninvasively quantify histological features of tissue, including intracellular, extracellular and vascular volume fractions, cell radius and blood flow. We report preliminary findings of a good correspondence between the ground truth and measured values.

3377 Computer 47

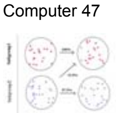

Two subgroups of mild TBI Patients Revealed by Diffusion TensorImaging and Cluster Analysis

Chuanzhu Sun[1], Lijun Bai[1], Hao Yan[2,3], Shan Wang[1], and Xiaocui Wang[1]

[1]Department of Biomedical Engineering, the Key Laboratory of Biomedical Information Engineering of the Ministry of Education, Xi'an Jiaotong University, Xi'an, People's Republic of China, [2]Department of Linguistics, Xidian University, Xi'an, People's Republic of China, [3]Center for Language and Brain, Shenzhen Institute of Neuroscience, Shenzhen University, shenzhen, People's Republic of China

More than 75% of traumatic brain injuries (TBI) seeking medical attention are mild, and the outcome of mild TBI (mTBI) is heterogeneous. Currently we are in badly need of the methods of classifying mTBI into more homogeneous subgroups since there is not a sensitive and valid biomarker identified right now. In current study, we aim to investigate whether different subgroups exist in a large cohort patients and to predict neuropsychological outcome in the future.

3378 Computer 48

Charatization of Peritumoral Regions of Cerebral Tumor with Neurite Orientation Dispersion and Density Imaging (NODDI)

Yi-Cen Ting [1], Chou-Ming Cheng[2], and Tzu-Chen Yeh[3]

[1]Institute of Brain Science, National Yang-Ming University, Taipei, Taiwan, [2]Department of Medical Research and Education, Taipei Veterans General Hospital, Taipei Veterans General Hospital, Taipei, Taiwan, [3]Department of Radiology, Taipei Veterans General Hospital, Taipei, Taiwan

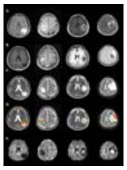

In this work, primary tumors of the central nervous system, including glioma and meningiomas, were studied with NODDDI. The parameters derived from NODDI was examined to differentiate peritumoral edema and characterize complex structural abnormalities using diffusion MRI (dMRI) of a clinical MRI scanners. As a result, a better understanding of this perplexity with the aid of modern imaging is clearly necessary to define the blurred tumor margins and confront the recurrences in long-term treatment.

Electronic Poster

Diffusion: Microstructure

Exhibition Hall — Monday 13:45 - 14:45

3379 — Computer 49

White matter microstructural properties are related to inter-individual differences in cognitive instability after sleep deprivation

yuanqiang zhu[1,2], lin liu[1], tian dai[1], ziliang xu[1], yibin xi[2], hong yin[2], and wei qin[1]

[1]xidian, xi'an, People's Republic of China, [2]xijing hospital, xi'an, People's Republic of China

ract-based spatial statistical analyses was used to investigate whether the individual differences in cognitive instability after SD was related to differences in WM structure. Resistant group exhibited significantly higher FA than vulnerable group, significant negative correlations were found between numbers of psychomotor vigilance task (PVT) lapses and FA in multiple regions. Our results also showed that 63% of individual variability in PVT lapse may be explained by variations in FA within superior longitudinal fasciculus and splenium of the corpus callosum. These findings suggested that cognitive instability after SD is closely associated with individual differences in WM integrity.

3380 — Computer 50

magna cum laude

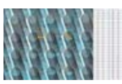

Axon diameter mapping using diffusion MR microscopy embedded in a Monte-Carlo based fingerprint approach

Delphine Estournet[1,2], Justine Beaujoin[1,2], Fabrice Poupon[2,3], Achille Teillac[1,2], Jean-François Mangin[2,3], and Cyril Poupon[1,2]

[1]CEA/I²BM/NeuroSpin/UNIRS, Gif-sur-Yvette, France, [2]Université Paris-Saclay, Orsay, France, [3]CEA/I²BM/NeuroSpin/UNATI, Gif-sur-Yvette, France

In this work, we demonstrate that Monte-Carlo simulations combined with fingerprint approaches can be used to develop decoding tools of the micro-structure using a dictionary learning approach. The validation has been done on a test object mimicking the mid-sagittal plane of a corpus callosum with axon diameters varying according to histological studies. The robustness of the decoding obviously depends on the richness of the dictionary, but, contrary to analytical approaches with highly non linear equations hard to fit practically, such MC approach do not have this kind of limitation, thus opening the way to decode more complex tissue cellular configurations.

3381 — Computer 51

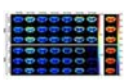

Microstructural Information from Modeling of the SDE and DDE MRI Signals in the Spinal Cord

Darya Morozov[1], Debbie Anaby[1], Inbar Seroussi[2], Nir Sochen[2], and Yoram Cohen[1,3]

[1]School of Chemistry, The Raymond and Beverly Sackler Faculty of Exact Sciences, Tel Aviv University, Tel Aviv, Israel, [2]School of Mathematical Sciences, The Raymond and Beverly Sackler Faculty of Exact Sciences, Tel Aviv University, Tel Aviv, Israel, [3]Sagol School of Neuroscience, Tel Aviv University, Tel Aviv, Israel

Various diffusion MRI approaches were suggested to study the complex water diffusion in neuronal tissues and gleaning microstructural information thereof. Nevertheless, to date, only few attempts were done to correlate between the microstructural features obtained from single diffusion encoding (SDE) and double diffusion encoding (DDE) MRI experiments. The main objective of the present study is to compare between the microstructural information obtained from both diffusion MRI methodologies, under similar experimental conditions, when performed on a fixed porcine spinal cord.

3382 — Computer 52

Biomarkers for fiber density: comparing Stejskal-Tanner diffusion encoding metrics with microscopic diffusion anisotropy from double-diffusion encoding imaging

Siawoosh Mohammadi[1,2,3], Isabel Ellerbrock[1], and Luke Edwards[2]

[1]Department of Systems Neuroscience, Medical Center Hamburg-Eppendorf, Hamburg, Germany, [2]Max Planck Institute for Human Cognitive and Brain Sciences, Leipzig, Germany, [3]UCL Institute of Cognitive Neurology, University College London

Different MRI biomarkers for fiber and myelin density have been proposed for MR g-ratio mapping, leaving open the question which biomarker is optimal. Here, we compare four different MRI biomarkers for fiber density using standard Stejeskal-Tanner diffusion encoding to the microscopic diffusion anisotropy (MA) measured by double-diffusion encoding. Thereby, we hypothesize that a better measure of the microscopic environment shows higher (and more significant) correlations to the MA metric. Our preliminary results showed that the marker by Kaden et al. (2016) shows higher correlation to MA than NODDI, suggesting it to be a better biomarker for fiber density.

3383 — Computer 53

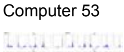

Double Diffusion Encoding vs Single Diffusion Encoding in Parameter Estimation of Biophysical Models in Diffusion-Weighted MRI

Santiago Coelho[1], Leandro Beltrachini[1,2,3], Jose M. Pozo[1], and Alejandro F. Frangi[1]

[1]Centre for Computational Imaging & Simulation Technologies in Biomedicine (CISTIB), Department of Electronic and Electrical Engineering, The University of Sheffield, Sheffield, United Kingdom, [2]School of Physics and Astronomy, Cardiff University, Cardiff, United Kingdom, [3]Cardiff University Brain Research Imaging Centre (CUBRIC), Cardiff University, Cardiff, United Kingdom

Biophysical tissue models are a solid tool for obtaining specific biomarkers with diffusion MRI. However, the assumptions they rely on are sometimes inaccurate and may lead to erroneous results. Some limitations of the Neurite Orientation Dispersion and Density Imaging (NODDI) model are tackled by NODDIDA (NODDI with Diffusivities Added), at the cost of an extended acquisition protocol. Here we adapt NODDIDA to a Double Diffusion Encoding scheme to improve the parameter estimation for reduced acquisition protocols. We demonstrate through *in silico* experiments that under similar experimental conditions, this novel approach increases both the accuracy and precision of the parameter estimates.

3384 Computer 54

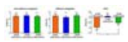

Oscillating gradient improves the sensitivity of diffusion functional MRI

Dan Wu[1], Hanbing Lu[2], Yihong Yang[2], and Jiangyang Zhang[3]

[1]Radiology, Johns Hopkins University School of Medicine, BALTIMORE, MD, United States, [2]Neuroimaging Research Branch, National Institute on Drug Abuse, Intramural Research Program, National Institutes of Health, Baltimore, MD, United States, [3]Radiology, New York University School of Medicine, NY, United States

Synopsis: Diffusion functional MRI (DfMRI) has been proposed to detect neuronal activations more directly than BOLD-fMRI, but its sensitivity to cell swelling associated with neuronal activities remains less known. Numerical simulations suggest that oscillating gradient spin echo (OGSE) diffusion MRI is more sensitive to changes in cell size than conventional pulsed gradient spin echo (PGSE) diffusion MRI. In adult rat brain DfMRI experiments with forepaw stimulation, ADC measured by OGSE showed significant reductions during stimulation, and the reductions were significantly larger than those measured by PGSE, suggesting OGSE may be more sensitive to cell swelling associated with neuronal activation than PGSE.

3385 Computer 55

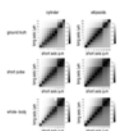

Effect of Realistic Timing Parameters on a Microscopic Diffusion Anisotropy Measure

Marco Lawrenz[1,2] and Jürgen Finsterbusch[1,2]

[1]Department of Systems Neuroscience, University Medical Center Hamburg-Eppendorf, Hamburg, Germany, [2]Neuroimage Nord, University Medical Centers Hamburg-Kiel-Lübeck, Hamburg-Kiel-Lübeck, Germany

Double diffusion encoding experiments with two weighting periods applied successively offer access to microscopic tissue properties and can provide information complementary to diffusion tensor imaging. The MA index derived from such measurements with long mixing times, depends on the cell eccentricities, i.e. the microscopic diffusion anisotropy, and can be determined in the human brain. However, its derivation is based on ideal timing parameters, infinitely short gradient pulses and long diffusion and mixing times that cannot be gained in practice. In this study, the effect of realistic timing parameters on the MA of restricted diffusion is investigated with Monte Carlo simulations.

3386 Computer 56

Quantification of pore size distributions using double diffusion encoding: assessment of the feasibility on a clinical system

Gaetan Duchene[1], Frank Peeters[1], Jorge Abarca-Quinones[1], and Thierry Duprez[1]

[1]Medical imaging dept, St-Luc University hospital, Université Catholique de Louvain, Brussels, Belgium

Recently, Double Diffusion Encoding (DDE) has been proposed for quantification of pore size distributions in a voxel or a Region Of Interest. Although the technique has been validated on animals with experimental MR systems, its translation to human scanners is challenging, mainly because of the limited gradient strength available on clinical systems. In this work, we present a validation of DDE on a clinical scanner on a biological phantom (asparagus). Furthermore, we restricted the acquisition time to 16 minutes which remains acceptable in clinical conditions.

3387 Computer 57

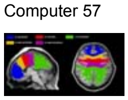

In-vivo Bundle-Specific Axon Diameter Distributions Estimation across the Corpus Callosum

Muhamed Barakovic[1], David Romascano[1], Gabriel Girard[1], Maxime Descoteaux[1,2], Jean-Philippe Thiran[1,3], and Alessandro Daducci[1,3,4]

[1]Signal Processing Lab (LTS5), École Polytechnique Fédérale de Lausanne, Lausanne, Switzerland, [2]Sheerbrooke Connectivity Imaging Laboratory (SCIL), University of Sheerbrooke, Canada, [3]University Hospital Center (CHUV) and University of Lausanne (UNIL), Switzerland, [4]Department of Computer Science, University of Verona, Italy

Over the last decade microstructure imaging has become commonly endorsed to estimate quantitative features of neuronal tissue. However, those techniques estimate the microstructure only locally. Microstructure informed tractography was recently proposed to bolster microstructure estimates by accounting for the structure of the white matter bundles. The purpose of this study was to extend this novel technique for evaluating bundle-specific axon diameter distributions and investigate bundle-specific properties in the human brain. The experiment was performed on the MGH adult HCP dataset. The findings suggest potential application in the estimation of the axon diameter distribution along white matter bundles in whole-brain tractograms.

3388 Computer 58

Phase retrieval from q-space imaging for diffusion pore imaging

Kerstin Demberg[1], Frederik Bernd Laun[1,2], Peter Bachert[1], Dieter Höpfel[3], and Tristan Anselm Kuder[1]

[1]Medical Physics in Radiology, Deutsches Krebsforschungszentrum (DKFZ, German Cancer Research Center), Heidelberg, Germany, [2]Institute of Radiology, University Hospital Erlangen, Erlangen, Germany, [3]Electrical Engineering & Information Technology, Karlsruhe University of Applied Science, Karlsruhe, Germany

Diffusion pore imaging enables the detection of the average shape of arbitrary closed pores in an imaging volume element. Until now, an experimentally challenging phase measurement, either by measuring with a long-narrow gradient profile or by employing double diffusion encodings, was a prerequisite to obtain the full information on the Fourier transform of the pore image. In this study, we present a first experiment, where the phase information is recovered alone from the magnitude information acquired by q-space imaging. To solve this phase problem, we adopted a phase retrieval algorithm that is widely applied to X-ray diffraction data.

3389 Computer 59

Analytical solution for restricted diffusion in multilayered cylinders using the extended Multiple Correlation Function approach.

Kevin GINSBURGER[1,2], Jean-François MANGIN[2,3], and Cyril POUPON[1,2]

[1]I2BM / Neurospin / UNIRS, CEA, Gif-sur-Yvette, France, [2]Université Paris-Saclay, Orsay, France, [3]I2BM / Neurospin / UNATI, CEA, Gif-sur-Yvette, France

In this work, we used the extended Multiple Correlation Function (MCF) method to derive analytical expressions of the NMR signal in multilayered cylinder geometries for an arbitrary direction of the magnetic field gradient. Each layer of the cylinder is characterized by a diffusion coefficient and a relaxation time and each boundary between adjacent layers is characterized by a value of permeability in order to allow the modeling of the multilayered structure of axons surrounded by its myelin sheat.

3390 Computer 60

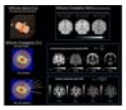

Comparison of diffusion propagator imaging metrics for accurate microstructure characterization in clinically acceptable scan times

Luis Miguel Lacerda[1,2], Gareth John Barker[2], and Flavio Dell'Acqua[2]

[1]Institute of Child Health, University College London, London, United Kingdom, [2]Neuroimaging, King's College London, London, United Kingdom

Despite the abundance of models to describe the diffusion propagator, its usefulness has not yet been explored in a clinical/clinical research setting. In this study, we have compared global diffusion propagator imaging metrics to recently described measures of anisotropy and probability profiles at different displacement scales to characterise microstructure. Moreover, we have shown that these metrics offer complementary information to the ones currently established. Finally we have also acquired a "Reference Dataset" with several different diffusion weightings and demonstrated that by choosing the right combination, accurate reconstruction of both types of metrics is possible for clinically acceptable scan times.

3391 Computer 61

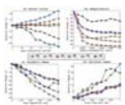

Validation of Sensitivity of Fast Kurtosis Measurements to Tissue Microstructural Changes

Ting Gong[1], Mu Lin[1], Hongjian He[1], Qiuping Ding[1], and Jianhui Zhong[1]

[1]Center for Brain Imaging Science and Technology, Department of Biomedical Engineering, Zhejiang University, Hangzhou, People's Republic of China

Diffusional kurtosis imaging (DKI) is a significant extension of diffusion tensor imaging, providing sensitive biomarkers to diseases at the cost of lengthy acquisition and post-processing time. Fast DKI method operating with kurtosis tensor and based on axially symmetric approximation was then proposed to overcome the disadvantage. To explore the clinical utility of fast DKI, a Monte Calo simulation was conducted on a tissue model to validate the sensitivity of fast kurtosis measurements to four microstructural changes. The results suggest that fast DKI method is reliable with reduced scan time but considerable sensitivity to microstructural Changes frequently occurred in neurological diseases.

3392 Computer 62

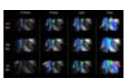

The spatial vs. angular resolution trade-off in diffusion MRI explored ex vivo at 9.4T

Giorgia Grisot[1,2], Joseph M. Mandeville[2], and Anastasia Yendiki[2]

[1]Harvard-MIT Health Sciences and Technology, Massachusetts Institute of Technology, Cambridge, MA, United States, [2]Athinoula A. Martinos Center for Biomedical Imaging, MGH, Charlestown, MA, United States

The time constraints of in vivo diffusion MRI require a compromise to be made between spatial and angular resolution. Given the lack of ground truth on the configuration of human brain connections, determining the optimal operating point along this trade-off is still an open problem. We use high-SNR ex vivo human data at microscopic resolution to study the effect of spatial and angular resolution on dMRI tractography accuracy. Our findings show that voxel size has a much more dramatic effect on tractography reconstruction of challenging white matter configurations than the number of gradient directions.

3393 Computer 63

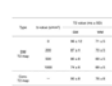

Measurement of the Diffusion-Selective T2 value in the Human Brain Using Diffusion-Weighted T2 map

Takuya Aoike[1], Noriyuki Fujima[2], Masami Yoneyama[3], Suzuko Aoike[1], Hiroyuki Sugimori[4], Kinya Ishizaka[1], and Kohsuke Kudo[2]

[1]Department of Radiological Technology, Hokkaido University Hospital, Sapporo, Hokkaido, Japan, [2]Department of Diagnostic and Interventional Radiology, Hokkaido University Hospital, [3]Philips Electronics Japan, [4]Faculty of Health Sciences, Hokkaido University

The purpose of this study was to assess the variation of T2 values by T2 map with the pre-pulse of diffusion gradient (=DW-T2 map). T2 value of GM was gradually decreased as b-value increased. From this result, water diffusivity based selective removal of tissue component such as perfusion fraction or extracellular extravascular space can be obtained using DW-T2 map technique. This technique can reveal the more detain in the human brain tissue characteristics.

3394 Computer 64

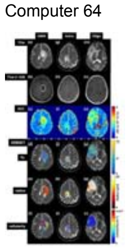

Quantifying microstructure in low and high-grade brain tumours using VERDICT MRI

Thomas A Roberts[1], Harpreet Hyare[2,3], Ben Hipwell[1], Andrada Ianus[4], James O Breen-Norris[1], Eleftheria Panagiotaki[4], David Atkinson[2], Shonit Punwani[2], Jeremy Rees[5], Sebastian Brandner[6], Daniel C Alexander[4], and Simon Walker-Samuel[1]

[1]Centre for Advanced Biomedical Imaging, University College London, London, United Kingdom, [2]Centre for Medical Imaging, Division of Medicine, University College London, London, United Kingdom, [3]UCL Institute of Neurology, Department of Brain Repair and Rehabilitation, London, United Kingdom, [4]Centre for Medical Image Computing, Department of Computer Science, University College London, London, United Kingdom, [5]National Hospital for Neurology and Neurosurgery, London, United Kingdom, [6]Division of Neuropathology, Institute of Neurology, University College London, United Kingdom

VERDICT (Vascular, Extracellular, and Restricted Diffusion for Cytometry in Tumours) MRI is a diffusion imaging technique which has shown promise in revealing information about tumour microstructure beyond ADC measures and structural imaging. We report the first application of VERDICT to human brain tumours. In this feasibility study, we characterise a mixed group of brain tumours using VERDICT, which includes a range of both low and high-grade gliomas; compare the VERDICT parameter maps with ADC maps, post-contrast T1w images and histological grading; and examine the repeatability of the technique.

3395 Computer 65

Rat brain development assessed by high-field neurite orientation dispersion and density imaging

Nicolas Kunz[1], Stéphane V Sizonenko[2], Rolf Gruetter[1,3], Petra S Hüppi[2], and Yohan van de Looij[1,2]

[1]Laboratoire d'imagerie fonctionnelle et métabolique, Ecole Polytechnique Fédérale de Lausanne, Lausanne, Switzerland, [2]Département développement et croissance, Université de Genève, Geneva, Switzerland, [3]Département de radiologie, Geneva and Lausanne, Switzerland

Diffusion tensor imaging (DTI) has been widely used to study rodent brain development. Nevertheless, the parameters derived from DTI are sensitive to, but non-specific to, the tissue's microstructure. Recently, NODDI (neurite orientation dispersion and density imaging) has been proposed. We aimed to estimate the real input of NODDI derived parameters in rodent brain development. ODI appears more accurate and specific to reflect GM (increase with dendritic arborization) and WM (decrease with myelination) development than FA and could be a very important parameter in the assessment of perinatal brain injuries. Conclusion about the other NODDI estimates requires further experiments.

3396 Computer 66

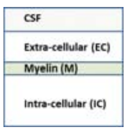

Disentangling myelination and axonal density using NODDI and mcDESPOT – a multimodal microstructure imaging approach

Samira Bouyagoub[1], Nicholas G. Dowell[1], Charlotte L. Clarke[1], Tobias C. Wood[2,3], Hui Zhang[4], and Mara Cercignani[1]

[1]Clinical Imaging Sciences Centre, Brighton and Sussex Medical School, Brighton, United Kingdom, [2]Neuroimaging, IoPPN, King's College London, London, United Kingdom, [3]Wellcome Trust Consortium for Neuroimmunology of Mood Disorders and Alzheimer's Disease, London, United Kingdom, [4]Centre for Medical Image Computing, University College London, London, United Kingdom

There is an increasing demand for specific tissue microstructure markers that can be related to demyelination and axonal loss. Quantitative MRI techniques are sensitive to microscopic changes but tend to be non-specific. We propose to combine NODDI, a popular MRI diffusion technique, with mcDESPOT, a multi-component relaxation analysis technique, to obtain separate estimates of the volumes of myelin, extra-cellular and intra-cellular spaces. This multimodal MR approach opens the possibility to disentangle changes to myelination and axonal density with the exciting prospect of achieving in vivo histology.

3397 Computer 67

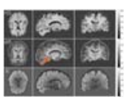

Negentropy: non-Gaussian characterization for Diffusion Spectrum Imaging

Gabriel Varela-Mattatall[1], Alexandra Tobisch[2,3], Rüdiger Stirnberg[2], Steren Chabert[4], Tony Stöcker[2,3], Cristian Tejos[1,5], and Pablo Irarrazaval[1,5]

[1]Biomedical Imaging Center, Santiago, Chile, [2]German Center of Neurodegenerative Diseases (DZNE), Bonn, Germany, [3]University of Bonn, Bonn, Germany, [4]Department of Biomedical Engineering, Pontificia Universidad Católica de Valparaíso, Valparaíso, Chile, [5]Department of Electrical Engineering, Pontificia Universidad Católica de Chile, Santiago, Chile

Measuring non-Gaussianity in the diffusion signal has revealed new possibilities for discovering new biomarkers for clinical applications. Therefore, it results desirable to incorporate and quantify the non-Gaussian trait of the diffusion propagator in Diffusion Spectrum Imaging. Unfortunately, the established index known as Kurtosis is sensitive to noise, making it unfeasible to obtain from the noisier, but higher resolution propagator. In this work, we propose an alternative index known as Negentropy. We demonstrate from noisy simulations and in-vivo DSI data the robustness of the Negentropy index against Kurtosis.

3398 Computer 68

Detection of distinct tract-specific axon diameter and density estimates in the in vivo human brain using TractCaliber MRI

Susie Y Huang[1], Thomas Witzel[1], Qiuyun Fan[1], Barbara Wichtmann[2], Aapo Nummenmaa[1], Lawrence L Wald[1], and Eric Klawiter[3]

[1]Athinoula A. Martinos Center for Biomedical Imaging, Department of Radiology, Massachusetts General Hospital, Harvard Medical School, Charlestown, MA, United States, [2]Computer Assisted Clinical Medicine, Medical Faculty Mannheim, Heidelberg University, Mannheim, Germany, [3]Department of Neurology, Massachusetts General Hospital, Harvard Medical School, Boston, MA, United States

In this work, we apply the TractCaliber approach to a group of healthy subjects and show that distinct tract-specific estimates of axon diameter may be obtained in different white matter tracts in the normal human brain. Larger diameter axons are consistently estimated in the corticospinal tracts and are shown to be distinct from those in the cingulum, an adjacent and orthogonal white matter tract. The development of robust tract-specific axon diameter-weighted maps may be useful for refining existing tractography algorithms.

3399 Computer 69

magna cum laude

A unified signal readout for reproducible multimodal characterisation of brain microstructure

Francesco Grussu[1], Marco Battiston[1], Ferran Prados[1,2], Torben Schneider[1,3], Enrico Kaden[4], Sébastien Ourselin[2], Rebecca S. Samson[1], Daniel C. Alexander[4], and Claudia A. M. Gandini Wheeler-Kingshott[1,5,6]

[1]UCL Institute of Neurology, Queen Square MS Centre, University College London, London, United Kingdom, [2]Translational Imaging Group, Centre for Medical Image Computing, Department of Medical Physics and Biomedical Engineering, University College London, London, United Kingdom, [3]Philips UK, Guildford, Surrey, United Kingdom, [4]Centre for Medical Image Computing, Department of Computer Science, University College London, London, United Kingdom, [5]Department of Brain and Behavioural Sciences, University of Pavia, Pavia, Italy, [6]Brain MRI 3T Mondino Research Center, C. Mondino National Neurological Institute, Pavia, Italy

Multimodal imaging is very promising for characterising brain microstructure in vivo, but it is usually performed employing a variety of signal readouts, which disrupts the spatial correspondence of the multimodal features. Here we demonstrate a multimodal imaging protocol for detailed characterisation of brain microstructure with unified single-shot EPI readout. Our aim is to provide macromolecular volume via inversion recovery spin echo, neurite morphology via diffusion imaging in close spatial alignment and thus to combine those for estimating myelin g-ratio. We show that our protocol enables the evaluation of parametric maps with high reproducibility that capture biological differences among healthy subjects.

3400 Computer 70

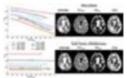

Probing Microstructure of Brain Tumor: A NODDI Study

Shin Tai Chong[1], Hung-Wen Kao[2], Chien-Yuan Eddy Lin[3,4], Chiao-Chi Chen[5], Ching-Po Lin[1], and Chen Chang[5]

[1]Institute of Neuroscience, National Yang-Ming University, Taipei city, Taiwan, [2]Department of radiology, Tri-Service General Hospital, National Defense Medical Center, Taiwan, [3]GE Healthcare, Taipei, Taiwan, [4]GE Healthcare MR Research China, Beijing, People's Republic of China, [5]Institute of Biomedical Sciences, Academia Sinica, Taiwan

We hypothesized that the model-based diffusion model, Neurite Orientation Dispersion and Density Imaging (NODDI), could help probing microstructures of brain tumos in different types and gradings. The model perfomed better than a conventional diffusion model in differetiating meningiomas and gliomas in different grades while the two models showed significant differences of the diffusion indices between meningiomas and gliomas. In the NODDI analysis, both VF_{ic} and VF_{ec} show great potential to probe the cellularity of brain tumors.

3401 Computer 71

Ex-vivo visualization of the human trigeminal pathways using 11.7T diffusion MRI and unique microscopy data

Dylan Henssen[1,2], Jeroen Mollink[1,3], Erkan Kurt[2], Jules Janssen Daalen[4], Robert van Dongen[5], Ronald Bartels[2], Tamas Kozicz[1], and Anne-Marie van Cappellen van Walsum[1]

[1]Department of Anatomy, Donders Institute for Brain, Cognition & Behaviour, Radboud University Medical Center, Nijmegen, Netherlands, [2]Department of Neurosurgery, Radboud University Medical Center, Nijmegen, Netherlands, [3]Oxford Centre for Functional MRI of the Brain, University of Oxford, United Kingdom, [4]Faculty of Medical Sciences, Radboud University, Nijmegen, Netherlands, [5]Department of Anesthesiology, Pain and Palliative Care, Radboud University Medical Center, Nijmegen, Netherlands

To optimize neuromodulation therapy of orofacial pain, a more profound insight in the trigeminal pathways in the human brainstem is of crucial importance. Using ex-vivo, 11.7T magnetic resonance imaging, polarized light microscopy and myelin staining methods, both the ventral and dorsal trigeminothalamic tracts can be visualized in humans. The combination of these visualization techniques strengthens the validity of these findings although the number of specimens forms a limitation. Future research must show whether these results are reproducible in more human brains and whether the described tracts could lead to new neuromodulation targets for the treatment of orofacial pain.

3402 Computer 72

Orientation-invariant and non-parametric Axon Diameter Distribution mapping using PGSE and regularized discrete linear modeling

David Romascano[1], Muhamed Barakovic[1], Anna Auría[1], Tim Bjørn Dyrby[2,3], Jean-Philippe Thiran[1,4], and Alessandro Daducci[1,4,5]

[1]Signal Processing Laboratory 5 (LTS5), EPFL, Lausanne, Switzerland, [2]Danish Research Centre for Magnetic Resonance, Center for Functional and Diagnostic Imaging and Research, Copenhagen University Hospital Hvidovre, Hvidovre, Denmark, [3]Department of Applied Mathematics and Computer Science, Technical University of Denmark, Lyngby, Denmark, [4]University Hospital Center (CHUV) and University of Lausanne (UNIL), Lausanne, Switzerland, [5]Computer Science department, University of Verona, Italy

Axon diameter distributions (ADDs) change during brain development and are altered in several brain pathologies. Mapping ADDs non-invasively using dMRI could provide a useful biomarker, but existing methods are either parametric, orientation-dependent, summarize the whole ADD as a single measure or use non-standard protocols. We propose to estimate the ADD from an orientation-invariant PGSE protocol optimized for axon diameter sensitivity, using a discrete linear model with smoothness and sparsity regularization. To our knowledge, we are the first to show that PGSE sequences can be used to extract orientationally invariant and non-parametric ADD estimates.

Electronic Poster

Diffusion: Body

Exhibition Hall Monday 13:45 - 14:45

3403 Computer 73

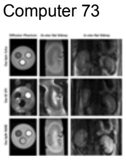

Diffusion-Weighted Split-Echo RARE Imaging Free Of Geometric Distortion for Renal MRI at Ultrahigh Fields

Joao Periquito[1], Katharina Paul[1], Till Huelnhagen[1], Yiyi Ji[1], Min-Chi Ku[1], Kathleen Cantow[2], Erdmann Seeliger[2], Bert Flemming[2], Dirk Grosenick[3], Andreas Pohlmann[1], and Thoralf Niendorf[1,4]

[1]Berlin Ultrahigh Field Facility (B.U.F.F.), Max Delbrueck Center for Molecular Medicine, Berlin, Germany, [2]Institut für Vegetative Physiologie, Charité - Universitätsmedizin Berlin, Berlin, Germany, [3]Physikalisch-Tecnische Bundesanstalt (PTB), Berlin, Germany, [4]Experimental and Clinical Research Center (ECRC), a joint cooperation between the Charité Medical Faculty and the Max Delbrueck Center for Molecular Medicine in the Helmholtz Association, Berlin, Germany

T_2^* mapping does not fully represent renal tissue oxygenation. Diffusion-weighted imaging (DWI) can provide information about confounding factors, which can be used to correct T_2^*. The most widely used DWI technique SE-EPI is sensitive to magnetic field inhomogeneities and hence prone to geometric distortions. In this work we propose a diffusion-weighted Rapid Acquisition Refocusing Enhancement (RARE) variant for DWI of the rat kidney free of geometric distortions. Phantom experiments validated the diffusion weighting implementation in the common RARE sequence. *Ex-vivo* and *in-vivo* experiments using diffusion-weighted RARE showed no geometric distortions at 9.4 Tesla.

3404 Computer 74

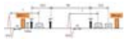

Improved algorithm for navigator-based free breathing cardiac diffusion tensor imaging

Fang Dong[1] and Shi Cheng[1]

[1]Siemens Shenzhen Magnetic Resonance Ltd., ShenZhen, People's Republic of China

Cardiac diffusion tensor imaging is an effective way to depict the fiber structure of the myocardium. A navigator(NAV)-based stimulated-echo (STEAM) method was proposed by Nielles-Vallespin to obtain cDTI in vivo. However, its use of a biofeedback process where the subjects had to adapt their breathing pattern in real-time can hinder its clinical implementation. In this abstract, we optimized the NAV accept/reject algorithm, using which the scanning efficiency and the image SNR were both largely improved. Therefore, our work laid a great foundation for the clinical use of free breathing cDTI in the future.

3405 Computer 75

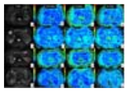

Application of diffusion kurtosis MR imaging in characterization of renal cell carcinomas with different pathological types and grades

Jie Zhu[1], Ying Sa Li[1], Jie Xiao Luo[1], Dan Dan Zheng[2], and Min Chen[1]

[1]Beijing Hospital, Beijing, People's Republic of China, [2]GE healthcare, MR research China, People's Republic of China

Identification of subtypes and pathological grades of renal cell carcinoma (RCC) prior to treatment has clinical significance in determining a treatment strategy and evaluating prognosis. In our research, we detected microstructural differences of RCC by using diffusion kurtosis imaging (DKI). The results showed that DKI had good inter- and intra-observer reproducibility of RCC as a new reliable noninvasive biomarker. Kurtosis metrics showed statistical differences between RCC and contralateral renal parenchyma, among the subtypes of RCC, and between low- and high- grade clear cell RCCs. Thus, DKI has the potential application in depicting the microstructural characteristics of RCC.

3406 Computer 76

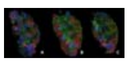

Origin of diffusion anisotropy in human kidney: a combined DTI and IVM study

Sophie van Baalen[1], Bart Vroling[1], Martijn Froeling[2], and Bennie ten Haken[1]

[1]Faculty of Science and Technology, University of Twente, Enschede, Netherlands, [2]Radiology, University Medical Centre Utrecht, Utrecht, Netherlands

To visualize the anisotropy of diffusion and pseudodiffusion, we have performed a two-tensor fit (**D** and **D***) on IVIM data in healthy volunteers. We have performed tractography on both tensors and compared the results with tractography perfomed using a conventional DTI tensor fit. Tracking was possible using both D and the D* derived tensors and resulted in patterns similar to conventional tractography. We conclude that diffusion and pseudodiffusion both have an anisotropic component that can be visualized using tractography, which indicates that they both likely contribute to the coherent diffusion anisotropy that is detected in conventional monoexponential DTI.

3407 Computer 77

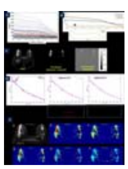

ICA based filtering of IVIM-DWI data to improve fidelity of parametric diffusion maps in breast cancer patients

Dattesh D Shanbhag[1], Tetsuya Wakayama[2], Reem Bedair[3], Andrew J Patterson[4], Fiona J Gilbert[3], Rakesh Mullick[1], and Martin J Graves[3,4]

[1]GE Global Research, Bangalore, India, [2]GE Healthcare, Hino, Japan, [3]Department of Radiology, University of Cambridge School of Clinical Medicine, Cambridge, United Kingdom, [4]Department of Radiology, Addenbrookes Hospital, Cambridge, United Kingdom

IVIM-DWI data can be potentially corrupted by eddy currents, susceptibility artifacts, motion and image reconstruction methods. We hypothesized that artifacts in IVIM imaging could be separated from true diffusion decay using an independent component analysis (ICA) methodology. In this work , we demonstrate that with ICA based filtering of raw IVIM data, transients in IVIM data are removed, with consequent improvement in IVIM model fit quality and reduction in saturated values in pseudo-diffusion D*maps. This should therefore improve confidence in interpreting IVIM parametric maps in clinical practice.

3408 Computer 78

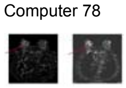

A multi-directional methodology for discriminating benign from malignant lesions on DWI for women with dense breasts

Alan Penn[1], Barry Reich[1], Etta Pisano[2], Vandana Dialani[3], Elodia Cole[2], David Brousseau[4], Milica Medved[5], Gregory S. Karczmar[5], Guimin Gao[5], and Hiroyuki Abe[6]

[1]Alan Penn & Assoc., Inc., Rockville, MD, United States, [2]Beth Israel Deaconess Medical Center, [3]Radiology, Beth Israel Deaconess Medical Center, [4]California Hospital Medical Center, [5]University of Chicago, [6]Radiology, University of Chicago

We describe a new methodology for discriminating benign from malignant breast lesions on DWI for women with dense breasts and show that the new methodology results in statistically significant improvement over standard ADC methods. The methodology uses computer models that can be constructed independently from the three directional DWI signals or from the trace signal. Preliminary results show improved discrimination is obtained using the multi-directional models when compared to using the trace. The methodology can be adapted for computer-aided-detection by tiling the image, independently marking each tile with areas of suspicion, and constructing a mosaic from the marked tiles.

3409 Computer 79

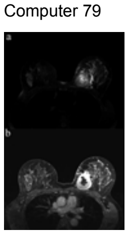

Optimization of Intravoxel Incoherent Motion Measurement in Diffusion-Weighted Imaging of Breast Cancer

Wengjing Chen[1], Juan Zhang[2], Dan Long[2], Zhenchang Wang[3], and Jianming Zhu[1]

[1]Biomedical Engineering, China Jiliang University, Hangzhou, People's Republic of China, [2]Radiology, Zhejiang Cancer Hospital, Hangzhou, People's Republic of China, [3]Radiology, Beijing Friendship Hospital, Beijing, People's Republic of China

The purpose was to use intra-voxel incoherent motion (IVIM) measurement in DWI to distinguish benign from malignant breast tissues. IVIM-derived parameter maps D, f, and D* were computed using segmented fitting method with proper threshold b-value. The region of interests were avoided the area of calcification. With pathological diagnosis as the gold standard, receiver operating characteristic (ROC) curves for three parameters and $f \times D^*$ reflect that the area under the curve (AUC) of D and $f \times D^*$ are 0.862 and 0.726, respectively. It suggested that these two parameters have high significance for the diagnosis of breast cancer lesions.

3410 Computer 80

Diffusion weighted MR imaging–derived histogram Metrics for quantitative assessment of response to neoadjuvant chemoradiotherapy in local advanced rectal cancer: Initial Experience and Comparison between Single-Section and Volumetric Analyses

Yanfen Cui[1], Xiaotang Yang [1], and Yong Zhang[2]

[1]Shanxi Province Tumor Hospital, Taiyuan, People's Republic of China, [2]MR Advanced Application and Research Center, GE Healthcare China, People's Republic of China

This retrospective study was to determine the diagnostic accuracy of apparent diffusion coefficient (ADC) values to assess the response to CRT in patient with local advanced rectal cancer by using histogram analysis derived from single-section (SS) and whole-tumor volume (WTV) regions of interest (ROIs). and found that Post-CRT ADC histogram metrics yield greater accuracy in discrimination between good and poor responders, especially in improving the specificity, compared with the mean ADC values.

3411 Computer 81

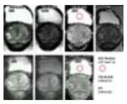

Distortionless diffusion weighted imaging of the prostate using a multi-shot Turbo Split Spin Echo BLADE sequence with bipolar diffusion gradients

Bart WJ Philips[1], Katharina Paul[2], Thoralf Niendorf[2], and Tom WJ Scheenen[1]

[1]Radiology and Nuclear Medicine, Radboud University Medical Centre Nijmegen, Nijmegen, Netherlands, [2]Berlin Ultrahigh Field Facility (BUFF), Max-Delbrueck-Center for Molecular Medicine in the Helmholtz Association, Berlin, Germany

Diffusion weighted imaging is an important modality in assessing and detecting prostate cancer, but often suffers from distortion artifact introduced by the EPI readout. We propose a TSE-BLADE split-echo sequence that has the potential for obtaining non-distorted diffusion weighted imaging of the prostate, while obtaining accurate ADC estimations. It is shown to be robust to motion and phase induced artifacts that pester multi-shot diffusion weighted imaging, in phantom measurements and initial patient results.

3412 Computer 82

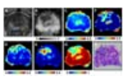

Multiparametric MRI-Defined Prostate Cancer Includes Heterogeneous Pathologies

Qingsong Yang[1], Ze-Zhong Ye[2], Joshua Lin[3], Peng Sun[4], Chunyu Song[5], Yasheng Zhu[6], Jianping Lu[1], and Sheng-Kwei Song[5]

[1]Department of Radiology, Changhai Hospital, Shanghai, China, shanghai, People's Republic of China, [2]Chemistry, Department of Chemistry, Washington University, St. Louis, MO, United States, [3]Department of Biology, Washington University, St. Louis, MO, United States, [4]Department of Radiology, Washington University, St. Louis, MO, United States, [5]Department of Biomedical Engineering, Washington University, St. Louis, MO, United States, [6]Department of Urology, Changhai Hospital, Shanghai, China

Due to the overlapping apparent diffusion coefficient of prostate cancer (PCa), inflammation, and benign prostatic hyperplasia (BPH), mpMRI commonly results in false-positive PCa diagnosis. Based on the histology of whole mount section from prostatectomy, heterogeneous pathologies was clearly seen in the mpMRI-defined cancer region. Our recently-developed diffusion MRI histology (D-Histo) approach successfully differentiated and quantified PCa, inflammation and BPH. We report mpMRI and D-Histo results on 178 PCa-suspicious patients to demonstrate the causes of mpMRI false-positive PCa diagnosis.

3413 Computer 83

Evaluation of Different Diffusion Models and Different B-value Ranges in the Detection of Peripheral Zone Prostate Cancer Using B-values up to 4500 s/mm2

Xiangde Min[1], Zhaoyan Feng[1], Liang Wang[1], and Zhongping Zhang[2]

[1]Tongji Medical College, Huazhong University of Science & Technology, Wuhan, People's Republic of China, [2]GE Healthcare China, Guangzhou 510080, China

We performed multi-b value diffusion-weighted imaging (DWI) to compare four phenomenological models (mono-exponential, bi-exponential, stretched exponential, and diffusion kurtosis imaging) with in vivo prostate cancer DWI data. A secondary aim is to compare results for different b-value ranges. The result showed that ADC derived from conventional mono-exponential model high b value (about 3200s/mm2) is an optional parameter for peripheral zone prostate cancer detection.

3414 Computer 84

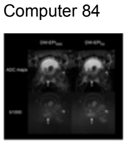

Feasibility of Accelerated Simultaneous Multi-Slice Diffusion-weighted MR Imaging of the Prostate

Jakob Weiss[1], Petros Martirosian[2], Jana Taron[3], Ahmed E Othman[3], Thomas Kuestner[4], Michael Erb[5], Jens Bedke[6], Fabian Bamberg[3], Konstantin Nikolaou[3], and Mike Notohamiprodjo[3]

[1]Diagnostic and Interventional Radiology, University of Tuebingen, Tuebingen, Germany, [2]Section on Experimental Radiology, University of Tuebingen, [3]Diagnostic and Interventional Radiology, University of Tuebingen, [4]University of Stuttgart, [5]Department of Biomedical Magnetic Resonance, University of Tuebingen, [6]Department of Urology, University of Tuebingen

Diffusion-weighted (DW) MRI of the prostate has increased the diagnostic accuracy for the detection of prostate cancer. However, acquisition time of DWI is still relatively long. Therefore, we evaluated the feasibility of simultaneous multi-slice (SMS) DWI for accelerated MRI of the prostate. Qualitative and quantitative image analyses in phantom, volunteer and patient measurements revealed similar image quality for DWI_{SMS} as compared to standard DWI sequences. Thus, DWI_{SMS} seems feasible for clinical routine in order to optimize patient throughput and economic efficiency, which is desirable, due to the recent implementation of prostate MRI into clinical guidelines and the expected increase in patient numbers.

3415 Computer 85

Effects of Echo Time on Diffusion Quantification of Prostate

Zhaoyan Feng[1], Xu Yan[2], Xiangde Min[1], and Liang Wang[1]

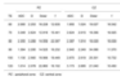

[1]Department of Radiology, Tongji Hospital, Tongji Medical College, Huazhong University of Science and Technology, Wuhan, People's Republic of China, [2]MR Collaboration NE Asia, Siemens Healthcare, Shanghai, People's Republic of China

We performed multi-b value and multi-TE diffusion imaging with two repetition on healthy human prostate to evaluate the influence of TE on reproducibility and quantification of IVIM diffusion model. The result showed that the Dstar and f parameters of IVIM model had high CVs and particularly high variability, while conventional ADC and D showed high reproducibility and a moderate TE-dependency in the peripheral zone and mild TE-dependency in the central zone. This work suggests that using diffusion parameters as quantitative biomarkers should consider the reproducibility and TE-dependency in clinical studies.

3416 Computer 86

Relationship between diffusion kurtosis imaging and RSI: application to prostate cancer

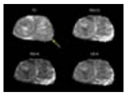

Roshan Karunamuni[1], Joshua Kuperman[1], Tyler Seibert[1], Natalie Schenker[1], Rebecca Rakow-Penner[1], Jose Teruel Antolin[1], Pal Erik Goa[2], David Karow[1], Anders Dale[1], and Nathan White[1]

[1]University of California San Diego, San Diego, CA, United States, [2]NTNU, Trondheim, Norway

This study explored the relationship between restriction spectrum imaging (RSI) and diffusion kurtosis imaging. Regions of interest for suspicious lesions and background tissue were identified in four patients with PIRADS 5 lesions. Kurtosis was estimated using either the signal fractions obtained from the RSI fit or the cumulant expansion for the NMR diffusion signal. A strong relationship was observed between RSI-derived restricted signal fraction and RSI-derived kurtosis. The performance of these two metrics was comparable in discriminating between suspicious lesions and background prostate tissue, and both outperformed the cumulant expansion approximation to kurtosis.

3417 Computer 87

Detection of peripheral zone prostate cancer using diffusion-weighted intravoxel incoherent motion imaging

Jin Shang[1], Hui Zhang[1], Miaoling Li[1], Jian Yang[1], and Rong Wang*[1]

[1]Department of radiology, the first affiliated hospital of medical college, Xi'an Jiaotong University, Xi'an, People's Republic of China

DWI has been proven to improve prostate cancer detection, and it reflects and measures the diffusion of water molecules within biological tissues due to thermal Brownian motion. However, to improve the significance of DWI, it is necessary to evaluate separately the two components of diffusion: the puremolecular diffusion and the perfusion-related diffusion originating from capillary microcirculation. IVIM-DWI, applying a bi-exponential fitting function, allows the extraction of pure molecular diffusion parameters (D) and perfusion-related diffusion parameters (D* and f). Therefore, the aim of this study is to further characterize and compare the biexponential nature of the diffusion related signal decay with multiple b-factors for PZ PCa and healthy PZ areas.

3418 Computer 88

Application of Fast SE-EPI-based T2 Mapping in Prostate, with Comparison to Conventional CPMG-Based T2 Mapping

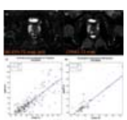

Xu Yan[1], Zan Ke[2], Minxiong Zhou[3], Caixia Fu[4], Xiangde Min[2], and Liang Wang[2]

[1]MR Collaboration NE Asia, Siemens Healthcare, Shanghai, People's Republic of China, [2]Department of Radiology, Tongji Hospital,Tongji Medical College, Huazhong University of Science and Technology, Wuhan, People's Republic of China, [3]Shanghai University of Medicine & Health Sciences, Shanghai, People's Republic of China, [4]Siemens Shenzhen Magnetic Resonance Ltd., Shenzhen, People's Republic of China

This study compared a fast SE-EPI-based T2 mapping method with a conventional CPMG-based method. The SE-EPI method is based on multi-TE data and can be integrated into a diffusion sequence with very fast acquisition speed (around 30 s). The voxel-by-voxel and region of interest (ROI)-based comparisons were performed using two methods, which showed that their T2 maps have a strong correlation. In addition, the clinical validation showed that the T2 maps of the two methods have similar statistical significance and can be used to differentiate between prostate cancer (PCa) and benign prostatic hyperplasia (BPH). This work suggests that the SE-EPI-based method is a quick quantification method, and could be used or combined with diffusion and other quantification methods for multi-parametric analysis. In addition, it may also have potential applications in body regions which are susceptible to motion artifacts.

3419 Computer 89

The ADC characteristics of the bone marrow within different anatomical parts: a DWI MR based study

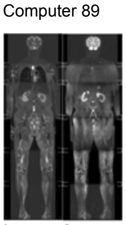

mi Yang[1], xiaodong Ji[2], Zhizheng Zhuo, and shuang Xia

[1]Department of Radiology, Tianjin first center hospital, Tianjin, People's Republic of China, [2]Department of Radiology

The diffusion weighted imaging has been widely used in clinical disease diagnosis, and the ADC value plays a key role in this progress. At present, the ADC values of normal organs and tissues have been reported, but few studies have been done on ADC values of normal bone marrow within different anatomical parts. In this study, the ADC values within different anatomical parts of bone marrow were measured and analyzed by using WB-DWI (whole body diffusion weighted imaging). And we furtherly evaluated the relationship of these ADC values with age and gender.

3420 Computer 90

Diffusion-Weighted Liver MRI in Forensic Medicine: A new radiological approach

Jin Yamamura[1], Tony Schmidt[2], Axel Heinemann, Roland Fischer[1,3], Gerhard Adam[1], and Sarah Keller[1]

[1]Diagnostic & Interventonal Radiology, University Medical Center Hamburg-Eppendorf, Hamburg, Germany, [2]KH Rostock, [3]Children's Hospital Oakland

In this original study and the first of its kind, the characteristic postmortem time course of liver ADC values were assessed over 24h after death. This results could be important as potential marker for tissue quality in liver transplantation. With the knowledge of the ex vivo data, DWI may be added to the MRI methods for a virtual autopsy.

3421 Computer 91

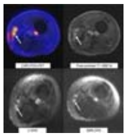

Simultaneous multislice diffusion weighted imaging in whole-body PET/MRI for accelerated multiparametric staging of oncologic patients.

Ferdinand Seith[1], Jana Taron[1], Christina Pfannenberg[1], Konstantin Nikolaou[1], Christina Schraml[1], and Petros Martirosian[2]

[1]Department of Diagnostic and Interventional Radiology, Eberhard-Karls-University Tuebingen, Germany, Tuebingen, Germany, [2]Section on Experimental Radiology, Eberhard-Karls-University Tuebingen, Germany, Tuebingen, Germany

Simultaneous multislice diffusion weighted imaging (SMS-DWI) is a promising technique to shorten scan time in MRI. Aim of our study was to compare the diagnostic performance of SMS-DWI to conventional DWI for multiparametric whole-body examinations of oncologic patients in PET/MRI. We performed an evaluation in three steps: First in a phantom study, second in a volunteer study and third in a patient study with 20 oncologic patients. We found that SMS-DWI led to a significant reduction of scan time and, although suffering from slightly impaired image quality, provided reliable ADC values and lesion conspicuity of PET positive lesions.

3422 Computer 92

Use of texture analysis of intravoxel incoherent motion (IVIM) in evaluating the expression of Ki67 of hepatitis B virus-related hepatocellular carcinoma (HCC)

Qungang Shan[1], Jingbiao Chen[1], Ronghua Yan[1], Yao Zhang[1], Hao Yang[1], Xin Li[2], Zhongping Zhang[3], Yunhong Shu[4], Churong Lin, Tianhui Zhang[1], Bingjun He[1], Zhuang Kang[1], Xi Long[1], and Jin Wang[1]

[1]Department of Radiology, the Third Affiliated Hospital, Sun Yat-sen University (SYSU), Guangzhou, People's Republic of China, [2]GE Healthcare MR Research China, Guangzhou, People's Republic of China, [3]MR Research China,GE Healthcare, Beijing, [4]Mayo Clinic

HCC is the second cause of cancer-related deaths and most HCC patients are accompanied with hepatitis B virus-related cirrhosis in China. Ki67 is a protein reflecting the proliferative activity of HCC and could be used as a predictor of prognosis. We assessed the value of the texture parameters in evaluating the expression of Ki67of HBV-related HCCs by whole tumor analysis. Our results showed that Dclusterprominence showed best diagnostic performance among all texture parameters. ADC and IVIM derived texture parameters might be used as useful and noninvasive biomarkers for evaluating the expression of Ki67 of HBV-related HCCs.

3423 Computer 93

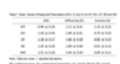

Feasibility of diffusion kurtosis imaging as a tool for differentiation between benign and malignant uterine lesions

Yoshihiko Fukukura[1], Yuichi Kumagae[1], Masanoari Nakajo[1], Kiyohisa Kamimura[1], Aya Umanodan[1], Takashi Iwanaga[2], Tomoyuki Okuaki[3], and Takashi Yoshiura[1]

[1]Radiology, Kagoshima University Graduate School of Medical and Dental Sciences, Kagoshima, Japan, [2]Radiological Technology, Kagoshima University Hospital, Kagoshima, Japan, [3]Philips Electronics Japan, TN, Japan

This study focused on the feasibility of DKI for differentiating benign from malignant uterine lesions. The ADC and D of malignant tumor (MT) were significantly lower than those of endometrial hyperplasia (EH) ($p=0.005$ and 0.004), uterine fibroid (UF) (both, $p<0.001$), normal endometrium (NE) (both, $p<0.001$), and normal myometrium (NM) (both, $p<0.001$), which indicative of the increased cellularity within uterine malignant tumor that resulted in restricted water diffusion. K was significantly higher in MT than in EH ($p=0.003$), UF ($p<0.001$), NE ($p<0.001$), and NM ($p<0.001$), possibly representing complexity of tissue microstructure in MT compared to benign lesions. DKI enables differentiate benign from malignant uterine lesions.

3424 Computer 94

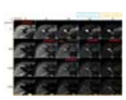

Zero-TE computed Diffusion Weighted Imaging Technique for the abdomen

Hiroshi Kusahara[1], Yuki Takai[1], and Yoshimori Kassai[1]

[1]MRI Systems Development Department, Toshiba Medical Systems Corporation, Tochigi, Japan

In this study is to adapt the short-TE cDWI (sTE-cDWI) technique, including the “Zero-TE”, validated previously in the brain[4] to the abdominal region. The algorithm under evaluation allows computing diffusion images for arbitrary combinations of TE and b-value based on three acquisitions (3-points method). With this method we demonstrate it is possible to suppress T2 shine-through effects and as well as improve the signal-to-noise and contrast-to-noise ratios of tissues with short T2 and low ADC. The clinical benefits of the method and the preliminary results on volunteers are discussed.

3425 Computer 95

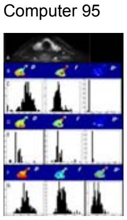

Comparison between IVIM combined with fuzzy clustering algorithm and IVIM combined with Bayesian method in the thyroid cancer

Kaining Shi[1], Fengmao Chiu[2], Yunlong Yue[3], Lee Jiang[4], Lili Zuo[3], and Yanfang Jin[3]

[1]Philips Healthcare (China), Beijing, People's Republic of China, [2]Philips Healthcare, Taipei, Taiwan, [3]Department of MR, Beijing Shijitan hospital of capital medical university, Beijing, People's Republic of China, [4]Philips Healthcare (China), Suzhou, People's Republic of China

To improve the stability of the nonlinear curve fitting of IVIM, the Fussy clustering technique (FCM) and data driven Bayesian approach are combined with IVIM in the imaging of thyroid tumors. Both FCM and Bayesian approach can improve the homogeneity of IVIM parameters. With limited sample size, FCM has similar diagnosis efficiency with conventional method using less calculation time, while Bayesian approach doesn’t increase the diagnosis efficiency.

3426 Computer 96

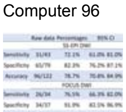

Evaluation of the reduced field-of-view Diffusion Weighted Imaging for staging of endometrial adenocarcinoma

Hiroki Hori[1,2], Toshio Yamaguchi[3], Hisashi Yoshihara[1], Youko Murakami[1], Yoshiyuki Konishi[2], Yoshihiro Muragaki[2,4], Jinichi Sasanuma[5], and Kazuo Watanabe[5]

[1]Radiology, Shin-Yurigaoka General Hospital, Kanagawa, Japan, [2]Faculty of Advanced Techno-Surgery (FATS), Institute of Advanced Biomedical Engineering and Science, Tokyo Women's Medical University, Tokyo, Japan, [3]Research Institute for Medical Imaging, Shin-Yurigaoka General Hospital, Kanagawa, Japan, [4]Neurosurgery, Tokyo Women's Medical University, Tokyo, Japan, [5]Neurosurgery, Shin-Yurigaoka General Hospital, Kanagawa, Japan

The objective of this retrospective study is to evaluate the differences of the accuracy in endometrial adenocarcinoma using FOCUS DWI compared to that using conventional SS-EPI DWI. We calculated the accuracy by the interpretation of magnetic resonance (MR) imaging and the pathology. The accuracy in the FOCUS DWI was significantly better than that in the SS-EPI DWI. This may be due to the decrease of distortion in DWI, which induced the artifacts. There was improvement of the accuracy using the FOCUS DWI in the patient who had suspected endometrial adenocarcinoma.

Electronic Poster

Metabolism, Diabetes, Fat Imaging

Exhibition Hall — Monday 13:45 - 14:45

3427 Computer 97

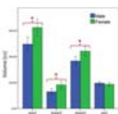

Sex and ethnic differences in abdominal fat partitioning and adipose tissue hydration in 4.5-year-old Asian children

Suresh Anand Sadananthan[1], Mya Thway Tint[2], Navin Michael[1], Kuan Jin Lee[3], Lynette Pei-Chi Shek[4], Yap Kok Peng Fabian[5,6], Keith M Godfrey[7], Melvin Khee-Shing Leow[8,9], Yung Seng Lee[1,4], Michael S Kramer[2,10,11], Peter D Gluckman[1,12], Yap Seng Chong[1,2], Christiani Jeyakumar Henry[8], Marielle Valerie Fortier[13], and S. Sendhil Velan[3]

*[1]Singapore Institute for Clinical Sciences, A*STAR, Singapore, [2]Department of Obstetrics & Gynaecology, Yong Loo Lin School of Medicine, National University of Singapore, Singapore, [3]Singapore BioImaging Consortium, A*STAR, Singapore, [4]Department of Paediatrics, Yong Loo Lin School of Medicine, National University of Singapore, Singapore, [5]Department of Paediatric Endocrinology, KK Women's and Children's Hospital, Singapore, [6]Lee Kong Chian School of Medicine, Nanyang Technological University, Singapore, [7]MRC Lifecourse Epidemiology Unit & NIHR Southampton Biomedical Research Centre, University of Southampton & University Hospital Southampton NHS Foundation Trust, Southampton, United Kingdom, [8]Clinical Nutrition Research Centre, Singapore Institute for Clinical Sciences, A*STAR, Singapore, [9]Department of Endocrinology, Tan Tock Seng Hospital, Singapore, [10]Department of Paediatrics, Faculty of Medicine, McGill University, Montreal, Canada, [11]Department of Epidemiology, Biostatistics and Occupational Health, Faculty of Medicine, McGill University, Canada, [12]Liggins Institute, University of Auckland, Auckland, New Zealand, [13]Department of Diagnostic and Interventional Imaging, KK Women's and Children's Hospital, Singapore*

In this study, we used MR-based estimation of abdominal fat distribution and the degree of adipocyte hypertrophy to study sex and ethnic differences in 4.5-year-old Asian children. Our results show sexual dimorphism in abdominal fat distribution in preschool children. Girls had higher subcutaneous fat depot volumes and lower adipose tissue hydration than boys. We also found that at 4.5 years, both deep and superficial subcutaneous fat volumes in Indian children were higher, while the ethnic difference in internal fat was non-significant. These differences may help explain why Indians are more susceptible to metabolic and cardiovascular diseases.

3428 Computer 98

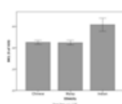

Inter-ethnic variation and SCD1 polymorphism predict risk for intramyocellular lipid accumulation in early childhood

Navin Michael[1], Varsha Gupta[1], Suresh Anand Sadananthan[1], Aparna Sampathkumar[1], Li Chen[1], Hong Pan[1], Mya Thway Tint[2], Kuan Jin Lee[3], Lynette Pei-Chi Shek[4], Yap Kok Peng Fabian[5,6], Keith M Godfrey[7], Melvin Khee-Shing Leow[8,9], Yung Seng Lee[1,4], Michael S Kramer[2,10,11], Yap Seng Chong[1,2], Christiani Jeyakumar Henry[8], Marielle Valerie Fortier[12], Peter D Gluckman[1,13], Neerja Karnani[1,14], and S. Sendhil Velan[3]

*[1]Singapore Institute for Clinical Sciences, A*STAR, Singapore, [2]Department of Obstetrics & Gynaecology, Yong Loo Lin School of Medicine, National University of Singapore, Singapore, [3]Singapore BioImaging Consortium, A*STAR, Singapore, [4]Department of Paediatrics, Yong Loo Lin School of Medicine, National University of Singapore, Singapore, [5]Department of Paediatric Endocrinology, KK Women's and Children's Hospital, Singapore, [6]Lee Kong Chian School of Medicine, Nanyang Technological University, Singapore, [7]MRC Lifecourse Epidemiology Unit & NIHR Southampton Biomedical Research Centre, University of Southampton & University Hospital Southampton NHS Foundation Trust, Southampton, United Kingdom, [8]Clinical Nutrition Research Centre, Singapore Institute for Clinical Sciences, A*STAR, Singapore, [9]Department of Endocrinology, Tan Tock Seng Hospital, Singapore, [10]Department of Paediatrics, Faculty of Medicine, McGill University, Montreal, Canada, [11]Department of Epidemiology, Biostatistics and Occupational Health, Faculty of Medicine, McGill University, Canada, [12]Department of Diagnostic and Interventional Imaging, KK Women's and Children's Hospital, Singapore, [13]Liggins Institute, University of Auckland, Auckland, New Zealand, [14]Department of Biochemistry, Yong Loo Lin School of Medicine, National University of Singapore, Singapore*

A large intramyocellular lipid (IMCL) pool is associated with early pathogenesis of insulin resistance and type 2 diabetes. Studies from mother-offspring cohorts indicate that, like obesity and metabolic traits, IMCL is also highly heritable. However, here have been not many studies on the effect of genetic variation on IMCL. Although a number of genome-wide association studies (GWAS) have established associations between several genetic loci and metabolic disorders, it is not yet known if these loci also contribute to IMCL levels, and help explain ethnic difference in IMCL levels. In this study, we examined the ethnic differences (Indian, Malay and Chinese) in IMCL in Singaporean children and the genetic risk variant(s) associated with these differences.

3429 Computer 99

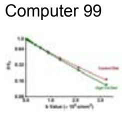

Determination of Droplet Size Distribution in Brown Adipose Tissues by Diffusion NMR Spectroscopy

Sanjay Kumar Verma[1], Jadegoud Yaligar[1], Navin Michael[2], Tian Xianfeng[1], Venkatesh Gopalan[1], Suresh Anand Sadananthan[2], Rengaraj Ananthraj[1], and S. Sendhil Velan[1,2]

[1]Laboratory of Molecular Imaging, Singapore Bioimaging Consortium, Singapore, Singapore, [2]Singapore Institute for Clinical Sciences, Singapore

Non-Invasive Imaging of Brown Adipose Tissue is of significant interest due to its potential to combat obesity and diabetes. In this study, we have utilized diffusion spectroscopy to estimate the droplet size distribution in chow and high-fat diet fed brown adipose tissues obtained from rodents. The high-fat diet BAT exhibited reduction in the restriction due to the increase in droplet size. The histology results confirm the droplet size distribution in both control and high-fat diet tissues.

3430

Detection of Brown Adipose Tissue: Hyperpolarized 129Xe MRI vs Xenon Enhanced CT

Computer 100

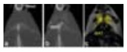

Rosa Tamara Branca[1,2], Andrew McCallister[1,2], Hong Yuan[2], Le Zhang[2,3], Alex Burant[1,2], and Michael Antonacci[1,2]

[1]Physics and Astronomy, University of North Carolina at Chapel Hill, Chapel Hill, NC, United States, [2]Biomedical Research Imaging Center, University of North Carolina at Chapel Hill, Chapel Hill, NC, United States, [3]Material Science, University of North Carolina at Chapel Hill, Chapel Hill, NC, United States

Despite histological evidence that all humans have brown adipose tissue, the detection of this tissue in overweight and obese subjects has proven to be a challenge. Here we demonstrate the combined used of hyperpolarized xenon gas (HP129Xe) MRI and xenon enhanced CT for the detection of BAT thermogenic activity and mass in lean and obese mouse phenotypes as well as our preliminary results in healthy young volunteers.

3431 Computer 101

Anti-FGFR1/KLB treatment reduces hepatic fat fraction in a murine model of NAFLD

Maj Hedehus[1], Mark Z. Chen[2], Jose Zavala-Solorio[2], Lance Kates[2], Oded Foreman[3], Junichiro Sonoda[2], and Richard A. D. Carano[1]

[1]Biomedical Imaging, Genentech, Inc., South San Francisco, CA, United States, [2]Molecular Biology, Genentech, Inc., South San Francisco, CA, United States, [3]Research Pathology, Genentech, Inc., South San Francisco, CA, United States

Anti-FGFR1/KLB is a novel experimental therapy to treat metabolic disorders and reverse lipid accumulation in the liver. MRI estimates of proton density fat fraction demonstrated a dose-dependent anti-FGFR1/KLB treatment effect in a murine model of NAFLD.

3432 Computer 102

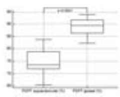

Supraclavicular and gluteal adipose tissue PDFF is associated to volumes of VAT and SAT and to anthropometric obesity markers in healthy adults

Daniela Franz[1], Dominik Weidlich[1], Friedemann Freitag[1], Christina Holzapfel[2], Thomas Baum[1], Holger Eggers[3], Ernst J. Rummeny[1], Hans Hauner[2], and Dimitrios C. Karampinos[1]

[1]Department of Diagnostic and Interventional Radiology, Technical University of Munich, Munich, Germany, [2]Else Kröner Fresenius Center for Nutritional Medicine, Technical University of Munich, Munich, Germany, [3]Philips Research Laboratory, Hamburg, Germany

Proton density fat fraction (PDFF) mapping has been emerging as important metabolic phenotyping parameter in obesity enabling spatially-resolved fat quantification in multiple organs. PDFF of adipose tissue has also recently gained significant attention due to the interest in developing biomarkers of brown fat which is assumed to be present in the adult supraclavicular fossa. However, it remains unknown how adipose tissue PDFF relates to other fat depots and anthropometric parameters. The present study aims to investigate the relationship of the supraclavicular and gluteal fat PDFF with SAT and VAT volumes and anthropometric obesity markers.

3433 Computer 103

Clinical evaluation of the early renal hypoxia in Type 2 Diabetes based on BOLD-MRI

Junjie Ren[1], Shengzhang Ji[1], Chunxia Li[2], Zhizheng Zhuo[3], and Hao Wang[1]

[1]The 4th center hospital of TianJin, Tianjin, People's Republic of China, [2]Inner Mongolia people's hospital, Inner Mongolia, People's Republic of China, [3]Philips Healthcare, Beijing, People's Republic of China

Till now the type 2 diabetes (T2DM) is more and more prevalent, and diabetic nephropathy (DN) has become the main leading cause of end-stage renal disease (ESRD). However the onset of DN is always ambiguous. In recent years, many studies focused on the change of renal oxygenation in diabetes and showed renal hypoxia especially in medulla. Blood oxygen level dependent magnetic resonance imaging (BOLD-MRI) is a non-invasive method that can assess hypoxia in prostate gland by utilizing the endogenous contrast generated by paramagnetic deoxyhemoglobin.

3434 Computer 104

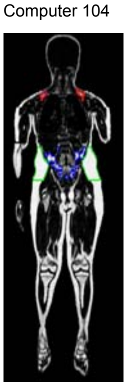

Characterization of brown and white adipose tissue in 7-year old children

Jonathan Andersson[1], Emma Kjellberg[2,3], Elin Lundström[1], Mathias Engström[4], Josefine Roswall[2,3], Stefan Bergman[5], Pär-Arne Svensson[6], Håkan Ahlström[1,7], Jovanna Dahlgren[2], and Joel Kullberg[1,7]

[1]Department of Radiology, Institution of Surgical Sciences, Uppsala University, Uppsala, Sweden, [2]Department of Pediatrics, the Institution of Clinical Sciences, The Sahlgrenska Academy, University of Gothenburg, Gothenburg, Sweden, [3]Department of Pediatrics, Halland Hospital, Halmstad, Sweden, [4]Applied Science Laboratory, GE Healthcare, Uppsala, Sweden, [5]Primary Health Care Unit, Department of Public Health and Community Medicine, Institute of Medicine, The Sahlgrenska Academy, University of Gothenburg, Gothenburg, Sweden, [6]Department of Pediatric Radiology, The Sahlgrenska University Hospital, Gothenburg, Sweden, [7]Antaros Medical, Mölndal, Sweden

The purpose of this study was to characterize and compare brown and white adipose tissue in 7 year-old overweight/obese and normal weight children using whole-body water-fat MRI. Correlations were also performed between the brown adipose tissue measurements and other measurements, such as VAT and SAT volumes. Results overall showed expected differences and associations to several measures relevant for obesity. We conclude that whole-body water-fat MRI of 7 year-old children is feasible and allows characterization of brown and white adipose tissue.

3435 Computer 105

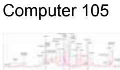

Urine Metabolic profiling of patients with colorectal cancer based on NMR and Pattern Recognition

Wang Zhening[1], Liang Jiahao[1], Huang Yao[1], Ma Changchun[2], Wu Renhua[1], Yang Jurong[3], Liu Xingmu[4], and Lin Yan[1]

[1]Radiology Department, Second Affiliated Hospital, Shantou University Medical College, Shantou, People's Republic of China, [2]Radiation Oncology, Affiliated Tumor Hospital, Shantou University Medical College, Shantou, People's Republic of China, [3]Shantou University Central Laboratory and NMR Unit, Shantou, People's Republic of China, [4]Surgery Deparment, Second Affiliated Hospital, Shantou University Medical College, Shantou, People's Republic of China

After our fecal metabonomic study of colorectal cancer (CRC) patients recently published in Oncotarget , we profiled urine metabolites from the same group of CRC patients, 40 age-matched healthy controls (HC), 18 esophageal cancers (EC), using proton nuclear magnetic resonance spectroscopy in conjunction with a multivariate statistics technique. OPLS-DA revealed that each stage of CRC could be clearly distinguished from HC and EC based on their different metabolomic profiles. These altered urine metabolites of CRC patients from HC potentially involved in the disrupted common pathways, and the different metabolites in CRC compare to EC indicated the special of the CRC.

3436 Computer 106

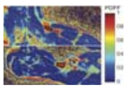

Spin Densities and Relaxation Parameters of the Spectral Components of Brown Fat and Subcutaneous Fat with Localized 1H-MRS at 3T.

Ronald Ouwerkerk[1], Aaron Cypess[2], Kong Chen[2], Peter Herscovitch[3], Robert Brychta[2], Brooks P Leitner[2], and Ahmed M Gharib[1]

[1]Biomedical and Metabolic Imaging Branch, NIDDK, Bethesda, MD, United States, [2]Diabetes, Endocrinology, and Obesity Branch, NIDDK, Bethesda, MD, United States, [3]PET, NIH Clinical Center, Bethesda, MD, United States

^{1}H-MRS was used to measure relaxation properties, lipid peak ratios and water content of white adipose tissue (WAT) and brown adipose tissue (BAT) in humans with the aim of providing information that can be used to improve MRI based methods for identifying BAT.

3437 Computer 107

Receiver operating characteristic analysis of fat fraction reveals no universal cut-off to reliably identify in vivo brown adipose tissue in adult humans

Terence Jones[1,2], Sarah Wayte[3], Narendra Reddy[4], Oludolapo Adesanya[1], Thomas Barber[2,4], and Charles Edward Hutchinson[1,2]

[1]Department of Radiology, University Hospitals Coventry & Warwickshire NHS Trust, Birmingham, United Kingdom, [2]Warwick Medical School, University of Warwick, Coventry, United Kingdom, [3]Medical Physics, University Hospitals Coventry & Warwickshire NHS Trust, Coventry, United Kingdom, [4]Department of Endocrinology, University Hospitals Coventry & Warwickshire NHS Trust, Birmingham, United Kingdom

Lower fat content within brown adipose tissue (BAT) compared to white adipose tissue (WAT) has been exploited using Dixon-based MRI imaging methods to visualize BAT but is subject to inter-rater variability. To determine the optimal fat fraction threshold for identifying BAT, receiver operating characteristic (ROC) analyses of fat fraction maps derived from 3 point IDEAL MRI scans were performed for sixteen subjects.

This method had good-to-excellent accuracy in four cases, and fair accuracy in two, but failed in ten. A single universal cut-off point to differentiate BAT and WAT could not be identified, instead the optimal thresholds varied between individuals.

3438 Computer 108

Adipose tissue and ectopic fat responses to an extended fast in healthy male adults

Alison Sleigh[1,2], Ajay Thankamony[3], Albert Koulman[4], Vlada Bokii[1], Graham J Kemp[5], Leanne Hodson[6], and David B Dunger[3]

[1]Wolfson Brain Imaging Centre, University of Cambridge, Cambridge, United Kingdom, [2]NIHR/WT Clinical Research Facility, Cambridge University Hospitals NHS Foundation Trust, Cambridge, United Kingdom, [3]Department of Paediatrics, University of Cambridge, Cambridge, United Kingdom, [4]MRC Human Nutrition Research, Cambridge, United Kingdom, [5]Department of Musculoskeletal Biology, University of Liverpool, Liverpool, United Kingdom, [6]Oxford Centre for Diabetes, Endocrinology and Metabolism, University of Oxford, Oxford, United Kingdom

We have investigated the response of different fat deposits to a 28 h fast in healthy nonobese males and shown significant increases in CH_2 IMCL in both the soleus and tibialis anterior muscles, and significant decreases in subcutaneous fat. Increases in TA and SOL IMCL correlated with oleic and palmitic acid FFA concentrations respectively. The compositional change of IMCL during the fast related inversely to the baseline composition, suggesting a selective efflux of unsaturated shorter chain IMCLs for preferential oxidation, which is in agreement with rat biopsy data, and supportive of the idea of IMCL as a flexible lipid store.

3439 Computer 109

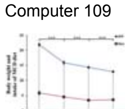

Identification and in vivo quantification of fatty acid metabolism in liver of a lipogenic methionine-choline-deficient diet-fed animal model by using magnetic resonance spectroscopy at 9.4 T

Kyu-Ho Song[1], Song-I Lim[1], Min Young Lee[1], Chi-Hyeon Yoo[1], and Bo-Young Choe[1]

[1]Department of Biomedical Engineering, and Research Institute of Biomedical Engineering, The Catholic University of Korea College of Medicine, Seoul, Korea, Republic of

Non-alcoholic steatohepatitis (NASH) is associated with metabolic syndrome as a result of insulin resistance and the accumulation of lipid droplets within hepatocytes. There is a need to diagnose and to accurately assess the progressive severity of hepatic steatosis with non-invasive biomarkers that are distinguishable from those in non-alcoholic fatty liver disease (NAFLD). Our findings demonstrate that fatty acid metabolism (saturated- and unsaturated-fatty acids) of hepatic steatosis induced by a methionine-choline diet can be distinguished from progressive NAFLD by using high-resolution magnetic resonance spectroscopy (MRS).

3440 Computer 110

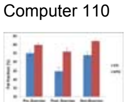

Metabolic Imaging of Brown Adipose Tissue Activation by Exercise in Control and High Fat Diet Fed Rats

Venkatesh Gopalan[1], Jadegoud Yaligar[1], Sanjay Kumar Verma[1], Suresh Anand Sadananthan[2], Anna Ulyanova[1], Navin Michael[2], Anantharaj Rengaraj[1], Tian Xianfeng[1], and S. Sendhil Velan[1,2]

[1]Laboratory of Molecular Imaging, Singapore Bioimaging Consortium, Singapore, Singapore, [2]Singapore Institute for Clinical Sciences, Singapore, Singapore

Exercise is an important intervention for correction of irregular fat-partitioning and treatment of metabolic dysfunction. There is a large interest in development of non-invasive methods for activation of brown adipose tissue (BAT) due to its potential to combat obesity. In this study we have investigated exercise induced BAT activation and IMCL from skeletal muscle of rodents fed with control and high fat diet. Our results show that exercise modulates the brown fat with reduction in fat fraction, increased UCP1 expression and reduction in “white” like adipocytes in control and high fat diet fed rats.

3441 Computer 111

Metabolic Imaging of Aging Adipose Tissues

Venkatesh Gopalan[1], Sanjay Kumar Verma[1], Jadegoud Yaligar[1], Anantharaj Rengaraj[1], Tian Xianfeng[1], Bhanu Prakash K N[1], Suresh Anand Sadananthan[2], Navin Michael[2], and S. Sendhil Velan[1,2]

[1]Laboratory of Molecular Imaging, Singapore Bioimaging Consortium, Singapore, Singapore, [2]Singapore Institute for Clinical Sciences, Singapore, Singapore

There is a global interest in healthy aging and also to avoid metabolic dysfunction. BAT and WAT play an important role in modulating the energy expenditure. In this study we have investigated the interscapular BAT and abdominal adipose tissues in young and old rats. During aging the iBAT activity is reduced due to the increase in "white" like adipocytes. The abdominal adipose tissues including VAT and SAT show increase in adipocyte size resulting in hypertrophy. Modulating these fat depots with nutritional interventions is of significant clinical interest.

3442 Computer 112

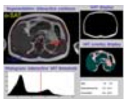

Automated MRI fat quantification in obese patients – impact of reader experience and degree of obesity on time exposure

Nicolas Linder[1,2], Alexander Schaudinn[1,2], Nikita Garnov[1,2], Roland Stange[1,2], Kilian Solty[1,2], Thomas Rakete[1,2], Nora Dipper[1,2], Sophia Michel[1,2], Thomas Karlas[2,3], Matthias Blüher[2,4], Stefanie Lehmann[2], Andreas Oberbach[2], Rima Chakaroun[4], Thomas Kahn[1], and Harald Busse[1]

[1]Diagnostic and Interventional Radiology, Leipzig University Hospital, Leipzig, Germany, [2]Integrated Research and Treatment Center (IFB) AdiposityDiseases, Leipzig University Medical Center, Leipzig, Germany, [3]Department of Internal Medicine, Neurology and Dermatology, Division of Gastroenterology and Rheumatology, Leipzig University Hospital, Leipzig, Germany, [4]Department of Internal Medicine, Neurology and Dermatology, Division of Endocrinology and Nephrology, Leipzig University Hospital, Leipzig, Germany

The last decades have seen an increasing socioeconomic impact of obesity and obesity-related diseases. Noninvasive measures like subcutaneous and visceral adipose tissue (SAT, VAT) amounts and are also increasingly correlated with other, often clinical or metabolic findings as well as independent patient characteristics, even interventional complication rates. MRI fat quantification is common but manual processing is often laborious and time consuming while fully automatic segmentation is prone to errors. This work takes a custom-made semiautomatic MRI tool and prospectively analyzes the processing and interaction times for readers with different experience as well as patients from different BMI groups.

3443 Computer 113

Preliminary study for the quantification of fatty composition and relation to metabolic syndrome using modified Dixon method.

Satoshi Goshima[1], Kimihiro Kajita[2], Tomoyuki Okuaki[3], Keita Fujimoto[1], Shoma Nagata[1], Yoshifumi Noda[1], Hiroshi Kawada[1], Nobuyuki Kawai[1], Hiromi Koyasu[1], and Masayuki Matsuo[4]

[1]Radiology, Gifu University Hospital, Gifu City, Japan, [2]Radiology, Gifu University Hospital, Gifu City, [3]Philips Healthcare, Tokyo, Japan, [4]Gifu University Hospital, Gifu City, Japan

We successfully quantified fatty acid composition in the liver, subcutaneous, and visceral fat tissue using modified Dixon technique with flexible six echo times and seven-peak spectral model with lipid components. Our results suggested that fatty acid composition of depot fat was varied among the patients with different metabolic status. We also demonstrated the possible relationship of unsaturated fatty acid in depot fat to cholesterol level and insulin tolerance.

3444 Computer 114

Liver and muscle energy metabolism in patients with organic acidemias using 31P and 1H MR spectroscopy

Alessandra Bierwagen[1,2], Daria Caspari[3], Maik Rothe[1,2], Klaus Straßburger[2,4], Jong-Hee Hwang[1,2], Michael Roden[1,2,5], and Regina Ensenauer[3]

[1]Institute for Clinical Diabetology, German Diabetes Center, Leibniz Institute for Diabetes Research, Heinrich Heine University, Duesseldorf, Germany, [2]German Center for Diabetes Research (DZD e.V.), Partner Düsseldorf, Duesseldorf, Germany, [3]Experimental Pediatrics and Metabolism, University Children's Hospital, Heinrich Heine University, Duesseldorf, Germany, [4]Institute for Biometrics and Epidemiology, German Diabetes Center, Leibniz Institute for Diabetes Research, Heinrich Heine University, Duesseldorf, Germany, [5]5Department of Endocrinology and Diabetology, Medical Faculty, Heinrich Heine University, Duesseldorf, Germany

This study assessed energy and fat metabolism in a well phenotyped cohort of patients with organic acidemias using non-invasive MR spectroscopy. ^{31}P and ^{1}H spectra of the liver as well as ^{1}H spectra of the muscle were acquired in 27 patients and 30 healthy controls (age-, sex-, BMI-matched). We found higher liver fat content in patients with propionic acidemia. The level of creatine in the soleus muscle was higher in patients with methylmalonic acidemia and propionic acidemia. In conclusion, the results provide evidence for previously unknown abnormalities of liver fat and muscle energy metabolism in patients with organic acidemias.

3445 Computer 115

Validity of estimating subcutaneous and visceral fat volume from single MRI slice in older adults with sarcopenia and sarcopenic obesity

Yu Xin Yang[1], Wee Shiong Lim[1,2], Mei Sian Chong[1], Laura Tay[1,2], Suzanne Yew[1], Audrey Yeo[1], and Cher Heng Tan[3]

[1]Institute of Geriatrics and Active Ageing, Tan Tock Seng Hospital, Singapore, Singapore, [2]Geriatric Medicine, Tan Tock Seng Hospital, Singapore, Singapore, [3]Diagnostic Radiology, Tan Tock Seng Hospital, Singapore, Singapore

The demand for measurements of fat quantities is driven by the rising prevalence of sarcopenia and sarcopenic obesity (SO). In order to reduce the time and the cost of image processing, several studies have estimated the subcutaneous fat (SF) and visceral fat (VF) volume from a single slice. However, the population of studies may not have necessarily included patients with either sarcopenia or SO. This study aims to determine the correlation between the cross-sectional areas in a single slice at different vertebra levels and the volumes of SF and VF in the abdomen for sarcopenic and SO populations using MRI.

3446 Computer 116

Water-fat MRI demonstrates seasonal proliferation of brown adipose tissue near the eyes of juvenile hibernators: An additive effect of cold exposure

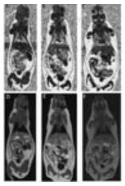

Amanda DV MacCannell[1], Kevin Sinclair [2], Lannete Friesen-Waldner[2], Charles A McKenzie[2], and James Staples[1]

[1]Biology, University of Western Ontario, London, ON, Canada, [2]Medical Biophysics, University of Western Ontario, London, ON, Canada

Hibernating mammals use brown adipose tissue (BAT) as a primary source of heat production. Volumes of both white adipose tissue (WAT) and BAT increase in the autumn even when temperatures are warm. Between Aug 19th and Oct 13th we used water-fat MRI to measure the dynamics of BAT and white adipose tissue as ground squirrels prepared for hibernation under either cold or thermoneutral temperatures. We found that the volume of a tissue that resembles BAT around the eye, increased significantly in cold exposed animals to warm exposed in October, as the animals are preparing for winter.

3447 Computer 117

Evaluation of renal hemodynamics and oxygenation with BOLD, oxygen extraction fraction (OEF) and ASL techniques in animal model of diabetic nephropathy

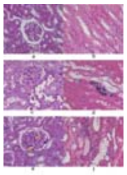

Rui Wang[1], Zhiyong Lin[1], Xueqing Sui[1], Kai Zhao[1], and Feng Wei[1]

[1]Radiology, Peking University First Hospital, Beijing, People's Republic of China

Our study was to investigate the feasibility of using blood oxygen level dependent (BOLD), oxygen extraction fraction (OEF) and arterial spin labeling (ASL) techniques for the detection of renal hemodynamics and oxygenation changes in rabbits with diabetic nephropathy (DN).

3448 Computer 118

The effects of sprint interval training on visceral, subcutaneous and hepatic fat stores: An MRI and 1H-MRS study of lipid content and composition

Stephen Bawden[1,2], Jack Sargeant[3], Liz Simpson[4], Mehri Kaviani[2], Myra Nimmo[5], Penny Gowland[2], Ian MacDonald[4], James King[3], and Guruprasad P Aithal[1]

[1]NIHR Nottingham Digestive Diseases Unit, Nottingham University Hospitals, University of Nottingham, Nottingham, United Kingdom, [2]Sir Peter Mansfield Imaging Center, Physics and Astronomy, University of Nottingham, Nottingham, United Kingdom, [3]NIHR The Leicester-Loughborough Diet, Lifestyle & Physical Activity Biomedical Research Unit, University Hospitals of Leicester and Loughborough University, [4]Metabolic Physiology Group, Faculty of Medicine and Health Sciences, University of Nottingham, United Kingdom, [5]College of Life and Environmental Sciences, University of Birmingham

In this study, 9 obese male participants underwent 6 weeks of sprint interval training (SIT) and changes in visceral, subcutaneous and intra-hepatocellular fat were measured using MRI and MRS at baseline, control (>4 weeks later) and post exercise. Change in liver lipid composition was also assessed.

3449 Computer 119

Multiparametric MR characterisation of a high-fat, high-cholesterol diet rodent model of liver disease

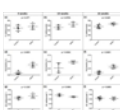

Manil Chouhan[1], Tim Bray[1], John Connell[2], Jane MacNaughtan[3], Alan Bainbridge[4], Helen Jones[3], Abeba Habtieson[3], Nathan Davies[3], Rajiv Jalan[3], Shonit Punwani[1], Tammy Kalber[2], Mark Lythgoe[2], Margaret Hall-Craggs[1], Rajeshwar Mookerjee[3], and Stuart Taylor[1]

[1]UCL Centre for Medical Imaging, University College London, London, United Kingdom, [2]UCL Centre for Advanced Biomedical Imaging, University College London, London, United Kingdom, [3]UCL Institute for Liver and Digestive Health, University College London, London, United Kingdom, [4]Department of Medical Physicist, University College London Hospitals NHS Trust, London, United Kingdom

There is a growing interest in the development of new animal models of non-alcoholic fatty liver disease. In this study, we use T1, proton density fat fraction (PDFF) and R2* mapping to characterise hepatic parenchymal tissue and the evolution of MR properties over time in a high-fat, high-cholesterol diet model of fatty liver disease.

3450 Computer 120

Longitudinal Assessment of Visceral and Subcutaneous Adipose Tissue in Obese Patients undergoing Weight Loss Surgery

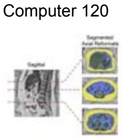

Curtis N Wiens[1], Cristobal Arrieta[2], Ignacio Osorio[2], Ben Ratliff[1], Timothy J Colgan[1], Alan B McMillan[1], Nathan S Artz[1,3], Luke Funk[4], Guilherme M Campos[4,5], Jacob Greenberg[4], Daniela Esparza[2], Sergio Uribe[6,7], Claude B Sirlin[8], and Scott B Reeder[1,9,10,11,12]

[1]Radiology, University of Wisconsin, Madison, WI, United States, [2]Electrical Engineering, Pontificia Universidad Catolica de Chile, Santiago, Chile, [3]Diagnostic Imaging, St. Jude Children's Research Hospital, Memphis, TN, United States, [4]Surgery, University of Wisconsin, Madison, WI, United States, [5]Surgery, Virginia Commonwealth University, Richmond, VA, United States, [6]Radiology, Pontificia Universidad Catolica de Chile, Santiago, Chile, [7]Biomedical Imaging Center, Pontificia Universidad Catolica de Chile, Santiago, Chile, [8]Radiology, University of California, San Diego, CA, United States, [9]Medical Physics, University of Wisconsin, Madison, WI, United States, [10]Medicine, University of Wisconsin, Madison, WI, United States, [11]Emergency Medicine, University of Wisconsin, Madison, WI, United States, [12]Biomedical Engineering, University of Wisconsin, Madison, WI, United States

This work monitored longitudinal changes in visceral (VAT) and subcutaneous (SCAT) adipose tissue in response to weight loss. Twenty-one patients undergoing clinical weight loss surgery (WLS) were recruited for 5 MRI studies: 2-3 weeks prior, 1 day prior to WLS and 1, 3, and 6 months post-WLS. Single breath-hold, chemical shift encoded acquisitions were analyzed using an Osirix semi-automated segmentation software to monitor changes in VAT and SCAT volumes. Continual reductions in VAT and SCAT were measured over the five visits. At every visit, each patient's relative body fat distribution remained relatively constant despite overall reductions in both VAT and SCAT.

Electronic Poster

Diffusion: Validation

3451 Computer 1

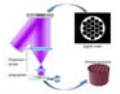

Quantitation of DTI changes associated with muscle injury using a 3D printed phantom

David B Berry[1], Shangting You[2], John Warner[2], Lawrence Frank[3], Shaochen Chen[2], and Samuel R Ward[1,3,4]

[1]Bioengineering, University of California, San Diego, San Diego, CA, United States, [2]Nanoengineering, University of California, San Diego, San Diego, CA, United States, [3]Radiology, University of California, San Diego, San Diego, CA, United States, [4]Orthopaedic Surgery, University of California, San Diego, San Diego, CA, United States

Diffusion tensor imaging has been proposed as a tool to non-invasively assess skeletal muscle microstructure, which would be of significant clinical value. However, its application to the assessment of changes in muscle microstructure associated with injury, pathology, or age remain poorly defined because it is difficult to precisely control muscle microstructural features in vivo. Recent advances in bottom up fabrication technologies allow precision-engineered diffusion phantoms with histology informed skeletal muscle geometry to be manufactured. Therefore, the goal of this study was to develop skeletal muscle phantoms at relevant size scales in order to relate microstructural features to MRI-based diffusion measurements.

3452 Computer 2

Accuracy of ADC measurements with an Ultrashort Echo Time Diffusion Weighted stimulated echo 3D Cones sequence (DW-STEAM 3D Cones UTE)

Paul Baron[1], Dirk H.J. Poot[1,2,3], Piotr A. Wielopolski[1], Edwin H.G. Oei[1], and Juan A. Hernandez-Tamames[1]

[1]Radiology and Nuclear Medicine, Erasmus Medical Center, Rotterdam, Netherlands, [2]Medical Informatics and Radiology, Erasmus Medical Center, Rotterdam, Netherlands, [3]Imaging Science and Technology, Delft University of Technology, Delft, Netherlands

Diffusion weighted STEAM with UTE readout is a promising acquisition method to measure diffusion in tissues with short T2 and T2*, such as tendons, ligaments and menisci. However, the accuracy of the ADC obtained with this method has not been studied before. Using experiments and Bloch simulations we show that the ADC can be biased, especially when a short TR is used, and that this bias depends on T1 and T2. Randomization of the diffusion gradient direction reduces the bias, providing clear suggestions to improve acquisition and/or post processing that reduces the ADC bias.

3453 Computer 3

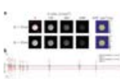

A biomimetic tumour tissue phantom for validating diffusion-weighted MRI measurements

Damien J. McHugh[1,2], Fenglei Zhou[1,2,3], Penny L. Hubbard Cristinacce[1], Josephine H. Naish[1], and Geoffrey J. M. Parker[1,2,4]

[1]Centre for Imaging Sciences, The University of Manchester, Manchester, United Kingdom, [2]CRUK and EPSRC Cancer Imaging Centre in Cambridge and Manchester, Manchester, United Kingdom, [3]The School of Materials, The University of Manchester, Manchester, United Kingdom, [4]Bioxydyn Ltd., Manchester, United Kingdom

This work investigates the stability of a water-based biomimetic tumour tissue phantom, and evaluates its potential as a tool for validating diffusion-weighted (DW) MRI measurements. As with biological tissue, and unlike most previous phantoms for tumour DW-MRI, the phantom's apparent diffusion coefficient depends on diffusion time, with values stable over six months. DW-MRI-based estimates of microstructural parameters exhibited bias, possibly indicating limitations in the analysis model or acquisition scheme. It is envisaged that such phantoms will aid investigation of DW-MRI tumour microstructural models, and more generally will act as realistic test objects for comparing DW-MRI-derived biomarkers obtained from different scanners/sites.

3454 Computer 4

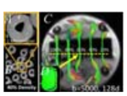

Providing Ground Truth Quantification of Anisotropic Diffusion MRI Imaging with a Hollow Textile Phantom

Sudhir Kumar Pathak[1], Catherine Fissell[1], David Okonkwo[2], and Walter Schneider[1]

[1]Psychology, University Of Pittsburgh, Pittsburgh, PA, United States, [2]Neurosurgery, University Of Pittsburgh Medical Center, PA, United States

A novel Textile Anisotropic Brain Imaging Phantom incorporating textile hollow fibers (taxons with inner/outer diameter 12/34 micron) is used to validate diffusion MRI imaging (dMRI). The taxon intra and extra spaces can be filled with water or deuterium. A taxon crossing pattern and a packing density pattern is manufactured to test orientation and the amount of taxons. NODDI based Intra-cellular volume fraction is correlated with the amount of taxons (r2=0.96) as compared to FA which is poor predictor with r2=0.11. Fiber crossings are estimated using Constrained Spherical Deconvolution techniques and can be resolved for angles greater then 45 degrees.

3455 Computer 5

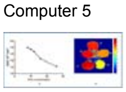

Cost effective 3D printed brain phantom for diffusion MRI

Arush Honnedevasthana Arun[1], Shivaprasad Ashok Chikop[1], Nithin N Vajuvalli[1], Rashmi Rao[1], and Sairam Geethanath[1]

[1]Dayananda Sagar Institutions, Bangalore, India

Diffusion weighted MRI is used to measure diffusion properties in the brain. In this paper, the method for the creation of an anatomically and mechanically realistic brain phantom from polyvinyl alcohol cryogel (PVA-C) and a 3D printable brain phantom using Poly Lactic Acid (PLA) PLA is proposed. PVA-C is material widely used in medical imaging phantoms because of its mechanical similarities to soft tissues. This brain phantom will allow testing and optimization of diffusion based MR methods.

3456 Computer 6

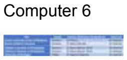

Robustness of Local Connectome Fingerprint Explored: Using a Multi-center and Multi-vendor Study

Vincent Kyu Lee[1,2], Ashok Panigrahy[1,2], Vincent J. Schmithorst[1,2], Thomas Chenevert[3], Borjan Gagoski[4], Deqiang Qiu[5], Peter S. LaViolette[6], Jeffrey I. Berman[7], Timothy D. Verstynen[8], and Fang-Cheng Yeh[9]

[1]Radiology, University of Pittsburgh, Pittsburgh, PA, United States, [2]Radiology, Children's Hospital of Pittsburgh UPMC, Pittsburgh, PA, United States, [3]Radiology, University of Michigan, Ann Arbor, MI, United States, [4]Radiology, Boston Children's Hospital, Boston, MA, United States, [5]Radiology and Imaging Sciences, Emory University School of Medicine, Atlanta, GA, United States, [6]Radiology, Medical College of Wisconsin, Milwaukee, WI, United States, [7]Radiology, Children's Hospital of Philadelphia, Philadelphia, PA, United States, [8]Psychology, Carnegie Mellon University, Pittsburgh, PA, United States, [9]Neurological Surgery, University of Pittsburgh, Pittsburgh, PA, United States

In this study we explore whether scanner-related-variabilities contribute to an individual's distinct fingerprint – and whether the fingerprint specificity would be robust as a biomarker by scanning the same subject across multiple vendors and multiple scanner in four institutions. Both Diffusion Tensor Imaging and Multi-shell Multi-band diffusion imaging (MSMBDI) was tested, and differences within acquisition type (using fractional anisotropy and normalized quantitative anisotropy) and between acquisition types comparisons (using q-space diffeomorphic reconstruction) analysis were examined. We found that scanner may contribute partly to the fingerprint patter, but the fingerprint was robust at maintaining pattern, especially in MSMBDI to warrant further studies.

3457 Computer 7

Quantitative evaluation of PROPELLER DWI using QIBA diffusion phantom

Joshua Yung[1], Hua Ai[1], Ho-Ling Liu[1], and R Jason Stafford[1]

[1]Imaging Physics, The University of Texas MD Anderson Cancer Center, Houston, TX, United States

The purpose of this study was to characterize ADC values when varying imaging parameters in a diffusion-weighted (DW) FSE sequence with Periodically Rotated Overlapping ParallEL Lines with Enhanced Reconstruction (PROPELLER) k-space trajectory. The QIBA diffusion phantom was used to quantitatively evaluate the different pulse sequences. The DW PROPELLER sequence showed good agreement with the QIBA SE EPI sequence with the ETL=20 and b-value of 0 and 2000 s/mm^2 sequence having with a r^2=0.9034. The DW PROPELLER sequence is promising for quantitative evaluation of ADC values and this study may help improve clinical protocols using diffusion weighted imaging.

3458 Computer 8

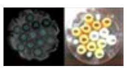

Quantitative evaluation of apparent diffusion coefficient in a large multi-unit institution using QIBA diffusion phantom

Joshua Yung[1], Yao Ding[1], Ken-Pin Hwang[1], Carlos E Cardenas[2,3], Hua Ai[1], Michael A Boss[4], Thomas L Chenevert[5], Clifton Fuller[6], and R Jason Stafford[1]

[1]Imaging Physics, The University of Texas MD Anderson Cancer Center, Houston, TX, United States, [2]Radiation Physics, The University of Texas MD Anderson Cancer Center, Houston, TX, United States, [3]The University of Texas Graduate School of Biomedical Sciences, Houston, TX, United States, [4]Physical Measurement Laboratory, National Institute of Standards and Technology, Boulder, CO, United States, [5]Radiology, University of Michigan, Ann Arbor, MI, United States, [6]Radiation Oncology, The University of Texas MD Anderson Cancer Center, Houston, TX, United States

The purpose of this study was to determine the quantitative variability of apparent diffusion coefficient values across a large fleet of MR systems. Using a NIST traceable magnetic resonance imaging diffusion phantom, imaging was reproducible and the measurements were quantitatively compared to known values. Significant differences in identical phantoms were not observed, but uncertainty in the measurements was seen at low apparent diffusion coefficient values. The same trend was observed when the diffusion phantoms were imaged in 20 different MR systems. The characterization of ADC variability for these systems provides an improved quality control for quantitative diffusion weighted imaging.

3459 Computer 9

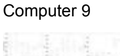

Reproducibility of DTI Metrics and the Influence of SNR on DTI metrics in a Longitudinal Multicenter Clinical Trial

Xiaopeng Zhou[1], Ken Sakaie[1], Josef Debbins[2], Robert Fox[1], and Mark J. Lowe[1]

[1]The Cleveland Clinic, Cleveland, OH, United States, [2]Barrow Neurological Institute, Phoenix, AZ, United States

SPRINT-MS is a large-scale longitudinal phase II trial including 27 3T MRI scanners to evaluate the treatment of progressive multiple sclerosis with Ibudilast. DTI measures showed high reproducibility in a longitudinal multicenter study, making it appropriate for use as a biomarker. The longitudinal design of the SPRINT-MS trial is expected to mitigate the systematic influence of SNR on DTI, but the observed trend may be useful as a correction factor in cross-sectional studies.

3460 Computer 10

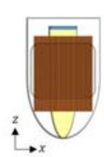

A Novel Yeast Cells- and Microcapillaries-Based Phantom for Validation of Diffusion MRI Models

Shir Levy[1], Darya Morozov[1], Inbar Seroussi[2], Leah Bar[2], Nir Sochen[2], and Yoram Cohen[1,3]

[1]School of Chemistry, The Raymond and Baverly Sackler Faculty of Exact Science, Tel Aviv University, Tel Aviv, Israel, [2]School of Mathematical Sciences, The Raymond and Beverly Sackler Faculty of Exact Science, Tel Aviv University, Tel Aviv, Israel, [3]Sagol School of Neuroscience, Tel Aviv University, Tel Aviv, Israel

Numerous different models provide detailed microstructure information from diffusion MRI data. In order to challenge them, there is a need for complex phantoms with known structural characteristics. For this purpose, we present a novel phantom, consists of spherical fixed yeast cells and cylindrical microcapillaries. Despite of its complexity, arising from the different size, geometry and size distribution of the restricted compartments, there is a good correlation between the known ground truth and the features that were extracted from fitting single diffusion encoding (SDE) MRI experimental data, assuming continued or discrete weight of size distribution.

3461 Computer 11

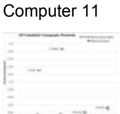

The use of novel validation methods to investigate optimal ROI location and probabilistic thresholds in tractography for presurgical planning in brain tumour patients.

Gideon Ayokunmi Oluniran[1,2], Marcelo Lemos[1], Jeorg Ederle[3], Jozef Jarosz[4], Gareth John Barker[1], and Jonathan Ashmore[4]

[1]Neuroimaging, King's College London, London, United Kingdom, [2]Physics, Federal University, Ndufu-Alike, Ikwo, Abakaliki, Ebonyi State, Nigeria, [3]Neuroradiology, King's College Hospital, London, United Kingdom, [4]Neuroradiology, King's College Hospital, London, United Kingdom

Although advanced tractography techniques exists and are well documented, many validation methods are not applicable to brain tumour cases and do not examine the possibility of proposing standard probabilistic thresholds. Using a novel approach, we investigate certain thresholds ('safe' thresholds) which can be applied to probabilistic tractography to reduce false representation of tracts, aid maximal tumour resection, and limit neurofunctional deficit from surgical treatments. We also examine optimal region of interest (ROI) location. 'Safe' thresholds can be determined, and with a wider confidence when tractography is defined with inclusion regions.

3462

Computer 12

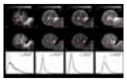

Theory, validation and application of blind source separation to diffusion MRI for tissue characterisation and partial volume correction

Miguel Molina-Romero[1,2], Pedro A Gómez[1,2], Jonathan I Sperl[2], Andrew J Stewart[3], Derek K Jones[4], Marion I Menzel[2], and Bjoern H Menze[1]

[1]Technische Universität München, Munich, Germany, [2]GE Global Research Europe, Garching, Germany, [3]EMRIC, Cardiff University, Cardiff, United Kingdom, [4]CUBRIC, Cardiff University, Cardiff, United Kingdom

Here we present blind source separation (BSS) as a new tool to analyse multi-echo diffusion data. This technique is designed to separate mixed signals and is widely used in audio and image processing. Interestingly, when it is applied to diffusion MRI, we obtain the diffusion signal from each water compartment, what makes BSS optimal for partial volume effects correction. Besides, tissue characteristic parameters are also estimated. Here, we first state the theoretical framework; second, we optimise the acquisition protocol; third, we validate the method with a two compartments phantom; and finally, show an in-vivo application of partial volume correction.

3463

Computer 13

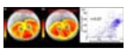

Histological validation of microstructural measures derived from the PICASO model

Lipeng Ning[1], Tanguy Duval[2], Julien Cohen-Adad[2], and Yogesh Rathi[1]

[1]Harvard Medical School, Boston, MA, United States, [2]Polytechnique Montréal

We propose to validate the PICASO (Precise Inference and Characterization of Structural Organization)[1] biophysical model of tissue microstructure using a full-slice histology of cat spinal cord. The PICASO model was fit to high resolution diffusion MRI (dMRI) of a cat spinal cord to estimate microstructural measures of diffusion disturbance, which is directly related to axonal packing and density. We found that the structural disturbance coefficient (SDC) in the direction orthogonal to the fiber orientation from the PICASO model was strongly correlated with the axonal density obtained from histology[2,] with a correlation coefficient of r=0.67. Thus, the SDC could provide very precise information about the microscopic arrangement of axons or cells in biological tissue.

3464

Computer 14

The histological validation analysis of diffusional kurtosis imaging with a cleared mouse brain.

Ryusuke Irie[1], Koji Kamagata[1], Aurelien Kerever[2], Suguru Yokosawa[3], Yosuke Otake[3], Hisaaki Ochi[3], Kazuhiko Tagawa[4], Hitoshi Okazawa[4], Ryo Ueda[5], Kohske Takahashi[6,7], Kanako Sato[1], Masaaki Hori[1], Eri Arikawa Hirasawa[2], and Shigeki Aoki[1]

[1]Radiology, Juntendo University School of Medicine, Tokyo, Japan, [2]Research Institute for Diseases of Old Age, Juntendo University Graduate School of Medicine, Tokyo, Japan, [3]Research & Development Group, Hitachi Ltd., Tokyo, Japan, [4]Neuropathology, Tokyo Medical and Dental University, Tokyo, Japan, [5]Radiological Sciences, Tokyo Metropolitan University Graduate School of Human Health Sciences, Tokyo, Japan, [6]Psychology, Chukyo University, Nagoya, Japan, [7]Araya Brain Imaging, Tokyo, Japan

Diffusional kurtosis imaging (DKI) is a sensitive technique to analyze brain microstructure but that has little histological foundation. In this study, we evaluated a relationship between DKI parameters with neurite density measured by a confocal microscopy of the cleared mouse brain. There was a strongly positive correlation between neurite density and DKI parameters in the caudate nucleus and putamen, whereas the correlation between neurite density and fractional anisotropy was moderate. DKI reflect neurite density in an area with crossing fibers, so that can evaluate more complex microstructures than diffusion tensor imaging.

3465

Computer 15

An affordable phantom for ADC/FA; a device for multi-site studies

Koji Sakai[1], Toshiaki Nakagawa[2], Ryusuke Nakai[3,4], Hiroyasu Ikeno[2], Seiji Yamaguchi[3], Hiroaki Takadama[3], and Kei Yamada[1]

[1]Kyoto Prefectural University of Medicine, Kyoto, Japan, [2]Kyoto Prefectural University of Medicine Hospital, [3]Chubu University, [4]Kyoto University

Multi-site study gives large statistical power for the results. Some intrinsic differences among scanners are recognizing as an inevitable property. Isotropic diffusion has already been discussing. In contrast, anisotropic diffusion has been evading the endeavor because of the absence of an easily available anisotropic diffusion phantom. We compared DTI measures among five different MR scanners at three different sites using commercially and easily available astriction cotton. The averaged coefficient of variation for longitudinal repeated acquisitions of DTI on five different MR scanners were stable. The scan-rescan properties of five different MR scanners can be comparable by anisotropic diffusion phantom.

3466

Computer 16

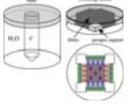

Reduction of susceptibility-induced field gradients in multi-fibre diffusion phantoms via susceptibility matching

Ezequiel Farrher[1], Johannes Lindemeyer[1], Farida Grinberg[1,2], Ana-Maria Oros-Peusquens[1], and N. Jon Shah[1,2,3]

[1]Institute of Neuroscience and Medicine 4, Forschungszentrum Jülich, Jülich, Germany, [2]Department of Neurology, Faculty of Medicine, RWTH Aachen University, Aachen, Germany, [3]JARA – BRAIN – Translational Medicine, RWTH Aachen University, Aachen, Germany

Studies performing diffusion-weighted MRI on anisotropic fibre phantoms suffer from microscopic background field gradients induced by differences in the magnetic susceptibility of the employed materials. We present a particularly promising approach that makes use of a matched magnesium chloride solution to eliminate these effects. The method is thoroughly studied and successfully validated on a crossing-fibre phantom containing two perpendicularly crossing fibre populations. The obtained results are no longer subject to any orientation-dependence with respect to $\mathbf{B}_0$.

3467 Computer 17

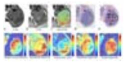

Diffusion radiomics analysis in intratumoral heterogeneity of murine prostate cancer following radiotherapy: pixel-wise correlation with histology

Yu-Chun Lin[1,2], Gigin Lin[1,2], and Chun-Chieh Wang[2,3]

[1]Dep. Medical Imaging and Intervention, Chang Gung Memorial Hospital, Taoyuan, Taiwan, [2]Chang Gung University, Taoyuan, Taiwan, [3]Dep. Radiation Oncology, Chang Gung Memorial Hospital, Taoyuan, Taiwan

To investigate the biological meaning of apparent diffusion coefficient (ADC) in tumors following radiotherapy. Five mice bearing TRAMP-C1 tumor were half-irradiated. Diffusion-weighted images were acquired using multiple b-values of up 0 to 3000 s/mm^2. The pixelwise ADC positively correlated with extracellular space and nuclear size, and negatively correlated with nuclear count, cytoplasmic space and nuclear space. Optimal ADC was achieved at b-value of 800 s/mm^2 in determining the treatment response. Pixelwise ADC values correlate with histology metrics might be a means of in vivo radiomics biomarkers for evaluating tumor heterogeneity and responses to radiotherapy.

3468 Computer 18

Hypoxia imaging of head and neck carcinoma: Correlation between DWI parameters and FAZA-PET activity

Akiko Imaizumi[1,2], Takayuki Obata[1], Yasuhiko Tachibana[1], Masayuki Inubushi[3], Mitsuru Koizumi[4], Kyosan Yoshikawa[5], Ming-Rong Zhang[6], Katsuyuki Tanimoto[7], Rintaro Harada[8], Takashi Uno[8], and Tsuneo Saga[9]

[1]Applied MRI Research, Molecular Imaging and Theranostics, National Institute of Radiological Sciences, National Institutes for Quantum and Radiological Science and Technology, Chiba, Japan, [2]Department of Oral and Maxillofacial Radiology, Tokyo Dental College, Tokyo, Japan, [3]Department of Nuclear Medicine, Kawasaki Medical School, [4]Department of Nuclear Medicine, Cancer Institute Hospital, Japanese Foundation for Cancer Research, [5]Molecular Imaging and Theranostics, National Institute of Radiological Sciences, [6]Department of Radiopharmaceuticals Development, National Institute of Radiological Sciences, [7]National Institute of Radiological Sciences Hospital, [8]Diagnostic Radiology and Radiation Oncology, Graduate School of Medicine, Chiba University, [9]Department of Diagnostic Imaging and Nuclear Medicine, Kyoto University

To investigate the usefulness of diffusion-weighted imaging (DWI) for visualizing hypoxia of head and neck carcinoma, the correlation between DWI parameter estimates and ^{18}F-fluoroazomycin arabinoside (FAZA) positron emission tomography (PET) activity was evaluated. The diffusion coefficients and fractions of the fast and slow compartments according to the 2-compartment model (D_{fast}, D_{slow} and F_{fast}, F_{slow}) were estimated. The diffusional kurtosis (K) and the corrected diffusion coefficient (D) were also obtained according to the diffusional kurtosis imaging (DKI) method. Amongst the DWI estimates, D_{slow} and K were significantly correlated with FAZA-PET activity, which suggests they might be useful as indicators of hypoxia.

3469 Computer 19

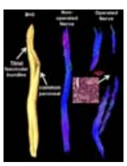

7.0 T Diffusion Tensor Imaging Evaluation of Rabbit Sciatic Nerve Microstructure with Histologic Correlation

Tina Jeon[1], Emil Stefan Vutescu[2], Eric Aronowitz[3], Henning U Voss[3], Jonathan P Dyke[3], and Darryl B Sneag[1]

[1]Radiology and Imaging, Hospital for Special Surgery, New York, NY, United States, [2]3Department of Hand and Upper Extremity Service, Hospital for Special Surgery, New York, NY, United States, [3]Citigroup Biomedical Imaging Center, Weill Cornell Medical College, New York, NY

High-resolution DTI is a promising tool to evaluate peripheral nerve regeneration following surgical repair of nerve injury. The spatial resolution achieved with 7.0 T allowed us to more confidently interrogate the nerve for measuring fractional anisotropy (FA) and diffusivity and to perform fiber tracking as compared to 3.0 T. Among DTI metrics, FA correlated the greatest with axonal density and diameter. These findings support that DTI has the potential to measure axonal regeneration in the peripheral nerves at preclinical and clinical field strengths.

3470 Computer 20

Diffusion-weighted MRI of node tissue: correlation of mean diffusivities and cellularity.

Mariaulpa Sahalan[1], Aritrick Chatterjee[1], Nyoman Kurniawan[2], Gary Cowin[2], Laurence Gluch[3], Carl Power[4], Geoffrey Watson[5], Kevin Tay[6], Julie Fletcher[7], David Taylor[8], and Roger Bourne[1]

[1]Faculty of Health Sciences, The University of Sydney, NSW, Australia, [2]Centre for Advanced Imaging, University of Queensland, Brisbane, Australia, [3]The Strathfield Breast Centre, NSW, Australia, [4]Biological Resources Imaging Laboratory, University of New South Wales, NSW, Australia, [5]Tissue Pathology and Diagnostic Oncology, Royal Prince Alfred Hospital, NSW, Australia, [6]Westmead Breast Cancer Institute, NSW, Australia, [7]Concord Repatriation General Hospital, NSW, Australia, [8]Vetnostics, NSW, Australia

Improvement of sensitivity and specificity in DWI-based assessment of nodal diseases is dependent on a better understanding of how nodal microstructures affect the water diffusivity in tissue. In this abstract we report the first diffusion microimaging investigation of formalin fixed node tissue with the aim of assessing any correlation between mean diffusivity and cellularity. Mean diffusivity was calculated in ROI corresponding to distinct node sub-structures. Nuclei were segmented semi-automatically to measure the cellularity metrics: nuclear count and nuclear area. The results showed there is no significant correlation between mean diffusivity with cellularity metrics in the nodal tissues.

3471 Computer 21

Reproducibility of SMT-Based Microscopic Diffusion Anisotropy Imaging on a Clinical MRI System

Cara Louise Foley[1], Enrico Kaden[2], Kiran Seunarine[1], Matt Hall[1], David Carmichael[1], Jonathan Clayden[1], and Chris Clark[1]

[1]Developmental Imaging & Biophysics, University College London, London, United Kingdom, [2]Centre of Medical Image Computing, University College London, London, United Kingdom

Diffusion Tensor Imaging (DTI) is a widely used neuroimaging technique, but it lacks specificity. Advanced diffusion models aim to yield greater biophysical information than DTI. This information is redundant if the parameters cannot be accurately reproduced across time-points. Multi-shell diffusion images were acquired on a single 3T scanner at two time-points for ten healthy adults. Mean parameter values from SMT-based microscopic diffusion anisotropy imaging and DTI were obtained in white matter, cortex and thalami. The advanced model performed similarly well to DTI in white matter, but was less consistent in the cortex and thalami, potentially due to its increased complexity.

3472 Computer 22

Scan-rescan of AxCaliber, macromolecular tissue volume and g-ratio in the spinal cord

Tanguy Duval[1], Victoria Smith[2], Eric Klawiter[2], Nikola Stikov[1,3], and Julien Cohen-Adad[1,4]

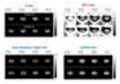

[1]NeuroPoly Lab, Institute of Biomedical Engineering, Polytechnique Montreal, Montreal, QC, Canada, [2]A.A. Martinos Center for Biomedical Imaging, Massachusetts General Hospital, Harvard Medical School, Boston, MA, United States, [3]Montreal Heart Institute, Montreal, QC, Canada, [4]Functional Neuroimaging Unit, CRIUGM, Montreal, QC, Canada

Translating quantitative MRI to clinical research raises many challenges in term of acquisition strategy, modeling of the MRI signal, artifact corrections (sensitivity to motion and distortion) and metric extraction (template registration and partial volume effects). In this work, we wanted to validate the repeatability of this entire framework, from the acquisition to the extraction of the metrics using a template-based approach. We took advantage of the 300 mT/m gradients from the connectome scanner for estimating robustly AxCaliber metrics, MTV, and g-ratio in the spinal cord of eight healthy subjects, scanned and rescanned in two different sessions. Our results show good scan-rescan repeatability (r>0.7, small deviations <5%), and demonstrate the capability of these metrics to detect inter-subjects (through ICC) and inter-fiber-pathways differences (through ANOVA analysis).

3473 Computer 23

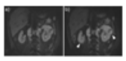

Reducing complexity of functional imaging: free-breathing imaging based ADC and IVIM measurements are as accurate as breath-hold measurements in renal cell carcinoma

Neil P Jerome[1,2], Matthew R Orton[2], James A d'Arcy[2], David J Collins[2], Martin O Leach[2], and Dow-Mu Koh[3]

[1]Department of Circulation and Medical Imaging, NTNU - Norwegian University of Science and Technology, Trondheim, Norway, [2]Radiotherapy & Imaging, The Institute of Cancer Research, London, United Kingdom, [3]Department of Radiology, The Royal Marsden Hospital, London, United Kingdom

Respiratory motion represents a serious confounding factor for abdominal imaging; for more complex diffusion models such as IVIM, acquisition of diffusion-weighted images in successive breath-holds offers control of motion for sharper images. In this patient study, DWI was performed in free-breathing and consecutive breath-holds, without registration, on successive days without intervention to determine repeatability. Derived tumour ROI parameters from ADC and IVIM models were not significantly affected between breathing regimes, but observed coefficients of variation for free-breathing were smaller for all pseudo-diffusion related parameters. Breath-holding is time inefficient, and free-breathing allows more data collection for development of robust DWI markers.

Electronic Poster

Diffusion: Tractography & Fiber Modeling

Exhibition Hall Monday 14:45 - 15:45

3474 Computer 25

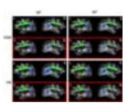

When does a volume of a bundle achieve saturation? A microstructure informed tractography study

Muhamed Barakovic[1], David Romascano[1], Gabriel Girard[1], Maxime Descoteaux[1,2], Jean-Philippe Thiran[1,3], and Alessandro Daducci[1,3,4]

[1]Signal Processing Lab (LTS5), École Polytechnique Fédérale de Lausanne, Lausanne, Switzerland, [2]Sheerbrooke Connectivity Imaging Laboratory (SCIL), University of Sheerbrooke, Canada, [3]University Hospital Center (CHUV) and University of Lausanne (UNIL), Switzerland, [4]Department of Computer Science, University of Verona, Italy

Volumetric analysis of bundles derived from tractography is a popular statistical measure used in neurological disorder studies. Recent research performed by Gauvin shows that different bundles saturate with different tractography parameters, however, to achieve that saturation millions of streamlines need to be computed. In this investigation, the aim was to use microstructure informed tractography, a novel technique that combine tractography and microstructure models, to study the saturation of the bundles. This study has found that generally microstructure informed tractography makes the volume estimation less sensitive to tracking parameters. The findings may have profound implications in volumetric analysis in group studies.

3475 Computer 26

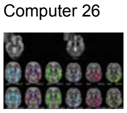

Structure tensor informed fibre tractography at 3T

Kwok-shing Chan[1], David G. Norris[1], and José P. Marques[1]

[1]Donders Centre for Cognitive Neuroimaging, Donders Institute for Brain, Cognition and Behaviour, Nijmegen, Netherlands

Structure tensor informed fibre tractography (STIFT) based on diffusion images at 3T and gradient-echo images at 7T has shown improvement in the accuracy of white matter bundles tracking in the presence of kissing and crossing fibres. In this study, we implemented STIFT using both DWI and GRE images at 3T. We further demonstrated white matter contrast presence in T_2* mapping and quantitative susceptibility mapping derived from GRE data can be used to compute structure tensor. The benefits of STIFT are shown in two tractography applications.

3476 Computer 27

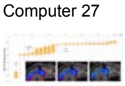

Stability metrics for optic radiation tractography: towards damage prediction after resective surgery

Stephan Meesters[1,2], Pauly Ossenblok[2,3], Louis Wagner[2], Olaf Schijns[2,4], Paul Boon[2], Luc Florack[1], Anna Vilanova[3,5], and Remco Duits[1]

[1]Mathematics and Computer Science, Eindhoven University of Technology, Eindhoven, Netherlands, [2]Academic Center for Epileptology Kempenhaeghe & Maastricht UMC+, Heeze, Netherlands, [3]Biomedical Engineering, Eindhoven University of Technology, Eindhoven, Netherlands, [4]Neurosurgery, Maastricht UMC+, Maastricht, Netherlands, [5]Mathematics and Computer Science, Delft University of Technology, Delft, Netherlands

An accurate delineation of the optic radiation (OR) is useful in reducing the risk of a visual field deficit after temporal lobe resective surgery. However, tractography, especially of the probabilistic kind, is prone to generate spurious (false-positive) streamlines that are poorly aligned with the surrounding bundle. Fiber-to-bundle coherence measures are applied to identify and remove spurious fibers, which together with test-retest parameter estimation can provide a reconstruction of the OR that is robust to the stochastic realization of probabilistic tractography. Pre- and post-operative comparison of the OR is performed for epilepsy patients to quantify the accuracy of damage prediction.

3477 Computer 28

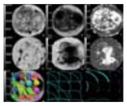

Structural Connectivity Within Neural Ganglia: A Default Small-World Network

Abdol Aziz O. Ould Ismail[1,2], Ghoncheh Amouzandeh[1,3], and Samuel Colles Grant[1,2]

[1]Center for Interdiscplinary Magnetic Resonance, Florida State University, Tallahassee, FL, United States, [2]Chemical & Biomedical Engineering, Florida State University, Tallahassee, FL, United States, [3]Physics, Florida State University, Tallahassee, FL, United States

Diffusion tensor imaging (DTI) provides a unique contrast based on the restricted directionality of water movement in an anisotropic environment. As such, DTI-based tractography can be used to characterize and quantify the structural connectivity within neural tissue. Here, structural connectivity within isolated abdominal neural ganglia of *Aplysia californica* (ABG) is assessed by integrating DTI and network theoretical analysis. For ABG, findings demonstrate a default structural network with preferential specific small-world properties when compared to simulated lattice and random networks that are equivalent in order and degree.

3478 Computer 29

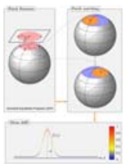

Atlas Construction in Diffusion MRI via Angular Patch Matching

Zhanlong Yang[1,2], Geng Chen[2], Dinggang Shen[2], and Pew-Thian Yap[2]

[1]College of Marine, Northwestern Polytechnical University, Xi'an, People's Republic of China, [2]Department of Radiology and BRIC, UNC Chapel Hill, Chapel Hill, NC, United States

Construction of brain atlases is generally carried out using a two-step procedure involving registering a population of images to a common space and then fusing the aligned images to form an atlas. In practice, image registration is not perfect and simple averaging of the images will blur structures and cause artifacts. In diffusion MRI, the problem is even more challenging, since the alignment of gross anatomical structures does not necessarily guarantee the alignment of the microstructural information captured in each voxel. In this situation, it is unclear for example how signals characterizing fiber bundles of varying orientations, which can occur naturally across subjects, should be fused to form the atlas. Moreover, the commonly used simple averaging method is sensitive to outliers.

3479 Computer 30

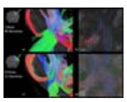

The impact of High-Q and High-K on complex fiber structures in the human brain

Iain Bruce[1], Christopher Petty[1], Hing-Chiu Chang[2], Nan-Kuei Chen[1,3], and Allen W Song[1]

[1]Brain Imaging and Analysis Center, Duke University Medical Center, Durham, NC, United States, [2]Department of Diagnostic Radiology, University of Hong Kong, [3]Biomedical Engineering, University of Arizona, Tuscan, AZ, United States

In this diffusion MRI study, we investigated the impact of high angular resolution (high-Q) and high spatial resolution (high-K) on complex fiber structures. It was found that while high-Q was able to resolve crossing fibers within a given region, high-K provided additional spatial details of these crossing fibers in the same location. In addition, diffusion data from high-K improved characterization of high-curvature fibers, which cannot be adequately resolved with high-Q. It is thus concluded that high-K is preferred when both crossing and high-curvature fibers need to be resolved, as in human connectome analysis.

3480 Computer 31

REPRODUCIBILITY OF GRAPH METRICS ESTIMATED FROM ALTERNATIVE STRATEGIES OF NETWORK WEIGHTING:EVIDENCES FROM REPEAT MRI SCANS

STAVROS I DIMITRIADIS[1,2], MARK DRAKESMITH[2], SONYA BELLS[3], GREG PARKER[3], DAVID LINDEN[3], and DEREK K JONES[4]

[1]SCHOOL OF MEDICINE, Institute of Psychological Medicine and Clinical Neurosciences, Cardiff University School of Medicin, CARDIFF, United Kingdom, [2]SCHOOL OF MEDICINE, Cardiff University Brain Research Imaging Center (CUBRIC), School of Psychology, Cardiff University, Cardiff, United Kingdom, CARDIFF, United Kingdom, [3]SCHOOL OF PSYCHOLOGY, Cardiff University Brain Research Imaging Center (CUBRIC), School of Psychology, Cardiff University, Cardiff, United Kingdom, CARDIFF, United Kingdom, [4]SCHOOL OF PSYCHOLOGY, CARDIFF, United Kingdom

Sinopsis:To evaluate the reliability of well-known network metrics over alternative weighting strategies using diffusion MRI. Methods: Using ten different network weighting strategies to construct structural networks from repeat dMRI scans, we estimated the reliability of network metrics estimated over the networks. Additionally, the recognition accuracy was estimated for each of the ten strategies. Results: We demonstrated excellent ICC for six network metrics for the seven out of network weighting strategies. Recogniton accuracy was 100% accurate for the number and percentage of streamlines and tract volume. Conclusions: Our results highlight the importance of reliable network metrics from structural brain networks.

3481 Computer 32

Visualizing White Matter Fiber Tracts of the Human Brain in Augmented Reality: Initial Experience with the Microsoft HoloLens

Nicole Wake[1], Steven H. Baete[1], Ying-Chia Lin[1], Fernando E. Boada[1], and Daniel K. Sodickson[1]

[1]Bernard and Irene Schwartz Center for Biomedical Imaging, Center for Advanced Imaging Innovation and Research, Department of Radiology, New York University School of Medicine, New York, NY, United States

The objective of this study was to create a workflow to view 3D fiber tracts derived from diffusion spectrum imaging (DSI) in augmented reality (AR) and to test the application of visualizing tractography models in AR. Visualizing tractography in AR may allow for enhanced comprehension of the connectivity in the brain which could impact patient care and management.

3482 Computer 33

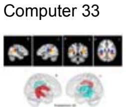

Hemispheric asymmetries and grey matter projections of the arcuate fasciculus: an along-tract study of diffusion and localization properties with deterministic and probabalistic tractography

Lia Talozzi[1], Claudia Testa[1], Stefano Zanigni[1], Stefania Evangelisti[1], Laura Ludovica Gramegna[1], Claudio Bianchini[1], Paola Fantazzini[2,3], Caterina Tonon[1], David Neil Manners[1], and Raffaele Lodi[1]

[1]Department of Biomedical and NeuroMotor Sciences, University of Bologna and Functional MR Unit, Policlinico S. Orsola - Malpighi, Bologna, Italy, [2]Department of Physics and Astronomy, University of Bologna, Italy, [3]Centro Enrico Fermi, Roma, Italy

We studied the arcuate fasciculus in both cerebral hemispheres in 29 healthy subjects, by evaluating GM projections and along-tract diffusion properties and tract curvature, obtained with three tractography methods: probabilistic ball-and-sticks model, deterministic and probabilistic spherical deconvolution. In all subjects we detected the arcuate in both hemispheres. For all the tractography methods we measured a bigger tract volume on the left, but detected more tracts branching towards GM terminations on the left only with the probabilistic methods, that influenced both the tract curvature and its diffusion parameters. The probabilistic tractography methods better described arcuate connectivity, which is more complex in the left hemisphere.

3483 Computer 34

Structural abnormalities in frontal lobe pathways in children with Attention-Deficit/Hyperactivity Disorder (ADHD)

Weining Wu[1,2], Hesham Hamoda[2], Lipeng Ning[2], Borjan Gagoski[3], Kiera Sarill[4], P. Ellen Grant[5], Martha E. Shenton[2], Deborah Waber[6], Nikos Makris[2], Gloria McAnulty[4], and Yogesh Rathi[2]

[1]College of Computer Science and Technology, Harbin Engineering University, Harbin, People's Republic of China, [2]Psychiatry Neuroimaging Laboratory, Brigham and Women's Hospital, Harvard Medical School, Boston, MA, United States, [3]Department of Radiology, Children's Hospital of Boston, Boston, MA, United States, [4]Department of Psychiatry, Children's Hospital of Boston, Boston, MA, United States, [5]Fetal-Neonatal Neuroimaging and Developmental Science Center, Children's Hospital of Boston, Boston, MA, United States, [6]Scientific Review and Behavioral Science Core, Children's Hospital of Boston, Boston, MA, United States

Structural abnormalities in frontal lobe connections have been observed in adults/children with ADHD in earlier studies using diffusion tensor imaging (DTI)[3]. This abstract investigates microstructural differences in frontal-lobe white matter connectivity using advanced diffusion imaging methods. 47 white matter fiber bundles connecting frontal areas as parcellated by Freesurfer were extracted using a novel whole-brain tractography algorithm[4,1], which allowed estimation of specific diffusion properties such as cellular volume and cellular density from advanced diffusion MRI (dMRI) data. After correcting for multiple comparisons, 6 significant white matter pathways were found to have lower cellular volume and density in ADHD compared to controls.

3484 Computer 35

Hyper-connectivity of the Seizure Onset Zone: A Potential Epilepsy Biomarker at 7T

Jack Rutland [1,2], Rebecca Feldman[1], Lara Marcuse [3], Madeline Fields [3], Bradley Delman [1], Priti Balchandani[1], and Rafael O'Halloran[1]

[1]Radiology, Icahn School of Medicine at Mount Sinai, New York, NY, United States, [2]Wake Forest University, Winston-Salem, NC, United States, [3]Neurology, Icahn School of Medicine at Mount Sinai, New York, NY, United States

The present study aims to identify the connectivity of the seizure onset zone (SOZ) in patients with MRI-negative epilepsy. Motivated by recent findings of aberrant white matter structure in epilepsy we hypothesized differences in structural connectivity. To test this we compared structural connectivity in a group of 8 epilepsy subjects and 8 healthy controls. We also investigated differences in connectivity in SOZ and non-SOZ areas in the epilepsy group. Hyper-connectivity was found in epilepsy subjects compared to controls. Additionally, hyper-connectivity was found in SOZ compared to non-SOZ related regions. These findings may have implications for diagnosis and surgical intervention in MRI-negative epilepsy.

3485 Computer 36

High-Throughput Diffusion Imaging Using Multiple Coils for Mouse Brain Connectomics

John Nouls[1,2], Alexandra Badea[1,2], Robert J. Anderson[1,2], Gary P. Cofer[1,2], and G. Allan Johnson[1,2]

[1]Center for In Vivo Microscopy, Duke University Medical Center, Durham, NC, United States, [2]Radiology, Duke University Medical Center, Durham, NC, United States

The complex neural architecture and brain connectivity of mouse models of human disease can be studied *ex vivo* by diffusion tensor imaging; however, acquisition times are long and make cohort studies prohibitively time-consuming. Throughput can be increased by the simultaneous use of multiple coils placed in proximity to the magnet isocenter. We quantify the impact of the multiple-coil configuration on throughput, on diffusion metrics used in tractography, and on mouse brain connectivity matrices. We show that fractional anisotropy is underestimated off-isocenter, while the main eigenvector direction is minimally affected. The effect on brain connectivity networks is currently being quantified.

3486 Computer 37

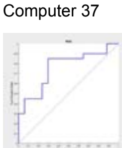

Prediction vision recovery of Neuromyelitis optica spectrum disorders (NMOSDs) with multivariate pattern analysis: a DTI study

Yuan Tian[1], Lin Ma[1], Zhenyu Liu[2], Zhenchao Tang[3], Xin Lou, Jie Tian, and Mingge Li

[1]radiology department, Chinese PLA General Hospital, beijing, People's Republic of China, [2]Key Laboratory of Molecular Imaging, Institute of Automation, Chinese Academy of Sciences, [3]School of Mechanical, Electrical & Information Engineering, Shandong University

To explore if a DTI protocol could provide a model to predict the degree of vision recovery in NMOSDs patients. 37 patients were employed in the study, including 20 patients of well vision recovery and 17 patients of poor vision recovery. With the diffusion measure of multiple white and grey matters as features, a Lasso-Logistic regression model and a Support Vector Machine (SVM)-based classification model were constructed. The results show area under curve (AUC) of 0.7618 (P=0.008) and accuracy (ACC) of 0.7297 (0.006). The method shows promising prediction performance, and it has the potential to improve the clinical treatment design.

3487 Computer 38

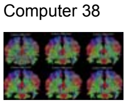

White Matter Fiber Tractography with Fiber Ball Imaging

Hunter Moss[1], George Russell Glenn[1], Emilie T. McKinnon[1], and Jens Jensen[1]

[1]Medical University of South Carolina, Charleston, SC, United States

An investigation into the minimum b-value necessary to characterize the fiber orientation density function (fODF) with fiber ball imaging (FBI) for white matter fiber tractography (WMFT) is presented. Using high angular resolution diffusion imaging (HARDI) data, we assessed the angular difference between principal directions across b-values using a high b-value benchmark, as well as the number of fiber crossings based on fODF peak detection. WMFT was performed using the reconstructed fODFs and was viewed qualitatively. Overall, the results indicated convergence near b = 4000 s/mm² suggesting this to be the minimum b-value needed for FBI-WMFT.

3488 Computer 39

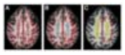

Impact of white-matter hyperintensities on tractography

Guillaume Theaud[1], Bixente Dilharreguy[2], Gwénaëlle Catheline[2], and Maxime Descoteaux[1]

[1]Sherbrooke Connectivity Imaging Lab (SCIL), Université de Sherbrooke, Sherbrooke, QC, Canada, [2]INCIA, UMR 5287, Université de Bordeaux, EPHE PSL Research University, Talence, France

A common way to seed tractography is thresholding the Fractional Anisotropy (FA). This technique is problematic for aging diffusion MRI studies because the FA decreases dramatically in regions of White Matter Hyperintensities (WMH) and thus, the tractography can erroneously start or stop in these WMH regions. We show the importance for tractography pipelines to correct for WMH in their tracking masks. We show that the non-correction can lead to approximately 15% erroneous streamlines, which are false connections that can pollute the structural connectome and lead to misinterpretations.

3489 Computer 40

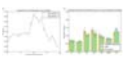

Effect of Different Seeding Strategies on Tractometry Reproducibility

Martin Cousineau[1,2], Maxime Descoteaux[1], and Hiromasa Takemura[2,3]

[1]Sherbrooke Connectivity Imaging Laboratory (SCIL), Université de Sherbrooke, Sherbrooke, QC, Canada, [2]Center for Information and Neural Networks (CiNet), National Institute of Information and Communications Technology (NICT), Suita, Japan, [3]Graduate School of Frontier Biosciences, Osaka University, Suita, Japan

Two common approaches to tractography seeding are using the whole-brain white matter mask, or the gray and white matter interface. Using a dataset with two acquisitions per subject and a state of the art processing pipeline, we compared the test-retest reproducibility of the shape and tract profiles of major white matter bundles for both seeding strategies. We found that both seeding strategies have regions in the brain where they are more reproducible. We propose an ensemble method combining both strategies as a possible way to make tractometry from white matter bundles more robust.

3490 Computer 41

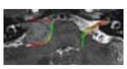

High Resolution Facial Nerve Tractography in Patient with Vestibular Schwannoma

Qiqi Tong[1], Ting Gong[1], Jing Jin[2], Xiujue Zheng[2], Lude Cheng[3], Hongjian He[1], and Jianhui Zhong[1]

[1]Center for Brain Imaging Science and Technology, Department of Biomedical Engineering, Zhejiang University, Hangzhou, People's Republic of China, [2]Department of Neurosurgery, The First Affiliated Hospital, School of Medicine, Zhejiang University, Hangzhou, People's Republic of China, [3]Application Team, Siemens Healthcare, Shanghai, People's Republic of China

Reliable tractography of specific abnormal brain nerves such as the facial nerve displaced by vestibular schwannoma is necessary for estimating risk before the surgery. Single-shot diffusion EPI sequence has been used previously to reconstruct tractography of facial nerve but suffered severe distortion in the basicranial region. Here we performed high resolution anatomical and diffusion scans in patients with vestibular schwannoma, in order to track the facial nerve and provide reliable result for the surgeons to evaluate the surgical risk.

3491 Computer 42

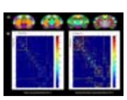

Towards a connectome atlas of the C57Bl6 mouse brain using ex vivo ultra-high field diffusion MRI

Ivy Uszynski[1,2], Hervé Mathieu[1,2,3,4], Jean-Christophe Deloulme[1,2], Emmanuel L. Barbier[1,2], and Cyril Poupon[5]

[1]Grenoble Institut des Neurosciences, Université Grenoble Alpes, Grenoble, France, [2]INSERM U1216, Grenoble, France, [3]Unité Mixte de Service IRMaGe, Grenoble Alpes Hospital, Grenoble, France, [4]Unité Mixte de Service 3552, CNRS, Grenoble, France, [5]NeuroSpin, CEA Saclay, Gif-sur-Yvette, France

Diffusion MRI is a powerful tool to investigate the structural connectivity of the brain and to characterize its microstructure. In this study, we propose to adapt the white matter bundles clustering approach - previously achieved on humans - to the mouse in order to establish the foundations of a novel atlas of the structural connectivity. To this aim, 3D High Angular Resolution Diffusion Imaging (HARDI) was performed ex vivo on C57Bl6 mice brains (100µm isotropic) at 9.4T and clusters of fibers were computed using an automated procedure across the entire brain.

3492 Computer 43

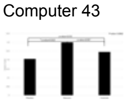

Tract covariance networks in expert dancers and pianists

Hsien-Te Su[1], Pin-Yu Chen[2], Yu-Jen Chen[1], Yung-Chin Hsu[1], Wei-Chi Li[3], Tzu-Yi Hong[3], Li-Fen Chen[3,4], Jen-Chuen Hsieh[3,4], and Wen-Yih Isaac Tseng[1,5]

[1]Institute of Medical Device and Imaging, National Taiwan University College of Medicine, Taipei, Taiwan, [2]Department of Life Science, National Taiwan University, Taipei, Taiwan, [3]Institute of Brain Science, National Yang-Ming University, Taipei, Taiwan, [4]Integrated Brain Research Unit, Division of Clinical Research, Department of Medical Research, Taipei Veterans General Hospital, Taipei, Taiwan, [5]Molecular Imaging Center, National Taiwan University, Taipei, Taiwan

To investigate plasticity of white matter tracts in expert dancers and pianists, we used diffusion spectrum imaging to measure generalized fractional anisotropy (GFA) of 76 major white matter tracts. A novel metric called tract covariance was defined as the correlation between each pair of tracts in variations of the mean GFA values across subjects. As compared with control subjects, expert dancers showed overall enhancement of the tract covariance, whereas expert pianists showed enhancement specific to sensory-motor processing. The findings underline the different effects on white matter tract plasticity following different types of long-term training.

3493 Computer 44

Exponential Decay Law for the Structural Brain Network of Maltreated Children

Moo K Chung[1], Jamie L Hanson[2], Nagesh Adluru[1], Andrew L Alexander[1], Richard J Davidson[3], and Seth D Pollak[3]

[1]Waksman Laboratory for Brain Imaging and Behavior, University of Wisconsin, Madison, WI, United States, [2]Department of Psychology, University of Pittsburgh, Pittsburgh, PA, United States, [3]Department of Psychology, University of Wisconsin, Madison, WI, United States

We present evidence that the structural brain network follows the exponential decay law; these data are inconsistent with the view the brain follows the more complicated truncated exponential power law. Our model is then used in application, to show that children exposed to high levels of early life stress have more sparsely connected hub nodes. These data are consistent with rodent models of the effects of stress on synaptogenesis.

3494 Computer 45

On Quantitatively Comparing Tractography Algorithms

Birkan Tunç[1], Drew Parker[1], and Ragini Verma[1]

[1]University of Pennsylvania, Philadelphia, PA, United States

Systematic comparison of tractography algorithms is rendered challenging by the differences in diffusion models and multiple parameters. In this work, we have defined a statistical framework to compare tractography algorithms, from two different perspectives: (1) the volume of generated tracts and (2) number of unbroken fibers. We applied our framework to compare six algorithms (four using tensor model and two using HARDI model) in reconstructing the contralateral corticospinal tract in ten brain tumor patients. Our results demonstrated significant differences between algorithms. These experiments establish our tractography comparison framework which can be used by researchers and tractography challenges for quantitative comparison.

3495 Computer 46

Inferior Fronto-occipital Fasciculus Tractography —— a Comparison of Reconstruction Methods

Ting Gong[1], Qiqi Tong[1], Hongjian He[1], Qiuping Ding[1], and Jianhui Zhong[1]

[1]Center for Brain Imaging Science and Technology, Department of Biomedical Engineering, Zhejiang University, Hangzhou, People's Republic of China

The anatomical definition and functional role of inferior fronto-occipital fascicle (IFOF) in human brain are important but still controversial. Post-mortem dissection has provided detailed and extended cortical terminations of IFOF while diffusion tractography further facilitates the definition of extended terminations through in vivo studies. A careful comparison of fiber reconstruction methods including diffusion tensor imaging, q-ball imaging, generalized q-sampling imaging and diffusion kurtosis imaging (DKI) was conducted. More integrated IFOF tracts were found with DKI, which could benefit the exploration of precise terminations of IFOF, thus a better understanding of its function.

3496 Computer 47

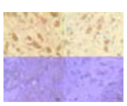

Comparison of rotenone-induced rat model and 6-OHDA-induced rat model of Parkinson's disease: FA and T2* values analysis

LanXiang Liu[1], Dan Du[1], Tao Zheng[2], Yuan Fang[1], Yansheng Chen[1], Huiling Yi[1], Qingyuan He[3], Dawei Gao[4], and Qinglei Shi[5]

[1]Qinhuangdao Municipal No. 1 Hospital, Hebei, People's Republic of China, [2]Hebei Medical University, Shijia Zhuang, Hebei, People's Republic of China, [3]Peking University Third Hospital, [4]Yanshan Univerisity, [5]Siemens Ltd

The fractional anisotropy (FA) and T2* values of rotenone (RT) and 6-OHDA-induced rat model of PD at different time points were quantitatively analyzed. A larger degree of quantitative parameters variation in 6-OHDA-induced rat group than RT-induced rat group were demonstrated when using quantitative parameters of FA and T2* values. The phenomena observed in this study may be of help in future studies about PD using rat model.

3497 Computer 48

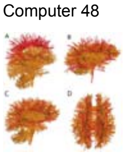

Important new insights for the reduction of false positives in tractograms emerge from streamline-based registration and pruning.

Tingyi Wanyan[1] and Eleftherios Garyfallidis[1]

[1]Intelligent Systems Engineering, Indiana University, Bloomington, IN, United States

Tractograms have large number of false positives. One possible solution is to use anatomically relevant atlases of bundles to create priors of known bundles and therefore concentrate on the true positives. However this requires registration with incomplete atlases that contain only a few known bundles. A new asymmetric cost function extensively advances the direct registration of tractograms to atlases with a small number of bundles. Furthermore, although existing ROI filtered atlases can miss important parts of bundles, by using a pruning method using streamline centroids, these parts can be found, and the false positives can be extensively reduced.

Electronic Poster

Diffusion: Acquisition & Reconstruction

3498 Computer 49

Comprehensive Correction of Motion and Nyquist Ghost Artifacts for Multi-shot Diffusion Imaging

Merry Mani[1], Mathews Jacob[2], Baolian Yang[3], and Vincent Magnotta[1]

[1]Department of Radiology, University of Iowa, Iowa City, IA, United States, [2]Department of Electrical and Computer Engineering, University of Iowa, Iowa City, IA, United States, [3]GE Healthcare

Echo planar imaging data are often corrupted by Nyquist ghost artifacts resulting from the eddy current induced shifts between the odd & even phase encodes. Current EPI methods often rely on calibration scans that are collected prior to the data acquisition to correct for Nyquist ghosts. Unfortunately, this approach is often insufficient for the recovery of diffusion-weighted (DW) data, since the ghosting artifacts also depend on the segmentation of the EPI read-outs and diffusion weighting. We introduce a comprehensive algorithm to simultaneously correct for the eddy-current errors as well as the motion-induced artifacts in DW images that does not require any calibration scans.

3499 Computer 50

Motion-tolerance Single-scan Diffusion Mapping

Lingceng Ma[1], Congbo Cai[2], Zhong Chen[1], Shuhui Cai[1], Hongyi Yang[3], and Kai Zhong[3]

[1]Department of Electronic Science, Department of Electronic Science, Xiamen University, Xiamen, People's Republic of China, [2]Department of Communication Engineering, Department of Communication Engineering, Xiamen University, Xiamen, People's Republic of China, [3]High Magnetic Field Laboratory, High Magnetic Field Laboratory, CAS, Hefei, People's Republic of China

A new diffusion imaging method, single-scan diffusion mapping through overlapping-echo detachment planar (DM-OLED) imaging sequence with corresponding separation algorithm, was proposed. The method can get reliable diffusion mapping by a single-scan in about 120ms.The diffusion mapping gained by DM-OLED has immunity to motion and higher time resolution compared with conventional multi-scan diffusion methods. Experimental results of mouse brains verified the accuracy and the motion-tolerance of DM-OLED. As a reliable fast diffusion measurement tool, DM-OLED can be boded well for further uses in clinical real-time measurements.

3500 Computer 51

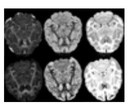

On the use of Gadolinium-staining for high resolution ex vivo NODDI measurements at 11.7T

Sophie Bernadette Sébille[1,2], Anne-Sophie Rolland[2], Romain Valabregue[1,2], Carine Karachi[2,3], Marie-Laure Welter[2,4], Stéphane Lehéricy[1,2], Eric Bardinet[1,2], and Mathieu David Santin[1,2]

[1]Center of NeuroImaging Research - CENIR, Paris, France, [2]Inserm U 1127, CNRS UMR 7225, Sorbonne Universités, UPMC Univ Paris 06 UMR S 1127, Institut du Cerveau et de la Moelle épinière, ICM, Paris, France, [3]AP-HP, Hôpital de la Pitié-Salpêtrière, Department of Neurosurgery, Paris, France, [4]AP-HP, Hôpital de la Pitié-Salpêtrière, Department of Neurology, Paris, France

The goal of this work was to compare diffusion and microstructure parameters estimation when the sample is soaked or not in gadolinium before imaging (Gd-staining). We found that Gd-staining is suitable for diffusion imaging experiment, leading to higher SNR and higher useful b-values. Meanwhile, care must be taken for several microstructure parameters estimation as T1 may vary during experiment.

3501 Computer 52

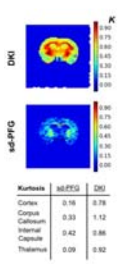

Differentiating Contributions To Diffusional Kurtosis in the Brain with Symmetrized Double-PFG MRI

Jeffrey Paulsen[1], Iris Yuwen Zhou[2], and Phillip Zhe Sun[2,3]

[1]Independent, Boston, MA, United States, [2]Athinoula A. Martios Center for Biomedical Imaging, MGH and Harvard Medical School, Charlestown, MA, United States, [3]Department of Radiology, University of Illinois at Chicago

Kurtosis imaging enables valuable diagnostics of stroke and other tissue pathologies. It can arise directly from restricted diffusion, but also from sub-voxel heterogeneity in the ADC. Utilizing double diffusion contrast, we are able to remove these heterogeneity contributions. We show this targeted 'microscopic' kurtosis contrast yields unique contrast in-vivo in a live rat brain: highlighting white/gray matter boundaries.

3502 Computer 53

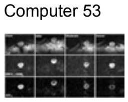

Improved Detection of Spinal Cord Injury in Rats with Reduced Field of View (rFOV) and Orthogonal Filter-Probe (OFP) Diffusion Weighted Imaging (DWI)

Nathan Skinner[1,2], Shekar Kurpad[3,4], Brian Schmit[5], L. Tugan Muftuler[3], and Matthew Budde[3]

[1]Biophysics Graduate Program, Medical College of Wisconsin, Milwaukee, WI, United States, [2]Medical Scientist Training Program, Medical College of Wisconsin, Milwaukee, WI, United States, [3]Neurosurgery, Medical College of Wisconsin, Milwaukee, WI, United States, [4]Clement J Zablocki Veterans Affairs Medical Center, Milwaukee, WI, United States, [5]Biomedical Engineering, Marquette University, Milwaukee, WI, United States

To improve image quality for investigation of spinal cord injury, a reduced field of view excitation scheme was implemented on a Bruker 9.4T imaging system. This was combined with an optimized orthogonal filter-probe diffusion weighted imaging sequence to improve specificity for axonal injury with a short acquisition time. Application in a rat spinal cord injury model showed sensitive detection of diffusivity changes 48 hours post-injury with improved image quality compared to a standard full field of view acquisition. These advances provide support for this technique as a potential biomarker of injury severity with the ability for translation into clinical systems.

3503 Computer 54

Whole-brain diffusional variance decomposition (DIVIDE) in 8 minutes: Technical feasibility at 1.5, 3, and 7 T

Filip Szczepankiewicz[1], Jens Sjölund[2,3,4], Freddy Ståhlberg[1,5,6], Jimmy Lätt[7], and Markus Nilsson[5,6]

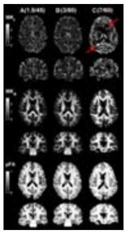

[1]Medical Radiation Physics, Lund University, Lund, Sweden, [2]Elekta Instrument AB, Kungstensgatan 18, Box 7593, SE-103 93 Stockholm, Stockholm, Sweden, [3]Department of Biomedical Engineering, Linköping University, Linköping, Sweden, [4]Center for Medical Image Science and Visualization, Linköping University, Linköping, Sweden, [5]Department of Clinical Sciences Lund, Lund University, Skåne University Hospital, Lund, Sweden, [6]Lund University Bioimaging Center, Lund University, Lund, Sweden, [7]Department of Imaging and Function, Skåne University Hospital, Lund, Sweden

Diffusion weighting along more than one direction at a time (tensor-valued encoding) can be used to probe features of the microstructure that are not accessible by conventional encoding. For example, it enables diffusional variance decomposition (DIVIDE) which can separate the effects of microscopic anisotropy, orientation dispersion, and heterogeneous isotropic diffusivity. Tensor-valued encoding is usually demanding with respect to gradient performance, limiting its applicability to high-performance MRI systems. However, a recent method for optimized encoding significantly reduced the demand on gradient performance, which warrants an investigation of the applicability of such encoding on a wider range of MRI hardware configurations. In this study, we demonstrate whole-brain diffusional variance decomposition (DIVIDE) in less than 8 minutes at a wide range of clinical MRI systems with different hardware configurations.

3504 Computer 55

Compressed sensing diffusion spectrum imaging as a forward-looking alternative to multi-shell diffusion MRI in population imaging

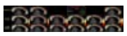

Alexandra Tobisch[1], Rüdiger Stirnberg[1], Robbert Leonard Harms[2], Thomas Schultz[3], Alard Roebroeck[2], Monique Breteler[1], and Tony Stöcker[1]

[1]German Center for Neurodegenerative Diseases (DZNE), Bonn, Germany, [2]Faculty of Psychology & Neuroscience, Maastricht University, Maastricht, Netherlands, [3]University of Bonn, Institute of Computer Science, Bonn, Germany

This study investigates the applicability of two advanced diffusion MRI protocols in population imaging: 3-shell High Angular Resolution Diffusion Imaging (HARDI) and Diffusion Spectrum Imaging accelerated through Compressed Sensing theory (CS-DSI). Group analysis of 20 subjects indicates that CS-DSI performs comparable to 3-shell HARDI in the estimation of microstructure parameters and adds the advantage of high b-value acquisitions, further complimentary biomarkers from the diffusion propagator and a high potential to deliver data well-suited for future developments.

3505 Computer 56

Quantitative Noise Analysis for Increased Homogeneity in Intra-voxel Incoherent Motion (IVIM) Perfusion Imaging in Brain

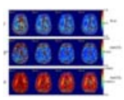

Harri Merisaari[1,2] and Christian Federau[3]

[1]Turku PET Centre, Turku University Central Hospital, Turku, Finland, [2]Department of Information Technology, University of Turku, Turku, Finland, [3]Department of Radiology, Uniklinik Balgrist, University Zürich, Zürich, Switzerland

Intravoxel incoherent motion (IVIM) perfusion imaging has been shown to be applicable in clinical brain examinations, but those images are known to be noisy. To better quantify the necessary conditions to produce homogenous IVIM perfusion images in the brain, we studied the properties of signal noise as function of b-value and of localization in the brain. We compared the image quality of the perfusion maps as function of number of average to the maximal quality IVIM perfusion maps obtained during a 1 hour acquisition time.

3506 Computer 57

High Resolution Cervical Spine Single-Shot DTI with Distortion Correction Using Modified Field-mapping Method

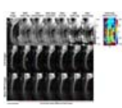

Yuhui Xiong[1], Xiaodong Ma[1], Zhe Zhang[1], Yishi Wang[1], and Hua Guo[1]

[1]Center for Biomedical Imaging Research, Department of Biomedical Engineering, School of Medicine, Tsinghua University, Beijing, People's Republic of China

Single-shot echo planar imaging (EPI) DTI (SS-DTI) has been commonly used in clinical cervical spine (C-spine) MR scans to get functional and pathologic information as it's fast and straightforward, but high resolution SS-DTI image suffers from severe geometric distortion. Field mapping method is a classical and simple distortion correction technique, but its performance in C-spine SS-DTI is limited. We used echo planar spectroscopic imaging (EPSI) sequence to acquire the field-map, and modified the conventional field-map post-processing method to promote the correction efficacy. The results show that the proposed method is effective and fast in C-spine SS-DTI distortion correction.

3507 Computer 58

High b-value Diffusion-Weighted MRI for Detection of Interscapular Brown Adipose Tissue in Rodent Model

Weiguo Li[1,2,3], Jin Gao[3], Andrew Gordon[2], Kejia Cai[4], Andrew Larson[2], and Richard Magin[3]

[1]Research Resource Center, University of Illinois at Chicago, Chicago, IL, United States, [2]Radiology, Northwestern University, Chicago, IL, United States, [3]Bioengineering, University of Illinois at Chicago, Chicago, IL, United States, [4]Radiology, University of Illinois at Chicago, Chicago, IL, United States

Brown adipose tissue (BAT) is increasingly considered a target organ for the treatment of metabolic disease. Persuasive evidence has shown that enhancement of the function of brown and beige adipocytes in humans could be very effective for treating type 2 diabetes and obesity. However, clinical studies have been limited by the lack of non-invasive tools for characterizing this tissue in humans. In this study, we explored the feasibility of using high b-value diffusion-weighted MRI for detecting the distribution of interscapular brown adipose tissue.

3508 Computer 59

Free-water elimination in diffusion MRI: pushing the limits towards clinical applications

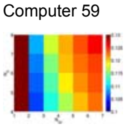

Ezequiel Farrher[1], Farida Grinberg[1,2], Zaheer Abbas[1,2], and N. Jon Shah[1,2,3]

[1]Institute of Neuroscience and Medicine 4, Forschungszentrum Jülich, Jülich, Germany, [2]Department of Neurology, Faculty of Medicine, RWTH Aachen University, Aachen, Germany, [3]JARA – BRAIN – Translational Medicine, RWTH Aachen University, Aachen, Germany

Free-water elimination allows one to reduce the bias in DTI metrics induced by partial-volume effects. In this work, we propose a versatile approach for the optimisation of the diffusion weighting settings, given a limited acquisition time, based on a parameterised Cramér-Rao lower-bound. The optimisation shows robust convergence.

3509 Computer 60

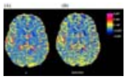

Assessing the Effect of Intravoxel Incoherent Motion on Diffusion Parameters in the Brain

Casey Robert Vieni[1,2], Benjamin Ades-Aron[1], Bettina Conti[1], Timothy M Shepherd[1], Yvonne W Lui[1], Dmitry Novikov[1], and Els Fieremans[1]

[1]Bernard and Irene Schwartz Center for Biomedical Imaging, Department of Radiology, New York University School of Medicine, New York University, New York, NY, United States, [2]Medical Scientist Training Program, New York University School of Medicine, New York, NY, United States

We investigated the effect of intravoxel incoherent motion (IVIM) on the brain diffusion MRI signal in a cohort of 143 control patients. We compared the diffusivities derived from a mono-exponential fit at b =0 and 1ms/μm² versus at b = 0.25 and 1 ms/μm². This allowed for a quantitative assessment of the IVIM signal fraction f* in specific brain matter types. Our results show a significant difference in the mean diffusivity of about 3% in white matter and up to 7% in grey matter, with corresponding f* estimated to be about 2% and 6% in white and grey matter respectively.

3510 Computer 61

magna cum laude

Design of a locally incoherent sampling scheme for improved joint k-q reconstruction of diffusion MRI

Wenchuan Wu[1], Peter J Koopmans[1], and Karla L Miller[1]

[1]FMRIB, University of Oxford, Oxford, United Kingdom

For joint k-q reconstruction, it's beneficial to incoherently under-sampling k-space for different q-space points to utilize the complimentary k-space information. As nearby q-space points in general share more similarities than distant points, it is hypothesized that locally-incoherent k-space sampling can further improve the joint k-q reconstruction. In this work, we propose a method to design locally-incoherent k-space sampling patterns based on a graph colouring algorithm. Results show the proposed method achieves better reconstruction than existing sampling schemes.

3511 Computer 62

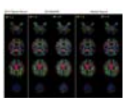

Model-Based Reconstruction for Undersampled High Resolution Diffusion Tensor Imaging Combined with Simultaneous Multi-Slice Acquisitions

Zijing Dong[1], Erpeng Dai[1], Fuyixue Wang[1,2], Yuantao Gu[3], Chun Yuan[1,4], and Hua Guo[1]

[1]Center for Biomedical Imaging Research, Department of Biomedical Engineering, School of Medicine, Tsinghua University, Beijing, People's Republic of China, [2]Harvard-MIT Health Sciences and Technology, MIT, Cambridge, MA, United States, [3]Department of Electronic Engineering, Tsinghua University, Beijing, People's Republic of China, [4]Vascular Imaging Laboratory, Department of Radiology, University of Washington, Seattle, WA, United States

Multi-shot interleaved EPI is an effective method to acquire high-resolution and less distorted diffusion weighted images, but with relatively low acquisition efficiency, especially for diffusion tensor imaging. Here, a novel model-based reconstruction is proposed for accelerated multi-shot diffusion imaging with simultaneous multi-slice (SMS) and partially parallel imaging (PPI). The method can directly estimate diffusion tensors from the undersampled k-space data, by integrating information of all shots and diffusion encoding directions. Simulation and in-vivo experiment demonstrated that the proposed method can achieve higher acceleration efficiency and improved accuracy in tensor estimation compared with conventional 2D GRAPPA.

3512 Computer 63

Accelerated High Resolution EPI DTI Using Model-Based Reconstruction

Zijing Dong[1], Fuyixue Wang[1,2], Zhe Zhang[1], Erpeng Dai[1], Xiaodong Ma[1], Yuantao Gu[3], and Hua Guo[1]

[1]Center for Biomedical Imaging Research, Department of Biomedical Engineering, School of Medicine, Tsinghua University, Beijing, People's Republic of China, [2]Harvard-MIT Health Sciences and Technology, MIT, Cambridge, MA, United States, [3]Department of Electronic Engineering, Tsinghua University, Beijing, People's Republic of China

Single-shot EPI is the most widely used sequence in diffusion tensor imaging. However, severe distortion in single-shot EPI limits its application for higher resolution images. Multi-shot EPI DTI can reduce distortion but results in longer acquisition time especially when a large number of diffusion-encoding directions are used. Here, we propose a model-based reconstruction framework for EPI DTI to estimate diffusion tensors from undersampled EPI sequences, in order to achieve high resolution diffusion imaging in a shorter scan time. The effectiveness of the proposed model-based method to get precise tensor estimation is validated by DTI simulation and in-vivo experiments.

3513 Computer 64

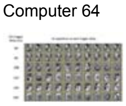

Quantification of Navigator Requirements for Multi-shot Diffusion Weighted Imaging

Joseph L Holtrop[1] and Bradley P Sutton[1]

[1]Bioengineering, University of Illinois at Urbana-Champaign, Urbana, IL, United States

The ability to use multiple shots in diffusion weighted imaging has enabled acquisitions with higher resolutions and higher SNRs. The methods currently being used to achieve higher resolutions rely on navigator information to correct for mismatches in coherent motion during the diffusion encoding between shots. The resolution of the navigator is a critical factor, too low and the corrections are incomplete, too high and there is a significant time or echo time penalty. This work presents an analysis for determining the resolution requirements for navigation. This work found that using a navigator resolution of 6 mm produces reliable results and allows shorter acquisitions to be used.

3514 Computer 65

Accelerated Body nCPMG SS-FSE Diffusion Weighted Imaging

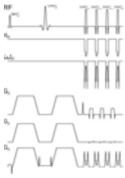

Eric Kenneth Gibbons[1], Patrick LeRoux[2], Shreyas Vasanawala[3], John Mark Pauly[4], and Adam Bruce Kerr[4]

[1]Department of Bioengineering, Stanford University, Stanford, CA, United States, [2]Praecedentia Libra, Palaiseau, France, [3]Department of Radiology, Stanford University, Stanford, CA, United States, [4]Department of Electrical Engineering, Stanford University, Stanford, CA, United States

This abstract presents a novel reconstruction for the nCPMG SS-FSE sequence. A theoretical justification for this approach is given. This reconstruction and sequence is demonstrated in phantom and *in vivo* and is shown to be quantitatively and qualitatively robust.

3515 Computer 66

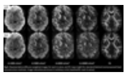

Feasibility of very high b-value diffusion imaging using a clinical scanner.

Steen Moeller[1], Essa Yacoub [1], Sudhir Ramanna[1], Emily Kittelson[1], Kamil Ugurbil[1], and Christophe Lenglet[1]

[1]Center for Magnetic Resonance Research, Minneapolis, MN, United States

The use of locally low-rank matrix approximation methods for noise variance reduction provides a powerful tool for diffusion MRI to increase the quality of very high b-value acquisitions. Using a clinical system, we demonstrate the feasibility of multi-shell high angular resolution diffusion imaging with b-value up to 10,000s/mm^2.

3516 Computer 67

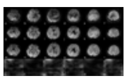

Multiband IRIS: A framework for diffusion-weighted image reconstruction integrating multiband, multishot, SENSE and 2D navigated motion correction

Ha-Kyu Jeong[1]

[1]Philips Korea, Seoul, Korea, Republic of

IRIS has been proposed for diffusion-weighted (DW) image reconstruction with 2D-navigated motion correction from highly aliased DW-MRI data using multishot and regularly subsampled SENSE implementations simultaneously. In this work, it is demonstrated that IRIS framework can be extended for multiband DW image reconstruction for reconstructing motion-free multiband multishot DW images.

3517 Computer 68

eIRIS — An Eigen-Analysis Motivated Approach for More Robust Multi-Shot Diffusion-Weighted Imaging

Li Guo[1], Zhongbiao Xu[1], Yingjie Mei[1,2], Wenxing Fang[3], Chenguang Zhao[3], Wufan Chen[1], Yanqiu Feng[1], and Feng Huang[4]

[1]Guangdong Provincial Key Laborary of Medical Image Processing, School of Biomedical Engineering, Southern Medical University, Guangzhou, People's Republic of China, [2]Philips Healthcare, Guangzhou, People's Republic of China, [3]Philips Healthcare (Suzhou), Suzhou, People's Republic of China, [4]Neusoft Medical System, Shanghai, People's Republic of China

IRIS corrects the motion-induced inter-shot phase errors for multi-shot diffusion-weighted imaging by extracting the phase information from an additional navigator data, which may cause the distortion mismatch between the image and navigator data. To solve the distortion mismatch issue in IRIS without using B0 field map, we propose to extract the coil sensitivities and phase information from navigator data by using an eigen-analysis scheme. The performance of the proposed method is demonstrated in both phantom and in vivo data sets.

3518 Computer 69

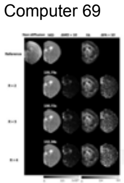

Accelerating Diffusion Tensor Imaging Using a Parametric Manifold Model

Chaoyi Zhang[1], Dan Wu[2], Jiangyang Zhang[3], Dong Liang[4], Jingyuan Lyu[1], Ukash Nakarmi[1], Rong-Rong Chen[5], and Leslie Ying[1,6]

[1]Electrical Engineering, University at Buffalo,State University of New York, Buffalo, NY, United States, [2]Radiology, Johns Hopkins University School of Medicine, Baltimore, MD, United States, [3]Radiology, New York University School of Medicine, New York City, NY, United States, [4]Biomedical and Health Engineering, Shenzhen Institutes of Advanced Technology, Shenzhen, People's Republic of China, [5]Electrical & Computer Engineering, University of Utah, Salt Lake City, UT, United States, [6]Biomedical Engineering, University at Buffalo, State University at New York, Buffalo, NY, United States

This abstract presents a novel method for diffusion tensor image (DTI) directly from highly under-sampled data acquired at multiple diffusion gradients. This method formulates the diffusion tensor estimation as a problem of parametric manifold recovery. We solve the recovery problem by alternatively shrinking the diffusion weighted images, estimating diffusion tensor, and enforcing data consistency constraint. The experimental results demonstrate that the proposed method is able to reconstruct the diffusion tensors accurately at high acceleration factors with low computational complexity.

Electronic Poster

Diffusion: Processing, Analysis & Visualization

Exhibition Hall Monday 14:45 - 15:45

3519 Computer 73

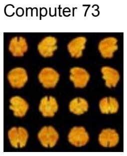

High Spatial Resolution White Matter Fibrography (WMF): Technique Optimization

Hernan Jara[1], Osamu Sakai[1], Stephan W Anderson[1], and Jorge A Soto[1]

[1]Boston University, Boston, MA, United States

Purpose: To test the high spatial resolution limits of the white matter fibrography (WMF) technique within the scan time constrains of clinical MRI of about ten minutes total scan time and to optimize the image processing algorithms for rendering the white matter (WM) connectome at the highest level of anatomic detail. Methods: Healthy volunteer was scanned with the quadra-FSE pulse at high spatial resolution in 10min. Results: WMF connectome was constructed using ultra-high b-value (34,000s/mm2) synthetic MRI. Conclusion: High spatial resolution direct rendering of the human brain connectome can be accomplished with a 10min scan.

3520 Computer 74

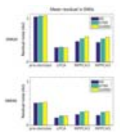

Comparing the LPCA and MPPCA denoising approaches for diffusion MRI using simulated human data

Qiuting Wen[1], Mark S. Graham[2], Sourajit M. Mustafi[1], Ivana Drobnjak[2], Hui Zhang[2], and Yu-Chien Wu[1]

[1]Indiana University, Indianapolis, IN, United States, [2]University of College London

In this study, we investigate two denoising methods for diffusion MRI: the local PCA approach and Marchenko-Pastur (MP) PCA approach. Ground-truth diffusion-weighted images of the human brain are developed and used for noise simulation. Two diffusion-weighting b-values and two noise levels are generated as input data for both denoisers. Metrics of diffusion tenor imaging (DTI) and neurite orientation distribution and density (NODDI) are computed after denoising and compared between denoise methods.

3521 Computer 75

magna cum laude

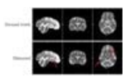

Quantitative assessment of susceptibility artefact correction techniques for diffusion-weighted MRI

Mark S Graham[1], Ivana Drobnjak[1], and Hui Zhang[1]

[1]Centre for Medical Image Computing and Department of Computer Science, University College London, London, United Kingdom

It is necessary to correct for susceptibility artefacts in DW-MR, but there are a number of available strategies to choose from. In this work we apply a simulation framework, previously used to assess motion and eddy current correction strategies, to quantitatively evaluate methods for susceptibility correction. Our results indicate that methods that use reversed phase-encoding data perform the best. Furthermore they show that non-linear registration of diffusion data to a structural target in insufficient to fully correct for the susceptibility artefact.

3522 Computer 76

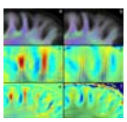

Multi-contrast diffeomorphic non-linear registration of orientation density functions

Maximilian Pietsch[1], David Raffelt[2], Thijs Dhollander[2], and J-Donald Tournier[1]

[1]Centre for the Developing Brain, Division of Imaging Sciences and Biomedical Engineering, King's College London, London, UK, London, United Kingdom, [2]Florey Institutes of Neuroscience and Mental Health, Melbourne, Australia

Spatial normalisation of high angular resolution diffusion images (HARDI) is an important prerequisite for group-level analysis of tissue microstructure. In this study, we extend a technique for non-linear registration of orientation density functions by including other non-WM tissue types into the metric driving the registration, and investigate the benefits this provides in terms of overall alignment. Our results show that including additional non-WM tissue types in the registration metric improves the performance of the registration, as assessed by visual inspection (sharper features), and in simulations (slight reduction in residuals)

3523 Computer 77

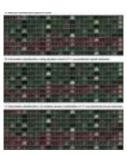

Transfer learning and convolutional neural net fusion for motion artefact detection

Christopher Kelly[1], Max Pietsch[1], Serena Counsell[1], and J-Donald Tournier[1]

[1]Centre for the Developing Brain, King's College London, London, United Kingdom

The first step in a diffusion MRI pre-processing pipeline typically involves the manual removal of heavily motion-corrupted volumes. However, this process is both time consuming and potentially subjective. We propose to automate this process by training multiple deep convolutional neural networks (CNNs) and decision trees to achieve near human-level accuracy for rejection of outliers.

3524 Computer 78

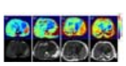

Diffusion Kurtosis Imaging with the breath hold method for staging of hepatic fibrosis: Potential as additional sequence in a clinical routine

Daisuke Yoshimaru[1,2], Toshiaki Miyati[2], Yuichi Suzuki[3], Yuhki Hamada[1], Nozomi Mogi[4], Ayumu Funaki[1], Ayumi Tabata[1], Maki Tobari[5], and Takayoshi Nishino[5]

[1]Department of Medical Technology Image Laboratory, Tokyo Women's Medical University Yachiyo Medical Center, Yachiyo, Japan, [2]Division of Health Sciences, Graduate School of Medical Sciences, Kanazawa University, kanazawa, Ishikawa, Japan, [3]Department of Radiological Service, The University of Tokyo Hospital, Japan, [4]Department of Radiological Service, Tokyo Women's Medical University Medical Center East, Japan, [5]Department of gastroenterological medicine, Tokyo Women's Medical University Yachiyo Medical Center, yachiyo, Japan

We evaluated hepatocellular degeneration using DKI analysis with the breath hold technique compared with the pathological appearance about chronic hepatic diseases and hepatic fibrosis. Using this DKI method in the liver the stage of hepatic fibrosis can be classified into normal hepatic fibrosis and early hepatic fibrosis, and into early hepatic fibrosis and advanced hepatic fibrosis. Thus, we consider that DKI analysis can reflect pathological classification accurately. We considere that this DKI method will be required to evaluate the degree of hepatic fibrosis and to monitor the progress of hepatic fibrosis as an additional sequence in a clinical routine.

3525 Computer 79

Quantitative estimation of IVIM parameters and response evaluation after neoadjuvant chemotherapy in Osteosarcoma

Esha Baidya Kayal[1], Devasenathipathy K[2], Kedar Khare[3], Raju Sharma[2], Sameer Bakhshi[4], and Amit Mehndiratta[1,5]

[1]Center for Biomedical Engineering, Indian Institute of Technology, New Delhi, India, [2]Radiodiagnosis, All India Institute of Medical Sciences, New Delhi, India, [3]Department of Physics, Indian Institute of Technology, New Delhi, India, [4]Medical Oncology, Dr. B.R.Ambedkar Institute-Rotary Cancer Hospital, All India Institute of Medical Sciences, New Delhi, India, [5]Department of Biomedical Engineering, All India Institute of Medical Sciences, New Delhi, India

Histological necrosis is the current gold standard for response evaluation in Osteosarcoma treated with neoadjuvant chemotherapy (NAC). However it is applicable only after tumour resection on completion of NAC. Thus, a non-invasive early marker of NAC response is desirable. We performed NAC response evaluation using Intra-voxel Incoherent Motion (IVIM) Diffusion weighted MRI using tumour volume change and histogram analysis. Tumour volume change and histogram analysis revealed similar and clinically useful information in chemotherapy response to Osteosarcoma.

3526 Computer 80

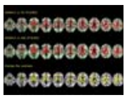

SHANK-3 gene mutation results in comprehensive white matter damage in children: a DTI-TBSS study

Dongyun Li[1], Chunxue Liu[1], Xiu Xu[1], Ed X. Wu[2], and Zhongwei Qiao[1]

[1]Children's Hospital of Fudan University, Shanghai, People's Republic of China, [2]Laboratory of Biomedical Imaging and Signal Processing, The University of Hong Kong, HongKong, Hong Kong

Autism spectrum disorder (ASD) is classified as a neuro-developmental disease with a dramatically increasing prevalence from 4 in 10000 to recently 1 in 68 children. SHANK-3 proteins are multidomain scaffold proteins of the postsynaptic density and also play a role in synapse formation and dendritic spine maturation. Recent human genetic studies suggest the potential association between molecular defects of SHANK-3 and ASD. DTI imaging and TBSS analysis was applied to study how SHANK-3 gene mutation results in severe microstructure of white matter. Results showed significant damage in SHANK-3 group but no positive findings between ASD and typical development controls. These results calls for attention to re-examine the previous neuroimaging studies of ASD or other neuro-developmental diseases where the positive correlations could be contaminated with unexplored genetic mutation influence.

3527 Computer 81

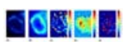

Qualitative and quantitative assessment of intravoxel incoherent motion (IVIM) parameters in hypoxic tumor of a mouse to find a relationship with 18F- misonidazole PET imaging

Eo-Jin Hwang[1], Joon-Yong Jung[1], Jin Kyoung Oh[2], and Mun Young Paek[3]

[1]Seoul St.Mary Hospital, The Catholic University of Korea, Seoul, Korea, Republic of, [2]Incheon St.Mary Hospital, The Catholic University of Korea, Incheon, Korea, Republic of, [3]Siemens Healthcare, Seoul, Korea, Republic of

Intravoxel incoherent motion (IVIM) based analysis of diffusion weighted imaging (DWI) has been suggested as a non-invasive tool to characterize tumor hypoxia, but no study has been performed to directly measure its parameters within the hypoxic tumor regions. In this study, we qualitatively and quantitatively compared IVIM parameters with ^{18}F- misonidazole PET imaging and tested the feasibility of using non-invasive imaging strategy to define tumor hypoxia. Our preliminary result successfully related perfusion fraction values to standardized uptake values (SUVs) from PET and showed a potential of DWI as a tool to evaluate tumor oxygenation.

3528 Computer 82

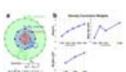

Model-free Fourier Reconstruction of the Diffusion Propagator from Multi-b-shell Diffusion Data

Qiyuan Tian[1,2], Grant Yang[1,2], Christoph W.U. Leuze[2], Ariel Rokem[3], Brian L. Edlow[4,5], and Jennifer A. McNab[2]

[1]Department of Electrical Engineering, Stanford University, Stanford, CA, United States, [2]Department of Radiology, Stanford University, Stanford, CA, United States, [3]eScience Institute, The University of Washington, Seattle, WA, United States, [4]Department of Radiology, Massachusetts General Hospital, Boston, MA, United States, [5]Department of Neurology, Massachusetts General Hospital, Boston, MA, United States

We propose a practical, model-free, Fourier reconstruction framework for obtaining the diffusion propagator and the diffusion orientation distribution function (ODF) from multi-b-shell diffusion data. Signals on each b-shell are scaled to account for non-uniform sampling density in q-space. Diffusion propagators and ODFs are obtained using a Discrete Fourier Transform and an analytic ODF solution. The method is demonstrated on data from the Human Connectome Project and shown to be both effective and broadly applicable to multi-b-shell data.

3529 Computer 83

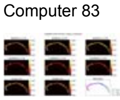

Statistical power and confounds for diffusion MRI microstructure modeling

Robbert Leonard Harms[1,2], Rainer Goebel[1,2], and Alard Roebroeck[1]

[1]Maastricht University, Maastricht, Netherlands, [2]Brain Innovation, Maastricht, Netherlands

Using high resolution HCP WU-Minn data and GPU accelerated software (MDT; https://github.com/cbclab), the aims of this study were to evaluate dMRI microstructure indices over white matter tracts, evaluate the effect sizes between tracts as an upper limit for effect size of diffusion microstructure indices between subjects and finally the influence of possible confounds on those other aims. We report sizeable effects between tracts within subjects for several indices. Also, two clear confounds for diffusion microstructure studies where identified, first, partial volume effects in small and large cross-section tracts, second, model selection on the number of intra-axonal model compartments.

3530 Computer 84

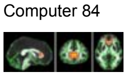

Brain correlates of apathy in Kleine Levin syndrome: a mean apparent propagator study

ANNE-CHARLOTTE PHILIPPE[1], LAVAULT SOPHIE[2], FICK RUTGER[3], WASSERMANN DEMIAN[3], VALABREGUE ROMAIN[1], DERICHE RACHID[3], LEVY RICHARD[2], ARNULF ISABELLE[2], and LEHERICY STEPHANE[1]

[1]Institut Cerveau Moelle – ICM,CENIR, ICM, Inserm – UPMC U1127, CNRS 7225, Paris, France, [2]Service des pathologies du sommeil, Hôpital de la Pitié Salpétrière, France, [3]Université Côte d'Azur, INRIA, France

Kleine-Levin syndrome (KLS) is a rare neurological disorder characterized by episodes of severe hypersomnia, apathy, cognitive impairment, derealization and behavioral disturbances. Between episodes, patients have normal sleep, mood and behavior. Apathy is a prominent clinical feature of KLS but its pathophysiology is not known. Here we used mean apparent propagator to investigate white matter changes in KLS and correlated diffusion changes with apathy scores. Results showed that the corpus callosum was involved in KLS during episodes and mean RTAP measures in the corpus callosum correlated with apathy scores. Results were in accordance with known motivation-based circuits involving the orbitomedial frontal cortex.

3531 Computer 85

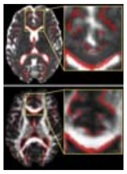

Reduction of Partial Volume Effects Using Diffusion-Kurtosis-Informed Template Improves the Atlas-Based Between-Group Comparison in Diffusion Kurtosis Imaging

Farida Grinberg[1,2], Ezequiel Farrher[1], Kerstin Konrad[3,4], Irene Neuner[1,5], and N. Jon Shah[1,2,6]

[1]Institute of Neuroscience and Medicine 4, Research Centre Jülich, Jülich, Germany, [2]Department of Neurology, Faculty of Medicine, RWTH Aachen University, Aachen, Germany, [3]Child Neuropsychology Section, Department of Child and Adolescent Psychiatry and Psychotherapy, RWTH Aachen University, Aachen, Germany, [4]Institute of Neuroscience and Medicine 3, Research Centre Jülich, Jülich, Germany, [5]Department of Psychiatry, Psychotherapy and Psychosomatics, RWTH Aachen University, Aachen, Germany, [6]JARA - BRAIN - Translational Medicine, RWTH Aachen University, Germany

Frequently used methods in between-group comparisons of diffusion tensor and diffusion kurtosis imaging metrics, such as region-of-interest analysis or atlas-based analysis, are subject to errors due to partial volume effects. In this work we demonstrate that the application of a simple diffusion-kurtosis-informed template significantly reduces partial volume effects and, in turn, improves the between-group atlas-based analysis. In particular, a better differentiation of diffusion metrics was achieved in the study of a group of children versus a group of adults.

3532 Computer 86

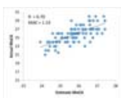

Prediction of the cognitive performance among Type 2 diabetes mellitus patients: a multivariable pattern analysis of Diffusion Tensor Imaging data

Zhenchao Tang[1], Zhenyu Liu[2], Xinwei Cui[3], Enqing Dong[1], and Jie Tian[2]

[1]School of Mechanical, Electrical & Information Engineering, Shandong University (Weihai), Weihai, People's Republic of China, [2]Key Laboratory of Molecular Imaging, Institute of Automation, Chinese Academy of Sciences, Beijing, People's Republic of China, [3]Cooperative Innovation Center of Internet Healthcare, Zhengzhou University, Zhengzhou, People's Republic of China

In the current study, we employed multivariate pattern analysis method together with Diffusion Tensor Imaging measures to make prediction on the cognitive performance of Type 2 diabetes mellitus (T2DM) patients, and explore the white matter tracts associated with cognitive changes in T2DM. The prediction model obtained relatively satisfying performance in the Montreal Cognitive Assessment (MoCA) scores estimation among T2DM patients, suggesting the effectiveness of the multivariable analysis method. The white matter identified in the current study mainly concerned the tracts closely related with cognitive function and memory performance, which were consistent with the finding of previous T2DM cognitive studies.

3533 Computer 87

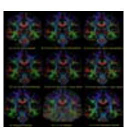

A unified framework for upsampling and denoising of diffusion MRI data

Samuel St-Jean[1], Max Viergever[1], and Alexander Leemans[1]

[1]Image Sciences Institute, University Medical Center Utrecht, Utrecht, Netherlands

Diffusion MRI suffers from relatively long scan times and low signal to noise ratio (SNR), which limits the acquired spatial resolution. In this work, we propose a unified framework for denoising and upsampling diffusion datasets based on a sparse representation of the diffusion signal. Our proposed method shows less blurring and increased anatomical details in the pons region when compared to denoising and subsequent spline interpolation. At the junction of the corpus callosum, the corticospinal tract and the cingulum, finer structures are also preserved as evidenced by a high resolution *invivo* acquisition.

3534 Computer 88

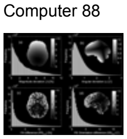

Investigating the adverse effect of gradient nonuniformities on diffusion MRI measures: Do we need to worry?

Hamed Y. Mesri[1], Martijn Froeling[2], Max A. Viergever[1], Anneriet M. Heemskerk[1], and Alexander A. Leemans[1]

[1]Image Sciences Institute, University Medical Center Utrecht, Utrecht, Netherlands, [2]Department of Radiology, University Medical Center Utrecht, Utrecht, Netherlands

Nonuniformities of gradient magnetic fields in diffusion-weighted MRI can introduce systematic errors in estimates of diffusion measures. While there are correction methods that can compensate for these errors, as presented in the Human Connectome Project, such non-linear effects are assumed to be negligible for typical applications and, hence, gradient nonuniformities are mostly left uncorrected. In this work, we evaluated the effect of ignoring such diffusion gradient nonuniformities on measures derived from diffusion tensor imaging. In particular, we simulated deviations from the ground-truth in terms of b-value and diffusion gradient orientation and investigated the resulting bias in fractional anisotropy and orientation of the first eigenvector. Our results demonstrate that not including a correction strategy to mitigate diffusion gradient imperfections especially for high quality data may lead to a significant bias for diffusion measure estimates.

3535 Computer 89

MuSHER: Multi-shell Spherical Harmonic Error Rejection

Greg Daniel Parker[1] and Derek K Jones[1]

[1]Cardiff University, Cardiff, United Kingdom

Diffusion weighted imaging is prone to artefacts. Sources including hardware instability, bulk motion and cardiac pulsation can all induce spurious signal intensities (i.e. corruption) which negatively affect derived measurements. To combat this an additional processing step may be added to detect (and subsequently reject) such corrupted data points; however, with the increasing use of multi-shell acquisitions a number of existing approaches (constrained to a single b-value shell and/or unsuitable diffusion tensor models) are no longer applicable, limiting available choices. With this abstract we propose a new multi-shell detection algorithm and provide preliminary experimental results.

3536 Computer 90

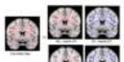

White Matter Microstructural Changes in Healthy Aging: The Impact of Free Water Elimination on DTI Metrics

Jordan Chad[1], Ofer Pasternak[2], David H. Salat[3], and J. Jean Chen[1,4]

[1]Rotman Research Institute, Baycrest Health Sciences, Toronto, ON, Canada, [2]Brigham and Women's Hospital, Harvard Medical School, Boston, MA, United States, [3]Massachusetts General Hospital, Harvard Medical School, Boston, MA, United States, [4]Medical Biophysics, University of Toronto, Toronto, ON, Canada

A Free Water Elimination (FWE) technique is applied to investigate changes in DTI parameters in the human white matter during healthy aging. Our results suggest that age-related changes in DTI metrics often reflect increased extracellular free water with age. DTI with FWE unmasks the effects of free water, revealing authentic tissue microstructure.

3537 Computer 91

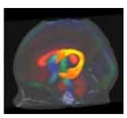

The Neonatal DTI fiber atlas for studies of brain development at birth

Rachel J Steiner[1,2], Sarah J Short[3], Rebecca Knickmeyer Santelli[3], Audrey Rose Verde[3], Aditya Gupta[3], François Budin[4], Katherine A Gilmore[3], Nagesh Adluru[5], Guido Gerig[6], John H Gilmore[3], and Martin A Styner[3,7]

[1]Center for Investigating Healthy Minds, University of Wisconsin-Madison, Madison, WI, United States, [2]Psychology, University of Wisconsin-Madison, Madison, WI, United States, [3]Psychiatry, University of North Carolina at Chapel Hill, [4]Kitware Inc., [5]Waisman Center, University of Wisconsin-Madison, [6]Tandon School of Engineering, Department of Computer Science & Engineering, NYU, [7]Department of Computer Science, University of North Carolina at Chapel Hill

Given the increasing popularity and wealth of DWI data in the field of neuroimaging, there is a critical need for the development of publically available resources that enable widespread application of a set of template fibers for atlas based along-tract analysis supporting an adequate and reliable analysis of DTI in newborns in both practice and in clinical research settings. To address this gap, we developed a Neonate DTI atlas that represents a typically developing human brain during the first few weeks of life. To the best of our knowledge, we are the first to develop a population atlas with this magnitude of quality and sample size, as well as with a comprehensive set of template fibers for semi-automatic tract based analysis. The DTI atlas and the tracts will be made available through NITRC.

3538 Computer 92

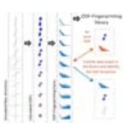

A fingerprinting approach to identifying fiber directions in Orientation Distribution Functions for Higher Order Diffusion MRI

Steven H. Baete[1,2], Ying-Chia Lin[1,2], and Fernando E. Boada[1,2]

[1]Center for Advanced Imaging Innovation and Research (CAI2R), NYU School Of Medicine, New York, NY, United States, [2]Center for Biomedical Imaging, Dept of Radiology, NYU School Of Medicine, New York, NY, United States

High quality diffusion acquisitions are routinely used to study white matter architecture and brain connectivity in vivo. A key step for successful tractography of neuronal tracts is correct identification of the tract directions in each voxel. Here we propose a fingerprinting-based methodology for identifying these fiber directions in Orientation Distribution Functions. This ODF-fingerprinting approach improves the detection of fiber pairs with small crossing angles whilst maintaining fiber direction precision. This improvement will aid fiber tracking algorithms in accurately displaying neuronal tracts and calculating brain connectivity.

3539 Computer 93

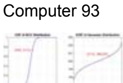

Non-Central Chi to Gaussian Transformation of Diffusion MRI Signals Improves Estimation of Fiber ODFs

Geng Chen[1], Dinggang Shen[1], and Pew-Thian Yap[1]

[1]Department of Radiology and BRIC, University of North Carolina at Chapel Hill, Chapel Hill, NC, United States

Many existing algorithms for estimation of the fiber orientation distribution function (ODF) inherently assume Gaussian noise distribution. Against this assumption, the non-central chi noise distribution of diffusion signals causes bias in fiber ODF estimation. In this work, we introduce a means of transforming the diffusion-weighted signals to have a Gaussian noise distribution with the help of the recently introduced *x-q* space non-local means (XQ-NLM) algorithm. We show that this signal mapping improves estimation of fiber ODFs.

3540 Computer 94

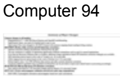

TORTOISE v3: Improvements and New Features of the NIH Diffusion MRI Processing Pipeline

Mustafa Okan Irfanoglu[1,2,3], Amritha Nayak[1,2,3], Jeffrey Jenkins[1,2], and Carlo Pierpaoli[1,2]

[1]Quantitative Medical Imaging Section, NIBIB/NIH, Bethesda, MD, United States, [2]SQUITS/NICHD/NIH, Bethesda, MD, United States, [3]Henry Jackson Foundation, Bethesda, MD, United States

Here we present a series of improvements and new features of the TORTOISE diffusion MRI data processing software (www.tortoisedt.org). TORTOISEv3 has been programmed in C++ and it is now significantly faster, can be batched and it fully benefits from modern multi-core CPU architectures. The DIFFPREP module brings a multitude of new and state-of-art features including DWI denoising, Gibbs ringing removal, and the ability to perform motion and eddy currents distortion correction for very high b-value data. The new DIFFCALC module can perform MAP-MRI propagator estimation and the output can be easily imported in other software packages for statistical analysis and atlas creation.

3541 Computer 95

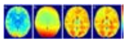

Bias Field Correction and Intensity Normalisation for Quantitative Analysis of Apparent Fibre Density

David Raffelt[1], Thijs Dhollander[1], J-Donald Tournier[2], Rami Tabbara[1], Robert E Smith[1], Eric Pierre[1], and Alan Connelly[1]

[1]Florey Institute of Neuroscience, Melbourne, Australia, [2]Centre for the Developing Brain, Division of Imaging Sciences and Biomedical Engineering, Kings College London, London, United Kingdom

Apparent Fibre Density (AFD) is a measure derived from un-normalised fibre orientation distributions. To make AFD quantitative across subjects, images need to be intensity normalised and bias field corrected. Here we present a fast and robust approach to simultaneous bias field correction and intensity normalisation by exploiting tissue compartment maps derived from multi-tissue constrained spherical deconvolution. We performed simulations to show that the method can accurately recover a ground truth bias field, while also demonstrating qualitative results on *in vivo* data.

3542 Computer 96

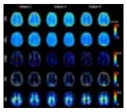

Multi compartment deconvolution with L2 regularization and priors improves repeatability of MD estimation through free water and IVIM elimination.

Alberto De Luca[1,2], Filippo Arrigoni[2], Alessandra Bertoldo[1], and Martijn Froeling[3]

[1]Department of Information Engineering, University of Padova, Padova, Italy, [2]Neuroimaging Lab, Scientific Institute IRCCS Eugenio Medea, Bosisio Parini (LC), Italy, [3]Radiology Department, University Medical Center Utrecht, Utrecht, Netherlands

Pseudo continuous description of the diffusion MRI (dMRI) signal through multi-compartment deconvolution is a promising technique to disentangle different water pools in the brain. In this work we verified whether a deconvolution based approach with L_2 regularized priors could improve the repeatability of DTI metrics computed on the brain data of 3 volunteers acquired twice. Signal fractions of free water and perfusion could reliably be quantified and removed from the diffusion signal, improving the repeatability of MD estimation both in gray and white matter.

Electronic Poster

Hepatopancreaticobiliary

Exhibition Hall Monday 14:45 - 15:45

3543 Computer 97

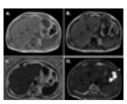

Comparing liver fat quantification obtained with Complex Chemical Shift-Encoded MRI and Conventional method in an oncologic population sample.

Alessandra Borgheresi[1], Davinia Ryan[1], Simone Krebs[1], Sarah Eskreis-Winkler[1], and Lorenzo Mannelli[1]

[1]Radiology, Memorial Sloan Kettering Cancer Center, New York, NY, United States

Chemotherapy is hepatotoxic. Since steatosis is an early sign of hepatotoxicity, an accurate estimation of the changing of fat liver concentration would be useful in the management of oncologic patients. The purpose of this study was to compare fat liver concentration estimated by T1-weightened-in-and-out-of-phase (IOP) imaging with the one obtained by IDEAL-IQ method in an oncologic patients population with unknown liver iron concentration. A statistical difference was demonstrated between fat fraction estimated with conventional IOP imaging and IDEAL-IQ method.

3544 Computer 98

Feasibility of computed diffusion-weighted MR imaging for visualization of pancreatic adenocarcinoma: comparison with acquired diffusion-weighted imaging

Yoshihiko Fukukura[1], Yuichi Kumagae[1], Hiroto Hakamada[1], Koji Takumi[1], Kiyohisa Kamimura[1], Masanoari Nakajo[1], Tomoyuki Okuaki[2], and Takashi Yoshiura[1]

[1]Radiology, Kagoshima University Graduate School of Medical and Dental Sciences, Kagoshima, Japan, [2]Philips Electronics Japan, TN, Japan

We compared directly acquired diffusion-weighted imaging (DWI) at b-values of 1500 s/mm^2 and 2000 s/mm^2 with computed DWI (cDWI) at the same b-values, which was calculated from directly acquired DWI data at b-values of 0 s/mm^2 and 1000 s/mm^2. Our main result is that the incidence of clear hyperintense pancreatic adenocarcinomas was significantly higher on cDWI at a b-value of 1500 s/mm^2 than on directly acquired DWI at a b-value of 1000 s/mm^2 ($P < 0.001$) and was comparable to the incidence on directly acquired DWI at a b-value of 1500 s/mm^2, suggesting that cDWI to a b-value of 1500 s/mm^2 has diagnostic merit.

3545 Computer 99

Hyperpolarized [1-13C]pyruvate reveals increase of hepatic LDH activity following a glucose challenge in pigs

Uffe Kjærgaard[1], Christoffer Laustsen[1], Thomas Nørlinger[1], Emmeli Mikkelsen[1], Rasmus Stilling Tougaard[2], Qi Haiyun[1], Lotte Bonde Bertelsen[1], Niels Jessen[3], and Hans Stødkilde-Jørgensen[1]

[1]MR Research Centre, Aarhus University Hospital, Aarhus, DK, Aarhus N, Denmark, [2]Department of Cardiology – Research, Aarhus University Hospital, Aarhus, DK, [3]Department of Clinical Medicine - Research Laboratory for Biochemical Pathology, Aarhus University, Aarhus, DK

Hepatic regulation of glucose homeostasis is of pivotal importance and thus in vivo interrogation of hepatic energetic alterations in disease and treatment non-invasively using [1-13C] pyruvate has been proposed as a novel modality for assessing metabolic status. Here we investigated the metabolic effect of a glucose challenge on the porcine liver. A hepatic metabolic shift towards a reduced gluconeogenesis (increased lactate pool size) was observed following the glucose challenge, confirming hyperpolarized 13C MR's ability to detect such changes. These findings support the use of hyperpolarized MR in metabolic challenge test in patients.

3546 Computer 100

4D-MRI with 3D radial sampling and self-gating-based K-space sorting: image quality improvement by slab-selective excitation

Zixin Deng[1,2], Wensha Yang[3], Jianing Pang[1,4], Richard Tuli[3], Behrooz Hakimian[3], Robert Reznik[3], Xiaoming Bi[5], Benedick Fraass[3], Debiao Li[1,2,6], and Zhaoyang Fan[1]

[1]Biomedical Imaging Research Institute, Cedars-Sinai Medical Center, Los Angeles, CA, United States, [2]Bioengineering, University of California, Los Angeles, Los Angeles, CA, United States, [3]Radiation Oncology, Cedars-Sinai Medical Center, [4]Siemens Healthcare R&D, Chicago, IL, United States, [5]Siemens Healthcare R&D, Los Angeles, CA, United States, [6]Medicine, University of California, Los Angeles, Los Angeles, United States

Stereotactic body radiation therapy with a simultaneous integrated boost (SBRT-SIB) has been used to improve tumor resection rate by sterilizing cancerous tissue that are surrounding the vessels. Accurate tumor imaging and tumor motion assessment will enhance the potential for SBRT-SIB. 4D-MRI (respiratory resolved, 3D volumetric images) has emerged as a promising imaging technique for characterizing tumor motion due to the absence of ionizing radiation and its superior soft tissue contrast. This study explored a slab-selective excitation approach to increase the blood vessel to tissue contrast with the goal of improving the accuracy of boost volume definition in radiation therapy.

3547 Computer 101

PET/MR in pancreatic cancer: correlation between overall survival and functional imaging biomarkers from DCE-MRI, DWI, MR spectroscopy and PET

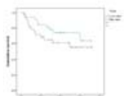

Bang-Bin Chen[1], Yu-Wen Tien[2], Ming-Chu Chang[3], Mei-Fang Cheng[4], Shih-Hung Yang[5], and Tiffany Ting-Fang Shih[6,7]

[1]Department of Medical Imaging and Radiology, National Taiwan University Medical School and Hospital, Taipei, Taiwan, [2]Department of Surgery, National Taiwan University Medical School and Hospital, [3]Department of Internal Medicine, National Taiwan University Medical School and Hospital, [4]Department of Nuclear Medicine, National Taiwan University Medical School and Hospital, [5]Department of Oncology, National Taiwan University Medical School and Hospital, [6]Departmen of Radiology, National Taiwan University Medical School and Hospital, Taipei, Taiwan, [7]Department of Medial Imaging, Taipei City Hospital

The purpose of this study is to evaluate the association of imaging biomarkers from PET/MR with overall survival in pancreatic cancer patients. Sixty-four patients with pathologically-proven pancreatic adenocarcinoma underwent PET/MRI before treatment. The imaging biomarkers included Ktrans and Peak from DCE-MRI, minimal apparent diffusion coefficient from DWI, choline from MR spectroscopy, standard uptake values, metabolic tumor volume, and total lesion glycolysis of the tumors. Among all imaging parameters, Peak was found to be an independent predictor for overall survival in these patients. Thus, the imaging biomarkers from PET/MRI reflect different tumor characteristics and may predict survival outcome in these patients.

3548 Computer 102

T1- MRI Assessment of Hepatobiliary Fibrosis in Cystic Fibrosis Patients: Significance for Chronic Liver Diseases

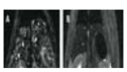

Shannon Donnola[1], Kimberly McBennett[2,3], David Weaver[3], Lan Lu[1,4], Xin Yu[1,5,6], James Chmiel[3], Michael Konstan[3], Mitchell Drumm[3,7], and Chris Flask[1,3,5]

[1]Radiology, Case Western Reserve University, Cleveland, OH, United States, [2]Medicine, University Hospitals of Cleveland, OH, United States, [3]Pediatrics, University Hospitals of Cleveland, Cleveland, OH, United States, [4]Urology, Case Western Reserve University, Cleveland, OH, United States, [5]Biomedical Engineering, Case Western Reserve University, Cleveland, OH, United States, [6]Physiology and Biophysics, Case Western Reserve University, Cleveland, OH, United States, [7]Genetics, Case Western Reserve University, Cleveland, OH, United States

Liver disease is the third leading cause of death in Cystic Fibrosis (CF). Unfortunately, conventional liver function tests cannot sensitively detect it.[1-3] Liver stiffness measurements via MRI and ultrasound have shown promise but are unfortunately impacted by other factors (e.g., hepatic fat) potentially resulting in over-estimation of fibrosis.[4,5] We recently validated a T1-MRI assessment of biliary dilatation and fibrosis in a rat model of congenital hepatic fibrosis (Figs. 1-3).[6] In this clinical study, we show that T1-MRI can be used to sensitively detect increased percent bile duct volumes in CF patients in comparison to control subjects with normal liver function.

3549 Computer 103

Reliable determination of bile acids from human gallbladder by 1H MRS - protocol optimization and estimation of reproducibility

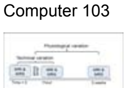

Gaelle Diserens[1], Roland Kreis[1], Dino Kroell[2], Philipp Nett[2], Guido Stirnimann[2], Peter Vermathen[1], and Reiner Wiest[2]

[1]Depts. Radiology and Clinical Research, University Bern, Bern, Switzerland, [2]Dept. Visceral Surgery and Medicine, University Inselspital, Bern, Switzerland

Bile exerts multiple functions in the liver and gut with a crucial role for triglyceride-, sterol- and carbohydrate-metabolism and is a key player in disease processes. The study purpose was to develop a reliable MRS protocol and to assess variability of bile acid determination in human gallbladder. Our study demonstrated higher stability and reliability of gallbladder spectra with subjects measured in prone position compared to back position. Relatively small coefficients of variation were obtained in a reproducibility study particularly within subjects, suggesting clinical applicability of the method, especially for longitudinal studies.

3550 Computer 104

MR Imaging Characteristics of Benign and Malignant Biliary Strictures

Nikhar Kinger[1], Peter Harri[1], Lauren F Alexander[1], Courtney Coursey Moreno[1], and Pardeep K Mittal[1]

[1]Department of Radiology and Imaging Sciences, Emory University School of Medicine, Atlanta, GA, United States

Wide spectrum of hepatobiliary and pancreatic diseases can lead to development of benign and malignant biliary strictures such as cholangiocarcinoma, pancreatic adenocarcinoma, ampullary carcinoma, PSC, autoimmune pancreatitis, ischemic strictures, post cholecystectomy, trauma etc. MRI characteristic of malignant strictures such as length, location, wall thickness, asymmetry, luminal regularity and enhancement will be discussed. CE_MRI helps to reach specific diagnosis and narrow differential diagnosis which is important for management and treatment planning

---

3551 Computer 105

Early Detection of Acute Pancreatitis (AP) Using MR Elastography (MRE) with Multislice Spin-echo Echo-planar Imaging

Yu Shi[1], qiyong guo[2], yin liu, and yanqing liu

[1]Shengjing Hospital, Shen Yang, People's Republic of China, [2]People's Republic of China

An accurate early diagnosis(<24h of admission) of acute pancreatitis is clinically important. Our work shows that MR elastography has significantly better diagnostic performance for detecting AP than that achieved using the conventional CT/MR imaging, with improved sensitivity and accuracy. Early MRE is a promising technique to diagnose AP in a noninvasive fashion on admission.

3552 Computer 106

Gadoxetate-disodium-enhanced T1-weighted R2* Mapping Improves Visualization of Biliary Anatomy in Liver Donor Candidates

Soudabeh Fazeli Dehkordy[1], Saya Igarashi[1], Carolina P Lamas Constantino[1,2], Jonathan Hooker[1], Cheng William Hong[1], Adrija Mamidipalli[1], Alan Hemming[3], and Claude B Sirlin[1]

[1]Liver Imaging Group, Department of Radiology, University of California San Diego, San Diego, CA, United States, [2]Dimagem Diagnóstico por Imagem, Rio de Janeiro, Brazil, [3]Department of Surgery, University of California San Diego, San Diego, CA, United States

Gadoxetate-disodium (Gd-EOB-DTPA)-enhanced 3D T1- weighted (T1W) MR cholangiography (MRC) is recognized as an efficient method for evaluation of biliary anatomy, which is critical in the preoperative evaluation of living liver donors. We hypothesize that bile duct visualization could be improved by acquiring Gd-EOB-DTPA-enhanced T1W multi-echo (ME) gradient-echo (GRE) images and generating parametric R2* map cholangiograms. In 10 liver donor candidates, we retrospectively compared biliary duct visualization on T1W-R2* maps vs. 3D T1W cholangiograms obtained 20 minutes after IV administration of gadoxetate disodium. T1W-R2* maps provided comparable visualization of the first-order bile duct branches and better visualization of the second-order branches (p<0.05).

3553 Computer 107

Evaluation of T1 Parametric Mapping using Inversion Recovery Fast Spoiled Gradient Echo: Application for Pre- and Post-Contrast Liver MRI

Puneet Sharma[1], Xiaodong Zhong[1,2], Marcel Dominik Nickel[3], Hiroumi Kitajima[1], and Pardeep Mittal[1]

[1]Department of Radiology and Imaging Sciences, Emory University, Atlanta, GA, United States, [2]MR R&D Collaborations, Siemens Healthcare, Atlanta, GA, United States, [3]MR Application Predevelopment, Siemens Healthcare, Erlangen, Germany

This investigation evaluates the performance and accuracy of a fast inversion recovery Look-Locker method for in vivo liver T1 mapping. Several parameters were assessed using T1 phantoms to describe accuracy trends and prevalence for artifacts. The method was also applied in vivo to demonstrate feasibility of fast T1 mapping of liver parenchyma and blood pool. The results offer insight into optimal imaging parameters, and showed good agreement with known T1 values at 1.5T.

3554 Computer 108

Black Blood T2-weighted Turbo Spin-Echo Imaging of the Liver with DANTE Preparation Module

Huimin Lin[1], Weibo Chen[2], Li Jiang[3], Lyu Li[2], Ruokun Li[1], and Fuhua Yan[1]

[1]Department of Radiology, Ruijin Hospital, Shanghai Jiao Tong University School of Medicine, Shanghai, People's Republic of China, [2]Philips Healthcare, Shanghai, People's Republic of China, [3]Philips Healthcare (Suzhou), Suzhou, People's Republic of China

The purpose is to implement high resolution black blood T2-weighted TSE liver imaging in order to facilitate focal liver lesion detection and characterization. DANTE black blood preparation module, T2 weighted Multivane XD multi-slice acquisition and respiratory trigger were combined together. 8 healthy volunteers underwent MRI scanning on 3T Ingenia MR Syste. The black blood T2-weighted sequence showed high image quality and no artifacts. Hepatic veins, portal vein and their main branches were all suppressed successfully. No significant difference was shown in the SNR between black blood and routine T2-weighted images. In conclusion, the black blood T2-weighted imaging could provide robust and good imaging quality.

3555 Computer 109

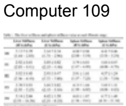

Splenic MR Elastography in Prediction of Hepatic Fibrosis Stage

Chen-Te Chou[1,2] and Ran-Chou Chen[3,4]

[1]Radiology, Chang-Hua Christian Hospital, Chang-Hua, Taiwan, [2]Biomedical Imaging and Radiological Sciences, National Yang-Ming University, Taipei, Taiwan, [3]Health Promotion Administration, Ministry of Health and Welfare, [4]Biomedical Imaging and Radiological Sciences, National Yang-Ming University, Taipei

The purpose of our study was to investigate the relationship between splenic MR elastography (MRE) and liver fibrosis stages. 109 patients underwent histological examination and abdominal MR examination within 3-months interval were enrolled in our study. MRE was performed with passive driver on right and left chest wall separately. The mean stiffness value of liver and spleen was determined and showed good correlation between hepatic/splenic stiffness and liver fibrosis stage. Our results demonstrated that spleen stiffness measured by MRE was significant correlated with liver fibrosis stage. Combination of the spleen/liver stiffness provide higher diagnostic value than liver stiffness alone.

3556 Computer 110

Hepatocyte Fraction: Correlation with non-invasive liver functional biomarkers

Yoshifumi Noda[1], Satoshi Goshima[1], Tomoyuki Okuaki[2], Kimihiro Kajta[1], Hiroshi Kawada[1], Nobuyuki Kawai[1], Hiromi Koyasu[1], and Masayuki Matsuo[1]

[1]Department of Radiology, Gifu University, Gifu, Japan, [2]Philips Healthcare, Tokyo, Japan

The hepatocyte fraction (HeF) is based on simple pharmacokinetics and can quantitatively estimate the fraction of hepatocyte. In our study, the HeF, quantitative liver-to-spleen contrast ratio (Q-LSC), and delta T1 value were compared and correlated with Child-Pugh and MELD score. The HeF demonstrated the highest correlations with Child-Pugh score (r = -0.58, P < 0.0001) and MELD score (r = -0.57, P < 0.0001). The HeF could be a useful biomarker for the evaluation of liver function, compared to conventional imaging based quantitative methods.

3557 Computer 111

Cardiac-induced liver deformation as a measure of liver stiffness: normal volunteer reproducibility and post-prandial stress studies

Manil Chouhan[1], Alex Menys[1], Alan Bainbridge[2], David Atkinson[1], Shonit Punwani[1], Rajeshwar Mookerjee[3], and Stuart Taylor[1]

[1]UCL Centre for Medical Imaging, University College London, London, United Kingdom, [2]Department of Medical Physicist, University College London Hospitals NHS Trust, London, United Kingdom, [3]UCL Institute for Liver and Digestive Health, University College London, London, United Kingdom

Liver stiffness measured with elastography has useful clinical applications but requires the use of expensive, specialist equipment. In this study, we acquire dynamic 'cine' data of the liver to capture cardiac-induced liver motion during cardiac cine MRI. We quantify these data by applying a registration algorithm and use the deformation fields as a surrogate for liver stiffness. We demonstrate feasibility and good seven-day reproducibility and evaluate the effects of physiological haemodynamic changes using a liquid meal challenge. This technique would be widely applicable to hospital MRI scanners without elastography equipment.

3558 Computer 112

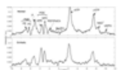

Investigation of liver cirrhosis using 31P-MRS at 7T

Lucian A. B. Purvis[1], William T. Clarke[1], Ladislav Valkovic[1], Christina Levick[1], Michael Pavlides[2], Eleanor Barnes[2], Jeremy F. Cobbold[2], Stefan Neubauer[1], Matthew D. Robson[1], and Christopher T. Rodgers[1]

[1]OCMR, Department of Cardiovascular Medicine, University of Oxford, Oxford, United Kingdom, [2]Translational Gastroenterology Unit, University of Oxford, Oxford, United Kingdom

Phosphorus (^{31}P) metabolites have potential value as markers in liver disease. The increase in field strength from 3 to 7T allows more accurate quantitation of the liver ^{31}P-MRS spectrum. Ten volunteers and eleven patients with liver cirrhosis were scanned using a 16-channel array and a 3D UTE-CSI sequence. Metabolite concentrations were calculated using an endogenous 2.5mM ATP reference. Significant reductions in inorganic phosphate and phosphoenolpyruvate/phosphatidylcholine concentrations were seen, as well as an increase in glycerophosphoethanolamine ($P<0.05$). The splitting of PDE into its constituent peaks allows more insight into changes in metabolism.

3559 Computer 113

Assessment of Liver Function of HBV-induced Cirrhosis using T1 Mapping on Gd-EOB-DTPA-Enhanced MRI

Xueqin Zhang[1], Jian Lu[1], Tao Zhang[1], Jifeng Jiang[1], Ding Ding[1], Sheng Du[1], and Weibo Chen[2]

[1]Nantong Third People's Hospital, Nantong University, Nantong, People's Republic of China, [2]Philips Healthcare, Shanghai, People's Republic of China

The purpose of this study was to investigate the ability of T1 mapping on Gd-EOB-DTPA-enhanced MRI for the assessment of liver function of HBV-induced cirrhosis. We used Look-Locker sequences to acquire T1 mapping images pre and post-contrast at 5, 10, 15 and 20 minutes after Gd-EOB-DTPA administration, T1 relaxation times of the liver parenchyma were measured, reduction rates of T1 relaxation times between pre- and post-contrast enhancement were calculated, our study showed that Gd-EOB-DTPA-enhanced T1mapping MRI is useful for the evaluation of Liver function of HBV-induced cirrhosis.

3560 Computer 114

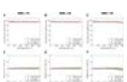

Assessment of Hepatic Iron Content by an Automatic Vessel Exclusion Technique in Patients with Iron Overload

Aaryani Tipirneni-Sajja[1], Ruitian Song[1], M. Beth McCarville[1], Ralf B. Loeffler[1], Jane S. Hankins[2], and Claudia M. Hillenbrand[1]

[1]Diagnostic Imaging, St. Jude Children's Research Hospital, Memphis, TN, United States, [2]Hematology, St. Jude Children's Research Hospital, Memphis, TN, United States

Extraction of liver parenchyma is an important step in the evaluation of R2*-based hepatic iron content. Traditionally this is performed by radiologists via thresholding, an iterative, time consuming process susceptible to interrater variability. Here, a new method based on Frangi vesselness filtering is presented that automatically removes hepatic vessels from liver tissue, thereby reducing potential bias and improving workflow. The method was evaluated in digital liver phantoms and 42 iron overloaded patients. Excellent agreement between manual and automated liver parenchyma segmentation was found which demonstrates accuracy and robustness of the proposed method.

3561 Computer 115

Steatohepatitic Hepatocellular Carcinoma: Distinctive MR Imaging Features with Pathologic and OPTN Correlation

Kelly Tung[1], Alvin Silva[1], Marcela Salomao[2], Christine Menias[1], Christine Zwart[1], Sukhdeep Singh[1], and Amy Hara[1]

[1]Radiology, Mayo Clinic Arizona, Phoenix, AZ, United States, [2]Pathology, Mayo Clinic Arizona, Phoenix, AZ, United States

Hepatocellular carcinoma (HCC) has specific imaging criteria such as arterial hyperenhancement, contrast washout, and pseudocapsule that allow it to be diagnosed with confidence and relative accuracy. However, a novel HCC variant, steatohepatitic hepatocellular carcinoma (SH-HCC), has been described which tends to not exhibit the classic HCC imaging features. In this study, we explored alternative secondary MR features of HCC such as T1 and T2 signal intensity, intralesional fat, and restricted diffusion which may be more applicable in diagnosing steatohepatitic hepatocellular carcinoma.

3562 Computer 116

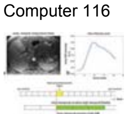

Retrospective reconstruction of hepatic arterial phases in gadoxetic acid-enhanced liver MR using continuous golden-angle radial sequence

Yoon-Chul Kim[1], Eunju Kim[2], Gabrielle Beck[3], Hans Peeters[3], and Young Kon Kim[4]

[1]Clinical Research Institute, Samsung Medical Center, Sungkyunkwan University School of Medicine, Seoul, Korea, Republic of, [2]Philips Healthcare, Seoul, Korea, Republic of, [3]Philips Healthcare, Best, Netherlands, [4]Radiology, Samsung Medical Center, Seoul, Korea, Republic of

We apply a 3D continuous golden-angle radial sparse parallel (GRASP) sequence to gadoxetic acid-enhanced imaging of the liver at 3 T. Arterial phase imaging may need high spatial and temporal resolution as well as correct timing of capturing arterial enhancement to obtain hemodynamic information of the tumor. Continuous golden-angle radial sampling provides a flexible retrospective selection of temporal window. We develop a technique that identifies the arterial peak from high temporal resolution data and reconstructs arterial phases with different temporal windows. The characteristics of hepatic arterial images after retrospective temporal resolution selection are demonstrated.

3563 Computer 117

Qualitative and Quantitative Comparison of 2D Gradient Recalled Echo and Rapid 2D Gradient Recalled Echo Magnetic Resonance Elastography

Ely R Felker[1], Steven S Raman[1], Bradley D Bolster[2], Holden Wu[1], Kyung Sung[1], Ning Jin[2], Brenda J Brown[1], and David S Lu[1]

[1]UCLA, Los Angeles, CA, United States, [2]Siemens Healthcare, United States

Conventional GRE-based MR elastography requires a breath hold of approximately 18 seconds per slice, which is difficult for some patients. We compared a rapid GRE-based sequence (9 second breath hold) to conventional GRE in terms of quantitative liver stiffness (LS) measurement and image quality score (IQS), based on wave propagation and confidence mask coverage, determined by two independent radiologists. The two sequences were equivalent in terms of LS measurement, but the rapid GRE sequence had significantly higher IQS for both readers. Rapid GRE-based MR elastography may be an improved alternative to GRE in patients with limited breath hold capacity.

3564 Computer 118

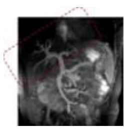

Evaluation of Portal Vein System Hemodynamics with Magnetic Resonance Angiographic Inflow-Sensitive Inversion Recovery

Di Zhu[1], Xianlun Zou[1], Hao Tang[1], Xiao Chen[1], Xiaoyan Meng[1], Zhen Li[1], and Daoyu Hu[1]

[1]Department of Radiology, Tongji Hospital, Tongji Medical College, Huazhong University of Science and Technology, Wuhan, People's Republic of China

To evaluate the ability of magnetic resonance angiographic inflow-sensitive inversion recovery (IFIR-MRA) to assess hemodynamics of portal vein system in patients with portal hypertension, we compared visualized portal vein branching grade scores at different blood suppression inversion time (BSP TI) settings and signal intensity contrast ratio of the vessles and the liver parenchyma with color Doppler ultrasonography (CDUS) measured hemodynamics. Statistically significantly correlation demonstrated that IFIR-MRA of portal vein system has the potential to suggest hemodynamic changes, especially for RPV.

3565 Computer 119

Validation of Feasibility of Magnetic Resonance Imaging for the Measurement of Depth of Tumor Invasion in Distal Bile Duct Cancer

Na Yeon Han[1], Min Ju Kim[1], Beom Jin Park[1], Deuk Jae Sung[1], Ki Choon Sim[1], Ki Choon Sim[1], and Sung Bum Cho[1]

[1]Korea University Anam Hospital, Seoul, Korea, Republic of

We performed the study to develop and validate a method for measuring the depth of tumor invasion (DoI) on magnetic resonance imaging (MRI) and to investigate the diagnostic performance of the measured DoI for stratifying T classification in patients with distal bile duct cancer. Our result showed that this newly developed method reliably measured DoI on T2-weighted MR images, and can be used for the preoperative T classification of distal bile duct cancer patients.

3566 Computer 120

Pancreatic exocrine function estimated by cine dynamic MRCP with a spatially selective IR pulse: Correlation with T1 mapping of the pancreatic parenchyma

Katsuyoshi Ito[1], Akira Yamamoto[1], Kazuya Yasokawa[1], Minoru Hayashida[1], Daigo Tanimoto[1], Akihiko Kanki[1], Tomohiro Sato[1], Hidemitsu Sotozono[1], Takeshi Fukunaga[1], Koji Yoshida[1], Kazunori Moriya[1], and Tomoyuki Okuaki[2]

[1]Radiology, Kawasaki Medical School, Kurashiki, Japan, [2]Philips Healthcare AsiaPacific, Japan

This study assessed the correlation between pancreatic exocrine function estimated by cine dynamic MRCP with a spatially selective IR pulse and T1 mapping of the pancreatic parenchyma on 3T MR imaging. There was a statistically significant correlation between the secretion grade of the pancreatic juice in cine-dynamic MRCP and T1 relaxation time of the pancreatic parenchyma. Therefore, T1 mapping of the pancreatic parenchyma will be used as collaborative, noninvasive technique of cine-dynamic MRCP with a spatially selective IR pulse for the estimation of pancreatic exocrine function.

Electronic Poster

Agent Developments & Technical Advances in Moleular MR Imaging

Exhibition Hall — Monday 16:15 - 17:15

3567 Computer 1

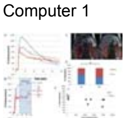

Detection of Acetaminophen-Induced Liver Damage using Contrast-Enhanced Dynamic MRI and T1 Maps

Christiane L Mallett[1], Matthew Latourette[1], Jeremy Hix[1], Alexander Wolf[1], and Erik M Shapiro[1]

[1]Radiology, Michigan State University, East Lansing, MI, United States

We are developing an MRI method to measure acetaminophen toxicity in the liver. We obtained dynamic T1 weighted images of the liver and T1 maps using the clinically approved contrast agent gadoxetate disodium (Eovist). After acetaminophen overdose, the uptake of contrast was decreased in the liver and increased in the kidney. T1 and variation in T1 were higher after acetaminophen. T1 was correlated with ALT, a serum measure of liver damage. This is a promising method for quantifying drug induced liver damage in vivo.

3568 Computer 2

A Transgenic Method to Enhance Intracellular Retention of Iron Oxide Nanoparticles and Prolong MRI Tracking

Xiaoyong Zhang[1], Ximei Qian[2], Sha Wang[1], and Xiaoping Hu[1]

[1]Bourns college of engineering, University of California, Riverside, CA, United States, [2]Department of Biomedical Engineering, Emory University

Iron oxide nanoparticles (IONPs) are widely used as labels for noninvasive cell tracking using magnetic resonance imaging (MRI). However, IONP induced contrast dilutes rapidly over time due to cell growth and division, limiting its applications in long-term cellular visualization. In the present work, unlike techniques focusing on modification of IONPs, we established a novel transgenic approach to increase IONP retention, significantly prolonging the tracking time of IONP labeled cells. In addition, this approach could be generalized to other cell types and magnetic nanoparticles, making it attractive for long-term cell tracking or tumor progression monitoring.

3569 Computer 3

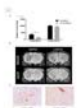

Comparison of USPIO and MPIO for molecular MRI across different field strengths

Niloufar Zarghami[1], Alexandr Khrapichev[1], Francisco Perez-Balderas[1], Manuel Sarmiento-Soto[1], and Nicola Ruth Sibson[1]

[1]Department of Oncology, University of Oxford, Oxford, United Kingdom

We have previously reported molecular MRI studies using Microparticles of Iron Oxide (MPIO) coupled to anti-VCAM-1 antibodies. However, Ultrasmall Superparamagnetic Iron Oxide (USPIO) are more commonly used in MRI applications. Although MPIO provide greater targeting valency and contrast per particle, their advantages over UPSIO for molecular MRI has not been demonstrated empirically. Here, we compared the sensitivity and specificity of VCAM-MPIO and VCAM-USPIO for molecular MRI; VCAM-MPIO, but not VCAM-USPIO, yielded marked and selective contrast in areas of cerebral inflammation. These results confirm the theoretical assumption that MPIO present a more viable platform for molecular MRI than USPIO.

3570 Computer 4

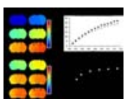

3 nm iron oxide nanoparticles as spin-lattice relaxation time enhancing contrast agents.

Joong Hee Kim[1], Taeghwan Hyeon[2], and David L. Brody[3]

[1]Neurology, Washington University School of Medicine in St. Louis, St. Louis, MO, United States, [2]Seoul National University, [3]Washington University School of Medicine in St. Louis

Relaxation based MR images have superior spatial resolution compared to other MRI approaches. In addition, structural MRI requires short scan time and yet has high signal to noise ratio. However, the greatest limitation of structural MRI is poor specificity and sensitivity to pathology. Thus a well characterized MR molecular contrast agent would be a major advance. Here we present 3 nm iron oxide nanoparticles (IONP) as a T1 contrast agent. The 3 nm IONP showed strong T1 effects up to 13.5 ms echo time. A fully functionalized 3 nm IONP would be an appropriate component for molecular contrast agents.

3571 Computer 5

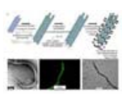

Engineered Protein-Iron Oxide Hybrid Biomaterial for MRI-monitoring of Drug Delivery

Lindsay Kathleen Hill[1,2,3], Che Fu Liu[3], Teeba Jihad[3], Youssef Zaim Wadghiri[2], and Jin Kim Montclare[3,4]

[1]Biomedical Engineering, SUNY Downstate Medical Center, Brooklyn, NY, United States, [2]Radiology, New York University School of Medicine, New York, NY, United States, [3]Chemical and Biomolecular Engineering, New York University Tandon School of Engineering, Brooklyn, NY, United States, [4]Chemistry, New York University, New York, NY, United States

Our goal is to create protein engineered biomaterials for dual drug delivery and MRI monitoring to improve the growing field of theranostics. Here we present a drug binding protein that is templated to USPIOs using a biomineralization-inspired biotemplation method. The agent shows promise for T2/T2*-weighted MRI.

3572 Computer 6

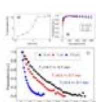

Direct hyperpolarization of micro- and nanodiamonds for bioimaging applications – considerations on particle size, functionalization and polarization loss

Grzegorz Kwiatkowski[1], Jonas Steinhauser[1], Patrick Wespi[1], Matthias Ernst[2], and Sebastian Kozerke[1]

[1]Institute for Biomedical Engineering, ETH Zurich, Zurich, Switzerland, [2]Physical Chemistry, ETH Zurich, Zurich, Switzerland

Due to the inherently long relaxation time of ^{13}C spins in diamonds, the nuclear polarization enhancement obtained with dynamic nuclear polarization can be preserved for a time on the order of ~1h, opening up a window for a new class of long-lived contrast agents. Up to now, no imaging with hyperpolarized micro and nanodiamonds has been reported. The present communication presents the feasibility of applying directly hyperpolarized diamonds in MR imaging including considerations for potential in-vivo applications.

3573 Computer 7

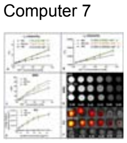

A novel multimodal mannan-based polymer system suitable for tumor and metastasis diagnosis

Andrea Galisova[1], Marketa Jiratova[1], Maria Rabyk[2], Martin Hruby[2], Milan Hajek[1], and Daniel Jirak[1]

[1]MR Unit, Institute for Clinical and Experimental Medicine, Prague, Czech Republic, [2]Institute of Macromolecular Chemistry, Prague, Czech Republic

Presented mannan-based polymers have promising properties for tumor and metastasis imaging due to their biocompatibility, nanosize and specificity for the immune cells. In this study, two mannan-based polymers were tested by multimodal imaging (MRI and fluorescence). The polymers showed superior imaging properties compared to a commercially available contrast agent. The polymer modified with oxazoline expressed slower elimination rate from the body. Both probes were visualized by MR and optical imaging modality at the injection sites and in the lymph nodes of the experimental mice suggesting their promising properties for cancer diagnosis.

3574 Computer 8

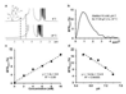

CEST MRI using sugar alcohol, maltitol, to detect cancer: Study on rat glioma model

Puneet Bagga[1], Mohammad Haris[2], Kevin D'Aquilla[1], Francesco Marincola[2], Hari Hariharan[1], Ravinder Reddy[1], and Puneet Bagga[3]

[1]Department of Rediology, University of Pennsylvania, Philadelphia, PA, United States, [2]Research Branch, Sidra Medical and Research Center, Doha, Qatar, [3]Perelman School of Medicine, University of Pennsylvania, Philadelphia, PA, United States

We show the use of a sugar alcohol sweetener, maltitol, in cancer MRI studies by exploiting its chemical exchange saturation transfer (malCEST) property. The tumor specific accumulation of maltitol in a rat glioma model provides localized, temporal changes in the CEST contrast, which corroborated the gadolinium-enhanced MRI. These findings illustrate the potential application of maltitol in the diagnosis and monitoring of the therapeutic response of cancers, including gliomas in preclinical studies.

3575 Computer 9

Detection of dynamic substrate binding using MRI

Nirbhay N. Yadav[1,2], Xing Yang[1], Yuguo Li[1,2], Wenbo Li[1,2], Guanshu Liu[1,2], and Peter C.M. van Zijl[1,2]

[1]Russell H. Morgan Department of Radiology and Radiological Science, The Johns Hopkins University School of Medicine, Baltimore, MD, United States, [2]FM Kirby Research Center, The Kennedy Krieger Institute, Baltimore, MD, United States

Magnetic Resonance Imaging (MRI) is rarely used for molecular binding studies and never without synthetic metallic labels. We designed an MRI approach that can selectively detect substrate-target interaction by exploiting the narrow resonance of protons in free substrate for selective radio-frequency (RF) labeling and, subsequently, the process of immobilisation upon binding to a solid-like target for fast dipolar transfer of this label over the protons in its backbone. This cascade of events is ultimately detected via the water MRI signal with enhanced sensitivity. We demonstrate the principle for caffeine binding *in vitro* and *in vivo*.

3576 Computer 10

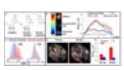

In vivo CEST MRI of specific activated T-cells population using the natural nucleoside cytidine

Hyla Allouche-Arnon[1] and Amnon Bar-Shir[1]

[1]Organic Chemistry, Weizmann Institute of Science, Rehovot, Israel

Non-invasive imaging of inflammation is crucial for understanding both inflammatory processes and immunotherapy. We propose a non-invasive and non-radioactive approach for longitudinal imaging of activated immune cells. We show that the use of the natural nucleoside cytidine as CEST imaging probe enable the monitoring of specific activated T-cells population with MRI. By using fluorescent analog of cytidine it is shown that CD8 T-cells are in situ labeled, underlying the specificity of nucleosides as potential probes for monitoring activated immune cells. We conclude that by using cytidine as a MRI-based probe one could monitor specific activated T-cells population during inflammation.

3577 Computer 11

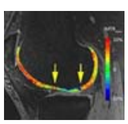

Prospective longitudinal evaluation of patients with low-grade cartilage injury using gagCEST at 7T

Markus Schreiner[1,2], Vladimir Mlynarik[1,3], Didier Laurent[4], Vladimir Juras[1], Pavol Szomolanyi[1], Stefan Zbyn[1,5], Celeste Scotti[4], Joerg Goldhahn[4], Harry Haber[4], Ewa Kubiak[4], Ronenn Roubenoff[4], Stefan Marlovits[6], Reinhard Windhager[2], and Siegfried Trattnig[1,3]

[1]High Field MR Centre, Department of Biomedical Imaging and Image-Guided Therapy, Medical University of Vienna, Vienna, Austria, [2]Department of Orthopaedics, Medical University of Vienna, Vienna, Austria, [3]Christian Doppler Laboratory for Clinical Molecular MR Imaging, Vienna, Austria, [4]Novartis Institutes for Biomedical Research, Basel, Switzerland, [5]Research Unit of Medical Imaging, Physics and Technology, University of Oulu and Oulu University Hospital, Oulu, Finland, [6]Depatment of Traumatology, Medical University of Vienna, Vienna, Austria

To the best of our knowledge, this is the first study that employs gagCEST for the longitudinal evaluation of untreated articular cartilage defects. We demonstrate that gagCEST at 7T has the potential of discriminating between cartilage defects, weight bearing and non-weight bearing femoral cartilage and therefore might serve as a biomarker for the evaluation of novel cartilage therapies. Furthermore, our study implies that proper fixation of the examined knee may help to increase the reliability of gagCEST experiments.

3578 Computer 12

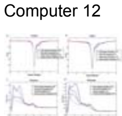

Lipo2-DG-CEST: a new theranostic agent for simultaneous tumour imaging and chemotherapy

Eleni Demetriou[1], Harriet Story[2], Robin Bofinger[2], Karin Shmueli[3], Helen Hailes[2], Alethea Tabor[2], and Xavier Golay[1]

[1]Brain Repair and Rehabilitation, Institute of Neurology, London, United Kingdom, [2]Department of Chemistry, University College of London, London, United Kingdom, [3]Department of Medical Physics & Bioengineering, University College of London, London, United Kingdom

2-DG has been shown to inhibit tumor growth in vivo; however, it cannot be used as a therapeutic agent in humans due to its toxicity. Here we show the potential for 2-DG-loaded liposomes to provide detectable Chemical Exchange Saturation Transfer (CEST) contrast, and thereby achieve simultaneous tumour imaging and chemotherapy by targeting areas of greater tumour metabolism. The CEST signal arising from 2-DG was compared to liposome-encapsulated 2-DG and to natural D-glucose, respectively. The results demonstrated an increase in signal for2-DG loaded liposomes when compared to both free 2-DG and glucose possibly due to a decrease in the global exchange rate.

3579 Computer 13

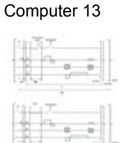

PRO-QUEST: A fast method for exchange rate quantification based on PROgressive saturation for Quantifying Exchange using Saturation Times in Chemical Exchange Saturation Transfer (CEST)

Eleni Demetriou[1], Mohamed Tachrount[1], Karin Shmueli[2], and Xavier Golay[1]

[1]Brain Repair and Rehabilitation, Institute of Neurology, London, United Kingdom, [2]Department of Medical Physics & Bioengineering, University College of London, London, United Kingdom

In this work we propose a novel pulse sequence for measuring chemical exchange rates through a progressive saturation recovery process PRO-QUEST (PROgressive saturation for Quantifying Exchange using Saturation Times). The water magnetization is sampled under non-steady state conditions and saturation is interleaved with the acquisition of images obtained in a single scan. Unlike previous approaches, it provides maps of T_1 and B_1 , needed for exchange-rate calculations, from the same dataset. The proposed pulse sequence has been successfully applied to obtain exchange rate maps in phantoms and healthy rat brains.

3580 Computer 14

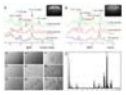

β−alanine Loaded Hollow Mesoporous Silica Nanospheres: A Potential Contrast Agent for Magnetic Resonance Spectroscopy Imaging of Brain Glioma

Jing Wang[1], Jianxun Qu[2], Tianyong Xu[2], and Zhenwei Yao[1]

[1]Radiology, Huashan Hospital of Fudan University, Shanghai, People's Republic of China, [2]GE Healthcare, Shanghai, People's Republic of China

The β−alanine loaded hollow mesoporous silica nanospheres (AMSNs) with a characteristic MRS spectrum are successfully synthesized and used for contrast enhanced magnetic resonance spectroscopy (MRS) imaging of brain glioma. Material characterizations, in vitro and in vivo cytotoxicity studies and contrast enhanced MRS imaging of both subcutaneously transplanted glioma and in situ glioma are conducted with the synthesized AMSNs.

3581 Computer 15

MR Imaging of Nanoparticle Uptake and 3D Intra-tumoral Distribution in Orthotopic Xenograft Mouse Models of Neuroblastoma

Ketan B Ghaghada[1], Saakshi Bhayana[1], Igor Stupin[1], Flavia Leao Barbosa[1], Chandresh Patel[1], Zbigniew Starosolski[1], and Ananth Annapragada[1]

[1]Pediatric Radiology, Texas Children's Hospital, Houston, TX, United States

Heterogeneity in tumor vasculature gives rise to variability in vascular permeability, one of the consequences being non-uniform intra-tumoral uptake and distribution of nanoparticle-based chemotherapeutics. An imaging agent that can assess tumor vascular heterogeneity and monitor uptake and distribution of nanoparticles could be useful for guiding and monitoring nanoparticle-based chemotherapy. In this work, we demonstrate, in orthotopic mouse models of solid tumors, that a high T1 relaxivity liposomal-gadolinium contrast agent (liposomal-Gd) enables MR imaging of nanoparticle uptake and 3D intra-tumoral distribution at clinically-relevant MR field strength.

3582 Computer 16

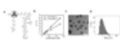

A high-relaxivity extradomain-B fibronectin targeting gadolinium metallofullerene for cancer detection and differential diagnosis in molecular MRI

Zheng Han[1] and Zheng-Rong Lu[1]

[1]Case Western Reserve University, Cleveland, OH, United States

Accurate cancer detection and characterization with MRI is hampered by the lack of safe and effective targeted MRI contrast agents. In this work, we have designed and synthesized a high-relaxivity targeted contrast agent by conjugating ZD2 peptide to hydroxylated Gd_3N@C80. ZD2-Gd_3N@C80 has a high T_1 relaxivity of 76.4 $mM^{-1}s^{-1}$ per Gd at 1.5 Tesla and a small diameter of 1 nm on average. At a low dose of 5 μmol Gd/kg, ZD2-Gd_3N@C80 is able to produce prominent contrast enhancement in the highly metastatic MDA-MB-231 triple-negative breast cancer model, but not in the estrogen-dependent MCF-7 tumors.

3583 Computer 17

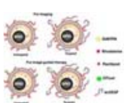

MR/optical image-guided liposomal drug delivery system for triple negative breast cancer

Sudath Hapuarachchige[1], Wenlian Zhu[1], Yoshinori Kato[1,2], Marina V. Backer[3], Susanta Sarkar[4], Joseph M Backer[1,3], and Dmitri Artemov[1,5]

[1]Radiology and Radiological Science, Johns Hopkins University School of Medicine, Baltimore, MD, United States, [2]Life Science Tokyo Advanced Research Center (L-StaR), Hoshi University School of Pharmacy and Pharmaceutical Science, Tokyo, Japan, [3]SibTech, Inc., Brookfield, CT, [4]CadenzaMed LLC, Wayne, PA, [5]Department of Oncology, The Sidney Kimmel Comprehensive Cancer Center, Johns Hopkins University School of Medicine, Baltimore, MD, United States

Noninvasive image-guided drug delivery is important in cancer drug development, and allows visualizing the delivery and predicting the outcome. In this study, the delivery and therapeutic effects of liposomes targeted to tumor vasculature was researched. Intravital microscopy and MRI were used for tracking the drug delivery and therapeutic effects were monitored in MDA-MB-231 mouse tumor model. Our experimental results suggest that targeting liposomes to VEGF receptors (VEGFRs) expressed on tumor endothelium, may inhibit EPR-mediated extravasation and accumulation of VEGFR-targeted liposomes.

3584 Computer 18

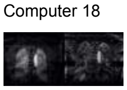

Use of Gadofosveset-enhanced Lung MRI to Assess Ongoing Lung Injury in Fibrotic Interstitial Lung Disease.

Sydney B Montesi[1], Rohan Rao[1], Lloyd Liang[1], Subba Digumarthy[2], Amita Sharma[2], Peter Caravan[2], Andrew Tager[1], and Ravi Seethamraju[3]

[1]Medicine, Pulmonary and Critical Care, Massachusetts General Hospital, Boston, MA, United States, [2]Radiology, Massachusetts General Hospital, Boston, MA, United States, [3]Siemens Healthcare, Boston, MA

Vascular leak is a cardinal response to injury, and prior assessments of alveolar-capillary permeability suggest that vascular leak is present in the lungs of patients, and that its extent is associated with progression and mortality. We hypothesized that the degree of vascular leak present reflects the extent of ongoing lung injury, and that measuring lung vascular permeability consequently could provide a much-needed metric for assessing ILD disease activity and predicting disease progression. Using magnetic resonance imaging with the albumin-binding contrast agent gadofosveset, we were able to detect increased vascular permeability in the lung of patients with fibrotic ILD.

3585 Computer 19

MRI assessment of spatial distribution of hypoxia in pre-clinical xenograft models of non-small cell lung cancer via GdDO3NI: A Novel Hypoxia-Binding T1 Contrast Agent

Shubhangi Agarwal[1], Nutandev B Jayadev[1], Carlos Renteria[1], Xiangxing Kong[2], Yanqing Tian[2,3], Landon J Inge[4], and Vikram D Kodibagkar[1]

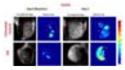

[1]Arizona State University, Tempe, AZ, United States, [2]Biodesign Institute, Arizona State University, Tempe, AZ, United States, [3]Department of Materials Science and Engineering, South University of Science and Technology of China, Shenzhen, People's Republic of China, [4]Norton Thoracic Institute, St. Joseph's Hospital and Medical Center, Phoenix, AZ, United States

Degree of tumor hypoxia and its spatial distribution could impact the therapeutic choices and lead to development of improved treatment plans. This study uses a hypoxia binding T1 contrast agent GdDO3NI, to evaluate the dependence of hypoxia activated pro-drug TPZ (Tirapazamine) on baseline tumor oxygenation and its effect on the oxygenation of two non-small cell lung cancer lines (NCI-H1975 and patient derived xenograft M112004). GdDO3NI was able to report the changes in hypoxia distribution in the tumor models in response to Tirapazamine therapy and correlation with therapeutic effect.

3586 Computer 20

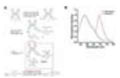

Aza-BODIPY Derivative for Gadolinium-enhanced MR and Near-infrared Fluorescence Dual Imaging

Hyunseung Lee[1], Eun-jung Kim[1], Hyun Min Kim[1], and Kwan Soo Hong[1,2]

[1]Bio-imaging Research Team, Korea Basic Science Institute, Cheongju, Korea, Republic of, [2]Graduate School of Analytical Science and Technology, Chungnam National University

A novel dual imaging probe for in vivo magnetic resonance imaging (MRI) and optical imaging was developed by combining gadolinium (Gd) -chelating MR probe and a near-infrared (NIR) fluorophore, aza-BODIPY (AB; BODIPY = borondipyrromethene). This aza-BODIPY-based bimodal contrast agent (AB-BCA) showed a significant fluorescence emission around the NIR range and an enhanced longitudinal relaxivity in MR modality. The probe was easily delivered to phagocytic cells of the innate immune system, together with macrophages and dendritic cells (DCs), and presented high-performance fluorescence and MR imaging without obvious cytotoxicity.

3587 Computer 21

Multi-parametric 11C-Methionine-PET/MRI for brain tumor imaging utilizing MR Fingerprinting.

Lale Umutlu[1], Jasmin Jaeger[1], Matthias Nittka[2], Stephan Kannengiesser [2], Josef Pfeuffer [2], Gregor Koerzdoerfer [2], Rainer Kirsch[2], Florian Meise[2], Harald Quick[3,4], Vikas Gulani[5], Mark Griswold[5], Ken Herrmann[6], Marcel Gratz[3,4], and Michael Forsting[1]

[1]Department of Diagnostic and Interventional Radiology and Neuroradiology, University Hospital Essen, Essen, Germany, [2]Siemens Healthcare GmbH, Erlangen, Germany, [3]University Duisburg-Essen, Erwin L. Hahn Institute for MR Imaging, Essen, Germany, [4]High Field and Hybrid MR Imaging, University Hospital Essen, Germany, [5]Case Western Reserve University, Cleveland, OH, [6]Department of Nuclear Medicine, University Hospital Essen, Essen, Germany

The successful implementation of integrated PET/MR systems has enabled a unique platform for simultaneous multi-parametric imaging comprising morphologic, functional and metabolic features of pathologic tissue. MR Fingerprinting has been recently presented as a robust and fast framework for simultaneous accurate quantification of multiple MR tissue properties. The results of our study, combining tissue characterization based on PET/MR imaging and MR Fingerprinting, indicate a correlation between tumor grading and changes in tissue features, demonstrating the high diagnostic potential of this novel approach for multi-parametric tissue characterization.

3588 Computer 22

A novel theranostic termoresponsive 19F probe for tumor imaging

Daniel Jirak[1], Andrea Galisova[1], Ondrej Sedlacek[2], Martin Hruby[2], and Milan Hajek[1]

[1]IKEM, Prague, Czech Republic, [2]Institute of Macromolecular Chemistry of the Academy of Sciences, Prague, Czech Republic

Novel ^{19}F MR probe with the ability of creation of a depot in the living system is presented. This agent is pH- and termoresponsible with the phase transition point from liquid into the solid state at the temperature above 20 ºC. The MR properties were assessed by relaxometry and ^{19}F spectroscopy/imaging. *In vivo* application confirmed efficiency of depot visualization; strong ^{19}F MR signal was detected in all animals. No adverse effects of the probe to the animals were observed. Sufficient MR sensitivity of the probe and its slow degradation in animals suggest potential for a theranostic use.

3589 Computer 23

Characterization of Inflammation Induced by Exposure to Primary Blast Waves in Rats using 19F MRI

Lesley M Foley[1], James C DeMar[2], Andrew B Batuure[2], William B Rittase[2], John G Rosenberger[2], Donna M Wilder[2], Patrick M Kochanek[3], Joseph B Long[2], and T Kevin Hitchens[1,4]

[1]Animal Imaging Center, University of Pittsburgh, Pittsburgh, PA, United States, [2]Center for Military Psychiatry and Neuroscience Research, Walter Reed Army Institute of Research, Silver Springs, MD, United States, [3]Safar Center for Resuscitation Research, University of Pittsburgh, Pittsburgh, PA, United States, [4]Department of Neurobiology, University of Pittsburgh, Pittsburgh, PA, United States

Our objective is to longitudinally monitor the nature and timing of immune cell guided inflammatory processes following multiple blasts in an animal model, in an effort to discern potential therapeutic windows. Blast, results in a heterogeneous whole-body inflammatory response that can be observed with a perfluorocarbon contrast agent and ^{19}F MRI. A second closely timed blast increased the amount of fluorine signal in injured rats, which most likely represents increased macrophage accumulation. Despite having potent anti-inflammatory properties, we did not observe that a diet rich in omega-3 fatty acids has a significant impact on the inflammatory response to blast injuries.

3590 Computer 24

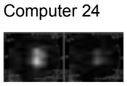

A Feedback System for Molecular Imaging of 19F FDG

Mirko Hrovat[1], James Balschi[2], Mike Dabaghyan[1], Mark Mattingly[3], and Neal Kalechofsky[2]

[1]Mirtech, Inc., Boston, MA, United States, [2]Millikelvin Technologies, LLC, Braintree, MA, United States, [3]Bruker BioSpin Corp., Billerica, MA, United States

A feedback system used in conjunction with a high concentration spin reservoir demonstrates an enhanced MRI signal from a molecular imaging target at low concentration. Enhanced images of a 10mM 19F FDG target obtained by a modified 3D Flash sequence are shown. Detectability curves reveal that for a 100ul voxel size, an imaging time of ~30 min is required to image 1mM 19F FDG with an SNR of 4.

Electronic Poster

Applications of Molecular Imaging & Hyperpolarized MRI

Exhibition Hall Monday 16:15 - 17:15

3591 Computer 25

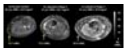

A novel application of quantitative sodium MRI for distinguishing lipedema from obesity

Rachelle Crescenzi[1], Adriana Marton[2], Paula MC Donahue[3,4], Helen B Mahany[1], Ping Wang[1], Joshua A Beckman[5], Manus J Donahue[1,6,7,8], and Jens Titze[2]

[1]Radiology and Radiological Sciences, Vanderbilt University Medical Center, Nashville, TN, United States, [2]Pharmacology and Physiology, Vanderbilt University, Nashville, TN, United States, [3]Physical Medicine and Rehabilitation, Vanderbilt University Medical Center, Nashville, TN, United States, [4]Vanderbilt Dayani Center for Health and Wellness, Nashville, TN, United States, [5]Cardiovascular Medicine, Vanderbilt University Medical Center, Nashville, TN, United States, [6]Neurology, Vanderbilt University Medical Center, Nashville, TN, United States, [7]Psychiatry, Vanderbilt University Medical Center, Nashville, TN, United States, [8]Physics and Astronomy, Vanderbilt University, Nashville, TN, United States

Sodium MRI is a molecular imaging tool that may be sensitive to the impact of lymphatic impairment on tissue homeostasis, yet has not been evaluated in a clinical population with a lymphatic disorder. Lipedema is a lymphatic fat-disorder that is under-recognized due to a need for further advanced MR imaging to diagnosis and assess treatment efficacy of the condition. Here, we apply quantitative 3T sodium imaging for the first time in a lipedema cohort to quantify tissue sodium levels and found elevated sodium concentration in the skin and muscle of patients with lipedema compared to BMI- and age-matched controls.

3592 Computer 26

The verification of the T2 distributed relaxation model (DRM) for a polydisperse nanoparticle system

Bashar Issa[1]

[1]Physics, UAE University, Al-Ain, United Arab Emirates

Theories describing *T2* enhancement due to the presence of superparamagnetic particles agree well with experimental and Monte Carlo simulation data under the condition that the particles are monodisperse both in size and magnetization. We present a *T2* distributed model that takes into account the particle size and magnetization distributions. The results shown confirm the ability of the distributed relaxation model to correctly predict *T2* values for a mixed MAR and SDR sample of MNP under a wide range of values of size, magnetization, volume fraction, etc. The new model will reduce the error in calculating *T2* values using the mean size and mean magnetization values when a distribution of MNP exists.

3593 Computer 27

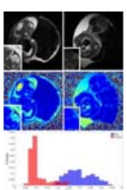

Chicken Embryo: An Excellent Platform for Monitoring Zika Virus Induced Microcephaly and Tracking Stem Cells

Qun Zhao[1], Forrest Goodfellow[2], Gregory Simchick[1], Thomas Hodge[3], Melinda Brindley[3], and Steven Stice[2]

[1]Bioimaging research Center, University of Georgia, Athens, GA, United States, [2]Regenerative Bioscience Center, University of Georgia, Athens, GA, United States, [3]Department of Infectious Diseases, University of Georgia, Athens, GA, United States

A chicken embryo is the developmental biology's oldest model organism. In ovo development of the chicken embryo closely mirrors human embryo development. The relatively large size, ease of access, and lack of maternal motion generated in pregnant mammals are distinct advantages the chicken embryo model provides. The chicken embryo provides an excellent platform for monitoring morphology and metabolism of central neural system (CNS) by using MRI or NMR spectroscopy over the course of development. In this presentation our recent work on monitoring Zika virus induced microcephaly and tracking stem cells are presented.

3594 Computer 28

Leucine deprivation causes hypothalamic neuronal inhibition accompanied by systemic metabolic changes.

Anna Ulyanova[1], Jadegoud Yaligar[1], Anantharaj Rengaraj[1], Tian Xianfeng[1], Venkatesh Gopalan[1], Sanjay K Verma[1], Christiani Jeyakumar Henry[2], and S Sendhil Velan[1]

*[1]Laboratory of Molecular Imaging, Singapore Bioimaging Consortium, A*STAR, Singapore, Singapore, [2]Clinical Nutrition Research Centre, Singapore Institute for Clinical Sciences, A*STAR, Singapore, Singapore*

The lack of dietary essential amino acid leucine influences energy metabolism via hypothalamic leptin signaling pathway. However, these neural circuits and its relationship with pathogenesis of obesity still remain unclear. In this work we investigated the hypothalamic neural pathway, abdominal fat and liver fat by multi-parametric imaging in leucine deficient diet fed mice. MEMRI results indicated that leu deficiency triggers neuronal inhibition in certain hypothalamic regions suggesting POMC neuronal pathway involvement in enhanced energy expenditure through leptin signaling pathway. Combined with systemic metabolic changes this may facilitate in understanding of amino acid sensing and metabolic regulatory network of energy homeostasis.

3595 Computer 29

Detecting neuronal activity in rat model of dementia with Lewy bodies by using MEMRI

Meng-Syuan Lin[1], Ying-Jui Ho[2], and Jun-Cheng Weng[1,3]

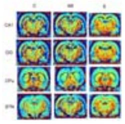

[1]Department of Medical Imaging and Radiological Sciences, Chung Shan Medical University, Taichung, Taiwan, [2]Department of Psychology, Chung Shan Medical University, Taichung, Taiwan, [3]Department of Medical Imaging, Chung Shan Medical University Hospital, Taichung, Taiwan

Dementia with Lewy bodies (DLB) is thought to be the second commonest cause of neurodegenerative dementia in older people, accounting 15 to 25% cases at autopsy. However, to date there are no reliable methods of instrumental and laboratory diagnosis of this disease while its treatment is based on reducing the symptoms. The drug X has been shown to have neuroprotective effects in neurodegenerative diseases. Therefore, we aimed to clarify the medicinal effectiveness of drug X through manganese-enhanced magnetic resonance imaging (MEMRI). Our results indicated that drug X may have clinical potential in the treatment of DLB.

3596 Computer 30

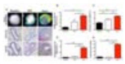

Aortic endothelial injury modifies plaque composition at a distally located site through increased monocyte extravasation

Begona Lavin Plaza[1], Alkystis Phinikaridou[1], Marcelo Andia Kohnenkampf[2], and Rene Botnar[1]

[1]Imaging Sciences and Biomedical Engineering, King's College London, London, United Kingdom, [2]Radiology Department, Universidad Catolica de Chile, Santiago de Chile, Chile

The deleterious impact of atherosclerosis on other cardiovascular diseases has recently been shown, but the effect of vascular alterations on plaque formation at a distal site, including the underlying mechanisms of this systemic response, has not been elucidated. In this study, we used an albumin-binding contrast agent to assess whether (1) endothelial injury in the abdominal aorta accelerates plaque progression in the brachiocephalic artery located distally to the site of injury and (2) whether monocytes can be the link between acute and systemic response.

3597 Computer 31

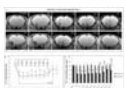

Precise longitudinal MRI tracking of systemically infused dual labelled mesenchymal stem cells and their regenerative potential in traumatic brain injury mice

Sushanta Kumar Mishra[1,2], Subash Khushu[1], and Gurudutta Gangenahalli[2]

[1]NMR Research Centre, Institute of Nuclear Medicine and Allied Sciences, Delhi, India, Delhi, India, [2]Division of Stem Cell and Gene Therapy Research, Institute of Nuclear Medicine and Allied Sciences, Delhi, India

Stem cells transplantation has emerged as a promising alternative therapeutic due to its potency at injury site. Thus, tracking of stem cells is very essential. Here, we have described a serial in vivo tracking of implanted stem cells through 7T MRI and its differentiation potential into neuronal precursors. T2*-weighted images and relaxation study demonstrated a significant signal loss and effective decrease in T2* relaxation time on day-3 at injury site. Expression of neuronal markers like GFAP, MAP2 and NeuN were observed in transplanted MSCs. The proposed procedure could be extrapolated for stem cell tracking and therapies in various neurodegenerative diseases.

3598 Computer 32

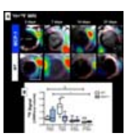

Molecular Imaging of the effects of monocyte chemoattractant protein-1 (MCP-1) on extracellular matrix remodeling following myocardial infarction

Isabel Teixeira Ramos[1,2], Markus Henningsson[1], Maryam Nezafat[1], Begoña Lavin[1], Silvia Lorrio[1], Alkystis Phinikaridou[1,2], Ulrich Flögel[3], Ajay Shah[2,4], and René Botnar[1,2]

[1]Division of Imaging Sciences and Biomedical Engineering, King's College London, London, United Kingdom, [2]Cardiovascular Division, The British Heart Foundation Centre of Excellence, King's College London, London, United Kingdom, [3]Heinrich Heine University Düsseldorf, Düsseldorf, Germany, [4]Cardiovascular Division, James Black Centre, King's College London, London, United Kingdom

After a myocardial infarction (MI) the degree of inflammation and its timely resolution, together with the degradation and deposition of extracellular matrix proteins are key processes in post-MI healing. Monocyte chemoattractant protein-1 (MCP1) plays an important role in the recruitment of monocytes/macrophages and its absence has revealed a significant reduction of inflammatory cell recruitment and subsequent ECM protein production in the infarcted area. Here, we explored the merits of multinuclear ^{1}H/^{19}F MRI for the simultaneous assessment of myocardial inflammation and remodelling in a murine model of MI. ^{19}F containing nanoparticle that is avidly taken up by macrophages was used to investigate inflammatory cell recruitment into injured myocardium[2], and a small molecular weight gadolinium-based elastin-specific MR contrast agent was used to evaluate changes of elastin content post-MI[3].

3599 Computer 33

19F-based MRI cell tracking shows that the density of tumour associated macrophages in breast tumours corresponds to tumour aggressiveness and metastatic potential

Ashley V Makela[1,2], Jeffrey M Gaudet[1,2], and Paula J Foster[1,2]

[1]Medical Biophysics, Western University, London, ON, Canada, [2]Robarts Research Institute, London, ON, Canada

Tumour associated macrophages (TAMs) have been associated with tumour aggressiveness, including tumour growth and metastatic potential. ^{19}F-based MRI is used in this study to track these cells *in vivo*, revealing the ability to differentiate TAM content between 3 murine models of breast cancer. Highly aggressive tumours had significantly higher ^{19}F signal when compared to the low and non aggressive variants. This information may be of use as a biomarker, to differentiate between tumours with high infiltration of TAMs, which have the propensity to metastasize and progress quicker, versus tumours with less TAMs, which may not advance as quickly.

3600 Computer 34

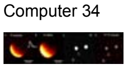

Post-mortem Cardiac and Skeletal Muscle 19F MRI of PFCE-labeled and FuGENE-transfected Cardiac Progenitor Stem Cells in the C57BL/6 Mouse

Christakis Constantinides[1], Ricardo Carnicer[1], Ayman Al Haj Zen[1], Mahon Maguire[1], Eileen McNeil[1], Edyta Swider[2], Mangala Srinivas[2], Carolyn A Carr[3], and Jurgen E Schneider[1]

[1]Cardiovascular Medicine, University of Oxford, Oxford, United Kingdom, [2]Department of Tumor Immunology, Radboud University, Nijmegen, Netherlands, [3]Physiology, Anatomy and Genetics, University of Oxford, Oxford, United Kingdom

Stem cell (SC) technologies constitute a potential new therapeutic approach aiming to achieve tissue regeneration. Despite advances in the visualization of pre-labeled SCs with SPIOs (^{1}H MRI), and of nanoparticles (NPs) containing perfluoro-crown-ethers (PFCE) [2-4] in ^{19}F MRI, there have been no prior reports on cardiac ^{19}F imaging with direct SC injections. We report herein the implementation of a fast acquisition protocol for cardiac and skeletal muscle ^{19}F imaging of the C57BL/6 mouse post-mortem, and identify the minimum cellular load for PFCE labels to achieve visualization following direct SC cell injections.

3601 Computer 35

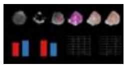

Characterizing the Tumor Microenvironment

Samata Kakkad[1], Balaji Krishnamachary[1], Marie-France Penet[1,2], Yelena Mironchik[1], Flonne Wildes[1], and Zaver M Bhujwalla[1,2]

[1]JHU ICMIC Program, Division of Cancer Imaging Research, The Russell H. Morgan Department of Radiology and Radiological Science, Johns Hopkins University School of Medicine, Baltimore, MD, United States, [2]Sidney Kimmel Comprehensive Cancer Center, Johns Hopkins University School of Medicine, MD, United States

Total choline in tumors is associated with increased aggressiveness. Since the distribution of total choline in tumors is usually heterogenous, here we have examined the relationship between high and low total choline, obtained with 1H MRSI, with hypoxia and necrosis in a human breast cancer xenograft model engineered to express red fluorescence protein under hypoxic conditions. We found that the highest total choline regions were associated with hypoxia. We also observed that overall total choline in tumors inversely correlated with the necrotic fraction, suggesting that reduced total choline may reflect increased cell death in tumors.

3602 Computer 36

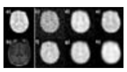

3D $CMRO_2$ Mapping in Human Brain with Direct ^{17}O-MRI: Comparison of Methods for Image Reconstruction and Partial Volume Correction

Dmitry Kurzhunov[1], Robert Borowiak[1,2,3], Marco Reisert[1], Axel Joachim Krafft[1], Ali Caglar Özen[1], and Michael Bock[1]

[1]Dept. of Radiology, Medical Physics, Medical Center – University of Freiburg, Freiburg, Germany, [2]German Cancer Consortium (DKTK), Heidelberg, Germany, [3]German Cancer Research Center (DKFZ), Heidelberg, Germany

This study presents a comparative analysis of different reconstruction techniques for quantification of 3D maps of the cerebral metabolic rate of oxygen consumption ($CMRO_2$) in human brain. $CMRO_2$ maps were calculated from a direct ^{17}O-MRI experiment at 3T in which ^{17}O gas was inhaled. Conventional Kaiser-Bessel reconstruction of ^{17}O MR images was compared to two iterative reconstruction methods using total variation (TV) and anisotropic diffusion (AD) of coregistered proton data as constraints. AD-constraint reconstruction, which acts as a non−homogeneous edge−preserving smoothing filter, enabled $CMRO_2$ mapping at clinical field strengths by increasing the SNR, and reducing partial volume effects.

3603 Computer 37

Multiparametric tumor characterization using simultaneous 1H-MRI, [18F]FDG PET and hyperpolarized [1-13C]pyruvate MRSI

Christian Hundshammer[1,2], Miriam Braeuer[1], Müller Christoph[3,4], Adam Espe Hansen[5], Jorge Cabello[1], Mathias Schillmaier[6], Benedikt Feuerecker[1], Stephan Duewel[1,2,7], Schachoff Sylvia[1], Birgit Blechert[1], Michael Michalik[1], Jan-Bernd Hövener[3,4], Steffen J. Glaser[2], Axel Haase[7], Franz Schilling[1], Andreas Kjaer[5], Stephan Nekolla[1], and Schwaiger Markus[1]

[1]Department of Nuclear Medicine, Klinkum rechts der Isar, Munich, Germany, [2]Department of Chemistry, Technical University Munich, Munich, Germany, [3]Department of Radiology, Medical Physics, Medical Center - University of Freiburg, Faculty of Medicine, University of Freiburg, Freiburg, Germany, [4]German Consortium for Translational Cancer Research (DKTK), Partnersite Freiburg, German Center for Cancer Research (DKFZ), Heidelberg, Germany, [5]Department of Clinical Physiology, Nuclear Medicine & PET, Rigshospitalet, Copenhagen, Denmark, [6]Department of Radiology, Klinikum rechts der Isar, Munich, Germany, [7]Deparment of Medical Engineering, Technical University Munich, Munich, Germany

In order to understand complex mechanisms of the tumor biology, multimodal imaging approaches are useful. Here we present a workflow to characterize subcutaneous MAT-B-III tumors in rats on a clinical 3T PET/MR. Proton imaging was used for tumor localization and to characterize tumor cellularity by diffusion-weighted imaging. Glucose uptake and downstream glucose metabolism of pyruvate by lactate dehydrogenase (LDH) was addressed by [^{18}F]FDG-PET and hyperpolarized [^{13}C]pyruvate metabolic imaging. The [^{18}F]FDG standard uptake values and the LDH activity were consistently and reproducibly higher compared to normal tissue.

3604 Computer 38

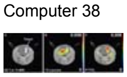

Imaging branched-chain amino acid metabolism in glioma using hyperpolarized [1-13C] alpha-ketoisocaproate

Eul Hyun Suh[1], Weijun Ou[1,2], Ian Corbin[1], Dean Sherry[1,3], and Jae Mo Park[1]

[1]Advanced Imaging Research Center, University of Texas Southwestern Medical Center, Dallas, TX, United States, [2]Organ Transplantation Center, Sun Yat-sen University, Guangzhou, People's Republic of China, [3]Chemistry, University of Texas Dallas, Richardson, TX, United States

Upregulated branched-chain amino transaminase 1 (BCAT1) expression is a common metabolic feature of most primary cancers with wild-type isocitrate dehydrogenase (IDH), including glioblastoma. In this study, ^{13}C-labeled a-ketoisocaproate (KIC) metabolism was investigated in a brain tumor-bearing rat to assess BCAT1 and branched-chain α-ketoacid dehydrogenase (BCKDH) activities in the tumor. Following an intravenous bolus injection of hyperpolarized [1-^{13}C]KIC, both [1-^{13}C]leucine and ^{13}C-bicarbonate were observed in the brain. We observed less [1-^{13}C]leucine but greater bicarbonate production in the tumor compared to normal, healthy brain tissue, suggesting downregulated chemical exchange of [1-^{13}C]KIC with leucine catalyzed by BCAT1 and upregulated BCKDH activity, respectively.

3605 Computer 39

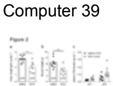

Metabolic changes in the heart precede functional changes in a rat model of doxorubicin-induced cardiotoxicity

Kerstin N Timm[1], Jack J Miller[1], Dragana Savic[1], Vicky Ball[1], Lucia Giles[1], Cher-Rin Chong[1], Michael S Dodd[1], and Damian J Tyler[1]

[1]Physiology Anatomy and Genetics, University of Oxford, Oxford, United Kingdom

Chemotherapeutic agents such as doxorubicin can cause serious adverse effects on the heart, leading to decreased left ventricular function and heart failure. The biochemical mechanisms for this are not fully understood, however, increased oxidative stress in cardiomyocytes as well as bioenergetic changes to the heart have been suggested as primary triggers for the functional decline. Here we show that hyperpolarized ^{13}C magnetic resonance spectroscopy and CINE magnetic resonance imaging of the heart can detect metabolic as well as functional changes in a clinically relevant rat model of doxorubicin-induced cardiotoxicity, and that metabolic changes may precede functional abnormalities.

3606 Computer 40

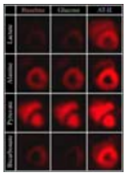

Acute afterload-imposed change in porcine cardiac metabolism imaged by hyperpolarized [1-13C]Pyruvate

Rasmus Stilling Tougaard[1,2], Esben Søvsø Szocska Hansen[2], Christoffer Laustsen[2], Jakob Lindhardt[2], Marie Schroeder[2], Hans Erik Bøtker[1], Won Yong Kim[1,2], Henrik Wiggers[1], and Hans Stødkilde-Jørgensen[2]

[1]Department of Cardiology - Research, Aarhus University Hospital, Aarhus N, Denmark, [2]MR Research Centre, Aarhus University, Aarhus N, Denmark

Deranged metabolism is now considered a key causal factor in heart failure and has therefore gained considerable scientific interest. The novel technique hyperpolarized MR has emerged as a leading methodological candidate to study these derangements. We employed a clinically relevant, large animal model of angiotensin-II-mediated acute hypertension to study cardiac metabolism in the setting of elevated afterload using hyperpolarized [1-^{13}C]Pyruvate MR. The method was able to detect acute increases in both anaerobic and aerobic cardiac metabolism, which, in the future could mean a useful way of monitoring a possible treatment response to afterload reduction by using hyperpolarized MR.

3607 Computer 41

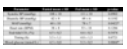

Hyperpolarized [1-13C]Pyruvate MRI identifies metabolic differences pertaining to the fasted and fed state in porcine cardiac metabolism

Rasmus Stilling Tougaard[1,2], Esben Søvsø Szocska Hansen[2], Christoffer Laustsen[2], Thomas Stokholm Nørlinger[2], Emmeli Mikkelsen[2], Jakob Lindhardt[2], Marie Schroeder[2], Per Mose Nielsen[2], Lotte Bonde Bertelsen[2], Hans Erik Bøtker[1], Won Yong Kim[1,2], Henrik Wiggers[1], and Hans Stødkilde-Jørgensen[2]

[1]Department of Cardiology - Research, Aarhus University Hospital, Aarhus N, Denmark, [2]MR Research Centre, Aarhus University, Aarhus N, Denmark

Standardized large animal models for cardiac hyperpolarized MR metabolic studies are becoming increasingly important as translation into human trials progresses. We employed a porcine (n=17) model of fasting/feeding to study these two states and to examine normal feeding as a standardized model for increasing hyperpolarized [1-^{13}C]Pyruvate signal in the heart. All metabolic ratios were higher in fed animals with no additional variance. This indicates the role of pyruvate uptake to be more important in pigs than in rodents, underlining the need for large animals in metabolic research, and also suggests feeding to be a feasible, standardized model for increasing signal.

3608 Computer 42

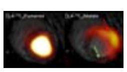

Fumarate to Malate Conversion in Infarcted Porcine Heart – a Pilot Study

Esben Søvsø Szocska Hansen[1,2], Rasmus Stilling Tougaard[1,3], Per Mose Nielsen[1], Jakob Lindhardt[1], Hans Stødkilde Jørgensen[1], and Christoffer Laustsen[1]

[1]The MR Research Centre, Aarhus University, 8200, Denmark, [2]Danish Diabetes Academy, Odense, Denmark, [3]Department of Cardiology, Aarhus University Hospital, 8200, Denmark

Hyperpolarized MR may be a key tool for investigation cardiac metabolism and cardiac treatment response. [1,4-$^{13}C_2$]Fumarate is an emerging and interesting candidate for measuring and visualizing cardiac injury after ischemia. In this study we showed an initial step for imaging cardiac cell death in a large animal model with [1,4-$^{13}C_2$]malate. The [1,4-$^{13}C_2$]malate signal correlated well with increased ^{13}C-lactate signal and ^{13}C-alanine absence. Overall, this shows increased metabolism in the infarcted area and ongoing necrosis.

3609 Computer 43

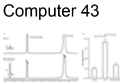

Molecular Detection of Inflammation in a Macrophage Cell Model Using Hyperpolarized 13C-Pyruvate

Renuka Sriram[1], Justin DeLos Santos[1], Julia Nguyen[1], Mark Van Criekinge[1], Seth Vigneron[2], John Kurhanewicz[1], and John MacKenzie[1]

[1]Radiology and Biomedical Imaging, University of California San Francisco, San Francisco, CA, United States, [2]University of California San Diego

Carbon-13 magnetic resonance with dynamic nuclear polarization is a potential molecular imaging strategy to detect and monitor inflammation. In this study we investigated hyperpolarized 13C-pyruvate and alterations in its conversion to 13C-lactate as an imaging biomarker for disease severity and monitoring treatment response in inflammatory disorders.

3610 Computer 44

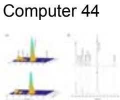

Metabolism of Hyperpolarized Pyruvate detects Knockout of Pyruvate Dehydrogenase Kinase

Gaurav Sharma[1], Cheng Yang Wu[2], R. Max Wynn[2,3], David T. Chuang[2,3], Craig R. Malloy[1,3], Chalermchai Khemtong[1], and A. Dean Sherry[1,4]

[1]Advanced Imaging Research Center, University of Texas Southwestern Medical Center, Dallas, TX, United States, [2]Biochemistry, University of Texas Southwestern Medical Center, Dallas, TX, United States, [3]Internal Medicine, University of Texas Southwestern Medical Center, Dallas, TX, United States, [4]Chemistry, University of Texas at Dallas, Dallas, TX, United States

The Pyruvate Dehydrogenase Complex (PDC) plays a critical role in the regulation of carbohydrate metabolism. Pyruvate Dehydrogenase Kinase (PDK) inhibits PDC via phosphorylation making it a novel therapeutic target for metabolic diseases. The present study aimed to evaluate whether the metabolism of HP-13C pyruvate is sensitive to PDK inhibition. Our results showed that higher production of HP-bicarbonate via PDC in PDK deficient livers. ^{13}C NMR isotopomer analysis of tissue extracts confirms higher 13C-enrichment of AcCo-A in the DKO livers than the control group. The result suggested that the appearance of HP-bicarbonate is a sensitive biomarker for monitoring the consequences of PDK inhibition.

3611 Computer 45

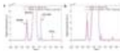

Optimization of redox-state assessment in rat liver using hyperpolarized [1-13C]alanine

Jae Mo Park[1,2], Ralph E Hurd[3], and Daniel M Spielman[2]

[1]Advanced Imaging Research Center, University of Texas Southwestern Medical Center, Dallas, TX, United States, [2]Radiology, Stanford University, Stanford, CA, United States, [3]Applied Science Laboratory, GE Healthcare, Menlo Park, CA, United States

In this study, we demonstrated the strategies of increasing signal sensitivities of ^{13}C-pyruvate and ^{13}C-lactate generated from an injection of hyperpolarized ^{13}C-alanine by (1) adjusting the alanine dose and (2) co-injecting unlabeled pyruvate. 120-mM alanine produced larger amount of labeled pyruvate and lactate as compared to when 80-mM or 40-mM alanine was injected. The co-injection of 7-mM unlabeled pyruvate showed up to 49% SNR increase in pyruvate and lactate peaks.

3612 Computer 46

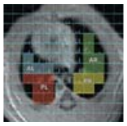

A Multi-Variate Regional Study of Acute Lung Injury Using Hyperpolarized [1-13C] Pyruvate

Hooman Hamedani[1], Mehrdad Pourfathi[1], Yi Xin[1], Stephen Kadlecek[1], Maurizio Cereda[2], Harrilla Profka[1], Ian Duncan[1], Sarmad Siddiqui[1], Nicholas Drachman[1], Kai Ruppert[1], and Rahim Rizi[1]

[1]Radiology, University of Pennsylvania, Philadelphia, PA, United States, [2]Anesthesiology and Critical Care, University of Pennsylvania, Philadelphia, PA, United States

In this study we seek to investigate the dependency of the changes of lactate-to-pyruvate ratio on various covariates in the settings of experimental acute lung injury using a random-effect model.

3613 Computer 47

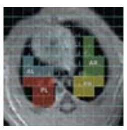

Regional Analysis of Hyperpolarized Lactate-to-Pyruvate Ratio Can Improve Sensitivity to Monitor Progression of Acute Pulmonary inflammation

Mehrdad Pourfathi[1], Hooman Hamedani[1], Yi Xin[1], Stephen Kadlecek[1], Maurizio Cereda[2], Harrilla Profka[1], Ian Duncan[1], Nicholas Drachman[1], Sarmad Siddiqui[1], Kai Ruppert[1], Joe Naji[1], and Rahim Rizi[1]

[1]Radiology, University of Pennsylvania, Philadelphia, PA, United States, [2]Anesthesiology and Critical Care, University of Pennsylvania, Philadelphia, PA, United States

In this hyperpolarized pyruvate imaging study of acute lung injury, we assessed alterations of regional lactate-to-pyruvate ratio during the progression of lung inflammation caused by acid aspiration. The study shows that posterior lactate-to-pyruvate ratio changes more significantly after injury compared to the anterior ratio. This is consistent with the pattern observed with proton MRI. We report good correlation between increased lactate-to-pyruvate ratio due to inflammation and increased proton image intensity as a result of formation of edema, especially in the posterior regions.

3614 Computer 48

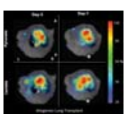

Metabolic characterization of rat lung transplantation using HP [1-13C]-pyruvate MRI

Sarmad Siddiqui[1], Mehrdad Pourfathi[1], Andreas Habertheuer[2], Yi Xin[1], Harrilla Profka[1], Hooman Hamedani[1], Stephen Kadlecek[1], Ali Naji[2], Prashanth Vallabhajosyula[2], and Rahim Rizi[1]

[1]Radiology, University of Pennsylvania, Philadelphia, PA, United States, [2]Surgery, University of Pennsylvania, Philadelphia, PA, United States

Orthotopic rat lung transplantation is a well-established animal model used for elucidating the mechanics of lung transplant surgery. However, most lung function assessment is conducted via invasive techniques. In this study, we demonstrated that hyperpolarized pyruvate MRI can be used to generate metabolic biomarkers that can be used for non-invasive lung function assessment after transplantation. In successful syngeneic lung transplants, the lactate-to-pyruvate ratio remains low in both lungs after transplant. However, in allogeneic or failed syngeneic lung transplantation, the native lung returns to baseline one week after surgery, whereas the transplanted lung shows a significant(~3-fold) increase in the lactate-to-pyruvate ratio.

Electronic Poster

Arterial Spin Labeling: Methodology

Exhibition Hall Monday 16:15 - 17:15

3615 Computer 49

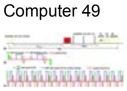

3D Whole-Brain Mapping of Cerebral Blood Flow using Velocity-Selective Pulse Trains: Evaluating Various Strategies for Background Suppression

Qin Qin[1,2]

[1]Johns Hopkins University, Baltimore, MD, United States, [2]Kennedy Krieger Institute, Baltimore, MD, United States

Velocity-selective arterial spin labeling (VSASL) has only been realized with 2D multi-slice acquisition. ASL with 3D readout is preferred for clinical applications and background suppression technique is essential for successful implementation of segmented 3D ASL. In this study, various strategies for background suppression are evaluated for 3D VSASL which are labeled with conventional T2prep VS pulse train, and new Fourier transform based velocity-selective saturation and inversion pulse trains, respectively. The optimal 3D whole-brain VSASL protocol is compared with PCASL for mapping cerebral blood flow on normal volunteers at 3T.

3616 Computer 50

Solving the dark-sides of multiband-ASL: A framework to correct for increased motion artefacts in MB-ASL due to sharp transitions in the level of background suppression

Yuriko Suzuki[1], Thomas W Okell[2], Wouter M Teeuwisse[1], Sophie Schmid[1], Merlijn van der Plas[1], Michael A Chappell[2,3], and Matthias JP van Osch[1]

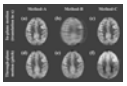

[1]C.J.Gorter Center for High Field MRI, Department of Radiology, Leiden University Medical Center, Leiden, Netherlands, [2]FMRIB Centre, Nuffield Department of Clinical Neurosciences, University of Oxford, Oxford, United Kingdom, [3]Institute of Biomedical Engineering, University of Oxford, Oxford, United Kingdom

Recently, incorporation of multi-band (MB-) EPI into ASL has been reported, enabling increased spatial coverage without compromising SNR of distal slices due to longer post-labeling delay time. However, the combination of MB-EPI and ASL with the background suppression (BGS) could potentially induce problems when motion correction (MoCo) is required. In this study, we demonstrate that subtraction artefacts can be introduced when performing MoCo of MB-BGS-pCASL and that these artefacts can degrade image quality considerably. We propose a new framework that corrects for image degradation caused by MoCo of MB-BGS-pCASL data, thereby greatly improving robustness and thus usefulness of MB-BGS-pCASL.

3617 Computer 51

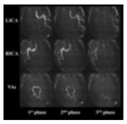

Improved spatial encoding for vessel-selective pCASL: improving efficiency, minimising mis-labeling, and shortening scan-time for artery specific MRA

Yuriko Suzuki[1], Matthias JP van Osch[1], and Thomas W Okell[2]

[1]C.J.Gorter Center for High Field MRI, Department of Radiology, Leiden University Medical Center, Leiden, Netherlands, [2]FMRIB Centre, Nuffield Department of Clinical Neurosciences, University of Oxford, Oxford, United Kingdom

Hadamard-encoded vessel-encoded pCASL is a vessel-selective ASL technique that enables SNR-efficient vascular territory mapping for perfusion MRI. For vessel-selective ASL-MRA, however, minimising the number of encodings is necessary to achieve clinically feasible scan times. The spatial modulation of inversion in ve-pCASL is gradual, which could potentially reduce SNR-efficiency and cause mislabeling of arteries when reducing the number of encodings. In this study, the modulation of ve-pCASL was optimized to achieve sharper inversion to avoid signal contamination of non-targeted arteries and achieve 4D-MRA with a minimal number of Hadamard-encodings.

3618 Computer 52

In-vivo evaluation of pCASL labeling scheme and position

Marta Vidorreta[1,2], Li Zhao[3], Sheila Shankar[4], Daniel H Wolf[4], David C Alsop[3], and John A Detre[1,2]

[1]Neurology, University of Pennsylvania, Philadelphia, PA, United States, [2]Radiology, University of Pennsylvania, Philadelphia, PA, United States, [3]Radiology, Beth Israel Deaconess Medical Center and Harvard Medical School, MA, United States, [4]Psychiatry, University of Pennsylvania, PA, United States

Despite recent consensus in the ASL community on pseudo-continuous ASL as preferred labeling method, several challenges still exist towards optimizing pCASL labeling efficiency in-vivo, including its sensitivity to vessel tortuosity and off-resonance effects. In this work, we assess the impact of labeling plane location and labeling scheme on the ASL perfusion signal.

3619 Computer 53

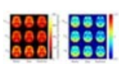

Bayesian model selection of Time Encoded Arterial Spin Labelling: effect of T1 and dispersion

Marco Castellaro[1], Erica Silvestri[1], Ilaria Boscolo Galazzo[2], Matteo Tonietto[1], Alessandro Palombit[1], Francesca Benedetta Pizzini[2], Stefania Montemezzi[2], Enrico Grisan[1], Matthias J.P. Van Osch[3], and Alessandra Bertoldo[1]

[1]Department of Information Engineering, University of Padova, Padova, Italy, [2]University of Verona, Verona, Italy, [3]Radiology, LUMC, Gorter Center for high field MRI, Leiden, Netherlands

Time-Encoded Arterial Spin Labelling (TE-ASL) has been proposed as a tool to efficiently sample the kinetics of the ASL signal. We propose a model comparison based on Bayesian Model Selection (BMS), to provide insights on which is the optimal model for the quantification of TE-ASL. Our results show how important it is to consider both T_1 decay and dispersion in the quantification process. When mainly interested in GM, it is advisable to incorporate the dispersion of the bolus in the model with a Gamma kernel dispersion model and to use a single T_1 value of 1.3s.

3620 Computer 54

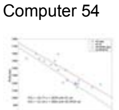

Defining the optimal post-labeling delay for pCASL using patient specific estimates of blood velocity in the carotid artery

Neville D Gai[1] and John A Butman[1]

[1]Radiology & Imaging Sciences, NIH Clinical Center, Bethesda, MD, United States

Pseudo-continuous arterial spin labeling (pCASL) with 3D non-segmented acquisition scheme allows assessment of full brain CBF with sufficiently high SNR and resolution in an efficient manner. Post-labeling delay is a critical parameter which needs to be determined preferably on a per subject basis since PLD can change based on the physiological condition of a subject. Multiple post-labeling delay (PLD) pCASL could address this issue. However, multiple PLD pCASL is not feasible for the 3D non-segmented acquisition scheme. In this work, we related the velocity in carotid artery (CA) measured using two schemes to PLD in ten volunteers. A relationship between the CA velocity and optimal PLD was derived which allows for optimal PLD to be determined on the fly for each subject.

3621 Computer 55

The reproducibility of absolute ASL-CBF: assessing the stability of absolute CBF, M0 and calibration images

Mareike Alicja Buck[1,2], Matthias Günther[1,2], and Federico Camilo von Samson-Himmelstjerna[1,2]

[1]Fraunhofer MEVIS, Bremen, Germany, [2]Universitaet Bremen, Bremen, Germany

In this abstract the reproducibility of absolute CBF as well as the M0- and an optional calibration-image is assessed during individual scanning-sessions and also over the entire day. Comparably high reproducibility was found for all three types of images, which agrees with similar earlier findings. However, also the uncertainty of the corresponding fits was found to be high.

3622 Computer 56

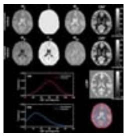

Improved Calculation of Arterial Blood Equilibrium Magnetization in Arterial Spin Labeling

André Ahlgren[1], Ronnie Wirestam[1], Freddy Ståhlberg[1,2,3], Linda Knutsson[1,4], and Esben Thade Petersen[5]

[1]Department of Medical Radiation Physics, Lund University, Lund, Sweden, [2]Diagnostic Radiology, Lund University, Lund, Sweden, [3]Lund University Bioimaging Center, Lund University, Lund, Sweden, [4]Department of Radiology (Adjunct), Johns Hopkins School of Medicine, Baltimore, United States, [5]Danish Research Centre for Magnetic Resonance, Copenhagen University Hospital Hvidovre, Copenhagen, Denmark

The calibration factor (equilibrium magnetization of arterial blood) in arterial spin labeling is usually calculated by dividing a PD image with a constant brain-blood partition coefficient, $$$\lambda$$$. A more accurate approach would be to divide a map corresponding to the PD of the perfused parenchymal tissue with a $$$\lambda$$$ map (i.e, taking into account different values of $$$\lambda$$$ in different tissue types). In this work, we demonstrate how this can be achieved using partial volume (PV) estimates. In vivo results are demonstrated and compared with the conventional method.

3623 Computer 57

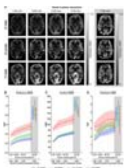

The influence of acquisition parameters on CBF and BOLD sensitivity in 3 and 7 Tesla ASL fMRI

Anna Gardumi[1], Dimo Ivanov[1], Roy Haast[1], Josef Pfeuffer[2], Benedikt A Poser[1], and Kamil Uludag[1]

[1]Maastricht University, Maastricht, Netherlands, [2]Application Development, Siemens, Erlangen, Germany

Arterial spin labeling (ASL) measures cerebral blood flow (CBF) non-invasively. Compared to the BOLD signal, CBF is quantitative and more directly linked to neural activation, albeit with lower SNR. Due to increased SNR and T1 relaxation time, ultra-high field MRI promises benefits for ASL. However, technical challenges remain to exploit its full potential. Here, we compared 3T and 7T ASL implementations and studied the influence of labeling schemes, resolution, parallel imaging, and field strength on the CBF and BOLD functional contrast. We found 3T pCASL being advantageous for low-resolution and 7T FAIR for high-resolution and acquisitions utilizing parallel imaging.

3624 Computer 58

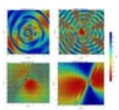

Improved labeling efficiency in Super-Selective Pseudo-Continuous Arterial Spin Labeling

Jonas Schollenberger[1], C. Alberto Figueroa[1,2], and Luis Hernandez-Garcia[1,3]

[1]Biomedical Engineering, University of Michigan, Ann Arbor, MI, United States, [2]Department of Surgery, University of Michigan, Ann Arbor, MI, United States, [3]Functional MRI Laboratory, University of Michigan, Ann Arbor, MI, United States

We investigate how to improve the SNR of vessel-selective ASL images by off-resonance compensation and label rotation scheme optimization.

3625 Computer 59

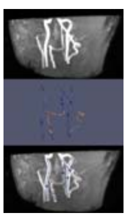

Automatic Planning for fast and robust Flow Territory Mapping

Michael Helle[1], Kim van de Ven[2], and Fabian Wenzel[1]

[1]Philips Research, Hamburg, Germany, [2]Philips Healthcare, Best, Netherlands

Super-Selective Pseudo-continuous Arterial Spin Labeling (pCASL) requires the labeling focus to be optimized to each artery of interest individually. This might be time-consuming especially for inexperienced users, and suboptimal results are possible as the labeling efficiency depends on the location of the labeling spot, as well as its angulation, which should be perpendicular to the artery. This study demonstrates an automatic planning approach for Super-Selective pCASL measurements in the major brain feeding vessels and subsequently compares the results to images acquired using a manual positioning of the labeling spot.

3626 Computer 60

A multi-compartment cerebral perfusion phantom to test territory selection using vessel encoded arterial spin labelling

Michael A Chappell[1], Bridget Fryer[1], Anton Firth[1], Robert Wight[1], Thomas Kirk[1], and Thomas W Okell[2]

[1]Institute of Biomedical Engineering, University of Oxford, Oxford, United Kingdom, [2]Oxford Centre for Functional MRI of the Brain, Nuffield Department of Clinical Neurosciences, University of Oxford, Oxford, United Kingdom

Vessel encoded arterial spin labelling allows the visualisation of perfusion territories in the brain. However, the accuracy of perfusion measurements from VE-ASL and the associated analysis methods is difficult to establish without ground truth. Perfusion phantom devices have been prosed for conventional ASL, but don't currently attempt to model the full cerebral vasculature anatomy of the brain, limiting their value in evaluation of VE-ASL methods. Thus in this work we set out to create a multi-compartment, multi 'artery' perfusion phantom based on normal vascular anatomy.

3627 Computer 61

Evaluation of 3D GRASE and 2D MB-EPI for Multi-Delay PCASL Imaging

Xiufeng Li[1], Xingfeng Shao[2], Dingxin Wang[1,3], Sudhir Ramanna[1], Steen Moeller[1], Kamil Ugurbil[1], Essa Yacoub[1], and Danny J.J. Wang[2]

[1]Radiology-CMRR, University of Minnesota, Minneapolis, MN, United States, [2]Laboratory of FMRI Technology, Stevens Neuroimaging and Informatics Institute, University of Southern California, CA, United States, [3]Siemens Medical Solutions USA Inc., MN, United States

Recently 2D multi-band (MB) imaging has emerged as a promising alternative to 3D acquisitions for arterial spin labeling imaging. As part of the Human Connectome Project, we evaluated a segmented 3D GRASE and 2D MB-EPI for multi-delay PCASL imaging in terms of test-retest repeatability and CBF/ATT quantification. The results indicated that compared to 3D GRASE, 2D MB-EPI is less sensitive to subject motion, provided comparable but more reproducible ATT and CBF estimates, and suffered less from data loss. 2D MB-EPI appears promising for multi-delay PCASL imaging, especially with limited imaging time and where higher spatial resolution is of interest.

3628 Computer 62

Robust 3D pCASL perfusion imaging using a Cartesian Acquisition with Spiral Reordering (CASPR)

Joshua S. Greer[1,2], Xinzeng Wang[2], Marco C. Pinho[2,3], Ivan Pedrosa[2,3], and Ananth J. Madhuranthakam[2,3]

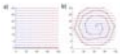

[1]*Bioengineering, UT Dallas, Richardson, TX, United States,* [2]*Radiology, UT Southwestern Medical Center, Dallas, TX, United States,* [3]*Advanced Imaging Research Center, UT Southwestern Medical Center, Dallas, TX, United States*

Arterial spin labeling can non-invasively measure perfusion, but offers low SNR compared to contrast-enhanced perfusion techniques. A novel 3D TSE with a Cartesian Acquisition with SPiral Reordering (CASPR) was implemented and combined with pCASL in the brain and kidneys. This sampling technique samples the center of k-space early in each echo train, and was shown to provide significantly improved 3D perfusion images compared to 3D linear acquisitions, and more extensive coverage than 2D acquisitions in a similar scan time.

3629 Computer 63

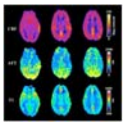

Single shot high resolution 3D arterial spin labeling using 2D CAIPI and ESPIRiT reconstruction

Xingfeng Shao[1] and Danny JJ Wang[1]

[1]*Laboratory of FMRI Technology (LOFT), Mark & Mary Stevens Neuroimaging and Informatics Institute, Keck School of Medicine, University of Southern California, Los Angeles, CA, United States*

We present a single-shot 3D GRASE pCASL technique, which reduces the data loss due to motion, using 2D CAIPI sampling strategy, and reconstruct the under-sampled data using ESPIRiT. Proposed sequence employs 4-fold acceleration and achieves whole brain volume with isotropic 3×3×3 mm^3 resolution. This technique was successfully applied for high resolution multi-delay ASL imaging, and CBF, ATT and T1 map could be simultaneously calculated in 4 min 14 sec.

3630 Computer 64

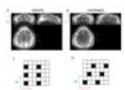

2D CAIPIRINHA improves accelerated 3D GRASE ASL

Dimo Ivanov[1], Josef Pfeuffer[2], Anna Gardumi[1], Kâmil Uludağ[1], and Benedikt A Poser[1]

[1]*Department of Cognitive Neuroscience, Maastricht University, Maastricht, Netherlands,* [2]*MR Application Development, Siemens Healthcare, Erlangen, Germany*

Arterial spin labelling (ASL) is the primary non-invasive MRI approach to measure cerebral blood flow in healthy subjects and patients. Recently, a consensus paper has recommended segmented versions of 3D spin-echo readouts like GRASE, but these are susceptible to motion and have poor temporal resolution. To alleviate these drawbacks, we propose to accelerate the 3D GRASE readout and utilize 2D CAIPIRINHA for the reconstruction. We demonstrate that our approach is superior or at least equivalent to the 2D GRAPPA technique, depending on the acceleration factor used. The proposed approach will particularly benefit functional and clinical ASL applications.

3631 Computer 65

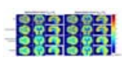

A Deconvolution Method for Improved CBF Quantification in 3D-GRASE ASL

Kenneth Wengler[1,2] and Xiang He[2]

[1]*Biomedical Engineering, Stony Brook University, Stony Brook, NY, United States,* [2]*Radiology, Stony Brook University, Stony Brook, NY, United States*

Pseudo-continuous arterial spin labeling (pCASL) with segmented 3D-GRASE acquisition is widely accepted as the optimal ASL technique. However, the method suffers from blurring along the partition direction caused by point spread function (PSF) broadening. In this study, a PSF deconvolution method for pCASL images with 3D-GRASE acquisition is developed and evaluated in simulations and in-vivo experiments. The deconvolution method greatly reduces the effects of the PSF and recover the perfusion signal for segmentation factors of at least 2_{PAR} x 2_{PE}. The proposed deconvolution method improves the accuracy of cerebral blood flow quantification and facilitates the use of lower segmentation factors.

3632 Computer 66

Optimization of Flip Angle Design for Reduced T2 Blurring of 3D Arterial Spin Labeling

Li Zhao[1] and David Alsop[1]

[1]*Radiology, Beth Israel Deaconess Medical Center and Harvard Medical School, Boston, MA, United States*

Conventional 3D arterial spin labeling images suffer from pronounced T2 blurring. In this work, new variable flip angle schemes, which can provide a Hann or Fermi window response across the slice direction, or which can be easily corrected to the designed window response and provide optimal SNR, were evaluated. Volunteers' results show reduced blurring, improved SNR and contrast with the proposed methods.

3633 Computer 67

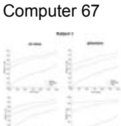

A denoising method for arterial spin labeling data based on total generalized variation (TGV) with a spatial varying regularization parameter

Stefan Manfred Spann[1], Kamil S Kazimierski-Hentschel[2], Christoph Stefan Aigner[1], and Rudolf Stollberger[1,3]

[1]*Institute of Medical Engineering, Graz University of Technology, Graz, Austria,* [2]*Institute for Mathematics and Scientific Computing, University of Graz, Graz, Austria,* [3]*BioTechMed-Graz, Graz, Austria*

Arterial spin labeling perfusion imaging permits a noninvasive approach to measure cerebral blood flow. The poor SNR of this technique makes denoising essential. ASL images are often corrupted with motion, physiological or scanning artifacts or acquired using parallel imaging leading to spatial dependent noise. To account for those artifacts and spatial varying noise we propose a denoising approach based on total generalized variation (TGV) using a spatial dependent regularization parameter. The performance of the proposed technique is evaluated on synthetic and in-vivo data and compared with the non-local means combined dual-tree complex wavelet transform (DT-CWT) denoising method.

3634 Computer 68

A Spatio-temporal Denoising Approach based on Total Variation Regularization for Arterial Spin Labeling

Cagdas Ulas[1,2], Stephan Kaczmarz[3], Christine Preibisch[3], Jonathan I. Sperl[2], Marion I. Menzel[2], Axel Haase[4], and Bjoern H. Menze[1]

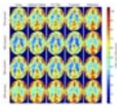

[1]Department of Computer Science, Technische Universität München, Munich, Germany, [2]GE Global Research, Munich, Germany, [3]Department of Neuroradiology, Technische Universität München, Munich, Germany, [4]Zentralinstitut für Medizintechnik, Technische Universität München, Munich, Germany

We present a new spatio-temporal denoising method for arterial spin labelling MR image repetitions, and mainly aim to improve the quality of perfusion-weighted images and cerebral blood flow (CBF) maps obtained from a subset of all dynamics available. Our technique is based on a two-step 3D total variation regularization, which is applied to subsets of control/label pairs in the first step and to resulting perfusion-weighted (difference) images in the second step. We demonstrate that our method leads to improved quality of perfusion-weighted images and CBF maps compared to existing spatial filtering techniques in short computation time.

3635 Computer 69

The effect of post-labeling delay on multiband pCASL based functional connectivity

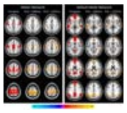

Alexander D. Cohen[1], Andrew S. Nencka[1], and Yang Wang[1]

[1]Radiology, Medical College of Wisconsin, Milwaukee, WI, United States

When too short a post-labeling delay (PLD) is used for ASL, intravascular artifacts can be present. This issue is amplified in multiband (MB) ASL where superior slices are acquired early in the acquisition. Here, MB pseudocontinuous ASL (pCASL) and a dual regression approach were used to analyze functional connectivity with PLD=1000ms and 1525ms. Increased whole-brain tSNR was observed for the PLD=1000ms data, but intravascular signal was present. Group connectivity was similar between PLDs, and no significant differences in mean or max z-score were seen between PLD. Thus, shorter PLDs may be appropriate for MB-ASL rsfMRI despite the presence of intravascular artifacts.

3636 Computer 70

Functional connectivity mapping using 3D GRASE arterial spin labeling MRI

Kalen J. Petersen[1], Daniel O. Claassen[2], and Manus J. Donahue[3]

[1]Chemical and Physical Biology, Vanderbilt, Nashville, TN, United States, [2]Neurology, Vanderbilt, [3]Radiology, Vanderbilt

The overall goal of this work is to optimize arterial spin labeling (ASL) MRI techniques to enable the use of baseline cerebral blood flow (CBF) fluctuations to identify major intrinsically-connected resting state networks (RSNs). We provide data in support of 3D GRASE pCASL being able to provide similar functional resting state networks as BOLD. Additionally, extremely low-frequency fluctuations, less than 0.01 Hz, were present in the CBF-weighted pCASL data, suggesting that application of pCASL may provide additional functional information relative to BOLD, which generally requires low-frequency filtering.

3637 Computer 71

Assessment of Resting State Perfusion and Coherent Large-Scale Brain Networks in Healthy Aging Using Arterial Spin Labeling Perfusion MRI

Alvaro Galiano[1], Reyes García de Eulate[1], Marta Vidorreta[2], Miriam Recio[3], and María Fernández-Seara[1,4]

[1]Radiology, University of Navarra Hospital, Pamplona, Spain, [2]Center for Functional Neuroimaging, University of Pennsylvania, Philadelphia, United States, [3]Neurology, University of Navarra Hospital, Pamplona, Spain, [4]Biomedical Engineering, TECNUN, University of Navarra, San Sebastian, Spain

Cognitive decline is associated with aging even in the absence of disease. In this study ASL perfusion fMRI was used to investigate changes in perfusion and resting state networks connectivity due to aging, by comparing two groups of healthy subjects (young and elderly). Results showed perfusion deficits in the elderly group, in association areas, related with advanced cognitive abilities. Disruptions in varios core RSNs were also detected. Assessment of perfusion and resting functional connectivity jointly could be a good predictor of cognitive decline and a good biomarker for treatments aiming to extend cognitive abilities.

3638 Computer 72

Trait Specificity of Regional Cerebral Blood Flow between Different Resting-State Conditions

Zhengjun Li[1], Marta Vidorreta[1], Daniel Wolf[2], and John A. Detre[1]

[1]Dept. of Neurology, University of Pennsylvania, Philadelphia, PA, United States, [2]Dept. of Psychiatry, University of Pennsylvania, Philadelphia, PA, United States

We used latent state-trait theory to examine trait specificity of regional cerebral blood flow (CBF) acquired using arterial spin labeled (ASL) perfusion MRI in four different resting-state conditions (eyes-open, eyes-closed, fixation, and a low-level attention task (psychomotor vigilance task, PVT)). Most brain regions accepted the latent state-trait model. Fixation exhibited the lowest latent trait specificity, while PVT, eyes-open, and eyes-closed showed progressively higher trait specificity. We confirmed that ASL CBF shows trait-like properties, which are optimally fit using eyes-open or eyes-closed conditions.

Electronic Poster

Electric Property Imaging & Clinical QSM

Exhibition Hall Monday 16:15 - 17:15

Computer 73

Investigating the relation between electrical conduction and tissue composition with proton and sodium MRI

Stefano Mandija[1], Paul W de Bruin[2], Andrew G Webb[2], Peter R Luijten[1], and Cornelis AT van den Berg[1]

[1]Center for Image Sciences, Center for Image Sciences, UMC Utrecht, Utrecht, Netherlands, [2]Radiology, Gorter Center for High-field MRI, LUMC Leiden, Leiden, Netherlands

3639

The focus of the presented work is to understand the relation between electrical conductivity and tissue composition in terms of ^{23}Na concentration and water fraction. This would be relevant to evaluate the potential value of electrical conductivity imaging as a new endogenous biomarker and the validity of accessing conductivity from water content. For this purpose, MR-EPT and waterEPT conductivity reconstructions are performed and compared to network analyzer measurements. To evaluate whether conductivity is directly related to the total sodium concentration in free water, ^{23}Na images are acquired at 7T and conductivity reconstruction are then performed using the Stogryn's model.

3640 Computer 74

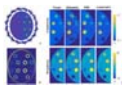

CONtrast Conformed Electrical Properties Tomography (CONCEPT) based on Multi-channel Transmission

Yicun Wang[1], Pierre-Francois Van de Moortele[2], and Bin He[1,3]

[1]Department of Biomedical Engineering, University of Minnesota, Minneapolis, MN, United States, [2]Center for Magnetic Resonance Research, University of Minnesota, Minneapolis, MN, United States, [3]Institute for Engineering in Medicine, University of Minnesota, Minneapolis, MN, United States

Magnetic Resonance based Electrical Properties Tomography holds promise to provide valuable information on tissue functional changes, such as Tumorigenesis. We propose a novel technique based on multi-channel transmission to reconstruct quantitative electrical properties maps by exploiting the intermediate contrast information with jointly promoted sparsity. The resultant optimization problem was solved by Alternating Direction Method of Multipliers within seconds. Numerical simulations, phantom and human subject experiments were performed at 7T using a multi-channel transceiver coils array, demonstrating improved accuracy and visual outcome. CONCEPT does not rely on anatomical assumptions, and therefore represents a general approach suitable for broader applications.

3641 Computer 75

Dictionary-based Electric Properties Tomography

Ulrich Katscher[1], Max Herrmann[1], Christian Findeklee[1], Mariya Doneva[1], and Thomas Amthor[1]

[1]Philips Research Europe, Hamburg, Germany

Electric Properties Tomography (EPT) derives tissue conductivity and permittivity according to the Helmholtz equation via the second derivative of the measured complex B1 map, or by iteratively solving the corresponding forward problem. This abstract presents a different type of EPT reconstruction: the measured B1 map is compared locally with entries of a dictionary, which are small B1 maps of a priori known electric properties. This "dictionary-based EPT" (db-EPT) could be able to solve the transceive phase problem as well as the boundary problem of EPT. This study applies db-EPT to numerical and experimental data comparing different types of dictionaries.

3642 Computer 76

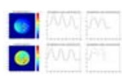

Spatial and Contrast Resolution of Phase Based MREPT

Yusuf Ziya Ider[1], Gokhan Ariturk[1], and Gulsah Yildiz[1]

[1]Electrical and Electronics Engineering, Bilkent University, Ankara, Turkey

Clarification of the contrast resolution (CR) and spatial resolution (SR) limits of phase based MREPT for conductivity imaging is essential for assessing its success success in clinical applications. Noise analysis of conventional phase based MREPT is performed to find the SNR needed for the MR sequence used for measuring B1-phase. It is found that with 1000-2000 SNR values about 0.01 S/m CR can be achieved. For SR evaluation, generalized phase based MREPT, which does not suffer from internal boundary artefacts, is considered. It is found by phantom experiments that 3.5mm spatial resolution is easily obtained with the state-of-art MR methods.

3643 Computer 77

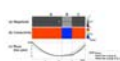

Adaptive Weighted Polynomial fitting in phase-based Electrical Property Tomography

Jun-Hyeong Kim[1], Jaewook Shin[1], Ho-Joon Lee[2], Kang-Hyun Ryu[1], and Donghyun Kim[1]

[1]Department of Electrical and Electronic Engineering, Yonsei University, seoul, Korea, Republic of, [2]Department of Radiology and Research Institute of Radiological Science, Severance Hospital, Yonsei University College of Medicine, seoul, Korea, Republic of

Weighted polynomial fitting method was proposed to resolve boundary artifact and noise amplification of Electrical Property Tomography. Weighted polynomial fitting method employs T1/T2 tissue contrast as prior information under assumption that pixels with similar magnitude intensity have similar conductivity. However, for non-simply connected structures make the fitting inaccurate. Therefore, in this study, we propose a modified weighted polynomial fitting technique including spatial constraint.

3644 Computer 78

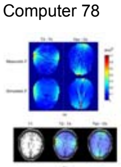

Current Density Measurements in the Brain using Magnetic Resonance Electrical Impedance Tomography in Healthy Volunteers

Aditya Kumar Kasinadhuni[1], Aprinda Indahlastari[2], Kevin Castellano[3], Christopher Saar[4], Casey Weigel[4], Bakir Mousa[4], Michael Schär[5], Munish Chauhan[2], Thomas Harold Mareci[6], and Rosalind Jane Sadleir[2]

[1]Biomedical Engineering, University of Florida, Gainesville, FL, United States, [2]School of Biological and Health Systems Engineering, Arizona State University, Tempe, AZ, United States, [3]University of Florida, Gainesville, FL, United States, [4]Arizona State University, Tempe, AZ, United States, [5]Radiology, Johns Hopkins University, Baltimore, MD, United States, [6]Biochemistry and Molecular Biology, University of Florida, Gainesville, FL, United States

Characterizing current density distributions in the brain of healthy volunteers can provide important information to guide electrical stimulation therapies. Current-induced magnetic fields, produced as a result of electrical stimulation, can be mapped from phase changes in the MR imaging then current density can be computed using Maxwell's equations. In this study, we present the first current density distribution induced magnetic field maps in healthy volunteers resulting from electrical stimulation using low frequency (10 Hz) transcranial alternating current simulation (tACS).

3645 Computer 79

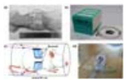

In Vivo Mapping of Liver Tissue Damage using MR-based Conductivity Imaging Method

Bup Kyung Choi[1], Nitish Katoch[1], Saurav ZK Sajib[1], Jin Woong Kim[2], Hyung Joong Kim[1], Oh In Kwon[3], and Eung Je Woo[1]

[1]Kyung Hee University, Seoul, Korea, Republic of, [2]Radiology, Chonnam National University Medical School, Gwangju, Korea, Republic of, [3]Konkuk University, Seoul, Korea, Republic of

Liver tissues mainly consist of single cell, the variations of ion concentration and mobility inside the liver have similar pattern. This indicates that liver tissues can exhibit uniform distribution of electromagnetic tissue properties such as electrical conductivity. MREIT is typical method which can provide electrical conductivity information of suspicious tissue using a current-injection MRI method. Mapping of liver tissue damage using MREIT conductivity imaging may provide direct, immediate, and high sensitive information based on the changes of ion concentration and mobility at cellular levels. This study experimentally imaged *in vivo* liver tissue damage based on the changes of tissue conductivity.

3646 Computer 80

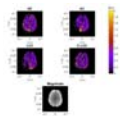

Data-Driven Background Phase Correction and Combination to Improve the Accuracy of MR-EPT with Multi-Channel Receivers

Kathleen Ropella[1] and Douglas C. Noll[1]

[1]Biomedical Engineering, University of Michigan, Ann Arbor, MI, United States

We propose a method for combining phase data from multiple receiver channels for phase-based conductivity mapping that does not require a reference scan or reference coil. The proposed method combines a background phase removal step, to reduce bias from individual coil phases, and local coil compression, which maximizes SNR in the combined phase data.

3647 Computer 81

magna cum laude

Volumetric Reconstruction of Tissue Electrical Properties from B1+ and MR Signals Using Global Maxwell Tomography: Theory and Simulation Results.

Jose E.C. Serralles[1], Ioannis Georgakis[2], Athanasios G. Polimeridis[2], Luca Daniel[1], Jacob K. White[1], Daniel K. Sodickson[3,4], and Riccardo Lattanzi[3,4]

[1]Research Laboratory of Electronics, Massachusetts Institute of Technology, Cambridge, MA, United States, [2]Center for Computational and Data-Intensive Science and Engineering, Skolkovo Institute of Science and Technology, Moscow, Russian Federation, [3]The Sackler Institute of Graduate Biomedical Science, New York University School of Medicine, New York, NY, United States, [4]Center for Advanced Imaging Innovation and Research, New York University School of Medicine, New York, NY, United States

Magnetic resonance-based inverse scattering has been proposed to extract tissue electrical properties (EP). We present an improved implementation of the Global Maxwell Tomography (GMT) EP mapping technique, with two new cost functions and an extension that uses piecewise linear basis functions to represent fields for higher accuracy. GMT does not make symmetry assumptions, is fully 3D, and is robust to noise. We validated the new GMT version with various numerical experiments, using a heterogeneous head model with realistic EP and a phantom with tissue-mimicking EP. We showed, for the first time, that artifact-free accurate reconstruction of EP is possible.

3648 Computer 82

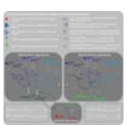

Longitudinal Atlas Construction for Normative Human Brain Development and Aging over the Lifespan using Quantitative Susceptibility Mapping (QSM)

Yuyao Zhang[1], Hongjiang Wei[1], Naying He[2], Christian Langkammer [3], Stefan Ropele [3], Fuhua Yan[2], and Chunlei Liu[1]

[1]University of California, Berkeley, berkeley, CA, United States, [2]Department of Radiology, Ruijin Hospital, Shanghai Jiaotong University School of Medicine, People's Republic of China, [3]Department of Neurology, Medical University of Graz, Graz, Austria

QSM is able to provide high contrast for iron-rich deep-brain nucleus. This is attributed to the sensitivity of magnetic susceptibility to the spatial variations of cellular components that exhibit different magnetic susceptibility properties, especially for brain iron and myelin. Although there have been atlases proposed for certain age groups, a longitudinal statistical atlas construction from general healthy population based on QSM is still lacking. We constructed longitudinal QSM atlases over the whole lifespan (from 1 to 83 years-old). One common QSM atlas is built for every 10-years interval to demonstrate the unique age-specific morphology and appearance of human brains.

3649 Computer 83

Does Total Iron Content in Deep Brain Nuclei Really Increase in Healthy Aging? A Study Based on Quantitative Susceptibility Mapping.

Yuyao Zhang[1], Hongjiang Wei[1], Naying He[2], Fuhua Yan[2], and Chunlei Liu[1]

[1]University of California, Berkeley, berkeley, CA, United States, [2]Department of Radiology, Ruijin Hospital, Shanghai Jiaotong University School of Medicine, People's Republic of China

The crucial role of iron for normal neurological function in human brain has been well recognized. The iron concentration evolution trajectories in human brain deep nucleus have been shown monotonously increased with aging. However, previous studies concern only on iron concentration. At the same time, atrophy occurs in healthy ageing brains. These two competing effects raise an interesting possibility that the total iron content in deep brain nuclei may decrease. Surprisingly, the iron content, investigated by QSM, in globus pallidus, substantia nigra and red nuclei appear to decrease after the iron content reaching a peak.

3650 Computer 84

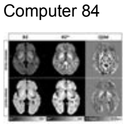

Paramagnetic ions quantification using QSM and EPR in human brain

Jeam Haroldo Oliveira Barbosa[1], Rafael Emidio[2], Ana Tereza Di Lorenzo Alho[2], Maria Conception Garcia Otaduy[2], Edson Amaro[2], Fernando Barbosa Junior[3], Oswaldo Baffa Filho[1], and Carlos Ernesto Garrido Salmon[1]

[1]InBrain Lab, Department of Physics, Faculty of Philosophy, Sciences and Letters of Ribeirão Preto, University of Sao Paulo, Ribeirao Preto, SP, Brazil, [2]Laboratory of Magnetic Resonance in Neuroradiology, LIM-44, Institute and Department of Radiology, University of Sao Paulo, Sao Paulo, SP, Brazil, [3]Department of Clinical Analyses, Toxicology and Food Sciences, School of Pharmaceutical Sciences of Ribeirão Preto, University of Sao Paulo, Ribeirao Preto, SP, Brazil

QSM, R2* and R2 values for post-mortem intra and extra cranial human brain samples were statistically correlated with only total iron and Fe3+ present in ferritin.

3651 Computer 85

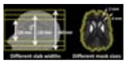

Importance of reference in QSM and a new differential ROI reference method

TaeHyun Hwang[1], JinGu Lee[1], JunYeol Choi[1], SangJoon Kim[2], GeonHo Jahng[3], and Jongho Lee[1]

[1]Department of Electrical and Computer Engineering, Seoul National University, Seoul, Korea, Republic of, [2]Department of Radiology, ASAN Medical Center, Korea, Republic of, [3]Department of Radiology, Kyung Hee University Hospital at Gangdong, Korea, Republic of

In this study, we developed a computer simulation to demonstrate the importance of reference in QSM. The results show that QSM values are substantially affected by spatial coverage for reconstruction. Only when the data are referenced using a neighboring region, the QSM results provide correct susceptibility values. Additionally, we suggest a new “differential ROI” reference method. This approach reports the susceptibility value as a difference between two (neighboring) ROIs. We demonstrate this new approach for a Parkinson’s disease patient study.

3652 Computer 86

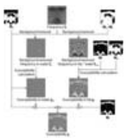

Quantitative susceptibility mapping with separate calculation in water and fat regions

Ryota Sato[1], Toru Shirai[1], Yo Taniguchi[1], Takenori Murase[2], Atsushi Kuratani[2], Taisei Ueda[2], Takashi Tsuneki[2], Yoshitaka Bito[2], Hisaaki Ochi[1], and Yoshihisa Soutome[1]

[1]Research and Development Group, Hitachi, Ltd., Tokyo, Japan, [2]Healthcare Business Unit, Hitachi, Ltd., Tokyo, Japan

To reduce the calculation error and artifacts of susceptibility in the boundary region between water and fat, a new reconstruction method is presented and applied to a prostate QSM. In the proposed method, susceptibility maps of the water region and the fat region are calculated separately and differently and then combined. Numerical simulation and human prostate imaging using a 3T-MRI are performed to evaluate accuracy and artifacts of the proposed method. The results suggest that the proposed method reduces calculation error and the shading artifacts in the boundary region between water and fat near the prostate.

3653 Computer 87

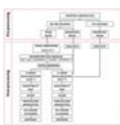

Localization of the implanted brachytherapy titanium seeds in presence of calcification on MR images using Quantitative Susceptibility Mapping (QSM) and 3D K-means clustering

Reyhaneh Nosrati[1,2], Abraam Soliman[3,4], Alexey V. Dimov[5,6], Hirohito Kan[7], Gerard Morton[8,9], Ana Pejović-Milić[10], and William Song[3,11]

[1]Medical Physics, Ryerson University, Toronto, ON, Canada, [2]Medical Physics, Sunnybrook Health Science Centre, Toronto, ON, Canada, [3]Medical Physics, Sunnybrook Health Sciences Centre, Toronto, ON, Canada, [4]Physical Sciences, Sunnybrook Research Institute, Toronto, ON, Canada, [5]Meinig school of Biomedical Engineering, Cornell University, Ithaca, NY, United States, [6]Radiology, Weill Medical College of Cornell University, New York, NY, United States, [7]Radiology, Nagoya City University Hospital, Nagoya, Japan, [8]Odette Cancer Centre, Sunnybrook Health Sciences Centre, Toronto, ON, Canada, [9]Radiation oncology, University of Toronto, Toronto, ON, Canada, [10]Physics, Ryerson University, Toronto, ON, Canada, [11]Medical Biophysics, University of Toronto, Toronto, ON

Post-implant dosimetry is an important quality assurance for prostate low-dose-rate (LDR) permanent seed brachytherapy. Despite the superior soft tissue contrast in MRI that is required for tumor delineation, there are some unresolved issues with seed depiction on MR images as they appear as signal void. In addition, calcified regions have similar characteristics on MR images making them indiscernible. This work investigates the feasibility of an MR-only workflow based on quantitative susceptibility mapping (QSM) and 3D k-means clustering for post-implant localization of the seeds.

3654 Computer 88

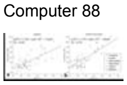

Image Quality Improvement by Applying Retrospective Motion Correction on Quantitative Susceptibility Mapping and R2*

Xiang Feng[1], Alexander Loktyushin[2,3], Andreas Deistung[1,4], and Jürgen R. Reichenbach[1,5,6]

[1]Medical Physics Group, Institute of Diagnostic and Interventional Radiology, Jena University Hospital - Friedrich Schiller University Jena, Jena, Germany, [2]Empirical Inference, Max Planck Institute for Intelligent Systems, Tübingen, Germany, [3]High-Field MR, Max Planck Institute for Biological Cybernetics, Tübingen, Germany, [4]Section of Experimental Neurology, Department of Neurology, Essen University Hospital, Essen, Germany, [5]Center of Medical Optics and Photonics, Friedrich Schiller University Jena, Jena, Germany, [6]Michael Stifel Center for Data-driven and Simulation Science Jena, Friedrich Schiller University Jena, Jena, Germany

The aim of this study was to quantitatively assess the improvement of image quality on motion corrupted quantitative susceptibility mapping (QSM) and the effective transverse relaxation rate (R_2*) maps, after applying retrospective motion correction. Image quality was assessed using the following metrics: SNR in different brain tissues, histogram analysis, and linear correlation between susceptibility and R_2* values in subcortical structures.

3655 Computer 89

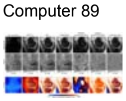

In-vivo phase imaging of growing epiphyseal human cartilage at 7 T.

Barbara Dymerska[1], Klaus Bohndorf[1], Paul Schennach[1], Alexander Rauscher[2], Siegfried Trattnig[1], and Simon Daniel Robinson[1]

[1]High Field MR Centre, Department of Biomedical Imaging and Image-guided Therapy, Medical University of Vienna, Vienna, Austria, [2]UBC MRI Research Centre, University of British Columbia, Vancouver, Canada

Growing epiphyseal cartilage of children contains vessels and more complex layer structure than adult hyaline cartilage. Phase imaging is sensitive to deoxyhemoglobin in venous blood and to orientation of magnetic tissues, but it is challenging since many established methods for combining and unwrapping data fail in the thin cartilage of the knee. In this study different phase reconstruction methods were tested at 7T and high resolution SWI was applied to visualize veins and collagen fiber architecture in healthy young subjects.

3656 Computer 90

Comparison of quantitative susceptibility mapping methods for evaluating cerebral microbleeds at 3T and 7T

Yicheng Chen[1], Clare B Poynton[2], Suchandrima Banerjee[3], and Janine M Lupo[2]

[1]UC Berkeley-UCSF Graduate Program in Bioengineering, University of California, Bekeley and University of California, San Francisco, San Francisco, CA, United States, [2]Department of Radiology, University of California, San Francisco, [3]Global Applied Science Laboratory, GE Healthcare

There is a growing interest in using QSM to detect and quantitatively evaluate cerebral microbleeds (CMBs). We compared several algorithms proposed in recent years for QSM on patients with CMBs after radiation therapy at 3T and 7T by quantitatively analyzing the noise and contrast of the susceptibility maps. Although RESHARP+ iLSQR had the least noise among methods, CMB and vessel contrast were more affected by incomplete background field removal, especially at 7T.

3657 Computer 91

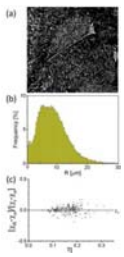

Quantitative susceptibility mapping: phase images and microstructure

Lukas R Buschle[1,2], Christian H Ziener[1], Michael O Breckwoldt[2], Artur Hahn[2], Julia Bode[3], Björn Tews[3], Martin Bendszus[2], Heinz-Peter Schlemmer[1], and Felix T Kurz[1,2]

[1]E010 Radiology, German Cancer Research Center, Heidelberg, Germany, [2]Neuroradiology, University Hospital Heidelberg, Heidelberg, Germany, [3]Schaller Research Group, University of Heidelberg and German Cancer Research Center, Heidelberg, Germany

In this work, the effect of inhomogeneous microstructure on quantitative susceptibility mapping (QSM) is simulated for typical microstructural geometries. The results suggest that the susceptibility of blood-filled capillaries can not be measured using quantitative susceptibility mapping due to the symmetry of the local Larmor frequency around a capillary. However, numerical simulations show that the concentration of spherically-shaped magnetic particles (contrast agents) is determinable with QSM. These results are therefore essential for a detailed analysis of quantitative susceptibility images.

3658 Computer 92

Variation of Regions of Interest (ROIs) using different tools for automatic ROI generation: The impact on reported magnetic susceptibility values in QSM

Emma Dixon[1], David L Thomas[2], Anna Barnes[3], and Karin Shmueli[1]

[1]Medical Physics and Biomedical Engineering, University College London, London, United Kingdom, [2]Leonard Wolfson Experimental Neurology Centre, University College London, Institute of Neurology, United Kingdom, [3]Institute of Nuclear Medicine, UCLH-NHS Foundation Trust, United Kingdom

Automatic Region of Interest (ROI) generation is useful for large clinical studies using Quantitative Susceptibility Mapping (QSM) as this allows mean susceptibility values for anatomical regions to be reported without manual intervention.

Several methods to generate ROIs are compared in this work. We found that methods based on T1 contrast showed little variation whether a typical magnitude image from a susceptibility protocol or a structural MPRAGE image was used. An additional method based on a QSM atlas showed greater variability in ROIs.

Mean susceptibility values for ROIs were shown to vary greatly depending on the method used to generate ROIs.

3659 Computer 93

Positive visualization of MR compatible nitinol stent using a susceptibility-based imaging method

Caiyun Shi[1], Xiaoyong Zhang[1,2], Shi Su[1], Hairong Zheng[1], Xin Liu[1], Guoxi Xie[1,3], and Jim Ji[4]

[1]Shenzhen Key Laboratory for MRI, Lauterbur Research Center for Biomedical Imaging, Shenzhen Institutes of Advanced Technology, Chinese Academy of Sciences, Shenzhen, People's Republic of China, [2]Centers for Biomedical Engineering, College of Information Science and Technology, University of Science and Technology of China, Hefei, People's Republic of China, [3]Beijing Center for Mathematics and Information Interdisciplinary Sciences, Beijing, People's Republic of China, [4]Department of Electrical and Computer Engineering, Texas A&M University, TX, United States

Previous studies have demonstrated that a susceptibility-based positive contrast MR method exhibits excellent efficacy for visualizing MR compatible metal devices by taking advantage of their high magnetic susceptibility. However, the method was not evaluated in the visualization of stents. Therefore, the purpose of this study is to assess whether the susceptibility-based positive method can be used to visualize the nitinol stents, with the comparison of two typical MR positive contrast techniques, i.e., SUMO and GRASP. Experiment results showed that the susceptibility-based method provides much better visualization and localization of the stent than SUMO and GRASP.

3660 Computer 94

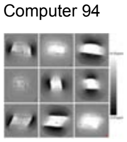

Magnetic Properties of Skeletal Muscle at 7T

Benjamin Tendler[1] and Richard Bowtell[1]

[1]Sir Peter Mansfield Imaging Centre, University of Nottingham, Nottingham, United Kingdom

The magnetic properties of skeletal muscle tissue were examined in a phantom consisting of a piece of muscle tissue embedded in agar. Frequency perturbation maps were generated from phase maps measured at 7T, with the phantom oriented at 29 angles to the external magnetic field. Using a novel minimisation technique, susceptibility and chemical exchange properties of the muscle tissue were obtained simultaneously. From this it was determined that skeletal muscle is significantly more diamagnetic than agar; there is a small anisotropic susceptibility component and a large, orientation independent positive offset within the tissue, hypothesised to be due to chemical exchange.

3661 Computer 95

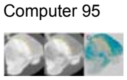

Correlations of SWI, QSM, and R2* map with neuromelanin and iron distributions from post-mortem human substantia nigra samples.

Hansol Lee[1], Se Young Chun[2], Jae-Hyeok Lee[3], Sun-Yong Baek[4], and HyungJoon Cho[1]

[1]Department of Biomedical Engineering, Ulsan National Institute of Science and Technology, Ulsan, Korea, Republic of, [2]Department of Electrical and Computer Engineering, Ulsan National Institute of Science and Technology, Ulsan, Korea, Republic of, [3]Department of Neurology, Pusan National University Yangsan Hospital, [4]Department of Anatomy, Pusan National University School of Medicine, Yangsan, Korea, Republic of

Spatial characterizations of neuromelanin and iron contents in human substantia nigra provide critical information in diagnosing and treating Parkinson's disease. In this work, MR investigations of susceptibility weighted imaging (SWI), R2* mapping, and quantitative susceptibility mapping (QSM) were performed with three post-mortem human substantia nigra samples at 7T and correlated with corresponding histological slides. Magnetization transfer (MT) based T1-weighted MRI technique was also conducted to validate its reputed neuromelanin sensitivity as well.

3662 Computer 96

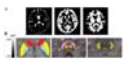

Changes in brain iron concentration after exposure to high altitude hypoxia by quantitative susceptibility mapping

Lin Chen[1], Congbo Cai[2], Tianhe Yang[3], Jianzhong Lin[3], Shuhui Cai[1], Jiaxing Zhang[4], and Zhong Chen[1]

[1]Department of Electronic Science, Xiamen University, Xiamen, People's Republic of China, [2]Department of Communication Engineering, Xiamen University, Xiamen, People's Republic of China, [3]Zhongshan Hospital, Xiamen, People's Republic of China, [4]Department of Physiology and Neurobiology, Xiamen University, Xiamen, People's Republic of China

Environmental factors may influence brain iron concentration. We investigated the changes of magnetic susceptibility and R_2^* values of cerebral regions especially in six deep gray matter nuclei of twenty-nine participants after high altitude exposure for four weeks. The results show that the susceptibility values of gray matter, especially in caudate nucleus, putamen, globus pallidus, substantia nigra, red nucleus, increased significantly. Traditional R_2^* maps verify the results of QSM evaluation except in red nucleus. Therefore, high altitude hypoxia can lead to significant increase of cerebral iron concentration.

Electronic Poster

QSM Technical Developments

Exhibition Hall Monday 16:15 - 17:15

3663 Computer 97

Optimization of Preconditioned Total Field Inversion for Whole head QSM and Cardiac QSM

Zhe Liu[1,2], Yan Wen[1,2], Pascal Spincemaille[2], and Yi Wang[1,2]

[1]Meinig School of Biomedical Engineering, Cornell University, Ithaca, NY, United States, [2]Department of Radiology, Weill Cornell Medical College, New York, NY, United States

Preconditioned Total Field Inversion (TFI) allows QSM for the entire head and chest. The preconditioner determines the TFI convergence. Can we choose a preconditioner that maximizes QSM quality within limited computational time? To answer this question, we conducted two numerical simulations specific to these applications to search for an optimal preconditioner. We found that preconditioner too small or too big for a targeted susceptibility distribution would have less computational acceleration and consequently greater errors for a given computational time. Our results here suggest that the optimal preconditioner should be identified to match the image content.

3664 Computer 98

magna cum laude

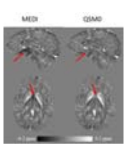

QSM0 - QSM with automatic uniform CSF zero reference

Zhe Liu[1,2], Yihao Yao[2], and Yi Wang[1,2]

[1]Meinig School of Biomedical Engineering, Cornell University, Ithaca, NY, United States, [2]Department of Radiology, Weill Cornell Medical College, New York, NY, United States

One challenge in Quantitative Susceptibility Mapping (QSM) identified in a recent QSM workshop is zero reference. Cerebrospinal fluid (CSF) with little cellular content has been a popular choice. However, current QSM often shows inhomogeneous CSF, which may be regarded as artifacts caused by surrounding anisotropic white matter fibers in the scalar dipole inversion. We propose a regularization of minimal CSF variation for projecting out CSF inhomogeneity artifacts. Our proposed new QSM incorporates automated segmentation and regularization specific to CSF and outputs susceptibility values with automatic and uniform CSF zero reference. Accordingly, we term this novel QSM method as QSM0

3665 Computer 99

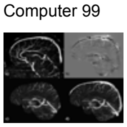

Susceptibility Mapping of the Dural Sinuses and Other Major Veins in the Brain

Sagar Buch[1], Yongsheng Chen[2], and E. Mark Haacke[1,2]

[1]The MRI Institute for Biomedical Research, Waterloo, ON, Canada, [2]Department of Radiology, Wayne State University, Detroit, MI, United States

In QSM, every effort is made to reduce background field induced by the air-tissue interfaces. In this abstract, we propose a method to: correct the phase of boundary regions by using background field extrapolation methods such as Taylor expansion; preserve the internal phase for the superior sagittal sinus (SSS) and transverse sinuses using an arterial-venous (MRAV) image; and predict the phase outside the brain and SSS using forward modeling. Further, we combine these steps to obtain an estimate of the venous oxygen saturation levels inside dural sinuses.

3666 Computer 100

Spatiotemporal dynamics of inter-subject magnetic susceptibility variations in the human brain

Balint P Sule[1], Robert Zivadinov[1,2], Jannis Hanspach[1], Michael G Dwyer[1], Jesper Hagemeier[1], Nicola Bertolino[1], Dhaval Shah[1], Niels P Bergsland[1,3], and Ferdinand Schweser[1,2]

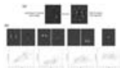

[1]Buffalo Neuroimaging Analysis Center, Department of Neurology, Jacobs School of Medicine and Biomedical Sciences, University at Buffalo, The State University of New York, Buffalo, NY, United States, [2]MRI Clinical and Translational Research Center, Jacobs School of Medicine and Biomedical Sciences, University at Buffalo, The State University of New York, Buffalo, NY, United States, [3]MR Research Laboratory, IRCCS, Don Gnocchi Foundation ONLUS, Milan, Italy

Magnetic susceptibility in the deep gray matter varies substantially between subjects of similar age or disease state. This work employs a blind source separation technique to 239 healthy controls to determine, without prior assumptions, the spatial patterns that drive inter-subject variation of magnetic susceptibility in the human brain.

3667 Computer 101

Accelerated B_{0} Mapping Using "X" Sampling in k-TE Space

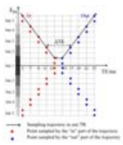

Xin Miao[1], Yi Guo[2], Krishna S. Nayak[1,2], and John C. Wood[1,3]

[1]Biomedical Engineering, University of Southern California, Los Angeles, CA, United States, [2]Ming Hsieh Department of Electrical Engineering, University of Southern California, Los Angeles, CA, United States, [3]Division of Cardiology, Children's Hospital Los Angeles, Los Angeles, CA, United States

High-resolution B_0 mapping suffers from long scan time, and issues with phase-wraps. We present an acquisition and reconstruction technique that resolves both problems. We utilize “X” sampling in ***k***-TE space, in which multiple phase-encoding lines are acquired exactly twice per TR. The echo spacing is shortest for central ***k***-space and largest for outer ***k***-space. A multi-scale reconstruction enables pixel-wise phase unwrapping. This technique may be particularly useful for quantitative susceptibility mapping (QSM), as it could a) shorten scan time while maintaining the sensitivity to high-order field variation and b) simplify phase-unwrapping, which are the key features of interest in QSM.

3668 Computer 102

Tikhonov regularization aided quantitative susceptibility mapping of whole brain without background field removal

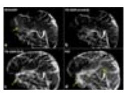

Hongfu Sun[1], Yuhan Ma[1,2], M. Ethan MacDonald[1], and G. Bruce Pike[1,2]

[1]Radiology, University of Calgary, Calgary, AB, Canada, [2]Biomedical Engineering, McGill University, Montreal, QC, Canada

An advanced dipole field inversion method for whole brain quantitative susceptibility mapping (QSM) without a traditional background field removal step, is proposed. To aid this ill-posed inversion process and obtain successful QSM, a Tikhonov regularization of the local susceptibility distribution is included. It is shown that the proposed method (Tikhonov-QSM) can substantially suppress reconstruction artefacts. More importantly, Tikhonov-QSM does not require edge erosion like in other QSM methods involving background field removal steps, preserving the cerebral cortex of the final images.

3669 Computer 103

A Fast Algorithm for Nonlinear QSM Reconstruction

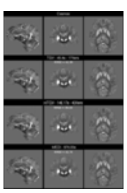

Carlos Milovic[1,2], Berkin Bilgic[3], Bo Zhao[3], Julio Acosta-Cabronero[4], and Cristian Tejos[1,2]

[1]Electrical Engineering, Pontificia Universidad Catolica de Chile, Santiago, Chile, [2]Biomedical Imaging Center, Pontificia Universidad Catolica de Chile, Santiago, Chile, [3]Martinos Center for Biomedical Imaging, Harvard Medical School, MA, United States, [4]German Center for Neurodegenerative Diseases (DZNE), Magdeburg, Germany

This abstract presents a fast nonlinear solver for the QSM reconstruction using the total generalized variation regularization. The proposed method utilizes the alternating direction method of multipliers to obtain close-form solution to each sub-problem. To handle the non-linear data fidelity, a two-step algorithm is described, including a global optimum search and a local Newton-Raphson iteration. Compared to conventional linear solvers, nonlinear solutions reduce streaking artifacts and better handle noise in poor SNR regions. Reconstruction results are at least comparable to nonlinear MEDI in quality, but with an order of magnitude improvement in the computational efficiency.

3670 Computer 104

Effect of Poisson kernel parameters on background field removal accuracy for QSM

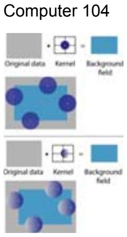

Debra E. Horng[1,2], Samir D. Sharma[1], Scott B. Reeder[1,2,3,4,5], and Diego Hernando[1,2]

[1]Radiology, University of Wisconsin, Madison, WI, United States, [2]Medical Physics, University of Wisconsin, Madison, WI, United States, [3]Biomedical Engineering, University of Wisconsin, Madison, WI, United States, [4]Medicine, University of Wisconsin, Madison, WI, United States, [5]Emergency Medicine, University of Wisconsin, Madison, WI, United States

The Poisson Estimation for Ascertaining Local fields (PEAL) kernel is a recently-introduced method for background field removal in quantitative susceptibility mapping (QSM). The PEAL kernel is determined by two parameters: radius and spatial shift. The choice of these two parameters may have a substantial effect on the accuracy of background field removal. In this work, we assessed the effect of PEAL kernel size and shift on the accuracy of background field removal and susceptibility estimation.

3671 Computer 105

Discrete frequency shift signatures explain GRE-MRI signal compartments

Shrinath Kadamangudi[1], Viktor Vegh[1], Surabhi Sood[1], and David Reutens[1]

[1]Centre for Advanced Imaging, University of Queensland, St Lucia, Australia

Ultra-high field GRE-MRI phase images present great promise for structural brain studies. Multi-echo GRE-MRI data has been shown to contain signal compartments, which may eventually be used to characterise brain microstructure. Existing studies considered three signal compartments, however it remains unclear how compartments co-localise throughout the brain. We compartmentalised the signal via frequency shift signatures in a mixture of grey-white matter brain regions and implemented quality of fit measures to select the most parsimonious model for each region. We utilised k-means cluster analyses to investigate signal compartment commonalities across different brain regions and found four dominant frequency shift signatures.

3672 Computer 106

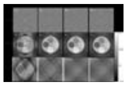

What causes streaking artifacts in QSM and how to efficiently suppress them?

Liangdong Zhou[1], Jae Kyu Choi[2], Youngwook Kee[3], Yi Wang[3,4], and Jin Keun Seo[1]

[1]Department of Computational Science and Engineering, Yonsei University, Seoul, Korea, Republic of, [2]Institute of Natural Sciences, Shanghai Jiao Tong University, Shanghai, People's Republic of China, [3]Department of Radiology, Weill Cornell Medical College, New York, NY, United States, [4]Department of Biomedical Engineering, Cornell University, New York, NY, United States

We provide a mathematical understanding for artifacts in QSM, particularly streaking artifacts. 1) The local field data can be decomposed into a dipole-compatible part and a dipole-incompatible part. 2) In spatially continuous space, the streaking-free susceptibility solution is obtained from the dipole-compatible field data only, and the dipole-incompatible data leads to artifacts defined by a wave propagator with z as time, specifically, streaking artifacts from granular noise and shadow artifacts from white matter noise error. Although it is not known how to filter out such dipole-incompatible data, its artifacts can be suppressed in regularization-based Bayesian methods such as MEDI, which can efficiently penalize streaking artifacts. k-space-truncation-based methods that generate additional dipole-incompatible data near the zero cone amplify streaking artifacts.

3673 Computer 107

Imaging Cerebral Arteries and Veins using Susceptibility Weighted Imaging with Ferumoxytol

Saifeng Liu[1], Jean-Christophe Brisset[2], Sagar Buch[1], Jing Jiang[3], E. Mark Haacke[1,3], and Yulin Ge[2]

[1]The MRI Institute for Biomedical Research, Waterloo, ON, Canada, [2]Radiology/Center for Biomedical Imaging, New York University School of Medicine, NY, United States, [3]Department of Radiology, Wayne State University, MI, United States

Susceptibility weighted imaging (SWI) has been widely used to image cerebral venous structures and in vivo iron content. However, it has not been used to image arteries, because of the lack of susceptibility contrast between arteries and the surrounding tissue. In this study, the susceptibility of the arterial blood was purposely modified to make it visible with SWI, by using the USPIO (ultra-small superparamagnetic iron oxide) agent Ferumoxytol. The purpose of this study is to determine the relationship between Ferumoxytol concentration and susceptibility using phantom and simulation studies, and compare these findings with those obtained from in vivo data.

3674 Computer 108

Coherence Enhancement in QSM via Anisotropic Weighting in Morphology-Enabled Dipole Inversion

Youngwook Kee[1], Pascal Spincemaille[1], Junghun Cho[1,2], and Yi Wang[1,2]

[1]Weill Cornell Medical College, New York, NY, United States, [2]Cornell University, Ithaca, NY, United States

The current regularization in morphology-enabled dipole inversion (MEDI) does not take into account orientation information in morphology between QSM and its corresponding magnitude image. In this abstract, we consider such orientation information to enhance structural coherence between the two images. In doing so, we achieve better image quality as well as higher RMSE (root mean square error) and HFEN (high frequency error norm) with respect to COSMOS and $$$\chi_{33}$$$.

3675 Computer 109

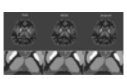

Improved Morphology Enabled Dipole Inversion for Quantitative Susceptibility Mapping by Using Prior Information

Yihao Guo[1], Li Guo[1], Yingjie Mei[1,2], Jijing Guan[1], and Yanqiu Feng[1]

[1]Guangdong Provincial Key Laboratory of Medical Image Processing,School of Biomedical Engineering, Southern Medical University, Guangzhou, People's Republic of China, [2]Philips Healthcare, Guangzhou, China.

Morphology enabled dipole inversion (MEDI) has been proposed to reconstruct QSM without obvious streaking artifacts at the smooth regions of susceptibility map. However, reconstruction errors or streaking artifacts near edges are not addressed by MEDI. In this work, we aim to improve MEDI by constraining the edges of susceptibility map with prior information.

3676 Computer 110

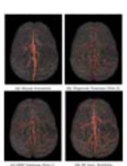

Automatic venous vessel segmentation in high field, multi-echo SWI using Random Forests

Albert Rechberger[1,2], Barbara Dymerska[2], Karin Poljanc[3], Georg Langs[1], and Simon Daniel Robinson[2]

[1]Computational Imaging Research Lab, Department of Biomedical Imaging and Image-guided Therapy, Medical University of Vienna, Vienna, Austria, [2]High Field MR Centre, Department of Biomedical Imaging and Image-guided Therapy, Medical University of Vienna, Vienna, Austria, [3]Atominstitut, TU Wien, Vienna, Austria

A method for automatic venous vessel segmentation is presented that uses a Random Forest classifier supplied with a number of appearance and shape features computed separately from magnitude images, phase images and QSMs of a multi-echo T2*-weighted GE scan. The importance of each feature, and thus each echo, is investigated. The approach was tested on whole-brain 7T scans of four subjects, two of which were manually annotated, and was effective in segmenting both internal and surface veins.

3677 Computer 111

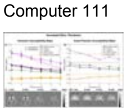

Resolution and Coverage for Accurate Susceptibility Maps: Comparing Brain Images with Simulations

Anita Karsa[1], Shonit Punwani[2], and Karin Shmueli[1]

[1]Department of Medical Physics and Biomedical Engineering, University College London, London, United Kingdom, [2]Centre for Medical Imaging, University College London, London, United Kingdom

Magnetic Susceptibility Mapping is moving closer to clinical application. To reduce scan time, clinical images are often acquired with reduced resolution and coverage in the through-slice dimension. The effect of these factors has been studied using only balloon phantoms and downsampled brain images. Here, we used MR images acquired at low resolution or low coverage and compared these with images simulated in volunteers and a realistic numerical phantom. Simulated susceptibility maps were very similar to maps from acquired images. Our results show that low resolution and very low coverage both lead to loss of contrast and errors in susceptibility maps.

3678 Computer 112

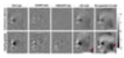

Phase processing for quantitative susceptibility mapping of regions with large susceptibility and lack of signal

Véronique Fortier[1,2] and Ives R. Levesque[1,2,3]

[1]Medical Physics Unit, McGill University, Montréal, QC, Canada, [2]Biomedical Engineering, McGill University, Montréal, QC, Canada, [3]Research Institute of the McGill University Health Centre, Montréal, QC, Canada

Phase unwrapping and background removal algorithms directly impact quantitative susceptibility maps. Phase processing techniques have been thoroughly studied for brain applications, but accuracy in the presence of large susceptibility and negligible signal, such as bone and air regions, is unknown. The performance of phase processing algorithms was evaluated quantitatively in simulations with a numerical head phantom and qualitatively *in vivo* in three head datasets. In these experiments, Laplacian-based unwrapping performed poorly. Accurate background removal remains an open question. Results suggest that Quality-Guided unwrapping should be preferred with background removal using Projection onto Dipole Fields.

3679 Computer 113

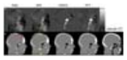

Evaluation of air/bone segmentation using susceptibility-based imaging methods

Emma Dixon[1], David L Thomas[2], Anna Barnes[3], and Karin Shmueli[1]

[1]Medical Physics and Biomedical Engineering, University College London, London, United Kingdom, [2]Leonard Wolfson Experimental Neurology Centre, University College London, Institute of Neurology, United Kingdom, [3]Institute of Nuclear Medicine, UCLH-NHS Foundation Trust, United Kingdom

Due to the difference in magnetic susceptibility of air, teeth and bone, magnetic susceptibility mapping has the potential to enable segmentation of these regions despite the absence of direct MRI signal. Several methods have been described which attempt to calculate the magnetic susceptibility within air and bone. Two datasets are used to test the ability of these methods to distinguish between air and bone. The performance of all methods varied between datasets and depended strongly on the parameters selected. None of the methods performed consistently better across groups, but all showed potential to improve air/bone segmentation using susceptibility mapping.

3680 Computer 114

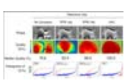

A comprehensive assessment of methods for combining phase data from array radio-frequency coils at 7 T

Simon Daniel Robinson[1], Korbinian Eckstein[1], José Rebelo Ferreira Marques[2], Berkin Bilgic[3], Siegfried Trattnig[1], and Ferdinand Schweser[4,5]

[1]Department of Biomedical Imaging and Image-guided Therapy, Medical University of Vienna, Vienna, Austria, [2]Donders Institute for Brain, Cognition and Behaviour, Radboud University Nijmegen, Netherlands, [3]Athinoula A. Martinos Center for Biomedical Imaging, Massachusetts General Hospital, MA, United States, [4]Department of Neurology, University at Buffalo, NY, United States, [5]MRI Clinical and Translational Research Center, University at Buffalo, NY, United States

Methods for combining phase data from array RF coils are quantitatively compared at 7 T. Of the reference-free approaches (which all leave arbitrary contributions to the total phase), the Virtual Reference Coil method yielded the best phase matching. The reference-free method COMPOSER removed non-B0-related phase but requires an artifact-free short echo-time reference measurement. Of the multi-echo methods, SVD, HIP and ASPIRE all had uniform phase matching. ASPIRE has higher CNR for a narrow range of echo times, but requires TE2=2 x TE1. The data and assessment scripts used in this study will be made publicly available.

3681 Computer 115

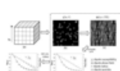

Evaluation of Accuracy of MR phase and R2* for susceptibility quantification

Yongquan Ye[1], Li Yang[2], Mengsu Zeng[2], Shengxiang Rao[2], Ying Ding[2], Jinguang Zong[3], and Xixi Wen[3]

[1]United Imaging of Healthcare America, Houston, TX, United States, [2]Department of Radiology, Shanghai Institute of Medical Imaging, Zhongshan Hospital, Fundan University, Shanghai, People's Republic of China, [3]Shanghai United Imaging of Healthcare, Shanghai, People's Republic of China

Computer simulation was performed to evaluate the relationship between a voxel's bulk susceptibility and its R_2* or phase behavior. A virtual voxel with multi-dipole model was created, and the effects of dipole properties on the accuracy and consistency of R_2* and phase on reflecting the voxel's bulk susceptibility was investigated. Linearity is only observed at low bulk susceptibility regime, and phase is much more robust against various susceptibility dipole properties than R_2*.

3682 Computer 116

Texture analyses of quantitative susceptibility maps to differentiate patients with Parkinson's disease from healthy controls

Gaiying Li[1], Guoqiang Zhai[1], Xinxin Zhao[1], Hedi An[2], Tian Liu[3], Yi Wang[1,3], Dongya Huang[2], and Jianqi Li[1]

[1]Shanghai Key Laboratory of Magnetic Resonance and Department of Physics, East China Normal University, Shanghai, People's Republic of China, [2]Department of Neurology, East Hospital, Tongji University School of Medicine, Shanghai, People's Republic of China, [3]Department of Radiology, Weill Medical College of Cornell University, NY, United States

QSM provides excellent contrast of iron-rich deep nuclei to quantify iron in the brains. Clinicians are interested in using QSM to diagnose patients with Parkinson's disease (PD). Texture analyses of QSM images in substantia nigra (SN) was performed to differentiate PD from healthy controls (HC). Most of the texture parameters were significantly different between PD and HC. The second-order textures were more efficient in differentiating PD from HC than did the first-order ,which suggests that the second-order texture parameters are more suitable and sensitive for the diagnosis of PD.

3683 Computer 117

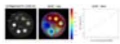

Ultrashort Echo Time Quantitative Susceptibility Mapping (UTE-QSM): Limitations in Quantifying High Iron Concentration

Xing Lu[1,2], Alexey Dimov[3], Qun He[1], Yajun Ma[1], Yi Wang[3], Eric Y Chang[1,4], and Jiang Du[1]

[1]Department of Radiology, University of California, San Diego, CA, United States, [2]Institute of Electrical Engineering, Chinese Academy of Science, Beijing, People's Republic of China, [3]Department of Radiology, Weill Cornell Medical College, New York, NY, United States, [4]Radiology Service, VA San Diego Healthcare System, San Diego, CA, United States

Iron overload can affect not only the central nervous system, but the liver, pancreas, myocardium, endocrine glands, and musculoskeletal structures. A reliable quantitative method to detect and measure high concentration iron in vivo would be of great clinical utility. Ultrashort echo time (UTE) sequences have echo times (TE) 100-1000 times shorter than clinical sequences, and may detect signal from high iron concentration. In this study, we aimed to evaluate the capability of UTE-QSM sequence in quantifying high iron concentration with an Iron phantom study and the results show that UTE-QSM techniques can quantify high iron concentration up to 22 mM or higher.

3684 Computer 118

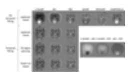

Comparison of Quantitative Susceptibility Mapping algorithms based on numerical and in vivo 3T data

Hanneke Geut[1], Louise van der Weerd[1], and Itamar Ronen[2]

[1]Radiology, Leiden University Medical Center, Leiden, Netherlands, [2]C.J. Gorter Center for High Field MRI Research, Leiden University Medical Center, Leiden, Netherlands

This study compares the currently publically available algorithms for quantitative susceptibility mapping, including different phase unwrapping, background field removal and dipole inversion methods. Numerical and human in vivo brain MRI data are used for a qualitative and quantitative assessment of the various methods. In 3T in vivo MRI data, phase unwrapping with combined spatial and temporal fitting and background field removal using V-SHARP results in the least artifacts. MEDI and iLSQR are currently the most accurate dipole inversion algorithms, with a significantly shorter processing time for the iLSQR method.

3685 Computer 119

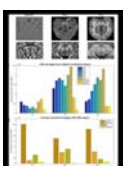

Biological underpinnings of different MR contrasts in the human midbrain using quantitative structural MR imaging at 9.4T: Validation with 14T ex-vivo measurements and PLI

Joana Loureiro[1], Gisela Hagberg, Elisa Tuzzi, Rolf Pohmann, Zora Schickardt, Marc Himmelbach, Thomas Ethofer, Matthias Valverde, Wolgang Grodd, and Klaus Scheffler

[1]High field MR, Max Planck Institute for Biological Cybernetics, Tuebingen, Germany

In this study we use relaxometry and susceptibility mapping to obtain enhanced contrast in the midbrain, in particular in the superior colliculus (SC). High resolution GRE images were obtained in 11 subjects at 9.4T. We calculated CNR values for each contrast for three midbrain regions (superior colliculus,red nucleus and aqueductal gray). were were obtained across 11 subjects in individual and MNI space. These measurement were validated with ex-vivo measurements in the 9.4T, 14.1T and PLI imaging.

3686 Computer 120

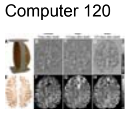

Investigation of Brain Tissue Fixation on Iron Concentration, Magnetic Susceptibility and Effective Transverse Relaxation Rate

Andreas Deistung[1,2], Verena Endmayr[3], Simon Hametner[3], Max Prihoda[4,5], Xiang Feng[1], Hans Lassmann[3], Jürgen Rainer Reichenbach[1], Simon Daniel Robinson[6], Evelin Haimburger[4], Christian Menard[7], Thomas Haider[8], Hannes Traxler[9], Siegfried Trattnig[6], and Günther Grabner[4,5,6]

[1]Medical Physics Group, Institute for Diagnostic and Interventional Radiology, Jena University Hospital – Friedrich Schiller-University, Jena, Germany, [2]Section of Experimental Neurology, Department of Neurology, Essen University Hospital, Essen, Germany, [3]Center for Brain Research, Medical University of Vienna, Vienna, Austria, [4]Department of Radiologic Technology, Carinthia University of Applied Sciences, Klagenfurt, Austria, [5]Institute for Applied Research on Ageing, Carinthia University of Applied Sciences, Klagenfurt, Austria, [6]High Field Magnetic Resonance Centre, Department of Biomedical Imaging and Image-guided Therapy, Medical University of Vienna, Vienna, Austria, [7]Department of Medical Engineering, Carinthia University of Applied Sciences, Klagenfurt, Austria, [8]University Clinic for Trauma Surgery, Medical University of Vienna, Vienna, Austria, [9]Center of Anatomy and Cell Biology, Medical University of Vienna, Vienna, Austria

We investigated the effect of brain tissue fixation on iron concentration and on quantitative maps of the magnetic susceptibility and effective transverse relaxation rate (R2*). Both R2* and susceptibility distributions of unfixed and fixed tissue were found to be similar, indicating similar underlying proportions of iron across tissues. Quantitatively, however, severe decreases of iron concentration of 25% in putamen and about 15% in white matter were measured after tissue fixation. The iron concentration change due to tissue fixation was captured by R2* and susceptibility which needs to be considered when directly comparing experiments performed with unfixed and fixed brain tissue.

Electronic Poster

Novel Probe & Pulse Sequence Design for Hyperpolarized 13C

Exhibition Hall Monday 17:15 - 18:15

3687 Computer 1 Simultaneous multislice acquisition without trajectory modification for hyperpolarized 13C experiments

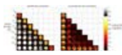

Angus Z. Lau[1,2], Albert P. Chen[3], Justin Y.C. Lau[1,2], and Charles H. Cunningham[1,2]

[1]Physical Sciences, Sunnybrook Research Institute, Toronto, ON, Canada, [2]Medical Biophysics, University of Toronto, Toronto, ON, Canada, [3]GE Healthcare, Toronto, ON, Canada

Recently we proposed using simultaneous multislice (SMS) acceleration to improve spatial coverage in the hyperpolarized ^{13}C experiment, and demonstrated that controlled aliasing improves conditioning of the inverse problem. For single-shot experiments this requires gradient modulation along z, which can be sensitive to gradient imperfections. Here, we show that inherent coil sensitivity variations can be sufficient for SMS acceleration in hyperpolarized ^{13}C experiments, without additional readout gradient modification. Two-fold acceleration with a 8 cm slice gap can be obtained with less than 20% SNR loss. We anticipate that this strategy will enable multiple organ ^{13}C imaging of in vivo metabolism.

3688 Computer 2

Slice Selective Adiabatic Refocusing Pulses for High Field, Pre-Clinical Hyperpolarized C-13 Imaging

Xucheng Zhu[1], Jeremy W Gordon[2], and Peder EZ Larson[1,2]

[1]Bioengineering, UCSF, Albany, CA, United States, [2]Radiology & Biomedical Imaging, University of California - San Francisco, CA, United States

Due to limited transmit coil volume, refocusing pulses spoil magnetization located around the edge of the coil even with adiabatic pulses. This is a major problem for hyperpolarized 13C MRI, as this can destroy precious magnetization. To overcome this drawback, we propose to use a high bandwidth slice-selective adiabatic pulse to replace the original non-selective pulse. We designed and optimized the pulse via simulation. Then the slice-selective double spin echo sequence was tested on both phantom and in vivo studies.

3689 Computer 3

Improved Off-Resonance Robustness for Spectral-Spatial Excitation and Echo-Planar Imaging of Hyperpolarized [1-13C]Pyruvate and Metabolites

Justin YC Lau[1,2], Benjamin J Geraghty[1,2], Yiping Gu[1], Albert P Chen[3], and Charles H Cunningham[1,2]

[1]Physical Sciences, Sunnybrook Research Institute, Toronto, ON, Canada, [2]Medical Biophysics, University of Toronto, Toronto, ON, Canada, [3]GE Healthcare, Toronto, ON, Canada

An interleaved multi-echo imaging sequence is proposed to improve off-resonance robustness for spectral-spatial excitation and echo-planar imaging of hyperpolarized [1-^{13}C]pyruvate. A non-iterative pointwise k-space signal decomposition approach for removing pyruvate hydrate contamination from lactate images is presented. Performance of the sequence and reconstruction pipeline was evaluated using an ethylene glycol phantom and a catalyzing enzyme system. Minimal signal loss and successful removal of pyruvate hydrate contamination were demonstrated in vivo for realistic cases of off-resonance.

3690 Computer 4

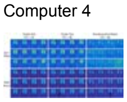

3D Hyperpolarized C-13 EPI with Calibrationless Parallel Imaging

Jeremy W Gordon[1], Yesu Feng[1], Peter Shin[1], Daniel B Vigneron[1], and Peder EZ Larson[1]

[1]Radiology & Biomedical Imaging, UCSF, San Francisco, CA, United States

With the translation of hyperpolarized ^{13}C to the clinic, imaging approaches will require large volumetric FOVs to support clinical applications. Parallel imaging techniques will be crucial to increasing volumetric scan coverage while minimizing RF requirements and temporal resolution. Calibrationless parallel imaging approaches are well-suited for this application because they eliminate the need to acquire coil profile maps or auto-calibration data. In this work, we explored the application of calibrationless parallel imaging (SAKE) and corresponding sampling strategies to accelerate and undersample hyperpolarized ^{13}C data using 3D blipped EPI acquisitions and multichannel receive coils.

3691 Computer 5

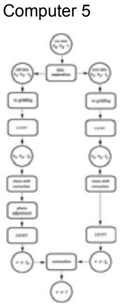

Echo Planar Spectroscopic Imaging of Hyperpolarized 13C in a Clinical System with Reduced Chemical Shift Artifacts

Abubakr Eldirdiri[1,2], Stefan Posse[3,4,5], Lars G. Hanson[1,2], Rie B. Hansen[1], Adam E. Hansen[6], and Jan Henrik Ardenkjær-Larsen[1]

[1]Center for Hyperpolarization in Magnetic Resonance, DTU Elektro, Technical University of Denmark, Kgs. Lyngby, Denmark, [2]Danish Research Center for Magnetic Resonance, Hvidovre Hospital, Hivdovre, Denmark, [3]Department of Neurology, University of New Mexico, Albuquerque, NM, United States, [4]Department of Physics and Astronomy, University of New Mexico, Albuquerque, United States, [5]Department of Electrical and Computer Engineering, University of New Mexico, Albuquerque, United States, [6]Department of Clinical Physiology, Nuclear Medicine and PET, Rigshospitalet, Copenhagen, Denmark

Fast and robust symmetric echo planar spectroscopic imaging sequence for hyperpolarized ^{13}C in a clinical system is presented. The sequence employs a reconstruction algorithm that re-grids the sampled data in the spatio-temporal frequency space to compensate for the chemical shift artifacts and achieve an improved reconstruction within a limited bandwidth. The sequence was tested on a clinical 3 T whole body scanner using dedicated ^{13}C coils and was compared with the conventional chemical shift imaging. Good tradeoff between speed, efficiency and SNR was achieved and the reconstruction was superior compared to the commonly used FFT reconstruction.

3692 Computer 6

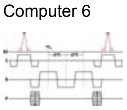

Multi-echo balanced steady state imaging of hyperpolarized [1-13C]-pyruvate at 9.4T

Christian Østergaard Mariager[1], Mette Ji Riis-Vestergaard[1], Haiyun Qi[1], Steffen Ringgaard[1], and Christoffer Laustsen[1]

[1]Department of Clinical Medicine, The MR Research Centre, Aarhus University Hospital, Aarhus N, Denmark

Hyperpolarized (HP) [1-^{13}C]-pyruvate imaging has gained increasing attention, as its ability to monitor metabolic changes in real-time is expected to have a great clinical impact. In this work we investigate the use of a fast multi-echo balanced steady state free precession (BSSFP) sequence to acquire spectroscopic images at 9.4T. We show that this technique, in combination with the iterative Dixon type reconstruction technique (IDEAL), yields dynamic high resolution spectroscopic maps in a ^{1}H phantom as well as for preliminary in vivo HP [1-^{13}C]-pyruvate experiments in rat kidneys.

3693 Computer 7

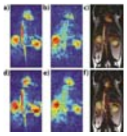

High Spatiotemporal Resolution bSSFP Imaging of Hyperpolarized ^{13}C Lactate and Pyruvate using Spectral Suppression of Alanine and Pyruvate-hydrate at 3T

Eugene Milshteyn[1,2], Cornelius von Morze[1], Jeremy W. Gordon[1], Zihan Zhu[1,2], Peder E. Z. Larson[1,2], and Daniel B. Vigneron[1,2]

[1]Radiology and Biomedical Imaging, UCSF, San Francisco, CA, United States, [2]UC Berkeley-UCSF Graduate Program in Bioengineering, UCSF and University of California, Berkeley, San Francisco, CA, United States

The bSSFP sequence provides high spatial and temporal resolution capabilities, but has a difficult to manage frequency response at 3T with regards to hyperpolarized [1-^{13}C]pyruvate and its products. The purpose of this project was to integrate a spectral suppression pulse, designed to suppress alanine and pyruvate-hydrate, with the bSSFP sequence to image [1-^{13}C]pyruvate and its conversion to [1-^{13}C]lactate. The results showed no significant effect on quantitative analysis of lactate-to-pyruvate ratios or k_{pl} after suppression of alanine and pyruvate-hydrate. Subsequently, dynamic imaging of [1-^{13}C]pyruvate and [1-^{13}C]lactate at high in-plane spatial resolution was achieved with the bSSFP sequence.

3694 Computer 8

Dynamic Nuclear Polarization across the barrier: a Focused Ultrasound approach

Tom H. Peeters[1], Thiele Kobus[1], Andor Veltien[1], Arend Heerschap[1], and Tom W.J. Scheenen[1]

[1]Radiology and Nuclear Medicine, Radboud university medical center, Nijmegen, Netherlands

The delivery of targeted metabolic compounds can be hindered by a natural barrier in the brain. Nowadays, focused ultrasound techniques allow temporarily opening of this blood-brain barrier (BBB). Here we investigated the feasibility to combine this technique with dynamic imaging of hyperpolarized (HP) pyruvate. After opening the BBB in a focal spot, we acquired *in vivo* HP pyruvate images of the mouse brain using a dynamic gradient-echo imaging acquisition scheme at 7T. This approach eventually allows investigations with hyperpolarized compounds in the brain that are usually hindered by the BBB or suffer from a too slow uptake for DNP-imaging.

3695 Computer 9

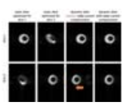

Dynamic shimming for multi-slice hyperpolarized metabolic imaging of the rat heart at 9.4T

Patrick Wespi[1], Jonas Steinhauser[1], Grzegorz Kwiatkowski[1], and Sebastian Kozerke[1]

[1]Institute for Biomedical Engineering, ETH and University Zurich, Zurich, Switzerland

In this work dynamic shimming was implemented for multi-slice hyperpolarized metabolic imaging of the rat heart at 9.4T. Phantom experiments were carried out to test the switching between different shim sets and eddy current effects. The method was subsequently applied to assess cardiac metabolism in healthy rats after injecting hyperpolarized [1-13C] pyruvate. It is demonstrated that B_0 inhomogeneity induced signal variations could be reduced with dynamic shimming when compared to static shimming.

3696 Computer 10

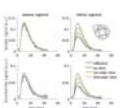

Effect of B0 inhomogeneity on the quantification of hyperpolarized metabolic data of the heart at 9.4T

Patrick Wespi[1], Jonas Steinhauser[1], Grzegorz Kwiatkowski[1], and Sebastian Kozerke[1]

[1]Institute for Biomedical Engineering, ETH and University Zurich, Zurich, Switzerland

The effect of B_0 inhomogeneity on the quantification of hyperpolarized metabolic data is studied using simulations based on B_0 maps acquired in-vivo in rat hearts at 9.4T. Kinetic modelling is compared to area-under-the-curve analysis and both methods are applied to average signals over myocardial segments and individual voxels, respectively.

3697 Computer 11

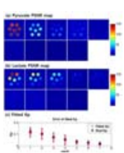

Analysis of the feasibility in using the SPICE technique for hyperpolarized 13C

Jae Eun Song[1], Hansol Lee[1], Eunhae Joe[1], Jaewook Shin[1], and Dong-Hyun Kim[1]

[1]Department of Electrical and Electronic Engineering, Yonsei University, Seoul, Korea, Republic of

In this study, using high spatial and/or spectral resolution CSI technique in 1H, the SPICE (SPectroscopic Imaging by exploiting spatiospectral CorrElation), we investigated the feasibility of using SPICE in hyperpolarized ^{13}C through numerical simulations for applications targeted for K_p estimation and high resolution studies. The error of the fitted K_p were within ±20% of the true value and the high spatial resolution rat brain image was reconstructed. It is seen that this method can be transferred to a hyperpolarized ^{13}C situation where due to the T1 decay and metabolite exchange the temporal basis can change dynamically.

3698 Computer 12

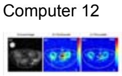

High resolution hyperpolarized 13C MRSI acquired by applying SPICE in mouse kidney

Hansol Lee[1], Jae Eun Song[1], Jaewook Shin[1], Eunhae Joe[1], Young-suk Choi[2], Ho-Taek Song[2], and Dong-Hyun Kim[1]

[1]Department of Electrical and Electronic engineering, Yonsei university, Seoul, Korea, Republic of, [2]Department of Radiology, Yonsei University College of Medicine, Seoul, Korea, Republic of

Hyperpolarized ^{13}C technique might be a practical challenge to achieve both high spatial and spectral resolution in spectroscopic images due to the amount of required data. Recently, an emerging technique called to SPectroscopic Imaging by exploiting spatiospectral CorrElation (SPICE) has been introduced for high spatiotemporal resolution in ^{1}H magnetic resonance spectroscopic image (MRSI). In this study, by applying this technique to hyperpolarized ^{13}C MRSI, a high resolution spectroscopic image was acquired.

3699 Computer 13

Overdiscrete Reconstruction for Signal Enhancement in Hyperpolarized 13C Spectroscopic Imaging

Eduardo Coello[1,2], Esben S. Hansen[3], Christoffer Laustsen[3], Bjoern Menze[1], Axel Haase[1], and Rolf Schulte[2]

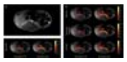

[1]Technische Universität München, Munich, Germany, [2]GE Global Research, Munich, Germany, [3]MR Research Centre, Aarhus University, Aarhus, Denmark

The overdiscrete reconstruction, originally proposed for ^{1}H MR Spectroscopic Imaging (MRSI), is adapted and applied to hyperpolarized ^{13}C MRSI. The method is demonstrated for in-vivo hyperpolarized [1-13C]-pyruvate scans of a pig's kidneys using phase encoded 2D-MRS. Linewidth and spectral separation were improved in addition to a significant signal enhancement for low concentrated downstream metabolites such as lactate, alanine and pyruvate-hydrate.

3700 Computer 14

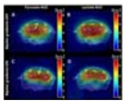

Repeatability of quantitative hyperpolarized ^{13}C MRSI measures of renal metabolism: impact of flow-sensitive gradients

Erin B Adamson[1], Kai D Ludwig[1], Benjamin L Cox[1,2,3], and Sean B Fain[1,4,5]

[1]Medical Physics, University of Wisconsin-Madison, Madison, WI, United States, [2]Morgridge Institute for Research, Madison, WI, United States, [3]Laboratory for Optical and Computational Instrumentation, University of Wisconsin-Madison, Madison, WI, United States, [4]Radiology, University of Wisconsin-Madison, Madison, WI, United States, [5]Biomedical Engineering, University of Wisconsin-Madison, Madison, WI, United States

Real-time quantification of *in vivo* metabolism with hyperpolarized ^{13}C magnetic resonance spectroscopic imaging (MRSI) is currently limited by partial volume effects from intense vascular signal. Flow-sensitive, bipolar gradients are an attractive option for suppressing vascular signal due to their minimal influence on static spins. This work looks at the impact of incorporating bipolar gradients on the quantification and repeatability of hyperpolarized ^{13}C MRSI metabolic measures of lactate-to-pyruvate area-under-the-curve ratios (AUC_{ratio}). The results suggest that incorporating bipolar gradients mitigates vascular partial voluming, increasing measured AUC_{ratio}, while reducing measurement repeatability, indicated by the larger repeatability coefficients.

3701 Computer 15

A Referenceless Workflow for Hyperpolarized 13C EPI

Jiazheng Wang[1], Alan Wright[1], Richard Hesketh[1], De-en Hu[1], and Kevin M Brindle[1,2]

[1]Cancer Research UK Cambridge Institute, University of Cambridge, Cambridge, United Kingdom, [2]Department of Biochemistry, University of Cambridge, Cambridge, United Kingdom

We have developed a workflow for hyperpolarized ^{13}C EPI phase correction that requires no reference scan. The workflow provides ghost-free images on phantoms with large or tight fields of view and where there are multiple signal sources. Dynamic images acquired from hyperpolarized [1-^{13}C]pyruvate and [1-^{13}C]lactate in a tumor showed comparable image quality to those corrected using a separate ^{13}C reference scan.

3702 Computer 16

Platform for Hyperpolarized 13C MRI of Breast Cancer

Benjamin Joseph Geraghty[1,2], Justin YC Lau[1,2], Logi Vidarsson[3], William Dominguez-Viqueira[4], Albert P Chen[5], and Charles Cunningham[1,2]

[1]Department of Medical Biophysics, University of Toronto, Toronto, ON, Canada, [2]Physical Sciences, Sunnybrook Research Institute, Toronto, ON, Canada, [3]LT Imaging Inc., Toronto, ON, Canada, [4]Moffitt Cancer Center, Tampa, FL, United States, [5]GE Healthcare, Toronto, ON, Canada

A platform consisting of a dual-echo 3D echo-planar pulse sequence and a custom coil system was implemented and tested for metabolic imaging of breast cancer. A two-channel unilateral breast ^{13}C receive array was designed for integration with the Sentinelle Vanguard Breast MRI system. A single-loop coil was designed for RF excitation. The highly ergonomic design enables the operator to swap between proton and ^{13}C breast coils without moving the patient, providing intrinsically registered anatomical and metabolic data. Phantom data and hyperpolarized ^{13}C pre-clinical rat images were obtained and are presented. The proposed coil system represents important progress towards a viable breast cancer patient study.

3703 Computer 17

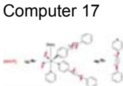

Cost-efficient hyperpolarization of long-lived nuclear spin states on carbon-13 spin pairs

Thomas Theis[1], Zijian Zhou[1], Jin Yu[1], Johannes Colell[1], and Warren Warren[1,2]

[1]Department of Chemistry, Duke University, Durham, NC, United States, [2]Departments of Physics, Radiology and BME, Duke University, Durham, NC, United States

Current hyperpolarization methods used in preclinical research are limited by high cost (>$2M) and short hyperpolarization lifetimes (<1 min). Here we demonstrate hyperpolarization of long-lived states with inexpensive equipment. Specifically, we use parahydrogen which is simple to produce (<$10k in equipment costs) and transfer its singlet hyperpolarization by non-reactive polarization transfer to long-lived singlet states on 13C spin pairs in molecular substrates. We detail polarization transfer mechanisms and obtain hyperpolarization lifetimes in excess of two minutes. Moving forward, we expect to achieve hyperpolarization lifetimes of hours as has been demonstrated on thermally polarized 13C spin pairs.

3704 Computer 18

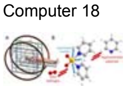

Simple, cost-efficient, and highly sensitive molecular imaging with hyperpolarized milliTesla MRI

Thomas Theis[1], Johannes F. P. Colell[2], David E. J. Waddington[3,4,5], Warren S. Warren[1,6], and Matthew S. Rosen[4,5,7]

[1]Department of Chemistry, Duke University, Durham, NC, United States, [2]Chemistry, Duke University, Durham, NC, United States, [3]School of Physics, University of Sydney, Sydney, Australia, [4]A. A. Martinos Center for Biomedical Imaging, Massachusetts General Hospital, Charlestown, MA, United States, [5]Department of Physics, Harvard University, Cambridge, MA, United States, [6]Departments of Physics, Radiology and BME, Duke University, Durham, NC, [7]Harvard Medical School, Boston, MA, United States

Hyperpolarized MRI is a powerful approach to non-invasive biomolecular imaging because of high sensitivity and excellent molecular specificity. However, current methods are limited by high cost (>$5M) and short hyperpolarized signal lifetimes (<1 min). We overcome both limitations by low field (6.5 mT) imaging of molecules polarized by non-reactive transfer of spin order from parahydrogen. Both, parahydrogen polarizers and low-field MRI hardware are simple technologies affordable on a modest budget (<$200k). At low fields, we establish hyperpolarization decay time constants of above 20 min, greatly exceeding current markers. This suggests highly sensitive biomolecular MR imaging could be done at the cost of an X-Ray.

3705 Computer 19

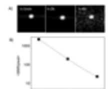

Development of nanometer size silicon nanoparticles for hyperpolarized MRI

Grzegorz Kwiatkowski[1], Jonas Steinhauser[1], Patrick Wespi[1], Matthias Ernst[2], and Sebastian Kozerke[1]

[1]Institute for Biomedical Engineering, ETH Zurich, Zurich, Switzerland, [2]Physical Chemistry, ETH Zurich, Zurich, Switzerland

Hyperpolarized silicon particles have been shown to exhibit enormously long T_1 relaxation at room temperature, making them favourable as novel imaging MR probes. To date, only large particles (average particle size (APS)=2.2 μm) could be efficiently polarized, restricting their in-vivo applicability.

The objective of the present work was to develop nanometre size hyperpolarized silicon-29 particles (APS= 55+/-12 nm) with superior MR properties. A maximum achievable polarization of 12.6% is reported with relaxation time of 42 min at room temperature. Applications of imaging of both solid and colloidal dispersion of silicon particles are demonstrated.

3706 Computer 20

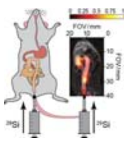

Hyperpolarized Magnetic Resonance Imaging of Silicon Microparticles Functionalized with Mucin Antibody: Towards Molecular Targeting of Colorectal Cancer

Nicholas Whiting[1], Jingzhe Hu[1,2], Julie X Liu[3], Klaramari Gellci[1,4], Pamela Constantinou[3], Jennifer Davis[5], Niki Zacharias Millward[1], David G Menter[6], Daniel Carson[3], and Pratip Bhattacharya[1]

[1]Department of Cancer Systems Imaging, The University of Texas MD Anderson Cancer Center, Houston, TX, United States, [2]Department of Bioengineering, Rice University, Houston, TX, United States, [3]Department of Biosciences, Rice University, Houston, TX, United States, [4]Department of Biomedical Engineering, Wayne State University, Detroit, MI, United States, [5]Department of Epidemiology, The University of Texas MD Anderson Cancer Center, Houston, TX, United States, [6]Department of Gastrointestinal Medical Oncology, The University of Texas MD Anderson Cancer Center, Houston, TX, United States

Hyperpolarized silicon nano- and microparticles hold great promise as targeted molecular imaging agents due to their overall biocompatibility and long-lasting enhanced MRI signals. We performed dynamic nuclear polarization on silicon microparticles that were functionalized with an antibody that targets Mucin overexpression in colorectal cancer. Conjugation of the antibody to the particle surface did not affect the ^{29}Si hyperpolarization characteristics, and *in vivo* imaging was attained 20 minutes after particle injection into a colorectal cancer mouse model. The goal is to develop these targeted particles as a platform technology that will allow non-invasive screening of colorectal cancer using ^{29}Si MRI.

3707 Computer 21

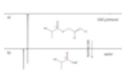

13C-MR Hyperpolarization of Lactate using ParaHydrogen and metabolic transformation in vitro.

Eleonora Cavallari[1], Carla Carrera[1], Silvio Aime[1], and Francesca Reineri[1]

[1]Department of Molecular Biotechnology and Health Sciences, University of Torino, Torino, Italy

Hyperpolarization (HP) of the 13C magnetic resonance signal of [1-13C]-lactate has been obtained using the ParaHydrogen Induced Polarization by means of Side Arm Hydrogenation (PHIP-SAH). Different ester derivatives of lactate have been tested in order to optimize the hydrogenation kinetics and the polarization level on the product. The metabolic transformation of hyperpolarized [1-13C]-lactate into pyruvate has been observed in vitro. The bio-compatibility of the aqueous solution and the good polarization level (7.9±0.4%) make the hyperpolarized metabolite thus obtained a good candidate for metabolic imaging studies.

3708 Computer 22

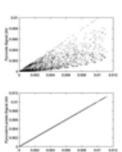

Combined Hyperpolarized Pyruvate and Lactate as a Proxy for Hyperpolarized Urea to Measure Tissue Perfusion

Christopher M Walker[1], Keith A Michel[1], Rafal J Zielinski[2], Waldemar Priebe[2], Dawid Schellingerhout[3], and James A Bankson[1]

[1]Department of Imaging Physics, UT MD Anderson Cancer Center, Houston, TX, United States, [2]Department of Experimental Therapeutics, UT MD Anderson Cancer Center, Houston, TX, United States, [3]Department of Diagnostic Radiology, UT MD Anderson Cancer Center, Houston, TX, United States

Hyperpolarized pyruvate can be used to noninvasively probe metabolism in vivo. However, quantitative measurement of metabolic processes is frequently complicated by tissue perfusion. Metabolic inert compounds such as hyperpolarized urea have been used to measure tissue perfusion. This work shows a strong correlation between hyperpolarized urea signal and the sum of hyperpolarized pyruvate and lactate signal, suggesting that the combination of pyruvate and lactate signals can be used to estimate tissue perfusion.

3709 Computer 23

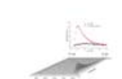

Measuring cerebral glucose metabolism in vivo using hyperpolarized 13C labelled glucose

Mor Mishkovsky[1,2], Brian Anderson[3], Magnus Karlsson[4], Mathilde H Lerche[4], A Dean Sherry[3], Rolf Gruetter[1,5,6], Zoltan Kovacs[3], and Arnaud Comment[2,7]

[1]Laboratory for Functional and Metabolic Imaging, Ecole Polytechnique Federale de Lausanne (EPFL), Lausanne, Switzerland, [2]Institute of Physics of Biological Systems, Ecole Polytechnique Federale de Lausanne (EPFL), Lausanne, Switzerland, [3]Advanced Imaging Research Center, University of Texas Southwestern Medical Center, Dallas, TX, United States, [4]Albeda Research, ApS, Copenhagen, Denmark, [5]Department of Radiology, Universite de Lausanne, Lausanne, Switzerland, [6]Department of Radiology, Geneva University Hospital and Faculty of Medicine, Geneva, Switzerland, [7]General Electric Healthcare, Buckinghamshire HP8 4SP, United Kingdom

Real-time glucose metabolism was observed in healthy mice brain following infusion of hyperpolarized [U-^{2}H, U-^{13}C]glucose and [U-^{2}H, 3,4-^{13}C] glucose. The evolution of lactate formation was readily observed. In addition, two glycolysis metabolites, namely 3-phosphoglycerate and pyruvate, were identified. Abnormalities in cerebral glucose metabolism is associated with large number of diseases so implementation of this method may prove useful in imaging brain metabolism in various animal models.

3710 Computer 24

Production of Highly Polarized Acetate by Rapid Decarboxylation of Pyruvate – Application to Hyperpolarized Cardiac Spectroscopy

Jonas Steinhauser[1], Grzegorz Kwiatkowski [1], Patrick Wespi[1], and Sebastian Kozerke[1]

[1]Institute for Biomedical Engineering, University and ETH Zurich, Zurich, Switzerland

In this work rapid decarboxylation of [1,2-13C]pyruvate using hydrogen peroxide was employed to obtain hyperpolarized [1-13C]acetate. 13C polarization was transferred completely and reproducibly. The application of the concept is demonstrated for detecting [1-13C]acetate and [1-13C]acetylcarnitine in the in-vivo heart.

Electronic Poster

Relaxation: Methods & Others

Exhibition Hall | Monday 17:15 - 18:15

3711 Computer 25

Development of magnetic resonance fingerprinting (MRF) combined with FISP and multi-echo SPGR acquisition for proton density, T1, T2, T2* and field mapping.

Dongyeob Han[1], Taehwa Hong[1], and Dong-Hyun Kim[1]

[1]School of Electrical & Electronic Engineering, Yonsei University, Seoul, Korea, Republic of

Magnetic resonance fingerprinting (MRF) is a novel technique which provides rapid proton density, T1 and T2 mapping. However, susceptibility related parameters such as T2* were not acquired simultaneously. In this study, FISP and multi-echo SPGR acquisition were combined within MRF scheme to allow proton density, T1, T2, T2* and field mapping.

3712 Computer 26

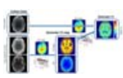

Direct Relaxation Measurement from Clinical Sequences

Kelly C McPhee[1] and Alan H Wilman[2]

[1]Physics, University of Alberta, Edmonton, AB, Canada, [2]Biomedical Engineering, University of Alberta, Edmonton, AB, Canada

Through exact sequence response modeling using the Bloch equations, we propose direct extraction of quantitative T1 and T2 relaxation maps from standard clinical MRI sequences. This approach eliminates the need for excess specialized and complex sequences by measuring relaxation directly from clinical sequences. We demonstrate this method to determine T2 and T1 using a standard brain protocol of fast spin echo images weighted by proton-density, T2 and FLAIR at 3 T. Our approach opens the door to wider use of quantitative MRI.

3713 Computer 27

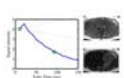

Whole Body Rapid T2 Quantification using Dual Echo Fast Spin Echo

Kelly C McPhee[1], Ashmita De[2], and Alan H Wilman[2]

[1]Physics, University of Alberta, Edmonton, AB, Canada, [2]Biomedical Engineering, University of Alberta, Edmonton, AB, Canada

We examine RF field variation on a modern 3T and illustrate T2 quantification using only PD and T2w fast spin echo images and a rapid flip angle map in the abdomen, spine, head, neck, and leg. Across the whole body at 3T or higher fields, RF field variation yields a wide variation in flip angles, requiring direct sequence modelling to achieve accurate T2.

3714 Computer 28

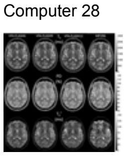

SNR Efficiency in Multi-Parameter Mapping (PD, T1 & T2*) at 3T: Comparison of MP2RAGE and VFA-FLASH

Jean-David Jutras[1], Keith Wachowicz[1,2], Guillaume Gilbert[3], and Nicola De Zanche[1,2]

[1]Oncology, University of Alberta, Edmonton, AB, Canada, [2]Medical Physics, Cross Cancer Institute, Edmonton, AB, Canada, [3]MR Clinical Science, Philips Healthcare Canada, Markham, ON, Canada

Quantitative parametric mapping is becoming increasingly promising for improving the diagnostic quality and reproducibility of structural brain MR images. The variable flip angle technique with FLASH (VFA-FLASH) is a popular technique for mapping the proton-density, T_1 and T_2^*. Recently, the MP2RAGE pulse sequence was developed to map T_1 with robustness to RF inhomogeneity. If a multi-echo (bipolar) MP2RAGE is employed, proton-density and T_2^* can also be mapped simultaneously. In this study we compare the SNR efficiency and accuracy of VFA-FLASH and MP2RAGE for multi-parameter mapping at 3T. Both methods yield comparable T_1-to-noise ratios, but VFA-FLASH is superior for PD and T_2^* mapping.

3715 Computer 29

Correction of off-resonance for T1 and T2 mapping using phase-cycled inversion-recovery balanced steady state free precession

Eric R. Muir[1] and Shengwen Deng[2,3]

[1]Research Imaging Institute and Ophthalmology, University of Texas Health Science Center, San Antonio, TX, United States, [2]Research Imaging Institute, University of Texas Health Science Center, San Antonio, TX, United States, [3]Biomedical Engineering, University of Texas at San Antonio, San Antonio, United States

Fast measurement of T1 and T2 can be made using inversion-recovery Look-Locker (LL) bSSFP methods. However, the LL-bSSFP signal is dependent on the off-resonance frequency which can affect calculated T1 and T2. In this study we develop and test methods to correct for effects of off-resonance on T1 and T2 calculation using multiple phase-cycled LL-bSSFP. The phase-cycled LL-bSSFP data could be combined with a maximum-T1* projection method to improve T1 and T2 accuracy in the case of off-resonance.

3716 Computer 30

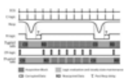

Whole Body T1 Mapping of Small Animals using Prospective Gating and Variable Flip Angle Imaging

Paul Kinchesh[1], Philip D Allen[1], John S Beech[1], Stuart Gilchrist[1], Ana L Gomes[1], Veerle Kersemans[1], Robert Newman[1], Borivoj Vojnovic[1], Michael Brady[1], Ruth J Muschel[1], and Sean C Smart[1]

[1]CRUK/MRC Oxford Institute for Radiation Oncology, University of Oxford, Oxford, United Kingdom

Prospective gating and automatic reacquisition of data corrupted by respiration motion were implemented in variable flip angle (VFA) and actual flip angle imaging (AFI) scans to enable cardio-respiratory synchronised T_1 mapping of the whole mouse. T_1 calculation for each mouse took approximately 6 s using a robust and efficient nonlinear least squares process. 16 cardio-respiratory gated VFA scans and a respiration gated AFI scan were acquired in less than 14 minutes. T_1 was calculated in the whole mouse with a voxel size of 0.075 mm^3 and with a standard deviation less than 6.2% within ROIs from multiple organs.

3717 Computer 31

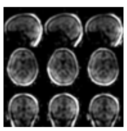

Motion Corrected T1 Mapping of the Pediatric Human Brain

Steven R Kecskemeti[1] and Andrew Alexander[1,2,3]

[1]Waisman Center, University of Wisconsin, Madison, WI, United States, [2]Psychiatry, [3]Medical Physics, University of Wisconsin, Madison, WI, United States

A method to retrospectively correct both in- and through-plane motions that occur during the acquisition of inversion recovery images is developed and used for motion-corrected T1-mapping of the pediatric human brain. Both intra- and inter-scan motions are corrected.

3718 Computer 32

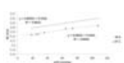

Fast T1 mapping with temperature correction via DWI thermometry, and it application to vitreous oxygen measurement

Shengwen Deng[1], Eric Muir[2], Wei Zhou[3], and Timothy Q. Duong[2]

[1]University of Texas Health Science Center at San Antonio, San Antonio, TX, United States, [2]University of Texas Health Science Center at San Antonio, [3]Radiology, Mayo Clinic

T1 mapping is showing great potential for mapping oxygen in human organs such as eyes and lungs. And yet, accuracy of oxygen using fast T1 imaging methods is of great concern especially in tissue with radical temperature changes. In the current study we improve fast T1 mapping with temperature correction and explore its potential in mapping oxygen in eyes. With combination of inversion-recovery Look-Locker bSSFP and diffusion weighted thermometry, we calibrate the temperature dependence of ADC and T1, and use it to adjust the R1 for measuring partial pressure of oxygen(pO2). Fast T1 mapping could be a reliable way to pO2 that well agrees with invasive oxygen-sensitive optic fibers.

3719 Computer 33

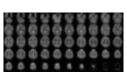

A rapid, whole-brain look-locker method for T1 mapping using inversion recovery EPIK

N. Jon Shah[1,2] and Seong Dae Yun[1]

[1]Institute of Neuroscience and Medicine, Medical Imaging Physics (INM-4), Forschungszentrum Juelich, Juelich, Germany, [2]Faculty of Medicine, Department of Neurology, JARA, RWTH Aachen University, Aachen, Germany

Quantitative measurement of the T_1 relaxation time is of great importance for the clinical diagnosis or optimisation of image contrast. Numerous Look-Locker method have been proposed for T_1 mapping. One of them demonstrated by the community is TAPIR which has been shown to be fast and robust. However, TAPIR still demands substantial acquisition time for whole-brain coverage. This work aims to develop a fast Look-Locker method with whole-brain coverage on a basis of EPIK. It was shown that the proposed method acquired whole-brain T_1 data (2.1 mm^2 resolution × 50 slices × 30 time-points) within 3.5 minutes.

3720 Computer 34

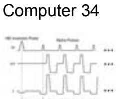

Rapid high-resolution 3D T1 mapping using a highly accelerated radial inversion-recovery FLASH technique

Zhitao Li[1], Ali Bilgin[2,3], Diego R. Martin[4], and Maria I. Altbach[4]

[1]Electrical and Computer Engineering, The University of Arizona, Tucson, AZ, United States, [2]Electrical and Computer Engineering, The University of Arizona, [3]Biomedical Engineering, The University of Arizona, [4]Department of Medical Imaging, The University of Arizona

A golden angle radial IR-FLASH technique and a principle component based iterative algorithm are developed for high-resolution T1 mapping using highly undersampled 3D radial data. The novel method yields T1 maps of a 3D volume with high spatial and temporal resolution and can cover 144 slices within 5 minutes.

3721 Computer 35

Quantitative 3D T1 mapping technique in rat brain using VFA-FLASH at 9.4T

Hedok Lee[1], Simon Sanggaard[2], Kristian Mortensen[2], Palle Koch[2], Maiken Nedergaard[2,3], and Helene Benveniste[1]

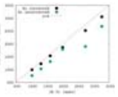

[1]Anesthesiology, Yale University, New Haven, CT, United States, [2]Center for Basic and Translational Neuroscience, University of Copenhagen, Copenhagen, Denmark, [3]Neurosurgery, University of Rochester, NY, United States

3D whole brain T1 mapping technique at 9.4T is studied because of a lack of methodological consideration in spite of its utility in pre-clinical paramagnetic and manganese contrast enhanced imaging studies. We report a simple and accurate 3D T1 mapping technique using variable flip angles spoiled gradient echo sequence with B1+ correction. Accuracy of the technique was validated using phantoms and a population averaged 3D rat T1 map was constructed.

3722 Computer 36

Model-Based Super-Resolution Reconstruction of T2 Maps

Tom Hilbert[1,2,3], Jose P Marques[4], Jean-Philippe Thiran[2,3], Reto Meuli[2], Gunnar Krueger[2,3,5], and Tobias Kober[1,2,3]

[1]Advanced Clinical Imaging Technology, Siemens Healthcare AG, Lausanne, Switzerland, [2]Department of Radiology, University Hospital (CHUV), Lausanne, Switzerland, [3]LTS5, École Polytechnique Fédérale de Lausanne, Lausanne, Switzerland, [4]Donders Institute, Radboud University, Nijmegen, Netherlands, [5]Siemens Medical Solutions USA, Inc., Boston, MA, United States

We propose an algorithm that can reconstruct 0.9mm³ isotropic T2 maps based on multiple 2D multi-echo spin-echo acquisitions that were highly undersampled. The data is reconstructed by combining a classical super-resolution approach with an iterative model-based reconstruction. Thereby, the reconstruction problem is split into multiple sub-problems to improve the convergence of the algorithm. Resulting T2 values within structures of the midbrain and the hippocampus from four healthy volunteers showed good reproducibility. This kind of high-resolution relaxometry may enable additional insight in pathologies of small brain structures and increased sensitivity to disease-induced changes.

3723 Computer 37

A time domain signal equation for multi-echo spin-echo sequences with arbitrary exciation and refocusing angle and phase

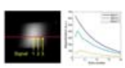

Andreas Petrovic[1], Christoph Stefan Aigner[1], and Rudolf Stollberger[1]

[1]Institute of Medical Engineering, Graz University of Technology, Graz, Austria

T_2 quantification with multi-echo spin-echo sequences is often hampered by flip angle inhomogeneities and non-rectangular slice profiles. Here, we present a novel time domain signal equation for multi-echo spin-echo sequences with arbitrary excitation and refocusing flip angles and phases. To evaluate the equation simulations and phantom measurements were compared. Excellent agreement was found for the simulated and measured evolution of the transverse magnetization across the slice profile in a CP and a CPMG sequence. T_2 mapping using the proposed signal equation and the incorporation of scanner specific RF pulse shapes will greatly improve T_2 quantification accuracy.

3724 Computer 38

Assessing the Accuracy of T2 and B1+ Maps Estimated from Multi-echo Spin Echo MRI Sequences Using Extended Phase Graph Signal Predictions

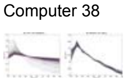

Nuno Saraiva Santos[1,2], Rui Pedro A G Teixeira[3], Joseph V Hajnal[3], and Rita G Nunes[1,2,3]

[1]Institute for Systems and Robotics / Department of Bioengineering, Instituto Superior Técnico, Universidade de Lisboa, Lisbon, Portugal, [2]Instituto de Biofísica e Engenharia Biomédica, Faculdade de Ciências, Universidade de Lisboa, Lisbon, Portugal, [3]Division of Imaging Sciences and Biomedical Engineering, King's College London, London, United Kingdom

Interpretation of T2-weighted images still remains highly reliant on subjective clinical evaluation. Quantitative mapping using the gold standard approach (single spin-echo), although appealing, remains unfeasible in clinical practice. Multi-SE sequences have emerged as viable solutions allowing much shorter scan times at the expense of signal contamination by indirect echoes. A method based on the MR Fingerprinting concept has recently been proposed, estimating T2 and B1+ maps from pre-computed Echo Modulation Curves. This study evaluated the performance of this method performing Monte Carlo simulations followed by an *in vivo* acquisition. The method provided accurate T2 maps, despite highly biased B1+ estimates.

3725 Computer 39

High-resolution 3D T2 mapping of the Brain Using T2-prepared Cartesian Spiral Phyllotaxis FLASH and Compressed Sensing

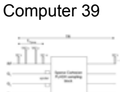

Emilie Priscille Claire Mussard[1,2,3], Tom Hilbert[1,2,3], Christoph Forman[4], Reto Meuli[2], Jean-Philippe Thiran[3], and Tobias Kober[1,2,3]

[1]Advanced Clinical Imaging Technology, Siemens Healthcare AG, Lausanne, Switzerland, [2]Department of Radiology, University Hospital (CHUV), Lausanne, Switzerland, [3]LTS5, École Polytechnique Fédérale de Lausanne (EPFL), Lausanne, Switzerland, [4]HC DI MR PI TIO CARD, Siemens Healthcare GmbH, Erlangen, Germany

Brain T2 relaxometry can provide sensitive biomarkers for pathological tissue alterations, especially inflammation. But their acquisition is often 2D-based and typically comes with long acquisition times. To improve through-slice resolution while keeping a clinically feasible scan time, we propose a centric T2-prepared variable-density Cartesian spiral phyllotaxis FLASH sequence combined with a compressed sensing reconstruction. Phantom experiments and a preliminary in-vivo scan show that T2 values can be reliably measured in 3D with high resolution. Parameter dependencies are evaluated and an initial protocol optimisation yields an acquisition time of 8.48min for a 1x1x1.2mm3 whole-brain acquisition.

3726 Computer 40

Approaching the Limits of Imaging Brain Tissue with Ultra Short T2

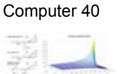

Christoph Alexander Rettenmeier[1] and V. Andrew Stenger[2]

[1]JABSOM, University of Hawai'i, Honolulu, HI, United States, [2]JABSOM, University of Hawai'i

A 3D radial UTE sequence optimized for the selective detection of fast relaxing tissue in the range of 500-60 µs using a composite hard pulse is presented. Its imaging properties on a T2-phantom are analyzed and used for the discussion of human brain images.

3727 Computer 41

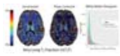

Exploring the Utility of Temporal Phase Correction in Multi-Echo T2 Relaxation at 3T

Emil Ljungberg[1], Alykhan Thobani[1], Thorarin A Bjarnason[2,3,4], Piotr Kozlowski[2], Alexander Rauscher[5], Jing Zhang[6], Anthony Traboulsee[1], Cornelia Laule[2,7,8], Alex MacKay[2,9], and Shannon Kolind[1,2]

[1]Medicine, University of British Columbia, Vancouver, BC, Canada, [2]Radiology, University of British Columbia, Vancouver, BC, Canada, [3]Diagnostic Imaging Services, Interior Health, Kelowna, BC, Canada, [4]Computer Science, Mathematics, Physics & Statistics, University of British Columbia, Kelowna, BC, Canada, [5]Pediatrics, University of British Columbia, Vancouver, BC, Canada, [6]GE Healthcare, Vancouver, BC, Canada, [7]Pathology & Laboratory Medicine, University of British Columbia, Vancouver, BC, Canada, [8]International Collaboration on Repair Discoveries, University of British Columbia, Vancouver, BC, Canada, [9]Physics and Astronomy, University of British Columbia, Vancouver, BC, Canada

T_2 relaxation using combined gradient and spin echo (GRASE) is a fast and robust approach for myelin water imaging in vivo. For long echo trains, when the noise floor is reached, the magnitude signal will converge towards a non-zero mean due to the Rician noise characteristics of the magnitude data. This can give rise to artificial long-T_2 components in analysis. In this study we employed temporal phase correction to multi-echo GRASE data and showed that for echo trains longer than 300ms, phase correction will effectively reduce artificial long-T_2 components, thus improving the ability to interpret the T_2 distribution.

3728 Computer 42

Correction of fixation effects in post-mortem T2 measurements using a kinetic tensor model

Feng Qi[1], Samuel A. Hurley[1], Menuka Pallebage-Gamarallage[2], Olaf Ansorge[2], Martin R. Turner[2], Ricarda A. L. Menke[2], Sean Foxley[1], and Karla L. Miller[1]

[1]FMRIB Centre, University of Oxford, Oxford, United Kingdom, [2]Department of Neurology, University of Oxford, Oxford, United Kingdom

MRI of fixed post-mortem tissue can be used to relate MR signals to histopathology. However, MR relaxation parameters are altered by the process of fixation. We propose a “kinetic tensor” model that simulates the influx of fixative into the brain using diffusion tensor data, and demonstrate a correction by fitting a fixative concentration map to quantitative T2 measurements. Compared to correction methods based on distance-to-surface or isotropic diffusion, our approach captures an individual brain’s morphology and microstructure, both of which influence fixation. T2 maps corrected with the kinetic tensor model are more homogeneous than those with alternate corrections.

3729 Computer 43

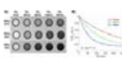

Ex vivo whole-blood $$$T_2$$$ versus $$$HbO_2$$$ calibration for $$$T_2$$$-prepared balanced steady-state free precession (bSSFP) at 1.5T

Ana E Rodríguez-Soto[1], Michael C Langham[1], Osheiza Abdulmalik[2], and Felix W Wehrli[1]

[1]Department of Radiology, University of Pennsylvania, Philadelphia, PA, United States, [2]Division of Hematology, The Children's Hospital of Philadelphia, Philadelphia, PA, United States

The transverse relaxation rate ($1/T_2$) of blood water protons is governed by deoxyhemoglobin concentration, therefore providing a means to determine oxygen saturation (HbO_2) in vivo. However, besides CPMG inter-pulse interval of the T_2 preparation and field strength, whole-blood T_2 depends on sequence-specific parameters. Balanced SSFP allows for rapid image acquisition and higher in-plane resolution and thus provides an ideal readout for T_2-based oximetry. Here, we quantified T_2 of human blood at 1.5T for the entire range of HbO_2 saturation levels using T_2-prepared bSSFP sequence. The data show the expected linearity of $1/T_2$ with $(1\text{-}HbO_2)^2$ with the y-intercept depending on hematocrit.

3730 Computer 44

Inversion-recovery Ultrashort Echo Time Imaging with Bi-component T2* Analysis of White Matter Signals in Native and Deuterated Ovine Brain Specimens

Shu-Juan Fan[1], Yajun Ma[1], Eric Y Chang[1,2], and Jiang Du[1]

[1]Dept. of Radiology, University of California, San Diego, San Diego, CA, United States, [2]Radiology Service, VA San Diego Healthcare System, San Diego, CA, United States

Myelin protons have ultrashort-lived MR signals and are not accessible by clinical MRI. Such signals were probed herein using ultrashort echo time imaging (UTE) and inversion-recovery UTE (IR-UTE) with bi-component analysis in native and deuterated ovine brain specimens. UTE detected a fraction of ultrashort T2 components (STC) of < 4% in native specimens, and up to ~54% in deuterated specimens. Choice of inversion time in IR-UTE significantly affected such bi-component signal decay behavior in native samples in heavily deuterated samples. These results support the application of UTE and IR-UTE in quantitative myelin imaging.

3731 Computer 45

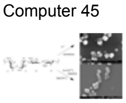

Novel nanogel-based MRI Contrast Agents

Brendan Garrett[1], Simon Duckett[2], David K. Smith[1], and Victor Chechik[1]

[1]Department of Chemistry, University of York, YORK, United Kingdom, [2]Centre for Hyperpolarisation in Magnetic Resonance, University of York, YORK, United Kingdom

We present here the preparation and properties of new Gd^{3+}-containing nanogel-based contrast agents. These gel nanoparticles are prepared by simple ionotropic gelation from sodium alginate and Gd^{3+}. The nanogels are 100-200 nm in diameter and have a high R_1 relaxivity of ≈ 30 mM^{-1} s^{-1} at 1 T, however, they have poor stability in high ionic strength media. Adding further covalent crosslinks with a suitable agent such as epichlorohydrin dramatically increased the relaxivity of the nanogels to ≈ 60 mM^{-1} s^{-1} at 1 T and provides a viable strategy to increases their stability against transmetallation.

3732 Computer 46

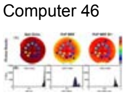

Quantitative validation of Spin Echo and Magnetic Resonance Fingerprinting derived Proton Density using the qMRI Phantom

Gregory Lemberskiy[1,2], Els Fieremans[1], Dmitry S Novikov[1], and Martijn Cloos[1]

[1]Radiology, NYU School of Medicine, New York, NY, United States, [2]Sackler Institute of Graduate Biomedical Sciences, NYU School of Medicine, New York, NY, United States

Proton density (PD) measurements derived from single Spin Echo and PnP-MRF, which is a fingerprinting protocol that enables simultaneous estimation of the excitation field (B1+), were validated using the ISMRM/NIST MRI system phantom that contains known D2O/H2O solutions at 14 different concentrations. We also expanded the PnP-MRF protocol by exploiting the symmetry between B1+ and the receive field, B1-, produced by a quadrature body coil at 3 Tesla in order to remove all B1 contribution from our PD. Ultimately, all methods showed remarkable correlation with the known water fraction from NIST samples (Pearson's rho>0.99).

3733 Computer 47

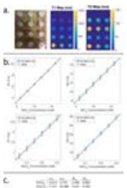

Toward 3D Printed, Anatomy-Mimicking, Quantitative MRI Phantoms

Karthik Gopalan[1], Jonathan I Tamir[1], Ana Claudia Arias[1], and Michael Lustig[1]

[1]Electrical Engineering and Computer Sciences, University of California, Berkeley, Berkeley, CA, United States

We aim to design and build reproducible phantoms with anatomy-mimicking resolution and image contrast. We mix solutions of paramagnetic ions in agar gel to target specific relaxation parameters. Chambers for different tissue types are 3D printed and filled with the agar gels. Microfiber cloths are added to create additional high-resolution structure. We validate the ability to reproduce target relaxation values through spin-echo imaging and quantitative mapping, and present two 3D printed phantom designs.

3734 Computer 48

Kitchen Safe T1 and T2 Phantom Creation

Kenneth O Johnson[1], N Okai Addy[1], Reeve Ingle[1], Michelle Nystrom[1], William Overall[1], Galen Reed[1], and Juan Santos[1]

[1]HeartVista, Los Altos, CA, United States

Typical magnetization prepared phantoms require paramagnetic salts such as copper, nickel and manganese chloride, which are toxic. Accordingly, governing bodies label these as hazardous materials requiring special storage, labeling and disposal. In search of a simpler and cheaper solution we have revisited this topic to make a kitchen-safe phantom recipe that is both cheap and easy to make. We used glycerine (a sweetener or for skin care) and Agar agar powder (a food additive for thickening or gel) to make phantoms with a physiological range of T1 and T2, and characterize these non-hazardous materials for 1.5 T MRI scanners.

Electronic Poster

CEST/MT/NOE: Animal Models & Human Translation

Exhibition Hall — Monday 17:15 - 18:15

3735 Computer 73

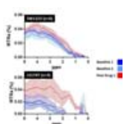

CEST imaging of an unlabelled chemotherapy agent (gemcitabine) 30 minutes after administration in a mouse model of colorectal cancer

Thomas A Roberts[1], May Zaw-Thin[1], Angela D'Esposito[1], Yanan Zhu[1], John J Connell[1], Mark F Lythgoe[1], and Simon Walker-Samuel[1]

[1]Centre for Advanced Biomedical Imaging, University College London, London, United Kingdom

Imaging of drug delivery is useful for improving our understanding of the physical factors that contribute to the efficacy of anticancer therapies. Gemcitabine, a standard chemotherapeutic agent, has two hydroxyl groups and one amine group, making it potentially amenable to CEST imaging via proton exchange with tissue water. Recently, Li et al. (2016) showed that many anticancer drugs can induce CEST contrast and demonstrated that liposome-encapsulated gemcitabine can be imaged 5-hours post-administration in a pre-clinical model of cancer[1]. Here, we extend this exciting work and investigate the use of CEST to image acute gemcitabine uptake within 30 minutes of administration.

3736 Computer 74

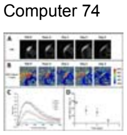

In Vivo Tracking of Hyaluronic Acid Hydrogel Degradation Using Temporal Evolution of Chemical Exchange Saturation Transfer Signal in a Mouse Subcutaneous Injection Model

Mohammed Salman Shazeeb[1], Rubina Corazzini[2], Dinesh Bangari[3], Robert Fogle[1], Jennifer Johnson[3], Paul J. Konowicz[2], Xiaoyou Ying[1], and Pradeep K. Dhal[2]

[1]Bioimaging, Translational In Vivo Models, Sanofi, Framingham, MA, United States, [2]Biomaterials, Sanofi, Framingham, MA, [3]Pathology, Translational In Vivo Models, Sanofi, Framingham, MA

Hyaluronic acid (HA) hydrogels have a wide range of applications in biomedicine from regenerative medicine to drug delivery applications. In vivo quantitative assessment of these hydrogels using magnetic resonance imaging (MRI) provides a powerful technique to assess the biodegradability of HA hydrogels. This study investigated the potential of chemical exchange saturation transfer (CEST) MRI in tracking HA hydrogels with varying degradation profiles in vivo in a mouse subcutaneous injection model over 77 days. Since CEST-MRI provides a unique chemical signature to visualize HA hydrogels, this technique can be used as a guide in hydrogel optimization process for drug delivery applications.

3737 Computer 75

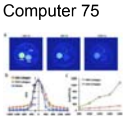

Magnetization Transfer MRI Noninvasively Detects Renal Fibrosis Swine Atherosclerotic Renal Artery Stenosis at 3.0 T

Kai Jiang[1], Christopher M. Ferguson[1], John R. Woollard[1], Roger C. Grimm[2], James D. Krier[1], Xiangyang Zhu[1], and Lilach O. Lerman[1]

[1]Division of Nephrology and Hypertension, Mayo Clinic, Rochester, MN, United States, [2]Department of Radiology, Mayo Clinic, Rochester, MN, United States

In this study, we tested the capability of magnetization transfer (MT) imaging for measuring renal fibrosis in a swine model of atherosclerotic renal artery stenosis (ARAS) at 3.0 T. A collagen phantom study was performed to select appropriate offset frequencies of MT pulses for collagen detection. In an in vivo study, the MT ratio (MTR) and percent change in MTR between two offset frequencies were quantified, and both showed a good correlation with renal fibrosis measured ex vivo by Picro-Sirius red staining, supporting the use of MT to assess renal fibrosis in swine ARAS.

3738 Computer 76

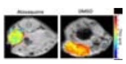

Modification of tumour hypoxia with Atovaquone measured by CEST MRI

Kevin J Ray[1], James Coates[1], Rathi Puliyadi[1], Thomas M Ashton[1], Paul Kinchesh[1], Sean Smart[1], Michael A Chappell[2], Geoff S Higgins[1], and Nicola R Sibson[1]

[1]*Oxford Institute for Radiation Oncology, Department of Oncology, University of Oxford, Oxford, United Kingdom,* [2]*Institute of Biomedical Engineering, Department of Engineering Science, University of Oxford, Oxford, United Kingdom*

Tumours often have areas of hypoxia, which renders cancer cells resistant to many therapies. Recently the anti-malarial drug Atovaquone has been shown to modify the oxygen consumption rate of cancer cells, reducing tumour hypoxia. Non-invasive mapping of tumour hypoxia would be particularly useful for translation of these preclinical findings into a clinical environment. Here, we tested the hypothesis that CEST MRI could be used to visualise changes in tumour hypoxia.

3739 Computer 77

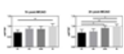

Investigation into the origin of the APT MRI signal in ischemic stroke

Kevin J Ray[1], James R Larkin[1], Brad A Sutherland[2,3], George Harston[2], Andrew Baldwin[4], Alastair M Buchan[2], Peter Jezzard[5], James Kennedy[2], Michael A Chappell[6], and Nicola R Sibson[1]

[1]*Oxford Institute for Radiation Oncology, Department of Oncology, University of Oxford, Oxford, United Kingdom,* [2]*Acute Stroke Programme and Acute Vascular Imaging Centre, Radcliffe Department of Medicine, University of Oxford, Oxford, United Kingdom,* [3]*School of Medicine, Faculty of Health, University of Tasmania, Hobart, Australia,* [4]*Physical and Theoretical Chemistry Laboratory, Department of Chemistry, University of Oxford, Oxford, United Kingdom,* [5]*Oxford Centre for Functional MRI of the Brain, Nuffield Department of Clinical Neurosciences, University of Oxford, Oxford, United Kingdom,* [6]*Institute of Biomedical Engineering, Department of Engineering Science, University of Oxford, Oxford, United Kingdom*

Studies employing CEST MRI to study ischemic stroke focus on the sensitivity of amide proton transfer (APT) MRI signals to tissue pH, assuming identical intracellular protein concentration as healthy tissue. This study shows that whilst cytoplasmic protein concentration remains stable in penumbral stroke regions, it decreases in the infarct core. By analysing APT MRI data with APTR*, which is specifically sensitive to amide proton exchange effects, we demonstrate that the APT signal change in infarct core is dominated by decreased protein concentration, whilst penumbral APT changes can be attributed to decreased tissue pH.

3740 Computer 78

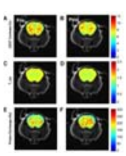

In Vivo Detection of Reactive Oxygen Species Using MRI with Endogenous Contrast

Rong-Wen Tain[1,2], Alessandro Scotti[1,2,3], Weiguo Li[4,5], Xiaohong Joe Zhou[1,2,3,6], Riya Thomas[7], Leon Tai[7], and Kejia Cai[1,2,3]

[1]*Radiology, University of Illinois at Chicago, Chicago, IL, United States,* [2]*Center for MR Research, University of Illinois at Chicago, Chicago, IL, United States,* [3]*Bioengineering, University of Illinois at Chicago, Chicago, IL, United States,* [4]*Research Resource Center, University of Illinois at Chicago, Chicago, IL, United States,* [5]*Radiology, Northwestern University, Chicago, IL, United States,* [6]*Neurosurgery, University of Illinois at Chicago, Chicago, IL, United States,* [7]*Anatomy and Cell Biology, University of Illinois at Chicago, Chicago, IL, United States*

Reactive oxygen species (ROS) contribute to pathogenesis of many human diseases including Parkinson’s and Alzheimer's diseases, cancer, and diabetes. There is a crucial need for using fully noninvasive imaging to further evaluate the role of ROS in pathogenesis and the potential treatment strategies. Our previous phantom studies demonstrated that ROS containing unpaired electrons can be detected with endogenous CEST and T_1 weighted contrasts. However, *in vivo* detection of ROS using MRI has not yet been demonstrated. This study therefore aimed to demonstrate the feasibility of *in vivo* ROS detection using endogenous MRI.

3741 Computer 79

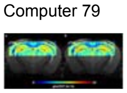

Imaging of neuronal compartment using gluCEST method

Jérémy Pépin[1], Pierrick Jego[1], Julien Valette[1], Gilles Bonvento[1], and Julien Flament[1,2]

[1]*Molecular Imaging Research Center (MIRCen), Commissariat à l’Energie Atomique (CEA), Fontenay-aux-Roses, France,* [2]*UMS27, INSERM, Fontenay-aux-Roses, France*

GluCEST imaging has been proposed to image brain glutamate distribution with a better resolution than spectroscopic methods and has many potential applications for the study of neurodegenerative diseases. In this study, we pushed further the limits of gluCEST imaging by combining high magnetic field and high performance cryoprobe to acquire gluCEST images with the best resolution so far. Thanks to the organization of hippocampal cell layers and the high resolution, we acquired gluCEST data in regions mostly reflecting the neuronal compartment.

3742 Computer 80

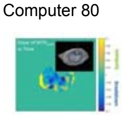

Assessment of hepatic glycogen metabolism ex vivo and in vivo in mice using chemical exchange saturation transfer MRI

Corin Miller[1], Jin Cao[1], Chunlian Zhang[1], Eduard Chekmenev[2], Bruce Damon[2], Alan Cherrington[3], and John Gore[2]

[1]*Translational Imaging Biomarkers, Merck & Co., Inc, West Point, PA, United States,* [2]*VUIIS, Vanderbilt University, Nashville, TN, United States,* [3]*Vanderbilt Medical Center, Vanderbilt University, Nashville, TN, United States*

Despite being integral to whole body glucose homeostasis, liver glycogen remains difficult to measure non-invasively. Recent works have demonstrated the feasibility of detecting liver glycogen using CEST MRI. In this presentation we present data that builds upon this observation and investigate whether CEST can be used to monitor glycogen synthesis and breakdown in mice in real time both ex vivo in a perfused liver system, and in vivo. Treatment with hyperglycemia or glucagon resulted in increases or decreases, respectively, in the CEST MTRasym AUC over time. This demonstrates that CEST-based approaches can be used to non-invasively monitor glycogen metabolism.

3743 Computer 81

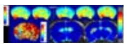

GlucoCEST MRI and brain blood barrier permeability in the mouse brain

Maria Yanez Lopez[1], Nicoleta Baxan[2], Miriam Ries[3], David Sharp[1], and Magdalena Sastre[3]

[1]The Computational, Cognitive and Clinical Neuroimaging Laboratory, Division of Brain Sciences, Department of Medicine, Imperial College London, London, United Kingdom, [2]The Imperial College Biological Imaging Centre, Department of Medicine, Imperial College London, London, United Kingdom, [3]Division of Brain Sciences, Department of Medicine, Imperial College London, London, United Kingdom

The aim of the study is to examine the feasibility of using GlucoCEST to evaluate subtle BBB dysfunction in the mouse brain, by comparing it with conventional gadolinium DCE. DCE and GlucoCEST showed no significant differences between WT and 5XFAD mice (3 months). However, the degree of the response after injection was similar for DCE and GlucoCEST for all animals except one, indicating shared contributions to the signal and supporting the potential for biodegradable d-glucose as a cheap, low-risk alternative/complement to DCE MRI. More work is required to assess GlucoCEST sensitivity to low-level BBB dysfunction, such as in Alzheimer's disease.

3744 Computer 82

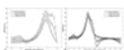

2-Deoxyglucose-Weighted MR Imaging in Rodent Brain Using Inverse Z-Spectrum Analytic Scheme

Ping-Huei Tsai[1,2,3], Fei-Ting Hsu[2,3], Hua-Shan Liu[3,4], Hsiao-Wen Chung[5], Yu-Chieh Kao[1,3], Chia-Feng Lu[1,3], Huai-Lu Chen[3,6], Paul Blakeley[3,6], Gilbert Aaron Lee[3,6], and Cheng-Yu Chen[1,2,3]

[1]Department of Radiology, School of Medicine, College of Medicine, Taipei Medical University, Taipei, Taiwan, [2]Department of Medical Imaging, Taipei Medical University Hospital, Taipei Medical University, Taipei, Taiwan, [3]Translational Imaging Research Center, College of Medicine, Taipei Medical University, Taipei, Taiwan, [4]School of Biomedical Engineering, College of Biomedical Engineering, Taipei Medical University, Taipei, Taiwan, [5]Graduate Institute of Biomedical Electrics and Bioinformatics, National Taiwan University, Taipei, Taiwan, [6]Department of Medical Research, Taipei Medical University Hospital, Taipei, Taiwan

Our proposed method provides an alternative to extract glucose profile and could be more robust to the field drift, which may be helpful in the implementation of in vivo brain glucoCEST imaging for further application.

3745 Computer 83

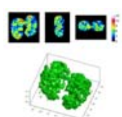

3D-CEST Imaging of a Mouse Model of Polycystic Kidney Disease

Shanrong Zhang[1], Matanel Yheskel[2], Vishal Patel[2], Masaya Takahashi[1], and A. Dean Sherry[1]

[1]Advanced Imaging Research Center, University of Texas Southwestern Medical Center, Dallas, TX, United States, [2]Department of Internal Medicine and Division of Nephrology, University of Texas Southwestern Medical Center, Dallas, TX, United States

The objective is to develop a new 3D-CEST imaging method (3-dimensional chemical exchange saturation transfer) to investigate a mouse model of polycystic kidney disease (PKD). It is based on 3D magnetization prepared rapid acquisition gradient echo sequence (3D MPRAGE) by applying a pre-saturation pulse consisting of three continuous Gauss shaped pulses.

3746 Computer 84

Z-spectrum acquisition and interpretation in the presence of fat: influence of imaging parameters

Shu Zhang[1], Jochen Keupp[2], Ivan E Dimitrov[3,4], Robert E Lenkinski[1,4], and Elena Vinogradov[1,4]

[1]Department of Radiology, UT Southwestern Medical Center, Dallas, TX, United States, [2]Philips Research, Hamburg, Germany, [3]Philips Medical Systems, Gainesville, FL, United States, [4]Advanced Imaging Research Center, UT Southwestern Medical Center, Dallas, TX, United States

CEST-MRI is increasingly evolving from brain to body applications. One of the known problems in body imaging is the presence of strong lipid signals. Their influence on the CEST signal is acknowledged but underexplored. The goal is to investigate the effects of lipids on the Z-spectrum taking TE into account. We performed simulations and verified the results in phantoms and *in vivo*. We demonstrate the mutual influence of fat fraction and TE on the Z-spectrum for gradient echo based sequences. This study provides a systematic understanding of lipid artifacts in CEST imaging and lays the foundations for their efficient removal.

3747 Computer 85

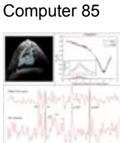

Monitoring neoadjuvant chemotherapy in breast cancer patients using CEST and 31P-MRS at 7 tesla

Erwin Krikken[1], Vitaliy Khlebnikov[1], Moritz Zaiss[2], Wybe J.M. van der Kemp[1], Tijl A. van der Velden[1], Hanneke W.M. van Laarhoven[3], Dennis W.J. Klomp[1], and Jannie P. Wijnen[1]

[1]Radiology, UMC Utrecht, Utrecht, Netherlands, [2]Max Planck Institute for Biological Cybernetics, Tubingen, Germany, [3]Oncology, Amsterdam Medical Center, Amsterdam, Netherlands

Treatment monitoring is of importance for breast cancer patients receiving systemic therapy. Metabolic imaging methods such as CEST and ^{31}P-MRS may have potential to predict treatment efficacy in an early stage of the treatment. In this study we assessed the amide proton transfer (APT) signal and the pH change in breast cancer patients before and after the first cycle of neoadjuvant chemotherapy to explore the relation between APT and pH. We observed changes in both the APT signal and the pH between the two measurements. These changes may serve as biomarkers for predicting treatment response to NAC in an early stage.

3748 Computer 86

Are MT and NOE (at -3.5 ppm) in z-spectroscopy coupled in the brain?

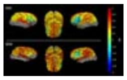

Nicolas Geades[1], Olivier E Mougin[1], Simon Shah[1], and Penny A Gowland[1]

[1]Sir Peter Mansfield Imaging Center, University of Nottingham, Nottingham, United Kingdom

The origin of the Nuclear Overhauser Enhancement (NOE) signal observed in the CEST spectrum of the brain is still under debate. The effect is detected upfield from water, in the frequency range of non-exchangeable aliphatic/olefinic protons, indicating that the transfer of magnetization is not occurring via proton or chemical exchange; furthermore the lineshape is relatively narrow, suggesting the signal is coming from mobile protons with T2 of the order of 300μs. This study investigates the correlation between NOE and MT in the human brain at 7T, and shows the two effects are strongly coupled, across a wide age range.

3749 Computer 87

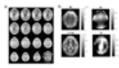

3D Quantitative CEST MRI of the human brain at 9.4T

Moritz Zaiss[1], Philipp Ehses[1], and Klaus Scheffler[1]

[1]Magnetic Resonance Center, Max-Planck-Institute for biological cybernetics, Tuebingen, Germany

Selective quantitative CEST MRI was shown to be feasible at 7T and for single-slice readout. In this study we extend qCEST MRI to a field strength of 9.4 T making use of the increase spectral resolution, and by employing a single-shot 3D CEST approach, more coverage of the human brain was realized.

3750 Computer 88

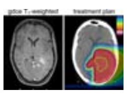

A longitudinal study of brain tumors in the course of radiotherapy using protein CEST MRI at 7T

Jan-Eric Meissner[1], Andreas Korzowski[1], Sebastian Adeberg[2], Steffen Goerke[1], Nicolas Behl[1], Heinz-Peter Schlemmer[3], Jürgen Debus[2], Mark E. Ladd[1], Peter Bachert[1], and Daniel Paech[3]

[1]Medical Physics in Radiology, German Cancer Research Center, Heidelberg, Germany, [2]Radiation Oncology, University Hospital of Heidelberg, Heidelberg, Germany, [3]Radiology, German Cancer Research Center, Heidelberg, Germany

Chemical Exchange Saturation Transfer (CEST) offers unique contrasts sensitive to micro environmental information such as protein concentration and pH. Thus CEST could be a promising biomarker to investigate radiotherapy-induced changes in tissue. In this study we examine brain tumor patients in the course of definitive radiotherapy on a 7 T whole-body scanner using the relaxation compensated contrast AREX. We compare the results of CEST imaging to Single Voxel Spectroscopy and high-resolution T_2-weighted imaging.

3751 Computer 89

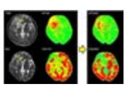

Voxel-wise comparison of amide proton transfer (APT) weighted image and fluorodeoxyglucose (FDG)-PET in brain tumors with a PET/MR system

Koji Sagiyama[1], Yuji Watanabe[2], Ryotaro Kamei[1], Sungtak Hong[3], Jochen Keupp[4], and Hiroshi Honda[1]

[1]Department of Clinical Radiology, Kyushu University Graduate School of Medical Sciences, Fukuoka, Japan, [2]Department of Molecular Imaging and Diagnosis, Kyushu University Graduate School of Medical Sciences, Fukuoka, Japan, [3]Healthcare, Philips Electronics Japan, [4]Philips Research

Amide proton transfer (APT) imaging has been reported to be useful for assessing malignancy or evaluating treatment efficacy. In this study, we evaluated the validity of APT signals in brain tumors by direct voxel-wise comparison with standardized uptake values (SUVs) from fluorodeoxyglucose positron emission tomography (FDG-PET) on a PET-magnetic resonance (PET/MR) system. APT imaging showed discrepancies with FDG-PET due to structural inhomogeneity, and the correlation between APT signals and SUVs was poor. The correlation was significantly improved after correcting for the apparent diffusion coefficient (ADC). APT/ADC could be a reliable metabolic marker with better correlation with SUVs.

3752 Computer 90

Repeatability study of APT CEST quantification techniques for identification of ischaemic penumbra in stroke

Yunus Msayib[1,2], George W. J. Harston[3], Yee K. Tee[4], Fintan Sheerin[3], Nicholas P. Blockley[5], Thomas W. Okell[5], Peter Jezzard[5], Stephen Payne[1], James Kennedy[3], and Michael A. Chappell[1]

[1]Engineering Science, University of Oxford, Oxford, United Kingdom, [2]Centre for Doctoral Training in Healthcare Innovation, University of Oxford, Oxford, United Kingdom, [3]Radcliffe Department of Medicine, University of Oxford, [4]Department of Mechatronics and Biomedical Engineering, Universiti Tunku Abdul Rahman, [5]Nuffield Department of Clinical Neurosciences, University of Oxford

The aim of this study was to identify the analysis technique with the optimum repeatability for quantifying APT CEST imaging for use in the clinical setting. The repeatability of eight quantification techniques was assessed across imaging time points in healthy subjects, and between the contralateral hemispheres of stroke patients. Model-based techniques exhibited better repeatability compared to simpler model-free methods, and are thus better-suited for use in clinical imaging at 3T.

3753 Computer 91

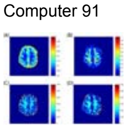

Chemical exchange rotation transfer (CERT) of human brain at 3 T

Eugene C. Lin[1], Hua Li[1], Zhongliang Zu[1], Elizabeth A. Louie[1], Xiaoyu Jiang[1], and Daniel F. Gochberg[1]

[1]Vanderbilt University Institute of Imaging Science, Nashville, TN, United States

It has been shown that the changes in chemical exchange saturation transfer (CEST), and specifically amide proton transfer (APT) and nuclear Overhauser effect (NOE), reflect abnormal tissues in tumor, stroke and other diseases. However, quantitative and specific imaging of these effects is challenging due to the influences from asymmetric magnetization transfer and direct water saturation. These obstacles can be avoided with chemical exchange rotation transfer (CERT), which is a pulsed version of CEST with the constraint of constant average power and varying rotation angle. In this study, we present initial CERT results in human brain at 3 T, with the goal of quantifying APT and NOE.

3754 Computer 92

The Chemical Exchange Saturation Transfer (CEST) and Nuclear Overhauser Enhancement (NOE) effects observed in human blood at 7 T under different physiological conditions.

Simon Shah[1], Olivier Mougin[1], Andrew Carradus[1], Nicolas Geades[1], William Morley[1], and Penny Gowland[1]

[1]Sir Peter Mansfield Imaging Centre, School of Physics and Astronomy, University of Nottingham, Nottingham, United Kingdom

CEST maps at 7T display higher APT and amine signal from the sagittal-sinus compared to elsewhere in the brain. We investigate CEST and NOE signals detected in *ex-vivo* blood under with varying oxygenation, haematocrit levels, pH and cell structure. Showing that human blood produces significant amounts of CEST and NOE, dominated by the cellular components of blood and independent of blood oxygenation. Clotting and lysing red-blood-cells has no impact on the observed CEST and NOE. We also observed increased APT and NOE with increasing pH. These result are important when interpreting exchange in conditions associated with blood volume change.

3755 Computer 93

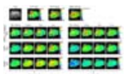

Optimization of Amide Proton Transfer (APT) Imaging Experimental Parameters for Brain Tumors: Does RF Saturation Length Always Increase APT Contrast?

Hye-Young Heo[1,2], Yi Zhang[1], Shanshan Jiang[1], and Jinyuan Zhou[1,3]

[1]Russell H Morgan Department of Radiology and Radiological Science, Johns Hopkins University, Baltimore, MD, United States, [2]F.M. Kirby Research Center for Functional Brain Imaging, Kennedy Krieger Institute, Baltimore, United States, [3]F.M. Kirby Research Center for Functional Brain Imaging, Kennedy Krieger Institute, Baltimore, MD, United States

Current APT imaging studies have used a moderate repetition time or relaxation delay to reduce the scan time. However, when a relatively short relaxation delay compared with T_1 is applied, the steady-state water longitudinal magnetization is reduced, resulting in a decrease in APT effect. Therefore, experimental parameters must be optimized on a combination of the RF saturation power, saturation length, and relaxation delay. Here, we quantitatively investigated the dependence of APT and NOE signals on the experimental parameters using Bloch simulations and rat brain tumor models at 4.7 T.

3756 Computer 94

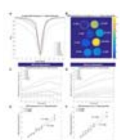

Development of Glutamate-Sensitive CEST at Clinical Field Strength for In Vivo Application

Kristin P. O'Grady[1,2], Samantha By[2,3], Bailey A. Box[1,2], and Seth A. Smith[1,2,3]

[1]Department of Radiology and Radiological Sciences, Vanderbilt University Medical Center, Nashville, TN, United States, [2]Vanderbilt University Institute of Imaging Science, Vanderbilt University Medical Center, Nashville, TN, United States, [3]Department of Biomedical Engineering, Vanderbilt University, Nashville, TN, United States

Cognitive impairment (CI) is a significant symptom of multiple sclerosis (MS), is the strongest predictor of unemployment in MS patients, and is critical to the decline of quality of life. There is an unmet need for imaging techniques that probe the pathological substrate of CI at a clinically relevant field strength. To address this need, we have investigated the translation of glutamate-sensitive chemical exchange saturation transfer (GluCEST) MRI to 3T, as glutamate abnormalities have been linked to CI in MS. Our results demonstrate the clinical feasibility of GluCEST imaging for application to studying cortical gray matter glutamate signals *in vivo*.

3757 Computer 95

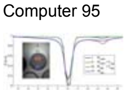

Correction of fat artifacts for unbiased CEST-MRI of the human breast at 7 T

Ferdinand Zimmermann[1], Steffen Görke[1], Johannes Breitling[1], Kerstin Klopries[2], Johannes Windschuh[1], Heinz-Peter Schlemmer[2], Mark Edward Ladd[1], Daniel Paech[2], and Peter Bachert[1]

[1]Medical Physics in Radiology, German Cancer Research Center, Heidelberg, Germany, [2]Division of Radiology, German Cancer Research Center, Heidelberg, Germany

Chemical Exchange Saturation Transfer (CEST) MRI in the mammary gland is affected by the high fat content in the human breast. Chemical shift induced artifacts are visible in the Z-Spectrum. We showed a method to test and verify water-fat separation techniques *in vitro*. Transfer of the gained insights to realize water-only CEST-MRI in the human breast is currently under investigation.

3758 Computer 96

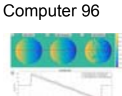

Interleaved B0-mapping during dynamic Creatine-CEST for correction of temporarily fluctuating B0 inhomogeneities during plantar flexion exercise at 7T

Esau Poblador Rodriguez[1], Philipp Moser[1], Barbara Dymerska[1], Siegfried Trattnig[1,2], and Wolfgang Bogner[1]

[1]High Field MR Centre. Biomedical Imaging and Image-guided Therapy, Medical University of Vienna, Austria, Vienna, Austria, [2]Christian Doppler Laboratory for Clinical Molecular MR Imaging, Vienna, Austria

Once the time resolution and specificity of Cr-CEST become comparable with 31P-MRS, it may replace it for the diagnosis of muscular disorders and treatment assessment due to its superior spatial resolution and sensitivity. The need of a complete Z-spectrum acquisition for B0 inhomogeneity correction limits the achievable time resolution and is unable to track temporal ΔB0 due to subject movement or B0 field drifts that occur during a CEST experiment. Temporal B0 field tracking allows independent B0 inhomogeneity correction for each z-spectral point, which may substantially improve the reliability of spectral CEST asymmetry analysis.

Electronic Poster

CEST: Acquisition, Quantification & Characterization

Exhibition Hall Monday 17:15 - 18:15

3759 Computer 49

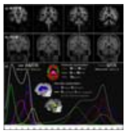

The inhomogeneous MT (ihMT) technique: Achievements and perspectives

Gopal Varma[1], Olivier M Girard[2], Valentin H Prevost[2], Samira Mchinda[2], Guillaume Duhamel[2], and David C Alsop[1]

[1]Radiology, Division of MR Research, Beth Israel Deaconess Medical Center, Harvard Medical School, Boston, MA, United States, [2]Aix Marseille Univ, CNRS, CRMBM, Marseille, France

The inhomogeneous (ihMT) technique represents a relatively simple addition to MT, but provides a different contrast that is sensitive to the dipolar relaxation time T_{1D}. A review is provided of: method(s) for its application; considerations for optimizing the ihMT signal; the use of models to obtain quantitative parameters and guide acquisition; and its application in vivo.

3760 Computer 50

On the Precision of Myelin Imaging: Characterizing Ex vivo Dog Spinal Cord with MRI and Histology

Manh-Tung Vuong[1,2], Tanguy Duval[1], Julien Cohen-Adad[1,3], and Nikola Stikov[1,2]

[1]NeuroPoly Lab, Polytechnique Montréal, Montréal, QC, Canada, [2]Montreal Heart Institute, Montréal, QC, Canada, [3]Functional Neuroimaging Unit, CRIUGM, Université de Montréal, Montréal, QC, Canada

There is an ongoing debate in the myelin imaging community about which MR-based biomarker has the greatest precision, sensitivity and specificity to myelin. In this work, we compared several MR-based myelin imaging techniques (quantitative magnetization transfer, myelin water fractions, and macromolecular tissue volume) by evaluating their repeatability and their relation to large-scale histology in dog spinal cord. Qualitatively the contrasts were similar, and all techniques had comparable scan-rescan and correlations with histology. Surprisingly, the correlations between the various myelin measures were almost as high as the scan-rescan correlations. The correlations decreased when only white matter was considered, which could be due to the small dynamic range of the measurement, or due to artifacts related to the preparation and panoramic scanning of the tissue.

3761 Computer 51

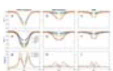

Assessment of Lipid Order in Model Myelin Membrane Systems with MT and ihMT

Scott D. Swanson[1], Mario L. Fabiilli[1], Dasha I. Malyarenko[1], Ashok Srinivasan[1], Zhongliang Zu[2], and Daniel F. Gochberg[2]

[1]Radiology, University of Michigan, Ann Arbor, MI, United States, [2]Radiology, Vanderbilt University, Nashville, TN

We report here a study of MT and enhanced MT (eMT), using dual-sided RF saturation, in model membrane system to measure lipid dynamics and structure in systems of known lipid order. The eMT signal generated by dual-sided RF saturation of phospholipid vesicles is well described by Gaussian line shape and T_{2b} is easily determined. T_{2b} of the lipids is related to the lipid order with T_{2b}(liquid disorder) > T_{2b}(liquid order) > T_{2b} (solid order). These tools provide a method to estimate lipid order *in vivo*.

3762 Computer 52

Combining multi gradient echo acquisitions with inversion recovery: estimating the residence time of myelin water from transient MT effects.

Peter van Gelderen[1] and Jeff H Duyn[1]

[1]Advanced MRI, LFMI, NINDS NIH HHS, Bethesda, MD, United States

Combining multi-gradient-echo (MGRE) acquisitions with inversion/saturation preparation pulses allows for separation of white matter signal in several water compartments and estimation of both their T_1 and exchange properties. A model of multiple myelin, myelin water and axonal/interstitial water compartments was implemented, including exchange from and across individual lipid bi-layers. Fitting this model to the inversion prepared MGRE-data resulted in T_1's and exchange rates for all compartments. The results from a corpus-callosum region of interest indicate that the single layer myelin water residence time is a few hundred microseconds, while the average residence time of all myelin water combined is around 15ms.

3763 Computer 53

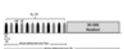

Characterization of the power dependency regimes of inhomogeneous Magnetization Transfer (ihMT)

Samira Mchinda[1], Gopal Varma[2], Valentin H Prevost[1], Arnaud Le Troter[1], Maxime Guye[1,3], Jean Pelletier[1,4], Jean-Philippe Ranjeva[1], David C Alsop[2], Guillaume Duhamel[1], and Olivier M Girard[1]

[1]Aix Marseille Univ, CNRS, CRMBM, Marseille, France, [2]Radiology, Division of MR Research, Beth Israel Deaconess Medical Center, Harvard Medical School, Boston, MA, United States, [3]Aix Marseille Univ, APHM, Hôpital de La Timone, Pôle d'Imagerie Médicale, CEMEREM, Marseille, France, [4]Aix Marseille Univ, APHM, Hôpital de La Timone, Pôle de Neurosciences Cliniques, Service de Neurologie, Marseille, France

Inhomogeneous magnetization transfer (ihMT) is a new MRI technique that shows promise for myelin imaging. A significant boost of the ihMT signal intensity is achievable when using a concentrated energy deposition scheme. Here we characterized the power dependency of ihMT for various energy deposition schemes (distributed vs. concentrated RF) and we identified distinct regimes with linear, sub-linear and saturated B1 dependency. This has a strong impact on the ihMT response to variable sequence configurations and on the most suitable conditions for different field strengths, e.g. to enhance sensitivity or provide immunity to $B1^+$ inhomogeneities.

3764 Computer 54

From in situ to ex vivo: the effect of autolysis and fixation on quantitative MRI markers for myelin

Siawoosh Mohammadi[1,2,3], Jan Sedlacik[4], Martina F Callaghan[2], Jens Fiehler[4], Gunther Helms[5], and Christian Sprenger[1,6]

[1]Department of Systems Neuroscience, Medical Center Hamburg-Eppendorf, Hamburg, Germany, [2]UCL Institute of Neurology, University College London, London, GA, United Kingdom, [3]Department of Neurophysics, Max Planck Institute for Human Cognitive and Brain Sciences, Leipzig, Germany, [4]Department of Neuroradiology, Medical Center Hamburg-Eppendorf, Hamburg, Germany, [5]Medical Radiation Physics, Lund University, Sweden, [6]Department of Engineering, University of Cambridge, United Kingdom

Ex vivo histology remains the gold standard against which MRI biophysical models, e.g. the MR g-ratio which characterises the fraction of a fibre's diameter that is myelinated, are evaluated. The MR g-ratio model requires a measure of myelin density, for which magnetization transfer saturation (MT) has been used as a biomarker. However, changes occurring post mortem, e.g. autolysis, temperature changes and fixation, significantly alter the MRI signal. Here we investigate how these changes impact MT. We found that MT decreased post mortem but greatly increased upon fixation. These effects are similar to reported changes of other established MRI myelin-markers.

3765 Computer 55

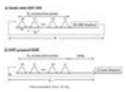

On the boost effect of inhomogeneous Magnetization Transfer (ihMT)

Valentin H Prevost[1], Olivier M Girard[1], Samira Mchinda[1], Gopal Varma[2], David C Alsop[2], and Guillaume Duhamel[1]

[1]Aix Marseille Univ, CNRS, CRMBM, UMR 7339, Marseille, France, [2]Division of MR Research, Beth Israel Deaconess Medical Center, Harvard Medical School, Boston, MA, United States

A new implementation of inhomogeneous magnetization transfer (ihMT) has recently been introduced, consisting of concentrating the RF energy deposition within the saturation period and demonstrating a significant boost of the ihMT sensitivity. The boost effect has been characterized in this study among different ihMT sequences, species and field strengths and reveals common features. The optimal sequence settings vary with the number of consecutive MT pulses and are presumably related to the timescale of the underlying T_{1D} components and magnetization exchange rates.

3766 Computer 56

Accelerating CEST Imaging with Experimental Undersampling and Compressed Sensing

Huajun She[1], Bian Li[1], Joshua S. Greer[1,2], Jochen Keupp[3], Ivan E. Dimitrov[1,4], Ananth Madhuranthakam[1,5], Robert Lenkinski[1,5], and Elena Vinogradov[1,5]

[1]Radiology, UT Southwestern Medical Center, Dallas, TX, United States, [2]Bioengineering, UT Dallas, Dallas, TX, United States, [3]Philips Research, Hamburg, Germany, [4]Philips Healthcare, Gainesville, FL, United States, [5]Advanced Imaging Research Center, UT Southwestern Medical Center, Dallas, TX, United States

Chemical exchange saturation transfer (CEST) is a new contrast mechanism in MRI. However, a successful application of CEST is hampered by its slow acquisition and fast acquisition is desired. Compressed sensing (CS) is powerful for perfect reconstruction of highly undersampled data. Existing works mostly focus on the retrospectively downsampled studies, but few implementation and analysis of truly undersampled scheme with CEST has been reported. This work experimentally implements the random Cartesian undersampled scheme and the golden angle radial sampling sequence for CEST. The results demonstrate influence of experimental conditions that are not accounted for in the retrospectively undersampled studies.

3767 Computer 57

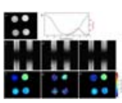

Robust image registration in CEST-acquisitions by exploiting a low-rank plus sparse decomposition of the Z-spectrum

Tobias Wech[1,2] and Herbert Köstler[1,2]

[1]Department of Diagnostic and Interventional Radiology, University Hospital of Würzburg, Würzburg, Germany, [2]Comprehensive Heart Failure Center, University Hospital of Würzburg, Würzburg, Germany

A robust motion correction technique for in vivo CEST-acquisitions is proposed. The algorithm exploits a low-rank plus sparse decomposition of the Z-spectrum to separate signal variations due to different off-resonance preparations from accompanying motion. The method was validated in a phantom study and subsequently used to register a CrCest acquisition of the human thigh during exercise.

3768 Computer 58

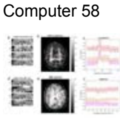

snapCEST – A single-shot 3D CEST sequence for motion corrected CEST MRI

Moritz Zaiss[1], Philipp Ehses[1], and Klaus Scheffler[1]

[1]Magnetic Resonance Center, Max-Planck-Institute for biological cybernetics, Tuebingen, Germany

In this study, we present a single-shot 3D MRI readout that allows acquisition of a CEST prepared volume within 2 s. This makes it possible to correct for motion, which otherwise can cause severe artifacts in CEST imaging.

3769 Computer 59

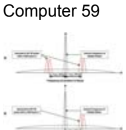

Multi-Band Enhanced Magnetization Transfer Contrast (MBE-MTC) Preparation

Xiufeng Li[1], Jialu Zhang[1,2,3], Wendy Elvendahl[1], Dingxin Wang[4], Kamil Ugurbil[1], and Gregory J. Metzger[1]

[1]Radiology-CMRR, University of Minnesota, Minneapolis, MN, United States, [2]Interdisciplinary Institute of Neuroscience and Technology, Zhejiang University, Hangzhou, People's Republic of China, [3]Department of Biomedical Engineering, Zhejiang University, Hangzhou, People's Republic of China, [4]Siemens Healthcare, Minneapolis, MN, United States

To overcome the limitations of traditional magnetization contrast (MTC) preparation methods, the Multi-Banded (MB) RF-pulse Enhanced Magnetization Transfer Contrast (MBE-MTC) preparation was proposed by using the multi-banded RF pulses for the MTC preparation. Such an approach has been evaluated via studies in the skeleton muscle, kidneys and the brain with demonstrated benefits. The proposed MBE-MTC preparation provides an alternative way for MTI either for increased MTC or simultaneous and symmetric capture of the MTC or its changes in tissue.

3770 Computer 60

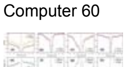

Separating out Fast and Slow Chemical Exchange Using Off-resonance Variable Delay Multiple Pulse (VDMP)

Lin Chen[1,2,3], Xiang Xu[2,3], Haifeng Zeng[2,3], Kannie W.Y. Chan[2,3,4], Nirbhay Yadav[2,3], Shuhui Cai[1], Kathryn J. Schunke[5], Nauder Faraday[5], Peter C. M. van Zijl[2,3], and Jiadi Xu[2,3]

[1]Department of Electronic Science, Xiamen University, Xiamen, People's Republic of China, [2]Russell H. Morgan Department of Radiology and Radiological Science, Johns Hopkins University School of Medicine, Baltimore, MD, United States, [3]F.M. Kirby Research Center for Functional Brain Imaging, Kennedy Krieger Research Institute, Baltimore, MD, United States, [4]Department of Mechanical and Biomedical Engineering, City University of Hong Kong, Hong Kong, People's Republic of China, [5]Department of Anesthesiology/Critical Care Medicine, Johns Hopkins University School of Medicine, Baltimore, MD, United States

We demonstrate that off-resonance VDMP can be used as an exchange rate filter to distinguish and quantify the slow- and fast-exchanging components in Z-spectra by applying an appropriate number of pulses and varying the mixing times. The method can be used to extract predominantly fast-exchanging protons by separating out the slow-MTC pool, and provides information about the chemical exchanging species in tissue that conventional MT/CEST technique cannot access.

3771 Computer 61

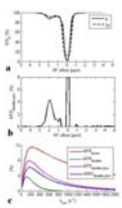

Chemical Exchange Rotation Transfer Imaging of CEST signal at 2ppm

Zhongliang Zu[1], Elizabeth A Louie[1], Eugene Lin[1], Xiaoyu Jiang[1], Mark D Does[1], John C Gore[1], and Daniel F Gochberg[1]

[1]Vanderbilt University, Nashville, TN, United States

The CEST signal around 2 ppm may have applications in cancer and muscle imaging and is likely related to an important energy molecule, creatine. In this work, we provide a specific metric to better quantify this signal based on modification of our previously developed CERT approach and an inverse analysis. Results show that the CEST signal at 2 ppm is hypointense in tumors which may be due to decreased creatine content.

3772 Computer 62

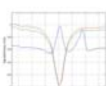

Chemical Exchange Saturation Transfer (CEST) with a Multiple Gradient Echo Chemical Shift Imaging (CSI) Sequence

Ken-Pin Hwang[1], Chunxiao Guo[2], Joshua Yung[1], Christopher J. MacLellan[1], Erik N.K. Cressmann[2], and R. Jason Stafford[1]

[1]Department of Imaging Physics, The University of Texas M.D. Anderson Cancer Center, Houston, TX, United States, [2]Department of Inverventional Radiology, The University of Texas M.D. Anderson Cancer Center, Houston, TX, United States

Chemical exchange saturation transfer (CEST) is observed by applying off-resonance saturation pulses at multiple frequencies and measuring the change in water signal. However, if lipid molecules are present, signals from both species contribute to overall voxel signal, confounding spectral measurement. A multiple gradient echo sequence was developed to simultaneously perform chemical shift imaging with CEST to decouple these signals and measure the independent effect of off-resonance saturation transfer to water. 2D spectra were reconstructed, from which individual water-only z-spectra were obtained. In data from a mixed species phantom, amide proton peaks were clearly visible despite the presence of lipid signal.

3773 Computer 63

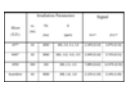

Chemical exchange-sensitive MRI at 9.4 T versus 15.2 T: Effect on Sensitivity and Background Signals

Julius Juhyun Chung[1,2], Wonmin Choi[1,3], Tao Jin[4], Jung Hee Lee[1,2,3,5], and Seong-Gi Kim[1,2,3]

[1]Center for Neuroscience Imaging Research, Institute for Basic Science (IBS), Suwon, Korea, Republic of, [2]Samsung Advanced Insitute for Health Sciences and Technology, SKKU, Seoul, Korea, Republic of, [3]Biomedical Engineering, Sungkyunkwan University, Suwon, Korea, Republic of, [4]Radiology, University of Pittsburgh, [5]Radiology, Sungkyunkwan University, Seoul, Korea, Republic of

With chemical-exchange sensitive imaging, increasing field narrows the linewidth of magnetization transfer effects and shifts relative exchange rates (exchange rate vs. chemical shift) toward a slower exchange regime. This study is intended to explore the interplay of contrast mechanisms and sensitivity benefits by comparing phantom and in-vivo data acquired at the fields of 9.4T and 15.2T. The linewidth narrowing effect between the fields is demonstrated in agar phantoms with nicotinamide as well as spectra from the rat cortex. Spectra taken at higher power shows increase of sensitivity by shifting toward a slower exchange regime.

3774 Computer 64

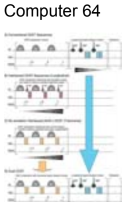

Dual-CEST: a novel 3D-CEST sequence exploiting simultaneous transverse and longitudinal CEST signal encoding.

Robert C. Brand[1], Nicholas P. Blockley[1], Michael A. Chappell[2], and Peter Jezzard[1]

[1]Department of Clinical Neurosciences, University of Oxford, Oxford, United Kingdom, [2]Department of Engineering Science, University of Oxford, Oxford, United Kingdom

We propose a novel 3D method called Dual-CEST, which simultaneously captures the CEST contrast stored in the longitudinal and transverse magnetisation of the bulk water. By including ADC events and a hexagonal spoiling scheme during the CEST preparation phase we collected the usually neglected transverse signal, generated by direct water saturation (a method we call NoXi-CEST). The unaffected longitudinal magnetisation is then acquired using a 3D-GRASE readout resulting in one (Dual-CEST) sequence (3:15 min) that provides XY-spectra, in addition to conventional Z-spectra, and producing additional CEST-contrast and B_0-maps without loss of contrast or additional scan time (compared with conventional imaging).

3775 Computer 65

Human cardiac creatine by CrCEST: potential improved fitting methods

Jane Ellis[1], Mabel Li[1], Michael Chappell[2], Mathew Robson[1], and Christopher Rodgers[1]

[1]OCMR, RDM Cardiovascular Medicine, University of Oxford, Oxford, United Kingdom, [2]Department of Engineering Science, University of Oxford, Oxford, United Kingdom

The development of a novel CEST technique optimised to measure creatine in the human heart. After unsuccessful measurement of *in vivo* creatine concentrations using MTR_{asym}, more robust model-based analysis methods based on spectral line shapes were tested and implemented on phantom data, with these model-based methods showing significant improvement to MTR_{asym} analysis. Going forward, the developed pulse sequence combined with the model-based analysis methods are a promising step towards human cardiac creatine CEST.

3776 Computer 66

Dominant pH-sensitive amide proton transfer effect during acute ischemic stroke - Quantification of multi-pool contribution to commonly used MTRasym analysis in a rat model of acute stroke

Yin Wu[1], Iris Yuwen Zhou[2], Jing Zhao[1], and Phillip Zhe Sun[2]

[1]Paul C. Lauterbur Research Center for Biomedical Imaging, Shenzhen Institutes of Advanced Technology, Chinese Academy of Sciences, Shenzhen, People's Republic of China, [2]Athinoula A. Martinos Center for Biomedical Imaging, Department of Radiology, Massachusetts General Hospital and Harvard Medical School, MA, United States

Routinely used magnetization transfer (MT) asymmetry in measurement of pH-sensitive amide proton transfer (APT) effect is susceptible to concomitant contributions, including semisolid MT and nuclear overhauser effect (NOE). In this study, multi-pool contribution from NOE, MT, CEST at 2 ppm and APT during the acute stroke was resolved with a sum of five Lorentzian functions. Results confirmed the changes in MT and NOE offset each other, and reduction of APT was approximately two-fold of the CEST effect decrease at 2 ppm, dominating the commonly observed pH-sensitive MTR_{asym} change during acute stroke.

3777 Computer 67

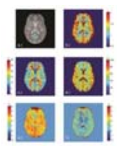

Towards Fast Quantitative CEST: A New Model for Quantifying the CEST Effect in the Presence of MT

Alex K Smith[1,2,3], Richard D. Dortch[2,3,4], and Seth A Smith[2,3,4,5]

[1]FMRIB, University of Oxford, Oxford, United Kingdom, [2]Vanderbilt University Institute of Imaging Science, Vanderbilt University, Nashville, TN, United States, [3]Department of Biomedical Engineering, Vanderbilt University, Nashville, TN, United States, [4]Department of Radiology and Radiological Sciences, Vanderbilt University, Nashville, TN, United States, [5]Department of Ophthalmology, Vanderbilt University, Nashville, TN, United States

Basic models to characterize the CEST effect in vivo suffer from competing magnetization transfer (MT) effects. Here, we use qMT to model the CEST effect and derive CEST indices that are independent of MT. Additionally, simultaneously assessing the MT and CEST effects provides more robust estimates of other elements of the MT effect. Simulations and initial in vivo findings suggest that combining MT and CEST fitting provides a more accurate fit of CEST z-spectra than a traditional single pool Lorentzian fit, and thus provides estimates of the CEST effect that are not dependent on the MT effect.

3778 Computer 68

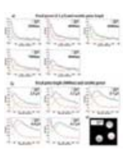

Overlap-resolved cest (orCEST) MRI: imaging gaba and glutamate at 16.4T

Frederico Severo[1] and Noam Shemesh[1]

[1]Champalimaud Centre for the Unknown, Lisbon, Portugal

Chemical Exchange Saturation Transfer (CEST) affords metabolic imaging at high spatial resolution, especially at ultrahigh fields. However, when spectral overlap exists downfield, metabolite maps may be contaminated by other unwanted signals. Here, we present a methodology termed overlap-resolved-CEST (orCEST), which, through subtraction in CESTasym spectra, provides enhanced specificity. We demonstrate how this technique can be used to resolve the signals of Glutamate and GABA – the Central Nervous System's primary neurotransmitters in vivo.

3779 Computer 69

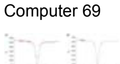

Model-Based Analysis of Partial Z-spectra for Rapid Quantification of Amide Proton Transfer MRI

Paula L. Croal[1], Kevin Ray[2], Yunus Msayib[1], James Larkin[2], Brad Sutherland[3,4], George Harston[3], Andy Baldwin[5], Alastair Buchan[3], Peter Jezzard[6], James Kennedy[3], Nicola Sibson[2], and Michael Chappell[1]

[1]Institute of Biomedical Engineering, University of Oxford, Oxford, United Kingdom, [2]Oxford Institute for Radiation Oncology, University of Oxford, Oxford, United Kingdom, [3]Acute Vascular Imaging Centre & Acute Stroke Programme, Radcliffe Department of Medicine, University of Oxford, Oxford, United Kingdom, [4]School of Medicine, Faculty of Health, University of Tasmania, Hobart, Australia, [5]Physical and Theoretical Chemistry Laboratory, Department of Chemistry, University of Oxford, Oxford, United Kingdom, [6]Oxford Centre for Functional MRI of the Brain, Nuffield Department of Clinical Neurosciences, University of Oxford, Oxford, United Kingdom

Model-based analysis of APT MRI has been shown to quantitatively outperform conventional approaches such as asymmetry analysis. However clinical application is hindered by slow acquisition of whole z-spectra, and processing times. Here, we demonstrate that by using only a subset of frequency offsets, acquisition and processing time can be reduced by ~70% and ~90%, respectively. Using an MCAO model of ischemic stroke, we demonstrate that our Reduced Frequency Offset approach is able to detect significant differences in APTR* between healthy and ischemic tissue.

3780 Computer 70

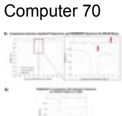

Peak RF Optimization for Baseline Enhancement (PROBE) for CEST/NOE with in-vitro application at 7T

Tobias Lenich[1], André Pampel[1], Toralf Mildner[1], Riccardo Metere[1], and Harald E. Möller[1]

[1]Max-Planck-Institute for Human Cognitive and Brain Sciences, Leipzig, Germany

In CEST/NOE experiments, induced saturation intended for certain metabolites also saturates other moieties, leading to mingled backgrounds in Z-spectra. Precise quantification of endogenous metabolites is impeded by slow acquisition times and confounding background contributions. We present an optimization framework targeting a flattened baseline in Z-spectra, with direct water saturation and non-specific macromolecular contributions fully compensated. Saturation pulse amplitudes as a function of frequency offset were derived using optimal-control-based calculation. Feasibility of this approach is demonstrated in vitro for NOE/CEST in the presence of tissue-like background and accelerated acquisition by distinct offset selection. Experimental results show good agreement with concentration levels.

3781 Computer 71

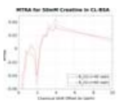

Volatility analysis for asymmetry-based CEST/NOE evaluation methods in the presence of multi-pool background systems with MT – Application to creatine CEST

Tobias Lenich[1], André Pampel[1], Toralf Mildner[1], Riccardo Metere[1], and Harald E. Möller[1]

[1]Max-Planck-Institute for Human Cognitive and Brain Sciences, Leipzig, Germany

Here, we aim to demonstrate the effects of complex multi-pool background systems with magnetization transfer (MT) on asymmetry and ratio-based analyses for CEST/NOE experiments. By using creatine in cross-linked BSA as a model, we show effects of background variations on such analyses for creatine CEST (CrCEST) based on experimentally obtained spin system parameters. For changes of up to 50% in background pool fractions, the CrCEST peak was found to change by up to 35% in asymmetry analysis. The necessity of model-based fitting with inclusion of complex background systems in contrast to conventional lineshape-based analysis is outlined.

3782 Computer 72

CEST and NOE signals in ischemic stroke at 9.4T evaluated using a Lorentzian multi-pool analysis: a drop, an increase or no change?

Yee Kai Tee[1], Badrul Abidin[1], Alexandr Khrapitchev[2], Brad A Sutherland[3,4], James Larkin[2], Kevin Ray[2], George Harston[4], Alastair M Buchan[4], James Kennedy[4], Nicola R Sibson[2], and Michael A Chappell[5]

[1]Department of Mechatronics and Biomedical Engineering, Universiti Tunku Abdul Rahman, Kajang, Malaysia, [2]Cancer Research UK & Medical Research Council Oxford Institute for Radiation Oncology, Department of Oncology, University of Oxford, United Kingdom, [3]School of Medicine, Faculty of Health, University of Tasmania, Australia, [4]Acute Stroke Programme, Radcliffe Department of Medicine, University of Oxford, United Kingdom, [5]Department of Engineering Science, Institute of Biomedical Engineering, University of Oxford, United Kingdom

CEST and NOE effects in ischemic stroke at 9.4T were studied using a Lorentzian multi-pool approach. It was found that both the CEST and NOE signals had significant changes in region of acute ADC reduction when compared with contralateral tissue. The contrast or relative values to the contralateral tissues of MTRasym(3.5 ppm) was found to correlate moderately strongly with the relative amide signal at 3.5 ppm but not the relative reference signal at –3.5 ppm, suggesting that it is should be used in the group analysis in a population-wide basis to assess the change of APT in the ischemic stroke.

Electronic Poster

Contrast Mechanisms: Miscellaneous

Exhibition Hall — Monday 17:15 - 18:15

3783 Computer 97

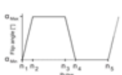

Flip Angle Optimization for Spin-Echo Based Sequences (RARE/TRAPS) for Hyperpolarized Nuclei

Sebastien Bär[1], Matthias Weigel[2], Dominik von Elverfeldt[1], Jürgen Hennig[1], and Jochen Leupold[1]

[1]Dept. of Radiology, Medical Physics, University Medical Center Freiburg, Freiburg, Germany, [2]Radiological Physics, University of Basel Hospital, Basel, Switzerland, Saint Helena

For applications like dynamic imaging, the relatively fast decaying hyperpolarized signal must be acquired over a higher number of sequence cycles and the optimal refocusing flip angle needs to be determined. Optimizing the RARE refocussing flip angles allow to optimize the signal exploitation. Furthermore, optimizing the flip angles of a RARE-based varying flip-angle TRAPS sequence enables an even longer prolongation of the signal lifetime.

3784 Computer 98

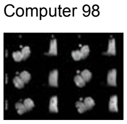

Longitudinal in vivo 19F MR imaging by ZTE of 19F labeled calcium phosphate cement implanted in bone defects in the rat

Weiqiang Dou[1], Simone Mastrogiacomo[2], Olga Koshkina[3], Andor Veltien[1], Mangala Srinivas[3], X. Frank Walboomers[2], and Arend Heerschap[1]

[1]Radiology, Radboud University Medical Centre, Nijmegen, Netherlands, [2]Biomaterials, Radboud University Medical Centre, Nijmegen, Netherlands, [3]Tumor Immunology, Radboud University Medical Centre, Nijmegen, Netherlands

To enhance MR image contrast of calcium phosphate cement (CPC) to bone, CPC was tagged with ^{19}F loaded nanoparticles. This ^{19}F labeled CPC material, after implantation into bone defects in rat legs, was monitored in vivo at 11.7T by longitudinal ^{19}F zero echo time (ZTE) MR imaging. We demonstrate that the overlay of ^{19}F ZTE images on ^{1}H images allows for an excellent qualitative view of CPC with no background. By a quantitative evaluation of the ^{19}F signal the in vivo degradation of CPC over weeks can be followed by MRI.

3785 Computer 99

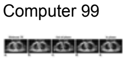

Image contrast at sub-millisecond echo times

Jinil Park[1,2], Soon Ho Yoon[3], Chanhee Lee[1], Jin Mo Goo[3], and Jang-Yeon Park[1,2]

[1]Center for Neuroscience Imaging Research, Institute for Basic Science (IBS), Suwon, Korea, Republic of, [2]Department of Biomedical Engineering, Sungkyunkwan University, Suwon, Korea, Republic of, [3]Department of radiology, Seoul National University Hospital, Seoul University College of Medicine, Seoul, Korea, Republic of

Some contrast mechanisms like in- and out-of-phase contrasts of fat and water come into play at sub-millisecond echo times(TE) at high field strengths above 3T, and under-recognition of them can lead to misunderstanding of signal intensities and inappropriate interpretation of normal and disease pathology. Here the TEs including the sub-millisecond ones were estimated at various field strengths and it was demonstrated by phantom and human lung imaging that contrast mechanisms are apparently seen at the sub-millisecond TE and thus should not be overlooked at high field strengths when using UTE imaging techniques that can cover the range of sub-millisecond TE.

3786 Computer 100

Threonine Manganese Chelate-a New Gastrointestinal Contrast Agent for MRI

Yan Luo[1], Hao Yu[1], and Yaqi Shen[1]

[1]Radiology Department, Tongji Hospital, Tongji Medical College, Huazhong University of Science and Technology, Wuhan, People's Republic of China

Threonine manganese chelate is a widely used nutritional food addictive. In this pilot study, we investigated the feasibility of threonine manganese chelate as a gastrointestinal contrast agent for MRI in rat models. Our study found that threonine manganese chelate aqueous solution created dark lumen on T1w, T2w and DWI images on rat models without obvious side effect. Threonine manganese chelate might be a promising enteral contrast agent for MRI on animal models.

3787 Computer 101

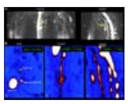

Non-invasive 3T lymphangiography using 3D velocity-suppressed T2-weighted MRI

Rachelle Crescenzi[1], Paula M.C. Donahue[2,3], Allison O Scott[1], Vaughn G Braxton[1], Helen B Mahany[1], Sarah K Lants[1], and Manus J Donahue[1,4,5,6]

[1]Radiology and Radiological Sciences, Vanderbilt University Medical Center, Nashville, TN, United States, [2]Physical Medicine and Rehabilitation, Vanderbilt University Medical Center, Nashville, TN, United States, [3]Vanderbilt Dayani Center for Health and Wellness, Nashville, TN, United States, [4]Neurology, Vanderbilt University Medical Center, Nashville, TN, United States, [5]Psychiatry, Vanderbilt University Medical Center, Nashville, TN, United States, [6]Physics and Astronomy, Vanderbilt University, Nashville, TN, United States

We demonstrate for the first time abilities to perform lymphangiography non-invasively using turbo-spin-echo 3.0T MRI pulse sequences. Contrast consistent with lateralizing disease was observed in patients with known secondary lymphedema from breast cancer treatment-related lymphedema, which also adjusted in an expected manner following manipulation of lymphatic stasis through manual lymphatic drainage therapy. These findings suggest that MRI may be well-suited to evaluate lymphatic functioning and lymphedema treatment response, and may have relevance for informing personalized lymphedema risk before surgery or following breast cancer therapies.

3788 Computer 102

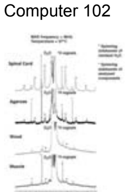

High Resolution Magic Angle Spinning (HR-MAS) NMR characterization of inhomogeneous magnetization transfer (ihMT) responsive samples

Olivier M. Girard[1], Victor Carvalho[1,2], Pierre Thureau[2], Valentin H. Prevost[1], Samira Mchinda[1], Gopal Varma[3], David C. Alsop[3], and Guillaume Duhamel[1]

[1]Aix Marseille Univ, CNRS, CRMBM, Marseille, France, [2]Aix Marseille Univ, CNRS, ICR, Marseille, France, [3]Division of MR Research, Beth Israel Deaconess Medical Center, Harvard Medical School

Inhomogeneous magnetization transfer (ihMT) is a promising technique for central nervous system imaging. Although ihMT signal is mostly observed in myelinated tissues, weaker ihMT signal may be revealed in other biological tissue. The fundamental relationship between the underlying NMR lineshape and the ihMT signal is still an open question. Here we investigate high resolution magic-angle spinning (HR-MAS) NMR to provide insight into the mechanisms underpinning line broadening of ihMT responsive samples. The resulting spectra evidence different dipolar Hamiltonian components contributing to line broadening and support ihMT as being dominated by inhomogeneous interaction in myelinated tissues.

3789 Computer 103

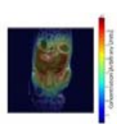

In Vivo Deuterium Labeling and Detection Of Organs Containing Rapidly Dividing Cells

Martin J Lizak[1], Natella Maglakelidze[2], Brittany Oliver[2], Don E Farthing[2], Hellmut Merkle[3], Ronald E Gress[4], and Nataliya P Buxbaum[5]

[1]Mouse Imaging Facility, NINDS, National Institutes of Health, Bethesda, MD, United States, [2]Experimental Transplantation and Immunology Branch, NCI, National Institutes of Health, Bethesda, MD, [3]Laboratory for Functional and Molecular Imaging, NINDS, National Institutes of Health, Bethesda, MD, United States, [4]Experimental Transplantation and Immunology Branch, NCI, National Institutes of Health, Betesda, MD, United States, [5]Experimental Transplantation and Immunology Branch, NCI, National Institutes of Health, Bethesda, MD, United States

In vivo deuterium labeling via ingestion of deuterated water was combined with magnetic resonance imaging to demonstrate a method for studying diseases with groups of rapidly dividing cells. This method was applied to a mouse model of chronic graft versus host disease to demonstrate feasibility.

3790 Computer 104

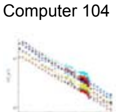

Fast Field-Cycling NMR of human glioma resections: characterization of heterogeneity

Lionel Marc Broche[1], Yang Huang[2], Sandra Pierre[2], Francois Berger[2], David J Lurie[1], Pascal Henry Fries[3], and Hana Lahrech[2]

[1]University of Aberdeen, Aberdeen, United Kingdom, [2]U1205 BrainTech Lab, INSERM, Grenoble, France, [3]INAC-SCIB, CEA, Grenoble, France

FFC-NMR is a unique tool for the measurements of molecular dynamics in the range of nano- to microseconds. With the development of FFC-MRI scanner, it is now possible to investigate new contrasts using field-dependant variations of T_1 to obtain quantitative markers in diseases. In this work we investigate what information FFC-NMR can provide in the context of glioma, using frozen human brain resection from glioma and epileptic surgery. We found that the quadrupolar peaks and T_1 dispersions values may be useful biomarkers.

3791 Computer 105

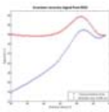

Optimisation of Fast Field-Cycling MRI pulse sequences by numerical simulation.

Nicholas R. Payne[1], Lionel M. Broche[1], and David J. Lurie[1]

[1]University of Aberdeen, Aberdeen, United Kingdom

Fast Field-Cycling MRI (FFC-MRI) has the ability to access contrast invisible to conventional scanners – that resulting from the dependence of T_1 on magnetic field strength. Simulating FFC-MRI sequences by iteratively applying the Bloch equations as the magnetic field strength changes with time was found to give highly accurate predictions of signal intensity at the end of each cycle. This information was used to optimise parameters of the FFC-MRI scans.

3792 Computer 106

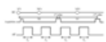

Measurement of R2 dispersion profiles using Fast Field Cycling MRI

Nicolas Chanet[1], Geneviève Guillot[1], and Ludovic de Rochefort[2]

[1]IR4M (Imagerie par Résonance Magnétique Médicale et Multi-modalités), Univ. Paris-Sud, CNRS, UMR8081, Université Paris-Saclay, Orsay, France, [2]Aix Marseille Univ., CNRS, CRMBM UMR 7339, Marseille, France

Fast Field Cycling (FFC) MRI enables rapid and precise relaxometry measurements as a function of magnetic field B_0. Up to now, it was possible to measure longitudinal R_1-NMRD profiles and to generate innovative R_1-dispersive contrasts. However, the ability to measure transverse R_2-NMRD profiles has still to be investigated. Here, a spin-echo based FFC sequence is developed to measure R_2-dispersion, and is applied to ferritin and Gd-DOTA in the range 1.15 to 1.85 T. It is shown that measurements of R2 dispersion could be obtained accurately with the FFC-MRI technology.

3793 Computer 107

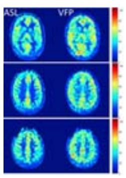

Vector field perfusion imaging

Pascal Spincemaille[1], Qihao Zhang[2], Thanh Dang Nguyen[3], and Yi Wang[3,4]

[1]Radiology, Weill Cornell Medicine, New York, NY, United States, [2]Weill Cornell Medicine, [3]Radiology, Weill Cornell Medicine, New York, NY, [4]Biomedical Engineering, Cornell University, Ithaca, NY

A vector field perfusion (VFP) approach is proposed to quantify three dimensional blood flow in tissue. The traditional lumped-element Kety equation for characterizing perfusion is fundamentally flawed with the indetermination of arterial input function. The standard continuity equation based on velocity vector field is proposed for fitting tomographic data. Preliminary analysis of dynamic contrast enhanced MRI and arterial spin labelled MRI of the brain demonstrate the feasibility of this VFP approach.

3794 Computer 108

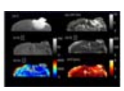

Diffusion effects on NMR transverse relaxation around randomly distributed capillaries

Lukas Reinhold Buschle[1,2], Christian H Ziener[1], Martin Rückl[3], Ke Zhang[1,2], Volker J Sturm[1,2], Gergely M Solecki[4], Frank Winkler[4], Martin Bendszus[2], Sabine Heiland[2], Heinz-Peter Schlemmer[1], and Felix T Kurz[1,2]

[1]E010 Radiology, German Cancer Research Center, Heidelberg, Germany, [2]Neuroradiology, University Hospital Heidelberg, Heidelberg, Germany, [3]Department of Physics, Humboldt University Berlin, Berlin, Germany, [4]Neurooncology, German Cancer Research Center, Heidelberg, Germany

The gradient echo and spin echo signal in brain tissue depend both on diffusion and susceptibility effects around and from capillaries, i.e. on structural and functional information that arise from the microvascular networks. In this work, the dependence of the relaxation rates R2 and R2* on capillary radius are considered for a random arrangement of capillaries in the strong collision approximation, and a closed-form solution is derived. Radius maps are then constructed for glioblastoma mice (N=8) to reveal an increased vessel radius in tumorous tissue as compared to non-affected brain tissue.

3795 Computer 109

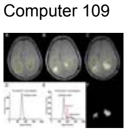

Quantitative, semiautomatic comparison of ferumoxytol and gadoteridol enhancement in treated glioma patients

Andrea Horváth[1], Csanad Varallyay[1], Daniel Schwartz[1], Joao Prola Netto[1], Peter Varallyay[2], Laszlo Szidonya[1], Gerda Toth[1], Rongwei Fu[1], Prakash Ambady[1], Peter Bogner[3], and Edward Neuwelt[1]

[1]Oregon Health and Science University, Portland, OR, United States, [2]National Institute of Clinical Neurosciences, Budapest, Hungary, [3]University of Pécs, Pécs, Hungary

Ferumoxytol is a nano-sized iron oxide particle approved for iron replacement therapy and may be used off label as an MRI contrast agent. While gadolinium-based contrast agents leak into the brain parenchyma where the blood brain barrier is not intact several minutes after administration, ferumoxytol remains intravascular for hours due to its high molecular weight, enabling excellent vascular visualization, with visible parenchymal enhancement peaking 24 hours after administration. In this study, we compared ferumoxytol T1 enhancement to standard of care gadoteridol enhancement with a quantitative method, which is an important step to develop ferumoxytol as an alternative MR imaging agent.

3796 Computer 110

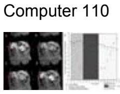

Dynamic Blood Volume Assessment in Extracranial Tissues using Gadofosveset

Tameshwar Ganesh[1,2], Marvin Estrada[3], James Duffin[4], and Hai-Ling Margaret Cheng[1,2,5,6]

[1]Leslie Dan Faculty of Pharmacy, University of Toronto, Toronto, ON, Canada, [2]Ted Rogers Centre for Heart Research, Translational Biology & Engineering Program, Toronto, ON, Canada, [3]Lab Animal Services, Hospital for Sick Children, [4]Anesthesia, University of Toronto, Canada, [5]The Edward S. Rogers Sr. Department of Electrical & Computer Engineering, University of Toronto, Toronto, ON, Canada, [6]Institute of Biomaterials & Biomedical Engineering, University of Toronto, Toronto, ON, Canada

The ability of blood vessels to modulate vascular tone (i.e. blood volume) is an important normal physiological function, which is compromised in multiple diseases, including diabetes and heart diseases. To date, there is no non-invasive imaging technique to assess dynamic microvascular blood volume response. Herein we present a novel MRI technique to assess vasoactive response in "near" real-time in extra-cranial tissues. We employ a blood-pool agent Gadofosveset (Vasovist) together with a variety of vasoactive gas stimuli. In-vivo results in kidney and liver demonstrate we can visualize dynamic changes in gas-induced blood volume changes, as confirmed on laser Doppler perfusion.

3797 Computer 111

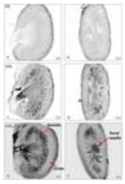

Comparison of MRI and optical CT measurements of murine kidney blood volume.

Ciara M McErlean[1], Yann Jamin[2], Jessica K R Boult[2], James A D'Arcy[2], Martin O Leach[2], David J Collins[2], Simon P Robinson[2], and Simon J Doran[2]

[1]CRUK Cancer Imaging Centre, Institute of Cancer Research, Sutton, United Kingdom, [2]CRUK Cancer Imaging Centre, Institute of Cancer Research

Functional MRI measurements of vasculature must be robustly validated pre-clinically. Optical computed tomography (CT) offers high-resolution *ex vivo* 3D imaging of perfused vasculature using India ink staining. We compared optical CT measurements of murine kidney blood volume with previously published MRI relative blood volume measurements. Fractional blood volumes of different kidney regions in optical CT images were calculated using Frangi vessel filtering, for three concentrations of India ink-staining. Significant positive correlations were found between optical CT and MRI measurements for 10% and 15% India ink staining. This is a potentially promising method for easily and cheaply validating MRI vasculature measurements.

3798 Computer 112

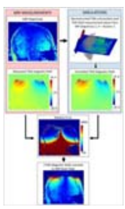

A novel MR-based framework for subject-specific guidance of TMS treatments

Stefano Mandija[1], Petar I Petrov[2], Jord JT Vink[2], Sanne Schuite-Koops[2], Peter R Luijten[1], Cornelis AT van den Berg[1], and Sebastian FW Neggers[2]

[1]Center for Image Sciences, UMC Utrecht, Utrecht, Netherlands, [2]Rudolf Magnus Institute of Neuroscience, UMC Utrecht, Utrecht, Netherlands

In the field of neurostimulation, Transcranial Magnetic Stimulation is gaining more and more momentum since it allows direct control on brain activation in a non-invasive and non-painful manner. However, accuracy of TMS administrations and precise knowledge on its biological effects are still limited. To better understand TMS induced effects, we propose a novel combined TMS-MRI framework which allows us to map the TMS induced magnetic field and to map subject-specific brain activation by means of concurrent TMS-MRI measurements. These subject-specific measurements, will allow us to validate neuronal models which are currently used to predict TMS induced brain activations.

3799 Computer 113

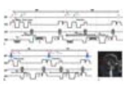

Mulitplexed OxFlow for Rapid Estimation of Whole-Brain Oxygen Consumption at Rest and During Apneic Challenge

Hyunyeol Lee[1], Michael C. Langham[1], Cheng Li[1], Ana E. Rodriguez-Soto[1], and Felix W. Wehrli[1]

[1]Radiology, University of Pennsylvania, Philadelphia, PA, United States

The OxFlow method provides a global CMRO2 estimation in a single pulse sequenc by combining phase-contrast-based flow mapping with estimation of venous oxygen saturation via susceptometry-based oximetry. However, four-interleave in convenional OxFlow makes it difficult to measure rapid changes of brain metabolic states such as response to apneic stimuli. Thus, in this work a highly efficient, multiplexed imaging based OxFlow method was developed and its feasibility was demonstrated in estimation of dynamic CMRO2 in response to an apneic challenge.

3800 Computer 114

Quantification of cerebral venous oxygenation using a two-compartment model of local phase evolution

Elena Kleban[1], Richard Bowtell[1], Penny Gowland[1], and Molly Bright[1]

[1]Sir Peter Mansfield Imaging Centre, University of Nottingham, UK, Nottingham, United Kingdom

We propose that a two-compartment model of the evolution of signal phase, processed using Frequency Difference Mapping, could be applied to study venous oxygenation and architecture at the microscopic scale. This study demonstrates proof-of-concept, quantifying Yv in large vessels, and tests the sensitivity of these values to hyperoxia. We discuss how this new method can be adapted to probe venous microstructure within grey matter, providing more sensitive measures of brain tissue function.

3801 Computer 115

magna cum laude

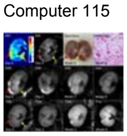

A feasibility study of using noninvasive renal oxygenation imaging to delineate different severities of renal ischemia in atheroembolic renal disease model

Chengyan Wang[1], Fei Gao[2], Hanjing Kong[1], Li Jiang[3], Wenjian Huang[1], Rui Wang[4], Kai Zhao[4], Yan Jia[5], Hui Xu[5], He Wang[6], Xiaodong Zhang[4], Li Yang[5], Jue Zhang[1,2], Xiaoying Wang[1,4], and Jing Fang[1,2]

[1]Academy for Advanced Interdisciplinary Studies, Peking University, Beijing, People's Republic of China, [2]College of Engineering, Peking University, Beijing, People's Republic of China, [3]Philips Healthcare, Suzhou, People's Republic of China, [4]Department of Radiology, Peking University First Hospital, Beijing, People's Republic of China, [5]Renal Division, Peking University First Hospital, Beijing, People's Republic of China, [6]Institute of Science and Technology for Brain-Inspired Intelligence, Fudan University, Shanghai, People's Republic of China

Since the use of angiographic and endovascular procedures increased rapidly during the past decades, the frequency of atheroembolic renal disease raised recently. This study demonstrates the feasibility of applying an MRI based oxygenation imaging to evaluate renal ischemia in an atheroembolic renal disease model. The average renal oxygen extraction fraction (OEFs) as well as the ratios between embolized kidney and contralateral kidney show significant differences between groups. Renal OEF measurement appears to be able to delineate different severities of renal ischemia by revealing information about the balance between tubular workload and delivery of oxygen.

3802 Computer 116

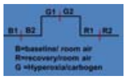

Differential modulation of arterial and venous oxygenation through inhalation of carbogen (95%O2/5%CO2) vs. 100% O2.

Harshan Ravi[1], Wen-Tung Wang[1], Dzung Pham[1], and John Butman[1,2]

[1]Center for Neuroscience and Regenerative Medicine, National Institute of Helath, Bethesda, MD, United States, [2]Radiology and imaging sciences, National Institute of Helath, Bethesda, MD, United States

Susceptibility-weighted imaging (SWI) is a MRI sequence which exploits the susceptibility contrast between various tissues by incorporating MRI phase data. In some clinical applications it may be useful to increase such contrast (e.g. identification of plaque associated veins) and in other cases it may be useful to suppress or decrease such contrast (e.g. visualization of microhemorrhage). Here we explore the use of gas inhalation (oxygen and carbogen) to modulate the conspicuity of brain vasculature.

3803 Computer 117

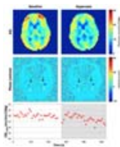

Estimation of arterial blood T1 during hyperoxic gas-mixture breathing

Erin K Englund[1], Zachary B Rodgers[1], Hyunyeol Lee[1], and Felix W Wehrli[1]

[1]Department of Radiology, University of Pennsylvania, Philadelphia, PA, United States

Hyperoxia gas mixture breathing causes additional oxygen to be dissolved in blood plasma thereby shortening the T_1 of arterial blood (T_{1a}). Here, we propose a method estimate T1a during hyperoxia gas breathing by solving a perfusion quantification model for T_{1a} given CBF measured during hyperoxia via phase contrast (PC) of the feeding arteries in the neck. The ratio between PC-based total CBF and ASL-based regional CBF was first determined at baseline, and then applied to normalize the expected ASL-based CBF during hyperoxia. T_{1a} was estimated as 1.46±0.09 s during hyperoxia gas mixture breathing, in reasonable agreement with previous reports.

3804 Computer 118

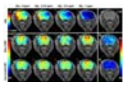

Tagging distance dependent Z-spectrum (TADDZ) for ASL MRI free from B0-inhomogeneity induced errors

Frederick C. Damen[1,2], Rong-Wen Tain[1,2], Weigo Li[3], Xiaohong Joe Zhou[1,2], Leon Tai[4], and Kejia Cai[1,2]

[1]Radiology, University of Illinois at Chicago, Chicago, IL, United States, [2]Center for Magnetic Resonance Research 3T Program, University of Illinois at Chicago, Chicago, IL, United States, [3]Research Resources Center, University of Illinois at Chicago, Chicago, IL, United States, [4]Anatomy and Cell Biology, Chicago, IL, United States

Arterial spin labeling (ASL) MRI, based on endogenous contrast from blood water, is used for research and diagnosis of cerebral vascular conditions. However, artifacts due to imperfect imaging conditions such as B_0 inhomogeneity could lead to variations in the quantification of cerebral blood flow (CBF). In this study, we investigated the CBF variation artifacts due to B_0–inhomogeneity using Signal Targeting with Alternating Radio frequency (STAR) based ASL. We developed a novel technique, TADDZ, similarly to the corrections for chemical exchange saturation transfer (CEST) experiments, to remove the B_0 inhomogeneity induced CBF artifacts.

3805 Computer 119

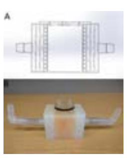

A 3D printed perfusion phantom for quality controlled measurement of arterial spin labeled perfusion

Joshua S. Greer[1,2], Xinzeng Wang[2], Keith Hulsey[2], Robert E. Lenkinski[2,3], and Ananth J. Madhuranthakam[2,3]

[1]Bioengineering, UT Dallas, Richardson, TX, United States, [2]Radiology, UT Southwestern Medical Center, Dallas, TX, United States, [3]Advanced Imaging Research Center, UT Southwestern Medical Center, Dallas, TX, United States

Arterial spin labeling (ASL) is a rapidly growing area of interest, primarily because of its ability to provide non-contrast quantitative perfusion maps. For the technique to be adopted for clinical use, these quantitative measurements need to be accurate and robust, which will require a quality controlled perfusion phantom to ensure consistency for different magnet strengths and manufacturers. In this study, we demonstrate a 3D printed perfusion flow phantom that can be easily replicated, and used to test the precision and repeatability of ASL perfusion measurements.

3806 Computer 120

Dynamic Magnetic Resonance Imaging with Vaginal and Rectal Contrast for the Observation of Vaginal Vault and Rectocele

Huici Zhu[1], Jianyu Liu[1], and Lizhi Xie[2]

[1]Radiology Department of Peking University Third Hospital, Beijing, People's Republic of China, [2]GE Healthcare, MR Research China, BeiJing, People's Republic of China

To determine which method is better for the observation of vaginal vault and rectocele, this research compared the routine dynamic MRI with the dynamic MRI with vaginal and rectum contrast. There was statistically significant difference between the dynamic MR imaging and dynamic MR imaging with vaginal and rectum contrast. For the observation of vaginal vault prolapse and rectocele, the dynamic MR imaging with vaginal and rectum contrast was better than the routine method.

Electronic Poster

Non-Proprietary Software/Hardware/Analysis

Exhibition Hall Tuesday 8:15 - 9:15

3807 Computer 1

NUFFT: Fast Auto-Tuned GPU-Based Library

Teresa Ou[1], Frank Ong[1], Martin Uecker[2], Laura Waller[1], and Michael Lustig[1]

[1]University of California, Berkeley, Berkeley, CA, United States, [2]University of Göttingen, Göttingen, Germany

We present a fast auto-tuned library for computing non-uniform fast Fourier Transform (NUFFT) on GPU. The library includes forward and adjoint NUFFT using precomputation-free and fully-precomputed methods, as well as Toeplitz-based operation for computing forward and adjoint NUFFT in a single step. Computation of NUFFT depends heavily on gridding parameters, desired accuracy, trajectory type, amount of undersampling, and level of precomputation. The library automatically chooses optimal gridding parameters and algorithms, and it can be easily extended to include implementations from other libraries. The library allows researchers to accelerate iterative reconstructions without the difficulties of choosing optimal parameters and algorithms.

3808 Computer 2

ASL-MRICloud: Towards a comprehensive online tool for ASL data analysis

Yang Li[1,2], Peiying Liu[1], Yue Li[3], Hongli Fan[1], Shin-Lei Peng[4], Denise C. Park[5], Karen M. Rodrigue[5], Hangyi Jiang[1], Andreia V. Faria[1], Can Ceritoglu[6], Michael Miller[6], Susumu Mori[1], and Hanzhang Lu[1]

[1]Department of Radiology, Johns Hopkins University School of Medicine, Baltimore, MD, United States, [2]Graduate School of Biomedical Sciences, UT Southwestern Medical Center, Dallas, TX, United States, [3]AnatomyWorks, LLC, Baltimore, MD, United States, [4]Department of Biomedical Imaging and Radiological Science, China Medical University, Taichung City, Taiwan, [5]Center for Vital Longevity, School of Behavioral and Brain Sciences, University of Texas at Dallas, Dallas, TX, United States, [6]Center for Imaging Science, Johns Hopkins University, Baltimore, MD, United States

ASL has drawn tremendous attention from both research and clinical community during recent years. Therefore, we deployed a cloud-based tool for ASL data analysis on top of MRICloud platform. Different from other downloadable ASL toolboxes, ASL-MRICloud features an automated interface via a web browser for data upload and results download. The computation is performed on the online server. Here we summarized the current functionalities, underlying algorithms, and representative results of ASL-MRICloud.

3809 Computer 3

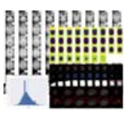

MRIQC: automated assessment and quality reporting of MRI scans

Oscar Esteban[1], Craig Anthony Moodie[1], William Triplett[2], Russell Alan Poldrack[1], and Krzysztof Jacek Gorgolewski[1]

[1]Department of Psychology, Stanford University, Stanford, CA, United States, [2]Department of Physical Therapy, University of Florida

Assessing the quality of MRI is necessary and time-consuming. MRIQC automates the quantification extracting a number of image quality measures (IQMs), and eases the individual inspection through specialized visual reports. MRIQC supports T1w, fMRI and dMRI brain images. MRIQC is an easy to use, “plug-and-play” tool, since it is multi-platform (including desktop and high performance clusters), and BIDS- and BIDS-apps compliant. The IQMs extracted automatically will yield unbiased exclusion criteria in MRI analyses.

3810 Computer 4

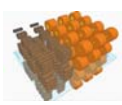

Simulation Reveals Evidence for Bias in Parameter Estimates for Compressed Sensing of Temporally Dynamic Systems

Nathan Murtha[1,2], James Rioux[1,2,3], Olliver Marriott[2], Chris Bowen[1,2,3], Sharon Clarke[1,2,3], and Steven Beyea[1,2,3]

[1]Physics and Atmospheric Science, Dalhousie University, Halifax, NS, Canada, [2]Biomedical Translational Imaging Centre, QE2 Health Sciences Centre, Halifax, NS, Canada, [3]Diagnostic Radiology, Dalhousie University, Halifax, NS, Canada

There exists no objective framework for assessment of acquisition and reconstruction methods in compressed sensing (CS) MRI involving temporal dynamics. We propose a simulation framework to address this gap. Image quality was assessed using two quantitative metrics, and temporal parameters were recovered using least-squares fitting. CS regularization weighting was varied to determine the effect on both image quality and accuracy of recovered temporal dynamic parameters. Image quality metrics displayed distinct optima, though bias, dependent on the underlying temporal dynamics, was introduced to temporal parameter estimates. These results support the need for an objective tool to characterize CS MRI methodologies.

3811 Computer 5

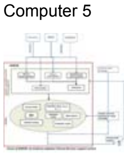

Developing an automated MRI Decision support system: MIROR a non-region specific modular analysis toolbox

Niloufar Zarinabad[1,2], Karen Manias[1,2], Katharine Foster[2], and Andrew Peet[1,2]

[1]University of Birmingham, Birmingham, United Kingdom, [2]Birmingham children hospital, Birmingham, United Kingdom

There is a need for an MRI diagnostic analysis-tool which can provide healthcare investigators with a platform for extraction of relevant information and allow for comparison with similar cases to aid decision-making. The aim of this study was to develop a modular, non-region-specific Medical-Image-Region-of-interest-analysis-tool and Repository (MIROR) in order for advanced MRI techniques to become a part of the clinical routine. Here, the first development phase is presented as applied to diffusion-weighted-imaging of pediatric body-tumors combined with comparison to a repository of cases. MIROR acts as a foundation which can be extended to more advanced image-analysis and sophisticated decision-support.

3812 Computer 6

Implementation of a parallel processing pipeline of multi-channel phase data

Timothy M Whelan[1], Martyn L Klassen[1], Igor Solovey[1], Junmin Liu[1], and Maria Drangova[1,2]

[1]Imaging Research Laboratories, Robarts Research Institute, London, ON, Canada, [2]Dept. of Medical Biophysics, Schulich School of Medicine & Dentistry, Western University, London, ON, Canada

Evidence exists to show that phase unwrapping performed before channel combination results in fewer artifacts (singularities, open ended fringe lines) than when phase unwrapping occurs after channel combination. We have implemented a fast and efficient pipeline designed to enable processing of multi-channel phase data. Specifically, non-iterative phase unwrapping and channel combination are employed within the pipeline that links the MR scanner to a DICOM server, which displays the final combined images, while preserving all metadata.

3813 Computer 7

An abstraction layer for simpler EPIC pulse programming on GE MR systems in a clinical environment

Stefan Skare[1,2], Enrico Avventi[1], Ola Norbeck[1], and Henric Ryden[1]

[1]Neuroradiology, Karolinska University Hospital, Stockholm, Sweden, [2]Karolinska Institutet, Stockholm, Sweden

A C-library that simplifies EPIC pulse programming on GE MR systems is presented, containing a large set of new structs and functions for EPIC. Three pulse sequences have been developed (GRE, FSE and EPI) using this library with EPIC. These sequences have most of the functionality expected in a clinical neuro MRI setting, including arbitrary scan planes, full user interface support, online/offline reconstruction, and with common generic sequence plugins/modules such as SpatialSat, FatSat, and Inversion. The KSFoundation library, pulse sequences and sequence modules can be used to quickly develop new pulse sequences with reduced amount of code.

3814 Computer 8

Implementation of Pulseq in GPI Lab

Keerthi Sravan R[1], Imam Ahmed Shaik[1], Stefan Kroboth[2], Maxim Zaitsev[2], and Sairam Geethanath[1]

[1]Medical Imaging Research Center, Dayananda Sagar Institutions, Bangalore, India, [2]Dept. of Radiology – Medical Physics, Medical Center, University of Freiburg, Germany

A major challenge for researchers in designing new pulse sequences is the limitation of needing to know vendor-specific programming environment. The Pulseq tool in Matlab has overcome this issue. This work demonstrates an open source implementation of Pulseq in GPI Lab to further access to Pulseq. Also, this enables a single platform on GPI to integrate the PSD with the rest of the MR research pipeline: simulation, reconstruction, image analysis and visualization. The Pulseq-GPI implementation is demonstrated through a gradient recalled echo. It is capable of designing all sequences/enhancements that Pulseq currently offers.

3815 Computer 9

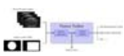

ImFEATbox: An MR Image Processing Toolbox for Extracting and Analyzing Features

Annika Liebgott[1,2], Sergios Gatidis[1], Petros Martirosian[1], Fritz Schick[1], Bin Yang[2], and Thomas Küstner[1,2]

[1]Diagnostic and Interventional Radiology, University Hospital of Tübingen, Tübingen, Germany, [2]Institute of Signal Processing and System Theory, University of Stuttgart, Stuttgart, Germany

In various image processing applications, finding appropriate mathematical descriptions which reflect or extract characteristics of the underlying content from acquired MR images is an important and crucial step. There exists a variety of features which can be used for MRI, but which ones are the most meaningful depends on the underlying scientific or diagnostic question/application as well as the image itself. To reduce the time spent searching for, implementing and testing features for a specific application, we provide a toolbox of features along with a GUI to easily choose and extract them, which will be made publicly available.

3816 Computer 10

PyMRT and DCMPI: two new Python packages for MRI data analysis

Riccardo Metere[1] and Harald E. Möller[1]

[1]NMR Unit, Max Planck Institute for Human Cognitive and Brain Sciences, Leipzig, Germany

Among the many packages available for data analysis in magnetic resonance imaging, only few offer specific tools for quantitative MRI. Additional limitations often come from implementation details, where fast development cycles and code maintainability can be difficult to achieve. Recently, Python has emerged as an ideal tool for the development of software for scientific computing.Here, we propose two easily extensible software packages implemented in Python: PyMRT for the analysis of MRI data, notably for quantitative applications; DCMPI for simplifying and automatize portions of the data collection step.

3817 Computer 11

A Matlab-based graphical user interface for processing dynamic CEST-MRI data

Neil Wilson[1], Hari Hariharan[1], and Ravinder Reddy[1]

[1]CMROI, University of Pennsylvania, Philadelphia, PA, United States

A graphical user interface was designed in Matlab to process dynamic CEST-MRI experiments. Field corrections due to B0 and B1 inhomogeneities are applied, ROIs are taken, CEST signal is fitted, and high quality figures are produced with minimal user input. Data is presented for an exercise-induced skeletal muscle creatine elevation experiment though the GUI is highly customizable.

3818 Computer 12

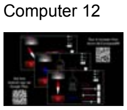

Day 1 of MRI and NMR education: Interactive visualization of MR basics

Lars G. Hanson[1,2]

[1]Center for Magnetic Resonance, DTU Elektro, Technical University of Denmark, Kgs. Lyngby, Denmark, [2]Danish Research Centre for MR, Centre for Functional and Diagnostic Imaging and Research, Copenhagen University Hospital, Hvidovre, Denmark

It is challenging to teach and learn the very basics of Magnetic Resonance as used in NMR and MRI. A simple approach is demonstrated that provides accurate understanding of basic MR phenomena, also for non-technical students. An interactive free simulation tool is used that invites student exploration of Compass and Nuclear MR via browser or app. This CompassMR simulator offers you a unique opportunity to finally make anybody intuitively understand MR in minutes, even your parents who always wanted to know what you are doing.

3819 Computer 13

IMAGING ON THE EARTH'S MAGNETIC FIELD

Ruth Agiobu-Alafun[1], Steven Sourbron[1], and Leonidas Georgiou[1]

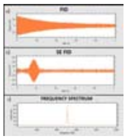

[1]Division of Biomedical Imaging, University of Leeds, Leeds, United Kingdom

This educational abstract is aimed at providing a better understanding of NMR principles and optimisation of scan parameters for imaging using graphical illustrations and images generated with the Terranova-MRI EFNMR system. It is benefitial to clinicians who seek a more intuitive way to educate themselves with regards to MRI; to students who need hands on experience to gain a better understanding of the underlying mechanisms of signal and image formation; and to academic researchers who are looking to introduce alternative teaching methods of MRI techniques in their institutions.

3820 Computer 14

3 Dimensional Image Reconstruction – Innovation Improves Diagnosis in Pediatric MRI

Dianna M.E. Bardo[1], Craig E Barnes[1], Robyn Augustyn[1], and Marrit Thorkelson[1]

[1]Diagnostic Radiology, Phoenix Children's Hospital, Phoenix, AZ, United States

3D and 2D image reconstruction and other image post-processing techniques are vital in developing a complete understanding of anatomy and pathology. The ability to visualize structures in 3 dimensions, perhaps showing pathology in the orientation a surgeon will see as they approach during surgery, provide information which allows planning a procedure before the patient is under anesthesia can improve care and reduce surgical or interventional times. Further, 3D images or printed 3D models a valuable resource for teaching a patient or a child's parent about the necessary care and treatment of their child.

3821 Computer 15

Segment Deep Gray Matter Nucleus from MR Images: An Automatic Computational Tool for Early Diagnosis of Parkinson's Disease

Pei Dong[1], Yanrong Guo[1], Yue Gao[2], Peipeng Liang[3], Yonghong Shi[4,5], Qian Wang[6], Dinggang Shen[1], and Guorong Wu[1]

[1]Department of Radiology and BRIC, The University of North Carolina at Chapel Hill, Chapel Hill, NC, United States, [2]School of Software, Tsinghua University, Beijing, People's Republic of China, [3]Department of Radiology, Capital Medical University, Beijing, People's Republic of China, [4]School of Basic Medical Sciences, Fudan University, Shanghai, People's Republic of China, [5]Shanghai Key Laboratory of Medical Imaging Computing and Computer-Assisted Intervention, [6]Med-X Research Institute, Shanghai Jiao Tong University, Shanghai, People's Republic of China

Accurate and automatic brainstem nuclei segmentation from MR images plays an important role in seeking for imaging-biomarkers of Parkinson's disease (PD). To address the segmentation challenge from regular MR images, we propose a novel multi-atlas patch based label fusion method where we use hyper-graph technique to handle the low image contrast issue. Our proposed method is successfully applied to a set of MR images from PPMI (Parkinson's Progression Markers Initiative) dataset, and we have achieved significant improvements in terms of segmentation accuracy compared to the state-of-the-art methods.

3822 Computer 16

Cerebra-QSM: An Application for Exploring Quantitative Susceptibility Mapping Algorithms

Marina Salluzzi[1,2], D Adam McLean[1,2], David G Gobbi[1,2], Cheryl R McCreary[2,3], M Louis Lauzon[2,3], and Richard Frayne[2,3]

[1]Calgary Image Processing and Analysis Centre, Foothills Medical Centre, Calgary, AB, Canada, [2]Departments of Radiology and Clinical Neurosciences, Hotchkiss Brain Institute, University of Calgary, Calgary, AB, Canada, [3]Seaman Family Research MR Centre, Foothills Medical Centre, Calgary, AB, Canada

Cerebra-QSM is a modular C++ application for quantitative susceptibility mapping that logs the inputs and results from each stage of the QSM processing pipeline. It provides a user interface for analysis, review and process validation, as well as a scripting interface for batch processing. It is flexible and intuitive, allowing rapid evaluation of algorithms and training of end-users on the specifics of QSM estimates. It has been adopted by multiple researchers, facilitating independent work. Cerebra-QSM provides a robust, simple and scalable framework for evaluation of processing pipelines.

3823 Computer 17

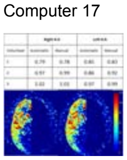

Hough-transform based detection of vascular structures applied to automate and accelerate planning of super-selective Arterial Spin Labeling

Thomas Lindner[1], Olav Jansen[1], and Michael Helle[2]

[1]Clinic for Radiology and Neuroradiology, University Hospital Schleswig-Holstein, Kiel, Germany, [2]Tomographic Imaging Department, Philips Research, Hamburg, Germany

Super-selective Arterial Spin Labeling (ASL) is a technique to perform non-contrast enhanced flow territory mapping. Prior to image acquisition, the labeling focus has to be positioned on each artery of interest separately. Depending on the arterial architecture, this process can be time-consuming, especially for untrained operators. In this study, an algorithm for automated vessel detection and planning is introduced to accelerate the planning procedure of super-selective ASL measurements, which is based on the Hough transform to detect circular structures (i.e. arteries) on a transversal time-of-flight (TOF) scan.

3824 Computer 18

Advanced platform-independent MR prototyping: From EPI to Arterial Spin Labeling without code compilation

Thorsten Honroth[1], Cristoffer Cordes[1,2], Saulius Archipovas[1], Federico von Samson-Himmelstjerna[1,2], Matthias Günther[1,2,3], and David Porter[1]

[1]Fraunhofer MEVIS, Bremen, Germany, [2]University of Bremen, Bremen, Germany, [3]mediri GmbH, Heidelberg, Germany

A previously demonstrated, platform-independent rapid prototyping environment for MR sequences that provides a workflow without code compilation has been extended with features that allow the creation of a FAIR Arterial Spin Labeling (ASL) sequence. Also, the calculation code for the necessary FOCI inversion pulse, which is protocol dependent and which needs to be executed during runtime on the scanner, can be implemented compilation-free using a scripting language.

3825 Computer 19

An online Cloud-ORiented Engine for advanced MRI simulations (coreMRI)

Christos G. Xanthis[1,2], Håkan Arheden[1], and Anthony H. Aletras[1,2]

[1]Lund Cardiac MR Group, Department of Clinical Physiology, Lund University, Lund, Sweden, [2]Laboratory of Computing and Medical Informatics, School of Medicine, Aristotle University of Thessaloniki, Thessaloniki, Greece

Despite high-performance, multi-GPU MR simulations are not widespread. In this study, we present coreMRI, an advanced simulation platform delivered as a web-service through an on-demand, scalable cloud-based and GPU-based infrastructure. coreMRI achieved with a 8xGPUs configuration a speedup of up to 63 when compared to a single-GPU configuration, bringing hour-long simulations down to a couple of minutes. In conclusion, coreMRI allows its users to exploit the highly-tuned computer performance of GPUs on MR simulations with neither upfront investment for purchasing advanced systems nor technical programming expertise.

3826 Computer 20

An Automated Phantom QA procedure for the Rhineland Study

Eberhard Daniel Pracht[1], Christian Schmickler[1], Monique Breteler[1], and Tony Stoecker[1,2]

[1]German Center for Neurodegenerative Diseases, Bonn, Germany, [2]Department of Physics and Astronomy, University of Bonn, Bonn, Germany

For the Rhineland study, a fully automated phantom QA procedure was developed to monitor the quality characteristics of the MRI scanners. Various QA metrics are investigated to characterize scanner stability and performance over time and across different sites. To ensure measurement reproducibility and consistency standardized phantoms were developed and a dedicated QA protocol as well as a processing pipeline was implemented. The QA scans are acquired each day after the last subject to be able to detect data inconsistencies and hardware defects as soon as possible. This ensures high-throughput data collection with minimal data loss.

3827 Computer 21

Development of 3D UTE Reconstruction Software Using Python Language

Eun-Kee Jeong[1,2], Kyle Jeong[1,3], Bijaya Thapa[1,4], and Insun Lee[1]

[1]Utah Center for Advanced Imaging Research, University of Utah, Salt Lake City, UT, United States, [2]Radiology and Imaging Sciences, University of Utah, Salt Lake City, UT, United States, [3]Biomedical Engineering, University of Utah, Salt Lake City, UT, United States, [4]Physics and Astronomy, University of Utah, Salt Lake City, United States

3D radial, such as ultra-short TE (UTE) MRI, is receiving a growing attention, because of its unique features, which include free of motion artifact and imaging of short T2* species. However, reconstruction of UTE data is very challenging, therefore, only a handful research institutes possess the reconstruction capability. We developed a GUI-based software to construct UTE images using Python and C++ languages. We will present details about the development of this software using Python, which includes difficulties.

3828 Computer 22

Implementation of a Dual Parameter Segmentation Tool for Identification of Brown Adipose Tissue on Magnetic Resonance Imaging

David Reading[1], Dana Mathews[2], Yee Ng[1], Binu Thomas[3], Orhan Oz[2], Jonathan Graff[4], and Takeshi Yokoo[5]

[1]Radiology, UT Southwestern Medical Center, Dallas, TX, United States, [2]Radiology, Division of Nuclear Medicine, UT Southwestern Medical Center, Dallas, TX, United States, [3]Advanced Imaging Research Center, UT Southwestern Medical Center, Dallas, TX, United States, [4]Department of Developmental Biology, UT Southwestern Medical Center, Dallas, TX, United States, [5]Radiology, Advanced Imaging Research Center, UT Southwestern Medical Center, Dallas, TX, United States

Defining regions of brown adipose tissue (BAT) on MRI remains challenging. Dissemination of existing methods is complicated by propriety algorithms, variability between institutions, and the need for time consuming manual segmentation. In this pilot imaging study, we implemented an online segmentation tool for the open-source OsiriX DICOM viewer platform (Pixmeo, Geneva) that can be used to identify regions of BAT on MRI through simultaneous fat fraction and T2* thresholding automatic segmentation. Since an OsiriX plugin is easily distributable and usable across different centers, our tool may facilitate future research studies of BAT using MRI.

3829 Computer 23

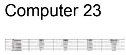

An Image Simulation Tool for 3D TSE Including Flow Effects

John W Grinstead[1], Gregor Koerzdoerfer[2], Gerhard Laub[2], William Rooney[3], and Mathias Nittka[2]

[1]Siemens Healthcare, Portland, OR, United States, [2]Siemens Healthcare, [3]Oregon Health & Science University, Portland, OR, United States

A 3D TSE simulation tool designed as both an educational tool as well as a guide for optimizing protocols is described. The pulse sequence protocol user interface triggers integrated Bloch simulations for a user-defined set of tissues based on current protocol settings including the variable flip angle scheme and reordering mode. The tool models tissue T1 & T2 as well as flow effects. We demonstrate applicability to the issue of flow-induced signal loss in CSF and compare simulations to in vivo measurements. The effects of parameter changes that would otherwise require lengthy in vivo comparisons can now be easily explored.

3830 Computer 24

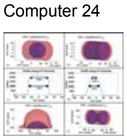

SNR and volume characterization of RF coils: A simple procedure and an automatic post-processing tool for a straightforward comparison

laurent Mahieu-Williame[1], Sophie Gaillard[1], Denis Grenier[1], Radu Bolbos[2], Jean-Baptiste Langlois[2], Franck Lamberton[2], Sorina Camarasu-Pop[1], and Olivier Beuf[1]

[1]Univ.Lyon, CREATIS, CNRS UMR 5220, Inserm U1206, INSA-Lyon, UJM- Saint Etienne Université Claude Bernard Lyon 1, Villeurbanne, France, lyon, France, Metropolitan, [2]CERMEP – imagerie du vivant, Lyon, France, lyon, France, Metropolitan

To choose the most suitable RF coil available for an MRI study, we propose a procedure which uses a calibrated phantom, a 3D gradient-echo sequence, and an automatic post-processing tool available on the web. This tool generates a report which contains the measurement of a SNR with uniform volumes located in the depth. The post-processing could be done on MR images acquired on most main MRI vendors (Siemens, GE, Philips and Bruker) with prior verification of applied scaling or filtering. RF coil characterization results performed on at 4.7T and 7T were compared. The tool can be used for quality control.

Electronic Poster

Multi-Band Pulses & Simultaneous Multi-Slice

Exhibition Hall — Tuesday 8:15 - 9:15

3831 Computer 25

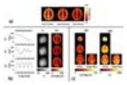

MR Fingerprinting ASL: multi-slice acquisition, sequence optimization, and validation with DSC

Pan Su[1,2], Yang Li[1,2], Deng Mao[1,2], Wenbo Li[1,3], Qin Qin[1,3], Jay J. Pillai[1], and Hanzhang Lu[1]

[1]Russell H. Morgan Department of Radiology and Radiological Science, Johns Hopkins University, Baltimore, MD, United States, [2]Graduate School of Biomedical Sciences, The University of Texas Southwestern Medical Center, Dallas, TX, United States, [3]F.M. Kirby Research Center for Functional Brain Imaging, Kennedy Krieger Institute, Baltimore, MD, United States

MR Fingerprinting (MRF) based Arterial Spin Labeling (ASL) has been recently proposed as a new approach to measure multiple hemodynamic parameters in a single scan. However, the previous implementation of MRF-ASL has several limitations, including a single-slice-only acquisition, incomplete optimization of the sequence, and an absence of comparison with existing techniques such as Look-Locker ASL and dynamic-susceptibility-contrast (DSC) MRI. In this work, we conducted a series of six studies to fill these technical gaps: we optimized several key imaging parameters in MRF-ASL and compared the results to existing methods.

3832 Computer 26

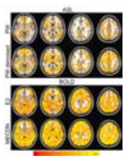

Using a Novel Multiband Multi-Echo Simultaneous ASL/BOLD Sequence to Measure Cerebrovascular Reactivity

Alexander D. Cohen[1], Andrew S. Nencka[1], and Yang Wang[1]

[1]Radiology, Medical College of Wisconsin, Milwaukee, WI, United States

A multiband, multi-echo simultaneous ASL/BOLD sequence was developed and used to estimate cerebrovascular reactivity (CVR) using a breath hold (BH) task. In addition, both the BOLD and ASL data were denoised using multi-echo independent component analysis (ME-ICA). ICA was used to extract the BH activation component from the data, which was then correlated with the whole brain. CVR was estimated as the percent signal change from the BH task. Denoising resulted in increased BH activation and more robust CVR maps. Furthermore, the data-driven approach used here eliminates the need to model for the complicated BH response.

3833 Computer 27

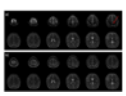

Comparison of Methods for Simultaneous Multi-Slice Balanced SSFP Imaging

Yuan Zheng[1], LeLe Zhao[2], Cong Zhang[2], Jian Xu[1], Ruchen Peng[3], and Weiguo Zhang[2]

[1]UIH America, Houston, TX, United States, [2]Shanghai United Imaging Healthcare Co., Ltd, Shanghai, People's Republic of China, [3]Medical Imaging Center, Beijing Luhe Hospital Affiliated to Capital Medical University, Beijing, People's Republic of China

Many previously reported SMS-bSSFP sequences use RF phase modulation for slice shifting, which inevitably shifts the bSSFP frequency band and is thus susceptible to banding artifacts. Another slice-shifting method is to modulate slice-select dephasing/rephasing gradients. We have studied these two strategies and showed that gradient modulation is more advantageous, since it does not modify the RF phase cycling scheme and bSSFP frequency selectivity is kept the same for all slices. We have acquired phantom and in-vivo head images using both approaches, and demonstrated that gradient modulation does not introduce banding artifacts and produces high quality images.

3834 Computer 28

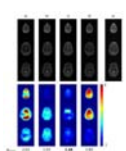

Tailored 3D RF pulses for g-factor reduction in phase-constrained simultaneous multislice imaging

Ádám Kettinger[1,2], Stephan A. R. Kannengiesser[3], Felix A. Breuer[4], Zoltán Vidnyánszky[1], and Martin Blaimer[4]

[1]Brain Imaging Centre, Research Centre for Natural Sciences, Hungarian Academy of Sciences, Budapest, Hungary, [2]Department of Nuclear Techniques, Budapest University of Technology and Economics, Budapest, Hungary, [3]MR Application Predevelopment, Siemens Healthcare GmbH, Erlangen, Germany, [4]Magnetic Resonance and X-ray Imaging Department, Fraunhofer Development Center X-ray Technology (EZRT), Würzburg, Germany

Simultaneous multislice imaging techniques are widely used to accelerate the acquisition process, however, non-ideal coil geometries can introduce noise enhancement. This effect can be reduced by using the virtual-conjugate-coil technique, in which case the g-factors will be dependent of the object background phase. It has been shown that an optimal phasemap exists that minimizes the g-factors. We have used 3D tailored RF pulses to approximate the optimal phase distribution in each simultaneously acquired slice to reduce the noise amplification in phantom and also in vivo. Our results imply that g-factors can be reduced significantly while flip angle homogeneity remains reasonable.

3835 Computer 29

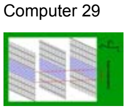

Quantitative Susceptibility Mapping Using 2D Simultaneous Multi-slice Gradient-echo Imaging at 7T

Wei Bian[1], Adam Bruce Kerr[2], Kongrong Zhu[2], Paymon Rezaii[1], Maged Goubran[1], Christopher Lock[3], May Han[3], Yi Wang[4], Zhe Liu[4], Sherveen Parivash[1], Brian Rutt[1], and Michael Zeineh[1]

[1]Department of Radiology, Stanford University, Stanford, CA, United States, [2]Department of Electrical Engineering, Stanford University, Stanford, CA, United States, [3]Department of Neurology and Neurological Sciences, Stanford University, Stanford, CA, United States, [4]Department of Radiology, Weill Cornell Medical College, New York, NY

A 2D multi-echo simultaneous multi-slice (SMS) gradient-echo imaging sequence was implemented for simultaneous anatomical imaging, R2* mapping and quantitative susceptibility mapping (QSM). Imaging acceleration in the slice direction speeds up the sequence to clinical scan times while using a longer TR and larger flip angle compared to 3D imaging. Evaluation from both healthy and multiple sclerosis subjects showed that, using the same acquisition time and imaging resolution as a 3D sequence, the proposed sequence improved tissue susceptibility contrast, suggesting 2D SMS GRE imaging may be a viable alternative for clinical applications of susceptibility-based imaging.

3836 Computer 30

Minimum-Duration Parallel Transmit Pulses for Simultaneous Multislice Imaging

Mihir Pendse[1] and Brian K Rutt[1]

[1]Stanford University, Stanford, CA, United States

We describe a procedure for obtaining minimum duration parallel transmit pulses for simultaneous multislice imaging. The strategy involves a combination of the IMPULSE parallel transmit pulse design algorithm for mitigating local SAR hotspots and enforcing flip angle homogeneity; an optimal control algorithm for intelligent design of slice selective subpulse shape with minimum power; and time-optimal VERSE for reducing peak power with minimum increase in pulse duration. Results indicate a reduction in pulse duration by a factor of 4.9 compared to a pTx-SMS pulse designed with conventional techniques.

3837 Computer 31

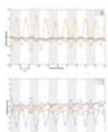

Super Resolution Motion Correction (SUPREMO) using Simultaneous Multi-Slice EPI based fMRI

Jose R. Teruel[1], Nathan S. White[1], Timothy T. Brown[2], Joshua M. Kuperman[1], and Anders M. Dale[1,2]

[1]Department of Radiology, University of California San Diego, La Jolla, CA, United States, [2]Department of Neurosciences, University of California San Diego, La Jolla, CA, United States

In this study, we describe a method to correct for motion in fMRI acquisitions with sub-TR temporal resolution, applying the Extended Kalman Filter framework, using each multi-slice EPI shot as its own navigator.

3838 Computer 32

Simultaneous Multislice MRF with Hadamard RF-Encoding

Alice Yang[1], Yun Jiang[1], Dan Ma[2], Kawin Setsompop[3], Vikas Gulani[2,4], and Mark Griswold[2]

[1]Biomedical Engineering, Case Western Reserve University, Cleveland, OH, United States, [2]Radiology, Case Western Reserve University, Cleveland, OH, United States, [3]Radiology, Massachusetts General Hospital, Athinoula A. Martinos Center for Biomedical Imaging, Charlestown, MA, United States, [4]Radiology, University Hospitals, Cleveland, OH, United States

Relaxation times can be measured efficiently with Magnetic Resonance Fingerprinting (MRF) but further acceleration of MRF is difficult as individual images are already highly undersampled. In this study Hadamard RF-encoding is utilized to acquire four slices simultaneously. It is demonstrated that the proposed method can provide T_1 and T_2 maps for simultaneously acquired slices at 2mm slice thickness.

3839 Computer 33

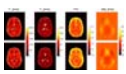

Simultaneous multi-slice triple-echo steady-state (SMS-TESS) T1, T2, PD, and B0 mapping in the human brain

Rahel Heule[1,2], Zarko Celicanin[1,2], Sebastian Kozerke[3], and Oliver Bieri[1,2]

[1]Division of Radiological Physics, Department of Radiology, University of Basel Hospital, Basel, Switzerland, [2]Department of Biomedical Engineering, University of Basel, Basel, Switzerland, [3]Institute for Biomedical Engineering, University and ETH Zurich, Zurich, Switzerland

Triple-echo steady-state (TESS) has so far been investigated mainly as a particular robust and intrinsically B_1-insensitive method for T_2 relaxation time mapping. Here, its potential for fast simultaneous multi-parametric (T_1, T_2, PD, and B_0) mapping of human brain tissues from a single scan is explored. TESS imaging is performed in 2D mode to mitigate motion sensitivity in the brain and accelerated by simultaneous multi-slice (SMS) imaging using CAIPIRINHA to excite two slices simultaneously providing similar SNR in half the acquisition time as compared to sequential single-slice imaging.

3840 Computer 34

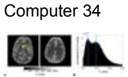

Snapshot whole-brain T1 mapping using 2D multi-slice variable flip angle spiral imaging with steady-state preparation

Rahel Heule[1,2], Josef Pfeuffer[3], and Oliver Bieri[1,2]

[1]Division of Radiological Physics, Department of Radiology, University of Basel Hospital, Basel, Switzerland, [2]Department of Biomedical Engineering, University of Basel, Basel, Switzerland, [3]Siemens Healthcare, Application Development, Erlangen, Germany

Spiral imaging substantially shortens MR fingerprinting acquisitions to tolerable scan times. Also more traditional “state-of-the-art” parametric mapping techniques can potentially benefit from the speed-up ability of fast spiral trajectories as opposed to Cartesian sampling. Here, a variable flip angle T_1 quantification approach based on an interleaved 2D spiral multi-slice spoiled gradient echo sequence is combined with a steady-state preparation scheme. The investigated method offers accurate whole-brain T_1 determination at clinically relevant resolution in only half a minute (including the B_1 mapping scan in about 40 s) with an acceleration factor of an order of magnitude compared to conventional Cartesian sampling.

3841 Computer 35

Improvements in Simultaneous Multislice Imaging Through the Use of SPIRiT and Virtual Conjugate Coils

Nikolai J Mickevicius[1] and Eric S Paulson[2]

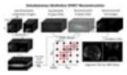

[1]Biophysics, Medical College of Wisconsin, Milwaukee, WI, United States, [2]Radiation Oncology, Biophysics, Radiology, Medical College of Wisconsin, Milwaukee, WI, United States

Simultaneous multislice (SMS) imaging is an attractive solution for accelerating MR acquisition due to its higher inherent SNR. However, further acceleration of SMS images along the phase encoding direction results in increased noise amplification. We demonstrate here the advantages of a combined virtual conjugate coil based phase-constrained SPIRiT reconstruction to minimize the g-factor penalty associated with highly accelerated SMS acquisitions.

3842 Computer 36

Slice-GRAPPA calibration using pre-scan data and application to simultaneous multi-slice PROPELLER

Kun Zhou[1], Wei Liu[1], Fang Dong[1], and Shi Cheng[1]

[1]Siemens Shenzhen Magnetic Resonance Ltd., Shenzhen, People's Republic of China

In simultaneous multi-slice imaging technique, the kernels used for unfolding the collapsed slices are estimated using integrated or separated reference scans, which require additional scan time. In this work a slice-GRAPPA calibration method utilizing the pre-scan data is developed to save the time for acquiring training data. This method has been applied to slice accelerated PROPELLER sequence. The result shows that the proposed method can correctly fit the SG kernel and reconstruct the slice undersampled images.

3843 Computer 37

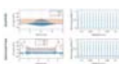

Application of time-optimal Simultaneous Multi-Slice refocusing to TSE/RARE

Christoph Stefan Aigner[1], Armin Rund[2,3], Berkin Bilgic[4,5], Borjan Gagoski[6], Kawin Setsompop[4,5], Karl Kunisch[2], and Rudolf Stollberger[1]

[1]Institute of Medical Engineering, Graz University of Technology, Graz, Austria, [2]Institute for Mathematics and Scientific Computing, University of Graz, Graz, Austria, [3]BioTechMed Graz, Graz, Austria, [4]Massachusetts General Hospital, Martinos Center for Biomedical Imaging, Charlestown, MA, United States, [5]Harvard Medical School, Boston, MA, United States, [6]Department of Radiology, Boston Children's Hospital, Boston, MA, United States

RF pulses for Simultaneous Multi-Slice imaging (SMS) are still limited by hardware and safety requirements leading to lengthy pulse durations. In this work we apply a bi-level time-optimal control method to design a minimum time SMS refocusing pulse for a multiband factor of 15 with 1mm slice thickness resulting in a refocusing duration of 4.58ms, which is 1.7x shorter than the state of the art MultiPINS pulse. The optimized RF pulse and the corresponding shaped slice selective gradient are tested in-vivo in a T2-TSE SMS wave-CAIPI scan of the whole head in 70s.

3844 Computer 38

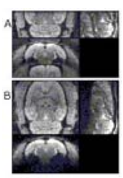

An optimized slice-GRAPPA reconstruction method to reduce leakage artifacts in small-animal multiband imaging

Hiroshi Toyoda[1], Sosuke Yoshinaga[2], Naoya Yuzuriha[2], Mitsuhiro Takeda[2], and Hiroaki Terasawa[2]

[1]Center for Information and Neural Networks, National Institute of Information and Communications Technology, Suita, Japan, [2]Department of Structural BioImaging, Kumamoto University, Kumamoto, Japan

Accurate slice separation for simultaneous multi-slice acquisition continues to be challenging, especially when animal scanners equipped with relatively few receiver coil elements are used. We propose an optimized slice-GRAPPA method to reconstruct the dual-band EPI of rat brains, in which the size-optimized kernel was iteratively estimated to reduce artifacts. The reconstructed images were evaluated in terms of inter-slice leakage, g-factor, and temporal variation across the repetitions. With the proposed method, inter-slice leakage artifacts and the g-factor were reduced, and the average signal-to-noise ratio was improved. Thus, the total reconstruction accuracy was improved in the multiband EPI in a small animal study.

3845 Computer 39

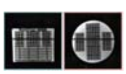

SOMS: Simultaneous Orthogonal Multi-Slice Imaging

Sebastian Rosenzweig[1,2] and Martin Uecker[1,2]

[1]Diagnostische und Interventionelle Radiologie, University Medical Center Göttingen, Göttingen, Germany, [2]Partner site Göttingen, German Centre for Cardiovascular Research (DZHK), Göttingen, Germany

Simultaneous multi-slice (SMS) MRI has become a popular technique in both research and clinical practice, as it provides information about multiple slices at the time of a conventional single-slice measurement. For technical reasons, SMS is commonly limited to the acquisition of parallel slices. Here, we propose a new Cartesian sequence for the simultaneous excitation of orthogonal slices. We dub this technique simultaneous orthogonal multi-slice (SOMS). In this proof of concept phantom study, we reconstruct two 2-fold undersampled, simultaneously acquired orthogonal slices.

3846 Computer 40

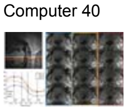

Evaluation of upper airway neuromuscular reflex and passive collapsibility using real-time multi-slice MRI during CPAP

Weiyi Chen[1], Emily Gillett[2], Sally L. Davidson Ward[2], Michael C.K. Khoo[1], and Krishna S. Nayak[1]

[1]University of Southern California, Los Angeles, CA, United States, [2]Children's Hospital Los Angeles, Los Angeles, CA, United States

We demonstrate a new imaging test that uses simultaneous multi-slice real-time MRI during continuous positive airway pressure (CPAP) to quantify upper airway neuromuscular reflex and passive collapsibility. Both are measured using cross-sectional area fluctuation during abrupt changes to CPAP. We applied this test to patients with obstructive sleep apnea (OSA) and healthy controls. Subjects with OSA showed 3-5x higher airway area fluctuation compared to healthy volunteers, and this difference was statistically significant ($p < 0.05$). Neuromuscular reflex and area fluctuation varied greatly among the OSA patients, suggesting a potential spectrum of active/physiological and passive/anatomical factors contributing to OSA.

3847 Computer 41

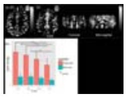

Multi-slice extension of iVASO for absolute cerebral blood volume mapping using a 3D GRASE readout

Swati Rane[1], Thomas J Grabowski[1], John C Gore[2,3,4], Jun Hua[5], and Manus J Donahue[2,6]

[1]Radiology, University of Washington Medical Center, Seattle, WA, United States, [2]Radiology and Radiological Sciences, Vanderbilt University Institute of Imaging Science, Nashville, TN, United States, [3]Biomedical Engineering, Vanderbilt University School of Medicine, Nashville, TN, United States, [4]Physics and Astronomy, Vanderbilt University School of Medicine, Nashville, TN, United States, [5]Radiology, Johns Hopkins University, Baltimore, MD, United States, [6]Neurology, Vanderbilt University School of Medicine, Nashville, TN, United States

We present a multi-slice approach to evaluate arterial cerebral blood volume with non-invasive inflow-vascular space occupancy (iVASO) approach using a 3D GRASE readout in conjunction with the iVASO preparation pulses.

3848 Computer 42

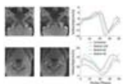

Simultaneous Multi-Slice Radial Phase Contrast MRI

Liyong Chen[1,2] and David Feinberg[1,2]

[1]Advanced MRI Technologies, LLC, Berkeley, CA, United States, [2]Helen Wills Neuroscience Institute, Univ of California, Berkeley, Berkeley, CA, United States

The purpose was to develop and evaluate a novel approach to MR phase imaging of blood flow by combining radial cine phase contrast (radial cine-PC) with simultaneous multi-slice (SMS) technique to measure velocity in several slice planes simultaneously. Comparisons were made between SMS radial and SMS Cartesian 2D cine-PC and the velocity curves measured in cerebral vessels were similar between them. The higher acquisition efficiency of SMS radial cine PC allows for simultaneous cross-sectional hemodynamic quantification and may be useful for medical diagnoses.

3849 Computer 43

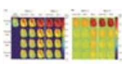

Improved unbiased multi-slice T1 measurement with compressed-sensing assisted variable-repetition-delay turbo-spin echo acquisition for ultra-high field preclinical applications

DongKyu Lee[1], Sohyun Han[1], and HyungJoon Cho[1]

[1]Bio-medical Engineering, Ulsan National Institute of Science and Technology, Ulsan, Korea, Republic of

The benefits of compressed-sensing (CS) assisted turbo-spin-echo (TSE), i.e. CS-TSE, acquisition for variable-repetition-delay T_1 measurement were investigated with two-dimensional multi-slice ex vivo and in vivo T_1 mappings at 7T preclinical scanner. The direct advantages resulting from replacing the refocusing pulses of TSE with CS acceleration included reduced scan times for multi-slice coverage and minimization of inter-slice interferences, which are all required in order to improve the accuracy of multi-slice T_1 measurement.

3850 Computer 44

Ultrafast 2D MRI method based on multi-slice spatiotemporal encoding with simultaneous image refocusing

Yao Luo[1], Jun Zhang[1], Shuhui Cai[1], and Congbo Cai[2]

[1]Department of Electronic Science, Xiamen University, Xiamen, People's Republic of China, [2]Department of Communication Engineering, Xiamen University, Xiamen, People's Republic of China

We propose a new ultrafast multi-slice spatiotemporally encoded (SPEN) MRI technique, termed SeMSPEN, which outmatches conventional multi-slice EPI in its capability in shortening sampling time by producing multiple images in single echo train, and in lowering the specific absorption rate by segmenting the slice-selective dimension. The feasibility of this new method is verified theoretically and experimentally.

3851 Computer 45

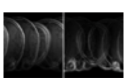

Improved CAIPIRINHA for Simultaneous Multislice Imaging Using Total Variation Regularization

Song Gao[1] and Yajun Ma[1]

[1]Medical Physics Department, Peking University, Beijing, People's Republic of China

The CAIPIRINHA (Controlled Aliasing in Parallel Imaging Results in Higher Acceleration), proposed for simultaneous multislice imaging, combines the multiband excitation and phase cycling techniques to reduce scan time and improve the subsequent imaging reconstruction.The total variation (TV) regularization uses an edge-preserving prior which imposes a relationship between neighboring pixels for image reconstruction. In this work, the TV regularization method is applied to further improve the CAIPIRINHA. In vivo data results demonstrate that the TV regularization is very powerful in suppressing noise, maintaining fine imaging details and reducing aliasing artifacts.

3852 Computer 46

Independent band-specific correction for B0 and B1 inhomogeneities in multiband 2D RF pulses

Yuxin Hu[1,2], Valentina Taviani[3], Bruce L. Daniel[1], and Brian A. Hargreaves[1]

[1]Department of Radiology, Stanford University, Stanford, CA, United States, [2]Department of Electrical Engineering, Stanford University, Stanford, CA, United States, [3]GE Healthcare, Menlo Park, CA, United States

2D in-plane multiband RF pulses have been developed to offer high-resolution diffusion-weighted imaging (DWI) with minimal distortion. However, B0 and B1 inhomogeneities may lead to significant and varying signal loss in different bands, that can in turn result in signal inconsistency between bands. In this work, correction for B0 and B1 variations was implemented by independently tuning the RF center frequency and amplitude for each band. Phantom images acquired with corrected pulses were shown to have higher signal amplitude and reduced slab boundary artifacts.

3853 Computer 47

Simultaneous multi-slice (SMS) imaging technique for radial trajectory using inter-slice shifting gradient.

Dongchan Kim[1], Jaejin Cho[2], Kinam Kwon[2], Byungjai Kim[2], Yeji Han[1], Jun-Young Chung[1], and HyunWook Park[2]

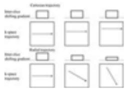

[1]Gachon University, Incheon, Korea, Republic of, [2]Korea Advanced Institute of Science and Technology, Daejeon, Korea, Republic of

SMS imaging techniques utilized phase modulated RF pulses, blipped gradients, or inter-slice shifting gradients to increase the use of sensitivity information of multi-channel coils. In this work, we extended the use of inter-slice shifting gradient based SMS techniques of a Cartesian trajectory to a radial trajectory. We modulated the ratio between inter-slice shifting gradient and readout gradient (*i.e.* view angle) with the cosine function. In addition, we adjusted the direction of shift of each slice by adjusting the offset of cosine function, thereby increase sampling efficiency of a radial trajectory when the imaging objects need an anisotropic field-of-view.

3854 Computer 48

Improved Simultaneous Multislice Pulse Design Directly Constraining Peak RF Amplitude

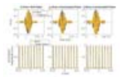

Sydney N Williams[1], Douglas C Noll[2], and Jeffrey A Fessler[3]

[1]Biomedical Engineering, University of Michigan, Ann Arbor, MI, United States, [2]BIomedical Engineering, University of Michigan, Ann Arbor, MI, United States, [3]Electrical Engineering and Computer Science, University of Michigan, Ann Arbor, MI, United States

In this abstract, we propose the design of SMS RF pulses using a new method based on the small-tip angle approximation that directly constrains peak amplitude using a least-square optimization. We compare our proposed method to the equivalent phase-modulated Shinnar-Le Roux (SLR) SMS pulse with optimized phase scheduling for minimal RF power. Our proposed method provides lower simulation error than SLR-based designs at equivalent pulse lengths and same error for shorter pulse lengths that are unrealizable (in the peak amplitude sense) with the SLR-based approach. In experiment we show sharp excitation slice profiles for our SMS designs.

Electronic Poster

Sparse & Low-Rank Reconstruction

Exhibition Hall — Tuesday 8:15 - 9:15

3855 Computer 49

Improved Accelerated Model-based Parameter Quantification with Total-Generalized-Variation Regularization.

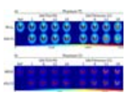

Oliver Maier[1], Matthias Schloegl[1], Andreas Lesch[1], Andreas Petrovic[1], Martin Holler[2], Kristian Bredies[2], Thomas Pock[3], and Rudolf Stollberger[1]

[1]Institute of Medical Engineering, Graz University of Technology, Graz, Austria, [2]Institute of Mathematics and Scientific Computing, University of Graz, Graz, Austria, [3]Insitute for Computer Graphics and Vision, Graz University of Technology, Graz, Austria

Incorporating TGV-regularization to accelerated model-based parameter-quantification can lead to improved image quality, however, adds non-differentiability to the problem which poses a problem for commonly used first order optimization methods like non-linear Conjugate-Gradient. The proposed method overcomes this limitation by handling the problem within a Gauss-Newton-framework and applying a Primal-Dual-algorithm to solve the inner TGV-regularized problem. Numerical simulations exhibit high agreement to references for four different parameter mapping problems up to 18-fold acceleration. In-vivo results for T1-VFA and T2-MESE models strengthen these findings. The proposed method offers huge acceleration potential for model-based parameter-quantification with similar quantification quality as fully sampled data.

3856 Computer 50

Comparison of Compressed Sensing Accelerated TOF MRA of the Neck with Conventional TOF MRA and Ultrasound in Clinical Cases

Takayuki YAMAMOTO[1], Tomohisa OKADA[2], Yasutaka FUSHIMI[1], Koji FUJIMOTO[3], Akira YAMAMOTO[1], Peter SPEIER[4], Michaela SCHMIDT[4], Yutaka NATSUAKI[5], and Kaori TOGASHI[1]

[1]Diagnostic Imaging and Nuclear Medicine, Kyoto University, Graduate School of Medicine, Kyoto, Japan, [2]Human Brain Research Center, Kyoto University, Graduate School of Medicine, Kyoto, Japan, [3]Center for Advanced Imaging Innovation and Research (CAI2R) and Bernard and Irene Schwartz Center of Biomedical Imaging, New York University School of Medicine, Ner York, NY, United States, [4]Siemens Healthcare GmbH, [5]Siemens Medical Solutions USA, Inc.

Compressed sensing (CS) can accelerate time-of-flight magnetic resonance angiography (TOF MRA) of the neck. The whole length of carotid arteries from the aortic arch to the skull base was scanned in 2 minutes with an acceleration factor of 7.5. Iterative reconstruction that exploits regularization in 3 spatial directions required less than 3 minutes on a GPU. The degree of stenosis at carotid bifurcation for 22 patients was subjectively evaluated on maximum intensity projection images. Results of CS accelerated TOF MRA and conventional TOF MRA were compared with stenotic rates measured by ultrasound, and showed an excellent correlation.

3857 Computer 51

High frame rate vocal tract MRI using compressed sensing on randomly sampled Cartesian spoiled fast gradient echo

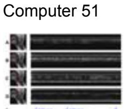

Pierre-André Vuissoz[1,2], Benjamin Elie[3], Freddy Odille[2,4], and Yves Laprie[3]

[1]IADI, Université de Lorraine, Nancy, France, [2]U947, INSERM, Nancy, France, [3]LORIA, INRIA/CNRS/Université de Lorraine, Nancy, France, [4]CIC-IT 1433, CHRU Nancy, Nancy, France

MRI becomes an important tool in the study of speech, in particular in the understanding of articulatory gestures. Distributed Compressed Sensing and Projection Onto Convex Sets are used to reconstruct dynamic sequences of vocal tract images at 33 frames per second with a spatial resolution enabling the extraction of vocal tract contours. 15 seconds long, spoiled gradient echo sequence acquisitions with pseudo random Cartesian sampling were recorded while subjects were repeating sentences. 76 sentences were recorded, representing the majority of the French phonemes. High frame rate dynamic vocal tract MRI will enable the study of coarticulation in French.

3858 Computer 52

Self-Calibrated Non-Cartesian Multi-shot Diffusion Imaging

Merry Mani[1], Arnaud Guidon[2], Baolian Yang[2], Vincent Magnotta[1], and Mathews Jacob[3]

[1]Radiology, University of Iowa, Iowa City, IA, United States, [2]GE Healthcare, [3]Electrical and Computer Engineering, University of Iowa, Iowa City, IA, United States

Non-Cartesian multi-shot sequences (e.g. spiral) offer several benefits over Cartesian counterparts in the context of high spatial resolution diffusion weighted imaging (DWI), including reduced B_0 & T2* artifacts, as well as improved SNR resulting from lower TE. However, their main drawback of the above scheme is the sensitivity of the multi-shot imaging to motion artifacts. To achieve motion compensation, the multi-shot reconstruction methods rely on a phase-calibration procedure, during which an estimate of motion induced phase map is computed. Not only is the phase-calibration step time consuming, it also involves heavy optimization of parameters. The main focus of this work is to develop a phase calibration-free motion-compensated reconstruction for multi-shot non-Cartesian diffusion imaging.

3859 Computer 53

Low Rank Alternating Direction Method of Multipliers Reconstruction for MR Fingerprinting

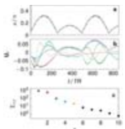

Jakob Assländer[1,2,3], Martijn A Cloos[1,2], Florian Knoll[1,2], Daniel K Sodickson[1,2], Jürgen Hennig[3], and Riccardo Lattanzi[1,2]

[1]Dept. of Radiology - Bernard and Irene Schwartz Center for Biomedical Imaging, New York University School of Medicine, New York, NY, United States, [2]Dept. of Radiology - Center for Advanced Imaging Innovation and Research, New York University School of Medicine, New York, NY, United States, [3]Dept. of Radiology - Medical Physics, University Medical Center Freiburg, Freiburg, Germany

The proposed reconstruction framework for MR-Fingerprinting (MRF) combines a low rank approximation of the signal's temporal evolution with the alternating direction method of multipliers. This general framework allows for incorporating parallel imaging and compressed sensing. The low rank approximation of the signal's temporal evolution reduces the number of fast Fourier transformations significantly and adresses the non-convexity of the MRF-reconstruction problem. Overall, the convergence is improved and undersampling artifacts are reduced, resulting in a fast, robust and flexible reconstruction framework.

3860 Computer 54

Multi-Compartment MR Fingerprinting via Reweighted-l1-norm Regularization

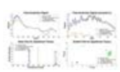

Sunli Tang[1], Jakob Asslaender[2], Lee Tannenbaum[3], Riccardo Lattanzi[2], Martijn Cloos[2], Florian Knoll[2], and Carlos Fernandez-Granda[1,3]

[1]Courant Institute of Mathematical Sciences, NYU, New York, NY, United States, [2]Center for Biomedical Imaging, NYU School of Medicine, [3]Center for Data Science, NYU

This work implements a Magnetic Resonance Fingerprinting (MRF) reconstruction that accounts for the presence of multiple compartments in a voxel. We estimate the contributions of the different tissues by incorporating a sparse-recovery method, based on reweighted-l1-norm regularization, within an iterative procedure that fits a multi-compartment model to the measured k-space data. The proposed approach is validated with simulated data, as well as with a controlled phantom experiment. In addition, we present preliminary results on in-vivo measurements of a brain.

3861 Computer 55

Compressed Sensing 3D GRASE with Group-Sparse Reconstruction for Brain Myelin Water Imaging

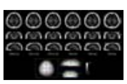

Henry Szu-Meng Chen[1], Emil Ljungberg[2], Alex L MacKay[1,3,4], and Piotr Kozlowski[3,5]

[1]Physics and Astronomy, University of British Columbia, Vancouver, BC, Canada, [2]Medicine, University of British Columbia, Vancouver, BC, Canada, [3]Radiology, University of British Columbia, Vancouver, BC, Canada, [4]UBC MRI Research Centre, Vancouver, BC, Canada, [5]UBC MRI Research Centre, Vancouer, BC, Canada

Myelin water fraction (MWF), which reflects myelin content, can be derived from multiple T2 weighted images. In this study, compressed sensing was used to accelerate 3D GRASE myelin water imaging in simulated experiments using a Cartesian undersampling scheme. Group-sparse reconstruction that exploits the correlation between the echoes, and different echo sampling schemes, were tested. Group-sparse reconstruction was found to improve the overall data quality, and identical phase encode undersampling for each echo was found to improve MWF map quality. Using both, MWF map quality remained usable for up to 4x acceleration.

3862 Computer 56

Fast 4D MRI Reconstruction Analytics using Low-Rank Tensor Imputation

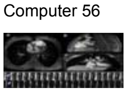

Morteza Mardani[1], Joseph Cheng[1,2], John Pauly[1], and Lei Xing[1]

[1]Stanford University, Stanford, CA, United States, [2]Stanford University, United States

An imaging analytic is proposed that efficiently reconstruct high-resolution 4D MR images using GPU computing. Modeling ***k***-space data low dimensionality with low PARAFAC rank of tensors, the correlation across different dimensions are captured via tensor subspaces, sequentially learned from the subsampled data, to impute the missing k-space entries. The novel analytics gain considerable computational saving relative to the state-of-the-art compressive sampling schemes, while achieving failry similar image quality.

3863 Computer 57

Compressive T2 Mapping with Non-Local Clustering and Subspace Constraints

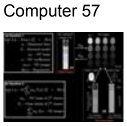

Sagar Mandava[1], Mahesh B Keerthivasan[1], Maria I Altbach[2], and Ali Bilgin[1,2,3]

[1]Electrical and Computer Engineering, University of Arizona, Tucson, AZ, United States, [2]Medical Imaging, University of Arizona, Tucson, AZ, United States, [3]Biomedical Engineering, University of Arizona, Tucson, AZ, United States

Subspace constrained T2 mapping uses PCA to reconstruct a few principal components instead of all the echo train images before T2 fitting. The temporal (contrast) subspace in these methods is estimated either from acquired training data or via training curves from a signal model. Typically, a single global PC basis is used for all the contrast signals. In this work we present a T2 mapping method based on non-local clustering of signal relaxation curves and tailor the PC bases for the curves in each cluster and compare it with the global PC basis approach.

3864 Computer 58

Respiratory motion-field reconstruction using low-rank plus sparse (L+S) approach for dynamic MRI of the lungs

Matthew John Muckley[1], Li Feng[1], Hersh Chandarana[1], Daniel K Sodickson[1], and Ricardo Otazo[1]

[1]Radiology, New York University, New York, NY, United States

A motion-guided low-rank plus sparse (L+S) approach for reconstruction of respiratory motion fields is presented for dynamic MRI of the lungs with high spatiotemporal resolution. Motion-guided L+S represents a paradigm shift where motion fields that describe deformations between respiratory phases are reconstructed instead of the respiratory phases themselves. The technique is demonstrated for normal and deep breathing imaging and compared against standard L+S reconstruction.

3865 Computer 59

Free-breathing and ungated cardiac imaging using calibrationless manifold smoothness regularization

Sunrita Poddar[1], Xiaoming Bi[2], Dingxin Wang[2], and Mathews Jacob[1]

[1]University of Iowa, Iowa City, IA, United States, [2]Siemens Healthcare

We introduce an image manifold smoothness regularization, coupled with spatial regularization, for high-resolution free-breathing and ungated cardiac cine imaging. Prior work in this area relied on additional navigators within each image frame to estimate the manifold structure. In this abstract, we focus on eliminating the need for navigators, which will provide improved sampling efficiency.

3866 Computer 60

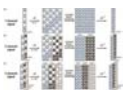

True Temporal Resolution TWIST Imaging using Annihilating Filter-based Low-rank wrap around Hankel Matrix

Eun Ju Cha[1], Kyong Hwan Jin[2], Eung Yeop Kim[3], and Jong Chul Ye[1]

[1]KAIST, Daejeon, Korea, Republic of, [2]EPFL, Lausanne, Switzerland, [3]Gacheon University Gil Medical Center, Incheon, Korea, Republic of

Temporal resolution is an important factor in dynamic enhanced contrast (DCE) MRI. Time-resolved angiography with interleaved stochastic trajectories (TWIST) has been widely used due to its improved temporal and spatial resolution. However, the temporal resolution of TWIST imaging is not a true one because of the view sharing. To provide more improved temporal resolution, we proposed a novel reconstruction algorithm based annihilating filter-based low rank Hankel matrix approach (ALOHA) which exploits the fundamental duality between sparsity in transform domain and low-rankness of Hankel matrix constructed using k-space data. Experimental result using in-vivo data showed the significantly improved temporal resolution than the conventional reconstruction.

3867 Computer 61

Total Generalized Variation as a Temporal Regularizer in Compressed Sensing MRI

Karthik Rao Aroor[1,2], Steven Kecskemeti[1,2], and Andrew Alexander[1,2]

[1]University of Wisconsin Madison, Madison, WI, United States, [2]Waisman Laboratory for Brain Imaging and Behavior, Madison, WI, United States

A novel compressed sensing temporal regularizer, Total Generalized Variation is introduced to enable accelerated temporal imaging. This regularizer eliminates the staircase artifacts typically observed when using a Total Variation regularizer.

3868 Computer 62

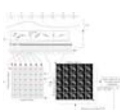

CARDIO-RESPIRATORY MOTION ESTIMATION FOR COMPRESSED SENSING RECONSTRUCTION OF FREE-BREATHING 2D CINE MRI

Javier Royuela-del-Val[1], Muhammad Usman[2], Lucilio Cordero-Grande[2,3], Federico Simmross-Wattenberg[1], Marcos Martin-Fernandez[1], Claudia Prieto[2], and Carlos Alberola-López[1]

[1]Image Processing Lab, University of Valladolid, Valladolid, Spain, [2]Division of Imaging Sciences and Biomedical Engineering, King's College London, London, United Kingdom, [3]Centre for the Developing Brain and Department of Biomedical Engineering, King's College London, London, United Kingdom

In this work a joint cardio-respiratory motion estimation technique is introduced for the compensation of both the respiratory and cardiac motion of the heart during free-breathing cardiac MRI examinations. The proposed technique is combined with an extra-dimensional reconstruction scheme in which respiratory and cardiac motions are resolved. Initial results for 2D cine cardiac MRI are presented for synthetic and real data.

3869 Computer 63

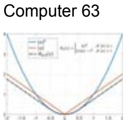

Robust GRASP: A novel approach using the Huber norm in projection space for robust data consistency in undersampled radial MRI

Marcelo V. W. Zibetti[1], Rebecca Ramb[2], Li Feng[2], Ricardo Otazo[2], Leon Axel[2], and Gabor T. Herman[3]

[1]NYU/CUNY/UTFPR, New York, NY, United States, [2]Radiology, NYU School of Medicine, New York, NY, United States, [3]Computer Science, CUNY, New York, NY, United States

Robust data consistency using the Huber norm is proposed for compressed sensing radial MRI to reduce artifacts associated with outliers in the acquired data that cannot be removed by the sparse reconstruction. System imperfections such as chemical shift can introduce this type of large data distortions, or outliers. The quadratic shape of the usually employed Euclidean norm for data consistency is very sensitive to very large errors. In the proposed method, named RObust Golden-angle Radial Sparse Parallel MRI (ROGRASP), the Huber norm enables large errors to remain in the data discrepancy, not transferring them to the reconstructed image. In vivo acquisitions with outlier-contaminated data illustrate this improvement in quality for free-breathing cardiac MRI.

3870 Computer 64

Parallel Imaging Reconstruction with Compressed Sensing Calibration for Real-time Neonatal Chest MRI

Yu Y. Li[1,2]

[1]Cardiac Diagnostic Imaging, St. Francis Hospital, Roslyn, NY, United States, [2]Radiology, Cincinnati Children's Hospital Medical Center, Cincinnati, OH, United States

In the presented work, a compressed sensing approach is introduced to calibrate k-t space parallel imaging reconstruction. This approach removes the need for calibration data and improves image reconstruction using data sparsity associated with narrow bandwidth of physiological motion signals. The new approach is used to enable real-time neonatal chest MRI. It is experimentally demonstrated that real-time imaging can provide high-quality cardiac and pulmonary images for improved clinical diagnosis in premature babies.

3871 Computer 65

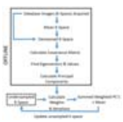

Real-time dynamic image reconstruction using Compressed Sensing and Principal Component Analysis (CS-PCA)

Bryson Dietz[1], Eugene Yip[1], Jihyun Yun[2], Gino Fallone[1,2], and Keith Wachowicz[1,2]

[1]Oncology, University of Alberta, Edmonton, AB, Canada, [2]Medical Physics, Cross Cancer Institute, Edmonton, AB, Canada

An online real-time reconstruction technique that combines compressed sensing with principal component analysis (CS-PCA) was developed for the purpose of adaptive radiotherapy using our Linac-MR system. Our technique uses a database of images, acquired prior to an incoherently accelerated acquisition, to fill in the missing lines of k-space using PCA. Our technique can reconstruct images ranging from 5-20 frames per second with minimal artefacts.

3872 Computer 66

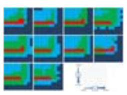

Evaluation of image quality of compressed sensing MRI with natural image quality evaluator

Thai Akasaka[1], Koji Fujimoto[2], Tomohisa Okada[1], Yasutaka Fushimi[1], Akira Yamamoto[1], Takayuki Yamamoto[1], Toshiyuki Tanaka[3], Masayuki Ohzeki[3], and Kaori Togashi[1]

[1]Diagnostic Imaging and Nuclear Medicine, Graduate School of Medicine, Kyoto University, Kyoto, Japan, [2]Center for Advanced Imaging Innovation and Research (CAI2R) and Bernard and Irene Schwartz Center for Biomedical Imaging, Department of Radiology, New York University School of Medicine, New York, NY, United States, [3]Department of Systems Science, Graduate School of Informatics, Kyoto University, Kyoto, Japan

Many image quality assessments (IQA) have been proposed for natural image assessment but few reports have applied them to MRI images, much less to reconstructed images by compressed sensing (CS). Ten subjects were scanned for time-of-flight MR angiography (TOF-MRA), retrospectively under-sampled, and reconstructed by CS. The reconstructed images were evaluated subjectively by radiologists and quantitatively by several IQAs. Structural similarity, scale-invariant feature transform and natural image quality evaluator correlate well with radiologists' perception and hence can be used to determine the optimal parameters for CS of TOF-MRA.

3873 Computer 67

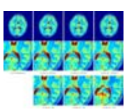

Highly Accelerated Quantitative MRI with ICTGV Regularized Reconstruction

Matthias Schloegl[1], Martin Holler[2], Oliver Maier[1], Thomas Benkert[3], Kristian Bredies[2], Kai Tobias Block[3], and Rudolf Stollberger[1]

[1]Institute of Medical Engineering, Graz University of Technology, Graz, Austria, [2]Institute of Mathematics and Scientific Computing, University of Graz, Austria, [3]Center for Advanced Imaging Innovation and Research (CAI2R), Department of Radiology, New York University School of Medicine, New York, NY, United States

This work describes the use of ICTGV regularization for highly accelerated T_1 and T_2 quantification. For increased robustness of quantitative MRI multiple parameter encodings are necessary. With conventional encoding, this strategy increases scan time, in particular for T_1. By using appropriate subsampling and iterative image reconstruction with ICTGV regularization, high quantification quality is achieved up to an acceleration factor of 16.

3874 Computer 68

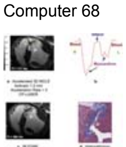

Accelerated Multicontrast Volumetric Imaging Using Compressed Sensing Parallel Imaging Reconstruction with Low Rank and Spatially Varying Edge-Preserving Constraints: In-Vivo Preclinical Validation for High-Resolution Myocardial Infarction Characterization

Li Zhang[1,2] and Graham Wright[1,2]

[1]Department of Medical Biophysics, University of Toronto, Toronto, ON, Canada, [2]Schulich Heart Research Program and Physical Sciences Platform, Sunnybrook Research Institute, Toronto, ON, Canada

To improve characterization of myocardial infarction using high-resolution multicontrast volumetric imaging, this work presents a new compressed sensing parallel imaging reconstruction using low rank and spatially varying edge-preserving constraints. The proposed method was validated in vivo in preclinical studies on pigs with chronic myocardial infarction with comparison to histopathology, demonstrating the promise of robust reconstruction of fine image detail from a single breath-hold multicontrast acquisition at an isotropic resolution of 1.5mm.

3875 Computer 69

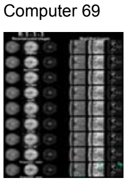

Joint Reconstruction of Multi-Contrast Images: Compressive Sensing Reconstruction using both Joint and Individual Regularization Functions

Emre Kopanoglu[1], Alper Gungor[1], Toygan Kilic[2,3], Emine Ulku Saritas[2,3], Tolga Cukur[2,3], and H. Emre Guven[1]

[1]Aselsan Research Center, Ankara, Turkey, [2]Electrical and Electronics Engineering, Bilkent University, Turkey, [3]National Magnetic Resonance Research Center (UMRAM), Bilkent University, Turkey

In many clinical settings, multi-contrast images of a patient are acquired to maximize complementary information. With the underlying anatomy being the same, the mutual information in multi-contrast data can be exploited to improve image reconstruction, especially in accelerated acquisition schemes such as Compressive Sensing (CS). This study proposes a CS-reconstruction algorithm that uses four regularization functions; joint L1-sparsity and TV-regularization terms to exploit the mutual information, and individual L1-sparsity and TV-regularization terms to recover unique features in each image. The proposed method is shown to be robust against leakage-of-features across contrasts, and is demonstrated using simulations and in-vivo experiments.

3876 Computer 70

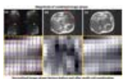

Self-Calibrating Multi-Coil Phase Combination Using The Localized Singular Value Decomposition

Jong Bum Son[1]

[1]*Department of Imaging Physics, The University of Texas MD Anderson Cancer Center, Houston, TX, United States*

MRI can encode clinically important information in the image-phase, thus has great potentials to extend its capability for clinical applications. However, if phase references are not available, the multi-coil phase combination using the weighted average suffers from dominant signal losses coming from phase cancellations due to uncompensated coil-dependent phase offsets.

In this work, we developed a self-calibrating multi-coil phase combining method which does not require any additional scans for phase references. When applied to a single-point Dixon imaging, we verified the proposed method could successfully estimate the global phase-map with the minimal signal loss only using a single-scan image.

3877 Computer 71

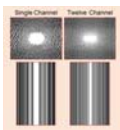

OEDIPUS: Towards optimal deterministic k-space sampling for sparsity-constrained MRI

Justin P. Haldar[1] and Daeun Kim[1]

[1]*Electrical Engineering, University of Southern California, Los Angeles, CA, United States*

We propose a novel approach to designing optimal k-space sampling patterns for sparsity-constrained MRI. The new approach, called OEDIPUS (Oracle-based Experiment Design for Imaging Parsimoniously Under Sparsity constraints), is inspired by insights and methods from estimation theory and the statistical design of experiments. Specifically, OEDIPUS combines the oracle-based Cramér-Rao bound for sparsity-constrained reconstruction with sequential greedy algorithms for observation selection. We demonstrate that OEDIPUS can be used to deterministically and automatically generate k-space sampling patterns that are tailored to specific hardware and application contexts, and which lead to better reconstruction performance relative to conventional sampling approaches for sparse MRI.

3878 Computer 72

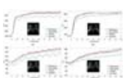

GenSeT: Reconstruction of k-space under-sampled DCE-MRI data using high-order generalized series and temporal constraint

Hien Minh Nguyen[1], Yuan Le[2], and Wei Huang[3]

[1]*Electrical Engineering & Information Technology, Vietnamese-German University, Binh Duong New City, Vietnam,* [2]*Department of Radiology, Mayo Clinic Arizona, Scottsdale, AZ, United States,* [3]*Advanced Imaging Research Center, Oregon Health & Science University, Portland, OR, United States*

A novel reconstruction method exploiting high-order generalized series and temporal sparsity constraint has been presented for sparsely-sampled DCE-MRI. The method uses a static reference to model high-resolution anatomical structures while extrapolating the missing k-space and imposing the sparsity of the time frame difference. Our initial experience with human breast DCE-MRI data shows that the proposed GenSeT method yields more accurate spatiotemporal dynamics and PK analysis than the conventional zero-filling and TWIST reconstruction methods. Further validation of the method as a useful reconstruction approach for sparsely-sampled DCE-MRI is warranted in a larger cohort and with data from different organs.

Electronic Poster

Multimodal & Multiparametric

Exhibition Hall — Tuesday 8:15 - 9:15

3879 Computer 73

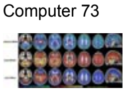

Correlating ZTE MRI signal to bone density to derive a patient-specific attenuation correction map in brain PET/MR

Maya Khalifé[1], Brice Fernandez[2], Olivier Jaubert[1], Michael Soussan[3], Irène Buvat[3], Vincent Brulon[3], and Claude Comtat[3]

[1]*Brain and Spine Institute (ICM), Hôpital de la Pitié-Salpêtrière, Paris, France,* [2]*Applications and Workflow, GE Healthcare, Orsay, France,* [3]*Laboratoire d'Imagerie Moléculaire In Vivo (IMIV), Commissarriat à l'Energie Atomique et aux Energie Alternatives (CEA), Orsay, France*

Attenuation correction (AC) is needed for an accurate PET image quantification in brain PET/MR. Regular MRI cannot distinguish between different tissue types based on electron density, thus, Zero Echo Time (ZTE) has been used to segment bone, air and soft tissue. Furthermore, a correlation has been established between histogram normalized ZTE intensity and measured CT density in Hounsfield Unit (HU) in bone on a CT-MR database of 16 patients. The patient-specific AC map generated by combining ZTE-based segmentation and linear scaling of normalized ZTE signal into HU showed to be a good substitute of the measured CT-AC map in brain PET/MR.

3880 Computer 74

Fully-Integrated 3D High-Resolution Multi-Contrast Abdominal PET-MR with High Scan Efficiency

Christoph Kolbitsch[1,2], Radhouene Neji[3], Matthias Fenchel[4], Andrew Mallia[2], Paul Marsden[2], and Tobias Schaeffter[1,2]

[1]*Physikalisch-Technische Bundesanstalt (PTB), Braunschweig and Berlin, Germany,* [2]*Division of Imaging Sciences and Biomedical Engineering, King's College London, London, United Kingdom,* [3]*MR Research Collaborations, Siemens Healthcare, Frimley, United Kingdom,* [4]*MR Oncology Application Development, Siemens Healthcare, Erlangen, Germany*

Abdominal PET-MR scans commonly combine free-breathing PET with breathhold or respiratory-triggered MR scans (T1/T2-weighted). This ensures high MR image quality but can lead to PET images impaired by motion blurring. Furthermore, PET can suffer from artefacts close to tissue-lung interfaces due to misalignment of breathhold MR-based attenuation correction (AC) information used for free-breathing PET. Here we present a free-breathing MR-technique which yields motion-compensated 3D T1-weighted and T2-weighted MR images. Respiratory-resolved AC maps and motion compensation improved uptake values (125±131%) and resolution (22±16%). Respiratory motion information is obtained with an accuracy of 1.3±0.1mm without an increase in scan time.

3881 Computer 75

Penta-contrast imaging: a Novel Pulse Sequence for Simultaneous Acquisition of Proton Density, T1, T2, T2* and FLAIR images

Jinhee Jeong[1], Yoonho Nam[2], and Jongho Lee[1]

[1]Department of electrical and computer engineering, Seoul National University, Seoul, Korea, Republic of, [2]Department of Radiology, Seoul Saint Mary's Hospital

A penta-contrast imaging sequence that generates proton density (PD), T1, T2, T2* and FLAIR images in a single scan is developed. Compared to conventional imaging sequences, the scan time is reduced by 50 %. Additionally, the new method generates T1 and T2 maps.

3882 Computer 76

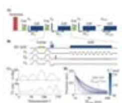

Magnetic Resonance Fingerprinting for T1 and T2* quantification with Cartesian readout

Benedikt Rieger[1], Fabian Zimmer[1], Jascha Zapp[1], Sebastian Weingärtner[1,2,3], and Lothar R. Schad[1]

[1]Computer Assisted Clinical Medicine, Heidelberg University, Mannheim, Germany, [2]Electrical and Computer Engineering, University of Minnesota, [3]Center for Magnetic Resonance Research, University of Minnesota

Magnetic resonance fingerprinting (MRF) has shown exceptional promise for simultaneous quantification of T_1 and T_2, based on numerous spiral readouts. We propose an implementation of the MRF paradigm for quantitative imaging using spoiled echo-planar imaging (EPI) with Cartesian readout for simultaneous assessment of T_1 and T_2^* within 10s. Joint T_1 and T_2^* parameter-maps acquired in phantoms with the proposed MRF method are in good agreement with reference measurements and demonstrate high quality in-vivo. This approach offers a rapid supplement to the non-Cartesian MRF portfolio, with potentially increased usability and robustness.

3883 Computer 77

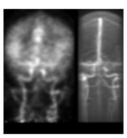

Validation of an Image Derived Input Function Method for PET/MR Brain Scans

Mohammad Mehdi Khalighi[1], Mathias Engström[2], Mark Lubberink[3], and Greg Zaharchuk[4]

[1]Applied Science Lab, GE Healthcare, Menlo Park, CA, United States, [2]Applied Science Lab, GE Healthcare, Uppsala, Sweden, [3]Nuclear Medicine & PET, Department of Surgical Sciences, Uppsala University, Uppsala, Sweden, [4]Radiology Department, Stanford University, Palo Alto, CA, United States

Accurate measurement of the arterial input function (AIF) is essential in quantitative analysis of cerebral blood flow (CBF) using ^{15}O-water PET imaging. The time-of-flight enabled SIGNA PET/MR scanner (GE Healthcare, Waukesha, WI, USA) provides high quality PET images, which can be used for non-invasive Image Derived Input Function (IDIF) estimation. AIF was measured using a proposed IDIF method on 4 patients and the results were compared with the gold standard, arterial blood sampling. The comparison shows excellent correspondence between IDIF and blood sampling, thus validating the IDIF method.

3884 Computer 78

Whole-body morphological and functional atlas using an integrated PET-MRI system and fat-water registration

Simon Ekström[1], Therese Sjöholm[1], Filip Malmberg[1,2], Lars Lind[3], Håkan Ahlström[1,4], Joel Kullberg[1,4], and Robin Strand[1,2]

[1]Division of Radiology, Department of Surgical Sciences, Uppsala University, Uppsala, Sweden, [2]Centre for Image Analysis, Uppsala University, Uppsala, Sweden, [3]Department of Medical Sciences, Uppsala University, Uppsala, Sweden, [4]Antaros Medical, Sweden

Today, when whole-body PET-MRI datasets are analyzed, the data is typically reduced to a few a priori specified measurements. New tools are developed in an attempt to utilize the full potential of large whole-body datasets. The purpose of this work was to build a preliminary whole-body atlas, containing both morphological (fat and water MR) and functional (FDG-PET) information on normality. An atlas was built out of 30 subjects using an integrated PET-MRI system together with an efficient registration method for fat-water MR images. The atlas was used in a proof-of-concept anomaly detection in FDG-PET using a pointwise *t*-test, which successfully detected anomalies in our test subject.

3885 Computer 79

Bayesian Experimental Design for Multi-Parametric T1/T2 Relaxometry and Diffusion

David Owen[1], Andrew Melbourne[2], Magdalena Sokolska[3], David L Thomas[2,4], Jonathan Rohrer[4], and Sebastien Ourselin[2]

[1]Translational Imaging Group, University College London, London, United Kingdom, [2]Translational Imaging Group, University College London, [3]Department of Medical Physics, University College London Hospitals, [4]Dementia Research Centre, University College London

Multi-parametric imaging, such as joint relaxometry and diffusion, can allow for a time-efficient measurement of several parameters of interest. However, it is unclear how best to make use of valuable scanner time when using such novel imaging techniques. In this work, we explore how Bayesian experimental design can be used to derive a maximally time-efficient joint imaging experiment.

3886 Computer 80

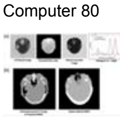

Rapid Dual Echo UTE MR-Based Attenuation Correction

Hyungseok Jang[1] and Alan B McMillan[1]

[1]Department of Radiology, University of Wisconsin, Madison, WI, United States

Recently, ultrashort TE imaging based MR-based attenuation correction (MRAC) has been proposed in literature to overcome the intrinsic difficulty in MRI to resolve bone contrast and hence enable more reliable estimation of attenuation map. However, the long acquisition time required for UTE imaging still remains challenging. In this study, we propose a novel, rapid dual echo method for UTE based MRAC, which allows segmentation of bone, air, fat, and water with high spatial resolution ($1mm^3$) in a single scan with extremely short scan time (35sec).

3887 Computer 81

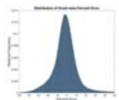

Atlas-based generation of synthesized transmission images for brain PETMR attenuation correction using MPRAGE

Karl D Spuhler[1], Nandita Joshi[2], Christine DeLorenzo[1,3], Ramin Parsey[3], and Chuan Huang[1,3,4]

[1]Biomedical Engineering, Stony Brook University, Stony Brook, NY, United States, [2]Electrical and Computer Engineering, Stony Brook University, Stony Brook, NY, United States, [3]Psychiatry, Stony Brook Medicine, Stony Brook, NY, United States, [4]Radiology, Stony Brook Medicine, Stony Brook, NY, United States

Attenuation correction remains a challenge in simultaneous PETMR, as MR signal is not directly related to attenuation. This is particularly problematic in PETMR studies of the brain, where accurate radiotracer quantification is extremely important. Here, we present a method for generating individual-specific transmission data for attenuation correction from an input MPRAGE MR volume. The method uses an atlas of matched MPRAGE and transmission images in order to achieve this. Our method does not add to scan time, as do common MR-based methods, and directly yields attenuation data for PET energies, unlike CT-based methods.

3888 Computer 82

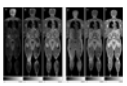

Intensity inhomogeneity correction of whole body fat-water images using fat and water fraction information on a 3T PET/MR scanner

Therese Sjöholm[1], Simon Ekström[1], Filip Malmberg[1,2], Robin Strand[1,2], Magnus Johansson[1], Lars Lind[3], Mathias Engström[4], Håkan Ahlström[1,5], and Joel Kullberg[1,5]

[1]Radiology, Uppsala University, Uppsala, Sweden, [2]Centre for Image Analysis, Uppsala University, Uppsala, Sweden, [3]Medical Sciences, Uppsala University, Uppsala, Sweden, [4]Applied Science Laboratory, GE Healthcare, Uppsala, Sweden, [5]Antaros Medical, Mölndal, Sweden

We describe and evaluate a method for intensity non-uniformity correction of whole-body fat-water MR data acquired with both surface and body coils on a 3T PET/MRI system. The proposed method consists of two steps. Abrupt station intensity changes are first supressed, followed by correction of smooth intensity changes using fat and water fraction information. Visual and quantitative evaluations of 42 corrected fat-water datasets show that the method gives improved adipose and lean tissue uniformity for both surface and body coil acquisitions. This renders the data suitable for continued analysis in a whole-body imaging framework.

3889 Computer 83

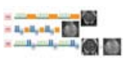

Multiple Instantaneous Switchable Scans interleaving T2W and DWI for Prostate Biparametric MRI

Wei WANG[1], Xiubo QIN[1], Juan WEI[2], and Xiaoying WANG[1]

[1]Peking University First Hospital, Beijing, People's Republic of China, [2]Philips Research China, Shanghai, People's Republic of China

Multiple Instantaneous Switchable Scans (MISS) is a type of interleaved scan method. In our study of prostate MRI, we combined the 3D-T2W and DWI by MISS into one scan, both of which are essential sequences for PIRADS v2. The combined sequences improved the scan efficiency (6min to 4min30s). The image quality and lesion display of MISS is similar to conventional T2W and DWI. The 3D-T2W in MISS showed better performance of seminal vesicles and lesion contrast and allowed for interactive multiplanar reformation.

3890 Computer 84

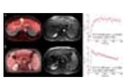

PET-MRI in hepatocellular carcinoma: Correlation of DCE-MRI perfusion quantification using shutter-speed model with FDG uptake

Stefanie Hectors[1], Mathilde Wagner[1], Cecilia Besa[1], Wei Huang[2], and Bachir Taouli[1]

[1]Translational and Molecular Imaging Institute, Icahn School of Medicine at Mount Sinai, New York, NY, United States, [2]Advanced Imaging Research Center, Oregon Health & Science University, Portland, OR, United States

Shutter-speed modeling (SSM) of DCE-MRI data allows for estimation of the mean intracellular water molecular lifetime (τ_i), which has been suggested to be associated with tissue metabolic activity. In this study, we assessed the correlation between SSM DCE-MRI parameters and FDG-PET uptake in hepatocellular carcinoma (HCC) lesions. While K^{trans} did show a significant negative correlation with the standardized uptake value (SUV) in the HCC lesions, τ_i was not significantly associated with FDG uptake. Our preliminary findings suggest that τi may not be associated with the up-stream tumor glucose metabolism as measured by FDG-PET.

3891 Computer 85

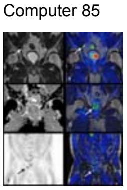

Detection of recurrent prostate cancer with 18F-Fluciclovine PET/MRI

Kirsten Margrete Selnæs[1,2], Mattijs Elschot[1], Brage Krüger-Stokke[1,3], Håkon Johansen[4], Per Arvid Steen[3], Sverre Langørgen[3], Bjørg Yksnøy Aksnessæther[5], Gunnar Indrebø[5], Torill Anita Eidhammer Sjøbakk[1], May-Britt Tessem[1], Siver Andreas Moestue[1], Heidi Knobel[6], Torgrim Tandstad[6], Helena Bertilsson[7,8], Arne Solberg[6], and Tone Frost Bathen[1,2]

[1]Department of Circulation and Medical Imaging, NTNU- Norwegian University of Science and Technology, Trondheim, Norway, [2]St. Olavs Hospital, Trondheim University Hospital, Trondheim, Norway, [3]Department of Radiology, St. Olavs Hospital, Trondheim University Hospital, [4]Department of Nuclear Medicine, St. Olavs Hospital, Trondheim University Hospital, [5]Ålesund sjukehus, Helse Møre og Romsdal HF, [6]Department of Oncology, St. Olavs Hospital, Trondheim University Hospital, [7]Department of Urology, St. Olavs Hospital, Trondheim University Hospital, [8]Department of Cancer Research and Molecular Medicine, NTNU- Norwegian University of Science and Technology, Trondheim, Norway

Simultaneous PET/MRI has the potential to improve the detection accuracy in recurrent prostate cancer, since it combines the excellent soft-tissue contrast of MRI with the high molecular sensitivity of PET in one imaging session. The aim of this observational study is to assess the detection rate of recurrent prostate cancer by simultaneous ^{18}F-Fluciclovine PET/MRI. We demonstrate that18F-Fluciclovine PET/MRI can detect suspicious lymph node, prostatic and bone lesions in patients with a wide range of PSA levels and that the number of equivocal findings is reduced when MR images are evaluated in conjunction with PET uptake. .

3892 Computer 86

Simultaneous acquisition of T1rho and T2 map of liver with black blood effect in a single breathhold

Weitian Chen[1], Vincent WS Wong[2], Queenie Chan[3], Yixiang J Wang[1], and Winnie CW Chu[1]

[1]Imaging and Interventional Radiology, The Chinese University of Hong Kong, New Territory, Hong Kong, [2]Medicine and Therapeutics, The Chinese University of Hong Kong, New Territory, Hong Kong, [3]Philips Healthcare, New Territory, Hong Kong

T1rho is promising for early detection of liver fibrosis. However, the richness of blood vessels in the liver coupled with respiratory motion makes T1rho measurement prone to errors. In this work, we propose a pulse sequence to simultaneously obtain a T1rho and a T2 map of liver in a single breathhold with black blood effect.

3893 Computer 87

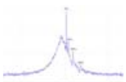

Using 31P-MRI of hydroxyapatite for bone attenuation correction in PET-MRI: proof of concept in the rodent brain

Vincent Lebon[1], Sébastien Jan[2], Yoann Fontyn[2], Brice Tiret[3], Géraldine Pottier[2], Emilie Jaumain[2], and Julien Valette[3]

[1]DRF/I2BM/SHFJ, CEA, Orsay, France, [2]DRF/I2BM/SHFJ/IMIV, CEA-Université Paris Saclay, Orsay, France, [3]DRF/I2BM/MIRCen/UMR9199, CEA-CNRS-Université Paris Saclay, Fontenay-aux-Roses, France

Current techniques for skull attenuation correction in PET-MRI provide indirect estimates of cortical bone density, leading to inaccurate estimates of brain activity. Here we propose an alternate method based on the detection of hydroxyapatite crystals by ^{31}P-MRI, providing individual and quantitative assessment of bone density. ^{31}P-MRI was performed in rodent to estimate the µ-map of the skull. FDG-PET data were acquired in the same animal and reconstructed with ^{31}P-based attenuation correction, demonstrating proper distribution of ^{18}F activity throughout the brain.

3894 Computer 88

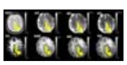

Water content, diffusion measures (DTI/DKI) and FET-PET in brain tumours: investigating similarities and differences

Ana-Maria Oros-Peusquens*[1], Ricardo Loucao*[1,2], Hugo Ferreira[2], Karl-Josef Langen[1], and Nadim Jon Shah[1]

[1]INM-4, Research Centre Jülich, Jülich, Germany, [2]Instituto de Biofísica e Engenharia Biomédica, Sciences Faculty, University of Lisbon, Lisbon, Portugal

Water content, diffusion measures and FET-PET measured simultaneously on a hybrid 3T scanner in 40 brain tumour patients were investigated. Despite reasonable expectations of finding some microscopic-structure-driven correlations between these parameters, compared here for the first time, low correlations were found in healthy tissue. Interestingly, the correlation between water content and diffusion indices -while still rather low - increased in tumour tissue. Importantly, this implies that each parameter reflects different aspects and thus their combination should be more powerful for oncology than using single parameters

---

3895 Computer 89

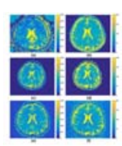

In Vivo T1 and T2 Mapping using Single-Shot EPI Fingerprinting

Cory Robert Wyatt[1,2], John Grinstead[3], and Alexander Guimaraes[1]

[1]Radiology, Oregon Health and Science University, Portland, OR, United States, [2]Advanced Imaging Research Center, Oregon Health and Science University, Portland, OR, United States, [3]Siemens Healthcare, Portland, OR, United States

MR fingerprinting (MRF) studies have been performed using heavily undersampled spiral acquisitions, which constantly rotate and use uncorrelated aliasing to fit quantitative T1 and T2 maps. On top of the usual spiral sensitivity to off-resonance, the undersampling used in MRF requires a slowly varying signal evolution to “see through” the aliasing artifacts. Echo-planar imaging (EPI) would avoid these aliasing issues while still having a short measurement time due to a single-shot acquisition and parallel imaging acceleration. In this study, a single-shot EPI sequence is combined with fingerprinting techniques to obtain T1 and T2 maps similar to those from spiral fingerprinting.

3896 Computer 90

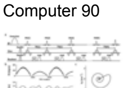

Fast Magnetic Resonance Fingerprinting of Mouse Brain Using a Spiral Trajectory

Yuning Gu[1], Charlie Wang[1], Christian Anderson[1], Yuchi Liu[1], Dan Ma[1], Yun Jiang[1], Mark A. Griswold[1,2], Chris A. Flask[1,2,3], and Xin Yu[1,2,4]

[1]Department of Biomedical Engineering, Case Western Reserve University, Cleveland, OH, United States, [2]Department of Radiology, Case Western Reserve University, Cleveland, OH, United States, [3]Department of Pediatrics, Case Western Reserve University, Cleveland, OH, United States, [4]Department of Physiology and Biophysics, Case Western Reserve University, Cleveland, OH, United States

In this study we developed spiral-based MRF sequences for fast T_1 and T_2 mapping of mouse brain at 7T. A variable density spiral trajectory that fully sampled the inner 10×10 k-space with 4 interleaves enabled up to 6-fold acceleration for both MRF-bSSFP and MRF-FISP sequences, corresponding to a 3-min scan to acquire 1024 time frames for simultaneous T_1 and T_2 mapping.

3897 Computer 91

PET-MR Motion Correction of Entire Listmode Data Sets Using Pilot Tone Navigation

Thomas Vahle[1], David Stephen Rigie[2], Ryan Brown[2], Tiejun Zhao, Li Feng[2], Matthias Fenchel[1], Peter Speier[1], and Fernando Boada[2]

[1]Siemens Healthcare GmbH, Erlangen, Germany, [2]Radiology, Center for Advanced Imaging Innovation and Research (CAI2R), New York University Langone Medical Center, New York, NY

The introduction of simultaneous PET-MR provides new opportunities for motion tracking and correction during PET imaging. The ideal clinical workflow for a PET-MR exam would allow for PET data to be continuously acquired alongside any desired MR sequences and to reconstruct a motion-corrected PET image utilizing the entire dataset. In this work we combine a surface coil driven by an external signal generator with an MR motion model to navigate PET data during an entire PET-MR exam. We demonstrate the approach on one human subject that underwent a PET-MR exam.

3898 Computer 92

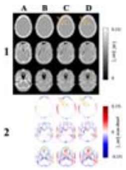

SPM-BASED SEGMENTATION OF AIR IN THE HUMAN HEAD FOR IMPROVED PET ATTENUATION CORRECTION IN SIMULTANEOUS PET/MR

Jakub Baran[1,2], Zhaolin Chen[1,3], Francesco Sforazzini[1], Sharna Jamadar[1,4,5], Nicholas Ferris[1,6], Nadim Jon Shah[1,7], Marian Cholewa[2], and Gary Egan[1,4,5]

[1]Monash Biomedical Imaging, Monash University, Melbourne, Australia, [2]Department of Biophysics, University of Rzeszow, Rzeszow, Poland, [3]Department of Electrical and Computer Systems Engineering, Monash University, Melbourne, Australia, [4]Monash Institute of Cognitive and Clinical Neurosciences and School of Psychological Sciences, Monash University, Melbourne, Australia, [5]Australian Research Council Centre of Excellence for Integrative Brain Function, Monash University, Melbourne, Australia, [6]Monash Imaging, Monash Health, Melbourne, Australia, [7]Institute of Neuroscience and Medicine, Forschungszentrum Jülich GmbH, Jülich, Germany

Dual-echo UTE MR sequences are widely used to estimate PET attenuation coefficients in simultaneous PET/MR imaging. However, due to susceptibility artefacts, air cavities in the head together with brain tissues and bones, can be misclassified, especially around air-tissue interface regions. In this work, we propose an SPM-based air and background segmentation method to improve the PET attenuation correction for simultaneous PET/MR imaging of the human brain. We compare air segmentation methods for more accurate air classification using an *in-vivo* MR-PET dataset and demonstrate improved PET image reconstruction accuracy.

3899 Computer 93

Impact of MR-based Motion Correction on clinical PET/MR data of patients with thoracic pathologies

Marcel Gratz[1,2], Verena Ruhlmann[3], Lale Umutlu[4], Matthias Fenchel[5], and Harald H. Quick[1,2]

[1]Erwin L. Hahn Institute, University Duisburg-Essen, Essen, Germany, [2]High Field and Hybrid MR Imaging, University Hospital Essen, Essen, Germany, [3]Department of Nuclear Medicine, University Hospital Essen, Essen, Germany, [4]Department of Diagnostic and Interventional Radiology and Neuroradiology, University Hospital Essen, Essen, Germany, [5]Siemens Healthcare GmbH, Erlangen, Germany

A new PET/MR method for MR-based motion correction of PET data was set up and evaluated in a clinical study to assess the potential gain of significance and visibility of lesions in the thorax for a free-breathing patient. The new method (MoCo) was applied to 20 patients and compared to reconstructions of a single respiratory state (gated) and the total non-corrected (static) dataset. Having a comparably high statistical confidence like the static PET imagery, the motion-corrected reconstruction shows superior image quality with sharper depiction of moving lesions and thus may facilitate the diagnosis of thoracic pathologies in routine PET/MR applications.

3900 Computer 94

MR-Based Respiratory and Cardiac Motion Corrected 18F-FDG-PET/MR in Cardiac Sarcoidosis

Philip M Robson[1], Nicolas A Karakatsanis[1], Maria Giovanna Trivieri[1], Ronan Abgral[2], Marc R Dweck[3], Jason C Kovacic[4], and Zahi A Fayad[1]

[1]Translational and Molecular Imaging Institute, icahn school of medicine at mount sinai, New York, NY, United States, [2]Department of Nuclear Medicine, European University of Brittany, [3]British Heart Foundation/University Centre for Cardiovascular Science, University of Edinburgh, [4]Cardiovascular Institute, Icahn School of Medicine at Mount Sinai

A major advantage of hybrid PET/MR systems is the radiation-free high spatial and temporal resolution of cardiac MR imaging that can be used to estimate respiratory and cardiac motion present during PET data acquisition. This information can be incorporated into algorithms to correct for the effects of motion in the PET data to reduce blurring and increase target-to-background ratios of PET hotspots. In this work, we demonstrate a method for respiratory and cardiac motion correction in patients with cardiac sarcoidosis.

3901 Computer 95

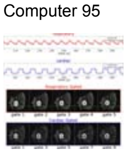

Automatic Extraction of Cardiac and Respiratory Motion via Self-Refocused Rosette Navigators and Independent Component Analysis

David Rigie[1], Thomas Vahle[2], Tiejun Zhao[3], Klaus Schäfers[4], Björn Czekalla [4], Lynn Frohwein[4], and Fernando Boada[1]

[1]Radiology, Center for Advanced Imaging Innovation and Research (CAI2R), New York University Langone Medical Center, New York, NY, United States, [2]Siemens Healthcare GmbH, Erlangen, Germany, [3]Siemens Healthcare, New York, NY, [4]European Institute for Molecular Imaging, University of Münster, Münster, Germany

Due to the recent availability of simultaneous PET-MR, there has been much interest in MR-based motion correction for PET imaging. A key component of any such scheme is a mechanism for tracking respiratory and cardiac motion phases throughout the entire exam. In this work, we present a robust, automated approach whereby respiratory and cardiac motion information is jointly encoded with rosette navigators and decoded via independent component analysis (ICA). This approach obviates the need for any external motion tracking devices (e.g. bellows or ECG) and requires just a contrast-neutral, self-refocused navigator echo (≈2ms) per repetition time and so may be easily incorporated into many clinical sequences.

Electronic Poster

System Characterization & Corrections

Exhibition Hall Tuesday 8:15 - 9:15

3902 Computer 97

Limitations of NMR Field Cameras for B0 Field Monitoring

Paul Chang[1,2], Sahar Nassirpour[1,2], and Anke Henning[1,3]

[1]MPI for Biological Cybernetics, Tuebingen, Germany, [2]IMPRS for Cognitive and Systems Neuroscience, Eberhard University of Tuebingen, Tuebingen, Germany, [3]Institute of Physics, Ernst-Moritz-Arndt University Greifswald, Greifswald, Germany

We compare the fields measured by a field camera to the fields obtained from B0 mapping at 9.4T. The B0 maps have higher spatial resolution and are therefore taken as a benchmark. We analyse the loss of spatial fidelity due to the lower spatial samples of the field camera and compare two different field probe position calibration and optimisation methods that would help alleviate the problem of discrepancies between field monitoring and field mapping.

3903 Computer 98

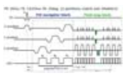

Estimating B0 inhomogeneities with projection FID navigator readouts

Alexander Loktyushin[1,2], Philipp Ehses[1,3], Bernhard Schölkopf[2], and Klaus Scheffler[1,3]

[1]High-field MRI, Max Planck Institute for Biological Cybernetics, Tübingen, Germany, [2]Empirical Inference, Max Planck Institute for Intelligent Systems, Tübingen, Germany, [3]Biomedical Magnetic Resonance, University of Tübingen, Tübingen, Germany

B0 field inhomogeneities can negatively impact the image acquisition process, cause artifacts such as ghosting and blurring and introduce physiological noise in fMRI time series. It is common to address the static inhomogeneity components by using shim coils. Physiological motion during the acquisition can lead to temporal variations in the field configuration. Dynamic shimming necessitates fast, real-time estimation of B0 distortions. In this work, we augment projection-encoded FID readouts with a simple projection-based spatial encoding and train a neural network to learn the mapping from projection FIDs to field maps, which we obtain using a double-echo EPI sequence.

3904 Computer 99

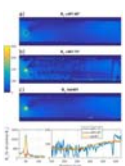

High-Dynamic-Range High-SNR B1+ Mapping Using Multiple Cyclic MR Signals

Mélina Bouldi[1], Tatiana Nemtanu[2,3], and Jan M Warnking[2,3]

[1]Département Ingénierie des Equipements de Travail, INRS, Nancy, France, [2]U1216, Inserm, Grenoble, France, [3]Grenoble Institut des Neurosciences, Université Grenoble Alpes, Grenoble, France

A method is presented to perform B_1^+-mapping simultaneously with high dynamic range and high SNR by optimally combining data from acquisitions with different acquisition parameters. Reconstruction of the B_1^+-maps is performed using dictionary matching methods. This approach is applicable to various B_1^+-mapping sequences. Examples based on the AFI sequence are shown in both numeric simulations and a phantom experiment in the presence of a severe B_1^+ hot-spot. The performance of the proposed methods largely exceeds that of classic AFI sequences, simultaneously matching low-flip-angle acquisitions in dynamic range and high-flip-angle acquisitions in SNR, at identical acquisition times.

3905 Computer 100

Assessment of Geometric Distortion in EPI with a SPAMM Tagged Acquisition

Ken-Pin Hwang[1], Joseph Meier[1], Joshua Yung[1], and R. Jason Stafford[1]

[1]Department of Imaging Physics, The University of Texas M.D. Anderson Cancer Center, Houston, TX, United States

Diffusion weighted EPI is susceptible to distortions due to multiple causes, and the amount of distortion is dependent on many interacting factors. Hence no good methodology currently exists for assessing and characterizing these distortions. In this work an EPI sequence is modified to include Spatial Modulation of Magnetization (SPAMM), a preparation technique that produces tagged grid lines in the imaged volume. This sequence is acquired to measure induced distortion in several phantoms in different coils with different sequence options, measuring distortion as it varies with parallel imaging acceleration, diffusion weighting direction, and susceptibility of various phantom materials.

3906 Computer 101

Encoding of Inductively Measured k-Space Trajectories in MR Raw Data

Jan Ole Pedersen[1,2], Christian G. Hanson, Rong Xue[3], and Lars G. Hanson[1,2]

[1]Centre for Magnetic Resonance, DTU Elektro, Technical University of Denmark, Kgs Lyngby, Denmark, [2]Danish Research Centre for Magnetic Resonance, Centre for Functional and Diagnostic Imaging and Research, Copenhagen University Hospital, Hvidovre, Denmark, [3]Institute of Biophysics, Chinese Academy of Sciences, State Key Laboratory of Brain and Cognitive Science, Beijing, People's Republic of China

For reconstruction of MRI from raw data, the k-space trajectory is needed. We propose to measure this simultaneously with the MRI signal using novel hardware and the scanner itself. As a first step, we demonstrate real-time processing of a gradient pickup coil voltage during scanning, modulation of this signal to a frequency within the MR acquisition bandwidth, and signal extraction from MR raw data. This principle is applied to measure k-space trajectories inductively and perform image reconstruction based on this. The resulting images have comparable quality to images reconstructed using nominal k-space trajectories. The method can potentially provide generic image reconstruction with limited hardware, even for challenging and dynamically updated gradient schemes.

3907 Computer 102

On the deviation of actual isocenter slice position in magnetic resonance imaging

Julian Emmerich[1], Sina Straub[1], and Frederik Bernd Laun[1,2]

[1]Medical Physics in Radiology, German Cancer Research Center (DKFZ), Heidelberg, Germany, [2]Institute of Radiology, University Hospital Erlangen, Erlangen, Germany

Due to imperfect laser positioning, actual isocenter slicepositions can deviate from manufacturer indication. Using MRI as tool for dose planning in MR guided radiation therapy, the geometric correct position of MR-slices is an essential quality parameter that can affect dose calculation and definition of the planning target volume (PTV). To evaluate the magnitude of the deviation of the actual slice position from the true isocenter of the scanner, a phantom study was performed. Scanner-dependent deviations in isocenter slice position occurred in the range of 1 mm - 5 mm.

3908 Computer 103

Robust B1 Mapping with Phase-sensitive Orthogonal Excitation RF Pulses

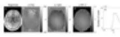

Jie Wen[1], Alexander Sukstansky[1], and Dmitriy Yablonskiy[1]

[1]Radiology, Washington University in St. Louis, St. Louis, MO, United States

Accurate B1 measurement is important in many MR related applications. In this study, we proposed and optimized a phase-sensitive approach for B1 mapping that relies on a multi-gradient-echo sequence with two successive orthogonal RF pulses used for signal excitation. We also proposed optimized methods for combining multi-channel data, allowing for optimal parameters' estimation. The method was validated on phantoms and tested on human participants. By applying this method on SMART (Simultaneous Multi-Angular Relaxometry of Tissue) MRI, we reaffirmed the importance of the B1 correction for quantifying biological tissues relaxation and magnetization transfer parameters.

3909 Computer 104

Implementation of a Gradient Pre-emphasis Based on the Gradient Impulse Response Function

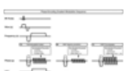

Manuel Stich[1], Tobias Wech[1], Anne Slawig[1], Ralf Ringler[2], Andrew Dewdney [3], Andreas Greiser[3], Gudrun Ruyters[3], Thorsten Bley[1], and Herbert Köstler[1]

[1]Department of Diagnostic and Interventional Radiology, University of Würzburg, Würzburg, Germany, [2]X-Ray & Molecular Imaging Lab, Technical University Amberg-Weiden, Weiden, Germany, [3]Siemens, Erlangen, Germany

The gradient impulse response function (GIRF) completely characterizes the gradient system as a linear and time-invariant (LTI) system, and has recently been used to correct for distorted k-space trajectories in image reconstruction. We now report on the implementation of a GIRF-based pre-emphasis, which is resulting in gradient waveforms already matching the desired k-space trajectory and rendering post-corrections obsolete. The method was successfully tested in a sequence with modulated phase-encoding gradients, as for example used in Wave-CAIPI.

3910 Computer 105

Spatiotemporal Magnetic Field Monitoring with Hall Effect Sensors

Koray Ertan[1], Soheil Taraghinia[1], Ayca Takmaz[2], Secil Eda Dogan[2], Safa Ozdemir[1], and Ergin Atalar[1]

[1]National Magnetic Resonance Research Center (UMRAM), Bilkent University, Ankara, Turkey, [2]Electrical and Electronics Engineering, Bilkent University, Ankara, Turkey

Hall effect sensors can be used to monitor the spatiotemporal field dynamics. However, measurement of the z component of the magnetic field (Bz) requires very large dynamic range for the Hall effect sensors due to superposition of encoding fields with main magnetic field (B0). Instead, we propose to measure the transverse components of the magnetic field in several spatial positions to reconstruct spatiotemporal dependency of Bz and we have demonstrated reconstruction of the first order spherical harmonic field distributions.

3911 Computer 106

Free breathing Motion-Robust Cardiac B1+ mapping at 3.0T based on DREAM

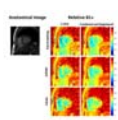

Teresa Rincón[1,2], Anne Menini[2], Ana Beatriz Solana[2], André Fischer[2,3], Guido Kudielka[2], and Wei Sun[4]

[1]Technische Universität München, Munich, Germany, [2]GE Global Research, Munich, Germany, [3]Cardiac Center of Excellence, GE Healthcare, Munich, Germany, [4]GE Healthcare, Waukesha, WI, United States

Radiofrequency (RF) field inhomogeneities affect image quality while performing body and cardiac imaging especially at high field strengths. RF shimming and quantitative MR applications such as T1 mapping can potentially benefit from an accurate knowledge of variations of the transmitted RF field (B_1^+).

The purpose of this work is to investigate spatial homogeneity of the B_1^+ in the myocardium at 3.0T. For this study, we developed a prospective ECG-gated method based on DREAM (Dual Refocusing Echo Acquisition Mode).

The presented approach allows free breathing multi-shot acquisition B_1^+ mapping and its feasibility is shown in vivo.

3912 Computer 107

Quality Assurance Phantoms and Procedures for UHF MRI – The German Ultrahigh Field Imaging (GUFI) Approach

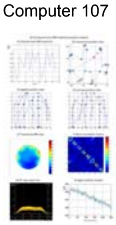

Maximilian N. Voelker[1], Oliver Kraff[1], Eberhard Pracht[2], Astrid Wollrab[3], Andreas K. Bitz[4], Tony Stöcker[2], Harald H. Quick[1,5], Oliver Speck[3,6], and Mark E. Ladd[1,4]

[1]Erwin L. Hahn Institute for Magnetic Resonance Imaging, University of Duisburg-Essen, Essen, Germany, [2]German Center for Neurodegenerative Diseases (DZNE), Bonn, Germany, [3]Otto-von-Guericke-University, Magdeburg, Germany, [4]Medical Physics in Radiology, German Cancer Research Center (dkfz), Heidelberg, Germany, [5]High Field and Hybrid MR Imaging, University Hospital Essen, University of Duisburg-Essen, [6]Leibniz Institute for Neurobiology, Magddeburg, Germany

The German Ultrahigh Field Imaging network (GUFI, www.mr-gufi.de) is a user group of 13 German and neighboring sites that all operate a UHF (7T or 9.4T) MRI system. Due to the lack of common quality assurance (QA) procedures for UHF, GUFI started an initiative to unify QA procedures at these sites. A QA phantom and measurement protocol were developed especially for UHF that is currently being rolled out to all member sites. The QA data allow monitoring of individual system performance based on long-term data analysis or by comparison to pooled data from all sites.

3913 Computer 108

Application of Magnetic Resonance Fingerprinting to evaluate degradation of Magnetic Resonance Imaging system

Imam Ahmed Shaik[1], Rajeshree Malage[1], and Sairam Geethanath[1]

[1]Medical Imaging Research Centre (MIRC), Dayanada Sagar Institutions, Bangalore, India

Detection of artefact and its automated correction is an active area of MRI research. The aim of this study is to evaluate MR system/sub-system degradation and detection of root cause for image quality degradation using Magnetic Resonance Fingerprinting (MRF). The method is demonstrated on Terranova, an earth's field MR imager as part of the preliminary studies. The 3 major coils: polarizer, gradient and Audio Frequency (AF) coils were considered for degradation evaluation. A dictionary similar to MRF with 64 entries for different ranges of inputs was generated. It is shown that based on dictionary a decision can be made about the status of the system.

3914 Computer 109

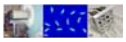

Characterization of a matrix gradient system using a magnetic field probe

Ying-Hua Chu[1,2], Sebastian Littin[2], Yi-Cheng Hsu[1,2], and Maxim Zaitsev[2]

[1]Institute of Biomedical Engineering, National Taiwan University, Taipei, Taiwan, [2]Medical Physics, Department of Radiology, University Medical Center Freiburg, Freiburg, Germany

Measuring GIRF using field probe and chirp gradient waveform is an efficient method to characterize the gradient behavior. We demonstrate that by measuring GIRF for each channel we are able to predict the response of simultaneously driven 12-channel gradient operation. Full characterization of the gradient system can be used to detect suboptimal matching of the amplifier and can be used to achieve desired performance also in such complex systems as matrix gradient coils.

3915 Computer 110

Accurate dynamic magnetic field monitoring and diffusion-weighted image reconstruction using uncorrelated local field measurements

Ying-Hua Chu[1], Yi-Cheng Hsu[1], and Fa-Hsuan Lin[1,2]

[1]Institute of Biomedical Engineering, National Taiwan University, Taipei, Taiwan, [2]Department of Neuroscience and Biomedical Engineering, Aalto University, Espoo, Finland

We proposed a method to decouple field probes and to improve the accuracy of dynamic magnetic field estimation. A sensitivity matrix of probes was measured and to decouple NMR signals. Diffusion weighted phantom images with off-resonance characterized by decoupled probes had a more invariant structure than by coupled probes when diffusion sensitivity gradients along different directions were applied. The phantom image reconstructed with field disturbances estimated from decoupled probes also shows a more homogeneous background than from coupled probes. Human brain images also demonstrated the improved image quality when decoupled probes were used.

3916 Computer 111

DREAM-based B1-shimming for cardiac imaging at 7 T

Bart R. Steensma[1], Ingmar Voogt[1], Luijten R. Peter[1], Tim Leiner[1], Dennis W.J. Klomp[1], van den Berg A.T. Nico[2], and Alexander J.E. Raaijmakers[1,3]

[1]Division Imaging, Department of Radiology, University Medical Center Utrecht, Utrecht, Netherlands, [2]Division Imaging, Department of Radiotherapy, University Medical Center Utrecht, Utrecht, Netherlands, [3]Biomedical Image Analysis, Eindhoven University of Technology, Eindhoven, Netherlands

RF shimming for multi-transmit systems is commonly performed by phase-only shimming. Improved B_1^+ homogeneity is reached by phase-amplitude shimming but this requires knowledge of the B_1^+ magnitude distributions. For cardiac imaging at 7 Tesla, the acquisition of these distributions is challenging. We present a DREAM-based acquisition series to reconstruct B_1^+ magnitude maps in the heart. This method is applied to homogenize the transmit field for three subjects using phase-amplitude shimming. Results demonstrate a clear improvement of transmit field homogeneity in the heart in comparison to phase-only shimming without B_1^+ magnitude information.

3917 Computer 112

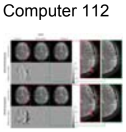

Interaction between trajectory deviations and B0 field inhomogeneity in readout-segmented EPI and spiral imaging

Yoko A Spirig[1,2], Nadine N Graedel[2], Lars Kasper[1], Karla L Miller[2], Robert Frost[2], Stuart Clare[2], Klaas P Pruessmann[1], and S Johanna Vannesjo[2]

[1]Institute for Biomedical Engineering, University of Zurich and ETH Zurich, Zurich, Switzerland, [2]FMRIB centre, Nuffield Department of Clinical Neurosciences, University of Oxford, Oxford, United Kingdom

We studied the effect of encoding imperfections due to gradient errors with a focus on their interaction with $$$B_0$$$ inhomogeneities. Using a simulation framework, we retrospectively sampled data using k-space trajectories of two fast imaging sequences and compared reconstructions based on nominal, gradient impulse response (GIRF) predicted and measured (ground-truth) trajectories for spiral and readout-segmented EPI sequences. We found that the detrimental impact of trajectory imperfections on image quality is strongly amplified by $$$B_0
$$$ inhomogeneities, especially for non-Cartesian trajectories. Furthermore, we confirmed that GIRF-predicted trajectory based reconstructions (requiring only a one-time calibration) allow effective artifact reduction.

3918 Computer 113

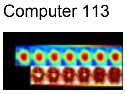

Robust Accelerated Reconstruction for Bloch-Siegert B1-mapping

Andreas Lesch[1], Matthias Schlögl[1], and Rudolf Stollberger[1,2]

[1]Institute of Medical Engineering, Graz University of Technology, Graz, Austria, [2]BioTechMed Graz, Graz, Austria

In this work we evaluate the performance and the robustness of an algorithm for the reconstruction of B1+-maps out of highly accelerated Bloch-Siegert data. The algorithm is based on variational modeling with a problem specific regularization approach. We evaluate the influence of different sampling patterns on the achievable accuracy and sampling efficiency and the influence of both regularization parameters on the final result. All results are compared to the fully-sampled reference using conventional reconstruction. We can show the general robustness of our algorithm and the most effective sampling pattern for this purpose.

3919 Computer 114

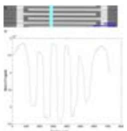

Computer Analysis of Linear-Array Resolution Insert

Alex C Karpilow[1,2], Kathryn E Keenan, Stephen E Russek, and Karl F Stupic

[1]NIST, Boulder, CO, United States, [2]University of Colorado, Boulder, CO, United States

Linear-array resolution inserts are considered for evaluations of MRI scanner performance in terms of spatial accuracy. The linear design allows for simple computer analysis of MR images, which can be used for a quick and quantitative comparison of MRI systems.

3920 Computer 115

Field Mapping using bSSFP Elliptical Signal Model

Meredith Taylor[1], Joseph Valentine[1], Steven Whitaker[1], Michael N Hoff[2], and Neal Bangerter[1]

[1]Electrical Engineering, Brigham Young University, Provo, UT, United States, [2]University of Washington

It is well known that the bSSFP signal is highly dependent on the precession frequency off-resonance value at each pixel. The bSSFP signal can be modeled as an ellipse in the complex plane that rotates about the origin, with the degree of rotation depending on the regional off-resonance value. If a specific point on the axis of the ellipse could be localized, the phase of that point could be used to produce a field map. Xiang and Hoff came up with a geometric solution (GS) which removes banding artifacts by estimating a consistent cross point within the ellipse.

3921 Computer 116

Magnetic Field Monitoring of Spiral Echo Train Imaging

Craig H Meyer[1], Gudrun Ruyters[2], John P. Mugler III[3], Samuel W. Fielden[4], Berthold Kiefer[5], and Josef Pfeuffer[5]

[1]Biomedical Engineering, University of Virginia, Charlottesville, VA, United States, [2]Physics, Siemens Healthineers GmbH, Erlangen, Germany, [3]Radiology & Medical Imaging, University of Virginia, Charlottesville, VA, United States, [4]Geisinger Health System, Lewisburg, PA, United States, [5]Application Development, Siemens Healthineers GmbH, Erlangen, Germany

The goal of this study was to characterize the k-space trajectories of a spiral echo train pulse sequence using a dynamic field camera. The spiral trajectories were quite repeatable, with typical measured error less than 0.01% of the maximum k-space magnitude. This was true for constant-density, dual-density, and spiral-in/out trajectories. A somewhat larger error was typically observed in the first echo. Overall, this study demonstrates that 3D spiral echo train imaging using the same k-space estimation method for all echoes was sufficient to achieve high image quality.

3922 Computer 117

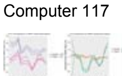

Assessing changes in MRI measurands incurred in a scanner upgrade: Is my study comprised?

Kathryn E Keenan[1], Slavka Carnicka[1], Sophia C Gottlieb[2], and Karl F Stupic[1]

[1]Physical Measurement Laboratory, National Insitute of Standards and Technology, Boulder, CO, United States, [2]Bates College, Lewiston, ME, United States

Scanner upgrades due to software and hardware changes are an inevitable part of MR research and, without quality assurance protocols, can jeopardize studies. We used two standardized phantoms to evaluate change in T_1 relaxation time and ADC measurements on a system that underwent an 'everything but the magnet' upgrade. Post-upgrade, the ADC measurements are comparable or better than the pre-upgrade measurements, while T_1 measurements (VFA and IR) are affected by the upgrade. Upgrades can have unintended consequences, and we recommend the development of standardized quality assurance protocols that test not only contrast, but also quantitative measurements to identify variations and enable corrections.

3923 Computer 118

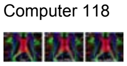

A within-subject comparison of anatomical and diffusion scans from Siemens TimTrio and Prisma scanners

Ross William Mair[1,2] and Stephanie McMains[1]

[1]Center for Brain Science, Harvard University, Cambridge, MA, United States, [2]Athinoula A. Martinos Center for Biomedical Imaging, Massachusetts General Hospital, Charlestown, MA, United States

Siemens' latest 3 Tesla scanner, the Magnetom Prisma, represents a significant upgrade in performance capability over the Magnetom TimTrio. To quantify the improvements offered by such a significant system upgrade, we scanned 8 subjects using a variety of anatomical, functional and diffusion protocols on the TimTrio platform, and then repeated the same protocols on the Prisma platform with the same subjects after the upgrade process. We found consistency in morphometric results from anatomical scans acquired using recommended T_1-weighted imaging protocols. Modest improvements in tSNR for high-resolution and highly-slice accelerated BOLD scans were seen, but more traditional 3mm resolution scans yielded no improvement presumably due to the dominance of physiological noise. The DTI scans conducted here benefit greatly from the new gradient coil in the Prisma, when protocols are optimized to reduce TE and bandwidth as allowed by the new gradient set.

3924 Computer 119

Compensating for Eddy Current Effects in Motion-compensated Diffusion-prepared TSE Sequences

Anh Tu Van[1], Barbara Cervantes[2], Hendrik Kooijman[3], and Dimitrios C Karampinos[2]

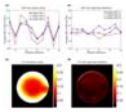

[1]IMETUM, Technical University of Munich, Garching, Germany, [2]Department of Diagnostic and Interventional Radiology, Technical University of Munich, Munich, Germany, [3]Philips Healthcare, Hamburg, Germany

Diffusion-prepared (dprep-TSE) TSE sequences are gaining attention for high-resolution distortion-free body DWI. However, dprep-TSE suffers from phase errors induced by both motion and eddy current effects. Motion compensation reduces motion effects, but eddy currents remain a source of phase errors. The present study investigates the performance of two alternative methods for compensating for eddy current effects in a motion-compensated dprep-TSE sequence: the use of phase cycling and the use of magnitude stabilizers.

3925 Computer 120

A Three-Dimensional Spiral-In/Out Turbo-Spin-Echo Technique with Long Readout Echo Train and Concomitant Phase Compensation

Zhiqiang Li[1], John P Karis[2], and James G Pipe[1]

[1]Imaging Research, Barrow Neurological Institute, Phoenix, AZ, United States, [2]Neuroradiology, Barrow Neurological Institute, Phoenix, AZ, United States

TSE is a rapid technique routinely used for T2 and FLAIR imaging. Three-Dimensional TSE with variable flip angles provides high scan efficiency, high SNR, and contiguous slice coverage. In this project we develop a 3D spiral TSE sequence employing a spiral-in/out readout for efficient acquisition but without the drawbacks associated with conventional spiral-out TSE. The variable flip angle schedule is adapted for long echo space to reduce waste in acquisition time. A concomitant phase compensation technique is incorporated to minimize the violation of the CPMG condition. Preliminary results demonstrate the feasibility of the proposed technique.

Electronic Poster

Motion Correction

Exhibition Hall — Tuesday 9:15 - 10:15

3926 Computer 73

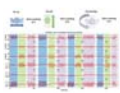

Robust EEG-fMRI using optical motion tracking: Retrospective EEG Motion Educated Gradient Artefact Suppression REEG-MEGAS

Danilo Maziero[1] and David W Carmichael[2]

[1]Department of Medicine, John A. Burns School of Medicine, University of Hawaii, Honolulu, HI, United States, [2]Developmental Imaging and Biophysics Section, University College London, London, United Kingdom

Here we present a method capable of suppressing motion-related EEG GA instabilities, induced EEG voltages and fMRI artefacts in simultaneous EEG-fMRI data. This correction method appeared to allow for the removal of harmonics associated with incomplete GA removal even in a moving subject. Therefore our findings might be helpful in improving both EEG quantification reliability and data quality in populations prone to movement e.g. children or for studying patients with epilepsy during seizures.

3927 Computer 74

Method of choice to increase the motion-robustness for free-breathing applications: Self-gating, motion-weighting, or extra-dimensional reconstruction

Thomas Benkert[1,2], Li Feng[1,2], Mark E Bittman[1,2], Justin Ream[1,2], Daniel K Sodickson[1,2], Ricardo Otazo[1,2], Kai Tobias Block[1,2], and Hersh Chandarana[1,2]

[1]Center for Advanced Imaging Innovation and Research (CAI2R), Department of Radiology, New York University School of Medicine, New York, NY, United States, [2]Bernard and Irene Schwartz Center for Biomedical Imaging, Department of Radiology, New York University School of Medicine, New York, NY, United States

Previously proposed techniques based on non-Cartesian or modified Cartesian sampling schemes allow for free-breathing acquisitions with solid motion-robustness. However, residual artifacts such as motion blurring often remain. Techniques including self-gating, motion-weighting, and extra-dimensional reconstruction have been proposed to further improve image quality.

Here, an analysis of these techniques is provided by performing multiple reconstructions of several volunteer and patient datasets, which were then evaluated by radiologists.

3928 Computer 75

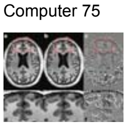

More than meets the eye: Quantitative evaluation of prospective motion correction at 7T

Hendrik Mattern[1], Falk Lüsebrink[1], Alessandro Sciarra[1], and Oliver Speck[1,2,3,4]

[1]BMMR, Otto-von-Guericke-University, Magdeburg, Germany, [2]German Center for Neurodegenerative Disease, Magdeburg, Germany, [3]Center for Behavioral Brain Sciences, Magdeburg, Germany, [4]Leibniz Institute for Neurobiology, Magdeburg, Germany

Prospective motion correction inherently does not provide uncorrected images. Thus, for image assessment usually motion corrected and uncorrected data from two different scans – therefore with different motion patterns – are qualitatively compared. In this study, prospectively corrected data from a highly trained cohort is retrospectively decorrected to enable a quantitative assessment with image-based and segmentation-based metrics. The results indicate that for the observed small-scale, involuntary subject motion quantitative rather than qualitative assessment is necessary to estimate the image degradation.

3929 Computer 76

PET motion correction by co-registering multiple MR contrasts in simultaneous brain MR-PET

Francesco Sforazzini[1], Richard McIntyre[1,2], Nicholas Ferris[1], Nadim Jon Shah[1,3,4], Gary Egan[1,5,6], and Zhaolin Chen[1,4]

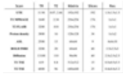

[1]Monash Biomedical Imaging, Monash University, Melbourne, Australia, [2]Monash Medical Centre, Clayton, Australia, [3]Forschungszentrum Jülich GmbH, Institute of Neuroscience and Medicine, Jülich, Germany, [4]Department of Electrical and Computer Systems Engineering, Monash University, Monash University, Melbourne, Australia, [5]Australian Research Council Centre of Excellence for Integrative Brain Function, Monash University, Melbourne, Australia, [6]Monash Institute of Cognitive and Clinical Neuroscience, Monash University, Melbourne, Australia

Head movement is a major issue in dynamic brain PET imaging. The introduction of a simultaneous MR-PET scanner enabled new opportunities to use MR information for PET motion correction. Here we present a novel method based on routinely acquired MRI sequences. Multi-contrast MR images are co-registered to extract motion parameters. These motion parameters are then used to guide PET image reconstruction. Results on both phantom and human data provide evidences that this method can significantly enhance image contrast and reduce motion artefact in brain PET images, without affecting MR protocol.

3930 Computer 77

A Novel Position and Orientation Sensor for MRI

James A. Smith[1], Glyn S. Spencer[1], Richard W. Bowtell[1], Penny A. Gowland[1], and Paul M. Glover[1]

[1]Sir Peter Mansfield Imaging Centre, University of Nottingham, Nottingham, United Kingdom

The effect of head motion is a significant problem for MRI. Here we present the early stages in the development of a novel device which is able to measure head pose within the scanner. By using a combination of a commercially available 3-axis MEMS accelerometer and an anisotropic magnetoresitive bridge sensor, the orientation of the device is monitored with root-mean-square accuracy of ±0.12° while translation is estimated using voltages induced in a single coil by time-varying magnetic field gradients with an accuracy of ±0.45mm. With further development, this device could be used effectively for prospective and retrospective motion correction.

3931 Computer 78

A Registration Framework for Prostate mpMRI via Combining Intensity and Shape Information

Xia Li[1], Sandeep Gupta[1], Rakesh Mullick[2], Oguz Akin[3], and Dattesh Shanbhag[2]

[1]GE Global Research Center, Niskayuna, NY, United States, [2]GE Global Research Center, Bengaluru, India, [3]Memorial Sloan-Kettering Cancer Center, New York, NY, United States

In prostate MRI, tissue alignment between T2w and DWI can be challenging due to elastic distortions in DWI induced by fast switching of gradients. In this work, we propose a joint approach to perform registration between DWI and T2w on the prostate data, by considering both image intensity and prostate gland shape information. After rigid alignment between segmented prostate masks, surface points on the prostate masks were extracted and Gaussian mixture model was used to build shape correspondence. The shape information was integrated into mutual-information based deformable registration to constrain undesired distortions. The proposed framework was compared with other strategies and demonstrated the best registration accuracy (DICE = 0.91 between T2 and DWI based prostate masks).

3932 Computer 79

Self-gated 4D-MRI of the Liver: Initial Clinical Results of Comprehensive Real-Time Imaging of Hepatic Enhancement

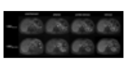

Jakob Weiss[1], Ahmed E Othman[2], Petros Martirosian[3], Marcel Dominik Nickel[4], Jana Taron[2], Manuel Kolb[2], Christer Ruff[2], Konstantin Nikolaou[2], and Mike Notohamiprodjo[2]

[1]Diagnostic and Interventional Radiology, University of Tuebingen, Tuebingen, Germany, [2]Diagnostic and Interventional Radiology, University of Tuebingen, [3]Section on Experimental Radiology, University of Tuebingen, [4]Siemens Healthcare

A remaining challenge of abdominal MRI are artifacts due to patient motion. In this study, we evaluated a prototype volume-interpolated breath-hold examination (VIBE) sequence with automated respiration self-gating and compressed sensing reconstruction ($VIBE_{SG-CS}$) for continuous dynamic contrast-enhanced (DCE) liver MRI in comparison to a standard multiphase breath-hold examination ($VIBE_{BH-STD}$). $VIBE_{SG-CS}$ provided similar overall image quality and lesion conspicuity and improved image sharpness as compared to $VIBE_{BH-STD}$. Therefore, $VIBE_{SG-CS}$ seems to be a promising approach to improve the validity and reliability of DCE-MRI of the liver, especially in patients with impaired breath-hold capabilities.

3933 Computer 80

Effect of head motion on B0 shimming based on magnetic field probes

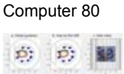

Joep Wezel[1], Andrew G. Webb[1], and Matthias J. van Osch[1]

[1]Radiology, Leiden University Medical Center, Leiden, Netherlands

Magnetic field probes (FP) can be used to monitor B_0-changes and this approach has shown great potential for real time correction of artifacts produced by such changes. When estimating B_0 fluctuations in the brain it is, however, not known how head motion influences the FP-based B_0-estimation. Head motion introduces a B_0-change both inside and outside the head, this study assesses the impact on field probe estimated B_0-distributions within the brain at 7 Tesla. FP based correction after head motion can actually lead to a higher error especially evident when using third order spherical harmonics. Improved performance is, however, identified when using first order spherical harmonics.

3934 Computer 81

A generalized prospective motion correction framework for improved spectroscopy, structural and angiographic imaging

Mads Andersen[1], Vincent Oltman Boer[2], Anouk Marsman[2], and Esben Thade Petersen[2,3]

[1]Philips Healthcare, Copenhagen, Denmark, [2]Danish Research Centre for Magnetic Resonance, Centre for Functional and Diagnostic Imaging and Research, Copenhagen University Hospital Hvidovre, Denmark, [3]Electrical Engineering, Technical University of Denmark, Lyngby, Denmark

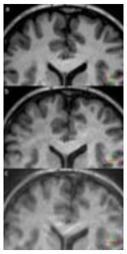

Subject motion is a major problem in brain imaging and spectroscopy, misleading diagnosis in the clinic and lowering data quality in research. A promising solution is to update the field-of-view in real time based on tracking with volumetric navigators. This was implemented using a new interleaved scanning framework and a product functionality for self-navigation of fMRI. The implementation is simple to use and very flexible, as the navigator and target sequence are simply defined as two different scans, that can be interleaved at any level. It was demonstrated to improve motion robustness in single voxel spectroscopy, T1-weighted imaging and angiography.

3935 Computer 82

One-Dimensional Phase Navigation of Diffusion-Weighted 3D TSE for High Resolution Musculoskeletal Diffusion Imaging

Barbara Cervantes[1], Anh T Van[2], Hendrik Kooijman[3], Kim van de Ven[4], Andreas Hock[3], Ernst J Rummeny[1], Jan S Kirschke[5], and Dimitrios C Karampinos[1]

[1]Department of Diagnostic and Inteventional Radiology, Technical University of Munich, Munich, Germany, [2]IMETUM, Technical University of Munich, Garching, Germany, [3]Philips Healthcare, Hamburg, Germany, [4]Philips Healthcare, Best, Netherlands, [5]Department of Neuroradiology, Technical University of Munich, Munich, Germany

Diffusion-prepared 3D TSE (dprep-3D-TSE) imaging has been recently applied for high-resolution distortion-free body and musculoskeletal DWI. Dprep-3D-TSE has been combined with magnitude stabilizers to reduce magnitude modulation effects induced by both motion and eddy current effects. In addition, velocity compensation has been proposed to reduce motion-induced phase modulation effects. However, given that dprep-3D-TSE is a multi-shot diffusion technique, it suffers from motion-induced phase variation effects across different shots and it requires phase navigation. The purpose of the present study is to develop an acquisition and phase correction scheme for one-dimensional phase navigation of dprep-3D-TSE imaging.

3936 Computer 83

Optical Motion Monitoring for Abdominal and Lung Imaging

Joseph Y. Cheng[1], Jonathan Lu[2], Grieg Scott[2], and Shreyas S. Vasanawala[1]

[1]Department of Radiology, Stanford University, Stanford, CA, United States, [2]Department of Electrical Engineering, Stanford University, Stanford, CA, United States

The accuracy to compensate or correct for MR image artifacts from motion depends on the ability to precisely measure patient motion. Optical cameras are a compelling solution as they simplify patient setup and do not negatively impact MR data acquisition. However, most efforts have been focused on integrating and applying optical cameras to neuroimaging. In this work, setup and methods for video processing were developed for lung and abdominal MRI where MRI acquisition is especially sensitive to motion. The proposed solution had high correlation with conventional approaches of respiratory bellows and MRI navigators; also, comparable image quality was achieved.

3937 Computer 84

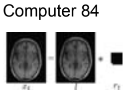

Joint Non-Rigid Motion Estimation and Image Reconstruction via Sparse Blind Deconvolution

Frank Ong[1] and Michael Lustig[1]

[1]Electrical Engineering and Computer Sciences, University of California, Berkeley, Berkeley, CA, United States

We propose a non-parametric method of jointly estimating non-rigid motion and the underlying image without the assumption of motion smoothness. We model non-rigid motion as local linear translation, which is equivalent to convolution with 1-sparse kernels. We then pose the non-rigid motion recovery problem as a sparse blind deconvolution problem. Our reconstruction results demonstrate that non-rigid motion can be well approximated as local translation motion using the proposed method. The proposed formulation can also be viewed as a generalization of locally low rank reconstruction.

3938 Computer 85

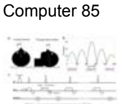

Exploring the Sensitivity of Magnetic Resonance Fingerprinting to Different Types of Motion and Possible Correction Mechanisms

Zidan Yu[1,2,3], Tiejun Zhao[1,2,4], Jakob Assländer[1,2], Riccardo Lattanzi[1,2,3], Daniel K Sodickson[1,2,3], and Martijn A Cloos[1,2,3]

[1]Bernard and Irene Schwartz Center for Biomedical Imaging, Department of Radiology, New York University School of Medicine, New York, NY, United States, [2]Center for Advanced Imaging Innovation and Research (CAI2R), Department of Radiology, New York University School of Medicine, New York, NY, United States, [3]The Sackler Institute of Graduate Biomedical Sciences, New York University School of Medicine, New York, NY, United States, [4]Siemens Medical Solutions USA, Inc., Siemens Healthineers, New York, NY, United States

In this work, we experimentally explore the sensitivity of Magnetic Resonance Fingerprinting (MRF) to various types of motion at different time intervals during the scan. Our results show that the T1 values are least affected by motion, but the maps may be blurred if the motion occurs early in the scan. Also, motion in the middle of the scan leads to a systematic underestimation in T2. In addition, we show that simply removing the corrupted time-points from the data can restore quantitative parameter values to the correct range.

3939 Computer 86

Image-Based Non-Rigid Motion Correction for Free-breathing 3D Abdominal MRI

Jun Lv[1], Ming Yang[2], Jue Zhang[1,3], Xiaoying Wang[1,4], and Jing Fang[1,3]

[1]Academy for Advanced Interdisciplinary Studies, Peking University, Beijing, People's Republic of China, [2]Philips Healthcare, Suzhou, People's Republic of China, [3]College of Engineering, Peking University, Beijing, People's Republic of China, [4]Department of Radiology, Peking University First Hospital, Beijing, People's Republic of China

Free breathing abdomen imaging requires non-rigid motion registration of the unavoidable respiratory motion in the 3D under-sampled datasets. In this work, pyramidal Lucas-Kanade based optical flow estimation is proposed to perform upper abdomen registration, which enables reconstruction of motion-free abdominal images throughout the respiratory cycle. Preliminary results on images acquired using 3D golden radial phase encoding eThrive scan demonstrate that our approach makes vessels in liver sharper and more consecutive when compared to traditional NMC and LREG based methods.

3940 Computer 87

Reconstruction of highly accelerated free-breathing 3D abdominal MRI using Stacked Convolutional Auto-Encoder Network

Jun Lv[1], Kun Chen[1], Ming Yang[2], Jue Zhang[1,3], Xiaoying Wang[1,4], and Jing Fang[1,3]

[1]Academy for Advanced Interdisciplinary Studies, Peking University, Beijing, People's Republic of China, [2]Philips Healthcare, Suzhou, People's Republic of China, [3]College of Engineering, Peking University, Beijing, People's Republic of China, [4]Department of Radiology, Peking University First Hospital, Beijing, People's Republic of China

Free-breathing 3D abdominal imaging is a challenging task for MRI since respiratory motion severely degrades image quality.Our purpose is to develop a novel reconstruction approach for highly accelerated free-breathing 3D abdominal images with stacked convolutional auto-encoders. The whole structure of our proposed method consists of 9 hidden layers except to input and output layer.The proposed method achieves similar quality to the whole sampling reconstruction with non-significant differences for structural similarity index measure (SSIM) (0.99 and 1.00, respectively). Moreover, the average reconstruction time is very short (about 0.25 s/image). Therefore, our method should be employed for a wide range of clinical applications.

3941 Computer 88

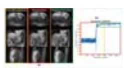

Real-time prospective bulk motion exclusion for robust 3D free-breathing abdominal imaging

Bjorn Stemkens[1,2,3], Thomas Benkert[2,3], Hersh Chandarana[2,3], Cornelis A.T. Van den Berg[1], Jan J.W. Lagendijk[1], Daniel K. Sodickson[2,3], Rob H.N. Tijssen[1], and Kai Tobias Block[2,3]

[1]Department of Radiotherapy, University Medical Center Utrecht, Utrecht, Netherlands, [2]Center of Advanced Imaging Innovation and Research (CAI2R), Department of Radiology, New York University School of Medicine, New York, NY, United States, [3]Bernard and Irene Schwartz Center for Biomedical Imaging, Department of Radiology, New York University School of Medicine, New York, NY, United States

3D free-breathing approaches have shown potential for abdominal imaging in patients who are unable performing breath-holds, such as pediatric patients and uncooperative adults. However, these free-breathing techniques fail when bulk motion occurs. This study proposes a method to detect and exclude such bulk motion to ensure diagnostic image quality, even in this challenging group of patients. Without requiring user interaction, this technique improves robustness for abdominal MR imaging, while minimizing the scan time on an individual basis, using a real-time implementation on the MRI system, which may enable robust non-sedated pediatric imaging.

3942 Computer 89

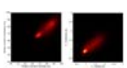

Radial MRI and model-based iterative reconstruction for motion robust quantification of the water content in the brain at 3 Tesla

Markus Zimmermann[1], Zaheer Abbas[1,2], Dominik Ridder[1], Ana-Maria Oros-Peusquens[1], and N. Jon Shah[1,2]

[1]Institute of Neuroscience and Medicine – 4, Medical Imaging Physics, Forschungszentrum Juelich GmbH, Juelich, Germany, [2]Department of Neurology, Faculty of Medicine, RWTH Aachen University, JARA, Aachen, Germany

Quantitative water content mapping is a promising technique to monitor brain diseases. However, established protocols suffer from long acquisition times and sensitivity to patient motion. To overcome these issues, we propose to use golden angle radial MRI and model-based iterative reconstruction. This allows accurate and precise estimation of water content and T_1 values, while providing significantly higher motion robustness, as shown in phantom and in vivo experiments. The golden angle-based k-space sampling allows for a nearly optimal k-space coverage even in the event of early termination of measurement. This opens the opportunity to apply such a technique in the clinic.

3943 Computer 90

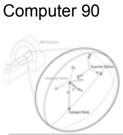

A head motion model for fusion of patient pose measurements from different sensing modalities.

Adam M. J. van Niekerk[1], Ernesta M. Meintjes[1], and Andre J. W. van der Kouwe[1,2,3]

[1]Division of Biomedical Engineering, Human Biology, University of Cape Town, Cape Town, South Africa, [2]Athinoula A. Martinos Center, Massachusetts General Hospital, Charlestown, MA, United States, [3]Radiology, Harvard Medical School, Boston, MA, United States

In this work we aim to address the challenges of fusing motion parameters measured using different sensing modalities, as temporal resolutions differ widely between navigator and external motion tracking techniques. A model is presented in which head motion is characterised as simple rolling motion. The resulting equations describe subject motion to within 2 mm when applied in an open loop manner. A filter, with feedback, is then implemented where navigator data is used to estimate model parameters. The filtered translation output is smooth without the cost of increased latency due to the fast orientation estimates.

3944 Computer 91

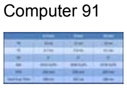

Accurate High-speed 3D-Registration of EPI vNavs for Head Motion Correction

Yingzhuo Zhang[1], Iman Aganj[2,3], André J.W. van der Kouwe[2,3], and Matthew Dylan Tisdall[4]

[1]John A. Paulson School of Engineering and Applied Sciences, Harvard University, Cambridge, MA, United States, [2]Athinoula A. Martinos Center for Biomedical Imaging, Radiology Department, Massachusetts General Hospital, Charlestown, MA, United States, [3]Department of Radiology, Harvard Medical School, Boston, MA, United States, [4]Department of Radiology, Perelman School of Medicine, University of Pennsylvania, Philadelphia, PA, United States

Low-resolution, whole-head volumes can be acquired rapidly with EPI-based volumetric navigators (vNavs). vNavs interspersed in a longer scan are widely used for prospective motion correction in a variety of sequences. To further improve the accuracy and flexibility of vNavs, we present a novel registration algorithm, tailored specifically for the vNavs application. Accuracy of the algorithm is tested on navigator volumes acquired with human volunteers at three isotropic resolutions, 6.4mm, 8mm, and 10mm, using a series of field of view (FOV) rotations and translations to provide ground truth rigid “motion”.

3945 Computer 92

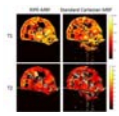

Regularly Incremented Phase Encoding Magnetic Resonance Fingerprinting (RIPE-MRF) for Enhanced Motion Suppression in Cartesian MRF

Christian Anderson[1], Charlie Wang[1], Yuning Gu[1], Mark Griswold[1,2], Xin Yu[1,2,3], and Chris Flask[1,2,4]

[1]Biomedical Engineering, Case Western Reserve University, Cleveland, OH, United States, [2]Radiology, University Hospitals Cleveland Medical Center, Cleveland, OH, United States, [3]Physiology and Biophysics, Case Western Reserve University, Cleveland, OH, United States, [4]Pediatrics, University Hospitals Cleveland Medical Center, Cleveland, OH, United States

Preclinical quantitative MRI is susceptible to the motion artifacts caused by the rapid respiratory motion and high heart rates present in small animals. This can be alleviated through the use of gating/triggering but these are difficult to implement in magnetic resonance fingerprinting due to the need for dynamic, coherent signal evolutions. We propose a method for an incremented phase encoding MRF acquisition that enhances motion suppression in Cartesian MRF. This phase incremented strategy distributes motion artifacts throughout the acquisition creating incoherent artifacts allowing the MRF method to “see through” the artifacts and produce artifact free T1 and T2 maps.

3946 Computer 93

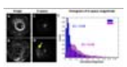

A novel and robust reconstruction method for free-breathing cine DENSE by minimizing k-space entropy

Xiaoying Cai[1], Kenneth C Bilchick[2], and Frederick H Epstein[1,3]

[1]Biomedical Engineering, University of Virginia, Charlottesville, VA, United States, [2]Medicine, University of Virginia, Charlottesville, VA, United States, [3]Radiology, University of Virginia

A reliable free-breathing (FB) cine DENSE method would benefit myocardial strain imaging in many patients. An echo due to T1 relaxation is an important source of artifacts, particularly for free-breathing acquisitions. We propose to optimize suppression of these echoes by minimizing k-space entropy. The method was tested in 10 subjects (6 healthy volunteers and 4 heart failure patients) and compared to a conventional diaphragm navigator method (dNAV). Image reconstruction by minimizing k-space entropy provided better image quality than the conventional dNAV method.

3947 Computer 94

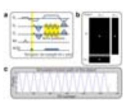

Motion-Robustness Evaluation and Motion Correction of Wave-Encoding

Feiyu Chen[1], Joseph Y Cheng[2], Tao Zhang[3], John M Pauly[1], and Shreyas S Vasanawala[2]

[1]Electrical Engineering, Stanford University, Stanford, CA, United States, [2]Radiology, Stanford University, Stanford, CA, United States, [3]Global MR Applications and Workflow, GE Healthcare, Houston, TX, United States

The motion-robustness of a 3D wave-encoded SPGR sequence was evaluated by simulating the acquisition of a Gaussian-profile object with periodic motion. Compared with non-wave-encoded sampling, wave-encoding provides better motion property because of wider diffusion of motion artifacts. A motion-correction method was also proposed for wave-encoding based on 3D translational motion estimates. This motion-correction method is demonstrated to effectively reduce motion artifacts in wave-encoded scans.

3948 Computer 95

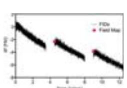

Simultaneous motion and B0 correction using FID-SNAVS

Patricia M Johnson[1,2], Junmin Liu[1], and Maria Drangova[1,2]

[1]Robarts Research Institute, London, ON, Canada, [2]Department of Medical Biophysics, Schulich School of Medicine and Dentistry, Western University, London, ON, Canada

Global B_0 shifts caused by subject motion and scanner heating, result in phase inconsistencies, which lead to image artefacts. In this work, an FID readout is added to Spherical Navigator Echoes (FID-SNAVs) in order to perform retrospective motion and frequency shift (Δf) correction. The accuracy of FID-SNAVs in measuring Δf is evaluated, and simultaneous Δf and motion measurement is demonstrated in phantom experiments. FID-SNAVs estimate Δf accurately, and shifts of approximately -10 to 6Hz are measured during translations of ±1.5cm. Combined Δf and motion correction demonstrates dramatic improvement of image quality compared to motion correction alone.

3949 Computer 96

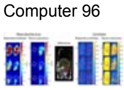

3D motion quantification based on the temporal evolution of the noise covariance matrix of a receive array

Robin J.M. Navest[1], Anna Andreychenko[1], Jan J.W. Lagendijk[1], Baudouin Denis de Senneville[1,2], and Cornelis A.T. van den Berg[1]

[1]Department of Radiotherapy, Center for Image Sciences, University Medical Center Utrecht, Utrecht, Netherlands, [2]IMB, UMR 5251 CNRS/University of Bordeaux, Bordeaux, France

Motion quantification is essential for successful MR imaging and MRI guided radiotherapy of mobile organs. Currently, 3D MRI is too slow to quantify organ displacements and a motion model could alternatively be used for tracking and/or motion compensation. A motion model trained on MRI data and driven by the noise covariance matrix (NCM) of a receive array is proposed to quantify internal anatomy motion. Passive thermal noise measurements have a high temporal resolution (~10ms) and do not interfere with or rely on MR signal. Abdominal organ displacement can be accurately estimated in 3D, through the NCM of the receive array.

Electronic Poster

Exhibition Hall | Tuesday 9:15 - 10:15

3950 Computer 1

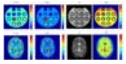

SNR analysis and sequence parameter optimization for T1 and T2 mapping using an ellipse fitting approach of phase cycled bSSFP data

Yulia Shcherbakova[1], Cornelis A.T. van den Berg[2], Chrit T.W. Moonen[1], and Lambertus W. Bartels[3]

[1]Center for Imaging Sciences/Imaging Division, University Medical Center Utrecht, Utrecht, Netherlands, [2]Dept. of Radiotherapy/Imaging Division, University Medical Center Utrecht, Utrecht, Netherlands, [3]Image Sciences Institute/dept. of Radiology, University Medical Center Utrecht, Utrecht, Netherlands

An ellipse fitting approach has been recently proposed for simultaneous estimation of the relaxation times T_1 and T_2 from phase-cycled balanced steady-state free precession (PC-bSSFP). In this work we present an analysis of the SNR sensitivity of the proposed method and optimization of the sequence parameter settings. We demonstrate, that it is feasible to perform an accurate and precise T_1 and T_2 mapping while using an optimal FA and TR combination for realistic SNRs.

3951 Computer 2

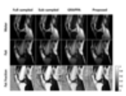

A Fast Interleaved Bipolar Imaging Method for Fat Quantification

JaeJin Cho[1], Hyunseok Seo[1], Kinam Kwon[1], Seohee So[1], Byungjai Kim[1], and HyunWook Park[1]

[1]Korea Advanced Institute of Science and Technology (KAIST), Daejeon, Korea, Republic of

The fat quantification using the bipolar multi-echo signals has several benefits such as fast imaging time, SNR, resolution, and robust separation. However, the fat quantification using the bipolar multi-echo signals suffers from the bipolar artifacts due to the imperfect gradient. In this abstract, to overcome these problems, fat quantification is independently performed for each polarity of the readout gradient. Because the acquisition of fully sampled data takes too much time, a new interpolation method for interleaved bipolar multi-gradient-echo acquisition is proposed, which uses the low-rankness of entire data. The experiment results show that the proposed method successfully quantifies the correct fat fraction without bipolar artifacts in a short imaging time.

3952 Computer 3

Using Pre-calculated Direct Signal Control Solutions for 7T 3D FLAIR Brain Imaging

Arian Beqiri[1], Alessandro Sbrizzi[2], Joseph V Hajnal[1,3], Shaihan J Malik[1], and Hans Hoogduin[2]

[1]Biomedical Engineering and imaging Sciences, King's College London, London, United Kingdom, [2]Image Sciences Institute, University Medical Centre Utrecht, Utrecht, Netherlands, [3]Centre for the Developing Brain, King's College London, London, United Kingdom

Direct Signal Control can be used for improving signal uniformity for TSE based 3D-FLAIR imaging at 7T by using dynamic RF shimming through the echo train. The need to calibrate and optimize on a subject-specific basis can be a workflow issue. In this work we evaluate generic solutions that are calculated in advance, in comparison with individual subject-specific optimizations.

3953 Computer 4

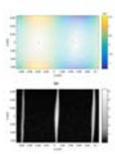

Gradient Field Design for RF Excitation in Simultaneous Multi-Slice and Simultaneous Multi-Slab Imaging by Using a Z-Gradient Array

Koray Ertan[1], Soheil Taraghinia[1], Hamed Mohammadi[2], and Ergin Atalar[1]

[1]National Magnetic Resonance Research Center (UMRAM), Bilkent University, Ankara, Turkey, [2]Electrical and Electronics Engineering, Bilkent University, Ankara, Turkey

Multiple locations inside the volume of interest can be mapped to same frequency by applying spatially oscillating magnetic fields (SOMFs) created by 9 channel z-gradient array. Such a mapping can lead to excitation of multiple slices or slabs with a single band RF pulse as well as doubling the number of slices excited by a multi-band RF pulse. Depending on the slice or slab locations, spatially oscillating magnetic fields can be shifted using a independent gradient amplifiers. We have demonstrated 2 slab excitation with a single band RF pulse and 6 slice excitation with a 3-band RF pulse.

3954 Computer 5

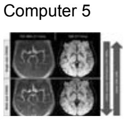

Simultaneous Variable-slab Dual-echo TOF MR Angiography and Susceptibility-Weighted Imaging

Won-Joon Do[1], Seung Hong Choi[2], and Sung-Hong Park[3]

[1]Dept. of Bio and Brain Engineering, KAIST, Daejeon, Korea, Republic of, [2]Dept. of Radiology, Seoul National University Hospital, Seoul, Korea, Republic of, [3]Dept. of Bio and Brain Enginnering, KAIST, Daejeon, Korea, Republic of

Multi-slab time of flight MR angiogram (TOF MRA) provides more detailed vascular structure than single-slab MRA, whereas single-slab susceptibility weighed imaging (SWI) provides better SNR than multi-slab SWI. In previous CODEA study, conflicting requirement on number of slab was not solved. In this study, we proposed and demonstrated an efficient method to acquire TOF MRA and SWI simultaneously with different number of slabs using variable-slab CODEA, which suppressed slab boundary artifacts in TOF MRA. Also demonstrated was acceleration of the variable-slab CODEA with a parallel imaging technique, GRAPPA. These improvements would provide more diverse clinical information in a limited scan time.

3955 Computer 6

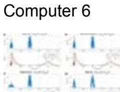

Root-flipped multiband pulses with inherently aligned echoes

Samy Abo Seada[1], Jo Hajnal[1], and Shaihan Malik[1]

[1]Division of Imaging Sciences and Biomedical Engineering, King's College London, London, United Kingdom

Root-flipped multiband pulses have peculiar spin-echo behaviour due to their non-linear phase profile. In spin-echo sequences, different slices will typically have different relaxation weightings. This work investigates the typical time-delays of the spin-echoes such pulses, and proposes a novel root-flipping method to minimize differences in relaxation weighting.

3956 Computer 7

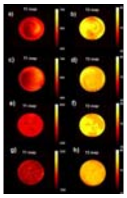

Spatial biases in Magnetic Resonance Fingerprinting parameter maps arising from undersampling patterns

Gregor Körzdörfer[1,2], Thomas Kluge[1], Josef Pfeuffer[1], Matthias Gebhardt[3], Dan Ma[4], Yun Jiang[4], Mark Griswold[4,5], and Mathias Nittka[1]

[1]Application Development, Siemens Healthcare, Erlangen, Germany, [2]Friedrich-Alexander Universität Erlangen-Nürnberg, Erlangen, Germany, [3]Physics department, Siemens Healthcare, [4]Department of Biomedical Engineering, Case Western Reserve University, OH, United States, [5]Dept. of Radiology, Case Western Reserve University and University Hospitals of Cleveland, OH, United States

Magnetic Resonance Fingerprinting (MRF) is an MR technique that generates parameter maps by matching pseudo randomly generated MR signals with a precalculated dictionary. In order to acquire the signals in a reasonable time, rapid imaging techniques with high undersampling factors are necessary. We show a detailed analysis of the artifacts originating from this and their impact on measured signals and subsequently on parameter maps. Additionally, an analytical approach of predicting undersampling artifacts is proposed. With the help of this approach, a more robust and time efficient sampling of signals in MRF can be designed.

3957 Computer 8

High-resolution 3D T2 mapping using a stack-of-stars radial FSE pulse sequence

Mahesh Bharath Keerthivasan[1], Manojkumar Saranathan[2], Ali Bilgin[1,2], Diego R Martin[2], and Maria Altbach[2]

[1]Electrical and Computer Engineering, University of Arizona, Tucson, AZ, United States, [2]Medical Imaging, University of Arizona, Tucson, AZ, United States

T2 mapping is a parametric imaging approach that provides quantification of T2-weighted images for a more accurate diagnosis of pathology. 2D multi-slice T2 estimation techniques cannot be used for thin slice isotropic imaging. To overcome this limitation, we present a T2 mapping technique using a 3D radial FSE pulse sequence with a variable flip angle scheme for optimal T2-weighting and T2 mapping within SAR constraints. Data is acquired in a stack-of-stars radial trajectory and T2 maps are reconstructed using model based iterative algorithms. The method is demonstrated in phantoms and in vivo brain and musculoskeletal imaging.

3958 Computer 9

Triple Quantum Filtering in Sodium Magnetic Resonance Imaging Using Strongly Modulated Pulses

Aliaksandra Shymanskaya[1], Wieland A. Worthoff[1], and N. Jon Shah[1,2]

[1]Institut of Neuroscience and Medicine - 4, Forschungszentrum Jülich GmbH, Jülich, Germany, [2]Department of Neurology, Faculty of Medicine, JARA, RWTH Aachen University, Aachen, Germany

^{23}Na-MRI can be used for non-invasive investigation of metabolic disease, based on discrimination between sodium signals arising from different tissue compartments due to development of multiple quantum coherences mainly in intracellular space. Strongly modulated pulses in NMR and MRI can be created using optimal control design to generate the most efficient transfer between the initial and target states of the nuclear spin ensemble, defined by the density matrix formalism. The Krotov algorithm and its implementation by Maximov of the optimal control design were used to modify the first hard RF pulse in the SISTINA sequence.

3959 Computer 10

Fast Interrupted Steady-State (FISS) Magnetic Resonance Imaging

Ioannis Koktzoglou[1,2] and Robert R Edelman[1,3]

[1]Radiology, NorthShore University HealthSystem, Evanston, IL, United States, [2]Radiology, University of Chicago Pritzker School of Medicine, Chicago, IL, United States, [3]Radiology, Northwestern University Feinberg School of Medicine, Chicago, IL, United States

We report an imaging approach, Fast Interrupted Steady-State (FISS), for retaining the high signal associated with true fast imaging with steady-state free precession (TrueFISP), while lessening its sensitivity flow artifacts.

3960 Computer 11

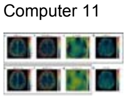

Magnetic Resonance Fingerprinting with Quadratic RF Phase for Simultaneous Measurement of δf, T1, T2, and T2*

Charlie Yi Wang[1], Simone Coppo[2], Bhairav Bipin Mehta[2], Nicole Seiberlich[1,2], Xin Yu[1,2], and Mark Alan Griswold[1,2]

[1]Biomedical Engineering, Case Western Reserve University, Cleveland, OH, United States, [2]Radiology, Case Western Reserve University, OH, United States

We propose a modified Magnetic Resonance Fingerprinting pulse sequence with quadratic RF excitation phase (qRF-MRF) for the purpose of simultaneous measurement of T_2* in addition to previously established spin parameters δ_f, T_1, and T_2. Existing bSSFP based MRF pulse sequence[1] was modified to incorporate excitation segments with quadratic RF phase to sensitize signal evolutions to T_2*. Measurements using qRF-MRF were performed in both phantom and in vivo. Maps from qRF-MRF were validated against traditional MRF, literature, and Multi-Echo GRE.

3961 Computer 12

Fast T1 Correction for Fat Quantification using a Dual-TR Chemical Shift Encoded MRI Acquisition

Xiaoke Wang[1,2], Diego Hernando[2,3], Curtis N Wiens[2], and Scott Reeder[1,2,3,4,5]

[1]Biomedical Engineering, University of Wisconsin-Madison, Madison, WI, United States, [2]Radiology, University of Wisconsin-Madison, Madison, WI, United States, [3]Medical Physics, University of Wisconsin-Madison, Madison, WI, United States, [4]Emergency Medicine, University of Wisconsin-Madison, Madison, WI, United States, [5]Medicine, University of Wisconsin-Madison, Madison, WI, United States

Dual flip angle (DFA) methods facilitate T1-corrected proton density fat-fraction (PDFF) quantification at the cost of doubling scan time compared to small flip angle (SFA) methods. In this study, a novel "dual-TR" (DTR) fat quantification strategy was proposed. It acquired 2 spoiled gradient echo (SGRE) dataset sequentially, one with a shortened echo train and reduced TR to alleviate scan time penalties. Monte-Carlo simulation and Cramer-Rao lower bound demonstrated improved noise performance using the proposed method compared with SFA and DFA methods. Phantom experiments demonstrated the feasibility of T1-corrected PDFF estimates using the proposed DTR method.

3962 Computer 13

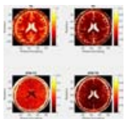

In-vivo Validation of MR-STAT: Simultaneous Signal Localization and Quantification of Tissue Parameters on a 3T Clinical MR-System

Oscar van der Heide[1], Alessandro Sbrizzi[1], Anna Kruseman[1], Martijn Cloos[2], Peter Luijten[1], and Nico van den Berg[1]

[1]UMC Utrecht, Utrecht, Netherlands, [2]NYU School of Medicine, New York, United States

MR-STAT is a framework for obtaining quantitative parameter maps from a single short scan. It is based on a time domain model. Large numerical inversion problems are solved to simultaneously localize signal and estimate tissue parameters. In this work we demonstrate the first experimental in-vivo results obtained with a clinical MR system.

3963 Computer 14

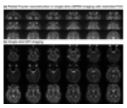

Partial Fourier techniques in single-shot cross-term spatiotemporal encoding (xSPEN) MRI

Zhiyong Zhang[1] and Lucio Frydman[1]

[1]Weizmann Institute of Science, Rehovot, Israel

xSPEN is a new single-shot imaging approach with exceptional resilience to field heterogeneities: its images do not suffer from miss-registrations, require a priori information nor use post-acquisition corrections, to deliver faithfully the spins' spatial distribution. xSPEN, however, suffers from SNR penalties due to its non-Fourier nature and its considerable diffusion losses –especially when desiring high resolution. This study introduces partial Fourier transform approaches that acting along either the readout or the spatiotemporally-encoded dimensions, reduce both of these penalties. The principles of these partial FT methods are given, and applications in materials, preclinical and human single-shot xSPEN imaging are presented.

3964 Computer 15

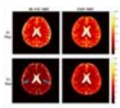

IR-TSE MRF: Rapid and Accurate Parametric Mapping Using Inversion-recovery Turbo Spin Echo and MR Fingerprinting

Congyu Liao[1], Xiaozhi Cao[1], Zhixing Wang[1], Qing Li[1], Ying Chen[1], Huihui Ye[1], Qiuping Ding[1], Hongjian He[1], and Jianhui Zhong[1]

[1]Center for Brain Imaging Science and Technology, Department of Biomedical Engineering, Zhejiang University, Hangzhou, People's Republic of China

This study proposes a rapid and accurate MR fingerprinting (MRF) framework based on inversion-recovery turbo spin echo (IR-TSE) sequence. Compared with the conventional quantitative imaging method and FISP-MRF, the proposed one can provide T2 maps with high accuracy in addition to T1 and proton density (PD) for whole brain in about 6 minutes. In this regard, this new MRF strategy would potentially aid in achieving high resolution quantitative mapping for T2-sensitive circumstances such as epilepsy and multiple sclerosis applications.

3965 Computer 16

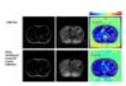

Optimized Trajectory Dual-Echo Fat and Water Separation

Hyungseok Jang[1] and Alan B McMillan[1]

[1]Department of Radiology, University of Wisconsin, Madison, WI, United States

Two-point Dixon methods enable robust fat suppression particularly in body and abdominal applications where large field of view imaging is required. However, a limitation of this approach is the decreased efficiency and longer TR's necessary to acquire multiple echoes. Furthermore, due to system performance constraints, flexible choice of image parameters necessary to obtain near in and out-of-phase echo times limits valid combinations of field of view, matrix size, and encoding bandwidth. In this study, we describe a novel, generalized framework to optimize a ramp-sampled readout, which allows reduced scan time, flexible parameter selection, and improved quantitative fat and water separation.

3966 Computer 17

Reference-Free Distortion Correction with Segmented Partial Fourier Acquisitions for High Resolution DTI at 7T

Michael Herbst[1], Benedikt A Poser[2], and Marco Reisert[1]

[1]Dept. of Radiology, Medical Physics, University Medical Center Freiburg, Freiburg, Germany, [2]Department of Cognitive Neuroscience, Maastricht Brain Imaging Centre (MBIC)

Single-Shot diffusion weighted echo planar imaging (EPI) is known for its strong distortions due to long imaging readouts. However, even for segmented acquisitions, high resolution diffusion weighted imaging suffers from image distortions. Our approach shows that intrinsic field information of a segmented DTI acquisition can be used for robust distortion correction without blurring effects. In addition this approach offers the advantage to reduce artifacts from partial Fourier (PF) acquisitions due to better data distribution in k-space. In combination with the MUSE approach, this promising technique is applied to whole brain DTI with a resolution of 1mm isotropic.

3967 Computer 18

Comparison of R2* and B0 Field in 2D and 3D Ferumoxytol-Enhanced Chemical Shift-Encoded MRI of the Healthy Rhesus Placenta

Ante Zhu[1,2], Ann Shimakawa[3], Sydney Nguyen[4], Kevin M. Johnson[2,5], Ian M. Bird[4], Ted Golos[4,6,7], Sean B. Fain[1,2,5], Dinesh M. Shah[6], Oliver Wieben[2,5], Scott B. Reeder[1,2,5,8,9], and Diego Hernando[2,5]

[1]Biomedical Engineering, University of Wisconsin-Madison, Madison, WI, United States, [2]Radiology, University of Wisconsin-Madison, Madison, WI, United States, [3]Global MR Applications and Workflow, GE Healthcare, Menlo Park, CA, United States, [4]Comparative Biosciences, University of Wisconsin-Madison, Madison, WI, United States, [5]Medical Physics, University of Wisconsin-Madison, Madison, WI, United States, [6]Obstetrics and Gynecology, University of Wisconsin-Madison, Madison, WI, United States, [7]Wisconsin National Primate Research Center, University of Wisconsin-Madison, Madison, WI, United States, [8]Medicine, University of Wisconsin-Madison, Madison, WI, United States, [9]Emergency Medicine, University of Wisconsin-Madison, Madison, WI, United States

A motion-robust 2D sequential chemical shift-encoded MRI (CSE-MRI) technique with a short temporal footprint for each slice is investigated for ferumoxytol-enhanced MRI of placental inflammation. In this study, the proposed 2D technique was compared with the reference 3D-CSE-MRI technique in healthy pregnant rhesus, which were anesthetized eliminating fetal motion. B0 field map boundary measurements, as well as R2* measurements in the placenta were compared across the two techniques to assess the accuracy of the 2D technique. High correlations between the measurements from 2D-CSE-MRI and 3D-CSE-MRI were demonstrated and thus provide promise for motion-robust imaging of human placental inflammation.

3968 Computer 19

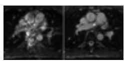

Improved Pulmonary Artery Non-Contrast Balanced Steady State Free Precession MR Imaging using Golden Angle Radial versus Cartesian Sampling

Alexander Fyrdahl[1,2], Roberto Vargas Paris[3,4], Sven Nyrén[1,4], Karen Holst[1,2], Magnus Båth[5,6], Martin Ugander[1,2], Peter Lindholm[3,4], and Andreas Sigfridsson[1,2]

[1]Department of Molecular Medicine and Surgery, Karolinska Institutet, Stockholm, Sweden, [2]Department of Clinical Physiology, Karolinska University Hospital, Stockholm, Sweden, [3]Department of Physiology and Pharmacology, Karolinska Institutet, Stockholm, Sweden, [4]Department of Radiology, Karolinska University Hospital, Stockholm, Sweden, [5]Department of Medical Physics and Biomedical Engineering, Sahlgrenska University Hospital, Gothenburg, Sweden, [6]Department of Radiation Physics, The Sahlgrenska Academy at University of Gothenburg, Gothenburg, Sweden

Free-breathing steady-state free precession MRI has shown promising results for pulmonary embolism diagnosis in preliminary studies. However, the acquisition is susceptible to artifacts from cardiorespiratory motion and flow. We propose a Golden Angle radial trajectory and show increased robustness to such artifacts in healthy volunteers, while providing added benefits such as sliding window reconstructions with higher temporal resolution than what is achievable by Cartesian sampling.

3969 Computer 20

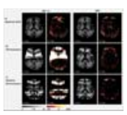

Evaluation of phase-cycled bSSFP for qMT mapping in the brain in off-resonance conditions

Nicholas G Dowell[1], Nathan Evans[2], and Mara Cercignani[1]

[1]CISC, BSMS, Brighton, United Kingdom, [2]Physics, University of Sussex, Brighton, United Kingdom

The balanced steady-state free precession acquisition approach is well-suited to quantitative magnetization transfer studies, owing to intrinsic MT weighting, rapid acquisition times and good SNR. However, the presence of off-resonance banding artefacts have limited its use, especially at B0>1.5T. This work is the first to evaluate a phase-cycled approach to bSSFP that can remove banding artefacts by taking maximum intensity projection MIP or taking a weighted mean as part of the qMT analysis. We conclude that neither MIP and weighted mean alone are capable of fully removing banding artefacts from qMT maps.

3970 Computer 21

Field-of-View Packing and k-Space Fast Sampling

Yudong Zhu[1]

[1]Zhu Consulting, Scarsdale, NY, United States

By natural or artificial arrangement, excited spins may cluster in discrete areas of a multi-dimensional image-space. By leveraging gaps in-between, one may under-sample k-space while preserving the ability to map the spin distribution. FOV-packing is a new technology that maximizes efficiency mapping gapped distribution (spatially, spectrally and etc.) and extends reach. When applied to simultaneous multi-slice MRI, it leads to a unique technique that is speedy (due to sampling of image space and acceleration of encoding), with $\sqrt{N}$ SNR scaling (due to volumetric encoding's noise averaging effect) and super-resolution capability (due to FOV packing and the option of resolving sub-slices).

3971 Computer 22

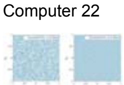

Density Optimized Low-Discrepancy k-Space Trajectory for Accelerated Single-Point Imaging

Tobias Speidel[1] and Volker Rasche[2]

[1]Core Facility Small Animal Imaging, University of Ulm, Ulm, Germany, [2]Department of Internal Medicine II, University of Ulm, Ulm, Germany

Single-point imaging (SPI) methods are a rarely discussed topic due to the related long acquisition times. However, single-point imaging sequences provide a powerful tool for the suppression of susceptibility and chemical shift artefacts. Additionally, single-point imaging methods exhibit the intrinsic possibility of arbitrary sampling, which makes them predestinated for the combination with imaging acceleration methods, such as Compressed Sensing as a type of non-linear optimization. In this work, we present a three-dimensional spherical SPI quasi-random MRI trajectory, generated using low-discrepancy algorithms with density-optimized centre-oversampling, capable of high undersampling and metal-artefact suppression.

3972 Computer 23

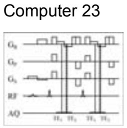

3D Dual-Echo Dixon Turbo Spin Echo Imaging of the Spine using Compressed Sensing

Holger Eggers[1], Xinzeng Wang[2], Christian Stehning[3], Ananth J Madhuranthakam[2], and Peter Börnert[1,4]

[1]Philips Research, Hamburg, Germany, [2]UT Southwestern Medical Center, Dallas, TX, United States, [3]Philips Healthcare, Hamburg, Germany, [4]Leiden University Medical Center, Leiden, Netherlands

The acceptance of 3D TSE sequences in spine imaging has been low up to now, mainly because of their long scan times. In this work, their acceleration by a combination of compressed sensing and parallel imaging was investigated. Moreover, their extension by an integration of chemical shift encoding was explored to obtain two contrasts simultaneously. For this purpose, a 3D dual-echo Dixon TSE sequence was implemented and evaluated in T_2-weighted imaging of the lumbar spine.

3973 Computer 24

B0 Mapping of Highly Inhomogeneous Fields using Missing-Pulse Steady-State Free Precession (MP-SSFP)

Naoharu Kobayashi[1], Djaudat Idiyatullin[1], Gregor Adriany[1], and Michael Garwood[1]

[1]Center for Magnetic Resonance Research,Department of Radiology, University of Minnesota, Minneapolis, MN, United States

A B_0 mapping of highly inhomogeneous fields is introduced. The method acquires refocused echo signals generated by a missing-pulse steady-state free precession (MP-SSFP) sequence with three-dimensional phase-encoding gradients. A B_0 map is calculated from the refocusing and dephasing of spin phase around the echo centers. Validation was performed in a phantom experiment conducted with a permanently inhomogeneous field produced by mounting a head gradient coil at 36 cm out of the isocenter of a 90-cm 4T magnet. Using the measured B_0 field map, we demonstrate correction of image distortion caused by the extremely nonlinear inhomogeneous B_0 field.

Electronic Poster

Artificial Intelligence & Machine Learning

Exhibition Hall Tuesday 9:15 - 10:15

3974 Computer 25

summa cum laude

Cascaded Convolutional Neural Network (CNN) for Reconstruction of Undersampled Magnetic Resonance (MR) Images

Taejoon Eo[1], Yohan Jun[1], Taeseong Kim[1], Jinseong Jang[1], and Dosik Hwang[1]

[1]Yonsei University, Seoul, Korea, Republic of

We propose cascaded CNN operating on k-space and image domain alternatively for reconstruction of undersampled MR images. Our cascaded CNN is capable of restoring most of detailed structures in the full-sampled image while sufficiently removing undersampling artifacts.

3975 Computer 26

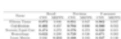

In-vivo Segmentation of Carotid Plaque MRI with Deep Convolutional Neural Networks

Yuxi Dong[1], Yuchao Pan[1], Rui Li[2], and Wei Xu[1]

[1]Institute for Interdisciplinary Information Sciences, Tsinghua University, Beijing, People's Republic of China, [2]Center for Biomedical Imaging Research, Tsinghua University, Beijing, People's Republic of China

MRI is gaining popularity for identifying atherosclerosis, a common disease caused by the accumulation of cholesterol in arteries. To identify vulnerable plaque, the components in plaque need to be segmented by radiologist manually, which is both hard and tedious. Previous attempts to solve the problem using probability maps are limited by their accuracy. We leverage the recently developed convolutional neural networks (CNN) to build a model based on 1,000 subjects automatically, achieving significantly better accuracy in almost every metric over traditional methods.

3976 Computer 27

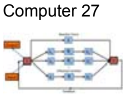

Deep network training based sparsity model for reconstruction

Jiahao Lin[1,2], Stamatios Lefkimmiatis[3], and Kyunghyun Sung[2]

[1]Electrical Engineering, University of California, Los Angeles, Los Angeles, CA, United States, [2]Radiology, University of California, Los Angeles, Los Angeles, CA, United States, [3]Skolkovo Institute of Science and Technology, Moscow, Russian Federation

One challenge for MR reconstruction is to heuristically select the appropriate regularizer for the optimization problem. This abstract proposes a novel deep learning based reconstruction approach for accelerated MR imaging. With the training using clinical MR images and their retrospectively undersampled noisy images, this algorithm learns the specific parameters of a general regularizer for the optimization problem, and uses this regularizer in the iterative reconstruction to achieves high image quality with high acceleration factors.

3977 Computer 28

Super resolution reconstruction in MRI by deep convolutional neural networks

zhengchao dong[1] and hong Wang[2]

[1]1. Columbia University, New York, NY, United States 2. New York State Psychiatric institute, New York, NY, United States, NY, United States, [2]1. Columbia University, New York, NY, United States 2. School of Science,Tianjin University, Tianjin, People's Republic of China

The sparse-representation-based super resolution is an efficient learning-based method. This method involves two key steps. One is to learn two dictionaries for low/high-resolution image patches, and the other is to learn a mapping between low resolution example patches and their corresponding high resolution patches from massive external images. We presented a super resolution method for MRI from reduced k-space acquisition sequences via deep convolutional neural networks. The proposed method directly learns an end-to-end mapping between the low/high-resolution images.Our proposed method is tested on the OpenfMRI database. It significantly outperforms the zero-filled reconstruction and an existing learning-based MRI SR method.

3978 Computer 29

Deep Learning Feature Classification for Predicting Treatment Decision: A Preliminary Study on Prostate Cancer Patients

Hansang Lee[1] and Junmo Kim[1]

[1]*School of Electrical Engineering, KAIST, Daejeon, Korea, Republic of*

We investigated the novel problem of predicting treatment decision for cancer patients using imaging feature analysis. We implemented deep learning feature classification framework consisting of feature computation with deep convolutional neural network (CNN) model and k-nearest neighbor (kNN) feature classification. The preliminary study on TCIA prostate cancer T2 MRI database showed the promising results and the potential of future researches.

3979 Computer 30

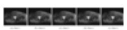

Automated reference-free assessment of MR image quality using an active learning approach: Comparison of Support Vector Machine versus Deep Neural Network classification.

Sergios Gatidis[1], Annika Liebgott[1], Martin Schwartz[1], Petros Martirosian[1], Fritz Schick[1], Konstantin Nikolaou[1], Bin Yang[2], and Thomas Küstner[1,2]

[1]*Department of Radiology, University of Tuebingen, Tuebingen, Germany,* [2]*Institute of Signal Processing and System Theory, University of Stuttgart*

In this study we compare the performance of Support Vector Machine (SVM)-based and Deep Neural Network (DNN)-based active learning for automated assessment of MR image quality. MR images were labeled by radiologists concerning perceived image quality and used as training and test data. DNN and SVM were trained to classify image quality on the training data. An active learning scheme was used for optimization of the training procedure. We found that using acitve learning with either SVM- or DNN- based classification allows for accurate and efficient automated assessment of MR image quality.

3980 Computer 31

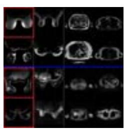

Fat/Water Classification Using a Supervised Neural Network

Anne Menini[1], Kang Wang[2], Zachary W. Slavens[3], and Christopher J. Hardy[4]

[1]*GE Global Research, Munich, Germany,* [2]*Global MR Applications & Workflow, GE Healthcare, Madison, WI, United States,* [3]*GE Healthcare, Waukesha, WI, United States,* [4]*GE Global Research, Niskayuna, NY, United States*

Fat/Water classification methods relying on image intensity histograms or hydrogen chemical-shift spectra can be subject to failure when assumptions in the algorithm are not met. In this study, we propose a new classification method based entirely on machine learning. Different neural network types were trained and tested on databases covering various anatomies, RF-coil types and image contrasts. A 2D paired classification using a fully connected neural network was capable of reliably classifying fat versus water with an accuracy of 100% on test data sets different from the training data, with a clinically relevant processing time of 0.05 s per case.

3981 Computer 32

Classification of Head Movements Inside an MRI Scanner using a Single Marker and Neural Networks

Aditya Singh[1], Brian Keating[1], Sara Hayama[1], Michael Herbst[1], and Thomas Ernst[1]

[1]*JABSOM, University of Hawaii, Honolulu, HI, United States*

Detection and classification of head motion may be required for optimal application of prospective motion correction techniques for brain imaging using external tracking systems. Supervised neural networks using various motion metrics were designed to classify head motion inside MR scanner into rigid-body motion and skin motion using single-marker 6-DOF information. The neural networks were trained using volunteer data and then applied to head motion data from 6 clinical in-patients. Neural networks could consistently achieve overall accuracy of 75% or greater.

3982 Computer 33

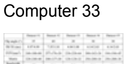

Artificial Neural Network for Suppression of Banding Artifacts in Balanced Steady-State Free Precession MRI

Ki Hwan Kim[1,2] and Sung-Hong Park[1,2]

[1]*Department of Bio and Brain Engineering, Korea Advanced Institute of Science and Technology (KAIST), Daejeon, Korea, Republic of,* [2]*Graduate School of Medical Science and Engineering, Korea Advanced Institute of Science and Technology (KAIST), Daejeon, Korea, Republic of*

This study is the first attempt for a learning-based algorithm to be applied to banding artifact suppression in balanced steady-state free precession (bSSFP). We trained multilayer perceptron (MLP) models with two or four phase−cycling datasets and banding-free datasets as inputs and outputs, respectively. We demonstrated that MLP was superior to existing methods in terms of banding artifact suppression and SNR efficiency, which was clearer in two phase−cycling datasets. Furthermore, MLP was widely applicable to various image sets, irrespective of scan parameters, body organs, and field strengths. The learning-based approach is promising for banding artifact suppression of bSSFP.

3983 Computer 34

Boosting SNR and/or Resolution of Arterial Spin Label (ASL) imaging using Multi-contrast Approaches with Multi-lateral Guided Filter and Deep Networks

Enhao Gong[1], John Pauly[1], and Greg Zaharchuk[2]

[1]*Electrical Engineering, Stanford University, Stanford, CA, United States,* [2]*Radiology, Stanford University, Stanford, CA, United States*

Arterial Spin Labeling (ASL) MRI is a powerful neuro imaging tool which provides quantitative perfusion maps. However, ASL perfusion maps typically suffer from low SNR and resolution. Averaging from multiple scans (high Nex value) can improve the SNR but at the cost of significantly increased acquisition time. In the work we proposed a technique for improved ASL image quality with boosted SNR and/or resolution by 1) incorporating the information of multi-contrast images 2) using nonlinear, non-local, spatial variant multi-lateral filtering, 3) training a deep network model to adaptively tune the final denoising level and further boost the SNR and improve image quality. Various in-vivo experiments demonstrate the superior performance of the proposed method which will significantly accelerate ASL acquisition and improve image quality.

3984 Computer 35

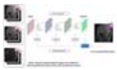

Undersampling trajectory design for fast MRI with super-resolution convolutional neural network

Shanshan Wang[1], Taohui Xiao[1,2], Sha Tan[1,3], Yuanyuan Liu[1], Leslie Ying[4], and Dong Liang[1]

[1]Paul C. Lauterbur Research Center for Biomedical Imaging, SIAT, Chinese Academy of Sciences, Shenzhen, People's Republic of China, [2]School of Physics and Optoelectronics, Xiangtan University, Xiangtan, People's Republic of China, [3]School of Information Engineering, Guangdong University of Technology, Guangzhou, People's Republic of China, [4]Department of Biomedical Engineering and Department of Electrical Engineering, The State University of New York, NY, United States

Deep learning based fast MR imaging (DeepLearnMRI) has been an appealing new research direction, which utilizes networks to draw valuable prior information from enormous existing high-quality MR images and then assists accurate MR image reconstruction from undersampled data. This paper explores optimal undersampling trajectory for DeepLearnMRI. Specifically, we designed hamming filtered asymmetrical 1D partial Fourier sampling scheme for fast MR imaging with our developed super-resolution convolutional neural network. Experimental results on in vivo dataset show that the proposed scheme allows DeepLearnMRI to reconstruct more accurate MR images with less time compared to the Classical GRAPPA and SPIRiT.

3985 Computer 36

Feasibility of Multi-contrast MR imaging via deep learning

Shanshan Wang[1], Tao Zhao[1,2], Ningbo Huang[1,3], Sha Tan[1,4], Yuanyuan Liu[1], Leslie Ying[5], and Dong Liang[1]

[1]Paul C. Lauterbur Research Center for Biomedical Imaging, SIAT, Chinese Academy of Sciences, Shenzhen, People's Republic of China, [2]College of Mining and Safety Engineering, Shandong University of Science and Technology, Qingdao, People's Republic of China, [3]School of Computer Science and Technology, Changchun University of Science and Technology, Changchun, People's Republic of China, [4]School of Information Engineering, Guangdong University of Technology, Guangzhou, People's Republic of China, [5]Department of Biomedical Engineering and Department of Electrical Engineering, The State University of New York, NY, United States

This paper develops a deep learning based multi-contrast MR imaging method. Unlike existing methods which mainly draw prior information from the target structure or a few reference images, we design a multi-contrast convolutional neural network to draw automatic feature descriptors for describing the multi-contrast correlations and identify the nonlinear mapping with the utilization of enormous existing multi-contrast MR images as training samples. Once the network is learned, it performs as a predicator for the online multi-contrast MR imaging. Experimental results on multi-contrast in vivo dataset show that the proposed method could restore lost information from the undersampled MR images while keeping their contrasts.

3986 Computer 37

Automatic Segmentation of MR Images of the Proximal Femur Using Deep Learning

Spencer Hallyburton[1,2], Gregory Chang[3], Stephen Honig[4], Kyunghyun Cho[5], and Cem M Deniz[1,6]

[1]Department of Radiology, Center for Advanced Imaging Innovation and Research (CAI2R) and Bernard and Irene Schwartz Center for Biomedical Imaging, New York University Langone Medical Center, New York, NY, United States, [2]Harvard College, Cambridge, MA, United States, [3]Department of Radiology, Center for Musculoskeletal Care, New York University Langone Medical Center, New York, NY, United States, [4]Osteoporosis Center, Hospital for Joint Diseases, New York University Langone Medical Center, New York, NY, United States, [5]Courant Institute of Mathematical Science & Centre for Data Science, New York University, New York, NY, United States, [6]The Sackler Institute of Graduate Biomedical Sciences, New York University School of Medicine, New York, NY, United States

Magnetic resonance imaging (MRI) of bones has added value for fracture risk assessment in osteoporosis, a disease of weak bones. However, manual segmentation of bone images is time-intensive, causing slow throughput for test results and inefficient risk assessment for patients. In this work, we implemented an automatic proximal femur segmentation algorithm by modeling a convolutional neural network (CNN) as a pixel-wise binary classification. The accuracy of automatic segmentation was investigated by analyzing similarity between automatic and manual ground-truth segmentation. In addition, we compared the time required for manual fine-tuning of the CNN segmentation with original manual segmentation.

3987 Computer 38

Performance comparison of artificial neural network and fuzzy deep learning algorithms for respiratory motion prediction in pseudocontinuous arterial spin labeling of the abdomen

H Michael Gach[1], Hao Song[2], Seonyeong Park[3], Yuichi Motai[3], Dan Ruan[4], Wenyang Liu[4], V Andrew Stenger[5], Rolf Pohmann[6], and Jingqin Luo[7]

[1]Radiation Oncology and Radiology, Washington University in St Louis, St Louis, MO, United States, [2]Imaging Physics, The University of Texas MD Anderson Cancer Center, Houston, TX, United States, [3]Electrical and Computer Engineering, Virginia Commonwealth University, Richmond, VA, United States, [4]Radiation Oncology, University of California Los Angeles, Los Angeles, CA, United States, [5]Medicine, University of Hawai'i at Manoa, Honolulu, HI, United States, [6]High-Field Magnetic Resonance Center, Max Planck Institute for Biological Cybernetics, Tubingen, Germany, [7]Biostatistics and Medicine, Washington University in St Louis, St Louis, MO, United States

Subtraction-based imaging methods like pseudocontinuous arterial spin labeling (pCASL) in the body are challenging due to physiological motion. Respiratory motion prediction (RMP) using an artificial neural network (ANN) and pencil beam navigators was previously integrated into a pCASL sequence to permit free-breathing perfusion MRI of the kidney. In an effort to improve the accuracy of the RMP, we compared the performance of a promising fuzzy deep learning (FDL) algorithm with ANN using navigator-echo displacements recorded from 8 volunteers during pCASL. FDL combines ANN with fuzzy logic. However, the ANN performance was significantly better than FDL for the pCASL application.

3988 Computer 39

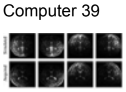

A Study of Simulated Training Data for Image Reconstruction from Subsampled MR Data using Artificial Neural Network

kinam kwon[1], Jaejin Cho[1], Seohee So[1], Byungjai Kim[1], Yoonmee Lee[1], kyungtak Min[1], and HyunWook Park[1]

[1]KAIST, Daejeon, Korea, Republic of

Recently, several works have applied the deep learning technique to medical imaging problems such as lesion classification and image reconstruction. The deep learning techniques have advantages of learning from big data, however, in medical imaging, collecting an amount of training data is not easy because of expense, privacy, and so on. Strategies to supplement insufficient training data are important topics for applying deep learning to medical imaging field. In this study, training data are generated from the simulated images and the acquired MR images, which are utilized to learn the architecture of multilayer perceptron to reduce imaging time.

3989 Computer 40

Robust and Efficient Dictionary Matching in Magnetic Resonance Fingerprinting with Neural Networks

Daniel Truhn[1], Christoph Haarburger[2], Volkmar Schulz[3], Dorit Merhof[2], and Christiane Kuhl[1]

[1]Radiology, University Hospital Aachen, Aachen, Germany, [2]Institute of Imaging and Computer Vision, [3]Physics of Molecular Imaging Systems

We implemented efficient and robust matching of signals acquired in magnetic resonance fingerprinting by use of neural networks and show its superiority in terms of speed and robustness to noise.

3990 Computer 41

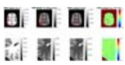

Deep Mapping: Using deep convolutional neural networks to estimate quantitative T1 maps trained on a 7 T minimum deformation average model

Steffen Bollmann[1], Andrew Janke[1], and Markus Barth[1]

[1]Centre for Advanced Imaging, University of Queensland, Brisbane, Australia

Deep convolutional neural networks are increasingly being used to solve challenging medical image processing tasks. The acquisition of high resolution quantitative parameter maps in MRI, such as T1 and quantitative susceptibility maps often require long or additional acquisitions and post-processing steps. We therefore trained a convolutional neural network on a minimum deformation model of MP2RAGE data acquired at 7 T and show the feasibility of computing T1 maps from single subject data.

3991 Computer 42

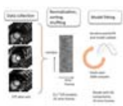

Dynamic cardiac MR image reconstruction models using machine learning on large training data sets

Johannes Schmidt[1] and Sebastian Kozerke[1]

[1]University and ETH Zurich, Zurich, Switzerland

An online learning algorithm is used to derive a generic model for dynamic cardiac MR data from a large set of training data. Image quality of reconstructed data could be improved and smoothing in time domain reduced.

3992 Computer 43

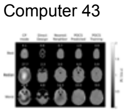

SAR-Efficient RF Shim Prediction via Machine Learning

Julianna D. Ianni[1,2], Zhipeng Cao[1,2], and William A. Grissom[1,2,3,4]

[1]Department of Biomedical Engineering, Vanderbilt University, Nashville, TN, United States, [2]Vanderbilt University Institute of Imaging Science, Vanderbilt University, Nashville, TN, United States, [3]Department of Radiology, Vanderbilt University, Nashville, TN, United States, [4]Department of Electrical Engineering, Vanderbilt University, Nashville, TN, United States

A method is presented for prediction of patient-tailored, SAR-efficient RF shims via machine learning. An iterative training scheme allows fast prediction of SAR-efficient shims for new head phantoms using little B_1^+ map data.

3993 Computer 44

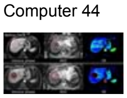

Machine-learning-based treatment response stratification for trans-arterial chemoembolization in HCC patients.

Atilla Peter Kiraly[1], Robert Grimm[2], Mounes Aliyari Ghasebeh[3], Li Pan[4], David Liu[1], Berthold Kiefer[2], and Ihab Roushdy Kamel[3]

[1]Medical Imaging Technologies, Siemens Medical Solutions USA, Princeton, NJ, United States, [2]MR Application Predevelopment, Siemens Healthcare, Erlangen, Germany, [3]The Russell H. Morgan Department of Radiology and Radiological Sciences, Johns Hopkins University School of Medicine, Baltimore, MD, United States, [4]Siemens Healthcare, Baltimore, MD, United States

In determining the effectiveness of chemoembolization in HCC, functional MRI has been shown to differentiate responders and non-responders earlier than anatomical measurements such as RECIST or EASL criteria. In previous studies, multiparametric response criteria based on thresholds of changes in ADC and venous enhancement (VE) intensities were proposed. We present improved stratification based on machine learning and image-based features. On a set of 57 chemoembolization patients, the proposed approach achieved a mean classification accuracy of 84% versus 66% for the previous threshold-based approach. These results further demonstrate the incremental value of functional MRI over traditional anatomical measures.

3994 Computer 45

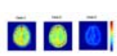

A Machine Learning Based Approach for Fast T1 estimation with Improved Accuracy

Anirban Sengupta[1], Rakesh Kumar Gupta[2], Sumeet Agarwal[3], and Anup Singh[4]

[1]CBME, IIT Delhi, New Delhi, India, [2]Radiology Department, FORTIS hospital,Gurgaon, India, [3]Electrical Engineering, IIT Delhi, India, [4]Centre for Biomedical Engineering, IIT Delhi; AIIMS Delhi, New Delhi, India

The purpose of this study is to propose a fast T1 estimation method with improved accuracy over existing approaches in a Multiple Flip Angle setting. A supervised machine learning based approach has been proposed that can be used to predict additional Flip Angle data using limited available Flip Angle data, thereby producing more accurate T1 estimation in reduced scan time. Both experimental as well as simulation results are shown to illustrate the efficacy of this approach. The accuracy of T1 estimation depends on the choice of Flip Angle data to be predicted.

3995 Computer 46

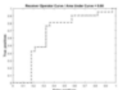

Semi-Automated Assessment for Distinguishing Glioblastoma and Solitary Brain Metastasis: A Machine Learning Approach

Nathaniel Swinburne[1], Javin Schefflein[1], Yu Sakai[2], Iris Chen[2], Ehsan Tadayon[2], and Kambiz Nael[1]

[1]Department of Radiology, Mount Sinai Medical Center, New York, NY, United States, [2]Mount Sinai Medical Center, New York, NY, United States

Although machine learning applications for non-medical imaging are well-established, its use in radiologic imaging interpretation remains nascent. We trained a support vector machine using advanced MR imaging to differentiate glioblastoma and brain metastasis with 72.6% balanced accuracy. The ability for machine learning to aid radiologists in differentiating pathologies with similar appearance on conventional imaging appears promising.

3996 Computer 47

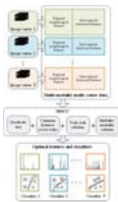

A Novel Multi-Center Classification Method for ASD Diagnosis via Sparse Multi-Modality Multi-Task Learning

Jun Wang[1,2], Qian Wang[3], Jialin Peng[1], Dong Nie[1], Feng Zhao[1], Chong-Yaw Wee[4], Shitong Wang[2], and Dinggang Shen[1]

[1]Department of Radiology and Biomedical Research Imaging Center, University of North Carolina at Chapel Hill, Chapel Hill, NC, United States, [2]School of Digital Media, Jiangnan University, Wuxi, People's Republic of China, [3]Med-X Research Institute, School of Biomedical Engineering, Shanghai Jiao Tong University, Shanghai, People's Republic of China, [4]Department of Biomedical Engineering, Faculty of Engineering, National University of Singapore, Singapore

Multi-task classification targeting multi-center ASD diagnosis is not well investigated yet. Taking advantages of the Autism Brain Imaging Data Exchange (ABIDE) database, we propose a novel multi-modality multi-center classification (M3CC) method for accurate ASD diagnosis. We formulate the diagnosis into a multi-task learning problem, as each task corresponds to the classification of the subjects of one center. Our comprehensive experiments show that, by incorporating multi-modality neuroimaging data and handling multiple centers jointly, the performance of computer-assisted ASD diagnosis is increased significantly.

3997 Computer 48

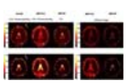

Application of Random Forest Regression for Fast and Robust MRF Dictionary Matching

Shivaprasad Ashok Chikop[1], Vimal Chandran[2], Imam Shaik[1], Mauricio Antonio Reyes Aguirre[2], and Sairam Geethanath[1]

[1]Medical Imaging Research Centre, Dayananda Sagar Institutions, Bangalore, India, [2]Institute of Surgical Technology and Biomechanics, University of Bern, Bern, Switzerland

Magnetic Resonance Fingerprinting (MRF) provides for simultaneous generation of MR multi-parametric maps from a single acquisition. In this work, a machine learning based regression method that does not require a dictionary has been demonstrated. A leave-one-out evaluation strategy was employed for numerical evaluation of the proposed MRF-RF approach. A comparative study was performed on two previously employed matching methods. Results depict that proposed MRF-RF method produces maps similar to the vector dot product approach, with a 10-fold saving in time. The method can also be extended to other non-linear maps such as B0 inhomogeneity, diffusion maps, and perfusion maps.

Electronic Poster

Non-Cartesian

Exhibition Hall — Tuesday 9:15 - 10:15

3998 Computer 49

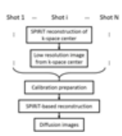

High-Resolution DWI Using Multishot Variable Density Spiral with SPIRiT-Based Reconstruction

Zijing Dong[1], Xiaodong Ma[1], Fuyixue Wang[1,2], Chun Yuan[1,3], and Hua Guo[1]

[1]Center for Biomedical Imaging Research, Department of Biomedical Engineering, School of Medicine, Tsinghua University, Beijing, People's Republic of China, [2]Harvard-MIT Health Sciences and Technology, MIT, Cambridge, MA, United States, [3]Vascular Imaging Laboratory, Department of Radiology, University of Washington, Seattle, WA, United States

Multishot variable density spiral is an efficient sequence for diffusion imaging with the oversampled k-space center serving as a navigator. However, the shot-to-shot phase variation of multishot acquisition due to motion must be corrected. To improve the reconstruction accuracy, we propose a novel reconstruction framework using SPIRiT-based reconstruction, integrating the information of phase variation and coil sensitivity in order to correct for the ghosting artifacts of multi-shot DWI. Both simulation and in-vivo experiment validated the superior performance of the proposed method to reconstruct more accurate images than CG-SENSE for VDS DWI.

3999 Computer 50

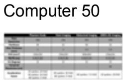

Golden-Ratio Rotated Stack-of-Stars Acquisition for Improved Volumetric MRI

Ziwu Zhou[1], Fei Han[1], Lirong Yan[2], Danny J.J. Wang[2], and Peng Hu[1]

[1]Radiological Sciences, University of California, Los Angeles, Los Angeles, CA, United States, [2]Neurology, University of Southern California, Los Angeles, CA, United States

In this abstract, we developed and evaluated an improved stack-of-stars (SOS) sampling strategy that can efficiently sample 3D k-space and reduce streaking artifacts. Compared with conventional SOS sampling strategies that collect the same radial angle for every slice, proposed method rotates the spokes in a golden-angle manner along the slice direction, which modifies the aliasing pattern resulted from k-space under-sampling. With either gridding reconstruction or more advanced methods, proposed rotated SOS sampling strategy provides improved image quality with reduced streaking artifacts and better delineation of fine structures.

4000 Computer 51

a-f SPARSE: Radial Extension to k-t SPARSE

Madison Kretzler[1], Jesse Hamilton[2], Mark Griswold[1,2,3], and Nicole Seiberlich[1,2,3]

[1]Electrical Engineering, Case Western Reserve University, Cleveland, OH, United States, [2]Biomedical Engineering, Case Western Reserve University, Cleveland, OH, [3]Radiology, University Hospitals, Cleveland, OH

a-f SPARSE is a new technique which enables the k-t SPARSE approach to be used for radial trajectories in the Radon domain. Its use for cardiac imaging retrospectively accelerated by a factor of 4 is presented.

4001 Computer 52

Unstreaking: Radial MRI with Automatic Streaking Artifact Reduction

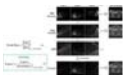

Li Feng[1], Hersh Chandarana[1], Daniel K Sodickson[1], and Ricardo Otazo[1]

[1]Center for Advanced Imaging Innovation and Research (CAI2R), New York University School of Medicine, New York, NY, United States

Streaking artifact is one of the major causes of image quality degradation in radial MRI. Since multicoil arrays are widely used in modern MR scanners, an easy way to reduce streaking artifacts is to identify coil elements that are contaminated by a high level of streaks, and then exclude them from image reconstruction. However, such an approach requires accurate clustering algorithms to automatically select unwanted coil elements. In this work, a method called “Unstreaking” is proposed for automatic streaking artifact reduction without the need to exclude coil elements. The method was tested for accelerated radial DCE-MRI of the liver.

4002 Computer 53

Rapid Non-Cartesian Regularized SENSE Reconstruction using a Point Spread Function Model

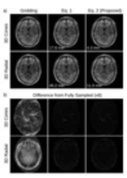

Corey A Baron[1], Nicholas Dwork[1], John M Pauly[1], and Dwight G Nishimura[1]

[1]Stanford University, Stanford, CA, United States

Iterative reconstructions of undersampled non-Cartesian data are computationally expensive because non-Cartesian Fourier transforms are much less efficient than Cartesian Fast Fourier Transforms. Here, we introduce an algorithm that does not require non-uniform Fourier transforms during optimization iterations, resulting in large reductions in computation times with no impairment of image quality.

4003 Computer 54

Rapid Two-Step 2D Filtered Backprojection for 3D radial-data reconstruction: Comparison of computatonal times with conventional methods

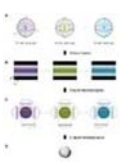

JeongTaek Lee[1,2], Seung-Kyun Lee[1,2], Jinil Park[1,2], and Jang-Yeon Park[1,2]

[1]Center for Neuroscience Imaging Research, Institute for Basic Science (IBS), Suwon, Korea, Republic of, [2]Department of Biomedical Engineering, Sungkyunkwan University (SKKU), Suwon, Korea, Republic of

3D-FFT via gridding is generally recognized as computationally faster than direct 3D filtered backprojection (FBP) in 3D radial-data reconstruction. To overcome the computational time issue of 3D-FBP, we investigated two-step 2D-FBP reconstruction having an alternative k-space trajectory. Computational requirements were theoretically analyzed to permit clear comparison among three reconstruction methods and computational burdens based on mathematical expressions were compared to actual computation times. In conclusion, two-step FBP provides considerable computational speed benefit over direct 3D-FBP and, under certain realistic conditions (e.g., with many channels), even over 3D-FFT, while showing almost same image quality in phantom and brain imaging.

4004 Computer 55

Comparison of Sequential and Joint Methods for Spiral Water-fat Separation and Deblurring

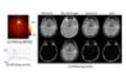

Dinghui Wang[1] and James G. Pipe[1]

[1]Imaging research, Barrow Neurological Institute, Phoenix, AZ, United States

Most previous approaches to spiral water-fat imaging perform the water-fat separation and deblurring sequentially based on the assumption that the phase accumulation and blurring are separable. A joint water-fat separation and deblurring method has been recently proposed using more accurate signal models. In this study, the sequential and joint methods are quantitatively compared. Simulation and experiments have demonstrated that the results of the joint method are significantly better in regions where the field inhomogeneity changes rapidly in space. The loss of signal-to-noise-ratio is minor for both approaches at optimal TEs when the noise in the field map $\Delta f0$ is negligible.

4005 Computer 56

Improved reconstruction of free breathing abdominal imaging using non-Cartesian iterative reconstruction and elastic image registration

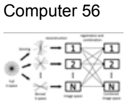

Jan Hendrik Wülbern[1], Mariya Doneva[1], Sven Kabus[1], and Peter Börnert[1]

[1]Philips Research Europe, Hamburg, Germany

Stack-of stars k-space trajectories following the golden angle scheme allow retrospective binning and reconstruction of data acquired from free-breathing patients, which is of particular interest in abdominal applications. Here we demonstrate that using an iterative non-Cartesian reconstruction in combination with an elastic registration algorithm produces images with high image quality for all motion states, regardless of the degree of under-sampling in the reference motion state.

4006 Computer 57

Rapid 3D imaging with multiplanar spirals

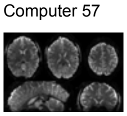

Maria Engel[1], Lars Kasper[1], and Klaas Paul Pruessmann[1]

[1]ETH, Zürich, Switzerland

Rapid 3D acquisition with long spiral readouts is enabled by multiplanar undersampling, array detection and an expanded signal model including off-resonance. Whole brain coverage with 1.5 mm isotropic resolution is achieved in 3.1 s.

4007 Computer 58

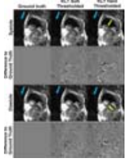

Automatic truncation of the Principal Component Analysis for improved image quality in radial cardiac real-time imaging

André Fischer[1,2], Peng Lai[3], and El-Sayed Ibrahim[4]

[1]GE Global Research Europe, Garching bei München, Germany, [2]Cardiac Center of Excellence, GE Healthcare, Garching bei München, Germany, [3]GE Healthcare, Menlo Park, CA, United States, [4]GE Healthcare, Waukesha, WI, United States

Radial cardiac real-time datasets are usually compromised by streaking artifacts. Truncated principal component analysis (PCA) has been proposed to remove streaking and improve apparent SNR of the images. However, a proper threshold for truncation of the PCA has to be selected to maintain good temporal fidelity. This work proposes a method for automatic truncation of the PCA and compares a soft against the standard hard thresholding approach. Results indicate that the proposed method in combination with soft thresholding offers reduced temporal blurring and streaking artifacts while improving apparent SNR.

4008 Computer 59

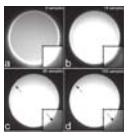

Implementation and Optimization of an Automatic k-Space Trajectory Correction for Ultrashort Echo Time Imaging

Simon Konstandin[1] and Matthias Günther[1,2]

[1]MR-Imaging and Spectroscopy, University of Bremen, Bremen, Germany, [2]Fraunhofer MEVIS, Bremen, Germany

Ultrashort echo time (UTE) sequences are usually applied for imaging of very short T_2^* tissues, for the evaluation of water content in the cortical bone and for X-nuclei imaging. The aim of this study was the implementation of an automatic calibration measurement to determine the actual k-space trajectory considering noisy data samples in UTE imaging. In contrast to most other studies, not only gradient delays were taken into account, but also gradient waveform distortions. It could be demonstrated that there exist an optimal number of samples used for correction (depending on signal-to-noise ratio) that should be determined by calibration scans.

4009 Computer 60

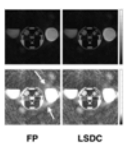

A Least Squares Optimal Density Compensation Function for Gridding

Nicholas Dwork[1], Corey Baron[1], Ethan Johnson[1], Adam B. Kerr[1], Dwight G. Nishimura[1], and John Pauly[1]

[1]Electrical Engineering, Stanford University, Stanford, CA, United States

Gridding is a relevant algorithm for both image reconstruction and pulse design. With Gridding, it is crucial to appropriately compensate for varying density of the sampling trajectory. In this paper, we present a technique to determine the weights by solving a least squares optimization problem.

4010 Computer 61

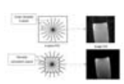

Reducing the effects of under-sampling in images acquired with a 3D radial sequence for the purposes of real-time navigation.

Leah Morgan[1], Ernesta Meintjes[1], and Andre van der Kouwe[1,2]

[1]Division of Biomedical Engineering, Department of Human Biology, University of Cape Town, Cape Town, South Africa, [2]Department of Radiology, Athinoula A. Martinos Center for Biomedical Imaging, Massachusetts General Hospital, Boston, MA, United States

Radial sequences hold great potential for real-time navigation in MRI. Navigator images can be produced off very few spokes of sampled data however, characteristic streaking artifacts appear due to under-sampling at the outer edges of the k-space field of view. In this study, a method is proposed to reconstruct navigator images with a reduced base resolution to minimize the effects of under sampling and reduce the appearance of streaking artifacts, improving the accuracy of motion-registration. The success of this method supports the pursuit of radial sequences for applications in real-time navigation.

4011 Computer 62

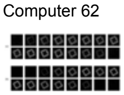

Ultrashort echo time imaging at 1.5 T using an insertable unshielded gradient coil and cone trajectories

Ayana Setoi[1] and Katsumi Kose[1]

[1]University of Tsukuba, Tsukuba, Japan

Ultrashort echo time (UTE) imaging with cone trajectories was installed to a 1.5T compact MRI system using an unshielded insertable gradient coil. K-trajectories of the 3D cone trajectory acquisition were measured using a small capillary phantom and used for image reconstruction. A LEGO block sample with T_2* of about 0.6 ms was successfully imaged with echo time of 0.05 ms to 0.6 ms. This result demonstrated that UTE imaging sequences with cone trajectories were successfully installed to our system.

4012 Computer 63

The efficacy of existing k-space correction methods for 2D golden angle radial sampling on clinical 1.5T and 3T systems

Tom Bruijnen[1], Bjorn Stemkens[1], Jan J. W. Lagendijk[1], Cornelis A. T. van den Berg[1], and Rob H. N. Tijssen[1]

[1]Center for image sciences, University Medical Center Utrecht, Utrecht, Netherlands

Golden angle radial acquisitions are sensitive to gradient imperfections leading to reduced image quality. Multiple methods are known to compensate for the zeroth and first order gradient waveform imperfections. Here we quantify the effect of these different methods on Philips 1.5T and 3T wide bore Ingenia scanners, and assess four direct correction methods on efficacy. We show that on these systems a gradient delay correction has minimal impact on the image quality, while phase correction provides a considerable improvement.

4013 Computer 64

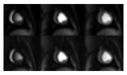

Evaluation of Rapid Radial Imaging Methods for Assessment of First Pass Myocardial Perfusion

James J Pilla[1], Gamaliel Isaac[1], Joseph H Gorman III[1], Robert C Gorman[1], and Lawrence Dougherty[1]

[1]University of Pennsylvania, Philadelphia, PA, United States

Rapid image acquisition is required to assess myocardial first-pass perfusion. K-t CS which uses compressed sensing has produced dynamic images with sufficient resolution. View sharing methods such as k-t VS could potentially provide similar results eliminating the need for regularization weights and significantly decreasing reconstruction time. K-t CS and k-t VS were investigated to determine their temporal and spatial response during first-pass myocardial perfusion. Results demonstrate that images reconstructed using each method had similar resolution and showed good correlation in assessing uptake kinetics. However, at higher acceleration, k-t CS showed increased SNR and smoother appearance while k-t VS used a less computationally intense and faster reconstruction.

4014 Computer 65

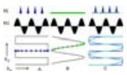

Variable-blipped-EPI (VB-EPI) for Lower Acoustic Noise and Higher Efficiency with non-Cartesian iterative Reconstruction

Patrick Liebig[1,2], Robin Martin Heidemann[2], Bernhard Hensel[1], and David Porter[3]

[1]University of Erlangen-Nuremberg, Erlangen, Germany, [2]Siemens Healthcare GmbH, [3]Fraunhofer MEVIS

Echo-Planar-Imaging[1] (EPI) with trapezoidal Readout (RO) and blipped Phase-Encoding (PE) gradients gives a high level of acoustic noise[2]. To reduce acoustic noise we suggest prolonging the duration of the blipped PE gradient in combination with a sinusoidal or trapezoidal RO gradient and continuous data sampling throughout the whole RO train. This results in a variable density sampling along PE (less dense at the edges, denser in the centre of k-space) with a non-Cartesian trajectory, where we use ESPIRiT[3] to reconstruct the data. The efficiency is improved due to continuous data sampling, resulting also in a reduced echo time.

4015 Computer 66

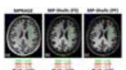

Partial Fourier Shells Trajectory with Non-Iterative Homodyne Reconstruction

Shengzhen Tao[1], Yunhong Shu[1], Joshua D Trzasko[1], Paul T Weavers[1], Erin M Gray[1], John Huston III[1], and Matt A Bernstein[1]

[1]Radiology, Mayo Clinic, Rochester, MN, United States

The 3D Shells trajectory-based MRI acquisition is a non-Cartesian acquisition technique that divides the 3D k-space into a series of concentric shells and samples each one with 3D helical readouts. Using the Shells trajectory, the inner k-space can be efficiently sampled within several interleaves, making it a maximally centric 3D acquisition. Partial Fourier (PF) acquisition is a commonly-used acceleration technique by exploiting the conjugate symmetry of k-space measurement. In this work, we present a new asymmetric 3D Shells trajectory design with PF acceleration to combine the advantages from both techniques, and develop a non-iterative homodyne reconstruction framework for it.

4016 Computer 67

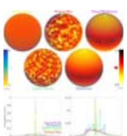

Spherical-surface Poisson disc point selection for radial-trajectory MRI

Ethan M Johnson[1], Kim Butts Pauly[2], and John M Pauly[1]

[1]Electrical Engineering, Stanford University, Stanford, CA, United States, [2]Radiology, Stanford University, Stanford, CA, United States

A design consideration for center-out ***k***-space trajectories is the angular distribution of trajectory endpoints (or equivalently, exit angles). Uniformity is desirable, but the regularity of spacing affects aliasing patterns, which can dictate undersampling performance. Here, a method for choosing points on a sphere with Poisson disc spacing is described, and its use in selecting angles for a 3D radial UTE sequence is validated.

4017 Computer 68

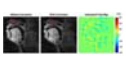

Correction of dynamic off-resonance in spiral 2D real-time MRI of speech

Yongwan Lim[1], Sajan Goud Lingala[1], Shrikanth Narayanan [1], and Krishna Nayak[1]

[1]Ming Hsieh Department of Electrical Engineering, University of Southern California, Los Angeles, CA, United States

Spiral real-time MRI (RT-MRI) is a valuable tool in speech production research. A key drawback is off-resonance blurring artifact that appears at the boundaries of important articulators. In this work, we demonstrate dynamic off-resonance estimation that is directly captured from phase of single echo-time dynamic images after coil phase compensation. Multi-frequency reconstruction then provides deblurring and improved depiction of articulator boundaries including the tongue, hard palate, and soft palate.

4018 Computer 69

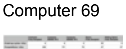

Sliding Slice 2D Spiral Time of Flight MRA

Nicholas R. Zwart[1] and James G. Pipe[1]

[1]MR Technology Design Group, Barrow Neurological Institute, Phoenix, AZ, United States

The scan technique and reconstruction method presented in this work are designed to reduce the scan duration of 2D time-of-flight angiography sequences. The acquisition makes use of a sliding-slice technique that eliminates the need for steady-state prep pulses, which are needed before each slice in time-of-flight. This reduces the total scan time of a 2D spiral time-of-flight sequence by almost half, without a reduction in k-space coverage.

4019 Computer 70

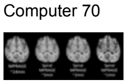

Spiral MPRAGE Acquisition and Segmentation

Kyoko Fujimoto[1,2], Brian R. Keating[2], and V. Andrew Stenger[1,2]

[1]Department of Electrical Engineering, University of Hawaii at Manoa, Honolulu, HI, United States, [2]Department of Medicine, John A. Burns School of Medicine, University of Hawaii, Honolulu, HI, United States

High-resolution MPRAGE has become a standard structural imaging sequence in clinical settings yet it is difficult to repeat the scan because of its relatively long acquisition time. Acceleration techniques allow the reduction of acquisition times although excessive acceleration can result in artifacts. We implemented a fast MPRAGE sequence using a spiral trajectory and demonstrated segmentation of acquired images. The spiral MPRAGE can acquire a whole-brain T_1 volume in less than 25% of the acquisition time of the conventional MPRAGE while maintaining comparable contrast and segmentation results.

4020 Computer 71

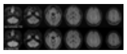

A Two-Dimensional Spiral Turbo-Spin-Echo Technique with T2-delay Correction and Concomitant Phase Compensation

Zhiqiang Li[1], Dinghui Wang[1], Ryan K Robison[1], John P Karis[2], and James G Pipe[1]

[1]Imaging Research, Barrow Neurological Institute, Phoenix, AZ, United States, [2]Neuroradiology, Barrow Neurological Institute, Phoenix, AZ, United States

Turbo spin-echo (TSE) is a rapid technique routinely used for T2 and FLAIR imaging. Two-dimensional spiral TSE is very challenging due to T2 signal decay. In this project we develop a 2D spiral TSE sequence employing a spiral-in/out readout for efficient acquisition without off-resonance phase errors, and a double encoding mechanism as well as signal demodulation to minimize T2 signal decay induced artifacts. A concomitant phase compensation technique is incorporated to mitigate the violation of the CPMG condition. Preliminary spiral TSE FLAIR results demonstrate comparable image quality to its Cartesian counterpart.

4021 Computer 72

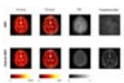

Spiral keyhole imaging for MR fingerprinting

Guido Buonincontri[1], Laura Biagi[1,2], Pedro A Gómez[3,4], Rolf F Schulte[4], and Michela Tosetti[1,2]

[1]IMAGO7 Research Center, Pisa, Italy, [2]IRCCS Stella Maris, Pisa, Italy, Pisa, Italy, [3]Technische Universität München, Munich, Germany, [4]GE Global Research, Munich, Germany

MR Fingerprinting can be used for a fast and quantitative estimation of physical parameters in MRI. For the fast acquisition of MRF, common approaches have used non-Cartesian sampling of k-space. Here, we introduce a method for non-iterative anti-aliasing of the spiral MRF time series, based on the concept of keyhole imaging. Our approach does not change acquisition or dictionary creation and matching procedures. As frames require only minimal density compensation in k-space, noise amplification during reconstruction is reduced. After applying our algorithm, individual images from the MRF time series are artifact-free and clearer parameter maps are obtained in a shorter time while preserving the accurate quantification of MRF.

Electronic Poster

Contrast Mechanisms: From A to ZTE

Exhibition Hall — Tuesday 9:15 - 10:15

4022 Computer 97

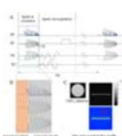

2D Zero TE Imaging Implemented with Gradient-Extended 2D Spiral-in Excitation and Spiral-out Acquisition (GRESS-ZTE)

Qing Li[1], Xiaozhi Cao[1], Congyu Liao[1], Hongjian He[1], and Jianhui Zhong[1]

[1]Center for Brain Imaging Science and Technology, Department of Biomedical Engineering, Zhejiang University, Hangzhou, Zhejiang, People's Republic of China

A 2D zero TE imaging technique was implemented with a gradient-extended 2D spiral-in excitation to excite a slice within 3mm full-width-half-maximum (FWHM) with pulse duration less than 6ms and spiral-out acquisition (GRESS-ZTE) strategy. Our preliminary data showed its ability to acquire signals in bones with very short T2*.

4023 Computer 98

High resolution dual-echo subtraction ZTE imaging at 7T with TE estimation based on multiple scaled trajectories

Hyo Min Lee[1], Markus Weiger[1], and Klaas Paul Pruessmann[1]

[1]Institute for Biomedical Engineering, University and ETH Zürich, Zürich, Switzerland

In dual-echo subtraction ZTE (DE-ZTE) MRI, it is crucial to correct for gradient delays in the second echo for high image quality. Linear phase fitting on the relative phase difference between projection pairs in image domain can be performed to estimate TE shifts, but it is not highly robust. Field camera can be used to externally provide TE shifts arising from gradient delays, but the probes tend to dephase at high resolution DE-ZTE scans. We demonstrate that gradient delays can be characterized as a linear function of gradient strength. Furthermore, we show that this can be exploited to reconstruct high resolution DE-ZTE data at 7T for high image quality.

4024 Computer 99

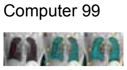

Ultra-short Echo-time MRI Lung Segmentation using High-Dimensional Features and Continuous Max-Flow

Fumin Guo[1], Khadija Sheikh[1], Robert Peters[2], Michael Carl[2], Aaron Fenster[1], and Grace Parraga[1]

[1]Robarts Research Institute, London, ON, Canada, [2]General Electric Healthcare, Milwaukee, WI, United States

Ultra-short-echo-time MRI may be used to generate imaging biomarkers to phenotype pulmonary abnormalities and facilitate the development of novel treatments but requires clinically-acceptable lung segmentation. We proposed an adaptive kernel K-means approach combining MRI signal intensity and neighbourhood location information for optimized lung segmentation. The resultant high dimensional features were implemented using a K-nearest neighbour graph and relaxed to a point-wise upper-bound formulation regularized by image edge information, which was implemented iteratively using a continuous max-flow optimization approach. Experimental results for 10 asthmatics demonstrated highly accurate, reproducible and computationally efficient lung segmentation for our approach consistent with clinical workflows.

4025 Computer 100

Whole-Body, Zero TE Based Pseudo CT Conversion

Florian Wiesinger[1], Sangtae Ahn[2], Sandeep Kaushik[3], Cristina Cozzini[1], Dirk Beque[1], Lishui Cheng[2], Jaewon Yang[4], Andrew Leynes[4], Dattesh Shanbhag[3], Thomas A. Hope[4], and Peder E. Z. Larson[4]

[1]GE Global Research, Munich, Germany, [2]GE Global Research, Schenectady, NY, United States, [3]GE Global Research, Bangalore, India, [4]Radiology and Biomedical Imaging, UCSF, San Francisco, CA, United States

Proton density (PD) weighted Zero TE (ZTE) MR imaging has been demonstrated to provide accurate bone depiction, segmentation and pseudo CT conversion in the head. However, when applied for the whole-body, discriminating between air and bone appears challenging (primarily because of SNR and RF shading). Here we present a novel method for decomposition of low ZTE signal intensity regions into bone and air based on connected component and shape analysis. The method is demonstrated for whole-body, pseudo CT conversion in three PET/MR patients.

4026 Computer 101

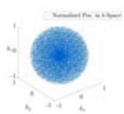

Accelerated Adaptive Quasi-Random Single-Point Imaging for in vivo Artefact Reduction

Tobias Speidel[1] and Volker Rasche[2]

[1]Core Facility Small Animal Imaging, University of Ulm, Ulm, Germany, [2]Department of Internal Medicine II, University of Ulm, Ulm, Germany

MR imaging of short relaxation times spin systems has been a widely discussed topic with serious clinical applications and led to the emergence of fast imaging ultra-short echo-time sequences such as UTE and ZTE. Nevertheless, these sequences suffer from image blurring due to the related point-spread function and are highly prone to imaging artefacts arising from e.g. chemical shifts or magnetic susceptibilities. In this work, we present a fully functional concept of spherical quasi-random single-point imaging that is highly acceleratable due to intrinsic undersampling properties and capable of strong metal artefact suppression with high tissue contrast.

4027 Computer 102

The Value of Ultrashort-Echo-Time (UTE) MR in Depiction of the Eustachian Tube at 3 Tesla

Wu Chao[1], Qian Tianyi[2], Wang Guangbin[1], Li Li[3], Wang Yuyu[4], Shi Honglu[1], Gao Fei[1], and Zhao Bin[1]

[1]Shandong Medical Imaging Research Institute, Shandong University, Jinan, People's Republic of China, [2]MR Collaborations NE Asia, Siemens Healthcare, [3]Shandong Provincial Hospital Affiliated with Shandong University, [4]Siemens Shenzhen Magnetic Resonance Ltd., Shenzhen, People's Republic of China

This study aimed to investigate the feasibility of ultrashort echo time (UTE) in visualizing the Eustachian tube (ET). Nineteen healthy volunteers were involved in this study. The quality of images was rated by two experienced radiologists using a double-blind method. Using the depiction of the cartilaginous part of the ET from standard T2-weighted images and that of the bony part from CT acquisition as reference points, UTE images were analyzed. The results indicate that UTE can not only display ET cartilage, but also display bone structure. This could lead to the application of whole-ET imaging in one MR exam.

4028 Computer 103

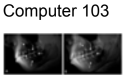

2D-UTE based pantomography with half-pulse excitation

Kilian Stumpf[1], Elena Kaye[2], Jan Paul[1], Stefan Wundrak[3], and Volker Rasche[1]

[1]Internal Medicine II, University Hospital of Ulm, Ulm, Germany, [2]Department of Medical Physics, Memorial Sloan Kettering Cancer Center, New York, NY, United States, [3]Dental Imaging, Sirona Dental Systems GmbH, Bensheim, Germany

Standard imaging methods in dental radiology are almost exclusively based on X-rays. Not only does magnetic resonance imaging (MRI) avoid ionizing radiation, but has also been shown to be superior in identifying carious lesions. In this work we present a 2D-UTE sequence with an echo time of 35μs, utilizing 240μs half-pulses to ensure reduced signal attenuation from tissues with short T2 relaxation during excitation. The feasibility of the method was demonstrated with the successful acquisition of in vivo MR pantomograms.

4029 Computer 104

An Iterative Gradient Delay Correction Method for 3D UTE Imaging

Qi Liu[1], Xiaomao Gong[2], Xiaolei Guan[2], Xueming Cao[2], Lingzhi Hu[1], Xiaodong Zhou[2], Jian Xu[1], and Weiguo Zhang[2]

[1]UIH America, Inc., Houston, TX, United States, [2]Shanghai United Imaging Healthcare Co., Ltd., Shanghai, People's Republic of China

Gradient imperfections such as gradient delay can cause image distortion and artifacts in UTE imaging. In this work, we report an iterative gradient delay correction method for 3D UTE imaging that allows use of arbitrary gradient waveform model, independent calibration of x, y, and z gradients, and subject-specific delay correction with an embedded prescan. The feasibility of improved image quality using this proposed method was demonstrated by volunteer data.

4030 Computer 105

Myelin and cortical bone short-T2 quantification using saturation and diffusion-based long-T2 suppression in a steady-state 3D-UTE sequence

Lucas Soustelle[1], Paulo Loureiro de Sousa[1], Julien Lamy[1], Mathieu D. Santin[2], François Rousseau[3], and Jean-Paul Armspach[1]

[1]Université de Strasbourg, CNRS, ICube, FMTS, Strasbourg, France, [2]ICM, CENIR, UPMC-Inserm U1127, CNRS 7225, Paris, France, [3]Institut Mines Télécom, Télécom Bretagne, INSERM LaTIM, Brest, France

Imaging of the very-short T_2 tissues in the head is challenging in that the signals decay very rapidly (T_2 < 1 ms), as well as their signal quantity being often overwhelmed by long-T_2 relaxing components (fat, free-water). In this work, we explore the feasibility of short-T_2 quantification in the white matter and in the cortical bone using a novel method for long-T_2 suppression based on diffusion and coherence effects in a steady-state 3D-UTE sequence.

4031 Computer 106

Long-T2 suppression based on saturation and diffusion in a steady-state 3D-UTE sequence

Lucas Soustelle[1], Julien Lamy[1], Paulo Loureiro de Sousa[1], François Rousseau[2], and Jean-Paul Armspach[1]

[1]Université de Strasbourg, CNRS, ICube, FMTS, Strasbourg, France, [2]Institut Mines Télécom, Télécom Bretagne, INSERM LaTIM, Brest, France

A new method for long-T_2 suppression in a prepared steady-state 3D-UTE sequence is introduced. The method is based on long-T_2 signal behavior in steady-state as the diffusion-inducing spoiling gradients are modified, giving a theoretical signal cancellation using appropriate coherence combinations. At the same time, short-T_2 signal quantity is optimized, offering a positive contrast over this component. Imaging experiments over a Lego brick soaked in doped water show an excellent agreement with theoretical predictions.

4032 Computer 107

Inversion-non-Recovery (InoR) method for long-T2 suppression in a steady-state 3D-UTE sequence for short-T2 imaging

Lucas Soustelle[1], Julien Lamy[1], Paulo Loureiro de Sousa[1], François Rousseau[2], and Jean-Paul Armspach[1]

[1]Université de Strasbourg, CNRS, ICube, FMTS, Strasbourg, France, [2]Institut Mines Télécom, Télécom Bretagne, INSERM LaTIM, Brest, France

A novel method for long-T_2 suppression in 3D-UTE imaging is introduced. The method is based on long- and short-T_2 components phase states in a dual-segment acquisition scheme (digital summation of two k-spaces before reconstruction, respectively acquired with and without adiabatic inversion), and offers a substantial contrast-to-noise ratio over the different components. We compare our method to the state-of-the-art IR-UTE. It shows higher performance and efficiency in terms of signal suppression and short-T_2 contrast.

4033 Computer 108

MR-embedded respiratory motion tracking in ZTE lung imaging for PET-MRI

Tanguy Boucneau[1], Brice Fernandez[2], Michael Soussan[3], Luc Darrasse[1], and Xavier Maître[1]

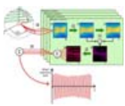

[1]Imagerie par Résonance Magnétique Médicale et Multi-Modalités, IR4M, CNRS, Univ Paris-Sud, Université Paris-Saclay, Orsay, France, [2]Applications & Workflow, GE Healthcare, Orsay, France, [3]Imagerie Moléculaire in Vivo, IMIV, Inserm, CEA, CNRS, Univ Paris-Sud, Université Paris-Saclay, Orsay, France

This study aims at showing the feasibility of MR-embedded respiratory motion tracking in ZTE lung imaging. It was shown that the motion information in a moving phantom as well as in free-breathing human volunteers and patients could be extracted from the off-center k-space data sampled during a ZTE acquisition with a faithful accuracy and precision in time and in amplitude with respect to a respiratory belt measurement. This new intrinsic motion follow-up method could be useful for retrospective motion correction of simultaneously acquired PET/MR images.

4034 Computer 109

Influence of k-space trajectory corrections on the proton density mapping precision with Ultrashort Echo Time Imaging.

Peter Latta[1], Zenon Starčuk[2], Marco Gruwel[3], and Boguslaw Tomanek[1,4]

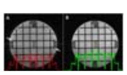

[1]Central European Institute of Technology, Masaryk University, Brno, Czech Republic, [2]Institute of Scientific Instruments, Academy of Sciences of the Czech Republic, Brno, Czech Republic, [3]Biological Resources Imaging Laboratory, Lowy Cancer Research Centre, Sydney, Australia, [4]University of Alberta, Edmonton, Canada

The ultrashort echo time (UTE) sequence is capable to provide information about tissues with short T2. On the other hand, as with all non-Cartesian data sampling schemes in general, it is sensitive to mismatching in the acquisition trajectory. This can be a potential source of errors, especially when used for quantitative applications such as proton density (PD) mapping. This problem can be reduced by calibration and correction of the k-space acquisition trajectories. The presented experiments demonstrate the importance of sampling trajectory corrections for UTE imaging, especially when applied for quantitative measurements.

4035 Computer 110

Fast, Volumetric and Silent Multi-contrast Zero Echo Time Imaging

Xin Liu[1,2], Pedro Gómez[1,2], Tim Sprenger[1,2], Ana Beatriz Solana[2], Florian Wiesinger[2], Marion Menzel[2], Jonathan Sperl[2], and Bjoern Menze[1]

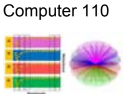

[1]Technical University Munich, Garching, Germany, [2]GE Global Research, Garching, Germany

The current work aims to provide a volumetric, fast and silent method for quantitative T1 mapping with Zero Echo Time (ZTE) imaging, and generate multiple T1-weighted images at virtual inversion times. By designing an interleaved radial trajectory for ZTE, and constraining the temporal behavior of the signal with low-dimensional subspace and spatiotemporal low rank regularization, we conducted a volumetric T1 mapping in 2 minutes with acoustic noise only 1.1dB higher than scanner background.

4036 Computer 111

A new ultrafast 3D gradient-echo magnetic resonance imaging method: RASE-I

JaeKyun Ryu[1,2], SoHyun Han[1,2], Joon-sung Lee[1,2], Seong-gi Kim[1,2], and Jang-Yeon Park[1,2]

[1]Center for Neuroscience Imaging Research, Institute for Basic Science (IBS), Suwon, Korea, Republic of, [2]Department of Biomedical Engineering Sungkyunkwan University (SKKU), Suwon, Korea, Republic of

One version of a new ultrafast ***gradient-echo-based*** 3D imaging technique using spatiotemporal encoding (RASE-I) is proposed which can provide very short TEs in some slices. RASE-I maintains most of appealing features of other ***spin-echo-based*** SPEN imaging methods including no Nyquist ghosting and high tolerance to field inhomogeneities. It is barely affected by T_2^* signal modulation and less sensitive to T_2^* effects due to local rephasing mechanism along the SPEN direction. Its performance is demonstrated by lemon and in-vivo mouse kidney imaging at 9.4T, including the measurement of dose-dependent arterial-input-function (AIF) of kidney-feeding artery.

4037 Computer 112

Ultra-high-bandwidth, high-resolution MRI of fast relaxing spins

Romain Nicolas Froidevaux[1], Markus Weiger[1], Manuela B. Rosler[1], Bertram Wilm[1], Franciszek Hennel[1], Roger Luechinger[1], Benjamin Dietrich[1], Jonas Reber[1], and Klaas Paul Pruessmann[1]

[1]University and ETH Zurich, Zürich, Switzerland

High resolution MRI of fast relaxing spins in human sets strong requirements on hardware and pulse sequences. Indeed, the acquisition duration is limited by the relaxation time of the protons of interest and high resolution can only be achieved with large magnetic field gradients. Also when large field-of-view is required, additional challenges appear. The sequence and receive hardware needs to be adapted to larger bandwidth. In this work, we image short T2 compounds in human scanners with gradient strengths up to 200 mT/m and bandwidth up to 1.63 MHz.

4038 Computer 113

Utilization of T1ρMR imaging in Sjögren's syndrome with normal appearing parotid glands: initial findings

Zhengyang Zhou[1], huayong zhang[2], and Weibo Chen[3]

[1]Department of Radiology, Drum Tower Hospital, School of Medicine, Nanjing University, Nanjing, People's Republic of China, [2]Department of Rheumatology, Drum Tower Hospital, School of Medicine, Nanjing University, People's Republic of China, [3]Philips Healthcare, Shanghai, People's Republic of China

Sixteen SS patients and age- and gender- match healthy volunteers underwent parotid MR imaging to evaluate whether T1ρ values could diagnose of SS patients. T1ρ values between the patients and healthy volunteers were compared. ROC analysis was used to evaluate the diagnostic performance of the T1ρ values. The T1ρ values of SS patients were significantly higher than those of healthy volunteers. With a cutoff value of 88.02 ms, the diagnostic sensitivity and specificity of the parotid T1ρ value was 75.0% and 100.0%, respectively. Parotid T1ρ MR imaging held the potential in the diagnosis of SS without morphological changes of glands.

4039 Computer 114

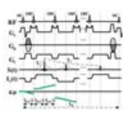

Human In-vivo MR Current Density Imaging (MRCDI) Based on Optimized Multi-echo Spin Echo (MESE)

Cihan Göksu[1,2], Lars Grüner Hanson[1,2], Philipp Ehses[3,4], Klaus Scheffler[3,4], and Axel Thielscher[1,2,3]

[1]Center for Magnetic Resonance, DTU Elektro, Technical University of Denmark, Kgs. Lyngby, Denmark, [2]Danish Research Centre for Magnetic Resonance, Centre for Functional and Diagnostic Imaging and Research, Copenhagen University Hospital, Hvidovre, Denmark, [3]High-Field Magnetic Resonance Center, Max-Planck-Institute for Biological Cybernetics, Tübingen, Germany, [4]Department of Biomedical Magnetic Resonance, University of Tübingen, Tübingen, Germany

MRCDI aims at imaging an externally injected current flow in the human body, and might be useful for many biomedical applications. However, the method requires very sensitive measurement of the current-induced magnetic field component $\Delta B_{z,c}$ parallel to main field. We systematically optimized MESE to determine its most efficient parameters. In one of the first human in-vivo applications of MRCDI, the optimized sequence was successfully used to image the $\Delta B_{z,c}$ distribution in the brain caused by a two-electrode montage, as confirmed by finite-element calculations of $\Delta B_{z,c}$. Further improvements will be performed to increase its robustness to field drifts.

4040 Computer 115

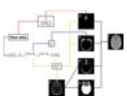

Tissue Relaxometry Defined (TRD) pseudo-CT imaging based on a single multi-gradient-echo MRI scan

Jie Wen[1], Bin Cai[2], Michael Gach[2], Olga Green[2], Christina Tsien[2], Jiayi Huang[2], Sasa Mutic[2], and Dmitriy Yablonskiy[1]

[1]Radiology, Washington University in St. Louis, St. Louis, MO, United States, [2]Radiation Oncology, Washington University in St. Louis, St. Louis, MO, United States

Generating MRI-based pseudo-CT images, providing electron density information for dose calculation, is the first step towards MRI-based radiation therapy treatment planning. Existing methods either require prior knowledge of a CT-MR atlas or require acquisition of multiple scans. In this study, we demonstrated the feasibility of producing pseudo-CT images by using a single multi-gradient-echo sequence. This method takes advantage of tissue-specific relaxation properties of MRI signal to provided segmentation of bone, air and other anatomical structures. Since all images are generated from a single scan and are naturally co-registered, this method is fast and avoids registration errors.

4041 Computer 116

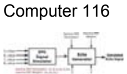

Multi-compartment T2 relaxometry Model using Gamma Distribution representations: A framework for Quantitative Estimation of Brain Tissue Microstructures.

Sudhanya Chatterjee[1], Olivier Commowick[2], Simon K. Warfield[3], and Christian Barillot[4]

[1]VisAGeS, IRISA U746, Universite de Rennes-1, Rennes, France, [2]VisAGeS Inserm U746, IRISA, Inria, Rennes, France, [3]Boston Children's Hospital, Boston, MA, United States, [4]VisAGeS, INRIA/IRISA, Inserm U746, CNRS, Rennes, France

Advanced MRI techniques (e.g. – d-MRI, MT, relaxometry etc.) can provide quantitative information of brain tissues. Image voxels are often heterogeneous in terms of microstructure information due to physical limitations and imaging resolution. Quantitative assessment of the brain tissue microstructure can provide valuable insights into neurodegenerative diseases (e.g. - Multiple Sclerosis). In this work, we propose a multi-compartment model for T2-Relaxometry to obtain brain microstructure information in a quantitative framework. The proposed method allows simultaneous estimation of the model parameters.

4042 Computer 117

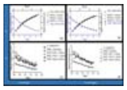

Fast, Robust and SimulTaneous (FRoST) relaxometry at polarizing field

Rashmi Rao[1], Shreyas Indurkar[1], Girish Koulagi[1], Nithin V Vajuvalli[1], Arush Honnedevasthana Arun[1], Sneha Potdar[1], and Sairam Geethanath[1]

[1]Medical Imaging Research Centre, Dayananda Sagar Institutions, Bangalore, India

T_1 and T_2 measurements in polarizing field systems have long acquisition times due to the inclusion of a polarizer pulse. Current work demonstrates Fast, RObust and SimulTaneous relaxometry ('FRoST') measurements at Earth's field on water and $CuSO_4$ phantoms. FRoST creates a variation of the net magnetization through a series of CPMG acquisitions by varying the polarizing pulse (τ_p) to obtain simultaneous T_1 and T_2 weighting. T_1 and T_2 values obtained are similar to standard sequences and the acquisition time is reduced by 55%-84%.

4043 Computer 118

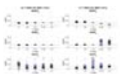

Impact of Magnetic Susceptibility Anisotropy at 3 T and 7 T on T2*-based Myelin Water Fraction Imaging

Eva Alonso Ortiz[1], Ives R. Levesque[1,2], and G. Bruce Pike[3]

[1]McGill University, Montreal, QC, Canada, [2]Research Institute, McGill University Health Centre, Montreal, QC, Canada, [3]University of Calgary, Calgary, AB, Canada

In this work we estimated the impact of myelin's magnetic susceptibility anisotropy on the Myelin Water Fraction (MWF) at 3T and 7T. We simulated realistic multicomponent T2* decay and then computed the MWF using three different fitting models. Our findings indicate that the effect of myelin's magnetic susceptibility anisotropy does not need to be considered when computing the MWF at 3T. However, failure to do so at 7T can lead to a significant bias in the MWF.

4044 Computer 119

A Fast Multi-Contrast Knee Imaging Method Using a Hybrid bSSFP Pulse Sequence

Hyunseok Seo[1], Seohee So[1], Byungjai Kim[1], Yoonmee Lee[1], Kyungtak Min[1], and HyunWook Park[1]

[1]Electrical Engineering, KAIST (Korea Advanced Institute of Science and Technology), Daejeon, Korea, Republic of

To increase the contrast between the bone and the cartilage, fat saturation techniques are additionally applied to the conventional imaging sequences. However, the fat saturation techniques eliminate most of the bone information. Thus, using the modified bSSFP (balanced steady-state free precession) pulse sequence called a hybrid bSSFP pulse sequence, the proposed method offers the multi-contrast knee images with very short imaging time (< 10 sec).

4045 Computer 120

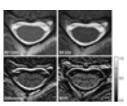

High Resolution Steady State Diffusion and Magnetization Transfer Imaging of the Spinal Cord

Matthias Weigel[1,2] and Oliver Bieri[1,2]

[1]Radiology, Radiological Physics, University Hospital Basel, Basel, Switzerland, [2]Dept. of Biomedical Engineering, University of Basel, Basel, Switzerland

The potential of high resolution steady state diffusion and magnetization transfer (MT) imaging approaches with short acquisition times of less than 2min were investigated for the depiction of the spinal cord. As a surprising result, diffusion weighted time-reversed fast imaging with steady state precession (PSIF) sequences are not able to generate notable diffusion based contrast in the spinal cord (identical diffusion quotient DQ = 1.96+-0.20). High resolution balanced steady state free precession (bSSFP) sequences, however, are able to depict MT induced signal saturation in spinal cord white matter (MT ratio = 0.30+-0.07).

Electronic Poster

MS: Longitudinal Studies

Exhibition Hall Tuesday 13:45 - 14:45

4046 Computer 1

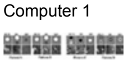

Longitudinal Study of MS lesions using Multi-contrast Ultra-high Field (7Tesla) MRI

SANJEEV CHAWLA[1], Ilya Kister[2], Tim Sinnecker[3], Jens Thomas Wuerfel[4], Friedemann Paul[5], and Yulin Ge[6]

[1]Radiology, UNIVERSITY OF PENNSYLVANIA, Philadelphia, PA, United States, [2]Neurology, Multiple Sclerosis Care Center, NYU School of Medicine, New York, NY, United States, [3]Neurology, Universitätsspital, Basel, Switzerland, [4]Medical Image Analysis Center, Basel, Switzerland, [5]NeuroCure Clinical Research Center, Charité-Universitätsmedizin, Berlin, Germany, [6]Radiology, NYU School of Medicine, New York, NY, United States

To track evolution of multiple sclerosis (MS) lesions, 9 patients underwent gradient-echo-T2* and quantitative susceptibility mapping on 7T MR system at baseline and at follow-up period (mean duration=2.4years). Majority of lesions were non-iron laden at baseline and most of them remained unchanged in size, morphology and susceptibility patterns. Some of these lesions accumulated iron deposition on follow-up. A minority of iron-laden lesions underwent redistribution of iron content. Small increase in lesion count was observed at follow-up. Interestingly, majority of these lesions were iron-enriched. This study may provide insights into pathophysiological features of MS lesions during the course of disease evolution.

4047 Computer 2

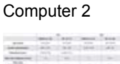

A longitudinal study of neurite orientation dispersion and density imaging in relapsing-remitting multiple sclerosis

Elda Fischi-Gomez[1,2,3], Guillaume Bonnier[1,2], Pavel Falkowskiy[3,4,5], David Romascano[3], Myriam Schluep[6], Renaud Du Pasquier[6], Alessandro Daducci[3], Jean-Philippe Thiran[3,4], Gunnar Kruger[7], and Cristina Granziera[1,2]

[1]Athinoula A. Martinos Center for Biomedical Imaging, Massachusetts General Hospital, Department of Radiology, Charlestown, MA, United States, [2]Harvard Medical School, Boston, MA, United States, [3]Signal Processing Laboratory (LTS 5), Ecole Polytechnique Fédérale de Lausanne (EPFL), Lausanne, Switzerland, [4]Department of Radiology, Centre Hospitalier Universitaire Vaudois (CHUV) and University of Lausanne (UNIL), Lausanne, Switzerland, [5]Advanced Clinical Imaging Technology (HC CMEA SUI DI BM PI), Siemens Healthcare AG, Lausanne, Switzerland, [6]Department of Clinical Neurosciences. Neuroimmunology and Neurology, Centre Hospitalier Universitaire Vaudois (CHUV) and University of Lausanne (UNIL), Lausanne, Switzerland, [7]Siemens Healthcare USA, Malvern, PA, United States

We explored the sensitivity of a novel diffusion MRI method i.e. “Neurite orientation dispersion and density imaging”, to detect and characterize brain microstructure alterations in relapsing-remitting multiple sclerosis patients that we followed up over 2 years. Cross-sectionally, NODDI revealed that an increase in orientation dispersion and a decrease in neurite density in NAWM and in lesions of RRMS patients compared to healthy subjects. Longitudinally, NODDI measured a decreased dispersion and an increased neurite density in MS lesions at 2 years follow-up. Also, NODDI metrics at baseline were highly related to cognition at both baseline and follow-up.

4048 Computer 3

Systematic Differences in High Angular Resolution Diffusion Imaging at Baseline in a Multicenter Longitudinal Clinical Trial

Ken Sakaie[1], Xiapeng Zhou[1], Josef Debbins[2], Mark Lowe[1], and Robert Fox[1]

[1]The Cleveland Clinic, Cleveland, OH, United States, [2]Keller Center for Imaging Innovation, Barrow Neurological Institute, Phoenix, AZ, United States

The lack of imaging biomarkers is a key obstacle to the development of treatment for progressive multiple sclerosis. While diffusion MRI is a promising biomarker, variability among scanners may limit its use. We examine site-related variability among multiple sclerosis patients to inform the design of multicenter trials.

4049 Computer 4

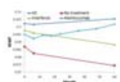

Myelin water imaging provides evidence of long-term remyelination and neuroprotection in Alemtuzumab treated multiple sclerosis patients

Irene Margaret Vavasour[1], Cornelia Laule[1,2], Shannon H Kolind[1,3], Roger Tam[1], David KB Li[1], Alex L MacKay[1,4], and Anthony L Traboulsee[3]

[1]Radiology, University of British Columbia, Vancouver, BC, Canada, [2]Pathology & Laboratory Medicine, University of British Columbia, Vancouver, BC, Canada, [3]Medicine (Neurology), University of British Columbia, Vancouver, BC, Canada, [4]Physics and Astronomy, University of British Columbia, Vancouver, BC, Canada

To test the potential neuroprotective and reparative properties of alemtuzumab (a highly effective disease modifying therapy for relapsing remitting MS), we used myelin water imaging to measure myelination in MS patients treated with either alemtuzumab, interferon, or no treatment. NAWM MWF showed a steady 4% increase in alemtuzumab-treated subjects whereas MWF in subjects treated with interferon or without treatment decreased by 10% over 5 years. Myelin recovery following treatment with alemtuzumab supports previous clinical trial findings, provides understanding of the biological mechanisms underlying observed clinical improvement and demonstrates that MWF is a powerful biomarker for neuroprotection and repair in MS.

4050 Computer 5

Myelin-Related MRI Metrics Demonstrate Longitudinal Differences for Relapsing MS Patients Treated with Ocrelizumab or Inteferon Beta-1a Over 96 Weeks

Shannon Kolind[1,2], Irene Vavasour[2], Roger Tam[2], Lisa Tang[3], Alexander Rauscher[2,4], Robert Carruthers[1], Rick White[5], Victoria Levesque[6], Hideki Garren[6], David Clayton[6], David Li[2], and Anthony Traboulsee[1]

[1]Neurology, University of British Columbia, Vancouver, BC, Canada, [2]Radiology, University of British Columbia, Vancouver, BC, Canada, [3]Biomedical Engineering, University of British Columbia, Vancouver, BC, Canada, [4]Pediatrics, University of British Columbia, Vancouver, BC, Canada, [5]Statistics, University of British Columbia, Vancouver, BC, Canada, [6]Genentech, South San Francisco, CA, United States

Conventional MRI scans cannot evaluate disease-related changes in normal-appearing white matter, and have limited sensitivity for detecting changes in chronic lesions. In this work, we employed 2 quantitative MRI measures related to myelin content, myelin water fraction and magnetization transfer ratio, to evaluate the effects a potential novel therapy for multiple sclerosis (ocrelizumab) compared to a commonly-used therapy (interferon beta-1a). Over 2 years, these myelin-related measurements increased or remained stable in all regions for patients taking ocrelizumab, while they decreased for interferon beta-1a. These results support the use of quantitative MRI measures for more efficient, biologically specific clinical trial outcomes.

4051 Computer 6

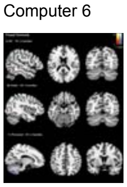

LONGITUDINAL ASSESSMENT OF LARGE-SCALE BRAIN FUNCTIONAL NETWORKS IN PATIENTS WITH MS: RELATIONSHIP WITH CLINICAL DISABILITY AND COGNITIVE IMPAIRMENT

Paola Valsasina[1], Maria Assunta Rocca[1], Fiammetta Pirro[1], Annalisa Colombi[1], Elisabetta Pagani[1], Ermelinda De Meo[1], Bruno Colombo[2], Paolo Preziosa[1], Vittorio Martinelli[2], Giancarlo Comi[2], Andrea Falini[3], and Massimo Filippi[1]

[1]Neuroimaging Research Unit, San Raffaele Scientific Institute, Vita-Salute San Raffaele University, Milan, Italy, [2]Department of Neurology, San Raffaele Scientific Institute, Vita-Salute San Raffaele University, Milan, Italy, [3]Department of Neuroradiology, San Raffaele Scientific Institute, Vita-Salute San Raffaele University, Milan, Italy

Aim of this study was to investigate the temporal evolution of resting state (RS) functional connectivity (FC) in patients with multiple sclerosis (MS) and its correlation with clinical and cognitive worsening. The predictive value of baseline functional network measures on the worsening of clinical disability/cognitive impairment was also explored. No significant RS FC changes were detected in healthy controls, while MS patients showed a complex pattern of longitudinal changes in the different networks, with a trend towards an increase (or stability) of RS FC in clinically stable MS patients, and a decrease of RS FC in clinically worsened MS patients.

4052 Computer 7

Longitudinal assessment of cervical cord atrophy across MS clinical phenotypes: a multicenter study

Paola Valsasina[1], Maria Assunta Rocca[1], Mohammad Ahmad Abdullah Ali Aboulwafa[1], Paolo Preziosa[1], Frederik Barkhof[2], Hugo Vrenken[2], Claudio Gobbi[3], Chiara Zecca[3], Alex Rovira[4], Xavier Montalban[5], Hugh Kearney[6], Olga Ciccarelli[6], Lucy Matthews[7], Jacqueline Palace[7], Antonio Gallo[8], Alvino Bisecco[8], Achim Gass[9], Philipp Eisele[9], Carsten Lukas[10], Barbara Bellenberg[10], Giancarlo Comi[11], and Massimo Filippi[1]

[1]Neuroimaging Research Unit, San Raffaele Scientific Institute, Vita-Salute San Raffaele University, Milan, Italy, [2]MS Centre Amsterdam, VU Medical Centre, Amsterdam, Netherlands, [3]Department of Neurology, Neurocenter of Southern Switzerland, Lugano, Switzerland, [4]Department of Radiology, Hospital Universitari Vall d'Hebron, Barcelona, Spain, [5]Department of Neurology, Hospital Universitari Vall d'Hebron, Barcelona, Spain, [6]Queen Square MS Centre, UCL Institute of Neurology, London, United Kingdom, [7]Nuffield Department of Clinical Neurosciences, University of Oxford, Oxford, United Kingdom, [8]MRI Center "SUN-FISM", Second University of Naples, Naples, Italy, [9]Universitaetsmedizin Mannheim, University of Heidelberg, Mannheim, Germany, [10]St Josef Hospital, Ruhr University Bochum, Bochum, Germany, [11]Department of Neurology, San Raffaele Scientific Institute, Vita-Salute San Raffaele University, Milan, Italy

Aims of this large, multicenter study were to characterize baseline cervical cord atrophy in patients with multiple sclerosis (MS) compared with healthy controls, and to evaluate the modification of cervical cord cross-sectional area (CSA) over one-year of follow-up in such patients. Results indicated that baseline cord atrophy was present in MS patients vs controls, with a differential effect across phenotypes and a greater severity of atrophy in the progressive forms of the disease. Significant CSA decrease over time was found in relapsing remitting, primary progressive MS and in clinically worsened patients.

4053 Computer 8

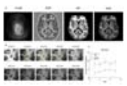

A longitudinal study of the effect of Multiple Sclerosis on surrounding white matter using z-spectrum imaging at 7T

Kingkarn Aphiwatthanasumet[1], Olivier Mougin[1], Nick Geades[1], Nikos Evangelou[2], Richard Bowtell[1], and Penny Gowland[1]

[1]Physics and Astronomy, Sir Peter Mansfield Imaging Centre, University of Nottingham, Nottingham, United Kingdom, [2]Neurology, Queen's Medical Centre, University of Nottingham, Nottingham, United Kingdom

MS lesions are known to evolve in time, many showing signs of remyelination. To investigate this, we considered the changes in the regions around existing lesions of varying ages, to test the hypothesis that there is ongoing tissue damage in the regions around white matter lesions in MS. We found that the quantitative MT measured at 7T values in the region surrounding MS lesions decreased over the period of a longitudinal 6 month study. No systematic trend was found for the lesion core. This supports the hypothesis that an MS lesion causes ongoing damage in the region surrounding the lesion.

4054 Computer 9

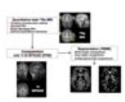

Brain sodium concentrations in healthy subjects are constant over time: a 3-year longitudinal 23Na MRI study at 3T

Adil Maarouf[1,2,3], Soraya Gherib[1], Elisabeth Soulier[1], Sylviane Confort-Gouny[1], Maxime Guye[1,2], Jean Pelletier[1,3], Jean-Philippe Ranjeva[1], and Wafaa Zaaraoui[1]

[1]Aix-Marseille Univ, CNRS, CRMBM, Marseille, France, [2]Aix-Marseille Univ, APHM, Hopital de la Timone, CEMEREM, Marseille, France, [3]Aix Marseille Univ, APHM, Hôpital de la Timone, Pôle de Neurosciences Cliniques, Service de Neurologie, Marseille, France

Longitudinal evaluation of brain sodium concentration in physiological conditions

---

4055 Computer 10

Manifold valued statistical models for longitudinal analysis of MRI data

Nagesh Adluru[1], Hyunwoo J Kim[2], Richard J Davidson[3], Andrew L Alexander[4], Sterling C Johnson[5], and Vikas Singh[6]

[1]Waisman Center, University of Wisconsin-Madison, Madison, WI, United States, [2]Computer Sciences, University of Wisconsin-Madison, [3]Psychology and Psychiatry, University of Wisconsin-Madison, [4]Medical Physics and Psychiatry, University of Wisconsin-Madison, [5]Medicine, University of Wisconsin-Madison, [6]Biostatistics and Computer Sciences, University of Wisconsin-Madison

This work presents novel statistical image analysis methods to characterize complex morphological brain changes using MRI data. Specifically, our procedure utilizes the fundamental representations of "longitudinal change" -- voxel-wise Jacobian matrices obtained from image registration. Currently their univariate summaries (for example determinants) are ubiquitously used in neuroimaging studies. Operating directly with representations of Jacobians namely Cauchy deformation tensors, which are elements of an abstract mathematical manifold of symmetric positive definite matrices, yields promising improvements in statistical power in detecting subtle but statistically significant effects. The key technical contributions are computational algorithms for estimating multivariate general linear models with manifold-valued response variables.

4056 Computer 11

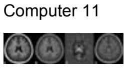

A preliminary study: the Values of Quantitative Susceptibility Mapping (QSM) in CIS and MS in Children

Hua CHENG[1], Hong ZHANG[1], Yang FAN[2], TongLi HAN[3], Yue LIU[1], and Yun PENG[1]

[1]Imaging Center, Beijing Children's Hospita, Capital Medical University, Beijing, People's Republic of China, [2]MR Research China, GE Healthcare, [3]Neurology Department, Beijing Children's Hospita, Capital Medical University, Beijing, People's Republic of China

Quantitative Susceptibility Mapping (QSM) has been well used in evaluating the iron quantity changes in adult patients with multiple sclerosis (MS). However, it has not been tested in pediatric MS patients. In the present study, QSM was applied to assess difference of iron quantity in clinically isolated syndrome (CIS) and MS in children. It is shown that QSM provides a superior sensitivity method in the detection iron of changes of MS-related tissue in children, which suggests that QSM may serve as a potential sensitive biomarker in pediatric MS.

4057 Computer 12

STRUCTURAL CONNECTIVITY ABNORMALITIES UNDERLYING COGNITIVE IMPAIRMENT IN PEDIATRIC MULTIPLE SCLEROSIS

Loredana Storelli[1], Maria Assunta Rocca[1], Ermelinda De Meo[1], Elisabetta Pagani[1], Lucia Moiola[2], Angelo Ghezzi[3], Pierangelo Veggiotti[4], Ruggero Capra[5], Maria Pia Amato[6], Agnese Fiorino[2], Lorena Pippolo[3], Maria Carmela Pera[4], Giancarlo Comi[2], Andrea Falini[7], and Massimo Filippi[1]

[1]Neuroimaging Research Unit, San Raffaele Scientific Institute, Vita-Salute San Raffaele University, Milan, Italy, [2]Department of Neurology, San Raffaele Scientific Institute, Vita-Salute San Raffaele University, Milan, Italy, [3]Multiple Sclerosis Center, Ospedale di Gallarate, Gallarate, Italy, [4]Fondazione "Istituto Neurologico Casimiro Mondino", Pavia, Italy, [5]Multiple Sclerosis Center, Spedali Civili di Brescia, Brescia, Italy, [6]Department of Neurology, University of Florence, Florence, Italy, [7]Department of Neuroradiology, San Raffaele Scientific Institute, Vita-Salute San Raffaele University, Milan, Italy

In this study, diffusion tensor (DT) magnetic resonance imaging (MRI) was applied to describe brain structural network architecture and connectivity abnormalities underlying cognitive dysfunction in 53 pediatric multiple sclerosis (MS) patients in comparison to 26 age- and gender-matched healthy controls (HC). Global and local network analyses were performed to assess between-group differences of connectivity metrics and cortical hubs. Cognitive impairment in pediatric MS patients seemed to be mainly associated to a reduced strength of connections of structural hubs and loss of efficiency in information transmission.

4058 Computer 13

Longitudinal Changes in Magnetic Resonance Spectroscopy Over 96 Weeks in Relapsing MS Treated with Ocrelizumab versus Interferon Beta-1a

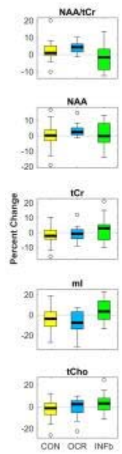

Erin L MacMillan[1], Julia J Schubert[1], Irene M Vavasour[1,2], Roger Tam[2], Alexander Rauscher[2], Rick White[3], Hideki Garren[4], David Clayton[4], Victoria Levesque[4], David KB Li[2], Anthony L Traboulsee[1], and Shannon H Kolind[1]

[1]Neurology, University of British Columbia, Vancouver, BC, Canada, [2]Radiology, University of British Columbia, Vancouver, BC, Canada, [3]Statistics, University of British Columbia, Vancouver, BC, Canada, [4]Genetech, Roche Pharmaceuticals, South San Francisco, CA, United States

Single voxel magnetic resonance spectroscopy (MRS) was performed in thirty-seven relapsing multiple sclerosis (MS) patients, who were enrolled in a phase III clinical trial of ocrelizumab versus interferon beta-1a, at baseline, 24, 48, and 96 weeks follow-up. 24 healthy controls were also scanned. MRS demonstrated a significant interaction between visit and treatment group in the NAA/tCr ratio. The change in absolute metabolite concentrations over 96 weeks revealed that this interaction was primarily driven by increased NAA and reduced inflammation in the ocrelizumab group, while the interferon beta-1a group exhibited a smaller increase in NAA and ongoing inflammation.

4059 Computer 14

Toward a standardized quantitative imaging protocol for multiple sclerosis: a multisite study of magnetization transfer and quantitative T1 imaging techniques

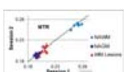

Ian Tagge[1], Daniel Schwartz[1], Katherine Powers[1], Rohit Bakshi[2], Peter Calabresi[3], Todd Constable[4], John Grinstead[1,5], Roland Henry[6], Govind Nair[7], Jiwon Oh[3,8], Li Pan[9], Nico Papinutto[6], Daniel Pelletier[10], Daniel S Reich[7], Nancy Sicotte[10], Jack Simon[1], William Stern[6], and William Rooney[11]

[1]Advanced Imaging Research Center, Oregon Health & Science University, Portland, OR, United States, [2]Brigham & Women's Hospital, Harvard Medical School, [3]Johns Hopkins, [4]Yale, [5]Siemens Medical Solutions, Portland, OR, [6]University of California San Francisco, [7]National Institute of Neurological Disease and Stroke, National Institute of Health, [8]University of Toronto, [9]Siemens Healthcare, Baltimore, MD, [10]University of Southern California, Keck School of Medicine, [11]Oregon Health & Science University, Portland, OR, United States

The current lack of standardization in MRI protocols leads to increased variability, particularly in semi-quantitative techniques such as MTR, and makes comparisons between studies almost impossible. A single subject with clinically stable RRMS travelled to seven North American sites and underwent two distinct 3T MRI sessions following a standardized MTR and qT_1 protocol at each site. Both MTR and qT_1 mapping have been shown to have potential in elucidating tissue characteristics and underlying pathology. This work demonstrated that use of carefully standardized protocols produces consistent quantitative and semi-quantitative measurements across sites in MS brain tissue in-vivo.

4060 Computer 15

Graph theoretical measures predict volumetric changes in multiple sclerosis

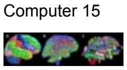

Thalis Charalambous[1], Carmen Tur[1], Ferran Prados[1,2], Steven H.P. van de Pavert[1], Declan T. Chard[1], David H. Miller[1], Sebastien Ourselin[2], Jonathan D. Clayden[3], Claudia A.M. Gandini Wheeler-Kingshott[1,4,5], Alan J. Thompson [1], and Ahmed T. Toosy[1]

[1]UCL Institute of Neurology, Queen Square MS Centre, University College London, London, United Kingdom, [2]Translational Imaging Group, Centre for Medical Image Computing, Department of Medical Physics and Biomedical Engineering, University College London, London, United Kingdom, [3]UCL GOS Institute of Child Health, University College London, London, United Kingdom, [4]Department of Brain and Behavioural Sciences, University of Pavia, Pavia, Italy, [5]Brain MRI 3T Mondino Research Center, C. Mondino National Neurological Institute, Pavia, Italy

Numerous studies demonstrated structural network changes in patients with multiple sclerosis (MS). However, the predictive nature of the graph-derived metrics is not yet examined. In this longitudinal study, we constructed baseline diffusion-based structural networks and we used multiple linear regression analysis to assess the ability of the network measures to predict follow-up increased lesion load and brain atrophy in MS (n=49). Our results suggest that edge density, global and local efficiency can predict follow-up brain atrophy after adjusting for the nuisance variables, signifying that network analysis can provide new insights into disease trajectories and offer potential biomarkers for MS progression.

4061 Computer 16

THE EVOLUTION OF CORTICAL AND SUB-CORTICAL LESION SIZE AND NUMBER CORRELATES WITH CHANGES IN COGNITION IN EARLY-STAGE RELAPSING-REMITTING MULTIPLE SCLEROSIS PATIENTS

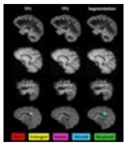

Alexandra Şorega[1], Mário João Fartaria [2,3,4], Guillaume Bonnier[5], Tobias Kober[2,3,4], Renaud Du Du Pasquier[6], Myriam Schluep[6], Gunnar Krueger[7], Meritxell Bach Cuadra[3,4,8], and Cristina Granziera[5,6]

[1]Department of Radiology, Valais Hospital, Sion, Switzerland, [2]Advanced Clinical Imaging Technology, Siemens Healthcare AG, Lausanne, Switzerland, [3]Department of Radiology, Centre Hospitalier Universitaire Vaudois (CHUV) and University of Lausanne (UNIL), Lausanne, Switzerland, [4]Signal Processing Laboratory (LTS 5), Ecole Polytechnique Fédérale de Lausanne (EPFL), Lausanne, Switzerland, [5]Martinos Center for Biomedical Imaging, Massachusetts General Hospital and Harvard Medical School, Boston, MA, United States, [6]Department of Clinical Neurosciences, Centre Hospitalier Universitaire Vaudois (CHUV) and University of Lausanne (UNIL), Lausanne, Switzerland, [7]Siemens Medical Solutions USA, Boston, MA, United States, [8]Medical Image Analysis Laboratory (MIAL), Centre d'Imagerie BioMédicale (CIBM), Lausanne, Switzerland

Lesion load and activity in multiple sclerosis (MS) patients, as identified by conventional magnetic resonance imaging (MRI), correlate only moderately with patients clinical status and evolution. Cortical lesion number and volume measured with advanced MRI may provide better correlates to cognitive dysfunction and disability. In this work, we studied the clinical impact of advanced MRI metrics of cortical and subcortical lesion evolution in a cohort of early relapsing-remitting MS patients. The number and volume of lesions that "shrunk", disappeared or remained stable over time were strong determinants of changes in cognition in our patients cohort.

4062 Computer 17

Longitudinal outer and inner cortical MTR abnormalities in different MS clinical phenotypes

Rebecca Sara Samson[1], Manuel J Cardoso[2,3], Nils Muhlert[1,4], Varun Sethi[1,5], Özgür Yaldizli[1,6], Maria A Ron[1], Ferran Prados [1,2], Sebastian Ourselin[2,3], David H Miller[1,7], Claudia A M Gandini Wheeler-Kingshott[1,8,9], and Declan T Chard[1,7]

[1]UCL Institute of Neurology, Queen Square MS Centre, University College London, London, United Kingdom, [2]Translational Imaging Group, Centre for Medical Image Computing, Department of Medical Physics and Biomedical Engineering, University College London, London, United Kingdom, [3]Dementia Research Centre, Department of Neurodegenerative Diseases, UCL Institute of Neurology, University College London, London, United Kingdom, [4]Division of Neuroscience and Experimental Psychology, University of Manchester, Manchester, United Kingdom, [5]Department of Neurology, Nottingham University Hospitals, Nottingham, United Kingdom, [6]Department of Neurology, University Hospital Basel, Basel, Switzerland, [7]National Institute for Health Research (NIHR) University College London Hospitals Biomedical Research Centre, United Kingdom, [8]Department of Brain and Behavioural Sciences, University of Pavia, Pavia, Italy, [9]Brain MRI 3T Center, C. Mondino National Neurological Institute, Pavia, Italy

Outer cortical magnetisation transfer ratio (cMTR) is potentially a sensitive measure of pathology linked to clinical disease progression in multiple sclerosis (MS). Here we aimed to investigate longitudinal outer and inner cMTR changes in healthy controls (HC) and people with MS of different clinical subtypes. Follow-up (FU) outer cMTR showed larger reductions in secondary progressive (SP)MS than other subtypes, and inner cMTR was also reduced more than in HC and relapsing-remitting (RR)MS, although cMTR was reduced in all MS patients at FU. This supports histopathological findings and suggests that cMTR measurement may be relevant to clinical disease progression in MS.

4063 Computer 18

Monitoring Disease Progression in Experimental Autoimmune Encephalitis using VDMP-CEST MRI

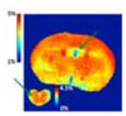

Aline Thomas[1], Jiadi Xu[2], Peter Van Zijl[2], and Jeff Bulte[3]

[1]Johns Hopkins School of Medicine, Baltimore, MD, United States, [2]Kennedy Krieger, [3]Johns Hopkins School of Medicine

VDMP-CEST MRI can spatiotemporally monitor disease progression in a mouse model of multiple sclerosis. Lower VDMP-CEST signals corresponded to a decreased lipid and metabolite content in the peri-ventricular region of the brain, characteristic of the disease, with magnetic resonance spectroscopy used as validation.

4064 Computer 19

ACCURACY AND REPRODUCIBILITY OF AN AUTOMATED LESION SEGMENTATION TOOL-LESIONQUANT

Weidong Luo[1], Kelly Leyden[1], Aziz M Ulug[1,2], Sebastian Magda[1], Julia Albright[1], Robert Haxton[1], and Chris Airriess[1]

[1]CorTechs Labs, San Diego, CA, United States, [2]Institute of Biomedical Engineering, Bogazici University, Istanbul, Turkey

Quantitative measures such as lesion volume and distribution have significant value for clinicians evaluating disease progression. Clinical standards for lesion evaluation include visual inspection of MRI images, or expert manual segmentation of lesions. These subjective measurements are often vulnerable to inter- and intra-rater variability, resulting in low reproducibility. CorTechs Labs' LesionQuant is a fully-automated lesion segmentation tool for clinical use designed to provide accurate and reproducible lesion segmentations. This study objectively evaluates the segmentation results of LesionQuant compared to expert manual segmentation.

4065 Computer 20

Automated Lateral Ventricle Segmentation in Multiple Sclerosis – Assessing Reliability and Clinical Impact in a 5-Years Follow-Up Cohort Study

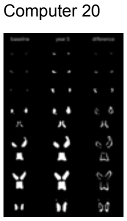

Esther Ruberte[1], Tim Sinnecker[1,2], Michael Amann[1,3], Yvonne Naegelin[2], Iris-Katharina Penner[4], Matteo Pardini[5], Jens Kuhle[2], Tobias Derfuss[2], Christoph Stippich[3], Ludwig Kappos[2], Jens Wuerfel[1], and Özgür Yaldizli[1,2]

[1]Medical Image Analysis Center AG, Basel, Switzerland, [2]Department of Neurology, Universitätsspital Basel, Basel, Switzerland, [3]Department of Neuroradiology, Universitätsspital Basel, Basel, Switzerland, [4]Department of Neurology, University Hospital Düsseldorf, Düsseldorf, Germany, [5]Department of Neuroscience, Rehabilitation, Ophthalmology, Genetics, Maternal and Child Health, University of Genoa and IRCCS S. Martino-IST, Genoa, Italy

As pars pro toto, lateral ventricle enlargement might give an indirect estimate of brain atrophy. In contrast to whole brain atrophy, ventricle enlargement is, however, clinically easy to assess and its quantification is robust to MR images of less than perfect quality. Here we investigate i) the applicability of an automatic lateral ventricle delineation algorithm (ALVIN) in multiple sclerosis (MS), and ii) the association between of lateral ventricle enlargement and clinical disability in MS longitudinally. We found that ALVIN reliably estimates the lateral ventricle volume in MS that is associated with whole brain atrophy and neurological as well as cognitive disability.

4066 Computer 21

Using multi-inversion time ASL to explore gray matter perfusion in patients with multiple sclerosis: repeatability and relationship to disease characteristics

Ilona Lipp[1], Catherine Foster[1], Rachael Stickland[1], Alison Davidson[1], Richard G Wise[1], and Valentina Tomassini[1,2]

[1]CUBRIC, Cardiff University, Cardiff, United Kingdom, [2]IRCCS Fondazione Santa Lucia, Rome, Italy

The first aim of this study was to investigate retest-reliability of gray matter perfusion estimates in patients with multiple sclerosis. Using multi-inversion time pulsed ASL, we demonstrate good repeatability of global and local perfusion estimates over a four-week interval. The perfusion estimates were consistently lower in the patients than in a group of healthy controls. The second aim was to relate GM perfusion to disease characteristics. We could not find an effect of disease duration or stage (relapsing-remitting vs progressive) on perfusion, but we did observe a weak correlation with cognition, supporting previous studies.

4067 Computer 22

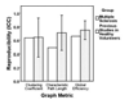

Reproducibility of Brain Network Metrics in People with Multiple Sclerosis

Thomas Welton[1], Dorothee P Auer[1], Cris S Constantinescu[2], and Rob A Dineen[1]

[1]Radiological Sciences, University of Nottingham, Nottingham, United Kingdom, [2]Clinical Neurology, University of Nottingham, Nottingham, United Kingdom

Knowledge of reproducibility of graph-theoretic brain network metrics in disease populations is critically important for applications in clinical studies but non-existent in published literature. We compared reproducibility of graph metrics over time in a cohort of MS patients to reported values in published studies of reproducibility in healthy volunteers. We found that reproducibility was good in MS patients but slightly lower than in healthy people. Reproducibility of graph-theoretic brain network metrics in MS patients is not greatly dissimilar to that in healthy populations, which supports their use in clinical studies.

4068 Computer 23

Progressive Iron Accumulation in Multiple Sclerosis Phenotypes Revealed by Sparse Classification of Deep Gray Matter

Ahmed M. Elkady[1], Dana Cobzas[1], Hongfu Sun[1], Gregg Blevins[2], and Alan H. Wilman[1]

[1]Biomedical Engineering, University of Alberta, Edmonton, AB, Canada, [2]Division of Neurology, University of Alberta, Edmonton, AB, Canada

Purpose: To create an anatomically-interpretable framework for localized analysis of brain iron accumulation/demyelination, and apply this framework to Multiple Sclerosis (MS) Deep Gray Matter (DGM).

Materials and Methods: Quantitative Susceptibility and R2* maps were computed for 110 MS and 75 control subjects.

Results: Significant iron accumulation and insignificant demyelination were detected in MS DGM. Common MS pathological volumes and their pathological effect size progressively increased with advanced phenotypes. The developed framework offered improved statistical power and iron specificity compared to whole structure and singular analysis.

Conclusion: Using a novel localized analysis pipeline, we demonstrated the progressive iron accumulation in MS DGM.

4069 Computer 24

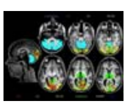

Predicting visual function clinical outcome in MS: a MRI and OCT metrics study.

Eduardo Caverzasi[1,2], Christian Cordano[1,3], Alyssa Zhu[4], Antje Bischof[1,5], Gina Kirkish[1], Nico Papinutto[1], Michael Devereux[1], Nicholas Baker[1], Sam Arnow[1], Justin Inman[1], Hao Yiu[1], Carolyn Bevan[1], Jeffrey M Gelfand[1], Bruce A Cree[1], Stephen L Hauser[1], Roland G Henry[1], and Ari J Green[1]

[1]Neurology, University of California, San Francisco, San Francisco, CA, United States, [2]University of Pavia, Italy, [3]DINOGMI, University of Genova, Italy, [4]Imaging Genetics Center, Stevens Neuroimaging and Informatics Institute, University of Southern California, United States, [5]Basel University Hospital, Switzerland

Fifty Multiple Sclerosis subjects were evaluated by optical coherence tomography and MRI, including multi-shell and putative myelin content imaging focused on primary visual area, thalamus and cerebellum. Predictive models of visual function performance, measured by visual evoked potentials and low contrast visual acuity were tested using a partial least square regression analysis. Combination of MRI and OCT metrics appears to strongly describe the visual function. Myelin content imaging, in particular, has a strong predictive value once there is history of optic neuritis. These preliminary results may improve the understanding of the pathological mechanisms underlying clinical dysfunction in multiple sclerosis.

Electronic Poster

Neuro: Animal Studies: Probing Disease

Exhibition Hall Tuesday 13:45 - 14:45

4070 Computer 49

Environmental enrichment changes neuroanatomy more than exercise and does not require CREB

Dulcie A Vousden[1,2], Alexander Friesen[1], Lily Qiu[1], Rylan Allemang-Grand[1,2], Jan Scholz[1], Sheena A Josselyn[3,4], Paul W Frankland[3,4], and Jason P Lerch[1,2]

[1]Mouse Imaging Centre, Hospital for Sick Children, Toronto, ON, Canada, [2]Dept. of Medical Biophysics, University of Toronto, Toronto, ON, Canada, [3]Hospital for Sick Children, Toronto, ON, Canada, [4]Dept. of Psychology, University of Toronto, Toronto, ON, Canada

Human and rodent imaging studies show that experience can lead to task-specific increases in brain structure, but the cellular and molecular basis of these changes is unknown. Here, we test the hypothesis that the these volume changes depend on the same signaling pathways required for learning and memory formation. We exposed mice lacking CREB (a transcription factor critical for memory) to an enriched housing environment, and imaged their brains longitudinally over two weeks. Surprisingly, enrichment altered the neuroanatomy of all mice, regardless of CREB genotype. These findings provide evidence that the volume changes are due to CREB-independent processes.

4071 Computer 50

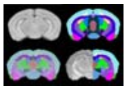

MEMRI atlas-based assessment of brain volumes in adult NSG mice irradiated at birth

Balasrinivasa R Sajja[1], Aditya N Bade[2], Mariano G Uberti[1], Michael D Boska[1,2], Howard E Gendelman[2], Santhi Gorantla[2], and Yutong Liu[1,2]

[1]Radiology, University of Nebraska Medical Center, Omaha, NE, United States, [2]Pharmacology & Experimental Neuroscience, University of Nebraska Medical Center, Omaha, NE, United States

Use of HIV-1 humanized mice allows the evaluation of brain morphology affected by disease and disease altering therapies. We posit that such studies can elucidate the pathobiology of HIV-1 associated neurological disorders. As irradiation, administered at birth, is a required step for long-term graft integrity we evaluated the effect of irradiation on mouse brain development using manganese-enhanced MRI (MEMRI) atlas-based segmentation. Brain size reductions in irradiated mice showed substantive morphological alterations. Thus, evaluation of irradiation effects on brain morphology is a requisite step in assessments of virus-induced brain pathology.

4072 Computer 51

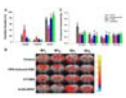

Resting-state functional connectivity reveals deep brain stimulation and 5-HT treated alteration in autism rat

Ssu-Ju Li[1], Hui-Yu Wang[1], Hui-Ching Lin[2,3], Ting-Chun Lin[1], Han-Fang Wu[2], Chi-Wei Lee[2], Yu-Chun Lo[4], You-Yin Chen[1], and Hsin-Yi Lai[5]

[1]Department of Biomedical Engineering, National Yang-Ming University, Taipei, Taiwan, [2]Department and Institute of Physiology, National Yang-Ming University, Taipei, Taiwan, [3]Brain Research Center, National Yang-Ming University, Taipei, Taiwan, [4]The PhD Program for Neural Regenerative Medicine, Taipei Medical University, Taipei, Taiwan, [5]Interdisciplinary Institute of Neuroscience and Technology, Zhejiang University, Hangzhou City, Zhejiang Province, People's Republic of China

This study demonstrates changes of functional connectivity in motor related brain areas and the motor cortex and striatum may be crucial areas for treatment and evolution of autism spectrum disorder (ASD). Our results indicate that both CT-DBS and 5-TH treatments can alter the social interaction and motor related functional connectivity VPA-induced ASD rats by modifying the motor cortico-striatal circuit. The rsfMRI has the potential to explore functional connectivity in the brain and monitor functional plasticity changes in a specific neuroanatomical pathway *in vivo*.

4073 Computer 52

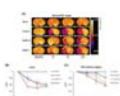

Effect of administration time of hydrogen sulfide on neuroprotective effects in the cerebral ischemia/reperfusion injury model

Chul-Woong Woo[1], Jae Im Kwon[1], Sang Tae Kim[1], Kyung won Kim[2], YoonSeok Choi[3], Jinil Kim[1], Jeong Kon Kim[2], Su Jeong Ham[1], Seul I Lee[1], Ho-jin Kim[1], Jeeheon Kang[1], and Dong-Cheol Woo[1]

[1]Asan Institute for Life Sciences, Asan Medical Center, Seoul, Korea, Republic of, [2]Department of Radiology, Asan Medical Center, [3]Medical research institute, Gangneung Asan Hospital

Recent evidence indicated that hydrogen sulfide is capable of attenuating ischemia/reperfusion (I/R) injury in brain. However, the influence of H_2S administration timing on its neuroprotective efficacy has not yet been assessed, thus we aimed to perform this study which used MRI and ^{1}H-MRS in rats with focal cerebral I/R injury. Our study demonstrated that hydrogen sulfide administration at 1 minute before reperfusion showed better neuroprotective effect than that at 30 minutes before reperfusion.

4074 Computer 53

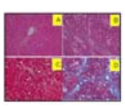

Neurochemical Alterations and Behavioral Impairments in Late Stage Alcoholic Liver Fibrosis in Mice

Su Xu[1,2], Wenjun Zhu[1,2], JiaBei Wang[3], Xi Chen[4], Rao P Gullapalli[1,2], Edward Herskovits[1], Elias Melhem[1], and Qi Cao[1]

[1]Radiology, University of Maryland School of Medicine, Baltimore, MD, United States, [2]Core for Translational Research in Imaging @Maryland, Baltimore, MD, United States, [3]Pharmaceutical Sciences, University of Maryland School of Pharmacy, Baltimore, MD, United States, [4]Harvard Medical School McLean Hospital, Belmont, MA, United States

A mouse model of late-stage alcoholic liver fibrosis (LALF) was used to investigate changes of neurochemical levels in specific brain regions that may relate to behavioral changes at LALF. Higher glutamine levels result in osmotic/oxidative stress were found in the thalamus and hippocampus of the alcohol-treated mice than in controls. Thalamic levels of taurine and creatine were significantly diminished and were strongly correlated with the alcohol-induced depressive behavior observed in an open field test. In addition, significant elevations in hippocampal glutamate were indicative of upregulated local glutamatergic activation. These pilot findings provide novel insight into the development of alcohol-induced HE.

4075 Computer 54

Diffusion MRI Quantifies Hippocampal CA1 Dendritic Loss and Inflammation in TMEV-Induced Epilepsy

Jie Zhan[1], Tsen-Hsuan Lin[2], Jane E. Libbey[3], Peng Sun[2], Ze-Zhong Ye[4], Chunyu Song[5], Michael Wallendorf[6], Honghan Gong[1], Robert S. Fujinami[3], and Sheng-Kwei Song[2,5,7]

[1]Radiology, The First Affiliated Hospital of Nanchang University, Nanchang, People's Republic of China, [2]Radiology, Washington University in St. Louis, St. Louis, MO, United States, [3]Pathology, University of Utah, Salt Lake City, UT, United States, [4]Chemsitry, Washington University in St. Louis, St. Louis, MO, United States, [5]Biomedical Engineering, Washington University in St. Louis, St. Louis, MO, United States, [6]Biostatistics, Washington University in St. Louis, [7]Hope Center for Neurological Disorders, Washington University in St. Louis, St. Louis, MO, United States

Hippocampal neuronal damage and inflammation are the hallmark pathologies of epilepsy. We demonstrate the capability of diffusion based spectrum imaging (DBSI) to quantify hippocampal CA1 neuronal dendritic injury/loss and inflammation in TMEV-induced epilepsy mice, followed by immunohistochemistry (IHC) validation. Results demonstrate that both DTI and DBSI metrics changed in CA1 region of TMEV-induced seizure mouse. DBSI-derived fiber fraction correlated with MAP2-positive area fraction, and DBSI-derived restricted isotropic diffusion fraction correlated with DAPI-positive nucleus density.

4076 Computer 55

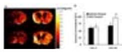

Effects of SHH Signaling Pathway in Post-Stroke Recovery Assessed by MRI

Yifan Zhang[1], Yongming Jin[2], Agnes Yu Luo[2], and Xin Yu[1]

[1]Biomedical Engineering, Case Western Reserve University, Cleveland, OH, United States, [2]Neurological Surgery, Case Western Reserve University, Cleveland, OH, United States

The current study investigated the effect of sonic hedgehog agonist (SAG) treatment in post-stroke recovery. SAG- and vehicle-treated mice were evaluated with MRI at day 2 and day 30 after middle cerebral artery occlusion (MCAO) surgery. Our results show that SAG treatment showed significantly increased cerebral perfusion in the ischemic penumbra at day 30, suggesting enhanced angiogenesis. In addition, SAG-treated mice also exhibited decreased T2, suggesting reduced neuronal damage. These results suggest that the sonic hedgehog signaling pathway can be a potential therapeutic target for stroke treatment.

4077 Computer 56

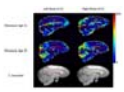

Myelin degeneration in cynomolgus macaques with advanced age using quantitative myelin imaging

Wenwen Yu[1], Zhe Wu[2], Hongjian He[2], Jianhui Zhong[2], and Zheng Wang[1]

[1]Institute of Neuroscience, Chinese Academy of Sciences, Shanghai, People's Republic of China, [2]Center for Brain Imaging Science and Technology, Department of Biomedical Engineering, Zhejiang University, Hangzhou, People's Republic of China

Effects of normal aging on myelin have drawn considerable attention for decades. Previous studies hypothesized that myelin sheath degeneration could result in the reduction of the fraction of myelin water due to the inflow of intra- or extra-cellular water between myelin sheath. This study investigates aging effects on myelin degeneration in elderly macaques using a multi-echo GRE sequence. Using a three-pool model, we observed a significant decrease in the fraction of myelin water in the body of corpus callosum and a negative correlation with ages in 8 monkeys (aged 21~25), indicating heterogeneous degradation of white matter infrastructure with aging.

4078 Computer 57

Effects of taurine on resting-state fMRI activity in rat model of attention deficit hyperactivity disorder

Hong-Chun Chou[1], Bor-Show Tzang[2], Vincent Chin-Hung Chen[3,4], and Jun-Cheng Weng[1,5]

[1]Department of Medical Imaging and Radiological Sciences, Chung Shan Medical University, Taichung, Taiwan, [2]Institute of Biochemistry, Microbiology and Immunology, Chung Shan Medical University, Taichung, Taiwan, [3]School of Medicine, Chang Gung University, Taoyuan, Taiwan, [4]Department of Psychiatry, Chang Gung Memorial Hospital, Chiayi, Taiwan, [5]Department of Medical Imaging, Chung Shan Medical University Hospital, Taichung, Taiwan

Attention deficit hyperactivity disorder (ADHD) is a most common developmental disorders in both children and adult population. However, the treatment for ADHD remains limited. To investigate the effects of taurine on ADHD, a spontaneously hypertensive rat (SHR) animal model was adopted in this study. The functional brain signals including functional connectivity (FC) and mean amplitude of low-frequency fluctuation (mALFF) were detected by using resting-state functional magnetic resonance imaging (rs-fMRI). Our findings in FC and mALFF suggested that taurine administration probably improves the hyperactive behavior in ADHD by changing brain functional signals in SHR rats.

4079 Computer 58

Ultra high resolution MR histology using ROI-extraction and SNR efficient gradient echo imaging

Joseph Guy[1,2], Robin Franklin[3], Kevin Brindle[1], and Daniel Reich[2]

[1]Biochemistry, Cambridge University, Cambridge, United Kingdom, [2]Translational Neuroradiology Section, National Institute of Neurologic Disorders and Stroke, Bethesda, MD, United States, [3]Clinical Neuroscience, Cambridge University, Cambridge, United Kingdom

Custom-built solenoid coils and 3D-printed rat brain slicers were used to identify and extract surgically placed inflammatory regions of interest within rat brains. The sequentially smaller and more sensitive coils combined with a highly-optimized gradient echo sequence, imaging setup, and registration algorithm achieved ultra high 25 µm isotropic resolution 3D MRI datasets. These images contained fully sampled k-space of the tissue pathology with preservation of the high frequency image details.

4080 Computer 59

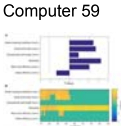

Social isolation in rats as a model for schizophrenia - a functional connectivity approach

Jonathan Rochus Reinwald[1], Robert Becker[1], Claudia Falfan-Melgoza[1], Anne Mallien[2], Dragos Inta[2], Peter Gass[2], Alexander Sartorius[1], and Wolfgang Weber-Fahr[1]

[1]Translational Imaging, Department of Neuroimaging, Central Institute of Mental Health, Medical Faculty Mannheim / Heidelberg University, Mannheim, Germany, [2]Animal Models in Psychiatry, Central Institute of Mental Health, Medical Faculty Mannheim / Heidelberg University, Mannheim, Germany

Post-weaning social isolation rats are a widely used translational animal model for schizophrenia based on its typical schizophrenic-like behavioral alterations. Nevertheless, effects of isolation on functional brain connectivity are highly understudied. We used resting-state functional magnetic resonance imaging with seed-based and graph analyses to investigate effects of social isolation in rats on brain connectivity. Our major findings consistently demonstrated dysmodularity, hypofrontality, posterior hyperconnectivity and reorganization of the somatosensory cortex. These features resemble alterations of functional brain connectivity commonly observed in schizophrenic patients and other translational animal models, underlining the potential use of isolated rats as a translational model of schizophrenia.

4081 Computer 60

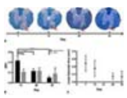

Characterizing the evolving property of de-and re-myelination in a mouse model using NODDI and MRI texture

Tim Luo[1], Peng Zhai[1], Olayinka Oladosu[2], Kahlil Rawji[1], and Yunyan Zhang[1]

[1]University of Calgary, Calgary, AB, Canada, [2]Queens University, Kingston, ON

Myelin injury and repair are associated with many neurological diseases including multiple sclerosis. We evaluated the utility of NODDI and MRI texture analysis for assessing myelin integrity using a mouse model of de- and re-myelination. Following lesion induction in mouse spinal cord, 9.4T MRI was conduced during demyelination (day 7) and ongoing remyelination (days 14, 28, and 35). With histological verification, both texture heterogeneity and neurite orientation dispersion (ODI) increased when demyelination occurs. But the latter showed persistent recovery with remyelination, similar to lesion size. These findings suggest the utility of ODI and texture heterogeneity as measures of myelin integrity.

4082 Computer 61

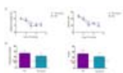

Patterns of resting-state functional connectivity in the prodromal phase of Alzheimer's disease: insights from a tauopathy mouse model (Thy-Tau22)

Laetitia Degiorgis[1], Meltem Karatas[1], Marion Sourty[1], Chrystelle Po[1], Thomas Bienert[2], Hsu Lei Lee, Dominik von Elverfeldt[2], Chantal Mathis[3], Anne-Laurence Boutillier[3], Frédéric Blanc[4], Jean-Paul Armspach[1], and Laura-Adela Harsan[1,2,5]

[1]ICube, Université de Strasbourg-CNRS, Strasbourg, France, [2]Department of Radiology, Medical Physics, University Medical Center Freiburg, Freiburg, Germany, [3]Laboratoire de Neurosciences Cognitives et Adaptatives, Université de Strasbourg-CNRS, Strasbourg, France, [4]Centres Mémoire de Ressources et de Recherche, CHU de Strasbourg, Services Neurologiques et Gériatriques, Strasbourg, France, [5]Département de Biophysique et Médecine Nucléaire, Hôpitaux Universitaires de Strasbourg, CHU de Hautepierre, France

Resting state functional magnetic resonance imaging (rsfMRI) has opened a new window into the brain and its connectome, proposing abnormal functional connectivity as a candidate biomarker of brain pathologies[1]. We explored this pathway and performed rsfMRI and network analysis in the Thy-Tau22 transgenic mouse model of Alzheimer's disease, evaluating possible network signatures of early pathological states. We mapped the brain functional connectivity patterns and found overactive resting state BOLD signal in core players of the memory and learning systems, including the hippocampal network. This correlates with subtle memory deficits characterizing a very early pathological phenotype of the Thy-Tau22 mouse model.

4083 Computer 62

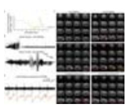

Imaging plasticity associated with hippocampal kindling using simultaneous LFP-ofMRI

Ben A Duffy[1], ManKin Choy[1], and Jin Hyung Lee[2]

[1]Department of Neurology, Stanford University, Stanford, CA, United States, [2]Departments of Neurology, Bioengineering, Neurosurgery, Electrical Engineering, Stanford University, Stanford, CA, United States

The kindling model of epilepsy is associated with a permanent form of synaptic potentiation, which is considered to be pathological. In this study we used optogenetic fMRI to observe changes in plasticity that occur following a kindling regime. Upon stimulation of the ventral hippocampus, post-kindling fMRI data displayed significantly more widespread activation, particularly in pre-frontal regions compared to pre-kindling acquisitions. Simultaneous LFP measurements were used to confirm the absence of epileptic activity that would confound the interpretation. This represents a powerful technique which can be used for understanding cognitive impairments or understanding the mechanism of anti-epileptogenic therapies.

4084 Computer 63

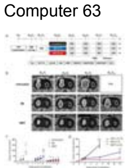

MRI monitoring of the in vivo permeability increase of brain tumor vessels induced by synchrotron microbeam radiation therapy

Audrey Bouchet[1,2], Marine Potez[3], Nicolas Coquery [3], Claire Rome[3], Benjamin Lemasson[3], Elke Bräuer-Krisch[4], Chantal Rémy[3], Jean Albert Laissue[5], Emmanuel Luc Barbier[3], Valentin Djonov[5], and Raphael Serduc[3]

[1]INSERM, Grenoble, France, [2]University of Bern, Bern, Switzerland, [3]INSERM, [4]ESRF, [5]University of Bern

Synchrotron microbeam radiation therapy (MRT), a spatially fractionated preclinical radiotherapy, is more efficient than broad beam irradiation (BB) at opening the blood-brain tumor barrier of intracranial rodent glioblastomas. MRT-induced increase of tumor vascular permeability is significantly greater, earlier and more prolonged than in the BB alone group, especially in highly proliferative areas. MRT targeted all tumor regions, including areas not impacted by BB. High dose microbeams might be used to facilitate the delivery of intravenously injected drugs to tumoral tissue: Adjuvant chemotherapy might thus be more effective when coupled with MRT than with homogeneous radiation fields used in conventional radiotherapy.

4085 Computer 64

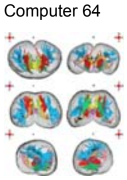

Diffusion Tractography Reveals Pervasive Asymmetry of Cerebral White Matter Tracts in the Bottlenose Dolphin

Alexandra Wright[1], Rebecca Theilmann[2], Sam Ridgway[3], and Miriam Scadeng[2]

[1]Scripps Institution of Oceanography, University of California San Diego, San Diego, CA, United States, [2]Radiology, University of California San Diego, San Diego, CA, United States, [3]National Marine Mammal Foundation, San Diego

Summary

Brain enlargement is associated with concomitant growth of interneuronal distance, increased conduction time, and reduced neuronal interconnectivity. Recognition of these functional constraints led to the hypothesis that large-brained mammals should exhibit greater structural and functional brain lateralization. As a taxon with the largest brains in the animal kingdom, Cetacea (whales, dolphins, and porpoises) provide a unique opportunity to examine asymmetries of brain structure and function. In the present study, diffusion tensor imaging (DTI) and tractography were used to investigate cerebral white matter asymmetry in the bottlenose dolphin.

4086 Computer 65

Mapping and modulation of Down Syndrome specific functional network in Dp(16)1yey mouse model

Laura-Adela Harsan[1,2,3], Meltem Karatas[1], Thu Lan NGUYEN[4], Anna Mechling[3], Tanzil Arefin [3], Thomas Bienert[3], Hsu-Lei Lee[3], Dominik von Elverfeldt[3], and Yann Herault[4]

[1]Engineering science, computer science and imaging laboratory (ICube), University of Strasbourg-CNRS France, Strasbourg, France, [2]Biophysics and Nuclear Medicine, Faculty of Medicine and University Hospital, Strasbourg, Strasbourg, France, [3]Medical Physics, AMIR, University Hospital, Freiburg, Freiburg, GA, Germany, [4]Translational medicine and neurogenetics, Institute of Genetics and Molecular Imaging, University of Strasbourg

Resting state functional MRI (rsfMRI) is currently the only non-invasive approach capable of giving insight into the large-scale cerebral networks architecture and its dynamic changes in pathology or following therapeutic interventions. With the aim of deciphering specific network signatures underlying memory and cognitive impairments in Down Syndrome pathology, we performed rsfMRI and network analysis in the Dp(16)1yey mouse model. We found perturbed synchrony of BOLD-signal in the hippocampal network of Dp(16)1yey mice. We further modulated this memory specific cerebral circuitry via therapeutic treatment with a DYRK1A kinase inhibitor, aimed at rescuing the memory and cognitive dysfunctions characterizing this mouse model.

4087 Computer 66

Integrated setup and characterization of an MRI-compatible PET camera for preclinical ultra-high field imaging

Nicola Bertolino[1], Yegor Sinelnikov[2], Dhaval Shah[1], Robert Zivadinov[1,3], and Ferdinand Schweser[1,3]

[1]Buffalo Neuroimaging Analysis Center, Department of Neurology, Jacobs School of Medicine and Biomedical Sciences, University at Buffalo, The State University of New York, Buffalo, NY, United States, [2]SynchroPET, Inc., Stony Brook, NY, United States, [3]MRI Clinical and Translational Research Center, Jacobs School of Medicine and Biomedical Sciences, University at Buffalo, The State University of New York, Buffalo, NY, United States

Simultaneous Positron Emission Tomography (PET) and Magnetic Resonance Imaging (MRI) in small animals would enable entirely new approaches to drug development and yield to a better functional understanding of living organisms. However, preclinical systems that allow truly simultaneous PET and MRI are not yet commercially available. We present the integration of an optimized microPET camera with ultra-high magnetic field strength MRI.

4088 Computer 67

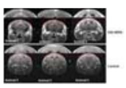

Preclinical detection of leptomeningeal inflammation using contrast-enhanced FLAIR at 9.4T in the EAE-MOG mouse model of Multiple Sclerosis

Nicola Bertolino[1], Suyog Pol[1], Robert Zivadinov[1,2], Natan Babek[1], Michelle Sudyn[1], Michele Sveinsson[1], Danielle Siebert[1], Marilena Preda[1,2], Dhaval Shah[1], and Ferdinand Schweser[1,2]

[1]Buffalo Neuroimaging Analysis Center, Department of Neurology, Jacobs School of Medicine and Biomedical Sciences, University at Buffalo, The State University of New York, Buffalo, NY, United States, [2]MRI Clinical and Translational Research Center, Jacobs School of Medicine and Biomedical Sciences, University at Buffalo, The State University of New York, Buffalo, NY, United States

Persistent clusters of inflammatory cells in the leptomeningeal compartment are thought to contribute directly to subpial cortical demyelination and neurodegeneration in MS patients. In human patients, post-contrast 3D T2-FLAIR allows the detection of leakage of contrast agent into inflammatory foci and the subarachnoid space. We propose a pulse sequence for LMI imaging in rodents and demonstrate its applicability in the EAE-MOG model of MS at 9.4T.

4089 Computer 68

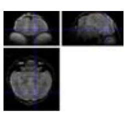

Correlation of striatal remodeling with changes in song performance: a longitudinal diffusion tensor imaging study of adult male zebra finches

Julie Hamaide[1], Kristina Lukacova[1,2], Lubica Kubikova[2], Marleen Verhoye[1], and Annemie Van der Van der Linden[1]

[1]Department of Biomedical Sciences, Bio-Imaging Lab, University of Antwerp, Wilrijk, Belgium, [2]Institute of Animal Biochemistry and Genetics, Slovak Academy of Sciences, Bratislava, Slovakia

In vivo diffusion tensor neuroimaging of adult male zebra finches was used to longitudinally monitor the effects of bilateral neurotoxic lesioning of a striatal component of the song control network and to explore possible causal relationships between the observed neuroplastic changes and specific alterations in song performance.

4090 Computer 69

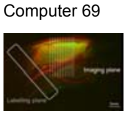

Application of multiphase pseudo-continuous ASL for quantitative blood flow measurement in rat brain metastasis

Manon A. Simard[1], James R. Larkin[1], Alexandre A. Khrapitchev[1], Kevin J. Ray[1], Michael A. Chappell[2], and Nicola R. Sibson[1]

[1]CRUK and MRC Oxford Institute for Radiation Oncology, Department of Oncology, University of Oxford, Oxford, United Kingdom, [2]Institute of Biomedical Engineering, Department of Engineering, University of Oxford, Oxford, United Kingdom

Arterial spin labelling (ASL) MRI is a useful clinical method of measuring blood flow in brain disorders such as tumours. This work presents a pre-clinical assessment of cerebral blood flow (CBF) by pseudo-continuous ASL in progressing rat breast cancer brain metastases. A statistically significant decrease in CBF of brain metastases was readily observed when tumours had grown sufficiently to breach the blood brain barrier, allowing gadolinium enhancement in T_1-weighted images. Upon histological analysis, the brain metastases proved to be hypoxic, consistent with a reduction in CBF in those regions.

4091 Computer 70

Brain-wide functional connectivity changes following self-administration of cocaine and a period of abstinence

Heather K. Decot[1,2], Sung-Ho Lee[3,4], Han Zhang[3,5], Fei Fei Wang[6], Regina M. Carelli[1,6], Yen-Yu Ian Shih[1,3,7,8], and Garret D. Stuber[1,2,9]

[1]Neuroscience curriculum, University of North Carolina at Chapel Hill, Chapel Hill, NC, United States, [2]Psychiatry, University of North Carolina at Chapel Hill, Chapel Hill, NC, United States, [3]Biomedical Research Imaging Center (BRIC), University of North Carolina at Chapel Hill, Chapel Hill, NC, United States, [4]Neurology, Chapel Hill, NC, United States, [5]Radiology, Chapel Hill, NC, United States, [6]Psychology, University of North Carolina at Chapel Hill, NC, United States, [7]Neurology, University of North Carolina at Chapel Hill, Chapel Hill, NC, United States, [8]Biomedical Engineering, Chapel Hill, NC, United States, [9]Cell Biology and Physiology, Chapel Hill, NC, United States*

Several different neural systems are likely to be dysregulated to promote maladaptive behaviors associated with drug addiction. Here, we investigate changes in global functional connectivity across the brain following self-administration of cocaine and a period of abstinence in rats. We found whole brain enhancement in synchronized activity immediately following cocaine self-administration compared to pre-cocaine. Furthermore, whole brain network connectivity continued to strengthen following a period of abstinence. These data suggest that the dynamic shifts in functional connectivity following cocaine exposure persist during periods of abstinence and may provide a critical mechanistic link to relapse susceptibility.

4092 Computer 71

Imaging of glutamate alterations in a mouse model of temporal lobe epilepsy

Niels Leonard Schwaderlapp[1], Philipp Janz[2], Jochen Leupold[1], Dominik von Elverfeldt[1], Jan Korvink[3], Jürgen Hennig[1], Carola Haas[2], and Pierre LeVan[1]

[1]Dept. of Radiology, Medical Physics, University Medical Center Freiburg, Freiburg, Germany, [2]Dept. of Neurosurgery, Experimental Epilepsy, University Medical Center Freiburg, [3]Institute of Microstructure Technology, Karlsruhe Institute of Technology

Hippocampal sclerosis involves neuronal loss in hippocampal subfields and is a common characteristic of temporal lobe epilepsy (TLE). Investigation of the metabolic alterations following a status epilepticus may lead to a better understanding of epileptogenesis and can reveal biomarkers for TLE. Overcoming the major disadvantages of single voxel ^{1}H MR spectroscopy, namely a low spatial and temporal resolution, this study investigates the capability of the glutamate chemical exchange saturation transfer (GluCEST) method to map endogenous glutamate alterations in a mouse model of TLE.

4093 Computer 72

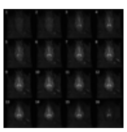

Hyperpolarized Water Perfusion in the Porcine Brain – a Pilot Study

Esben Søvsø Szocska Hansen[1,2], Kasper Wigh Lipsø[3], Rasmus Stilling Tougaard[1,4], Christoffer Laustsen[1], and Jan Henrik Ardenkjær-Larsen[3,5]

[1]The MR Research Centre, Aarhus University, 8200, Denmark, [2]Danish Diabetes Academy, Odense, Denmark, [3]Department of Electrical Engineering, Technical University of Denmark, [4]Department of Cardiology, Aarhus University Hospital, Denmark, [5]GE Healthcare, Denmark

Dynamic Contrast-Enhanced MR (DCE-MR) perfusion assessment with gadolinium contrast agents is currently the most widely used cerebral perfusion MR method. Hyperpolarized water has recently been shown to succeed 13C probes as angiography probe. In this study, we demonstrate the feasibility of hyperpolarized water for visualizing the brain vasculature of a large animal in a clinically relevant setting. In detail, reference perfusion values were obtained and large to small arteries could be identified.

Electronic Poster

Fetal & Pediatric Neuroimaging

Exhibition Hall — Tuesday 13:45 - 14:45

4094 Computer 73

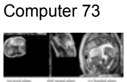

The development of automatic 3D fetal brain MRI analysis methods for depicting growth trajectories of fetal brain tissues

YISHAN LUO[1,2], LIN SHI[3,4,5], DANTONG MIAO[6], XIN ZHANG[6], Queenie Chan[7], Winnie CW CHU[1], BING ZHANG[6], and DEFENG WANG[1,8]

[1]Department of Imaging and Interventional Radiology, The Chinese University of Hong Kong, Hong Kong, Hong Kong, [2]Shenzhen Research Institute,The Chinese University of Hong Kong, Shenzhen, People's Republic of China, [3]Chow Yuk Ho Technology Center for Innovative Medicine, Hong Kong, [4]Therese Pei Fong Chow Research Centre for Prevention of Dementia, [5]Department of Medicine and Therapeutics, The Chinese University of Hong Kong, Hong Kong, [6]Department of Radiology, Nanjing Drum Tower Hospital,The Affiliated Hospital of Nanjing University Medical School, Nanjing, People's Republic of China, [7]Philips Healthcare, Hong Kong, [8]Shenzhen Research Institute, The Chinese University of Hong Kong, Shenzhen, People's Republic of China

In this paper, we proposed a set of fetal brain MRI analysis methods to quantify the fetal brain tissue volume. We used deep learning-based brain mask extraction method to obtain brain mask and reconstructed 3D fetal brain volumes using registration-based reconstruction method. Then an age-specific atlas-based segmentation method was applied to segment three major tissues (White Matter, cortical Gray Matter, cerebrospinal fluid). The changes of intracranial volume and the three brain tissue volumes across different gestational ages were calculated and fitted with both linear and quadratic curves. The results demonstrated the effectiveness of the automatic 3D fetal MRI quantification methods.

4095 Computer 74

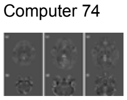

Developmental Susceptibility changes from neonate to early childhood using Quantitative Susceptibility Mapping (QSM)

Takuya Hinoda[1], Yasutaka Fushimi[1], Tomohisa Okada[1,2], Akira Yamamoto[1], Tsutomu Okada[1], and Kaori Togashi[1]

[1]Department of Diagnostic Imaging and Nuclear medicine, Graduate school of Medicine, Kyoto University, Kyoto, Japan, [2]Human Brain Research Center, Graduate School of Medicine, Kyoto University

To assess the susceptibility changes in early childhood (0 45 months) and these consistencies with previous reports. In our study, 35 children were enrolled and QSM was calculated from 3D gradient-echo images. Susceptibility values in deep gray matter structures showed positive correlation with the subjects' age and theoretical iron contents, and these in white matter structures showed negative correlation in posterior peduncle of internal capsule and optic radiation. These results reflect the normal neural development in the early childhood and QSM can provide us quantitative methods to evaluate brain development.

4096 Computer 75

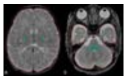

Quantification of myelin in children using multi-parametric quantitative MRI

Hyun Gi Kim[1], Jin Wook Choi[1], Sung-Min Gho[2], Young Ju Lee[2], and Ha Young Shin[3]

[1]*Radiology, Ajou University School of Medicine, Suwon, Korea, Republic of,* [2]*MR Apps & WF, GE Healthcare, Korea, Republic of,* [3]*Neurology, Yonsei University College of Medicine, Seoul, Korea, Republic of*

Clinical usage of myelination quantification is wide in children. With multi-parametric quantitative MRI, it is possible to acquire T1-weighted or T2-weighted contrast image simultaneously with absolute values of R1 and R2 relaxation rates and proton density. Using the absolute values, myelination water fraction (MWF) can be calculated.

4097 Computer 76

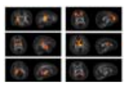

Patterns of Microstructural Correlations in the White Matter of the Neonatal Brain

Douglas C Dean III[1,2], Elizabeth M Planalp[1,3], William Wooten[2], Nagesh Adluru[1], H Hill Goldsmith[1,3], Richard J Davidson[1,2,3,4], and Andrew L Alexander[1,4,5]

[1]*Waisman Center, University of Wisconsin-Madison, Madison, WI, United States,* [2]*Center for Healthy Minds, University of Wisconsin-Madison, Madison, WI, United States,* [3]*Psychology, University of Wisconsin-Madison, Madison, WI, United States,* [4]*Psychiatry, University of Wisconsin-Madison, Madison, WI, United States,* [5]*Medical Physics, University of Wisconsin-Madison, Madison, WI, United States*

Quantitative MRI affords a unique opportunity to map dynamic patterns of neurodevelopment and provide insight into relations between brain maturation and emerging cognition. Using a data-driven technique, we investigated underlying patterns of white matter microstructure and subsequently examined the relationships of these microstructural correlations with respect to gestation-corrected age. We demonstrate that patterns of white matter development may be informative to studies of early brain development.

4098 Computer 77

Assessment of subcortical white matter myelination progression based on T2WI visual evaluation during the age of 6-48 months: a DTI-based validation study

Congcong Liu[1], Zhijie Jian[2], Xianjun Li[2], Chao Jin[3], Miaomiao Wang[3], Heng Liu[3], and Jian Yang[3]

[1]*Department of Diagnostic Radiology, the First Affiliated Hospital of Xi'an Jiaotong University, Xi'an,China, People's Republic of China,* [2]*Department of Diagnostic Radiology, the First Affiliated Hospital of Xi'an Jiaotong University, Xi'an 710061, P.R. China,* [3]*Department of Diagnostic Radiology, the First Affiliated Hospital of Xi'an Jiaotong University, Xi'an 710061, P.R. China, People's Republic of China*

Assessment of WM myelination is important to diagnose WM disorders in infants and children. We retrospectively evaluated 109 subjects (age of 6-48 months) using modified Cecilia Parazzini's scoring method based on T2WI visual evaluation. A significantly positive correlation was found between age and total scores of WM myelination with non-linear correlation coefficient of 0.948 (p<0.01). TBSS results demonstrated WM myelination progressed rapidly during age of 6-20 months and relatively stable during age of 21-48 months. The modified scoring method was more applicable to assess the WM myelination in infant with age of 6-20 months.

4099 Computer 78

Left	Right
Thalamic radiations	Centrum semiovale
Internal capsule (anterior limb)	Lateral splenium CC
Internal capsule (genu)	Lateral genu CC
Cerebral peduncle	Lateral anterior body CC
Optic radiations	Fornix
	External Capsule

White Matter Brain Asymmetries in Preterm and at Term Newborns

Paola Scifo[1,2], Pasquale Anthony Della Rosa[2,3], Elisa Marchetta[2,3], Silvia Pontesilli[2,3], Roberta Scotti[2,3], Antonella Poloniato[4], Andrea Falini[2,3], and Cristina Baldoli[2,3]

[1]*Nuclear Medicine Dept, San Raffale Scientific Institute, Milan, Italy,* [2]*CERMAC, San Raffaele University, Milan, Italy,* [3]*Neuroradiology Dept, San Raffaele Scientific Institute, Milan, Italy,* [4]*Pediatrics Dept, San Raffaele Scientific Institute, Milan, Italy*

Aim of this study is to investigate, through DTI, structural white matter (WM) asymmetries in newborns and compare these differences in control and in preterm newborns scanned at term. Both controls and preterms show multiple regions of asymmetries in all the DTI indices. A small area localised in the talamic radiations was found to have a significant difference of WM brain asymmetries between the two groups of subjects.

4100 Computer 79

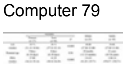

Axon development revealed by directional diffusivities in intra-axonal and extra-axonal compartments

Xianjun Li[1,2], Miaomiao Wang[1], Heng Liu[1,2], Jie Gao[1], Xiaocheng Wei[3], and Jian Yang[1]

[1]*Department of Radiology, the First Affiliated Hospital, Xi'an Jiaotong University, Xi'an, People's Republic of China,* [2]*Department of Biomedical Engineering, the Key Laboratory of Biomedical Information Engineering of the Ministry of Education, School of Life Science and Technology, Xi'an Jiaotong University, Xi'an, People's Republic of China,* [3]*MR Research China, GE Healthcare, Bei Jing, People's Republic of China*

White matter in human brain undergoes a complex and long lasting process. It is not likely that conventional diffusion parameters are specific enough to distinguish axon-related and myelin-related processes. This study investigates directional diffusivities in intra-axonal and extra-axonal compartments on preterm neonates, term neonates, infants, and adults. Two change patterns of extra-axonal axial and radial diffusivities are found during development. This may be related to premyelination and myelination. Developmental changes of the fiber dispersion and intra-axonal diffusivities are observed in both pre-myelination and myelination periods. Directional diffusivities in intra-axonal and extra-axonal compartments provide more detailed information to evaluate axonal development.

4101 Computer 80

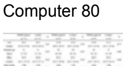

Characterization of Extensive Microstructural Variations Associated with Punctate White Matter Lesions in Preterm Neonates

Xianjun Li[1,2], Jie Gao[1], Miaomiao Wang[1], Edward S. Hui[3], Xiaocheng Wei[4], and Jian Yang[1]

[1]*Department of Radiology, the First Affiliated Hospital, Xi'an Jiaotong University, Xi'an, People's Republic of China,* [2]*Department of Biomedical Engineering, the Key Laboratory of Biomedical Information Engineering of the Ministry of Education, School of Life Science and Technology, Xi'an Jiaotong University, Xi'an, People's Republic of China,* [3]*Department of Diagnostic Radiology, the University of Hong Kong, Hong Kong, People's Republic of China,* [4]*MR Research China, GE Healthcare, Bei Jing, People's Republic of China*

Punctate white matter lesions (PWML) are common in preterm neonates. Neurodevelopmental outcome of the neonates is related to the lesion extensions. This study aimed to characterize the extent of microstructural variations for different PWML grades. White matter microstructural variations were different across PWML grades. The severe PWML were associated with extensive microstructural changes. Pattern of increased AD, increased RD, and reduced/unchanged FA was found proximal to the PWML. Unchanged AD, increased RD, and reduced/unchanged FA were observed in the vast regions distal from the PWML. These findings may help in determining outcomes of PWML and treatment strategies.

4102 Computer 81

Convolutional Neural Networks for Identifying Preterm Infants at High Risk of Developmental Disorders

Ahmed Serag[1], Emma J Telford[1], Scott Semple[1], and James P Boardman[1]

[1]*University of Edinburgh, Edinburgh, United Kingdom*

Preterm birth is a major cause of neuropsychiatric impairment in childhood and leads to significant long-term clinical, educational and social problems. A major issue confronting clinicians who work with preterm infants and their families is the identification of infants who are most at risk for subsequent neurodevelopmental disability and who may benefit from early intervention services. We designed a system for the identification of preterm infants at high risk of developmental disorders using convolutional neural networks (CNN). The designed network yields an accuracy of 83.33%, and is applicable to the automated analysis of larger study cohorts.

4103 Computer 82

Music training enhances functional connectivity in preterm newborns

Serafeim Loukas[1,2], Lara Lordier[1,3], Frédéric Grouiller[4], Didier Grandjean[3], François Lazeyras[5], Dimitri Van de Ville[2,5], and Petra S. Hüppi[1]

[1]*Division of Development and Growth, Department of Pediatrics, University Hospital of Geneva, Geneva, Switzerland,* [2]*Institute of Bioengineering, Ecole Polytechnique Fédérale de Lausanne, Lausanne, Switzerland,* [3]*Neuroscience of Emotion and Affective Dynamics Lab, Department of psychology, University of Geneva, Geneva, Switzerland,* [4]*Swiss center for affective neurosciences, University of Geneva, Geneva, Switzerland,* [5]*Department of Radiology and Medical Informatics, University of Geneva, Geneva, Switzerland*

In this study we examined the impact of the environmental enrichment of preterm newborns with music on auditory cortex functional connectivity. A group of preterm infants listened to music from 33 weeks gestational age until term equivalent age. Two control groups were used: preterm and full-term infants without music. Auditory cortex functional connectivity with cerebral regions known to be implicated in tempo and familiarity processing were identified for preterm newborns that had music training during their stay in the NICU using Psychophysiological Interaction (PPI) analyses. Our results suggest that music training during hospitalization can modify functional connectivity in the newborn brain.

4104 Computer 83

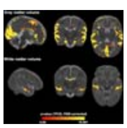

Early life predictors of brain development at term-equivalent age in infants born across the gestational ages.

Deanne K Thompson[1,2,3], Claire E Kelly[1], Jian Chen[1,4], Richard Beare[1,4], Marc L Seal[1,3], Peter J Anderson[1,3], Lex W Doyle[1,5,6], Alicia J Spittle[1,5,7], and Jeanie LY Cheong[1,5,6]

[1]*Murdoch Childrens Research Institute, Melbourne, Australia,* [2]*Florey Institute of Neuroscience and Mental Health, Melbourne, Australia,* [3]*Department of Paediatrics, The University of Melbourne, Melbourne, Australia,* [4]*Department of Medicine, Monash Medical Centre, Monash Univeristy, Melbourne, Australia,* [5]*Royal Women's Hospital, Melbourne, Australia,* [6]*Department of Obstetrics and Gynaecology, The University of Melbourne, Melbourne, Australia,* [7]*Department of Physiotherapy, The University of Melbourne, Melbourne, Australia*

Many early life factors contribute to how well a preterm child will develop, and these affect the brain differently based on how early the infant is born. The current study found that earlier gestational age is related to smaller brain volumes and less mature white matter at term-equivalent age. Correlated with these brain measures were lower birthweight SD score, multiple birth or high social risk. We show that infants born moderate and late preterm have altered brain development, not just those born very preterm, and there is a differential effect of early life predictors based on gestational age.

4105 Computer 84

Investigating early brain-behaviour relationships in infants born preterm using whole brain, multimodal magnetic resonance imaging

Claire E Kelly[1], Alicia J Spittle[1,2,3], Jeanie LY Cheong[1,3,4], Jian Chen[1,5], Joy E Olsen[1,3], Abbey L Eeles[1], Jennifer M Walsh[1,3,4,6], Marc L Seal[1,7], Peter J Anderson[1,7], Lex W Doyle[1,3,4,7], and Deanne K Thompson[1,7,8]

[1]*Murdoch Childrens Research Institute, Melbourne, Australia,* [2]*Department of Physiotherapy, The University of Melbourne, Melbourne, Australia,* [3]*Newborn research, Royal Women's Hospital, Melbourne, Australia,* [4]*Department of Obstetrics and Gynaecology, The University of Melbourne, Melbourne, Australia,* [5]*Department of Medicine, Monash Medical Centre, Monash University, Melbourne, Australia,* [6]*Pediatric, Infant, Perinatal Emergency Retrieval (PIPER), Royal Children's Hospital, Melbourne, Australia,* [7]*Department of Paediatrics, The University of Melbourne, Melbourne, Australia,* [8]*Florey Institute of Neuroscience and Mental Health, Melbourne, Australia*

The neonatal period is critical for brain development, however relationships between the brain and behaviour early in life are poorly understood. This study investigated relationships between whole brain, multimodal, quantitative magnetic resonance imaging (MRI) measures and neurobehavioural function in 257 preterm infants at term-equivalent age. Voxel-based morphometry and tract-based spatial statistics identified regions where grey and white matter volume and white matter microstructure were associated with various aspects of neurobehavioural function, with regions varying depending on the function. Thus, this study improves knowledge of brain-behaviour relationships early in life, which may help with predicting long-term outcomes and assessing early interventions to improve outcomes.

4106 Computer 85

Neonatal whole brain volume and microstructure in infants born preterm and neurodevelopmental outcomes at 2 years of age

Claire E Kelly[1], Jeanie LY Cheong[1,2,3], Alicia J Spittle[1,2,4], Jian Chen[1,5], Marc L Seal[1,6], Peter J Anderson[1,6], Lex W Doyle[1,2,3,6], and Deanne K Thompson[1,6,7]

[1]Murdoch Childrens Research Institute, Melbourne, Australia, [2]Newborn research, Royal Women's Hospital, Melbourne, Australia, [3]Department of Obstetrics and Gynaecology, The University of Melbourne, Melbourne, Australia, [4]Department of Physiotherapy, The University of Melbourne, Melbourne, Australia, [5]Department of Medicine, Monash Medical Centre, Monash Univeristy, Melbourne, Australia, [6]Department of Paediatrics, The University of Melbourne, Melbourne, Australia, [7]Florey Institute of Neuroscience and Mental Health, Melbourne, Australia

Infants born preterm are at risk of neurodevelopmental delays in childhood, and MRI may improve knowledge of underlying cerebral changes. Relationships were investigated between whole brain volumes and microstructure in 256 preterm infants and neurodevelopmental outcomes at age 2 years using voxel-based morphometry and tract-based spatial statistics. Lower grey and white matter volumes and altered white matter microstructure were associated with poorer outcomes. In general, relatively widespread brain regions were associated with cognition, more central regions with cerebral palsy, and more peripheral regions with language. This study provides further understanding of how brain structure in preterm infants is related to longer-term outcomes.

4107 Computer 86

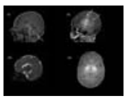

The type and prevalence of incidental findings on magnetic resonance imaging of the low risk term born neonatal brain.

Emer J Hughes[1], Olivia Carney[2], Nora Tusor[1], Kelly Pegoretti[1], Sophie Arulkumaran[1], Lucilio Cordeo-Grande[3], Christopher Kelly[1], Madeline Barnett[1], Michelle Krishnan[1], Johannes Steinweg[1], Joanna Allsop[1], Ana Dos Santos Gomes[1], Julia Wurie[1], Jose Bueno-Conde[1], Matthew Fox[1], Amber Strang[1], Maryanne Sharma[1], Suresh Victor[1], Counsell J Serena[1], David A Edwards[1], Joseph V Hajnal[3], and Mary A Rutherford[1]

[1]Perinatal Imaging and Health, Kings College London, London, United Kingdom, [2]Paediatric radiology, Great Ormond Street Hospital, London, United Kingdom, [3]Biomedical engineering and imaging sciences, Kings College London, London, United Kingdom

The aim of this study was to ascertain the prevalence and type of incidental findings present in the low risk term brain using MRI. Out of 200 infants, 105 had incidental findings, with 8 requiring follow-up assessment. Common findings included subdural haemorrhage, punctate and cystic lesions and hyperintense signal of the basal ganglia. Findings requiring further assessment included subarachnoid, cerebellar, and germinal matrix haemorrhages, ectopic posterior pituitary lobe, subepenymal heterotopia and venous infarcts. Prevalence of incidental findings in this cohort is significant. Communicating to parents the possibility of detecting abnormalities and referral pathways are important considerations in neonatal research.

4108 Computer 87

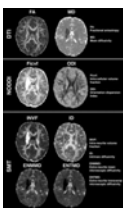

Characterizing brain microstructural changes in childhood arterial ischemic stroke using multi-shell diffusion magnetic resonance imaging

Joseph Yuan-Mou Yang[1,2,3], Richard Beare[3,4], Belinda Stojanovski[2,5], Wirginia J Maixner[1,2], Marc L Seal[3,6], and Mark T Mackay[2,5]

[1]Neurosurgery, Royal Children's Hospital, Melbourne, Australia, [2]Neuroscience Research, Murdoch Childrens Research Institution, Melbourne, Australia, [3]Developmental Imaging, Murdoch Childrens Research Institution, Melbourne, Australia, [4]Stroke and aging research group, Department of Medicine, Monash University, Melbourne, Australia, [5]Neurology, Royal Children's Hospital, Melbourne, Australia, [6]Paediatrics, University of Melbourne, Melbourne, Australia

Imaging markers that can infer microstructural changes occurring in childhood arterial ischemic stroke (CAIS) may lead to a better understanding of the disease's neurobiological substrates. We applied both the Neurite Orientation Dispersion and Density Imaging (NODDI) and the Spherical Mean Technique (SMT) diffusion compartment models to two-shell diffusion data acquired in four acute CAIS patients. We demonstrate that parameter estimates derived from the stroke-affected regions were consistent with known microstructural changes described in acute stroke histopathology. The magnitudes of parameter changes were associated with stroke severity, and the motor outcomes at follow-up.

4109 Computer 88

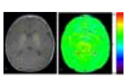

Amide proton transfer imaging of neonatal brain injury: a preliminary study

Yang Zheng[1], Xiaoming Wang[2], and Xuna Zhao[3]

[1]Shengjing Hospital of China Medical University, shenyang, People's Republic of China, [2]Shengjing Hospital of China Medical University, People's Republic of China, [3]Philips Healthcare, People's Republic of China

The environment of the brain dynamically changes with neonatal brain development, and the topic of whether the application of magnetic resonance imaging (MRI) can reflect these brain environment changes is a recent one. In recent years, a new magnetic resonance contrast technology called amide proton transfer (APT) imaging has emerged which can detect protein and peptides through the signal from water (1), reflecting in vivo pH and protein concentration at the cellular and molecular level. The so-called amide proton mainly refers to the amide proton from the free protein and the polypeptide backbones.

4110 Computer 89

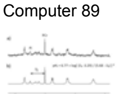

Deep grey matter brain alkalosis in neonatal encephalopathy measured using 31P ISIS is associated with seizure burden and poor outcomes

David Price[1], Cristina Uria-Avellanal [2], Magdalena Sokolska[1], Subhabrata Mitra[2], Alan Bainbridge[1], Xavier Golay[3], and Nicola Robertson[4]

[1]Medical Physics and Biomedical Engineering, UCLH NHS Trust, London, United Kingdom, [2]Neonatology, UCLH NHS Trust, London, United Kingdom, [3]Institute of Neurology, University College London, [4]Institute for Women's Health, University College London

31P image selected in vivo spectroscopy was used to measure deep grey matter intracellular pH in 43 neonates with hypoxic-ischaemic encephalopathy. All neonates had previously received therapeutic hypothermia, the current standard of care. Brain alkalosis was associated with poor outcomes reproducing what was found from whole-brain pH measurements in the pre-cooling era. Brain alkalosis was associated with increased seizure burden, the first time this has been shown in babies. Avoiding brain alkalosis could be a new objective for treating seizures and for neuroprotection in neonatal encephalopathy.

4111 Computer 90

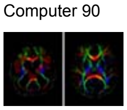

Diffusion-Weighted MR Signal Sparsity Indicates Impaired White Matter Organization in Lissencephaly

Vishal Patel[1] and Noriko Salamon[1]

[1]University of California, Los Angeles, Los Angeles, CA, United States

We demonstrate a novel technique for studying white matter pathology by examining the statistical properties of the DWI signal. We apply a sparse coding method, K-SVD, to decompose a diffusion-weighted series. We then quantify the efficiency of the resulting encoding by computing the Gini coefficient. We show that this measure is abnormally decreased in a cohort of lissencephaly patients compared to age-matched control subjects. Our results support the hypotheses that more organized white matter can be more sparsely encoded and that the sparsity of the encoding may thus be used to infer pathological white matter states.

4112 Computer 91

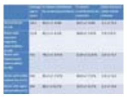

VOLUMETRIC BRAIN FINDINGS IN CHILDREN WITH SEIZURES

PhuaHwee TANG[1] and HsiaoPiau NG

[1]*Diagnostic and Interventional Imaging, KK Women's and Children's Hospital, Singapore, Singapore*

Retrospective study of MRI brains with volumetric measurements done using voxel based morphology was conducted for children with seizures imaged in KK Women's and Children's Hospital since 2006. There was decreased cerebral volume and increased ventricular volume in children with hippocampal abnormalities compared to children with structurally normal brain, the difference in volumes exceeding 1 standard deviation, not statistically significant likely on account of the small sample sizes. Relative reduced grey matter to white matter is seen in children with hippocampal abnormalities as well as in children with neuronal migration abnormalities, reaching statistical significance in both groups.

4113 Computer 92

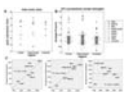

Imaging Genomics of Young Children with Global Developmental Delay: Preliminary DTI connectome study correlated with Allen brain atlas gene expression level

Jeong-Won Jeong[1,2], Harry Chugani[3], Michael Behen[1,2], and Senthil Sundaram[1,2]

[1]*Pediatrics and Neurology, Wayne State University, Detroit, MI, United States,* [2]*Translational Imaging Lab, Children's Hospital of Michigan, Detroit, MI, United States,* [3]*Neurology, Nemours DuPont Hospital for Children, Wilmington, DE, United States*

This study is to investigate if different types of genetic mutations observed in children with global developmental delay (GD) are associated with white matter dysmorphologies and neuropsychological assessments. Eight children with GD having different mutations underwent a 3T MRI including diffusion tensor imaging with topological whole brain connectome analysis. Four of eight GD-associated mutations having high gene expression level in frontal and hippocampal regions showed apparently increased connectivity strengths in frontal and hippocampal regions which were significantly correlated with three behavioral phenotypes (IQ, memory, communication) suggesting that white matter abnormalities in different regions are perhaps driven by different genetic mutations.

4114 Computer 93

CEREBELLAR TRACTOGRAPHY STUDY ON ADOLESCENT IDIOPATHIC SCOLIOSIS

Cindy Xue[1], Lin Shi[2], Steve C.N Hui[1], Tsz-ping Lam[3], Bobby K.W Ng[3], Jack C.Y Cheng[3], and Winnie C.W Chu[4]

[1]*Department of Imaging and Interventional Radiology, The Chinese University of Hong Kong, Hong Kong, Hong Kong,* [2]*Department of Medicine and Therapeutics, The Chinese University of Hong Kong,* [3]*Department of Orthopedics and Traumatology, The Chinese University of Hong Kong,* [4]*Department of Imaging and Interventional Radiology, The Chinese University of Hong Kong*

Adolescent Idiopathic Scoliosis (AIS) is a 3-dimensional spinal deformity which occurs predominantly in adolescent girls. Impaired postural balance and tonsillar ectopia are reported findings in AIS. This study sought to investigate and compare white matter integrity of the cerebellar pathways in AIS with matched controls. Anatomically-guided deterministic tractography was used to reconstruct the cerebellar pathways. Lower FA value was found in spinocerebellar tract and in intracerebellar tract in AIS, suggestive of, reduced white matter integrity of the cerebellar pathway, which is in agreement with similar changes in other white matter pathways within the brain of AIS patients.

4115 Computer 94

Increased Global Functional Connectivity in Hormonal Maturation Girls: a Resting-State Functional MRI Study

Wenjing Zhang[1], Yaxin Zhu[2], Di Yang[2], Peining Liu[3], Zhihan Yan[2], and Su Lui[1]

[1]*Huaxi MR Research Center (HMRRC), Department of Radiology, West China Hospital of Sichuan University, Chengdu, People's Republic of China,* [2]*Radiology, The Second Affiliated Hospital & Yuying Children's Hospital of Wenzhou Medical University, Wenzhou, People's Republic of China,* [3]*Child Health Care, The Second Affiliated Hospital & Yuying Children's Hospital of Wenzhou Medical University, Wenzhou, People's Republic of China*

To investigate the impact of hormone maturation on brain function and psychological development, seventy-three girls aged 6-11 years were enrolled. Using the global voxel-wise functional connectivity, we found that girls with hormonal maturation showed significantly greater functional connectivity strength mainly in the default mode network and limbic system, relative to girls who were not hormonally maturated. While these two networks contribute substantially to the social cognition, cognitive processing and emotion regulation, our finding suggested that the hormonal maturation manifested its effects greatly on regions which are crucial to the social, self-referencial, and emotional cognition development.

4116 Computer 95

Longitudinal Hypergraph Learning: A Consistent Segmentation Method for Measuring the Growth Trajectory of Infant Hippocampus from Brain MR Images

Yanrong Guo[1,2], Pei Dong[1], Guorong Wu[1], Weili Lin[1], and Dinggang Shen[1]

[1]*Department of Radiology and BRIC, The University of North Carolina at Chapel Hill, Chapel Hill, NC, United States,* [2]*School of Computer and Information, Hefei University of Technology, Hefei, People's Republic of China*

Automatic and consistent hippocampus segmentation from longitudinal infant brain MR image sequences is crucial for the measurement and analysis of its growth trajectory during early brain developing stage. To achieve this goal, we propose to use the longitudinal hypergraph method for joint learning the MR images from multiple acquisition time-points. We apply the proposed method to segment hippocampus from infant brain MR dataset which contains five time-points from 2 weeks to 12 months of age. According to the experimental results, our method outperforms other state-of-the-art label fusion methods in terms of both segmentation accuracy and consistency.

4117 Computer 96

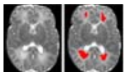

Early Prediction of Cognitive Deficits in Very Preterm Infants using Machine Learning Algorithms

Lili He[1,2] and Nehal A. Parikh[1,2]

[1]Perinatal Institute, Cincinnati Children's Hospital Medical Center, Cincinnati, OH, United States, [2]Department of Pediatrics, University of Cincinnati College of Medicine, Cincinnati, OH, United States

By school age, 30-50% of very preterm infants exhibit cognitive deficits. Unfortunately, cognitive deficits cannot be reliably diagnosed until 3 to 5 years of age. These early years are now recognized as critical for neuroplasticity when early intervention therapies can enhance infants' ability to reach their full cognitive potential. Diffuse white matter abnormality (DWMA) is seen on term-equivalent age MRI in 50-75% of very preterm infants and is predictive of cognitive deficits. In this study, we examined features of DWMA and conducted personalized prediction in very preterm infants, soon after birth, using machine learning algorithms.

Electronic Poster

Alzheimer's Disease

Exhibition Hall Tuesday 13:45 - 14:45

4118 Computer 97

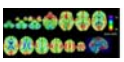

Detecting Perfusion Deficit in AD and MCI by Resting-State Functional MRI

Tianyi Qian[1], Zhigang Qi[2], and Kuncheng Li[2]

[1]MR Collaboration NE Asia, Siemens Healthcare, Beijing, People's Republic of China, [2]Radiology, Xuanwu Hospital Capital Medical University, Beijing, People's Republic of China

Resting-state fMRI has been widely used to investigate the functional deficits of Alzheimer's disease (AD) and mild cognitive impairment (MCI). In this study, we applied this method to investigate the differences in tissue perfusion deficits between MCI, AD, and normal control (NC) groups. The results show that the AD and MCI groups have areas with less fast perfusion than normal controls. While the MCI group has more perfusion deficits in the frontal lobe, the AD group has more perfusion deficits in the parietal and occipital lobe.

4119 Computer 98

Degeneracy between apolipoprotein E ε3 and ε4 alleles predicts elderly episodic memory variation: a longitudinal study with independent validation

Hao Shu[1,2], Gang Chen[2], Zan Wang[1], Duan Liu[1], Guangyu Chen[2], B. Douglas Ward[2], Chunxian Yue[1], Fan Su[1], Lihua Gu[1], Feng Bai[1], Shi-Jiang Li[2], and Zhijun Zhang[1]

[1]Department of Neurology, Affiliated ZhongDa Hospital, Neuropsychiatric Institute and Medical School of Southeast University, Nanjing, People's Republic of China, [2]Department of Biophysics, Medical College of Wisconsin, Milwaukee, WI, United States

We reported distinct EM neural correlates among APOE alleles in elderly subjects but still unclear whether and how the APOE ε4 carriers' distinct EM neural correlates contribute to an increased risk of AD onset. This study found that higher HFC strength in the EM neural correlates correlated with better longitudinal EM performance in the APOE ε3ε3 subjects but associated with inferior longitudinal EM performance in the ε4 carriers. These findings indicate that the degeneracy of EM function advance differential AD onset risk among APOE alleles, and provide a potential tool to predict APOE ε4 carriers with impending cognitive decline.

4120 Computer 99

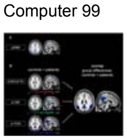

Reduced BOLD connectivity is related to hypoperfusion in Alzheimer's disease

Jens Goettler[1], Isabelle Riederer[1], Lorenzo Pasquini[1], Stephan Kaczmarz[1], Claus Zimmer[1], Christine Preibisch[1], and Christian Sorg[1]

[1]Department of Neuroradiology, Technische Universität München, Munich, Germany

BOLD-functional connectivity (BOLD-FC) is decreased in Alzheimer's disease (AD), and suggested to reflect reduced coherence of neural activity. However, the BOLD signal is based on vascular hemodynamics, therefore, impaired perfusion might also contribute to reduced BOLD-FC. Here, 32 AD patients and 22 controls underwent a simultaneous MR/PET, assessing BOLD-FC by resting-state fMRI, baseline CBF by pASL, and neuronal activity by FDG-uptake. Patients' BOLD-FC, CBF, and FDG-uptake were reduced within the same precuneal regions. BOLD-FC was positively associated with mean CBF, specifically in patients and independently from FDG-uptake. Data indicate that impaired vascular hemodynamics contribute to reduced BOLD-FC in AD.

4121 Computer 100

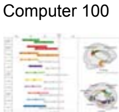

Fibre-specific white matter changes in Alzheimer's disease: novel insights from Fixel-Based Analysis

Remika Mito[1,2], David Raffelt[1], Thijs Dhollander[1], David N Vaughan[1,2,3], Olivier Salvado[4], Amy Brodtmann[1,2,5], Christopher Rowe[6,7], Victor L Villemagne[2,6,7], and Alan Connelly[1,2]

[1]Florey Institute of Neuroscience and Mental Health, Melbourne, Victoria, Australia, [2]Florey Institute of Neuroscience and Mental Health, University of Melbourne, Melbourne, Victoria, Australia, [3]Department of Neurology, Austin Health, Victoria, Australia, [4]Health & Biosecurity, CSIRO, Brisbane, Queensland, Australia, [5]Eastern Clinical Research Unit, Box Hill Hospital, Monash University, Victoria, Australia, [6]Department of Medicine, Austin Health, University of Melbourne, Victoria, Australia, [7]Department of Molecular Imaging & Therapy, Centre for PET, Austin Health, Heidelberg, Victoria, Australia

Alzheimer's disease (AD) is characterised by extensive white matter disruption, however voxel-based studies have been unable to provide fibre-specific insight into how this alters brain connectivity. Here, we applied fixel-based analysis (FBA) to diffusion MRI data to investigate changes in AD and mild cognitive impairment (MCI) patients. AD patients exhibited significant reductions in both fibre density and cross-section across multiple fibre tracts, while significant decreases in MCI were only evident in the posterior cingulum and uncinate, upon tract-of-interest analysis. This work demonstrates the value of FBA in identifying both macroscopic and microscopic changes to specific fibre pathways in the investigation of AD.

4122 Computer 101

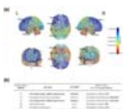

Machine learning on resting state fMRI classifies the prevalent underlying disease in subjects with mixed dementia

Gloria Castellazzi[1,2], Letizia Casiraghi[2,3], Giovanni Savini[2,4], Fulvia Palesi[2,5], Paolo Vitali[6], Nicoletta Anzalone[7], Elena Sinforiani[8], Giovanni Magenes[1], Cristina Cereda[9], Claudia AM Gandini Wheeler-Kingshott[3,6,10], Giuseppe Micieli[11], and Egidio D'Angelo[2,3]

[1]Department of Electrical, Computer and Biomedical Engineering, University of Pavia, Pavia, Italy, [2]Brain Connectivity Center, C. Mondino National Neurological Institute, Pavia, Italy, [3]Department of Brain and Behavioral Sciences, University of Pavia, Pavia, Italy, [4]Department of Physics, University of Milan, Mialn, Italy, [5]Department of Physics, University of Pavia, Pavia, Italy, [6]Brain MRI 3T research center, C. Mondino National Neurological Institute, Pavia, Italy, [7]Scientific Institute H.S. Raffaele, Milan, Italy, [8]Neurology Unit, C. Mondino National Neurological Institute, Pavia, Italy, [9]Genomic and Post-Genomic Center, C. Mondino National Neurological Institute, Pavia, Italy, [10]Queen Square MS Centre Department of Neuroinflammation, UCL Institute of Neurology, London, United Kingdom, [11]Department of Emergency Neurology, C. Mondino National Neurological Institute, Pavia, Italy

Evidence from recent studies suggests that machine learning applied on MRI can be used to reliably differentiate Alzheimer disease from other major dementia diseases, e.g. Vascular Dementia (VD). In this work we used a machine learning approach applied on features derived from resting state fMRI (rs-fMRI) to build a model that is able not only to differentiate AD from VD, but also to classify the prevalent underlying disease (AD or VD) in a group of early dementia patients for whom clinical profile presented major overlap between symptoms of AD and symptoms of VD (i.e. mixed dementia subjects, MXD).

4123 Computer 102

Constant decline in Alzheimer's disease: A brain morphometry study.

Jeam Haroldo Oliveira Barbosa[1], Silvio Ramos Bernardes da Silva Filho[2], Carlo Rondinoni[2], Antonio Carlos Santos[2], Carlos Ernesto Garrido Salmon[1], Nereida Kilza Costa Lima[2], Eduardo Ferriolli[2], and Júlio César Moriguti[2]

[1]InBrain Lab, Department of Physics, Faculty of Philosophy, Sciences and Letters of Ribeirão Preto, University of Sao Paulo, Ribeirão Preto, SP, Brazil, [2]Ribeirao Preto Medical School, University of Sao Paulo, Ribeirao Preto, SP, Brazil

Constant atrophy in Alzheimer's disease is observed until the later DAD stages.

4124 Computer 103

Towards automated MP2RAGE-based hippocampal volumetry for routine clinical practice

Bénédicte Maréchal[1,2,3], Sophie Espinoza[4], Wadie Ben Hassen[5], Tobias Kober[1,2,3], Christophe Habas[4], and Alexis Roche[1,2,3]

[1]Advanced Clinical Imaging Technology, Siemens Healthcare HC CEMEA SUI DI PI, Lausanne, Switzerland, [2]Department of Radiology, CHUV, Lausanne, Switzerland, [3]LTS5, EPFL, Lausanne, Switzerland, [4]Service de NeuroImagerie, Centre Hospitalier National d'Ophtalmologie des XV-XX, Paris, France, [5]Siemens Healthcare S.A.S., Saint-Denis, France

We investigate the potential of an automated method to provide hippocampal volume estimates using T1-weighted images obtained from the MP2RAGE sequence. Scheltens visual medial temporal atrophy scores from 27 patients undergoing clinical brain MRI for workup of cognitive decline were compared to automated volumetric measures using multinomial logistic regression. Strong correlation was observed which suggests that the employed hippocampal volumetry method may help supporting diagnosis of neurodegenerative diseases.

4125 Computer 104

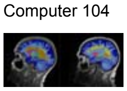

Diagnostic Decision Support in Alzheimer's Disease: Predicting Typical and Mixed Forms from Combined Routine Brain Volumetry and Cognitive Assessment

Alexis Roche[1,2,3], Daniel Damian[4], Frédéric Pedron[1], Bénédicte Maréchal[1,2,3], Patric Hagmann[1], Philippe Maeder[1], Reto Meuli[1], Tobias Kober[1,2,3], and Jean-François Démonet[4]

[1]Department of Radiology, CHUV, Lausanne, Switzerland, [2]Advanced Clinical Imaging Technology, Siemens Healthcare AG, Lausanne, Switzerland, [3]LTS5, EPFL, Lausanne, Switzerland, [4]Leenaards Memory Centre, CHUV, Lausanne, Switzerland

We implemented an automated classifier using T1-weighted magnetic resonance imaging-based brain volumetry and the Montreal Cognitive Assessment test to predict whether patients of a University Memory Clinic with suspected neurocognitive disorders have subjective complaints, or suffer from either typical or mixed forms of Alzheimer's disease. The classifier achieved an accuracy of 80.8% and was found to require both psychometric and brain morphometric data to perform best.

4126 Computer 105

The effects of a Western-type diet on the cerebrovascular response to hypercapnia in a double transgenic mouse model for Alzheimer's Disease

Kristof Govaerts[1], Jessica Sternisa[1], Tom Dresselaers[2], Fred Van Leuven[3], and Uwe Himmelreich[1]

[1]Imaging & Pathology, KU Leuven, Leuven, Belgium, [2]Radiology, UZ Leuven, Leuven, Belgium, [3]Human Genetics, KU Leuven, Leuven, Belgium

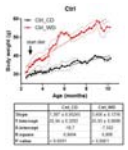

Alzheimer's Disease (AD) is the most common neurodegenerative disease, and is influenced by various environmental factors. In this study, we evaluate the effect of a high-fat, high-sugar 'Western-type' diet on the on the vascular response capacity to hypercapnia in a double transgenic (APP/PS1) mouse model of AD. We make use of Arterial Spin Labelling to investigate basal perfusion and cerebrovascular response to hypercapnia (CVR) in the hippocampus, cortex and thalamus.

4127 Computer 106

Can measuring hippocampal atrophy over a 3 year interval with a fully automatic method be substantially less noisy than manual?

Keith S Cover[1], Ronald A van Schijndel[2], Adriaan Versteeg[2], Alberto Redolfi[3], Paolo Bosco[3], Soheil Damangi[4], Bob W van Dijk[1], Hugo Vrenken[1,2], Giovanni B Frisoni[3,5], and Frederik Barkhof[2]

[1]Physics and Medical Technology, VU University Medical Center, Amsterdam, Netherlands, [2]Radiology, VU University Medical Center, Amsterdam, Netherlands, [3]IRCCS SanGiovannidiDioFatebenefratelli, Italy, [4]KarolinskaInstitutet, Stockholm, Sweden, [5]University Hospitals and University of Geneva, Switzerland

The segmentation noise of hippocampal atrophy measurement methods can be measured using the back-to-back (BTB) reproducibility with the ADNI1 data set. Previous studies have only measured the segmentation noise over a one year interval. In the current study, two methods are shown to be substantially less noisy than manual hippocampal atrophy measurements over both 1 and 3 years - MAPS-HBSI and the recent FreeSurfer 6.0 Beta B (Build 20161008). Scatter plots of the 1 year versus 3 year BTB differences were found to be a particularly simple and effective way to display the segmentation noise of a method.

4128 Computer 107

The disturbed subcortical local intrinsic activity synchronism in mild cognitive impairment and its association with spatial navigation ability: a resting-state fMRI study

Zhao Qing[1], Weiping Li[1], Wenbo Wu[1], Fangfang Wang[1], Renyuan Liu[1,2], Zuzana Nedelska[3,4], Jakub Hort[3], Hui Zhao[2], Weibo Chen[5], Queenie Chan[6], Bin Zhu[1], Yun Xu[2], and Bing Zhang[1]

[1]Department of Radiology, Affiliated Drum Tower Hospital of Nanjing University Medical School, Nanjing, China, NanJing, People's Republic of China, [2]Department of Neurology, Affiliated Drum Tower Hospital of Nanjing University Medical School, Nanjing, China, NanJing, People's Republic of China, [3]Memory Disorders Clinic, Department of Neurology, Charles University in Prague, 2nd Faculty of Medicine and Motol University Hospital, Prague, Czech Republic, Czech Republic, [4]International Clinical Research Center, St.Anne's University Hospital Brno, Brno, Czech Republic, Czech Republic, [5]Philips Healthcare, Shanghai, People's Republic of China, People's Republic of China, [6]Philips Healthcare, HongKong, People's Republic of China, People's Republic of China

Loss of spatial navigation skills is a typical feature in mild cognitive impairment. Here we investigate intrinsic activity using resting-stat functional magnetic resonance imaging within the subcortical regions, which is previously reported to be important in spatial navigation. Right hippocampus, pallidum and thalamus showed significant decreased regional homogeneity of local intrinsic activity in the patients, and the correlational trend between regional homogeneity and allocentric navigation performance showed significantly difference between patients and normal aging controls. These results showed evidences for the intrinsic subcortical activity damage and a possible compensatory mechanism of spatial navigation in the early mild cognitive impairment.

4129 Computer 108

A multi-modal study of the neural mechanisms behind the beneficial effects of repetitive TMS over the precuneus of MCI patients

Matteo Mancini[1,2], Mara Cercignani[2,3], Sonia Bonnì[4], Silvia Picazio[4], Viviana Ponzo[4], Maria Concetta Pellicciari[4], Elias Casula[4], Laura Serra[2], Carlo Caltagirone[4], Giacomo Koch[4,5], and Marco Bozzali[2]

[1]University of Rome "Roma Tre", Rome, Italy, [2]Neuroimaging Laboratory, Santa Lucia Foundation, Rome, Italy, [3]Clinical Imaging Sciences Centre, University of Sussex, Brighton, United Kingdom, [4]Non-Invasive Brain Stimulation Unit, Santa Lucia Foundation, Rome, Italy, [5]Stroke Unit, Policlinico Tor Vergata, Rome, Italy

We present a double-blind randomized cross-over clinical study that aims to investigate the efficacy of two weeks of repetitive transcranial magnetic stimulation (TMS) in modulating cognitive performances in patients with mild cognitive impairment (MCI) and to characterize in vivo brain connectivity changes in MCI patients after rTMS. We used a multi-modal approach based on behavioural tests, TMS-EEG, DWI and fMRI. The behavioural and neurophysiological results support the role of medial parietal region in memory process. Moreover, our findings suggest that TMS may be a potential effective strategy in treatment of MCI patients for whom, currently, there is no available therapy.

4130 Computer 109

HYPOTHALAMIC-PITUITARY-GONADAL AXIS DYSREGULATION ALTERS RESTING STATE FUNCTIONAL CONNECTIVITY IN A MOUSE MODEL OF ALZHEIMER'S DISEASE

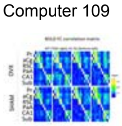

FIRAT KARA[1], Michael Belloy[1], Garima Yadav[1], An Langbeen[2], Jules Jacobs[3], Disha Shah[1], Steffen Roßner[4], Peter Ponsaerts[5], Marleen Verhoye[1], and Annemie Van Der Linden[1]

[1]Bioimaging Lab, Antwerp University, Antwerp, Belgium, [2]Laboratory of Veterinary Physiology and Biochemistry, Antwerp University, Antwerp, Belgium, [3]Mathematics, Leiden University, Netherlands, [4]Paul Flechsig Institute for Brain Research, University of Leipzig, Leipzig, Germany, [5]Experimental Cell Transplantation Group, Antwerp University, Antwerp, Belgium

Dysregulation of hypothalamic pituitary gonadal (HPG) axis signaling with menopause is considered as a risk factor for Alzheimer's disease (AD). Menopause leads to decreased sex steroid signaling and increased luteinizing hormone signaling which may have profound effects on many cellular processes that predispose to neurodegeneration and impairment in cognitive function. The effects of amyloid production on resting state BOLD fMRI using functional connectivity analysis in a mouse model of AD have been previously published. However how HPG axis dysregulation affect resting state functional connectivity in a mouse model of AD has not been studied. Here we show that ovariectomized AD mice, a commonly used animal model to study menopause related hormonal changes in the HPG axis, exhibit alterations in resting state connectivity in the mouse default mode network connectivity. These findings establish a causal link between AD and HPG axis dysregulation.

4131 Computer 110

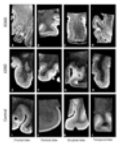

Changes in susceptibility-weighted MRI contrast reflect differences in cortical spreading of pathology in early-onset and late-onset Alzheimer patients

Marjolein Bulk[1,2], Boyd Kenkhuis[1], Linda M. van der Graaf[1,2], Ingrid M. Hegeman[3], Mark A. van Buchem[1], Remco Natté[3], and Louise van der Weerd[1,2]

[1]Radiology, Leiden University Medical Center, Leiden, Netherlands, [2]Human Genetics, Leiden University Medical Center, Leiden, Netherlands, [3]Pathology, Leiden University Medical Center, Leiden, Netherlands

Changes in susceptibility-based MRI contrast and histological correlates of post-mortem brain tissue have been used to distinguish differences in spreading patterns of AD pathology over the cortex between AD subtypes. Susceptibility-based MRI allowed us to clearly distinguish early-onset and late-onset AD patients. The MRI contrast in the different regions closely reflected the overall severity of pathology. This study confirms iron deposition as the underlying source of MRI contrast in all cortical regions, and demonstrates that iron deposition is a putative biomarker for disease progression, with a spatial and temporal spreading pattern independent of amyloid and tau.

4132 Computer 111

Simultaneous measurement of regional cerebral perfusion and glucose metabolism in frontotemporal dementia.

Udunna C Anazodo[1], Elizabeth Finger[2], Claes Nøhr Ladefoged[3], Frank S Prato[1], Jonathan D Thiessen[1], and Keith S St Lawrence[1]

[1]Medical Biophysics, Lawson Health Research Institute, London, ON, Canada, [2]Clinical Neurological Sciences, London, ON, Canada, [3]Rigshospitalet (Copenhagen University Hospital), Copenhagen, Denmark

This study examined regional associations of hypoperfusion to hypometabolism in frontotemporal dementia patients using simultaneous PET/MRI acquisitions. Concordance between modalities was observed across regions. In general ASL-CBF appears to complement PET-FDG measurements

---

4133 Computer 112

3D DCE-MR imaging shows compromised brain waste transport in spontaneously hypertensive rats

Kristian Nygaard Mortensen[1], Simon Sanggaard[1], Hedok Lee[2], Palle Koch[3], Maiken Nedergaard[1,4], Bjørn Quistorff[3], and Helene Benveniste[2]

[1]Center for Basic and Translational Neuroscience, University of Copenhagen, Copenhagen, Denmark, [2]Department of Anesthesiology, Yale University, New Haven, CT, United States, [3]Cellular and Metabolic Research & NMR, University of Copenhagen, Copenhagen, Denmark, [4]Department of Neurosurgery, University of Rochester, Rochester, NY, United States

The link between hypertension and cerebral small vessel disease is key to understanding pathobiology of certain types of dementia. We studied the effects of mild hypertension on a newly discovered pathway for clearance of solutes from the brain parenchyma in young spontaneously hypertensive rats using DCE-MRI after intrathecal infusion of a paramagnetic contrast agent. We found normal-to-increased tracer influx and decreased efflux to and from the brain parenchyma, consistent with a lowered efficiency of brain solute clearance. This suggests that a compromised brain waste transport system may be implicated in the development of cerebral small vessel disease and dementia.

4134 Computer 113

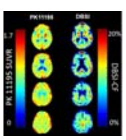

A promising endogenous, non-radioactive method to quantify neuroinflammation in Alzheimer Disease

Qing Wang[1], Yong Wang[1], Jon Christensen[1], Yi Su[1], Lisa Cash[1], John Morris[1], Mark Mintun[2], and Tammie Benzinger[1]

[1]Washington University in St. Louis, St. Louis, MO, United States, [2]Avid Radiopharmaceuticals, Inc., Philadelphia, PA, United States

Accumulation of amyloid beta (Aβ) plaques and neurofibrillary tau tangles are the neuropathological hallmarks of Alzheimer disease (AD). However, increasing evidence points to the involvement of neuroinflammation in early AD and disease progression. Diffusion basis spectrum imaging (DBSI) is a novel non-invasive and non-radioactive multi-parametric diffusion MRI technique to quantify neuroinflammation in AD. We demonstrated that DBSI derived neuroinflammation marker significantly correlated with 11C-PK11195 PET imaging, a marker for microglia activation and neuroinflammation, suggesting DBSI as a promising endogenous, non-radioactive method to quantify neuroinflammation in AD.

4135 Computer 114

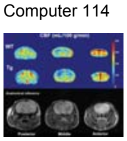

Using time-encoded pCASL to study vascular function in a mouse model of Alzheimer's disease

Leon P. Munting[1,2], Lydiane Hirschler[3,4,5], Ernst Suidgeest[1], Emmanuel L. Barbier[3,4], Matthias J. P. van Osch[1], and Louise van der Weerd[1,2]

[1]Radiology, Leiden University Medical Center, Leiden, Netherlands, [2]Human Genetics, Leiden University Medical Center, Leiden, Netherlands, [3]Grenoble Institut des Neurosciences, Université Grenoble Alpes, Grenoble, France, [4]Inserm U836, Grenoble, France, [5]Bruker Biospin, Ettlingen, Germany

Cerebral Blood Flow (CBF) as measured with ASL-MRI is an emerging Alzheimer's Disease (AD) biomarker. However, vascular pathology may delay the arterial transit time (ATT) of the magnetic label and influence the measurement. Thus, ATT estimation can potentially reveal vascular pathology and benefit CBF quantification. To evaluate CBF and ATT as read-out markers in AD mouse models, time-encoded ASL was used to measure ATT and CBF in the APPswe/PS1ΔE9 AD model. No major CBF difference was found when ATT was taken into account. However, AD mice showed increased ATT in the thalamus and decreased CBF in the cortex and striatum.

4136 Computer 115

Longitudinal progression of white matter deficits in Young Onset Alzheimer's Disease and Its Syndromic Variants using NODDI

Jiaying Zhang[1], Catherine F Slattery[2], Ross W Paterson[2], Alexander JM Foulkes[2], Laura Mancini[3,4], David L Thomas[3,4], Marc Modat[1], Nicolas Toussaint[1], David M Cash[1,2], John S Thornton[5], Daniel C Alexander[1], Sebastien Ourselin[1], Nick C Fox[2], Jonathan M Schott[2], and Hui Zhang[1]

[1]Department of Computer Science and Centre for medical image computing, University College London, London, United Kingdom, [2]Department of Neurodegenerative disease, Institute of Neurology, University College London, London, United Kingdom, [3]Neuroradiological Academic Unit, Department of Brain Repair and Rehabilitation, UCL Institute of Neurology, London, UK, University College London, London, United Kingdom, [4]Lysholm Department of Neuroradiology, National Hospital for Neurology and Neurosurgery, UCLH NHS Foundation Trust, London, UK, University College London, [5]Lysholm Department of Neuroradiology, National Hospital for Neurology and Neurosurgery, UCLH NHS Foundation Trust, London, UK, University College London, London, United Kingdom

Young Onset Alzheimer's disease (YOAD) is characterised by its syndromic diversity, which may be underpinned by different patterns of white matter (WM) network breakdown. This prompts considerable interest in studying WM. We have previously shown that NODDI, a multi-shell diffusion MRI technique, is more sensitive at detecting WM changes in YOAD than standard DTI and demonstrated unique profiles of WM deficits in its syndromic variants. Here we investigated longitudinal WM changes in YOAD patients using NODDI, and explored the patterns of longitudinal WM changes associated with syndromic variants using tract-based spatial statistics (TBSS).

4137 Computer 116

Automated Fiber Quantification Identifies the Extent of White Matter Integrity Loss Concurrent to Hippocampal Atrophy

Joseph A Helpern[1], George Russell Glenn[1], Andreana A Benitez[2], Fatima A Falangola[3], Rachael A Deardorff[1], and Jens A Jensen[1]

[1]Radiology, Medical University of South Carolina, Charleston, SC, United States, [2]Neurology, Medical University of South Carolina, Charleston, SC, United States, [3]Neuroscience, Medical University of South Carolina, Charleston, SC, United States

Automated fiber quantification with white matter tract integrity metrics identified subtle changes in brain microstructure occurring in the early stages of Alzheimer’s pathology. These metrics were found to be significantly different in the posterior section of the parahippocampal white matter in cognitively normal older adults with hippocampal atrophy as compared to those without. Axonal water fraction distinguished those with hippocampal atrophy versus those without with the largest effect size (Cohen’s $d = 0.86$, $p = 0.004$). As expected, the metrics for these two groups did not differ in the arcuate fasciculus, a tract typically unaffected in Alzheimer’s disease.

4138 Computer 117

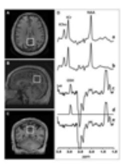

Relationships among Cortical Glutathione Levels, Brain Amyloidosis, and Memory in Normal Older Adults Investigated in vivo with 1H MRS and PiB PET

Gloria C Chiang[1], Xiangling Mao[2], Guoxin Kang[3], Eileen Chang[2], Sneha Pandya[2], Shankar Vallabhajosula[2], Richard Isaacson[2], Lisa D Ravdin[2], and Dikoma C. Shungu[1]

[1]Radiology, Weill Cornell Medicine, New York, NY, United States, [2]Radiology, Weill Cornell Medicine, [3]Radidology, Weill Cornell Medicine

Oxidative stress has been implicated as an important pathological mechanism in the development of Alzheimer’s disease (AD). The purpose of this study was to assess whether J-edited ^{1}H MRS levels of glutathione (GSH) – the primary antioxidant in living tissue – are associated with brain amyloidosis, as assessed with PET, and memory in a community-dwelling cohort of nondemented older adults. The results showed an inverse association relating GSH, a sensitive marker of oxidative stress, and amyloidosis, one of the pathological hallmarks of AD, and a weaker association with memory, thereby collectively further implicating oxidative stress in AD pathophysiology.

4139 Computer 118

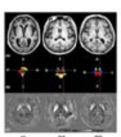

Differentiation of deep gray matters in patients with Alzheimer’s disease (AD), dementia with Lewy bodies (DLB) and Parkinson’s disease dementia (PDD) using T1 weighted images and quantitative susceptibility maps (QSM)

Eo-Jin Hwang[1], Hyun Seok Choi [1], Jinhee Jang[1], Seung Eun Jung[1], So-Lyung Jung[1], Kook-Jin Ahn[1], Bum-soo Kim[1], and Joong-Seok Kim[1]

[1]Seoul St.Mary Hospital, Seoul, Korea, Republic of

The purpose of this study was to differentiate Alzheimer’s disease (AD), dementia with Lewy bodies (DLB) and Parkinson’s disease dementia (PDD) by evaluating deep gray matter regions of the three subject groups. The 3D T1 weighted images and quantitative susceptibility maps (QSM) were segmented into 15 deep gray matter structures to estimate volumes and mean susceptibility values, and differences among the three groups were evaluated using a one-way analysis of covariance (ANCOVA) with age and gender as covariates. A multivariate logistic regression and receiver operating characteristic curve analyses were performed to determine associated imaging features and diagnostic performance.

4140 Computer 119

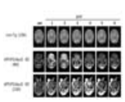

Development of the oligomeric amyloid-beta targeted MRI contrast agents to diagnose the early stage of Alzheimer’s disease

Geon-Ho Jahng[1], Sang-Tae Kim[2], Peter Verwilst[3], Hyug-Gi Kim[4], Jee-Hyun Cho[5], Kwan Soo Hong[5], Ki Woong Kim[2], Jong Seung Kim[3], Wook Jin[1], Eui Jong Kim[6], and Dal Mo Yang[1]

[1]Radiology, Kyung Hee University Hospital at Gangdong, Seoul, Korea, Republic of, [2]Bundang Hospital of Seoul National University, Kyunggeedo, Korea, Republic of, [3]Korea University, Seoul, Korea, Republic of, [4]Kyung Hee University, Seoul, Korea, Republic of, [5]Korea Basic Science Institute, Cheongju, Korea, Republic of, [6]Radiology, Kyung Hee University Hospital, Seoul, Korea, Republic of

A new T1 molecular MRI contrast agent specifically designed to be specific for oligomeric Aβ was developed by combining the commercially available gadolinium (Gd)-Dota with an oligomeric Aβ-specific DNA aptamer. We confirmed the protein size with Aβ polymerization in aspect of molecular masses when polymers were formed. We performed the following experiment in the cell level and AD-model mice. We identified a particular region with a significantly distinct T1 MRI signal, allowing for distinguishing Alzheimer's disease model mice from non-Tg mice.

4141 Computer 120

Functional MRS in patients with mild cognitive impairment and Alzheimer’s disease: Three-year longitudinal study

Soo Hyun Cho[1], Geon-Ho Jahng[2], Jang-Hoon Oh[3], Hyug-Gi Kim[3], Hak Young Rhee[4], Chang Woo Ryu[2], Key-Chung Park[1], Dal Mo Yang[2], Eui Jong Kim[5], and Wook Jin[2]

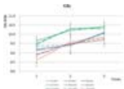

[1]Kyung Hee University Hospital, Seoul, Korea, Republic of, [2]Radiology, Kyung Hee University Hospital at Gangdong, Seoul, Korea, Republic of, [3]Kyung Hee University, [4]Kyung Hee University Hospital at Gangdong, [5]Radiology, Kyung Hee University Hospital, Seoul, Korea, Republic of

To measure temporal changes of the metabolite level during a memory task, proton functional MRS (fMRS) data with a single-voxel PRESS sequence were acquired at the precuneus and posterior cingulate brain region during a face-name association task using a 3 Tesla MRI scanner for the 28 cognitive normal elderly, 16 amnestic mild cognitive impairment, and 12 Alzheimer's disease individuals. We measured the fMRS data three times at the eight-month interval. All of the acquired data were analyzed using LCModel software. Glx at the second trial increased significantly compared to that of the first trial in the novel condition.

Electronic Poster

Neurodegeneration

Exhibition Hall — Tuesday 13:45 - 14:45

4142 — Computer 25

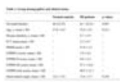

Quantitative susceptibility mapping (QSM) as a biomarker for evaluating white matter alterations in Parkinson's disease

Xiaojun Guan[1], Peiyu Huang[1], Qiaoling Zeng[1], Chunlei Liu[2], Min Xuan[1], Quanquan Gu[1], Xiaojun Xu[1], Nian Wang[2], Nian Wang[2], Xinfeng Yu[1], Xiao Luo[1], Jingjing Xu[1], Wei Luo[3], Yong Zhang[4], and Minming Zhang[1]

[1]Radiology, Second Affiliated Hospital of Zhejiang University School of Medicine, Hangzhou, People's Republic of China, [2]Brain Imaging and Analysis Center, Duke University School of Medicine, Durham, NC, United States, [3]Neurology, Second Affiliated Hospital of Zhejiang University School of Medicine, Hangzhou, People's Republic of China, [4]MR Research, GE Healthcare, Shanghai, People's Republic of China

Myelinated white matter showing diamagnetic susceptibility is important for information transfer in the brain. In Parkinson's disease, the white matter is damaged secondary to nigral degeneration. Quantitative susceptibility mapping is a novel technique for noninvasive assessment of regional white matter ultrastructure, and provides different information to standard diffusion tensor imaging.

4143 — Computer 26

The quantitative susceptibility mapping and non-motor symptoms of patients with early Parkinson disease

Chae Won Shin[1], Sun-Won Park[2,3], Jee-Young Lee[1], Jongho Lee[4], Seon Lee[5], Jae Myung Kim[4], and Jung Hyo Lhim[2]

[1]Department of Neurology, SNU-SMG Boramae Medical Center, Seoul, Korea, Republic of, [2]Department of Radiology, SNU-SMG Boramae Medical Center, Seoul, Korea, Republic of, [3]Department of Radiology, College of Medicine, Seoul National University, [4]Department of Electrical and Computer Engineering, Seoul National University, Seoul, Korea, Republic of, [5]Department of Mechanical and Aerospace Engineering, Seoul National University, Seoul, Korea, Republic of

This study is to evaluate the impact of quantitative susceptibility mapping (QSM) on regional distribution of iron deposition and its correlations with non-motor symptoms in patients with early Parkinson disease (PD). The QSM values of deep nuclei and clinical data using validated scales were obtained from patients. There were no differences in regional QSM values between patients and controls, and the QSM values were not correlated with any of motor or non-motor symptoms in PD patients. This study suggests that the QSM may not be a sensitive tool enough to use in patients with early PD.

4144 — Computer 27

Co-activation Pattern Analysis in Parkinson's Disease

Xiaowei Zhuang (co-first)[1], Ryan R Walsh (co-first)[1], Zhengshi Yang[1], Virendra Mishra[1], Karthik Sreenivasan[1], and Dietmar Cordes[1,2]

[1]Cleveland Clinic Lou Ruvo Center for Brain Health, Las Vegas, NV, United States, [2]University of Colorado Boulder, Boulder, CO, United States

In this study, we explored the dynamics of Parkinson's disease (PD) brain network function utilizing the co-activation pattern (CAP) analysis emphasizing sensorimotor network (SM) function during resting-state. We modified the routine to calculate group dominant CAPs (d-CAPs) and proposed a novel way to obtain within-subject CAP switching-rate. Reduced dynamics of the SM network in PD was demonstrated by both decreased number of d-CAPs and decreased switching-rate, which corroborates electrophysiologic data.

4145 — Computer 28

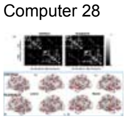

Distinct structural backbone-network in early Parkinson's disease (PD) subjects: Insights from Parkinson's Progressive Markers Initiative (PPMI) dataset

Virendra Mishra[1], Karthik Sreenivasan[1], Christopher Bird[1], Dietmar Cordes[1], and Ryan R Walsh[1]

[1]Cleveland Clinic Lou Ruvo Center for Brain Health, Las Vegas, NV, United States

In vivo imaging that reliably captures the impact of the spreading pathology of Parkinson's disease (PD), including its impact on both white and gray matter, remains elusive. In this study, we applied graph-theoretical techniques to multi-site diffusion-MRI data from a cohort of early PD-subjects in Parkinson's Progressive Markers Initiative (PPMI) database. A distinctive structural backbone-network was revealed in early PD-subjects without any a-priori assumptions involving cortical and subcortical regions that are known to be involved in various stages of PD, including early PD (Olfactory-cortex, globus-pallidum, and striatum). Our study opens new avenues to understanding progression of PD from a graph-theoretical approach.

4146 — Computer 29

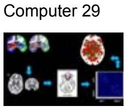

Characterizing diffusion MRI based structural connectome of the human brain in Parkinson's disease

Apurva Shah[1], Shivali Amit Wagle[1], Jitendra Saini[2], Pramod Pal[3], and Madhura Ingalhalikar[1]

[1]Electronics and Telecommunication, Symbiosis Institute of Technology, pune, India, [2]Department of Neurology, NIMHANS, Banglore, [3]Department of Neurology, NIMHANS, Banglore, India

This study aims at assessing the large scale structural network changes in Parkinson's disease. The structural connectome is computed using probabilistic fiber tracking on diffusion MRI between 95 regions of interest. Graph theoretic analysis on the connectome is carried out at several levels of granularity: global, local (nodal) and lobar. We find that patients with PD demonstrate lower network clustering capability and lower neural connectivity as well as significantly reduced nodal influence of the hippocampus. Additionally, widespread patterns of reduced connectivity are observed in the temporal and occipital areas. These deficits could potentially mark the non-motor symptoms indicated in PD.

4147 Computer 30

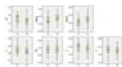

Altered Topological Properties of Structural Connectome in Early-Stage, Drug-naive PD Revealed by Graph Theoretical Analysis

Xueling Suo[1], Du Lei[2], Nannan Li[3], Lan Cheng[3], Lei Li[1], Fuqin Chen[4], Meiyun Wang[5], Rong Peng[3], and Qiyong Gong[1]

[1]Radiology, West china hospital, Chengdu, People's Republic of China, [2]Psychosis Studies, Institute of Psychiatry, Psychology & Neuroscience, King's College London, United Kingdom, [3]Neurology, West china hospital, People's Republic of China, [4]Medical Information Engineering, School of Electrical Engineering and Information, Sichuan University, People's Republic of China, [5]Radiology, Henan Provincial People's Hospital & the People's Hospital of Zhengzhou University, People's Republic of China

To use diffusion tensor imaging (DTI) and graph theory approaches to explore the brain structural connectome in patients with early-stage drug-naive Parkinson's disease (PD). The structural connectome was constructed by using deterministic tractography and thresholding the mean fractional anisotropy of 90 brain regions to yield 90*90 partial correlation matrixes. The decreased characteristic path length L_p and increased global efficiency E_{glob} in the PD patients relative to healthy controls indicated that structural networks are closer to randomization, providing a structural basis for functional alterations of PD.

4148 Computer 31

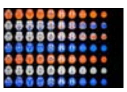

Altered Dynamic Functional Connectivity State Patterns of Patients with Idiopathic Parkinson's Disease

Naying He[1,2], Shiyang Chen[3], Jason Langley[4], Yong Zhang[5], Fuhua Yan[1], and Xiaoping Hu[4,6]

[1]Radiology, Ruijin Hospital,Shanghai Jiao Tong University School of Medicine, Shanghai, People's Republic of China, [2]Center for Advanced Neuroimaging, University of California, Riverside, Riverside, CA, United States, [3]Department of Biomedical Engineering, Georgia Institute of Technology and Emory University, Atlanta, GA, United States, [4]Center for Advanced Neuroimaging, University of California, Riverside, Riverside, Riverside, CA, United States, [5]MR Research, GE Healthcare, Shanghai, People's Republic of China, [6]Department of Bioengineering, University of California, Riverside, Riverside, Riverside, CA, United States

Parkinson's disease (PD) is a neurodegenerative disorder characterized by nigral-striatal dopamine deficiency and motor symptoms. Neuroimaging studies have shown that functional connectivity within cortical-striatal networks and related connections are disturbed in PD. But these are based on conventional static resting-state analyses which assume functional connectivity being static over time. Recent studies have demonstrated that resting state brain activity is highly dynamic. In this work, we applied Gaussian Hidden Markov Model to investigate dynamic functional connectivity in PD and compared it with that in normal controls. Our results show alterations in sensorimotor, DMN, and visual networks in PD.

4149 Computer 32

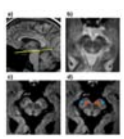

Quantitative Magnetization Transfer Imaging of the Substantia Nigra in Parkinson's Disease

Paula Trujillo[1,2], Paul E. Summers[2], Alex K. Smith[3], Seth A. Smith[4,5], Antonella Costa[2], and Daniel O. Claassen[1]

[1]Neurology, Vanderbilt University Medical Center, Nashville, TN, United States, [2]Neuroradiology, Fondazione IRCCS Ca' Granda - Ospedale Maggiore Policlinico, Milan, Italy, [3]FMRIB, University of Oxford, Oxford, United Kingdom, [4]Vanderbilt University Institute of Imaging Science, Vanderbilt University, Nashville, TN, United States, [5]Radiology and Radiological Sciences, Vanderbilt University, Nashville, TN, United States

Parkinson's disease (PD) is characterized by the loss of pigmented dopaminergic neurons in the substantia nigra pars compacta (SNc). The aim of the study was to evaluate the feasibility of rapid magnetization pool size ratio (PSR) mapping as a subset of the magnetization transfer (MT) properties of the SNc in healthy subjects and patients with PD. These results demonstrated the feasibility of performing quantitative PSR mapping in human SN within reasonable scan times, and that PSR is likely the quantitative MT parameter most relevant for PD.

4150 Computer 33

Abnormal Brain White Matter Connectivity in Diabetic Neuropathy: A Magnetic Resonance Diffusion Tensor Imaging Study.

Dinesh Selvarajah[1], Joseph Harding[1], Shillo Pallai[1], Solomon tesfaye[2], and Iain Wilkinson[1]

[1]University of Sheffield, Sheffield, United Kingdom, [2]Sheffield Teaching Hospitals NHS Foundation Trust, Sheffield, United Kingdom

This study for the first time has shown alterations in white matter MD in patients with DSPN. Increased MD in the primary somatosensory cortex in patients with diabetic neuropathy (DN) is suggestive of white matter microarchitecture degeneration, and supports the evidence of neuronal loss in the somatosensory cortex in patients with . Furthermore, these results also support the previous evidence of thalamic neuronal dysfunction in DN on MR spectroscopy. Changes in the degree of white matter structure might provide a pathophysiological underpinning of spinal cord atrophy and brain volume reduction in DN.

4151 Computer 34

Brain gray matter changes in type 2 diabetes mellitus: A meta-analysis of whole-brain voxel-based morphometry study

lin lin[1] and Guangyao wu[1]

[1]radiology, Affiliated Zhongshan Hospital of Dalian University, Dalian, People's Republic of China

To our knowledge, this is the first whole-brain VBM meta-analysis showing a reduced volume of whole and regional gray matter (GM) in the brains of type 2 diabetes mellitus (T2DM) patients. we used a new meta-analytic tool, signed differential mapping to identify consistent results about global and regional abnormalities in T2DM, and explore the relationship between cognitive and GM alternations. We showed educed volume of whole and regional GM in T2DM patients, particularly in the temporal lobe, the GM volumes of the right insula were positively correlated with MMSE scores, and those changes may indicate a risk of dementia.

4152 Computer 35

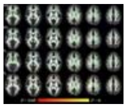

Altered White Matter Microstructure in Middle-Aged Type 2 Diabetic Patients: A Diffusional Kurtosis Imaging Study Based on Two-compartment White Matter Model

Jie Gao[1], Min Tang[1], Xin Zhang[1], Xiaoling Zhang[1], Kaining Shi[2], and Xiaohong Wu[1]

[1]Shaanxi Provincial People's Hospital, Xi'an, People's Republic of China, [2]Clinical science, Philips Healthcare China

This study aims to use a two-compartment diffusion model of white matter based on diffusional kurtosis imaging (DKI) to explore early white matter alternations in middle-aged type 2 diabetes mellitus (T2DM) . 33 T2DM patients and 13 healthy control were enrolled. All diffusion parameters (FA=fractional anisotropy, MD=mean diffusivity, AD=axial diffusivity, RD=radial diffusivity, MK=mean kurtosis, AK=axial kurtosis, RK=radial kurtosis, D_a=intra-axonal diffusivity, $D_{e\|}$=axial extra-axonal space diffusivity, $D_{e\perp}$= radial extra-axonal space diffusivity) were compared. $D_{e\perp}$ was demonstrated to be the most sensitive in detecting the diffusion changes. These increased $D_{e\perp}$ (extra-axonal diffusivity) and unchanged D_a (intra-axonal diffusivity) reflected the increased water and/or demyelination.

4153 Computer 36

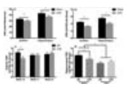

An animal model of comorbid cerebral hypoperfusion and metabolic syndrome

Jessica Livingston-Thomas[1], Greg O. Cron[2,3,4], Therese Gagnon[5], Anthony Carter[6], Matthew Jeffers[5], and Dale Corbett[5,6]

[1]Cellular and Molecular Medicine, The University of Ottawa, Ottawa, ON, Canada, [2]Medical Imaging, The Ottawa Hospital, Ottawa, ON, Canada, [3]The Ottawa Hospital Research Institute, Ottawa, ON, Canada, [4]Radiology, The University of Ottawa, Ottawa, ON, Canada, [5]Cellular and Molecular Medicine, The University of Ottawa, [6]Canadian Partnership for Stroke Recovery

Vascular cognitive impairment (VCI) arises from chronic cerebral hypoperfusion and is characterized by executive dysfunction, memory problems, and motor impairments. In countries where people eat highly processed, energy-dense food, there are high rates of VCI. Poor diet is also linked to metabolic syndrome, which is also associated with cognitive dysfunction. Metabolic syndrome and VCI commonly coexist within cardiovascular patients. Due to the translational failure of many promising preclinical treatments for cardiovascular disease, researchers are trying to incorporate human comorbidities within animal disease models. Here, we develop a rat model which combines cerebral hypoperfusion with an unhealthy diet.

4154 Computer 37

MR-NODDI Evaluating Amyotrophic Lateral Sclerosis: a Tract Based Spatial Statistics Analysis

Rifeng Jiang[1], Wenzhen Zhu[2], Qing Duan[1], Yunjing Xue[1], Yihao Yao[2], Jingjing Shi[2], and Linying Guo[2]

[1]Fujian Medical University Union Hospital, Fuzhou, People's Republic of China, [2]Tongji Hospital, HUST, Wuhan, People's Republic of China

This study uses NODDI, a novel tool, to quantify changes of white matter (WM) skeleton in patients with ALS. By TBSS analysis, significant FA reductions were demonstrated within the (pre)frontal WM, partial parietal WM, corpus callosum and partial corticospinal tract. Similarly, significant Ficvf reductions were found within almost all the WM skeleton, which was more extensive than that of FA. In contrast, ODI showed no significant changes in all the WM skeleton. Therefore, NODDI is a more potential tool to demonstrating the neurite density reductions for ALS patients, which will help lead to earlier diagnosis and treatment for ALS.

4155 Computer 38

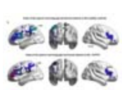

Reorganization of Brain Connectivity in the Speech and Language Network in the Non-fluent variant of PPA

Maria Luisa Mandelli[1], Christa Watson[1], Eduard Vilaplana[2], Jesse A Brown[1], Zachary A Miller[1], Isabel H Honey[1], Ariane Welch[1], Miguel A Santos-Santos[3], Howard J Rosen[1], Bruce L Miller[1], William W Seeley[1], and Maria Luisa Gorno-Tempini[1]

[1]Memory and Aging Center, Neurology, University of California, San Francisco, San Francisco, CA, United States, [2]Memory Unit, Department of Neurology, Hospital de la Santa Creu i Sant Pau - Biomedical Research Institute Sant Pau – Universitat Autonoma de Barcelona, Spain, [3]Fundació ACE, Alzheimer Research Center, Institut Català de Neurociències Aplicades, Barcelona, Spain Cognition and Brain Plasticity Group, Bellvitge Biomedical Research Institute, Barcelona, Spain

Graph theory analysis is a method recently introduced to study the brain as a network. In this study we investigate the topological distribution of the speech and language functional network in nfvPPA patients characterized by isolated and progressive language impairments. We identified the hubs of the speech and language network in healthy controls and nfvPPA. In patients, the network presented an abnormal topological distribution where right-sided brain regions were recruited. These findings suggest that in nfvPPA this network reorganizes in the presence of localized gray matter volume loss.

4156 Computer 39

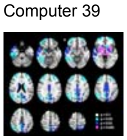

Sporadic Jakob-Creutzfeld Disease quantitative diffusion profiles and resting state functional correlates

Matteo Paoletti[1], Eduardo Caverzasi[2], Maria Luisa Mandelli[3], Jesse A. Brown[3], William W. Seeley[3], Roland G. Henry[2,4], Howard J. Rosen[3], Bruce L. Miller[3], Maria Luisa Gorno-Tempini[3], Stefano Bastianello[5,6], and Michael D. Geschwind[3]

[1]Institute of Radiology, University of Pavia, Pavia, Italy, [2]Department of Neurology, University of California, San Francisco, San Francisco, CA, [3]Memory and Aging Center, University of California, San Francisco, San Francisco, CA, [4]Department of Radiology and Biomedical Imaging, University of California, San Francisco, San Francisco, CA, [5]Department of Neuroradiology, IRCCS C. Mondino Neurological Institute, University of Pavia, Pavia, Italy, [6]Department of Brain and Behavioral Sciences, University of Pavia, Pavia, Italy

Diffusion restriction on MRI is an important diagnostic finding in sporadic Jakob-Creutzfeld disease. We performed group-wise quantitative cortical and subcortical grey matter mean diffusivity analysis at 3.0 T and tested feasibility of single-subject diffusivity restriction maps, that, compared to group-wise analysis, can better describe variable patterns of involvement in sJCD. DMN-related regions demonstrated prominent diffusion restriction; thus DMN functional connectivity was evaluated. DMN showed a increased connectivity in sJCD, that based on cross-sectional analysis seems to decrease along with clinical worsening. Resting-state fMRI may be a promising candidate to evaluate involvement in sJCD especially during the preclinical phase.

4157 Computer 40

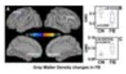

Structural and Functional MRI Characterization of Trial Spinal Cord Stimulation Responders in Failed Back Surgery Syndrome

Guangyu Chen[1], Andrew S. Nencka[2], Hao Shu[1,3], Shekar N. Kurpad[4], Shi-Jiang Li[1], and Peter A. Pahapill[4]

[1]Biophysics, Medical College of Wisconsin, Milwaukee, WI, United States, [2]Radiology, Medical College of Wisconsin, Milwaukee, WI, United States, [3]Neuropsychiatric Institute and Medical School, Southeast University, Nanjing, People's Republic of China, [4]Neurosurgery, Medical College of Wisconsin, Milwaukee, WI, United States

Chronic pain is an important and growing problem in aging populations. A key challenge to treating chronic pain is the absence of effective, objective methods of assessment. This study, from a homogeneous group of chronic pain patients with failed back surgery syndrome, demonstrated that the functional interaction strength between the limbic striatum and neocortex were very tightly correlated with the patients' pain scores. We believe this index may form the basis for an objective, non-invasive biomarker for chronic lower back pain, and may be generalizable to other types of chronic pain.

4158 Computer 41

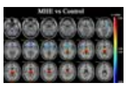

The Grey Matter Density of the Thalamus Correlates with the Cirrhotic Indexes and Child-Pugh Score in Cirrhotic Patients: A Voxel-Based Morphometry Study.

Chun-Qiang Lu[1], Yun Jiao[2], and Shenghong Ju[3]

[1]ZhongDa Hospital, Nanjing, People's Republic of China, [2]Information Department, ZhongDa Hospital, Nanjing, People's Republic of China, [3]Radiology Department, ZhongDa Hospital, Nanjing, People's Republic of China

Altered brain structure in cirrhotic patients have been seen in previously reported studies. Many studies focus on the grey matter change of the caudate putamen, while few study investigate the relationship of thalamus grey matter change and cirrhotic symptoms. Our study reveal that the grey matter density of thalamus is closely correlated with the clinical makers of the cirrhosis, which may help to clarify the mechanism of the thalamus structural change.

4159 Computer 42

Imaging Impairment of the Glymphatic System after Diabetes

Quan Jiang[1,2], Li Zhang[1], Guangliang Ding[1], Esmaeil Davoodi-Bojd[1], Qingjiang Li[1], Lian Li[1], David Hearshen[3], Michael Chopp[1,2], and Zhenggang Zhang[1]

[1]Neurology, Henry Ford Health System, Detroit, MI, United States, [2]Physics, Oakland University, Rochester, MI, United States, [3]Radiology, Henry Ford Health System, Detroit, MI, United States

The recently discovered glymphatic system has fundamentally altered the traditional model of cerebrospinal fluid (CSF) hydrodynamics and shown promising results in applications for understanding neurological diseases1, 2. However, little is known how diabetes affects the glymphatic system. The current study is the first investigation of the effect of diabetes on the glymphatic system and the relationship between glymphatic system and cognitive impairment in diabetic rats using MRI and fluorescence imaging.

4160 Computer 43

Volumetric MR analysis of brain areas identifies SCA 1, 2 and 3 by applying random forest classifier

Dibashree Tamuli[1], Tavpritesh Sethi[2], Anup Singh[3,4], S. Senthil Kumaran[5], Ashok Kumar Jaryal[1], Achal Kumar Srivastava[6], and Kishore Kumar Deepak[1]

[1]Physiology, All India Institute of Medical Sciences (AIIMS), NewDelhi, India, [2]Pediatrics, All India Institute of Medical Sciences (AIIMS), New Delhi, India, [3]Center for Biomedical Engineering (CBME), Indian Institute of Technology (IIT), New Delhi, India, [4]Center for Biomedical Engineering (CBME), All India Institute of Medical Sciences (AIIMS), NewDelhi, India, [5]NMR, All India Institute of Medical Sciences (AIIMS), NewDelhi, India, [6]Neurology, All India Institute of Medical Sciences (AIIMS), NewDelhi, India

Brain volumetric analysis of SCA 1, 2 and 3 shows differential measurements with reference to cortical thinning and volumes of brain stem and cerebellum. Therefore, to find a solution to classify SCA1, 2 and 3, we have applied machine learning approach for feature selection followed by random forest modeling using volumetric features of the brain.

4161 Computer 44

Altered Structural Connectivity Networks in Young Adults Perinatally-infected with HIV

Mohammed Z Goryawala[1], Elizabeth J Willen[2,3,4], Anai M Cuadra[2], and Varan Govind[1]

[1]Radiology, University of Miami, Miami, FL, United States, [2]Pediatrics, University of Miami, Miami, FL, [3]Pediatrics, University of Missouri, Kansas City, MO, [4]Developmental and Behavioral Sciences, Children's Mercy, Kansas City, MO

Milder forms of HIV-associated neurocognitive disorders (HAND) are frequently observed in approximately half of the HIV-infected individuals, even with treatment for HIV infection. Cognitive deficits observed in them can be associated with injury to the frontal and temporal lobes of their brains. The goal of this study was to assess the impact of HIV infection on vulnerable structural connections in these lobar regions in adults perinatally-infected with HIV. Our results indicate that altered connectivity in frontal lobe regions with differentiated modularity and significant alterations in hub patterns at the temporo-parietal junction occurred in the HIV group.

4162 Computer 45

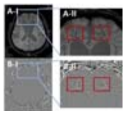

Susceptibility-related phase contrast associated with the alterations of myelo-architecture in adult-onset leukoencephalopathy with neuroaxonal spheroids and pigmented glia

Hansol Lee[1], Minkyeong Kim[2], HyungJoon Cho[1], Se Young Chun[3], Gi Yeong Huh[4], Eun-Joo Kim[5], and Jae-Hyeok Lee[6]

[1]Department of Biomedical Engineering, Ulsan National Institute of Science and Technology, Ulsan, Korea, Republic of, [2]Department of Neurology, Pusan National University Yangsan Hospital, Yangsan, Korea, Republic of, [3]Department of Electrical and Computer Engineering, Ulsan National Institute of Science and Technology, Ulsan, Korea, Republic of, [4]Department of Forensic Medicine, Pusan National University Yangsan Hospital, Yangsan, Korea, Republic of, [5]Department of Neurology, Pusan National University Hospital, Busan, Korea, Republic of, [6]Department of Neurology, Pusan National University Yangsan Hospital

To investigate the origin of susceptibility-weighted imaging (SWI) contrast in frontal white matters of adult-onset leukoencephalopathy with neuroaxonal spheroids and pigmented glia (ALSP), we performed a combined post-mortem magnetic resonance imaging (MRI) and histological study of ALSP pathology. The myelin architectural changes, marked central myelin loss with preserved U-fibers beneath cortical gray matter, mainly contributed to the susceptibility contrast.

4163 Computer 46

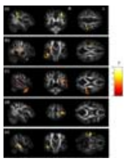

Assessment of chemotherapy-induced brain structural alterations in breast cancer patients using GQI and its correlation with cognitive performance

Tsung-Yuan Li[1,2], Vincent Chin-Hung Chen[3,4], Shu-Ling Huang[5], Dah-Cherng Yeh[6], Jyh-Wen Chai[2], Clayton Chi-Chang Chen[2], and Jun-Cheng Weng[1,7]

[1]Department of Medical Imaging and Radiological Sciences, Chung Shan Medical University, Taichung, Taiwan, [2]Department of Radiology, Taichung Veterans General Hospital, Taichung, Taiwan, [3]School of Medicine, Chang Gung University, Taoyuan, Taiwan, [4]Department of Psychiatry, Chang Gung Memorial Hospital, Chiayi, Taiwan, [5]Department of Psychology, Chung Shan Medical University, Taichung, Taiwan, [6]Breast Center, Taichung Tzu Chi Hospital, Taichung, Taiwan, [7]Department of Medical Imaging, Chung Shan Medical University Hospital, Taichung, Taiwan

Neuroimaging studies suggest that white matter and cognitive function changes were affected by breast cancer and its treatments. Our study interested in the early effect of the brain by chemotherapy. This study included 19 breast cancer survivors who had completed their chemotherapy and 20 healthy control group. Generalized q-sampling imaging (GQI) with voxel-based analysis was performed to show the brain structural differences between two groups. Multiple regression was also used to detect the correlation between Mini-Mental State Examination (MMSE) and the indices of GQI. Our results provided further evidence that breast cancer and adjuvant chemotherapy are associated with adverse effects on white matter.

4164 Computer 47

The association of MRI-detected brain volume change with prenatal exposure to Perfluoroalkyl Substances in teenage

Chao-Yu Shen[1,2,3], Shu-Li Wang[4], Jeng-Dau Tasi[5], Ju-Chien Wu[2], and Jun-Cheng Weng[2,3]

[1]Institute of Medicine, Chung Shan Medical University, Taichung, Taiwan, [2]Department of Medical Imaging and Radiological Sciences, Chung Shan Medical University, Taichung, Taiwan, [3]Department of Medical Imaging, Chung Shan Medical University Hospital, Taichung, Taiwan, [4]National Institute of Environmental Health Sciences, National Health Research Institutes, Miaoli, Taiwan, [5]School of Medicine and Department of Pediatrics, Chung Shan Medical University and Hospital, Taichung, Taiwan

The current study was to explore the relationship between prenatal exposure to PFASs, determined in maternal blood collected during the third trimester of pregnancy and the children's brain volume difference at the age of 13-15 years old. The results showed a significant negative correlation between the maternal blood PFASs concentrations and the children's brain MRI in multiple different brain areas, including both gray matter and white matter.

4165 Computer 48

Diffusion magnetic resonance imaging for predicting changes in the severity of Progressive Supranuclear Palsy

Xiang-An Zhao[1], Lin Sung-Han[1], Tsai Chih-Chien[1], Wu Yi-Ming[2], Lin Wey-Yil[3], Weng Yi-Hsin[3], Lu Chin-Song[3], and Wang Jiun-Jie[1]

[1]Medical Imaging and Radiological Sciences, Chang Gung University, Taoyuan City, Taiwan, [2]Medical Imaging and Intervention, Chang Gung Memorial Hospital, Taoyuan City, Taiwan, [3]Neurology, Chang Gung Memorial Hospital, Taoyuan City, Taiwan

Progressive Supranuclear Palsy (PSP) is an atypical Parkinsonism, which shared similar symptoms with Parkinson's disease (PD) and PSP progressed typically much faster than PD and the prognosis is often poor. The linear regression analysis demonstrated the capability of diffusion MRI indices as measured from multiple brain regions in the prediction of two-year clinical severity. Strong predictive power can be observed in mHY, motor subscale of UPDRS and PIGD. The two-year clinical decay in patients with PSP can be accurately predicted by using diffusion tensor derived parameters as measured from distinct brain regions.

Electronic Poster

Brain Tumor: Diffusion, Perfusion, fMRI & Vascular Imaging

Exhibition Hall Tuesday 14:45 - 15:45

4166 Computer 1

An application of histogram analysis for multiparameters from multimodal MRI combining DCE, IVIM-DWI and 3D-Asl in predicating the Glioma grading and survival

Lin-Feng Yan[1], Xin Zhang[1], Yu Han[1], Yu-Chuan Hu[1], Hai-Yan Nan[1], Ying-Zhi Sun[1], Zhi-Cheng Liu[1], Yang Yang[1], Wen Wang[1], and Guang-Bin Cui[1]

[1]Tangdu Hospital, Xi'an, People's Republic of China

To find the early biomarkers for predicting the histological grading and prognosis of glioma, the study compared the discriminating efficiency of multiple metrics from DCE, Multi-b DWI and 3D-ASL with a histogram analysis approach, and further evaluated the combined accuracy and the survival association. The accuracy of assessing glioma grading and survival would not significantly improved by a univariate parameter, but highly promoted by combining the multiple parameters of histogram analysis from various MRI modality. We will further utilize the machine learning to evaluate the classifying accuracy.

4167 Computer 2

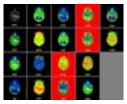

ADC-Map Based Computer Aided Radiological Diagnostics (CARD) for the Initial Differential Diagnosis of Medulloblastoma versus Pilocytic Astrocytoma – A Reproducibility Study.

Urspeter Knecht[1], Nicole Porz[2], Beate Sick[3], Elvis Murina[4], Nuno Miguel Pedrosa de Barros[5], Philippe Schucht[6], Evelyn Herrmann[7], Jan Gralla[1], Roland Wiest[1], Marwan El-Koussy[5], and Johannes Slotboom[8]

[1]Neuroradiology, University Hospital Bern, Bern, Switzerland, [2]Neurosurgery, University Hospital Bern, Bern, Switzerland, [3]Department of Biostatistics, Institute of Epidemiology, Biostatistics and Prevention, University of Zürich, Zürich, Switzerland, [4]Institute for Data Analysis and Process Design, ZHAW, Switzerland, [5]Neuroradiology, University Bern, University Hospital, Bern, Switzerland, [6]Neurosurgery, University Hospital Bern, Bern, [7]Radiooncology, University Bern, University Hospital, Bern, Switzerland, [8]Neuroradiology, University Hospital Bern, Switzerland

The diagnosis of brain tumors using visual criteria is very challenging. A novel computational method for computer aided radiologic diagnostics (CARD) is described based on quantitative textural features from ADC-maps, and a machine learning algorithm (Random-Forest classification). The reproducibility of the method was examined with 3 human raters was performed, and the Fleiss'-Kappa-test revealed high inter-rater agreement of κ=0.821 (p-value<<0.001) and an intra-rater agreement of κ =0.822 (p-value<<0.001). The method significantly improves the differential diagnosis of medulloblastoma versus pilocytic-astrocytomas.

4168 Computer 3

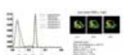

3D Parametric Histogram Analysis of Extravascular Extracellular Space for Identifying Subpopulations of Glioblastoma Related to Survival

Ka-Loh Li[1], Natale Quartuccio[1], Xiaoping Zhu[1], Samantha Mills, and Alan Jackson[1]

[1]Division of Informatics, Imaging and Data Sciences, The University of Manchester, Manchester, United Kingdom

Histogram Analysis of v_e was used for quantification of heterogeneity in glioblastomas and to study whether heterogeneity is related to survival. 27 patients with GBM were imaged. v_e histograms were processed by using a 4-mixture Gaussian distribution. Patients with short survival show an increasing proportion of the third Gaussian distribution. The mean of the 2nd Gaussian component, μ2, (p = 0.00015) and the weight of the 3rd components, w3 (p = 0.0066) were the most predictive for survival. The identification of tissue components, characterized by Gaussian fitting of v_e values suggests that these represent, in some way, separate tissue subpopulations.

4169 Computer 4

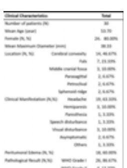

Evaluation of the Applicability of Territorial Arterial Spin Labelling in Meningiomas for Presurgical Assessments Compared with 3-Dimensional Time-of-Flight Magnetic Resonance Angiography

Yiping Lu[1], Bo Yin[1], Shihai Luan[2], Li Liu[3], Ji Xiong[1], Jianbo Wen[1], Jianxun Qu[4], and Daoying Geng[1]

[1]Department of Radiology, Huashan Hospital, Fudan University, Shanghai, People's Republic of China, [2]Department of Neurosurgery, Huashan Hospital, Fudan University, Shanghai, People's Republic of China, [3]Department of Radiology, Shanghai Cancer Center, Shanghai, People's Republic of China, [4]MR Research China, GE Healthcare, Shanghai, People's Republic of China

In this research, territorial Arterial Spin Labelling (t-ASL) and unenhanced 3D-TOF-MRA were used to evaluate the usage in identification of the feeding vasculature of meningiomas in 20 consecutive patients. Results showed that the inter-observer agreement was excellent for the identification of the origin of the feeding arteries by t-ASL, which was better than the inter-observer agreement of 3D-TOF-MRA. The inter-modality agreement between t-ASL and 3D-TOF-MRA for the feeding arteries was moderate. The information about feeding arteries was potentially related to patients' symptoms and pathology, making it crucial for neurosurgeons in planning surgery and evaluating prognosis.

4170 Computer 5

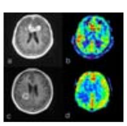

Three-dimensional pseudo-continuous arterial spin labeling(3D-pcASL) in differentiating tumor progression from treated effects in glioma

Yuelei Lyu[1,2], Bo Hou [1], Shuai Liu [3], Hui You[1], Yu Wang[3], Wenbin Ma [3], and Feng Feng[1]

[1]Department of Radiology, Peking Union Medical College Hospital, Beijing, People's Republic of China, [2]Department of Radiology, Beijing Chao-Yang Hospital, Beijing, People's Republic of China, [3]Department of Neurosurgery, Peking Union Medical College Hospital, Beijing, People's Republic of China

This study investigates the role of 3D-pcASL in discriminating between glioma progression(TP)and treatment related changes(TRC). We found that the maximum CBF (absolute value and its normalized values) in the lesion from 3D-pcASL were significantly higher in the TP group than in the TRC group. The ROC curve analysis showed the maximum CBF has an excellent performance in differentiating TP from TRC in patients with newly diagnosed glioma who have undertaken radiotherapy or chemoradiotherapy.

4171 Computer 6

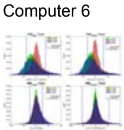

Proposed thresholds for parametric response mapping using intravoxel incoherent motion diffusion weighted imaging (IVIM-DWI) for the assessment of brain tumor treatment response

Ashley M Stokes[1], Jack T Skinner[2], Laura C Bell[1], Adrienne N Dula[3], Thomas E Yankeelov[3], and C. Chad Quarles[1]

[1]Translational Bioimaging Group, Barrow Neurological Institute, Phoenix, AZ, United States, [2]Imaging Programs, National Comprehensive Cancer Network (NCCN), Philadelphia, PA, United States, [3]University of Texas - Austin

The purpose of this study is to establish thresholds for parametric response mapping (PRM) using apparent diffusion coefficients (ADC) and intra-voxel incoherent motion (IVIM) parameters in healthy controls and to apply these thresholds in a cohort of brain tumor patients to study regional treatment-induced changes in diffusion and perfusion. We obtained thresholds (95% confidence intervals) of 0.38 and 0.32 x10^{-3} mm^2/s for ADC and IVIM-*D*, respectively. For the perfusion-related distributions, the thresholds were 10 ml/100g (IVIM-f_p) and 54 ml/100g/min (IVIM-f_pD^*). This multi-parametric sensitivity to local tumor changes could be useful to simultaneously evaluate treatment-induced changes in perfusion and cellularity.

4172 Computer 7

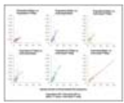

Repeatability of ktrans derived from DCE-MRI in newly diagnosed glioblastoma across multiple baseline images and processing methods.

Andrew L Beers[1], Yi-Fen Yen[2], Kyrre Eeg Emblem[3], Elizabeth R Gerstner[4], Bruce Rosen[2], and Jayashree Kalpathy-Cramer[2]

[1]Radiology, Massachusetts General Hospital, Boston, MA, United States, [2]Radiology, Massachusetts General Hospital, [3]Oslo University Hospital, [4]Neurology, Massachusetts General Hospital

We evaluate the reproducibility of ktrans values derived from dynamic contrast MRI images in patients with newly diagnosed glioblastoma. Particular focus is put on the reproducibility across choices of T1 values and arterial input functions (AIFs) to the Tofts-Kermode model. Reproducibility is assessed across multiple pre-therapy baseline visits in a 45 patient cohort. Our model based on static population AIFs and static global T1 values had excellent reproducibility compared to other models including unique individual AIFs and T1 maps. There is relatively little concordance between all tested models, but individual AIFs led to higher mean ktrans values.

4173 Computer 8

Influence of Preload and Post-Processing Methods on the Consistency of Cerebral Blood Volume Values from Dynamic Susceptibility Contrast MRI

Laura C. Bell[1], Leland S. Hu[2], Ashley M. Stokes[1], Samuel C. McGee[1], Leslie C. Baxter[1], and C. Chad Quarles[1]

[1]Barrow Neurological Institute, Phoenix, AZ, United States, [2]Mayo Clinic, Phoenix, AZ

With DSC-MRI, contrast agent leakage effects in high-grade gliomas must be resolved for accurate CBV measurements. Our aim is to compare CBV values across 1) varying preload doses, 2) two different previously published leakage correction methods, 3) normalized to either the AIF or normal appearing white matter (NAWM), and 4) different CBV integration limits. This was accomplished by acquiring six consecutive DSC-MRI with varying preloads in 14 glioma patients. We found that leakage corrected CBV measurements exhibit high consistency across variable preload doses, particularly when data is integrated under the “First Pass Only” and normalized to the AIF.

4174 Computer 9

True progression versus radiation necrosis in glioma: a comparative study of arterial spin labelling and dynamic susceptibility contrast imaging

Qian Xu[1], Kai Xu[1], Qi Liu[1], Hong Ma[1], Jiangfen Wu[2], and Jianxun Qu[2]

[1]Department of radiology, Affiliation hospital of Xuzhou Medical University Department of Radiology, Xuzhou, People's Republic of China, [2]GE Healthcare, Shanghai, People's Republic of China

Differentiation of treatment-related radiation necrosis from recurrent neoplasm is often difficult and dynamic susceptibility contrast perfusion MR imaging (DSC-MRI) is reported to be a surrogate marker for distinguishing them. However, DSC technique is invasive and has its disadvantage. Three dimensional pseudo-continuous ASL (3D-pcASL) can provide noninvasive absolute cerebral blood flow (CBF) measurement with insensitivity to permeability, and it is especially necessary for the evaluation of the postoperative gliomas patients where the blood-brain barrier (BBB) is completely broken with much more leakage effects. This study aimed to differentiate true progression from radiation necrosis of gliomas by using 3D-pcASL and DSC-MRI.

4175 Computer 10

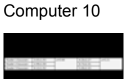

Cerebral Blood Volume (CBV) Normalization for Dynamic Susceptibility Contrast (DSC) MRI in Glioblastoma Patients

Lei Qin[1], Xiang Li[2], Jinrong Qu[2], Katherine Leung[3], Angie Li[3], and Geoffrey S Young[3]

[1]Dana-Farber Cancer Institute, Boston, MA, United States, [2]Radiology, Affiliated Cancer Hospital of Zhengzhou University, [3]Radiology, Brigham and Women's Hospital

Gaussian normalization generates more consistent nCBV maps than the gold standard, manual NAWM normalization. The ease of implementation and automated aspect of Gaussian normalization makes it an appealing method that could be successfully implemented in the clinical setting.

4176 Computer 11

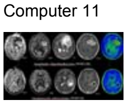

Preliminary Analysis of Neurite Orientation Dispersion and Density Imaging in Grading of Gliomas

Jing Zhao[1], Jian-ping Chu[2], Jing-yan Wang[2], and Xu Yan[3]

[1]The First Affiliated Hospital of Sun Yat-sen University, Guang Zhou, People's Republic of China, [2]The First Affiliated Hospital of Sun Yat-sen University, [3]Shang Hai

Neurite orientation dispersion and density imaging (NODDI) was an advanced DWI. Our study is to quantitatively evaluate the diagnostic efficiency of NODDI in grading gliomas. 29 patients were recruited and they underwent whole-brain DWI which were collected at three b value (0, 1000 and 2000 s/mm2) and 1000 and 2000 s/mm2 with 30 directions. Compared with LGG, ficvf and ODI are significantly higher in HGG and the mean value of ficvf showed the highest diagnostic value. Quantitative parameters from NODDI can aid in gliomas grading and the mean value of ficvf showed the highest diagnostic power.

4177 Computer 12

Diffusion kurtosis imaging: a novel tool to evaluate survival of glioma patients

Rifeng Jiang[1], Wenzhen Zhu[2], Lingyun Zhao[2], Qing Duan[1], Yunjing Xue[1], and Jingjing Jiang[2]

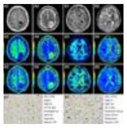

[1]Fujian Medical University Union Hospital, Fuzhou, People's Republic of China, [2]Tongji Hospital, HUST, Wuhan, People's Republic of China

DKI is a promising tool to predict the survival of glioma patients. MK, MD and ADC were significantly correlated with overall survival (OS) of patients with astrocytic tumor. By univariate Kaplan-Meier survival analyses, OS of the patients was related to tumor grade, Ki-67 LI, resection status, enhancement degree, edge, edema degree, lesion number, MK, MD and ADC (log rank $p < 0.05$ for all). Multivariate Cox regression analysis indicated that MK is an independent predictor of OS in these patients, and it is a risk factor ($P = 0.006$, HR=2.142 and 95% CI=1.247-3.679 for MK increasing every 0.1). These results are helpful to clinic.

4178 Computer 13

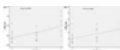

Predicting WHO grade of brain glioma using inflow-based vascular-space-occupancy MR imaging at 3 Tesla

Yuankui Wu[1], Shukun Liao[1], Danni Wang[2], Lichao Ma[1], Jun Hua[3,4], Yingjie Mei[2], Jun Wang[5], Jun Zhou[6], and Yikai Xu[1]

[1]Department of Medical Imaging, Nanfang Hospital, Southern Medical University, Guangzhou, People's Republic of China, [2]School of Biomedical Engineering, Southern Medical University, Guangzhou, People's Republic of China, [3]Neurosection, Division of MRI Research, Department of Radiology, Johns Hopkins University School of Medicine, Baltimore, Maryland, USA, [4]F.M. Kirby Research Center for Functional Brain Imaging, Kennedy Krieger Institute, Baltimore, Maryland, United States, [5]Department of Neurosurgery, Nanfang Hospital, Southern Medical University, Guangzhou, People's Republic of China, [6]Department of Pathology, Nanfang Hospital, Southern Medical University, Guangzhou, People's Republic of China

The purpose of this study is to investigate the feasibility of grading primary brain gliomas with inflow-based vascular-space-occupancy (iVASO) MRI. The iVASO MRI perfusion approach enables the quantitative analysis of physiological information of tumor without using exogenous contrast agent. The measured arteriolar cerebral blood volume (CBVa) showed a significant association with tumor grades as well as the capability to predict tumors grades. When exogenous contrast agent administration is difficult or contraindicated in certain patient populations, iVASO MRI may used as an option for the clinical management of brain tumors.

4179 Computer 14

Clinical Applications of Simultaneous Multi-slice (SMS) Imaging with High-angular-resolution Diffusion Imaging (HARDI) : a Comparative Study of Brain Tumor Pre-operative Evaluation with and without SMS

Louis-Olivier Bouchard[1,2], Christian Berthelot[2], and Maxime Villeneuve[3]

[1]Radiology, Université Laval, Québec, QC, Canada, [2]Radiology, CHU de Québec, Québec, QC, Canada, [3]CHU de Québec, QC, Canada

Diffusion MRI can be helpful in pre-operative brain tumor evaluation to assess white matter tracts involved. It is however a time-consuming sequence, a problem that Simultaneous Multi-slice Imaging was designed to solve, although it has to demonstrate its quality non-inferiority. We compared in five patients tractographic data (using HARDI), acquired with and without SMS techniques, to evaluate the quality of imaging data as measured by the number of fibers between two regions of interest. We found that SMS-factor 2, cut time down by 37%, which is clinically relevant. We also found that SMS-2 is indeed non-inferior (alpha=0,03125) and can be used without quality compromise.

4180 Computer 15

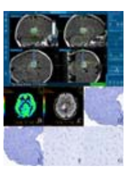

Perfusion imaging of brain gliomas using arterial spin labeling: Correlation with histopathological vascular density in MRI-guided biopsies

Haopeng Pang[1], Ningning Di[1], Chengjun Yao[2], Yan Ren[1], Jingsong Wu [3], Yong Zhang[4], Jianxun Qu [4], and Zhenwei Yao [1]

[1]Radiology, Huashan Hospital, Shanghai, People's Republic of China, [2]Glioma Surgery Division, Huashan Hospital, Shanghai, People's Republic of China, [3]Neurosurgery, Huashan Hospital, Shanghai, People's Republic of China, [4]MR Research China, GE Healthcare, Shanghai, People's Republic of China

This study was designed to determine if CBF derived from ASL perfusion imaging could be used to quantitatively evaluate the MVD of brain gliomas on a “point-to-point” basis. The study enrolled 47 patients with treatment-naive brain gliomas who underwent preoperative ASL before stereotactic surgery. We histologically quantified MVD from CD34-stained sections of stereotactic biopsies and co-registered biopsy locations with localized CBF measurements. CBF showed a statistically significant positive correlation with MVD. ASL can be a quantitative and noninvasive perfusion MR method for evaluating the MVD of brain gliomas, and may reflect the microvascularity of gliomas.

4181 Computer 16

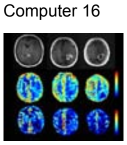

Non-invasive, contrast-exempt (NICE) assessment of glioblastoma (GBM) using multi-slice ASL and iVASO imaging

Jalal B. Andre[1], S Kristie McKown[2], and Swati Rane[2]

[1]Radiology, University of Washington, Seattle, WA, United States, [2]University of Washington

Assessment of cerebral and tumor perfusion has frequently been advocated for initial prognostication, and evaluation for possible progression, of primary brain tumors, historically accomplished via intravenous injection of a gadolinium-based contrast agent (GBCA). The potential for intracranial and corporeal deposition of GBCA invites the development and optimization of non-invasive, contrast-exempt (NICE) methods to assess cerebral perfusion. We sought to develop and implement NICE spin-label-based methods incorporating cerebral blood flow (CBF) and volume (CBV) assessment, applied in treated GBM patients.

4182 Computer 17

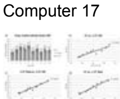

Intraoperative Arterial Spin Labeling – feasibility and first results

Thomas Lindner[1], Isabel Lübbing[2], Christian von der Brelie[2,3], Michael Helle[4], Olav Jansen[1], Michael Synowitz[2], and Stephan Ulmer[1,5]

[1]Clinic for Radiology and Neuroradiology, University Hospital Schleswig-Holstein, Kiel, Germany, [2]Clinic for Neurosurgery, University Hospital Schleswig-Holstein, Kiel, Germany, [3]Clinic for Neurosurgery, University Hospital Göttingen, Göttingen, Germany, [4]Tomographic Imaging Department, Philips Research, Hamburg, Germany, [5]Medizinisch Radiologisches Institut, Zurich, Switzerland

Performing MRI studies in an intraoperative setting is generally limited due to hardware and patient positioning restrictions. Structural imaging alone might not be sufficient to gather all required information. The goal of this study was to implement pseudo-continuous ASL in the intraoperative neurosurgical setting with limited hardware available and compare the images with measurements obtained pre-, and postoperatively on different clinical MRI scanners. The first application in a patient shows the potential of intraoperative ASL imaging with regards to visualizing residual tumor mass already during the surgical intervention in similar image quality.

4183 Computer 18

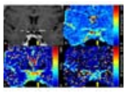

Evaluation of intravoxel incoherent motion in pituitary adenoma using turbo spin-echo diffusion-weighted imaging

Kiyohisa Kamimura[1], Masanori Nakajo[1], Yoshihiko Fukukura[1], Shingo Fujio[2], Takashi Iwanaga[3], Tomoyuki Okuaki [4], and Takashi Yoshiura[1]

[1]Radiology, Kagoshima University Medical and Dental Hospital, Kagoshima, Japan, [2]Neurosurgery, Kagoshima University Medical and Dental Hospital, Kagoshima, Japan, [3]Clinical Engineering Department Radiation Section, Kagoshima University Hospital, Kagoshima, Japan, [4]Philips Healthcare, Tokyo

Our purpose was to evaluate the intravoxel incoherent motion (IVIM) in the pituitary adenoma using turbo spin-echo diffusion-weighted imaging (TSE-DWI). The f (perfusion fraction) in the pituitary adenoma was significantly lower than that in the normal pituitary gland, which is consistent with histopathologically known lower microvascular density in adenomas compared to normal pituitary tissue. There was no significant correlation between the f and the volume in pituitary adenomas. TSE-DWI-based IVIM imaging is a viable imaging technique for assessment of vascularity in skull base lesions including pituitary adenoma.

4184 Computer 19

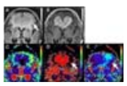

Histogram Analysis of Intravoxel Incoherent Motion in Peritumoral Edema for Distinguishing between Central Nervous System Lymphoma and Other Brain Tumors

Kazuhiro Murayama[1], Takashi Fukuba[2], Shigeharu Ohyu[3], Ayako Ninomiya[3], Kazuhiro Katada[4], and Hiroshi Toyama[1]

[1]Radiology, Fujita Health University, Toyoake, Japan, [2]Radiology, Fujita Health University Hospital, Toyoake, Japan, [3]Toshiba Medical Systems Corporation, Japan, [4]Joint Research Laboratory of Advanced Medical Imaging, Fujita Health University, Toyoake, Japan

Additional benefits of quantitative analysis of peritumoral edema for distinguishing between brain tumors by diffusion weighted image or dynamic susceptibility contrast MRI has been described. Our aim was to investigate the hypothesis that quantitative analysis of intravoxel incoherent motion (IVIM) in peritumoral edema may be a useful parameter for distinguishing between central nervous system lymphoma (CNSL) and other brain tumors. Quantitative analysis of IVIM indicates that *D** and ***f*** maps of CNSL visually showed increase values in peritumoral edema. Our results indicate that these IVIM parameters have been successfully applied to obtain quantitative estimates of the vascularity and perfusion in peritumoral edema for differenciating CNSL and others without gadolinium contrast agent.

4185 Computer 20

Independent Component-based Denoising for Mapping Cerebrovascular Reactivity with Resting-State Fluctuation of BOLD Signal Amplitude in Patients with Gliomas

AI-LING HSU[1], Ping-Ni Wang[2], Jyh-Horng Chen[3], and Ho-Ling Liu[4]

[1]Imaging Physics, The University of Texas MD Anderson Cancer Center, Houston, TX, United States, [2]Department of Medical Physics, University of Wisconsin-Madison, [3]Institute of Biomedical Electronics and Bioinformatics, National Taiwan University, [4]Department of Imaging Physics, The University of Texas MD Anderson Cancer Center

Cerebrovascular reactivity (CVR) with hypercapnia challenges, such as a breath-hold (BH) task, has been proposed to indicate areas with neurovascular uncoupling potentials for presurgical fMRI. Previous studies have shown that BH response correlated with resting-state fluctuation of amplitude (RSFA) in healthy adults. This study explores the use of RSFA for indicating sites with neurovascular uncoupling potentials in presurgical fMRI of patients with gliomas. The RSFA with ICA-based denoising approaches was found to perform superior to the traditional approaches. Unlike BH, RS-fMRI is less dependent on patient performance thus can be widely applied in clinical practice.

4186 Computer 21

Active and passive fMRI for preoperative localization of motor function areas in brain tumor patients

Chen Niu[1], Xiao Ling[1], Pan Lin[2], Kun Zhang[3], Xin Liu[4], Liping Guo[1], Wenfei Li[1], Hao Song[2], Ming Zhang[1], and Maode Wang[5]

[1]Department of Medical Imaging, The First Affiliated Hospital of Xi'An Jiaotong University, Xi'An, People's Republic of China, [2]Key Laboratory of Biomedical Information Engineering of Education Ministry, Institute of Biomedical Engineering, Xi'an Jiaotong University, [3]Department of Electronics Engineering, Northwestern Polytechnical University, [4]Technical University Munich, [5]Department of neurosurgery, The First Affiliated Hospital of Xi'An Jiaotong University, Xi'An, People's Republic of China

The aim of this study is to investigate whether there is consistency between active and passive movement in patients with brain tumors. Two motor tasks (active and passive hand movement) were applied to brain tumor patients. Our results demonstrate that there is no statistical difference of activation intensity between active hand movement and passive hand movement in patients with brain tumors. Our results suggest that passive movement fMRI provides a potential method for presurgical mapping in cases where patients are unable to comply with task instructions.

4187 Computer 22

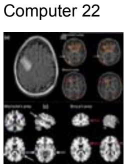

Predicting pre-surgical language lateralization using resting state fMRI in patients with neuropathologies

Bradford A Moffat[1], Sarah Kalus[2], Christopher Steward[2], Chris Kokkinos[3], Patricia M Desmond[2], and Pramit Phal[3]

[1]Anatomy and Neuroscience, The University of Melbourne, Parkville, Australia, [2]Radiology, The University of Melbourne, Parkville, Australia, [3]Epworth Medical Imaging, Richmond, Australia

We present a quantitative resting state fMRI method for determining the laterality of language processing in patients undergoing neurosurgical procedures. The results show that laterality indices based on the resting state fMRI can predict a patient's laterality based on a language task fMRI. This has potential for guiding neurosurgical interventions in patients unable to perform task fMRI exams or during surgery with an interventional MRI scanner.

4188 Computer 23

Brain Structural Network of Working Memory and Processing Speed for ALL Survivors

Junyu Guo[1], John O. Glass[1], JungWon Hyun[1], Yimei Li[1], Heather Conklin[1], Lisa Jacola[1], Ching-Hon Pui[1], Sima Jeha[1], and Wilbrun E. Reddick[1]

[1]St Jude Children's Research Hospital, Memphis, TN, United States

Acute lymphoblastic leukemia survivors may have significant deficits in processing speed and working memory even when treated with only chemotherapy. We investigate the relationship of diffusion tensor imaging metrics in an a priori brain structural network with neurocognitive functions such as processing speed and working memory. We found that fractional anisotropy values in the structural network were significantly positively associated with processing speed performance in two MR exams two years apart, and axial diffusivity values were negatively associated with working memory in the MR exam at the end of therapy. These findings may provide potential evidence for a structural neurocognitive network.

4189 Computer 24

magna cum laude

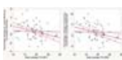

Altered network topology in patients with primary brain tumors after fractionated radiotherapy

Naeim Bahrami[1], Tyler Seibert [1], Roshan Karunamuni[1], Jona Hattangadi-Gluth[1], Nikdokht Farid[1], Anders Dale[1], and Carrie McDonald[1]

[1]University of California, San Diego, San Diego, CA, United States

The purpose of this study is to determine whether brain structural network properties change in brain tumor patients following fractionated, partial brain radiotherapy(RT). We applied graph theory to MRI-derived cortical thickness estimates in 54 patients pre and post-RT and examine global and local changes in network topology. Increases in global efficiency, transitivity, and modularity were observed post-RT compared to pre-RT. Decreases in local efficiency and clustering coefficient were seen in regions receiving higher doses of RT. Our findings demonstrate alterations in global and local network topology following RT in patients with primary brain tumors.

Electronic Poster

Neuro Educational

Exhibition Hall Tuesday 14:45 - 15:45

4190 Computer 25

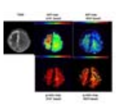

The pitfalls of MR fiber g-ratio mapping in neurological disease patients.

Masaaki Hori[1], Kouhei Kamiya[2], Yuichi Suzuki[2], Ryuji Nojiri[3], Yasuaki Turushima[3], Ryo Ueda[1,4], Issei Fukunaga[1], Misaki Nakazawa[1,4], Akifumi Hagiwara[2], Christina Andica[1], Koji Kamagata[1], Keiichi Ishigame[3], Kanako Kunishima Kumamaru[1], and Shigeki Aoki[1]

[1]Radiology, Juntendo University School of Medicine, Tokyo, Japan, [2]Radiology, The University of Tokyo Hospital, Tokyo, Japan, [3]Radiology, Tokyo Medical Clinic, Tokyo, Japan, [4]Health Science, Tokyo Metropolitan University, Tokyo, Japan

The purpose of this exhibit is to present the pitfalls of generating MR fiber g-ratio mapping in neurological disease patients, and to propose possible solutions. While the g-ratio maps can help to make comprehensive diagnosis together with clinical information (i.e. symptoms), probable differential diagnosis and conventional MR imaging findings can help to avoid the misuse of MR fiber g-ratio maps in the clinical setting.

4191 Computer 26

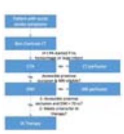

State of the art stroke imaging

Olivier Clerk-Lamalice[1] and John W Chen[1]

[1]Neuroradiology, Massachusetts General Hospital, Boston, MA, United States

This work will review key concepts of our current understanding of stroke pathophysiology, imaging protocol with an interest on specific MRI sequences. This review will also introduce important concepts regarding stroke-related neuroinflammation.

4192 Computer 27

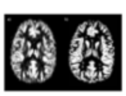

Partial Volume Effects in Arterial Spin Labelling: Something to Live With or Correct For?

Michael A Chappell[1], Iris Asllani[2], Xavier Golay[3], Matthias Günther[4,5,6], Juan A Hernández-Tamames[7], and Matthias J.P van Osch[8]

[1]Institute of Biomedical Engineering, University of Oxford, Oxford, United Kingdom, [2]Department of Biomedical Engineering, Rochester Institute of Technology, Rochester, NY, United States, [3]Department of Brain Repair and Rehabilitation, UCL Institute of Neurology, London, United Kingdom, [4]Fraunhofer MEVIS, Bremen, Germany, [5]University Bremen, Bremen, Germany, [6]mediri GmbH, Heidelberg, Germany, [7]Radiologie & Nucleaire Geneeskunde, Erasmus MC, Rotterdam, Netherlands, [8]C.J. Gorter Center for High Field MRI, Leiden University Medical Center, Leiden, Netherlands

Partial Volume Effects have a profound influence on the perfusion images generated using Arterial Spin Labelling. We are only starting to appreciate how this influences our interpretation of the images and what we can discover when using perfusion imaging in studies. This e-poster seeks to outline the key issues, underlying theory about what effects PVE might have, methods to correct for them, and when correction may or may not be a good idea.

4193 Computer 28

Optimizing pediatric leptomeningeal metastasis detection: technical considerations

Julie H Harreld[1], Muhammad Ayaz[1], Claudia M Hillenbrand[1], Ralf Loeffler[1], Scott N Hwang[1], Junyu Guo[1], and Zoltan Patay[1]

[1]Diagnostic Imaging, St. Jude Children's Research Hospital, Memphis, TN, United States

MRI has assumed a central role in the detection of leptomeningeal metastasis for risk stratification of pediatric CNS tumors, but not all sequences are created equal for detection of tumor in CSF. In this presentation, we describe the strengths, weaknesses and tradeoffs of sequences commonly used for this purpose, and suggest guidelines for a targeted imaging protocol with increased sensitivity for leptomeningeal tumor, in less scan time.

4194 Computer 29

Malformations of cortical development: MRI evaluation

Maria Camila Arango-White[1], Diego Herrera[2], and Sergio Alberto Vargas[3]

[1]radiology, Universidad de Antioquia, Medellin, Colombia, [2]Radiology, CEDIMED, medellin, Colombia, [3]Radiology, CEDIMED, Medellin, Colombia

Cortical development malformations are relatively uncommon conditions but have an enormous impact in children with neuro-developmental delay, disability and epilepsy. We aim to present cases from our clinical practice to illustrate the pathology spectrum and review the existing literature about these malformations. We emphasize the importance of an MRI approach to elaborate a differential diagnosis which can be useful to focus genetic tests, and to establish prognosis in these patients.

4195 Computer 30

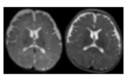

Expanding the Role of the Rapid Sequence MRI in Pediatric Neuroimaging

Cory Pfeifer[1], Amber Pokorney[1], and Patricia Cornejo[1]

[1]Phoenix Children's Hospital, Phoenix, AZ, United States

The Image Gently campaign has resulted in increased awareness of radiation risks in the pediatric population. A major effect of this is a reduction in computed tomography in pediatric hospitals. While MRI may be able to achieve many of the goals of CT, risks related to sedation and the need for increased resources to perform sedated MRI must also be considered for children with conditions known to require follow-up imaging. In cases where children have external ventricular shunts in place over a long term, rapid sequence MRI has been well-described in its role to assess ventricular size while avoiding both ionizing radiation and sedation. Here we describe the use of our version of the rapid sequence MRI to assess additional indications, as more than half of the patients undergoing this study in our facility do not have indwelling ventricular shunt catheters at the time of imaging. Limitations of this technique are also discussed.

4196 Computer 31

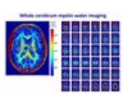

Magnetic Resonance Imaging of Myelin Water: Principles and Applications

Cornelia Laule[1,2,3], Irene M. Vavasour[1], Shannon H. Kolind[1,4], Thorarin A. Bjarnason[1,5,6], Jing Zhang[1], Donna J.M. Lang[1], Hanwen Liu[3,7], Emil Ljungberg[4], Roger Tam[1], Erin L. MacMillan[4], John K. Kramer[3,8], Sandra Sirrs[4], Piotr Kozlowski[1,3,7], Alexander Rauscher[1,9], Lara Boyd[10], G.R. Wayne Moore[2,3,4], Anthony L. Traboulsee[4], David K.B. Li[1,4], and Alexander L. MacKay[1,7]

[1]Radiology, University of British Columbia, Vancouver, BC, Canada, [2]Pathology & Laboratory Medicine, University of British Columbia, Vancouver, BC, Canada, [3]International Collaboration on Repair Discoveries, University of British Columbia, Vancouver, BC, Canada, [4]Medicine, University of British Columbia, Vancouver, BC, Canada, [5]Interior Health, Kelowna, BC, Canada, [6]Computer Science, Mathematics, Physics & Statistics, University of British Columbia Okanagan, Kelowna, BC, Canada, [7]Physics & Astronomy, University of British Columbia, Vancouver, BC, Canada, [8]Kinesiology, University of British Columbia, Vancouver, BC, Canada, [9]Pediatrics, University of British Columbia, Vancouver, BC, Canada, [10]Physical Therapy, University of British Columbia, Vancouver, BC, Canada

Myelin water imaging (MWI) provides quantitative and specific mapping of myelin content in-vivo. Water trapped between myelin bilayers have a short T_2 relaxation time; the fractional proportion of this myelin water signal correlates strongly with histological staining for myelin. MWI has successfully been used to study both the brain and spinal cord where it can increase our understanding of development, aging and disease processes, and may also improve accuracy of diagnosis, prognosis and assessment of therapeutic response. Moving forward, MWI is expected to play an important role in the development and monitoring of new treatments targeted at remyelination and neuroprotection.

4197 Computer 32

The adaptive learning processing of establishing a research imaging core lab

Marina Salluzzi[1,2], Nicole Blenkin[1,2], and Richard Frayne[2,3]

[1]Calgary Image Processing and Analysis Centre, Foothills Medical Centre, Calgary, AB, Canada, [2]Departments of Radiology and Clinical Neurosciences, Hotchkiss Brain Institute, University of Calgary, Calgary, AB, Canada, [3]Seaman Family Research MR Centre, Foothills Medical Centre, Calgary, AB, Canada

As institutions, agencies and governing bodies move toward increased value for invested research funds, core laboratory facilities have been found to be an effective solution to researcher needs. The Calgary Image Processing and Analysis Centre was envisioned as a core lab to support the local research community, and today it provides an evolving suite of services to facilitate the translation efforts in medical imaging research. CIPAC's evolution has been possible due to the synergy with local researchers striving for a quality solution to research image data management needs.

4198 Computer 33

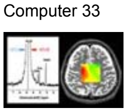

Relation between brain temperature and cerebral perfusion and metabolism in human brain

Shunrou Fujiwara[1,2], Takaaki Beppu[1,3], Kuniaki Ogasawara[1], and Yoshichika Yoshioka[2,4]

[1]Department of Neurosurgery, Iwate Medical University, Morioka, Japan, [2]WPI Immunology Frontier Research Center, Osaka University, Suita, Japan, [3]Department of Hyperbaric Medicine, Iwate Medical University, Morioka, Japan, [4]Center for Information and Neural Networks (CiNet), NICT and Osaka University, Suita, Japan

Brain temperature (BT) had traditionally been discussed whether it may be a simple parameter depending on body (core) temperature or it may regulate the neural activities; however, recent reports with magnetic resonance imaging (MRI) system demonstrated BT was strongly associated with the cerebral perfusion and metabolism in patients with ischemic change. Here, we reviewed BT measurement techniques with a MRI system and discussed the pathologic conditions causing BT alteration relating to the cerebral perfusion and metabolism.

4199 Computer 34

Clinical Application of Synthetic MRI: Benefits and Pitfalls

Christina Andica[1], Akifumi Hagiwara[1,2], Misaki Nakazawa[1,3], Masaaki Hori[1], and Shigeki Aoki[1]

[1]Radiology, Juntendo University, Tokyo, Japan, [2]Radiology, The University of Tokyo Graduate School of Medicine, Tokyo, Japan, [3]Radiological Sciences, Tokyo Metropolitan University Graduate School of Human Health Sciences, Tokyo, Japan

Synthetic MRI is a method of imaging based on the quantification of T1, T2, PD and B1 field by a single scan. The features of synthetic MRI such as; quantitative maps, tailored contrast-weighted imaging, brain tissue and myelin segmentation and volumetry show some advantages in the evaluation of brain disorders. However, some limitations were also noted.

4200 Computer 35

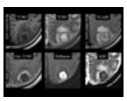

Brain abscess due to odontogenic infection: Insights from dental CT for differential diagnosis.

Daiji Uchiyama[1], Katsumi Nakamura[1], and Takehisa Tsuji[2]

[1]Radiology, Tobata Kyoritsu Hospital, Kitakyushu, Japan, [2]Neurosurgery, Kitakyushu, Japan

We herein report the 4 cases of brain abscess secondary to odontogenic infection due to an untreated tooth decay. In all cases, there were no abnormalities on physical and intraoral examinations, nor overt trismus or facial swelling. Dental CT showed a periapical radiolucency around the root tips of a decayed tooth, which revealed periodontal abscess. After the multidisciplinary therapy including antibiotics, abscess drainage, and dental treatments, all the patients recovered and discharged.

4201 Computer 36

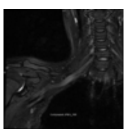

Navigating the Brachial Plexus: An MRI Visual Primer

Manu Singh[1], Bernard Chow[1], and Kai Kinder[1]

[1]Radiology, Santa Barbara Cottage Hospital, Santa Barbara, CA, United States

This educational exhibit provides an up-to-date, practical approach for MRI evaluation of the brachial plexus.

4202 Computer 37

The Review of Age-Related White Matter Changes in Alzheimer's Disease Trials

Dewen Yang[1]

[1]ICON Clinical Research, North Wales, PA, United States

Age-related white matter changes (ARWMC) are prevalent brain imaging findings and important substrates for cognitive impairment in the elderly. The true pathogenesis of ARWMC is not well understood. Previous studies verified that ARWMC also associate with cognitive decline. In Alzheimer's disease, ARWMC is also common findings on MRI images. The clinical importance of ARWMC in AD trials is reviewed.

4203 Computer 38

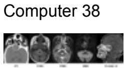

Imaging features of myoepithelial carcinoma in the nasopharynx and paranasal sinus

Chunyan Zhang[1], Jingliang Cheng[1], Yong Zhang[1], Kangkang Xue[1], and Shaoyu Wang[2]

[1]MRI Division, the First Affiliated Hostipal of Zhengzhou University, Zhengzhou,China, People's Republic of China, [2]Siemens Healthcare Ltd., People's Republic of China

This study aimed to explore the diagnostic points of myoepithelial carcinoma（MEC）in the nasopharynx analyze through analysing the imaging features.11 patients with MEC in the nasopharynx and paranasal sinus confirmed by pathology were analyzed retrospectively. CT and MRI appearances can localize the tumors，show tumors'size, and delineate the relationship of the 1esions with the surrounding tissue．On CT findings, MEC easily has osteolytic destruction and on MR and ADC vuale it owns certain characteristic features.These characteristics are conducive to the early diagnosis and rational treatment in clinics.

4204 Computer 39

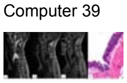

Intraspinal bronchogenic cyst: Series of case reports and literature review

Xueying Ma[1], Dun Ding[1], Fengli Liang[1], Zhuonan Wang[1], Haining Li[1], Yingxiang Sun[1], and Ming Zhang[1]

[1]Imaging Medical, The First Affiliated Hospital of Xi'an Jiaotong University, Xi'an, People's Republic of China

The purpose of this study was to provide a deeper knowledge of clinical presentation, imaging diagnosis, differential diagnosis and the management of the intraspinal bronchiogenic cysts. We retrospectively studied three cases of SBCs which were registered in our department and analyzed eight case reports which were all published in English. The SBCs can occur anywhere in the spinal canal, but they are more likely to present at the cervical canal and might be along with some developmental malformations of spine. We emphasize the role of MRI findings in the diagnosis before surgery. It is recommended that the lesion should be removed as completely as possible on the premise of protecting the spinal cord from being injured.

4205 Computer 40

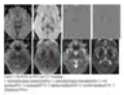

The study of brain iron by SWI and T2 * imaging in Parkinson's disease

Lixia Yang[1] and Yu Cheng[1]

[1]Department of image center, Shanghai Xuhui central hospital,Shanghai, Shanghai, People's Republic of China

Both Susceptibility Weighted Imaging (SWI) and T2 star (T2*) imaging can measure the brain iron deposition. However, the two ways by which the brain iron is measured are not compared. This study measured the brain iron of healthy volunteers and Parkinson's disease patients by SWI and T2* imaging. we found that SWI and T2* imaging could estimate the brain iron, and the SWI radiant values of SNr and RN were significance difference between healthy volunteers and Parkinson's disease patients, suggesting the SWI had better reliability to diagnose the Parkinson's disease than the T2* imaging.

4206 Computer 41

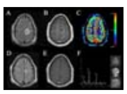

Imaging Mimics of Brain Tumors: Radiologic-Histopathologic Correlation

Ozden Kilinc[1], Sara Dastmalchian[1], Michael Coffey[1,2], Mark Cohen[2,3], Jeffrey Sunshine[1,2], Andrew Sloan[2,4], and Chaitra Badve[1,2]

[1]Department of Radiology, Case Western Reserve University School of Medicine, Cleveland, OH, United States, [2]University Hospitals Cleveland Medical Center, Cleveland, OH, United States, [3]Department of Pathology, Case Western Reserve University School of Medicine, Cleveland, OH, United States, [4]Department of Neurological Surgery, Case Western Reserve University School of Medicine, Cleveland, OH, United States

Neuroimaging plays critical diagnostic and prognostic role in the management of brain tumors. However, there can be a significant overlap in the imaging features between neoplastic and various non-neoplastic pathological processes in the brain. The knowledge of key differentiating features of such non-neoplastic entities is essential for a radiologist to facilitate accurate and timely diagnosis. Additionally, in such settings, judicious use of advanced imaging techniques such as perfusion imaging and spectroscopy can help the radiologist as problem-solving tools. In this exhibit, we review the conventional and advanced imaging features of different disease processes that are encountered in day-to-day clinical practice and can mimic brain neoplasms on imaging.

4207 Computer 42

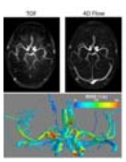

Image Quality Comparison of High Resolution PC-MRA (4D-Flow) with Time of Flight in Healthy Volunteers

Warren Chang[1], Michael Loecher[1], Daniel B Ennis[1], Aichi Chien[1], and J. Pablo Villablanca[1]

[1]Department of Radiological Sciences, University of California, Los Angeles, CA, United States

In this study, image quality of high resolution PC-MRA (4D Flow) and 3D-TOF was compared. Ten healthy volunteers were scanned with high resolution 4D-Flow and 3D-TOF angiograms at 0.5 mm isotropic spatial resolution in clinically-useful scan times of 7 and 12 minutes. There was no significant difference in image quality between 4D Flow and 3D-TOF in both source images and MIPs. 4D Flow acquisitions were velocity encoded, allowing hemodynamic evaluation of intracranial structures. This study demonstrated that phase-contrast techniques such as 4D-Flow have comparable image quality to 3D-TOF while obtaining velocity measurements, showing promise as a viable alternative to 3D-TOF.

Electronic Poster

Psychiatric Neuroimaging

Exhibition Hall Tuesday 14:45 - 15:45

4208 Computer 49

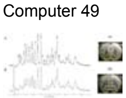

Individual metabolic differences in murine nucleus accumbens (NAc) measured by 1H-MRS at 14.1 Tesla is associated with trait-anxiety levels

Antoine Cherix[1], Thomas Larrieu[2], Arantxa Duque Moreno[3], Hongxia Lei[4], Santiago Moléon[3], Carmen Sandi[2], and Rolf Gruetter[1,5,6]

[1]Laboratory for Functional and Metabolic Imaging (LIFMET), Ecole Polytechnique Fédérale de Lausanne, Lausanne, Switzerland, [2]Laboratory of Behavioral Genetics (LGC), Ecole Polytechnique Fédérale de Lausanne, Lausanne, Switzerland, [3]Department of Psychobiology, University of Valencia, Valencia, Spain, [4]Center for Biomedical Imaging (CIBM), Ecole Polytechnique Fédérale de Lausanne, Lausanne, Switzerland, [5]Department of Radiology, University of Geneva, Geneva, Switzerland, [6]Department of Radiology, University of Lausanne, Lausanne, Switzerland

^{1}H-MRS was used to study metabolic changes associated with basal anxiety levels in nucleus accumbens (NAc) and medial prefrontal cortex (mPFC) of naive mice. Results indicate some neuroenergetic differences specific to the NAc, which supports the idea that this structure plays a critical role in the etiology of anxiety.

4209 Computer 50

Elevated Glycine and Glutamate Metabolite Levels in Patients with First-Episode Psychotic Disorders Measured by TE-averaged PRESS at 4 T

Sang-Young Kim[1,2], Marc J. Kaufman[1,3], Bruce M. Cohen[4], Joseph T. Coyle[5], Fei Du[1,2], and Dost Öngür[2]

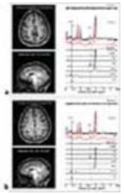

[1]McLean Imaging Center, McLean Hospital, Harvard Medical School, Belmont, MA, United States, [2]Psychotic Disorders Division, McLean Hospital, Harvard Medical School, Belmont, MA, United States, [3]Translational Imaging Laboratory, McLean Hospital, Harvard Medical School, Belmont, MA, United States, [4]Program for Neuropsychiatric Research, McLean Hospital, Harvard Medical School, Belmont, MA, United States, [5]Laboratory for Psychiatric and Molecular Neuroscience, McLean Hospital, Harvard Medical School, Belmont, MA, United States

In this work, we present the advantage of TE-averaged PRESS approach to reliably quantify brain glutamate and glycine levels in vivo in patients with psychosis. Since glutamtergic dysregulation and NMDA receptor hypofunction are implicated in the pathophysiology of major psychiatric conditions, non-invasive in vivo assessments of glutamate and its NMDA receptor modulator, glycine, would be of great importance. We found significantly elevated glutamate and glycine levels in the anterior cingulate cortex and parieto-occipital cortex of patients with first-episode psychosis as compared to healthy controls, suggesting increased brain glutamatergic activity with compensatory attempts to correct for NMDA receptor hypofunction.

4210 Computer 51

Modular organization of functional connectivity in schizophrenia patients beyond the resolution limit

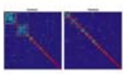

Cecile Bordier[1], Carlo Nicolini[1], and Angelo Bifone[1]

[1]Center for Neuroscience and Cognitive Systems, Istituto Italiano di Tecnologia, Rovereto (TN), Italy

Graph theoretical methods have been widely applied to study the modular organization of functional connectivity networks in neuropsychiatric disorders like Schizophrenia. However, current methods are affected by a resolution limit that prevents detection of modules that are smaller than a scale determined by the size of the entire network. We have developed a resolution-limit-free method, dubbed Surprise, and applied it to study resting state functional connectivity networks in a large cohort of Schizophrenia patients and matched controls. Improved resolution reveals substantial reorganization of resting state connectivity structure in patients, with previously undetected fragmentation and merging of sensory and associative modules.

4211 Computer 52

Decreased Brain Nicotinamide Adenine Dinucleotide (NAD) Levels in Adolescent Bipolar Disorder

Young-Hoon Sung[1,2], Xian-Feng Shi[1,2], Perry F. Renshaw[1,2,3], and Douglas G. Kondo[1,2,3]

[1]Brain Institute, Salt Lake City, UT, United States, [2]University of Utah Department of Psychiatry, Salt Lake City, UT, United States, [3]Veterans Administration Rocky Mountain MIRECC for Suicide Prevention, Salt Lake City, UT, United States

Converging evidence implicates mitochondrial dysfunction in bipolar disorder (BPD). Treatments of adolescent BPD have limited efficacy, and are associated with significant toxicity. Phosphorus magnetic spectroscopy imaging (^{31}P MRSI) may shed light on the pathophysiology and neural markers of adolescent BPD. In the present study, nicotinamide adenine dinucleotide (NAD) levels were measured using ^{31}P MRSI in 15 adolescents with BPD and 23 healthy controls (HC). BPD adolescents had significantly decreased NAD levels compared to HC. Clinical trials of NAD precursors are required to determine whether restoration of NAD levels is feasible, and can serve as a treatment for adolescent BPD.

4212 Computer 53

White matter structure asymmetry of drug-naïve first-episode schizophrenia patients under different genetic load

Wenbin Li[1], Huaiqiang Sun[1], Su Lui[1], and Qiyong Gong[1]

[1]West China Hospital, Chengdu, People's Republic of China

We analyzed the white matter (WM) asymmetry in a relatively large sample of drug-naïve schizophrenia patients under different genetic load. Based on this method, our findings demonstrated similar overall WM brain torque in sporadic and familial schizophrenia patients and healthy controls. Furthermore, our observation that familial illness was associated with more abnormal brain asymmetry compared to sporadic patients and that these specific changes were mainly located in a functional network associated with auditory hallucinations suggesting genetic factors may play critical roles in impacting risk for the most common form of hallucinations in schizophrenia.

4213 Computer 54

Connectome-wide exploration of altered resting-state connectivity in combat veterans with and without PTSD and real-time fMRI neurofeedback training effect on abnormal connectivity

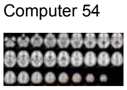

Masaya Misaki[1], Raquel Phillips[1], Vadim Zotev[1], Chung Ki Wong[1], Frank Krueger[2], Matthew Feldner[3], and Jerzy Bodurka[1,4]

[1]Laureate Institute for Brain Research, Tulsa, OK, United States, [2]Department of Psychology, George Mason University, Fairfax, VA, United States, [3]Deptartment of Psychological Science, University of Arkansas, Fayetteville, AR, United States, [4]College of Engineering, Stephenson School of Biomedical Engineering, University of Oklahoma, Tulsa, OK, United States

In combat veterans with and without PTSD diagnosis, we performed connectome-wide exploration of the whole-brain voxel-by-voxel fMRI connectivity using multivariate distance-based matrix regression (MDMR) analysis to determine connectivity abnormalities without a priori hypothesis. PTSD veterans showed increased connectivity across sensory motor areas and the superior temporal to default mode network (DMN) areas compared to non-trauma-exposed control. Veterans without PTSD also showed altered connectivity in the bilateral insula compared to control. This abnormal connectivity pattern was normalized after real-time fMRI neurofeedback training focused on learning to control left amygdala activity with positive autobiographical memory recall.

4214 Computer 55

Substructural Volumes of the Thalamus in Alcoholism

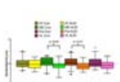

Natalie M Zahr[1,2] and Manojkumar Saranathan[3]

[1]Psychiatry and Behavioral Sciences, Stanford University, Stanford, CA, United States, [2]Neurosciences, SRI International, Menlo Park, CA, United States, [3]Medical Imaging, Univ. of Arizona, Tucson, AZ, United States

Volumes of the thalamus and 4 thalamic substructures (i.e., anterior (AT), mediodorsal (MD), ventrolateral (VL), pulvinar (Pul)) were quantified using a novel automated segmentation algorithm in 18 individuals meeting criteria for Alcohol Use Disorders (AUD) and 28 healthy controls (Con). Multiple regressions considered contributions of diagnosis (i.e., Con vs. AUD), age, sex, and intracranial volume on substructural volumes. Volumes of AT, VL, and Pul were smaller with increasing age. Volumes of MD and Pul were affected by diagnosis: both were smaller in the AUD relative to the Con group. These results suggest that thalamic substructures have differential vulnerability to pathological processes.

4215 Computer 56

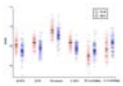

Localized connectivity in obsessive-compulsive disorder: An insight from univariate and multivariate pattern analyses

Xinyu Hu[1], Ming Zhou[1], Lu Lu[1], Lianqing Zhang[1], Xiaoxiao Hu[1], Xuan Bu[1], Hailong Li[1], Yanchun Yang[2], Qiyong Gong[1], and Xiaoqi Huang[1]

[1]Department of Radiology, Huaxi MR Research Center (HMRRC), West China Hospital of Sichuan University, Chengdu, People's Republic of China, [2]Department of Psychiatry, Mental Health Center, West China Hospital of Sichuan University, Chengdu, People's Republic of China

The current study, for the first time, integrated voxel-wise univariate analysis and multivariate pattern classification approach to evaluate the alterations of localized neural connectivity in a relatively large sample of drug-naive patients with obsessive-compulsive disorder (OCD). Our findings (i) suggested the disequilibrium between the fronto-parietal circuit and the cerebellum might be associated with the pathophysiology of OCD, (ii) indicated the translational role of the localized neural connectivity as a potential discriminative pattern to identify OCD at the individual level and (iii) highlighted the hyperactivation of the prefrontal cortex in the pathophysiologic process of OCD.

4216 Computer 57

The ability of magnetic resonance spectroscopy to measure metabolite changes in response to ketamine in major depression at 7T

Jennifer Evans[1], Niall Lally[1], Li An[1], Allison Nugent[1], and Carlos Zarate[1]

[1]NIMH, NIH, Bethesda, MD, United States

This study investigates the feasibility of measuring glutamate and glutamine metabolites by 7T 1H-MRS after a ketamine infusion in a double blind placebo cross-over study in major depression. MRS data was acquired from the pre-genual anterior cingulate in 15 depressed and 13 healthy controls. Glutamate levels, but not glutamine, were found to be significantly different between groups.

4217 Computer 58

Aberrant fronto-limbic effective connectivity during repeated fearful face stimuli in body dysmorphic disorder and anorexia nervosa

D Rangaprakash[1,2], Nathan L Hutcheson[1], Katherine E Lawrence[1], Teena D Moody[1], Sarah Madsen[1,3], Sahib Khalsa[1,4,5], Michael Strober[1], Cara Bohon[6], and Jamie D Feusner[1]

[1]Department of Psychiatry and Biobehavioral Sciences, University of California Los Angeles, Los Angeles, CA, United States, [2]AU MRI Research Center, Department of Electrical and Computer Engineering, Auburn University, Auburn, AL, United States, [3]Imaging Genetics Center, Department of Neurology, University of Southern California, Los Angeles, CA, United States, [4]Oxley College of Health Sciences, University of Tulsa, Tulsa, OK, United States, [5]Laureate Institute for Brain Research, University of Tulsa, Tulsa, OK, United States, [6]Department of Psychiatry and Behavioral Sciences, Stanford University, Stanford, CA, United States

Anorexia nervosa (AN) and body dysmorphic disorder (BDD) share distorted perception of appearance, anxiety, and depression, yet their common and distinguishing neural phenotypes of emotion processing remain unknown. To address this, we studied fronto-limbic connectivity using functional MRI data obtained while participants (N=94) viewed fearful faces and rated their own subjectively experienced fearfulness. Healthy controls exhibited, as predicted, significant bidirectional medial prefrontal (mPFC)-amygdala connectivity, which increased across blocks. However, BDD participants exhibited significant mPFC-to-amygdala but not amygdala-to-mPFC connectivity (indicating limbic hypo-responsiveness), while AN exhibited no significant prefrontal-amygdala connectivity. This study suggests distinct, aberrant fronto-limbic modulatory connectivity in AN and BDD.

4218 Computer 59

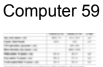

Accumulation of Prefrontal Lactate Levels in Chronic Schizophrenia

Lijing Xin[1], Philipp S Baumann[2,3], Raoul Jenni[2,3], Luis Alameda[2,3], Carina Ferrari[2,3], Philippe Conus[3], Rolf Gruetter[4,5], and Kim Q Do[2]

[1]Center for Biomedical Imaging (CIBM), Ecole Polytechnique Fédérale de Lausanne, Lausanne, Switzerland, [2]Unit for Research in Schizophrenia, Center for Psychiatric Neuroscience, Department of Psychiatry, Lausanne University Hospital (CHUV), Lausanne, Switzerland, [3]Service of General Psychiatry, Department of Psychiatry, Lausanne University Hospital (CHUV), Lausanne, Switzerland, [4]Laboratory of Functional and Metabolic Imaging, Ecole Polytechnique Fédérale de Lausanne, Lausanne, Switzerland, [5]Departments of Radiology, University of Lausanne and Geneva, Lausanne and Geneva, Switzerland

Mitochondrial dysfunction including altered brain energy metabolism has been implicated in the pathophysiology of schizophrenia. The aim of this study was to investigate prefrontal lactate(Lac) levels in patients with chronic schizophrenia. An increase of $[Lac_{mPFC}]$ was observed in patients with chronic schizophrenia relative to healthy controls. This may be associated with glucose metabolism impairment and mitochondrial dysfunction resulting from oxidative stress. Indeed, oxidative damages can impair mitochondrial oxidative phosphorylation and enzyme activities of pyruvate dehydrogenase, leading to Lac production. Therefore, this study provides in vivo evidence supporting that oxidative stress and mitochondrial dysfunction may be involved in schizophrenia.

4219 Computer 60

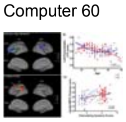

Brain Cortical Thickness in Adolescents from Multiplex Alcohol Dependence Families

Bharath Holla[1], Rajanikanth Panda[2], Ganesan Venkatasubramanian[3], Rose Dawn Bharath[2], and Vivek Benegal[1]

[1]Centre for Addiction Medicine and Department of Psychiatry, National Institute of Mental Health & Neuro Sciences (NIMHANS), Bangalore, India, [2]Cognitive Neuroscience Centre and Department of Neuroimaging and Interventional Radiology (NIIR), National Institute of Mental Health & Neuro Sciences (NIMHANS), Bangalore, India, [3]Translational Psychiatry Laboratory and Department of Psychiatry, National Institute of Mental Health & Neuro Sciences (NIMHANS), Bangalore, India

Adolescents with high familial-loading of alcoholism exhibit altered premorbid subcortical and cerebellar brain-volumes compared to their peers. They also differ in brain-activity during executive-functioning, reward, and emotion-processing tasks. However, the changes in the maturation of the cortical thickness during the adolescence in these high-risk (HR) individuals and their relationship with the externalizing-behaviors have never been examined. Our findings reveal wide-spread delays in cortical maturation in HR subjects, which may ultimately contribute to their addiction vulnerability. More importantly, these effects reduce with age by late-adolescence in the absence of substance-misuse. Additionally, cortical thinning was associated with better behavioral control across groups

---

4220 Computer 61

Proton magnetic resonance spectroscopy study of amygdala, anterior cingulate cortex and thalamus in pediatric post-traumatic stress disorder patients

Weina Wang[1], Xiaorui Su[2], Qiyong Gong[2], and Qiang Yue[2]

[1]Department of Radiology, West China Hospital of Sichuan University, Chengdu, People's Republic of China, [2]West China Hospital of Sichuan University, People's Republic of China

PTSD is associated with a variety of structural and functional brain abnormalities, but the molecular pathophysiological mechanisms are unknown. 25 pediatric PTSD and 24 matched healthy control subjects underwent single voxel 1H-MRS. Right amygdala NAA was significantly increased in pediatric PTSD subjects than in controls, and the other metabolites did not differ significantly between the groups. We hypothesis that long-term excessive activation in amygdala after traumatic events may lead to increase density and activity of the neurons in pediatric PTSD patients with increased NAA concentration, which may be an adaptive response to traumatic stimulation in the human brain. Our findings add the neurochemical abnormality evidence in pediatric PTSD.

4221 Computer 62

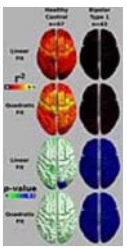

Disruptions in T1-weighted MRI signal trajectories over age in Bipolar Disorder Type-1

Christopher Dennis Rowley[1], Manpreet Sehmbi[1], Luciano Minuzzi[2], Benicio Frey[2], and Nicholas Bock[3]

[1]Neuroscience, McMaster University, Hamilton, ON, Canada, [2]Psychiatry and Behavioural Neurosciences, McMaster University, Hamilton, ON, Canada, [3]Psychology, Neuroscience & Behaviour, McMaster University, Hamilton, ON, Canada

T_1-weighted signal is known to be correlated with age and myelin content. T_1-weighted images with optimized intracortical contrast were taken in subjects aged 17-45. The half cortical depth signal was mapped in 67 healthy controls and 43 individuals diagnosed with bipolar disorder type-1. We investigated the trajectory of the signal with age in each group and it was found that healthy signal trajectory follows a quadratic form with age, while no correlation with age was found in bipolar disorder. We have shown that it is possible to map signal trajectory changes in clinical populations across the cortex.

4222 Computer 63

Resting-state functional connectivity abnormalities associated with posttraumatic stress disorder and traumatic stress: a graph-based analysis

Lei Li[1], Xinyu Hu[1], Xiaoqi Huang[1], and Qiyong Gong[1]

[1]Department of Radiology, Huaxi MR Research Center, Chengdu, People's Republic of China

Previous studies have clarified that differentiating the disease- and traumatic stress-related brain changes may elucidate the core neural mechanism of PTSD. This study is to investigate brain functional alterations in PTSD and the traumatic exposed controls (TEC) relative to the non-traumatized healthy controls (HC) separately, using a data-driven graph theoretical approach--whole-brain functional connectivity strength (FCS) mapping. The current study provided the preliminary evidence of common and separate abnormalities of neural correlates at whole-brain level associated with PTSD and traumatic stress. The disequilibrium between the DMN and the SN might be associated with the pathophysiology of PTSD.

4223 Computer 64

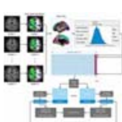

Discrimination of patients with first episode schizophrenia via quantitative cortical morphology features and machine learning methods

Huaiqiang Sun[1], Ying Chen[1], Haoyang Xing[1], Su Lui[1], and Qiyong Gong[1]

[1]Huaxi MR research center, Department of Radiology, West China Hospital, Sichuan University, Chengdu, People's Republic of China

A multivariable analysis framework for schizophrenia prediction with quantitative cortical morphology features features extracted at individual level.

4224 Computer 65

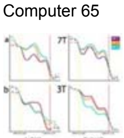

Detailed T1-weighted laminar profiles from the human cortex measured in vivo at 3T and validated at 7T

Bart Ferguson[1], Natalia Petridou[2], Alessio Fracasso[2,3], Martijn P Van den Heuvel[1], Rachel M Brouwer[1], Hilleke E Hulshoff Pol[1], Rene S Kahn[1], and Rene C W Mandl[1,4]

[1]Psychiatry, UMC Utrecht, Utrecht, Netherlands, [2]Radiology, UMC Utrecht, Utrecht, Netherlands, [3]Experimental Psychology, Utrecht University, Utrecht, Netherlands, [4]CNSR, Psykiatrisk Center Glostrup, Glostrup, Denmark

Patients with schizophrenia show cortical gray matter thinning but it is unknown whether all six cortical layers are implicated or that specific layers are affected. Knowing which layers are involved gives more insight in the underlying pathophysiological processes of schizophrenia. Here we present a method to compute detailed laminar profiles per brain area from conventional 3T T1-weighted scans, which can be used to obtain information on relative layer organization. We validate this method by comparing average profiles computed from conventional 3T scans to profiles computed from high resolution scans, acquired at ultra-high field MRI (7T).

4225 Computer 66

The acute pharmacological MRI response to a citalopram challenge is modulated by earlier selective serotonin reuptake inhibitor exposure in an age dependent manner

Michelle Solleveld[1,2], Anouk Schrantee[1], Henk-Jan Mutsaerts[1,3], Paul Lucassen[2], and Liesbeth Reneman[1]

[1]Department of Radiology, Academic Medical Center Amsterdam, Amsterdam, Netherlands, [2]Swammerdam Institute for Life Sciences, Center for Neurosciences, University of Amsterdam, Amsterdam, Netherlands, [3]Sunnybrook Research Institute, University of Toronto, Toronto, Canada

Preclinical studies have shown that selective serotonin reuptake inhibitor (SSRI) treatment, when applied to the developing brain, is associated with long-term changes in the adult serotonergic system. Using pharmacological MRI (phMRI), we here investigated whether SSRIs can also induce such age-dependent changes in the human serotonergic system. We found that the phMRI response to citalopram was decreased in the amygdala only in adult female subjects who had been first exposed to SSRIs early in life, whereas a blunted response was found in subjects first exposed at a later age.

4226 Computer 67

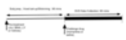

Utility of MR-Spectroscopy in Early Drug Discovery: Characterization of Psychiatric Dysfunctions & Psycho-active Drug Effects

Sakthivel Sekar[1], Joanes Grandjean [1], Joanne Garnell[1], Sankar Seramani[1], Marc Ceuster[2], Hilde Lavreysen[2], and Kishore Bhakoo[1]

[1]Singapore Bioimaging Consortium, Singapore, Singapore, [2]Neuroscience Therapeutic Area, Janssen Pharmaceuticals R&D, Belgium

MR-Spectroscopy offers a unique potential to characterize underlying neuronal mechanisms of psychiatric dysfunctions and the effects of psychoactive drugs, at a fundamental neuro-metabolite level in-vivo. We studied two preclinical disease models: the chronic mild unpredictable stress (CMUS) model, a putative model for depression, and a sub-chronic memantine (NMDA antagonist) model, a putative model for psychosis using single voxel spectroscopy (SVS). Our results represents metabolic fingerprinting of dysfunctions utilising live metabolic flux profiling; documenting neuro-metabolic effects of novel psycho-active drugs, presenting novel insights in-vivo. Our results and unique approach, exemplifies the potential value of SVS in early stage drug discovery and its potential translation to clinical research.

4227 Computer 68

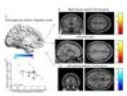

Altered causal connectivity of the anterior cingulate cortex in obsessive compulsive disorder

Fei Li[1], Su Lui[1], Li Yao[1], Xiaoqi Huang[1], Yanchun Yang[2], and Qiyong Gong[1]

[1]Huaxi MR Research Center (HMRRC), Department of Radiology, West China Hospital of Sichuan University, Chengdu, People's Republic of China, [2]Department of Psychiatry, West China Hospital of Sichuan University, Chengdu, People's Republic of China

In order to explore the role of anterior cingulate cortex (ACC) in the pathophysiology of obsessive-compulsive disorder (OCD), we used the resting-state functional magnetic resonance imaging (rfMRI) and Granger causality analysis (GCA) and found that the left pregenual ACC of OCD showed decreased amplitude of low-frequency fluctuation (ALFF) than controls. The areas with altered ALFF exhibited decreased driving effect to right dorsal superior frontal gyrus (dSFG) and left precuneus, and a significant increase in the causal influence from left ventral SFG (vSFG) to the left pregenual ACC in OCD compared to controls.

4228 Computer 69

Evaluation of abnormal structural changes in major depressive disorder with self-harm using generalized q-sampling MRI

Kung-Te Chu[1], Vincent Chin-Hung Chen[2,3], Te-Wei Kao[1], and Jun-Cheng Weng[1,4]

[1]Department of Medical Imaging and Radiological Sciences, Chung Shan Medical University, Taichung, Taiwan, [2]School of Medicine, Chang Gung University, Taoyuan, Taiwan, [3]Department of Psychiatry, Chang Gung Memorial Hospital, Chiayi, Taiwan, [4]Department of Medical Imaging, Chung Shan Medical University Hospital, Taichung, Taiwan

Major depressive disorder (MDD) is a significant brain dysfunction that might cause self-harm behavior. The abnormal brain structures between MDD and healthy control have been investigated by using diffusion tensor imaging (DTI) in several studies. However, few studies discussed the brain structure changes in MDD patients with self-harm behavior. Moreover, there were some limitations in DTI. Therefore, our study aimed to find the abnormalities of neurological structure of white matter among MDD without self-harm behavior (MDD_N), MDD with self-harm behavior (MDD_S), and healthy control (HC), using generalized q-sampling imaging (GQI). We found the significant differences in the corpus callosum, superior longitudinal fasciculus (SLF), cingulum, and frontal lobe of GQI indices in individual groups.

4229 Computer 70

Altered Hippocampus Microstructure in Schizophrenia: A Diffusional Kurtosis Imaging and Magnetic Resonance Spectroscopy Imaging Study

Mariana Lazar[1], Maia Boudzinskaia[2], Emma Meyer[2], Dolores Malaspina[2], James Babb[1], and Oded Gonen[1]

[1]Radiology, New York University School of Medicine, New York, NY, United States, [2]Psychiatry, New York University School of Medicine, New York, NY, United States

Diffusional Kurtosis Imaging (DKI) and Magnetic Resonance Spectroscopy Imaging were employed to assess microstructural changes of hippocampus in patients with schizophrenia. Increased mean kurtosis and mean diffusivity were observed for both left and right hippocampi in patient compared to the control group. In patients, mean kurtosis showed a strong negative correlation with N-acetylaspartate concentration. These results suggest disorganized hippocampal microstructure, likely due to neuroinflammatory processes such as micro- and astrogliosis and/or disorganized neuronal domains. DKI's apparent sensitivity to microstructural deficits may ultimately be employed to identify individuals with microscopic hippocampal impairment.

4230 Computer 71

Measuring Alanine in Schizophrenia using 2D Correlation Spectroscopy

Adrienne Lee[1], Luke Wang[1,2], Benjamin Rowland[1], Vicky Liao[1], Elisabetta Del Re[3], Robert McCarley[3], and Alexander Lin[1]

[1]Center for Clinical Spectroscopy, Brigham and Women's Hospital, Boston, MA, United States, [2]Department of Anesthesiology, Perioperative and Pain Medicine, Boston Children's Hospital and Harvard Medical School, Boston, MA, [3]Laboratory of Neuroscience, Veterans Affairs Boston Healthcare System, Boston, MA

Degree of schizophrenia (SZ) was determined by phase-locking factor (PLF) acquired through an electroencephalogram (EEG). Correlation spectroscopy (COSY) spectra of the chronic SZ patients and age-matched healthy controls were then compared. A significant difference ($p < 0.05$) between SZ and controls was found in the concentrations of alanine supported by a strong correlation between PLF and alanine levels. These results suggest further studies to examine alanine as a potential biomarker for schizophrenia.

4231 Computer 72

Regional Brain Volume Changes in Alcohol-dependent Individuals during Short-term and Long-term Abstinence

Xiaowei Zou[1,2], Timothy C. Durazzo[3,4], and Dieter J. Meyerhoff[1,2]

[1]Department of Radiology and Biomedical Imaging, University of California San Francisco, San Francisco, CA, United States, [2]Center for Imaging of Neurodegenerative Diseases, San Francisco VA Medical Center, San Francisco, CA, United States, [3]Department of Psychiatry and Behavioral Sciences, Stanford University, Stanford, CA, United States, [4]Mental Illness Research and Education Clinical Centers and Sierra-Pacific War Related Illness and Injury Study Center, VA Palo Alto Health Care System, CA, United States

The general goal of this study is to determine the volume changes of cortical and subcortical brain regions in smoking and currently non-smoking alcohol-dependent individuals during short-term and long-term abstinence from alcohol, compared with non-/light-drinking controls. Preliminary results from paired t-tests within each group show that the anterior cingulate cortex, dorsolateral prefrontal cortex, orbitofrontal cortex, insula, and hippocampus have different recovery patterns, which suggest potentially different neuropathological changes and/or injuries. More statistical analyses will test for cross-sectional and longitudinal differences between the groups for a better interpretation of the regional volume changes and their cognitive and behavioral correlates.

Electronic Poster

Brain Tumor: Molecular Imaging, Machine Learning & Emerging Techniques

Exhibition Hall — Tuesday 14:45 - 15:45

4232 Computer 73

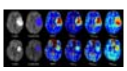

RAFF, T1ρ and T2ρ mapping of human gliomas: association with IDH mutation, 1p19q co-deletion and Ki67

Harri Merisaari[1,2,3], Ivan Jambor[3,4], Marko Pesola[3,4], Maria Gardberg[5], Janek Frantzén[6], Pekka Jokinen[6], Hannu Aronen[3,4], Timo Liimatainen[7,8], Heikki Minn[9], and Aida Kiviniemi[3,4]

[1]Turku PET Centre, University of Turku, Turku, Finland, [2]Department of Information Technology, University of Turku, Turku, Finland, [3]Medical Imaging Centre of Southwest Finland, Turku University Hospital, Turku, Finland, [4]Department of Diagnostic Radiology, University of Turku, Turku, Finland, [5]Department of Pathology, University of Turku and Turku University Hospital, Turku, Finland, [6]Division of Clinical Neurosciences, Department of Neurosurgery, Turku University Hospital, Turku, Finland, [7]Department of Biotechnology and Molecular Medicine, A.I. Virtanen Institute for Molecular Sciences, University of Eastern Finland, Kuopio, Finland, [8]Diagnostic Imaging Center, Kuopio University Hospital, Kuopio, Finland, [9]Department of Oncology and Radiotherapy, Turku University Hospital, Turku, Finland

Our aim was to study the feasibility of quantitative RAFF, $T1\rho_{cw}$, $T1\rho_{adiab}$ and $T2\rho_{adiab}$ imaging for the first time in human gliomas and to assess their ability to differentiate gliomas with specific genetic profile. FLAIR lesion segmentation and histogram analysis from parametric maps were applied. Both IDH mutated and 1p19q codeleted gliomas demonstrated a tendency for lower relaxation values compared to IDH wild-type and 1p19q intact gliomas, respectively. Additionally, T2ρ, adiab significantly correlated to Ki-67 and tumor aggressiveness. We conclude that RAFF, $T1\rho_{cw}$, $T1\rho_{adiab}$ and $T2\rho_{adiab}$ imaging of gliomas is feasible and carry a potential for improving non-invasive glioma characterization.

4233 Computer 74

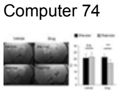

Detecting treatment response of a novel immune stimulator in an animal model of glioblastoma with conventional and cell tracking MRI

Runze Yang[1], Susobhan Sarkar[2], V. Wee Yong[2], and Jeff F Dunn[1,2]

[1]Radiology, University of Calgary, Calgary, AB, Canada, [2]Clinical Neuroscience, University of Calgary

Glioblastoma Multiforme (GBM) is an aggressive brain cancer. Immunotherapy is a promising avenue of exploration for treatment of GBM. We discovered a new drug capable of stimulating innate immunity and showed that it is able of reducing tumor growth in a mouse model of GBM. We used ultrasmall iron oxide nanoparticles (USPIO) to track the migration of stimulated immune cells and showed that this drug related response can be detected with as little as 7 days of treatment. MRI tracking of immune cells using USPIO is a promising tool that can be easily translated into the clinical setting.

4234 Computer 75

Metabolic imaging with Gallium-68 citrate PET and 3D MRSI in patients with glioma

Yan Li[1], Spencer Behr[1], Susan Chang[2], Sarah J Nelson[1], and Michael Evans[1]

[1]Department of Radiology and Biomedical Imaging, University of California San Francisco, San Francisco, CA, United States, [2]Department of Neurological Surgery, University of California San Francisco, San Francisco, CA, United States

This study evaluated the feasibility of using combined metabolic imaging methodologies, namely 3D lactate-edited proton magnetic resonance spectroscopic imaging and Gallium-68 citrate PET, in patients with glioma using a PET/MR scanner.

4235 Computer 76

MRI Signal Enhancement in Early-Stage GBM Detection by Nonlinear Spin Dynamics using Active Feedback Fields

Huimin Yang[1], Chaohsiung Hsu[2], and Yung-Ya Lin[1]

[1]Chemistry and Biochemistry, University of California, Los Angeles, Los Angeles, CA, United States, [2]Chemistry, National Taiwan University, Taipei, Taiwan

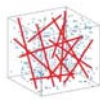

Application of MR imaging is very limited in imaging sensitivity and contrast in regards to the detection of brain tumor at an early stage because of tiny variations between healthy tissue and early-stage tumor. The radiation damping effect provides insight about the nonlinear spin evolution. Taking advantage of nonlinear spin evolution, we confirmed theoretically and experimentally that MR imaging provides a more stable and significant contrast in comparison to conventional methods.

4236 Computer 77

Ferumoxytol Iron Nanoparticle Enhanced MR Imaging is a Noninvasive Biomarker of Isocitrate Dehydrogenase Mutational Status in Recurrent Glioblastoma and Pseudoprogression

Ramon Francisco Barajas Jr[1,2], Bronwyn E Hamilton[1], David R Pettersson[1], Daniel L Schwartz[2,3], Jenny Firkins[3], Prakash Ambady[3], Andrea Horvath[3], Heather L McConnell[3], Joao Prola-Netto[1,3], Csanad Varallyay[1,3], Jerry J Jaboin[4], Charlotte D Kubicky[4], Ahmed M Raslan[5], Aclan Dogan[5], Jeremy Ciporen[5], Leslie L Muldoon[3], William Rooney[2], and Edward A Neuwelt[3,5]

[1]Radiology, Oregon Health & Science University, Portland, OR, United States, [2]Advanced Imaging Research Center, Oregon Health & Science University, Portland, OR, United States, [3]Neurology, Oregon Health & Science University, Portland, OR, United States, [4]Radiation Medicine, Oregon Health & Science University, Portland, OR, United States, [5]Neurological Surgery, Oregon Health & Science University, Portland, OR, United States

Ferumoxytol iron nanoparticles are used as an off label molecular MR imaging contrast agent in patients with reduced renal function precluding gadolinium administration. Glioblastoma molecular features are now recognized as an integral component of glioma pathogenetic classification and clinical outcome. IDH1 mutation accounts for approximately 10% of glioblastoma. The absence of a reliable noninvasive biomarker of glioblastoma IDH mutation prompted this retrospective study to determine if Ferumoxytol MR Imaging is diagnostic of IDH mutational status. We observed that the presence of increased Ferumoxytol to Gadolinum enhancing ratio was a significant 3T MR imaging biomarker for IDH mutational status in recurrent glioblastoma and the differentiation of pseudoprogression.

4237 Computer 78

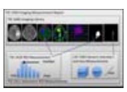

Standard DICOM Structured Reports as a Vehicle for Multi-Modal Region-of-Interest MR Analysis Results for Clinical Workflows and Radiomic Studies for Brain Tumor Patients

Marram P Olson[1], Jason C Crane[1], Janine Lupo[1], Marisa Lafontaine[1], and Sarah J Nelson[1]

[1]Radiology and Biomedical Imaging, UCSF, San Francisco, CA, United States

Quantitative analysis of metabolic and dynamic imaging data produces maps of parameters that show promise for improving medical diagnosis and therapeutic monitoring for patients with brain tumors. Statistical ROI analysis of these maps can be used to quantitatively summarize multi-modality imaging metrics and longitudinal changes. In this work we demonstrate a standards-based mechanism for generating and communicating minable, quantitative Region of Interest (ROI) analysis results that can easily be integrated into clinical workflows and radiomic studies.

4238 Computer 79

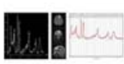

Prediction of IDH Mutation Status of Diffuse-Gliomas Based on Short-Echo Time Magnetic Resonance Spectroscopy at 3T

Esin Ozturk-Isik[1], Sevim Cengiz[1], Koray Ozduman[2,3], Alpay Ozcan[3,4], Cengiz Yakicier[5], M. Necmettin Pamir[2,3], and Alp Dincer[3,6]

[1]Institute of Biomedical Engineering, Bogazici University, Istanbul, Turkey, [2]Department of Neurosurgery, Acibadem University, Istanbul, Turkey, [3]Neuroradiology Research Center, Acibadem University, Istanbul, Turkey, [4]Department of Medical Engineering, Acibadem University, Istanbul, Turkey, [5]Department of Molecular Biology and Genetics, Acibadem University, Istanbul, Turkey, [6]Department of Radiology, Acibadem University, Istanbul, Turkey

The tumor biology of diffuse-gliomas is best reflected by their molecular profile. Isocitrate dehydrogenase (IDH) mutation status has the strongest correlation to treatment response and patient survival among all molecular markers. The aim of this study is to predict IDH mutation status of gliomas based on short-echo time MR spectroscopic (MRS) biomarkers by using machine learning algorithms at 3T. Our results indicated that MRS based biomarkers were able to discriminate between IDH-mutant and IDH-wild type patients with up to 91% sensitivity, %78 specificity, and 86.9% accuracy by using an ensemble of bootstrap-aggregated decision trees classification with a three-fold cross validation.

4239 Computer 80

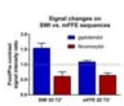

Minimizing the confounding effect of gadolinium contrast on subsequent ferumoxytol MRI in the brain

Csanad Gyorgy Varallyay[1], Andrea Horvath[2], Gerda Toth[2], Laszlo Szidonya[2], Emily Youngers[2], and Edward Neuwelt[3]

[1]Dept. of Radiology, Oregon Health and Science University, Portland, OR, United States, [2]Oregon Health and Science University, Portland, OR, United States, [3]Dept. of Neurology, Oregon Health and Science University, Portland, OR, United States

Ferumoxytol as an MRI contrast agent has the advantage of long intravascular phase and strong transverse relaxivity, allowing high resolution depiction of abnormal vasculature and steady state blood volume (SS-CBV) mapping. In clinical studies it would be beneficial to use ferumoxytol as an immediate extension of standard of care gadolinium enhanced MRI, instead of imaging on two separate days. This study concludes that the 3D T2* weighted acquisition has substantial T1 weighting, while the 2D acquisition does not, therefore the latter one is preferable for ferumoxytol vascular imaging if gadolinium is on board.

4240 Computer 81

Comparison of gadoterate meglumine and gadobutrol in MRI diagnosis of brain tumors: a double-blind randomized intra-individually controlled in cross-over study (the REMIND study)

Kenneth Maravilla[1], Daniel San Juan Orta[2], Sang Joon Kim[3], and Guillermo Elizondo Riojas[4]

[1]Radiology, University of Washington, Seattle, WA, United States, [2]Clinical Research Institute S.C., Tlanepantla de Baz, Mexico, [3]Asan medical center / Radiology, Seoul, Korea, Democratic People's Republic of, [4]Universidad Autonoma de Nuevo Leon, Hospital Universitario Dr. Jose Eleuterio Gonzalez, Monterrey, Mexico

This double-blind randomized cross-over study was conducted to demonstrate non-inferiority of gadoterate meglumine vs. gadobutrol in MRI diagnosis of brain tumors. Images from two identical MRIs with each agent were evaluated by three independent off-site readers. Overall lesion visualization and characterization was scored as "good" or "excellent" in >90% of patients by all readers. Despite a small difference in signal intensity measurements in favor of gadobutrol, similar results were observed with the two agents regarding overall lesion visualization and characterization or qualitative efficacy criteria. Non-inferiority of gadoterate meglumine vs. gadobutrol in diagnosis of brain tumors by MRI was demonstrated.

4241 Computer 82

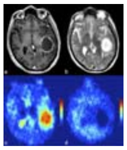

23Na-MRI demonstrates a sodium gradient within gliomas as a biomarker of tumor heterogeneity

Fulvio Zaccagna[1], Frank Riemer[1], Mary A. McLean[2], James T. Grist[1], Joshua Kaggie[1], Rolf F Schulte[3], Sarah Hilborne[1], Tomasz Matys[1], Jonathan H. Gillard[1], Colin Watts[4], Stephen J. Price[4], Martin J. Graves[1], and Ferdia A. Gallagher[1]

[1]Department of Radiology, University of Cambridge, Cambridge, United Kingdom, [2]Cancer Research UK Cambridge Institute, University of Cambridge, Cambridge, United Kingdom, [3]GE Global Research, Munich, Germany, [4]Neurosurgery Unit, Department of Clinical Neurosciences, University of Cambridge, Cambridge, United Kingdom

Glioma grade and the extent of local infiltration are important factors for guiding management. Imaging tumor heterogeneity may also improve diagnosis and therapy planning. ^{23}Na-MRI has been used here to demonstrate a gradient in sodium concentration across gliomas: necrosis greater than viable tissue greater than edema. This gradient was evident in all 17 tumors analyzed and is consistent with the expected underlying histopathology; concentration is increasing throughout the evolution from edema, dominated by the extracellular compartment, to the necrotic core, dominated by dead cells and broken sodium pumps. ^{23}Na-MRI may therefore represent an imaging biomarker of tumor heterogeneity in glioma.

4242 Computer 83

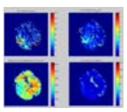

CEST and binding water MT separation in brain tumor by multi pool model CEST Peak Extraction method

Mitsuharu Miyoshi[1], Masafumi Harada[2], Yuki Kanazawa[2], and Hiroyuki Kabasawa[1]

[1]Global MR Applications & Workflow, GE Healthcare Japan, Hino, Tokyo, Japan, [2]Graduate School of Biomedical Sciences, Tokushima University, Tokushima, Japan

Although MTR asymmetry is often used as a CEST parameter, it is not quantitative. In this study, CEST Peak Extraction (CPE) method was used to separate CEST and MT parameters. CEST peaks in brain tumor could be fitted with Lorentzian function on CPE spectrum. Each fitted parameter had a quantitative meaning in multi pool model, which includes CEST pool, binding water MT pool and free water pool.

4243 Computer 84

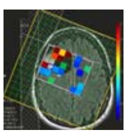

Spectroscopic Imaging-based detection of 2-hydroxyglutarate (2HG) in IDH1 mutant human gliomas on 3T Clinical

Gaurav Verma[1], Sanjeev Chawla[1], Harish Poptani[2], MacLean Nasrallah[3], Michael Albert Thomas[4], Arati Desai[5], Steven Brem[6], and Suyash Mohan[7]

[1]Neuroradiology, University of Pennsylvania, Philadelphia, PA, United States, [2]Cellular and Molecular Physiology, University of Liverpool, Liverpool, United Kingdom, [3]Pathology, University of Pennsylvania, Philadelphia, PA, United States, [4]Radiology, University of California Los Angeles, Los Angeles, CA, United States, [5]Hematology Oncology, University of Pennsylvania, Philadelphia, PA, United States, [6]Neurosurgical Oncology, University of Pennsylvania, Philadelphia, PA, United States, [7]Radiology, University of Pennsylvania, Philadelphia, PA, United States

Mutations in isocitrate dehydrogenase (IDH) play an increasing role in clinical assessment of human gliomas and determination of treatment. The performance of Chemical Shift Imaging (CSI) to detect 2-hydroxyglutarate (2HG) in mutant-IDH gliomas was assessed in the routine clinical environment. Specificity of 80% and sensitivity of 63% was achieved in a cohort of 15 patients scanned with the technique at 3T. Greater sensitivity, through longer acqusition or more sensitive equipment could result in reliable non-invasive detection of this putative biomarker present in a majority of Grade II/III gliomas.

4244 Computer 85

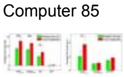

Differentiation of Radiation Necrosis from Tumour Progression Using Chemical Exchange Saturation Transfer (CEST)

Hatef Mehrabian[1,2], Hany Soliman[3], Arjun Sahgal[3], and Greg J Stanisz[2]

[1]Radiology and Biomedical Imaging, University of California, San Francisco, San Francisco, CA, United States, [2]Physical Sciences, Sunnybrook Research Institute, Toronto, ON, Canada, [3]Radiation Oncology, Sunnybrook Research Institute, Toronto, ON, Canada

Radiation necrosis is the most common side-effect of stereotactic radiosurgery (SRS) and has similar characteristics to tumor progression on standard anatomical MRI. Differentiating these two conditions is a major long standing clinical challenge. In this study the potential of chemical exchange saturation transfer (CEST) in differentiating the two conditions in patient with brain metastases is investigated. The results showed that the magnetization transfer ratio (MTR) of amide and NOE peaks provided the best separation of radiation necrosis cases from tumor progression cases. However, the commonly used amide proton transfer (APT) was unable to differentiate the two conditions.

4245 Computer 86

High resolution 7 T magnetic resonance spectroscopic imaging of glioma in the brain

Gilbert Hangel[1], Eva Heckova[1], Bernhard Strasser[1], Michal Považan[1,2], Stephan Gruber[1], Elisabeth Springer[1], Georg Widhalm[3], Matthias Preusser[4], Siegfried Trattnig[1,2], and Wolfgang Bogner[1,2]

[1]High Field MR Centre, Medical University of Vienna, Vienna, Austria, [2]Christian Doppler Laboratory for Clinical Molecular MR Imaging, Vienna, Austria, [3]Department of Neurosurgery, Medical University of Vienna, [4]Department of Medicine I, Division of Oncology, Medical University of Vienna

We present the application of single-slice high-resolution FID-MRSI with short acquisition delay at 7T that provides whole-slice metabolite maps in eight patients with different types of glioma. With six minutes measurement time, it could be easily integrated into a standard imaging protocol. The results show that it is possible to resolve metabolic deviations in an extended number of biochemical compounds in tumors with unprecedented spatial details, thereby offering deeper insight into the neurochemical profiles of different glioma types. This suggests that the demonstrated method has a high potential for the research of glioma.

4246 Computer 87

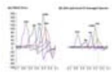

Detection 2-Hydroxyglutarate in IDH-Mutant Gliomas using TE-Averaged PRESS at 3T

Vivek TIWARI[1], Sandeep Ganji, ZhongXu An, and Changho Choi

[1]UT Southwestern Medical Center, Dallas, TX, United States

Gliomas harboring mutations in Isocitrate-Dehydrogenase (IDH) 1/2 exhibits a neomorphic-activity resulting in production of 2-hydroxyglutarate (2HG) by 2-3 orders of magnitude. Non-invasive detection of 2HG using conventional 1H Magnetic Resonance Spectroscopy (MRS) is challenging due to extensive overlap with the resonances of neighboring metabolites. Here we have designed a TE-Averaged PRESS 1H-MRS that reduces the spectral-overlaps of GABA, Gln, Glu and glutathione signals on 2HG-2.25ppm-resonance that provides a reliable-detection of 2HG. We have also estimated T2 in each brain-tumor by taking the advantage of multiple-TEs used in TE-averaging acquisitions, and used patient-specific T2 for estimation of 2HG.

4247 Computer 88

Characterizing CRT-Induced Vascular Injury in the Developing Brain

Melanie A Morrison[1], Erin Felton[2], Angela Jakary[1], Andrew Leynes[1], Peder Larson[1], Sabine Mueller[2], and Janine Lupo[1]

[1]Radiology & Biomedical Imaging, University of California San Francisco, San Francisco, CA, United States, [2]Neurology, University of California San Francisco, CA, United States

In the treatment of pediatric medulloblastomas, cranial radiation therapy (CRT) may induce long-term effects including CRT-induced vascular injury and cognitive impairments. 7T Susceptibility-weighted MRI was used to characterize CRT-induced injury in the form of cerebral microbleeds (CMBs) as potential markers of cognitive deficits. The majority of CMBs were located in the frontal lobe, which develop late in the adolescent brain. CMB density was associated with deficits in working and visual memory as a function of time since CRT. This work supports a modification of future standards for defining radiation target volumes, with evidence for early intervention with cognitive rehabilitation strategies.

4248 Computer 89

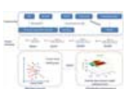

Optimizing Statistical Texture Model to Improve the Classification Accuracy of Tumor Grade in Glioma Patients with Machine Learning Based on Multimodality MR Images

Yang Yang[1], Lin-Feng Yan[1], Xin Zhang[1], Hai-Yan Nan[1], Yu-Chuan Hu[1], Yu Han[1], Jin Zhang[1], Wen Wang[1], and Guang-Bin Cui[1]

[1]Tangdu Hospital, Fourth Military Medical University, Xi'an, People's Republic of China

Texture analysis is a powerful image analysis method to assess the heterogeneous distribution of tumor quantitatively. Different statistical models have been applied in texture analysis to classify glioma grade and level. It has not been evaluated that which model is the most efficient. The aim of this study is to compare four texture models in glioma grading. Texture features were extracted from multimodality MR images in 3D ROIs. After machine learning and leave-one-out cross validation, the gray-level run-length matrix was found as the best model while gray-level was set as 256.

4249 Computer 90

Texture analysis of quantitative ADC maps to differentiate low from high grade glioma

Yingqiu Liuyang[1], Jin Shang[1], Yanwei Miao[1], Shesnia Salim Padikkalakandy Cheriyath[1], and Yan Guo[2]

[1]First Affiliated Hospital of Dalian Medical University, Dalian, People's Republic of China, [2]GE Healthcare,Lifescience,China

The objective of this study, was to differentiate low from high grade glioma using texture analysis of quantitative ADC maps, and further aimed at revealing the microscopic changes of glioma in the evolution of low grade to high grade.Conclusion that texture analysis of ADC signal value based on entire tumor could provide more information in differentiation of low and high grade glioma. Through logistic regression analysis we obtain skewness, entropy,long run emphasis are the independent influence factors, and joint application of them showed superior diagnostic value.

4250 Computer 91

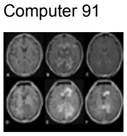

A morphological classification of primary central nervous system lymphoma: new insights of the imaging analysis to facilitate treatment planning

Jing Liu[1,2], Kannie W.Y. Chan[3], Bin Zhang[1], Guan Shu Liu[2], and Shui Xing Zhang[1]

[1]Department of Radiology, Guangdong Academy of Medical Sciences/Guangdong General Hospital, Guangzhou, People's Republic of China, [2]Russell H. Morgan Department of Radiology and Radiological Sciences, The Johns Hopkins University School of Medicine, Baltimore, MD, United States, [3]Department of Mechanical and Biomedical Engineering, City University of Hong Kong, Hong Kong, People's Republic of China

A preliminary classification of primary central nervous system lymphoma (PCNSL) was reported based on the MRI radiographical features. We classified the 90 PCNSL patients based on the T1 contrast-enhanced MRI findings and assessed treatment responses. The goal is to provide some guidelines and additional information for diagnosis and treatment planning. We categorized these patients into four distinctive types of PCNSL according to the T1 findings and observed the treatment response rate, which we found the highest in type Ia. This could potentially facilitate the diagnosis and treatment plan of PCNSL in a routine clinical setting.

4251 Computer 92

Radiogenomic analysis of distinct tumor sub-compartments on T2 and FLAIR predict distinct molecular subtypes in Lower Grade Gliomas

Niha Beig[1], Ramon Correa[1], Prateek Prasanna[1], Jhimli Mitra[1], Ameya Nayate[2], Anant Madabhushi[1], and Pallavi Tiwari[1]

[1]Biomedical Engineering, Case Western Reserve University, Cleveland, OH, United States, [2]Radiology, University Hospitals, Cleveland, OH, United States

The recent categorization of low-grade Glioma (LGG) has been modified based on the molecular aberrations associated with IDH mutations (IDHmut or IDH-WT) and 1p19q co-deletions (codel or non-codel). We explored the utility of radiogenomic analysis to identify radiomics signatures (computer extracted features from MRI) that distinguish IDHmut codel, IDHmut noncodel, and IDH-WT LGG tumors on T2 and FLAIR sequences. Initial results indicate that radiomic features from non-enhancing regions on T2 and infiltrative edges on FLAIR can segregate the 3 subgroups. A non-invasive means of discerning molecular subtypes on MRI may allow clinicians to determine prognosis, and inform treatment strategy.

4252 Computer 93

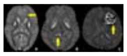

Textural Analysis Tool for Grading of Astrocytoma on Quantitative Susceptibility Mapping

Yihao Yao[1], Ilhami Kovanlikaya[2], Ramin Jafari[3], Yi Wang[2,4], and Wenzhen Zhu[1]

[1]Department of Radiology, Tongji Hospital, Tongji Medical College, Huazhong University of Science & Technology, Wuhan, People's Republic of China, [2]Department of Radiology, Weill Cornell Medical College, New York, NY, United States, [3]Department of Biomedical Engineering, Cornell University, Ithaca, NY, United States, [4]Biomedical Engineering, Cornell University, Ithaca, NY, United States

The accuracy of grading astrocytic brain tumors using texture analysis (TA) on quantitative susceptibility mapping (QSM) was studied. For texture analysis training data set, most discriminant factor (MDF1) values were significantly different for low grade and high grade astrocytomas (p<0.01), as well as Grade II and III, Grade II and IV, Grade III and IV (p<0.01). For texture analysis test data set, 19/20 cases in differentiating low grade from high grade astrocytomas, 16/20 cases in Grade II, III and IV differentiation were correctly classified. TA promises to be a useful tool for grading astrocytoma on QSM.

4253 Computer 94

Voxel-based Multiparametric Analysis of Magnetic Resonance Imaging Data for Differentiating Recurrent Glioblastoma from Delayed Radiation Necrosis

Ra Gyoung Yoon[1], Ho Sung Kim[2], Myeong Ju Koh[3], and Sang Joon Kim[2]

[1]Radiology, Catholic Kwandong University International St. Mary's Hospital, Incheon, Korea, Republic of, [2]Radiology and Research Institute of Radiology, Asan Medical Center, Seoul, Korea, Republic of, [3]Jeju National University Hospital

We evaluated a volume-weighted voxel-based multiparametric (MP) clustering method as an imaging biomarker for differentiating recurrent glioblastoma from delayed radiation necrosis, comparing to the single imaging parameters of DWI, DSC and DCE perfusion MR. In an area under the receiver operating characteristic curve analysis, volume-weighted voxel-based MP clustering demonstrated better diagnostic accuracy for discriminating these two conditions than single imaging parameters. When performed with use of an optimal cutoff, volume-weighted voxel-based MP clustering improved the overall sensitivity. Therefore, quantitative analysis using volume-weighted voxel-based MP clustering is superior to single imaging parameter measurements for differentiating recurrent glioblastoma from delayed radiation necrosis.

4254 Computer 95

Medulloblastomas in adults: An MRI radiogenomic approach to an extremely rare disease

Vera Catharina Keil[1], Monika Warmuth-Metz[2], Christina Reh[1], Jonas Enkirch[1], Torsten Pietsch[3], Hans Heinz Schild[1], Elke Hattingen[1], and Peter Hau[4]

[1]Radiology, University Hospital Bonn, Bonn, Germany, [2]Institute for Diagnostic and Interventional Neuroradiology, University Hospital Wuerzburg, Wuerzburg, Germany, [3]Institute for Neuropathology, University Hospital Bonn, Bonn, Germany, [4]Wilhelm Sander-Therapieeinheit NeuroOnkologie and Clinic and Policlinic for Neurology, University Hospital Regensburg, Regensburg, Germany

Medulloblastoma in adults is very rare and shows prognostically relevant histological and genetic subtypes. Within a nation-wide multicenter study, pre-surgical MRIs of 28 cases were analysed to identify imaging biomarkers, which may be used to non-invasively predict these subtypes based on a radiophenotype. Molecular genetic subtypes SHH p53wt, WNT and non-WNT/non-SHH (Group 4) were significantly distinct in their relation to the 4th ventricle and lower rhombic limb, and extent of edema. Further imaging biomarkers could be identified that differentiate histological subtypes and nuclear-ß-catenin expression patterns. Imaging biomarkers were not congruent to markers identified in pediatric patients implying possible age-related differences.

4255 Computer 96

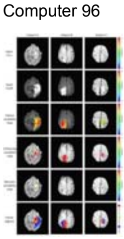

Measuring Tumor Boundary Variability to Improve Automated Segmentation of Brain Tumors Using Multimodal MRI.

Edgar A. Rios Piedra[1,2], Benjamin M. Ellingson[1,2], Suzie El-Saden[1,2], Ricky K. Taira[1,2], Alex A. T. Bui[1,2], and William Hsu[1,2]

[1]Department of Radiological Sciences, David Geffen School of Medicine., University of California, Los Angeles, Los Angeles, CA, United States, [2]Department of Bioengineering, David Geffen School of Medicine., University of California, Los Angeles, Los Angeles, CA, United States

We present an automated brain tumor segmentation framework to measure the variability associated to the tumor boundary that is observed on multimodal MRI; this is a vital task to accomplish as quantitative and automated tumor measurements and assessment become the standard in neuro-oncology for disease diagnosis, treatment planning, and clinical monitoring.

Electronic Poster

Normal & Aging Brain

Exhibition Hall Tuesday 14:45 - 15:45

4256 Computer 97

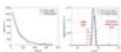

Enhanced Quality of Myelin Water Fraction Mapping from GRASE Imaging Data of Human Brain using a New Nonlocal Estimation of multi-Spectral Magnitudes (NESMA) Filter

Mustapha Bouhrara[1], Michael C. Maring[1], David A. Reiter[1], Jean-Marie Bonny[2], and Richard G. Spencer[1]

[1]NIA, National Institutes of Health, Baltimore, MD, United States, [2]QuaPa, INRA, Clermont-Ferrand, France

Changes in myelin water fraction (MWF) represent a biomarker for central nervous system disease. However, high quality mapping of MWF is challenging, requiring very high signal-to-noise ratio for accurate and stable results. In this work, we demonstrate the potential of a new multispectral filter to permit high quality MWF mapping using in-vivo GRASE brain imaging datasets. Indeed, unlike conventional averaging filters, our filter permits substantial reduction of the random variation in derived MWF estimates while preserving edges and small structures. Finally, our results regarding patterns of MWF as a function of age are consistent with recent literature.

4257 Computer 98

Quantitative cerebral arteriolar vasomotor function mapping by spectral analysis of time series MR signal fluctuations

Minghui Tang[1], Keigo Nishi[2], and Toru Yamamoto[1]

[1]Faculty of Health Sciences, Hokkaido University, Sapporo, Japan, [2]Department of Radiology, National Hospital Organization Hokkaido Medical Center, Sapporo, Japan

Cerebral arteriolar vasomotor function would be a biomarker for early diagnosis of dementia. We developed a quantitative mapping technique for cerebral arteriolar vasomotor function without administrating any agents. The natural respiratory fluctuation of CO_2 in arterial blood was used, which alters cerebral blood flow and venous blood oxygenation, and hence modulates the MRI signal. This new technique is based on our finding of a strong correlation in MR signals between the cardiac fluctuation in brain parenchyma and the respiratory fluctuation at the sagittal sinus. Using this new mapping technique, the degeneration of arteriolar vasomotor function associated with aging was observed.

4258 Computer 99

Cardiovascular risk factors, cerebral blood flow, and cognitive functions: preliminary results in a community based study in Chinese elders

Xin Hong[1], Sei Hwan Oh[1], Ying Hwey Nai[1], Saima Hilal[2,3], Suz-Chieh Sung[1], Mohammad Kamran Ikram[3,4], Christopher Chen[2,3], and Kai-Hsiang Chuang[1]

[1]Singpare Bioimaging Consortium, Agency for Science Technology and Research, Singapore, Singapore, [2]Department of Pharmacology, National University of Singapore, [3]Memory Aging & Cognition Centre, National University of Singapore, [4]Singapore Eye Research Institute, Singapore National Eye Center

Cerebral blood flow (CBF) is an important biomarker of the brain function and has been shown to correlate with cognitive performance in diseases. Since cardiovascular and metabolic complications are common in elders, to understand the influence of vascular confound in cognitive correlation, we investigated how cardiovascular risk factors may affect the relationship between cognitive functions and CBF in non-demented elders. We found that mean arterial blood pressure, haematocrit, blood cholesterol and glucose levels had significant negative effects on CBF. This suggests that cardiovascular risk factors shall be taken into consideration when analyzing CBF in aging, cognitive impairment, and neurodegenerative diseases.

4259 Computer 100

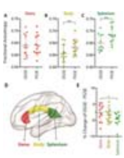

Oscillating Gradient Spin Echo Diffusion Tensor MRI of the Corpus Callosum with Typical Aging

Pascal Tétreault[1], Diana Valdés Cabrera[1], Robert Stobbe[1], Corey Baron[1], and Christian Beaulieu[1]

[1]Biomedical Engineering, University of Alberta, Edmonton, AB, Canada

This study compared short diffusion time (4 ms) oscillating gradient spin echo (OGSE) relative to regular long diffusion time (40 ms) pulsed gradient spin echo (PGSE) DTI in healthy individuals over a 40 year age span (n=12, 24 to 67 years old) to identify unique microstructure organization and reveal potential age related changes in three portions of the corpus callosum. Diffusivity and anisotropy were shown to depend on the diffusion time, mostly in the splenium, and these changed with age possibly reflecting alterations of restrictive dimensions such as the loss of specific axon diameters with aging.

4260 Computer 101

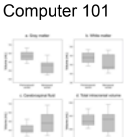

Brain morphological alterations and functional changes during visually stimulated sexual arousal in menopausal women

Gwang-Won Kim[1], Chung-Man Moon[1], and Gwang-Woo Jeong[1,2]

[1]Research Institute of Medical Imaging, Chonnam National University Medical School, Gwangju, Korea, Republic of, [2]Department of Radiology, Chonnam National University Hospital

The aging process and menopausal transition are important factors in sexual dysfunction of menopausal women. Until now, it has been unknown how menopause synchronously influences brain morphology and brain function during visually stimulated sexual arousal in menopausal women. We used structural and functional magnetic resonance imaging (fMRI) in parallel to evaluate menopause-related brain morphological and functional alterations during visually stimulated sexual arousal in menopausal women.

4261 Computer 102

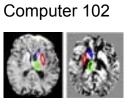

MR R2* and Quantitative Susceptibility Mapping: Variability in Normal Subjects across the Adult Lifespan

Christopher M O'Neill[1,2], Cheryl R McCreary[1,2], and Richard Frayne[1,2]

[1]Radiology and Clinical Neurosciences, Hotchkiss Brain Institute, University of Calgary, Calgary, AB, Canada, [2]Seaman Family MR Research Centre, Foothills Medical Centre, Alberta Health Serivces, Calgary, AB, Canada

R2* relaxation and susceptibility measurements are both candidate biomarkers for studying brain change. The relative variability of R2* and quantitative susceptibility mapping (QSM) approaches was studied in six deep brain regions in 182 normal subjects (18-89 years). The variability of R2* measures (average coefficient of variation, CoV: 0.33, mean ± standard deviation over regions) was found to be significantly less than QSM measurements (average CoV: 5.72). The variability in R2* measurements was found to vary with age, unlike QSM which showed no age effects. The increased variability observed in QSM measurements, however, may obscure smaller age effects.

4262 Computer 103

The Effects of Long-Term Physical Intervention for Active Ageing on the White Matter Hyperintensities in Older Adults

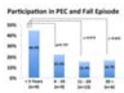

Toshiharu Nakai[1,2], Noriko Ogama[3], Takashi Sakurai[4], Mika Ueno[1], Sachiko Kiyama[1,5], and Ayuko Tanaka[1,6]

[1]NeuroImaging & Informatics, National Center for Geriatrics & Gerontology, Ohbu, Japan, [2]Department of Radiological Science, Nagoya University Graduate School of Medicine, Nagoya, Japan, [3]Center for Comprehensive Care and Research on Memory Disorders, National Center for Geriatrics and Gerontology, Ohbu, Japan, [4]Center for Comprehensive Care and Research on Memory Disorders, National Center for Geriatrics & Gerontology, Ohbu, Japan, [5]College of Liberal Arts and Sciences, Mie University, Tsu, Japan, [6]Faculty of Human Sciences, Kobe Shoin Women's University, Kobe, Japan

The relationship between the history of participation in community based physical exercise activity and the volume of white matter hyperintensity was evaluated in order to investigate the long-term effects of physical exercises on the neurophysiological status of brain to support cognitive processing in older adults. The FLAIR MR images obtained from 54 community dwelling older adults were segmented semi-automatically and the WMH volumes were quantified. It was suggested that long-term physical exercises more than 5 years for 90 minutes once per week may potentially reduce the progress of WMH lesions as well as the risk of fall.

4263 Computer 104

QSM and R2* texture analysis in the aging brain

Arturo Cardenas-Blanco[1,2], Matthew J Betts[1], Peter J Nestor[1], Emrah Düzel[1,2], and Julio Acosta-Cabronero[1]

[1]DZNE, Magdeburg, Germany, [2]Institute of cognitive neurology and dementia research (IKND), Magdeburg, Germany

To date, several studies have shown the value of quantitative susceptibility mapping (QSM) and R2* to detect aging-associated neurobiological mechanisms often based on single parametric features, either mean or median values, to characterise QSM/R2* behaviours in regions of interest (ROIs). In this study we propose the use of Haralick texture features to probe regional distribution characteristics of voxel intensities in R2*/QSM images. The results demonstrate that Haralick texture features add value to study the aging brain since they increase significantly the accuracy in subcortical R2*/QSM differentiation between elderly and young subjects.

4264 Computer 105

Changes in myelination and cortical thickness with advancing age

Andrew John Carradus[1], Benjamin Hunt[1], Prejaas Tewarie[1], Nicolas Geades[1], Simon Shah[1], Olivier Mougin[1], Matthew Brookes[1], and Penny Gowland[1]

[1]Sir Peter Mansfield Imaging Centre, University of Nottingham, Nottingham, United Kingdom

This study explores the relationships that cortical myelination and cortical thickness have with age, and expands on existing literature by investigating whether the previously reported trends are still present when only looking at individual lobes of the brain. We find that quadratic variations occur in all four lobes of the brain in regards to myelination, and that cortical thickness declines linearly with age in all lobes except the temporal. We also find that myelination levels and cortical thickness appear to change independently of each other.

4265 Computer 106

Cross-Sectional Assessment of Diffusion Parameters in Specific Brain Tracts correlated with Cortical Thinning throughout Healthy Aging

Maíra Siqueira Pinto[1], Antônio Carlos dos Santos[2], and Carlos Ernesto Garrido Salmon[1]

[1]InBrain Lab, Department of Physics, Faculty of Philosophy, Sciences and Letters of Ribeirão Preto, University of São Paulo, Ribeirão Preto, Brazil, [2]Department of Internal Medicine, Ribeirão Preto Medical School, University of São Paulo, Ribeirão Preto, Brazil

The human brain is a complex structure that undergoes continuous, non-linear changes over the lifespan. We used anatomic and diffusion data from 165 healthy subjects, collected retrospectively from CCIFM/HC-FMRP. T1-weighted images were used for cortical parcellation, thus 102 of 148 cortical regions had statistically significant decrease with age. Three fiber tracts were selected: Corpus Callosum, Uncinate Faciculus and Corticospinal Tract, their diffusion parameters, FA and MD, showed significant relationship with cortical thickness of the biggest cortical area in the ending of each tract. Despite these correlations, it was possible to verify that age is the pivotal variable in this relationship.

4266 Computer 107

Human Connectome Project (HCP) Lifespan Pilot: age-course of structural, microstructural and functional parameters in the hubs of the default mode network

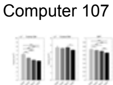

Daniele Mascali[1], Emily Kittelson[2], Keith Jamison[2], Kâmil Uğurbil[2], Essa Yacoub[2], Shalom Michaeli[2], Lynn Eberly[3], Melissa Terpstra[2], Federico Giove[1], and Silvia Mangia[2]

[1]Museo Storico della Fisica e Centro Studi e Ricerche “Enrico Fermi”, Rome, Italy, [2]Center for Magnetic Resonance Research, Dept. of Radiology, University of Minnesota, Minneapolis, MN, United States, [3]Division of Biostatistics, University of Minnesota, Minneapolis, MN, United States

Age-courses of multiple MRI outcomes were here characterized with a specific focus to default mode network (DMN) regions. Data were collected with unprecedented sensitivity and spatial resolution using the Human Connectome Project Lifespan Pilot protocol from 65 subjects divided in 4 age-groups (teen, young, middle-age and older adults). Age-related decreases of grey matter volumes, mean diffusivity, amplitude of resting-state oscillations and regional homogeneity were observed in both anterior and posterior DMN, and were more pronounced in anterior than in posterior DMN. Connectivity between posterior and anterior DMN regions remained relatively stable during the lifespan.

4267 Computer 108

Investigating the compensatory mechanisms of the ageing brain in response to a sub-maximal exercise task

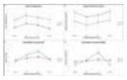

Andrew Hale[1,2], Penny Gowland[1], Paul Greenhaff[1,2], and Susan Francis[1]

[1]Sir Peter Mansfield Imaging Centre, University of Nottingham, Nottingham, United Kingdom, [2]MRC/ARUK Centre for Musculoskeletal Ageing Research, University of Nottingham, Nottingham, United Kingdom

Age-related alterations in cerebral vascular function may be better understood by investigating cerebral response to exercise. We performed a MR study involving low/moderate intensity exercise in healthy young and older subjects. We assess the effect of exercise on CBF response, cerebral oxygenation, and $CMRO_2$. We also investigate the relationship of GM-volume and physical fitness with ageing. At rest, there was no difference between CBF and $CMRO_2$ but an increase in oxygen extraction with age. On exercise the age-related increase in OEF remained, however CBF and $CMRO_2$ were blunted in older subjects. GM-volume was found to be associated with VO_{2max}.

4268 Computer 109

A two-region approach to assess brain iron changes as a function of age in basal ganglia, midbrain and dentate nuclei of healthy subjects using quantitative susceptibility mapping

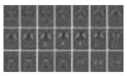

Kiarash Ghassaban[1], Sean K Sethi[1], Shuang Xia[2], and E. Mark Haacke[1,3]

[1]Magnetic Resonance Innovations Inc., Detroit, MI, United States, [2]Department of Radiology, Tianjin First Central Hospital, Tianjin, People's Republic of China, [3]Department of Radiology, Wayne State University, Detroit, MI, United States

In this work, 81 healthy subjects were recruited to assess iron deposition as a function of age in eight major brain nuclei using quantitative susceptibility mapping. By thresholding out high iron content region for each structure, seven basal ganglia and midbrain structures were evaluated locally and compared with the literature. Global (the entire structure) and regional (high iron content) susceptibility changes versus age were also analyzed for the dentate nucleus. In addition to the global analysis being consistent with the literature, regional analysis showed more sensitivity and precision as well as the left hemisphere dominance in terms of iron deposition.

4269 Computer 110

High Resolution Magnetic Resonance Histology of the Human Brain Temporal Lobe

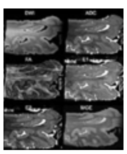

Alexandra Badea[1], Nian Wang[1], Gary P Cofer[1], Simon W Davis[2], John F Ervin[2], Dianne A Cruz[3], and G Allan Johnson[1]

[1]Center for InVivo Microscopy, Department of Radiology, Duke University Medical Center, Durham, NC, United States, [2]Department of Neurology, Duke University Medical Center, Durham, NC, United States, [3]Departments Psychiatry and Behavioral Science, Duke University Medical Center, Durham, NC, United States

Detecting early brain changes in neurodegenerative diseases such as Alzheimer's disease (AD) is essential for enabling interventions. We thus need to increase our ability to accurately localize areas that change, and to quantifying changes. The temporal lobe is essential for memory function. This is where AD hallmarks such as plaques, tangles, and neuronal death happen first. White matter has been proposed to have a role in early AD. We use high resolution magnetic resonance histology and diffusion tensor imaging to characterize the temporal lobe and its tracts. A compressed sensing acquisition with cluster based reconstruction increased efficiency four-fold.

4270 Computer 111

Effects of Working Memory Training on Microstructural Brain Changes in HIV-positive and Seronegative Subjects

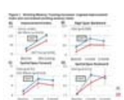

Chad Otoshi[1], Thomas Ernst[1], Kenichi Oishi[2], Hua Jun Liang[1], David Greenstein[1], and Linda Chang[1]

[1]Department of Medicine, University of Hawaii John A. Burns School of Medicine, Honolulu, HI, United States, [2]Department of Radiology and Radiological Science, Johns Hopkins Medicine, Baltimore, MD, United States

Microstructural brain changes before, 1-month and 6-months and after working Memory Training was evaluated in both HIV-positive and seronegative individuals. While working memory training improved performance in both trained and non-trained working memory tasks, brain diffusivities increased in most brain regions after training in both groups, more in HIV than controls in some regions. These findings suggest ongoing brain inflammation associated with normal aging or HIV may mask the training-related changes in DTI measures.

4271 Computer 112

Aging effects on kurtosis measures of limbic and association white matter tracts

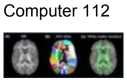

Qinmu Peng[1,2], King Kevin[3,4], Minhui Ouyang[1], Hanzhang Lu[5], and Hao Huang[1,2]

[1]Department of Radiology, Children's Hospital of Philadelphia, Philadelphia, PA, United States, [2]Department of Radiology, Perelman School of Medicine, University of Pennsylvania, Philadelphia, PA, United States, [3]Department of Imaging, Huntington Medical Research Institutes, [4]Department of Radiology, University of Texas Southwestern Medical Center, [5]Department of Radiology, Johns Hopkins University

Numerous studies have revealed that DTI-derived metrics are sensitive to the microstructural changes of the aging white matter tracts. However, microstructural changes associated with non-Gaussian water diffusion cannot be quantified by DTI-derived metrics, but uniquely quantified by DKI-derived metrics. Little is known on the progressive white matter microstructural changes measured by DKI-derived metric during aging. In this study, we found that the measurements of DKI-derived mean kurtosis (MK) decrease heterogeneously across white matter tracts, characterized with significant MK decreases in limbic tracts including fornix and cingulum and insignificant MK decreases in the association tracts.

4272 Computer 113

Longitudinal Cerebrovascular Analysis of the Aging Mouse Brain using Contrast Enhanced-MRA

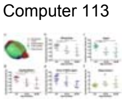

Lindsay Kathleen Hill[1,2,3], Dung Minh Hoang[2], Willis Chen[4], and Youssef Zaim Wadghiri[5]

[1]Biomedical Engineering, SUNY Downstate Medical Center and New York University, New York, NY, United States, [2]Radiology, NYU School of Medicine, New York, NY, United States, [3]Chemical and Biomolecular Engineering, NYU Tandon School of Engineering, Brooklyn, NY, United States, [4]NYU School of Medicine, New York, NY, United States, [5]New York University School of Medicine, New York, NY, United States

Here we study normal brain aging in wild type C57BL/6 mice and have detected a decline in cerebrovasculature over the two year aging process

4273 Computer 114

Age Related Differences in the geomT2 Relaxation Assessed Using Multi-Echo T2 Imaging

Muzamil Arshad[1,2], Jeffrey A. Stanley[1], and Naftali Raz[3,4]

[1]Psychiatry and Behavioral Neurosciences, Wayne State University School of Medicine, Detroit, MI, United States, [2]MD/PhD Program, Wayne State University School of Medicine, Detroit, MI, United States, [3]Psychology, Wayne State University, [4]Institute of Gerontology, Wayne State University

Multi-echo T_2 imaging (ME-T_2) enables the investigation of multiple white matter compartments. The short T_2 compartment has been the focus of recent investigations due to its specificity for the myelin water compartment. However, the much larger intra/extra cellular (IE) compartment has been relatively less explored. Here we investigate age differences in the geometric mean T_2 (geomT_{2IEW}) of the IE compartment in subcortical white matter tracts. We demonstrate that the effects of age on geomT_{2IEW} are not uniform across white matter tracts and suggest that this index may offer additional value in the characterization of age differences of white matter microstructure.

4274 Computer 115

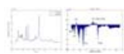

Quantification of Brain Metabolites in Alcohol Dependent Patients Using MRS with Experimental Basis Sets at 3T

Hyeon-Man Baek[1,2] and Yeong-Jae Jeon[1,2]

[1]Korea Basic Sicence Institute, Ochang, Korea, Republic of, [2]Dept. Bio-Analytical Science, Univ of Science & Technology, Daejeon, Korea, Republic of

In this study, in vivo quantification of brain metabolites measured on the dorsolateral prefrontal cortex (DLPFC) was carried out with LCModel using a priori knowledge based on experiment metabolite basis set signals. The main observation in this work was the significant reduction of tCho and Ins, and increase of GSH and Glx concentrations in the left DLPFC of alcohol dependent patients compared to healthy control subjects.

4275 Computer 116

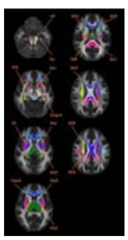

Anomalous diffusion γ metrics detects physiological and microstructural changes in brain normal aging

Michele Guerreri[1,2], Alessandra Caporale[1,3], Marco Palombo[4], Emiliano Macaluso[5], Marco Bozzali[6], and Silvia Capuani[1]

[1]CNR ISC UOS Sapienza University of Rome, Rome, Italy, Rome, Italy, [2]SAIMLAL Dept., Morphogenesis and Tissue Engineering, Sapienza University of Rome, Rome, Italy, [3]SAIMLAL Dept., Morphofunctional Sciences, Sapienza University of Rome, [4]MIRCen, CEA/DSV/I2BM, Fontenay-Aux Roses, France, [5]ImpAct Team, Lyon Neurosince Research Center, Lyon, France, [6]Neuroimaging Laboratory, Santa Lucia Foundation, Rome, Italy

The intent of this study was to test the potential of parameters extracted by the so-called anomalous diffusion (AD) stretched exponential γ-imaging model, to detect microstructural modifications occurring in brain during normal aging. Conventional DTI metrics was also considered. 27 healthy volunteers with age range 21-77y underwent DW acquisitions. Parametric maps of Mean γ (Mγ) and γ Anisotropy (γA) were obtained and a quantitative analysis was carried in different regions of White and Deep Grey Matter. We found that AD and DTI parameters correlations with age indicate changes in different brain regions diversifying thus aging patterns.

4276 Computer 117

Sub-clinical trait anxiety relates to cerebral blood flow in brain regions related to autonomic arousal

William J Cottam[1,2,3], Diane Reckziegel[1,2,3], Marianne M Drabek[1,2,3], and Dorothee P Auer[1,2,3]

[1]Radiological Sciences, Division of Clinical Neuroscience, University of Nottingham, Nottingham, United Kingdom, [2]Arthritis Research UK Pain Centre, University of Nottingham, Nottingham, United Kingdom, [3]Sir Peter Mansfield Imaging Centre, University of Nottingham, Nottingham, United Kingdom

Arterial spin labelling is a powerful, non-invasive tool to map cerebral blood flow (CBF) in the study of neural activity patterns underpinning spontaneous behaviour or personality traits. In this study we sought to directly investigate the effects of negative affect, specifically trait anxiety on local cerebral blood flow in a group of patients with chronic pain known to have mildly elevated anxiety scores. This study found widespread cerebral blood flow in osteoarthritis subjects with chronic pain that correlate significantly with trait anxiety, overlapping with regions previously reported to relate to autonomic functions. fMRI studies should account for increased physiological arousal.

4277 Computer 118

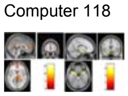

Evaluation of aging effects on cerebral hemodynamics by Magnetic Resonance Imaging

João Paulo Santos Silva[1], Ícaro Agenor Oliveira[1], André Monteiro Paschoal[1], and Renata Ferranti Leoni[1]

[1]Physics, University of Sao Paulo, Ribeirao Preto, Brazil

Recently, the effects of aging on human brain tissue, mainly how structural changes may be related to functional changes, have been extensively discussed. However, there is still no agreement on which brain regions have altered perfusion and how it is related with dementia. Therefore, in the present study, we investigated regional changes in perfusion and gray matter concentration in healthy aging, Mild Cognitive Impairment and Alzheimer's disease. The results indicate a significant age- and disease-related reduction of regional cerebral perfusion associated with brain atrophy. Therefore, these alterations may be important biomarkers for neurodegeneration.

4278 Computer 119

Both Rostral and Dorsal Anterior Cingulate Cortices Exhibit Age-related Metabolic Changes

Pui Wai Chiu[1,2], Hui Zhang[1], Savio Wai Ho Wong[3], Tianyin Liu[4], Gloria Hoi Yan Wong[5], Queenie Chan[6], and Henry Ka Fung Mak[1,2,7]

[1]Department of Diagnostic Radiology, The University of Hong Kong, Hong Kong, Hong Kong, [2]State Key Laboratory of Brain and Cognitive Sciences, The University of Hong Kong, Hong Kong, Hong Kong, [3]Department of Special Education and Counselling, The Education University of Hong Kong, Hong Kong, Hong Kong, [4]Sau Po Centre on Ageing, The University of Hong Kong, Hong Kong, Hong Kong, [5]Department of Social Work and Administration, The University of Hong Kong, Hong Kong, Hong Kong, [6]Philips Healthcare, Hong Kong, Hong Kong, Hong Kong, [7]Alzheimer's Disease Research Network, The University of Hong Kong, Hong Kong, Hong Kong

Rostral ACC displays a characteristic task-induced deactivation, while dorsal ACC displays positive BOLD responses in cognitive tasks. Nevertheless, the effect of age on the rostral ACC and dorsal ACC has never been investigated within the same cohort. In this study, quantitative proton magnetic resonance spectroscopy was used to investigate the metabolic changes in the rostral ACC and dorsal ACC in a local Chinese cohort at 3.0T. Both rostral ACC and dorsal ACC showed age-related metabolic changes. Rostral ACC may reveal greater degree of compensation compared to dorsal ACC.

4279 Computer 120

Memory Recall Accuracy is Associated with Glutamatergic Neurotransmission in the Right Hippocampus

Pui Wai Chiu[1,2], Hui Zhang[1], Savio Wai Ho Wong[3], Tianyin Liu[4], Gloria Hoi Yan Wong[5], Queenie Chan[6], and Henry Ka Fung Mak[1,2,7]

[1]Department of Diagnostic Radiology, The University of Hong Kong, Hong Kong, Hong Kong, [2]State Key Laboratory of Brain and Cognitive Sciences, The University of Hong Kong, Hong Kong, Hong Kong, [3]Department of Special Education and Counselling, The Education University of Hong Kong, Hong Kong, Hong Kong, [4]Sau Po Centre on Ageing, The University of Hong Kong, Hong Kong, Hong Kong, [5]Department of Social Work and Administration, The University of Hong Kong, Hong Kong, Hong Kong, [6]Philips Healthcare, Hong Kong, Hong Kong, Hong Kong, [7]Alzheimer's Disease Research Network, The University of Hong Kong, Hong Kong, Hong Kong

Memory for face–name associations is an important type of memory in our daily lives, and often declines in older adults, but the neural mechanisms underlying such decline are still unknown. In this study, quantitative proton magnetic resonance spectroscopy was used to investigate the metabolic changes in the bilateral hippocampi in a local Chinese cohort at 3.0T. The relationship between metabolite concentrations and memory recall accuracy from a face-name recognition task was also assessed. Right hippocampus revealed the plausibility of compensation activity during aging, and the memory recall accuracy was associated with alterations in glutamatergic neurotransmission.

Electronic Poster

RF Simulation & Design Strategies

Exhibition Hall Tuesday 16:15 - 17:15

4280 Computer 97

Visualizing the role of ideal current patterns in minimizing sample noise using dark mode current patterns for a spherical sample

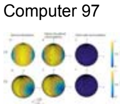

Manushka V. Vaidya[1,2,3], Daniel K. Sodickson[1,2,3], Christopher M. Collins[1,2,3], and Riccardo Lattanzi[1,2,3]

[1]Center for Advanced Imaging Innovation and Research (CAI2R), Department of Radiology, New York University School of Medicine, New York, NY, United States, [2]Bernard and Irene Schwartz Center for Biomedical Imaging, Department of Radiology, New York University School of Medicine, New York, NY, United States, [3]Sackler Institute of Graduate Biomedical Sciences, New York University School of Medicine, New York, NY, United States

We show that the ideal surface current patterns maximizing internal signal-to-noise ratio (SNR) are composed of a) signal-optimizing current patterns which maximize the signal sensitivity without considering sample noise, and b) “dark mode” current patterns which minimize sample noise without affecting signal. For a central voxel in a spherical sample, the absence of dark mode current patterns on an encircling sphere suggests that optimally tracking the precessing spin while ignoring sample noise is sufficient to achieve the best possible SNR. For an off-center voxel, however, the dark mode current patterns form high magnitude localized currents that efficiently minimize sample noise.

4281 Computer 98

The Twisted Solenoid RF Phase Gradient Transmit Coil for TRASE Imaging

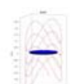

Stephanie Yong[1], Boguslaw Tomanek[2], and Jonathan C. Sharp[2]

[1]Physics, University of Alberta, Edmonton, AB, Canada, [2]Oncology, University of Alberta, Edmonton, AB, Canada

TRASE is a k-space encoding method that uses RF transmit phase gradient fields to achieve mm-level resolution. However, image quality is critically dependent upon the efficient generation of B_1 fields with uniform magnitude and strong phase gradients. We present a new family of phase gradient coil designs based upon a solenoid twisted about a transverse axis. Four twisted solenoids wound on a single cylindrical former are sufficient to encode two spatial dimensions. The design has many attractive geometric, electrical and magnetic characteristics, including the ability to encode in the B_0-direction, previously not possible for transverse-B_0 magnet geometries.

4282 Computer 99

Alternative approach for modeling a geometrically complex RF coil for evaluation in simulation.

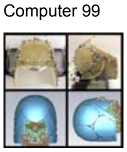

Gillian G Haemer[1,2,3], Nicole Wake[1,2,3], Martijn Cloos[1,2], Christopher Collins[1,2,3], Daniel K Sodickson[1,2,3], and Graham C Wiggins[1,2]

[1]The Center for Advanced Imaging Innovation and Research (CAI2R), Department of Radiology, New York University School of Medicine, New York, NY, United States, [2]The Bernard and Irene Schwartz Center for Biomedical Imaging, Department of Radiology, New York University School of Medicine, New York, NY, United States, [3]The Sackler Institute of Graduate Biomedical Sciences, New York University School of Medicine, New York, NY, United States

An alternative approach for generating a digital model of an RF coil is described that avoids the use of geometric priors and ensures structural accuracy. This approach is demonstrated on a helmet-shaped transmit-receive coil, and the resulting simulations are compared to experimental data.

4283 Computer 100

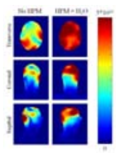

Evaluation of a high permittivity helmet for use as a coil former for an 8ch transmit/receive array with dodecahedral symmetry.

Gillian G Haemer[1,2,3], Manushka V Vaidya[1,2,3], Christopher Collins[1,2,3], Daniel K Sodickson[1,2,3], and Graham C Wiggins[1,2]

[1]The Center for Advanced Imaging Innovation and Research (CAI2R), Department of Radiology, New York University School of Medicine, New York, NY, United States, [2]The Bernard and Irene Schwartz Center for Biomedical Imaging, Department of Radiology, New York University School of Medicine, New York, NY, United States, [3]The Sackler Institute of Graduate Biomedical Sciences, New York University School of Medicine, New York, NY, United States

A helmet shaped coil former made of high permittivity material is simulated with an 8 channel transmit/receive coil as an evaluation step towards coil construction. The addition of the high permittivity material improves performance in both transmit and receive but the choice of a permittivity that is too high may lead to undesired split-resonance effects.

4284 Computer 101

EM-Circuit Co-Simulation Experience with a 7T 16-ch Array: Challenge, Errors, Speeding Factor, and Simulation Protocol towards Simulation Automation

Jinfeng Tian[1], Xiaoping Wu[1], Brian Hanna[1], John Strupp[1], Kamil Ugurbil[1], Gregor Adriany[1], and J. Thomas Vaughan[1,2]

[1]Center for Magnetic Resonance Research, University of Minnesota, Minneapolis, MN, United States, [2]Columbia University, New York, NY, United States

A complete MRI RF simulation has at least two parts involved: S-parameter optimization including frequency tuning, impedance matching and channel decoupling, and RF field generation. Previous EM-Circuit co-simulation work used every port data for field synthesis. In this abstract, the speeding factor, or the CPU/GPU time reduction factor, of the co-simulation method against the traditional broadband calculation, is present. We also compared the accuracy of field synthetization from every port data, vs. from every channel data, and propose a highly automatic optimal simulation flow that offers best field accuracy, minimum computer disk space and memory requirement, and fast data processing.

4285 Computer 102

Simulation of B1 Efficiency in 64-Channel Phased Head Arrays at 7T and 10.5T.

J. W. Radder[1], S. Moeller[1], G. Adriany[1], P.-F. Van de Moortele[1], B. Tramm[2], E. Auerbach[1], and K. Ugurbil[1]

[1]CMRR University of Minnesota, Minneapolis, MN, United States, [2]Life Services, LLC, Minneapolis, MN, United States

Simulation results are presented for 64-channel phased arrays operating at frequencies of 296.5 MHz (7T) and 447 MHz (10.5T) with 4.5 cm element loop diameters. FDTD simulations were performed per channel to obtain B1 receive fields of the coil array placed around a 2 mm resolution voxel anatomical head model. Sum-of-squares B1 efficiency maps show improved performance of the array at 10.5T compared to 7T over the whole head region.

4286 Computer 103

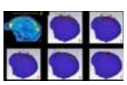

Mixed Dipole and Loop Coil for Macaque Brain Imaging at 7T: A Simulation Study

Yang Gao[1,2], Weidao Chen[1,2], Jinfeng Tian[3], Yi Sun[4], Gang Chen[1,2], Anna Wang Roe[1,2], and Xiaotong Zhang[1,2]

[1]Interdisciplinary Institute of Neuroscience and Technology, Zhejiang University, Hangzhou, People's Republic of China, [2]College of Biomedical Engineering & Instrument Science, Zhejiang University, Hangzhou, People's Republic of China, [3]Center for Magnetic Resonance Research, University of Minnesota, Minneapolis, United States, [4]MR Collaboration Northeast Asia, Siemens Healthcare, Shanghai, People's Republic of China

For monkey brain functional MR imaging, sufficient SNR is essential to reveal significant functional activities. Through a series of numerical simulation, we have demonstrated that under 7T environment, to image macaque brain whose size is much smaller than the natural resonate dimension of a dipole antenna, combining dipole and loop can feasibly provide considerably high SNR in both local cortical and deep brain regions. It is believed that such design will effectively benefit functional MRI over macaque with much enhanced signal quality.

4287 Computer 104

Ultimate Intrinsic SNR Based on Expansion Coefficient Optimization for Realistic 3D Macaque Head Model

Yang Gao[1,2], Weidao Chen[1,2], and Xiaotong Zhang[1,2]

[1]Interdisciplinary Institute of Neuroscience and Technology, Zhejiang University, Hangzhou, People's Republic of China, [2]College of Biomedical Engineering and Instrument Science, Zhejiang University, Hangzhou, People's Republic of China

We have calculated the ultimate SNR at a particular voxel located at monkey cortex through finding the optimized expansion coefficient. Our proposed method enables us to find the relative contribution of divergence free and curl free in UISNR at particular position in the realistic model.

4288 Computer 105

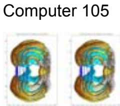

Degree of RF MRI Coil Detuning and SAR Variations over an Anatomically Realistic Respiratory Cycle Modeled with the Finite Element Method

Anh Tran[1], Sergey Makarov[1,2], and Harshal Tankaria

[1]Worcester Polytechnic Institute, Worcester, MA, United States, [2]NEVA Electromagnetics, LLC, Yarmouth Port, MA, United States

Respiratory motion is an important problem in Magnetic Resonance Imaging (MRI), contributing to image blurring during data acquisition and coil detuning. Using the concept of an ideal (perfectly matched and tuned at all available ports) RF transmit coil and the VHP-Female v4.0 dynamic CAD model, we estimate the detuning of a full-body RF coil detuning during the respiratory cycle. Our results show that the computed resonant capacitance values change by at most 0.5%.

4289 Computer 106

Design of Elliptical Birdcage Coil with Constant Ring-capacitor Value

Yoshihisa Soutome[1], Shin-ichiro Suzuki[2], Hideta Habara[2], Takahide Shimoda[2], and Yoshitaka Bito[2]

[1]R&D Group, Hitachi, Ltd., Kokubunji, Japan, [2]Healthcare Business Unit, Hitachi, Ltd., Tokyo, Japan

The value of ring capacitors in elliptical birdcage coil (EBC) should be varied gradually according to the location of the ring capacitor in order to generate uniform B_1^+ field distribution. Usually, it is difficult to adjust the value of the ring capacitor precisely by using fixed capacitors, because the value of the fixed capacitor is discretized. To realize the easy fabrication of EBC, we have designed EBC with constant ring-capacitor value at 1.5T. Simulation and experimental results indicated that the designed EBC generated uniform B_1^+ field distribution and showed the same transmission efficiency as the conventional EBC.

4290 Computer 107

Ultra-high field RF coils with adjustable longitudinal coverage: Traveling-wave meets standing-wave

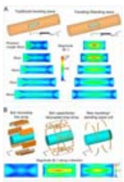

Xinqiang Yan[1,2], John C. Gore[1,2,3], and William A. Grissom[1,2,3]

[1]Institute of Imaging Science, Vanderbilt University, Nashville, TN, United States, [2]Department of Radiology and Radiological Sciences, Vanderbilt University, Nashville, TN, United States, [3]Department of Biomedical Engineering, Vanderbilt University, Nashville, TN, United States

7T scanners currently are not equipped with body coils, so for MR imaging of relatively short coverage along the z-direction (head, knee and prostate), local transmit coils with standing-wave behavior are commonly used to achieve high efficiency. For MR imaging that requires long coverage such as the legs, traveling wave MRI is potentially a competitive choice since it is extremely simple to implement and enables large FOV imaging. In this study, we propose a coverage-adjustable transmit coil which combines the concepts of traveling-wave and standing-wave. The new design exhibits excellent efficiency over short regions, but maintains the ability to cover longer areas for MR imaging of the legs or whole body.

4291 Computer 108

Improved traveling wave efficiency in 7T human MRI using wireless local loop and dipole arrays

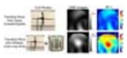

Xinqiang Yan[1,2], Xiaoliang Zhang[3,4], John C. Gore[1,2,5], and William A. Grissom[1,2,5]

[1]Institute of Imaging Science, Vanderbilt University, Nashville, TN, United States, [2]Department of Radiology and Radiological Sciences, Vanderbilt University, Nashville, TN, United States, [3]Department of Radiology and Biomedical Imaging, University of California San Francisco, San Francisco, CA, United States, [4]UCSF/UC Berkeley Joint Graduate Group in Bioengineering, San Francisco, CA, United States, [5]Department of Biomedical Engineering, Vanderbilt University, Nashville, TN, United States

Traveling-wave MRI has robust matching performance and capability for large field-of-view (FOV) imaging. However, the efficiency of traveling-wave MRI is much lower than conventional methods, which limits its application. One way to improve the efficiency is to place local wireless resonators around the subject. The feasibility of this approach has been demonstrated in previous works using a single small loop. However, it is not clear whether other kinds of coils (such as electric dipoles) can be used as local elements, and it is not clear how much the improvements can be maintained in human imaging using an array design. By using wireless local loop coil and transverse dipole arrays, the transmit efficiency (B_1^+) of traveling-wave MRI can be improved by 3.4-fold in the brain and 2-fold in the knee. The coil types (loops or dipoles) should be carefully chosen for brain or knee imaging to maximize the improvement since they exhibit different types of coupling to the TE_{11} mode, and the enhancement depends on the local body configuration

---

4292 Computer 109

New resonator geometries for ICE decoupling of loop arrays

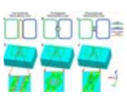

Xinqiang Yan[1,2], John C. Gore[1,2,3], and William A. Grissom[1,2,3]

[1]Institute of Imaging Science, Vanderbilt University, Nashville, TN, United States, [2]Department of Radiology and Radiological Sciences, Vanderbilt University, Nashville, TN, United States, [3]Department of Biomedical Engineering, Vanderbilt University, Nashville, TN, United States

To overcome B1 inhomogeneities and technological difficulties in building large-sized volume resonators, multi-channel arrays are commonly used for transmission at ultra-high fields. One of the main challenges in designing transmit arrays is to minimize the coupling among coil elements. The induced current elimination (ICE) method, which uses additional resonator elements to cancel coils' mutual electromagnetic (EM) coupling, has proven to be a simple and efficient approach to decouple loop, stripline and dipole arrays. However, in previous embodiments the decoupling elements acted as "magnetic-walls", blocking the magnetic field and leading to MR signal loss near the elements. In this study, we improved the ICE method to avoid the signal cancellation by using overlapped and perpendicular decoupling loops.

4293 Computer 110

An analytic expression for the ultimate intrinsic SNR in a uniform sphere

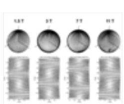

Hong-Hsi Lee[1], Daniel K. Sodickson[1], and Riccardo Lattanzi[1]

[1]Center for Biomedical Imaging, New York University, New York, NY, United States

Ultimate intrinsic SNR (UISNR) is the theoretically highest SNR for given geometry and electrical properties, independent of the coil design. Here, we introduce an analytic exact expression to calculate the UISNR at the sphere center, enabling to directly analyze the dependence on main magnetic field, sample geometry and electric properties. The analytic expression can approximate the UISNR near the center with < 5% error. This work can enable people without access to the full simulation code to calculate UISNR and use it, for example, as an absolute reference to assess the performance of head coils with spherical phantoms.

4294 Computer 111

A Novel Optimization Method for the Design of Permanent Magnet Array and its Application to a Portable Magnetic Resonance Imaging (MRI) System

Zhi Hua Ren[1] and Shao Ying Huang[1,2]

[1]EPD, Singapore University of Technology and Design, Singapore, Singapore, [2]Department of Surgery, National University of Singapore, Singapore, Singapore

Permanent magnet array is a welcome option to provide main magnetic field for portable magnetic resonance imaging (MRI). In this abstract, we propose an efficient and fast optimization method which can optimize the filed strength and homogeneity for the design of permanent magnet arrays. The magnetic field of permanent magnets with the interference of irons is calculated by applying boundary integral method (BIM). For optimization, genetic algorithm particle swarm optimization (GAPSO) is applied which offers highly diversified options and converges fast. A permanent magnet array is optimized with significantly improved performance, and it will be built for low-field portable MR imaging.

4295 Computer 112

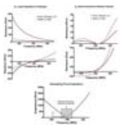

Decoupling and Integration of Electric Dipoles into RF Arrays

Ian Robert Oliphant Connell[1,2] and Ravi S Menon[1,2]

[1]Centre for Functional and Metabolic Mapping, Robarts Research Institute, London, ON, Canada, [2]Medical Biophysics, University of Western Ontario, London, ON, Canada

To-date, increasing interest in adapting dipole antennae for imaging at ultra-high field strengths has spawned the design and construction of many dipole-based RF arrays. However, increased electric-field interactions between dipole-to-sample and dipole-to-dipole provide an implementation barrier due to mutual coupling and load-sensitivity. This study presents an analysis of dipole-to-dipole coupling and implements a filter design method to isolate dipole elements in a highly-conformal array designed for human brain imaging at 7 Tesla.

4296 Computer 113

RF Pulse Design - based Parallel Transmit Array Design

Zhipeng Cao[1,2], Xinqiang Yan[2], Jun Ma[1,2], and William A. Grissom[1,2]

[1]Biomedical Engineering, Vanderbilt University, Nashville, TN, United States, [2]Institue of Imaging Science, Vanderbilt University, Nashville, TN, United States

A novel parallel transmit array design method is proposed that integrates both Maxwell and Bloch equations. The method is demonstrated to be better than traditional coils in dynamic multiband shimming and reduced field-of-view imaging scenarios to achieve better excitation accuracy and lower RF energy deposition, as well as robustness across multiple subjects and excitation schemes.

4297 Computer 114

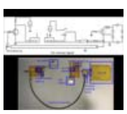

Wireless Q-spoiling of Receive Coils at 1.5T MRI

Jonathan Y Lu[1], Fraser Robb[2], John Pauly[1], and Greig Scott[1]

[1]Electrical Engineering, Stanford University, Stanford, CA, United States, [2]Advanced Coils, GE Healthcare Inc, Aurora, OH, United States

In this work, we demonstrate wireless Q-spoiling of an MRI surface coil in a 1.5T scan using commercial Linx LR series modules. These modules send a digital data stream wirelessly using an On-Off-Keying (OOK) protocol and a carrier frequency of 418MHz. With the simple Linx modules for wireless scanner state detection, it becomes possible to perform tasks such as wirelessly Q-spoiling MRI receive coils and beginning readout of receive coil data. Such steps are necessary for the ultimate goal of wireless MRI.

4298 Computer 115

A Simple Setup to Measure the Noise Figure of MRI Preamplifiers

Roland Müller[1] and Harald E. Möller[1]

[1]Max Planck Institute for Human Cognitive and Brain Sciences, Leipzig, Germany

Noise figure measurements have the reputation of being intricate and needing special equipment. Here, we will demonstrate that a simple setup involving an RTL-SDR dongle achieves convenient results. It requires, besides the inexpensive dongle, only common equipment, which should be available in all MRI coil labs.

4299 Computer 116

Practical aspects of preamplifier designs for 13C imaging.

Daniel Højrup Johansen[1], Juan D. Sanchez-Heredia[1], Vitaliy Zhurbenko[1], and Jan H. Ardenkjær-Larsen[1]

[1]Department of Electrical Engineering, Technical University of Denmark, Kgs. Lyngby, Denmark

This abstract presents two preamplifier designs for ^{13}C imaging optimized either for single or array coil usage. For single coil usage the preamplifier is designed to minimize noise yielding a noise figure of 0.25 dB. For array coils coupling between elements is a problem when the input impedance of the preamplifier is high. Hence the main contribution of this work is a low resistance, inductive input impedance preamplifier yielding better decoupling for array coils, while maintaining acceptable gain (20 dB) and noise figure (0.75 dB).

4300 Computer 117

Comparison of different RF coil designs for short T2* samples

Agazi Samuel Tesfai[1], Johannes Fischer[1], Ali Caglar Özen[1], and Michael Bock[1]

[1]Dept. of Radiology, Medical Physics, Medical Center – University of Freiburg, Freiburg, Germany

MRI of short T_2* samples is possible with ultra-short echo time sequences (UTE) which can be further improved using dedicated RF coils optimized for short-TE imaging. This work compares the performance of a commercial wrist coil with two custom-built coils (birdcage, solenoid) for UTE imaging of a mummy hand (low water content, short T_2*), and an *in-vivo* measurement of a human hand in which short-T_2* tissues such as tendons are highlighted by UTE image subtraction.

4301 Computer 118

Effect of Mismatching on the Transmit and Receive Performance of a Human Head 9.4T Tight-Fit Transceiver Phased Array.

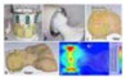

Nikolai I. Avdievich[1], Ioannis A. Giapitzakis[1], and Anke Henning[1,2]

[1]Max Planck Institute for Biological Cybernetics, Tübingen, Germany, [2]Institute of Physics, Ernst-Moritz-Arndt University, Greifswald, Germany

Tight-fit multi-channel ultra-high field (UHF, ≥7T) transceiver (TxRx) phased arrays improve transmit (Tx) efficiency in comparison to larger Tx-only arrays. However, tight-fit TxRx-arrays may require matching for each subject. To evaluate a potential use of tight-fit TxRx-arrays without matching, we investigated both numerically and experimentally an effect of a strong mismatch on performance of a 9.4T 8-channel human head TxRx-array. We demonstrated that mismatching caused only ~5% decrease of the B_1^+ field, while may have stronger effect on the maximum local SAR. Additionally it also effects the SNR distribution. While overmatching favors SNR, undermatching may enhance Tx-efficiency evaluated as $B_1^+/\sqrt{SAR_{10g}}$.

4302 Computer 119

ANALYTICAL RF COILS DECOUPLING: A THEORETICAL APPROACH FOR PARALLEL TRANSMISSION

Angelo Galante[1,2,3], Marco Fantasia[1], Piero Sebastiani[4], Antonello Sotgiu[4], and Marcello Alecci[1,2,3]

[1]Department of Life, Health and Environmental Sciences, L'Aquila University, L'Aquila, Italy, [2]Laboratori Nazionali del Gran Sasso, Istituto Nazionale di Fisica Nucleare, L'Aquila, Italy, [3]Istituto SPIN-CNR, CNR, L'Aquila, Italy, [4]Imaging Technology Abruzzo, L'Aquila, Italy

We show, by Finite Elements Modelling, the tuning and matching feasibility of a highly coupled parallel transmission (PTx) array by means of two degrees of freedom (two capacitances values) and decouple them a posteriori. This approach could be useful to simplify the design of PTx arrays avoiding complex procedures to geometrically and/or electrically decouple the elements. The procedure is stable for small parameters changes and this suggests a possible experimental verification of the results.

Electronic Poster

RF Coils & Systems

Exhibition Hall Tuesday 16:15 - 17:15

4303 Computer 49

magna cum laude

Experimental realization of a novel dual-nuclei coil for small animal imaging at 7 Tesla based on periodic structures of metal strips

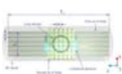

Anna A. Hurshkainen[1], Anton V. Nikulin[1], Stanislav B. Glybovski[1], Irina V. Melchakova[1], Pavel A. Belov[1], Benoit Larrat[2], Elodie Georget[2], Stefan Enoch[3], Pierre Sabouroux[3], Ana L. Neves[3], and Redha Abdeddaim[3]

[1]Department of Nanophotonics and Metamaterials, ITMO University, Saint-Petersburg, Russian Federation, [2]DRF/I2BM/Neurospin/UNIRS, CEA-Saclay, Paris, France, [3]CNRS, Institut Fresnel, Aix-Marseille Université, Marseille Cedex, France

In order to acquire image or MR spectra at two different nuclei dual-frequency RF-coils are used. Conventional approaches of tuning and matching a coils at several frequencies employ expensive non-magnetic capacitors which also introduce dissipative losses. We propose an alternative method of tuning and matching the coils at multiple desired frequencies. This method is based on resonant excitation of hybridized eigenmodes of periodic structures of metal strips. The proposed method allows one to build cheap coil with reduced dissipative losses resonating on two different frequencies simultaneously.

4304 Computer 50

magna cum laude

32-Channel In-Vivo Parallel Transmit Body Imaging at 7 Tesla

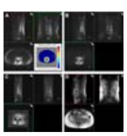

Sören Johst[1], Sascha Brunheim[1,2], Marcel Gratz[1,2], Harald H Quick[1,2], Mark E Ladd[1,3], and Stephan Orzada[1]

[1]Erwin L. Hahn Institute for MRI, University Duisburg-Essen, Essen, Germany, [2]High Field and Hybrid MR Imaging, University Hospital Essen, Essen, Germany, [3]Division of Medical Physics in Radiology (E020), German Cancer Research Center (DKFZ), Heidelberg, Germany

In this work we present phantom and in-vivo pTx excitation results acquired with a 32-channel add-on pTx system based on a 1-channel 7T MRI system. The add-on system uses custom-built I/Q modulators and custom-built amplifiers located inside the magnet room. The single exciter channel is split into 32 sub-channels, whereby the modulators control the phase and amplitude of the individual pTx RF pulses. The modulators and pre-calculated pTx gradients are synchronized via trigger signals generated in the imaging sequence. With the 32-channel pTx system, reduced FOV imaging of the lumbar vertebrae during free breathing was possible.

4305 Computer 51

A 8-channel pTx transceive coil for hip imaging at 7 T

Jin Jin[1], Ewald Weber[1], Kieran O'Brien[2], Aurelien Destruel[1], Bassem Henin[3], Craig Engstrom[1], and Stuart Crozier[1]

[1]University of Queensland, St Lucia, Australia, [2]Siemens Ltd, Brisbane, Australia, Australia, [3]American University of the Middle East, Kuwait

This paper presents the initial in vivo imaging results from a new unilateral 8-channel pTx transceive array designed and constructed for 7 T MRI of the hip joint. With subject-specific RF shims, 3D sequences (DESS and MEDIC) provided sufficient coverage, uniform image intensity and excellent contrast. The RF techniques employed in the construction of the array promote efficient use of RF power, enabling turbo spin echo sequences with full coverage of hip joint to be performed with adequate excitation. Comprehensive and conservative RF safety procedures ensure that local RF energy absorption is well below regulatory limits.

4306 Computer 52

Comparison of a 32-channel remote body coil for 7 Tesla with local and remote 8- and 16-channel transmit coil arrays

Thomas M. Fiedler[1], Martina Flöser[1], Stefan H. G. Rietsch[2,3], Stephan Orzada[2], Harald H. Quick[2,3], Mark E. Ladd[1,2], and Andreas K. Bitz[1]

[1]Medical Physics in Radiology, German Cancer Research Center (DKFZ), Heidelberg, Germany, [2]Erwin L. Hahn Institute for MRI, University Duisburg-Essen, Essen, Germany, [3]High Field and Hybrid MR Imaging, University Hospital Essen, Essen, Germany

The RF shimming performance of a 32-channel remote body coil is compared to ideally and non-ideally decoupled local and remote arrays consisting of 8 and 16 channels by evaluation of the singular values as well as evaluation of the RF shimming performance in axial and coronal slices with L-curves. For high-field body imaging, multi-ring remote coil arrays provide high degrees of freedom for RF shimming and can achieve higher B1+ homogeneity, especially for coronal slices. However, to utilize the full RF shimming potential of remote multi-ring transmit arrays, high local SAR has to be taken into account during safety assessment.

4307 Computer 53

Occipital-parietal coil with variable-density element distribution for 7T functional imaging

Kyle M Gilbert[1], Joseph S Gati[1], and Ravi S Menon[1]

[1]Centre for Functional and Metabolic Mapping, The University of Western Ontario, London, ON, Canada

A 32-channel receive coil with variable-density element distribution, in conjunction with an 8-channel transmit coil, was developed for imaging of the occipital-parietal regions of human brain at 7T. Spatial SNR maps demonstrate targeted sensitivity to the peripheral occipital pole, with a smoothly varying SNR proximal to this region. The temporal SNR of the occipital-parietal coil attained 35% higher SNR in the visual cortex than a whole-head coil.

4308 Computer 54

64-channel Double-Octagon Tx Head Coil for 7T Imaging

Tales Santini[1], Narayanan Krishnamurthy[2], Sossena Wood[3], Shailesh Raval[3], Yujuan Zhao[3], Anthony Fischetti[3], Minseok Koo[3], Howard Aizenstein[3], and Tamer Ibrahim[3]

[1]University of Pittsburgh, Pittsburgh, PA, United States, Pittsburgh, PA, United States, [2]University of Pittsburgh, PA, United States, [3]University of Pittsburgh

This work presents the design of a 64-channel double-rowed head coil (16 octagons with 4 Tx channels on each octagon). The magnetic field ( ) and the specific absorption rate (SAR) generated by the new coil were then compared with the TEM and 16-channel Tic Tac coils using Finite-Difference Time Domain (FDTD) simulations. Preliminary data shows significant improvements in all of performance parameters: coefficient of variation (CV) = 14.9% (field distribution) and maximum/minimum (Max/Min) = 2.45 (field intensity) across the whole head above and including the cerebellum; and peak/average SAR = 4.97/1.51 W/Kg/10g.

4309 Computer 55

Optimization of the Receive Performance of a Tight-Fit Transceiver Phased Array for Human Brain Imaging at 9.4T.

Nikolai I. Avdievich[1], Ioannis A. Giapitzakis[1], and Anke Henning[1,2]

[1]Max Planck Institute for Biological Cybernetics, Tübingen, Germany, [2]Institute of Physics, Ernst-Moritz-Arndt University, Greifswald, Germany

Tight-fit ultra-high field (UHF) ($\geq$7T) surface loop transceiver (TxRx)-phased arrays improve transmit (Tx) efficiency in comparison to Tx-only arrays built larger to accommodate for receive (Rx)-only array inserts. However, the number of elements in TxRx-arrays is restricted by the number of available RF Tx-channels (commonly 8 or 16), which limits the Rx-performance. A prototype of a 16-element array, which consists of 8 TxRx-surface loops circumscribing a head and 8 additional “vertical” Rx-only loops positioned in the center of each TxRx-loop perpendicularly, was constructed. This addition improves the Rx-performance substantially and has a minimal effect on both the Tx-efficiency and maximal local SAR.

4310 Computer 56

Lightweight Size Optimized Printed Pediatric Receive Array

Joseph Corea[1], Balthazar Lechene[1], Shreyas Vasanawala[2], Ana Clauda Arias[1], and Micheal Lustig[1]

[1]UC Berkeley, Berkeley, CA, United States, [2]Stanford Hospital

The current landscape of pediatric body MRI lacks dedicated high-density arrays, especially for small children. Therefore many centers use existing arrays designed for adults. These arrays are much larger than the patients, reducing the effective number of elements. Adult arrays are heavy for children and are supported by additional padding, increasing the distance from the patient and reducing image quality. Here, we present an appropriately sized blanket-like array designed from patient data for torso and chest/abdominal imaging of 0-2 and 3-5 year olds respectively. This pediatric array is fabricated using screen-printed electronics to produce an extremely lightweight and flexible coil.

4311 Computer 57

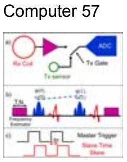

Software Synchronization of Independent Receivers by Transmit Phase Tracking

Greig Scott[1], Fraser Robb[2], John Pauly[1], and Pascal Stang[3]

[1]Electrical Engineering, Stanford University, Stanford, CA, United States, [2]GE Healthcare, Aurora, OH, United States, [3]Procyon Engineering, San Jose, CA

For add on receiver electronics, and wireless receiver coils, a major challenge is the synchronization of on-coil digitizers without a physical connection to the scanner. We propose that a digitizer that multiplexes the RF pulse and FID to an ADC can then use the transmit data to phase and frequency correct the MRI image data. We demonstrate frequency estimator and pulse sequence frequency tracking feasibility with a test bench that synthesizes the wireless MRI data acquisition and artifact-free image reconstruction.

4312 Computer 58

Fast method to get an upper bound of the maximum SAR_{10g} for body coil arrays

Ettore Flavio Meliadò[1,2], Alexander J.E. Raaijmakers[1,3], Peter R. Luijten[1], and Cornelis A.T. van den Berg[1]

[1]Center for Image Sciences, University Medical Center Utrecht, Utrecht, Netherlands, [2]MR Code BV, Zaltbommel, Netherlands, [3]Biomedical Image Analysis, Eindhoven University of Technology, Eindhoven, Netherlands

One of the most demanding challenges with ultra-high field MRI is the SAR_{10g} assessment during a multi-channel transmit MRI examination. A worst-case estimate is often used. In this work a fast method is presented to assess the upper bound of the maximum SAR_{10g} for body coil arrays with knowledge on only the power distribution among the channels. The performance is assessed for prostate imaging at 7T using our database with 23 realistic subject-specific models. The mean overestimation factor is 1.58 and the mean reduction in overestimation is 0.75 compared to a recently presented alternative estimation method.

4313 Computer 59

Measurement of Phosphocreatine and BOLD Kinetics in the Lower Extremity Muscles using a Dual-Frequency Coil Array

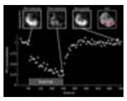

Ryan Brown[1,2], Oleksandr Khegai[1,2], and Prodromos Parasoglou[1,2]

[1]Center for Advanced Imaging Innovation and Research (CAI2R), New York University School of Medicine, New York, NY, United States, [2]Bernard and Irene Schwartz Center for Biomedical Imaging, New York University School of Medicine, New York, NY, United States

MRI provides the unique ability to study metabolic and microvasculature functions in skeletal muscle using phosphorus and proton measurements. However, the low sensitivity of these techniques can make it difficult to capture dynamic muscle activity due to the temporal resolution required for kinetic measurements during and after exercise tasks. We developed a dual-nuclei coil array to enable proton and phosphorus MRI of the human lower extremities with SNR more than double that of a birdcage coil in the gastrocnemius muscles. This enabled the local assessment of phosphocreatine recovery kinetics following a plantar flexion exercise using an efficient sampling scheme with a 6 s temporal resolution. The integrated proton array demonstrated image quality approximately equal to that of a clinical state-of-the-art knee coil, which enabled fat quantification and dynamic blood oxygen level-dependent measurements that reflect microvasculature function.

4314 Computer 60

29-channel Receive-only Dense Dipole Head Array for 7T MRI

Bei Zhang[1], Gang Chen[1,2], Martijn Cloos[1], Zidan Yu[1,2], Jerzy Walczyk[1], Christopher Collins[1,2], Ryan Brown[1], Riccardo Lattanzi[1,2], Daniel Sodickson[1,2], and Graham Wiggins[1]

[1]Bernard and Irene Schwartz Center for Biomedical Imaging, Department of Radiology, New York University School of Medicine, New York, NY, United States, [2]The Sackler Institute of Graduate Biomedical Sciences, New York University School of Medicine, New York, NY, United States

Inspired by recent theoretical work indicating that z-oriented currents could capture most of the optimal SNR and outperform loops in reception at high frequencies, we constructed and evaluated a close-fitting dense dipole receive-only head array with 29 elements. The array was combined with a dual-channel transmit birdcage for experiments. SNR was good throughout a head phantom at 7T and outperformed a commercial head coil in regions above and below the center. Future work will focus on detuning mechanisms for dipole elements to enable safe in-vivo measurements.

4315 Computer 61

An open 8-channel pTx coil for 7-Tesla MRI of the knee and ankle joints at multiple postures

Ewald Weber[1], Craig Engstrom[1], Kieran O'Brien[2], Aurelien Destruel[1], Bassem Henin[3], Jin Jin[1], and Stuart Crozier[1]

[1]University of Queensland, St Lucia, Australia, [2]Siemens Ltd, Brisbane, Australia, [3]American University of the Middle East, Kuwait

This paper presents the initial *in vivo* imaging results from a new open 8-channel pTx transceive array designed and constructed for 7 T MRI of the knee and ankle joints. The open design of the coil provides easy access and conformable accommodation of both joints, while enabling the joints to be imaged at multiple angles for enhanced pathological assessment. With individualized RF shims, the array provided full coverages and uniform excitations for both joints, demonstrated with high quality 2D TSE and 3D GRE (DESS and MEDIC) images.

4316 Computer 62

Utilization of Slotted Antennas for Capturing Ideal Current Patterns at Ultra High Field

Leeor Alon[1,2], Christopher M. Collins[1,2], Daniel K. Sodickson[1,2], and Riccardo Lattanzi[1,2]

[1]Center for Advanced Imaging Innovation and Research (CAI2R), New York University School of Medicine, New York, NY, United States, [2]Center for Biomedical Imaging, New York University School of Medicine, New York, NY, United States

Slotted antennas were demonstrated to be highly efficient coils for ultra high field magnetic resonance imaging. In this work, we elucidate the performance of such antennas using the ideal current patterns theoretical work.

4317 Computer 63

Combining loops and dipoles at 7 T and 10.5 T: a simulation study

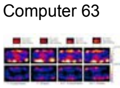

Bart R. Steensma[1], M. Arcan Ertürk[2], Kamil Uğurbil[2], Luijten R. Peter[1], Dennis W.J. Klomp[1], van den Berg A.T. Nico[3], Gregory J. Metzger[2], and Alexander J.E. Raaijmakers[1,4]

[1]Division Imaging, Department of Radiology, University Medical Center Utrecht, Utrecht, Netherlands, [2]Center for Magnetic Resonance Research, Department of Radiology, University of Minnesota, Minnesota, United States, [3]Division Imaging, Department of Radiotherapy, University Medical Center Utrecht, Utrecht, Netherlands, [4]Biomedical Image Analysis, Eindhoven University of Technology, Eindhoven, Netherlands

The combined use of loops and dipoles as transmit elements is investigated at 7 T and 10.5 T. A 8 channel loop/8 channel dipole setup is compared to a 16 channel dipole setup at both field strengths. It is found that combining loops and dipoles enhances transmit performance at both field strengths. The 8 loop/8 dipole transmit setup is the best performing setup at both field strengths. Additionally, increasing the channel count from 8 to 16 channels provides an almost 50% reduction in $SAR_{10g}/(B_1^+)^2$ at 10.5 T.

4318 Computer 64

Metamaterial Double-loop RF Head Coil for UHF MRI: A Numerical Evaluation and Experimental Verification at 7T

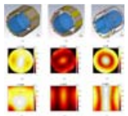

Elizaveta Motovilova[1], Yang Gao[2,3], Zhihua Ren[1], Xiaotong Zhang[2,3], and Shao Ying Huang[1,4]

[1]Engineering Product Development, Singapore University of Technology and Design, Singapore, Singapore, [2]Interdisciplinary Institute of Neuroscience and Technology, Zhejiang University, Hangzhou, People's Republic of China, [3]College of Biomedical Engineering & Instrument Science, Zhejiang University, Hangzhou, People's Republic of China, [4]Department of Surgery, National University of Singapore, Singapore, Singapore

This study presents a numerical evaluation of a novel RF coil array for human head imaging at 7T. The 8-element coil was developed using a metamaterial concept. As the main advantage of a metamaterial transmission line is that the uniformity of RF-magnetic near field does not dependent of the TL's physical length, we applied this meta-TL concept to a loop in order to achieve a larger coverage of B_1^+-field. Numerical comparison to conventional designs demonstrate an improved B_1-field homogeneity of the proposed coil. Preliminary experimental studies show a reasonable agreement with simulations.

4319 Computer 65

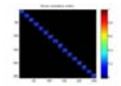

The potential of a 256-Channel receive-only Array Coil for accelerated Cardiac Imaging at 3T

Bernhard Gruber[1,2], Arjan D. Hendriks [1], Cezar B.S. Alborahal[3], Bas Brussen[3], Tim Leiner[1], Gustav Strijkers[1], Dennis W. J. Klomp[1,3], and Martijn Froeling[1]

[1]Department of Radiology, University Medical Center Utrecht, Utrecht, Netherlands, [2]Institute of Biomedical Mechatronics, Johannes Kepler University, Linz, Austria, [3]MR Coils B.V., Zaltbommel, Netherlands

High-density coil arrays can be used to accelerate MRI. Here we present the results from measurement-based extrapolations of a 256 Channel Cardiac Array Coil obtained by 16 sequential scans of a 16 Channel Array to assess acceleration performance and sensitivity constraints for 3T MRI. With element sizes of 55 mm x 33 mm, tissue load remains dominant at the 3T Larmor frequency of water, while SENSE accelerations can go up to 20-fold at low g-factors. These results motivate the design of a 256 channel cardiac array for accelerated 3T MRI.

4320 Computer 66

A bent dipole antenna and 4-channel loop array for 1H/31P brain application at 3 T MRI

Suk-Min Hong[1], Chang-Hoon Choi[1], Jörg Felder[1], Arthur W. Magill[1,2], and N. Jon Shah[1,3]

[1]Institute of Neuroscience and Medicine - 4 Medical Imaging Physics Forschungszentrum Juelich GmbH, Juelich, Germany, [2]Current Address: Medical Physics in Radiology, German Cancer Research Centre (DKFZ), Heidelberg, Germany, [3]Department of Neurology, Faculty of Medicine, RWTH Aachen University, JARA, Aachen, Germany

A dipole antenna achieves good isolation from a loop coil when it is located over the centre of a loop coil. Such an arrangement can be used as a dual-tuned coil, by tuning the dipole and the loop to the ^{1}H and X frequencies, respectively. At 3 T, however, the length of a dipole antenna is too long to be of use for brain applications. In this study, we bent the dipole antenna around the head to overcome the length problem. We then evaluated the feasibility of combining two dipole antennae and a 4-loop array for ^{1}H/^{31}P application.

4321 Computer 67

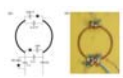

PIN-diode switched dual-tuned RF coils

YongHyun Ha[1], Arthur W. Magill[1,2], Chang-Hoon Choi[1], and N. Jon Shah[1,3]

[1]Institute of Neuroscience and Medicine - 4, Forschungszentrum Juelich, Juelich, Germany, [2]Current Address: Medical Physics in Radiology, German Cancer Research Centre (DKFZ), Heidelberg, Germany, [3]Faculty of Medicine, Department of Neurology, JARA, RWTH Aachen University, Aachen, Germany

In this work we investigate the transmit and receive performance of a probe employing such switching, using a simple loop coil tuned to 45 and 169 MHz for the detection of ^{23}Na and ^{1}H, respectively, at 4T. PIN diode switched-capacitor networks work well under forward bias, but perform poorly in reverse bias. Specifically, a high reverse bias voltage is required to allow operation over a realistic range of RF transmit voltages. This makes such switched-capacitor networks unsuitable for use in transmit probes. However, they can be used in receive-only probes, because the voltages present on the loop are much smaller.

4322 Computer 68

Folded four-ring double-tuned birdcage coil design

YongHyun Ha[1], Chang-Hoon Choi[1], and N. Jon Shah[1,2]

[1]Institute of Neuroscience and Medicine - 4, Forschungszentrum Juelich, Juelich, Germany, [2]Faculty of Medicine, Department of Neurology, JARA, RWTH Aachen University, Aachen, Germany

In this work, we designed a double-tuned ^{1}H/^{23}Na four-ring birdcage coil with a modification that entailed folding the outer end-rings by 90 degrees to overcome the available space limitation. And ^{23}Na SNR of the folded four-ring birdcage coil reached more than 93% of that obtained with the single-tuned birdcage coil. One benefit of folded four-ring birdcage coil compared to conventional four-ring birdcage coil is that there is no space restriction. This helps to build double-tuned coils that have a smaller diameter, leading to higher filling factors.

4323 Computer 69

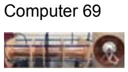

Half-wave Cavity Resonator for MR Coils Cable Assembly Testing

Victor Taracila[1], Louis Vannatta[1], Robert Rainey[1], Miguel Navarro[1], Aleksey Zemskov[1], and Fraser Robb[1]

[1]GE Healthcare Coils, Aurora, OH, United States

In MR coils or MR table there are multiple cables. Their presence is not desirable because they distort the B1 field; therefore multiple RF traps are distributed along the cable length to minimize induced cable currents. Tuning and performance of the MR cable traps', also called cable baluns, on the cable are always difficult to predict, because the cable shape and position may vary. A coaxial half-wave cavity resonator is shown to be a precise tool to test cable balun assembly. It facilitates precise measurement of a balun's coupling to the cable, its loss, and coupling to neighboring baluns.

4324 Computer 70

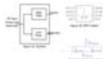

A General Approach to Interfacing Multi-Nuclear RF Coils

karthik lakshmanan[1], Ryan Brown[1], Christopher Collins[1], and Graham C Wiggins[1]

[1]NYU School of Medicine, Newyork, NY, United States

RF coils for multi-nuclear imaging require scanner-specific front-end interfaces that can limit their compatibility to one particular scanner platform. On the other hand, an intermediate interface that allows legacy coil compatibility with modern scanner architecture can be valuable in large institutions that operate a variety of scanners. In this work we describe the tools to build an intermediate interface with electronically controlled low-loss RF and DC signal pathways to provide a flexible means to route signals between the coil and scanner. While the tools are generally applicable to a variety of platforms, we focus on enabling compatibility between legacy multinuclear coils and a current scanner platform.

4325 Computer 71

Initial tests of a 4-channel building block for a local 32-channel Rx-only body coil at 7T

Stefan HG Rietsch[1,2], Stephan Orzada[1], Sarah Handtke[1], Sascha Brunheim[1,2], Mark E Ladd[1,3], and Harald H Quick[1,2]

[1]Erwin L. Hahn Institute for MR Imaging, University of Duisburg-Essen, Essen, Germany, [2]Highfield and Hybrid MR Imaging, University Hospital Duisburg-Essen, Essen, Germany, [3]Medical Physics in Radiology, German Cancer Research Center (DKFZ), Heidelberg, Germany

Receive-only (Rx) radiofrequency (RF) arrays are widely used in the clinical environment at 1.5 and 3T. At 7T, there is by default no integrated RF body coil. Yet, a 32-channel Tx/Rx body coil built into a 7T MRI system was recently presented. Consequently, this paves the way for 7T body imaging using this coil for Tx and local coils to receive the RF signal. In this work we present a 32-channel Rx-only coil for 7T and evaluate SNR boost and acceleration capabilities of one 4-channel building block.

4326 Computer 72

Optimization of Remote RF Transmit Coil Elements and Arrays for 7T UHF Body MRI

Stefan HG Rietsch[1,2], Stephan Orzada[1], Andreas K Bitz[3], Marcel Gratz[1,2], Mark E Ladd[1,3], and Harald H Quick[1,2]

[1]Erwin L. Hahn Institute for MR Imaging, University of Duisburg-Essen, Essen, Germany, [2]Highfield and Hybrid MR Imaging, University Hospital Duisburg-Essen, Essen, Germany, [3]Medical Physics in Radiology, German Cancer Research Center (DKFZ), Heidelberg, Germany

Remote radiofrequency (RF) body coils are broadly used as built-in body RF coils for signal transmission in clinical MR systems at 1.5 and 3T. For ultra highfield MR at 7T, remote body coils in conjunction with pTx systems have recently been presented. In this work we present a modified micro stripline RF element with meanders and investigate the performance of a 7T remote RF transmit array for body imaging applications featuring 8 of these elements concerning coupling, degrees of freedom within the B_1^+ fields, distribution of losses, power efficiency, and SAR efficiency.

Electronic Poster

Gradient, Shim & Magnet Technology

Exhibition Hall — Tuesday 16:15 - 17:15

4327 Computer 73

A comparative study of coil winding techniques of a full body 1.5 T MgB_2 based MRI magnets.

Abdullah Al Amin[1], Bhumi Bhusal[2], Tanvir Noor Baig[2], Robert Deissler[2], Laith Sabri[2], Ozan Akkus[1], and Michael Martens[2]

[1]Mechanical & Aerospace Engineering, Case Western Reserve University, Cleveland, OH, United States, [2]Department of Physics, Case Western Reserve University, Cleveland, OH, United States

Control of strain development in an MgB_2 based full body MRI magnet is a challenge towards realizing a conduction cooled system. It is possible to alter the strain development in an MRI magnet by modifying the coil winding support conditions and by varying the winding stress on the wire across the layers. A multiscale multiphysics model is employed to study the strain comparison by varying support conditions and winding prestress. Results conclude, radial support with constant winding prestress generates about 50% less stress and 42% less strain compared to no mandrel support.

4328 Computer 74

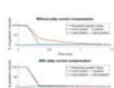

Concurrent use of 4 gradient axis enables eddy current compensation of an unshielded gradient insert coil

Tijl A van der Velden[1], Quincy van Houtum[1], Vincent O. Boer[1,2], Peter R. Luijten[1], Jeroen C.W. Siero[1,3], and Dennis W.J. Klomp[1]

[1]Radiology, University Medical Center Utrecht, Utrecht, Netherlands, [2]Danish Research Centre for Magnetic Resonance, Copenhagen University Hospital Hvidovre, Denmark, [3]Spinoza Center for Neuroimaging, Amsterdam, Netherlands

In this work, a method is presented where a whole-body gradient system corrects for eddy currents induced by an unshielded gradient insert coil. A single-axis unshielded gradient breast insert coil was positioned in a 7 tesla whole body MR system. Field cameras were used to analyze the eddy currents and validate the proposed method.

4329 Computer 75

A lightweight gradient insert coil for high resolution brain imaging

Tijl A van der Velden[1], Carel C. van Leeuwen[1], Erik R. Huijing[1], Martino Borgo[2], Peter R. Luijten[1], Dennis W.J. Klomp[1], and Jeroen C.W. Siero[1,3]

[1]Radiology, University Medical Center Utrecht, Utrecht, Netherlands, [2]Futura Composites B.V., Heerhugowaard, Netherlands, [3]Spinoza Center for Neuroimaging, Amsterdam, Netherlands

A lightweight insert gradient coil was constructed for high resolution brain imaging. The coil was designed as a single-axis unshielded coil to accelerate EPI readouts. The resulting coil weighs 45 kg and can be quickly positioned in the scanner by two persons. Theoretically, a gradient strength of 210 mT/m can be achieved with a slew rate of 1088 $T*m^{-1}*s^{-1}$ when driven at 400V/600A. In a 7 tesla scanner, an efficiency of 0.35 $mT*m^{-1}*A^{-1}$ with a slew rate of 800 $T*m^{-1}*s^{-1}$ was measured. Experiments on five healthy volunteers resulted in no experiences of nerve stimulation.

4330 Computer 76

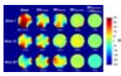

Global and dynamic shimming with the scanner's inbuilt shim system and a custom-made multi-coil setup at 9.4 T

Ali Aghaeifar[1,2], Irena Zivkovic[1], Christian Mirkes[1], Theodor Steffen[1], and Klaus Scheffler[1,3]

[1]Max Planck Institute for Biological Cybernetics, Tübingen, Germany, [2]IMPRS for Cognitive and Systems Neuroscience, University of Tübingen, Tübingen, Germany, [3]Department of Biomedical Magnetic Resonance, University of Tübingen, Tübingen, Germany

The homogenization of static magnetic field (B0) is necessary for MR imaging. The unwanted B0 inhomogeneity becomes more pronounced in ultra high field, and the scanner's inbuilt shim setup can not compensate the B0 fluctuation as is needed. Here we propose to use combined setup of the multi-coil approach and the scanner's shim setup to achieve higher homogeneity of B0 field. We employed custom-built multi-coil for slice-wise shimming in combination with the scanner's shim setup for global shimming. The results show improvement about 50% compare to dynamic shimming alone in the most of the slices.

4331 Computer 77

A Compact Affordable Three-Bore Cryogen-Free Superconducting Magnet for Extremity Imaging

Shahin Pourrahimi[1], Jerome L. Ackerman[2,3], John E. C. William[1], Nadder Pourrahimi[1], and Alexey Kaplan[1]

[1]Superconducting Systems, Inc., Billerica, MA, United States, [2]Martinos Center, Dept of Radiology, Massachusetts General Hospital, Charlestown, MA, United States, [3]Department of Radiology, Harvard Medical School, Boston, MA, United States

In a project to develop a compact MRI limb scanner for orthopedic and metabolic bone disease applications we developed a three-bore 1.5T magnet with the following design goals: ability to operate the magnet in a small point-of-care space, elimination of liquid cryogens for installation or operation, a comfortable patient experience while scanning knees, ability to tilt the magnet to accommodate patients rather than requiring patients to accommodate to the magnet, and capability for conventional and solid state proton and phosphorus MRI for metabolic bone disease assessment.

4332 Computer 78

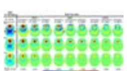

The numerical limitation of Multi-coil shim and Orthogonal RF-Shim coil

Jiazheng Zhou[1], Pu-Yeh Wu[1], Jason P. Stockmann[2,3], and Fa-Hsuan Lin[1,4]

[1]Institute of Biomedical Engineering, National Taiwan University, Taipei City, Taiwan, [2]A. A. Martinos Center for Biomedical Imaging, Massachusetts General Hospital, Charlestown, MA, United States, [3]Harvard Medical School, Boston, MA, United States, [4]Department of Neuroscience and Biomedical Engineering, Aalto University, Espoo, Finland

We used numerical simulations to study the relationship between attainable field homogeneity and the number as well as the orientation of shim coils in a multi-coil shim array. We found that, constrained the same number of shim coils, arranging shim coils in three orthogonal directions can provide the best shimming. Inspired by simulations, we propose a design of the integrated RF-shim coil at 3 T to place shim and RF coil orthogonally.

4333 Computer 79

Controlled E-peak field gradient coil

Hector Sanchez Lopez[1,2], Luca Zilberti[3], Oriano Bottauscio[3], Mario Chiampi[3,4], Xiaodong YANG[2], and Yajie XU[2]

[1]ARKFIELD PTY LTD, Brisbane, Australia, [2]Medical Imaging Department, Suzhou Institute of Biomedical Engineering and Technology (SIBET), Suzhou, People's Republic of China, [3]Division of Metrology for Quality of Life, Istituto Nazionale di Ricerca Metrologica (INRIM), Torino, Italy, [4]Energia Department, Politecnico di Torino, Torino, Italy

This work presents a new shielding method capable to reduce E-peak field values by minimizing the infinite norm of the induced current density. The target volume ("organ") is surrounded by a conductive surface "shell" where the infinite norm of the induced current density is minimized thereby producing a uniform distribution of the E-field inside the target volume and its surrounding. The method was effectively applied in the design of a whole body gradient coil with E-field control. E-field reduction larger than 10% are registered in a human phantom model. Further reductions in E-field is possible by compromising the coil performance.

4334 Computer 80

Design of an MRI Gradient Field Exposure System for Medical Device Testing

Daniel J Martire[1], William B Handler[1], Colin M McCurdy[1], Justin C Peterson[1], and Blaine A Chronik[1]

[1]Physics and Astronomy, Western University, London, ON, Canada

A method to design and numerically optimize a gradient field exposure system for testing medical devices is presented. Magnet windings are modelled as small current elements in space, and dimensions of a coil capable of emulating the switching rate and strength of MRI gradient fields are chosen by a grid search of parameter space. A buildable option capable of achieving 1.2% homogeneity over an 8 cm DSV, a slew rate of 246 T/s, and a maximum field shift of 68 mT was determined to be sufficient for our application and for satisfying relevant elements of ISO/TS 10974.

4335 Computer 81

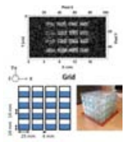

Very low field MRI setup for brain imaging

Reina Ayde[1] and Claude Fermon[1]

[1]Commissariat à l'enegie Atomique, Saclay, France, Metropolitan

Mixed sensors coupled to tuned flux transformer could more effective than classical tuned coils in detecting MRI signals on a very low field range. In order to compare later on their effectiveness, first, a very low field head MRI system (8.4 mT) is developed. Homogeneity, gradients strength, excitation and reception coils were adjusted. A homogeneity of 84 ppm was achieved in a quasi-open configuration. The amplitude of each gradient was 100 times lower than at high field but sufficiently high to achieve a resolution of less 2 mm x 2 mm x 2 mm. Images with a 3D imaging acquisition without pre-polarization technique nor magnetic shielding room were achieved.

4336 Computer 82

A new method for optimizing performances of gradient coils based on singular value decomposition and genetic algorithm

Koki Matsuzawa[1], Katsumi Kose[1], and Yasuhiko Terada[1]

[1]Institute of Applied Physics, University of Tsukuba, Tsukuba, Japan

Designing gradients coils with arbitrary geometries has been realized by matrix inversion optimization techniques. Use of a truncated singular value decomposition (SVD) is promising because magnetic field accuracies are controlled by choosing the appropriate SVD eigenmodes. However, in the SVD method, the gradient performances, such as inductance and power dissipation, cannot be optimized. Here we proposed a new strategy to optimize a desired coil performance. A key feature is the use of a genetic algorithm to optimize the appropriate combination of SVD eigenmodes. The concept is demonstrated for a biplanar geometry, and would be readily applicable to arbitrary geometries.

4337 Computer 83

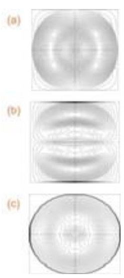

Oval gradient coils for a vertical magnetic field MRI

Koki Matsuzawa[1], Katsumi Kose[1], and Yasuhiko Terada[1]

[1]University of Tsukuba, Tsukuba, Japan

Small gradients are ideal in performance. Vertical-field MRI systems use biplanar gradient coils, and the coil sizes are no smaller than the magnet gap. Here we propose the oval geometry for gradient coils for vertical-field MRI to increase coil performance, Oval coils could be smaller than biplanar coils with maintaining the high accessibility and gradient linearity. Moreover, oval coils are preferable from the viewpoint of heating problems, because the gradient heat is efficiently cooled by air. In this study, we designed and constructed oval gradient coils for a 0.3 T, open MR scanner, and demonstrated the validity of the concept.

4338 Computer 84

B0 shimming in a small volume at 9.4T – irregular coil geometry setup vs. loop coil setup

Irena Zivkovic[1], Iliya Tolstikhin[2], Bernhard Schoelkopf[2], and Klaus Scheffler[1,3]

[1]High Field MRI, Max Planck Institute for Biological Cybernetics, Tuebingen, Germany, [2]Empirical Inference, Max Planck Institute for Intelligent System, Tuebingen, Germany, [3]Dept. for Biomedical Magnetic Resonance, University of Tuebingen, Tuebingen, Germany

At high magnetic fields B0 inhomogeneities are more pronounced and B0 shimming becomes very important. Dynamic or slice based shimming always provides better results than global or shimming in a volume. For shimming in a small volume, we propose a setup composed of irregularly shaped coils. Performances of the proposed setup are compared to performances of the configuration composed of only loop elements. The setup with irregular coils shows improved performances over the setup containing only loop elements. Future work should validate performances of the proposed setup on different volume sizes and different brain's B0 maps.

4339 Computer 85

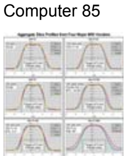

Measuring Slice Profiles Across the Industry With the ACR Phantom

Moriel NessAiver[1]

[1]Simply Physics, Baltimore, MD, United States

As part of mandated yearly performance evaluations on over 120 GE, Siemens, Philips and Toshiba 1.5T scanners, the ACR phantom was used to make 2555 measurements of RF slice profiles and thicknesses. Aggregated slice profiles are plotted showing clear differences between vendors both in terms of 'squareness' and FWHM thickness. With a target slice thickness of 5.0 mm the measured thicknesses ranged from 4.21 to 6.65 mm! The affect that interslice gap has on measured profiles (RF crosstalk) is demonstrated for T1 weighted sequences. A very surprising dependence of measured thickness on slice position on the ACR phantom is demonstrated.

4340 Computer 86

Continuous SWIFT: Analog Leakage Compensation Utilizing an Embedded System

Jonathan Weine[1], Florian Maier[1], Daniel Polak[1], and Reiner Umathum[1]

[1]German Cancer Research Center, Heidelberg, Germany

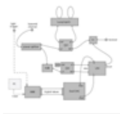

Methods for simultaneous excitation and acquisition enable measurements of signals with ultrashort T2* relaxation times. In this work, a method was developed and implemented to analogously compensate leakage of the excitation pulse into the receiver channel due to imperfections in coil tuning and the quadrature hybrid utilized in cSWIFT setups. The setup was enhanced with an embedded system, a vector modulator and a summing unit to subtract the leakage from the signal. Feasibility of the real-time compensation was demonstrated. Leakage was reduced by up to -40 dB.

4341 Computer 87

High field MRI in-vivo setup for observing brain plasticity in Eastern Fenced Lizards

Yee Eun Kim[1], Thomas Neuberger[2], Gangchea Lee[1], and Lara LaDage[3]

[1]PSU, University Park, PA, United States, [2]HUCK Institute, PSU, University Park, PA, United States, [3]PSU, Altoona, PA, United States

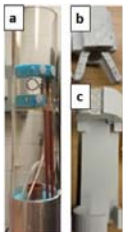

In this work, Eastern Fenced lizards, a non-model species known for high neurogenesis, were used to explore the extent of adult brain plasticity after exposing the animals to a complex environment and inmates. To conduct this study a MR setup for *in-vivo* lizard imaging was designed, constructed and tested. High resolution baseline in-vivo three dimensional lizard brain MR microscopy data sets were acquired and analyzed. The high quality of the images will allow to detect any brain volume changes after exposing the lizards to the enriched environment and having them scanned a second time.

4342 Computer 88

An open source waveform generator based on PulSeq for matrix coils

Huijun Yu[1], Mohamed Hamed[2], Sebastian Littin[1], Feng Jia[1], Stefan Kroboth[1], and Maxim Zaitsev[1]

[1]Department of Radiology, University Medical Center Freiburg, Freiburg, Germany, [2]Faculty of Engineering, University of Freiburg, Freiburg, Germany

An open source waveform generator based on Pulseq (open-source pulse sequence programming environment) for emerging matrix coils was developed, with the channel count of up to 64. The FPGA development board integrated with USB3.0 is used to store the waveform data and generate the waveform in real-time when external trigger signal is activated. The generator software was written in Python 2.7 with a queue structure.

4343 Computer 89

Using machine learning with dynamic exam block lengths to decrease patient wait time and optimize MRI schedule fill rate.

Michael C. Muelly[1], Paul B. Stoddard[1], and Shreyas S. Vasanwala[1]

[1]Department of Radiology, Stanford University, Stanford, CA, United States

MRI has advantages compared to other radiologic modalities in terms of tissue visualization, versatility, and lack of risks associated with ionizing radiation. However, cost of MRI is often the limiting factor favoring other modalities. Using historical scanner data and a Monte Carlo type discrete event simulation, we investigated how estimating exam length on the basis of patient demographics and dynamic block lengths affect mean patient wait times and schedule fill rate. In our simulation we are able to significantly lower mean patient wait times and optimize the schedule fill rate, which would theoretically result in lower cost per exam while enhancing patient satisfaction.

4344 Computer 90

Automated quality control of MR images using deep convolutional neural networks

Michael C. Muelly[1], Paul B. Stoddard[1], and Shreyas S. Vasanwala[1]

[1]Department of Radiology, Stanford University, Stanford, CA, United States

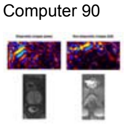

The complexity of MR scanners results in significant variability in the quality of images produced, in some cases requiring clinical expertise to recognize suboptimal images. Deep convolutional neural networks are an emerging technique with potential clinical applications. We aim to investigate whether deep convolutional neural networks could be trained for three MR image quality control classification tasks: 1) Recognize adequacy of MR elastography wave propagation, 2) determine whether rectal gas susceptibility artifact obscuring the prostate is present, and 3) determine scan technique in unlabeled images. Using the Inception v4 deep convolutional neural network we found high classification accuracy for two out of these three problems suggesting the potential to automate certain aspects of MR quality control.

4345 Computer 91

Evaluation of an Anthropomorphic Phantom with In-Vivo Using Quantitative MRI

Sossena Wood[1], Tales Santini[1], Narayanan Krishnamurthy[1], Shailesh Raval[1], and Tamer S. Ibrahim, PhD[1,2]

[1]Bioengineering, University of Pittsburgh, Pittsburgh, PA, United States, [2]Radiology, University of Pittsburgh, PA, United States

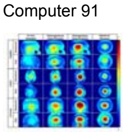

In this work, a developed refillable multi-compartment 3D-printed head phantom (established from MRI scans obtained in-vivo) was compared to a homogeneous commercial spherical phantom, the phantom itself with homogeneous loading in all of its compartments and in-vivo (the same volunteer on whom the phantom was based). Through B1 mapping and SAR analysis within an RF coil, the heterogeneous multi-compartment head phantom results were most accurate to the in-vivo volunteer.

4346 Computer 92

Real time gain stabilization for PET detectors in PET/MR

Floris Jansen[1], Mark Fries[1], Tuoyu Cao[1], Mehdi Khalighi[2], and Chang Kim[1]

[1]GE Healthcare, Waukesha, WI, United States, [2]GE Healthcare, Palo Alto, CA, United States

Accurate quantitation in PET requires good stability of the detector gain. The challenging thermal environment of the detector in a PET/MR system (proximity to gradients, induced eddy currents, heat from RF shield, ...) makes accurate temperature compensation important. Current solutions rely on characterization of detector response together with real time temperature measurement for a predictive (open loop) gain control. This work presents a method of gain control that operates in real time by analyzing spectral information of singles events, permitting closed loop gain control in the presence of temperature gradients or count rate variations.

4347 Computer 93

Prototype Hardware of FPGA Controlled Multi-Channel All-Digital RF Transmitter for Parallel Magnetic Resonance Imaging

Filiz Ece Filci[1], Aylin Dogan[1], Gokhan Cansiz[1], Bulent Sen[1], Volkan Acikel[1], and Ergin Atalar[2,3]

[1]Aselsan Inc., Ankara, Turkey, [2]Electrical-Electronics Engineering Department, Ihsan Dogramaci Bilkent University, Ankara, Turkey, [3]National Magnetic Resonance Center, Ihsan Dogramaci Bilkent University, Ankara, Turkey

In this study, prototype hardware of FPGA Controlled Multi-Channel All-Digital Transmitter for Parallel Magnetic Resonance Imaging is presented. The transmitter system consists of a RF power amplifier and a digital signal generator to feed each channels and a user interface computer to control the signal type, amplitude, phase, and frequency of targeted pulse. Digital signal generator uses a novel method which is IQ Pre-Modulation Delta Sigma Modulation Based Digital Single Side Band modulator and enables frequency, phase, and amplitude modulation schemes. The prototype hardware is produced to feed a 12-channel RF-coil, thus RFPA module consists of 12-PA are implemented.

4348 Computer 94

Cost-effective RF Signal Transmit-Receive chain at 9.5mT

Samarth Singh[1], Darshan Shivaramu Keelara[1], Chennagiri Rajarao Padma[1], Rashmi Rao[1], Imam Ahmed Shaik[1], and Sairam Geethanath[1]

[1]Medical Imaging Research Centre, Dayanand Sagar Institutions, Bangalore, India

A cost-effective RF Signal Transmit-Receive chain with independent transmit and receive coil was designed with inexpensive off-the-shelf electronic components, costing around 175 US dollars. A Direct Digital Synthesizer (DDS) module was controlled using an Arduino Uno R3 microcontroller board. RF pulses were timed to precision using Arduino IDE, and the 405 kHz sine wave required to operate a 9.5 mT system was pulsed to a transmit coil. This signal was detected successfully by a custom-made surface coil. While the transmit, pulse was at 1.12Vpp from the DDS module, the surface coil successfully picked up a 1.75 Vpp signal.

4349 Computer 95

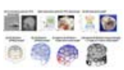

Unified Coils (UNIC) for Simultaneous RF Reception and Targeted Local B0 Shimming

HUI HAN[1], John Stager[1], Hsin-Jung Yang[1], Na Zhang[1], Sizhe Guo[1], Zhuoqi Li[1], Yicheng Wang[1], and Debiao Li[1]

[1]Biomedical Imaging Research Institute, Cedars-Sinai Medical Center, LOS ANGELES, CA, United States

We propose a new general MR coil concept with integrated RF and Bo shimming applicable to almost all MRI coils and systems. Innovative geometrical decoupling methods are proposed to bring the distance between separate shim and RF loops to zero millimeters and to make shim loops physically free from the RF loops. Therefore, both RF and shim coils can be in close proximity to the subject and be designed independently to maximize the performance of each function. It also opens a new window to integrate shim and RF coils or other coils in the constricted scanner bore space.

4350 Computer 96

Design and Construction of Shielded Enclosures for MRI

Jonathan Howard[1] and Rexford Newbould[1]

[1]Imanova Ltd, London, United Kingdom

A significant limiting factor for electronic devices within the scanner room is the electromagnetic interference (EMI) that they generate. Also, electromagnetic radiation from the scanner can interfere with the safe operation of electronics in close proximity to the scanner. We describe the development of an approach that enables researchers to fabricate inexpensive and reliable shielded enclosures without access to extensive engineering facilities. Our investigation explores the relative advantages and disadvantages in the design and construction of three different shielded enclosures and concludes with a performance evaluation by measuring the frequency dependent attenuation of electromagnetic signal intensity.

Electronic Poster

Cancer Treatment Response

Exhibition Hall — Tuesday 16:15 - 17:15

4351 Computer 1

A multi-parametric MRI-based radiomics approach to predict the high level of microsatellite instability in colorectal cancer

Zaiyi Liu[1], Yanqi Huang[1], Xin Chen[2], Zhongping Zhang[3], Lan He[1], and Xiaomei Huang[1]

[1]Radiology, Guangdong General Hospital, Guangzhou, People's Republic of China, [2]Radiology, Guangzhou First Hospital, Guangzhou, People's Republic of China, [3]MR Research China, GE Healthcare, Beijing, People's Republic of China

Microsatellite instability (MSI) is the condition of genetic hypermutability that results from impaired DNA mismatch repair (MMR). High levels of microsatellite instability (MSI-H) is regarded as a prognostic marker and predictor of the response to chemotherapy in colorectal cancer (CRC). This study presented a multi-parametric radionics classifier for preoperative and individualized prediction of MSC-H status in CRC patients. The potential application of this radiomics approach may aid the prognostic evaluation and decision-making in CRC patients.

4352 Computer 2

Magnetic Resonance Spectroscopic Early Predictors of 2-Year Progression Free Survival in IDH Mutated WHO II and III Gliomas

Min Zhou[1], Raymond Huang[2], Huijun Liao[1], Benjamin Rowland[1], Yue Zhou[1], Nils Arvold[3], and Alexander Lin[1]

[1]Center for Clinical Spectroscopy, Brigham and Women's Hospital, Boston, MA, United States, [2]Radiology, Brigham and Women's Hospital, Boston, MA, United States, [3]Radiation Oncology, Brigham and Women's Hospital, Boston, MA, United States

Most MR spectroscopy studies of patients with IDH-mutated gliomas have focused on the sensitivity and specificity of the 2-hydroxyglutarate measures but none that have examined the predictive value of 2HG in comparison to other brain metabolites for treatment outcome. This prospective longitudinal study measured MRS at baseline and two time points after radio/chemotherapy of IDH-mutated gliomas. Results showed that Cho/NAA shows the greatest predictive value followed by Cho/Cr, NAA/Cr, and Lac/Cr ratios but that all three time points 2HG levels were not predictive of outcome demonstrating that it is likely reflective of pathways distinct from membrane proliferation.

4353 Computer 3

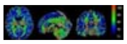

Radiation-induced changes in normal-appearing brain in patients with nasopharyngeal carcinoma: a MR T1ρ imaging study

Xiang Xiao[1], Yikai Xu[1], Yuankui Wu[1], Yingjie Mei[2], and Queenie Chan[3]

[1]Medical Imaging Center, Nanfang Hospital of Southern Medical University, Guangzhou, People's Republic of China, [2]Philips Healthcare, Guangzhou, People's Republic of China, [3]Philips Healthcare, Hongkong, People's Republic of China

Radiation encephalopathy is the primary complication in patients with nasopharyngeal carcinoma (NPC) following radiotherapy (RT). In order to detect early radiation-induced alterations in the brain of NPC patients after RT, we recruited NPC patients before RT and after RT with normal-appearing brain for MR T1ρ examinations. We found abnormal microstructural changes of gray matter and white matter in NPC patients after RT can be detected by MR T1ρ even when routine MRI findings are negative. MR T1ρ may be used to predict early radiation-induced alterations of the brain following RT for NPC patients.

4354 Computer 4

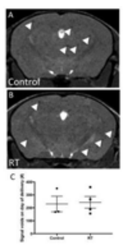

Using MRI to investigate the impact of radiation-induced damage on promoting tumor growth in a mouse model of brain metastasis

Amanda M Hamilton[1], Eugene Wong[2], and Paula J Foster[1,2]

[1]Imaging Research Laboratories, Robarts Research Institute, London, ON, Canada, [2]Medical Biophysics, University of Western Ontario, London, ON, Canada

Whole brain radiotherapy (RT) is the standard of care for breast cancer patients with multiple brain metastases but there are multiple negative consequences associated with the irradiation of normal brain tissue. In our study we investigated the influence that RT-induced damage of healthy brain has on the arrest and growth of metastatic breast cancer cells in a mouse model of breast cancer brain metastasis. We observed that irradiated but otherwise healthy neural tissue had an increased propensity to support metastatic growth compared to control. Elucidating the impact of RT on normal neural tissue could have implications in clinical patient management.

4355 Computer 5

Quantitative assessment of water diffusivity in bladder tumors: can response be predicted prior to neoadjuvant chemotherapy?

Huyen Thanh Nguyen[1], Amir Mortazavi[2], Kamal K Pohar[3], Lai Wei[4], Zarine K Shah[1], Debra L Zynger[5], Guang Jia[6,7], and Michael V Knopp[1]

[1]Wright Center of Innovation in Biomedical Imaging, Department of Radiology, The Ohio State University, Columbus, OH, United States, [2]Department of Internal Medicine, The Ohio State University, Columbus, OH, United States, [3]Department of Urology, The Ohio State University, Columbus, OH, United States, [4]Center for Biostatistics, The Ohio State University, Columbus, OH, United States, [5]Department of Pathology, The Ohio State University, Columbus, OH, United States, [6]Department of Physics and Astronomy, Louisiana State University, Baton Rouge, LA, United States, [7]Pennington Biomedical Research Center, Baton Rouge, LA, United States

This study is to correlate the degree of tumor heterogeneity in Apparent Diffusion Coefficient (ADC) at baseline with chemotherapeutic response in bladder cancer patients. MRIs of twenty muscle-invasive bladder cancer patients were performed with Diffusion weighted MRI (DWI). Freehand ROIs were placed on the whole tumor volume on ADC maps to obtain a dataset of voxel-wise ADC values for each patient. Histogram analysis was performed on each patient's ADC dataset to calculate uniformity (U) and entropy (E) at baseline. These quantities were then correlated with the patient's chemotherapeutic response. Our data showed that there was a strong correlation of tumor heterogeneity, which is characterized by U and E, and the patient's chemotherapeutic response. While U was significantly higher, E was significantly lower in responders (both $P<0.01$) compared to non-responders. In conclusion, quantification of tumor ADC heterogeneity can provide useful information that enables the ability to predict chemotherapeutic response prior to the treatment, to improve the patient outcomes.

4356 Computer 6

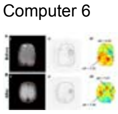

Simultaneous imaging of tumor size with contrast-enhanced MRI and response to therapy with extracellular pH readout from BIRDS

Jyotsna Upendra Rao[1,2], John Walsh[3], Maxime Parent[2], Yuegao Huang[2], Meser Ali[4], Daniel Coman[2], and Fahmeed Hyder[2,3]

[1]Cardiff University School of Medicine, Cardiff, United Kingdom, [2]Radiology and Biomedical Imaging, Yale School of Medicine, New Haven, CT, United States, [3]Biomedical Engineering, Yale University, New Haven, CT, United States, [4]Neurology, Henry Ford Hospital, Detroit, MI, United States

Acidic extracellular pH (pHe) of gliomas promotes tumor growth and builds resistance to therapy. Thus, to monitor therapeutic response, we used Biosensor Imaging of Redundant Deviation in Shifts (BIRDS), to generate pHe maps of rat brains bearing U251 tumors. Upon TmDOTP5-infusion, MRI identified tumor boundary and BIRDS imaged the intratumoral and peritumoral pHe gradient (DpHe). Two weeks post implantation of U251 glioma cells, animals were either treated with temozolomide (40 mg/kg) or were left untreated. The results of both terminal and longitudinal studies suggest that temozolomide therapy hinders tumor growth and normalizes intratumoral pHe.

4357 Computer 7

Anatomical sites' dependency of 3.0 T whole-body MRI's signal fat fraction and apparent diffusion coefficient in multiple myeloma focal lesions

Arash Latifoltojar[1], Margaret Hall-Craggs[1], Alan Bainbridge[2], Neil Rabin[2], Rakesh Popat[1], Ali Rismani[2], Kwee Yong[1], and Shonit Punwani[1]

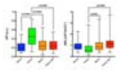

[1]University College London, London, United Kingdom, [2]University College London Hospital, United Kingdom

The increasing utility of MRI's quantitative imaging biomarkers for disease characterisation and response monitoring necessitates a better understanding of underlying pathophysiological changes.

This might be more pertinent when heterogeneous organ such as skeletal system is being investigated. In this work, we carry out a study into the heterogeneity of multiple myeloma's focal lesions on the basis of the various anatomical locations in skeleton.

4358 Computer 8

HCC treated with 90Yttrium radioembolization: can pre-treatment and 6week post-treatment volumetric ADC histogram measurements predict subsequent tumor response?

Sonja Gordic[1,2], Mathilde Wagner[1,3], Riccardo Zanato[1], Stefanie Hectors[1], Cecilia Besa[1], Edward Kim[4], and Bachir Taouli[1,4]

[1]Translational and Molecular Imaging Institute, New York, NY, United States, [2]Institute of Diagnostic and Interventional Radiology, University Hospital Zurich, Zurich, Switzerland, [3]Radiology, Groupe Hospitalier Pitié Salpêtrière, Paris, France, [4]Department of Radiology, Icahn School of Medicine at Mount Sinai, New York, NY, Switzerland

We evaluated the potential of volumetric ADC histogram measurements (vADC) obtained pre- and 6 weeks (6w) post-treatment for prediction of HCC response to ^{90}Yttrium radioembolization (RE). 22 patients underwent MRI at baseline and 6w after RE using a routine liver MRI protocol including DWI. Tumor response was assessed by mRECIST at 6 months post treatment. vADC mean, median and mode obtained at 6w post-treatment were significantly different between patients with partial/complete response vs. those with stable/progressive disease, and were a significant predictor of complete tumor response at 6 months, with vADC mode performing best. Pre-treatment vADC did not have any predictive value for response.

4359 Computer 9

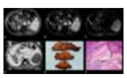

Evaluation of HCC Response to Loco-regional Therapy: Validation of Response Criteria with MRI using Explant as a Reference

Sonja Gordic[1,2], Idoia Corcuera-Solano[3], Ashley Stueck[4], Pamela Argiriadi[3], Preethi Guniganti[3], Michael King[3], Edward Kim[3], Swan Thung[4], and Bachir Taouli[1,3]

[1]Translational and Molecular Imaging Institute, New York, NY, United States, [2]Institute of Diagnostic and Interventional Radiology, University Hospital Zurich, Zurich, Switzerland, [3]Department of Radiology, Icahn School of Medicine at Mount Sinai, New York, NY, United States, [4]Department of Pathology, Icahn School of Medicine at Mount Sinai, New York, NY, United States

We assessed the performance of various imaging response criteria for the prediction of complete pathologic necrosis (CPN) of hepatocellular carcinoma post locoregional therapy on liver explant. Patients who underwent liver transplantation after locoregional therapy were included in this retrospective study. All patients underwent MRI using routine liver protocol within 90 days of liver transplant. RECIST, mRECIST, EASL, percentage of necrosis on subtraction images, and DWI (signal intensity and ADC) were assessed. CPN was retrospectively assessed in all tumors at histopathology. mRECIST, EASL, percentage of necrosis and signal intensity on DWI were all significant predictors of CPN while RECIST and ADC criteria were not.

4360 Computer 10

Value of Tumor Stiffness Measured with MR Elastography for Assessment of Response of Hepatocellular Carcinoma to Locoregional Therapy

Sonja Gordic[1,2], Jad Bou Ayache[3], Paul Kennedy [1], Cecilia Besa[1], Mathilde Wagner[1], Octavia Bane[1], Richard Ehman[4], Edward Kim[3], and Bachir Taouli[1,3]

[1]Translational and Molecular Imaging Institute, Icahn School of Medicine at Mount Sinai, New York, NY, United States, [2]Institute of Diagnostic and Interventional Radiology, University Hospital Zurich, Zurich, Switzerland, [3]Department of Radiology, Icahn School of Medicine at Mount Sinai, New York, NY, United States, [4]Department of Radiology, Mayo Clinic, Rochester, MN, United States

We correlated tumor stiffness (TS) measured with MR elastography (MRE) to degree of tumor enhancement and necrosis on contrast-enhanced T1-weighted imaging (CE-T1WI) in hepatocellular carcinomas (HCC) treated with locoregional therapy. Patients with HCC who underwent locoregional treatment and controls with newly diagnosed untreated HCC were included. TS values were obtained by placing regions of interest (ROIs) over HCCs on stiffness maps. Visual assessment of tumor necrosis on subtraction images and calculation of enhancement ratios by placing ROIs over tumors on CE-T1WI was performed. TS measured with MRE showed a significant correlation with tumor enhancement and necrosis.

4361 Computer 11

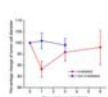

in vivo detection of tumor response to radiotherapy using Imaging Micro-structural Parameters Using Limited Spectrally Edited Diffsuion

xiaoyu jiang[1], hua li[1], zou yue[1], junzhong xu[1], and john Gore[1]

[1]vanderbilt university institute of imaging science, nashville, TN, United States

The changes that occur over a cell cycle play a vital role in mediating a cell’s sensitivity towards radiation therapy. Radiation exposure is expected to arrest cells at a particular cell cycle phase which improves the effectiveness of subsequent doses of radiation/chemotherapy. Cells in different phases have different sizes that can be detected by diffusion MRI with appropriate diffusion times. In this study, we evaluate the hypothesis in a rat glioma model that measurements of mean tumor cell size provides a means to quantify changes of cell phase distributions, and hence is capable of monitoring tumor response to radiotherapy.

4362 Computer 12

ADC and Kurtosis parameters show early response to anti-angiogenic therapy in patients with liver metastases

Mihaela Rata[1], Khurum Khan[1], David Collins[1], Matthew Orton[1], James d'Arcy[1], Nina Tunariu[1], Maria Bali[1], Ian Chau[1], Nicola Valeri[1], David Cunningham[1], Martin O Leach[1], and Dow-Mu Koh[1]

[1]CR-UK Cancer Imaging Centre, The Institute of Cancer Research and Royal Marsden Hospital, London, United Kingdom

Diffusion Weighted Imaging (DWI) is a valuable method of characterising tumour cellularity and assessing tumour response to therapy. Diffusion Kurtosis Imaging (DKI) is now being investigated outside of the brain, as the diffusional kurtosis metrics are strongly linked to cellular microstructure and heterogeneity in tissues. This work assesses tumour response to anti-angiogenic therapies as derived from DWI and DKI data in a cohort of patients with liver metastases enrolled on an early phase clinical trial. Our results demonstrate a significant cohort response to treatment of the ADC parameter, but also observed significant non-Gaussian diffusion behaviour.

4363 Computer 13

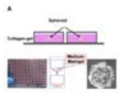

Impacting cancer cells via mechanical waves: can we change cellular behaviour?

Marlies Christina Hoelzl[1], Frederic Festy[2], Gilbert Fruhwirth[3], and Ralph Sinkus[4]

[1]Biomedical Engineering, King's College London, London, United Kingdom, [2]Tissue Engineering & Biophotonics, King's College London, [3]Imaging Chemistry and Biology, King's College London, London, United Kingdom, [4]Biomedical Engineering, King's College London, Lodon, United Kingdom

90% of cancer related deaths are caused by cancer metastasis, a process where cells leave the primary tumour, disseminate and form outgrowth at the secondary metastatic site. The tumour microenvironment provides crucial signals ((bio)chemical, mechanical) to regulate tumour formation, progression, and cell spread throughout the body. Translation of mechanical forces, displacements and deformations into biochemical signals (i.e. mechanotransduction) affects their cell behaviour (adhesion, spread, survival).[1,2] We show here that multiple treatment of tumour spheroids (solid tumour model in vitro) with focussed shear waves operating at specific frequency and amplitude results in reduced growth and reduced invasive behaviour of cancer cells.

4364 Computer 14

Evaluation of tumor oxygenation following radiation and PS-targeting antibody therapy in an orthotopic lung cancer model

Heling Zhou[1], Olivier Belzile[2], Zhang Zhang[3], Debabrata Saha[3], Jo Wagner[1], Brock Sishc[3], Strahinja Stojadinovic[3], Rolf Brekken[2,4], and Ralph P Mason[1]

[1]Radiology, Univ Texas Southwestern Medical Center, Dallas, TX, United States, [2]Hamon Center for Therapeutic Oncology Research, Univ Texas Southwestern Medical Center, Dallas, TX, United States, [3]Radiation Oncology, Univ Texas Southwestern Medical Center, Dallas, TX, United States, [4]Surgery, Univ Texas Southwestern Medical Center, Dallas, TX, United States

Combining phosphatidylserine (PS)-targeting monoclonal antibodies with radiation therapy can potentially enhance treatment efficacy. Oxygenation is important in radiation therapy response and could influence future treatment design. Oxygen enhanced MRI was used to examine changes in oxygenation in orthotopic lung tumors in rats treated by radiation or radiation plus a PS-targeting antibody. Orthotopic tumors were well oxygenated and responsive to oxygen breathing challenges before and after treatment. Combination therapy appeared to be more effective in tumor control than radiation alone.

4365 Computer 15

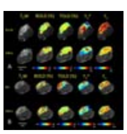

Multiparametric MRI assessment of tumor physiological changes during hypofractionated SABR

Heling Zhou[1], Zhang Zhang[2], Rebecca Denney[1], Jessica S Williams[3], Jeni Gerberich[1], Strahinja Stojadinovic[2], Debabrata Saha[2], John M Shelton[3], and Ralph P Mason[1]

[1]Radiology, Univ Texas Southwestern Medical Center, Dallas, TX, United States, [2]Radiation Oncology, Univ Texas Southwestern Medical Center, Dallas, TX, United States, [3]Internal Medicine, Univ Texas Southwestern Medical Center, Dallas, TX, United States

Hypofractionated stereotactic body radiation therapy, a new radiation treatment scheme, may be particularly susceptible to tumor hypoxia. We applied oxygen enhanced MRI together with DCE MRI to observe tumor physiological changes induced by a radiation fraction in a human lung cancer xenograft rat model. This study showed reduced vascular oxygenation 24 hours after the first fraction of 12 Gy, as indicated by the significant decrease in T_2* compared to baseline, but no significant response in dynamic contrast enhanced MRI. DCE parametric maps revealed a multinodular structure in the tumor as confirmed by histology.

4366 Computer 16

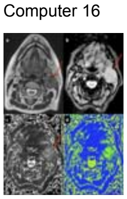

Absence of oxygen enhanced changes in T2* within head and neck cancer metastatic cervical lymph nodes is associated with local disease recurrence within 2-years following chemoradiotherapy

Harbir Singh Sidhu[1], Chiara Tudisca[1], David Price[2], Sola Adeleke[1], Marianthi-Vasiliki Papoutsaki[1], Martin Forster[3], Ruheena Mendes[4], Stuart Andrew Taylor[1], and Shonit Punwani[1]

[1]Centre for Medical Imaging, University College London, London, United Kingdom, [2]Medical Physics, University College London Hospital, London, United Kingdom, [3]Research Department of Oncology, University College London, London, United Kingdom, [4]Radiotherapy Department, University College London Hospital, London, United Kingdom

Hypoxia within head and neck squamous cell cancer metastatic lymph nodes is associated with poorer outcomes following chemoradiotherapy when measured directly using polarographic probes.

The utility of non-invasive pretreatment T2* measurement in prediction of chemoradiotherapeutic response was investigated. Our data suggest, however, that nodes demonstrating sustained post-therapy complete local response based on two-year follow-up are significantly more hypoxic compared with relapsing-nodes and paradoxically demonstrate a significant increase in hypoxia on breathing 100%-oxygen.

Following further work to ascertain the mechanisms of these observed changes, the differential response to oxygen and lower baseline oxygenation in responding-nodes could be exploited in risk stratification.

4367 Computer 17

Prediction of Individual Breast Tumor Therapeutic Response

Charles S. Springer, Jr.[1], Xin Li[1], Megan L. Troxell[2], Karen Y. Oh[3], Arpana Naik[4], Kathleen A. Kemmer[5], Aneela Afzal[1], May H. Mishal[1], Alina Tudorica[3], and Wei Huang[1]

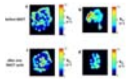

[1]Advanced Imaging Research Center, Oregon Health & Science University, Portland, OR, United States, [2]Pathology, Oregon Health & Science University, Portland, OR, [3]Radiology, Oregon Health & Science University, Portland, OR, [4]Surgical Oncology, Oregon Health & Science University, Portland, OR, [5]Medical Oncology, Oregon Health & Science University

Synopsis: A k_{io} parametric image maps Na^+,K^+ATPase activity with intra-tumor resolution. For breast tumors, the k_{io} hot spot fraction decreases after one NACT cycle if the tumor goes on to be cancer-free after NACT completion, but not if it maintains residual cancer. Also, though k_{io} hot spots are reduced after one NACT cycle, new ones appear in different *loci*. This is consistent with metabolic competition between different cancer cell populations within the tumor.

4368 Computer 18

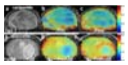

In-vivo Detection of Acute Intracellular Acidification in Glioblastoma Multiforme by AACID CEST MRI Following a Single Dose of Cariporide and Quercetin

Mohammed Albatany[1,2], Alex Li[2], Susan Meakin[3], and Robert Bartha[1,2]

[1]Department of Medical Biophysics, University of Western Ontario, London, ON, Canada, [2]The Centre for Functional and Metabolic Mapping, Robarts Research Institute, University of Western Ontario, London, ON, Canada, [3]Department of Biochemistry, University of Western Ontario, London, ON, Canada

Identification of tumor boundaries is challenging due to the infiltrative nature of the cancer. Cariporide and quercetin are drugs approved for human use that target different pH regulatory mechanisms in cancer. The goal of the current study is to determine whether chemical exchange saturation transfer (CEST) MRI is sensitive to tumor acidification after cariporide or quercetin injection. In mice with U87 glioblastoma brain tumors, we found both drugs significantly reduced tumor pH within two hours of treatment measured by CEST MRI. The physiological change induced by cariporide or quercetin could help localize brain cancer and monitor tumor response to chemotherapy. This unique approach to cancer detection does not require injection of an imaging contrast agent.

4369 Computer 19

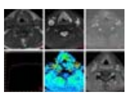

The use of DCE MRI in predicting early chemo-radiotherapy treatment response for Larynx and hypopharynx carcinoma

Wei Guo[1], Dehong Luo[1], Xinyi Chen[2], Bing Wu[3], Meng Lin[1], Lin Li[1], Yanfeng Zhao[1], Xinming Zhao[1], and Chunwu Zhou[1]

[1]Radiology, Peking Union Medical College, Cancer Institute & Hospital, Chinese Academy of Medical Sciences, BeiJing, People's Republic of China, [2]Radiology, The Second Affiliated Hospital, Zhejiang University School of Medicine, HangZhou, People's Republic of China, [3]GE MR Research China

In this work, we evaluated the utility of pretreatment semi-quantitative dynamic contrast-enhanced magnetic resonance imaging (MRI) in predicting early response to CRT (chemo-radiotherapy) in patients with larynx and hypopharynx carcinoma from primary tumors. To our knowledge, few studies correlate DCE-MRI semi-quantitative parameters on larynx and hypopharynx carcinoma. These quantitative methods do not require high computational power and were very suitable for clinical application.

4370 Computer 20

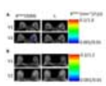

DCE-MRI Assessment of Breast Cancer Response to Neoadjuvant Chemotherapy: Early Prediction of Response and Evaluation of Residual Disease

Alina Tudorica[1], Karen Y Oh[1], Kathleen A Kemmer[1], Megan L Troxell[1], Arpana Naik[1], Neda Jafarian[1], Yiyi Chen[1], Stephen YC Chui[1], Eric Goranson[1], Nicole Roy[1], Aneela Afzal[1], May Mishal[1], Megan L Holtorf[1], Charles S Springer[1], Xin Li[1], and Wei Huang[1]

[1]Oregon Health & Science University, Portland, OR, United States

DCE-MRI was performed on 47 breast cancer patients (49 primary tumors) before, during, and after neoadjuvant chemotherapy (NACT). DCE-MRI data were subjected to Tofts model (TM) and Shutter-Speed model (SSM) pharmacokinetic (PK) analysis. Imaging metrics and the corresponding percent changes were correlated with binary pathologic complete response (pCR) and non-pCR endpoints, as well as residual cancer burden (RCB) index values. By NACT midpoint, several DCE-MRI PK parameters and percent changes are good early predictors of pCR vs. non-pCR, while tumor size is a poor predictor. Both PK parameters and tumor size after NACT completion are good markers of RCB. TM and SSM parameters perform equally well for prediction of NACT response and evaluation of RCB.

4371 Computer 21

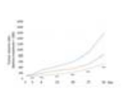

Near infrared photoimmunotherapy for lung cancer in a transgenic mouse model evaluated by MRI

Yuko Nakamura[1,2], Marcelino Bernardo[1], Zoe Weaver Ohler[3], Tadanobu Nagaya[1], Shuhei Okuyama[1], Fusa Ogata[1], Peter L. Choyke[1], and Hisataka Kobayashi[1]

[1]National Cancer Institute, Bethesda, MD, United States, [2]Diagnostic Radiology, Hiroshima University, Hiroshima, Japan, [3]Frederick National Laboratory for Cancer Research

Near infrared photoimmunotherapy (NIR-PIT) is a new cancer treatment that combines the specificity of antibodies for targeting tumors with the toxicity induced by photoabsorbers after irradiation with NIR light. The purpose of this study was to determine whether MRI can monitor the therapeutic effect of NIR-PIT in spontaneously occurring lung cancers that express epidermal growth factor receptor. Tumor volume ratio was inhibited significantly in the NIR-PIT group compared with control group. Thus, MRI can be a useful imaging modality for monitoring the therapeutic effects of NIR-PIT for cancer.

4372 Computer 22

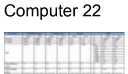

Rapid MR Pancreatic and Ovarian Screening Imaging for Patients with BRCA Mutation Undergoing Screening Breast MRI – Pilot Study

Sandra Huicochea Castellanos[1], Mitchell C. Raeside, Andrea Agostini, Richard K.G. Do, Amita Amita Shukla-Dava, David Aramburu Nunez, Ramesh Ramesh , Olga Smelianskaia, Monika Khan, Yuliya Lakhman, Evis Sala, and Lorenzo Mannelli

[1]MSKCC, New York, NY, United States

The purpose of this study was to develop and optimize a rapid MR pancreas and ovarian screening protocol to be performed in conjunction with breast MRI screening in BRCA mutation carriers. Images were acquired with the patient in the prone position, with the breast coil still in place, but using the built-in body coil on a 3T magnet, and evaluated for image quality and detection of lesions. 30 women had research MR for pancreatic screening and 5 of them also underwent for rapid ovarian MR screening which provided diagnostic quality images within a short time of acquisition.

4373 Computer 23

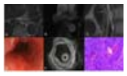

Preoperative T Staging of Potentially Resectable Esophageal Cancer: 3T MRI based on T2-TSE-BLADE and contrast-enhanced free-breathing radial VIBE (StarVIBE) vs endoscopic ultrasound

Jinrong Qu[1], Hongkai Zhang[1], Hui Liu[2], Xu Yan[2], Zhaoqi Wang[1], Hailiang Li[1], Kiefer Berthold[3], Nickel Marcel Dominik[3], and Ihab R. Kamel[4]

[1]Radiology, the Affiliated Cancer Hospital of Zhengzhou University, Henan Cancer Hospital, Zhengzhou, People's Republic of China, [2]MR Collaboration, Siemens Healthcare, [3]MR Pre-development, Siemens Healthcare, [4]Radiology, Johns Hopkins University School of Medicine

This study compared MRI based on the combination of T2-TSE-BLADE and contrast-enhanced T1 radial VIBE (StarVIBE) against endoscopic ultrasound (EUS) for T staging of potentially resectable esophageal cancer (EC). The histology confirmation of the T stage was used as reference. The results showed that the combination of T2-TSE-BLADE and StarVIBE is comparable to EUS in T staging of potentially resectable EC with lesions of T1/T2 stage, and is superior to EUS with lesions of T3/T4 stage.

4374 Computer 24

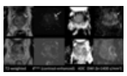

Appearance of Changes From Focal Therapy on Multiparametric Prostate Magnetic Resonance Imaging

Daniel Margolis[1], Ely Felker[2], Shyam Natarajan[3], Chris Alabastro[4], and Leonard Marks[3]

[1]Department of Radiology, Weill Cornell Medical College, New York, NY, United States, [2]Radiology, UCLA Geffen School of Medicine, Los Angeles, CA, United States, [3]Urology, UCLA Geffen School of Medicine, Los Angeles, CA, United States, [4]School of Medicine, UCLA Geffen School of Medicine, Los Angeles, CA, United States

Understanding the changes corresponding to focal therapy of prostate cancer on MRI is paramount to appropriate management, as serum tests may fail to accurately monitor these patients.

Electronic Poster

Perfusion, Permeability & Diffusion in Cancer

Exhibition Hall Tuesday 16:15 - 17:15

4375 Computer 25

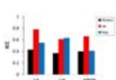

The Effects of AIF Quantification Variations on DCE-MRI Prediction of Soft Tissue Sarcoma Response to Preoperative Therapy: A Preliminary Multicenter Study

Kimberly Li[1,2], Yiyi Chen[2], Yun Yu[2], Xia Li[3], Andriy Fedorov[4], Guido Jajamovich[5], Dariya Malyarenko[6], Madhava Aryal[6], Peter LaViolette[7], Matthew Oborski[8], Finbarr O'Sullivan[9], Richard Abramson[10], Kourosh Jafari-Khouzani[11], Aneela Afzal[2], Alina Tudorica[2], Brendan Moloney[2], Sandeep Gupta[3], Cecilia Besa[5], Jayashree Kalpathy-Cramer[11], James Mountz[8], Charles Laymon[8], Mark Muzi[12], Paul Kinahan[12], Kathleen Schmainda[7], Yue Cao[6], Thomas Chenevert[6], Bachir Taouli[5], Fiona Fennessy[4], Thomas Yankeelov[13], Xin Li[2], and Wei Huang[2]

[1]International School of Beaverton, Beaverton, OR, United States, [2]Oregon Health & Science University, Portland, OR, United States, [3]GE Global Research, [4]Brigham and Women's Hospital, [5]Icahn School of Medicine at Mt Sinai, [6]University of Michigan, [7]Medical College of Wisconsin, [8]University of Pittsburgh, [9]University College, [10]Vanderbilt University, [11]Massachusetts General Hospital, [12]University of Washington, [13]The University of Texas at Austin

Soft tissue sarcoma DCE-MRI data collected at baseline and after one chemotherapy cycle were shared among nine centers and individual arterial input functions (AIFs) were quantified with center-specific methods. Pharmacokinetic (PK) modeling of the data was performed with these AIFs and the Tofts model. Considerable variations in estimated PK parameters and the corresponding percent changes were observed due to AIF variations. k_{ep} is less susceptible to AIF variation than K^{trans} and may be a more robust imaging biomarker of microvasculature. k_{ep} percent change correlates in a uniformly negative relationship with necrosis percentage of resection specimen across all individually measured AIFs.

4376 Computer 26

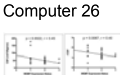

Predicting MGMT expression levels in glioma patients using multi-inversion-time PASL

Yuchao Liang[1], Yinyan Wang[1], Tianyi Qian[2], Josef Pfeuffer[3], Shaowu Li[4], Tao Jiang[1,5], and Lei Wang[1]

[1]Neurosurgery, Beijing Tiantan Hospital, Beijing, People's Republic of China, [2]MR Collaborations NE Asia, Siemens Healthcare, Beijing, People's Republic of China, [3]Application Development, Siemens Healthcare, Erlangen, Germany, [4]Neuroimaging center, Beijing Neurosurgical Insitute, Beijing, People's Republic of China, [5]Neurosurgery, Beijing Neurosurgical Insitute, Beijing, People's Republic of China

To evaluate the differences in cerebral blood flow between glioma patients with high MGMT expression and those with low MGMT expression, we retrospectively compared cerebral blood flow in pre-operative MR images acquired using multi-inversion-time PASL from glioma patients with histopathologically confirmed high MGMT expression and those with histopathologically confirmed low MGMT expression. The results demonstrate that MGMT expression status significantly correlates with both quantitative CBF and relative CBF.

4377 Computer 27

Utilizing correlations between Ktrans and plasma volume fraction estimates improves extended Kety modelling of DCE-MRI data

Matthew R Orton[1], Mihaela Rata[1], David J Collins[1], James A d'Arcy[1], and Martin O Leach[1]

[1]CRUK Cancer Imaging Centre, Division of Radiotherapy and Imaging, Institute of Cancer Research, Sutton, United Kingdom

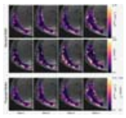

The extended Kety model is widely used for deriving quantitative perfusion and vascularity measures from DCE-MRI. In practice the signal contribution from the plasma space can be low compared to the signal-to-noise ratio (SNR) of the data which leads to cases where Ktrans is non-zero (indicating delivery of contrast to the tissues), but where the plasma volume fraction is estimated as zero: a logical contradiction. This work describes a model and fitting methodology to overcome this that makes use of a relationship between Ktrans and the plasma volume fraction to ensure both are positive or both are zero.

4378 Computer 28

Application of dynamic contrast-enhanced MRI in differential diagnosis of benign and malignant lung lesions

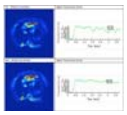

Zhi-yun Jiao[1], Fang Du[1], Jianxun Qu[2], Ling He[1], Chao Xu[1], Xia Ye[1], and Jiangfen Wu[3]

[1]Department of Radiology, First People's Hospital of Yangzhou, Yangzhou, People's Republic of China, [2]MR Research China, GE Healthcare, Shanghai, People's Republic of China, [3]GE Healthcare

Dynamic contrast enhancement (DCE) MRI is rarely used in lung lesions in previous studies, because of the influence of heart rate and respiratory motion. With the development of 3D non-rigid registration algorithm, high resolution dynamic enhanced MRI application in lung disease is increasing. After registration, the image is more clearer and the quantitative parameters are more accurate. The quantitative parameters Ktrans and Kep are capable of differentiating benign and malignant lung lesions, which has an important value in clinical work.

4379 Computer 29

Differential diagnosis of hepatocellular carcinoma and hepatic metastases using Radiomics Features from Quantitative DCE-MRI

Ye Li[1], Lian Ai Liu, Ning Huang[2], and Yan Guo[2]

[1]First Affiliated Hospital of Dalian Medical University, Dalian, People's Republic of China, [2]GE Healthcare, Lifescience, China

To evaluate the value of K^{trans} and HPI (hepatic arterial perfusion index), and their radiomics features in the differential diagnosis of hepatocellular carcinoma (HCC) and hepatic metastases from colorectal cancer (HM) using dynamics contrast enhanced MRI (DCE-MRI). Exchange model with dual input-based arterial input function was used to obtain the radiomics features that can provide a comprehensive assessment of tumors' physiologic properties including vascular permeability, microcirculation and hemodynamic information. Our results indicated that IDM (K^{trans}), inertia and correlation (HPI) are of great significance to differentiate HM and HCC.

4380 Computer 30

R2* relaxation affects pharmacokinetic analysis of DCE-MRI at high field strength

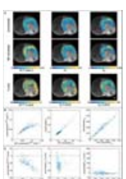

Eugene Kim[1], Jana Kim[1], and Siver Andreas Moestue[1]

[1]MR Cancer Group, Department of Circulation and Medical Imaging, NTNU Norwegian University of Science and Technology, Trondheim, Norway

In DCE-MRI, the effect of the r2* relaxivity of gadolinium-based contrast agents is often assumed to be negligible. Here, the validity of this assumption at 7T was tested. DCE-MRI was performed on two preclinical cancer models using a spoiled multiple gradient-echo acquisition, which enabled correction for transverse relaxation. Not accounting for R2* resulted in underestimation of the Tofts pharmacokinetic parameters, with K^{trans} being the most affected and v_p the least. Simulations showed that the R2* effect can be significant even at 3T in highly perfused regions but can be mitigated by decreasing TE and TR or increasing the flip angle.

4381 Computer 31

Arterial Input Function Selection in DSC-MRI of Brain Tumors Using Differential Evaluation Clustering Method

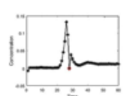

Hossein Rahim Zadeh[1], Anahita Fathi Kazerooni[1,2], Mohammad Reza Deevband[3], and Hamidreza Saligheh Rad[1]

[1]Quantitative MR Imaging and Spectroscopy Group, Research Center for Molecular and Cellular Imaging, Tehran University of Medical Sciences, Tehran, Iran, [2]Department of Medical Physics and Biomedical Engineering, Tehran University of Medical Sciences, Tehran, Iran, [3]Shahid Beheshti University of Medical Sciences, Tehran, Iran

Proper arterial input function (AIF) selection is a critical step for accurate quantification of dynamic susceptibility contrast enhanced (DSC) MRI in brain tumor patients. In this study, we have employed differential evaluation (DE) clustering method on processed perfusion images for accurate AIF selection. The procedure consists of two main steps: preprocessing for eliminating non-arterial curves including tissue, noisy and those contaminated with partial volume effects; and AIF selection using DE clustering method. The performance of this clustering method was compared to K-means and Hierarchical Clustering techniques and the results show the superiority of the proposed approach for accurate AIF selection.

4382 Computer 32

Quantitative Perfusion Imaging in Rectal Cancer – Choice and Influence of the Arterial Input Function to Perfusion Parameters

Tanja Gaa[1], Sonja Sudarski[2], Lothar R. Schad[1], and Frank G. Zöllner[1]

[1]Computer Assisted Clinical Medicine, Medical Faculty Mannheim, Heidelberg University, Mannheim, Germany, [2]Institute of Clinical Radiology and Nuclear Medicine, Medical Faculty Mannheim, Heidelberg University, Mannheim, Germany

Quantitative perfusion analysis in rectal cancer with DCE-MRI is highly dependent on the choice of the arterial input function (AIF). In nineteen patients it was investigated whether the selection affects the quantification of plasma flow (PF) applying with three different perfusion models (fast deconvolution algorithm, two-compartment uptake model, two-compartment exchange model). Results show disagreements in PF between the two AIFs for all three models with significant differences for the two-compartment exchange and uptake model.

4383 Computer 33

Model-based and Non-model-based Perfusion-related Predictors of Response to Chemotherapy in Intrahepatic Cholangiocarcinoma

Kristen Zakian[1], Aditi Iyer[1], Aditya Apte[1], Taryn Boucher[2], William Jarnagin[3], Nancy Kemeny[4], and Richard Do[2]

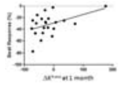

[1]Medical Physics, Memorial Sloan-Kettering Cancer Center, New York, NY, United States, [2]Radiology, Memorial Sloan-Kettering Cancer Center, New York, NY, United States, [3]Surgery, Memorial Sloan-Kettering Cancer Center, New York, NY, United States, [4]Medicine, Memorial Sloan-Kettering Cancer Center, New York, NY, United States

Hepatic arterial infusion of floxuridine has shown benefit in intrahepatic cholangiocarcinoma. Due to the complexity and expense of this treatment, a pre-treatment or early biomarker of efficacy would be advantageous. We employed non-model-based (NMB) analysis to maximize information from breath-motion degraded DCE-MRI in 24 patients. Model-based and NMB parameters were compared to RECIST response. The kurtosis value of pre-treatment time-to-half-maximum correlated with response, as did 1 month changes in perfusion parameters (K^{trans} and signal at half maximum). NMB analysis resulted in fewer voxels being discarded due to motion and thus may be more representative of tumor physiology while not requiring modeling.

4384 Computer 34

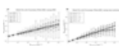

Optimization of acquisition and modelling parameters for accurate and precise estimation of tumor vascular permeability using modified K-CNR

Thomas S.C. Ng[1], Ravi T. Seethamraju[2], and Ritu R. Gill[1]

[1]Radiology, Brigham and Women's Hospital, Boston, MA, United States, [2]Siemens Healthcare USA

Adoption of quantitative clinical DCE-MRI remains limited given the challenges in accurate and precise estimation of kinetic parameters. Simulations are being increasingly used to guide protocol optimization1, but the relative effects of altering protocol variables are seldom considered. We used a modified K-CNR metric to quantify tumor Ktrans estimation. K-CNR provided a simple way to compare how input variables affect Ktrans output. The extended Toft's model was shown to be robust for tumor relevant Ktrans. Lengthening baseline time can improve Ktrans estimation. Care must be taken when using nested model analysis; wrong model convergence can occur with non-optimized acquisition variables.

4385 Computer 35

Robust and Efficient Perfusion Parameter Estimation for DCE-MRI of the Prostate Utilizing the Variable Projection (VARPRO) Method

Soudabeh Kargar[1], Eric Stinson[2], Eric Borisch[2], Adam Froemming[2], Akira Kawashima[3], Lance Mynderse[4], Joshua Trzasko[2], and Stephen Riederer[1,2]

[1]Biomedical Engineering and Physiology, Mayo Graduate School, Rochester, MN, United States, [2]Radiology, Mayo Clinic, Rochester, MN, United States, [3]Radiology, Mayo Clinic, Scottsdale, AZ, United States, [4]Urology, Mayo Clinic, Rochester, MN, United States

Dynamic contrast enhanced-MRI is essential for assessment of tissue microvasculature, and thus improved methods of parameter estimation for evaluation of tissue perfusion can be valuable. This work demonstrates how application of Variable Projection (VP) in perfusion analysis increases the robustness and computation efficiency compared to the conventional Levenberg-Marquardt (LM) method. A numeric simulation is used to validate the perfusion estimation and evaluate the robustness with respect to noise. The computation speed of VP is shown to be improved about 5× faster compared to LM method. VP-based perfusion analysis is demonstrated in eight patients with known prostate cancer.

4386 Computer 36

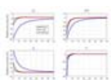

Weighted Total Least Squares for Parameter Estimation with the Two Compartment Exchange Model

Anders Garpebring[1] and Tommy Löfstedt[1]

[1]Radiation Sciences, Umeå University, Umeå, Sweden

When using linear least squares to estimate pharmacokinetic model parameters in dynamic contrast-enhanced MRI there is a risk of introducing bias due to noise correlations. By using a weighted total least squares (WTLS) method instead, these correlations are taking into account. The results of this study shows that the WTLS method is able to reduce the bias considerably compared to the linear least squares method for the two compartment exchange model, however, at the expense of increased computational time.

4387 Computer 37

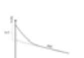

Diffusion-weighted MRI of rectal cancer: baseline tumour perfusion fraction predicts chemoradiotherapy response and survival

Kine Mari Bakke[1,2], Knut Håkon Hole[3], Svein Dueland[4], Krystyna Grøholt[5], Kjersti Flatmark[6,7,8], Anne Hansen Ree[1,8], Therese Seierstad[3], and Kathrine Røe Redalen[1]

[1]Department of Oncology, Akershus University Hospital, Lørenskog, Norway, [2]Institute of physics, University of Oslo, Oslo, Norway, [3]Department of Radiology and Nuclear Medicine, Oslo University Hospital, [4]Department of Oncology, Oslo University Hospital, [5]Department of Pathology, Oslo University Hospital, [6]Department of Tumor Biology, Oslo University Hospital, [7]Department of Gastroenterological Surgery, Oslo University Hospital, [8]Institute of Clinical Medicine, University of Oslo

More accurate diagnostics for prediction of treatment responses in locally advanced rectal cancer is warranted. We employed a simplified approach to the intravoxel incoherent motion imaging method to estimate the tumour perfusion fraction from diffusion-weighted MRI. The perfusion fraction was predictive of the histologic tumour response after chemoradiotherapy ($p = 0.02$), and in combination with tumour volume this parameter was also predictive of five-year progression-free survival of the patients ($p = 0.002$). This simplified approach does not require substantial extra scan time in a routine diagnostic scanning, and may offer a clinically feasible approach to stratifying patients to individualised treatment.

4388 Computer 38

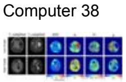

Anomalous diffusion in cerebral gliomas assessed using a fractional motion model

Boyan Xu[1], Lu Su[2], Zhenxiong Wang[3], Yaoyu Zhang[1], Yang Fan[4], Bing Wu[4], Gaolang Gong[5], Wenzhen Zhu[3], Peiyi Gao[2], and Jia-Hong Gao[1]

[1]Center for MRI Research, Peking University, Beijing, People's Republic of China, [2]Department of Radiology, Beijing Tiantan Hospital, Capital Medical University, Beijing, People's Republic of China, [3]Department of Radiology, Tongji Hospital, Tongji Medical College, Huazhong University of Science and Technology, Wuhan, People's Republic of China, [4]MR Research China, GE Healthcare, Beijing, People's Republic of China, [5]State Key Laboratory of Cognitive Neuroscience and Learning, Beijing Normal University, Beijing, People's Republic of China

Several models have been proposed to explain the anomalous diffusion in biological tissues. Among them, the fractional motion (FM) model was considered more appropriate. In this study, the FM model was applied in gliomas to assess its feasibility for grading gliomas. It was found that the FM model could improve the diagnostic accuracy in differentiation low- and high-grade gliomas, indicating the potential of the FM model to facilitate future studies of neuro-pathological changes in clinical populations.

4389 Computer 39

Discriminatory ability of MRSI and DW-MRI in prostatic diseases in biopsy naïve men with PSA 4-10 ng/ml

Durgesh Kumar Dwivedi[1,2], Rajeev Kumar[3], Alok Kumar Dwivedi[4], Girdhar S. Bora[3], Sanjay Thulkar[5], Sanjay Sharma[5], Siddhartha Datta Gupta[6], and Naranamangalam R. Jagannathan[1]

[1]Department of NMR and MRI Facility, All India Institute of Medical Sciences, New Delhi, Delhi, India, [2]Department of Radiodiagnosis, King George's Medical University, Lucknow, India, [3]Department of Urology, All India Institute of Medical Sciences, New Delhi, Delhi, India, [4]Division of Biostatistics and Epidemiology, Department of Biomedical Sciences, Texas Tech University Health Sciences Center, El Paso, Texas, TX, United States, [5]Department of Radiodiagnosis, All India Institute of Medical Sciences, New Delhi, New Delhi, India, [6]Department of Pathology, All India Institute of Medical Sciences, New Delhi, New Delhi, India

Multivariate approach of including different MR parameters offer a holistic view of entire data, which could provide better approach in differentiating various prostatic diseases. This approach may help in reducing the burden of unnecessary biopsy in men with PSA 4-10 ng/ml. we evaluated discriminatory ability of MRSI and DW-MRI in prostatic diseases in biopsy naïve men with PSA 4-10 ng/ml. The combined model (PSA + ADC + metabolite ratio) showed highest discriminatory ability in various prostatic diseases with AUC of 89% in men with clinically challenging group of PSA.

4390 Computer 40

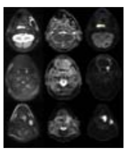

Diffusion Weighted Fast Spin Echo for tumor delineation in head-and-neck radiotherapy: a comparison with FDG-PET

Tim Schakel[1], Boris Peltenburg[1], Jan-Willem Dankbaar[2], Carlos Cardenas[3], Michalis Aristophanous[3], Chris Terhaard[1], Hans Hoogduin[2], and Marielle Philippens[1]

[1]Department of Radiotherapy, UMC Utrecht, Utrecht, Netherlands, [2]Department of Radiology, UMC Utrecht, Utrecht, Netherlands, [3]Department of Radiation Physics, MD Anderson Cancer Center, TX, United States

DWI shows high contrast between tumor and surrounding tissue, which shows potential for target volume delineation in head-and-neck radiotherapy treatment planning. In this study we assess the performance of a diffusion weighted fast spin echo sequence (DW-SPLICE) for target delineation in terms of interobserver agreement and spatial concordance with PET. Fifteen patients underwent both PET and DW-SPLICE. PET was segmented using a Gaussian mixture model, DW-SPLICE was delineated by 3 observers. Target volume delineation using DWI is feasible in head-and-neck radiotherapy. Using an optimized DWI sequence, target volumes could be defined with good interobserver agreement and large similarity with PET.

4391 Computer 41

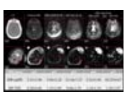

Distortion-Free Diffusion MRI using an MRI-Guided Tri-Cobalt 60 Radiotherapy System: Sequence Validation and Preliminary Clinical Experience

Yu Gao[1,2], Minsong Cao[2,3], Tania Kaprealian[3], Mitchell Kamrava[3], Michael Wang[3], John Neylon[3], Daniel Low[2,3], Yingli Yang[2,3], and Peng Hu[1,2]

[1]Radiology, University of California, Los Angeles, Los Angeles, CA, United States, [2]Physics and Biology in Medicine IDP, University of California, Los Angeles, Los Angeles, CA, United States, [3]Radiation Oncology, University of California, Los Angeles, Los Angeles, CA, United States

Limited resolution, severe distortion, and inaccurate quantification in low SNR scenarios associated with the conventional DW-ssEPI are problematic for adaptive radiotherapy based on tumor response. In this study, we sought to develop a reliable, accurate and distortion-free diffusion sequence that is practicable for longitudinal assessment of tumor response using an MRI-guided radiotherapy system. Quantitative phantom studies validated the superiority of the proposed technique over standard DW-ssEPI in terms of geometric fidelity and ADC accuracy. Excellent ADC reproducibility makes it a promising candidate for tumor response monitoring. Preliminary patient study demonstrated its feasibility to be used for tumor response assessment.

4392 Computer 42

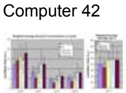

Proton Magnetic Resonance Spectroscopy of the Lipid Metabolic Response of a Murine Tumor Model to Radiation Therapy

Anthony G. Tessier[1], Atiyah Yahya[1,2], Matthew Larocque[1,2], B. Gino Fallone[1,2], and Alasdair Syme[3,4]

[1]Medical Physics, Cross Cancer Institute, Edmonton, AB, Canada, [2]Oncology, University of Alberta, Edmonton, AB, Canada, [3]Radiation Oncology, Dalhousie University, Halifax, NS, Canada, [4]Medical Physics, QEII Health Sciences Centre, Nova Scotia Health Authority, Halifax, NS, Canada

The temporal dependence of the lipid metabolic response to single fraction radiation therapy of human glioblastoma multiforme xenografts in NIH III nude mice was assessed with *in vivo* ^{1}H magnetic resonance spectroscopy (MRS) on a 9.4T magnetic resonance system. Lipid MRS can measure fat polyunsaturation, and therapeutic response can be monitored. The methylene:methyl peak ratio (CH_2/CH_3) can assess drug treatment and disease progression. Herein, lipid parameters and their response to radiotherapy in tumors are studied, including methyl, lactate + methylene, diallylic, and allylic protons, protons in α position to the carbonyl group, CH_2/CH_3, and mean polyunsaturation.

4393 Computer 43

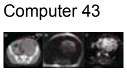

Longitudinal diffusion MRI for treatment assessment of sarcoma patients with pre-operative radiation therapy

Yingli Yang[1], Minsong Cao[1], Yu Gao[2], Mitchell Kamrava[1], Anusha Kalbasi[1], Nzhde Agazaryan[1], James Lamb[1], Ke Sheng[1], Daniel Low[1], and Peng Hu[2]

[1]Radiation Oncology, UCLA, Los Angeles, CA, United States, [2]Radiology, UCLA, Los Angeles, CA, United States

Diffusion weighted MRI (DWI) is promising for early prediction of tumor response to radiation therapy. We report our results of using longitudinal DWI approach performed on ViewRay system for predicting the response of sarcoma patient to pre-op RT. Six sarcoma patients were recruited in this study. Each patient subsequently underwent surgery. The tumor necrosis score was then used to compare to the ADC values to assess the predictive value of longitudinal DWI. Each patient successfully underwent 3–5 diffusion MRI scans. Based on the data from 6 patients, our longitudinal changes in tumor ADC matched well with pathology necrosis results.

4394 Computer 44

Integrated volumetric diffusion-weighted MR imaging and HPV genotyping in outcome prediction for stage IB-IV cervical cancer patients following chemoradiation therapy

Gigin Lin[1], Chyong-Huey Lai[1], and Yu-Chun Lin[1]

[1]Medical Imaging and Intervention, Chang Gung Memorial Hospital, Linkou, Taiwan

We evaluated the values of integration of pretreatment volumetric ADC analysis with human papillomavirus (HPV) genotyping in prediction of survival and recurrence for women with locally advanced cervical cancer in 82 women following concurrent chemoradiation therapy (CCRT). Independent poor prognostic indicators for OS and DFS by stepwise multivariate analysis, i.e., lower ADC10, advanced T or M stage and high-risk HPV status were composed to generate a novel outcome-predicting model, in which death was found in all the high-risk group patients whiles none of the low-risk group died or recurred during the follow up.

4395 Computer 45

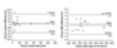

Longitudinal assessment of tumor volume and apparent diffusion coefficient in patients on active surveillance: a good way of monitoring disease progression?

Veronica A Morgan[1], Christopher Parker[2], and Nandita M deSouza[1]

[1]CRUK Imaging Centre, The Institute of Cancer Research, Surrey, United Kingdom, [2]Academic Urology Unit, The Royal Marsden Hospital NHS Foundation Trust, Sutton, United Kingdom

Tumor growth on T2-W MRI in 151 men with low-risk prostate cancer managed by active surveillance was related to tumor apparent diffusion coefficient (ADC). Volume increases greater than the 95% upper Limits of Agreement of reproducibility (~60%, n=20) were seen in 52 (34.4%) men. ADC was more reproducible (~5% variability). Baseline ADC values did not differ between those with and without measurable growth (p=0.06) but change in ADC did (-6.8±12.3% for those with measurable growth vs. 0.23±10.1% for those without, p=0.0005). A 5.6% reduction in ADC with time indicated a measurable increase in tumor volume (specificity 77.0%, sensitivity 54.9%, AUC=0.67).

4396 Computer 46

Textural Analysis based Segmentation of Bone tumours using Diffusion Weighted MR Image

Amit Mehndiratta[1,2], Esha Baidya Kayal[3], Rishabh Gupta[3], Abhimanyu Sahai[3], Jayendra Tiru Alampally[4], Sameer Bakhshi[5], Raju Sharma[4], and Devasenathipathy Kandasamy [4]

[1]Centre for Biomedical Engineering, Indian Institute of TechnologyDelhi, New Delhi, India, [2]Department of Biomedical Engineering, All India Institute of Medicine, New Delhi, India, [3]Centre for Biomedical Engineering, Indian Institute of TechnologyDelhi, [4]Department of Radio Diagnosis, All India Institute of Medical Sciences, [5]Institute-Rotary Cancer Hospital, All India Institute of Medical Sciences

Diffusion weighted imaging (DWI) plays a crucial role in diagnosis and prognosis of cancerous diseases. Proper demarcation of tumour on DWI is therefore necessary for qualitative assessment as well as quantitative image analysis like ADC or IVIM. Manual demarcation of tumour on each DWI slice is time consuming, prone to error and hard to reproduce. Automated and semi-automated algorithms were implemented and tested to segment bone tumours specifically on DWI. Experimental results reveal that semi-automated Active-Contours performed tumor segmentation better than other methods with acceptable levels of accuracy with considerable less time and manual effort.

4397 Computer 47

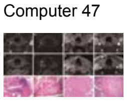

MR imaging in the prediction of aggressive histological features in papillary thyroid carcinoma

Bin Song[1] and Hao Wang[1]

[1]Radiology, Central Hospital of Minhang District, Fudan University, Shanghai, People's Republic of China

Purpose To investigate the value of magnetic resonance imaging (MRI) features for prediction of tumor aggressiveness in papillary thyroid cancer (PTC). Method A consecutive series of 119 lesions with PTC were preoperatively evaluated by MR imaging. A multivariate analysis was performed to predict tumor aggressiveness by 18 independent variables. Results Multivariate analysis demonstrated that lesion size classification and tumor margin on delayed contrast-enhanced images were the independent predictors of high aggressive PTC. Conclusion Lesion size classification and tumor margin on delayed contrast-enhanced images can be used preoperatively to estimate the risk of high aggressive of PTC.

4398 Computer 48

Optimization of b-values in iShim diffusion-weighted MR imaging of the thyroid gland: to improve the visualization of malignant thyroid nodules and the accuracy in differentiating malignant from benign thyroid nodules

Qingjun Wang[1], Qinglei Shi[2], Tianyi Qian[3], Alto Stemmer[4], and Yong Guo[1]

[1]Department of Radiology, Chinese Navy General Hospital, Beijing, People's Republic of China, [2]Scientific Marketing, Siemens Healthcare, People's Republic of China, [3]MR Collaobration, HC NEA MR COL, Siemens Healthcare, People's Republic of China, [4]MR Application Predevelopment, Siemens Healthcare GmbH

To investigate the optimal b-values of diffusion-weighted imaging (DWI), a prototype sequence with integrated slice-specific shimming (iShim) was applied for visualizing thyroid malignant nodules and making accurate differentiation between benign and malignant nodules. DWI images were acquired with five b-values including 0, 800, 1000, 2000 and 3000 sec/mm^2. The results show that the iShim-DWI with b-value of 800 s/mm^2 can present the clearest delineation of malignant thyroid nodules and that the images with b-value of 3000 s/mm^2 had the best performances in differentiating malignant from benign thyroid nodules.

Electronic Poster

UHF Imaging & Spectroscopy

Exhibition Hall | Tuesday 17:15 - 18:15

4399 Computer 73

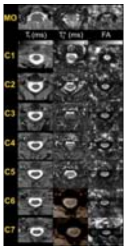

From medulla to lower cervical levels, a multi-parametric quantitative MR investigation dedicated to the diffuse alterations of the spinal cord at 7T: first insights into Amyotrophic Lateral Sclerosis

Aurélien Massire[1,2,3], Henitsoa Rasoanandrianina[1,2,3], Thorsten Feiweier [4], Manuel Taso[1,2,3], Aude-Marie Grapperon[5], Shahram Attarian[5], Maxime Guye[1,2], Jean-Philippe Ranjeva[1,2,3], Annie Verschueren[5], and Virginie Callot[1,2,3]

[1]Aix-Marseille Université, CNRS, CRMBM UMR 7339, Marseille, France, Marseille, France, [2]AP-HM, Hôpital de la Timone, Pôle d'imagerie médicale, CEMEREM, Marseille, France, Marseille, France, [3]iLab-Spine - Laboratoire international associé - Imagerie et Biomécanique du rachis, France/Canada, Marseille, France, [4]Siemens Healthcare GmbH, Erlangen, Germany, [5]Service de Neurologie et Maladies neuromusculaires, Hôpital de La Timone, AP-HM, Marseille, France

Amyotrophic lateral sclerosis (ALS) may benefit from unique contrasts and high-spatial resolutions provided by ultra-high field brain MRI. This also stands for spinal cord; nevertheless spinal cord imaging at 7T has lagged considerably behind brain investigations until recently. In this work, we propose a multi-parametric quantitative MR imaging protocol (T_1, T_2*, DTI, CSA), in an acquisition time compatible with clinical research (50min), to comprehensively investigate spinal cord diffuse alterations in neurodegenerative diseases such as ALS. With imaging along the whole cervical cord and medulla, theses multi-parametric acquisitions have the potential to provide new insights for the study of ALS.

4400 Computer 74

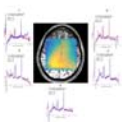

Density Weighted Concentric Rings K-Space Trajectory for 1H MRSI with gradient offset independent adiabatic pulses at 7T

Mark Chiew[1], Wenwen Jiang[2], Peder Larson[2,3], Brian Burns[4], Peter Jezzard[1], Albert Thomas[5], and Uzay E Emir[1]

[1]Oxford Centre for Functional MRI of the Brain (FMRIB), University of Oxford, Oxford, United Kingdom, [2]UC Berkeley-UCSF Graduate Program in Bioengineering, University of California, Berkeley and University of California, San Francisco, CA, United States, [3]Department of Radiology and Biomedical Imaging, University of California, San Francisco, CA, United States, [4]Department of Oncology, University of Oxford, Oxford, United Kingdom, [5]Department of Radiological Sciences, University of California, Los Angeles, CA, United States

In this study, we have developed and demonstrated a GOIA-semi-LASER sequence with density-weighted (DW)-concentric rings trajectory (CRT) that performs robustly at 7 Tesla and within a clinically feasible acquisition time. DW-CRT has been validated in a series of phantom experiments and its feasibility assessed in a healthy volunteer with an in-plane resolution of 5×5 mm^2. Experiments qualitatively demonstrate the advantage of DW-CRT over uniformly-weighted (UW)-CRT in terms of its improved resolution and reduced contamination of spectra from neighboring voxels.

4401 Computer 75

A form-fitted 1H/13C transceive coil array for MR spectroscopy in the human calf muscles at 7 T: initial results

Sigrun Goluch[1], Roberta Frass-Kriegl[1], Michael Pichler[1], Martin Gajdošík[2,3], Juergen Sieg[1], Ewald Moser[1], Martin Meyerspeer[1], Martin Krššák[2,3,4], and Elmar Laistler[1]

[1]Division MR Physics, Center für Medical Physics and Biomedical Engineering, Medical University of Vienna, Vienna, Austria, [2]High-Field MR Center, Department of Biomedical Imaging and Image-Guided Therapy, Medical University of Vienna, Vienna, Austria, [3]Christian Doppler Laboratory for Clinical Molecular MR Imaging, Medical University of Vienna, Vienna, Austria, [4]Division of Endocrinology and Metabolism, Medical University of Vienna, Vienna, Austria

Carbon-13 (^{13}C) MR spectroscopy (MRS) requires RF coils enabling acquisition at two different Larmor frequencies, namely at the ^1H frequency (f_{1H}=297.2 MHz) for scout imaging, B_0 shimming and proton decoupling, as well as at the ^{13}C frequency (f_{13C}=74.7 MHz) for acquisition of the carbon spectra at 7T. In this work we present preliminary data on the development of a dual tuned $^{13}C/^1H$ coil array for calf muscle studies at 7 T, including simulation, bench and MR measurements in a glucose phantom.

4402 Computer 76

Quantitative MRI of extra-ocular muscles in the clinical evaluation of systemic diseases

Luc van Vught[1,2], Robert de Meel[3], Jedrzej Burakiewicz[2], Stijn Genders[1], Martine Jager[1], Irene Notting[1], Jan Verschuuren[3], Hermien Kan[2], and Jan-Willem Beenakker[1,2]

[1]Ophthalmology, LUMC, Leiden, Netherlands, [2]Radiology, CJ Gorter center for high field MRI, LUMC, Leiden, Netherlands, [3]Neurology, LUMC, Leiden, Netherlands

Current diagnostic tools fail to accurately assess the condition of the eye muscles and orbital fat in ocular diseases. We have developed a high-resolution 7 Tesla quantitative MRI-protocol of the eye and evaluated its clinical value for Graves' orbitopathy and myasthenia gravis. The scan protocol proved to be robust against eye-motion and extra-ocular muscles were easily segmented from the orbital fat. Patient data showed elevated muscle fat fractions for both conditions compared to healthy subjects. Since the method quantifies the condition of the tissues, which otherwise can only be assess via an invasive biopsy, it potentially is an efficient technique to assess treatment response.

4403 Computer 77

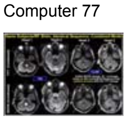

Towards Homogeneous 7T Neuro Imaging: Findings and Comparisons between 7T TTT and NOVA RF Coil Systems

Tamer S Ibrahim[1,2], Tales Santini[1], Shailesh Raval[1], Narayanan Krishnamurthy[1], Sossena Wood[3], Jung-Hwan Kim[1], Yujuan Zhao[1], Xiaoping S Wu[4], Essa S Yacoub[4], Howard S Aizenstein[5], and Tiejun Zhao[6]

[1]Bioengineering, University of Pittsburgh, Pittsburgh, PA, United States, [2]Radiology, University of Pittsburgh, Pittsburgh, PA, United States, [3]Bioengineering, University of Pittsburgh, Cranberry Twp, PA, United States, [4]Radiology, University of Minnesota, Minneapolis, MN, United States, [5]Psychiatry, University of Pittsburgh, Pittsburgh, PA, United States, [6]Siemens Medical Solutions, United States

Several major obstacles still face neuro UHF imaging including scanning and preparation time for every subject (for TX arrays) and RF intensity limitations due to increased local/global power deposition. The solutions provided and compared in this work represent non-subject specific configurations (combined mode NOVA coil system, PTX NOVA coil system operating in quadrature, and combined mode 16Tx/32Rx Tic-Tac-Toe coil system) and subject specific configurations (PTX NOVA coil system RF-shimmed for each subject). Experimental results shows significant drop in the B1+ field intensity in the left temporal lobe and cerebellum in the NOVA coil systems, issue alleviated with the Tic-Tac-Toe design.

4404 Computer 78

A Feasibility Study on Bilateral Monopole Antenna with Two Common Grounds for 7T MRI

Han-Joong Kim[1], Hyunwoo Song[1], Sang-Doc Han[1], Phil Heo[1], Donghyuk Kim[2], Yeonjin Choi[3], and Kyoung-Nam Kim[3]

[1]Department of Health Sciences and Technology, Gachon University, Incheon, Korea, Republic of, [2]Neuroscience Research Institute, Gachon University, Incheon, Korea, Republic of, [3]Department of Biomedical engineering, Gachon University, Incheon, Korea, Republic of

In this study, a bilateral monopole antenna was proposed to have ring element of existing ring-monopole as common ground and to consist of two interlocking monopole antennas along ***z***-axis to improve lopsided $|B_1|$ field toward the ground plate. Geometry of the proposed bilateral monopole antenna was optimized with EM simulation then optimized antenna was compared with a transceiver array coil and a birdcage coil for quality verification. Even with worse power consumption, the proposed bilateral monopole antenna can be an alternative for existing RF coils such as transceiver array coil and birdcage coil due to its improved $|B_1^+|$ field uniformity.

4405 Computer 79

Unified Proton and Fluorine Imaging of Small and Low Spin Density Samples at a Human Whole-Body 7 T MRI

Christian Bruns[1], Tim Herrmann[1], Markus Plaumann[1], Chang-Hyun Oh[2], Chulhyun Lee [3], Suchit Kumar[4], and Johannes Bernarding[1]

[1]Department for Biometrics und Medical Informatics, Otto-von-Guericke University, Magdeburg, Germany, [2]Department of Electronics and Information Engineering, and Korea Artificial Organ Center, Korea University, Seoul, Korea, Republic of, [3]Bioimaging Research Team, Korea Basic Science Institute, Ochang, Korea, Republic of, [4]Department of Biomicrosystem Technology and Korea Artificial Organ Center, Korea University, Seoul, Korea, Republic of

In order to provide a system, which allows imaging of ^{19}F MR contrast agents, an in-house-built ^{19}F/^{1}H transmit/receive system for 7 T was successfully tested in a human whole-body 7 T MRI system. This system enables the measurement of concentrations of 1.85 mM. For this approach we used a ^{19}F tuned coil which provided still enough signal gain at the proton frequency to allow ^{1}H imaging for comparison. This showed the possibility of using ^{19}F as contrast agents with a quite simple coil design in comparison to other dual tuned approaches.

4406 Computer 80

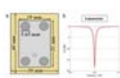

Newly Designed Miniaturized Patch Antenna with High Dielectric Material Plugs

Gangchea Lee[1], Navid Pourramzan Gandji[2], Seokwon Jung[3], Elena Semouchkina[2], Michael Lanagan[4], and Thomas Neuberger[1,5]

[1]Bio Engineering, Pennsylvania State University, University Park, PA, United States, [2]Electrical and Computer Engineering, Michigan Tech University, Houghton, MI, United States, [3]Mechanical and Nuclear Engineering, Pennsylvania State University, University Park, PA, United States, [4]Engineering Science and Mechanics, Pennsylvania State University, University Park, PA, United States, [5]Huck Institutes of the Life Sciences, Pennsylvania State University, University Park, PA, United States

High performance Radio Frequency resonators (RF resonators) produce strong and homogeneous magnetic fields. Due to their large sizes, patch antennas have hardly been considered to be used as RF resonators in Magnetic Resonance Imaging (MRI), especially at high fields. In this work, a newly developed miniaturized patch antenna with high dielectric material plugs was designed, simulated, built and tested at 14.1 T. The simulated and experimental magnetic fields were compared to confirm the performance of the fabricated patch antenna as a RF resonator for MRI.

4407 Computer 81

Multi Scroll Coil Setup for Simultaneous Acquisition of MR Microscopy Data of 3D Printed Cells

Gangchea Lee[1], Jeongin Choi[2], Eberhard Munz[3,4], Ibrahim Tarik Ozbolat [5], Michael Lanagan[5], and Thomas Neuberger[1,6]

[1]Bio Engineering, Pennsylvania State University, University Park, PA, United States, [2]Physics, Pennsylvania State University, University Park, PA, United States, [3]Experimental Physics 5, University of Wurzburg, Wurzburg, Germany, [4]Leibniz Institute of Plant Genetics and Crop Plant Research, Gatersleben, Germany, [5]Engineering Science and Mechanics, Pennsylvania State University, University Park, PA, United States, [6]Huck Institutes of the Life Sciences, Pennsylvania State University, University Park, PA, United States

High resolution, and high Signal to Noise Ratio (SNR) images in Magnetic Resonance Imaging (MRI) require long imaging times. In this work a setup for two separate shielded scroll coils with a common gradient and magnet was introduced to produce two independent three dimensional MRI data sets for MR microscopy. The RF coils and shields were designed, fabricated, and tested. 3-D printed cell samples were imaged using the fabricated set up. Overall, two samples could be acquired with a larger field of view and a similar SNR in the same time compared to a single sample in a solenoid.

4408 Computer 82

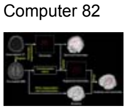

Co-localization of individual neuroanatomical structures and intracranial electrodes to assist brain mapping for pre-surgical evaluation of epilepsy

Syu-Jyun Peng[1] and Yue-Loong Hsin[2]

[1]National Chiao Tung University, Hsinchu, Taiwan, [2]Chung Shan Medical University and Chung Shan Medical University Hospital, Taichung, Taiwan

We proposed a method to precisely visualize subdural strip and grid electrodes in relation to underlying Brodmann’s area labeled cortical gyration. We transformed a reference brain labeled with Brodmann’s areas to match individual brain. Then we registered the digitalized electrodes from post-implant CT onto the anatomically labeled brain MRI.

4409 Computer 83

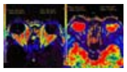

Characteristics of fat in orbits of patients with early-stage hyperthyroidism

Huajie Jiao[1], Rongrong Zhu[2], Kaining Shi[3], Yong Yang[4], and Weiheng He[4]

[1]Ningxia people's hospital, yinchuan, People's Republic of China, [2]Medical Imaging center, Ningxia people's hospital, People's Republic of China, [3]Philips HealthCare, Beijing,china, People's Republic of China, [4]People's Republic of China

Summary: Exophthalmos caused by muscle thickening and fat increasing in orbit is the typical symptom in hyperthyroidism, which impairs multiple systems as the auto-immune disease. From this study, we found the increase of percentage of fat and T2* value using the fat quantification analysis package, which indicate the accumulation and differentiation of fat-oriented cells, inflammation cells infiltration and collagen mucous change. Therefore, the characteristics of fat change in orbit can be evaluated by the transverse six-echo proton density fat fraction (PDFF) sequence (mDIXON-quant) technique in early-stage hyperthyroidism without significant manifestation of eyes.

4410 Computer 84

Human brain tissue equivalent MRI phantom for well defined T1 and T2 times at 3 and 7 Tesla

Michael Woletz[1], Sigrun Goluch[1], Allan Hummer[1], and Christian Windischberger[1]

[1]Division MR Physics, Center for Medical Physics and Biomedical Engineering, Medical University of Vienna, Vienna, Austria

Tissue-equivalent phantoms with well-defined T_1- and T_2-relaxation behaviour are often required for sequence optimisation and quality control purposes. Based on numerous T_1 and T_2 measurements at 3T and 7T with varying concentrations of Agarose and gadopentetate dimeglumine (Magnevist), we herein present a formula for creating phantoms with T_1-values between 700 ms and 3000 ms and T_2-values between 30 ms to 250 ms at both field strengths.

4411 Computer 85

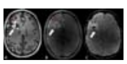

Qualitative and Quantitative Assessment of Arteriovenous Malformation Architecture at 7 Tesla

Bixia Chen[1,2], Toshinori Matsushige[2,3], Sören Johst[1], Stefan Maderwald[1], Lale Umutlu[1,4], Ulrich Sure[2], Harald H Quick[1,5], Mark Edward Ladd[1,6], and Karsten H Wrede[1,2]

[1]Erwin L. Hahn Institute for MRI, University of Duisburg-Essen, Essen, Germany, [2]Department of Neurosurgery, University Hospital Essen, University of Duisburg-Essen, Essen, Germany, [3]Department of Neurosurgery, Graduate School of Biomedical and Health Sciences, Hiroshima University, Japan, [4]Institute of Diagnostic and Interventional Radiology and Neuroradiology, University Hospital Essen, University of Duisburg-Essen, Essen, Germany, [5]High Field and Hybrid MR Imaging, University Hospital Essen, University of Duisburg-Essen, Essen, Germany, [6]Medical Physics in Radiology, German Cancer Research Center (DKFZ), Heidelberg, Germany

General advantages of ultra-high-field MRI at 7 T in cerebral arteriovenous malformations (AVM) imaging have been shown recently. This prospective clinical study (10 adult patients) aims to evaluate signal characteristics of AVM feeders, nidus and drainage using 7 T MRI (TOF, MPRAGE, SWI). AVM feeders, nidus and drainage were evaluated by 2 raters. Additionally, AVMs were segmented manually and signal intensity histograms were calculated for the extracted feeders, nidus and drainage, respectively. As previously shown, 7 T MRI has excellent imaging results regarding vessel delineation in AVMs. However, identification of the AVM architecture remains challenging due to signal heterogeneity.

4412 Computer 86

Magnetic Resonance Imaging of Collateral Networks in Moyamoya Angiopathy at 7 Tesla

Bixia Chen[1,2], Toshinori Matsushige[2,3], Markus Kraemer[4], Philipp Dammann[1,2], Sören Johst[1], Stefan Maderwald[1], Marc Schlamann[5], Harald H Quick[1,6], Mark Edward Ladd[1,7], Ulrich Sure[2], and Karsten H Wrede[1,2]

[1]Erwin L. Hahn Institute for MRI, University of Duisburg-Essen, Essen, Germany, [2]Department of Neurosurgery, University Hospital Essen, University of Duisburg-Essen, Essen, Germany, [3]Department of Neurosurgery, Graduate School of Biomedical and Health Sciences, Hiroshima University, Japan, [4]Department of Neurology, Alfried Krupp Hospital, Essen, Germany, [5]Institute of Diagnostic and Interventional Radiology and Neuroradiology, University Hospital Giessen, Giessen University, Giessen, Germany, [6]High Field and Hybrid MR Imaging, University Hospital Essen, University of Duisburg-Essen, Essen, Germany, [7]Medical Physics in Radiology, German Cancer Research Center (DKFZ), Heidelberg, Germany

Collateral networks in Moyamoya angiopathy (MMA) have a complex angioarchitecture. Delineation of deeply seated collateral networks (DSCNs) and image quality were prospectively evaluated in 10 patients using 7 Tesla TOF MRA and MPRAGE in comparison with conventional DSA. Seventy DSCNs were detected in DSA, 79 in TOF MRA, and 54 in MPRAGE. Detection of DSCNs was significantly better in TOF MRA than in DSA and MPRAGE. TOF MRA and DSA image quality were comparable, both were better than MPRAGE. Delineation of DSCN pathways in MMA using 7 Tesla TOF MRA was excellent and comparable to DSA.

4413 Computer 87

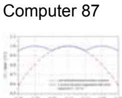

Microstrip Resonator for High Field MRI with Capacitor-Segmented Strip and Ground Plane

Vitaliy Zhurbenko[1], Vincent Boer [2], and Esben Thade Petersen [1,2]

[1]Technical Univ. of Denmark, Kgs. Lyngby, Denmark, [2]Danish Research Centre for Magnetic Resonance, Centre for Functional and Diagnostic Imaging and Research, Copenhagen University Hospital, Hvidovre, Denmark

High field MRI coils are often based on transmission line resonators. Due to relatively short wavelength of RF fields, such coils produce uneven field patterns. Here we show, that it is possible to manipulate magnetic field patterns of microstrip resonators in both planes (sagittal and transverse) segmenting stripe and ground plane of the resonator with series capacitors. The design equations for capacitors providing symmetric current distribution are derived. The performance of two types of segmented resonators are investigated experimentally. To authors' knowledge, a microstrip resonator, where both, strip and ground plane are capacitor-segmented, is shown here for the first time.

4414 Computer 88

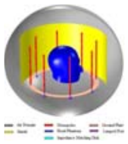

Monopole Antenna Array for UHF Magnetic Resonance Imaging

A S M Zahid Kausar[1], David Reutens[1], Ewald Weber[2], and Viktor Vegh[1]

[1]Center for Advanced Imaging, University of Queensland, Brisbane, Australia, [2]School of Information Technology and Electrical Engineering, University of Queensland, Brisbane, Australia

Birdcage coils have a number of limitations, especially at ultra-high field. Monopole antenna arrays have been proposed as an alternative to birdcage coils, as the design is simpler and they do not use capacitors. We evaluated the potential of using monopole arrays for 3T and 7T MRI brain scans. To be able to benchmark performance, we compared the field produced by the monopole array with the field produced by the birdcage coil. We show that monopole arrays can potentially achieve better field homogeneity and sensitivity than the birdcage coil. We fabricated a monopole array and demonstrated decoupling between individual monopoles.

4415 Computer 89

The TEM horn: A new array element for high-field imaging

Atefeh Kordzadeh[1] and Nicola De Zanche[2]

[1]Biomedical Engineering, University of Alberta, Edmonton, Canada, [2]Medical Physics, University of Alberta, Canada

This abstract introduces the TEM horn antenna as an efficient element for imaging the human body at high fields. The horn was designed for 200.4 MHz, simulated in HFSS adjacent to a torso-size phantom, and fabricated using 3-D printing. Transmit/receive imaging measurements were performed at 4.7T. Flip angle maps are compared to the simulation results.

4416 Computer 90

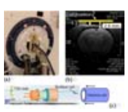

34 µm Isotropic Resolution MRI of Rat Brain using 55K cryo-probe

Kurt H Bockhorst[1], Jarek Wosik[2,3], and Ponnada A Narayana[1]

[1]Diagnostic and Interventional Imaging, University of Texas, Health Science Center-Houston Medical School, Houston, TX, [2]Electrical and Computer Engineering, University of Houston, Houston, TX, United States, [3]Texas Center for Superconductivity

We report on the performance and development of a 300-MHz (7 T) cryogenic receive- only surface coil for MRI of rat brain. Practical performance limits of the cryo-coil were tested such as SNR gains at 55 K for a 19 mm in diameter Cu coil and its frequency stability over long (up to a few days) scans. 3D-RARE isotropic images of ex-vivo rat brain up to 512 slices with outstanding isotropic resolution of 34 µm were acquired showing structural details not seen with conventional small animals coils. In addition, a comparison of such images with matching histological plates is discussed.

4417 Computer 91

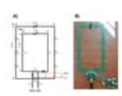

A simple frequency selectable method controlled by PIN diode in the double layered multi-nuclei RF coil at 7T

Sang-Doc Han[1], Hyunwoo Song[1], Phil Heo[1], Han-Joong Kim[1], Donghyuk Kim[2], Yeonjin Choi[3], Yeunchul Ryu[4], and Kyoung-Nam Kim[3]

[1]Department of Health Sciences and Technology, Gachon University, Incheon, Korea, Republic of, [2]Neuroscience Research Institute, Gachon University, Incheon, Korea, Republic of, [3]Department of Biomedical engineering, Gachon University, Incheon, Korea, Republic of, [4]Department of Radiological Science, Gachon University, Incheon, Korea, Republic of

With the facilitated approach of ultra-high frequency (UHF, over 7T) magnetic resonance imaging (MRI) system, multi-nuclei (MN)-MRI can be regarded as one of critical means for diagnose due to its capability of acquiring non-invasive metabolic information[1, 2]. In this study, a radiofrequency (RF) coil that can selectively receive two nuclei signals, the proton (^{1}H) and the sodium (^{23}Na), by controlling PIN diodes is proposed. Since ^{1}H images show clear anatomical structure where ^{23}Na show critical in-vivo metabolisms, acquired MN magnetic resonance (MR) images using the proposed MN RF coil have capabilities to assist diagnose visually[3].

4418 Computer 92

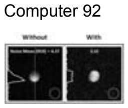

Improvement of Magnetic Field Uniformity of 19F Imaging using the Inductive Coupling at 7.0T

Bu Sik Park[1], Sunder S. Rajan[1], Joe Murphy-Boesch[2], William Koch[1], Charity Stagg[1], and Brent McCright[1]

[1]FDA, Silver Spring, MD, United States, [2]NIH

Numerical simulations and experimental verification of the feasibility are shown to improve B_1 uniformity of a commercial ^{19}F RF coil with addition of a secondary resonator using inductive coupling without changing the RF coil at 7.0T animal MRI. The designed resonator was placed on the opposite side of the imaging object from the ^{19}F surface coil to improve the field uniformity. Numerical simulations and related experiments using a ^{19}F phantom show significant improvement of $|B_1^+|$ and image uniformity, i.e., about 26%. The mouse leg image of ^{19}F/^{1}H with the designed resonator is shown as an example of potential pre-clinical applications.

4419 Computer 93

A method to experimentally assess "coil loss" of a dipole antenna for Ultra-High-Field (UHF) MRI

Gang Chen[1,2], Christopher M. Collins[1,2], Daniel K. Sodickson[1,2], and Graham C. Wiggins[1]

[1]Center for Advanced Imaging Innovation and Research (CAI2R), New York University School of Medicine, New York, NY, United States, [2]The Sackler Institute of Graduate Biomedical Science, New York University School of Medicine, New York, NY, United States

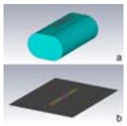

At clinical field strengths, the contribution of coil noise is often characterized by the Q-ratio, the ratio of the loaded Q and unloaded Q. Because of the inconsistent contribution of radiation loss and frequency drift in unloaded and loaded cases, it is difficult to characterize the body noise dominance of a dipole antenna by conventional Q ratio at 7T. Here we propose a new approach using a measure of Q when a dipole antenna is well shielded. The shielded/loaded Q ratio estimates the relative noise contribution from coil loss, similar to unloaded/loaded Q ratio for surface coil at low frequencies.

4420 Computer 94

A new RF coil for foot and ankle imaging at 7T MRI

Tales Roberto de Souza Santini[1], Junghwan Kim[1], Sossena Wood[1], Narayanan Krishnamurthy[1], Shailesh Raval[1], and Tamer Ibrahim[1]

[1]University of Pittsburgh, Pittsburgh, PA, United States

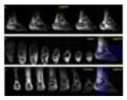

7T Foot and ankle has been previously explored1. A four-channel Tic-Tac-Toe (TTT) transmit-only (Tx-only) array2,3 and a four-channel receive-only array were developed and combined to demonstrate the feasiability of high signal-to-noise ratio (SNR) foot and ankle imaging at 7T MRI. The experimental measurements of magnetic field distribution responsible for excitation (B1+) is in agreement with the finite-difference time-domain (FDTD) simulations and the SAR is within the FDA safety limits for the entire lower leg and foot (peak SAR ~ 7W/Kg/10g of tissue, average SAR ~ 1W/Kg/10g of tissue per continuous average field B1+ = 1.97uT). In-vivo proton density TSE and T2DESS images were acquired.

4421 Computer 95

Improving Image Quality by Adjusting Relative Phases of Channels with a Two-element Rotating Coil Array at 9.4T

Mingyan Li[1], Ewald Weber[1], Jin Jin[1], Yasvir Tesiram[2], Thimo Hugger[3], Simon Stark[3], Feng Liu[1], Sven Junge[3], and Stuart Crozier[1]

[1]School of Information Technology and Electrical Engineering, The University of Queensland, Brisbane, Australia, [2]Centre for Advanced Imaging, The University of Queensland, Brisbane, Australia, [3]Bruker BioSpin MRI GmbH, Ettlingen, Germany

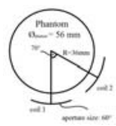

This work investigates the feasibility of incorporating an additional RF element to the rotating RF coil (RRFC) to improve imaging performance. The transmit profiles of the two-element rotating coil array were optimised by adjusting the interference patterns formed by two channels with varied relative phase. Combined with the previously developed rotating imaging scheme, an optimal relative phase was determined to produce an image uniformity of 93%.

4422 Computer 96

A Compact Planar Triple-Nuclear Coil for Small Animal 1H, 13C, and 31P Metabolic MR Imaging at 14.1 T

Andrew Palmera Leynes[1], Yiran Chen[1], Subramaniam Sukumar[1], Duan Xu[1], and Xiaoliang Zhang[1]

[1]Radiology and Biomedical Imaging, University of California San Francisco, San Francisco, CA, United States

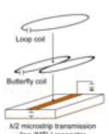

The development and test of a triple-nuclear surface coil for simultaneous 1H, 13C, and 31P small animal imaging at 14.1 Tesla.

Electronic Poster

Hybrid & Novel Technology

Exhibition Hall Tuesday 17:15 - 18:15

4423 Computer 49

EKG-based detection of deep brain stimulation (DBS) for fMRI studies

Eric Fiveland[1], Julia Prusik[2], Renee Linton[3], Jeffrey Ashe[1], Julie Pilitsis[2], and Ileana Hancu[1]

[1]GE Global Research Center, Niskayuna, NY, United States, [2]Albany Medical College, Albany, NY, United States, [3]Medtronic, Minneapolis, MN, United States

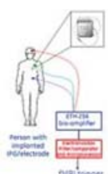

A detector for measuring and predicting the on/off state of cycling deep brain stimulation (DBS) was developed and tested in 6 patients. 3-electrode EKG measurements, amplified by a commercial bio-amplifier, were used as input for a custom electronics box (e-box). The e-box transformed the DBS waveforms into transistor-transistor logic (TTL) pulses and recorded their timing. Following locking to each patient's individual waveform, the e-box was shown to predict stimulation onset with an average absolute error of 112ms, 30 minutes after disconnecting from the patients.   Using this detector, stimulation can be accurately synchronized to fMRI acquisitions.

4424 Computer 50

Fast 3D Design of High-Permittivity Pads for Dielectric Shimming using Model Order Reduction and Nonlinear Optimization

Jeroen van Gemert[1], Wyger Brink[2], Andrew Webb[2], and Rob Remis[1]

[1]Circuits and Systems, Delft University of Technology, Delft, Netherlands, [2]Radiology, Leiden University Medical Center, Leiden, Netherlands

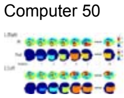

High-permittivity pads can be used to improve B_1^+ homogeneity and intensity in neuroimaging and body applications. Normally, finding the "optimal" pad for a specific region of interest involves evaluating many different pad designs using electromagnetic simulations, which is a very time-consuming approach taking hours to days of computation time. We propose a nonlinear optimization method based on model order reduction that allows us to design high-permittivity pads in less than 30 seconds.

4425 Computer 51

Improved local sensitivity in magnetic resonance spectroscopy at 3 T using a new flexible and compact metasurface

Rita Schmidt[1], Assaf Tal[2], and Andrew Webb[1]

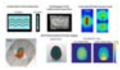

[1]Radiology, Leiden University Medical Center, Leiden, Netherlands, [2]Chemical Physics, Weizmann Institute of Science, Rehovot, Israel

Magnetic resonance spectroscopy is a powerful technique for in-vivo measurement of metabolites, however its sensitivity is limited due to very low concentration of the metabolites. This is especially valid for studies of neurotransmitters such as glutamate and GABA. In this study, a new hybrid metasurface comprising of conducting strips and agar-gel was designed to improve MR sensitivity at 3T. The metasurface forms a compact and flexible pad which is placed in the vicinity of the region of interest. The measurements focused on MRS acquisitions including PRESS and MEGA-PRESS, showing an improvement in SNR of a factor of 1.75, 2 cm from the pad.

4426 Computer 52

A Practical Imaging Scheme for a Rotating RF Coil (RRFC) at 9.4T by Applying Dynamic Sensitivity Averaging

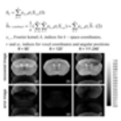

Mingyan Li[1], Jin Jin[1], Ewald Weber[1], Yasvir Tesiram[2], Thimo Hugger[3], Simon Stark[3], Sven Junge[3], Feng Liu[1], and Stuart Crozier[1]

[1]School of Information Technology and Electrical Engineering, The University of Queensland, Brisbane, Australia, [2]Centre for Advanced Imaging, The University of Queensland, Brisbane, Australia, [3]Bruker BioSpin MRI GmbH, Ettlingen, Germany

Precise image recovery for the rotating coil requires sensitivity estimation and iterative algorithm to remove motion artifact, but inaccurate sensitivity estimation can affect image reconstruction accuracy. Previously we developed a radial sampling scheme for the RRFC which avoids sensitivity mapping procedures by manipulating oversampled central k-space data. However, the overall reconstruction inaccuracy results from relatively sparse sampled outer k-space still remained. As a more robust and preferred imaging scheme in routine MRI scans, the Cartesian trajectory will be employed to develop an imaging scheme for the RRFC to overcome the abovementioned limitations and further reduce motion artifact.

4427 Computer 53

Efficient Analysis of Dielectric Materials in Coupled RF Coil Configurations

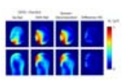

Wyger M. Brink[1], Jan Paska[2], Jiying Dai[1], Jeroen H.F. van Gemert[3], Gang Chen[2], Graham C. Wiggins[2], Rob F. Remis[3], Christopher M. Collins[2], and Andrew G. Webb[1]

[1]Leiden University Medical Center, Leiden, Netherlands, [2]NYU School of Medicine, [3]Delft University of Technology

Dielectric materials enable additional control of the RF field in a particular RF coil. In this work we present a hybrid domain decomposition method, which allows for an efficient analysis of dielectric materials in the presence of coupled RF coil structures or coil array configurations.

4428 Computer 54

Real-time Percutaneous Transluminal Angioplasty with Traveling Wave Magnetic Particle Imaging

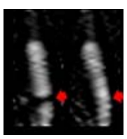

Patrick Vogel[1,2], Stefan Herz[1], Philip Dietrich[1], Thomas Kampf[2,3], Volker C Behr[2], and Thorsten A Bley[1]

[1]Department of Diagnostic and Interventional Radiology, University Hospital Würzburg, Würzburg, Germany, [2]Department of Experimental Physics 5 (Biophysics), University of Würzburg, Würzburg, Germany, [3]Department of Diagnostic and Interventional Neuroradiology, University Hospital Würzburg, Würzburg, Germany

A percutaneous transluminal angioplasty (PTA) is a procedure to widen stenotic blood vessels in medical conditions such as coronary heart disease or peripheral artery disease. With the assistance of fluoroscopic guidance and radiopaque contrast agents, guidewires and balloon catheters are used to treat vascular stenoses. Magnetic Particle Imaging (MPI) is a very fast and sensitive tomographic imaging modality with the potential of real-time radiation-free 3D imaging. In this work the feasibility of performing a MPI-guided PTA in artificial stenoses with a traveling wave MPI scanner is demonstrated.

4429 Computer 55

Prescan consistency of ZTE-based attenuation map generation

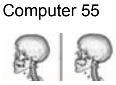

Gaspar Delso[1], Roie Manavaki[2], Florian Wiesinger[3], David Goldhaber[4], and Floris Jansen[4]

[1]GE Healthcare, Cambridge, United Kingdom, [2]Department of Radiology, University of Cambridge, United Kingdom, [3]GE Global Research, Germany, [4]GE Healthcare, United States

We present an evaluation, across multiple clinical sites, of the impact of prescan variability on head attenuation maps based on zero echo time imaging.

4430 Computer 56

WiFi-enabled RF Coil for Simultaneous MR Image Acquisition and Wireless Communication

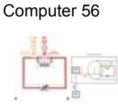

Dean Darnell[1], Jonathan Cuthbertson[1], Yixin Ma[1], Naomi Morales-Medina[1], Sebastian Luce[1], Allen W Song[1], and Trong-Kha Truong[1]

[1]Brain Imaging and Analysis Center, Duke University, Durham, NC, United States

Implementation of wireless communications in an MRI scanner will reduce the complexity of the scanner by decreasing the number of wired connections and connectors. To enable wireless communication in the scanner, a new RF coil design is proposed which allows RF currents at the Larmor and wireless data frequencies to flow on the same coil element, thus enabling simultaneous MRI image acquisition and wireless data transfer with the same coil.

4431 Computer 57

Battery-Powered Integrated Parallel Reception, Excitation, and Shimming (iPRES) Head Coil Array for Plug-and-Play Localized B_0 Shimming

Dean Darnell[1], Devin Willey[1], Sebastian Luce[1], Allen W Song[1], and Trong-Kha Truong[1]

[1]Brain Imaging and Analysis Center, Duke University, Durham, NC, United States

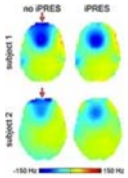

Integrated parallel reception, excitation, and shimming (iPRES) coil arrays enable RF excitation/reception and localized B_0 shimming with a single coil array, but so far use an external DC power supply and require a B_0 map and a shim optimization for each subject, which takes additional time. Here, we propose a novel iPRES head coil array powered by an on-board MR-compatible battery that delivers fixed DC currents optimized in advance to shim an average subject's brain. This stand-alone, plug-and-play system does not require any subject-specific shim optimization, thus enabling a wider adoption of iPRES in clinical applications.

4432 Computer 58

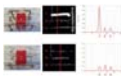

An evaluation of RF coil materials for 1H/31P for use in a hybrid MR-PET scanner at 3T

Chang-Hoon Choi[1], Lutz Tellmann[1], Jörg Felder[1], Christoph Lerche[1], and N. Jon Shah[1,2]

[1]Institute of Neuroscience and Medicine-4, Forschungszentrum Juelich, Juelich, Germany, [2]Faculty of Medicine, Department of Neurology, JARA, RWTH Aachen University, Aachen, Germany

In a simultaneous MR-PET experiment, an RF resonator for MRI is placed inside the field-of-view of the PET scanner. Attenuation caused by RF coil components can cause severe artefacts in PET images if not adequately corrected. Although it may be possible to minimise subject-specific attenuation and scatter effects, correcting those due to the RF coil is still a challenging task. In this work, we have designed and constructed a number of RF coils constructed utilising a variety of copper conductors and evaluated their characteristics from the MR and PET points of view.

4433 Computer 60

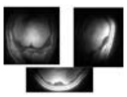

Progress in adapting SWIFT to a clinical scanner

Steen Moeller[1], Naoharu Kobayashi[1], Gregor Adriany[1], Djaudat Idiyatullin[1], Mike Garwood[1], and Edward Auerbach[1]

[1]University of Minnesota, Minneapolis, MN, United States

The development of a programmable high-speed triggering to enable progress in implementation of SWIFT on a Siemens scanner. First in-vivo images, at 50khz, using a linear T/R coil.

4434 Computer 61

Tunable Electropermanent System for Magnetic Resonance Imaging and Magnetic Particle Propulsion

Alek Nacev[1], Ryan Hilaman[1], Sahar Jafari[1,2], Sagar Chowdhury[1], Lamar Mair[1], Pavel Stepanov[1], Dhruv Patel[1], and Irving Weinberg[1]

[1]Weinberg Medical Physics, Inc., North Bethesda, MD, United States, [2]Biomedical Engineering, George Mason University, VA, United States

Directing magnetic nanoparticles to sites within biological tissues requires both strong magnetic field gradients and accurate images of the particles and underlying anatomy. Most modern MR imaging systems require always-on magnetic field sources such as permanent magnets or superconducting coils. These field sources limit the ability to control magnetic particles within the imaging volume. Due to these field sources having a high strength always-on magnetic field, there are additional safety concerns when attempting to integrate these sources into an intraoperative arena. We built a new magnetic field source design that is capable of adjusting its magnetic field strength while retaining a low power usage to improve portability.

4435 Computer 62

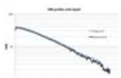

Low-attenuation RF surface coils for linac-MR hybrids: compromise between radiation dose to the skin and SNR

Radim Barta[1], Andrei Ghila[1], Satyapal Rathee[1,2], B Gino Fallone[1,2], and Nicola De Zanche[1,2]

[1]Oncology, University of Alberta, Edmonton, AB, Canada, [2]Medical Physics, Cross Cancer Institute, Edmonton, AB, Canada

Aluminum and copper conductors are compared for constructing radiologically transparent MRI surface coil detectors for use in a hybrid MRI - linear accelerator. Radiation dose to skin can cause serious reactions and skin dose is enhanced when materials are placed in the radiation beam. Therefore increases in skin dose due to surface coils must be minimized by optimized construction. A copper conductor causes a three-fold increase in skin dose compared to a similar thickness aluminum conductor. An aluminium coil (20µm thick) was used to image a phantom, yielding 93% of the SNR achieved with a copper tape coil (32µm thick).

4436 Computer 63

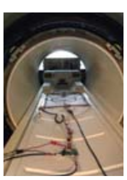

A MRI Compatible Class-EF Power Amplifier Designed to Drive a Wireless Power Transfer System

Kelly Byron[1], Fraser Robb[2], Shreyas Vasanawala[3], John Pauly[1], and Greig Scott[1]

[1]Electrical Engineering, Stanford University, Stanford, CA, United States, [2]GE Healthcare, Aurora, OH, [3]Radiology, Stanford University, Stanford, CA

A compact wireless power transfer (WPT) system being used to power wireless patient coils would require a compact power amplifier that can operate inside the MRI bore. A Class-EF power amplifier is designed and implemented that uses air-core inductors and is capable of driving the coupled resonant coils used for WPT with similar efficiency to a system that uses a large and expensive power amplifier that is outside the scan room. This new power amplifier is very compact and is also very cost-effective.

4437 Computer 64

CANTILEVER SYSTEM TO REDUCE PHASE NOISE CAUSED BY VIBRATIONS IN 11.1T

Malathy Elumalai[1], Joshua E Slade[1], Huadong Zheng[1], and Thomas H Mareci[2]

[1]AMRIS facility, University of Florida, Gainesville, FL, United States, [2]Department of Bio-chemistry and Molecular Biology, University of Florida, Gainesville, FL, United States

Magnetic Resonance Imaging at higher field strengths has several design challenges that must be addressed for optimal performance and image resolution. We have developed a cantilever system that is suspended in the magnet to eliminate phase noise that are produced due to vibrations generated by gradient coils. The cantilever system has features such as detachable quadrature RF coils, animal cradle system with in-built water & anesthesia and tuning/matching capability outside the bore. The system is not only centered in all three axes but also has tuning capability in the z-direction from outside the bore so we could move the subject in and out to center in the bore.

4438 Computer 65

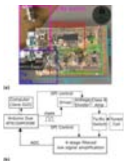

Compact NMR Spectrometer for ^{129}Xe Polarization Monitoring with Java Based Signal Processing and User Interface

Adam Maunder[1], Graham Norquay[1], Madhwesha Rao[1], and Jim M Wild[1]

[1]Unit of Academic Radiology, University of Sheffield, Sheffield, United Kingdom

Monitoring of the ^{129}Xe polarization by NMR during spin-exchange optical pumping (SEOP) is vital for quality control and for experimental investigations into optimizing system running parameters. In this study, we present a compact NMR spectrometer designed to improve user flexibility and reduce cost for online polarimetry on a ^{129}Xe SEOP system. A Java-based user interface was developed to control the system with an Arduino based hardware control. The performances of the user interface and hardware in routine ^{129}Xe NMR spectrometer measurements are demonstrated herein.

4439 Computer 66

RF Coil Performances in Compact Hybrid MR/PET Scanner Design Using an Integrated Shielding

Arne Berneking[1], Adam Mehina, and N. Jon Shah

[1]Institute of Neuroscience and Medicine, Forschungszentrum Juelich GmbH, Juelich, Germany

The goal of this study is to demonstrate hybrid MR/PET scanner design optimization methods from an RF coil perspective with a focus on UHF MRI. Here, coil performances are investigated depending on different shielding distances to present simulation and measurement methods to include RF coil performances into the hybrid MR/PET scanner design. Moreover, integration of PET detector shielding and RF coil shield is investigated. The results of this study clarify that a trade of between a compact design, PET and RF coil performances is necessary and that RF coil performances can be optimized by an integrated shielding with an optimized configuration.

4440 Computer 67

A compact handheld MR spectrometer system for mobile MR applications

John Zhen[1], Robin Dykstra[1], and Sergei Obruchkov[2]

[1]School of Engineering, Victoria University of Wellington, Wellington, New Zealand, [2]School of Chemical and Physical Sciences, Victoria University of Wellington, Wellington, New Zealand

Magnetic Resonance Imaging has established itself as indespensible utility in health sector for over 3 decades, yet remained inflexible in its form factor. By taking advantage of modern advances in miniturisation and improved efficiency of electronic devices along with the developments of single sided magnet probes this abstract presents a handheld, battery powered portable MR spectrometer system which can be used for tissue analysis and sample charectarisation outside of an imaging suite.

4441 Computer 68

A novel method to maintain PET detector performance in the presence of MR gradient induced heating

Mohammad Mehdi Khalighi[1], Tuoyu Cao[2], Mark Fries[3], Timothy W. Deller[2], Floris Jansen[2], and Gary Glover[4]

[1]Applied Science Lab, GE Healthcare, Menlo Park, CA, United States, [2]PET/MR engineering, GE Healthcare, Waukesha, WI, United States, [3]Imaging Subsystems, GE Healthcare, Waukesha, WI, United States, [4]Radiology Department, Stanford Unviersity, Palo Alto, CA, United States

In a simultaneous ToF-enabled SiPM PET/MR scanner, eddy currents induced by the changing gradient field lead to increased temperature around the PET detectors; this can change the detector gain and shift the position of the photopeak in the spectrum, reducing accuracy of the reconstructed image. Conventionally, peak stability is achieved by thermal monitoring system and adjusting the gain based on the temperature. A more accurate gain control algorithm is presented, which analyzes the spectrum of single events detected on each device. Reconstructed activity of a PET phantom in extreme MR gradient switching is measured to remain stable, better than 0.5%.

4442 Computer 69

Virtual Reality to read MR Angiography

Xiaoqi Wang[1], Hong Bai[2], and Yadong Cui[3]

[1]Clinical Science, Philips Healthcare, Beijing, People's Republic of China, [2]Digital Rubic, [3]Department of Radiology, Beijing Hospital

A first attempt in utilizing the state of art visualizing technology - Virtual Reality to read MR angiography images.

4443 Computer 70

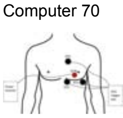

Ultrasound-based Cardiac Gating for MRI

Frank Preiswerk[1], Cheng-Chieh Cheng[1], Pei-Hsin Wu[1], Lawrence P. Panych[1], and Bruno Madore[1]

[1]Department of Radiology, Brigham and Women's Hospital, Harvard Medical School, Boston, MA, United States

Clinical cardiac MRI typically requires the use of electrocardiogram (ECG) leads to detect R-waves and synchronize the MRI acquisition accordingly. The magnetohydrodynamic effect can corrupt the ECG signal, sometimes making R-wave detection difficult, especially at higher field strengths. We are proposing here a practical and low cost ultrasound-based solution for detecting cardiac activity in a manner immune to the presence and strength of the B0 field. Equivalence was shown in cases where ECG gating worked well. In the future, the approach should prove most helpful as an alternative to ECG when the latter proves impractical, especially at higher field strengths.

4444 Computer 71

RF-sensing for Trigger-based Synchronization of Auxiliary Devices, and Pulse-sequence Debugging

Frank Preiswerk[1], Jiarui Cai[2], Cheng-Chieh Cheng[1], W. Scott Hoge[1], Pei-Hsin Wu[1], Lawrence P. Panych[1], and Bruno Madore[1]

[1]Department of Radiology, Brigham and Women's Hospital, Harvard Medical School, Boston, MA, United States, [2]Beijing University of Posts and Telecommunications, Beijing, People's Republic of China

Voltage or laser-light triggers are often used to synchronize auxiliary devices to the MR acquisition process. A very simple RF antenna and associated circuit is proposed here instead. The device is used here to trigger ultrasound probe firings, as part of a hybrid ultrasound-MRI system, but could be used for other purposes as well. Compared to scanner-generated triggers, advantages include: 1) vendor- and software release-independent, 2) available in the scan room, 3) no change to product sequences needed, and 4) the little device proved handy for pulse sequence debugging as well.

4445 Computer 72

A Novel Cryogenic Radio-Frequency Probe for High Spatial Resolution Fluorine-19 MRI of Brain Inflammation

Andreas Pohlmann[1], Jason M Millward[1], Paula Ramos Delgado[1], Daniel Marek[2], Didier Wecker[3], Ralph Wissmann[3], Helmar Waiczies[4], Thoralf Niendorf[1,5], and Sonia Wacizies[1]

[1]Berlin Ultrahigh Field Facility (B.U.F.F.), Max Delbrueck Center for Molecular Medicine, Berlin, Germany, [2]Bruker BioSpin AG, Fällanden, Switzerland, [3]Bruker BioSpin MRI GmbH, Ettlingen, Germany, [4]MRI TOOLs GmbH, Berlin, Germany, [5]Experimental and Clinical Research Center (ECRC), a joint cooperation between the Charité Medical Faculty and the Max Delbrueck Center, Berlin, Germany

MRI using i.v. administered fluorine-19 loaded nanoparticles (NPs) allows the tracking of inflammatory cell migration. The inherently low SNR limits the precise localization of 19F-labeled inflammatory cells, because large voxel sizes are needed to collect sufficient signal. To overcome this, we show here the first use of a novel 19F cryogenic quadrature RF surface probe at ultrahigh field to substantially boost SNR beyond that of state-of-the-art room temperature RF coils, while facilitating the acquisition of better spatially-resolved images within shorter scan times.

Electronic Poster

Studying Value of MRI

Exhibition Hall — Tuesday 17:15 - 18:15

4446 Computer 97

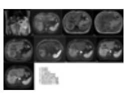

A clinically-validated, fast and semi-automated MR workflow for Liver Evaluation

Qingsong Yang[1], Yukun Chen[1], Caixia Fu[2], Bernd Kuehn[3], Berthold Kiefer[3], Zhen Wang[1], Xu Yan[4], Chao Ma[1], Dehe Weng[2], Luguang Chen[1], and Jianping Lu[1]

[1]Department of Radiology, Changhai Hospital of Shanghai, the Second Military Medical University, Shanghai, People's Republic of China, [2]Application development, Siemens Shenzhen Magnetic Resonance Ltd., Shenzhen, People's Republic of China, [3]MR Applications Predevelopment, Siemens Healthcare, Erlangen, Germany, [4]MR Collaboration NE Asia, Siemens Healthcare, Shanghai, People's Republic of China

A fast and semi-automated MRI workflow for liver examinations with approximately 12mins of total examination time was proposed and evaluated with liver patients using CT or histo-pathology as reference. 28 patients suspected of liver disease were enrolled in this study. The results show a good concordance between findings on MRI and the chosen reference standard. This indicates that the proposed fast MRI workflow has the capability to be used for diagnostic purposes in clinical routine while being highly time efficient at the same time.

4447 Computer 98

Increasing value of MRI in evaluation of gynecologic malignancies by decreasing scan time and reducing artifacts through the replacement of fast spin echo (FSE) with variable refocusing flip angle single-shot FSE (vrfSSFSE)

Paul Benjamin Stoddard[1], Valentina Taviani[2], Daniel V. Litwiller[2], Michael C. Muelly[1], Shreyas S. Vasanawala[1], and Andreas M. Loening[1]

[1]Radiology, Stanford University, Stanford, CA, United States, [2]Global MR Applications and Workflow, GE Healthcare

Variable refocusing flip angle single-shot fast spin echo (vrfSSFSE) with outer volume suppression (OVS) improves upon standard single-shot fast spin echo (SSFSE or HASTE): 1) decreasing average flip angles thereby reducing specific absorption rate (SAR) limited acquisition times, 2) reducing blurring from T2 decay, 3) allowing full-Fourier acquisitions. Although improving upon conventional SSFSE, it remains unknown if vrfSSFSE with OVS can approach the image quality and diagnostic capability of fast spin echo (FSE). We found vrfSSFSE comparable to FSE in signal-to-noise and contrast and superior to FSE in coherent artifact reduction, depending on the plane of imaging.

4448 Computer 99

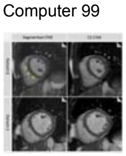

Robust high−throughput Cardiac MR featuring Compressed Sensing

Michaela SCHMIDT[1], Peter WEALE[2], Kavin JAYAWARDHANA[3], Christoph FORMAN[1], Sue J THOMAS[3], Carmel HAYES[1], and Russell Bull[3]

[1]Siemens Healthcare, Erlangen, Germany, [2]Siemens Healthcare Ltd, Frimley, Surrey, United Kingdom, [3]Department of Radiology, Royal Bournemouth Hospital, Bournemouth, United Kingdom

A standard CMR protocol for the evaluation of cardiac function and myocardial damage in patients with ischemic or non-ischemic heart-disease was compared to a new approach which drastically reduces the scan time. This was achieved by introducing a highly accelerated compressed sensing cine sequence which facilitated significant work-flow optimization. Image quality scores of both methods were equivalent and quantitative results showed good agreement. The mean examination time was reduced from 26:29 ± 5:45 min to 16:15 ± 2:47 min, which corresponds to a 38 % reduction in examination time.

4449 Computer 100

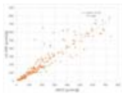

Gradient Echo vs. Spin Echo MRI to Determine Liver Iron Concentration

Arthur Peter Wunderlich[1,2], Holger Cario[3], Mario Teigeler[1], Meinrad Beer[1], and Stefan Andreas Schmidt[1]

[1]Diagnostic and Interventional Radiology, Ulm University, Medical Center, Ulm, Germany, [2]Section for Experimental Radiology, Ulm University, Medical Center, Ulm, Germany, [3]Department of Pediatrics and Adolescent Medicine, Ulm University, Medical Center, Ulm, Germany

To evaluate an alternative to an established method for liver iron content (LIC) determination based on spin-echo (SE) MRI, we analyzed 195 MRI scans, including both SE and gradient echo (GRE) protocols, of regularly transfused patients suspected for liver iron overload. A relationship was derived between reference LIC obtained by Ferriscan® and GRE data. From this, LIC was determined using GRE acquisitions and these values correlated to reference LIC. Considering the LIC threshold of 80 µmol/g (4.5 mg/g) relevant for therapy, diagnostic accuracy of the GRE approach was quite good, with sensitivity and specificity of 99/98 % compared to Ferriscan®.

4450 Computer 101

Development of an artificial intelligence algorithm to automatically assign MR abdomen/pelvis protocols from free-text clinical indications.

Jae Ho Sohn[1], Joseph Mesterhazy[1], Fouad Al Adel[1], Thienkhai Vu[1], Alex Rybkin[1], and Michael A Ohliger[1]

[1]Radiology & Biomedical Imaging, UCSF Medical Center, San Francisco, CA, United States

Timely and accurate MR protocoling is important to ensure best efficiency and diagnostic value in radiology departments. We propose and validate an artificial intelligence based natural language classifier that can assign MR abdomen/pelvis protocols based on free-text clinical indications. We achieve an overall classification accuracy rate of 93% on a test set consisting of 83 free-text clinical indications.

4451 Computer 102

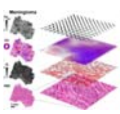

Mapping cell shape and cell density by diffusion variance decomposition (DIVIDE): Towards rapid non-invasive diagnostic and prognostic assessment of tumors

Danielle van Westen[1], Filip Szczepankiewicz[2], Karin Bryskhe[3], Pia Sundgren[1,4], and Markus Nilsson[1]

[1]Diagnostic Radiology, Lund University, Lund, Sweden, [2]Medical Radiation Physics, Lund University, Lund, Sweden, [3]CR Development, Lund, Sweden, [4]Center for Imaging and function, Skane University hospital, Sweden

In this work we present a novel approach based on tensor-valued diffusion encoding to quantify tumor tissue characteristics such as cell shape and cell density variation — features considered in histopathology. This approach constitutes a promising framework for non-invasive diagnostic and prognostic assessment of tumors that may improve patient care by non-invasively capturing histopathological information on cell shape and cell density heterogenity.

4452 Computer 103

Limited MRI protocol for ischemic stroke

CC Tchoyoson Lim[1,2], Wai Yung Yu[1,2], Francis Hui[1,2], Wing Lok Au[2,3], and Yih Yian Sitoh[1,2]

[1]National Neuroscience Institute, Singapore, Singapore, [2]Duke-NUS School of Medicine, Singapore, [3]Neurology, National Neuroscience Institute, Singapore, Singapore

We describe adapting a Limited Stroke Protocol of unenhanced MRI pulse sequences (including diffusion-weighted images to diagnose recent cerebral infarction and TOF MR angiography to detect large intracranial vessel stenosis/occlusion), for hospital inpatients and the Emergency Room patients with suspected recent ischemic stroke. Although this abbreviated, targeted limited MRI protocol may be challenging in subtle diagnosis, it improves patient access, enables image-guided decision-making, and results in rapid throughput.

4453 Computer 104

Diagnostic value of using SSFP and UTE subtraction MRI for the management of critical limb ischemia patients

Trisha L. Roy[1,2], Howard Chen[1], Andrew D. Dueck[1], and Graham A. Wright[1,3]

[1]Schulich Heart Program, Sunnybrook Research Institute, Toronto, ON, Canada, [2]Division of Vascular Surgery, University of Toronto, Toronto, ON, Canada, [3]Department of Medical Biophysics, University of Toronto, Toronto, ON, Canada

There are two treatment options for revascularizing patients with critical limb ischemia: bypass surgery and percutaneous vascular intervention (PVI). PVI is less invasive but has high immediate technical failure rates (20%) and high re-intervention rates (20%). The most common mode of immediate failure is the inability to enter/cross the lesion. With current imaging (X-ray angiography, CTA, Duplex ultrasound) it is difficult to predict which lesions will be soft enough to cross with a wire to make PVI possible. Physicians have responded with a "percutaneous-first" strategy where they attempt PVI in all patients and perform surgery if PVI fails. This requires more procedures per index limb at significant cost to healthcare systems and delays definitive revascularization. Additionally, there is evidence that surgical bypass after failed PVI results in worse outcomes, including higher amputation rates within 1 year.

These issues highlight the critical need for improved diagnostic accuracy to inform patient selection. We have developed and validated MR methods to distinguish hard PAD lesions (densely calcified or collagenous) that would be at high risk of PVI failure from soft lesions that would be amenable to PVI. The impact of this work will help to reduce PVI failure rates, reduce time to definitive revascularization and reduce costs for additional procedures and investigations.

4454 Computer 105

Can replacement sagittal diffusion images increase MR value of spinal imaging in patients with suspected malignant disease?

Saurabh Singh[1], Timothy James Pengilley Bray[1], Alan Bainbridge[1], Magdalena Sokolska[1], Shonit Punwani[1], and Margaret A Hall-Craggs[1]

[1]Centre of Medical Imaging, University College London, London, United Kingdom

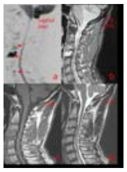

To increase the MR value of spinal imaging in patients with suspected or known malignant disease, we propose the use of sagittal diffusion weighted imaging as replacement for traditional image types such as STIR and T2W TSE. The impact of this protocol is threefold. Scan times are reduced from potentially 50 minutes to 15 minutes for the whole spine; making scans more tolerable for patients with back pain, reducing cost and increasing scanner capacity. Reader confidence is increased in detecting malignant infiltration especially when diffuse. Finally, read times are reduced as there are fewer images to review.

4455 Computer 106

MR arthrography of the hip using 3D isotropic SPGR reconstructed with ESPIRiT compressed sensing reconstruction and two-point Dixon fat-water separation

Kathryn Jane Stevens[1], Tao Zhang[2], Marcus T Alley[3], and Shreyas S Vasanawala [4]

[1]Department of Radiology, Stanford University School of Medicine, Stanford, CA, United States, [2]GE Healthcare, [3]Department of Radiology, Stanford University School of Medicine, CA, United States, [4]Stanford University School of Medicine, CA, United States

A single volumetric SPGR sequence reconstructed with ESPIRiT compressed sensing reconstruction and two-point Dixon fat-water separation was added to routine hip MR arthrogram and compared to the conventional 3-plane 2D-FSE fat-saturated T1-weighted sequences in identification of hip pathology in 25 patients. SPGR compared favorably well with T1 FS, but failed to identify 3 subtle labral tears, 1 chondral delamination and 3 low-grade ligamentum teres tears, possibly due to increased blurring associated with SPGR, decreasing overall image quality of SPGR. The relative time saving of SPGR and ability to subsequently reformat data makes this a viable technique for hip MR arthrograms.

4456 Computer 107

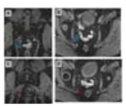

USPIOs for metastatic lymph node detection in prostate cancer: back on the block

Tom W Scheenen[1], Ansje Fortuin[1], Janine van der Linden[2], Ilia Panfilov[1], Bas Israel[1], Roger Brüggeman[2], and Jelle Barentsz[1]

[1]Radiology and Nuclear Medicine, Radboud university medical center, Nijmegen, Netherlands, [2]Pharmacology, Radboud university medical center, Nijmegen, Netherlands

The presence of nodal metastases in patients with prostate cancer is a key factor determining prognosis and treatment. With the reintroduction of ferumoxtran-10-enhanced MRI in local clinical practice, small metastases in lymph nodes down to 2 mm in size can be detected non-invasively, avoiding diagnostic surgical lymph node dissections and guiding personalized treatment of patients with prostate cancer at intermediate and high risk for metastatic spread.

4457 Computer 108

Whole-body MRI for initial assessment of plasma cell disorders including multiple myeloma

Arash Latifoltojar[1], Margaret Hall-Craggs[1], Alan Bainbridge[2], Neil Rabin[2], Ali Rismani[2], Rakesh Popat[1], Kwee Yong[3], and Shonit Punwani[4]

[1]University College London, London, United Kingdom, [2]University College London Hospital, United Kingdom, [3]University College London, [4]University College London, United Kingdom

Whole body MRI (WB-MRI) is increasingly being used to assess plasma cell disorders (PCDs). The adoption of WB-MRI provides a niche to further incorporate novel imaging technique into assessment of PCDs, streamlining decision making progress in a cost-effective way.

4458 Computer 109

Quality Assessment in the Multicenter MR Imaging Study of the German National Cohort (NAKO)

Jochen G. Hirsch[1], Alexander Köhn[2], Daniel C. Hoinkiss[1], Jonas Singe[2], Eyyub Ebu-Bekir Öztürk[1], Matthias Günther[1], and the NAKO MRI Study Investigators[3]

[1]MR Physics and Imaging, Fraunhofer MEVIS, Bremen, Germany, [2]Software Development, Fraunhofer MEVIS, Bremen, Germany, [3]Central Executive Office of the German National Cohorte, Heidelberg, Germany

A fully automated workflow for image-based quality assessment (QA) was set up in a large, multi-center cohort whole-body MR imaging study, part of the National Cohort Study Germany NAKO. Study design, data management, workflow, and objectives have been described previously. Standardized quality assessment including technical aspects like program and protocol parameter truth, as well as image-based estimates of various quality indices demonstrate a high degree of stability and homogeneity of image quality across the 5 contributing MR centers. Furthermore, QA ensures short-term intervention procedures with respect to quality control, and offer valuable quantitative information for subsequent scientific data evaluation.

4459 Computer 111

MRI evaluation of suspected appendicitis in pediatric patients

Christina L Sammet[1,2], Cindy Rigsby[1,2], Barb Karl[1], Laura Gruber[1], and Jie Deng[1,2]

[1]Medical Imaging, Lurie Children's Hospital of Chicago, Chicago, IL, United States, [2]Radiology, Northwestern University, Chicago, IL, United States

Appendicitis is prevalent in pediatric populations and currently CT imaging is used to triage children to emergency surgery. As of early 2015 we have been able to replace this CT scan with a limited abdomen/pelvis study using MRI. This limited MRI appendicitis protocol is rapid, cost-neutral (equal in cost to our previous CT study for appendicitis), and confers less potential risk to the child by eliminating radiation exposure. Using state-of-the-art rapid MRI imaging techniques, we have been successful in imaging suspected appendicitis in children as young as five years old.

4460 Computer 112

Using Hippocampus Volume to Predict Treatment Outcome in Major Depressive Disorder

Xiaoxiao Hu[1], Lianqing Zhang[1], Ming Zhou[1], Lu Lu[1], Xinyu Hu[1], Qiyong Gong[1], and Xiaoqi Huang[1]

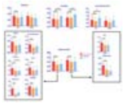

[1]Department of Radiology, Huaxi MR Research Center (HMRRC), West China Hospital of Sichuan University, Chengdu, People's Republic of China

The current study aimed to use structural data of hippocampus volume obtained from magnetic resonance imaging to predict treatment outcome in major depressive disorder. Our findings demonstrated that there was a relationship between left hippocampus volume and medication efficiency in major depressive disorder group. Meanwhile, our results threw light on the predictive value as a marker of treatment responsiveness in major depressive disorder.

4461 Computer 113

Voxel-wise meta-analysis of resting-state functional activity in type 2 diabetes

Taiyuan Liu[1], Jia Liu[2], Wenhui Wang[1], Lun Ma[1], Xiaoyue Ma[1], Shaojie Shi[1], Qiyong Gong[3], and Meiyun Wang[1]

[1]Henan Provincial People's Hospital, Zhengzhou, People's Republic of China, [2]Huazhong University of Science and Technology, Wuhan, People's Republic of China, [3]Department of Radiology, West China Hospital of Sichuan University, Zhengzhou, People's Republic of China

Previous studies about resting-state functional activity reported that altered brain activity was demonstrated with type 2 diabetes and their findings were inconsistent ,which have not been quantitatively reviewed. Therefore, we conducted a quantitative meta-analysis including resting-state functional activity studies of patients with type 2 diabetes. Meta-analysis of pooled and subgroup meta-analyses found that type 2 diabetes patients showed abnormal brain activity mainly in default mode network(DMN) and visual-related regions. Our finding supports that type 2 diabetes could lead to diabetic brain activity alterations, which may correlate with cognitive impairment of type 2 diabetes patients.

4462 Computer 114

Simultaneous Perfusion Imaging with Consecutive Echoes (SPICE)

Michael Schmainda[1]

[1]Imaging Biometrics, LLC, Elm Grove, WI, United States

SPICE (simultaneous perfusion imaging with consecutive echoes) is a method that permits simultaneous estimation of DSC- and DCE-MRI parameters, in one acquisition, using a single dose of contrast agent. Conventional algorithms are used to obtain the perfusion and permeability parameters corrected for confounding recirculation and leakage effects. The proposed method does not require administration of a loading dose of contrast agent (traditionally employed for DSC), and pre-contrast spin density and native T1 calibration scans (traditionally required for DCE) have been eliminated.

4463 Computer 115

Open Source Imaging Initiative (OSI²) – Update and Roadmap

Felix Arndt[1], Sebastian Aussenhofer[2], Eva Behrens[3], Christian Blücher[3], Peter Blümler[4], Janko Brand[5], Kate Michi Ettinger[6], Ariane Fillmer[7], William Grissom[8], Bernhard Gruber[9,10], Bastien Guerin[11,12], Sergej Haas[13], Haopeng Han[3], Michael Hansen[14], Christopher Jordan Hasselwander[8], Russ Hodge[3], Werner Hoffmann[7], Bernd Ittermann[7], Marcin Jakubowski[15], Andre Kühne[16], Stefan Klein[17], Stefan Kroboth[18], Mark Ladd[19,20], Kelvin Layton[21], Brian Leiva, Sebastian Littin[18], Blanca López-Aranguren Blázquez, Kasper Marstal[17], Ralf Mekle[22], Manuel Moritz[23], Raphael Moritz[3], Thoralf Niendorf[3,16,24], Ruben Pellicer[25], Mihir Pendse[26], Athanasios Polimeridis[27], Tobias Redlich[23], Henning Reiman[3], Reiner Seemann[7], Frank Seifert[7], Ludger Starke[3], Jason Stockmann[28], Tony Stoecker[29], Kazuyuki Takeda[30], Lukas Thiele, Martin Uecker[31], Florian von Knobelsdorff-Brenkenhoff[32], Robert Wahlstedt[33], Andrew Webb[34], Simone Winkler[35], Lukas Winter[3], Huijun Yu[18], and Maxim Zaitsev[18]

[1]Facility for Antiproton and Ion Research in Europe GmbH, Darmstadt, Germany, [2]Noras MRI products GmbH, Höchberg, Germany, [3]Berlin Ultrahigh Field Facility (B.U.F.F.), Max Delbrück Center for Molecular Medicine in the Helmholtz Association, Berlin, Germany, [4]Institute of Physics, University of Mainz, Mainz, Germany, [5]One World Doctors, Berlin, Germany, [6]Mural Institute, San Francisco, CA, United States, [7]Physikalisch Technische Bundesanstalt (PTB), Berlin, Germany, [8]Biomedical Engineering, Vanderbilt University, Nashville, TN, United States, [9]Institute of Biomedical Mechatronics, Johannes Kepler University, Linz, Austria, [10]Department of Radiology, University Medical Center Utrecht, Utrecht, Netherlands, [11]Department of Radiology, Massachusetts General Hospital, Charlestown, MA, United States, [12]Harvard Medical School, Boston, MA, United States, [13]Haasdesign, Erkrath, Germany, [14]National Heart, Lung, and Blood Institute, National Institutes of Health, Bethesda, MD, United States, [15]Open Source Ecology, MO, United States, [16]MRI.TOOLS GmbH, Berlin, Germany, [17]Biomedical Imaging Group Rotterdam, Depts. of Medical Informatics & Radiology, Erasmus MC, Rotterdam, Netherlands, [18]Department of Radiology – Medical Physics, Medical Center - University of Freiburg, Freiburg, Germany, [19]Medical Physics in Radiology, German Cancer Research Center (DKFZ), Heidelberg, Germany, [20]Erwin L. Hahn Institute for Magnetic Resonance Imaging, University of Duisburg-Essen, Essen, Germany, [21]Institute for Telecommunications Research, University of South Australia, Mawson Lakes, Australia, [22]Center for Stroke Research Berlin (CSB), Charité Universitätsmedizin, Berlin, Germany, [23]Institute for Production Engineering, Helmut Schmidt University, Hamburg, Germany, [24]Experimental and Clinical Research Center (ECRC), a joint cooperation between the Charité Medical Faculty and the Max Delbrück Center for Molecular Medicine, Berlin, Germany, [25]Centre for Advanced Imaging, University of Queensland, Brisbane, Australia, [26]Stanford University, Stanford, CA, United States, [27]Skolkovo Institute of Science and Technology, Moscow Region, Russian Federation, [28]A. A. Martinos Center for Biomedical Imaging, Massachusetts General Hospital, Charlestown, MA, United States, [29]German Center for Neurodegenerative Diseases (DZNE), Bonn, Germany, [30]Division of Chemistry, Graduate School of Science, Kyoto University, Kyoto, Japan, [31]Institute for Diagnostic and Interventional Radiology, University Medical Center Göttingen, Göttingen, Germany, [32]Cardiology at Agatharied Hospital, University of Munich, Hausham, Germany, [33]Regenerative Science Institute Spokane, Washington, WA, United States, [34]C.J. Gorter Center for High Field MRI, Dept of Radiology, Leiden University Medical Center, Leiden, Netherlands, [35]Lucas Center for Imaging, Dept of Radiology, Stanford University, Stanford, CA, United States

*authors are listed in alphabetical order

The aim of the open source imaging initiative (OSI²) is to collaboratively share research in MR technology and building a quality, affordable open source MR scanner. Combining innovation and open source (OS) approaches will generate global value by reproducible science and development and will allow a major reduction of investments and operational costs with the guiding principle: From the community, for the community. OSI² (www.opensourceimaging.org) was presented for the first time at the ISMRM 2016. Here we present an update and a roadmap towards the fulfillment of our vision.

4464 Computer 116

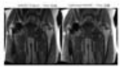

Clinical Impact of Reduced Spectral Acquisitions in Calibrated 3D Multi-Spectral Imaging Near Metal Implants

Rajeev R Mannem[1], Sujan Fernando[1], Sean Lehner[1], Suryanarayanan Kaushik[2], and Kevin Koch[1]

[1]Radiology, Medical College of Wisconsin, Milwaukee, WI, United States, [2]Applications and Workflow, GE Healthcare

We present the clinical evaluation results of a novel approach for acquisition time reduction in 3D multispectral imaging near implants. Two musculoskeletal radiologists compared standard MAVRIC SL sequences to spectrally calibrated MAVRIC SL sequences for exams of instrumented hips, knees, and shoulders. Initial results demonstrated maintenance of diagnostic information in the hips when the calibration is utilized. Rotator cuff evaluation was still limited in the shoulder using the calibrated technique but evaluation of the other structures was nearly equivalent. Calibrated imaging of the knee showed reductions of SNR, which will inform future adjustment of targeted calibrated protocols in this joint.

Electronic Poster

Preclinical Imaging in Cancer

Exhibition Hall — Tuesday 17:15 - 18:15

4465 Computer 1

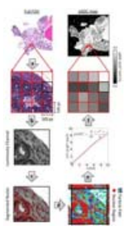

Histology-Derived pseudo-ADC correlates with measured ADC and extranuclear space in a transgenic model of prostate cancer, identifying contribution of luminal space to measured ADC.

Matthew David Blackledge[1,2], Konstantinos Zormpas-Petridis[1], Andreas Heindl[3], Siver A. Moestue[4], Yinyin Yuan[3], Dow Mu Koh[1,2], David J Collins[1,2], Yann Jamin[1], Tone F. Bathen[4], Martin O Leach[1,2], and Deborah K. Hill[4]

[1]Division of Radiotherapy and Imaging, The Institute of Cancer Research, London, United Kingdom, [2]MRI Unit, The Royal Marsden NHS Foundation Trust, Sutton, United Kingdom, [3]Division of Molecular Pathology & Centre for Evolution and Cancer, The Institute of Cancer Research, London, United Kingdom, [4]Institute of Circulation and Medical Imaging, NTNU - Norwegian University of Science and Technology, Trondheim, Norway

In this preclinical study we investigate the utility of in-silico simulations of the pseudo-apparent diffusion coefficient (pADC) of water within extra-nuclear regions segmented on large field-of-view haematoxylin, eosin, and saffron (HES) slides from a transgenic mouse model of prostate cancer. We demonstrate that pADC is correlated within in-vivo measurements of the apparent diffusion coefficient (ADC) measured by diffusion-weighted magnetic resonance imaging and may thus be used as a surrogate for exploring the effect of tissue structure on measured ADC values. Furthermore, we demonstrate that ADC is correlated with fractional space occupied by lumen, derived from semi-automatic segmentation of HES slides.

4466 Computer 2

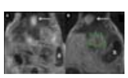

Tumor vasculature differs between cell and fragment derived murine orthotopic models of hepatocellular carcinoma

Sibu P Kuruvilla[1], Colleen A Crouch[2], and Joan M Greve[2]

[1]Materials Science and Engineering, University of Michigan at Ann Arbor, Ann Arbor, MI, United States, [2]Biomedical Engineering, University of Michigan at Ann Arbor, Ann Arbor, MI, United States

We report the use of semi-quantitative dynamic contrast enhanced (DCE)-MRI to identify differences in the growth and vascular environment seen within two murine hepatocellular carcinoma (HCC) models - cellular orthotopic injection (COI) (representing a traditional tumor model) or surgical orthotopic implantation (SOI) of tumor fragments (representing a patient-derived orthotopic xenograft model, or PDOX). Uptake curves of gadolinium contrast agent indicate differences in vasculature between the two models, highlighting important considerations to be made when trying to use PDOX methods to model HCC in the clinic.

4467 Computer 3

Intrinsic susceptibility MRI predicts response to the vascular endothelial growth factor receptor inhibitor cediranib in the Th-*MYCN* model of neuroblastoma

Yann Jamin[1], Evon Poon[2], Neil P. Jerome[1], Alexander Koers[2], Laura S. Danielson[2], Dow-Mu Koh[1], Louis Chesler[2], and Simon P. Robinson[1]

[1]Division of Radiotherapy and Imaging, The Institute of Cancer Research, London, London, United Kingdom, [2]Division of Cancer Therapeutics and Division of Clinical Studies, The Institute of Cancer Research, London, London, United Kingdom

In this study we demonstrate that the transverse relaxation rate R_2* predicts response to the vascular endothelial growth factor receptor (VEGFR) inhibitor cediranib in the Th-*MYCN* genetically-engineered murine model of neuroblastoma, a childhood cancer of the developing nervous system.

4468 Computer 4

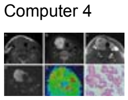

Papillary thyroid carcinoma with hobnail pattern: unique MRI features and correlated with the histopathologic findings

Lanyun Wang[1]

[1]Shanghai Minhang District Central Hospital, shanghai, People's Republic of China

Hobnail papillary thyroid carcinoma (HPTC) is a moderately differentiated PTC variant with aggressive clinical behavior and significant mortality.The purpose of this study was to recognize the unique MRI features of HPTC .61 patients with PTC confirmed histopathologically[19 lesions of HPTC and 42 NHPTC （PTC without hobnail features）lesions] undergoing MRI with T1W, T2W,DWI and contrast material–enhanced sequences prior to thyroidectomy were included retrospectively. there was a significant tendency toward T2WI significantly high signal 、T2WI linear low signal 、Lace levy 、Gyrus-like structure 、higher ADC values 、irregular shape present in HPTCs. HPTC lesions have unique MRI features.

4469 Computer 5

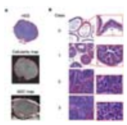

Cell Nuclear Size and Shape are Associated with ADC, Cellularity, and Histological Class in a Transgenic Mouse Model of Prostate Cancer

Leslie R. Euceda[1], Matthew D. Blackledge[2], Andreas Heindl[2], Yinyin Yuan[2], Dow-Mu Koh[2,3], David Collins[2,3], Siver A. Moestue [1], Martin O. Leach[2,3], Tone F. Bathen[1], and Deborah K. Hill[1]

[1]Institute of Circulation and Medical Imaging, NTNU - Norwegian University of Science and Technology, Trondheim, Norway, [2]Institute of Cancer Research, London, United Kingdom, [3]MRI Unit, Royal Marsden Hospital, London, United Kingdom

The relationship between tissue microstructure and ADC is poorly understood in cancer. We identified quantitative nuclear characteristics from haematoxylin, eosin, and saffron stained prostatic histology samples. ADC maps were calculated for transgenic prostate cancer mice and healthy controls. Matched histology images of excised prostates were used to determine cellularity and histological class. ADC and cellularity correlated with a set of nuclear features (describing texture, lightness, radius, and shape), which exhibited mirrored trends, implying an inverse relationship between ADC and cellularity. The same nuclear features correlated with histological class. This will be useful for underpinning relationships between ADC and tissue microstructure.

4470 Computer 6

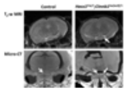

A Genetically Engineered Mouse Model Recapitulates Radiological Features of Human Adamantinomatous Craniopharyngioma

Jessica KR Boult[1], Ciaran Hutchinson[2], John R Apps[3], Gabriela Carreno[3], Laura S Danielson[4], Laura M Smith[4], Alex K Virasami[2], Alexander Koers[4], Louis Chesler[4], Owen J Arthurs[2], Juan Pedro Martinez-Barbera[3], and Simon P Robinson[1]

[1]Division of Radiotherapy and Imaging, The Institute of Cancer Research, London, United Kingdom, [2]Histopathology Department, Great Ormond Street Hospital for Children NHS Foundation Trust, London, United Kingdom, [3]Birth Defects Research Centre, Institute of Child Health, University College London, London, United Kingdom, [4]Division of Clinical Sciences, The Institute of Cancer Research, London, United Kingdom

Tumours in $Hesx1^{Cre/+};Ctnnb1^{lox(ex3)/+}$ mice resemble human adamantinomatous craniopharyngioma (ACP) molecularly and histologically. MRI and *ex vivo* micro-CT were used to assess the radiology of this model for the first time. Early enlargement and heterogeneity of $Hesx1^{Cre/+};Ctnnb1^{lox(ex3)/+}$ pituitaries was evident; enlargement of a solid tumour, and development of cysts and haemorrhage subsequently occurred. Solid components showed heterogeneous T_1-weighted signal enhancement following Gd-DTPA administration, and in some animals cysts were hyperintense on FLAIR and T_1-weighted images, both emulating clinical observations. Cyst calcification was not observed by micro-CT but we show that $Hesx1^{Cre/+};Ctnnb1^{lox(ex3)/+}$ tumours faithfully recapitulate the MRI radiology of the human disease.

4471 Computer 7

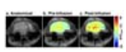

Probing tumor metabolism using dynamic lactate chemical exchange saturation transfer MRI

Puneet Bagga[1], Mohammad Haris[2], Pranav Jain[1], Alekya Bheemreddy[1], Francesco Marincola[2], Hari Hariharan[1], and Ravinder Reddy[1]

[1]Department of Rediology, University of Pennsylvania, Philadelphia, PA, United States, [2]Research Branch, Sidra Medical and Research Center, Doha, Qatar

Lactate CEST (LATEST) MRI method has been shown to be applicable in detecting and imaging changes in the lactate level in human subjects post heavy exercise and to measure the lactate in a mouse model of lymphoma. In this study, LATEST was implemented to probe the lactate dehydrogenase (LDH) activity in vivo in a rat glioma model. Following the administration of pyruvate, the LATEST contrast is elevated in the tumor region while it is unaltered in the unaffected region.

4472 Computer 8

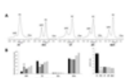

Molecular effects of various chemotherapeutic agents on choline phospholipid metabolism of triple-negative breast cancer cells

Menglin Cheng [1], Zaver M. Bhujwalla[1], and Kristine Glunde[1]

[1]Russell H. Morgan Department of Radiology and Radiological Science, The Johns Hopkins University School of Medicine, Baltimore, MD, United States

The MRS-detected total choline (tCho) signal is a promising non-invasive surrogate marker of chemotherapy response in breast cancer patients. The molecular mechanisms by which common chemotherapeutic drugs affect the tCho signal, consisting of glycerophosphocholine (GPC), phosphocholine (PC), and free choline (Cho), are unknown. We have employed widely used cancer chemotherapeutic drugs including doxorubicin, paclitaxel, and vinorelbine to treat triple-negative human MDA-MB-231 breast cancer cells to elucidate their molecular effects on choline phospholipid metabolism using high-resolution ^{1}H MRS to detect changes in cellular choline metabolite profiles, and quantitative RT-PCR to assess the corresponding changes in the expression levels of choline-metabolizing enzymes.

4473 Computer 9

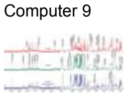

The Metabolic Secretome of Cachexia Inducing Pancreatic Ductal Adenocarcinoma

Santosh K Bharti[1], Paul T Winnard Jr.[1], Louis Dore-Savard[2], Yelena Mironchik[1], Marie-France Penet[1,3], and Zaver M Bhujwalla[1,3]

[1]JHU ICMIC Program, Division of Cancer Imaging Research, The Russell H. Morgan Department of Radiology and Radiological Science, The Johns Hopkins University School of Medicine, Baltimore, MD, United States, [2]Experimental Therapeutics and Metabolism Program, McGill University Health Center, Montreal, QC, Canada, [3]Sidney Kimmel Comprehensive Cancer Center, The Johns Hopkins University School of Medicine, Baltimore, MD, United States

Tumor interstitial fluid (TIF) contains the secretome of cancers that can impact most phenotypic aspects of cancer. One characteristic phenotype of pancreatic ductal carcinoma (PDAC) is its ability to induce profound weight loss or cachexia through a multifactorial syndrome that affects multiple organs. To understand the interaction between cancer cells and body organs, here, for the first time, we have characterized the metabolomic profile of TIF from cachexia and non-cachexia inducing pancreatic cancer xenografts and identified clear differences in the metabolic secretome between cachexia inducing and the non-cachexia inducing tumors.

4474 Computer 10

Metabolic reprogramming in a relevant IDH1-mutated human glioma xenograft model

Tom Peeters[1], Krissie Lenting[2], Jack van Asten[1], William Leenders[2], and Arend Heerschap[1]

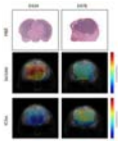

[1]Radiology and Nuclear Medicine, Radboud university medical center, Nijmegen, Netherlands, [2]Pathology, Radboud university medical center, Nijmegen, Netherlands

Understanding metabolic aberrations in IDH-mutated gliomas requires xenograft models growing in a relevant tissue microenvironment and resembling its human genetic counterparts. We performed *in vivo* ^{1}H MRSI of human-derived oligodendroglioma xenograft models to map lactate and total choline concentrations. Lactate levels were significantly lower and total choline higher in mutated tumor tissue compared to non-tumor brain in the same animal, or to its wild-type counterpart model. This outcome was correlated with expression levels of enzymes and transporters in both lactate- and phospholipid-related metabolic pathways. The findings point to a metabolic reprogramming of aerobic glycolysis and lipid synthesis by the IDH1 mutation.

4475 Computer 11

Intratumoral vessel evaluation using magnetic resonance micro-angiography with a vascular pool Gd-DOTA-dendron liposomal contrast agent

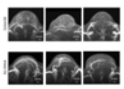

Nobuhiro Nitta[1,2], Daisuke Kokuryo[3], Sayaka Shibata[1], Kenji Kono[4], Akihiro Tomita[5], Jeff Kershaw[1], Ichio Aoki[1], and Masafumi Harada[2]

[1]Department of Molecular Imaging and Theranostics, National Institute of Radiological Sciences, National Institutes for Quantum and Radiological, Chiba, Japan, [2]Radiology and Radiation Oncology, Graduate School of Medicine, Tokushima University, Tokushima, Japan, [3]Graduate School of System informatics, Kobe University, Hyogo, Japan, [4]Graduate School of Engineering, Osaka Prefecture University, Osaka, Japan, [5]Graduate School of Medicine, Nagoya University, Aichi, Japan

Evaluation of the intratumor environment, such as cell distribution and vessel structure, are important for understanding the characteristics of tumors. In particular, the vessel structure and its permeability is critical for the malignant potential of the tumor and drug-targeting. The purpose of this work was to non-invasively visualize intratumoral vessels using MR micro-angiography (MRmA) and a liposomal contrast agent having long blood half-life. In addition, we tried to identify differences in the vascular structures for Colon26 and SU-DHL6 cells. The proposed method visualized the intratumoral vessels clearly and revealed differences in the structure depending on the cell type.

4476 Computer 12

MR image analysis to identify habitats through comparison with histology and immunohistochemistry in breast cancer

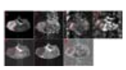

Bruna V. Jardim-Perassi[1,2], William Dominguez-Viqueira[2], Mikalai Budzevich[2], Epifanio Ruiz[2], Suning Huang[2], Jan Poleszczuk[3], Alex S Lopez[4], Debora APC Zuccari[1], Gary Martinez[2], and Robert Gillies[2]

[1]Molecular Biology, Faculdade de Medicina de Sao Jose do Rio Preto, Sao Jose do Rio Preto, Brazil, [2]Cancer Imaging and Metabolism, Moffitt Cancer Center, Tampa, FL, United States, [3]Nalecz Institute of Biocybernetics and Biomedical Engineering, Poland, [4]Oncologic Sciences, Moffitt Cancer Center, Tampa, FL, United States

Breast cancer shows significant heterogeneity at both inter- and intratumoral levels. In this study, a distribution clustering of multiple MRI pulse sequences was used in combination with a 3D printed approach, and showed a qualitatively comparable pattern of intratumoral heterogeneity (habitats) in MRI and histological images. This approach could potentially be used as a non-invasive imaging method for the monitoring of the intratumoral heterogeneity following the therapy in breast cancer.

4477 Computer 13

Electric field and current density mapping during reversible Electroporation

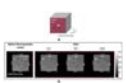

Munish Chauhan[1], Neeta Ashok Kumar[1], Vikram D Kodibagkar[1], and Rosalind J Sadleir[1]

[1]School of Biological and Health Systems Engineering, Arizona State University, Tempe, AZ, United States

Electroporation is popular in cancer therapy and gene or drug delivery. Magnetic Resonance Electrical Impedance Tomography (MREIT) was used to monitor the applied electric field and current density during electroporation. Electroporation fields were applied by novel low-susceptibility carbon fiber electrodes in a bovine liver tissue sample. Projected current density (J^P) and Electric field (E) were computed from MR data collected under electroporation fields. Susceptibility artifacts around the pair of carbon fiber electrodes were greatly reduced. In this study, we demonstrated the feasibility of MREIT technique to monitor the current density and electric field distribution during ex-vivo tissue electroporation.

4478 Computer 14

Diffusion Kurtosis Imaging Evaluating Epithelial–mesenchymal Transition in Colorectal Carcinoma Xenografts Model: Initial Experience

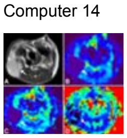

Huanhuan Liu[1], Caiyuan Zhang[2], Jinning Li[2], Weibo Chen[3], and Dengbin Wang[2]

[1]Department of Radiology, Xinhua hospital, Shanghai Jiaotong University School of Medicine, Shanghai, People's Republic of China, [2]Department of Radiology, Xinhua hospital, Shanghai Jiaotong University School of Medicine, People's Republic of China, [3]Philips Healthcare, People's Republic of China

Colorectal cancer (CRC) is one of the most common malignant tumors in gastrointestinal tract. Tumor recurrence and metastasis are still a major cause of death in rectal cancer patients. Epithelial-mesenchymal transition (EMT) is reported a critical process providing tumor cells with the ability to migrate and metastasize to distant sites, leading to a poor prognosis in CRC. The diffusion kurtosis imaging (DKI) could quantify non-Gaussian behavior of water diffusion and provide more precise information of tissue characteristics. Our study demonstrated that DKI could be used to identify EMT in CRC xenograft models.

4479 Computer 15

Telomerase expression enhances pentose phosphate pathway flux resulting in an MR-detectable increase in reduced glutathione levels in mutant IDH1 glioma cells

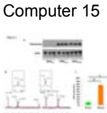

Pavithra Viswanath[1], Russell O Pieper[2], and Sabrina M Ronen[1]

[1]Radiology and Biomedical Imaging, University of California San Francisco, San Francisco, CA, United States, [2]Neurological Surgery, University of California San Francisco, San Francisco, CA, United States

Telomerase is the enzyme responsible for maintenance of telomeres, which are special capped structures that protect chromosomal ends from degradation. Telomerase activation and metabolic reprogramming have both emerged as hallmarks of cancer. Here, we investigated the link between telomerase and metabolism in mutant isocitrate dehydrogenase 1 (IDH1) glioma cells with the goal of identifying MR-detectable biomarkers of telomerase expression. Using ^{13}C- and ^{1}H- MRS, we show that telomerase expression is associated with elevated flux through the pentose phosphate pathway resulting in increased levels of reduced glutathione (GSH). Thus, GSH is a potential biomarker of telomerase expression in mutant IDH1 gliomas.

4480 Computer 16

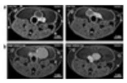

Dietary Fat Results in Increased Tumor Burden in a Mouse Model of Human Triple-Negative Breast Cancer Based on Magnetic Resonance Imaging and Histology

Devkumar Mustafi[1], Sully Fernandez[2], Erica Markiewicz[1], Xiaobing Fan[1], Marta Zamora[1], Jeffrey Mueller[3], Matthew J Brady[2], Suzanne D Conzen[4], and Gregory S Karczmar[1]

[1]Radiology, The University of Chicago, Chicago, IL, United States, [2]Medicine, Sections of Adults and Pediatric Endocrinology, Diabetes and Metabolism, The University of Chicago, Chicago, IL, United States, [3]Pathology, The University of Chicago, Chicago, IL, United States, [4]Medicine, the Section of Hematology and Oncology, The University of Chicago, Chicago, IL, United States

Breast cancer is the most commonly diagnosed malignancy among women in the United States and the second leading cause of cancer mortality worldwide. Epidemiological studies suggest an increase in the risk of triple-negative breast cancer (TNBC) in association with a high animal fat diet. Based on previous MRI studies in SV40Tag mice, we examined the effect of pre-pubertal exposure to high dietary fat in this model of TNBC. The results reported here demonstrate that a high animal fat diet significantly increased the number of aggressive cancers detected by MRI in a mouse model of human TNBC.

4481 Computer 17

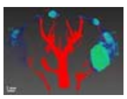

Magnetic Resonance Angiography Shows Increased Arterial Blood Supply Associated with Murine Mammary Cancer

Devkumar Mustafi[1], Abby Leinroth[1], Xiaobing Fan[1], Erica Markiewicz[1], Marta Zamora[1], Jeffrey Mueller[2], Suzanne D Conzen[3], and Gregory S Karczmar[1]

[1]Radiology, The University of Chicago, Chicago, IL, United States, [2]Pathology, The University of Chicago, Chicago, IL, United States, [3]Medicine, the Section of Hematology and Oncology, The University of Chicago, IL, United States

Breast cancer is a major cause of morbidity and mortality in Western women. Tumor neo-angiogenesis may be an MRI-detectable prognostic marker for cancer progression. Clinical practice uses DCE-MRI to detect cancers based on increased blood flow and capillary permeability. However, DCE-MRI requires repeated injections of contrast media; therefore we used time-of-flight MR angiography to measure the number and size of arteries feeding mammary glands with and without cancer, and demonstrated that blood vessels in and near mammary glands grew significantly as invasive cancers developed.

4482 Computer 18

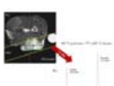

In vivo hyperpolarized [1-13C]pyruvate and [18F]-FDG PET/CT studies of prostate cancer metastasis xenografts in mice

Frits H.A. van Heijster[1], Sandra Heskamp[1], Andor A. Veltien[1], Tom H. Peeters[1], Tom W.J. Scheenen[1], Otto C. Boerman[1], and Arend Heerschap[1]

[1]Radiology and Nuclear Medicine, Radboud University Medical Center, Nijmegen, Netherlands

Understanding the underlying mechanisms of aggressiveness is important for better staging and treatment of prostate cancer. In this study two murine xenograft models of early and late stage prostate cancer were investigated. [1-^{13}C]pyruvate was hyperpolarized by Dynamic Nuclear Polarization (DNP) and pyruvate metabolism is followed by ^{13}C-MR. This is combined with [^{18}F]FDG-PET/CT to study glucose metabolism. We found differences in pyruvate conversion and glucose uptake *in vivo* in the murine models.

4483 Computer 19

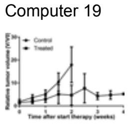

Multi-agent dynamic contrast enhanced MRI to assess vascular changes induced by prolonged VEGFR2 inhibition in oesophageal cancer

Remy Klaassen[1,2], Anne Steins[1,2], Matthias C Schabel[3,4], Igor Jacobs[5], Maarten F Bijlsma[2], Aart J Nederveen[6], Gustav J Strijkers[7], and Hanneke WM van Laarhoven[1]

[1]Medical Oncology, Academic Medical Center, Amsterdam, Netherlands, [2]LEXOR, Academic Medical Center, Amsterdam, Netherlands, [3]Advanced Imaging Research Center, Oregon Health & Science University, Portland, OH, United States, [4]Utah Center for Advanced Imaging Research, University of Utah, Salt Lake City, UT, [5]Biomedical NMR, Department of Biomedical Engineering, Eindhoven University of Technology, Eindhoven, Netherlands, [6]Radiology, Academic Medical Center, Amsterdam, Netherlands, [7]Biomedical Engineering and Physics, Academic Medical Center, Amsterdam, Netherlands

The effective vascular changes induced by prolonged VEGFR2 inhibition and the resulting changes in vascular function are difficult to monitor in vivo and therefore largely unexplored. In this study we show a multi-agent DCE-MRI approach, using 3 different-sized contrast agents, to quantify effects on vascularization induced by prolonged VEGFR2 inhibition in an oesophageal cancer mouse model. Effects on vascularization were predominantly observed in parameters dependent on the larger-sized contrast agents, where no effects where found for the traditional low-molecular weight contrast agent.

4484 Computer 20

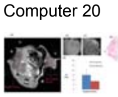

In-vivo targeting and imaging of super-paramagnetic iron-oxide particles to subcutaneous tumour models

Mohammad Mohseni[1], John Connell[1], Stephen Patrick[1], May Zaw-Thin[1], Tammy Kalber[1], Tom Roberts[1], Quentin Pankhurst[2], Mark Lythgoe[1], and Bernard Siow[1]

[1]CABI, UCL, london, United Kingdom, [2]UCL, london, United Kingdom

Magnetic targeting of drug-conjugated iron oxide nanoparticles has the potential to increase the concentration of therapeutic agents to tumours whilst reducing off-target side effects of current chemotherapy methods. This preclinical work demonstrates that SPION accumulation can be increased in subcutaneous tumours using magnetic fields and can then be detected by MRI. In addition, key physiological parameters can be measured before magnetic targeting for future optimisation of the strategy.

4485 Computer 21

Imaging Collagenase-Induced Changes in the Mechanical Phenotype of Orthotopic BT474 Breast Cancer Xenografts Using Magnetic Resonance Elastography

Jin Li[1], Jessica K.R. Boult[1], Craig Cummings[1], Jeffrey C. Bamber[1], Ralph Sinkus[2], Yann Jamin[1], and Simon P. Robinson[1]

[1]Division of Radiotherapy & Imaging, The Institute of Cancer Research, London, United Kingdom, [2]Division of Imaging Sciences and Biomedical Engineering, King's College London, King's Health Partners, St. Thomas' Hospital, London, United Kingdom

We tested the hypothesis that MRE can inform on collagenase-induced matrix degradation in orthotopic BT474 breast carcinoma xenografts *in vivo*. An acute reduction in the absolute value of the complex shear modulus |G*| was detected in tumour just 5 hours after collagenase administration, mostly likely a consequence of both collagen degradation and reduction of interstitial fluid pressure. The study highlights the utility of MRE-derived quantitation of tumour viscoelasticity for monitoring the response of stromal rich tumours to modification of the extracellular matrix.

4486 Computer 22

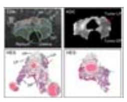

Multiparametric MRI for optimal prostate cancer detection in TRAMP mice

Jana Kim[1], Eugene Kim[1], Deborah K. Hill[1], Dan E. Meyer[2], Karina Langseth[3], Frits A. Thorsen[4], Tone F. Bathen[1], and Siver A. Moestue[1]

[1]Department of Circulation and Medical Imaging, NTNU - Norwegian University of Science and Technology, Trondheim, Norway, [2]Diagnostics, Imaging and Biomedical Technologies, GE Global Research Center, Niskayuna, NY, United States, [3]GE Healthcare AS, Oslo, Norway, [4]Department of Biomedicine, University of Bergen, Bergen, Norway

Multiparametric MRI is the standard for the detection and characterization of prostate cancer. In this study we compared the diagnostic value of clinically used DW-MRI and DCE-MRI in a transgenic mouse model of prostate cancer (TRAMP). Additionally, we investigated the potential utility of SSC-MRI using a USPIOs contrast agent for prostate cancer detection. The results of this study confirm the utility of DW-MRI and the potential value of DCE-MRI in early-stage detection and monitoring of prostate cancer. SSC-MRI appears to be less useful for this task in the TRAMP model, but further analysis is required to draw a clear conclusion.

4487 Computer 23

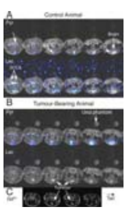

Transport across the blood-brain-barrier may be limiting for hyperpolarized [1-13C]pyruvate neuro-oncology studies

Jack Julian James Jenkins Miller[1,2,3], James Larkin[4], Katherine R Fisher[1], Vicky Ball[1], Kevin J Ray[4], Sebastien Serres[5], Damian John Tyler[1,2], Angus Zoen Lau[1,6], and Nicola Ruth Sibson[4]

[1]Department of Physiology, Anatomy & Genetics, University of Oxford, Oxford, United Kingdom, [2]Oxford Centre for Clinical Magnetic Resonance Research, University of Oxford, Oxford, United Kingdom, [3]Department of Physics, University of Oxford, Oxford, United Kingdom, [4]Cancer Research UK and Medical Research Council Oxford Institute for Radiation Oncology, University of Oxford, Oxford, United Kingdom, [5]School of Life Sciences, University of Nottingham, Nottingham, United Kingdom, [6]Physical Sciences, Sunnybrook Research Institute, Toronto, ON, Canada

Hyperpolarized pyruvate has previously been used to probe primary brain cancer. Through imaging the delivery and metabolism of both hyperpolarized [1-^{13}C]pyruvate and ethyl-[1-^{13}C]pyruvate in a rodent model of cancer metastasis to the brain, we show that the transport of [1-^{13}C] pyruvate across the blood brain barrier may be limiting until it is compromised by metastatic cell infiltration.

4488 Computer 24

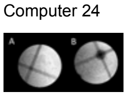

Validation of an efficient and robust MRI-guided radiotherapy planning approach for targeting abdominal organs and tumours in the mouse.

Veerle Kersemans[1], John S Beech[1], Stuart Gilchrist[1], Paul Kinchesh[1], Philip D Allen[1], James Thompson[1], Ana L Gomes[1], Zenobia D'Costa[1], Luke Bird[1], Iain DC Tullis[1], Robert G Newman[1], Abul Azad[1], Ruth J Muschel[1], Borivoj Vojnovic[1], Mark A Hill[1], Emmanouil Fokas[1], and Sean C Smart[1]

[1]CRUK/MRC Oxford Institute for Radiation Oncology, University of Oxford, Oxford, United Kingdom

The aim was to develop and validate a robust and accurate method of MR-IGRT delivery to abdominal targets in the mouse that takes advantage of the strengths of each of its components: MRI for soft tissue contrast and target identification, CBCT for accurate dose calculation and IGRT for accurate, collimated X-ray beam delivery. A multimodality cradle was developed and evaluated to enable transfer of the mouse between MR and the IGRT platform. Additionally, each step of the MG-IGRT process was validated, both in vitro using BANG gel dosimeters and in vivo by targeting the adrenal glands in mice.

Electronic Poster

General Cancer Including Preclinical

Exhibition Hall — Tuesday 17:15 - 18:15

4489 Computer 25

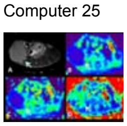

Diffusion kurtosis imaging can stratify differentiation of colorectal cancers: a preliminary study

Huanhuan Liu[1], Caiyuan Zhang[2], Jinning Li[3], Weibo Chen[4], and Dengbin Wang[3]

[1]Department of Radiology, Xinhua hospital, Shanghai Jiaotong University School of Medicine, Shanghai, People's Republic of China, [2]Department of Radiology, Xinhua hospital, Shanghai Jiaotong University School of Medicine, [3]Department of Radiology, Xinhua hospital, Shanghai Jiaotong University School of Medicine, People's Republic of China, [4]Philips Healthcare, People's Republic of China

Colorectal cancer (CRC) is the third most common cancer in the world and its incidence is on the rise. Management is particularly challenging technically for surgeon and local recurrence is a common result of treatment failure. Tumor differentiation grade is one of the factors that influence the choice of individual management, then affecting the prognosis. Diffusion kurtosis imaging (DKI) could quantify non-Gaussian behavior of water diffusion and provide more precise information of tissue characteristics. Our study demonstrated that DKI is conducive to distinguishing the various differentiations of CRC models, and reflecting the proliferation indirectly in tumor cells.

4490 Computer 26

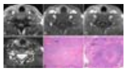

Multi-phase contrast-enhanced magnetic resonance imaging with respiratory gating in papillary thyroid carcinoma

Hao Wang[1] and Bin Song[2]

[1]Radiology, Central Hospital of Minhang District, Fudan University, Shanghai, People's Republic of China, [2]Radiology, Central Hospital of Minhang District, Fudan University, People's Republic of China

Purpose To investigate the role of multi-phase contrast-enhanced MR imaging in papillary thyroid carcinoma (PTC). **Methods** A consecutive series of 62 lesions with PTC were prospective evaluated by MR imaging. Lesions were evaluated for location, size, shape, margin, rim, degree and pattern of enhancement. **Results** 52 (83.9%) lesions showed moderate enhancement. 45 (72.6%) lesions showed ring-enhancement and 42 (67.7%) showed central washout enhancement during the delayed phase. 36(58.1%) manifested ill-defined margin and irregular rim (49, 79.0%) after administration of the contrast medium. Nine nodules (14.5%) showed extrathyroidal extension. **Conclusion** PTC commonly manifest moderate enhancement during the initial phase, with ill-defined margin and irregular rim. Central wash out enhancement and ring-enhancement occur during delayed contrast –enhanced phase.

4491 Computer 27

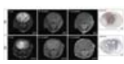

Radiological comparisons of 3D and 2D-cell culture derived tumours in an orthotopic mouse xenograft model of paediatric glioblastoma

Mariama Fofana[1], Jessica KR Boult[1], Maria Vinci[1], Valeria Molinari[1], Sergey Popov[1], Alan Mackay[1], Angel M Carcaboso[2], Chris Jones[1], and Simon P Robinson[1]

[1]The Institute of Cancer Research, London, United Kingdom, [2]Department of Oncology, Hospital Sant Joan de Déu, Barcelona, Spain

Primary patient-derived paediatric glioblastoma (pGBM) cells, cultured under conditions designed to maintain stem-like phenotypes, provide valuable platforms for pre-clinical research. Culturing tumour cells in suspension (3D) or adherent on laminin (2D) may influence their growth behaviour *in vivo*. Longitudinal, anatomical MRI showed that orthotopic HSJD-GBM-001 xenografts derived from 3D-cultured cells grew significantly faster than those from 2D-culture. Infiltrative tumour growth, maintenance of the blood brain barrier and high ADC, T_1 and T_2, associated with histopathologically confirmed tumour-oedema, were observed in both cohorts. The study highlights the influence of *in vitro* cell culture conditions on *in vivo* tumour growth characteristics.

4492 Computer 28

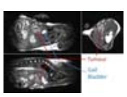

Application of Cardio-Respiratory Gated High Resolution 3D Balanced SSFP to Liver Tumour Imaging in the Mouse

Ana L Gomes[1], Paul Kinchesh[1], Stuart Gilchrist[1], Alex Gordon-Weeks[1], Ruth J Muschel[1], and Sean C Smart[1]

[1]CRUK/MRC Oxford Institute for Radiation Oncology, University of Oxford, Oxford, United Kingdom

Prospective gating and automatic reacquisition of data corrupted by respiration motion were implemented in 3D balanced steady-state free precession (bSSFP) to provide contrast that enables unambiguous detection of liver tumours in the whole mouse liver with 200 µm isotropic resolution and in scan times that are routinely less than 7 minutes. The method was used for orthotopic tumour burden quantification in 8 female C57BL/6 mice at days 7, 9, and 11 post intra-hepatic injection of MC38-GFP cells, and enabled measurement of tumour volumes less than 1 mm^3.

4493 Computer 29

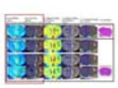

Early Detection of Glioblastoma Multiforme by the Magnetic Susceptibility Effect from Deoxyhemoglobin

Zhao Li[1], Chaohsiung Hsu[1], and Yung-Ya Lin[1]

[1]Chemistry and Biochemistry, UCLA, Los Angeles, CA, United States

Early detection of high-grade malignancy, such as glioblastoma multiforme (GBM), using new contrast mechanism and enhanced MRI techniques significantly increases not only the treatment options available, but also the patients' survival rate. For this purpose, the local magnetic-field gradient variations due to irregular water contents and deoxyhemoglobin concentration in early GBM is detected sensitively to provide the needed cancer contrast. Statistical results (N=22) for in vivo orthotopic xenografts GBM mouse models at various cancer stages validate the superior contrast and robustness of this approach (tumor time constant differs from that of the healthy brain tissue by +24%) towards early GBM detection than conventional T1-weighted (+2.6%) and T2-weighted images (-3.1%). This novel approach provides 4-8 times of improvements in early GBM tumor contrast, as measured by "tumor to normal tissue contrast", "contrast-to-noise ratio" (CNR) or "Visibility".

4494 Computer 30

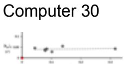

On Molecular Aspects of K^{trans} and Angiogenesis: Cerebral Gliomas

Charles S. Springer, Jr.[1], Xin Li[1], Seymur Gahramanov[2], Martin M. Pike[1], William D. Rooney[1], and Edward A. Neuwelt[3]

[1]Advanced Imaging Research Center, Oregon Health & Science University, Portland, OR, United States, [2]Neurosurgery, University of New Mexico, Albuquerque, NM, United States, [3]Blood Brain Barrier Program, Oregon Health & Science University, Portland, OR, United States

It is often thought that tumor K^{trans} value differences correspond to changes in capillary contrast agent (CA) permeability. We show this is not the case for implanted glioma in rat brain. Over an almost eight-fold K^{trans} change, the tumor CA extravasation rate constant k_{pe} remains relatively fixed, as if regulated, but at a value greater than normal. The K^{trans} changes reflect cerebral blood volume fraction changes.

4495 Computer 31

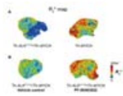

Intrinsic susceptibility MRI detects phenotypic alteration induced by a potent anaplastic lymphoma kinase inhibitor in a transgenic model of neuroblastoma

Yann Jamin[1], Elizabeth R. Tucker[2], Evon Poon[2], Alexander Koers[2], Laura S. Danielson[2], Louis Chesler[2], and Simon P. Robinson[1]

[1]*Division of Radiotherapy and Imaging, The Institute of Cancer Research, London, London, United Kingdom,* [2]*Division of Cancer Therapeutics and Division of Clinical Studies, The Institute of Cancer Research, London, London, United Kingdom*

In this study we demonstrate that the transverse relaxation rate R_2^* affords a biomarker of response to a potent anaplastic lymphoma kinase inhibitor in the Th-*ALK*^{F1174L}/Th-*MYCN* genetically engineered murine model of neuroblastoma, a childhood cancer of the nervous system

---

4496 Computer 32

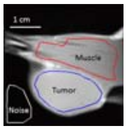

Numerical Model of Bi-Exponential T2 Decay-Based Magnetic Resonance Oximetry Imaging (MOXI).

Tatsuya J Arai[1], Donghan M Yang[1], James Campbell [1], and Ralph P Mason[1]

[1]*Radiology, UT Southwestern Medical Center, Dallas, TX, United States*

The present work seeks to explore the accuracy and precision of proton MR oximetry imaging (MOXI) in silico. MOXI technique relies on the separation of oxygen sensitive T_{2Blood} from the bi-exponential nature of overall T_2 decay. The bi-exponential T_2 decay models with Rician distribution noise were numerically generated, simulating the preclinical prostate tumor model experiments. The present in silico study showed the feasibility of the proton based MOXI technique. However, the results suggest that the MOXI technique may lack the accuracy and precision of measuring short T_{2Blood} (< 30 ms), which is essential to measure hypoxia in a tumor.

4497 Computer 33

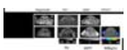

Improved quantification of SPIO in peripheral tumor xenografts using QSM

Kofi Deh[1], Marjan Zaman, Pascal Spincemaille, Moonsoo Jin, and Yi Wang

[1]*Weill Cornell Medical College, New York, NY, United States*

The use of MRI relaxometry for super-paramagnetic iron oxide (SPIO) quantification in a murine peripheral tumor xenograft, a frequently performed procedure in drug development research, may result in inaccurate estimates because of the dependence of relaxivity on tissue microenvironment. SPIO complexes conjugated to PET radiotracers have been proposed for more accurate SPIO quantification, but these have disadvantages of a cyclotron requirement, low spatial resolution and confounding tumoricidal effects. We demonstrate that SPIO quantification in peripheral tumor xenografts using new quantitative susceptibility mapping (QSM) algorithms has good agreement with quantification using PET suggesting that QSM may provide value for quantification in drug development research.

4498 Computer 34

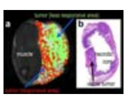

Probing Tumor Oxygenation Response to Hypoxic Gas Breathing

Donghan Mo Yang[1], Tatsuya J Arai[1], James Campbell[1], and Ralph P Mason[1]

[1]*Radiology, The University of Texas Southwestern Medical Center, Dallas, TX, United States*

Tumor oxygenation response to hypoxic gas breathing is studied in rat 13762NF breast tumors using BOLD and TOLD MRI, with hyperoxic gas breathing as reference. Time course of R_2^* and R_1-weighted signal is analyzed for 100%, 16%, and 14% O_2 breathing challenges, respectively. Evidence for decreased blood oxygen saturation (sO_2) and decreased tissue oxygen partial pressure (pO_2) is observed, revealing different patterns depending on the tumor size.

4499 Computer 35

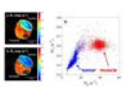

Characterization of Intratumoral Heterogeneity Based on BOLD Effect: A Study in 13762NF Breast Tumor

Donghan Mo Yang[1], Tatsuya J Arai[1], James Campbell[1], and Ralph P Mason[1]

[1]*Radiology, The University of Texas Southwestern Medical Center, Dallas, TX, United States*

Characterization of intratumoral heterogeneity is crucial for the accuracy and specificity of MRI evaluation of cancer. BOLD MRI, which is widely used for investigating tumor oxygenation, is sensitive to the structure and function of tumor vasculature. We present a method, based on BOLD effect (R_2^* dynamics), for differentiating subregions in rat 13762NF tumors that show different degrees of sensitivity with respect to hyperoxic and hypoxic gas breathing challenges. We further show the potential connection between the classified heterogeneity and tumor growth.

4500 Computer 36

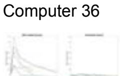

Diffusion MRI can provide non-invasive early biomarkers of the outcome of irreversible electroporation tumor treatment in a mouse model.

Matteo Figini[1], Zhanliang Su[1], Tianchu Lyu[1], Xifu Wang[1], Xiaoke Huang[1], Daniel Procissi[1], Andrew Christian Larson[1], and Zhuoli Zhang[1]

[1]*Radiology, Northwestern University, Chicago, IL, United States*

This study investigates diffusion MRI changes after treatment with irreversible electroporation (IRE) in a murine cancer model. The mean and standard deviation of the ADC in regions of interest covering the whole tumors increased 1 day after treatment and then returned gradually to the pre-treatment values. A strong correlation was found between the volume increase and the maximum relative change in ADC mean and standard deviation. Therefore we propose diffusion MRI as an early tool to predict the outcome of IRE treatment in tumors.

4501 Computer 37

Extracting oxygen-enhancing components from OE-MRI using ICA

Firas Moosvi[1], Jennifer H.E. Baker[2], Andrew Yung[3], Piotr Kozlowski[3], and Stefan Reinsberg[1]

[1]*Department of Physics & Astronomy, University of British Columbia, Vancouver, BC, Canada,* [2]*Department of Integrative Oncology, BC Cancer Research Centre,* [3]*UBC 7T MRI Research Centre, University of British Columbia*

MRI methods to assess tissue oxygenation have recently flourished. Here we explore how a common signal processing technique (independent component analysis) can be used to extract and amplify signal from oxygen stimuli in mouse tumours. With just dynamic T1-weighted images and ICA to extract the enhancing pixels, we can create rich parameter maps corresponding to a response to an oxygen challenge.

4502 Computer 38

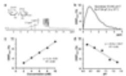

Extracellular-extravascular accumulation of non-caloric sweetener (sucralose) provides CEST contrast for cancer detection

Puneet Bagga[1], Mohammad Haris[2], Kevin D'Aquilla[1], Francesco Marincola[2], Hari Hariharan[1], and Ravinder Reddy[1]

[1]Department of Rediology, University of Pennsylvania, Philadelphia, PA, United States, [2]Research Branch, Sidra Medical and Research Center, Doha, Qatar

We show the utility of a non-nutritive sweetener, sucralose, as a contrast agent in cancer MRI studies by exploiting its chemical exchange saturation transfer (sucCEST) property. The extracellular-extravascular accumulation of sucralose in a glioma model provides localized, temporal changes in the CEST contrast, corroborating the gadolinium-enhanced MRI. These findings illustrate the potential of sucCEST for diagnosis and monitoring of the therapeutic response of cancers, including gliomas in preclinical studies.

4503 Computer 39

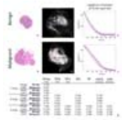

Characterization of lymph nodes in colorectal cancer using non-exponential modeling of T2* decay

Inês Santiago[1], Andrada Ianus[1,2], Celso Matos[1], and Noam Shemesh[1]

[1]Champalimaud Research, Champalimaud Centre for the Unknown, Lisbon, Portugal, [2]Centre for Medical Image Computing, Dept. Computer Science, University College London, London, United Kingdom

Lymph node staging is determinant in the management of cancer patients. Noninvasive imaging modalities have limited accuracy to distinguish malignant form benign lymph nodes. For that purpose, we investigated putative nonexponential (multicompartmental) and potentially non-monotonic decay in simple multi-gradient-echo(MGE) MRI in colorectal cancer. We find that frequency offsets arising from multicompartment models distinguish malignancy from normal tissues (as identified from histopathology), while relaxation rates or fractions do not. Such experiments are potentially suggestive of a simple yet useful tool for nodal staging.

4504 Computer 40

Evaluation of PET and MR datasets in integrated 18F-FDG PET/MRI: a comparison of different MR sequences for whole-body restaging of breast cancer patients.

Johannes Grueneisen[1], Axel Wetter, Julian Kirchner, Sonja Kinner, Verena Ruhlmann, Michael Forsting, and Lale Umutlu

[1]Diagnostic and Interventional Radiology, University Hospital Essen, Essen, Germany

Simultaneous PET/MR imaging has been successfully implemented for whole-body staging of numerous tumor entities within the last four years. However, to date, the introduced study protocols were acquainted with prolonged examination times, potentially impeding patient comfort and patient compliance. The present results demonstrate the high diagnostic capability of integrated PET/MR imaging for staging patients with suspected breast cancer recurrence. Furthermore, facing the need for an optimization of dedicated MR study protocols for whole-body PET/MR imaging on oncological purposes, the present data support the application of fast, yet morphologically adequate PET/MR protocols, leaving the application of contrast-agent and DWI debatable.

4505 Computer 41

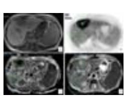

A novel DTI derived heterogeneity index discriminating liver metastasis from normal appearing liver tissue: a PET-MRI study

DAN STEIN[1,2], Natalia Goldberg [1], Liran Domachevsky [1], Hanna Bernstine[1], Meital Nidam [1], Dorit Stern [1], Ifat Abadi-Korek[1], Jacob Sosna , and David Groshar[1]

[1]Radiology, Assuta Medical Center, Tel-Aviv, Israel, [2]Anatomy & Anthropology, Tel-Aviv University

This study's purpose was to compare DTI heterogeneity index with F18 fluorodeoxyglucose (FDG) standardized uptake value (SUVpeak) in liver metastases and in normal appearing liver tissue. The newly defined diffusion coefficient index (DCV) showed a stronger correlation to SUVpeak ($r=0.714$, $p<0.001$) than any other MR metrics evaluated. A threshold of DCV >0.05 and SUVpeak>2.88, correctly classified 28/35 (80%) and 32/35 (91.43%) liver metastases with AUC of 0.939 and 0.989, respectively. DCV, may provide quantitative data of tissue heterogeneity associated with liver metastases. In addition, DCV introduces a potential biomarker index as a quantitative discriminator of liver metastases.

4506 Computer 42

Exploring flow effects on BOLD MRI with oxygen challenge in orthotopic lung tumor model

Heling Zhou[1], Zhongwei Zhang[1], Zhang Zhang[2], Jo Wagner[1], James Campbell[1], Shanrong Zhang[3], Debabrata Saha[2], Masaya Takahashi[3], and Ralph P Mason[1]

[1]Radiology, Univ Texas Southwestern Medical Center, Dallas, TX, United States, [2]Radiation Oncology, Univ Texas Southwestern Medical Center, Dallas, TX, United States, [3]Advanced Imaging Research Center, UT Southwestern Medical Center, Dallas, TX, United States

Blood oxygen level dependent (BOLD) is sensitive to deoxyhemoglobin providing information on tumor oxygenation. However, the measurements are affected by blood flow. This study explored the extent of flow sensitivity by comparing the BOLD signal intensity and T_2* values with and without flow suppression using an orthotopic lung tumor model. T_2* appeared to be insensitive to flow for the tumor regions as observed in this preliminary study, while semi-quantitative ΔSI was strongly affected by flow and is a potential caveat. For well vascularized normal tissue (such as liver), flow suppression will be necessary for accurate measurements.

4507 Computer 43

A probabilistic approach to automated classification of distinct pathological regions in soft tissue sarcoma using diffusion and T2 relaxation

Shu Xing[1,2], Carolyn Freeman[3], Sungmi Jung[4], and Ives Levesque[1,2,5]

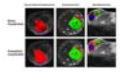

[1]Physics, McGill University, Montreal, QC, Canada, [2]Medical Physics Unit, McGill University, Montreal, QC, Canada, [3]Radiation Oncology, McGill University Health Centre, Montreal, QC, Canada, [4]Pathology, McGill University Health Centre, Montreal, QC, Canada, [5]Research Institute of the McGill University Health Centre, Montreal, QC, Canada

In this work, we propose a novel probabilistic reference-region-based segmentation method to automatically distinguish various pathological tissue regions within soft tissue sarcoma, including high cellularity, high T2 and necrosis. The classification is based on a calculation of the probability that a tumour voxel belongs to a given class using the quantitative diffusion and T2 information when compared to a reference tissue. The probabilistic approach provides a more realistic classification of the complex tumour microenvironment compared to the previous proposed binary classification method.

4508 Computer 44

Microenvironmental changes in prostatic tissues in relation to tumor growth in low risk prostate cancer

Hugh Harvey[1], Veronica A Morgan[1], Christopher Parker[2], and Nandita M deSouza[1]

[1]CRUK Imaging Centre, The Institute of Cancer Research, Surrey, United Kingdom, [2]Academic Urology Unit, The Royal Marsden Hospital NHS Foundation Trust, Sutton, United Kingdom

In 50 men with prostate cancer managed by active surveillance, changes in diffusion and perfusion within normal prostate and tumor were compared between those whose tumors did (“Growers”) or did not grow. 14% had >50% increase in tumor volume on MRI at 1-year. In these men, ADC of normal PZ was lower and more homogenous and remained unchanged over time; vascular metrics also remained stable. In TZ, no changes occurred in ADC or vascular metrics. In tumor, K_{ep} increased with time in growers and ADC histogram metrics showed a left-shift indicating changes in tumor vascular and cellular microstructure with progression.

4509 Computer 45

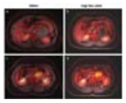

Optimized Fast High-Resolution Whole-Body Imaging Protocols for Clincial Oncologic PET/MRI

Simone Angela Winkler[1], Anne Muehe[1], Ashok Theruvath[1], Maryam Aghighi[1], Sandra Luna-Fineman[1], Neyssa Marina[1], Ranjana Advani[1], Valentina Taviani[2], Samantha J Holdsworth[1], Praveen Gulaka[1], and Heike Daldrup-Link[1]

[1]Stanford University, Stanford, CA, United States, [2]GE Healthcare

We present a fast sequence with high diagnostic accuracy to move towards high-throughput clinical whole-body cancer staging using PET/MRI. Ferumoxytol-contrast enhanced T1-weighted LAVA-Flex is acquired at 16s/bed, at a voxel size of 3.4x1.5x1.9mm. This contrast-enhanced sequence offers superior vessel contrast and resolution to existing T1 co-registration modalities that are most commonly based on MR attenuation correction sequences or longer T1-weighted sequences. Integration of this sequence in a clinical protocol bears the promise of dramatically accelerated whole-body cancer staging with durations <20min, thus offering similar exam times to the more radiation-invasive alternative of PET/CT.

4510 Computer 46

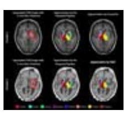

Localization of Subcortical Structures with the Presence of Lesions in Clinical Brain MRI

Long Xie[1,2], Yanhui Ding[3], James C. Gee[1,4,5], Andreas M. Rauschecker[4], and Jeffrey D. Rudie[4]

[1]Penn Image Computing and Science Laboratory (PICSL), Department of Radiology, University of Pennsylvania, Philadelphia, PA, United States, [2]Bioengineering, University of Pennsylvania, Philadelphia, PA, United States, [3]School of Information Science and Engineering, Shandong Normal University, Jinan, People's Republic of China, [4]Department of Radiology, University of Pennsylvania, Philadelphia, PA, United States, [5]School of Computer Science & Engineering, University of Electronic Science and Technology of China, Chengdu, People's Republic of China

In this study, we proposed a pipeline to locate subcortical structures in patients with deep gray matter lesions using clinical brain MRI images. Due to altered signal intensity profile caused by lesions and high slice thickness (~5mm), segmentation of clinical MRI images provide challenges for state-of-the-art algorithms. Our proposed pipeline generates better subcortical structure segmentations, including better lesion coverage and more reliable segmentations than other widely used algorithms. The proposed pipeline may have help in automating the diagnosis of subcortical lesions, potentially improving current clinical practice.

4511 Computer 47

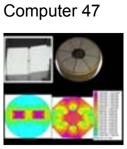

An experimental and computational study of magnetic nanoparticle movement in response to an external magnetic force

Areej Alghamdi[1], Munitta Muthana[1], and Martyn Paley[2]

[1]Oncology and Metabolism, University of Sheffield, Sheffield, United Kingdom, [2]Academic Radiology, University of Sheffield, Sheffield, United Kingdom

This study investigates the ability of two different magnet arrays to capture magnetic nanoparticles from a flow system located at different distances from the magnet face. The magnet fields and gradients and hence magnetic forces were simulated using FEMM software. MR Images were acquired to qualitatively assess the trapping which were compared with quantitative iron concentrations measured using inductively coupled plasma mass spectrometry.

4512 Computer 48

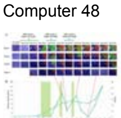

Multi slice MRSI-based generation of nosological images of therapy response using a semi-supervised source extraction approach in preclinical glioblastoma.

Nuria Arias-Ramos[1,2], Silvia Lope-Piedrafita[2,3], Victor Mocioiu[2,4], Margarida Julià-Sapé[1,2,4], Carles Arús[1,2,4], and Ana Paula Candiota[1,2,4]

[1]Departament de Bioquímica i Biologia Molecular, Unitat de Bioquímica de Biociències, Universitat Autònoma de Barcelona, Cerdanyola del Vallès, Spain, [2]Networking Research Center on Bioengineering, Biomaterials and Nanomedicine (CIBER-BBN), Cerdanyola del Vallès, Spain, [3]Servei de Ressonància Magnètica Nuclear, Universitat Autònoma Barcelona, Cerdanyola del Vallès, Spain, [4]Institut de Biotecnologia i de Biomedicina, Universitat Autònoma de Barcelona, Cerdanyola del Vallès, Spain

Glioblastoma (GBM) is the most common aggressive primary brain tumour in adults and characterization of response to treatment turns out to be crucial for improving patient survival. In this work we obtained 3D-like information, from preclinical GBM under temozolomide (TMZ) treatment, with a multi-slice MRSI approach using source-based nosological images as response biomarker. A “Tumour Response Index” (TRI) was defined as the percentage of responding tumor pixels divided by the total tumour pixels. Heterogeneous response patterns with cyclical longitudinal variations were observed in several mice while responding pixels were mostly seen at the first 2 upper grids.

Electronic Poster

TBI: Mechanisms & Therapies

Exhibition Hall — Wednesday 8:15 - 9:15

4513 — Computer 1

Decreased apparent fibre density in an experimental model of traumatic brain injury

David K Wright[1,2], Leigh A Johnston[2,3], Jeff Kershaw[4], Roger Ordidge[5], Terence J O'Brien[6], and Sandy R Shultz[6]

[1]Department of Anatomy and Neuroscience, The University of Melbourne, Melbourne, Australia, [2]The Florey Institute of Neuroscience and Mental Health, Parkville, Australia, [3]Department of Electrical & Electronic Engineering, The University of Melbourne, Australia, [4]National Institute of Radiological Sciences, Japan, [5]Department of Anatomy and Neuroscience, The University of Melbourne, Australia, [6]Department of Medicine, The University of Melbourne, Australia

Apparent fibre density (AFD) is postulated to be a sensitive marker of white matter damage and, as it is derived from a continuous fibre orientation distribution, may identify changes along single fibre bundles in regions containing multiple fibre groups. Here, we compared AFD to traditional DTI metrics in an experimental model of traumatic brain injury (TBI). We found that rats given a TBI had widespread regions of reduced AFD when compared to sham-injured rats as well as significant, but less extensive changes in DTI metrics. These results support the use of AFD in assessing disease progression and treatment following TBI.

4514 — Computer 2

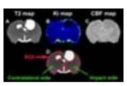

Therapeutic Effect of Bone Marrow Stromal Cells on Vascular Permeability and Hemodynamic Alteration in Traumatic Injured Brain: A long-term MRI Study

Lian Li[1], Michael Chopp[1,2], Guangliang Ding[1], Changsheng Qu[3], Qingjiang Li[1], Asim Mahmood[3], and Quan Jiang[1,2]

[1]Neurology, Henry Ford Health System, Detroit, MI, United States, [2]Physics, Oakland University, Rochester, MI, United States, [3]Neurosurgery, Henry Ford Health System, Detroit, MI, United States

Cerebral vascular permeability and hemodynamic alteration in a broad normal appearing brain tissue in response to the transplantation of hMSCs after TBI were longitudinally investigated up to 3-months post-injury. Our data reveal the evidence that a quicker recovery of vascular integrity, as a result of cell transplantation, is associated with a higher level of cerebral perfusion, and acute cell administration after TBI significantly promotes these global therapeutic effects. The findings of the current study indicate that BBB reconstitution plays an essential role in CBF restoration in the injured brain, which in turn, contributes to the improvement of functional outcome.

4515 — Computer 3

Automated Versus Manual Analysis of DTI and Blood Flow in Adolescents with Chronic Post-Concussive Symptoms

Samuel Barnes[1], Brenda Bartnik-Olson[1], Holshouser Barbara[1], and Stephen Ashwal[2]

[1]Radiology, Loma Linda University, Loma Linda, CA, United States, [2]Pediatrics, Loma Linda University, Loma Linda, CA, United States

Adolescents who sustained a concussion and had persistent symptoms were scanned with DSC-PWI, to assess blood flow, and DTI. Images were compared with controls using automatically defined ROIs by registration to an atlas, and manually drawing ROIs. While both techniques showed similar trends manual ROIs has less variance within groups and therefore greater sensitivity. To detect subtle imaging changes after concussion on an individual basis, manual ROIs, despite being time intensive to define, should still be considered due to their greater sensitivity.

4516 — Computer 4

magna cum laude

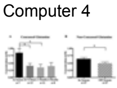

Reduced Brain Glutamine in Female Varsity Rugby Athletes after Concussion

Amy L Schranz[1,2], Kathryn Y Manning[1,2], Gregory A Dekaban[3,4], Lisa Fischer[5], Kevin Blackney[3,4], Christy Barreira[3], Tim Doherty[6], Douglas Fraser[7], Arthur Brown[3,8], Ravi S Menon[1,2], and Robert Bartha[1,2]

[1]Centre for Functional and Metabolic Mapping, Robarts Research Institute, London, ON, Canada, [2]Medical Biophysics, University of Western Ontario, London, ON, Canada, [3]Robarts Research Institute, London, ON, Canada, [4]Microbiology and Immunology, University of Western Ontario, London, ON, Canada, [5]Family Medicine and Fowler Kennedy Sport Medicine Clinic, University of Western Ontario, London, ON, Canada, [6]Physical Medicine and Rehabilitation, University of Western Ontario, London, ON, Canada, [7]Paediatrics Critical Care Medicine, London Health Sciences Centre, London, ON, Canada, [8]Anatomy and Cell Biology, University of Western Ontario, London, ON, Canada

The effect of concussion on female athletes is underreported in the literature. This study found reduced glutamine in the prefrontal white matter of female varsity rugby athletes after concussion and in non-concussed athletes after a season of play using proton magnetic resonance spectroscopy (MRS). Additionally, using diffusion tensor imaging, decreased fractional anisotropy and increased radial diffusivity were found within the spectroscopy voxel in athletes after a season of play. The observed changes were uncorrelated with clinical test scores suggesting these imaging metrics may be more sensitive to brain injury and could aid in concussion diagnosis and monitoring.

4517 — Computer 5

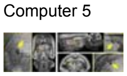

9.4 Tesla in vivo Quantitative Susceptibility Mapping (QSM) detects thalamic calcium influx associated with repeated mild traumatic brain injury (mTBI)

Ferdinand Schweser[1,2], Austin Poulsen[3], Dhaval Shah[1], Nicola Bertolino[1], Marilena Preda[1,2], Jenni Kyyriäinen[4], Asla Pitkänen[4], Robert Zivadinov[1,2], and David J Poulsen[3]

[1]Buffalo Neuroimaging Analysis Center, Department of Neurology, Jacobs School of Medicine and Biomedical Sciences, University at Buffalo, The State University of New York, Buffalo, NY, United States, [2]MRI Clinical and Translational Research Center, Jacobs School of Medicine and Biomedical Sciences, University at Buffalo, The State University of New York, Buffalo, NY, United States, [3]Department of Neurosurgery, Jacobs School of Medicine and Biomedical Sciences, University at Buffalo, The State University of New York, Buffalo, NY, United States, [4]Department of Neurobiology, A. I. Virtanen Institute for Molecular Sciences, University of Eastern Finland, Kuopio, Finland

This work investigated if Quantitative Susceptibility Mapping (QSM) can detect thalamic Ca^{2+} influx associated with an alteration of the N-methyl-D-aspartate receptor in a rodent model of mild TBI (mTBI). We found significant concentrations of calcium after repeated mTBI, but not after single mTBI, suggesting that persistent calcium deposits represent a primary pathology of repeated injury.

4518 Computer 6

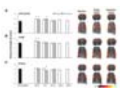

Evolving Functional Connectivity in Rats following Mild Traumatic Brain Injury

Yu-Chieh Jill Kao[1,2], Chia-Feng Lu[1,2,3], Huai-Lu Chen[1,4], Ping-Huei Tsai[1,2,5], Fei-Ting Hsu[1,5], Hua-Shan Liu[1,6], Gilbert Aaron Lee[1,4], Paul Blakeley[1,4], Li-Chun Hsieh[1,5], Bao-Yu Hsieh[7], and Cheng-Yu Chen[1,2,5]

[1]Translational Imaging Research Center, College of Medicine, Taipei Medical University, Taipei, Taiwan, [2]Department of Radiology, School of Medicine, Taipei Medical University, Taipei, Taiwan, [3]Department of Biomedical Imaging and Radiological Sciences, National Yang-Ming University, Taipei, Taiwan, [4]Department of Medical Research, Taipei Medical University Hospital, Taipei, Taiwan, [5]Department of Medical Imaging, Taipei Medical University Hospital, Taipei, Taiwan, [6]School of Biomedical Engineering, College of Biomedical Engineering, Taipei Medical University, Taipei, Taiwan, [7]Department of Biomedica, China Medical University, Taichung, Taiwan

Longitudinal rsfMRI showed the hyper-connectivity in the primary somatosensory cortex and DMN in the acute phase after experimental impact acceleration injury. This is the first demonstration of functional connectivity change with the preserved brain structure after mTBI in rats.

4519 Computer 7

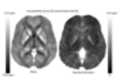

Longitudinal Quantitative Susceptibility Changes after Mild Traumatic Brain Injury

Kevin Koch[1], Robin Karr[1], Brad Swearingen[2], Ashley LaRoche[2], Casey Anderson[1], Timothy B Meier[2], Michael McCrea[2], and Andrew Nencka[1]

[1]Radiology, Medical College of Wisconsin, Milwaukee, WI, United States, [2]Neurosurgery, Medical College of Wisconsin, Milwaukee, WI, United States

We present findings of longitudinal quantitative susceptibility mapping measurements on a cohort of contact sport athletes that were imaged longitudinally (24 hour, 8 day, 6 month) following diagnosed sport-related concussions (N=22). A cohort (N=29) of contact sport controls was imaged longitudinally using the same protocol and allowed stability assessment stability of the measurement. In regions of high stability, changes in susceptibility after injury were assessed in comparison to an atlas constructed from the control data. Substantial susceptibility variations after injury were found in the deep brain nuclei, which recovered and stabilized in the following two measurement points.

4520 Computer 8

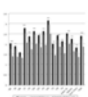

Early NAA Reductions predict Neuropsychological Outcomes after Pediatric TBI

Barbara Holshouser[1], Jamie Pivonka-Jones[2], Joy Nichols[2], Udo Oyoyo[1], Karen Tong[1], and Stephen Ashwal[3]

[1]Radiology, Loma Linda University, Loma Linda, CA, United States, [2]Pediatric Psychology, Loma Linda University, Loma Linda, CA, United States, [3]Pediatric Neurology, Loma Linda University, Loma Linda, CA, United States

The primary aim of this prospective study was to test the hypothesis that early 3D MR spectroscopic (MRSI) changes in discrete regions of the brain after TBI predict neuropsychologic outcomes 1 year after injury. MRSI was acquired at 3T in 68 pediatric mild to severe TBI subjects and 72 controls. Subacute NAA/Cr and NAA/Cho ratios were significantly reduced in TBI patients in all brain regions. A binary logistic regression analysis using combined subcortical NAA/Cr ratios alone predicted dichotomized neurologic outcome (93%), Full Scale IQ (78%), General Memory (82%) and General Attention (88%).

4521 Computer 9

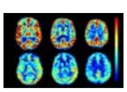

Detecting perfusion deficits in concussive blast subjects using arterial spin labeling

Swati Rane[1], Jalal B Andre[2], and Christine MacDonald[3]

[1]Radiology, University of Washington Medical Center, Seattle, WA, United States, [2]Neuroradiology, University of Washington Medical Center, Seattle, WA, United States, [3]Neurological Surgery, University of Washington Medical Center, Seattle, WA, United States

This work applied ASL imaging to understand perfusion abnormalities in concussive brain injury. Results show overall reduction in cerebral perfusion, with significant decreases in the frontal and temporal lobes as well as the insula.

4522 Computer 10

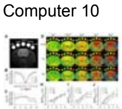

Mapping of endogenous glucose content on the detection of hypometabolic syndrome in experimental traumatic brain injury by glucoCEST

Tsang-Wei Tu[1], Wael Ibrahim[2], Neekita Jikaria[3], Dima Hammoud [3], and Joseph Frank[3]

[1]Radiology and Imaging Sciences, National Institutes of Health, Bethesda, MD, United States, [2]National Library of Medicine, National Institutes of Health, [3]Radiology and Imaging Sciences, National Institutes of Health

The current study investigated the feasibility of using glucoCEST technique, without delivering exogenous glucose as contrast agent, to measure the endogenous glucose content in brain by optimizing the saturation power and duration. The glucoCEST data were compared to the gold-standard ^{14}C-2-deoxyglucose autoradiography for testing the sensitivity and specificity in the detection of hypometabolic syndrome in a rat model of diffuse traumatic brain injury (TBI). The glucoCEST showed comparable results to the 2DG-autoradiography showing glucose uptake largely decreased after TBI. Our findings suggest that glucoCEST could be a robust and reliable imaging modality capable of monitoring glucose metabolism non-invasively.

4523 Computer 11

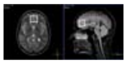

Increased cerebral level of GABA- in the acute phase of children's mild traumatic brain injury.

Petr Menshchikov[1,2], Tolibjon Akhadov[2], Olga Bozhko[2], and Natalia Semenova[1,2]

[1]Semenov Institute of Chemical Physics, Russian Academy of Sciences, Moscow, Russian Federation, [2]Clinical and Research Institute of Urgent Pediatric Surgery and Trauma, Moscow, Russian Federation

There is not any information about [GABA] and [GABA]/[GLX] balance in human brain in acute phase of mTBI, but animal studies have shown alterations in concentrations of major inhibitory and excitatory neurotransmitters. [GABA-], [GABA+] and [GLX] were studied *in vivo* using MEGA-PRES pulse sequence in young patients (mean age - 16±2) with acute phase of mTBI. [GABA-]/[GLX] was significantly increased (p<0.05) in patients and [GABA-]/[tCr] had a trend for increase (p=0.09). This results correlates with animals experiments. [GABA+] didn't show any effects. Thus, [GABA-] MEGA-PRESS is more preferable for accurate [GABA] estimation.

4524 Computer 12

Increased regional cerebral venous oxygen saturation in mild traumatic brain injury is correlated with neurophysiological function: a magnetic susceptibility mapping study

Chao Chai[1], Chao Zuo[2], Linlin Fan, Tianyi Qian, E Mark Haacke, Shuang Xia, and Wen Shen

[1]Radiology Department, Tianjin First Central Hospital, Tianjin, People's Republic of China, [2]Department of Nuclear Medicine, Cangzhou Central Hospital

The aim of this study is to explore the changes of regional cerebral venous oxygen saturation (SvO_2) in patients with mild traumatic brain injury (mTBI) using susceptibility mapping (SWIM). SWIM was reconstructed from magnitude and phase data of SWI to measure the susceptibility of cerebral veins in mTBI patients and healthy controls. The results suggested that overall regional cerebral SvO_2 was higher in mTBI patients than controls. The regional cerebral SvO_2 shows that decreased to normal levels along with an increase in elapsed time post trauma and a high-SvO_2 condition is an evidence of neurophysiological deficit.

4525 Computer 13

Fronto-Parietal Brain Metabolites Changes Following Traumatic Brain Injury

Ping-Hong Yeh[1], Chen-Haur Yeh[1], Gerard Riedy[1], Wei Liu[1], Grant Bonavia[1], and John Ollinger[1]

[1]National Intrepid Center of Excellence, United States, MD, United States

Changes of the fronto-parietal brain metabolites following traumatic brain injury can be reflected in cognitive performance and self-reported psychological function. These results suggest that MRSI might be sensitive to the disturbance of brain metabolites in chronic military mTBI.

4526 Computer 14

Symptom-related Alterations of Thalamocortical Connectivity in mild Traumatic Brain Injury: An fMRI Connectome Study

Chia-Feng Lu[1,2,3], Li-Chun Hsieh[1,4], Yu-Chieh Jill Kao[1,2], Ho-Fang Huang[1,5], Wen-Jin Hsieh[1,4], Fei-Ting Hsu[1,4], Ping-Huei Tsai[1,2,4], Hua-Shan Liu[1,6], Hui-Hsien Lin[1,4], Huai-Lu Chen[1,5], and Cheng-Yu Chen[1,2,4]

[1]Translational Imaging Research Center, College of Medicine, Taipei Medical University, Taipei, Taiwan, [2]Department of Radiology, School of Medicine, College of Medicine, Taipei Medical University, Taipei, Taiwan, [3]Department of Biomedical Imaging and Radiological Sciences, National Yang-Ming University, Taipei, Taiwan, [4]Department of Medical Imaging, Taipei Medical University Hospital, Taipei, Taiwan, [5]Department of Medical Research, Taipei Medical University Hospital, Taipei, Taiwan, [6]School of Biomedical Engineering, College of Biomedical Engineering, Taipei Medical University, Taipei, Taiwan

Disrupted thalamocortical networks and elevated connectivity between thalamic nuclei can reveal the clinical symptoms in mild traumatic brain injury.

4527 Computer 15

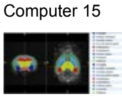

High-Resolution DTI and Volumetric Analysis in a Mouse Model of Mild-to Moderate TBI

Talaignair N Venkatraman[1], Chris Petty[2], Haichen Wang[3], John Nouls[4], Allen W Song[2], and Chris D Lascola[1]

[1]Radiology, Duke University Medical Center, Durham, NC, United States, [2]BIAC, Duke University Medical Center, Durham, NC, [3]Neurology, Duke University Medical Center, Durham, NC, [4]CIVM, Duke University Medical Center, Durham

3D High-Resolution DTI and volumetric analyses in a mouse model of sub-acute injury after TBI with and without neuroprotective therapy.

4528 Computer 16

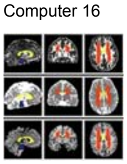

How strictly are traumatic microbleeds related to the actual diffuse axonal injury?

Arnold Toth[1], Balint Kornyei, Noemi Kovacs, Andras Buki, Tamas Doczi, Peter Bogner, and Attila Schwarcz

[1]Department of Neurosurgery, University of Pécs, Pécs, Hungary

This study aims to reveal the relation between traumatic microbleeds (TMBs) on susceptibility weighted imaging and diffuse axonal injury (DAI). Regional TMB and diffusion tensor imaging (DTI) data were collected from 38 traumatic brain injury patients, and 20 control subjects. Analyses included multiple linear regression among TMB parameters, clinical variables and DTI data. Only basal ganglia area TMBs were found to be significantly related to DTI alteration indicating DAI. In general, TMBs might be rather due to microvascular vulnerability than actual DAI, however, specifically basal ganglia area TMBs might be still regarded as markers of DAI.

4529 Computer 17

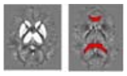

Quantitative Susceptibility Mapping of Hockey Players After Mild Traumatic Brain Injury

Anna Pukropski[1], Alexander Weber[1], Michael Jarrett[1], Christian Kames[2], Shiroy Dadachanji, David K. B. Li[3], Jack Taunton[4], and Alexander Rauscher[5]

[1]Pediatrics, University of British Columbia, Vancouver, BC, Canada, [2]University of British Columbia, Vancouver, BC, Canada, [3]Radiology, University of British Columbia, Vancouver, BC, Canada, [4]Division of Sports Medicine, University of British Columbia, Vancouver, BC, Canada, [5]Pediatrics, University of British Columbia, BC, Canada

We followed 45 varsity hockey players during one season of play, and scanned all players at the beginning of the season. 11 players received a concussion, and were scanned within 72hrs post-concussion, and then again after 2 weeks and 2 months. Quantitative Susceptibility Maps were created from the multi-echo 3D gradient-echo data, and susceptibility values were measured in deep grey matter (caudate, pallidum, putamen, and thalamus) and frontal and posterior WM in the corpus callosum (genu and splenium). A linear mixed-effect model analysis of the regions of interest revealed no significant changes over time compared to baseline.

4530 Computer 18

Characterizing White Matter Microstructural Changes After Mild Traumatic Brain Injury Based On Diffusion White Matter Tract Integrity And Shannon Entropy

Sohae Chung[1,2], Els Fieremans[1,2], Xiuyuan Wang[1,2], Dmitry S. Novikov[1,2], Farng-Yang A. Foo[3], Steven R. Flanagan[4], and Yvonne W. Lui[1,2]

[1]Center for Advanced Imaging Innovation and Research (CAI2R), Department of Radiology, New York University School of Medicine, New York, NY, United States, [2]Bernard and Irene Schwartz Center for Biomedical Imaging, Department of Radiology, New York University School of Medicine, New York, NY, United States, [3]Department of Neurology, New York University Langone Medical Center, New York, NY, United States, [4]Department of Rehabilitation Medicine, New York University Langone Medical Center, New York, NY, United States

Mild traumatic brain injury (MTBI) is a growing public health problem and some patients may suffer from long-term symptoms. This study shows that there are both microstructural changes as well as regional textural changes after MTBI affecting the corpus callosum within 4 weeks of injury. We demonstrate the potential for compartment specific white matter tract integrity (WMTI) metrics such as tortuosity of the extra-axonal space (a marker of misalignment of fibers or demyelination), and Shannon entropy (reflecting complexity or uncertainty) to be useful as early biomarkers of MTBI-related WM injury.

4531 Computer 19

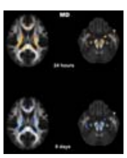

Identifying potential sites of brain injury in an individual concussed football player using a normative database based on diffusion kurtosis imaging

L. Tugan Muftuler[1], Daniel V. Olson[2], and Michael A. McCrea[1]

[1]Department of Neurosurgery, Medical College of Wisconsin, Milwaukee, WI, United States, [2]Department of Biophysics, Medical College of Wisconsin, Milwaukee, WI, United States

Mild traumatic brain injury (mTBI) is a prevalent health problem, especially in full-contact sports[1, 6]. Despite its prevalence, there is still a lack of reliable, unbiased biomarkers of brain injury and recovery following mTBI. Diffusion weighted MRI techniques have gained attention recently in studies of mTBI. Diffusion kurtosis tensor imaging (DKTI) is an extension of the conventional DTI, which estimates non-Gaussianity of bulk diffusion in each voxel. Our studies indicated that DKTI might be potential biomarker to detect subtle changes in brain tissues[5]. Here, we introduce a workflow to detect sites of brain injury in an individual concussed subject.

4532 Computer 20

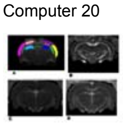

Measurements of Microstructural Changes after Sildenafil Treatment of Experimental Traumatic Brain Injury in Rats using Diffusion Tensor Imaging

Asamoah Bosomtwi[1,2], Alexandru Korotcov[1,2], Angela Pronger[3], Margalit Haber[1], Andrew Hoy[2,3], Ramon Diaz-Arrastia[3,4], and Bernard J Dardzinski[2,3]

[1]Center for Neuroscience and Regenerative Medicine, Henry Jackson Foundation, Bethesda, MD, United States, [2]Radiology and Radiological Sciences, Uniformed Services University of Health Sciences, Bethesda, MD, United States, [3]Center for Neuroscience and Regenerative Medicine, Uniformed Services University of Health Sciences, Bethesda, MD, United States, [4]Neurology, Uniformed Services University of Health Sciences, Bethesda, MD, United States

The long-term dynamic response of microstructural changes in rat brain to the administration of sildenafil after traumatic brain injury (TBI) using non-invasive MRI techniques have been investigated. Our results demonstrate that the treatment of diffuse traumatic brain injury with sildenafil reverses several changes in brain microstructure at 30 days post injury. Diffusion tensor imaging (DTI) data suggests that sildenafil treatment improves white matter reorganization after TBI in rats compared with saline treatment.

4533 Computer 21

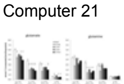

Improved Anaplerotic Metabolism Following Sodium Pyruvate, Ethyl Pyruvate or Glucose Supplementation after Experimental Traumatic Brain Injury

Brenda Bartnik Olson[1], Katsunori Shijo[2], Sima Ghavim[2], Neil Harris[2], and Richard Sutton[2]

[1]Radiology, Loma Linda University, Loma Linda, CA, United States, [2]Neurosurgery, David Geffen School of Medicine at UCLA

Traumatic brain injury initiates a cascade of events including increased oxidative stress that contributes to the period of generalized metabolic depression. Previously, sodium and ethyl pyruvate and glucose supplementation were shown to reduce cell death and improve recovery following experimental TBI. In this study we used ^{13}C NMR spectroscopy to determine if sodium pyruvate, ethyl pyruvate or glucose supplementation influences the activity of metabolic pathways associated with the intracellular redox state and oxidative metabolism. Our findings show improvements in astrocyte anaplerotic metabolism following all fuel treatments. Only animals treated with sodium pyruvate showed improved oxidative metabolism in neurons. None of the fuel treatments reduced the amount of glucose metabolized via the pentose phosphate pathway. The restoration of astrocyte metabolism by these fuels may partially underlie their abilities to improve cerebral glucose utilization and to reduce neuronal loss following experimental TBI.

4534 Computer 22

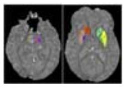

TBI Patients with Cerebral Microhemorrhage Exhibit Increased Magnetic Susceptibility in the Cerebral Hemispheres, but Reduced Magnetic Susceptibility in the Basal Ganglia

Wei Liu[1,2], Gerard Riedy[1], Ping-Hong Yeh[1,2], Dominic E. Nathan[1,2], Grant H. Bonavia[1], and John Ollinger[1]

[1]National Intrepid Center of Excellence, Walter Reed National Military Medical Center, Bethesda, MD, United States, [2]The NorthTide Group, LLC, Dulles, VA, United States

Magnetic susceptibilities of the basal ganglia, as well as the right and left cerebral hemispheres of TBI patients with cerebral microhemorrhage (CMH) were analyzed. Compared to patients without CMH and controls, patients with CMH demonstrated increased magnetic susceptibility in both the left and right hemispheres but decreased magnetic susceptibility in the basal ganglia. This finding suggests disrupted brain iron hemostatsis due to CMH in the chronic phase of TBI.

4535 Computer 23

Longitudinal changes in cortical thickness in collegiate high contact sports

Maged Goubran[1], Sherveen Parivash[1], Paymon Rezaii[1], Wei Bian[1], Brian Boldt[1], Huy Do[1], David Douglas[1], Eugene Wilson[1], Lex Mitchell[1], Mansi Parekh[1], Scott Anderson[1], Gerald Grant[1], and Michael Zeineh[1]

[1]Stanford University, Stanford, CA, United States

There is emerging evidence that cumulative sports-related concussions may lead to long-term neurological abnormalities. The extent to which changes are occurring in collegiate athletes is still undetermined, and the progression of these changes is poorly understood. Cross sectional studies with small cohorts have found that concussions maybe be associated with cortical thinning in young football players [(1,2)]. We analyze the longitudinal changes occurring in high vs. low contact sports over the course of 3-4 years.

4536 Computer 24

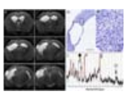

Chronically elevated Taurine in the putative seizure onset zone during posttraumatic epileptogenesis identifies epilepsy-prone rats

Riikka Johanna Immonen[1], Amna Yasmin[1], Asla Pitkänen[1], and Olli Gröhn[1]

[1]Neurobiology, A.I.Virtanen Institute, Univ. Eastern Finland, Kuopio, Finland

In lateral fluid percussion rat model for posttraumatic epilepsy 50% of animals have slowly developed epilepsy 1 year after the head injury.[1] The seizures presumably originate in the perilesional cortex that appears normal in conventional MRI.2 We targeted localized magnetic resonance spectroscopy (MRS) to this cortical area 6 months post-injury, and found elevated Taurine and elevated macromolecule concentration to differentiate the subpopulation (19%) of injured animals with higher susceptibility to seizures in EEG recorded PTZ test. The preliminary immunohistochemical analysis of the underlying complex pathology revealed swollen neurons that may associate with the increase of osmoregulator taurine.

Electronic Poster

Novel Neuroimaging Techniques

Exhibition Hall Wednesday 8:15 - 9:15

4537 Computer 25

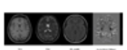

Learning how to see the invisible - using machine learning to find underlying abnormality patterns in reportedly normal MR brain images from patients with epilepsy

Oscar Bennett[1], M. Jorge Cardoso[1], John Duncan[2,3], Gavin Winston[2,3], and Sebastien Ourselin[1]

[1]Translational Imaging Group, Centre for Medical Image Computing, University College London, London, United Kingdom, [2]Department of Clinical and Experimental Epilepsy, UCL Institute of Neurology, London, United Kingdom, [3]Epilepsy Society MRI Unit, Chalfont St Peter, United Kingdom

The visual identification of subtle abnormalities in MR brain images that underlie focal epilepsies is a challenging problem. In this study, we used machine learning techniques to uncover patterns of abnormality that exist within reportedly normal brain images from individuals with epilepsy. Our results demonstrated that abnormalities exist in MR images reported to be normal by a human reader, and that these abnormalities exist in a different spatial pattern to that seen in visually apparent cases. We obtained novel insights into why visual assessment may be ineffective in these visually normal cases and provide suggestions on how to improve this situation.

4538 Computer 26

Water exchange in a white matter tissue phantom measured using clinically feasible diffusion exchange spectroscopy (DEXSY) MRI

Dan Benjamini[1], Michal E Komlosh[1,2], and Peter J Basser[1]

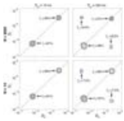

[1]Quantitative Imaging and Tissue Sciences, National Institutes of Health, Bethesda, MD, United States, [2]Center for Neuroscience and Regenerative Medicine, Bethesda, MD, United States

Studying the axons' membrane permeability at different white matter tracts could clarify the role of aquaporins. Diffusion exchange spectroscopy (DEXSY) is an assumption-free approach to measure water exchange, allowing for any number of exchange processes between any number of compartments. It has never been applied in biological MRI owing to its exceptionally long scan time requirements. Here we present a method to reduce the number of required acquisitions, making DEXSY-MRI clinically feasible for the first time. We apply this method on a nerve tissue phantom, and demonstrate that 14 acquisitions are sufficient to determine the exchange spectrum.

4539 Computer 27

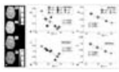

The Anomalous Diffusion γ-parameter depends on local magnetic susceptibility differences when quantified in human brain tissue by MRI

Alessandra Caporale[1,2], Marco Palombo[3,4], Emiliano Macaluso [5], Michele Guerreri[4,6], Marco Bozzali[7], and Silvia Capuani[8]

[1]SAIMLAL Dept., Morpho-functional Sciences, Sapienza University of Rome, Rome, Italy, [2]CNR ISC UOS Roma Sapienza, Rome, Italy, [3]MIRCen, Commissariat à l'Energie Atomique, France, Italy, [4]Physics Department, CNR ISC UOS Roma Sapienza, Rome, Italy, [5]ImpAct Team, Lyon Neuroscience Research Center, Lyon, France, France, [6]SAIMLAL Dept., Morphogenesis & Tissue Engineering, Sapienza University of Rome, Rome, Italy, [7]NeuroImaging Laboratory, Santa Lucia Foundation, Rome, Italy, [8]Physics Dept., CNR ISC UOS Roma Sapienza, Rome, Italy

Motivated by previous results obtained in vitro, we investigated the dependence of the anomalous diffusion γ-parameter on local magnetic susceptibility differences ($\Delta\chi$) in human brain. We performed diffusion weighted experiments varying diffusion gradient strengths in eight healthy subjects at 3.0T and measured the rate of relaxation ($R2^*$). We found significant strong linear correlations between γ and $R2^*$ both in white and gray matter selected regions. Conversely, DTI-parameters did not correlate with $R2^*$. Consequently AD-γ depends on $\Delta\chi$ due to differences in myelin orientation and iron content. This makes AD-imaging even more appealing for clinical neuroimaging investigations.

4540 Computer 28

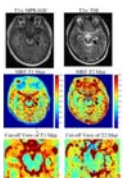

Rapid and Quantitative Parametric Mapping for Mesial Temporal Lobe Epilepsy Using MR Fingerprinting

Congyu Liao[1], Kang Wang[2], Xiaozhi Cao[1], Dengchang Wu[2], Qiuping Ding[1], Hongjian He[1], and Jianhui Zhong[1]

[1]Center for Brain Imaging Science and Technology, Department of Biomedical Engineering, Zhejiang University, Hangzhou, People's Republic of China, [2]Department of Neurology, The First Affiliated Hospital, School of Medicine, Zhejiang University, Hangzhou, People's Republic of China

A recently proposed MR fingerprinting (MRF) technique was used to acquire quantitative multi-parametric maps in about 3 minutes for diagnosis of mesial temporal lobe epilepsy in 20 patients. The results could improve the reliability and sensitivity of MRI evaluations in such patients compared with conventional MRI diagnosis methods.

4541 Computer 29

Single-scan, whole-brain functional network mapping using optogenetic fMRI with CBV

Andrew J Weitz[1], ManKin Choy[2], Ben A Duffy[2], Jia Liu[2], and Jin Hyung Lee[1,2,3,4]

[1]Bioengineering, Stanford University, Stanford, CA, United States, [2]Neurology and Neurological Sciences, Stanford University, Stanford, CA, United States, [3]Neurosurgery, Stanford University, Stanford, CA, United States, [4]Electrical Engineering, Stanford University, Stanford, CA, United States

Optogenetic fMRI studies have traditionally required significant scan averaging to achieve signal-to-noise ratios sufficient for whole-brain functional network mapping. As a result, more scan time is required, and measurements may not directly translate to accompanying behavioral paradigms that employ a single stimulation. Here, we used a SPION-based MRI contrast agent to enable single-scan functional network mapping with CBV during optogenetic stimulation of the thalamic submedial nucleus. Measurement of CBV led to significant activations detected at the site of stimulation and downstream mono- and polysynaptically connected regions. In comparison, single-scan BOLD measurements led to minimal detectable responses to stimulation.

4542 Computer 30

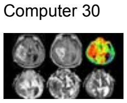

The Relationship between Diffusivity and Electrical Conductivity: Initial Results of an In Vivo Assessment by MRI

Khin Khin Tha[1], Ulrich Katscher[2], Shigeru Yamaguchi[3], Shunsuke Terasaka[3], and Hiroki Shirato[1]

[1]Department of Radiation Medicine, Hokkaido University, Sapporo, Japan, [2]Philips Research Laboratories, Hamburg, Germany, [3]Department of Neurosurgery, Hokkaido University, Japan

Correlation between diffusion kurtosis imaging indices and electrical conductivity was tested in 24 patients with grade II to grade IV gliomas. The results suggest association of electrical conductivity with complexity of tissue microstructure.

4543 Computer 31

Advances in imaging the human brain with inhaled hyperpolarized xenon-129 MRI at 1.5 T

Madhwesha Rao[1], Neil Stewart[1], Paul Griffiths[1], Graham Norquay[1], and Jim Wild[1]

[1]University Of Sheffield, Sheffield, United Kingdom

The feasibility of imaging human brain ***tissue-perfusion*** using inhaled hyperpolarized ^{129}Xe magnetic resonance imaging is demonstrated. Enhancement of ^{129}Xe gas polarization and a custom brain RF coil array have together enabled imaging of hyperpolarized ^{129}Xe dissolved in the human brain at 1.5 T with a quality and signal-to-noise hitherto unseen. The images clearly demonstrate the uptake and washout of ^{129}Xe in the brain with time and could provide novel insights into cerebral perfusion and blood brain barrier permeability without the use of intravenous contrast.

4544 Computer 32

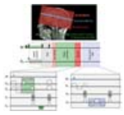

Interleaved pulse sequence for calibrated BOLD based on MRI measurement of venous oxygen saturation

Erin K Englund[1], Maria A Fernandez-Seara[2], Hyunyeol Lee[1], Zachary B Rodgers[1], John A Detre[3], and Felix W Wehrli[1]

[1]Department of Radiology, University of Pennsylvania, Philadelphia, PA, United States, [2]Department of Radiology, University of Navarra, Pamplona, Spain, [3]Department of Neurology, University of Pennsylvania, Philadelphia, PA, United States

An improved interleaved pulse sequence termed “OxBOLD” is presented for calibrated fMRI. OxBOLD measures ASL-based perfusion and BOLD signal changes with whole-brain coverage, in addition to global measures of blood flow and venous oxygen saturation by concatenating background-suppressed 3D-GRASE pCASL, phase contrast, 2D-multi-slice EPI, and dual-echo GRE sequences. The OxBOLD pulse sequence is combined with the Y_v-based calibration model to derive the calibration factor, M, which relates perfusion and BOLD signal changes to the cerebral metabolic rate of oxygen ($CMRO_2$). M-maps derived from OxBOLD have similar M values averaged over grey matter as compared to the traditional Davis calibration model.

4545 Computer 33

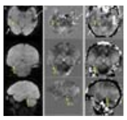

Advancing Quantitative Brain Injury Lesion Imaging Using Total Field Inversion QSM

Salil Soman[1], Zhe Liu[2], Ursula Nemec, Samantha Holdsworth, Keith L Main, Jerome Yesavage, David Hacknkey, Ansgar J Furst, Maheen M Adamson, Yi Wang, Pascal Spincemaille, and Michael Moseley

[1]Radiology, Harvard Medical School / BIDMC, Boston, MA, United States, [2]Cornell University

Traumatic brain injury often results in brain lesions which are subtle. Current conventional MRI techniques (GRE and SWI) are field strength and echo time dependent, causing lesions to possible be missed. QSM methods can overcome this, but with many artifacts and missed lesions due to masking artifacts. TFI QSM can overcome this issue, as we demonstrate in this study of TBI patients.

4546 Computer 34

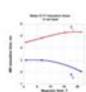

The first observation of 17O MRI in normal rats at 21.1 T

Victor D. Schepkin[1], Andreas Neubauer[2], Christian Schuch[3], Tilo Glaeser[3], Michael Kievel[3], Steven L. Ranner[1], William W. Brey[1], Shannon Helsper[1], and Lothar Schad[2]

[1]CIMAR, NHMFL/FSU, Tallahassee, FL, United States, [2]University of Heidelberg, Mannheim, Germany, [3]NUKEM Isotopes, Alzenau, Germany

The capability of ^{17}O MRI in a rat head was evaluated at the high magnetic field of 21.1 T (NHMFL, Tallahassee). The results demonstrated that ^{17}O MR relaxation times are dependent on the magnetic field strength which correlates with experimental observations for sodium. Well separated MR peaks of ^{17}O water and 6-^{17}O glucose provided the time courses of water distribution and glucose consumption in vivo. 3D ^{17}O MRI is possible with a resolution of 1 mm^3 in normal rats. ^{17}O MRI is a promising tool for future tumor detection and evaluation of tumor glucose consumption rates.

4547 Computer 35

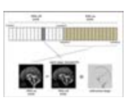

Improvement of dynamic improved motion-sensitized driven-equilibrium steady-state free precession (dynamic iMSDE SSFP) to visualize the irregular motion of cerebrospinal fluid

Tomohiko Horie[1], Nao Kajihara[1], Shuhei Shibukawa[1], Susumu Takano[1], Toshiki Saitou[1], Tetsu Niwa[2], Mitsunori Matsumae[3], Kagayaki Kuroda[4], Makoto Obara[5], Tetsuo Ogino[5], and Isao Muro[6]

[1]Department of Radiology, Tokai University Hospital, Isehara, Japan, [2]Department of Radiology, Tokai University School of Medicine, Isehara, Japan, [3]Department of Neurosurgery, Tokai University School of Medicine, Isehara, Japan, [4]Course of Electrical and Electronic Engineering, Graduate School of Engineering, Tokai University, Hiratsuka, Japan, [5]Healthcare, Philips Electronics Japan Ltd, Shinagawa, Japan, [6]Department of Radiology, Tokai University Hospital, Hachiouji, Hachiouji, Japan

We reported a new technique to visualize the irregular motion of cerebrospinal fluid (CSF) by using dynamic improved motion-sensitized driven-equilibrium steady-state free precession (dynamic iMSDE SSFP). The purpose of this study was to optimize the sequence parameters of dynamic iMSDE SSFP. As a result, the slow and irregular CSF motions were sensitively detected using the following parameters: T2prepTE: 30 ms, dynamic interval: 700 ms, flow VENC: 1 cm/s and the directions of MSG: 3axes. Therefore, optimized dynamic iMSDE SSFP is suggested to contribute to the diagnosis of various diseases in the CSF space.

4548 Computer 36

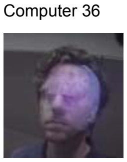

Holographic visualization of brain MRI with Real-Time Alignment to a Human Subject

Christoph Leuze[1], Subashini Srinivasan[1], Michael Lin[1], Brian A Hargreaves[1], Bruce L Daniel[1], and Jennifer A McNab[1]

[1]Stanford, Stanford, CA, United States

In this work we use the Microsoft Hololens for holographic visualization of brain MR imaging data aligned to the real world human body. This provides a way to directly “look inside” the subject’s head instead of treating image and subject as two separate entities.

4549 Computer 37

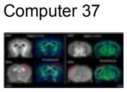

Validation of inhomogeneous Magnetization Transfer (ihMT) as a myelin biomarker

Valentin H Prevost[1], Olivier M Girard[1], Myriam Cayre[2], Gopal Varma[3], Samira Mchinda[1], Jean-Philippe Ranjeva[1], Jean Pelletier[4], Pascale Durbec[2], David C Alsop[3], and Guillaume Duhamel[1]

[1]Aix Marseille Univ, CNRS, CRMBM, UMR 7339, Marseille, France, [2]Aix Marseille Univ, CNRS, IBDM, UMR 7288, Marseille, France, [3]Division of MR Research, Beth Israel Deaconess Medical Center, Harvard Medical School, Boston, MA, United States, [4]Aix Marseille Univ, APHM, Hôpital de La Timone, Pôle de Neurosciences Cliniques, Service de Neurologie, Marseille, France

The ihMT (inhomogeneous Magnetization transfer) signal qualitatively demonstrates sensitivity for myelinated structures. However, image intensity and contrast vary with the saturation parameters, further questioning the specificity of ihM for myelin. This study validated ihMT as a myelin biomarker by demonstrating for various ihMT sequences, linear relationships between ihMT signal and intensity of fluorescence microscopy (a quantitative myelin specific histology technique) collected in plp-GFP mouse brain.

4550 Computer 38

Hybrid EEG and fMRI platform for multi-modal neurofeedback

Marsel Mano[1,2], Elise Bannier[2,3], Lorraine Perronnet[1,2], Anatole Lécuyer[1], and Christian Barillot[2,4,5,6]

[1]Hybrid Team, Inria, Rennes, France, [2]VisAGeS Project-Team, Inria, Rennes, France, [3]Service de Radiologie, CHU Pontchaillou, Rennes, France, [4]VisAGeS U746, Inserm, Rennes, France, [5]UMR CNRS 6074, IRISA, Rennes, France, [6]University of Rennes, Rennes, France

Neurofeedback (NFB) relies on neurosignals for the estimation of brain activity. There exist a wide variety of NFB applications that use one type of neurosignals like fMRI or electroencephalography (EEG). Recently, the combination of two or more neurosignals has been receiving a lot of attention in the research community, but still very few multi-modal NFB applications exist. This is primarily because of the lack of commercial multi-modal NFB systems and the associated technical difficulties in building them.

Here we are going to describe a bi-modal EEG and fMRI NFB platform that we have build in our lab. Our platform is designed to maximize modularity and parallel processing in order to be able to provide real-time NFB with high level of synchronization and minimal delays. We have successfully used our platform to conduct over 100 uni-modal and bi-modal NFB experiments with more than 30 healthy subjects.

4551 Computer 39

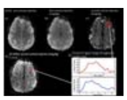

Brain parenchyma pulsatility assessed with ferumoxytol enhanced T2* MRI.

Leonardo A Rivera Rivera[1], Patrick Turski[1,2], Oliver Wieben[1,2], Scott B Reeder[2], Tilman Schubert [2], and Kevin M Johnson[1]

[1]Dept. of Medical Physics, University of Wisconsin-Madison, MADISON, WI, United States, [2]Dept. of Radiology, University of Wisconsin-Madison, Madison, WI, United States

Pulsatility differences in large intracranial arteries and veins have been observed in patients with dementia using 4D flow MRI. How microvascular pulsatility is affected, however, is unclear. Non-invasive methods to monitor capillary pulsatility are still lacking. In this work, we present a method to assess brain parenchyma microvascular pulsatility using T2* signal changes over the cardiac cycle using ferumoxytol enhanced MRI. Significant differences in PI of the cortical gray matter were found when compared to white matter PI values. This method to assess microvascular blood volume pulsatility over the cardiac cycle might serve as a marker to study capillary pulsatility.

4552 Computer 40

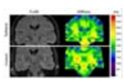

Hippocampal stiffness in mesial temporal sclerosis epilepsy measured by MR elastography: Initial results

Daniel R Smith[1], Hillary Schwarb[2], Ryan Pohlig[3], William C Oliviero[4,5], Bradley P Sutton[4], Tracey M Wszalek[4,5], Graham R Huesman[4,5,6], and Curtis L Johnson[1]

[1]Biomedical Engineering, University of Delaware, Newark, DE, United States, [2]Beckman Institute for Advanced Science and Technology, University of Illinois at Urbana-Champaign, Urbana, IL, [3]College of Health Sciences, University of Delaware, Newark, DE, United States, [4]Beckman Institute for Advanced Science and Technology, University of Illinois at Urbana-Champaign, Urbana, IL, United States, [5]Carle Neuroscience Institute, Carle Foundation Hospital, Urbana, IL, United States, [6]Department of Molecular and Integrative Physiology, Univerity of Illinois Urbana-Champaign, Urbana, IL, United States

Mesial temporal sclerosis (MTS), or hippocampal sclerosis, is the most common form of temporal lobe epilepsy and can be effectively treated by surgery if it is able to be reliably detected. In this work we examine whether hippocampal stiffness measured by magnetic resonance elastography (MRE) is sensitive to MTS. In our preliminary sample of five patients with MTS and seven controls, we found the hippocampus to be softer bilaterally in MTS (-13.4% and -15.2% differences for affected and unaffected sides). This preliminary evidence suggests MRE may provide highly sensitive markers that could aid the diagnosis and treatment of MTS.

4553 Computer 41

N-Acetylcysteine Supplementation Elevates Human Brain Glutathione In Vivo: A Proof-of-Concept Study using J-edited 1H MRS

Nora Weiduschat[1], Xiangling Mao[1], Diana Vu[2], Michelle Blate[2], Guoxin Kang[1], Halinder S. Mangat[3], Amanda Artis[4], Yize Zhao[4], Gudrun Lange[2], Claire Henchcliffe [3], Benjamin H. Natelson[2], and Dikoma C. Shungu[1]

[1]Radiology, Weill Cornell Medicine, New York, NY, United States, [2]Neurology, Mount Sinai Beth Israel Medical Center, New York, NY, United States, [3]Neurology and Neuroscience, Weill Cornell Medicine, New York, NY, United States, [4]Healthcare Policy and Research, Weill Cornell Medicine, New York, NY, United States

A prior finding of robust cortical glutathione (GSH) deficits in patients with chronic fatigue syndrome (CFS) and major depressive disorder (MDD) provided a compelling rationale for this pilot study that aimed to assess whether 4 weeks of daily supplements of 1800mg of the GSH synthetic precursor N-acetylcysteine (NAC) would normalize brain GSH in CFS patients, as measured *in vivo* with J-edited MRS. The study's main finding was that NAC supplementation significantly increased cortical GSH levels in CFS patients compared to controls, while levels of the antioxidant remained statistically unchanged in controls despite a slight numerical increase.

4554 Computer 42

T1 mapping from variable flip angle SPGR and IR-SPGR data using DESPOT1-HIFI

Mohammad Kayvanrad[1,2]

[1]Amirkabir University of Technology, Tehran, Iran, [2]Robarts Research Institute, London, Canada

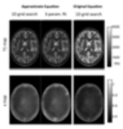

This work aims at improving the calculation of T1 maps at high magnetic fields from a set of VFA SPGR and IR-SPGR images for direct correction of B1 inhomogeneities using DESPOT1-HIFI. In the present work we (i) call attention to an erroneous assumption regarding the IR-SPGR signal intensity equation in the original DESPOT1-HIFI method and derive an alternative equation, and (ii) propose a reduced-dimensions least-squares fitting method, which turns the complex multi-parameter fitting into a simple one-dimensional search.

4555 Computer 43

Ex-vivo Quantitative Susceptibility Mapping of Human Brain Hemispheres

Arnold M. Evia[1], Aikaterini Kotrotsou[1], Robert J. Dawe[1,2,3], Sue E. Leurgans[2,4], Julie A. Schneider[2,4,5], David A. Bennett[2,4], and Konstantinos Arfanakis[1,2,3]

[1]Department of Biomedical Engineering, Illinois Institute of Technology, Chicago, IL, United States, [2]Rush Alzheimer's Disease Center, Rush University Medical Center, Chicago, IL, United States, [3]Department of Diagnostic Radiology, Rush University Medical Center, Chicago, IL, United States, [4]Department of Neurological Sciences, Rush University Medical Center, Chicago, IL, United States, [5]Department of Pathology, Rush University Medical Center, Chicago, IL, United States

In order to establish the role of quantitative susceptibility mapping (QSM) as a diagnostic tool in aging, it is essential to combine QSM with direct assessments of age-related brain pathologies on the same individuals. Using ex-vivo QSM for this purpose may be more advantageous than in-vivo QSM, since ex-vivo QSM assesses the brain in the same condition as histology, and allows imaging of older adults independent of frailty level. However, being able to translate ex-vivo QSM findings to in-vivo is crucial. Therefore, our goal was to investigate the effects of death and fixation on brain QSM data collected ex-vivo.

4556 Computer 44

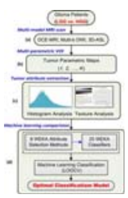

Investigation of machine learning techniques in preoperative glioma grading based on multi-parametric MRI data

Xin Zhang[1], Linfeng Yan[1], Yang Yang[1], Haiyan Nan[1], Yu Han[1], Yuchuan Hu[1], Jin Zhang[1], Ying Yu[1], Yingzhi Sun[1], Qian Sun[1], Zhicheng Liu[1], Wen Wang[1], and Guangbin Cui[1]

[1]Department of Radiology, Tangdu Hospital, Fourth Military Medical University, Xi'an, People's Republic of China

This study demonstrates the significance of integrating multi-parametric MRI attributes and effective machine learning techniques in preoperative glioma grading. A comprehensive scheme combining tumor attribute extraction, attribute selection and classification model was proposed and tested. The tumor attributes were collected from histogram and texture analysis of multi-parameter MRI maps within the whole tumor. The classification performances of 25 commonly used classifiers combined with 8 kinds of attribute selection strategies in differentiating low grade gliomas from high grade gliomas were investigated. Support vector machine (SVM) combined with SVM-RFE attribute selection method were found to exhibit superior performance to others.

4557 Computer 45

Quantitative and qualitative evaluation of "Flexible PET/MRI" images in brain

Mizue Suzuki[1], Yasutaka Fushimi[1], Tomohisa Okada[2], Takuya Hinoda[1], Ryusuke Nakamoto[1], Yuji Nakamoto[1], and Kaori Togashi[1]

[1]Department of Diagnostic Imaging and Nuclear Medicine, Kyoto University Graduate School of Medicine, Kyoto, Japan, [2]Human Brain Research Center, Kyoto University Graduate School of Medicine, Kyoto, Japan

A newly developed " Flexible PET (fxPET)" is a prototype of MR-compatible mobile PET system. We tried to investigate the clinical feasibility of the fxPET with a 1.5T MRI compared with PET/CT for brain imaging. Twenty-one patients (including 12 patients with known intracranial masses) were enrolled in this study. We compared misregistration between fxPET/MRI and PET/CT, and compared the image quality of fxPET and PET in both qualitative (visual rating) and quantitative (standardized uptake value (SUV)-based analysis) manner. Consequently, fxPET/MRI showed acceptable misregistration and enough image quality, revealing clinical feasibility comparable to that of PET/CT.

4558 Computer 46

MR Fingerprinting in paediatric neuroradiology: our initial experience

Graziella Donatelli[1], Guido Buonincontri[2], Rosa Pasquariello[3], Mauro Costagli[2], Raffaello Canapicchi[3], and Michela Tosetti[2,3]

[1]Università di Pisa, Pisa, Italy, [2]IMAGO7 Research Institute, [3]IRCCS Stella Maris, Pisa Italy

In paediatric neuroimaging, young children have often to be sedated in order to obtain diagnostic MRI images. Magnetic Resonance Fingerprinting (MRF) is a potential alternative to sedation in children, as it achieves a fast exam with reduced sensitivity to patient motion. MRF acquisitions can be used to acquire a fully-quantitative anatomical exam in less than five minutes at a standard resolution. We performed a preliminary evaluation of MRF in 15 paediatric patients, acquiring both the standard protocol and MRF at 1.5T. Detection of brain alterations was possible, if present, in all patients. Only a few small lesions were unrevealed. MRF could be a promising tool for a fast and diagnostic exam in children, and due to its low sensitivity to motion it has the potential to allow exams without sedation.

4559 Computer 47

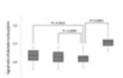

Contrast Agent-Induced High Signal Intensity in Dentate Nucleus on Unenhanced T1-Weighted Images: Comparison of Gadodiamide and Gadoxetic Acid

Shintaro Ichikawa[1], Utaroh Motosugi[1], Yoshie Omiya[1], and Hiroshi Onishi[1]

[1]Department of Radiology, University of Yamanashi, Chuo-shi, Japan

Hyperintensity in the dentate nucleus (DN) on unenhanced T1-weighted images was associated with previous administration of gadodiamide but not gadoxetic acid. There were no significant differences in DN-to-pons ratio between patients who received five or more administrations of gadoxetic acid and those without gadolinium-based contrast agent administration or chronic liver disease. Hyperintensity in the dentate nucleus on unenhanced T1-weighted images is not associated with up to fifteen previous administrations of gadoxetic acid. Therefore, gadolinium deposition in the brain might be difficult despite a history of repeated gadoxetic acid administration.

4560 Computer 48

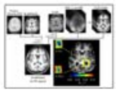

In vivo measurement of water exchange at the human blood-cerebrospinal fluid barrier

Valerie C Anderson[1], Xin Li[1], Aaron Doud[1], Ian J Tagge[1], Eric M Baker[1], Joseph F Quinn[2], Jeffrey A Kaye[2], and William D Rooney[1]

[1]Advanced Imaging Research Center, Oregon Health & Science University, Portland, OR, United States, [2]Dept. of Neurology, Oregon Health & Science University, Portland, OR, United States

Epithelial cells of the choroid plexus contain the blood-CSF barrier and play a pivotal role in brain water homeostasis. Here, DCE-MRI was used to investigate choroid plexus water exchange in 25 older individuals. A marked non-linearity of blood and tissue R_1 values was observed, indicating that water exchange departs the fast exchange limit at clinical blood contrast agent levels. Using a two-site model that explicitly incorporates water exchange between intra- and extraventricular compartments, a mean rate constant for ventricular water efflux, k_{io}, of 0.26 ± 0.13 s^{-1} was obtained. Significant associations of k_{io} with age and cognitive status were found.

Electronic Poster

Cerebrovascular Disease

Exhibition Hall — Wednesday 8:15 - 9:15

4561 Computer 49

Evaluating brain tissue oxygen extraction fraction changes following transfusion therapy using TRUST MRI in adults with sickle cell anemia

Meher R Juttukonda[1], Manus J Donahue[1], Melissa C Gindville[2], and Lori C Jordan[2]

[1]Radiology and Radiological Sciences, Vanderbilt University Medical Center, Nashville, TN, United States, [2]Pediatrics - Division of Pediatric Neurology, Vanderbilt University Medical Center, Nashville, TN, United States

Brain tissue oxygen extraction fraction (OEF) and cerebral blood flow (CBF) have been identified as potential imaging biomarkers for triaging adults with sickle cell anemia (SCA) for aggressive blood transfusion therapy for stroke prevention; however, little is known regarding how tissue-level hemodynamics are affected by transfusions. We utilized noninvasive MRI methods to assess OEF and CBF before and after transfusions in adults with SCA. Our results showed that OEF significantly reduces after transfusion and that this reduction parallels increases in blood oxygen content, while CBF is unchanged.

4562 Computer 50

Evaluation of hemodynamic impairments in healthy elderly participants and patients with high-grade unilateral carotid artery stenosis

Stephan Kaczmarz[1], Jens Göttler[1], Vanessa Griese[1], Jan Petr[2], Kim van de Ven[3], Michael Helle[4], Hendrick Kooijman[5], Anne Kluge[6], Dimitrios C. Karampinos[7], Claus Zimmer[1], Christian Sorg[1,8], and Christine Preibisch[1,8,9]

[1]Department of Neuroradiology, Technical University of Munich, Munich, Germany, [2]PET center, Institute of Radiopharmaceutical Cancer Research, Helmholtz-Zentrum Dresden-Rossendorf, Dresden, Germany, [3]Philips Healthcare, Best, Netherlands, [4]Philips Research, Hamburg, Germany, [5]Philips Healthcare, Hamburg, Germany, [6]Department of Radiation Oncology and Radiotherapy, Charité Berlin, Berlin, Germany, [7]Department of Radiology, Technical University of Munich, Munich, Germany, [8]TUM Neuroimaging Center, Technical University of Munich, Munich, Germany, [9]Clinic for Neurology, Technical University of Munich, Munich, Germany

Internal carotid-artery stenosis (ICAS) causes complex and not yet well understood physiological impairments. We present preliminary data from an ongoing clinical study in ICAS patients and healthy, age-matched participants. The major aims were to evaluate the reliability of a multimodal MRI-protocol and investigate physiological changes. For ICAS patients, regionally impaired vascular-reactivity as well as hypo-perfusion were found. In accordance with literature, we did not find ICAS-induced changes in oxygen extraction on group level. The presented preliminary results thus imply successful application of multimodal MRI methods and are highly promising with respect to gaining a deeper insight into ICAS-related physiological changes.

4563 Computer 51

The brain metabolite change of magnetic resonance spectroscopy for evaluating he Rehabilitation therapy effect of intra-cerebral hemorrhage rat animal model

Sang-Hun Jang[1] and Seung-Man Yu[2]

[1]Gimcheon University, Gimcheon, Korea, Republic of, [2]Gimcheon University, Gimcheon, Korea, Korea, Republic of

The objective of this study were to examine the brain metabolite concentration quantification change by in-vivo 1H-MRS analysis in animal hemorrhage model, and we determined the bio-marker that was shown the effect of exercise treatment in hemorrhage disease. No significant difference in the concentration levels of experimental and control group were observed (p=0.839). There was great significance in revealing that (Glu+Gln)/tCr value was increased, and tCho/tCr concentration level was decrease applying exercise treatment methods on hemorrhage animal model. Therefore, the metabolite concentration change of (Glu+Gln)/tCr and tCho/tCr can be used as a powerful bio-marker that represented an exercise treatment in hemorrhage patients.

4564 Computer 52

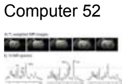

Longitudinal metabolic evolution of rat cortex upon global ischemia: an ultra-short echo time 1H MRS study

Mario G Lepore[1] and Hongxia Lei[1,2]

[1]Biomedical Imaging Research Center, Ecole Polytechnique Fédérale de Lausanne, Lausanne, Switzerland, [2]University of Geneva, Geneva, Switzerland

Stroke is a leading cause for disability. Metabolic evolution of transient ischemia attack might shed insights for diagnosis and prognosis. We aimed to ^{1}H MRS study metabolic evolution of cortex before, during and immediately after 15-min complete global ischemia. Combination of MR angiography (MRA) and ^{1}H MRS allows execution of vascular occlusion models directly in the magnet as well as proper identification and characterization of complete stroke.

4565 Computer 53

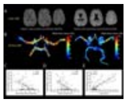

Associations between white matter lesions, age, and 4D flow MRI hemodynamics in 69 patients with Sickle Cell Disease

Lena Vaclavu[1], Zelonna Baldew[1], Sanna Gevers[1], Veronica van der Land[2], Henri JMM Mutsaerts[3], Karin Fijnvandraat[2], John C Wood[4], Charles BLM Majoie[1], Ed T vanBavel[5], Bart J Biemond[6], Aart J Nederveen[1], and Pim van Ooij[1]

[1]Radiology, Academic Medical Center, Amsterdam, Netherlands, [2]Pediatric Hematology, Emma Children's Hospital, Academic Medical Center, Amsterdam, Netherlands, [3]Sunnybrook Research Institute, Toronto, Canada, [4]Cardiology, Children's Hospital Los Angeles, Los Angeles, CA, United States, [5]Biomedical Engineering and Physics, Academic Medical Center, Amsterdam, Netherlands, [6]Internal Medicine, Hematology, Academic Medical Center, Amsterdam, Netherlands

Hemodynamic parameters such as wall shear stress(WSS) may be adversely affected in Sickle Cell Disease(SCD). Vaso-occlusion is a common complication leading to ischemic organ damage. We investigated how impaired hemodynamics (velocity, WSS, flow and lumen area) relate to ischemic white matter lesions(WMLs). Our aim was to quantify age-related changes in hemodynamics and to investigate their relationship with WMLs. 14 controls and 69 patients underwent 4D-flow MRI. We assessed intracranial velocity, WSS, flow and lumen area in the circle of Willis. We show that 4D-flow parameters are decreased in patients with WMLs, but age is an important factor in this relationship.

4566 Computer 54

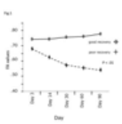

Fractional anisotropy values of pyramidal tract and motor functional recovery: intracerebral hemorrhage patients study

Takashi Inoue[1], Yasutaka Kuzu[2], Yoshiyuki Kanbara[2], Shunro Fujiwara[2], Kuniaki Ogasawara[2], and Teiji Tominaga[3]

[1]Neurosurgery, Sendai Medical Center, Sendai, Japan, [2]Neurosurgery, Iwate Meical University, Morioka, Japan, [3]Neurosurgery, Tohoku University Graduate School of Medicine, Sendai, Japan

Patients with ICH are sometimes treated with surgical evacuation. However, the efficacy of surgery remains unclear for recovery of motor function. We assessed the relationship between motor function outcome and sequential change of FA in patients, to explore whether motor function outcome can be predicted in the early phase. The FA values of the cerebral peduncle on day 3 could predict the motor function outcome on day 90. Patients with severe motor paresis and FA value of greater than 0.7 should be considered for surgical evacuation.

4567 Computer 55

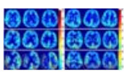

Comparison of the Arterial transit artifact of pcASL between stroke patients with cerebral artery stenosis and normal controls

Le He[1], Shuo Chen[1], Zhensen Chen[1], Lixia Yang[2], Xihai Zhao[1], Chun Yuan[1,3], and Huijun Chen[1]

[1]Center for BioMedical Imaging Research,Tsinghua, Beijing, People's Republic of China, [2]Department of Image Center, Shanghai Xuhui Center Hospital, Shanghai, People's Republic of China, [3]Department of radiology, University of Washington, Seattle, WA, United States

Cerebral blood flow (CBF) reduction below a certain threshold is a main cause leading to cerebral ischemia . Arterial Spin Labeling (ASL) is a noncontrast MRI perfusion technique that can quantify CBF. Although ATA may be problematic for CBF quantification, there are evidences suggest that ATA may be a useful imaging biomarker to represent collateral flow and indicate better outcomes , this study aims to investigate the difference of ATA prevalence between stroke patients with cerebral artery stenosis and healthy volunteers. It was found that the stroke patients have more brain regions with long arterial transit time compared with healthy volunteers using a manual review method to estimate the overall CBF of subject while allowing ATA detection, suggesting ATA could be a potential imaging biomarker.

4568 Computer 56

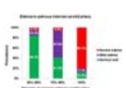

Association between Occluded Extra-cranial Carotid Artery Disease and Arterial Wall Edema in Ipsilateral Petrous Internal Carotid Artery: A 3D MR Vessel Wall Imaging Study

Xiaoyi Chen[1,2], Huilin Zhao[3], Zechen Zhou[4], Le He[2], Rui Li[2], Chun Yuan[2,5], and Xihai Zhao[2]

[1]Beijing Institute for Brain Disorders, Capital Medical University, Beijing, People's Republic of China, [2]Center for Biomedical Imaging Research, Department of Biomedical Engineering, Tsinghua University, Beijing, People's Republic of China, [3]Department of Radiology, Renji Hospital, School of Medicine, Shanghai Jiao Tong University, Shanghai, People's Republic of China, [4]Philips Research China, Philips Healthcare, Beijing, People's Republic of China, [5]Department of Radiology, University of Washington, Seattle, United States

Carotid artery severe stenosis or occlusion will lead to decreases in blood flow and ischemia in downstream arterial segments. It has been shown that ischemia within vessel wall may lead to wall edema which will affect the vascular revascularization after interventional treatment for the severe stenotic or occluded diseases. This study investigated the correlation between extra-cranial carotid artery stenotic diseases and arterial wall edema in ipsilateral petrous internal carotid artery (ICA) using 3D MR vessel wall imaging. We found that proximal ICA severe stenosis was independently associated with wall edema in ispilateral petrous ICA (OR=2.45, 95% CI 1.65-3.63, P<0.001).

4569 Computer 57

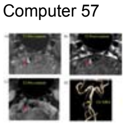

Prevalence and Clinical Relevance of Intraplaque Haemorrhage in Stenotic and Non-stenotic Basilar Artery Intracranial Atherosclerotic Plaque

Chengcheng Zhu[1], Xia Tian[2], Andrew Degnan[3], Zhongzhao Teng[4], Jianping Lu[2], David Saloner[1], and Qi Liu[2]

[1]Radiology, University of California, San Francisco, San Francisco, CA, United States, [2]Radiology, Changhai Hospital, Shanghai, People's Republic of China, [3]Radiology, University of Pittsburgh, PA, United States, [4]Radiology, University of Cambridge, Cambridge, United Kingdom

Intraplaque hemorrhage (IPH) in intracranial arteries is a possible marker of increased stroke risk. While previous studies focused on stenotic arteries, non-stenotic arteries also cause fatal stroke. We studied 100 patients using high-resolution MRI and found IPH was prevalent (>20%) in both stenotic and non-stenotic basilar arteries, and was a strong predictor of symptoms with an odd ratios of 15.4. IPH has a very high specificity (97.1%) to predict symptoms. Specifically, IPH may be useful in selecting high risk stroke patients with clinically non-significant stenosis, who may benefit from more aggressive treatment.

Computer 58

Cerebral perfusion characteristics show differences in younger vs. older children with sickle cell anaemia: results from a multiple inflow-time arterial spin labelling study

Jamie M Kawadler[1], Patrick W Hales[1], Fenella J Kirkham[1], and Chris A Clark[1]

4570

[1]Developmental Neurosciences, UCL Great Ormond Street Institute of Child Health, London, United Kingdom

Sickle cell disease (SCD) is associated with chronic anaemia and oxygen desaturation, which elevates cerebral blood flow (CBF) and increases risk of stroke. Cerebral haemodynamics are abnormal and techniques for assessing CBF using a single inflow-time may not be sufficient. This study investigated haemodynamic parameters from a multi-inflow-time acquisition in younger and older children with SCD and healthy controls. CBF was elevated globally in both groups of patients, but in older children, patients had significantly shorter bolus arrival time. This may indicate increasing disparity between patients and controls with age and may be related to longer standing burden of disease.

4571 Computer 59

4D Flow assessment of ophthalmic artery flow in patients with atherosclerotic internal carotid artery stenotic disease

Tetsuro Sekine[1], Ryo Takagi[1], Yasuo Amano[1,2], Yasuo Murai[3], Yoshimitsu Fukushima[1], Erika Orita[1], Takahiro Andoh[1], Yoshio Matsumura[3], and Shin-ichiro Kumita[1]

[1]Radiology, Nippon Medical School, Tokyo, Japan, [2]Radiology, Nihon University School of Medicine, Tokyo, Japan, [3]Neurosurgery, Nippon Medical School, Tokyo, Japan

We performed 4D Flow MRI assessment of the ophthalmic artery (OphA) flow in patients with internal carotid artery stenosis (ICS). Twenty-one consecutive patients with unilateral ICS were recruited. 4D Flow MRI and acetazolamide-stress brain perfusion SPECT were performed. The flow direction on the affected-side OphA was categorized into native flow and non-native flow based on 4D Flow MRI. In the affected-side MCA territory, the ratio of rest cerebral blood flow to normal control ($RCBF_{MCA}$) and cerebral vascular reserve (CVR_{MCA}) were calculated from SPECT dataset. Eleven patients had native OphA flow and the remaining 10 had non-native OphA flow. $RCBF_{MCA}$ and CVR_{MCA} were significantly lower in non-native flow group (84.9±18.9% vs. 69.8±7.3%, p<0.05; 36.4±20.6% vs. 17.0±15.0%, p<0.05). Four patients in the non-native flow group and none in the native flow group were confirmed as high-risk (Sensitivity/Specificity, 1.00/0.65). The 6 min-standard 4D Flow MRI assessment of OphA in patients with ICS can predict intracranial hemodynamic impairment.

4572 Computer 60

Slower Information Processing Speed is related to White-Matter Integrity in Sickle Cell Disease

Hanne Stotesbury[1], Fenella J Kirkham[1], Chris A Clark[1], and Jamie M Kawadler [1]

[1]Developmental Neurosciences, UCL Great Ormond Street Institute of Child Health, London, United Kingdom

Sickle cell disease (SCD) is associated with stroke[1] and slower processing[2]. Slower processing in the absence of stroke may be related to hypoxic-ischaemic white-matter (WM) injury[3]. Cognitive assessments and tract-based spatial statistics analyses using diffusion tensor imaging (DTI), were conducted in 84 patients with SCD, stratified by degree of hypoxic-anaemic exposure. Processing speed indices (PSI) were related to WM integrity, and there were differences in PSI and WM integrity as a function of daytime oxygen-desaturation, but not SCI. The results provide links between oxygen desaturation, PSI, and WM integrity, and may indicate amelioration of function by interventions that reduce hypoxic exposure.

4573 Computer 61

Cerebral perfusion and reactivity in Impaired Glucose Tolerance and Type-2 Diabetes using arterial spin labeling

Maria-Eleni Dounavi[1,2], Aneurin J. Kennerley[2,3], Solomon Tesfaye[4], Christopher Martin[2,3], Dinesh Selvarajah[4], Elaine Boland[1], and Iain D. Wilkinson[1,2]

[1]Academic Unit of Radiology, University of Sheffield, Sheffield, United Kingdom, [2]Neuroimaging in Cardiovascular Disease (NICAD) Network, University of Sheffield, Sheffield, United Kingdom, [3]Department of Psychology, University of Sheffield, Sheffield, United Kingdom, [4]Academic Unit of Diabetes, University of Sheffield, Sheffield, United Kingdom

This study evaluates cerebral perfusion and cerebrovascular reserve (CVR) in impaired glucose tolerance and patients with type-2 diabetes using QUASAR Arterial Spin Labeling. CVR was evaluated as the change in gray matter CBF in response to a pharmacological stimulus. The developed processing pipeline was based on published QUASAR theory, modified to account for excessive motion and partial volume effects. Results show that baseline CBF is within the expected range. In patients with T2DM and IGT there is a significantly lower value of Cerebrovascular Reserve compared to healthy, normoglycaemic individuals.

4574 Computer 62

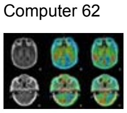

The use of Arterial Spin Labeling to Evaluate Posterior Circulation Ischemia in the elderly group (>80 years)

Rui Jia[1], Ningyu An[2], Xian Xu, and Bing Wu[3]

[1]Department of Radiology, General Hospital of the People's Liberation Army, Beijing, People's Republic of China, [2]General Hospital of the People's Liberation Army, [3]GE Healthcare company

Contrast free arterial spin labeling approach is used to assess the perfusion changes in PCI in the elderly group (>80yrs)compared with normal control elderly group. Lower perfusion level was seen in PCI group, also a long PLD time is more effective in detecting the PCI group in case of slower perfusion rate. The lower level of increment with a long PLD in PCI group also indicates the weakened perfusion ability in the posterior circulation.

4575 Computer 63

Serial MRI of Lateral Ventricular Enlargement to Measure Rate of Brain Atrophy in Patients with Ischemic Stroke

Muhammad E. Haque[1], Refaat E. Gabr[1], Khader M Hasan[1], Jerome Jeevarajan[1], Jonathan Izygon[1], Duyen M Nghiem[1], Clark W Sitton[1], Ponnada A Narayana[1], and Sean I Savitz[1]

[1]UTHealth Science Center of Houston, Houston, TX, United States

The primary objective of this longitudinal study is to determine the rate of ipsilesional and contralesional lateral ventricular volume (LVv) enlargement in six mild chronic ischemic stroke patients who underwent serial brain MRI at four time points over one year. Infarct volumes, National Institutes of Health Stroke Scale (NIHSS), LVv, gray matter volume (GMv) and white matter volume (WMv) were also measured. Our results show the ipsilesional increase in LVv and the decrease in WMv suggests post-stroke progression of unilateral atrophy. These changes appear to be independent of the decrease in NIHSS during this same period. This study suggests that MRI can detect pathology that is not reflected by NIHSS.

4576 Computer 64

Study on the correlation between carotid bifurcation anatomy and atherosclerotic plaque by high resolution MR

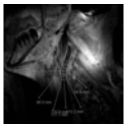

Xiao Gao[1], Shengzhang Ji[1], Yulong Gao[1], Jinyu Song[1], Ran Du[1], Zhizheng Zhuo[2], and Shengli Chen[1]

[1]Tianjin 4th Center Hospital, Tianjin, People's Republic of China, [2]Philips Healthcare, Beijing, People's Republic of China

Based on carotid MR imagings performed on a 3.0T MR scanner with an eight-channel phased-array carotid coil, including 3D TOF, BB-T1WI, BB-T2WI, 3D MP-RAGE, 3D MERGE, We investigated the characteristics of the internal carotid artery angle and common carotid artery bifurcation angle, and compare different forms of carotid bifurcation, analyzed the occurrence of the vulnerable plaques and plaque components, found that bifurcation angles of the internal carotid artery and the common carotid artery have a close relationship with the occurrence of atherosclerosis. Vulnerable plaque with LRNC is more likely to occur at the large angle of the internal carotid artery.

4577 Computer 65

The Sensorimotor Network Dysfunction in Migraineurs WithoutAura: A Resting-state fMRI study

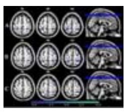

Jilei Zhang[1], Jingjing Su[2], Mengxing Wang[1], Qian Yao[2], Haifeng Lu[1], Hui Zhang[1], Jianqi Li[1], Jian-Ren Liu[2], and Xiaoxia Du*[1]

[1]Shanghai Key Laboratory of Magnetic Resonance and Department of Physics, School of Physics and Materials Science, East China Normal University, Shanghai, People's Republic of China, [2]Department of Neurology and Jiuyuan Municipal Stroke Center, Shanghai Ninth People's Hospital, Shanghai Jiao Tong University School of Medicine, Shanghai, People's Republic of China

In current study, we analyzed resting-state fMRI data for the first time to evaluate the dysfunction of the sensorimotor network in migraineurs without aura by applying regional homogeneity (ReHo), amplitudes of low-frequency fluctuation (ALFF) and degree centrality (DC) analysis methods. The ReHo, DC and ALFF values were decreased in the S1 and PMC indicating the sensorimotor network dysfunction in migraineurs without aura. These changes may result in disruption of discrimination of sensory features of pain, thereby affecting nociception pathways. Non-invasive brain stimulation could be applied to sensorimotor network to modulate headache pain in future therapies.

4578 Computer 66

Ischemic brain lesions and cognition in patients with aneurysmal subarachnoid hemorrhage.

Mariska E Hendriks[1], Irene MC Huenges-Wajer[2], Theo D Witkamp[3], Jeroen Hendrikse[4], Gabriel JE Rinkel[4], Johanne MA Visser-Meily[4], Mervyn DI Vergouwen[4], and Jill B De Vis[5]

[1]Radiology, University Medical Center Utrecht, Utrecht, Netherlands, [2]Rehabilitation, University Medical Center Utrecht, [3]University Medical Center Utrecht, Netherlands, [4]University Medical Center Utrecht, [5]Radiology, University Medical Center Utrecht, Washington, DC, United States

A significant amount of patients with aneurysmal subarachnoid hemorrhage suffer from cognitive impairment. The exact origin of this cognitive impairment is unclear. Lesions developing in relation to the event have been hypothesized as the mechanism of action. However, literature on this topic is inconclusive. We aimed to scrutinize this by analyzing our cohort of patients. Lesions were found in 60% of patients, no relation was found with cognitive outcome, This could be due to selection bias as most of the included patients had a good or mild impaired clinical status at admission and demonstrated 'no cognitive impairment' at follow-up.

4579 Computer 67

Water Diffusion Heterogeneity in Cytoxic Edema

Kevin Midlash[1], Yong Jeong[2], Charles Cantrell[2], Keigo Kawaji[1], Greg Christoforidis[1], and Timothy J. Carroll[1]

[1]University of Chicago, Chicago, IL, United States, [2]Northwestern, Evanston, IL, United States

Modern stroke research and treatment depend on the ability to accurately characterize and quantify diffusion volume. Current methods for segmentation and quantification of diffusion volumes are largely manual and time intensive. In this paper, we explored and validated a method of automatic segmentation of diffusion volumes. This algorithm was validated against known values from previous studies. We then studied the number of angles required to accurately predict diffusion volumes. We determined accurate volumes can be determined with as few as 3 directional vectors while accurate infarct mapping requires only 7 allowing for reduced scan time.

4580 Computer 68

Sickle hemoglobin vs. normal hemoglobin: Any changes in susceptibility?

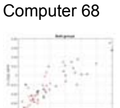

Cihat Eldeniz[1], Michael Binkley[2], Dustin K. Ragan[3], Melanie Fields[3], Kristin Guilliams[3], Liam Comiskey[3], Yasheng Chen[3], Andria L Ford[3], Jin-Moo Lee[3], and Hongyu An[1]

[1]Mallinckrodt Institute of Radiology, Washington University in St. Louis, St. Louis, MO, United States, [2]Washington University in St. Louis, St. Louis, MO, United States, [3]Washington University in St. Louis

Alterations in cerebral oxygenation may be helpful as an imaging biomarker to predict stroke risk in sickle cell disease (SCD). Such measurement requires the knowledge of susceptibility properties of sickle hemoglobin, HbS. In this study, we aimed at measuring volume susceptibility difference between fully-oxygenated and full-deoxygenated blood, $\Delta\chi o$, of HbS and HbA. The measured $\Delta\chi o$ of HbA is consistent with literature reported range, and $\Delta\chi o$ of HbS is greater than that of HbA. However, this difference does not reach statistical significance.

4581 Computer 69

How does acute hypertensive crisis affect brain volume? A structural MRI study

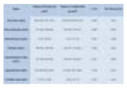

Arzu Ceylan Has[1], Mehmet Yasir Pektezel[2], Mehmet Akif Topcuoglu[2], Rahsan Gocmen[3], Bulent Erbil[4], Nalan Metin Aksu[4], Ethem Murat Arsava[2], and Kader K. Oguz[3]

[1]National Magnetic Resonance Research Center (UMRAM), Ankara, Turkey, [2]Department of Neurology, Faculty of Medicine, Hacettepe University, Ankara, Turkey, [3]Department of Radiology, Faculty of Medicine, Hacettepe University, Ankara, Turkey, [4]Department of Emergency Room, Faculty of Medicine, Hacettepe University, Ankara, Turkey

Acute elevations in systemic blood pressure can lead to a wide spectrum of central nervous system manifestations, including catastrophic scenarios like intracerebral hemorrhage. We hypothesized that brain swelling occurs in hypertensive crisis patients, assessed by structural MRI. We prospectively collected MRI data from a consecutive series of patients admitted to the emergency department with a diagnosis of hypertensive urgency but no neurologic symptoms. A second MRI was obtained at 3-months follow-up of blood pressure normalization. MRI analysis revealed reductions in cortical and sub-cortical gray matter after normalization of blood pressure.

4582 Computer 70

Visualization of Post Stroke Revascularization on a Rat Model Using Dual R1- and Compressed Sensing Assisted R2*-MRAs

MungSoo Kang[1] and HyungJoon Cho[1]

[1]Department of Biomedical Engineering, Ulsan National Institute of Science and Technology, Ulsan, Korea, Republic of

The visualization of post stroke revascularization is of particular importance for the prognosis and therapeutic measures. In this work, using dual contrast R_1-R_2^*-MRAs, visualization of post stroke revascularization on a rat model was performed. R_1-R_2^*-MRAs were used to visualize surface and inner regions of rat brain, respectively. As a result of post stroke revascularization, all MRAs clearly showed thickened vessel structures in ipsilateral hemisphere.

4583 Computer 71

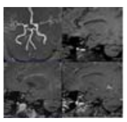

The Value of High-resolution MRI and Perfusion Weighted Imaging in the Middle Cerebral Artery Atherosclerotic Stenosis

Shanshan Xie[1], Jingliang Cheng, Yong Zhang, and Chengru Song

[1]The First Affiliated Hospital of Zhengzhou University, Zhengzhou, People's Republic of China

This study aimed to explore the assessment value of HRMRI and PWI in patients of TIA with unilateral MCA atherosclerotic stenosis. 43 patients with MCA territory symptoms underwent preliminary DWI and MRA to exclude acute cerebral infarction and ascertain unilateral stenosis of MCA M1 segment. Thereafter, all the patients underwent HRMRI and PWI. HRMRI gets 155 positive slices，type Ⅲ of plaque 49 (31.6%), Ⅳ~Ⅴa 41 (26.5%), Ⅴb 4 (2.5%), Ⅵ 13 (8.4%), Ⅴc 48 (31.0%). The soft plaques(type Ⅳ~Ⅴa and VI) adds up to 54 (34.8%), hard plaques (type III, Ⅴb and Ⅴc) 101 (65.2%). HRMRI diagnosed four cases of mild stenosis, 11 moderate, 22 severe and 6 occlusion. 42 patients has hemisphere perfusion difference between the affected and normal MCA perfusion districts, with lower rCBF , longer rMTT and TTP (P <0.05) in the affected side. HRMRI can assess AHA sub-type and stability of atherosclerotic plaque, and stenosis rate of MCA, MTT, TTP can be found changes in early ischemic events, which are sensitive parameters to diagnose TIA.

4584 Computer 72

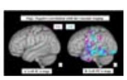

NODDI revealed the brain microstructural damage in patients with moyamoya disease

Shoko Hara[1,2], Masaaki Hori[1], Syo Murata[1], Ryo Ueda[1], Misaki Nakazawa[1], Yoji Tanaka[2], Taketoshi Maehara[2], Shigeki Aoki[1], and Tadashi Nariai[2]

[1]Department of Radiology, Juntendo University, Tokyo, Japan, [2]Department of Neurosurgery, Tokyo Medical and Dental University, Tokyo, Japan

We applied Neurite Orientation Dispersion and Density Imaging (NODDI) and neurophysiological batteries to 13 patients with moyamoya disease (10 females, age 16-61 yo). We found that intracellular volume fraction (Vic) and orientation dispersion index (OD) decreased as the stages of vascular lesion progressed, and many neurocognitive tasks correlated with the decrease in Vic and OD among different parts of brain. Interestingly, some tasks were much more correlated with the Vic and OD among posterior part of brain than among frontal part. This finding may suggest the importance of PCA lesions in neurocognitive disturbance in patients with moyamoya disease.

Electronic Poster

Functional MRI: Miscellaneous

Exhibition Hall — Wednesday 8:15 - 9:15

4585 Computer 73

In vivo evidence of negative fMRI response without decrease in neuronal activity: a combined optogenetic fMRI and electrophysiology study

Brittany Katz[1,2,3], Daniel Albaugh[2,3,4], Chunxiu Yu[5], Martin J MacKinnon[1,2], Warren Grill [5], and Yen Yu Ian Shih [2,6]

[1]Biomedical Research Imaging Center, University of North Carolina Chapel Hill, Chapel Hill, NC, United States, [2]Neurology, University of North Carolina Chapel Hill, Chapel Hill, NC, United States, [3]Neurobiology, University of North Carolina Chapel Hill, Chapel Hill, NC, United States, [4]Biomedical Research Imaging Core, University of North Carolina Chapel Hill, Chapel Hill, NC, United States, [5]Biomedical Engineering, Duke University, Durham, NC, United States, [6]Biomedical Research Imaging Center, Unveristy of North Carolina Chapel Hill, Chapel Hill, NC, United States

Neurovascular coupling is the central principle of functional magnetic resonance imaging (fMRI), and thus critical for the interpretation of most fMRI data. While the strong majority of studies support such a tight coupling between neuronal and vascular activity changes in the cortex, the case may not be so straightforward in brain areas containing different cell types such as the striatum, wherein negative fMRI response has been observed to be positively correlated with1, 2, or uncorrelated with electrophysiologically-measured neuronal activity3, 4. Thus, the rodent striatum is an attractive platform to mechanistically dissect the rules governing neurovascular coupling, providing a novel case in which known coupling rules are violated. Taking this path, we began by asking a simple yet critical question: are neuronal activity increases in striatum causal in striatal negative fMRI response? Our results, employing an optogenetic-fMRI approach coupled with correlative in vivo electrophysiology, reveal that, indeed, selective excitation of striatal neurons drives large-scale local negative fMRI response. However, complementary electrophysiological data also described here suggests that the link between striatal neuronal activity and hemodynamics is more complicated than straightforward negative coupling

---

4586 Computer 74

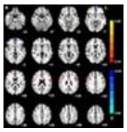

Abnormal resting-sate functional connectivity of thalamus in patients with paroxysmal kinesigenic dyskinesia

Guangxiang Chen[1], Du Lei[1], Jiechuan Ren[2], Xiaoqi Huang[1], Dong Zhou[2], and Qiyong Gong[1]

[1]Huaxi MR Research Center (HMRRC), Department of Radiology, West China Hospital, Sichuan University, Chengdu, People's Republic of China, [2]Department of Neurology, West China Hospital, Sichuan University, Chengdu, People's Republic of China

The underlying pathophysiological mechanisms of paroxysmal kinesigenic dyskinesia are still not fully understood. The aim of this study was to investigate the patterns of resting-sate functional connectivity of thalamus in patients with paroxysmal kinesigenic dyskinesia. Our novel findings of abnormal resting-sate functional connectivity from thalamus to precentral gyrus and medial frontal gyrus provided direct evidence that the basal ganglia-thalamo-cortical circuit may play an important role in the pathogenesis of paroxysmal kinesigenic dyskinesia.

4587 Computer 75

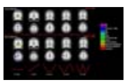

Associative areas and cerebellum show non-linear modulation of fMRI signal when using the non-dominant hand

Adnan A.S. Alahmadi[1,2], Rebecca S. Samson[1], Matteo Pardini[1,3], Egidio D'Angelo[4,5], Karl J. Friston[6], Ahmed T. Toosy[1], and Claudia AM Gandini Wheeler-Kingshott[1,4,7]

[1]UCL Institute of Neurology, Queen Square MS Centre, University College London, London, United Kingdom, [2]Department of Diagnostic Radiology, Faculty of Applied Medical Science, KAU, Jeddah, Saudi Arabia, [3]Department of Neurosciences, Rehabilitation, Ophthalmology, Genetics and Maternal and Child Health, University of Genoa, Genoa, Italy, [4]Department of Brain and Behavioural Sciences, University of Pavia, Pavia, Italy, [5]Brain Connectivity Centre, C. Mondino National Neurological Institute, Pavia, Italy, [6]Wellcome Centre for Imaging Neuroscience, University College London, London, United Kingdom, [7]Brain MRI 3T Mondino Research Center, C. Mondino National Neurological Institute, Pavia, Italy

We investigated linear and non-linear BOLD-grip force (GF) relationships in the brain using dominant (DH) and non-dominant hands (NDH). The NDH revealed widespread brain activations compared to DH, irrespective of GF. Looking at the BOLD-GF effects, both hands showed increased activations with increased GF within the contralateral M1 and ipsilateral anterior cerebellum. Non-linear BOLD-GF relationships (up to 4^{th} order) were found, typically in posterior M1, premotor, sensory, parietal, and cerebellar areas. Finally, the consistent bilateral involvement of the cerebral and cerebellar areas suggests their involvement in error tracking or in synkinetic processes between DH and NDH.

4588 Computer 76

Neural correlates of cognitive load on working memory in organic-solvent exposed brain using fMRI

Kyung Eun Jang[1], Jeehye Seo[2], Hyejeong Choi[1], Hyunsil Cha[1], Eunji Kim[1], Moojin Yang[1], Jiung Yang[1,3], Huijin Song[2], and Yongmin Chang[1,4]

[1]Medical & Biological Engineering, Kyungpook National University, Daegu, Korea, Republic of, [2]Institute of Biomedical Engineering Research, Kyungpook National University, Daegu, Korea, Republic of, [3]Daegu Kyungpook Medical Innovation Foundation, Daegu, Korea, Republic of, [4]Radiology and Molecular Medicine, College of Medicine, Kyungpook National University, Daegu, Korea, Republic of

Several neuroimaging studies demonstrated that solvent-exposed subjects showed significantly poor performance on the working memory task than did controls [1,2]. However, no investigations have examined how solvent-exposed subjects are influenced by the cognitive load of a working memory task. Therefore, we performed N-back tasks with different cognitive demands using fMRI to investigate the neural basis for possible association between working memory load and memory deficit in the subjects with neurotoxicant solvent exposure. We found a positive correlation between response time of the 1-back task and percent BOLD signal changes in the left inferior parietal cortex, but a positive correlation was not founded of the 2-back task.

4589 Computer 77

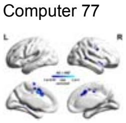

Altered structure and functional connectivity of the post-insular in uremic restless legs syndrome patients

DUN DING[1], XueYing Ma[1], WangHuan Dun[1], Peng Li[1], ZhuoNan Wang[1], and ZHANG MING[1]

[1]Radiology Department, First Affiliated Hospital of Xi'an Jiaotong University, XI'AN, People's Republic of China

To investigate the structure and functional changes in the insulars in uremic RLS patients using a resting-state function magnetic resonance imaging (fMRI)paradigm,We examined cortical thickness,and investigage the abnormal functional connectivity in maintenance dialysis patients. The clinical parameters and RLS severity were correlated analyzed. The characteristics of uremic RLS patients were compared to those of the controls.

4590 Computer 78

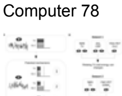

Vascular-metabolic and GABAergic inhibitory modulation of neural variability. A combined fMRI and PET study

Pengmin Qin[1,2], Niall W Duncan[2], David Yen-Ting Chen[3], Zirui Huang[4], Chien-Yuan Eddy Lin[5,6], Christine Wiebking[7], Chien-Mu Lin[8], Che-Ming Yang[8], Ying-Chi Tseng[3], Georg Northoff[9], and Timothy Lane[2]

[1]Guangdong Key Laboratory of Mental Health and Cognitive Science, South China Normal University, Guangzhou, People's Republic of China, [2]Brain and Consciousness Research Centre, Taipei Medical University-Shuang Ho Hospital, New Taipei City, Taiwan, [3]Department of Radiology, Taipei Medical University - Shuang Ho Hospital, New Taipei City, Taiwan, [4]Mind, Brain Imaging and Neuroethics Research Unit, Institute of Mental Health Research, University of Ottawa, Ottawa, Canada, [5]GE Healthcare, Taipei, Taiwan, [6]GE Healthcare MR Research China, Beijing, People's Republic of China, [7]Applied Emotion and Motivation Research, Institute for Psychology and Education, Universität Ulm, Ulm, Germany, [8]Department of Nuclear Medicine, Shuang-Ho Hospital, Taipei Medical University, New Taipei City, Taiwan, [9]Brain and Mind Research Institute, Centre for Neural Dynamics, Faculty of Medicine, University of Ottawa, Ottawa, Canada

We sought to investigate the mechanism involved in temporal variability (TV) changes between two basic behavioral states, namely having the eyes open (EO) or eyes closed (EC). The aim of this study was to use the change between the EC and EO states to identify the potential mechanisms involved in TV modulation.

4591 Computer 79

Differentiation of Functional Activity within the Thalamus during Rest and Visual Task

Wolfgang Grodd[1], Philip Ehses[1], Klaus Scheffler[1], and Vinod Kumar[1]

[1]Dep. of Magnetic Resonance, Max Planck Institute for Biological Cybernetics, Tuebingen, Germany

The presented study explores the capability of high resolution functional MRI (fMRI) at 9.4 Tesla to study functional changes in the primary visual cortex and the human thalamus during rest and natural picture viewing. We found increased intrinsic thalamic connectivity during both eyes open (EO) and eyes closed (EC) condition in the viewing task compared to rest.

4592 Computer 80

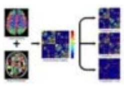

Analysis of the network properties of structural brain network of elderly people with obstructive sleep apnea

Min-Hee Lee[1], Areum Min[1], Yoon Ho Hwang[1], Dong Youn Kim[1], Bong Soo Han[2], Seung Ku Lee[3], Chang-Ho Yun[4], and Chol Shin[3]

[1]Department of Biomedical Engineering, Yonsei University, Wonju, Korea, Republic of, [2]Department of Radiological Science, Yonsei University, Wonju, Korea, Republic of, [3]Institute of Human Genomic Study, College of Medicine, Korea University Ansan Hospital, Ansan, Korea, Republic of, [4]Department of Neurology, Seoul National University Bundang Hospital, Seongnam, Korea, Republic of

Obstructive sleep apnea (OSA) is a common and progressive condition that is accompanied by affective, cognitive and autonomic nervous system changes. Recent studies have demonstrated abnormalities in the brains of OSA subjects. However, no study has illustrated alterations in brain structural connectivity caused by OSA. To assess alterations of brain structural connectivity, we constructed a structural brain network from diffusion tensor imaging (DTI) and examined global network properties for control and OSA subjects. OSA subjects showed lower global efficiency, local efficiency and strength. Brain network analysis may improve understanding of global architecture of anatomical connection patterns in OSA.

4593 Computer 81

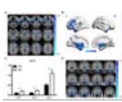

Abnormally functional connectivity density and network pattern in lifelong premature ejaculation patient: A resting-state fMRI study

Jiaming Lu[1], Xin Zhang[1], Yun Chen[2], Jiadong Xia[2,3], Zhao Qing[1], Fei Chen[4], Huiting Wang[1], Weibo Chen[5], Queenie Chan[6], Yutian Dai[2], Bing Zhang[7], and Bin Zhu[8]

[1]Department of Radiology, Affiliated Drum Tower Hospital of Nanjing University Medical School, Nanjing, Jiangsu, China, NanJing, People's Republic of China, [2]Department of Andrology, Affiliated Drum Tower Hospital of Nanjing University Medical School, Nanjing, Jiangsu, China, NanJing, People's Republic of China, [3]Department of Urology, The First Affiliated Hospital of Nanjing Medical University, Nanjing, Jiangsu, China., [4]Department of Radiology, The Affiliated Yancheng Hospital of Southeast University Medical College, Yancheng, Jiangsu, China, NanJing, People's Republic of China, [5]Philips Healthcare, Shanghai, People's Republic of China, People's Republic of China, [6]Philips Healthcare, HongKong, People's Republic of China, People's Republic of China, [7]Department of Radiology, Affiliated Drum Tower Hospital of Nanjing University Medical School, Nanjing, China, NanJing, People's Republic of China, [8]Department of Radiology, ffiliated Drum Tower Hospital of Nanjing University Medical School, Nanjing, Jiangsu, China., NanJing, People's Republic of China

Premature ejaculation (PE) is considered the alteration in dopaminergic reward system. Functional connectivity density along with network pattern methodology provides an opportunity to assess the functional integrity of brain activity in implicated circuits and it was applied to analysis the inter-group difference in SFCD and LFCD. Network constructing and graph theoretical were used to compare the network property. In conclusion, this study demonstrated the weaken connection inner brain areas and strengthened connection inter brain areas in dopaminergic reward system along with the functional network pattern has changed in the lifelong PE patient for the first time.

4594 Computer 82

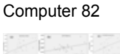

An fMRI investigation of the neural efficiency of abstract reasoning as a function of trait anxiety

Shilpi Modi[1], Mukesh Kumar[1], Sanjeev Nara[1], and Subash Khushu[1]

[1]NMR Research Centre, INMAS, Delhi, India

According to the Attentional Control Theory, trait anxiety has a greater adverse effect on processing efficiency (i.e. performance effectiveness/effort) than on accuracy. Functional magnetic resonance imaging (fMRI) provides a measure of task-related effort in the form of neural activity elicited during cognitive processing. fMRI was used to assess the neural activation (Blood Oxygen Level Dependent (BOLD) contrast estimates) in a priori regions of interest for a reasoning task. Our results indicate that a compensatory increased neural effort is required by high trait anxious individuals to maintain an equivalent task performance as that of low anxiety individuals.

4595 Computer 83

Altered resting state functional connectivity by autogenic training

Takashi Shizukuishi[1], Osamu Abe, Takahiro Shinozaki, Haruyasu Yamada, Akihiko Wada, Ryutaro Kohashi, and Yoshiki Imamura

[1]Radiology, Nihon University School of Medicine, Tokyo, Japan

Objective: We investigated whether autogenic training (AT) altered resting state functional connectivity. Methods: 7 volunteers familiar with AT participated in this study. Rs-fMRI was performed pre and post AT, and 3D-T1WI was acquired. Group analysis was performed to explore the alteration of resting functional connectivity after autogenic training by using CONN functional connectivity toolbox. Results: Greater connectivity between 1. right amygdala and right caudate, 2. precuneus and left pallidum, and 3. right supratemporal gyrus and left pallidum, were demonstrated. Conclusion: AT could have positive effects not only to restore the automatic nervous system but also to alter RS functional connectivity.

4596 Computer 84

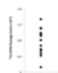

Evidence of a link between brain structure and function and gut permeability: a combined RS-fMRI and DTI investigation of the brain-gut axis in healthy women

Suzanne T Witt[1], Olga Bednarska[2], Adriane Icenhour[1,2], Sigrid Elsenbruch[3], Johan D Söderholm[2], Maria Engström[1,4], Emeran A Mayer[5], Åsa Keita[2], and Susanna Walter[1,2]

[1]CMIV, Linöping University, Linköping, Sweden, [2]Dept. of Clinical and Experimental Medicine, Linköping University, [3]Institute of Medical Psychology & Behavioral Immunobiology, University of Duisburg-Essen, Essen, Germany, [4]Dept. of Medical and Health Sciences, Linköping University, [5]Dept. of Medicine, UCLA, Los Angeles, CA, United States

The brain-gut axis is thought to play a key role in the regulation of the gastrointestinal system with overall physical and emotional health. In diseases, such as irritable bowel syndrome, dysfunction within brain-gut interactions have been proposed to underlie symptoms of chronic abdominal pain. This study demonstrated that variations in gut mucosal permeability affected both resting-state functional connectivity in the DMN and white matter microstructure properties in healthy adult women. Variations within brain function and structure were apparent even when variations in gut permeability were small and remained within the normal range, indicating that brain-gut interactions may be quite sensitive.

4597 Computer 85

Chronic exposure to air pollutants alters the functional network and spatiotemporal dynamics of the resting brain: Graph theory and dynamic functional connectivity analysis.

Suhnyoung Jun[1,2], Sanghoon Han[1,2,3], Chang Soo Kim[2,4], and Seung-Koo Lee[2,5]

[1]Psychology, Yonsei University, Seoul, Korea, Republic of, [2]Integrative Neurocognitive Functional Imaging Center, Yonsei University, Seoul, Korea, Republic of, [3]Cognitive Science Interdisciplinary Program, Yonsei University, Seoul, Korea, Republic of, [4]Department of Preventive Medicine, Yonsei University, Seoul, Korea, Republic of, [5]Radiology, Yonsei University, Seoul, Korea, Republic of

Detrimental effects of air pollutants on cognitive function are gaining considerable concern. The present study compared high-risk and low-risk group, defined based on the level of exposure to air pollutants, using graph theory-based approach and sliding window correlation analysis. Despite the undifferentiated cognitive functions between the groups, our study demonstrated the changes of the large-scale functional networks and dynamic brain activity of the high-risk group. Thus, our findings provide strong evidence of the influence of chronic high-dose exposure to air pollutants on the neural correlates, and offer new ways to understand the functional neural networks and dynamics.

4598 Computer 86

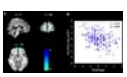

Hope and the brain: trait hope mediates the protective role of the medial orbitofrontal cortex spontaneous activity against anxiety

Xin Xu[1,2], Song Wang[1], and Qiyong Gong[1]

[1]Huaxi MR Research Center (HMRRC), Department of Radiology, West China Hospital of Sichuan University, Chengdu, People's Republic of China, [2]Department of Psychiatry, West China Hospital of Sichuan University, Chengdu, People's Republic of China

As a personality trait, hope refers to the motivational tendency for initiating actions and generating routes to achieving goals and plays a protective role in anxiety. Here, we investigated the neural basis of hope in 231 adolescents using resting-state functional magnetic resonance imaging (RS-fMRI). We found that trait hope was negatively associated with the spontaneous activity in the bilateral medial orbitofrontal cortex (mOFC). Further mediation analyses revealed that trait hope mediated the relationship between the mOFC activity and trait anxiety. Taken Together, our findings might provide the initial evidence for the brain-personality mechanisms protecting against anxiety.

4599 Computer 87

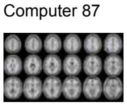

Improving attention through network-based neurofeedback training

Gustavo Pamplona[1], Frank Scharnowski[2], Yury Koush[3], and Carlos Salmon[1]

[1]InBrain Lab, Department of Physics, Faculty of Philosophy, Sciences and Letters of Ribeirão Preto, University of São Paulo, Ribeirão Preto, SP, Brazil, [2]Swiss Institute of Technology, University of Zürich, Zurich, Switzerland, [3]Department of Radiology and Medical Imaging, Yale University, New Haven, CT, United States

Being able to sustain attention for longer without mind-wandering would improve our performance. The brain correlates underlying both sustained attention and mind-wandering – the so-called sustained attention and default mode networks, respectively – have been well identified. Nevertheless, this knowledge has not yet been translated in advanced brain-based attention training protocols. Here we propose to use a novel brain imaging technique based on real-time fMRI to provide participants with information about ongoing levels of activity. We thus purpose a neurofeedback training of this difference between brain networks, what could lead to a boost in sustained attention ability, which is not reported yet.

4600 Computer 88

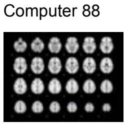

Traffic-Related Air Pollution Associated with Activation in a Functional MRI Verb Generation Task of a Longitudinally Studied, Pediatric Cohort

Kim M Cecil[1], Thomas Maloney[1], Mekibib Altaye[2], Rachel Severs[2], Christopher Wolfe[2], Zana Percy[3], Travis Beckwith[1], Kimberly Yolton[2], Grace LeMasters[3], and Patrick Ryan[2]

[1]Radiology/Imaging Research Center, Cincinnati Children's Hospital Medical Center, Cincinnati, OH, United States, [2]Cincinnati Children's Hospital Medical Center, Cincinnati, OH, United States, [3]University of Cincinnati College of Medicine, Cincinnati, OH, United States

Traffic-related air pollution (TRAP) is strongly associated with adverse cardiopulmonary health effects. Evidence suggests the developing brain may also be a target organ for particulate matter due to translocation either from the respiratory system or through the olfactory nerve. Using a pediatric cohort, we tested the hypothesis that exposure to TRAP during critical windows of brain development is significantly associated with changes in brain functioning during a language task. Children with high exposure levels were associated with reduced activation within the frontal lobe compared with children at low exposure.

4601 Computer 89

Associations between clinical risk factors, neurocognitive performance and brain activity in survivors of childhood Acute Lymphoblastic Leukemia treated on a chemotherapy-only protocol

Slim Fellah[1], Matthew A. Scoggins[1], Ping Zou[1], Lisa M. Jacola[2], Ching-Hon Pui[3], Robert J. Ogg[1], and Wilburn E. Reddick[1]

[1]Diagnostic Imaging, St Jude Children's Research Hospital, Memphis, TN, United States, [2]Psychology, St Jude Children's Research Hospital, Memphis, TN, United States, [3]Oncology, St Jude Children's Research Hospital, Memphis, TN, United States

ALL survivors treated with chemotherapy alone remain at elevated risk for neurocognitive impairment. We used fMRI to investigate associations between clinical risk factors, neurocognitive performance and brain activity in survivors of ALL. Ninety-two survivors completed Verbal and Object N-back tasks during fMRI at end of therapy. Measures of working memory were completed as part of a neurocognitive evaluation. Working memory-related brain activation was associated with important clinical risk factors and neurocognitive performance. The pattern of behavioral and imaging responses provides evidence for both compromised and compensatory changes in regional brain function. fMRI may help in selecting patients for remedial intervention.

4602 Computer 90

Low-frequency Visual Entrainment Enhances Bilateral Resting-state fMRI Connectivity in Primary Sensory Cortices

Eddie Wong[1,2], Celia M. Dong[1,2], Russell W. Chan[1,2], Leon C. Ho[1,2], Alex T. L. Leong[1,2], Condon Lau[3], and Ed X. Wu[1,2]

[1]Laboratory of Biomedical Imaging and Signal Processing, The University of Hong Kong, Hong Kong, Hong Kong, [2]Department of Electrical and Electronic Engineering, The University of Hong Kong, Hong Kong, Hong Kong, [3]Department of Physics and Materials Science, City University of Hong Kong, Hong Kong, Hong Kong

Entrainment is known to alter or synchronize brain rhythm and may enhance task performance. However, whether and how sensory entrainment may modulate the long-range brain functional networks are unknown. We investigated the effects of frequency-dependent visual entrainment on resting state functional connectivity in distinct sensory cortical networks. Our findings provide the first and direct evidence that only low frequency visual entrainment can modulate the long-range non-visual sensory networks. They suggest that the entrained neural oscillation at low frequency can actively contribute to the long-range interactions between primary sensory cortical functional networks that underlie the brainwide connectivity measured by resting-state fMRI.

4603 Computer 91

Disrupted Brain Connectivity Patterns in patients with Attention-deficit/hyperactivity disorder

Ming Zhou[1], Chuang Yang[2], Xuan Bu[1], Haixi Lin[2], Yan Liang[2], Lu Lu[1], Lianqing Zhang[1], Xinyu Hu[1], and Xiaoqi Huang[1]

[1]Department of Radiology, Huaxi MR Research Center, Chengdu, People's Republic of China, [2]Department of Psychiatry, The First Affiliated Hospital of Wenzhou Medical University, People's Republic of China

In the current study, we used a graph theory-based network measurements named degree centrality (DC) to identify main cortical hubs in the brain network architecture at voxel level affected in ADHD. Then, functional connectivity maps were generated with seeded at altered DC to detect the brain changes at large-scale level. Finally, we found the disconnection within cortico-thalamus and cortico-striatal loops in ADHD patients, which may associated with inattention and cognitive function deficits.

4604 Computer 92

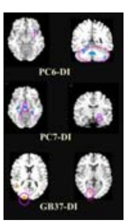

Neural mechanism of acupoint specificity underlying the antiemetic efficacy: an fMRI study.

Tong Yang[1] and Xuan Niu[1]

[1]The First Affiliated Hospital of Xi'An Jiaotong University, Xi'an, People's Republic of China

This paper presents an original research to investigate the underlying neural mechanism on acupoint specificity underlying the antiemetic efficacy. Our findings further suggested that acupuncture at different acupoints may exert distinct modulation effects on the brain activity patterns. Notably, we also may provide preliminary evidence for understanding the gut–brain communication.

4605 Computer 93

Changes in fMRI activation pattern during different levels of sacral nerve stimulation for overactive bladder

Pallab Bhattacharyya[1], Bradley Gill[2], Javier Pizarro-Berdichevsky[2,3,4], Howard Goldman[2], Mark Lowe[1], and Stephen Jones[1]

[1]Imaging Institute, Cleveland Clinic, Cleveland, OH, United States, [2]Glickman Urology & Kidney Institute, Cleveland Clinic, Cleveland, OH, United States, [3]Urogynecology Unit, H. Dr. Sotero del Rio, Santiago, Chile, [4]Division Obstetricia y Ginecologia, Pontificia Universidad Católica de Chile

Sacral nerve stimulation (SNS) is an effective treatment for refractory overactive bladder(OAB). For patient-specific and therapeutic efficacy, stimulus at levels below or above the sensory level are sometimes applied on OAB patients. Previous functional brain studies suggested that few forebrain circuits acting primarily on midbrain periacqueductal grey is responsible for facilitating voiding reflex and a sensation of voiding. The neural circuits underlying the action of SNS, and its response to different levels of stimulus is studied by functional MRI (fMRI). Differences in activation patterns resulting from subsensoy, sensory and supresensory stimulation are reported.

4606 Computer 94

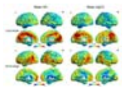

[Abnormal Brain Functional connectivity strength in the Absence of the Corpus Callosum: A Resting-State fMRI Study]

Long Zuo[1], Shuangkun Wang, Hua Gu[2], Junliang Yuan[2], and Yang Zhou[2]

[1]Beijing Chao-Yang hospital, Beijing, People's Republic of China, [2]Beijing Chao-Yang hospital

The problem

The whole-brain functional connectivity strength on long-range and short-range in the AgCC is still unknown.

Methods

A novel voxel-based FCS analysis were performed on the whole-brain resting-state functional images.

Results

Compared with the healthy control subjects, the AgCC groups exhibits statistical differences of FCS on long-range and short-range connecvity respectively.

Conclusions

Anatomical distance affects functional connectivity strength in AgCC individuals.

4607 Computer 95

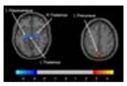

Abnormal Local Functional Connectivity Density in Major Depressive Disorder Patients with Suicidal Behavior

Ziqi Chen[1], Mingrui Xia[2], Weihong Kuang[3], Zhiyun Jia[1,4], Yong He[5], and Qiyong Gong[1,6]

[1]Huaxi MR Research Center (HMRRC), Department of Radiology, West China Hospital of Sichuan University, Chengdu, People's Republic of China, [2]State Key Laboratory of Cognitive Neuroscience and Learning, Beijing Normal University, Beijing, People's Republic of China, [3]Department of Psychiatry, West China Hospital of Sichuan University, Chengdu, People's Republic of China, [4]Department of Nuclear Medicine, West China Hospital of Sichuan University, Chengdu, People's Republic of China, [5]State Key Laboratory of Cognitive Neuroscience and Learning, Beijing Normal University, [6]Department of Psychology, Sichuan University, Chengdu, People's Republic of China

Previous studies suggested abnormal functional connectivity related to suicide behavior, which however relied on priori selection of seed regions. We applied functional connectivity density (FCD) to investigate the short-range and long-range functional connectivity patterns in major depressive disorder (MDD) patients with suicidal behavior. Relative to healthy controls, MDD patients with suicidal behavior showed reduced short-range FCD in bilateral thalamus, left hippocampus and increased short-range FCD in left precuneus. This study demonstrated altered local connectivity density at voxel level in MDD patients with suicidal behavior and highlighted that the thalamus, hippocampus and precuneus were important brain network hubs for these patients.

4608 Computer 96

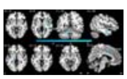

Resting Functional Connectivity and Anatomical Basis in Patients with Hepatic Myelopathy After Transjugular Intrahepatic Portosystemic Shunt

Long-Biao Cui[1], Yi-Bin Xi[1], Ling-Li Zeng[2], Guo-Hong Han[3], and Hong Yin[1]

[1]Department of Radiology, Xijing Hospital, Fourth Military Medical University, Xi'an, People's Republic of China, [2]National University of Defense Technology College of Mechatronic Engineering and Automation, Changsha, People's Republic of China, [3]Xijing Hospital of Digestive Diseases, Xijing Hospital, Fourth Military Medical University, Xi'an, People's Republic of China

We investigated whether motor system in the brain shows altered functional connectivity and what the anatomical basis behind it is in patients with hepatic myelopathy (HM) after transjugular intrahepatic portosystemic shunt (TIPS), a rare and likely overlooked complication in chronic liver disease patients with portosystemic shunts characterized by severe and mostly irreversible neurologic symptoms. HM patients exhibited hypoconnectivity between the right SMA and right insula, which revealed decreased gray matter volume. The positive correlation was observed between the strength of this connectivity and folic acid level in HM patients, which could discriminate HM from Non-HM with a high level of accuracy.

Electronic Poster

Cerebrovascular Disease

Exhibition Hall — Wednesday 8:15 - 9:15

4609 Computer 97

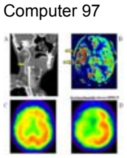

Correlation of cerebrovascular reserve assessed by acetazolamide-stress SPECT with collaterals on arterial spin-labeling MRI in patients with carotid occlusive disease

Hyunkoo Kang[1] and Keuntak Roh[1]

[1]Department of Radiology, Seoul Veterans Hospital, Seoul, Korea, Republic of

We evaluated the correlation between cerebrovascular reserve (CVR) on acetazolamide-stress single photon emission computed tomography (SPECT) brain scans and collaterals on arterial spin-labeling (ASL) magnetic resonance imaging (MRI) in internal carotid artery (ICA) stenosis.With acetazolamide stress SPECT, the 21/74 (28%) patients showed evidence of decreased CVR. In 7/53 (13%) of the normal CVR group and 10/21 (48%) of the reduced CVR from the SPECT results, ASL showed ATA in ipsilateral to the stenosis. Significant relationship was observed between reduced CVR group and ATA showing group in ICA stenosis patients on ASL brain perfusion (p=0.004).

4610 Computer 98

Differentiation of Intracerebral Hemorrhage from Ischemic Stroke at Early Stage Using a Novel Scheme of Length and Offset VARied Saturation (LOVARS) MRI

Yan Bai[1,2], Meiyun Wang[1], Yue Li[3], Xiaowei He[4], Xiaoyue Ma[1], Panli Zuo[5], Yucheng Li[1], and Xiaolei Song[2]

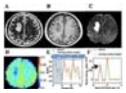

[1]Henan Provincial People's Hospital, Zhengzhou, People's Republic of China, [2]The Johns Hopkins University School of Medicine, Baltimore, MD, United States, [3]AnatomyWorks LLC, Baltimore, MD, United States, [4]Northwest University, Xi'an, People's Republic of China, [5]Siemens Healthcare China, Beijing, People's Republic of China

This study investigated the diagnostic capability of a novel scheme of Length and Offset VARied Saturation (LOVARS) CEST method, for detecting and differentiating intracerebral hemorrhage from ischemic stroke at early stage. With the saturation offsets of 2 ppm and -3.5 ppm, the new LOVARS real image is able to separate ischemic lesion from hemorrhagic lesion by the opposite signal appearances for all patients enrolled. i.e. the former is hypointensity while the latter is hyperintensity. Our results revealed that the LOVARS real signals are significantly higher in hemorrhage than in ischemic stroke, which may serve as an imaging marker.

4611 Computer 99

Measurement of mean transit time changes in response to Acetozalomide challenge in patients with cerebral steno-occlusive disease: a study using dynamic susceptibility contrast MR perfusion imaging.

Kyle Pate[1], Junjie Wu[1], Seena Dehkharghani[2], Fadi Nahab[1], Jason Allen, and Deqiang Qiu[1]

[1]Emory University, Atlanta, GA, United States, [2]New York University

In this paper, 9 patients with chronic cerebrovascular disease underwent a two day MR perfusion study with a Diamox challenge in order to quantify cerebrovascular reserve with a focus on MTT and Tmax parameters. Parametric maps were generated and used to compare regional differences in four perfusion parameters between the left and right hemispheres, MCA and ACA vascular territories, and the cerebellum. This approach demonstrated an unexpected increase in MTT and Tmax augmentation in the anterior circulation over augmentation in the cerebellum.

4612 Computer 100

Preliminary Study of High b-value Diffusion MRI for Characterizing White Matter Damage in A Mouse Model of Amyotrophic Lateral Sclerosis

Jin Gao[1], Rodolfo G Gatto[2], Richard Magin[1], Andrew C Larson[3], and Weiguo Li[1,3,4]

[1]Bioengineering, University of Illinois at Chicago, Chicago, IL, United States, [2]Anatomy and Cell Biology, University of Illinois at Chicago, Chicago, IL, United States, [3]Radiology, Northwestern University, Chicago, IL, United States, [4]Research Resource Center, University of Illinois at Chicago, Chicago, IL, United States

Amyotrophic lateral sclerosis (ALS), a progressive motor neuron disease, is characterized by severe cervical spinal cord damage caused by degeneration of the corticospinal tracts and loss of lower motor neurons. Although MR imaging of spinal cord is challenging, the ubiquity and non-invasive nature of MRI has supported its continued development and a leading role in ALS biomarker discovery. In this study, we investigated the feasibility of exploiting high b-value diffusion MRI to evaluate alterations of the spinal cord in a mouse model of ALS.

4613 Computer 101

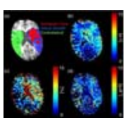

Quantitative Brain Oxygenation Measurements Made using Streamlined-qBOLD in Acute Stroke Patients: Further Investigation using a Detailed Voxel-Wise Analysis of Tissue Outcome

Alan J Stone[1], George WJ Harston[2], Davide Carone[2], Radim Licenik[2], James Kennedy[2], and Nicholas P Blockley[1]

[1]FMRIB, Nuffield Department of Clinical Neurosciences, University of Oxford, Oxford, United Kingdom, [2]Acute Vascular Imaging Centre and Acute Stroke Programme, Radcliffe Department of Medicine, University of Oxford, Oxford, United Kingdom

Streamlined-qBOLD is a baseline brain oxygenation measurement technique that has qualitatively shown promising results for the early identification of the ischaemic penumbra. Here regional definitions of tissue outcome are used to further investigate the application of this technique in acute stroke. Quantitative brain oxygenation parameters are demonstrated to vary between regions with different tissue outcomes.

4614 Computer 102

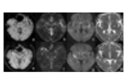

A quantitative analysis using susceptibility mapping of unilateral middle cerebral artery thrombosis in patients with acute cerebral infarction

Shuang Xia[1], Chao Chai[2], Qingyuan Yang, Tianyi Qian, E Mark Haacke, and Wen Shen

[1]Tianjin First Central Hospital, Tianjin, People's Republic of China, [2]Radiology Department, Tianjin First Central Hospital, Tianjin, People's Republic of China

The aim of this study was to explore the correlation between thrombus length, thrombus susceptibility, CBS, DWI-ASPECTS, and admission and discharge NIHSS scores between patients with single-segment and multiple-segment thrombi using susceptibility mapping (SWIM). SWIM, reconstructed from magnitude and phase images acquired by an SWI sequence, was used to measure thrombus susceptibility in patients with acute infarction. A higher susceptibility of thrombus was correlated with lower DWI-ASPECTS and increased NIHSS scores. The patients with multiple-segment thrombi had a larger area of cerebral infarction, more severe symptoms, and worse clinical outcomes.

4615 Computer 103

The potential of MRI as a biomarker in elderly patients with asymptomatic unilateral internal carotid artery stenosis

Pedro Henrique Rodrigues Silva[1], Ana Paula Afonso Camargo[2], André Monteiro Paschoal[1], Octavio M Pontes-Neto[2], and Renata Ferranti Leoni[1]

[1]Department of Physics, FFCLRP, University of Sao Paulo, Ribeirao Preto, Brazil, Ribeirão Preto, Brazil, [2]Department of Neurosciences and Behavioral Science, FMRP, University of Sao Paulo, Ribeirao Preto, Brazil, Brazil

Asymptomatic unilateral internal carotid stenosis is associated with brain hemodynamic changes and cognitive impairment. However, the effects on Gray Matter (GM) volume, Cerebral Blood Flow (CBF) and Functional Connectivity (FC) are not clear. Therefore, the present study aims to assess changes in brain volume, CBF, resting-state FC and their relation to cognitive decline in a group of patients at presymptomatic stage using MRI. This study confirmed abnormalities in GM volume, CBF, RSBNs and RS-FC in patients, showing that MRI have great potential as biomarker of the disease and may provide additional information to predict cases at risk of brain ischemia.

4616 Computer 104

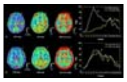

Identifying Perfusion Deficit Patterns in Unilateral Middle Cerebral Artery Stenosis Patients using Multi-Inversion Time Arterial Spin Labeling

Shuang Yan[1], Tianyi Qian[2], Li Zhang[3], Josef Pfeuffer[4], Mingli Li[1], Bin Peng[3], and Zhengyu Jin[1]

[1]Department of Radiology, Peking Union Medical College Hospital, Peking Union Medical College, Chinese Academy of Medical Sciences, Beijing, China, Beijing, People's Republic of China, [2]Siemens Healthcare, MR Collaborations NE Asia, Beijing, China, [3]Department of Neurology, Peking Union Medical College Hospital, Peking Union Medical College, Chinese Academy of Medical Sciences, Beijing, China, Beijing, People's Republic of China, [4]Siemens Healthcare, ApplicationDevelopment, Erlangen, Germany

To investigate the perfusion pattern in patients with unilateral middle cerebral artery stenosis, a multi-inversion time pulsed arterial spin labeling technique was used to measure the cerebral blood flow and bolus arrival time (BAT). The preliminary results indicatethat patients with cerebral infarction (CI) had longer BAT than patients with transient ischemic attack (TIA). Assuming CBF valuesare corrected in the areas with BAT longer than 1300ms and combine the corrected CBF with the BAT, we can distinguish TIA and CI cases from their perfusion deficits patterns.

4617 Computer 105

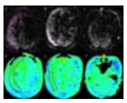

Stable CBF fluctuation in 4-day follow up after carotid artery stenting compared with carotid endarterectomy revealed by 3D pCASL

Wang Ting [1], Xing Xinbo[1], Wu Bing [2], Ma Lin [1], and Lou Xin [1]

[1]Radiology, Chinese PLA General Hospital, Beijing, People's Republic of China, [2]GE healthcare China

Carotid endarterectomy (CEA) and carotid artery stenting (CAS) are two commonly used surgical treatment methods for severe internal carotid artery (ICA) stenosis, hence, our objective was to investigate the CBF difference before and in 4-day follow up after CEA and CAS using 3D pCASL technique. As it demonstrated, the CBF values showed no significant ($P>0.05$) differences in various time points prior to the operations between CAS and CEA, whereas compared to the patients after CEA, the CBF values were stable fluctuated in various time points ($P<0.05$). This proves that 3D pCASL is useful for quantifying CBF changes after CAS or CEA; moreover, the stable fluctuation CBF may indicate that CAS has a lower hyperperfusion syndrome and death rate compared to CEA in the future.

4618 Computer 106

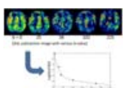

Evaluation of water permeability for ischemic lesion in the brain using DW-ASL

Noriyuki Fujima[1], Tomoyuki Okuaki, Takuya Aoike, Suzuko Aoike, and Kohsuke Kudo

[1]Hokkaido University Hospital, Sapporo, Japan

Diffusion-weighted arterial spin labeling technique was described to depict the tissue water permeability in the brain non-invasively; this information was also described to reflect the degree of blood-brain barrier damage. This study revealed that tissue water permeability can be useful for the evaluation of ischemic lesion more in detail than conventional technique such as T2WI or FLAIR for the determination of severity of ischemia and the prediction how fast the ischemia will progress.

4619 Computer 107

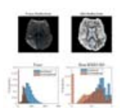

Correlation of microstructure differences in diffusion MRI scans with Fugl-Meyer assessment scores in stroke subjects

Kyler Hodgson[1], Ganesh Adluru[2], Lorie Richards[3], Jennifer Majersik[4], and Edward DiBella[5]

[1]Biomedical Engineering, University of Utah, Salt Lake City, UT, United States, [2]Radiology and Imaging Sciences, University of Utah, [3]Occupational Therapy, University of Utah, Salt Lake City, UT, United States, [4]Neurology, University of Utah, [5]Radiology and Imaging Sciences, Biomedical Engineering, University of Utah, Salt Lake City, UT, United States

Improved characterization of brain microstructure is important for image-based methods for diagnosing stroke. We explored the extent to which microstructural maps including Fractional Anisotropy (FA), Generalized Fractional Anisotropy (GFA), and Neurite Orientation Dispersion Density Index (NODDI) detect ipsilateral and contralateral differences in stroke patients as a measure of stroke severity. The difference between hemispheres was correlated with Fugl-Meyer Assessment motor function scores and the results of 16 patient scans reported. Results suggest that the Orientation Dispersion Index (ODI) contains information that could be clinically useful in understanding stroke recovery.

4620 Computer 108

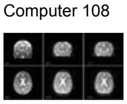

Clinical application of Half Fourier Acquisition Single Shot Turbo Spin Echo (HASTE) imaging with multiband (MB) excitation and PINS refocusing pulses

Jenni Schulz[1], José P. Marques[1], Annemieke ter Telgte[1], Frank-Erik de Leeuw[1,2], Frederick J.A. Meijer[3], and David G. Norris[1,4]

[1]Donders Institute for Brain, Cognition and Behaviour, Radboud University Nijmegen, Nijmegen, Netherlands, [2]Department of Neurology, Radboud University Medical Centre, Nijmegen, Netherlands, [3]Department of Radiology and Nuclear Medicine, Radboud University Medical Centre Nijmegen, Nijmegen, Netherlands, [4]Erwin L. Hahn Institute for Magnetic Resonance Imaging, University Duisburg-Essen, Essen, Germany

In this abstract, we demonstrate a clinical application of a MB-PINS-HASTE sequence with TRAPS and compare it to a standard HASTE protocol which is used in daily clinical practice. The modified MB-PINS-HASTE sequence offers the possibility to overcome limitations related to its typically high energy deposition and can accelerate the acquisition by acquiring several slices simultaneously. The reconstructed images show good diagnostic quality for the evaluation of the overall brain and CSF spaces in patients with small vessel disease. MB-PINS HASTE therefore offers the possibility of using ultrafast spin-echo imaging to acquire anatomical T2-weighted images and follow dynamic signal changes.

4621 Computer 109

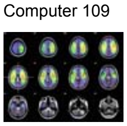

Voxel-based Lesion Mapping of Cardiogenic Cerebral Embolism

Masatoshi Takagaki[1], Yuki Togami[1], Akira Murasawa[1], Kazutami Nakao[1], and Manabu Kinoshita[2]

[1]Neurosurgery, Kawachi general hospital, Higashi Osaka, Japan, [2]Neurosurgery, Osaka Medical Center for Cancer and Cardiovascular Diseases, Osaka, Japan

Although outcome of acute cardiogenic cerebral embolism patients improved dramatically due to development of interventional devices, sub-acute cases over the golden period still follow miserable clinical courses requiring to elucidate the pathology of cerebral ischemia. The authors attempted to unveil the correlation of clinical features following cardiogenic cerebral embolism and the locations or sizes of the infarction using voxel-based lesion mapping (VBLM). Our result revealed a correlation between spatial characteristics of infarction and clinical features. Larger ischemic volume at the left hemisphere is correlated with patient's outcome and cerebral herniation was strongly influenced by ischemic volume after standardization.

4622 Computer 110

Correlating clinical outcome with voxel-based quantitative multiparametric MRI analysis in chronic ischemic stroke

Rui He[1,2], Olivier Detante[2,3], Alexandre Krainik[2,3], Assia Jaillard[2,3], Emmanuel Luc Barbier[1,2], and Benjamin Lemasson[1,2]

[1]U836, Inserm, Grenoble, France, [2]Université Grenoble Alpes, Grenoble Institut des Neurosciences, Grenoble, France, [3]Grenoble University Hospital, Grenoble, France

Predicting clinical outcome following stroke remains a challenge for magnetic resonance imaging (MRI). In this study, we acquired longitudinally (3 sessions) multiparametric MRI data sets including diffusion-weighted and perfusion-weighted images of 30 patients with chronic ischemic stroke. All of the diffusion and perfusion MRI parameters were analyzed by the classic whole-lesion approach and the parametric response map (PRM), a voxel-based post-processing approach at each time point. The results emphasized the superiority of the PRM over the whole-lesion approach for the prediction of long-term outcome based on early MRI data.

4623 Computer 111

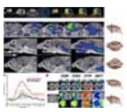

Magnetic particle imaging - The future of acute stroke imaging and treatment?

Peter Ludewig[1], Nadine Gdaniec[2], Jan Sedlacik[3], Kannan M. Krishnan[4], Christian Gerloff[1], Tobias Knopp[2], and Tim Magnus[1]

[1]Neurology, University Medical Center Hamburg-Eppendorf, Hamburg, Germany, [2]Institute of Biomedical Imaging, University Medical Center Hamburg-Eppendorf, Hamburg, Germany, [3]Neuroradiology, University Medical Center Hamburg-Eppendorf, Hamburg, Germany, [4]Materials Science and Engineering Department, University of Washington, Seattle, United States

Magnetic particle imaging (MPI) is a new tomographic imaging modality with superior temporal and spatial resolution compared to other imaging techniques, allowing 3D real-time assessment of vasculature and perfusion without X-rays or nephrotoxic contrast agents. For the first time we show that MPI can used for the diagnosis of acute pathologies like ischemic stroke by showing the first MPI stroke images in a murine stroke model. Additionally, we give an outlook how MPI may revolutionize not only stroke imaging but also stroke treatment, as the magnetic fields of the MPI can be used for catheter guidance and targeted drug delivery.

4624 Computer 112

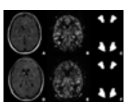

Decreased borderzone perfusion is related to brain parenchymal volume loss after subarachnoid hemorrhage

Lisa A. van der Kleij[1], Carlo Lucci[1], Esben T. Petersen[2], Mervyn D.I. Vergouwen[3], Gabriel J.E. Rinkel[3], Jeroen Hendrikse[1], and Jill B. De Vis[1]

[1]Department of Radiology, University Medical Center Utrecht, Utrecht, Netherlands, [2]Danish Research Centre for Magnetic Resonance, Copenhagen University Hospital Hvidovre, Denmark, [3]Department of Neurology and Neurosurgery, Brain Center Rudolf Magnus, University Medical Center Utrecht, Netherlands

Brain injury after aneurysmal subarachnoid hemorrhage (aSAH) has been linked to cerebral hypoperfusion in the acute and subacute disease stage. The areas most prone to hypoperfusion are the borderzone regions. In this study we obtained cerebral blood flow measurements in the subacute stage after aSAH, and longitudinal volumetric data. We found a moderate correlation between the ratio of borderzone/whole-brain perfusion and percentage brain volume loss. Thereby, perfusion in the watershed areas in the subacute stage could identify patients at a higher risk for future brain parenchymal volume loss. Consequently, increasing perfusion in these regions could be a future therapeutic target.

4625 Computer 113

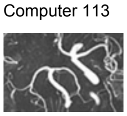

Assessment of cerebral perfusion changes in asymptomatic internal carotid artery stenosis using multi-parametric arterial spin-labeling MRI

Ya-Fang Chen[1], Sung-Chun Tang[2], Yen-Shu Kuo[3,4], and Wen-Chau Wu[5,6]

[1]Medical Imaging, National Taiwan University Hospital, Taipei, Taiwan, [2]Neurology, National Taiwan University Hospital, Taipei, Taiwan, [3]Graduate Institute of Biomedical Electronics and Bioinformatics, National Taiwan University, Taipei, Taiwan, [4]Radiology, Cathay General Hospital, Taipei, Taiwan, [5]Graduate Institute of Oncology, National Taiwan University, Taipei, Taiwan, [6]Graduate Institute of Clinical Medicine, National Taiwan University, Taipei, Taiwan

Internal carotid artery stenosis (ICAS) has been identified as a risk factor of ischemic stroke, with altered flow velocity and narrowed lumen commonly assessed by ultrasonography and angiography. However, hemodynamic change/compensation in microvasculature cannot be ruled out before symptoms. In this study, we investigated cerebral perfusion changes in asymptomatic ICAS by simultaneously assessing cerebral blood flow (CBF), arterial transit time (ATT), and flow territory, derived from arterial spin-labeling (ASL) MRI. Our data suggest that ATT and flow territory may be better predictors of high-grade unilateral ICA stenosis (≥70 %) than CBF in asymptomatic patients.

4626 Computer 114

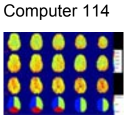

FEAST based Arterial Transit Time Measurement using Pseudo Continuous Arterial Spin Labeling in Patients with Sickle Cell Disease

Yihao Xia[1], Yaqiong Chai[2,3], Adam M Bush[2], Natasha Lepore[3], Thomas Coates[4], and John Wood[3,5]

[1]Department of Electrical Engineering, University of Southern California, Los Angeles, CA, United States, [2]Department of Biomedical Engineering, University of Southern California, Los Angeles, CA, United States, [3]Radiology, Children's Hospital of Los Angeles, Los Angels, CA, United States, [4]Section of Hematology, Children's Hospital of Los Angeles, Los Angels, CA, United States, [5]Division of Cardiology, Children's Hospital of Los Angeles, Los Angels, CA, United States

Sickle cell disease (SCD) is a genetic blood disorder with a high prevalence of cerebral vasculopathy and stroke. Arterial Transit Time (ATT) refers to the time it takes blood to flow from the labeling plane, to the vascular imaging compartment and reflects cerebrovascular impairment in SCD. We used pseudo continuous arterial spin labeling to measure ATT with flow encoding arterial spin tagging technique in patients with SCD and ethnicity matched, healthy controls. Our findings demonstrated sensitivity of ATT to vasculopathy.

4627 Computer 115

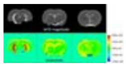

Electric properties tomography in a rodent model of ischemic stroke: Results of a combined ex-vivo and in-vivo pilot study.

Ulf Jensen-Kondering[1], Ruwen Böhm[2], Liang Shu[1], Olav Jansen[1], and Ulrich Katscher[3]

[1]Department of Radiology and Neuroradiology, UKSH, Kiel, Germany, [2]Department of Experimental and Clinical Pharmacology, UKSH, Kiel, Germany, [3]Research Laboratories, Philips GmbH Innovative Technologies, Hamburg, Germany

Electric properties tomography (EPT) is a new contrast in MRI which delivers information on tissue electrical conductivity. Up to now, it has been mostly used for tumor mapping. Ischemic cerebral stroke is another promising application. Seven male Wistar rats were used in this study. Five culled animals from another stroke study, three of which were subjected to MCAO and two live animals which were also subjected to MCAO were examined. Healthy cortical grey matter, white matter and cerebrospinal fluid could be well differentiated Conductivity was altered within the infarct. EPT is feasible in a rodent model of stroke.

4628 Computer 116

Measure Cerebral Microstructure Changes in Brain Small Vessel Disease Using Diffusion Kurtosis Imaging

Wenjing Lan[1], Shuang Xu[1], Yang Liu[1], Kaining Shi[2], and Lizhi Xie[3]

[1]The First Hospital of Jilin University, Changchun, People's Republic of China, [2]Philips Healthcare (China), Beijing, People's Republic of China, [3]GE Healthcare, MR Research China, Beijing, People's Republic of China

Diffusion tensor imaging (DTI) has been the most commonly used modality among diffusion MRI methods in the studies of ageing and development in the current study, we investigated diffusional modifications arising from brain small vessel disease, as compared with age and educational level matched healthy controls. Diffusion kurtosis imaging (DKI) was applied throughout the study, which is a recent novel extension of DTI to provide additional metrics quantifying non-Gaussianity of water diffusion in brain tissues.

4629 Computer 117

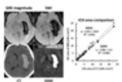

Quantitative Susceptibility Mapping of Intracranial Hemorrhage: Time Evolution and Comparison to CT

Hongfu Sun[1,2], Derek J. Emery[3], Kenneth Butcher[4], and Alan H. Wilman[2]

[1]Radiology, University of Calgary, Calgary, AB, Canada, [2]Biomedical Engineering, University of Alberta, Edmonton, AB, Canada, [3]Radiology and Diagnostic Imaging, University of Alberta, Edmonton, AB, Canada, [4]Division of Neurology, Department of Medicine, University of Alberta, Edmonton, AB, Canada

To follow the time evolution of intracranial hemorrhage (ICH) using quantitative susceptibility mapping (QSM) and compare to CT. Twenty ICH patients were followed using a clinical MRI protocol typically performed on day 2, 7 and 30. The ICH areas and mean values were compared between the CT and QSM on 18 patients (average 1.7 days apart). Time evolution of ICH was also investigated by QSM. In conclusion, QSM can be used to measure the size of ICH and track susceptibility evolution of the blood degradation products, providing a means to track iron evolution.

4630 Computer 118

Feasibility of 1H-MRS brain temperature map to detect hemodynamic abnormality in patients with unilateral chronic major cerebral artery steno-occlusive disease

Takamasa Namba[1], Kuniaki Ogasawara[1], Hideaki Nishimoto[1], Daiya Ishigaki[1], Yoshichika Yoshioka[2,3], Toshiyuki Murakami[1], Makoto Sasaki[4], Masakazu Kobayashi[1], Kenji Yoshida[1], Ikuko Uwano[4], Shunrou Fujiwara[1], Kazunori Terasaki[5], and Akira Ogawa[1]

[1]Department of Neurosurgery, School of Medicine, Iwate Medical University, Morioka, Japan, [2]Center for Information and Neural Networks (CiNet), NICT and Osaka University, Suita, Japan, [3]Biofunctional Imaging, Immunology Frontier Reseach Center, Osaka University, Suita, Japan, [4]Division of Ultra-High Field MRI, School of Medicine,Iwate Medical University, Morioka, Japan, [5]Cyclotoron Reseach Center, School of Medicine, Iwate Medical University

Deep cerebral white matter (CWM) like the centrum semiovale is vulnerable to ischemic injury. Brain temperature (BT) was associated with cerebral hemodynamic abnormalities in patients with chronic ischemia. We investigated whether the BT distribution map by multi-voxel ^{1}H-MRS were associated with the cerebral hemodynamic abnormalities assessed by positron emission tomography (PET) in the CWM region of patients with unilateral chronic major cerebral artery steno-occlusive disease. The BT map quantitatively and qualitatively correlated with PET images, especially oxygen extraction fraction. This may help to identify the patients at high risk for the stroke recurrence.

4631 Computer 119

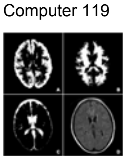

BRAIN PARENCHYMAL VOLUME CHANGES AFTER ANEURYSMAL SUBARACHNOID HEMORRHAGE

Carlo Lucci[1], Lisa A. van der Kleij[1], Mervyn D.I. Vergouwen[2], Gabriël J.E. Rinkel[2], Jeroen Hendrikse[1], and Jill B. De Vis[1]

[1]Department of Radiology, University Medical Center Utrecht, Utrecht, Netherlands, [2]Department of Neurology and Neurosurgery, Brain Center Rudolf Magnus, University Medical Center Utrecht, Netherlands

Aneurysmal Subarachnoid Hemorrhage (aSAH) accounts for only 5% of all strokes, but it is a disabling disease because of the cognitive deficits that occur in many survivors. We hypothesize these deficits to be caused by an accelerated brain atrophy process that develops after the event. To investigate this hypothesis, we evaluated brain volume changes in aSAH patients over time.

4632 Computer 120

Measurement of Blood-Brain Barrier Permeability using Dynamic Contrast-Enhanced Magnetic Resonance Imaging with Reduced Scan Time

Jonghyun Bae[1], Jin Zhang[1], Orlando Aristizabal[1], Willis Chen[1], Youssef Zaim Wadghiri[1], Yulin Ge[1], and Sungheon Gene Kim[1]

[1]Center for Advanced Imaging Innovation and Research, Radiology, New York University School of Medicine, New York, NY, United States

The purpose of this study is to investigate the feasibility of reducing the scan time while maintaining the sensitivity to BBB permeability changes. We propose a new model, extended Patlak model (EPL), where plasma flow is added to the Patlak model. The numerical simulation and in vivo mouse data in this study suggest that the proposed EPL model can be used to measure BBB permeability change with DCE-MRI scan time of 10 min or less.

Electronic Poster

Metabolic Neuroimaging

Exhibition Hall — Wednesday 9:15 - 10:15

4633 Computer 1

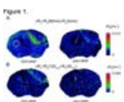

2-deoxy-D-glucose-conjugated magnetonanoparticles (2DG-MNP) uptake as a measure of metabolic activity in glioblastoma murine model

Jelena Lazovic[1], Whitney Pope[2], and Massoud Akhtari

[1]preclinical imaging, Vienna Biocenter Core Facilities, Vienna, Austria, [2]Radiology, University of California, Los Angeles, CA, United States

In the current study we tested if accumulation of non-radioactive 2-deoxy-D-glucose (2DG)-conjugated magnetonanoparticles (2DG-MNP) can be used as a measure of metabolic activity in glioblastoma. To quantify 2DG-MNP uptake across brain ΔR_2 maps are proposed. The difference in R_2 relaxation rates prior to and at different times following 2DG- or unlabeled (plain) MNP administration represents ΔR_2. Significant changes in ΔR_2 between brain and glioblastoma, reflecting increased metabolic rate of glioblastoma were found for glucose labeled MNP and not for plain-MNP. Our results suggest that 2DG-MNP have potential to be utilized in metabolic imaging as non-radioactive 2-^{18}[F]-fluoro-deoxy-D-glucose analogue.

4634 Computer 2

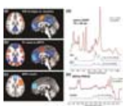

Regional GABA concentrations modulate inter-network resting-state functional connectivity

Xi Chen[1], Xiaoying Fan[1], Yuzheng Hu[2], Chun Zuo[1], Dost Ongur[1], and Fei Du[1]

[1]McLean Hospital, Belmont, MA, United States, [2]National Institute on Drug Abuse, Baltimore, MD, United States

The resting-state functional connectivity (rsFC) and task evoked fMRI, involving the default mode network (DMN) and control network (CN) was performed, with GABA, glutamate and glutamine measured at MPFC and DLPFC, in order to explore the underlying molecular mechanism of the DMN-CN interaction. We found that MPFC GABA concentrations significantly modulate DMN deactivation during a working memory task, and resting state anti-correlation between DMN and CN, while DLPFC GABA correlations modulate DMN-CN anti-correlation in the opposite direction. These findings suggest that MPFC and DLPFC GABA make a major but differential impact on task related activation and inter-network rsFC. The neurochemical characteristics of DMN and CN may provide novel insights into abnormal network activity in neuropsychiatric diseases and provide opportunities for novel interventions.

4635 Computer 3

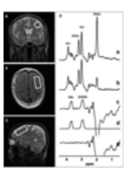

Sleep-Disordered Breathing Severity in Elderly is Associated with Decreased GABA in the Dorsolateral Prefrontal Cortex: A J-edited 1H MRS and Polysomnography Study

Ana C Pereira[1], Xiangling Mao[2], Caroline S Jiang[3], Guoxin Kang[2], SAra Milrad[4], Bruce S McEwen[3], Ana C Krieger[4], and Dikoma C. Shungu[5]

[1]Laboratory of Neuroendocrinology, The Rockefeller University, New York, NY, United States, [2]Radiology, Weill Cornell Medicine, [3]Laboratory of Neuroendocrinology, The Rockefeller University, [4]Medicine, Neurology and Neuroscience, Weill Cornell Medicine, [5]Radiology, Weill Cornell Medicine, New York, NY, United States

Sleep-disordered breathing (SDB) is a disorder characterized by repeated episodes of hypopnea and apnea during sleep that lead to sleep fragmentation and intermittent hypoxia. A leading model of model of SDB that posits GABAergic and glutamatergic dysregulations that lead to hyperexcitability and neuronal damage, which this study aimed to investigate using J-edited MRS and polysomnography. The main results were a robust DLPFC GABA decrease and associations between GABA and hypoxia as well as disease severity. The state of hyperexcitability observed in SDB is interpreted as likely the result of disinhibition (GABA) that might lead to excitotoxicity and neuronal damage.

4636 Computer 4

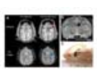

MR Imaging & Spectroscopy in a Non-Human Primate Model of Ebola Makona Aerosol Exposure

Margaret R Lentz[1], Anna N Honko[1], Jordan K Bohannon[1], Matthew G Lackemeyer[1], Jeffrey M Solomon[2], Louis M Huzella[1], Gene G Olinger[1], Lisa E Hensley[1], and Peter B Jahrling[1,3]

[1]NIAID/Integrated Research Facility, National Institutes of Health, Frederick, MD, United States, [2]Clinical Research Directorate & Clinical Monitoring Research Program, Leidos Biomedical Research, Inc., Frederick, MD, United States, [3]NIAID, Emerging Viral Pathogens Section, National Institutes of Health, Frederick, MD, United States

The purpose of this study was to use MRI and magnetic resonance spectroscopy (MRS) to determine if structural or metabolic alterations occur in the brain of rhesus macaques exposed to Ebola virus via inhalation of aerosolized small particles. Unlike intramuscular inoculation with Ebola virus, small-particle aerosol exposure of macaques did not result in uniform changes in brain volume or vascular alterations 8-9 days after exposure. However, most animals had reductions in N-acetyl aspartate and increases in choline levels, indicating spectroscopy may be useful in identifying early alterations in brain metabolism due to Ebola virus disease.

4637 Computer 5

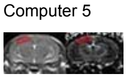

The impact of inflammation on grey matter metabolism, quantified using a novel NIRS/MRI system

Thomas Wade Johnson[1], James A Rogers[2], and Jeff F Dunn[1]

[1]Radiology, University of Calgary, Cumming School of Medicine, Calgary, AB, Canada, [2]Clinical Neurosciences, University of Calgary, Cumming School of Medicine, Calgary, AB, Canada

Cerebral metabolic rate for oxygen ($CMRO_2$) in gray matter (GM) is a sensitive marker for abnormalities in oxidative metabolism. We combined a near-infrared spectroscopy (NIRS) system with 9.4.T MRI to quantify regional $CMRO_2$ in the experimental autoimmune encephalomyelitis (EAE) mouse model of multiple sclerosis. Increases in $CMRO_2$ were seen in EAE mice and positive inflammation (CFA) controls at day 35 post-induction when compared to naïve controls. In addition, EAE and CFA mice showed increased $CMRO_2$ from day 14 to 35. These data indicate that inflammation alone, not necessarily linked to a white matter autoimmune disease, could cause abnormal $CMRO_2$ in GM.

4638 Computer 6

Individual mapping of neuronal damage in early relapsing-remitting MS using [11C]Flumazenil PET

Emilie Poirion[1,2], Benedetta Bodini[1], Marco Battaglini[3], Theodore Soulier[1], Léorah Freeman[1], Daniel Lorenzo-Garcia[1], Géraldine Bera[1], Michel Bottlaender[4], and Bruno Stankoff[1]

[1]Institut du Cerveau et de la Moelle Epinière/CNRS UMR 7225/INSERM 1127/UPMC UM75, Paris, France, Paris, France, [2]CEA, DRF, I2BM, Neurospin, UNIRS, Paris, France, [3]rtement of medecine, Surgery and Neuroscience, University of Siena, Siena, Italy, Italy, [4]CEA, DRF, I2BM, Neurospin, UNIACT, Paris, France

We explored the neuronal component of grey matter damage in the earliest phase of multiple sclerosis (MS) with [^{11}C]Flumazenil positron emission tomography (PET). Using a novel post-processing approach based on the generation of individual maps of neuronal pathology, we found a significant neuronal damage in the cortical lesions of patients with MS which preceded the occurrence of cortical atrophy, and correlated with white matter lesion load. These results suggest that cortical demyelination, together with retrograde degeneration of transected axons within white matter lesions, are among the key pathogenic contributors to neuronal cortical damage at the earliest stage of the disease.

4639 Computer 7

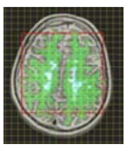

Proton Spectroscopic Imaging of Secondary Progressive Multiple Sclerosis in the MS-SMART trial

Ian Marshall[1], Michael J Thrippleton[1], Mark E Bastin[1], Daisy Mollison[1], David A Dickie[1], Francesca Chappell[1], Scott IK Semple[2], Annette Cooper[3], David Miller[4], Sue Pavitt[5], Gavin Giovannoni[6], Claudia AM Gandini Wheeler-Kingshott[7,8,9], Bhavana S Solanky[7], Christopher Weir[10], Nigel Stallard[11], Clive Hawkins[12], Basil Sharrack[13], Moira Ross[10], Jeremy Chataway[4], Peter Connick[1], Siddharthan Chandran[1], and the MS-SMART trialists

[1]Centre for Clinical Brain Sciences, University of Edinburgh, Edinburgh, United Kingdom, [2]Centre for Cardiovascular Sciences, University of Edinburgh, Edinburgh, United Kingdom, [3]Clinical Research Imaging Centre, University of Edinburgh, Edinburgh, United Kingdom, [4]Queen Square Multiple Sclerosis Centre, Department of Neuroinflammation, UCL Institute of Neurology, University College London, London, United Kingdom, [5]Dental Translational and Clinical Research Unit, School of Dentistry, Faculty of Medicine and Health, University of Leeds, Leeds, United Kingdom, [6]Department of Neurology, Barts and the London NHS Trust, London, United Kingdom, [7]UCL Institute of Neurology, Queen Square MS Centre, University College London, London, United Kingdom, [8]Department of Brain and Behavioural Sciences, University of Pavia, Pavia, Italy, [9]Brain MRI 3T Mondino Research Center, C. Mondino National Neurological Institute, Pavia, Italy, [10]Edinburgh Clinical Trials Unit, Usher Institute of Population Health Sciences and Informatics, University of Edinburgh, Edinburgh, United Kingdom, [11]Division of Health Sciences, University of Warwick, United Kingdom, [12]Institute for Science and Technology in Medicine, Keele University, United Kingdom, [13]Academic Department of Neuroscience, Royal Hallamshire Hospital, Sheffield, United Kingdom

^{1}H MR Spectroscopy yields metabolic information and has proved to be a useful addition to structural imaging in neurological diseases. We applied short-TE Spectroscopic Imaging combined with linear modelling with respect to brain tissue type in a homogeneous cohort of 42 patients with Secondary Progressive Multiple Sclerosis. Metabolite levels were significantly different in lesions compared with normal appearing tissues, suggesting axonal damage (reduced NAA) and increased glial activity (increased myo-inositol) yet relatively stable lesions (reduced Glx).

4640 Computer 8

MRS-based classification of Spinocerebellar Ataxias 1, 2, 3, and 6 at 7T: A distance-weighted discrimination approach

James Joers[1], Dinesh Deelchand[1], Tianmeng Lyu[2], Uzay Emir[1,3], Diane Hutter[1], Christopher M Gomez[4], Khalaf O Bushara[5], Lynn E. Eberly[2], and Gulin Oz[1]

[1]Center for Magnetic Resonance Research, University of Minnesota, Minneapolis, MN, United States, [2]Division of Biostatistics, University of Minnesota, Minneapolis, MN, United States, [3]University of Oxford, Oxford, United Kingdom, [4]Department of Neurology, University of Chicago, Chicago, IL, [5]Department of Neurology, University of Minnesota, Minneapolis, MN

We investigated the sensitivity of ultra-high field MRS to distinguish 4 hereditary neurodegenerative diseases with substantial overlap in clinical presentation and conventional MRI. We carried out pairwise classifications of spinocerebellar ataxias (SCAs) 1,2,3 and 6 using distance weighted discrimination (DWD) on 7T MRS from 3 brain regions of 68 SCA patients. Each subject contributed to the DWD model a 50-dimensional vector of concentrations. SCA6 was classified from SCAs 1-3 with high reliability (90%) and SCA2 was classified from SCA3 with moderate success (84%), while SCA1 could not reliably be classified from SCA2 (62%) or SCA3 (48%) with the current model.

4641 Computer 9

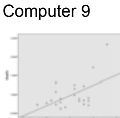

Abnormal Thalamic Metabolism in End-Stage Renal Disease Patients with Restless Legs Syndrome

Xueying Ma[1], Dun Ding[1], Peng Li[2], Fengli Liang[1], Zhuonan Wang[1], Yingxiang Sun[1], Haining Li[1], and Ming Zhang[1]

[1]Medical Imaging, The First Affiliated Hospital of Xi'an Jiaotong University, Xi'an, People's Republic of China, [2]Imaging Department, NO.215 Hospital of Shaanxi Nuclear Industry, Xianyang, People's Republic of China

Restless legs syndrome (RLS) was very common among ESRD patients. However, the physiopathologic mechanisms of RLS in ESRD patients were largely unclear. Here we analyzed the thalamic metabolites using 1H MRS and the correlation between sleep/RLS score and metabolites, compared with corresponding normal controls. The results showed that the Cho/Cr ratio increased and NAA/Cr ratio decreased in thalamus of ESRD patients. The correlation between Cho/Cr ratio and RLS score was significant. It indicated that the sleep disturbance in ESRD patients with RLS might be associated with the abnormal thalamocortical activation of human sleep regulation system.

4642 Computer 10

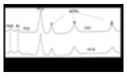

The influence of mild hypercapnia on brain intracellular pH, phosphate metabolites and cerebral blood flow a multinuclear (1H/31P) MR study at 7T.

Devashish Das[1], Aneurin James Kennerley[1], Samuel Harris[1], and Jason Berwick[1]

[1]University of Sheffield, Sheffield, United Kingdom

Permissive hypercapnia is commonly used as vasodilatory challenge in clinical applications and basic research. During fMRI experiments continuous exposure to mild (3-10%) CO2 can be applied to derive stimulus induced changes in the cerebral rate of oxygen consumption (CMRO2) by measuring cerebral blood flow and blood oxygenation dependent (BOLD) signal. Previous data from anesthetized primate during hypercapnia suggested increase in CBF are accompanied by decreases in neuronal activity. In this context, using multinuclear (31P/1H) and multi-parametric MR we show that mild exposure to hypercapnia elevates regional CBF, and can cause marginal but consistent drop in intracellular pH of rat brain, despite constant [ADP ~25-35μM] and [ATP ~3-2.4mM] to that of resting brain. Our findings support the view that unspecific drop in brain pH may likely elevate regional CBF, thereby sustain oxygen supply-to-demand ratio in rat brain.

4643 Computer 11

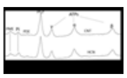

The influence of mild hypercapnia on brain intracellular pH, phosphate metabolites and cerebral blood flow a multinuclear (1H/31P) MR study at 7T

Devashish Das[1], Aneurin James Kennerley[1], Samuel Harris[1], Jason Berwick[1], and Devashish Das[1]

[1]University of Sheffield, Sheffield, United Kingdom

Permissive hypercapnia is commonly used as vasodilatory challenge in clinical applications and basic research. During fMRI experiments continuous exposure to mild (3-10%) CO2 can be applied to derive stimulus induced changes in the cerebral rate of oxygen consumption (CMRO2) by measuring cerebral blood flow and blood oxygenation dependent (BOLD) signal. Previous data from anesthetized primate during hypercapnia suggested increase in CBF are accompanied by decreases in neuronal activity. In this context, using multinuclear (31P/1H) and multi-parametric MR we show that mild exposure to hypercapnia elevates regional CBF, and can cause marginal but consistent drop in intracellular pH of rat brain, despite constant [ADP ~25-35μM] and [ATP ~3-2.4mM] to that of resting brain. Our findings support the view that unspecific drop in brain pH may likely elevate regional CBF, thereby sustain oxygen supply-to-demand ratio in rat brain.

4644 Computer 12

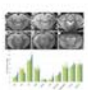

Longitudinal 7T MRI and MRS in a sheep model of Tay-Sachs disease and the effect of AAV gene therapy.

Heather Gray-Edwards[1], Elise Diffie[1], Ashley Randle[1], Amanda Gross[1], Nouha Salibi[2], Lauren Ellis [1], Ronald Beyers[1], Miguel Sena-Esteves[3], Thomas Denney[1], and Douglas Martin[1]

[1]Auburn University, Auburn, AL, United States, [2]MR R&D, Seimens Healthcare, Malvern, PA, United States, [3]University of Massachusetts, Worcester, MA, United States

Tay-Sachs Disease (TSD) is a fatal neurodegenerative disorder of children and the sheep model of TSD is a powerful tool to study the disease and evaluate novel therapies. One such therapy, adeno associated viral (AAV) gene therapy has resulted in a 2-fold increase in lifespan and biomarkers are needed for clinical trials. 7T MRI shows white and gray matter alterations and MR spectroscopic abnormalities that worsen with TSD disease progression. At humane endpoint the AAV treated sheep has normalization of gray and white matter intensities, but cortical atrophy and MRS alterations persist. 7T MRI and MRS reflect TSD disease severity.

4645 Computer 13

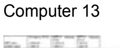

Dependence of degree of motor impairment on the association between motor performance and sensorimotor GABA level in relapsing remitting multiple sclerosis

Pallab Bhattacharyya[1], Micheal Phillips[1], Lael Stone[2], and Mark Lowe[1]

[1]Imaging Institute, Cleveland Clinic, Cleveland, OH, United States, [2]Neurological Institute, Cleveland Clinic, Cleveland, OH, United States

Gamma aminobutyric acid (GABA), a major inhibitory neurotransmitter, has been implicated as a metabolic marker of multiple sclerosis (MS). Previously it has been shown that sensorimotor cortex GABA level is higher in relapsing remitting MS (RRMS) patients with poorer motor performance. In this study, the association between cortical GABA level and motor performance, as measured by 9-hole peg test score, has been studied for groups of patients with RRMS with different degrees of motor impairment. The results suggest that cortical GABA has more involvement in motor performance in early stage of RRMS or in less impaired patients.

4646 Computer 14

Baseline of Chemical Exchange Saturation Transfer Imaging for Brain

Yuki Kanazawa[1], Masafumi Harada[1], Mitsuharu Miyoshi[2], Yuki Matsumoto[3], Hiroaki Hayashi[1], Toshiaki Sasaki[4], and Natsuki Ikemitsu[5]

[1]Graduate School of Biomedical Sciences, Tokushima University, Tokushima, Japan, [2]Global MR Applications and Workflow, GE Healthcare, [3]Graduate school of Health Science, Tokushima University, [4]School of Health Sciences, Tokushiama University, [5]School of Health Sciences, Tokushima University

The purpose of this study is to assess the CEST effect and contrast of various brain regions in normal for phase cycle-CEST MR imaging. Subjects were five healthy volunteers. All slice positions were set on the nucleus basalis level. ROIs were set as thalamus, frontal, occipital, putamen, and gray matter on right and left brain hemispheres of each subject There was no significant difference in mean MTR_{asym} values among each brain region (P > 0.01 for all). CEST effects for normal brain tissue had no dependency on region and/or left-right hemispheres.

4647 Computer 15

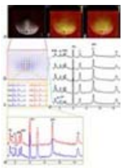

31P MR Spectroscopic Imaging of the Human Brain at 7T

Jimin Ren[1], Ty Shang[2], A. Dean Sherry[1,3], and Craig R. Malloy[1,4]

[1]Advanced Imaging Research Center, University of Texas Southwestern Medical Center, Dallas, TX, United States, [2]Department of Neurology and Neurotherapeutics, University of Texas Southwestern Medical Center, Dallas, TX, United States, [3]Department of Chemistry, University of Texas at Dallas, Richardson, TX, [4]VA North Texas Health Care System, Dallas, TX, United States

^{31}P MRS is capable of probing cerebral metabolism in vivo, but clinical applications are limited by poor spatial resolution. This study demonstrates that ^{31}P MRS imaging (MRSI) at 7T can offer high quality spectral data that enables cross-sectional mapping of various phosphorus-bearing metabolites in normal human brain. In a patient with prior ischemic stroke, high-energy phosphates were depleted and extracellular inorganic phosphate was increased in the stroke lesion.

4648 Computer 16

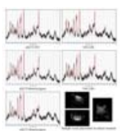

Striatal 7T 1H-MRS in two Huntington's Disease Mouse Models (zQ175 and YAC128)

Bretta Russell-Schulz[1], Andrew Yung[1], Austin Hill[2], Alex L MacKay[1,3], Piotr Kozlowski[1], and Blair R Leavitt[2]

[1]Radiology, University of British Columbia, Vancouver, BC, Canada, [2]Centre for Molecular Medicine and Therapeutics, University of British Columbia, Vancouver, BC, Canada, [3]Physics and Astronomy, University of British Columbia, Vancouver, BC, Canada

Two Huntington's disease (HD) mouse models with difference rates of disease progression, zQ175 and YAC128, were examined using 7T proton magnetic resonance spectroscopy of mice aged 6-7 months. zQ175 heterozygous and homozygous genotypes showed significantly decreased [tNAA] and increased [mI] compared to wild type. No differences in metabolite concentrations were found between YAC128- (wild type) and YAC128+ mice. A slow HD disease course in YAC128+ genotype may be the reason for lack of measured metabolite concentration differences.

4649 Computer 17

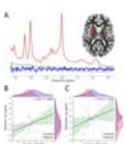

QSM meets MRS: The influence of subcortical iron on glutamatergic neurotransmission in a movement disorder population

Ahmad Seif Kanaan[1,2], Alfred Anwander[1], Andreas Schäfer[3], Berkin Bilgic[4], Torsten Schlumm[1], Jamie Near[5], Kirsten Müller-Vahl[2], and Harald E. Möller[1]

[1]Max Planck Institute for Human Cognitive and Brain Sciences, Leipzig, Germany, [2]Department of Psychiatry, Social Psychiatry and Psychotherpay, Hannover Medical School, Hannover, Germany, [3]Diagnostic Imaging, Magnetic Resonance, Research & Development, Siemens Healthcare GmbH, Erlangen, Germany, [4]Martinos Center for Biomedical Imaging, Charlestown, MA, United States, [5]Douglas Mental Health University Institute and Department of Psychiatry, McGill University, Montreal, QC, Canada

We use a combination of Quantitative Susceptibility Mapping and 1H-MRS to examine the role of iron and its association with glutamatergic signalling in Gilles de la Tourette syndrome (GTS). GTS is a neurodevelopmental movement disorder with abnormalities in the neurotransmission of dopamine and GABA and, as shown more recently, also in subcortical glutamate (Glu) and glutamine (Gln). In this work, we observed that GTS patients exhibit reductions in cerebral iron levels and report a general association between iron and the Gln:Glu ratio. This work provides a good example of utilizing multi-modal neuroimaging methods to interrogate pathophyiology at multiple scales.

4650 Computer 18

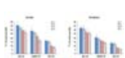

Effects of astrocytic Nrf2 activation on recently-identified ^{13}C and ^{1}H MRS flux-based biomarkers of mitochondrial energetics and neurotransmitter cycling in Huntington's Disease

Golam M. I. Chowdhury[1], Peter Dixon[2], Robin de Graaf[3], Xiaoxian Ma[4], Johnson A Johnson[5], Jeffrey A Johnson[5], Larry Park[6], Gerard Sanacora[1], Douglas L Rothman[4], and Kevin L Behar[1]

[1]Department of Psychiatry, Yale University School of Medicine, New Haven, CT, United States, [2]Department of Psychiatry, Yale University School of Medicine, [3]Department of Radiology and Biomedical Imaging, Yale University School of Medicine, New Haven, United States, [4]Department of Radiology and Biomedical Imaging, Yale University School of Medicine, New Haven, CT, United States, [5]School of Pharmacy, School of Pharmacy, University of Wisconsin, Madison, WI, United States, [6]CHDI Management, CHDI Management/CHDI Foundation, Los Angeles, United States

Alterations in brain glucose and energy metabolism is observed in Huntington's Disease (HD) and HD animal models. 1H-[13C]-MRS can be readily adapted to measure metabolic pathway flux by use of 13C-labeled substrates. In this study we assessed whether activation of the astroglial Nrf2-ARE pathway in the R6/2 mouse model of HD, which has shown therapeutic potential in HD animal models, can reverse the reduction in 13C labeling seen previously in R6/2 mice. In cortex and striatum, astroglial Nrf2 activation led to increased amino acid 13C labeling, suggesting a degree of improvement in mitochondrial and neurotransmitter fluxes in the R6/2 mice.

4651 Computer 19

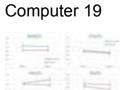

Longitudinal Changes of Metabolites Measured by Proton Magnetic Resonance Spectroscopy and Their Correlations with Behavioral Outcomes in a Rat Model of Kainic Acid Induced Spinal Cord Injury

Mingming Zhu[1], Alice Shum-Siu[2], Emily Martin[2], Abby Wade[2], Darlene Burke[2], David S Magnuson[2], and Chin K Ng[1]

[1]Diagnostic Radiology, University of Louisville School of Medicine, Louisville, KY, United States, [2]Neurological Surgery, University of Louisville School of Medicine, Louisville, KY, United States

We measured the profile of major metabolites longitudinally using MRS in spinal cord gray matter of kainic acid (KA) injured rats at both 7 and 14 days post KA administration and correlated their concentrations with functional outcomes assessed by the Basso, Bresnahan, and Beattie (BBB) Open Field Locomotor scores. Our preliminary findings indicate that metabolite concentrations in the lower lumbar spinal cord gray matter, caudal to the injury epicenter, as detected by in vivo 1H-MRS, could be used as injury and recovery biomarkers in SCI animal models.

4652 Computer 20

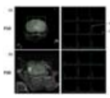

A metabolic study of hypoxic ischemia during mouse brain development using hyperpolarized 13C

Yiran Chen[1,2], Byongsop Lee[3,4], Robert Bok[1], Ilwoo Park[1], Subramaniam Sukumar[1], R Ann Sheldon[3,4], A James Barkovich[1,4], Donna M Ferriero[3,4], and Duan Xu[1,2]

[1]Department of Radiology and Biomedical Imaging, UCSF, San Francisco, CA, United States, [2]Joint UCSF/UC Berkeley Graduate Group in Bioengineering, UCSF, San Francisco, CA, United States, [3]Department of Neurology, UCSF, San Francisco, CA, United States, [4]Department of Pediatrics, UCSF, San Francisco, CA, United States

In this study, we applied dynamic nuclear polarization (DNP) technique to investigate C1 labeled ^{13}C pyruvate to lactate conversion on hypoxic ischemia (HI) injured neonatal mouse brains during development. Our results showed that lower pyruvate level and higher lactate to pyruvate ratio on the injured hemisphere in comparison to the non-injured hemisphere at the day of injury (P10). This difference narrows as the brain matures. With this technique, we are able to examine individuals' response to HI in vivo during brain development.

4653 Computer 21

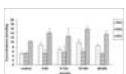

Correlation between dynamic changes of glutamate metabolism and microcirculatory perfusion in basal ganglia after hypoxic–ischemic brain damage

Yuxue Dang[1], Xiaoming Wang[2], and Kaining Shi[3]

[1]Department of Radiology, Shengjing Hospital of China Medical University, Shenyang, People's Republic of China, [2]Department of Radiology, Shengjing Hospital of China Medical University, Shenyang, China, People's Republic of China, [3]Department of Imaging Systems Clinical Science, Philips Healthcare (China), Beijing, People's Republic of China

The excitotoxicity of glutamate metabolism as well as hemodynamic disorders of the brain are both risk factors for neonatal hypoxic–ischemic brain damage (HIBD). To investigate the combined application of intravoxel incoherent motion (IVIM) and ^{1}H-magnetic resonance spectroscopy (MRS) in exploring the possible mechanisms. This study was undertaken to examine basal ganglia metabolites (by means of ^{1}H MRS) and microcirculation (by means of IVIM) in a piglet model of hypoxic-ischemia (HI). It is concluded that elevation of glutamate occurs in parallel to perfusion disruption reflected by changes in perfusion fraction ***f*** after HI.

4654 Computer 22

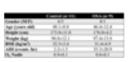

Implications of Obstructive Sleep Apnea on Global Cerebral Metabolic Rate of Oxygen

Ana E Rodríguez-Soto[1], Yulin Chang[1], Wen Cao[1], Zachary B Rodgers[1], John A Detre[2], Erin K Englund[1], Sarah Leinwand[3], Richard Schwab[3], Michael C Langham[1], and Felix W Wehrli[1]

[1]Department of Radiology, University of Pennsylvania, Philadelphia, PA, United States, [2]Department of Neurology, University of Pennsylvania School of Medicine, Philadelphia, PA, United States, [3]Division of Sleep Medicine, Department of Medicine, University of Pennsylvania, Philadelphia, PA, United States

Obstructive sleep apnea (OSA) is a chronic disorder caused by intermittent obstruction of the upper airways during sleep. Neurocognitive deficits in this population have previously been associated with altered brain metabolism. In fact, a recent pilot study suggests that global cerebral metabolic rate of oxygen ($CMRO_2$) may be a potential marker of oxygen metabolic dysfunction in this population. Here, we present preliminary results from an ongoing study designed to quantify $CMRO_2$ in subjects with OSA and matched controls. Initial results suggest that apneics have overall lower baseline $CMRO_2$ and increased response to volitional apnea, a paradigm to mimic spontaneous apneas.

4655 Computer 23

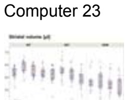

Mutant huntingtin dosage effect on incidence of high striatal Glutamine in a mouse model of Huntington's disease – a symptom of liver pathophysiology?

Thomas Mueggler[1], Andreas Bruns[1], Laurence Ozmen[1], Herve Schaffhauser[1], Basil Künnecke[1], and Markus von Kienlin[1]

[1]Roche Pharma Research and Early Development, Hoffmann-La Roche Pharmaceuticals Ltd, Basel, Switzerland

In contrast to transgenic models of Huntington's disease (HD) newly available knock-in models, such as the HttQ175, recapitulate the heterozygosity present in the clinically observed pathophysiology. Here we report a longitudinal assessment of striatal metabolites using 1H-MRS and volumetry in 30+ brain regions in both male and female HttQ175 mice. Apart from a genotype-specific, progressive neurodegenerative phenotype present in both genders, we discovered an entirely novel feature in mouse models of HD, namely individuals with abnormally high glutamine (Gln) levels, whose incidence increased with mutant Htt gene dosage. In line with emerging data on a widespread peripheral metabolic perturbation in HD, we hypothesize that this excessive Gln is a consequence of disordered hepatic metabolism.

4656 Computer 24

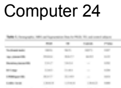

Inhibitory Motor Dysfunction in Parkinson's Disease Subtypes

Tao Gong[1,2], Guangbin Wang[3], Richard Edden[4], Fei Gao[3], Yuanyuan Xiang[5], and Weibo Chen[6]

[1]MRI, Shandong Medical Imaging Research Institute, Shandong University, Jinan, People's Republic of China, [2]Russell H. Morgan Department of Radiology and Radiological Science, Johns Hopkins university, Baltimore, MD, United States, [3]MRI, Shandong Medical Imaging Research Institute, [4]Russell H. Morgan Department of Radiology and Radiological Science, Johns Hopkins university, Baltimore, MD, [5]Shandong University, [6]MRI, Philips Healthcare, Shanhai, People's Republic of China

This study was aimed to evaluate the differences between PD motor subtypes of GABA+ levels using MEGA-PRESS. PD patients were classified into PIGD and TD groups; sixteen healthy controls were recruited. All subjects underwent 3T MR examination including MEGA-PRESS. We found that GABA+ concentration was lower in PD compared with controls; furthermore, the TD group was lower than PIGD. In PD patients, the GABA+ levels were correlated with UPDRS scores. The results suggest that GABAergic dysfunction may play an important role in the pathogenesis of Parkinson’s disease. MEGA-PRESS provides a valuable examination method to discriminate between PD motor subtypes.

Electronic Poster

Head, Neck, Spine

Exhibition Hall — Wednesday 9:15 - 10:15

4657 Computer 25

In Vivo Study of the Human Ear Canal Using Contrast-Enhanced MRI

Sune Darkner[1], Søren Jønsson[2], and Stefan Sommer[1]

[1]Computer Science, University of Copenhagen, Copenhagen, Denmark, [2]Brüel & Kjaer, Denmark

We present the first MRI-based study of the anatomy of the human outer ear. We show that on 45 subjects we can accurately retrieve the anatomy of this outer cavity using a focussing coil, a T2-weighted sequence and vegetable oil. As validation, we show that from the retrieved anatomies of the population we can, using standard methodology, compute an average ear canal that has distinct anatomical landmarks as well as the acoustical properties, which are almost identical to that of a real ear-canal anatomy.

4658 Computer 26

Does MR of the neck improve the credibility of victims after manual strangulation?

Isabella Klasinc[1,2], Kathrin Ogris[2], Thomas Ehammer[1], Thomas Widek[1], Thorsten Schwark[1,2], and Eva Scheurer[3]

[1]Ludwig Boltzmann Institute Clinical Forensic Imaging, Graz, Austria, [2]Institute of Forensic Medicine, Medical University of Graz, Graz, Austria, [3]Institute of Forensic Medicine, University of Basel - Health Department Basel, Switzerland

Former studies have already shown, that MRI findings in victims after survived strangulation allow the diagnosis of strangulation. Native 3T MR scans of the neck were performed in strangulation victims without external findings. All subjects showed strangulation specific MRI findings. Therefore, MRI of the neck is indicated in cases of reported manual strangulation.

4659 Computer 27

Investigating the use of arterial spin labeling perfusion as a substitute to DCE-MRI in primary tumor perfusion of nasopharyngeal carcinoma

Meng Lin[1], Xiaoduo Yu[1], Bing Wu[2], Dehong Luo[1], Han Ouyang[1], and Chunwu Zhou[1]

[1]Cancer Hospital, Chinese Academy of Medical Sciences, Beijing, People's Republic of China, [2]GE Healthcare MR research China, Beijing

Assessment of perfusion is important in tumor diagnosis, stage and therapeutic effect evaluation. This study aimed to investigate the relationship between arterial spin labeling (ASL) (with PLD=1.0, 1.5 and 2.0s) and DCE-MRI parameters of nasopharyngeal carcinoma (NPC). Two observers measured the tumor blood flow (TBF) by ASL and DCE derived parameters including MaxSlop, CER, IAUGC, Ktrans, Kep and Ve. TBF showed moderate to strong correlations between all three TBF and DCE-MRI parameters except between all TBF with Ve and between TBF of PLD1.5s and CER. ASL is a feasible non-invasive tool in NPC to quantitatively assess the perfusion.

4660 Computer 28

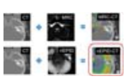

Detectability and anatomical location identification of cholesteatoma with thin-slice non-echo planar imaging diffusion-weighted image (nEPID) using fused nEPID and CT(nEPID-CT)

Toshitada Hiraka[1], Masafumi Kanoto[1], Yuuki Toyoguti[1], Yoshihiro Konno[1], Yasuhiro Sugai[1], and Takaaki Hosoya[1]

[1]Diagnostic Radiology, Yamagata University Faculty of Medicine, Yamagata, Japan

Non-echo planar imaging diffusion-weighted imaging (nEPID) is a useful tool for diagnosing middle ear cholesteatoma. The cut-off value of nEPID has not yet been determined, however, as fused thin-slice nEPID and computed tomography (nEPID-CT) color imaging cannot correctly distinguish cholesteatoma from other soft tissue. We examined the detectability of cholesteatoma with nEPID using nEPID-CT color images obtained as preoperative studies. The appropriate cut-off value of the signal intensity ratio on nEPID is 0.925 on the receiver operating characteristic (ROC) curve with Youden’s index. Here, we evaluate the efficacy of nEPID-CT color images based on this nEPID cut-off value.

4661 Computer 29

B0 and B1 Field Inhomogeneity Consideration in Pseudo-continuous ASL Due to the Presence of Carotid Artery Stenting

Chien-Yuan Eddy Lin[1,2], Jianxun Qu[2], Ai-Chi Chen[1], Yen-Chien Wu[3], David Yen-Ting Chen[3], Ying-Chi Tseng[3], and Chi-Jen Chen[3]

[1]GE Healthcare, Taipei, Taiwan, [2]GE Healthcare MR Research China, Beijing, People's Republic of China, [3]Department of Radiology, Taipei Medical University - Shuang Ho Hospital, New Taipei City, Taiwan

Pseudo-continuous arterial spin labeling (pCASL) has been recently used for investigating cerebral hemodynamic change on the patient receiving carotid artery stenting (CAS) because it permits repeated measurement of absolute cerebral blood flow in a short interval without MR contrast agent or radioactive material. However, labeling efficiency of pCASL has been proved to be dependent on B_0 and B_1 inhomogeneity. The aim of this study was to understand how inhomogeneous of the B_0 and B_1 at labeling position of pCASL and find the remedies of the pCASL measurement for the CAS patient.

4662 Computer 30

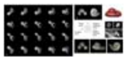

Modified 3D T2W DRIVE sequence for high resolution inner ear imaging at 7T

Kingkarn Aphiwatthanasumet[1], Gerry O'Donoghue[2], Paul Glover[1], Xiao Liang[1,3], and Penny Gowland[1]

[1]Sir Peter Mansfield Imaging Centre, University of Nottingham, Nottingham, United Kingdom, [2]Ear Nose and Throat, University of Nottingham, Nottingham, United Kingdom, [3]Beijing University of Chemical Technology, People's Republic of China

Despite the promise of increased sensitivity, non-contrast-enhanced imaging of inner ear at 7T is challenging due to local variations in B1 and B0. Here we optimize T2-weighted scanning to improve image quality in the inner ear and evaluate the normal variation in the geometry of the cochlea using 3D T2W DRIVE sequence with dielectric pads and RF shimming. The resulting images show well-defined internal structure of the cochlea and the branches of cranial nerve.

4663 Computer 31

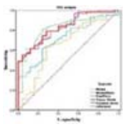

Dynamic Contrast-Enhanced MRI Predicts Short-Term Control of Nasopharyngeal Carcinoma within 5 fractions Intensity-Modulated Radiotherapy

Dechun Zheng[1], Yunbin Chen[1], Meng Liu[1], Hao Lin[1], Xiaoxiao Zhang[1], Qiuyuan Yue[1], Wang Ren[1], Weibo Chen[2], and Queenie Chan[3]

[1]Radiology, Fujian Cancer Hospital & Fujian Medical University Cancer Hospital, Fuzhou, People's Republic of China, [2]MR Clinical Science, Philips Healthcare, [3]Philips Healthcare

Many quantitative DCE-MRI based studies suggested it had utility in early monitoring radiotherapy and chemotherapy sensitivity in anti-tumor treatment. However, there are a few studies investigated whether it could been used for predicting IMRT effect and to what extend of its performance would be. This study enrolled 87 patients who received DCE-MRI one week before NAC and one week after IMRT treatment and suggested there were collaboration the kinetic parameters of quantitative DCE-MRI in early assessing IMRT treatments in NPC.

4664 Computer 32

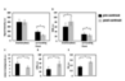

The application of enhanced MRI with 3D-STIR-SPACE for Brachial Plexus lesions

Lan Zhang[1] and Wen Chang Chen[2]

[1]MRI, The 1st affiliated hospital of Henan university of TCM, Zhengzhou, People's Republic of China, [2]Chang Gung Memorial Hospital, Chiayi Branch, Taiwan

Imaging the brachial plexus is a challenge due to its complicated structure. The purpose of this study is to improve the diagnosis ability for brachial plexus 3D-STIR-SPACE technique with contrast agent administration. After contrast agent administration, signals of adjacent vessels were suppressed due to reduction in its T1 relaxation time which became similar to that of fat. The outlines of nerves would be clearer with respect to surrounding tissues.The image of 3D-STIR-SPACE technique with contrast agent was superior to that without contrast agent. It might be a better way to evaluate anatomies and pathologies of the brachial plexus.

4665 Computer 33

One shot 3D flow sensitive cine MR imaging using improved motion sensitized driven equilibrium(iMSDE)

Nao Kajihara[1], Tomohiko Horie[1], Syuhei Shibukawa[1,2], Susumu Takano[1], Toshiki Saito[1], Makoto Obara[3], Tetsuo Ogino[3], Tetsu Niwa[4], and Yutaka Imai[4]

[1]Department of Radiology, Tokai University Hospital, Kanagawa, Japan, [2]Graduate School of Medical Science, Kanazawa University, Kanazawa, Japan, [3]Healthcare department, Philips Electronics Japan, Tokyo, Japan, [4]Department of Radiology, Tokai University School of Medicine, Kanagawa, Japan

Dynamic improved motion-sensitized driven-equilibrium steady-state free precession (dynamic iMSDE SSFP) has been introduced to visualize the irregular flow of cerebrospinal fluid (CSF), which obtains this data in 2D. To improve visibility of CSF space at a wide range, we here proposed a new technique using 3D-free factor. The results showed that fluid motions were sensitively suppressed by iMSDE, similar to 2D acquisition. Thus, this technique may detect irregular CSF motion at the wide range.

4666 Computer 34

Positional variation of parotid glands in the treatment position of head and neck radiotherapy with immobilization: a pilot study on healthy volunteers using high spatial resolution 3D MRI at 1.5T

Jing Yuan[1], Yihang Zhou[1], Oilei Wong[1], Winky Wing Ki Fong[2], George Chiu[2], Kin Yin Cheung[1], and Siu Ki Yu[1]

[1]Medical physics and research department, Hong Kong Sanatorium & Hospital, Happy Valley, Hong Kong, [2]Department of Radiotherapy, Hong Kong Sanatorium & Hospital, Happy Valley, Hong Kong

Investigation of positional and geometric variations of organ-at-risk (OAR) in head-and-neck (HN) radiotherapy (RT) is greatly limited by the poor soft tissue contrast of X-ray-based imaging. We investigated the positional variation of parotid glands (PG) in the immobilized HN-RT treatment position on healthy volunteers using high-spatial-resolution 3D-MRI at 1.5T. The results showed that PGs generally had sub-millimeter and sub-degree group mean error, systematic error and random error under immobilization. Although PGs generally showed insignificant positional variations from global HN, individual left and right PG might move independently and resulted in insignificant positional correlations with each other and global HN.

4667 Computer 35

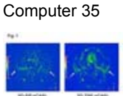

Measurement of blood flow in normal parotid glands using pseudo-continuous arterial spin labeling: comparison between 2D echo-planar and 3D turbo spin-echo sequences.

Katsuhiro Inoue[1], Maki Umino[2], Ryohei Nakayama[3], Shinichi Takase[1], Tsunehiro Yamahata[1], Makoto Obara[4], Masayuki Maeda[5], and Hajime Sakuma[6]

[1]Department of Radiology, Mie University Hospital, Mie, Japan, [2]Department of Radiology, Mie University School of Medicine, Mie, Japan, [3]Department of electronic and Computer Engineering, Ritsumeikan University, Shiga, [4]Philips Electronics Japan, Tokyo, Japan, [5]Department of Advanced Diagnostic Imaging, Mie University School of Medicine, Mie, Japan, [6]Department of Radiology, Mie University School of Medicine, Tsu, Mie, Japan

Evaluation of parotid blood flow (PBF) may provide an insight into the pathophysiology of parotid diseases. We evaluated and compared the blood flow of normal parotid glands in six volunteers using 2D-echo-planar (EP) and 3D-turbo-spin-echo (TSE) pseudo-continuous ASL (pCASL) sequences. Visual assessment indicated that 3D-TSE pCASL maps were significantly better for delineating normal parotid glands. 3D-TSE pCASL showed larger PBF values than 2D-EP pCASL. Fewer measurement errors were observed in 3D-TSE pCASL data. We concluded that 3D-TSE pCASL is more suitable for the evaluation of PBF than 2D-EP pCASL.

4668 Computer 36

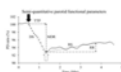

Semi-quantitative Parametric Evaluation of Parotid Gland Function Using Proton Density Magnetic Resonance Imaging

Yu-Chia Cheng[1], Yi-Jui Liu[2], Yi-Hsiung Lee[3,4], Hing-Chiu Chang[5], Hui-Chu Chiu[6], Ta-Wei Chiu[7], Kang Hsu[8], Hsian-He Hsu[4,9], and Chun-Jung Juan[4,9]

[1]Master 's Program of Biomedical Informatics and Biomedical Engineering of Feng Chia University, Taichung, Taiwan, Taichung, Taiwan, [2]Department of Automatic Control Engineering, Feng Chia University, Taichung, Taiwan, Republic of China, [3]Ph.D. program in Electrical and Communication Engineering in Feng Chia University, Taichung, Taiwan, Republic of China, [4]Department of Radiology, Tri-Service General Hospital, Taipei, Taiwan, Republic of China, [5]Department of Diagnostic Radiology, The University of Hong Kong, Hong Kong, [6]Ph.D. program of Technology Management, Chung Hua University, Hsinchu, Taiwan, Republic of China, [7]Department of Medicine, Taipei Medical University, Taipei, Taiwan, Republic of China, [8]Department of Dentistry, National Defense Medical Center, Taipei, Taiwan, Republic of China, [9]Department of Radiology, National Defense Medical Center, Taipei, Taiwan, Republic of China

The parotid gland function is evaluated by gustatory stimulation using scintigraphy in clinic. It is supposed to measure the water component of parotid gland using PD MRI instead of scintigraphy. In this study, we initially developed the evaluation of parotid gland function by PD MRI, and 10 healthy volunteers underwent double echo EPI with gustatory stimulation. Maximal drop ratio (MDR), time to peak (TTP), drop slope (DS), recovery slope (RS) and recovery ratio (RR) were calculated. The signal intensity dropped significantly after gustatory stimulation on PD image (P<0.01). MRI allows quantification of parotid gland function using semi-quantitative functional parameters.

4669 Computer 37

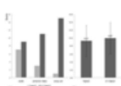

3D pituitary dynamic MR imaging using the TWIST and Iterative reconstruction TWIST

Yusuke Yokota[1], Yasutaka Fushimi[1], Tomohisa Okada[2], Akira Yamamoto[1], Tsutomu Okada[1], Aurelien Stalder[3], Christoph Forman[3], Michaela Schmidt[3], and Kaori Togashi[1]

[1]Department of Diagnostic Imaging and Nuclear Medicine, Graduate School of Medicine, Kyoto University, Kyoto, Japan, [2]Human Brain Research Center, Graduate School of Medicine, Kyoto University, Kyoto, Japan, [3]Siemens Healthcare GmbH, Erlangen, Germany

The aim of this study is to perform a comparison between 3D pituitary dynamic study using time-resolved angiography with interleaved stochastic trajectories (TWIST) and TWIST with iterative reconstruction (IT-TWIST). IT-TWIST was retrospectively reconstructed from the raw data of TWIST by using L1 wavelet regularization in space and time. One neuroradiologist put regions of interest in pituitary stalk and anterior lobe and made time intensity curve. The slope of enhancement in the early phase was evaluated. In addition, image quality was visually evaluated. IT-TWIST yielded higher slope of enhancement in the early phase in anterior lobe and better image quality.

4670 Computer 38

Correlation of humanpapilloma virus status with quantitative perfusion/diffusion MRI parameters and metabolic 18F-FDG-PET parameters in oral cavity and oropharyngeal squamous cell carcinoma : Comparison between primary tumor lesions and metastatic lymph nodes

Miran HAN[1], Jin Wook Choi[1], and Su Jin Lee[2]

[1]Radiology, Ajou University Medical Center, Suwon, Korea, Republic of, [2]Nuclear medicine, Ajou University Medical Center, Suwon, Korea, Republic of

We evaluated association between perfusion/diffusion MRI parameters, metabolic ^{18}F-FDG PET parameters and HPV status in not only primary oral cavity-oropharyngeal squamous cell carcinoma but also its metastatic lymph nodes. Any significant difference was not found in quantitative perfusion, diffusion, metabolic parameters of primary tumor between HPV-positive and HPV-negative groups. In case of metastatic lymph node, only metabolic parameters were significantly higher in HPV-positive group. In our study population, HPV status of primary OC-OPSCC and metastatic lymph nodes did not translate into different perfusion/diffusion parameters. Larger study population is needed to establish whether imaging parameters can represent the HPV status.

4671 Computer 39

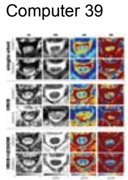

Reduced FOV with Multi-shot IRIS Provides Improved Diffusion Tensor Imaging in the Cervical Spinal Cord

Samantha By[1,2], Ed Mojahed[2,3], Saikat Sengupta[2], and Seth A. Smith[1,2,4]

[1]Biomedical Engineering, Vanderbilt University, Nashville, TN, United States, [2]Vanderbilt University Institute of Imaging Science, Vanderbilt University Medical Center, Nashville, TN, United States, [3]Philips Healthcare, Nashville, TN, United States, [4]Radiology and Radiological Sciences, Vanderbilt University Medical Center, Nashville, TN, United States

Spinal cord DTI is technically challenging, primarily due to the small size of the cord and physiological motion. We compare three different sequences to address these challenges: 1) single-shot EPI (ss-EPI), 2) multi-shot EPI with 2D navigation (IRIS), and 3) multi-shot EPI with reduced FOV (IRIS+iZOOM). Results indicate that IRIS alleviates geometric distortion present in ss-EPI. The combination of IRIS and iZOOM, however, provides the most consistent and least distorted diffusion-weighted images. These effects are clearly seen in the fractional anisotropy, axial diffusivity, and radial diffusivity maps, where exceptional contrast between gray and white matter are observed with IRIS+iZOOM.

4672 Computer 40

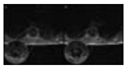

Suppression of CSF-flow-artifacts for T1-w Spin-echo Spine Imaging

Ola Norbeck[1,2], Enrico Avventi[1,2], Henric Rydén [1], and Stefan Skare[1,2]

[1]Neuroradiology, Karolinska University Hospital, Stockholm, Sweden, [2]Clinical Neuroscience, Karolinska Institutet, Stockholm, Sweden

We propose a simple method to suppress cerebrospinal fluid pulsatile-flow-artifacts in axial 2D T1-weighted spin-echo images of the spine. Widening the spatial width of the excitation pulse is shown to remove artifacts that otherwise could obscure or mimic tumors in the spinal canal.

4673 Computer 41

Simple Modification of Arms Position Improves B1+ and Signal Homogeneity in the Thoracolumbar Spine at 3T

Kinya Ishizaka[1], Kohsuke Kudo[2], Kuniaki Harada[3], Toru Shirai[4], and Taro Fujiwara[1]

[1]Department of Radiological Technology, Hokkaido University Hospital, Sapporo, Japan, [2]Division of Diagnostic and Interventional Radiology, Hokkaido University Hospital, Sapporo, Japan, [3]Hitachi, Ltd., Healthcare Company, [4]Hitachi, Ltd., Research and Development Group

To evaluate the homogeneity of B1+ and signal intensity of the thoracolumbar spine with different arm positions. Twenty volunteers were scanned with 4-channel RF transmit coil at 3T. Three arm positions were used; arms on the bed, arm lift, and arm up position. Axial B1+ maps and sagittal T1WI were obtained individually with each arm position. Mean and SD values of FA, and CNR with arm lift and arm up position were significantly superior with arms on the bed position. Inhomogeneities of B1+ and signal intensities were improved by simply changing the arm position at 3T thoracolumbar spine imaging.

4674 Computer 42

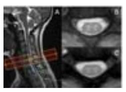

Motor-task based fMRI of the spinal cord reveals neural activity in gray matter horns

Satoshi Maki[1], Benjamin N. Conrad[1], Robert L. Barry[2,3], Lydia J. McKeithan[1], John C. Gore[1,4], and Seth A. Smith[1,4]

[1]Vanderbilt University Institute of Imaging Science, Nashville, TN, United States, [2]Athinoula A. Martinos Center for Biomedical Imaging, Department of Radiology, Massachusetts General Hospital, Charlestown, MA, United States, [3]Department of Radiology, Harvard Medical School, Boston, United States, [4]Department of Radiology and Radiological Sciences, Vanderbilt University Medical Center, Nashville, TN, United States

In spinal cord functional magnetic resonance imaging (fMRI) studies, localization of functional activation is still limited due to low signal to noise ratio and low spatial resolution. We studied blood oxygen level dependent signal changes in individual gray matter horns of the cervical spinal cord using a 3D gradient-echo sequence for fMRI during an upper extremity motor task. Visualization and delineation of neural activity in gray matter of cervical spinal cord elicited by the motor task was successfully demonstrated at fine spatial scales suggesting the potential for noninvasive monitoring of spinal cord function.

4675 Computer 43

Feasibility of Grey Matter and White Matter Segmentation of the Conus Medullaris: A Pilot In Vivo Investigation in the Neurologically Intact Spinal Cord

Martina D Liechti[1,2], Nuttakarn Budtarad[1], Daniel R Altmann[1,3], Xixi Yang[1,2], Ahmed T Toosy[1], Jalesh N Panicker[2], Claudia AM Gandini Wheeler-Kingshott[1], and Marios Yiannakas[1]

[1]UCL Institute of Neurology, Queen Square MS Centre, University College London, London, United Kingdom, [2]UCL Institute of Neurology, Uro-Neurology, Department of Brain Repair & Rehabilitation, University College London, London, United Kingdom, [3]Translational Imaging Group, Centre for Medical Image Computing, Department of Medical Physics and Biomedical Engineering, University College London, London, United Kingdom

Spinal cord (SC) atrophy as a consequence of neurodegeneration, and its association with clinical scores of disability, may be assessed indirectly by means of cord, grey matter (GM) and white matter (WM) segmentation from magnetic resonance images. Neuropathological evidence suggests that in certain neurological conditions, early degeneration may occur as low as the sacral SC, potentially implicating neural pathways that are essential for the functioning of the lower urinary tract. In this work, the feasibility of GM/WM segmentation of the conus medullaris is assessed *in vivo* using a clinical 3T system.

4676 Computer 44

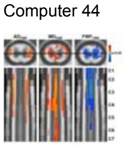

Free Water Estimation Improves in vivo Diffusion MRI Remote from the Lesion Site in Rat Spinal Cord Injury

Matthew Budde[1], Nathan Skinner[2], Brian Schmit[3], and Shekar Kurpad[1]

[1]Neurosurgery, Medical College of Wisconsin, Milwaukee, WI, United States, [2]Medical College of Wisconsin, Milwaukee, WI, United States, [3]Biomedical Engineering, Marquette University, Milwaukee, WI, United States

Diffusion tensor imaging (DTI) of the spinal cord remote from the site of injury has been shown to be a surrogate marker of spinal cord injury (SCI) severity. In this work, detection of injury severity with in vivo diffusion MRI of the rat cervical cord following a thoracic SCI was improved with advanced diffusion MRI signal modelling compared to DTI.

4677 Computer 45

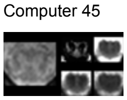

Investigating trauma-induced microstructural changes at the lumbosacral enlargement after spinal cord injury

Gergely David[1], Eveline Huber[1], Nikolaus Weiskopf[2,3], Siawoosh Mohammadi[3,4], and Patrick Freund[1,2,3]

[1]Spinal Cord Injury Center, Balgrist University Hospital, Zurich, Zurich, Switzerland, [2]Department of Neurophysics, Max Planck Institute for Human Cognitive and Brain Sciences, Leipzig, Germany, [3]Wellcome Trust Centre for Neuroimaging, UCL Institute of Neurology, London, United Kingdom, [4]Department of Systems Neuroscience, University Medical Center Hamburg-Eppendorf, Hamburg, Germany

Neuroimaging of the cervical cord has demonstrated above-level neurodegeneration after traumatic spinal cord injury. In this study, we investigated below-level neurodegeneration with optimized high-resolution MRI sequences, including diffusion tensor imaging and structural imaging, applied to the lumbar cord in patients with cervical injury. Our results demonstrate that atrophy and axonal degeneration are prominent in the lumbar cord reflected by structural and diffusivity changes. Furthermore, the extent of these changes is related to clinical impairment. This study shows neurodegeneration below the level of injury and demonstrates the clinical feasibility of acquiring readouts of tissue-specific changes in the lumbar cord.

4678 Computer 46

Voxel-based analysis of grey and white matter degeneration above the level of injury in cervical spinal cord injury

Eveline Huber[1], Gergely David[1], Niklaus Weiskopf[2,3], Siawoosh Mohammadi[3,4], and Patrick Freund[1,2,3,5]

[1]University Hospital Balgrist, University of Zurich, Zurich, Switzerland, [2]Department of Neurophysics, Max Planck Institute for Human Cognitive and Brain Sciences, Leipzig, Germany, [3]Wellcome Trust Centre for Neuroimaging, UCL Institute of Neurology, University College London, London, United Kingdom, [4]of Systems Neuroscience, University Medical Center Hamburg-Eppendorf, Hamburg, Germany, [5]Department of Brain Repair and Rehabilitation, UCL Institute of Neurology, University College London, London, United Kingdom

We studied the extent of cervical grey and white matter neurodegeneration above the level of injury after traumatic spinal cord injury (SCI) using high-resolution structural and diffusion MRI data. We found marked atrophy of both white and grey matter alongside diffusivity changes associated with axonal degeneration within the major spinal tracts. The extent of structural decline related to clinical impairment. These tract specific changes and clinicopathological relationships shed light into underlying neurodegenerative disease mechanisms, and therefore these measureable changes hold potential to serve as neuroimaging biomarkers of cord pathology.

4679 Computer 47

summa cum laude

The Utility of DTI and NODDI for Assessment of Disease Severity and in Predicting Postoperative Neuronal Recovery: An Atlas-based Tract Specific Study

Tomohiro Takamura[1], Ryo Ueda[2], Masaaki Hori [1], Ryusuke Irie[1], Koji Kamagata[1], Michimasa Suzuki[1], and Shigeki Aoki[1]

[1]Juntendo University, Tokyo, Japan, [2]Tokyo Metropolitan University

Quantification of disease severity and prediction of postoperative outcome were essential in management of cervical spondylotic myelopathy (CSM). The purpose of this study was to investigate correlation between diffusion metrics, including DTI or NODDI in spinal cord pathways, and the severity of CSM, as well as their predictive ability for postoperative recovery. We elucidated that the disease severity was significantly correlated with FA and ODI, and postoperative recovery correlated with RD and MD. The lateral funiculi and lateral corticospinal tract seemed to be the predominant spinal cord pathway that correlated with disease severity and postoperative recovery.

4680 Computer 48

Microstructural assessment of the cervical spinal cord using high-resolution, 1 dimensional MRI

Rexford Newbould[1] and Paul M Matthews[2]

[1]Imanova, London, United Kingdom, [2]Division of Brain Sciences, Imperial College London, London, United Kingdom

A 1-dimensional MR sequence termed Fine Structural Analysis (fineSA) was applied to the human cervical spinal cord in order to determine if spinal tracts and nerve fibres of the dorsal horn could be identified from the spectral regularity of their myeloarchitecture. Repeatable 60 µm peaks could be attributed to the dorsal horn as opposed to projective nerve tracts of the cord. This analysis might be able to identify the loss of neurons via changes in packing density that would be proximal to macrostructural atrophy detectable on more classical MR sequences.

Electronic Poster

Brain Anatomy: Techniques & Applications

Exhibition Hall Wednesday 9:15 - 10:15

4681 Computer 49

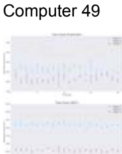

(free)Surfing ANTs: a comparative study

Santi Puch[1], Paulo Rodrigues[1], David Moreno-Dominguez[1], Marc Ramos[1], and Vesna Prčkovska[1]

[1]Mint Labs, Barcelona, Spain

Robust and automated tools such as *FreeSurfer* or *ANTs* for brain segmentation and quantification have been of utmost importance in the recent advancements in the Neuroimaging field. However, the reproducibility and variability of their results are often uncertain. In this study, we analyzed their reproducibility and compared their outputs for different brain structures. We observe that both tools give high reproducibility for volumetric studies and give similar results in most of the examined cases. However, in some structures (pallidum, rostral-anterior cingulate) there are more pronounced and significant differences. Our results also indicate slightly better reproducibility of *ANTs* over *FreeSurfer*.

4682 Computer 50

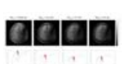

Dura Mater imaging with UTE T_2^* Mapping

Yuki Kanazawa[1], Masafumi Harada[1], Mitsuharu Miyoshi[2], Yuki Matsumoto[3], Hiroaki Hayashi[1], Toshiaki Sasaki[4], Natsuki Ikemitsu[4], and Michael Carl[2]

[1]Graduate School of Biomedical Sciences, Tokushima University, Tokushima, Japan, [2]Global MR Applications and Workflow, GE Healthcare, [3]Graduate school of Health Science, Tokushima University, [4]School of Health Sciences, Tokushima University

To assess signal of dura mater acquired from UTE imaging, we evaluated this component with T_2^* mapping derived from a multi-echo UTE sequence of healthy volunteers. We then compared measured T_2^* values of cranium and dura mater. The mean T_2^* value of dura mater in five healthy volunteers was significantly higher than that of cranium (P < .05). It is found that the T_2^* decay of dura mater was faster than the cranium components. UTE T_2^* mapping makes it possible to obtain detailed information for meningeal abnormalities.

4683 Computer 51

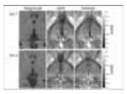

Reproducibility of human habenula characterization with high-resolution quantitative susceptibility mapping at 3T

Seung-Kyun Lee[1,2], Seulki Yoo[1,2], and Anup S Bidesi[1,2]

[1]Department of Biomedical Engineering, Sungkyunkwan University, Suwon, Korea, Republic of, [2]Center for Neuroscience Imaging Research, Institute for Basic Science, Suwon, Korea, Republic of

We investigated scan-rescan reproducibility of human habenula susceptibility measurement using quantitative susceptibility mapping (QSM) at a 0.5x0.5x0.8 mm^3 resolution. Although previously reported paramagnetic enhancement in the habenula (Schenck et al., ISMRM 2015) was confirmed, the paramagnetic center was highly localized within the habenula mass to make the susceptibility quantification vulnerable to partial volume effects. This appeared to limit the reproducibility of peak susceptibility measurements in the habenula to 10~40%, with significant variation among subjects. High resolution scans and reliable coil combination of phase data would be needed to make QSM a more reliable tool for human habenula characterization.

4684 Computer 52

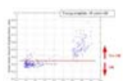

Characterization Of Registration Errors To Screen Aberrant Subject Results Prior To Voxel-Wise Whole Brain Analysis

Roman Fleysher[1,2], Namhee Kim[1,2], Asif Suri[1,2], Michael L Lipton[1,2], and Craig A Branch[1,2]

[1]Gruss Magnetic Resonance Research Center, Albert Einstein College of Medicine, Bronx, NY, United States, [2]Radiology, Albert Einstein College of Medicine, Bronx, NY, United States

Voxel-wise analyses of DTI, fMRI or any other MRI-derived metric, be it for comparing groups or one patient to a control group, require quality registration of images to a template. One or several poorly registered images may skew the distributions of the metric in several voxels leading to incorrect inferences. We propose an approach to screen poorly registered images prior to voxel-wise analysis by comparing subject-wise mean displacements of anatomical landmarks between morphed images and the template estimated using FreeSurfer. We apply this proposed algorithm to demonstrate morph accuracy characterization using two age extreme (18 and 86 year old) templates.

4685 Computer 53

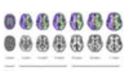

Automatic Segmentation of Human Brain MRI using Sliding Window and Random Forests

Ahmed Serag[1], Emma J Telford[1], Scott Semple[1], and James P Boardman[1]

[1]University of Edinburgh, Edinburgh, United Kingdom

Volumetric analysis of brain MRI acquired across the life course may be useful for investigating long-term effects of risk and resilience factors for brain development and healthy ageing, and for understanding early life determinants of adult brain structure. We developed an automatic segmentation method for human brain MRI, where a sliding window approach and a multi-class random forest classifier were applied to high-dimensional feature vectors for accurate segmentation. The method performed well on brain MRI data acquired from 179 individuals, analysed in three age groups: newborns (38-42 weeks gestational age), children and adolescents (4-17 years) and adults (35-71 years).

4686 Computer 54

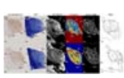

Post-mortem and In Vivo Thalamic Nuclei Identification at 7T with Comparison to Histology

Mobeen Ali[1], Ian Scott[2], Alain Pitiot[3], Karen Mullinger[1,4], Andy Bagshaw[4], Penny Gowland[1], and Richard Bowtell[1]

[1]Sir Peter Mansfield Imaging Centre, University of Nottingham, Nottingham, United Kingdom, [2]Department of Cellular Pathology, Nottingham University Hospitals NHS Trust, Nottingham, United Kingdom, [3]School of Psychology, University of Nottingham, Nottingham, United Kingdom, [4]Centre for Human Brain Health (CHBH), University of Birmingham, Birmingham, United Kingdom

The thalamus plays a major role in regulating the transfer of information through the brain and is also implicated in many neurodegenerative diseases. It is therefore crucial to improve our understanding of this key brain structure. Structural differentiation of thalamic nuclei in post-mortem 7T MRI was investigated. Thalamic sub-regions were identified in magnitude, R2*, R1 and magnetisation transfer ratio maps from six post-mortem brains. Edge detection, k-means clustering algorithms and thin-plate spline warping to the Morel atlas were used to systematically identify thalamic nuclei. These data showed good correlation with stained histological sections and in vivo MRI data.

4687 Computer 55

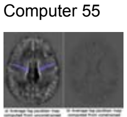

Strategies for Building a Morphologically Faithful Average Brain Template from Population Diffusion MRI Data

Mustafa Okan Irfanoglu[1,2,3], Neda Sadeghi[2], Amritha Nayak[1,2,3], and Carlo Pierpaoli[1,2]

[1]Quantitative Medical Imaging Section, NIBIB/NIH, Bethesda, MD, United States, [2]SQUITS/NICHD/NIH, Bethesda, MD, United States, [3]Henry Jackson Foundation, Bethesda, MD, United States

The availability of anatomically accurate MRI atlases, which can be used as target templates for registration, is essential for quantitative analysis of MRI data. Ideally the computed atlas should be representative of the average features of the population at each voxel location. In this work, we investigate the ability of the most common atlasing approach (i.e. iterative registration followed by averaging) of assuring morphological accuracy. We also evaluate whether constraining the individual deformation fields with deformation-based information helps achieving this goal. We perform our atlas creation tests from full DTI data, using a novel diffusion tensor based diffeomorphic registration technique. We conclude that current atlasing techniques lead to templates that do not faithfully represent the average morphology of the population but that by applying appropriate constraints significant improvements toward this goal can be achieved.

4688 Computer 56

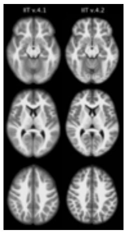

IIT Human Brain Atlas: Enhancement of T1-weighted Template, Tissue Probability Maps and Gray Matter Atlas

Xiaoxiao Qi[1], Shengwei Zhang[1], and Konstantinos Arfanakis[1]

[1]Department of Biomedical Engineering, Illinois Institute of Technology, Chicago, IL, United States

The IIT Human Brain Atlas contains anatomical, DTI, HARDI templates, probabilistic gray matter (GM) labels, probabilistic connectivity-based white matter labels, and major fiber-bundles of the young adult brain. During development of the atlas, spatial normalization was accomplished based on diffusion data. Consequently, matching of the anatomical information of T1-weighted images was not maximized, blurring the T1-weighted template and tissue probability maps, increasing the noise of the T1-weighted template, and lowering confidence of GM labeling and GM label precision. The present work enhanced the quality of the T1-weighted template, tissue probability maps, and GM labels of the IIT Human Brain Atlas.

4689 Computer 57

Multi-modal characterization of white matter for studying language and hand motor function

Yuichi Suzuki[1], Kouhei Kamiya[1], Minoru Mitsuda[1], Akira Kunimatsu[1], Masaaki Hori[2], Harushi Mori[1], Katusya Maruyama[3], Kenji Ino[1], Yasushi Watanabe[1], Jiro Sato[1], Shigeki Aoki[2], Keiichi Yano[1], and Osamu Abe[1]

[1]Department of Radiology, The University of Tokyo Hospital, Tokyo, Japan, [2]Radiology, Juntendo University School of Medicine, Tokyo, Japan, [3]Siemens Japan K.K., Tokyo, Japan

We present a preliminary experience of a fiber g-ratio technique using a combination (MT_sat and NODDI) in multi-modal characterization of the white matter bundles relevant to language and hand motor function. Tract-specific analyses of the pyramidal tract, accurate fasciculus, and frontal aslant tract were performed using the tractography as volume of interest. The fiber g-ratio, MVF, AVF, and FA were measured, and differences between the the hemispheres and among the bundles were tested. This study suggested we can be more sensitive to the lateralities of these bundles by combining myelin imaging and diffusion.

4690 Computer 58

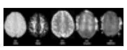

Gender Dimorphism in Cerebral White Matter Architecture: Insights from Diffusion Spectrum Imaging and Whole Brain Echo-Planar Spectroscopic Imaging

Khin Khin Tha[1,2], Kagari Abiko[3], Yuta Urushibata[4], Sinyeob Ahn[5], Osamu Manabe[6], Naoya Hattori[6], Kohsuke Kudo[1], and Hiroki Shirato[1]

[1]Department of Radiation Medicine, Hokkaido University, Sapporo, Japan, [2]Global Station for Quantum Medical Science and Engineering, Sapporo, Japan, [3]Department of Rehabilitation, Hokkaido University, Sapporo, Japan, [4]Siemens Health Care, Japan, [5]Siemens Health Care, San Francisco, CA, United States, [6]Department of Nuclear Medicine, Hokkaido University, Japan

Gender dimorphism in white matter architecture was evaluated by using DSI and whole brain EPSI. Several white matter areas revealed gender differences in the major DSI indices, of which some area had gender difference in NAA/Cr.

4691 Computer 59

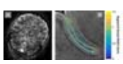

Measuring Transcortical Vasculature with Ultra-high Field (7T) MRI

Allen Timothy Newton[1], Isabel Gauthier[2], and Rankin W McGugin[2]

[1]Radiology and Radiological Sciences, Vanderbilt University Medical Center, Nashville, TN, United States, [2]Psychology, Vanderbilt University, Nashville, TN, United States

Direct visualization of intracortical vascular structure holds promise for detection of pathologic conditions currently invisible with conventional clinical MRI. However, imaging of these structures with MRI has been rare, and no validation of the technique has been performed. Here, we use 7T SWI to directly image intracortical vasculature on the microscopic scale with the goal of understanding the within and between subject variance. We found intracortical vascular measurements were reproducible within subjects and were sensitive to between subject variability, indicating that the measurements may be useful as a biomarker of disease processes affecting vasculature within the cortex.

4692 Computer 60

MRI to monitor the impact of positional changes in the airway of sleep apnea patients – A Phase I methodology demonstration at 3T

Huyen Thanh Nguyen[1], Ulysses Magalang[2], Amir Abdujiliah[1], Saba Elias[1], Petra Schmalbrock[1], Preethi Subramanian[1], Shivangi Vora[1], Wenbo Wei[1], Samantha Rojas[2], Kirsten Emmons[3], David Ribble[3], and Michael V Knopp[1]

[1]Wright Center of Innovation in Biomedical Imaging, Department of Radiology, The Ohio State University, Columbus, OH, United States, [2]Division of Pulmonary, Allergy, Critical Care, and Sleep Medicine, The Ohio State University, Columbus, OH, United States, [3]Hill-Rom

We aimed to develop a non-invasive quantitative MRI methodology to assess positional and rotational impact on the airway opening in subjects with history of sleep apnea for a proposed clinical trial. An equipment and software analysis approach was implemented to perform a feasibility demonstration using 9 volunteers. All data analysis was performed on IntelliSpace Portal (ISP) (Philips Healthcare) to validate the angles and perform the assessment of the airway opening in the RP and RG regions. We have established a prototype table setup that enables us to image 7 positions of various head and chest support angles to investigate the best positional changes to improve the airway opening of sleep apnea subjects. The results showed that the actual angles were within 0.10-0.30 from the targeted angles. In conclusion, the developed 3T MRI methodology appears robust to assess the impact of head and chest positional changes on the airway in sleep apnea patients.

4693 Computer 61

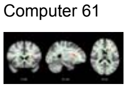

Inter-individual variability in rapid eye movement sleep is associated with brain white matter structure

Shuqin Zhou[1], Qihong Zou[2], Jing Xu[2], Jiahui Deng[3], Zihui Su[2], Tianyi Qian[4], Thomas Beck[5], Changwei Wu[6], Hongqiang Sun[3], and Jia-Hong Gao[2]

[1]Department of Biomedical Engineering, Peking University, Beijing, People's Republic of China, [2]Center for MRI Research and Beijing City Key Lab for Medical Physics and Engineering, Peking University, Beijing, People's Republic of China, [3]Sixth Hospital, Peking University, Beijing, People's Republic of China, [4]MR Collaborations NE Asia, Siemens Healthcare, Beijing, People's Republic of China, [5]Application Development, Siemens Healthcare, Erlangen, Germany, [6]Graduate Institute of Humanities in Medicine, Taipei Medical University, Taipei, Taiwan

Previous animal studies indicated that sleep is important for cell membrane and myelin maintenance in the brain. Research further suggests that variability in sleep structure may be associated with brain white matter microstructure. In this study, we investigate the relationship between sleep structure parameters evaluated with polysomnography and brain white matter characteristics, as measured by MR diffusion tensor imaging. We find that inter-subject variability of regional white matter characteristics may explain the differences in sleep structure across participants.

4694 Computer 62

Relationship between cortical Grey Matter quantitative Magnetization Transfer and corresponding sub-cortical White Matter in healthy adults

Olivier E. Mougin[1], Prejaas K. Tewarie[1], Benjamin A.E. Hunt[1], Nicolas Geades[1], Peter G. Morris[1], Matthew J. Brookes[1], and Penny A. Gowland[1]

[1]Sir Peter Mansfield Imaging Centre, School of Physics and Astronomy, University of Nottingham, Nottingham, United Kingdom

The aim of this study is to estimate the correlation between myelination in the cortical ribbon and the underlying subcortical WM fibres in healthy adults, using quantitative Magnetization Transfer to assess myelination. The results shows that GM myeloarchitectonic is reflected in the underlying WM in healthy adults.

4695 Computer 63

Relationship between nicotine dependence and the structural changes in the brain of young and middle-aged male smokers: a voxel-based morphometry study

Peng Peng[1], Min Li[1], Ya-Ru Tian[1], Yang Yu[1], Bin Jing[2], Qing-Lei Shi[3], and Tao Jiang[1]

[1]Radiology, Beijing Chao-Yang Hospital, Beijing, People's Republic of China, [2]School of Biomedical Engineering, Capital Medical University, Beijing, People's Republic of China, [3]MR Scientific Marketing, Siemens Healthcare Ltd. Diagnostic Imaging

This study aimed to research the relationship between the volume changes of brain and smoking extent/nicotine dependence. A voxel-based morphometry study between smokers grouped by smoking amount and dependence level was conducted. This study demonstrated the volume of many brain areas decreased with the increase in smoking extent and an opposite correlation between some brain areas and smoking dependence was observed. This study indicated that dependence had limited ability to predict smoking-related brain structure changes. A comprehensive assessment of the situation should be consulted, when clinicians make treatments options.

4696 Computer 64

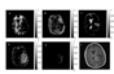

Exploring Subvoxel Structures in Brain Tumors using Magnetic Resonance Fingerprinting

Debra McGivney[1], Anagha Deshmane[2], Chaitra Badve[3], Dan Ma[1], Vikas Gulani[1,3], and Mark Griswold[1,2]

[1]Radiology, Case Western Reserve University, Cleveland, OH, United States, [2]Biomedical Engineering, Case Western Reserve University, Cleveland, OH, [3]Radiology, University Hospitals, Cleveland, OH, United States

We apply a partial volume analysis to MR fingerprinting brain tumor data. In the analysis, the number and types of tissues that make up a given voxel are not assumed to be known ***a priori***, which is particularly important in the case of abnormal tissues, such as tumors or edema. We examine the partial volume results in a patient with a glioblastoma multiforme (GBM) and another with a metastasis to look for patterns in healthy tissues, tumor, and the peritumoral region.

4697 Computer 65

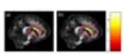

Prenatal exposure to phthalate esters and later brain structure change revealed by generalized q-sampling MRI

Yen-Ning Hsu[1], Jun-Cheng Weng[1,2], Jeng-Dau Tasi[3], Chao-Yu Shen[1,2,4], and Shu-Li Wang[5]

[1]Department of Medical Imaging and Radiological Sciences, Chung Shan Medical University, Taichung, Taiwan, [2]Department of Medical Imaging, Chung Shan Medical University Hospital, Taichung, Taiwan, [3]School of Medicine and Department of Pediatrics, Chung Shan Medical University and Hospital, Taichung, Taiwan, [4]Institute of Medicine, Chung Shan Medical University, Taichung, Taiwan, [5]National Institute of Environmental Health Sciences, National Health Research Institutes, Miaoli, Taiwan

Phthalate esters are a group of chemicals that are widely used everywhere. There is an emerging public health issue that the prevalent use of phthalates may affect children’s brain development. Therefore, we tried to use generalized q-sampling imaging (GQI) to identify the neurological structure changes of white matter of children’s brain induced by prenatal phthalate exposure. The altered GQI indices in the corpus callosum, corona radiata, superior longitudinal fasciculus (SLF), internal capsule, and superior frontal gyrus were found in the children’s brain who were prenatal exposure to phthalate esters.

4698 Computer 66

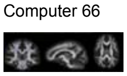

Measuring white matter structure in solid tumor survivors: a fixel-based versus voxel-based approach

Charlotte Sleurs[1,2], Jurgen Lemiere[1], Daan Christiaens[3], Thibo Billiet[4], Marjolein Verly[2], Ronald Peeters[2], Stefan Sunaert[2], Anne Uyttebroeck[1], and Sabine Deprez[2]

[1]Department of Pediatric Hematology and Oncology, University Hospitals Leuven, Leuven, Belgium, [2]Department of Radiology, University Hospitals Leuven, Leuven, Belgium, [3]Centre for the Developing Brain, King’s College London, [4]Imaging Biomarker Experts, Icometrix

Neurotoxicity of multi-agent chemotherapy in survivors of solid non-CNS tumors during childhood, has limitedly been investigated. Nowadays, diffusion-weighted imaging (DWI) is implemented in clinical studies to examine potential white matter changes. However, standard voxel-based analyses of diffusion measures such as fractional anisotropy (FA), only provide information about local white matter structure on a voxel-level, but lack specific information about fiber populations within a voxel. Therefore, we compared a fixel-based versus voxel-based group comparison analysis of DWI images in survivors of pediatric solid tumor versus healthy age-matched controls.

4699 Computer 67

High resolution volumetric 3D-SoS MPRAGE detection of carotid intraplaque hemorrhage

J. Scott McNally[1], Laura Eisenmenger[1], Seong-Eun Kim[1], Rock Hadley[1], Adam De Havenon[2], Jason Mendes[1], Gerald Treiman[3], and Dennis Parker[1]

[1]Radiology, University of Utah, Salt Lake City, UT, United States, [2]Neurology, University of Utah, Salt Lake City, UT, United States, [3]Surgery, Salt Lake City VA Medical Center

To provide a better method of detection and quantification of carotid intraplaque hemorrhage (IPH), we developed a motion-robust 3D radial stack of stars (SoS) MPRAGE sequence. 3D SoS MPRAGE outperformed 3D TOF in the detection and quantification of carotid IPH when compared with histology. The sequence was robust to motion and flow related artifacts. This sequence, when combined with high-SNR neck shape specific coils, can help identify stroke etiology, determine future stroke risk, and evaluate treatment response by quantifying IPH volume in future clinical trials aimed at decreasing carotid IPH.

4700 Computer 68

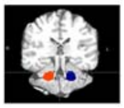

Extraction of Dentatorubrothalamic Fiber Tracts in Human Brain Using Probabilistic Fiber Tracking and Unsupervised Clustering Algorithm

Qing Ji[1], Angela Edward[1], John O. Glass[1], Zoltan Patay[1], and Wilburn E. Reddick[1]

[1]Diagnostic Imaging, St.Jude Children's Research Hospital, Memphis, TN, United States

We proposed a novel robust method to extract the dentatorubrothalamic tract (DRTT) in the human brain from DTI images. First, the method was tested on healthy control subjects, then on 30 medulloblastoma patients who had undergone resection of their posterior fossa tumors. Patterns of bilateral, left only, right only and even no DRTT were observed. Validation with multiple manual ROIs along the known pathway confirmed the extracted DRTTs. This suggests that the proposed method may provide an object way to access the DRTTs in medulloblastoma patients post-surgery.

4701 Computer 69

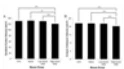

Grey matter atrophy measured in-vivo with 9.4T MRI in the experimental autoimmune encephalomyelitis mouse model of multiple sclerosis

A. Max Hamilton[1,2,3,4], Nils D. Forkert[1,2], Runze Yang[1,2,3,4], Ying Wu[1,2,3,4], James A. Rogers[2,3], V. Wee Yong[2,3], and Jeff F. Dunn[1,2,3,4]

[1]Department of Radiology, University of Calgary, Calgary, AB, Canada, [2]Hotchkiss Brain Institute, University of Calgary, Calgary, AB, Canada, [3]Department of Clinical Neurosciences, University of Calgary, Calgary, AB, Canada, [4]Experimental Imaging Center, University of Calgary, Calgary, AB, Canada

Grey matter atrophy has become a clinically relevant marker of progressive disability in multiple sclerosis (MS). To better study atrophy in MS, mouse models that have grey matter loss are needed. A possible candidate is the experimental autoimmune encephalomyelitis (EAE) mouse model. We used high-resolution magnetic resonance imaging (MRI) and atlas-based regional volumetrics to measure the volumes of 62 structures in the brains of EAE mice, 66 days post-induction. We identified atrophy in 19 structures including the cortex, cerebellum, striatum, thalamus, hippocampus, and corpus callosum. Using MRI we can study atrophy in this inflammatory model of MS.

4702 Computer 70

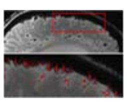

Mapping veins on the surface of the human cerebral cortex

Günther Grabner[1,2], Thomas Haider[3], Alexander Rauscher[4], Hannes Traxler[5], Siegfried Trattnig[1], and Simon Daniel Robinson[1]

[1]High Field Magnetic Resonance Centre, Department of Biomedical Imaging and Image-guided Therapy, Medical University of Vienna, Vienna, Austria, [2]Department of Radiologic Technology, Carinthia University of Applied Sciences, Klagenfurt, Austria, [3]University Clinic for Trauma Surgery, Medical University Vienna, Austria, [4]UBC MRI Research Centre, University of British Columbia, Canada, [5]Center of Anatomy and Cell Biology, University of Vienna, Austria

Image-guided neurosurgery uses information from a wide spectrum of imaging methods which are registered to the patient's skull so that they correspond to the intraoperative macro- and microscopic view at the start of the operation. During neurosurgical intervention the correspondence between imaging and optical systems breaks because of brain shift down. In this study we demonstrate that Susceptibility-Weighted Imaging and automatic vessel segmentation can be used for visualization and segmentation of superficial cortical veins which can be used as additional reference system during operation.

4703 Computer 71

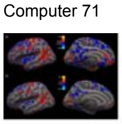

Cortical thickness and morphometric volumes derived from Multi-Echo MPRAGE scans acquired with different head coils

Ross William Mair[1,2] and Andre J. van der Kouwe[2]

[1]Center for Brain Science, Harvard University, Cambridge, MA, United States, [2]Athinoula A. Martinos Center for Biomedical Imaging, Massachusetts General Hospital, Charlestown, MA, United States

Variations in modern head-coil design lead to sensitivity differences, changes in intensity profiles, and image SNR. As morphometric analysis is based on automated analysis of image intensity and contrast variations, such variation of head coil may be expected to provide variation in morphometric results. We investigated the morphometric results from MEMPRAGE scans on subjects scanned in pairs of different head coils. We saw very limited variation in basic morphometric results from subjects scanned on the same day in different head coils. Cortical thickness variations are generally less than 50 µm, although some larger values were observed in portions of the temporal lobe. Larger differences were observed in volumes of small sub-cortical structures. These structures often have high variability in repeat measurements. However, intensity and SNR variations between coils are often most felt in the deeper regions of the brain, perhaps contributing to wider variation for these structures.

4704 Computer 72

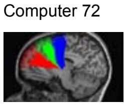

Is the length of the white matter fiber bundles underlying the thalamo-cortical loop associated with sleep spindles? – a preliminary study

Pierre-Olivier Gaudreault[1,2], Julie Carrier[1,2,3], Maxime Descoteaux[4], and Samuel Deslauriers-Gauthier[4]

[1]Center for advanced research in sleep medicine, Hôpital du Sacré-Coeur de Montréal, Montreal, QC, Canada, [2]Department of Psychology, University of Montreal, Montreal, QC, Canada, [3]Research Center, Institut universitaire de gériatrie de Montréal, Montreal, QC, Canada, [4]Sherbrooke connectivity imaging lab, Computer science Department, University of Sherbrooke, Sherbrooke, QC, Canada

Sleep spindles, an EEG manifestation generated by the thalamo-cortical loop and implicated in sleep-dependent learning were recently associated to voxel-based metrics of brain white matter. Thus, we aimed to investigate if specific bundles of streamlines underlying the thalamo-cortical loop will be associated to sleep spindles variables in twenty-five young subjects. Our study showed that the median fiber length of streamlines connecting the thalamus to the anterior and middle part of the superior frontal gyrus significantly predicted sleep spindles amplitude and frequency measured on frontal and central electrodes.

Electronic Poster

Neurovascular Methods

Exhibition Hall — Wednesday 9:15 - 10:15

4705 — Computer 73

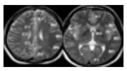

Evaluation of collaterals: comparison between cerebral perfusion using 3D TASL and FVH in unilateral internal carotid artery stenosis

Xinbo Xing[1,2], Ting Wang[1], Jinhao Lv[1], Xiaoxiao Ma[1], Jiafei Yang[2], Lin Ma[1], and Xin Lou[1]

[1]Radiology, Chinese PLA general hospital, Beijing, People's Republic of China, [2]Radiology, First affiliated hospital of Chinese PLA general hospital, Beijing, People's Republic of China

As a critical result in different researches the sign of FHV refers to the hemodynamic impairment and slow retrograde flow in leptomeningeal collaterals with or without good clinical outcome. We collected MR imaging data of 32 patients with unilateral ICA stenosis-occlusion who all underwent MR examinations by using 3D tASL perfusion imaging and T2-FLAIR. The tASL perfusion scores were compared between in FVH(-) group (14 patients) and FVH(+) group (18 patients), and there was no difference in the 2 groups. The result showed that 3D tASL perfusion MRI may be a useful non-invasive tool to identify the collateral flow.

4706 — Computer 74

Intracranial Vessel Analysis (IVA): A Toolkit for Semi-Automatic Morphological Quantification of Intracranial Atherosclerotic Plaque

Feng Shi[1], Zhangbin Yi[2], Qi Yang[1,3], Debiao Li[1], and Zhaoyang Fan[1]

[1]Biomedical Imaging Research Institute, Cedars Sinai Medical Center, Los Angeles, CA, United States, [2]Electrical and Computer Engineering, University of Michigan, MI, United States, [3]Department of Radiology, Xuanwu Hospital, Beijing, People's Republic of China

Intracranial atherosclerosis is a disease in which a sticky substance called plaque builds up inside the arteries. In practice, plaque analysis based on high resolution MRI is largely conducted manually by neuroradiologists with qualitative results. In this study, we propose a framework for intracranial vessel analysis (IVA), for semi-automatic morphological quantification of intracranial atherosclerotic plaque. Briefly, the framework includes functions of vessel path tracking, 3D MPR, vessel wall segmentation, measurement calculation, and report generation, with minimal user intervention required. Experiments show that plaque existence and location could be easily determined from the resulting vessel wall measures.

4707 — Computer 75

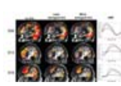

ICA-based overt speech artifact removal leads to improved estimation of deconvolution-based hemodynamic response function in aphasics

Venkatagiri Krishnamurthy[1,2], Lisa C. Krishnamurthy[2,3], Michelle L. Benjamin[4], Kaundinya Gopinath[5], and Bruce A. Crosson[1,2,6]

[1]Dept. of Neurology, Emory University, Atlanta, GA, United States, [2]Center for Visual and Neurocognitive Rehabilitation, Atlanta VAMC, Decatur, GA, United States, [3]Dept. of Physics & Astronomy, Georgia State University, Atlanta, GA, United States, [4]University of Florida, Gainesville, FL, United States, [5]Dept. of Radiology & Imaging Sciences, Emory University, Atlanta, GA, United States, [6]Dept. of Psychology, Georgia State University, Atlanta, United States

Overt speech task functional Magnetic Resonance Imaging (fMRI) paradigms are very attractive to study aphasic patients, but are also plagued by task-correlated motion (TCM). Speech involves movements of the mouth and soft palate, and causes a change in air volume around these areas leading to localized motion and susceptibility artifacts. These artifacts become more severe in patients with Aphasia. The goal of this study is to utilize existing FSL-based semi-automated ICA tools, and optimize them to go beyond removing standard fMRI artifacts by also mitigating TCM artifacts to obtain meaningful hemodynamic response function (HRF) in aphasic patients. Our preliminary results to utilize ICA for TCM-based artifact removal is promising as evidenced by the improved sensitivity and specificity, but needs further optimization. Optimal denoising of overt speech task fMRI in aphasic patients will also help us to delineate their task-based networks in an effort to monitor plastic changes due to language behavior interventions.

4708 — Computer 76

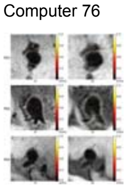

Improved Visualization and Measurement of Intracranial Aneurysmal Walls: Comparison between 7T and 3T Black-blood MRI.

Zihao Zhang[1], Zhaoyang Fan[2], Chengcheng Zhu[3], Xinke Liu[4], Qi Yang[2,5], Xianchang Zhang[1,6], Qingle Kong[1,6], Jing An[7], and Lin Chen[1,6]

[1]State Key Laboratory of Brain and Cognitive Science, Beijing MR Center for Brain Research, Institute of Biophysics, Chinese Academy of Sciences, Beijing, People's Republic of China, [2]Biomedical Imaging Research Institute, Cedars-Sinai Medical Center, Los Angeles, CA, United States, [3]Department of Radiology and Biomedical Imaging, University of California San Francisco, San Francisco, CA, United States, [4]Department of Interventional Neuroradiology, Beijing Neurosurgical Institute and Beijing Tiantan Hospital, Beijing, People's Republic of China, [5]Xuanwu Hospital, Beijing, People's Republic of China, [6]University of Chinese Academy of Sciences, Beijing, People's Republic of China, [7]Siemens Shenzhen Magnetic Resonance Ltd., Shenzhen, People's Republic of China

Black-blood MRI (BB-MRI) has been used to evaluate the walls of intracranial aneurysms at both 3T and 7T. However, there is no quantitative comparison between the two field strengths in terms of delineation quality of aneurysmal wall by using BB-MRI. In this study, we analyzed black-blood images acquired from the same group of patients at both 7T and 3T. Higher wall-to-lumen signal ratio (WLSR) and lower inside wall thickness (IWT) were obtained from 7T black-blood images. Our results suggest that 7T BB-MRI can provide improved visualization and measurement of intracranial aneurysmal walls.

4709 Computer 77

Comparative study of zero TE ASL MRA and 3D-TOF MRA in diagnostic value of cerebral arteriovenous malformations at 1.5T

Juan Huang[1], Yan Song, Peng Qi, Sheng Jiao, Hong Wang, Min Chen, and Bing Wu

[1]Beijing Hospital, Beijing, People's Republic of China

3D TOF MRA is susceptible to hemodynamic artifacts and is not sensitive to the slow blood flow, which results in the unsatisfied image quality for the diagnosis of AVMs. So we compared the use of zero TE ASL MRA (zTE MRA) and traditional 3D-TOF MRA in assessment of AVMs at 1.5T, taking DSA as standard. It was demonstrated that ASL MRA features significantly better consistency with DSA for AVMs as compared to TOF. In detail, zTE MRA can demonstrate the size, internal details, the feeding arteries and draining veins more clearly and accurately compared with TOF MRA.

4710 Computer 78

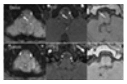

Intramural Hematoma Detection by Susceptibility-weighted Angiography (SWAN) in Intracranial Vertebral Artery Dissection

Hideki Ishimaru[1], Minoru Morikawa[1], Reiko Ideguchi[1], Yohei Ikebe[1], and Masataka Uetani[1]

[1]Radiology, Nagasaki University Hospital, Nagasaki, Japan

Vessel wall susceptibility on SWAN with no calcification on CT indicates intramural hematoma (IMH) associated with vertebral artery dissection (VAD). The early detection of IMH in VAD can be enhanced with the use of SWAN.

4711 Computer 79

A preliminary study on the amplitude of low frequency fluctuations in CADASIL

Mengxing Wang[1], Jingjing Su[2], Jilei Zhang[1], Hui Zhang[1], Jian-ren Liu[2], and Xiaoxia Du*[1]

[1]Shanghai Key Laboratory of Magnetic Resonance and Department of Physics, School of Physics and Materials Science, East China Normal University, Shanghai, People's Republic of China, [2]Department of Neurology and Jiuyuan Municipal Stroke Center, Shanghai Ninth People's Hospital, Shanghai Jiao Tong University School of Medicine, Shanghai, People's Republic of China

The purpose of this study was to investigate spontaneous low-frequency fluctuations in CADASIL patients during resting-state fMRI scans. Eleven patients (aged, 33-66 years, 6 female) and 11 age- and gender-matched healthy controls were recruited. Amplitude of low-frequency fluctuation (ALFF) was calculated to measure spontaneous brain activity. The results showed that CADASIL patients exhibited significantly decreased ALFF in the bilateral precuneus, and increased ALFF in the midbrain/ pons, the insula/ temporal pole, and the anterior cingulate gyrus/ corpus callosum. Our study first provides empirical evidence for altered spontaneous neuronal activity in CADASIL patients.

4712 Computer 80

T2*-weighted imaging of the mouse neurovasculature without contrast agent

Jérémie P. Fouquet[1], Luc Tremblay[1], and Martin Lepage[1]

[1]Centre d'imagerie moléculaire de Sherbrooke, department of Médecine nucléaire et radiobiologie, Université de Sherbrooke, Sherbrooke, QC, Canada

While standard isoflurane anesthesia does not easily allow visualization of small vessels in mice using T2*-weighted imaging, ketamine/xylazine anesthesia enables the visualization of an impressive fraction of the vasculature, without the need of an external contrast agent. Visualization can be further modulated by modifying the breathing gas.

4713 Computer 81

Analysis of capillary permeability index and stiffness variation during Ischemic Stroke: A first step towards evaluation of compressibility and neurodegenerative changes in Brain MRE

Raghu Prasad[1], Jaganathan Vellagoundar[2], and Kathryn M McMillan[3]

[1]GE Healthcare, Bangalore, India, [2]GE Healthcare, India, [3]GE Healthcare, Milwaukee, WI, United States

Evaluation of compressibility and neurodegenerative changes is critical for planning the therapy for ischemic stroke disorders. A key factor that was not analyzed till date is the capillary permeability of blood-brain-barrier (BBB) perturbations and localized mechanical degenerative changes inside the infarct region during ischemic stroke. Our results clearly indicate a decrease in stiffness of stroke-affected infarct tissue. CPI was observed to be less in the weak BBB regions.The results demonstrate through CP and stiffness maps that extent of tissue integrity that is degraded inside the infarcted region can be assessed efficiently

---

4714 Computer 82

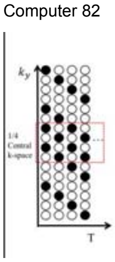

Accelerated Time Resolved Phase Contrast Cerebral MRA to Evaluate Pulse Wave Velocity

Tzu Cheng Chao[1,2], Yu-Chia Cheng[3], Wen-Chau Wu[4,5], Hsu-Hsia Peng[6], Tzu-Chao Chuang[7], Hsiao-Wen Chung[5,8], Teng-Yi Huang[9], and Yi-Jui Liu[3]

[1]Department of Computer Science and Information Engineering, National Cheng Kung University, Tainan, Taiwan, [2]Institute of Medical Informatics, National Cheng Kung University, Tainan, Taiwan, [3]Department of Automatic Control Engineering, Feng-Chia University, Taichung, Taiwan, [4]Graduate Institute of Oncology, National Taiwan University, Taipei, Taiwan, [5]Graduate Institute of Biomedical Electronics and Bioinformatics, National Taiwan University, Taipei, Taiwan, [6]Department of Biomedical Engineering and Environmental Sciences, National Tsing Hua University, Hsinchu, Taiwan, [7]Department of Electrical Engineering, National Sun Yat Sen University, Kaohsiung, Taiwan, [8]Department of Electrical Engineering, National Taiwan University, Taipei, Taiwan, [9]Department of Electrical Engineering, National Taiwan University of Science and Technology, Taipei, Taiwan

Time-resolved PCMRI has been applied to measure pulse wave velocity (PWV) for the assessment of aortic stiffness. However, longer scan time hinders its practice to achieve a high spatial and temporal resolution scan, especially required for the arteries inside of the head and neck. In the present work, an accelerated Time-resolved PCMRA was implemented to shorten scan time. The reconstruction combines temporal strategy and self-reference information to retain reasonable imaging quality. The results suggest that the proposed method differentiate PWV delay time from Common-Carotid artery to Middle-Cerebral arteries via Internal-Carotid artery with good quality within a 10-minute scan.

4715 Computer 83

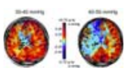

Development of a clinically useful cerebrovascular stress test using CO2 and BOLD-MRI

Olivia Sobczyk[1], James Duffin[2,3], Adrian P Crawley[4], Kevin Sam[4], Julien Poublanc[4], Lashmi Venkatraghavan[3], Daniel M Mandell[4], David J Mikulis[1,4], and Joseph A Fisher[1,2,3]

[1]Institute of Medical Sciences, University of Toronto, Toronto, ON, Canada, [2]Department of Physiology, University of Toronto, Toronto, ON, Canada, [3]Department of Anaesthesia and Pain Management, University Health Network, Toronto, ON, Canada, [4]Joint Department of Medical Imaging and the Functional Neuroimaging Laboratory, University Health Network, Toronto, ON, Canada

Current methods of measuring cerebrovascular reactivity (CVR) have shown promise for aiding in clinical diagnosis and management of patients with various neurovascular diseases. However, CVR measurement is currently limited to a research setting and transition to clinical utility requires a universal standardized measurement method. Using BOLD-MRI CO_2 measured CVR, we present experimentally developed concepts for standardization and post processing, which have the potential to provide a clinically useful brain stress test.

4716 Computer 84

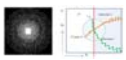

Accelerated Intracranial Vessel Wall Imaging using Compressed Sensing

Chengcheng Zhu[1], Bing Tian[2], Sinyeob Ahn[3], Esther Raithel[4], Gerhard Laub[3], and David Saloner[1]

[1]Radiology, University of California, San Francisco, San Francisco, CA, United States, [2]Radiology, Changhai Hospital, Shanghai, People's Republic of China, [3]Siemens Healthcare, CA, United States, [4]Siemens Healthcare, Erlangen, Germany

Current 3D black-blood high-resolution MRI (0.4-0.6mm isotropic) of intracranial vessel wall is limited by long scan times (~10 minutes). This study implemented a compressed sensing SPACE (CS-SPACE) sequence to reduce the scan time. The scan and reconstruction parameters were optimized in volunteers and then validated in patients. The optimized CS-SPACE protocol achieved good image quality and reliable vessel area measurements compared with SPACE, with a 37% time reduction. 0.5mm isotropic resolution can be achieved in <7 minutes, and $0.6mm^3$ is possible in 4 minutes. This fast intracranial vessel wall technique has potential for use in a clinical setting.

4717 Computer 85

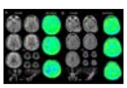

Determinants of the Presence and Intensity of Hyperintense Vessels on Fluid-Attenuated Inversion Recovery Imaging in Intracranial Atherosclerotic Stenosis or Occlusion

Jinhao Lyu[1], Ning Ma[2], Xiaoxiao Ma[3], Bing Wu[4], Lin Ma[3], and Xin Lou[3]

[1]Radiology, Chinese PLA General Hospital, Beijing, People's Republic of China, [2]Beijing Tiantan Hospital, Capital Medical University, Beijing, People's Republic of China, [3]Radiology, Chinese PLA General Hospital, People's Republic of China, [4]GE healthcare China, People's Republic of China

The correlation of fluid-attenuated inversion recovery imaging (FLAIR) vascular hyperintensity (FVH) and collateral are still in discrepancy in intracranial atherosclerotic stenosis or occlusion. In the present study, we used territorial arterial spin labeling (ASL) and two post labeling delay (1.5s and 2.5s) ASL to study the leptomeningeal collateral and hemodynamic status in patients with different intensity of FVH, and concluded that FVH may be related to poor collateralization and hemodynamic impairments.

4718 Computer 86

A time efficient, high resolution 3D vessel wall MRI (vwMRI) of the head and neck vessels in a single scan

Seong-Eun Kim[1], J Rock Hadley[1], Michael J Beck[1], J Scott McNally[1], Adam DeHavenon[2], Bradley D Bolster, Jr. [3], Gerald S Treiman[4], and Dennis L Parker[1]

[1]UCAIR, Department of Radiology and Imaging Sciences, University of Utah, Salt Lake City, UT, United States, [2]Department of Neurology, University of Utah, [3]Siemens Healthcare, [4]Department of Veterans Affairs, VASLCHCS

Vessel wall MRI(vwMRI) increases diagnostic accuracy for stroke etiologies without overt luminal irregularities, such as mild atherosclerosis, subtle dissection, or vasculitis. Prior vwMRI research has focused on the head or neck in isolation. We developed a set of two neck-shape-specific(NSS) coil that fit two different neck sizes and configured them to integrate with the existing commercial head coils. The purpose of this work was to develop a 3D vwMRI protocol, leveraging the NSS coil array, which permits simultaneous imaging of the head and neck vessels in a single scan. By allowing an efficient examination and identifying patients at high risk of future recurrent stroke, this technique will enable detection of cryptogenic stroke sources and optimal personalized management of vascular disease.

4719 Computer 87

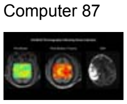

Non-invasive MR Thermometry in a Non-human Primate Model of Acute Ischemic Stroke

Seena Dehkharghani[1], Candace Fleischer[2], Deqiang Qiu[3], and Frank Tong[4]

[1]Radiology, New York University, New York, NY, United States, [2]Radiology and Imaging Sciences, Emory University, Atlanta, GA, United States, [3]Radiology, Emory University, Atlanta, GA, United States, [4]Radiology, Emory University

Temperature dysregulation is deeply implicated in potentiation of cerebrovascular ischemia. We present a multi-phasic, MR thermographic study in a non-human primate (NHP) model of MCA infarction, hypothesizing detectable brain temperature disturbances and brain-systemic temperature decoupling. Successful physiologic and continuous post-ischemic cerebral MR thermography was conducted, and prescribed in an NHP infarction model to facilitate translatability. The results confirm hypothesized temperature disturbance and decoupling of physiologic brain-systemic temperature gradients. These findings inform a developing paradigm of brain thermoregulation, and the applicability of brain temperature as a neuroimaging biomarker in CNS injury.

4720 Computer 88

Scheme optimization for inflow and outflow visualization in non-contrast enhanced dynamic MRA based on pseudo-continuous arterial spin labeling

Makoto Obara[1], Osamu Togao[2], Noriyuki Fujima[3], Shuhei Shibukawa[4], Masami Yoneyama[1], Tomoyuki Okuaki[5], Msanobu Nakamura[1], and Marc Van Cauteren[5]

[1]Philips Electronics Japan, Tokyo, Japan, [2]Clinical Radiology, Graduate School of Medical Sciences, Kyushu University, Fukuoka, Japan, [3]Department of Radiology, Hokkaido University Hospital, Hokkaido, Japan, [4]Department of Radiology, Tokai University Hospital, Kanagawa, Japan, [5]Asia Pacific, Philips Healthcare, Tokyo, Japan

A new scheme for non-contrast enhanced intracranial three-dimensional dynamic magnetic resonance angiography (4D-MRA) using pseudo-continuous arterial spin labeling (4D-PCASL) is proposed for visualizing inflow and outflow dynamics. The 4D-PCASL procedure was accelerated with contrast-enhanced timing-robust angiography (CENTRA)-Keyhole and the view-sharing techniques (4D-PACK). Images acquired from four volunteers were compared between the 4D-PCASL and 4D-PACK approaches. We show that this new scheme accelerates data acquisition and provides dynamic inflow and outflow information.

4721 Computer 89

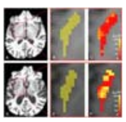

Spectral Diffusion IVIM Analysis of Enlarged Perivascular Spaces in Cerebral Small Vessel Disease

Sau May Wong[1], Jacobus F.A. Jansen[1], C. Eleana Zhang[2], Julie Staals[2], Paul A.M. Hofman[1], Robert J. van Oostenbrugge[2], and Walter H. Backes[1]

[1]Radiology and Nuclear Medicine, Maastricht University Medical Centre, Maastricht, Netherlands, [2]Neurology, Maastricht University Medical Centre, Maastricht, Netherlands

The conventional IVIM model assumes a two-compartment model; this might not apply for regions with enlarged perivascular spaces (PVS) in cerebral small vessel disease (cSVD). Regularized non-negative least squared was used to deconvolve the IVIM signal in multiple diffusion components. Sixty-three cSVD patients and thirty-five controls received IVIM imaging and visual scoring of enlarged PVS. An additional component to the assumed parenchymal and perfusion components was revealed. We show that the fraction of this component is related to the amount of scored enlarged PVS. Quantifying PVS is a time-consuming process and this method might aid the development of automatic quantification.

4722 Computer 90

Triple Magnetic Resonance Angiography (triple-MRA) for planning of Gamma Knife Radiosurgery of brain arteriovenous malformations

Alvaro Rojas Villabona[1,2], Magdalena Sokolska[3,4], Enrico De Vita[4], Mary Murphy[2], Thomas Solbach[5], Joan Grieve[2], Prem Rangi[5], Yuriko Suzuki[6], Matthias JP Van Osch[6], David Atkinson[7], Emma Biondetti[3], Karin Shmueli[3], Xavier Golay[4], Ian Paddick[1], Neil Kitchen[2], and Hans Rolf Jäger[4,5]

[1]The Gamma Knife Centre at Queen Square, National Hospital for Neurology and Neurosurgery, London, United Kingdom, [2]Department of Neurosurgery, National Hospital for Neurology and Neurosurgery, London, United Kingdom, [3]Medical Physics and Biomedical Engineering, University College London, London, United Kingdom, [4]Academic Neuroradiological Unit, Department of Brain Repair and Rehabilitation, Institute of Neurology, University College London, London, United Kingdom, [5]The Lysholm Department of Neuroradiology, National Hospital for Neurology and Neurosurgery, London, United Kingdom, [6]C. J. Gorter Center for High Field MRI, Department of Radiology, Leiden University Medical Center, Leiden, Netherlands, [7]Centre for Medical Imaging, University College London, London, United Kingdom

This study investigates whether a combination of three MRA techniques, referred to as triple-MRA, could be used as an alternative to DSA for visualisation and delineation of brain AVMs for GKR targeting. The AVMs of 13 patients undergoing GKR were delineated using triple-MRA and the resultant target volumes were compared to the radiosurgical targets generated by the neurosurgical team using DSA and volumetric contrast T1/T2 imaging. Target volumes obtained using triple-MRA are comparable to target volumes obtained with DSA and used for delivery of GKR. In conclusion, triple-MRA is a robust method for non-invasive identification and delineation of brain AVMs.

4723 Computer 91

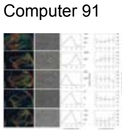

Susceptibility based characterization of brain arteriovenous malformations

Till M. Schneider[1,2], Markus Möhlenbruch[1], Sebastian Schmitter[3,4], Mark Ladd[3], Heinz-Peter Schlemmer[2], Martin Bendszus[1], and Sina Straub[3]

[1]Department of Neuroradiology, Universityhospital Heidelberg, Heidelberg, Germany, [2]Department of Radiology, German Cancer Research Center (DKFZ), Heidelberg, Germany, [3]Department of Medical Physics in Radiology, German Cancer Research Center (DKFZ), Heidelberg, Germany, [4]Physikalisch-Technische Bundesanstalt (PTB), Braunschweig und Berlin, Germany

Brain arteriovenous malformations (bAVM) are congenital lesions detected incidentally or following symptomatic events like hemorrhage, seizure or headache. In bAVM patients, the most feared complication is intracranial hemorrhage with a general risk ranging between 2-4%[1] and further functional and hemodynamic characterization of bAVMs may improve risk assessment and ultimately aid in patient management[2, 3]. In this study, bAVMs have been investigated using quantitative susceptibility mapping and phase contrast based flow measurements. Susceptibility across the bAVM nidus is studied in relation to flow characteristics.

4724 Computer 92

Semi-automatic Analysis of Carotid Plaque Composition from Multicontrast Magnetic Resonance Imaging

Chien-Yuan Eddy Lin[1,2], Ai-Chi Chen[1], Liang-Yu Shyu[3], Yen-Chien Wu[4], David Yen-Ting Chen[4], Ying-Chi Tseng[4], and Chi-Jen Chen[4]

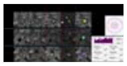

[1]GE Healthcare, Taipei, Taiwan, [2]GE Healthcare MR Research China, Beijing, People's Republic of China, [3]Biomedical Engineering Department, Chung Yuan Christian University, Chungli, Taiwan, [4]Department of Radiology, Taipei Medical University - Shuang Ho Hospital, New Taipei City, Taiwan

Accurate tracking of plaque composition would be very useful clinically to determine the status of atherosclerosis and to understand the potential risk under myocardial infraction, stroke, and peripheral vascular disease. We developed a semi-automatic software to evaluate the carotid plaque types using four contrast-weighted MRI (pre- and post-contrast T1-weighted, time-of-flight, T2-weighted). Working with the proposed software with the minimal operator input reduces the process time of plaque component identification and minimizes the possibility of random and systematic errors. As a result, proposed software is capable of assisting the radiologist/clinician in imaging interpretation and decision-making in managing carotid artery atherosclerosis.

4725 Computer 93

Automatic Quantification of Haematoma and Surrounding Oedema in MRI of Acute Spontaneous Intracerebral Haemorrhage: Preliminary Results for the TICH-2 MRI Sub-study

Stefan Pszczolkowski[1], Rebecca G. Gallagher[2,3], Zhe K. Law[1,4], Dewen Meng[1], David J. Swienton[2,5], Paul S. Morgan[6], Philip M. Bath[1], Nikola Sprigg[1], and Robert A. Dineen[1]

[1]Division of Clinical Neuroscience, University of Nottingham, Nottingham, United Kingdom, [2]Department of Neuroradiology, Nottingham University Hospitals, United Kingdom, [3]Department of Radiology, Royal Derby Hospital, United Kingdom, [4]Department of Medicine, National University of Malaysia, Malaysia, [5]Imaging Department, Leicester Royal Infirmary, United Kingdom, [6]Department of Medical Physics and Clinical Engineering, Nottingham University Hospitals, United Kingdom

In this work, we propose to take advantage of improved contrast seen on magnetic resonance (MR) images of patients with acute spontaneous intracerebral haemorrhage (SICH), and introduce an automated algorithm for haematoma and oedema segmentation from these images. To our knowledge, there is no previously proposed segmentation technique for SICH that utilises MR images directly. The method is based on k-means clustering of image intensities for haematoma segmentation and voxel-wise dynamic thresholding of hyper-intensities for oedema segmentation. Preliminary results using the Dice score metric to measure segmentation overlaps between labellings yielded by the proposed algorithm and five different expert raters show that our technique has the potential to be an effective way to automatically delineate haematoma and perihaematoma oedema extent directly from MR images.

4726 Computer 94

A Retrospective Study of Amide Proton Transfer Imaging in Acute Ischemic Stroke

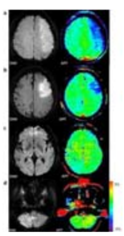

Guodong Song[1], Min Chen[1], Chunmei Li[1], and Jinyuan Zhou[2]

[1]Department of Radiology, Beijing Hospital, Beijing, People's Republic of China, [2]Department of Radiology, Johns Hopkins University, BALTIMORE, MD

This study was performed to investigate the imaging features of Amide Proton Transfer (APT) MR imaging in different subtypes of acute ischemic stroke (AIS) . By figuring out the detailed APTw features in AIS patients, it would be helpful for further clinical applications of APT MRI technique.

4727 Computer 95

Arterial transit time measured by multi-delay ASL perfusion for evaluating major cerebral artery stenosis/occlusive disease: correlation with 15O-H2O and 15O2 gas PET-CBF and OEF

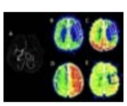

Kayo Takeuchi[1], Makoto Isozaki[2], Masayuki Kanamoto[1], Yoshifumi Higashino[2], Hidehiko Okazawa[3], Kenichiro Kikuta[2], R Marc Lebel[4], and Hirohiko Kimura[1]

[1]Department of Radiology, University of Fukui, Fukui, Japan, [2]Department of Neurosurgery, University of Fukui, Fukui, Japan, [3]Biomedical Imaging Center, University of Fukui, Fukui, Japan, [4]GE Healthcare, Calgary, Canada

Positron emission computed tomography (PET) is used for evaluating cerebral hemodynamic ischemic stages in patients with major cerebrovascular stenosis/occlusion for treatment indication. Using a rapid, low-resolution pre-scan method, arterial transit time (ATT) and corrected cerebral blood flow (CBF) could be obtained, even in the immediate clinical setting. This study aimed to clarify whether ATT is hemodynamically related to misery perfusion stratified with $^{15}O\text{-}H_2O/^{15}O_2$-gas PET data. There was a significant correlation between ASL and PET CBF before and after ATT correction (r^2=0.27, 0.55). ATT also significantly correlated with PET-OEF (r^2=0.11) and is a useful parameter to classify cerebral ischemia.

Electronic Poster

Advanced Neuroimaging Methods

Exhibition Hall — Wednesday 9:15 - 10:15

4728 Computer 97

Imaging changes in cardiorespiratory pulsation amplitude of the brain during breathold - an MREG-study.

Lauri Raitamaa[1], Vesa Korhonen[1], and Vesa Kiviniemi[1]

[1]OFNI/Radiology, Oulu University Hospital, Oulu, Finland

Glymphatic pulsation mechanisms clear the brain by using physiological pulsations to drive CSF through the brain tissue. Magnetic resonance encephalography (MREG), an ultra-fast inverse imaging technique, was recently able to map three basic mechanisms driving the glymphatic brain clearance; arterial pulsations, respiratory venous pulses and slow vasomotor waves. In this study we demostrate that the MREG can also detect changes in the amplitudes of the pulsations driving the clearance. The mapping of the physiological pulsation amplitude changes can be used to quantify changes in glymphatic clearing mechanims that precede neurodegeneration.

4729 Computer 98

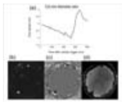

Cardiac-induced pulsatility of blood flow resolved in sub-millimeter cerebral veins using phase contrast MRI at 7 Tesla

Ian D Driver[1], Fabrizio Fasano[2], and Richard G Wise[1]

[1]CUBRIC, School of Psychology, Cardiff University, Cardiff, United Kingdom, [2]Siemens Healthcare Ltd, Frimley, Caberley, United Kingdom

We report the first measurement of venous flow pulsatility in cerebral veins with sub-millimeter diameters using phase contrast MRI. This work exploits the increased signal and finer spatial resolution available at 7 Tesla, over lower field strengths. We suggest that the observed venous pulsatility is a passive response to intracranial pressure changes caused by arterial pulsatility. These measurements may be applied to pathology in which there is compromised venous flow, extending such investigations to the smaller cerebral veins and offering a better understanding of the temporal dynamics of cerebral venous flow.

4730 Computer 99

Cross-validation of $$$T_2$$$-prepared bSSFP blood oximetry $$$in$$$ $$$vivo$$$

Ana E Rodríguez-Soto[1], Michael C Langham[1], and Felix W Wehrli[1]

[1]Department of Radiology, University of Pennsylvania, Philadelphia, PA, United States

Susceptometry-based oximetry is a well-established, robust method for quantifying hemoglobin oxygen saturation (HbO_2) *in vivo*; but the method is somewhat limited by the orientation of the vessel of interest relative to B_o. T_2-based oximetry, based on the dependence of blood water T_2 on HbO_2, provides greater flexibility with respect to vessel geometry. However, the measured T_2 critically depends on B_o and sequence-specific imaging parameters. Here, a T_2-prepared bSSFP sequence and appropriate calibration curve were used to extract HbO_2 at the superior sagittal sinus and the results were compared to susceptometry-based oximetry. The agreement between both methods was excellent with 2% bias.

4731 Computer 100

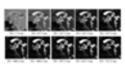

Visualization of CSF flow using multi spin echo acquisition cine imaging (MUSACI)

Tatsuhiro Wada[1], Chiaki Tokunaga[1], Osamu Togao[2], Yasuo Yamashita[1], Kouji Kobayashi[1], Masami Yoneyama[3], and Yasuhiko Nakamura[1]

[1]Division of Radiology, Department of Medical Technology, Kyushu university hospital, Fukuoka, Japan, [2]Department of Clinical Radiology, Graduate School of Medical Sciences, Kyushu University, [3]Philips Electronics Japan

This study demonstrates a new CSF flow imaging using multi spin echo acquisition cine imaging (MUSACI). MUSACI can obtain the high resolution CSF flow images more than the conventional phase contrast technique, moreover it is simple method because need not use a labeling pulse such as the time-SLIP technique. MUSACI can provide both morphological and physiologic information regarding CSF flow in a single scan.

4732 Computer 101

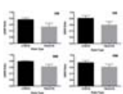

Improving Multiband EPI pCASL Imaging with Dynamic Frequency Feedback

Dingxin Wang[1,2], Gregory Metzger[2], Kamil Ugurbil[2], and Xiufeng Li[2]

[1]Siemems Healthcare, Minneapolis, MN, United States, [2]Center for Magnetic Resonance Research-Radiology, University of Minnesota, Minneapolis, MN, United States

Dynamic frequency feedback to multiband (MB) EPI PCASL excitation, fat saturation, and labeling RF pulse frequency can improve spatial and temporal perfusion signal-to-noise ratio (sSNR and tSNR) and cerebral blood flow (CBF) measurement reproducibility of MB-EPI PCASL. Dynamic frequency feedback helps maintain optimal labeling efficiency, achieve stable fat saturation, and correct scanner drift during MB-EPI PCASL measurements.

4733 magna cum laude Computer 102

Inversion Recovery Ultrashort Echo Time Imaging of Short T2 Tissue Components in Ovine Brain: A Sequential D2O Exchange Study

Shu-Juan Fan[1], Yajun Ma[1], Graeme M. Bydder[1], and Jiang Du[1]

[1]Dept. of Radiology, University of California, San Diego, San Diego, CA, United States

Myelin produces ultrashort-lived MRI signals, and cannot be directly imaged using conventional MRI sequences that typically have TEs of several milliseconds or longer. This study explored the potential of inversion recovery ultrashort echo time (IR-UTE) sequences in direct myelin imaging in an ovine brain D_2O exchange model. The IR-UTE signals survived D_2O exchange. Myelin T2* was measured to be 200-300 μs both before and after exchange. These results support myelin to be the major source of the ultrashort T2* signals seen on IR-UTE images, and IR-UTE sequence as a tool for assessing myelin loss in multiple sclerosis and other diseases.

4734 Computer 103

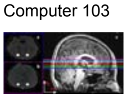

Superior sagittal sinus venous oxygen saturation based on fully automated MR susceptometry : effects of slice dependent even-odd echo discrepancy and vascular angle correction

Chou-Ming Cheng[1,2], Tzu-Chen Yeh[3,4], Jen-Chuen Hsieh[2,4], and Hsiao-Wen Chung[1]

[1]Graduate Institute of Biomedical Electronics and Bioinformatics, National Taiwan University, Taipei, Taiwan, [2]Department of Medical Research, Taipei Veterans General Hospital, Taipei, Taiwan, [3]Department of Radiology, Taipei Veterans General Hospital, Taipei, Taiwan, [4]Institute of Brain Science, National Yang-Ming University, Taipei, Taiwan

Venous oxygen saturation (SvO_2) for estimation of global cerebral metabolic rate of oxygen is measured using MR susceptometry from the phase information obtained with multi-echo gradient-echo imaging. Automatic selection and segmentation of the superior sagittal sinus is performed with slice dependent even-odd discrepancy to avoid operator dependency. Results from 12 healthy subjects suggested that phase values of the vessel showing minimal even-odd echo discrepancy could be used as a useful information guiding selection of the appropriate vessel segment for SvO_2 estimations by taking into consideration the three dimensional vasculature.

4735 Computer 104

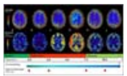

MRI submerging into The Big Blue: A comparative 3D-pCASL and IVIM-MRI brain perfusion study to elucidate circulatory adaptation during prolonged freediving

Vera Catharina Keil[1], Lars Eichhorn[2], Burkhard Mädler[3], Jürgen Gieseke[3], Frank Träber[1], Wolfgang Block[1], Martin Alois Sprinkart[1], Andreas Müller[1], Christine Schneider[4], Lukas Scheef[1], Hans Heinz Schild[1], Dariusch Reza Hadizadeh[1], and Elke Hattingen[1]

[1]Department of Radiology, University Hospital Bonn, Bonn, Germany, [2]Department of Anesthesiology, University Hospital Bonn, Bonn, Germany, [3]Clinical Science Department, Philips Healthcare, Germany, [4]Department of Neurology, University Hospital Bonn, Bonn, Germany

Freedivers can endure severe hypoxemia during breathhold without any apparent neurological deficit. Little is known on how brain circulation adapts to deliberate breathhold. We examined 14 experienced freedivers during breathholds of 5 to 7.5 minutes at a 3T MRI applying 3D-pCASL and IVIM-MRI sequences to reveal dynamic alterations of cerebral blood flow (rCBF) and in order to elucidate the relationship of rCBF and perfusion fraction (PF) of IVIM-MRI. rCBF increased to 3.2-fold the baseline levels and negatively correlated to blood oxygen levels, but not to PF, which initially dropped during breathhold and therefore appears to represent another underlying physiological mechanism.

4736 Computer 105

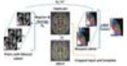

A method for near-realtime automated segmentation of thalamic nuclei

Francis Tyson Thomas[1], Jason Su[2], Brian K Rutt[2], and Manojkumar Saranathan[3]

[1]Electrical and Computer Engineering, Univ. of Arizona, Tucson, AZ, United States, [2]Radiology, Stanford University, Stanford, CA, United States, [3]Medical Imaging, Univ. of Arizona, Tucson, AZ, United States

Thalamic nuclei are often hard to visualize on most anatomical sequences. White-matter-nulled MPRAGE imaging provides sufficient intra-nuclear contrast to enable manual segmentation, which is very tedious. We have developed fast multi-atlas based segmentation schemes that can provide accurate segmentation of all the major thalamic nuclei in under 15 minutes.

4737 Computer 106

Small vessel specific cerebrovascular reactivity with 7 tesla 2D Qflow MRI.

Lennart J. Geurts[1], Alex Bhogal[1], Jeroen C. W. Siero[1,2], Geert Jan Biessels[3], and Jaco J. M. Zwanenburg[1]

[1]Radiology, UMC Utrecht, Utrecht, Netherlands, [2]Spinoza Center for Neuroimaging, Amsterdam, Netherlands, [3]Brain Center Rudolf Magnus, UMC Utrecht, Utrecht, Netherlands

We aimed to measure cerebrovascular reactivity (CVR) specifically at the level of the superficial perforating arteries with 7T 2D Qflow, to develop a method to assess small vessel function for cerebral small vessel disease research. 7T 2D Qflow acquisitions through the semi oval center (CSO) and through the medial cerebral artery (M1) were acquired at baseline and during hypercapnia. CVR_{M1} corresponded to CVR values from Qflow literature and, while an order of magnitude smaller, CVR_{CSO} corresponded to CVR values from ASL literature. This shows proof of concept that CVR of perforating arteries can be measured using 7T 2D Qflow.

4738 Computer 107

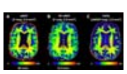

Segmented EPI readout Variable Flip-angle Magnetization Transfer (EP-vfMT) imaging for 7 T quantitative MT (qMT) Imaging

Se-Hong Oh[1,2] and Mark J. Lowe[1]

[1]Imaging Institute, Cleveland Clinic Foundation, Cleveland, OH, United States, [2]Department of Biomedical Engineering, Hankuk University of Foreign Studies, Yongin, Korea, Republic of

Because of the much higher SAR and longer acquisition time, patient studies using qMT at UHF have not been clinically feasible. In this work, we demonstrated a new approach (EP-vfMT) for whole brain 7T qMT data in a clinically reasonable time. EP-vfMT provides similar image quality to that obtained with conventional MT imaging, and shortens the scan time by utilizing segmented EPI readout and avoiding from SAR limitation. EP-vfMT generates qMT map in reasonable scan time and it exhibits similar myelin density distribution with qMT result from vdMT and aMWF map from ViSTa. Moreover, it maintains sensitivity to MS lesions.

4739 Computer 108

Parallel transmission (pTx) on an in-vivo human brain at 7T: a new approach using global B1 coefficient template

Se-Hong Oh[1,2], Tiejun Zhao[3], Ken Sakie[1], Stephen E. Jones[1], and Mark J. Lowe[1]

[1]Imaging Institute, Cleveland Clinic Foundation, Cleveland, OH, United States, [2]Department of Biomedical Engineering, Hankuk University of Foreign Studies, Yongin, Korea, Republic of, [3]Siemens Healthcare, New York, NY, United States

Improving B_1-uniformity by calibration procedure is crucial for the pTx imaging and commonly individual B_1 coefficient estimation is conducted in the beginning of each patient scan protocol. However, B_1 calibration procedure increase the scan time by approximately 10~15 mins increasing discomfort to the patient. Here we propose using global B_1 coefficient template to reduce scan time while maintaining acceptable B_1 profile. The approach using global B_1 coefficient template is assumed to have limited inter-individual variation of B_1 coefficient between subjects. We demonstrate the feasibility of scan with global B_1 coefficient template and provide a perception of in-vivo scan with pTx.

4740 Computer 109

Toward Real Time Estimation and Quality Assurance for Myelin Water Mapping in the Human CNS

Khader M Hasan[1], Refaat E Gabr[1], John A Lincoln[2], and Ponnada A Narayana[1]

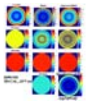

[1]Diagnostic and Interventional Radiology, University of Texas Health Science Center at Houston, Houston, TX, United States, [2]Neurology, University of Texas Health Science Center at Houston, Houston, TX, United States

Reliable *in vivo* quantification and visualization of myelin spatio-temporal changes in the developing and aging human central nervous system (CNS) would help provide important surrogate markers of white matter integrity. However, high resolution whole brain myelin water fraction (MWF) mapping methods remain challenging and are not well-standardized and are not widely adopted due to ill-posed solutions of the sum-of-exponents problem in the presence of noisy measurements and excessive computation time due to iterative solutions. In this work, we report a rapid method to initialize the solution of the bi-exponential multi-compartment fit which was used along with a host of quality assurance measures to speed up the estimation of the MWF and corresponding compartmental T2 relaxation times using an improved and regularized non-negative least-squares (rNNLS). The sensitivity of the method to signal-to-noise ratio (SNR) and different values of MWF was investigated using a digital phantom. This method was applied to healthy and multiple sclerosis (MS) patients. Our analysis strategy accelerated the accurate mapping of high resolution MWF in the entire human brain in seconds and provided the spatial variability MWF across the corticospinal tract (CST) and callosal pathways.

4741 Computer 110

ΔR1ρ, a potential indication for myelin concentration in white matter?

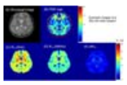

Ping Wang[1], Richard Dortch[1], and John C. Gore[1]

[1]Radiology and Radiological Sciences, Vanderbilt University Institute of Imaging Science, Nashville, TN, United States

Previous studies have demonstrated that at high fields (3T and beyond), the difference of $R_{1\rho}$ between low and high spin-locking fields ($\Delta R_{1\rho}$) may reflect chemical exchange processes in biological tissues. This study aimed to investigate the possibility of using $\Delta R_{1\rho}$ to assess the content of exchangeable protons in myelin in white matter by comparing $\Delta R_{1\rho}$ with PSR (macromolecular to free pool size ratio from magnetization transfer imaging). The results show that $\Delta R_{1\rho}$ and PSR have a much stronger correlation in white matter than in gray matter, inferring that $\Delta R_{1\rho}$ might have a potential to evaluate myelin integrity.

4742 Computer 111

Comparison of R1ρ dispersion in human brain between 3T and 7T

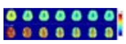

Ping Wang[1], Henry Zhu[1], and John C. Gore[1]

[1]Radiology and Radiological Sciences, Vanderbilt University Institute of Imaging Science, Nashville, TN, United States

Previous studies have indicated that $R_{1\rho}$ (= $1/T_{1\rho}$) dispersion may be dominated by chemical exchange processes at higher fields, and the dispersion may be used to quantify exchange processes between water and labile protons, mainly amides and hydroxyls. At 3T some biological tissues with high macromolecular protein content may demonstrate a considerable dispersion, but fat and water rich tissues typically have a negligible $R_{1\rho}$ dispersion. In this study, we observed that the degree of $R_{1\rho}$ dispersion in white matter at 7T was more than three times the dispersion at 3T, confirming that chemical exchange is a major contribution to $R_{1\rho}$ and suggesting $R_{1\rho}$ dispersion at higher fields may help to characterize tissue physicochemical properties.

4743 Computer 112

COnstrained Data Extrapolation (CODE): A New Approach for High Resolution MR Angiographic Image Reconstruction.

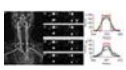

Yang Song[1], Ehsan Hamtaei[2], Guang Yang[1], Haibin Xie[1], and Mark Haacke[1,2,3]

[1]Shanghai Key Laboratory of Magnetic Resonance, East China Normal University, Shanghai, People's Republic of China, [2]Magnetic Resonance Innovations, Inc., Detroit, MI, United States, [3]Radiology, Wayne State University, Detroit, MI, United States

We propose a “COnstrained Data Extrapolation” (CODE) algorithm to reconstruct high-resolution MRA images from k-space with a lower resolution thereby accelerating acquisition of the data. We found that CODE can estimate a 50% (70%) stenosis of a vessel with a diameter equal to 7 (10) pixels in the high-resolution image to within 5% of the correct result when the SNR=4:1 or better. Both phantom simulations and in-vivo 3D contrast enhanced MRA data demonstrate that CODE is robust to noise and can be used to speed up conventional data acquisition by a factor of four.

4744 Computer 113

Non-Invasive Cerebrovascular Pulsatility Measurement via Cardiac Sorting of BOLD Data: An Investigative Study Using Exercise-Induced Hypotension in Adolescents

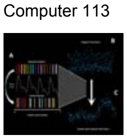

Athena Theyers[1,2,3], Benjamin Goldstein[2,3], Arron Metcalfe[2,3], Andrew Robertson[2,3], and Bradley MacIntosh[1,2,3]

[1]University of Toronto, Toronto, ON, Canada, [2]Sunnybrook Research Institute, Toronto, ON, Canada, [3]Heart & Stroke Foundation Canadian Partnership for Stroke Recovery, Toronto, ON, Canada

Arterial pulsatility increases with age and is linked to small vessel damage and neurodegeneration. Our group has developed a method that fits a pulsatility model to BOLD temporal volumes based on their cardiac cycle position. We test this method in a healthy adolescent group before and after a physiological stressor, i.e. 20 minutes of moderate intensity exercise. Brain pulsatility was significantly lower in BOLD scans taken 20 minutes after exercise cessation, supporting the viability of this method to track brain arterial stiffness non-invasively.

4745 Computer 114

Using Hyperpolarized 129Xe in Human Participants to Perform Functional Magnetic Resonance Imaging (fMRI)

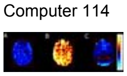

Francis Hane[1], Tao Li[1], Jane M Lawrence-Dewar[2], Ayman Hassan[3], Karl Granberg[3], Raiili Pellizzari[1], Jennifer Anne Plata[4], and Mitchell Albert[1,5]

[1]Lakehead University, Thunder Bay, ON, Canada, [2]Thunder Bay Regional Research Institute, Thunder Bay, ON, Canada, [3]Thunder Bay Regional Health Sciences Centre, [4]Lakehead University, [5]Northern Ontario School of Medicine, ON, Canada

We demonstrate the use of hyperpolarized (HP) 129Xe MRI as a novel fMRI modality. We successfully obtained axial HP Xe fMRI maps from healthy humans throughout the conduct of a 1-back memory task. Our preliminary results suggest that HP 129Xe fMRI may have a sensitivity of up to an order of magnitude more than BOLD fMRI.

4746 Computer 115

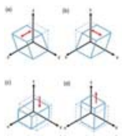

Mechanical stiffness of human brain tissue is inversely correlated with FA and MTR

Christoph Birkl[1], Silvia Budday[2], Gerhard Sommer[3], Melanie Bauer[2], Paul Steinmann[2], Johannes Haybaeck[4,5], Ellen Kuhl[6], Gerhard A. Holzapfel[3,7], Franz Fazekas[1], Stefan Ropele[1], and Christian Langkammer[1]

[1]Department of Neurology, Medical University of Graz, Graz, Austria, [2]Department of Mechanical Engineering, University of Erlangen-Nuermberg, Erlangen, Germany, [3]Institute of Biomechanics, Graz University of Technology, Graz, Austria, [4]Department of Neuropathology, Institute of Pathology, Medical University of Graz, Graz, Austria, [5]Department of Pathology, Medical Faculty, Otto-von-Guericke-University, Magdeburg, Germany, [6]Departments of Mechanical Engineering and Bioengineering, Stanford University, CA, United States, [7]Faculty of Engineering Science and Technology, Norwegian University of Science and Technology (NTNU), Trondheim, Norway

In this study, we investigated the mechanical stiffness of human brain tissue assessed by triaxial testing of post-mortem tissue specimens in relation to magnetization transfer ratio (MTR) and diffusion tensor MRI. Our results showed a strong inverse correlation of MTR and FA with the tissue stiffness. Anisotropy of the stiffness was not observed, which indicates that the neuronal fiber orientation does not mechanically support the tissue.

4747 Computer 116

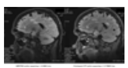

Improved T2-weighted 3D FLAIR from a compact, lightweight 3T scanner with high-performance gradients

Paul T Weavers[1], Norbert Campeau[1], Yunhong Shu[1], Shengzhen Tao[1], Joshua D Trzasko[1], Erin M Gray[1], Thomas K.F. Foo[2], Matt A Bernstein[1], and John Huston III[1]

[1]Radiology, Mayo Clinic, Rochester, MN, United States, [2]MRI, GE Global Research, Niskayuna, NY, United States

A compact, low-cryogen 3T MRI scanner has been developed employing high-performance gradients capable of simultaneously achieving 80 mT/m and 700 T/m/s. A comparison study of T2-weighted 3D FLAIR in 16 clinical patients graded by two neuroradiologists has been performed. The compact 3T system performed equally well to a standard whole-body system in terms of motion artifacts and cerebellar folia conspicuity, and performed better in terms of signal-to-noise ratio, lesion conspicuity, gray/white contrast, and overall exam quality.

4748 Computer 117

T1 Shortening in the Globus Pallidus after Macrocyclic Gadolinium Contrast Agent Administration assessed with Multi-Dynamic, Multi-Echo (MDME) Sequence

Koung Mi Kang[1], Seung Hong Choi, Moonjung Hwang, Ji-hoon Kim, Chul-Ho Sohn, and Tae Jin Yun

[1]Seoul National University Hospital, Seoul, Korea, Republic of

Although a few studies reported the possibility of Gd deposition in the brain by macrocyclic GBCAs, the final determination of deposition with macrocyclic GBCAs has not been performed. Because Synthetic MRI with MDME sequence enables quantitative measurements with relatively short time, our study aimed to investigate whether T1 relaxation time in globus pallidus was influenced by gadobutrol administrations by using the quantitative MR imaging. This study revealed that T1 shortening in globus pallidus occurs by gadobutrol administrations. Additional studies are needed to investigate the clinical significance of these findings.

4749 Computer 118

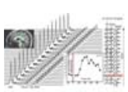

Glucose Tolerance Test in the Human Brain: 1H MRS study at 7 Tesla

Lana Galina Kaiser[1], Ben Inglis[2], Hirokazu Kawaguchi[1], Masaki Fukunaga[3], Norihiro Sadato[3], and Tomohisa Okada[4]

[1]Diagnostics, Siemens Healthcare Japan, Tokyo, Japan, [2]Psychology, UC Berkeley, Berkeley, CA, United States, [3]NIPS, Okazaki, Japan, [4]Department of Diagnostic Radiology, Kyoto University, Japan

The goal of this study is to perform an oral glucose tolerance test (GTT) in the healthy human brain tissue *in vivo* and to evaluate the performance of the recently developed ^{1}H MRS technique. The observed glucose level curve shape showing increase and washout during the ^{1}H MRS GTT test is consistent with the medical GTT blood measurements obtained in healthy subjects. This study demonstrates the initial steps towards better understanding of potential utility of ^{1}H MRS in experiments on glucose metabolism in vivo in the context of nutrition, brain function, and various neurological disorders with impaired glucose utilization.

4750 Computer 119

magna cum laude

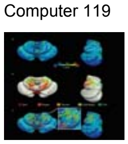

Quantitative T1 mapping and somatotopic organization of the cerebellum at 7T : is there a link?

Yohan Boillat[1], Pierre-Louis Bazin[2], Rolf Gruetter[1,3,4], and Wietske Van der Zwaag[5,6]

[1]Laboratory of Functional and Metabolic Imaging, Ecole Polytechnique Fédérale de Lausanne, Lausanne, Switzerland, [2]Department of Neurophysics, Max Planck Institute for Human Cognitive and Brain Sciences, Leipzig, Germany, [3]Department of Radiology, University of Lausanne, Lausanne, Switzerland, [4]Department of Radiology, University of Geneva, Geneva, Switzerland, [5]Biomedical Imaging Research Center, Ecole Polytechnique Fédérale de Lausanne, Lausanne, Switzerland, [6]Spinoza Centre for Neuroimaging, Amsterdam, Netherlands

In this study, the spatial relationship between the somatotopy and the pattern of myelination (as measured by quantitative T_1-maps) in the cerebellum was investigated. Subject-specific surfaces were generated on which were mapped T_1 values and somatotopic maps. Consistent somatotopic gradients organized through several lobules were present in the anterior and posterior lobes. Despite being more complex, changes of T_1 values across the cerebellar surface were also observed and showed a similar orientation as the somatotopic organization. This study showed the potential structure-function relationship of the cerebellum observed at macroscale level.

4751 magna cum laude

Computer 120

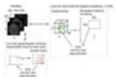

Accelerated Multi-UTE MRI for Direct Myelin Measurements at 7T

Peng Cao[1], Tanguy Boucneau[2], and Peder Larson[1]

[1]Department of Radiology and Biomedical Imaging, UCSF, San Francisco, CA, United States, [2]Université Paris-Sud, France

Recent study demonstrated a multiple and ultrashort echo time (multi-UTE) MRI method for direct detection of methylene protons in myelin membranes on normal brains. However, such multi-UTE MRI requires prohibitively long scan time; therefore, acceleration method is needed. The objective of this study was to accelerate the multi-UTE imaging in order to reduce the scan time and enable such measurements routinely on our 7T human MRI.

Electronic Poster

Image Processing

Exhibition Hall — Wednesday 13:45 - 14:45

4752

Computer 1

Optimized PC-MRA using a New Processing Workflow for 4D Flow MRI Data

Lingzi Tashakkor[1], Susanne Schnell[1], Alex J Barker[1], Kelly Jarvis[1], Emilie Bollache[1], and Michael Markl[1]

[1]Northwestern University, Chicago, IL, United States

A new workflow was developed based on the information from 4D flow MRI to optimize the phase contrast MR angiogram. Five new PC-MRA algorithms were tested on 15 patients, and compared with and without the proposed pre-processing. Histogram equalization/remapping was applied to improve the dynamic signal range for easier segmentation and reduced user interaction. Results showed higher-quality PC-MRAs when the proposed pre-processing was applied.

4753

Computer 2

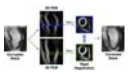

Slice Realignment for Motion-Corrupted Stacks of Short-Axis Cine Cardiac MR Images based on 3D Probabilistic Edge Maps

Giacomo Tarroni[1], Ozan Oktay[1], Andreas Schuh[1], Wenjia Bai[1], Antonio de Marvao[1], Declan O'Regan[1], Stuart Cook[1], and Daniel Rueckert[1]

[1]Imperial College London, London, United Kingdom

Short-axis cine cardiac MR image stacks are acquired during multiple breath-holds, which often causes a misalignment of several slices. We propose a technique for in-plane spatial realignment of motion-corrupted short-axis slices which uses probabilistic edge maps of the myocardium (generated with decision forests) as input to image registration. The proposed technique was quantitatively tested on a dataset of motion-free stacks artificially corrupted by in-plane motion. Overlap measures such as the Dice coefficient - computed on myocardial masks segmented respectively on motion-free, motion-corrupted and motion-corrected stacks - suggest that the proposed technique is able to correctly compensate for slice misalignment.

4754

Computer 3

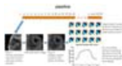

Semi-Automatic Ejection Fraction Calculation from Cardiac Low-Rank Tensor Images Based on Unsupervised Machine Learning

Zihao He[1,2], Anthony G. Christodoulou[1,3], Hua Guo[2], and Debiao Li[1,4]

[1]Biomedical Imaging Research Institute, Cedars-Sinai Medical Center, Los Angeles, CA, United States, [2]Center for Biomedical Imaging Research, Department of Biomedical Engineering, School of Medicine, Tsinghua University, Beijing, People's Republic of China, [3]Cedars-Sinai Heart Institute, Cedars-Sinai Medical Center, Los Angeles, CA, United States, [4]Department of Bioengineering, University of California Los Angeles, Los Angeles, CA, United States

Calculation of the ejection fraction from cardiac cine MR images requires segmenting multiple images of the left ventricle. This process, which is often performed manually, is time-consuming and observer-dependent. In this work, an unsupervised machine learning algorithm, combining hidden Markov random field and optical flow, has been proposed to perform semi-automatic tissue segmentation on T1/T2-weighted low-rank tensor images that have a built-in feature space due to low-rank factorization performed during image reconstruction. The segmentation results then allow automatic EF calculation. Demonstrated results have higher efficiency and similar accuracy compared with manual segmentation, and were stable with respect to different initializations.

4755

Computer 4

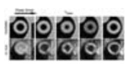

Non-rigid Groupwise Image Registration for Myocardial Strain Quantification from High-Resolution 3D Tagging

Valery Vishnevskiy[1], Christian Stoeck[1], and Sebastian Kozerke[1]

[1]Institute for Biomedical Engineering, ETH Zurich, Zurich, Switzerland

Cardiac motion can be efficiently assessed using 3D-tagged MR sequences for diagnostic purposes. However, there is a lack of robust post-processing tools to derive regional motion and strain data. Current registration methods tend to underestimate radial strain in the left ventricle. In order to provide accurate strain estimates we leverage temporal smoothness of displacements and low-rank structure of aligned images. The herein proposed method is 38% more accurate for radial strain, 27% for circumferential strain and 25% for longitudinal strain estimation than state-of-the-art registration implemented in Elastix while increasing computational speed by a factor of six.

4756

Computer 5

Cardiac image acquisition by SENSE combined compressed sensing with three dimensional quantification

Jong-Hyun Yoon[1], Pan-ki Kim[2], Young-Joong Yang[1], Jinho Park[3], Jin-Soo Kim[1], Byoung Wook Choi[2], and Chang-Beom Ahn[1]

[1]Department of Electrical Engineering, Kwangwoon University, Seoul, Korea, Republic of, [2]Department of Radiology, Severance Hospital, Yonsei University College of Medicine, Seoul, Korea, Republic of, [3]Brain Research Laboratory, Children's National Health System, Washington, DC, United States

SENSE combined compressed sensing technique is applied to multi-slice cardiac CINE imaging with breath holds. As to the compressed sensing, ITSC is used, which truncates small transformed coefficients in r-f domain to make data sparse, and it restores the measured data in k-t domain iteratively until the reconstructed images converge. Variation of ejection fraction (EF) is measured for two set of experiments, one from regenerated data set by resampling the original data set, and the other from real measurements. Using the variation of EF and normalized mean square error clinical usefulness of the technique is demonstrated.

4757 Computer 6

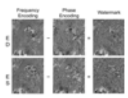

Motion tracking in cardiac MRI: Cine Watermark tracking of myocardial strain

Davis Marc Vigneault[1,2,3], Ronald J Beyers[4], Chia Ying Liu[2], Alison J Noble[1], Thomas Denney[4], and David A Bluemke[2]

[1]Department of Engineering Science, University of Oxford, Oxford, United Kingdom, [2]Radiology and Imaging Sciences, National Institutes of Health, Bethesda, MD, United States, [3]Sackler School of Graduate Biomedical Sciences, Tufts University School of Medicine, Boston, MA, United States, [4]Auburn University MRI Research Center, Auburn University, Auburn, AL, United States

Quantification of regional cardiac function is of central importance in cardiology, but has yet to be adopted into clinical practice due to limitations of the current techniques. Here we present a method requiring minimal human intervention for tracking "cine watermark" images, in which features have been encoded into the *phase image* of a cardiac cine series. The method employs nonlinear least squares optimization, which allows the sum of squared wrapped phase differences between patches in successive frames to be minimized globally across all frames, while regularizing over physically-motivated metrics. Preliminary results in healthy human volunteers show robust tracking.

4758 Computer 7

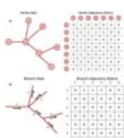

Automated 4D Flow Conservation Utilizing Adjacency Matrices

Carson Anthony Hoffman[1], Gabe Shaughnessy[1], and Oliver Wieben[1]

[1]Medical Physics, University of Wisconsin Madison, Madison, WI, United States

4D flow magnetic resonance imaging (MRI) can provide comprehensive information on vessel anatomy and hemodynamics for complex vessel system. Adjacency matrices are often used in computer science to help simplify complex graphs into a binary encoded matrix. The adaptation of adjacency matrices to 4D flow MRI can help reduce the complexity for analysis by structuring the data into an efficient binary matrix. One application of this new analysis method allows for flow conservation to be completed for complex volumes at all junctions. The conservation of flow at every junction can then be used to find segments of potential erroneous measurements.

4759 Computer 8

MRI vessel slice tool visualization with an interactive 3-D display

Carson Anthony Hoffman[1], Eric Schrauben[1], and Oliver Wieben[1,2]

[1]Medical Physics, University of Wisconsin Madison, Madison, WI, United States, [2]Radiology, University of Wisconsin Madison, Madison, WI, United States

The comprehensive information on vessel anatomy and hemodynamics presented by 4D Flow MRI can be difficult to visualize. We introduce a new viewing mode using a 'slice tool'. The use of this display algorithm can provide benefits for scalar visualization by preserving spatial location and avoiding ambiguities in cases of overlapping vessels. This novel approach can thus offer an improved understanding of complex hemodynamics within the body when used in conjunction with previously existing visualization methods eg. MIP images, pathline, and streamline visualizations.

4760 Computer 9

SUPER-RESOLUTION RECONSTRUCTION OF LATE GADOLINIUM ENHANCEMENT CARDIOVASCULAR MAGNETIC RESONANCE IMAGES USING A RESIDUAL CONVOLUTIONAL NEURAL NETWORK

Archontis Giannakidis[1,2], Ozan Oktay[3], Jennifer Keegan[1,2], Veronica Spadotto[1,4], Inga Voges[1], Gillian Smith[1], Iain Pierce[1], Wenjia Bai[3], Daniel Rueckert[3], Sabine Ernst[1], Michael A Gatzoulis[1], Dudley J Pennell[1,2], Sonya Babu-Narayan[1], and David N Firmin[1,2]

[1]NIHR Cardiovascular Biomedical Research Unit, Royal Brompton Hospital, London, United Kingdom, [2]National Heart & Lung Institute, Imperial College London, London, United Kingdom, [3]Biomedical Image Analysis Group, Imperial College London, London, United Kingdom, [4]Department of Cardiac, Thoracic and Vascular Sciences, University of Padua

Late gadolinium enhancement cardiac magnetic resonance (LGE-CMR) has enabled the accurate myocardial tissue characterization. Due to practical considerations, the acquisition of anisotropic two-dimensional (2D) stack volumes, with low through-plane resolution, still prevails in the clinical routine. We propose a deep learning-based method for reconstructing a super-resolved three-dimensional LGE-CMR data-set from a low resolution 2D short-axis stack volume. The method directly learns the residuals between the high and low resolution images. Results on clinical data-sets show that the proposed technique outperforms the state-of-the-art with regard to image quality. The fast speed of our model furthers facilitates its adoption for practical usage.

4761 Computer 10

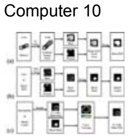

Fully automatic bullseye analysis on short-axis MOLLI mapping: LV segmentation and AHA 17 parcellation

Yun-Wen Wang[1], Chun-Yu Huang[1], Hsiao-Hui Huang[1], and Teng-Yi Huang[1]

[1]Department of Electrical Engineering, National Taiwan University of Science and Technology, Taipei, Taiwan

The free-breathing MOLLI (FB-MOLLI) presented in our previous study allowed T1 mapping in vivo without breath-hold. In this study, we attempted to implement unsupervised reconstruction for FB-MOLLI data sets and used a deformable method for image registration to improve the reliability of free-breathing T1 mapping. The results supported that the method improved the image alignments of the FB-MOLLI data sets and thus increased the quality of the T1 map. The variations of the repeated T1 measurements were significantly reduced in the anterolateral of the LV walls.

4762 Computer 11

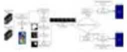

Fully automatic myocardial ECV mapping: deformable image registration, LV segmentation and a cloud computing pipeline

Yun-Wen Wang[1], Chiao-Ning Chen[1], Teng-Yi Huang[1], and Ming-Ting Wu[2]

[1]Department of Electrical Engineering, National Taiwan University of Science and Technology, Taipei, Taiwan, [2]Deptartment of Radiology, Kao-Hsiung Veterans General Hospital, Kao-Hsiung, Taiwan

In this study, we developed an automatic pipeline and segmentations of left ventricle walls for mapping myocardial extracellular volume fraction (ECV) and calculating global ECV values. The system combined with user-friendly web-based user interface was packaged into a software container. We used this system to analyze myocardial T1 images obtained from subjects with tetralogy of Fallot (TOF). The ECV values of the TOF data sets were significantly higher than those of the normal subjects. This automatic pipeline could be a practical tool for clinical evaluations of myocardial fibrosis with MR MOLLI T1 images.

4763 Computer 12

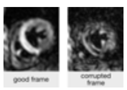

Automatic detection of corrupted frames in cardiac DTI with machine learning

Francesca Cavallo[1], Pedro Ferreira[1], Zohya Khalique[1], Andrew Scott[1], Sonia Nielles-Vallespin[2], and David Firmin[1]

[1]Cardiovascular BRU, Royal Brompton Hospital, London, United Kingdom, [2]NHLBI, National Institutes of Health, MD, United States

In vivo cardiac DTI is capable of probing the microstructure of the myocardium and its dynamics throughout the cardiac cycle. The typical cardiac DTI scan data will contain corrupted frames due to cardiac and respiratory motion. Currently an experienced observer identifies corrupted frames by means of a visual assessment and manually removes them. In this work we show that machine learning can be used to accurately assess DTI corrupted frames, reducing the user input, accelerating analysis and removing human subjectivity.

4764 Computer 13

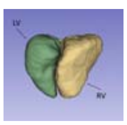

A Novel 4D Semi-automatic Segmentation Algorithm for Whole-heart 3D Cine Magnetic Resonance Imaging

Ruizhi Liao[1], Danielle F. Pace[1], Andrew J. Powell[2], Polina Golland[1], and Mehdi Hedjazi Moghari[2]

[1]Massachusetts Institute of Technology, Cambridge, MA, United States, [2]Boston Children's Hospital, Boston, MA, United States

Three-dimensional (3D) time-resolved (cine) whole-heart magnetic resonance imaging promises to greatly facilitate comprehensive and evaluation of cardiac function and morphology. We present here a robust semi-automatic 4D segmentation algorithm, using patch-based volumetric segmentation and a temporal image registration method, to reduce the segmentation time of 3D cine datasets to less than 30 minutes and to enable wide clinical use. Resulting volumetric measurements of the left ventricle and right ventricle are aligned with measurements from the current clinical routine. By visualizing the anatomy and dynamics of the heart, we show that 3D cine datasets promise to enhance surgical planning for patients with complex congenital heart disease.

4765 Computer 14

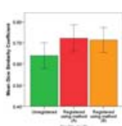

Non-iterative model for synthetic image-based registration of MOLLI cardiac T1 mapping images

Laura Claire Saunders[1], Neil Stewart[1], David Kiely[2], Martin Graves[3], Andy Swift[1], and Jim Wild[1]

[1]Academic Radiology, University of Sheffield, Sheffield, United Kingdom, [2]Pulmonary Vascular Disease Unit, Sheffield Teaching Hospitals NHS Trust, [3]University of Cambridge

Cardiac T1 maps rely upon the acquisition of spatially aligned images. When patients fail to maintain breath hold, respiratory motion can cause T1 map inaccuracies due to poor image alignment. In the method demonstrated here, images are registered by co-registration to synthetic images, which are created via a non-iterative, automatic, model-based method. This method is compared to an iterative registration method using an energy minimisation process for quantitative registration accuracy and speed. Both methods were found to significantly improve image registration. The resultant registrations from both methods did not significantly differ, however the non-iterative model-based method reduced processing time by 1/5th.

4766 Computer 15

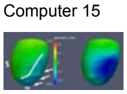

An MRI based High-Resolution Geometrical Framework to Quantify Left Ventricular Remodeling in Murine Model of Myocardial Infarction

Siamak Ardekani[1], Geoffrey Gunter[1], Jiadi Xu[1], Robert G Weiss[2], and Laurent Younes[1]

[1]Johns Hopkins University, Baltimore, MD, United States, [2]Johns Hopkins Medical Institutions, Baltimore, MD, United States

Computational models of left ventricular (LV) geometry and function that characterize regional cardiac response to injury can provide valuable diagnostic and predictive information. We have developed a mathematical tool to non-rigidly match a high-resolution surface mesh of the LV geometry to a set of LV epi and endocardial contours that are extracted from cardiac MR. We have applied our algorithm on murine model of myocardial infarction to quantify cardiac remodeling process. This approach enables us to perform statistical analysis of LV 3D geometry and function using only sparse sets of 2D plane contours, therefore facilitating cross-subject examination of shape variation.

4767 Computer 16

Texture analysis of native T1 mapping in dilated cardiomyopathy

Xiaoning Shao[1], Yingjie Sun[1], Yong Zhang[1], Jingliang Cheng[1], and Shaoyu Wang[2]

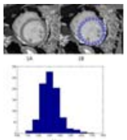

[1]MRI, The first affiliated hospital of Zhengzhou University, Zhengzhou, People's Republic of China, [2]MR, Siemens Healthcare Ltd, Shanghai, People's Republic of China

MR native T1 mapping technique was found have the ability of detecting diffuse myocardial fibrosis which was found in histological examination of dilated cardiomypathy (DCM). Texture analysis of T1 mapping had been proved to be able to provide more information besides T1 value. We found several histogram parameters (statistical class of texture analysis) were significantly higher in DCM than that of healthy volunteers. The areas under the receiver operating characteristic curve of histogram parameters were calculated. The results indicate that texture analysis of T1 mapping may be helpful for the diagnosis of DCM.

4768 Computer 17

Improving Precision of Arrhythmia-Insensitive Rapid Cardiac T1 Maps using a Non-Local Means Filter

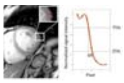

Suvai Gunasekaran[1], KyungPyo Hong[2], Jeremy Collins[2], James Carr[2], and Daniel Kim[1,2]

[1]Biomedical Engineering, Northwestern University, Chicago, IL, United States, [2]Radiology Department, Feinberg School of Medicine, Chicago, IL, United States

Compared with other investigations, images produced from arrhythmia-insensitive rapid (AIR) cardiac T_1 mapping pulse sequences contain significant random noise which limits the accuracy of quantitative measurements. Therefore, denoising filters were used to reduce noise present in the images. From our analysis, the non-local means filter was best able to reduce the amount of noise while still maintaining accurate T_1 measurement data.

4769 Computer 18

Validation of dMRI-Derived Fiber Orientations Using PLI in Human Fetal Hearts

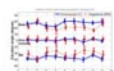

Feng Yang[1,2], YueMin Zhu[2], Gabrielle Michalowicz[3], Yves Usson[3], Laurent Fanton[2], Magalie Viallon[2,4], Patrick Clarysse[2], Pierre-Simon Jouk[3], and Pierre Croisille[2,4]

[1]Department of Computer Science, School of Computer and Information Technology, Beijing Jiaotong University, Beijing, People's Republic of China, [2]Univ.Lyon, INSA-Lyon, Université Claude Bernard Lyon 1, UJM-Saint Etienne, CNRS, Inserm, CREATIS UMR 5220, U1206, F-69621, LYON, France, Villeurbanne, France, [3]Equipe DYCTIM, Laboratoire TIMC-IMAG, UMR5525 CNRS, Université Grenoble Alpes, La Tronche, France, France, [4]Jean-Monnet University, Saint-Etienne, France, Saint-Etienne, France

To validate to what extent the fiber orientations derived from diffusion MRI (dMRI) reveal anatomical reality, polarized light imaging (PLI) allowing the fiber orientations of the human heart to be physically measured with high spatial resolution was used. The dMRI and PLI orientation measurements of the same hearts are then compared using a multimodal registration-based framework. Experimental results show that dMRI and PLI have similar variation patterns of elevation or azimuth angles, except that dMRI introduced a decrease of about 24° in transmural elevation angle range. No significant differences were observed on azimuth angle in both modalities.

4770 Computer 19

Regularized Curve Fitting Improves T1 Bias in Cardiac T2 Mapping

Galen D Reed[1], Kenneth O Johnson[1], Michelle M Nystrom[1], Okai Addy[1], Reeve Ingle[1], Bob Hu[1], Juan Santos[1], and William Overall[1]

[1]HeartVista, Los Altos, CA, United States

Bias error is studied in T2-prepared single shot SSFP cardiac T2 mapping. Phantom experiments showed that although centric phase encode ordering reduces bias from T1 relaxation during single shot readouts, a residual bias of approximately 20% remains in the 1000 ms T1 regime. A regularized, three parameter exponential fitting model reduces this bias and generates T2 maps with low variance using 4 echo times.

4771 Computer 20

The Myocardial Feature Tracking of LA, LV and RV: Age-related in Normal Chinese

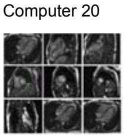

Junping Peng[1], Mingwu Lou[2], Lei Zhao[3], Zhanming Fan[3], Xiaohai Ma[3], Liang Zhong[4], Xiaodan Zhao[4], Hui Chen[3], Zheng Wang[3], and Shuang Leng[4]

[1]Department of Radiology, Shenzhen Longgang District Center Hospital, Shenzhen, People's Republic of China, [2]Department of Radiology, [3]Department of Radiology, Beijing Anzhen Hospital，Capital Medical University, [4]National Heart Centre Singapore

To quantify the age-related global cardiac deformation, GLS and GCS derived from feature-tracking cardiovascular magnetic resonance were measured using post-processing software in 81 healthy Chinese volunteers. It was found that age significantly influenced GLS of LV and LA. This is an important indicator for further research of quantitation MR Myocardial Feature Tracking.

4772 Computer 21

Workflow Improvement with a Cardiac MRI Positioning Assist Function

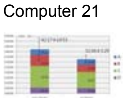

Kensuke Shinoda[1], Shuhei Takemoto[1], and Shuhei Nitta[2]

[1]MRI Systems Division, Toshiba Medical Systems Corporation, Tochigi, Japan, [2]Corporate Research & Development Center, Toshiba Corporation

In this study, we evaluated how the Cardiac MRI positioning assist function can reduce the operation steps and times in CMRI. When using the assist function, the total number of the operation steps was reduced to about 25% for both the experts and the beginners. The operation time was also reduced to about 25%. The mean and SD of the elapsed time for the CMRI procedure performed by experts were reduced from 42m17s±10m53s to 32m46s±3m29s, and those for coronary angiography were reduced from 20m42s±8m5s to 15m22s±2m49s.

4773 Computer 22

4D Flow MRI based aortic wall shear stress analysis using two different software tools and datasets from MRI scanners of two different appliance brands

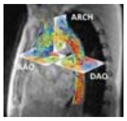

Michael Peter Beldoch[1], Thekla Helene Oechtering[1], Victoria Schultz[1], Peter Hunold[1], Joerg Barkhausen[1], and Alex Frydrychowicz[1]

[1]*Clinic for Radiology and Nuclear Medicine, University Hospital Schleswig-Holstein, Lübeck, Germany*

Wall shear stress (WSS) is an increasingly used vessel wall parameter derived from 4D Flow-MRI data. There is no reference standard for evaluating WSS and different software approaches are available. However, their comparability is not known. Hence, it was the aim of this study to compare two available software tools (GTFlow and FlowTool). To achieve this goal, data from 21 healthy volunteers scanned on MRI scanners of different vendors were analyzed with respect to average and segmental WSS. Results showed good agreement between tools.

4774 Computer 23

Free-Breathing cardiovascular imaging: comparing central k-space amplitude vs. phase based self-gating approaches

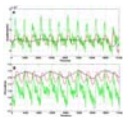

Feifei Qu[1], Uday Krishnamurthy[1,2], Brijesh Kumar Yadav[1,2], Ewart Mark Haacke[1,2], and Jaladhar Neelavalli[1,2]

[1]*Department of Radiology, Wayne State University, Detroit, MI, United States,* [2]*Department of Biomedical Engineering, Wayne State University, Detroit, MI, United States*

Two self-gating approaches to reconstruct free-breathing cardiovascular image generated by Golden Angle radial trajectory MRI were compared. The results show that both central k-space magnitude and phase self-gated image have comparable quality with breathhold Cartesian CINE image, and the phase self-gating signal is less sensitive to the coil sensitivity compared to the magnitude based self-gating signal.

4775 Computer 24

Evaluation of three-dimensional magnetic resonance imaging of autopsied human heart specimens for computational modeling of congenital heart diseases

Yoshiaki Morita[1], Wataru Ueki[1], Ryo Haraguchi[2], Takaaki Matsuayama[3], Yoshiaki Watanabe[1], Tatsuya Nishii[1], Atsushi Kono[1], Naoaki Yamada[1], and Tetsuya Fukuda[1]

[1]*Department of Radiology, National Cerebral and Cardiovascular Center, Suita, Osaka, Japan,* [2]*Division of Medical informatics, National Cerebral and Cardiovascular Center, Suita, Osaka, Japan,* [3]*Department of Pathology, National Cerebral and Cardiovascular Center, Suita, Osaka, Japan*

This study aimed to compare the visibility of a formalin-fixed heart using various 3D MRI sequences as well as to determine the optimal sequence for computational modeling of congenital heart diseases. Our results demonstrated that MPRAGE showed the best contrast with good image quality for imaging of the myocardium and the vascular structure when surrounded by normal saline in a plastic container. We believe that computational cardiac modeling of human autopsied heart specimens using MPRAGE plays a critical role in education and/or research.

Electronic Poster

Prostate Cancer

Exhibition Hall — Wednesday 13:45 - 14:45

4776 Computer 25

FOCUS diffusion-weighted imaging for prostate cancer at high b-values: An analysis of image quality, diagnostic accuracy and observer agreement.

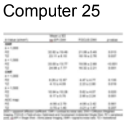

Tom Syer[1], Keith Godley[2], Donnie Cameron[1], and Paul Malcolm[2]

[1]*Norwich Medical School, University of East Anglia, Norwich, United Kingdom,* [2]*Radiology, Norfolk and Norwich University Hospital*

To assess FOCUS diffusion-weighted imaging (DWI) for prostate cancer assessment, 30 consecutive biopsy-proven patients underwent both FOCUS and conventional DWI. Sensitivity and specificity was not significantly different between sequences but inter-observer agreement improved from moderate to substantial when using FOCUS. There was significantly lower SNR and CNR for FOCUS on *b*-value images, but similar CNR on ADC maps. Mean ADC values were significantly lower using FOCUS and both sequences showed excellent discrimination between malignant and benign prostate with no statistical difference. FOCUS DWI improves agreement between observers of varying experience while maintaining diagnostic accuracy despite lower SNR and CNR.

4777 Computer 26

Target performance of MRI-ultrasound fusion guided prostate biopsy in a cohort of patients suspicious for prostate cancer

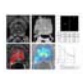

Matthias Gergely Zadory[1], Jean-Luc Fehr[2], Claudius Moeckel[2], Seife Hailemariam[3], Johannes Malte Froehlich[1], and Michael Patak[4]

[1]*Pharmaceutical sciences institute, ETHZ, Zurich, Switzerland,* [2]*Zentrum für Urologie, Hirslanden Klinik, Zurich, Zurich, Switzerland,* [3]*Institut für histologische und zytologische Diagnostik, Aarau, Switzerland,* [4]*Radiologie, Hirslanden Klinik, Zurich, Zurich, Switzerland*

Conventional systematic core biopsies might fail to detect clinical significant prostate cancer. ARTEMIS MRI-ultrasound fusion guided prostate biopsy (ART-PBx) might overcome this issue by improving the targeting of suspicious lesions. In a retrospective clinical study including 194 patients (243 lesions) we determined a target performance of 56.3 % positive biopsies related to histopathology. The detection rate rises up to 71.4% for high score lesions (PIRADS 5) but did not show any correlation with lesion's size. This target methodology based on MRI achieves greater detection rate of clinical significant prostate cancer, improving the ability to appropriately counsel patients regarding therapy.

4778 Computer 27

Role of DWI in guiding MRI-TRUS fusion biopsy in patients with prostate cancer: a prospective cohort study

Chandan J Das[1], Rohit Kaushal[2], Sanjay Sharma[1], Rajeev Kumar[3], P N Dogra[3], and S DattaGupta[4]

[1]*Radiology, All India Institute of Medical Sciences, New Delhi, India, NewDelhi, India,* [2]*Uology, All India Institute of Medical Sciences, New Delhi, India, NewDelhi, India,* [3]*Urology, All India Institute of Medical Sciences, New Delhi, India, NewDelhi, India,* [4]*Pathology, All India Institute of Medical Sciences, New Delhi, India, NewDelhi, India*

Transrectal ultrasound (TRUS) guided 12 core biopsy of prostate has a sensitivity of 39-52%. We prospectively evaluated the role of DWI in guiding MRI-TRUS fusion biopsy. MRI was performed on a 3 Tesla system. PIRAD score was assigned and PIRAD 3-5 score were subjected to targeted fusion biopsy using the Artemis device along with standard 12 core biopsies. Targeted biopsy detected a higher number (93%) of clinically significant cancers and 71% cancers were upgraded to significant cancer on targeted biopsy. Fusion biopsies guided by DWI thus provide incremental information over standard TRUS biopsies in the diagnosis of significant prostate cancer.

4779 Computer 28

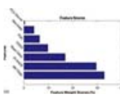

MR-based machine learning analysis can help to predict pathological outcome of biopsy-proven Gleason score 3+3 prostate cancer

Chen-Jiang Wu[1], Yu-Dong Zhang[1], and Hai-Bin Shi[1]

[1]Department of Radiology, the First Affiliated Hospital with Nanjing Medical University, Nanjing,China, People's Republic of China

Machine learning-based analysis of multi-parametric was used to predict pathological outcome of biopsy-proven Gleason score 3+3 prostate cancer and proven to be better compared with single any MR or clinical paremeter in predicting pathological outcome.

4780 Computer 29

Diffusion-Kurtosis imaging predicts tumor upgrading in biopsy-proven Gleason score = 6 prostate cancers

Chen-Jiang Wu[1], Yu-Dong Zhang[1], and Hai-Bin Shi[1]

[1]Department of Radiology, the First Affiliated Hospital with Nanjing Medical University, Nanjing,China, People's Republic of China

The study investigated the feasibility of Diffusion Kurtosis Imaging (DKI) in predicting surgical result upgrading of biopsy-proven Gleason Score (GS) = 6 prostate cancer. The predicting efficiency of clinical variables (tumor volume, PSA level) and MRI variables (ADC, Dapp, Kapp) were compared by ROC analysis. DKI was found feasible to predict surgical result upgrading of biopsy-proven GS = 6 prostate cancer and Dapp-minimun had the highest Az value.

4781 Computer 30

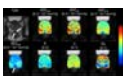

DWI of prostate cancer beyond ADC: correlation with histopathology

Stefanie Hectors[1], Sahar Semaan[1], Christopher Song[1], Ashutosh Tewari[2], George K Haines[3], and Bachir Taouli[1]

[1]Translational and Molecular Imaging Institute, Icahn School of Medicine at Mount Sinai, New York, NY, United States, [2]Department of Urology, Icahn School of Medicine at Mount Sinai, New York, NY, United States, [3]Department of Pathology, Icahn School of Medicine at Mount Sinai, New York, NY, United States

In this study, we correlated advanced DWI [diffusion kurtosis imaging (DKI), stretched-exponential (SE) DWI and diffusion tensor imaging DTI)] parameters with fractional tissue fractions of nuclei, cytoplasm, cells, stroma and lumen and the nuclear-cytoplasmic ratio in prostate cancer (PCa) lesions. We found that all assessed diffusion methods showed significant correlations with cytoplasmic, cellular and/or stromal tissue fractions. Specifically, DKI seems promising for characterization of PCa tissue composition, since multiple significant correlations between histology parameters and both ADC_{DKI} and kurtosis parameter K were observed.

4782 Computer 31

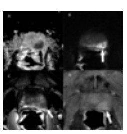

Mixed performance of PIRADS v2: a validation study

James Walton[1], Sajal Pokharel[1], E. David Crawford[2], Kavita Garg[1], Kimberly E. Lind[1], Emma Murugaverl[3], and Nayana U. Patel[1]

[1]Radiology, University of Colorado School of Medicine, Aurora, CO, United States, [2]Urology, University of Colorado School of Medicine, Aurora, CO, United States, [3]Lake Erie College of Osteopathic Medicine

The second version of the Prostate Imaging Reporting and Data System (PIRADSv2) is the new standard for interpreting prostate MRI. Validation studies have been performed of this scheme, but many have used targeted biopsies as the reference standard. Our validation study is unique in utilizing 3D trans-perineal mapping biopsy (3DTMB) as the reference standard. With a total of 41 MRI lesions, PI-RADSv2 score = 5 lesions had a PPV for cancer of 1.0. However, when all significant lesions (PI-RADSv2 score ≥3) were included, the PPV is 0.29, with equal PPV of PI-RADS 3 and 4 lesions.

4783 Computer 32

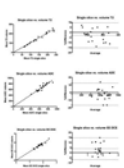

Single Slice vs. Volumetric Analysis of Multiparametric Prostate MRI Metrics

Edward William Johnston[1], Clare Allen[2], Michela Antonelli[3], Nikolaos Dikaios[1], Sebastien Ourselin[3], and Shonit Punwani[1]

[1]Centre for Medical Imaging, University College London, London, United Kingdom, [2]Radiology, University College London Hospitals, London, United Kingdom, [3]Centre for Medical Image Computing, University College London, London, United Kingdom

Despite consensus guidelines advising volumetric analysis of tumours over single slice region-of-interest analysis, there is little data in the literature to support this recommendation. In this study we compare the reproducibility between each of these two methods in 20 patients with prostate cancer and also determine the intraobserver repeatability of each method. We show high levels of agreement and intraobserver repeatability in both of these methods. This study suggests that region-of-interest analysis is a perfectly acceptable analytical method and may have higher intraoberver repeatability than volumetric analysis, and could expedite the analysis of multiparametric prostate MRI datasets in clinical trials.

4784 Computer 33

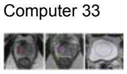

Improving the Reproducibility of Quantitative Imaging Metrics for Multicentre Multiparametric Prostate MRI Trials

Edward William Johnston[1], Michela Antonelli[2], Nikolaos Dikaios[1], Sebastien Ourselin[2], David Atkinson[1], and Shonit Punwani[1]

[1]Centre for Medical Imaging, University College London, London, United Kingdom, [2]Centre for Medical Image Computing, University College London, London, United Kingdom

Whilst multi-scanner studies provide the most robust evidence for quantitative imaging trials, they tend to be limited by poor reproducibility of scans performed on different scanners. In this study, 14 patients underwent paired multiparametric prostate MRI within 3 months of each other. We found that normalisation of T2 signal to the bladder improved the reproducibility of both peripheral zone and transition zone metrics considerably when compared with the current convention of using obturator internus. Whilst ADC also met sufficient levels of reproducibility, semiquantiative and quantitative DCE analysis and histographic features failed to do so.

4785 Computer 34

Lower Normalised T2 Signal Intensity is Associated with Higher Intratumoural Heterogeneity: A Radiogenomic Study in High-Risk Prostate Cancer

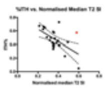

Edward William Johnston[1], Mark Linch[2], Gerald Goh[2], Crispin Hiley[3], Yaalini Shanmugabavan[4], Michela Antonelli[5], Marco Gerlinger[6], Andrew Rowan[2], Yien Ning Sophia Wong[2], Helen King [2], Andrew Furness[7], Alexander Freeman[8], Linares Linares[7], Ayse Akarca[7], Javier Herrero[7], Stephan Dentro[9], Nathalie Harder[10], Guenter Schmidt[10], Gareth A Gareth[3], Nicholas McGranahan[3], Nicolai Birkbak[3], Richard Mitter[3], Paul Cathcart[11], Rebecca Scott[4], Michelle Hung[4], Mark Emberton[4], Gert Attard[12], Zoltan Szallasi[13], Sergio Quezada[7], Teresa Marafioti[8], Sebastien Ourselin[5], Hashim Ahmed[4], Charles Swanton[3], and Shonit Punwani[1]

[1]Centre for Medical Imaging, University College London, London, United Kingdom, [2]Translational Cancer Therapeutics Laboratory, University College London, London, United Kingdom, [3]Translational Cancer Therapeutics Laboratory, Francis Crick Institute, London, United Kingdom, [4]Division of Surgery and Interventional Science, University College London, London, United Kingdom, [5]Centre for Medical Image Computing, University College London, London, United Kingdom, [6]Centre for Evolution and Cancer, The Institute of Cancer Research, [7]Cancer Immunology Unit, University College London, [8]Department of Pathology, University College London Hospital, University Street, United Kingdom, [9]Department of Bioinformatics and Biostatistics, University College London, [10]Definiens AG, [11]Urology, Guy's and St. Thomas' NHS Trust, [12]Treatment Resistance Laboratory, The Institute of Cancer Research, [13]Centre for Biological Sequence 47 Analysis, Technical University of Denmark

Intratumoural heterogeneity (ITH) has been shown to predict overall survival in prostate cancer, and non-invasive biomarkers that can measure this genetic diversity would be welcome. In this study, we correlated imaging metrics derived from multiparametric prostate MRI with genomic heterogeneity indices and showed that low values of normalised T2 signal intensity within tumours are associated with a higher degree of mutational ITH. Our study shows the potential to use diagnostic imaging as a surrogate for genomic ITH in order to risk stratify patient for guiding management decisions.

4786 Computer 35

Preliminary application of magnetization transfer imaging and amide proton transfer imaging of prostate cancer at 3.0 tesla

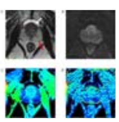

Xiangde Min[1], Zhaoyan Feng[1], Liang Wang[1], and Zhongping Zhang[2]

[1]Tongji Medical College, Huazhong University of Science & Technology, Wuhan, People's Republic of China, [2]GE Healthcare, Guangzhou, People's Republic of China

Magnetization transfer (MT) imaging and amide proton transfer (APT) imaging have reported many promising results. However, little is known about their usefulness for prostate cancer (PCa). In this study, MT-APT imaging were performed for 39 patients with pathological proven PCa. The feasibility of MT imaging and APT imaging for PCa detection was assessed, and their differential diagnostic values for PCa were compared. The results revealed that MTR(16.5 ppm) increased in cancerous tissues compared with normal PZs, and MT imaging outperformed APT imaging for PCa diagnosis. MT imaging showed promising role in the diagnosis of PCa.

4787 Computer 36

Evaluation of prostate cancer on diffusion weighted imaging; Can FOCUS and synthetic diffusion weighted imaging with FOCUS contribute to the Prostate Imaging Reporting and Data System (PI-RADS) version 2.0?

Motoyuki Katayama[1], Takayuki Masui[1], Kei Tsukamoto[1], Mitsuteru Tsuchiya[1], Masako Sasaki[1], Yuki Hayashi[1], Takahiro Yamada[1], Mitsuharu Miyoshi[2], Tetsuya Wakayama[2], and Harumi Sakahara[3]

[1]Radiology, Seirei Hamamatsu General Hospital, Hamamatsu, Japan, [2]GE Healthcare Japan, Japan, [3]Radiology, Hamamatsu University School of Medicine, Hamamatsu, Japan

We evaluated 47 patients suspected of having prostate cancers on synthetic DWI calculated from FOCUS DWI with PI-RADS version 2.0. Compared with conventional FOV DWI, FOCUS DWI is more useful for evaluation of prostate cancer with high spatial resolution and less distortion. S-DWI is able to enhance diagnostic ability of FOCUS without image degradation, which might be one of the best combinations, and contribute to the Prostate Imaging Reporting and Data System (PI-RADS) version 2.0.

4788 Computer 37

Prostate Cancer Diffusion Signal Analysis: Combination of Multiple Fit Parameters Improves Tissue Discrimination

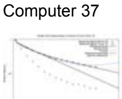

Stephan E. Maier[1,2], Thiele Kobus[3], Andriy Fedorov[1], Fredrik Langkilde[2], Ruth Dunne[1], Robert V. Mulkern[4], and Clare M. Tempany[1]

[1]Radiology, Brigham and Women's Hospital, Harvard Medical School, Boston, MA, United States, [2]Radiology, Sahlgrenska Academy, Gothenburg University, Gothenburg, Sweden, [3]Department of Radiology and Nuclear Medcine, Radbound University Medical Center, Netherlands, [4]Radiology, Children's Hospital, Harvard Medical School, Boston, MA, United States

Diffusion signals over an extended b-factor range 0-3500 s/mm^2 were measured with an endorectal coil at 3 Tesla in 56 prostate cancer patients. For each pixel, signal decay fits were computed assuming biexponential, kurtosis, stretched exponential and gamma distribution diffusion signal models. The potential of individual parameters and linear parameter combinations to differentiate normal from cancerous tissue was evaluated with ROC analysis. For the kurtosis and stretched exponential models, single parameters yield the highest AUCs, whereas for the biexponential and gamma distribution models, only combinations of parameters produce the comparably high AUCs.

4789 Computer 38

3T DCE-MRI Performance in Prostate Cancer Detection: Correlation of Different Kinetic Parameters in the Transition and Peripheral Zone Stratified by Gleason Score and Scanner B1+ field Heterogeneity

Nazanin H Asvadi[1], Kyung Hyun Sung[2], Pooria Khoshnoodi[3], Pornphan Wibulpolprasert[4], Tristan Grogan[5], Anthony Sisk[6], Robert Reiter[7], and Steven Raman[8]

[1]Radiology, David Geffen School of Medicine at UCLA, Los Angeles, CA, United States, [2]Department of Radiological Sciences, Bioengineering, and Biomedical Physics IDP, UCLA, Los Angeles, CA, United States, [3]David Geffen School of Medicine at UCLA, Los Angeles, CA, United States, [4]Radiology, Ramathibodi Hospital, Bangkok, Thailand, [5]Division of General Internal Medicine and Health Services Research, UCLA, Los Angeles, CA, United States, [6]Pathology, David Geffen School of Medicine at UCLA, Los Angeles, CA, United States, [7]Urology, David Geffen School of Medicine, Los Angeles, CA, United States, [8]Radiology, David Geffen School of Medicine, Los Angeles, CA, United States

To correlate 3T dynamic contrast-enhanced MRI (DCE-MRI) kinetic parameters in prostate cancer (PCa) in the transition zone (TZ) and peripheral zone (PZ) confirmed by whole mount histopathology (WMHP) stratified by Gleason Scores (GS) and inter-scanner B1+ field variation. This study demonstrates that clinically relevant heterogeneity between kinetic parameters in low and high grade PCa in the TZ & PZ exists.

4790 Computer 39

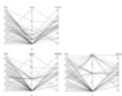

Using Natural Language Processing to explore the correlation of prostate MR findings and prostate biopsy

Yi Liu[1], Shuai Ma[1], Rui Wang[2], Ge Gao[3], En Ouyang[4], Zuofeng Li[4], Juan Wei[4], and Xiaoying Wang[3]

[1]Peking University First Hospital, Beijing, People's Republic of China, [2]Peking University First Hospital, [3]Peking University First Hospital, People's Republic of China, [4]Philips Research China, People's Republic of China

Natural language processing (NLP) provides techniques that aid the conversion of text into a structured representation, which is potentially a valuable source of information for improving clinical care and supporting research in medical domain.[1,2] Used on radiology reports and biopsy results, NLP techniques enable automatic identification and extraction of information. For most patients suffer from prostate diseases, they always conduct tests including radiology and biopsy. And it is an interesting task to explore the prostate MR findings and prostate biopsy, which have not been studied in other research center.

4791 Computer 40

Ex vivo MRI evaluation of prostate cancer: localization and margin status prediction of prostate cancer in fresh radical prostatectomy specimens

Jan Heidkamp[1], Martijn Hoogenboom[1], Iringo Kovacs[2], Andor Veltien[1], Arie Maat[2], Michiel Sedelaar[3], Christina Hulsbergen-van de Kaa[2], and Jurgen Fütterer[1]

[1]Radiology and Nuclear Medicine, Radboud university medical center, Nijmegen, Netherlands, [2]Pathology, Radboud university medical center, Nijmegen, Netherlands, [3]Urology, Radboud university medical center, Nijmegen, Netherlands

This study investigated the ability of high field ex vivo MRI to localize prostate cancer (PCa) and to predict the margin status in fresh radical prostatectomy (RP) specimens using histology as gold standard. In twelve specimens, ex vivo MRI localized 17 (47%) of 36 PCa lesions confirmed by histological examination. Ex vivo MRI identified none of the 4 histological positive surgical margins (sensitivity 0%) and 9 of the 13 negative margins (specificity 69%). Our results indicate accurate localization of PCa in fresh RP specimens by ex vivo MRI, yet the technique did not perform well in predicting the margin status.

4792 Computer 41

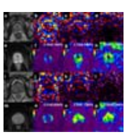

Clinical Evaluation of a Simple Approach for Improving Shear Wave Illumination in Magnetic Resonance Elastography of the Prostate

Jin Wang[1], Tianhui Zhang[1], Kevin J. Glaser[2], Jingbiao Chen[1], Jun Chen[2], Phillip J. Rossman[2], Bingjun He[1], Arvin Arani[2], Ziying Yin[2], Zhuang Kang[1], Qungang Shan[1], Jun Pang[3], and Richard L. Ehman[2]

[1]Department of Radiology, the Third Affiliated Hospital, Sun Yat-sen University (SYSU), Guangzhou, People's Republic of China, [2]Department of Radiology, Mayo Clinic, Rochester, United States, [3]Department of Urology, the Third Affiliated Hospital, Sun Yat-sen University (SYSU), Guangzhou, People's Republic of China

Conventional prostate magnetic resonance elastography (MRE) is performed using an external driver to transmit shear waves into the prostate. It is a challenge to produce shear waves in the prostate with adequate amplitude at a suitably high frequency because the prostate is a deep-seated organ. We evaluated the hypothesis that the placement of a urinary catheter would improve the shear wave illumination of the prostate when waves are emitted from an external driver. Our results in 30 BPH patients show that the commercially available liver MRE driver used in combination with a catheter can improve MRE image quality at higher frequencies.

4793 Computer 42

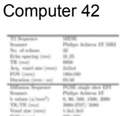

Linking a multi-compartment T2 model to diffusion microstructure in prostate cancer

William Devine[1], Edward Johnston[1], Elisenda Bonet-Carne[2], Shonit Punwani[1], Daniel Alexander[2], and David Atkinson[1]

[1]Centre for Medical Imaging, University College London, London, United Kingdom, [2]Centre for Medical Image Computing, University College London, London, United Kingdom

This work develops a multi-compartment T2 model for prostate imaging. We investigate whether this model can provide information about differences in tissue microstructure, such as those between normal prostate tissue and tumour, by comparing it to the VERDICT diffusion model6. The high correlations found between a number of the parameters suggest that the proposed model is capable of detecting some microstructural differences. In the future this method may be able to provide different and complementary microstructural information to current diffusion models.

4794 Computer 43

Magnetic Resonance Elastography of the Prostate: Impact of Driver Size on Image Quality

Tianhui Zhang[1], Jin Wang[1], Kevin J. Glaser[2], Phillip J. Rossman[2], Jun Chen[2], Bingjun He[1], Jun Pang[3], Ziying Yin[2], Zhuang Kang[1], Qungang Shan[1], Jingbiao Chen[1], Arvin Arani[2], and Richard L. Ehman[2]

[1]Department of Radiology, the Third Affiliated Hospital, Sun Yat-sen University (SYSU), Guangzhou, People's Republic of China, [2]Department of Radiology, Mayo Clinic, Rochester, United States, [3]Department of Urology, the Third Affiliated Hospital, Sun Yat-sen University (SYSU), Guangzhou, People's Republic of China

Conventional prostate MRE uses an external driver located on the surface of the body to transmit shear waves into the prostate. However, the conventional large-diameter driver produces poorer image quality at higher frequencies. In this study we compared the performance of a large- and small-diameter Pelvic Wall driver at multiple frequencies using 2D and 3D MRE. Our results show that the smaller Pelvic Wall driver performs better than the larger driver in terms of image quality and success rate.

4795 Computer 44

TRUS Biopsy Has a Lower Cancer Detection Rate in Large Prostate Volumes: Can In-Bore MRI-Guided Biopsy Do Better?

Kareem K Elfatairy[1], Christopher P Filson[2], Adeboye O Osunkoya[3], Rachel G Geller[3], and Sherif G Nour[1]

[1]Radiology, Emory University-School of Medicine, Atlanta, GA, United States, [2]Urology, Emory University-School of Medicine, GA, United States, [3]Pathology, Emory University-School of Medicine, Atlanta, GA, United States

TRUS biopsy known to have low cancer detection rates in patients with large prostate volumes. With the proved advantages of MRI guided biopsy (MRGB), it may offer a better alternative to those patients. We compared between cancer detection rates of TRUS biopsy and MRGB in 49 patients as related to their prostate volumes. MRGB showed better detection of clinically significant cancers in prostate volumes between 30-59 mL . Adopting MRGB in patients with gland volumes ≥ 30 mL may save patients the need for repeated TRUS biopsies, provide better disease risk stratification, and reduce the healthcare costs associated with unnecessary biopsies.

4796 Computer 45

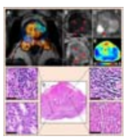

Quantitatively Differentiating Prostate Cancer, Prostatitis and Benign Prostatic Hyperplasia (BPH) by Diffusion MRI Histology (D-Histo)

Ze-Zhong Ye[1], Qingsong Yang [2], Peng Sun [3], Yasheng Zhu[4], Chunyu Song[5], Joshua Lin[6], Jianping Lu[2], Yinghao Sun[4], and Sheng-Kwei Song[3,5,7]

[1]Chemistry, Washington University, St. Louis, MO, United States, [2]Radiology, Changhai Hospital, Shanghai, People's Republic of China, [3]Radiology, Washington University, St. Louis, MO, United States, [4]Urology, Changhai Hospital, Shanghai, People's Republic of China, [5]Biomedical Engineering, Washington University, St. Louis, MO, United States, [6]Biology, Washington University, St. Louis, MO, United States, [7]Hope Center for Neurological Disorder, Washington University, St. Louis, MO, United States

A recent consensus established mpMRI for PCa detection has not had the needed sensitivity or specificity to distinguish prostatitis from PCa. Thus, PCa diagnosis by MRI remains uncertain, resulting in over-diagnosis and over-treatment. For the first time, we demonstrate that the new method, diffusion MRI histology (D-Histo), accurately localizes and quantifies PCa, prostatitis, and BPH. With improved diagnosis accuracy, D-Histo affords effective guidance of treatment planning, and assessment of treatment efficacy.

4797 Computer 46

Modified Dispersion Model in Prostate Dynamic Contrast-Enhanced MRI

Kyunghyun Sung[1], Xinran Zhong[2], and Holden Wu[2]

[1]Radiological Sciences, University of California, Los Angeles, Los Angeles, CA, United States, [2]Radiology, University of California, Los Angeles, Los Angeles, CA, United States

The dispersion imaging has shown great promise in prostate DCE-MRI, but there still exist practical limitations due to the complex model fitting. We describe a modified dispersion model to overcome these limitations by adapting a simple dispersion factor into the existing population-averaged arterial input function. We use the regions of interest, derived from the histological analysis, to evaluate both the quality of the model fitting and the ability of DCE-MRI parameters to delineate between cancerous and normal prostate tissues using 25 prostate patient cases available with the whole-mount histopathology.

4798 Computer 47

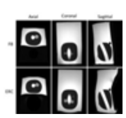

A Transverse External RF Surface Coil for Prostate MR Imaging at 3T

Keith Hulsey[1], Alexander Ivanishev[1], Ivan Dimitrov[2,3], and Robert E. Lenkinski[1,2]

[1]Radiology, UT Southwestern Medical Center, Dallas, TX, United States, [2]Advanced Imaging Research Center, UT Southwestern Medical Center, Dallas, TX, United States, [3]Philips Medical Systems, Cleveland, OH, United States

MRI is playing an increasingly important role in the work up of prostate cancer. This increased demand for prostate imaging has caused a debate in the field regarding the necessity of an endo-rectal coil for these studies. While the endo-rectal coil has distinct advantages it also has some drawbacks in both work-flow and cost. Current external coils do not provide images at comparable SNR to endo-rectal coil images (at the same field strength). Here we describe our initial experience with a transverse external RF coil designed to be placed on the perineum for high quality images.

4799 Computer 48

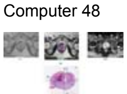

3T Restriction Spectrum Imaging Association with Prostate Cancer Gleason Score, PI-RADS v2 Score and Tumor Diameter on Whole Mount 3D-Mold-Sectioned Histopathology

Pooria Khoshnoodi[1], Sepideh Shakeri[1], Ashkan Shademan[1], Naznin Asvadi[1], Leila Mostafavi[1], Nathan White[2], David S. Karow[2], Daniel Margolis[3], Anthony Sisk[4], Robert Reiter[5], and Steven Raman[1]

[1]Radiological Sciences, UCLA, Los Angeles, CA, United States, [2]Radiological Sciences, UCSD, La Jolla, CA, United States, [3]Radiology, Cornell University, New York, NY, United States, [4]Pathology, UCLA, Los Angeles, CA, United States, [5]Urology, UCLA, Los Angeles, CA, United States

Multiparametric MRI is becoming a crucial imaging for prostate cancers. A novel advanced, diffusion-based technique, restriction spectrum imaging (RSI) has been applied for prostate cancer imaging recently. In this work we will investigate the RSI performance in prostate cancer evaluation verified by post-surgery whole mount histopathology slides.

Electronic Poster

Female Pelvis, Fetal & Placenta

Exhibition Hall — Wednesday 13:45 - 14:45

4800 Computer 49

DECIDE: Diffusion-rElaxation Combined Imaging for Detailed Placental Evaluation

Andrew Melbourne[1], Rosalind Pratt[1,2], David Owen[1], Magdalena Sokolska[3], Alan Bainbridge[3], David Atkinson[4], Giles Kendall[2], Jan Deprest[5], Tom Vercauteren[1], Anna David[2], and Sebastien Ourselin[1]

[1]University College London, London, United Kingdom, [2]Institute for Women's Health, University College Hospital, London, United Kingdom, [3]Medical Physics, University College Hospital, London, United Kingdom, [4]Centre for Medical Imaging, University College Hospital, London, United Kingdom, [5]UZ Leuven

We propose a new multi-compartment model for the tissue signal in MRI and apply this to images of liver and placenta. Motivated by different flow characteristics in these organs, a three compartment model comprising fast and slowly circulating fluid pools and a tissue pool is fitted to overlapping multi-echo T2 relaxometry and an intra-voxel incoherent motion diffusion acquisition with low b-values. We compare and contrast parametric maps for regions of interest in liver and placenta.

4801 Computer 50

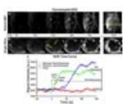

Perfusion MRI of the Placenta: Preliminary Results using ASL FAIR and Ferumoxytol DCE MRI in the Rhesus Macaque

Kai D. Ludwig[1], Sean B. Fain[1,2,3], Sydney Nguyen[4], Thaddeus G. Golos[4,5], Scott B. Reeder[1,2,3,6,7], Ian M. Bird[5], Oliver E. Wieben[1,2], Dinesh M. Shah[5], and Kevin M. Johnson[1]

[1]Medical Physics, University of Wisconsin - Madison, Madison, WI, United States, [2]Radiology, University of Wisconsin - Madison, Madison, WI, United States, [3]Biomedical Engineering, University of Wisconsin - Madison, Madison, WI, United States, [4]Comparative Biosciences, University of Wisconsin - Madison, Madison, WI, United States, [5]Obstetrics and Gynecology, University of Wisconsin - Madison, Madison, WI, United States, [6]Medicine, University of Wisconsin - Madison, Madison, WI, United States, [7]Emergency Medicine, University of Wisconsin - Madison, Madison, WI, United States

Non-contrast enhanced methods are needed to quantify placental perfusion to detect and monitor pathophysiological changes during pregnancy. We evaluate the potential of an endogenous perfusion labeling perfusion technique, Arterial Spin Labeled Flow-sensitive Alternating Inversion Recovery (ASL FAIR), and compare with ferumoxytol dynamic contrast enhanced (DCE) MRI. Three pregnant rhesus macaque were imaged with both FAIR and ferumoxytol DCE. Localized regions of ASL perfusion were observed that coincided with regions of early contrast enhancement seen in DCE. Ferumoxytol DCE measured perfusion with extended transit times across the placenta beyond those typically used for ASL labeling.

4802 Computer 51

Evaluation of Placenta Motion throughout Gestation

Thomas Martin[1,2], Dapeng Liu[2], Teresa Chanlaw[3], Sherin U. Devaskar[3], Carla Janzen[4], Tess Armstrong[1,2], Yutaka Natsuaki[5], Daniel Margolis[2], Rinat Masamed[2], Holden Wu[1,2], and Kyunghyun Sung[1,2]

[1]Biomedical Physics, University of California, Los Angeles, Los Angeles, CA, United States, [2]Radiological Sciences, University of California, Los Angeles, Los Angeles, CA, United States, [3]Department of Pediatrics, University of California, Los Angeles, Los Angeles, CA, United States, [4]Department of Obstetrics and Gynecology, University of California, Los Angeles, Los Angeles, CA, United States, [5]Siemens Healthcare, Los Angeles, CA, United States

Proper placental function is essential for normal fetal development. MRI can easily assess the growth and development of the placenta throughout gestation due to its capabilities in functional imaging. However, uterine contractions, and fetal and maternal motion can lead to inaccuracies in the quantitative assessments. In this we assessed the impact of extraneous motion on placental imaging by using a 3D multi-echo golden angle radial sequence to generated dynamic images of the placenta.

4803 Computer 52

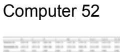

Differentiating metastatic from nonmetastatic lymph nodes by using monoexponential, biexponential, and stretched exponential diffusion-weighted imaging in cervical cancer patients

Qingxia Wu[1], Dandan Zheng[2], Ligang Shi[3], Mingbo Liu[4], Meiyun Wang[1], and Dapeng Shi[1]

[1]Radiological Department, Henan Provincial People’s Hospital (Zhengzhou University People’s Hospital), Zhengzhou, People's Republic of China, [2]MR Research China, GE Healthcare, Beijing, People's Republic of China, [3]Pathological Department, Henan Provincial People’s Hospital (Zhengzhou University People’s Hospital), Zhengzhou, People's Republic of China, [4]Radiotherapeutical Department, Henan Provincial People’s Hospital (Zhengzhou University People’s Hospital), Zhengzhou, People's Republic of China

The aim of our study was to judge whether diffusion parameters derived from different models of multi-b value DWI could be used to discriminate metastatic from nonmetastatic pelvic lymph node (LN) status in patients with cervical cancer. A statistical significant difference in the mean D, f and α values between metastatic and nonmetastatic LNs, with metastatic LNs presenting with higher D values, lower f values and higher α values than nonmetastatic ones. This study revealed that metastatic LNs had their respective diffusion parameters compared with nonmetastatic LNs.

4804 Computer 53

Comparison of 18F-FDG PET/MRI and MRI alone for pretherapeutic tumor staging of patients with primary cancer of the uterine cervix.

Johannes Grueneisen[1], Lino Morris Sawicki, Axel Wetter, Julian Kirchner, Michael Forsting, Verena Ruhlmann, and Lale Umutlu

[1]Diagnostic and Interventional Radiology, University Hospital Essen, Essen, Germany

This study demonstrates a successful attempt to utilize and evaluate the diagnostic potential of integrated PET/MRI for staging patients with primary cervical cancer. According to the results, 18F-FDG PET data do not seem to provide useful additional information to MRI for the determination of the local extent of the primary tumors. However, the present results show a better performance of simultaneously acquired 18F-FDG PET and MR datasets for the detection of nodal and distant metastases if compared to MRI alone. Therefore, integrated PET/MR imaging may provide valuable information for treatment planning and to predict prognosis.

4805 Computer 54

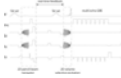

Full 3D high-resolution BOLD imaging of the human placenta with prospective navigation and 2D spatially selective excitation

Glen R. Morrell[1], Matthias C. Schabel[2], Robert M. Silver[3], Christopher D. Kroenke[2], and Antonio E. Frias[2]

[1]Radiology and Imaging Sciences, University of Utah, Cottonwood Heights, UT, United States, [2]Oregon Health & Science University, [3]Department of Obstetrics and Gynecology, University of Utah

Full 3D high-resolution human placenta BOLD imaging at 3T was performed with a free-breathing prospectively navigated sequence using 2D spatially selective excitation. Advantages of this sequence over conventional multi-slice breath hold BOLD include increased SNR, no breath hold recovery periods leading to better time efficiency, and elimination of artifacts from respiratory and fetal motion. T2* maps clearly show the cotyledon architecture of the human placenta.

4806 Computer 55

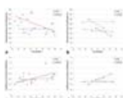

Non-invasive placental perfusion imaging in pregnancies complicated by fetal heart disease using velocity-selective arterial spin labeling

Zungho Zun[1,2,3], Greg Zaharchuk[4], Nickie Niforatos-Andescavage[1,2], Samantha Bauer[1], Mary T Donofrio[2,3,5], and Catherine Limperopoulos[1,2,3]

[1]Division of Diagnostic Imaging and Radiology, Children's National Medical Center, Washington, DC, United States, [2]Division of Fetal and Transitional Medicine, Children's National Medical Center, Washington, DC, United States, [3]Departments of Radiology and Pediatrics, George Washington University, Washington, DC, United States, [4]Department of Radiology, Stanford University, Stanford, CA, United States, [5]Division of Cardiology, Children's National Medical Center, Washington, DC, United States

Recent data have reported that placental dysfunction may be present in the setting of complex fetal congenital heart disease (CHD). We performed placental perfusion imaging using velocity-selective arterial spin labeling in pregnancies complicated by fetal CHD and healthy pregnancies. We demonstrated that global placental perfusion and regional variation of perfusion were significantly correlated with GA in pregnancies complicated by fetal CHD, but not in healthy controls. Our findings suggest that placental ASL may have the potential to serve as an early biomarker of placental dysfunction in fetal CHD.

4807 Computer 56

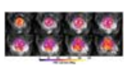

Measuring human placental blood flow with multi-delay 3D GRASE pseudo-continuous arterial spin labeling at 3 Tesla

Xingfeng Shao[1], Dapeng Liu[2], Thomas Martin[2], Teresa Chanlaw[3], Sherin U. Devaskar[3], Carla Janzen[4], Daniel Margolis[2], Kyunghyun Sung[2], and Danny JJ Wang[1]

[1]Laboratory of FMRI Technology (LOFT), Mark & Mary Stevens Neuroimaging and Informatics Institute, Keck School of Medicine, University of Southern California, Los Angeles, CA, United States, [2]Department of Radiology, David Geffen School of Medicine at UCLA, Los Angeles, CA, United States, [3]Department of Pediatrics, David Geffen School of Medicine at UCLA, Los Angeles, CA, United States, [4]Department of Obstetrics and Gynecology, Division of Perinatology, David Geffen School of Medicine at UCLA, Los Angeles, CA, United States

We presented a multi-delay pCASL combined with inner-volume GRASE imaging technique to measure placental blood flow (PBF) and arterial transit time (ATT) simultaneously, and report PBF and ATT evolution along different gestational ages during the second trimester. More blood flew through placenta with a slightly shorter transit time was seen with fetal development. Overall, PBF and ATT for the second trimester were 129.8±44.7 ml/min/100g and 786.8±174.1 ms respectively.

4808 Computer 57

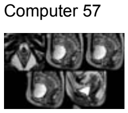

Pelvic Floor Structural Alterations of Primipara with Stress Urinary Incontinence After Vaginal Delivery：A MRI Study

yujiao zhao[1], zhizheng zhuo[2], and wen shen[1]

[1]Department of Radiology, Tianjin First Center Hospital, Tianjin, People's Republic of China, [2]Philips Healthcare, Beijing, China, beijing, People's Republic of China

Vaginal childbirth women have an increasing incidence of stress urinary incontinence(SUI). There are few studies on pathogenesis of SUI and the relationship between the SUI and pelvic floor structure changes. In this study, static and dynamic MRI imaging are performed to describe and assess pelvic floor structure changes in patients with stress urinary incontinence. The results showed that pelvic floor structures changed significantly in the primipara suffering from SUI after vaginal delivery, which suggest a series of pathological state.

4809 Computer 58

Characterization of the placental vascular tree using MRI: an ex-vivo study

Daphna Link[1,2], Ariel Many[3], Liat Ben Sira[4], Shaul Harel[1,5], and Dafna Ben Bashat[1,2,6]

[1]Sackler Faculty of Medicine, Tel Aviv University, Tel Aviv, Israel, [2]Functional Brain Center, The Wohl Institute for Advanced Imaging, Tel Aviv Sourasky Medical Center, Tel Aviv, Israel, [3]Department of Obstetrics and Gynecology, Lis Maternity Hospital, Tel Aviv Sourasky Medical Center, Tel Aviv, Israel, [4]Division of Pediatric Radiology, Tel Aviv Sourasky Medical Center, Tel Aviv, Israel, [5]Pediatric Neurology, Tel Aviv Sourasky Medical Center, Tel Aviv, Israel, [6]Sagol School of Neuroscience, Tel Aviv University, Tel Aviv, Israel

Placental vascular dysfunction is a major cause of pregnancy complications, such as intrauterine growth restriction (IUGR). However, current knowledge on human placental vascular architecture is limited. In this study, for the first time, we characterized the structure of the placental vascular system ex-vivo, using MRI. Fifteen normal placentas and one with IUGR were studied using a novel method, and the vascular structure was analyzed with an automatic algorithm. Results provided information regarding: cord insertion location; branching pattern; branching generation; and daughter to mother diameters of normal placentas. Preliminary results from one IUGR placenta suggest significant differences from normal placentas.

4810 Computer 59

Safety of 3T MRI Scan for pregnant women: Effect of Maternal Size, Maternal Position and Twin Pregnancy

Esra Abaci Turk[1], Filiz Yetisir[2], Borjan Gagoski[1], Bastien Guerin[3,4], Natalie Copeland[1], Lawrence Wald[3,4,5], Elfar Adalsteinsson[2,5], and P. Ellen Grant[1]

[1]Fetal-Neonatal Neuroimaging & Developmental Science Center, Boston Children's Hospital, Boston, MA, United States, [2]Department of Electrical Engineering and Computer Science, Massachusetts Institute of Technology, Cambridge, MA, United States, [3]Harvard Medical School, Boston, MA, United States, [4]A. A. Martinos Center for Biomedical Imaging, Department of Radiology, Massachusetts General Hospital, Charlestown, MA, United States, [5]Harvard-MIT Health Sciences and Technology, Massachusetts Institute of Technology, Cambridge, MA, United States

Possible temperature increase due to RF exposure during MRI scan of pregnant women can be critical for the fetus. In this study, we perform electromagnetic and temperature simulations using different pregnant women models with different postures. We assess the variability of in-utero RF induced heating in a 3T birdcage coil for different models generated by segmenting structural MR images.

4811 Computer 60

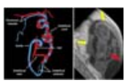

4D Flow MRI in the Rhesus Macaque Fetus

Jacob Macdonald[1], Philip Corrado[1], Sydney Nguyen[2], Kevin M Johnson[1,3], Christopher J Francois[3], Ian Bird[2], Dinesh Shah[4], Thaddeus G Golos[2,4,5], and Oliver Wieben[1,3]

[1]Medical Physics, University of Wisconsin - Madison, Madison, WI, United States, [2]Comparative Biosciences, University of Wisconsin - Madison, Madison, WI, United States, [3]Radiology, University of Wisconsin - Madison, Madison, WI, United States, [4]Obstetrics and Gynecology, University of Wisconsin - Madison, Madison, WI, United States, [5]Wisconsin National Primate Research Center, University of Wisconsin - Madison, Madison, WI, United States

4D flow measurements were performed with PC-VIPR in rhesus macaque monkeys undergoing healthy pregnancies to determine the feasibility of flow measurements in the fetal vasculature and umbilical cord. Flow measures appeared to be viable for the larger fetal vessels (aorta and IVC), but more variable in smaller vessels with slower flow (umbilical vessels). Image quality improved for later gestational ages as a result of increased vessel area.

4812 Computer 61

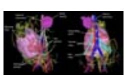

Ferumoxytol MRA in the Pregnant Rhesus Macaque

Jacob Macdonald[1], Philip Corrado[1], Sydney Nguyen[2], Christopher J Francois[3], Scott Reeder[1,3,4,5,6], Ian Bird[2], Dinesh Shah[7], Thaddeus G Golos[2,7,8], Oliver Wieben[1,3], and Kevin M Johnson[1,3]

[1]Medical Physics, University of Wisconsin - Madison, Madison, WI, United States, [2]Comparative Biosciences, University of Wisconsin - Madison, Madison, WI, United States, [3]Radiology, University of Wisconsin - Madison, Madison, WI, United States, [4]Biomedical Engineering, University of Wisconsin - Madison, Madison, WI, United States, [5]Medicine, University of Wisconsin - Madison, Madison, WI, United States, [6]Emergency Medicine, University of Wisconsin - Madison, Madison, WI, United States, [7]Obstetrics and Gynecology, University of Wisconsin - Madison, Madison, WI, United States, [8]Wisconsin National Primate Research Center, University of Wisconsin - Madison, Madison, WI, United States

Both maternal and fetal complications arise from poor vascular adaptation to pregnancy. Assessing utero-placental vessels with contrast-enhanced MR Angiography may be valuable, but Gadolinium based contrast agents commonly used for MR angiography are contraindicated during pregnancy. In this work, we tested the feasibility of ultrashort echo time contrast-enhanced angiography with Ferumoxytol in a small cohort of pregnant rhesus macaques. Ferumoxytol allowed for detailed visualization of utero-placental vessels without detectable uptake in fetal tissues.

4813 Computer 62

Myometrial invasion in endometrial cancer: Comparison of reduced field-of-view diffusion-weighted imaging and dynamic contrast-enhanced magnetic resonance imaging

Mayumi Takeuchi[1], Kenji Matsuzaki[2], and Masafumi Harada[1]

[1]Department of Radiology, Tokushima University, Tokushima, Japan, [2]Department of Radiological Technology, Tokushima Bunri University, Sanuki-city, Japan

The depth of myometrial invasion was evaluated in 25 patients with surgically proven endometrial cancer by T2WI, reduced field-of-view DWI (rFOV-DWI) and 3D dynamic contrast-enhanced MRI (DCE-MRI). The depth of myometrial invasion (stage S: <50% vs stage D: ≥50%) on MRI was correlated with surgical pathology results. The staging accuracy was 68% for T2WI, 92% for DCE-MRI, and 96% for rFOV-DWI. Combination of rFOV-DWI reading together with T2WI improved the assessment of myometrial invasion with a diagnostic accuracy of up to 100%. Especially, rFOV-DWI has an advantage in assessing the depth of myometrial invasion in cases with coexisting adenomyosis.

4814 Computer 63

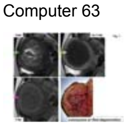

Red degeneration of uterine leiomyoma: Clinical utility of susceptibility-weighted MR imaging

Mayumi Takeuchi[1], Kenji Matsuzaki[2], and Masafumi Harada[1]

[1]Department of Radiology, Tokushima University, Tokushima, Japan, [2]Department of Radiological Technology, Tokushima Bunri University, Sanuki-city, Japan

Red degeneration of uterine leiomyoma (RDL) is hemorrhagic infarction caused by peripheral venous thrombosis. Peripheral high intensity rim on T1WI due to methemoglobin of blood products confined to thrombosed vessels is characteristic, however, it may not be observed at acute phase. We evaluated MR images including SWI of 17 RDL and 12 usual leiomyomas (UL). High intensity rim on T1WI, low intensity rim on T2WI and on SWI were observed in 47%, 47%, and 100% of RDL, whereas 0%, 8%, and 0% of UL, respectively. SWI may be helpful for the diagnosis of RDL in distinguishing from UL or sarcomas.

4815 Computer 64

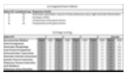

Preliminary Experience Using Motion-Robust Dynamic MRI to Visualize Fetal Congenital Heart Disease: Comparison to Static MRI

Christopher W. Roy[1,2], Mike Seed[3,4], and Christopher K. Macgowan[1,2]

[1]Medical Biophysics, University of Toronto, Toronto, ON, Canada, [2]Physiology and Experimental Medicine, Hospital for Sick Children, Toronto, ON, Canada, [3]Pediatric Cardiology, Hospital for Sick Children, ON, Canada, [4]Pediatric and Diagnostic Imaging, University of Toronto, Toronto, ON, Canada

Recent advances in cardiac MRI have enabled powerful new methods for assessing the fetal heart in utero. Using a novel reconstruction framework, combining methods for motion correction, retrospective gating, and accelerated imaging, motion-robust CINE images are reconstructed and compared to conventional static MRI of the fetal heart. Preliminary evaluation of fetal congenital heart disease with this technique is demonstrated in multi-slice axial acquisitions of four subjects.

4816 Computer 65

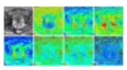

MR non-Gaussian diffusion model of female cervix: a diffusion kurtosis imaging study

Wenhui Guo[1], Kuang Fu[1], and Lizhi Xie[2]

[1]Department of MR, The Second Affiliated Hospital of Harbin Medical University, Harbin, People's Republic of China, [2]GE Healthcare, MR Research China, BeiJing, People's Republic of China

To assess the fitted parameters of DKI in female cervix and to investigate their potential in distinguishing tumors from diverse healthy tissues. The presence of rich collagen and fibers in healthy cervix helps to differentiate itself from the heterogeneious and cell-rich malignancies. It is concluded that DKI can be performed as a feasible technique to depict the real phenomenon of non-Gaussian water diffusion behavior in female cervix.

4817 Computer 66

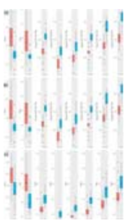

Histogram analysis of intravoxel incoherent motion parameters in assessing tumour diffusion and perfusion heterogeneity in cervical cancer before and after chemoradiotherapy

Jose Angelo Udal Perucho[1], Elaine Yuen Phin Lee[1], Wing Chi Lawrence Chan[2], Nanjie Gong[3], and Queenie Chan[4]

[1]Department of Diagnostic Radiology, The University of Hong Kong, Hong Kong, Hong Kong, [2]Department of Health Technology and Informatics, The Hong Kong Polytechnic University, Hong Kong, [3]University of California, Berkeley, CA, United States, [4]Philips Healthcare, Hong Kong, Hong Kong

Histogram analysis of intravoxel incoherent motion (IVIM) diffusion-weighted MRI (DWI) could be a promising quantitative approach in assessing tumour heterogeneity. We retrospectively studied twenty-five patients with cervical cancer who had paired IVIM MRI examinations before and at week-4 of chemoradiotherapy treatment (CRT). We observed histogram skewness and kurtosis significantly decreased while mean and all percentiles significantly increased in apparent diffusion coefficient (ADC), true diffusion coefficient (D) and perfusion fraction (f) following treatment. Furthermore, these significant differences were not correlated with a change in primary tumour volume (PTV) following treatment.

4818 Computer 67

Radial segmented echo-planar readout for fast fetal angiography – feasibility test

Brijesh Kumar Yadav[1,2], Uday Krishnamurthy[1,2], Pavan Kumar Jella[2], Edgar Hernandez-Andrade[3,4], Swati Mody[2], Feifei Qu[2], Anabela Trifan[2], Sonia S Hassan[3,4], Roberto Romero[4], Ewart Mark Haacke[1,2], and Jaladhar Neelavalli[2]

[1]Department of Biomedical Engineering, Wayne State University, Detroit, MI, United States, [2]Department of Radiology, Wayne State University, Detroit, MI, United States, [3]Department of Obstetrics and Gynecology, Wayne State University, Detroit, MI, United States, [4]Perinatology Research Branch, NICHD/NIH/DHHS, Bethesda, MD, United States

A simulation study showing the potential benefit of a radial-trajectory based data acquisition technique named as "radial segmented echo-planar readout (radialSEPI)" for faster fetal angiography is presented. The results indicate that at echo train length of 2 and echo-spacing of 6.1 ms can provide good quality fetal/adult MRA reconstructions providing a potential factor 2 improvement in time.

4819 Computer 68

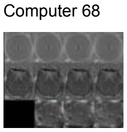

Radial-SWI in Human Fetal Imaging

Brijesh Kumar Yadav[1,2], Uday Krishnamurthy[1,2], Pavan Kumar Jella[2], Edgar Hernandez-Andrade[3,4], Swati Mody[2], Feifei Qu[2], Anabela Trifan[2], Sonia S Hassan[3,4], Roberto Romero[4], Ewart Mark Haacke[1,2], and Jaladhar Neelavalli[2]

[1]Department of Biomedical Engineering, Wayne State University, Detroit, MI, United States, [2]Department of Radiology, Wayne State University, Detroit, MI, United States, [3]Department of Obstetrics and Gynecology, Wayne State University, Detroit, MI, United States, [4]Perinatology Research Branch, NICHD/NIH/DHHS, Bethesda, MD, United States

Radial-SWI in human fetal imaging is presented which includes: (a) determining the minimum number of radial projections necessary for fast measurement of intravascular phase in the blood vessels in human adult and fetus, without loss of accuracy; and (b) exploring the feasibility of fetal venography using radial-SWI. Results of this study illustrate that (a) in both fetal and adult imaging, accurate quantification of intravascular phase from the superior-sagittal-sinus is possible from radial SWI with just 161 projections, and (b) venograms in fetal brain were presented using radial-SWI.

4820 Computer 69

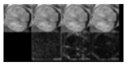

Accelerated HASTE-Based Fetal MRI with Low-Rank Modeling

Bo Zhao[1,2], Borjan Gagoski[2,3], Elfar Adalsteinsson [4], P. Ellen Grant[2,3], and Lawrence L. Wald[1,2]

[1]Martinos Center for Biomedical Imaging, Chalestown, MA, United States, [2]Department of Radiology, Harvard Medical School, Boston, MA, United States, [3]Boston Children's Hospital, Boston, MA, United States, [4]Department of Electrical Engineering and Computer Science, Massachusetts Institute of Technology, Cambridge, MA, United States

HAlf-fourier Single-shot Turbo spin Echo (HASTE) sequence is one of the most common acquisitions in fetal MRI due to its T2 contrast and relative robustness to fetal motion. In this work, we present a low-rank model-based imaging method to accelerate HASTE acquisitions. The proposed method is fully compatible with the k-space sampling strategy implemented by vendor-provided pulse sequences, and provides improved image quality and/or noise robustness compared to the conventional half-Fourier and GRAPPA reconstruction, and compressive sensing reconstruction.

4821 Computer 70

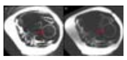

Pseudo-fat in the fetal liver with two-point Dixon water-fat separation

Stephanie A Giza[1], Barbra de Vrijer[2,3], and Charles A McKenzie[1,3]

[1]Medical Biophysics, The University of Western Ontario, London, ON, Canada, [2]Obstetrics and Gynaecology, The University of Western Ontario, London, ON, Canada, [3]Division of Maternal, Fetal and Newborn Health, Children's Health Research Institute, London, ON, Canada

2-point Dixon water-fat imaging is a widely available sequence that can be used to generate fat images. Increased fat was seen in the livers of a 35+4 week anencephalic fetus and a 37 week normal fetus on 2-point Dixon images, but not with IDEAL water-fat imaging. When applied to the fetus late in gestation, caution should be taken as a shortened fetal liver T2* may appear as false liver fat. IDEAL water-fat imaging corrects for changes in T2* and is a more appropriate sequence for fetal water-fat separated imaging in the third trimester.

4822 Computer 71

Application of Texture Analysis to Apparent Diffusion Coefficient Images of the Normal Human Placenta

Quyen N. Do[1], Matthew A. Lewis[1], Ananth J. Madhuranthakam[1,2], Yin Xi[1,3], April Bailey[1,4], and Diane Twickler[1,4]

[1]Radiology, University of Texas Southwestern Medical Center, Dallas, TX, United States, [2]Advanced Imaging Research Center, University of Texas Southwestern Medical Center, Dallas, TX, United States, [3]Department of Clinical Science, University of Texas Southwestern Medical Center, Dallas, TX, United States, [4]Obstetrics & Gynecology, University of Texas Southwestern Medical Center, Dallas, TX, United States

The human placenta is a complex structure with unique capabilities. It has a 40-week average life span, during which it facilitates the exchange between the maternal and fetal cardiovascular systems. There is little known about the development and maturation of the placenta throughout the gestational period during normal pregnancy. It is however recognized that the placenta appears more heterogeneous on various imaging modalities as the pregnancy progresses. In this work, we propose to characterize the placenta heterogeneity as a function of gestational age through the application of grey-scale texture analysis to ADC maps using a large retrospective MRI database.

4823 Computer 72

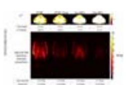

Potential of parallel transmission for fetal imaging in reducing SAR and mitigating flip angle inhomogeneities: a simulation study at 3T

Filiz Yetisir[1], Esra Abaci Turk[2], Bastien Guerin[3,4], Ellen Patricia Grant[2], Lawrence L. Wald[3,4,5], and Elfar Adalsteinsson[1,5,6]

[1]Electrical Engineering and Computer Science, Massachusetts Institute of Technology, Cambridge, MA, United States, [2]Fetal-Neonatal Neuroimaging & Developmental Science Center, Boston Children's Hospital, Harvard Medical School, Boston, MA, United States, [3]Athinoula A. Martinos Center for Biomedical Imaging, Massachusetts General Hospital, Charlestown, MA, United States, [4]Department of Radiology, Harvard Medical School, Boston, MA, United States, [5]Harvard-MIT Division of Health Sciences and Technology, Massachusetts Institute of Technology, Cambridge, MA, United States, [6]Institute for Medical Engineering and Science, Massachusetts Institute of Technology, Cambridge, MA, United States

In this work we evaluate the potential benefits of parallel transmission for fetal imaging in reducing local SAR and mitigating flip angle inhomogeneities. Our results show that compared to single channel transmission, using 2 channel parallel transmission with a 2 port birdcage coil, local SAR can be reduced by a factor of up to 5 and flip angle inhomogeneity can be mitigated by up to 66% for realistically long RF pulses.

Electronic Poster

Body: Emerging Techniques

Exhibition Hall — Wednesday 13:45 - 14:45

4824 Computer 73

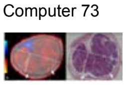

Comparing the invasive depth of esophageal carcinoma in 3.0 T ex vivo T2-mapping MR imaging with histopathological findings

Dandan Zheng[1], Yi Wei[2], and Shaocheng Zhu[2]

[1]MR Research China, GE Healthcare, Beijing, People's Republic of China, [2]Radiology, Zhengzhou University People's Hospital, Zhengzhou, People's Republic of China

Esophageal carcinoma is the eighth most common cancer worldwide with a rising incidence. It has been demonstrated that the normal esophageal wall can be depicted as eight layers in T2 weighted MRI , however only qualitative assessment has been made so far. In this work, an ex vivo experiment was conducted on 3.0T clinical scanner to prospectively establish the quantitative T2 value as a means of depicting the normal esophageal wall by T2-mapping and evaluate the depth of the carcinoma invasion using histopathological as a reference.

4825 Computer 74

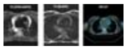

Whole body functional and anatomical MRI: Accuracy in staging of Childhood and Adolescent Hodgkin's Lymphoma compared to conventional multimodality imaging

Arash Latifoltojar[1], Shonit Punwani[1], Paul Humphries[1], Leon Menezes[2], Deena Neriman[2], Stephen Daw[2], Ananth Shankar[2], Bilyana Popova[1], Paul Smith[1], Ka Man Condne[1], Andre Lopes[1], and Stuart Taylor[1]

[1]University College London, London, United Kingdom, [2]University College London Hospital, London, United Kingdom

Current gold standard imaging for assessment of paediatric Hodgkin's lymphoma is PET-CT. Anatomical and functional whole-body MRI (WB-MRI) provides an alternative/adjunct radiation free imaging technique.

The aim of this prospective single centre study is to investigate the diagnostic accuracy of WB-MRI against reference standard imaging for staging of paediatric Hodgkin's lymphoma.

4826 Computer 75

A Novel Retrospective Sorting Strategy Utilizing both Respiratory Profile and Internal Surrogate Position for Generating Free-Breathing Abdominal 4D-MRI

Yihang Zhou[1], Oi Lei Wong[1], Jing Yuan[1], George Chiu[2], Kin Yin Cheung[1], and Siu Ki Yu[1]

[1]Medical Physics and Research Department, Hong Kong Sanatorium & Hospital, Happy Valley, Hong Kong, [2]Department of Radiotherapy, Hong Kong Sanatorium & Hospital, Happy Valley, Hong Kong

Four-dimensional (4D) image are widely used to capture the respiration-induced motion of the abdominal organs in free-breathing radiotherapy. However, due to the breathing variability, appropriate assignment of images to each phase is critical in revealing the motion of anatomy structures. In this study, we proposed a novel approach to develop high-quality retrospective 4D-MRI. Instead of sorting images only based on their respiratory phases, the proposed strategy sorted the images using both the respiratory phases and the internal surrogate positions. The proposed strategy was tested using in-vivo human abdominal images.

4827 Computer 76

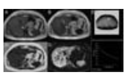

Complex Chemical Shift-Encoded MRI to Estimate Fat in Livers with Elevated Iron Content

Sarah Eskreis-Winkler[1,2], Simone Krebs[1], Alessandra Borgheresi[1], Davinia Ryan[1], Scott Reeder[3], and Lorenzo Mannelli[1]

[1]Memorial Sloan Kettering Cancer Center, New York, NY, United States, [2]New York Presbyterian Hospital/Weill Cornell Medicine, New York, NY, United States, [3]University of Wisconsin

In patients with elevated liver iron, in-and-out-of-phase and IDEAL-IQ methods yield very different proton density fat fractions. In these patients, IDEAL-IQ could potentially serve as a more sensitive marker of hepatic steatosis than in-and-out-of-phase imaging, although larger studies are needed to confirm these findings. Irrespective of liver fat and liver iron content, conventional and IDEAL-IQ R2* values are highly correlated.

4828 Computer 77

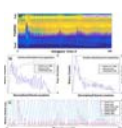

Amplitude-probability sorting for single-pass, retrospective 4D-MRI using 2D bSSFP MRI with interleaved cylindrical navigators

Erik Tryggestad[1], Ersin Bayram[2], Yanle Hu[3], Daniel Litwiller[4], Dan Rettmann[2], Matthew Walb[1], Darin White[5], and Kiaran McGee[5]

[1]Radiation Oncology, Mayo Clinic, Rochester, MN, United States, [2]GE Healthcare, Waukesha, WI, United States, [3]Radiation Oncology, Mayo Clinic, Phoenix, AZ, United States, [4]GE Healthcare, New York, NY, United States, [5]Radiology, Mayo Clinic, Rochester, MN, United States

With MRI being increasingly incorporated in the radiotherapy workflow, the multidisciplinary community has a strong interest in developing "4D-MRI" techniques for both offline (tumor motion characterization for treatment planning) and online (tumor motion tracking) applications. In a cohort of 10 volunteers, the present study applied 2D (coronal) bSSFP with interleaved cylindrical navigators monitoring the liver dome to retrospectively derive 4D-MRI comparing two sorting methods, namely phase and amplitude-probability. Amplitude-probability binning was shown, both qualitatively and quantitatively, to reduce "volume inconsistencies" caused by variable breathing.

4829 Computer 78

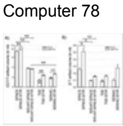

3D MSVAT-SPACE-STIR or 2D SEMAC-STIR for high resolution dental MRI?

Tim Hilgenfeld[1], Marcel Prager[2], Alexander Heil[2], Daniel Gareis[3], Mathias Nittka[4], David Grodzki[4], Martin Bendszus[2], and Sabine Heiland[2]

[1]Heidelberg University, Heidelberg, Germany, [2]Heidelberg University, [3]NORAS MRI products GmbH, [4]Siemens Healthcare GmbH

Dental MRI is a new and promising diagnostic tool. Unfortunately, in presence of implants image quality is impaired by failure of fat suppression and susceptibility artifacts. Here, we for the first time systematically evaluated fat saturated MR sequences for artifact reduction for dental MRI. Smallest artifact volume was noted for SEMAC-STIR and TSE-STIR sequences. But, higher and isotropic resolution was only achieved with MSVAT-SPACE-STIR sequence. No artifact reduction was measured for SEMAC-STIR compared to standard TSE-STIR. In contrast, MSVAT-SPACE-STIR reduced artifacts up to 70% compared to standard SPACE-STIR. Since imaging of dental structures benefit from isotropic high resolution MSVAT-SPACE-STIR is advantageous.

4830 Computer 79

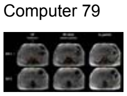

SAR-Constrained kT-Points Pulse Design Applied to B1 Inhomogeneity Mitigation in the Human Abdomen at 3T

Raphaël Tomi-Tricot[1], Vincent Gras[1], Franck Mauconduit[2], Nicolas Boulant[1], Pierre Zerbib[3], Alain Rahmouni[3], Alexandre Vignaud[1], Alain Luciani[3], and Alexis Amadon[1]

[1]CEA-DRF-I2BM-NeuroSpin-UNIRS, Gif-sur-Yvette, France, [2]Siemens Healthineers France, Saint-Denis, France, [3]Department of Radiology, AP-HP, CHU Henri Mondor, Créteil, France

High field MRI systems offer better performance in terms of signal-to-noise ratio but are burdened with dielectric resonance artefacts inducing zones of weak excitation with major consequences on Signal and Contrast to Noise Ratios. In this work, the interest of subject-tailored k_T-points pulse design with joint SAR control over current patient-specific RF-shimming technique is investigated, in the context of human liver imaging at 3T. T1w acquisitions are performed in-vivo to compare quadrature, tailored RF-shimming, and k_T-points pulses. The interest of k_T-points is clearly demonstrated in terms of signal, contrast and diagnostic power.

4831 Computer 80

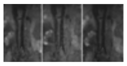

Compressed Sensing Black Blood SPACE for Abdominal Aortic Aneurysmal Vessel Wall Imaging

Sinyeob Ahn[1], Chengcheng Zhu[2], Esther Raithel[3], Christoph Forman[3], Gerhard Laub[1], and David Saloner[4]

[1]Siemens Healthcare, San Francisco, CA, United States, [2]Radiology and Biomedical Imaging, UCSF, San Francisco, CA, United States, [3]Siemens Healthcare, Erlangen, Germany, [4]UCSF, San Francisco, CA, United States

Abdominal aortic vessel wall imaging has been interested and used for studying pathological vasculature. In this study, compressed sensing (CS) 3D SPACE DANTE technique is proposed for imaging abdominal aortic aneurysm (AAA) vessel wall to accelerate imaging acquisition. Its scan/reconstruction parameters were optimized on normal volunteers then, used for patient scan. DANTE provided sufficiently dark blood signal at a large vessel like the aorta, which is essential to delineate the vessel wall. CS SPACE DANTE provided comparable image quality and vessel wall-lumen signal contrast as compared to non-accelerated SPACE DANTE technique.

4832 Computer 81

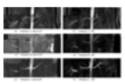

Quantitative comparison of time-SLIP and Triple Inversion Recovery (TIR) non-contrast enhanced MRI for renal angiography

Suzanne Franklin[1], Torben Schneider[2], Marcelo E Andia[3], Markus Henningsson[4], and Rene M Botnar[4]

[1]Eindhoven University of Technology, Eindhoven, Netherlands, [2]Philips Healthcare, Guildford, United Kingdom, [3]Pontificia Universidad Católica de Chile, Escuela de Ingeniería, Santiago, Chile, [4]King's College London, Division of Imaging Sciences, and Biomedical Engineering, St. Thomas' Hospital, London, United Kingdom

Renal artery stenosis (RAS) has been associated with hypertension, chronic kidney disease and an increased risk of vascular events. This study quantitatively compares two non-contrast enhanced magnetic resonance angiography (NC-MRA) techniques for renal angiography, based on SNR, CNR, vessel sharpness and number of renal branches. TIR has shown promising results in suppressing background signal and provided overall better image quality than outflow time-SLIP. TIR has the advantage over time-SLIP that tissues can be nulled over a wide range of T1 -values. To further shorten scan time the TIR technique could be combined with more advanced image based motion correction techniques.

4833 Computer 82

Comparison of diffusion imaging microstructure models of the human placenta at 3T

Paddy J. Slator[1], Jana Hutter[2,3], Laura McCabe[2], Ana Dos Santos Gomes[2], Anthony N. Price[2,3], Mary A. Rutherford[2], Joseph V. Hajnal[2,3], and Daniel C. Alexander[1]

[1]Centre for Medical Image Computing, Department of Computer Science, University College London, London, United Kingdom, [2]Centre for the Developing Brain, King's College London, London, United Kingdom, [3]Biomedical Engineering Department, Division of Imaging Sciences, King's College London, London, United Kingdom

Developmental abnormalities in placental vascular formation are associated with major complications of pregnancy, such as fetal growth restriction and early onset pre-eclampsia. Multi-shell diffusion MRI at 3T has been shown to be capable of capturing fine microstructural information in a wide variety of organs and disease states, and could prove valuable for studying the human placenta in-vivo. We develop a rich scanning protocol, and use the data to investigate the complexity of models supported by the placental diffusion MRI signal. We demonstrate the feasibility of using this non-invasive approach to quantify microstructure in the human placenta and surrounding tissue.

4834 Computer 83

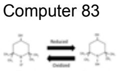

Quantitative Assessment of Markers of Oxidative Stress in Mice Model of Renal Artery Stenosis

Behzad Ebrahimi[1,2], Alvin Ihsani[2], Arkadiusz Sitek[2], Slobodan I Macura[3], and Lilach O Lerman[1]

[1]Nephrology, Mayo Clinic, Rochester, MN, United States, [2]Radiology, Harvard/MGH, Boston, MA, United States, [3]Biochemistry and Molecular Biology, Mayo Clinic

Inability of cells to detoxify reactive oxidative species (ROS) is responsible for numerous degenerative pathological conditions. Currently there is no clinical method to assess reduction-oxidation (redox) state in vivo. In this study, using a cyclic nitroxide T_1 MR probe with unique characteristics, we propose a two-tissue compartment model which provides quantitative information of markers of oxidative stress. Results demonstrated the feasibility of redox status assessment in vitro and in vivo in the stenotic mouse kidney. In the stenotic kidney, our method indicated increased renal ROS production, accompanied by preserved ability to detoxify ROS compared to the contralateral kidney.

4835 Computer 84

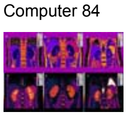

Quantitative BOLD MRI and T1 Mapping in Acute Kidney Injury Patients: A preliminary study

Yingjie Mei[1,2], Xiang Xiao[3], Zihan Lei[4], Jie Feng[3], Yuankui Wu[3], Ruiying Chen[3], Qiangqiang Gang[3], Min Liang[4], Yikai Xu[3], and Yanqiu Feng[1]

[1]School of Biomedical Engineering, Guangdong Provincial Key Laboratory of Medical Image Processing, Southern Medical University, Guangzhou, People's Republic of China, [2]Philips Healthcare, Guangzhou, People's Republic of China, [3]Medical Imaging Center, Nanfang Hospital of Southern Medical University, Guangzhou, People's Republic of China, [4]Division of Nephrology, Nanfang Hospital, Southern Medical University, Guangzhou, People's Republic of China

Hypoperfusion and hypoxia are thought to be important factors in the pathogenesis of AKI and in the progression from AKI to chronic kidney disease. Previous studies have demonstrated the correlation between MR relaxation time (T1 and T2*) and tissue oxygenation. The result of this preliminary study suggests BOLD and T1 mapping are potential to diagnose AKI at early stage and predict the progression of AKI non-invasively.

4836 Computer 85

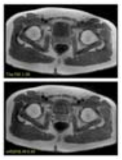

Fast, Motion-Robust T1-weighted Body Imaging with Single-Shot Fast Spin Echo via Centric Partial Fourier Encoding and Variable Refocusing Flip Angle

Daniel V Litwiller[1], Valentina Taviani[2], Lloyd Estkowski[2], and Ersin Bayram[3]

[1]Global MR Applications & Workflow, GE Healthcare, New York, NY, United States, [2]Global MR Applications & Workflow, GE Healthcare, Menlo Park, CA, United States, [3]Global MR Applications & Workflow, GE Healthcare, Houston, TX, United States

Here we present a single-shot fast spin echo sequence optimized for fast, motion-robust T1-weighted body imaging through the use of inversion recovery preparation, and the introduction of variable refocusing flip angle configured for centric, partial Fourier encoding.

4837 Computer 86

Automated scan prescription for an oblique plane through the aortic arch for bolus tracking in DCE-MRI

Takao Goto[1], Miki Araki[1], and Kenji Asano[1]

[1]MR Engineering, GE Healthcare, Hino-shi, Japan

Accurate placement of a 2D plane across the aorta arch while examining scout images is a complex task that makes the operator’s workflow difficult when bolus tracking in DCE-MRI. We present a novel method for automated scan prescription for an oblique plane delineating the entire aortic arch used to monitor bolus arrival. The oblique plane was prescribed automatically by selecting the optimal oblique angle using regression forests. A dataset with 31 volunteers was tested, and all cases depicted the cross section of the aortic arch clearly. This automation will assist the operator and decrease the total examination time.

4838 Computer 87

The direct and indirect findings of pulmonary embolism found on contrast enhanced pulmonary Magnetic Resonance Angiography exams: A pictorial essay approach for the imager based on the real world findings found in over 600 patients

Mark Schiebler[1], Donald Benson[1], Christopher Francois[1], and Scott Nagle[1]

[1]Radiology, UW Madison School of Medicine and Public Health, Madison, WI, United States

The use of contrast enhanced pulmonary magnetic resonance angiography (CE-MRA) is being used as a primary modality for the diagnosis of pulmonary embolism (PE) at our institution. We have found both direct and indirect findings of PE on CE-MRA images. It is of critical importance to have a thorough understanding of the pitfalls in the diagnosis of PE using this modality. This pictorial essay will help to educate imaging physicians about these pitfalls and the associated indirect findings that can point to the presence of this important disease.

4839 Computer 88

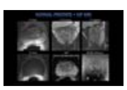

The role of Multiparametric prostate MRI in the detection, biopsy, and staging of prostate cancer.

Mathew Cherny[1] and Robert Villani[1]

[1]Radiology, Northwell Health, Manhasset, NY, United States

Prostate cancer is the second cause of cancer related death in men. Historically, screening has consisted of serum PSA, digital rectal exams, and random US guided transrectal biopsy. Compared to older methods, mp-MRI is superior for the detection and staging of prostate cancer due to its improved visualization and lesion characterization. The PI-RADS classification system is a schema developed concordantly with mp-MRI in order to better characterize the clinical significance of imaging findings. Increasingly, mp-MRI is taking a central role in detection, staging and biopsy of prostate neoplasm. In the future it may emerge as a primary screening tool.

4840 Computer 89

Can Thoracic MRI Add Value to Your Practice?

Chi Wan Koo[1], Darin B White[1], and Geoffrey B Johnson[1]

[1]Radiology, Mayo Clinic, Rochester, MN, United States

After reviewing state-of-the art clinical applications of thoracic MRI, reader will become cognizant of potentials and limitations of thoracic MRI and be the judge of whether thoracic MRI can add value to clinical practice.

4841 Computer 90

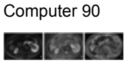

Magnetic Resonance Imaging Features of Immunoglobulin G4 Related Kidney Disease

Qiang Huang[1], Jinpeng Liu[1], Feng Chen[1], Wenjie Liang[1], and Wenbo Xiao[1]

[1]Radiology, The Fisrt Affiliated Hospital, College of Medicine, Zhejiang University, Hangzhou, People's Republic of China

Immunoglobulin G4 related disease (IgG4-RD) is a recently recognized distinct disease entity that can affect many organs/tissues. The kidney is a frequently involved organ with tubulointerstitial nephritis (TIN), and the renal lesions are collectively referred to as IgG4-related kidney disease (IgG4-RKD). Although definitive diagnosis requires histopathologic analysis, imaging plays a crucial role in demonstrating the involved organs/tissues. We retrospectively reviewed the magnetic resonance (MR) imaging findings of 13 patients diagnosed as IgG4-RKD. Various features were assessed, including renal size, margin between cortex and medulla, signal intensity on T1, T2 and diffusion weighted MR images, contrast enhancement, collecting system and/or renal fascia changes. MR imaging features, such as morphology changes, signal intensity abnormality especially on DWI, collecting system and/or renal fascia involvement enables the diagnosis of IgG4-RKD.

4842 Computer 91

A Review of the Magnetic Resonance Findings in Abnormal Placental Implantation.

Caron Parsons[1,2] and Charles Hutchinson[1]

[1]Population, Evidence & Technologies, University of Warwick, Coventry, United Kingdom, [2]Department of Radiology, University Hospital Coventry Warwickshire, Coventry, United Kingdom

This presentation will cover the normal anatomy, variants and physiology of the human placenta, as well as magnetic resonance imaging techniques for the evaluation of the placenta, and the spectrum of magnetic resonance findings in abnormal placental implantation. The implications for the mother and foetus will be discussed.

4843 Computer 92

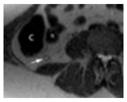

MRI of Non-obstetric Acute Pelvic Pain in Pregnant Patients

Francisco Lazaga[1], Laura Miller[2], and Yogesh kumar[1]

[1]Radiology, Yale New Haven Health Bridgeport Hospital, Bridgeport, CT, United States, [2]Yale New Haven Health Bridgeport Hosptial, Bridgeport, CT, United States

Acute abdominopelvic pain is a common concern during pregnancy. The differential diagnosis for pelvic pain is extensive and includes multiple non-obstetric etiologies. MRI is effective in evaluating pregnant patients with acute abdominopelvic pain.

MRI provides a complete cross-sectional evaluation of the abdomen and pelvis without radiation exposure or the need for intravenous contrast. MRI can help with the diagnosis in pregnant women with acute pelvic pain expediting treatment, especially when ultrasound results are indeterminate. MRI can also prevent unnecessary surgical exploration which carries a high risk to the pregnancy secondary to preterm uterine contractions.

We provide a list and MR imaging examples of differential diagnoses of acute non-obstetric pelvic pain in pregnancy.

4844 Computer 93

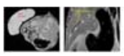

Quantitative Susceptibility Mapping to Characterise Hepatic Hyperoxia in Mice

Eoin Finnerty[1], Rajiv Ramasawmy[1], James O'Callaghan[1], John Connell[1], Karin Shmueli[2], David L Thomas[3], and Simon Walker-Samuel[1]

[1]Centre for Advanced Biomedical Imaging, University College London, London, United Kingdom, [2]Medical Physics and Biomedical Engineering, University College London, London, United Kingdom, [3]Institute of Neurology, University College London, United Kingdom

Information gleaned from Hepatic Venous Oxygen Saturation (ShvO2) can be beneficial in the post-operative care of those who have undergone a partial hepatectomy. Previously this has been performed invasively. We hypothesise that Quantitative Susceptibility Mapping (QSM) can do so non-invasively. The ShvO2 of a healthy cohort of mice was manipulated with a hyperoxic gas challenge. Susceptibility was measured under normoxic and hyperoxic conditions, and ShvO2 was calculated from the measurements. Significant differences were measured in susceptibility and ShvO2 in response to the gas challenge. We conclude that QSM can non-invasively measure changes in ShvO2 in the pre-clinical liver in-vivo.

4845 Computer 94

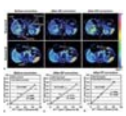

A novel portable perfusion phantom for quantitative DCE-MRI of the abdomen

Harrison Kim[1], Mina Mousa, Patrick Schexnailder, Mark Bolding, Robert Hergenrother, Vinoy Thomas, and Desiree Morgan

[1]University of Alabama at Birmingham, Birmingham, AL, United States

We developed a perfusion phantom that reduced variability in quantifying perfusion parameters of human abdominal tissues across different MR units. The phantom is compact enough to be imaged with the human subject and large enough to not suffer from partial volume effect, thus MR system calibration can be implemented simultaneously with patient imaging. Since it is composed of inexpensive materials, the phantom can be constructed as a disposable device. It is simple to use, so clinical MRI technologists should be able to operate it routinely. This phantom has the potential to facilitate multi-institutional clinical trials employing quantitative DCE-MRI to evaluate various abdominal malignancies.

4846 Computer 95

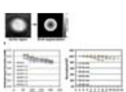

Semiautomatic determination of arterial input function in breath-hold DCE-MRI of the abdomen

Harrison Kim[1] and Desiree Morgan[2]

[1]University of Alabama at Birmingham, Birmingham, AL, United States, [2]University of Alabama at Birmingham

We developed a semiautomatic technique to determine the arterial input function (AIF) in breath-hold DCE-MRI of the abdomen. The error in AIF was significantly reduced by tracking the motion of aorta. Also, we confirmed that the semiautomatic segmentation of the aortic region can reduce error in AIF induced by manual segmentation up to 15%.

4847 Computer 96

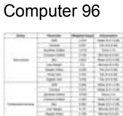

Hepatocellular carcinoma (HCC) screening with contrast-enhanced liver MRI: View-sharing artifact reduction with retrospective compressed sensing reconstruction

Paul Benjamin Stoddard[1], Evan Levine[2], Stephanie T. Chang[3], Qiong Song[1], Michael C. Muelly[1], Brian A. Hargreaves[2], Shreyas S. Vasanawala[1], and Andreas M. Loening[1]

[1]Radiology, Stanford University, Stanford, CA, United States, [2]Electrical Engineering and Radiology, Stanford University, Stanford, CA, United States, [3]Radiology, Veteran Affairs Palo Alto Health Care System

Hepatocellular carcinoma (HCC) screening is a common indication for contrast-enhanced liver MRI. Dynamic contrast-enhanced (DCE) acquisitions often utilize view-sharing (VS) to optimize spatiotemporal resolution, but MRI can often be degraded by respiratory motion. VS introduces temporal blurring of high spatial frequencies that propagate coherent motion artifacts across phases. Compressed sensing (CS) can reduce the need for VS by recovering missing k-space data from pseudo-random undersampling, thus potentially reducing temporal blurring while maintaining spatial resolution. CS results in greatly reduced ghosting artifacts despite a more synthetic appearance.

Electronic Poster

4848 Computer 97

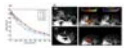

Assessing placenta injury with anatomical and IVIM-diffusion MRI in a mouse model of intrauterine inflammation

Dan Wu[1], Jun Lei[2], Solange Eloundou[2], and Irina Burd[2]

[1]Radiology, Johns Hopkins University School of Medicine, BALTIMORE, MD, United States, [2]Gynecology and Obstetrics, Johns Hopkins University School of Medicine, BALTIMORE, MD, United States

In this study, we investigated the placenta anatomy and function in a mouse model of intrauterine inflammation, using T2-weighted MRI and introvoxel incoherent motion (IVIM) MRI to measure placental perfusion. The high-resolution T2-weighted images demonstrated altered placenta anatomy in response to the acute inflammatory injury, which agreed with the histological measurements. IVIM of the mouse placenta was acquired with diffusion-weighted echo-planar imaging in a reduced field-of-view. The pseudo-diffusion fraction (***f***) and coefficient (*D**) fitted from IVIM model indicated reduced perfusion volume (***f***) and velocity (***f***·*D**) in the injured placentas compared to the shams.

4849 Computer 98

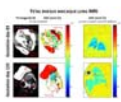

Water diffusion MRI as a biomarker of fetal lung development

Xuefeng Cao[1,2], Xiaojie Wang[3], Jinbang Guo[1,4], Nara S. Higano[1,4], Susan E. Wert[5], Christopher D. Kroenke[3], and Jason C. Woods[1,2,4,6]

[1]Center for Pulmonary Imaging Research, Cincinnati Children's Hospital Medical Center, Cincinnati, OH, United States, [2]Department of Physics, University of Cincinnati, Cincinnati, OH, United States, [3]Advanced Imaging Research Center, Oregon Health & Science University, Portland, OR, United States, [4]Department of Physics, Washington University in St. Louis, St. Louis, MO, United States, [5]Pulmonary Biology, Cincinnati Children's Hospital Medical Center, Cincinnati, OH, United States, [6]Department of Radiology, CCHMC, Cincinnati, OH, United States

In the developing fetal lung of both humans and rhesus macaques, the amount of interstitial tissue decreases during the transition from the canalicular to saccular stage. We hypothesize that this change corresponds to a decrease in restricted 1H diffusion in fetal lungs. 17 rhesus fetal lungs (in-vivo and ex-vivo) were imaged at gestation days 83-85, 110, and 133-135 with diffusion-weighted MRI. The apparent diffusion coefficients (ADCs, normalized by free-diffusion) significantly increased with gestational age for both in-vivo and ex-vivo experiments. These results demonstrate that ADC in the fetal lung can be used as a biomarker for the degree of alveolarization.

4850 Computer 99

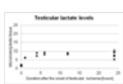

Magnetic Resonance Spectroscopy of the Testis under Ischemic Condition

Masayuki Yamaguchi[1], Hidehiro Watanabe[2], Nobuhiro Takaya[2], Fumiyuki Mitsumori[2], and Hirofumi Fujii[1]

[1]Division of Functional Imaging, National Cancer Center, Kashiwa, Japan, [2]National Institute for Environmental Studies, Tsukuba, Japan

Testicular ischemia is an acute disorder, which requires an accurate diagnosis whether the testis function is reversible or irreversible at the time of presentation; however, diagnostic test that predicts the functional reversibility of the ischemic testis has yet been established. This paper reports temporal metabolite changes for up to 24 hours after the onset of experimental testicular ischemia by using a 9.4-tesla magnetic resonance spectroscopy. We found the reduction in creatine levels in the testis under prolonged ischemic condition; hence, the alteration in creatine levels could be a possible metabolite marker that indicates the functional reversibility of the ischemic testis.

4851 Computer 100

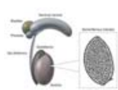

Imaging Seminiferous Tubules in a Mouse Model at 9.4 T – Feasibility for In Vivo Fertility Research

Mari Herigstad[1], Sofia Granados Aparici[2], Rachel Rodham[3], Allan Pacey[2], Martyn Paley[1], and Steven Reynolds[1]

[1]Academic Unit of Radiology, University of Sheffield, Sheffield, United Kingdom, [2]Department of Oncology and Metabolism, University of Sheffield, Sheffield, United Kingdom, [3]Biological Services Unit, University of Sheffield, Sheffield, United Kingdom

Damage to gonads, including the seminiferous tubules or epididymis, can diminish male fertility. Fertility research often employs mouse models, yet biopsy procedures may sometimes be incompatible with longitudinal studies. A viable non-invasive alternative may be MR. We scanned 8 mice at 9.4T, showing that internal testicular structure can be clearly observed, accurate measurements of seminiferous tubules (volume, diameter) obtained, extra-testicular tissues (e.g. epididymis) identified and spectroscopy peaks spatially localized across different tissues. This indicates that MRI/MRS could be useful in mouse models of fertility and possibly extended to human fertility studies in the future.

4852 Computer 101

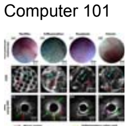

MR- and optical-based multimodal and multiscale protocol for mice colorectal diseases diagnosis

Hugo Dorez[1], Raphaël Sablong[1], Hélène Ratiney[1], Laurence Canaple[2], Hervé Saint-Jalmes[3], Sophie Gaillard[1], Driffa Moussata[1,4], and Olivier Beuf[1]

[1]Univ Lyon, INSA‐Lyon, Université Lyon 1, UJM-Saint Etienne, CNRS, Inserm, CREATIS UMR 5220, U1206, Lyon, France, [2]Institut de Génomique Fonctionnelle de Lyon, Université de Lyon 1, UMR 5242 CNRS, Ecole Normale Supérieure de Lyon, Lyon, France, [3]LTSI; INSERM U642; Université Rennes 1, Rennes, France, [4]Hôpital Régional Universitaire de Tours - Service hépato-gastroentérologie, Tours, France

A multimodal and multiscale protocol was defined for the diagnosis of mice colorectal diseases. Based on endoluminal MRI, using dedicated endorectal coils, and optical modalities the protocol was assessed on a mouse model of colorectal cancer for a six-month period. Optical modalities were used for microscopic characterization of the surface of the colon wall where endoluminal MRI was used for in-depth macroscopic characterization and staging of lesions from inflammation to cancer. The protocol was then used to support in vivo MRS signal analysis that was used to assess the biochemical content of various anatomical structures (colon wall, visceral fat…).

4853 Computer 102

Arterial Spin Labeling imaging of kidney after administration of 2 types of iodinated contrast medium: a time course study in CIN animal models

Kai Zhao[1], Xueqing Sui[1], Rui Wang[1], Zhiyong Lin[1], Xiaodong Zhang[1], Jian Luo[1], and Xiaoying Wang[1]

[1]Department of Radiology, Peking University First Hospital, Beijing, People's Republic of China

ASL imaging is a preeminent noninvasive method to quantify renal blood flow, which may be helpful to understand the pathogenesis of CIN. Our time course study indicates that the iodinated contrast medium can reduce the blood flow in the different zones of kidney. And some differences do exist on the renal blood flow after the two kinds of iodinated CM administration.

4854 Computer 103

BOLD imaging of kidney after administration of 2 types of iodinated contrast medium: a time course study in CIN animal models

Kai Zhao[1], Xueqing Sui[1], Rui Wang[1], Zhiyong Lin[1], Xiaodong Zhang[1], Jian Luo[1], and Xiaoying Wang[1]

[1]Department of Radiology, Peking University First Hospital, Beijing, People's Republic of China

BOLD is a preeminent noninvasive method to quantify renal function, which may be helpful to understand the pathogenesis of CIN. Our time course study indicates that the iodinated contrast medium can induce some affect to the different zone of kidneys. And some differences do exist on the renal oxygen consumption after the two kinds of iodinated CM administration.

4855 Computer 104

Oxygen Extraction Fraction imaging of kidney after administration of 2 types of iodinated contrast medium: a time course study in CIN animal models

Kai Zhao[1], Xueqing Sui[1], Rui Wang[1], Zhiyong Lin[1], Xiaodong Zhang[1], Jian Luo[1], and Xiaoying Wang[1]

[1]Department of Radiology, Peking University First Hospital, Beijing, People's Republic of China

MEGSE imaging is a preeminent noninvasive method to quantify renal oxygen extraction fraction, which may be helpful to understand the pathogenesis of CIN. Our time course study indicates that the iodinated contrast medium can inrease the OEF in different zones of kidney. And some differences do exist on the renal Oxygen Extraction Fraction (OEF) after the two kinds of iodinated CM administration.

4856 Computer 105

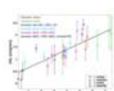

Comparison of Renal Blood Flow Measurements obtained using ASL-MRI and CT Perfusion

Vanessa L. Landes[1], Christopher M. Ferguson[2], Hung P. Do[1], John R. Woollard[2], James D. Krier[2], Lilach O. Lerman[2], and Krishna S. Nayak[1]

[1]University of Southern California, Los Angeles, CA, United States, [2]Mayo Clinic, Rochester, MN, United States

Computed tomography perfusion (CTP) is a validated method for assessment of single-kidney renal blood flow (RBF), but is limited by the use of exogenous contrast (i.e. iodine) injection and ionizing radiation. Arterial Spin Labeling (ASL)-MRI is an emerging technique that quantitatively measures RBF without any contrast agents or ionizing radiation. We compared renal perfusion (RBF/gram tissue) obtained using CTP and ASL-MRI in the left and right cortex and medulla of the same pigs (n=6), and observed a linear fit of ASL-MRI = 0.24*CTP+0.42 ml/ml/min with correlation r^2=0.71.

4857 Computer 106

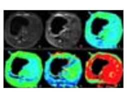

Intravoxel Incoherent Motion MR Study of Rabbit Liver Fibrosis Model

Lisui Zhou[1], Guangnan Quan[2], and Xiaocheng Wei[2]

[1]Department of Radiology, Affiliated hospital of Chengdu University, Chengdu, People's Republic of China, [2]GE Research China, GE Healthcare, Beijing, People's Republic of China

Staging of liver fibrosis is of great clinical value, because early stage fibrosis is reversible under proper treatment. Liver biopsy, which is currently the golden standard for fibrosis staging, has many limitations. In this study, we evaluated non-invasive IVIM diffusion imaging technique on rabbit liver fibrosis models. As a result, IVIM parameters show significant difference between normal, early and advanced fibrosis liver models. Our study suggests that IVIM parameters have potential to become the biomarker for liver fibrosis staging.

4858 Computer 107

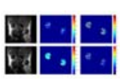

Assessment of unilateral renal infarction with VTE-ASL in comparison with DCE-MRI

Hanjing Kong[1], Chengyan Wang[1], Fei Gao[2], Bihui Zhang[3], Haochen Wang[3], Xiaodong Zhang[4], Min Yang[3], Jue Zhang[1,2], Xiaoying Wang[1,4], and Jing Fang[1,2]

[1]Academy for Advanced Interdisciplinary Studies, Peking University, Beijing, People's Republic of China, [2]College of Engineering, Peking University, Beijing, People's Republic of China, [3]Interventional radiology and vascular surgery, Peking University First Hospital, Beijing, People's Republic of China, [4]Department of Radiology, Peking University First Hospital, Beijing, People's Republic of China

DCE-MRI and ASL are promising method in evaluating renal disease. However, their application on renal infarction is lagging behind. In this study, we aim to investigate the value of VTE-ASL and DCE-MRI in renal infarction assessment and further compare the results with histological findings.

4859 Computer 108

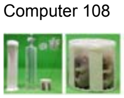

Whole body, high throughput mouse embryo 3D phenotyping using multi gradient echo and ultra short echo time with computed tomography validation.

Orlando Aristizabal[1], Dung Minh Hoang[2], Sebastian Mendoza[3], Daniel H. Turnbull[2], and Youssef Zaim Wadghiri[2]

[1]Structural Biology, Skirball Institute of Biomolecular Medicine, New York, NY, United States, [2]Radiology, NYU School of Medicine, [3]NYU School of Medicine

In this study a combination of 3D multi gradient echo (MGE) and ultrashort echo time (UTE) 100 micron isotropic resolution where acquired from 6 fixed mouse embryos at embryonic day 16. The embryos where littermates from an engrailed knockout mouse whose mutant embryos die at birth. The data from the UTE was validated with a high resolution CT scan. Results verify the utility of this approach to image both soft tissue and the skeletal system in a high throughput manner. The expected phenotype was easily identifiable and the 3D reconstruction of the skeletal system was equivalent to CT.

4860 Computer 109

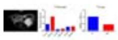

Evaluation of unilateral obstructive uropathy using co-polarized 13C-pyruvate and 13C-urea

Per Mose Nielsen[1], Rikke Nørregaard[2], and Christoffer Laustsen[1]

[1]MR Research Centre, Skejby University hospital, Aarhus N, Denmark, [2]Clinical institute, Skejby University hospital, Aarhus N, Denmark

Unilateral obstructive uropathy (UUO) is a cause of acute kidney injury and can also lead to chronic kidney diseases. A common cause for UUO is kidney stones and is also often the cause of end-stage renal diseases in children because of congenital development defects. Here we used a unilateral obstruction model with obstruction release after 5 days, and injection of co-polarized 13C-pyruvate and 13C-urea 2 days after release. We saw a marked elevation in lactate/pyruvate ration in the UUO kidney of the animals and also a reduction of approx. 50% in kidney bldflow measured by 13C-urea. The mechanisms involved must be investigated further. We believe that injection of co-polarized 13C-pyruvate and 13C-urea can be used as a clinical tool to follow kidney metabolic status and bldflow after surgical release of ureter obstruction.

4861 Computer 110

Evaluation of renal oxygenation change by functional MRI with administration of furosemide in diabetic nephropathy model

Rui Wang[1], Zhiyong Lin[1], and Xueqing Sui[1]

[1]Radiology, Peking University First Hospital, Beijing, People's Republic of China

Our study was to assess renal hemodynamics and oxygenation using blood oxygen level dependent (BOLD) and oxygen extraction fraction (OEF) imaging in diabetic nephropathy (DN) rabbits following administration of furosemide.

4862 Computer 111

A multicenter in vivo study to evaluate gadoxetate DCE-MRI as a preclinical biomarker of liver function

Paul Hockings[1,2], Anastassia Karageorgis[3], Stephen Lenhard[4], Brittany Yerby[5], Mikael Forsgren[6,7], Serguei Liachenko[8], Edvin Johansson[3], Richard Peterson[9], Xi Yang[8], Dominic Williams[10], Sharon Ungersma[5], Ryan Morgan[5], Kim Brouwer[11], and Beat Jucker[4]

[1]Antaros Medical, Molndal, Sweden, [2]MedTech West, Chalmers University of Technology, Gothenburg, Sweden, [3]AstraZeneca, Molndal, Sweden, [4]GlaxoSmithKline, King of Prussia, PA, United States, [5]Amgen Inc., Thousand Oaks, CA, United States, [6]Linköping University, Linköping, Sweden, [7]Wolfram MathCore, Linköping, Sweden, [8]National Center for Toxicological Research, U.S. Food and Drug Administration, Jefferson, AR, United States, [9]AbbVie, North Chicago, IL, United States, [10]AstraZeneca, Cambridge, United Kingdom, [11]University of North Carolina, Chapel Hill, NC, United States

Gadoxetate dynamic contrast-enhanced MRI (DCE-MRI) seems promising for non-invasive quantification of liver function. Here we tested the reproducibility of gadoxetate DCE-MRI at four MRI sites using an acute clinical dose of the antibiotic rifampicin. We found significant differences between sites in maximum relative enhancement (RE) in vehicle treated rats. However, highly significant differences in maximum RE between vehicle and rifampicin treated rats was detected at all sites. To our knowledge this is the first multicenter preclinical reproducibility study of an imaging biomarker.

4863 Computer 112

Characterization of renal parenchyma impairment in partial unilateral ureteral obstruction in mice with Intravoxel Incoherent Motion MR imaging

Maguelonne Pons[1], Benjamin Leporq[2], Liza Ali[3], Marianne Alison[3], Miguel Albuquerque[1], Michel Peuchmaur[4], Marie-Laurence Poli Mérol[5], Ulrich Blank[1], Simon Auguste Lambert[2], and Alaa El Ghoneimi[4]

[1]INSERM UMR 1149, Paris, France, [2]Univ Lyon, INSA-Lyon, Université Claude Bernard Lyon 1, [3]Hôpital Robert Debré, APHP, Université Paris Diderot, Sorbonne Paris Cité, [4]Pediatric Surgery and Urology, Hôpital Robert Debré, APHP, Université Paris Diderot, Sorbonne Paris Cité, [5]Université Reims Champagne Ardennes,American Memorial Hospital

Ureteropelvic junction obstruction constitutes a major cause of progressive pediatric renal disease. To date the follow-up of patients is difficult because there is a lack of non-invasive biomarkers. Here we propose to quantitatively characterize impairment of the kidney parenchyma after partial unilateral ureteral obstruction (pUUO) on mice using an intravoxel incoherent motion diffusion sequence. The results suggest that an f reduction is associated with a decrease in the volume of the renal parenchyma, which could be related to decreased renal vascularization. The later may occur before impairment by fibrosis and the findings are in accordance with the literature on pUUO.

4864 Computer 113

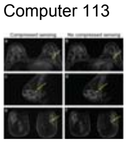

Evaluation of compressed sensing for 3D T1-weighted fat-suppressed breast MRI

Courtney K. Morrison[1], Jacob M. Johnson[2], Yuji Iwadate[3], Kevin King[4], James H. Holmes[2], Frank R. Korosec[1,2], Roberta M. Strigel[1,2,5], and Kang Wang[6]

[1]Department of Medical Physics, University of Wisconsin, Madison, WI, United States, [2]Department of Radiology, University of Wisconsin, Madison, WI, United States, [3]Global MR Applications and Workflow, GE Healthcare, Hino, Japan, [4]Global MR Applications and Workflow, GE Healthcare, Waukesha, WI, United States, [5]Carbone Cancer Center, University of Wisconsin, Madison, WI, United States, [6]Global MR Applications and Workflow, GE Healthcare, Madison, WI, United States

Spatial resolution has typically been prioritized at the expense of temporal resolution in the setting of dynamic contrast-enhanced breast MRI. In this work, we evaluated the use of compressed sensing (CS) with intermittent fat suppression for improved temporal resolution by comparing quality of fat suppression and overall image quality between a sequence accelerated using CS to one without CS.

4865 Computer 114

Correlations between R2* value and liver fibrosis in radiation-treated rats at early stage

Rong Ma[1], Dong Zhang[1], Changzheng Shi[1], Zhongping Zhang[2], and Liangping Luo[1]

[1]Medical Imaging Center, The First Affiliated Hospital of Jinan University, Guangzhou, People's Republic of China, [2]MR Research China, GE Healthcare, Beijing

At the early stage of liver fibrosis in radiation-treated rats, R2* value increased significantly. This suggests that R2* value could be a feasible biomarker to early evaluate liver fibrosis in vivo.

4866 Computer 115

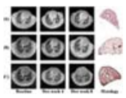

Quantifying tidal volume and pulmonary fibrosis in a TGF-α transgenic mouse model with retrospective self-gating UTE MRI

Jinbang Guo[1,2], Zackary I. Cleveland[1], William D. Hardie[3], Cynthia Davidson[3], Xuefeng Xu[3], and Jason C. Woods[1,2]

[1]Center for Pulmonary Imaging Research, Cincinnati Children's Hospital Medical Center, Cincinnati, OH, United States, [2]Physics, Washington University in St. Louis, St. Louis, MO, United States, [3]Division of Pulmonary Medicine, Cincinnati Children's Hospital Medical Center, Cincinnati, OH, United States

Pulmonary fibrosis has high morbidity and mortality, but remains poorly understood. Many experimental and clinical studies have implied or demonstrated the role for transforming growth factor (TGF)-α in the pathogenesis of pulmonary fibrosis. We demonstrate the utilization of retrospective self-gating UTE MRI with ellipsoidal k-space coverage to measure the burden of pulmonary fibrosis in a TGF-α transgenic mouse model, with the dynamic progression of fibrotic burden well quantified longitudinally by both high-density lung volume percentage and tidal volume.

4867 Computer 116

Ferumoxytol-Enhanced Quantitative Susceptibility Mapping of the Rhesus Placenta

Ante Zhu[1,2], Samir D. Sharma[2], Sydney Nguyen[3], Kevin M. Johnson[2,4], Ian M. Bird[3], Ted Golos[3,5,6], Sean B. Fain[1,2,4], Dinesh M. Shah[5], Oliver Wieben[2,4], Scott B. Reeder[1,2,4,7,8], and Diego Hernando[2,4]

[1]Biomedical Engineering, University of Wisconsin-Madison, Madison, WI, United States, [2]Radiology, University of Wisconsin-Madison, Madison, WI, United States, [3]Comparative Biosciences, University of Wisconsin-Madison, Madison, WI, United States, [4]Medical Physics, University of Wisconsin-Madison, Madison, WI, United States, [5]Obstetrics and Gynecology, University of Wisconsin-Madison, Madison, WI, United States, [6]Wisconsin National Primate Research Center, University of Wisconsin-Madison, Madison, WI, United States, [7]Medicine, University of Wisconsin-Madison, Madison, WI, United States, [8]Emergency Medicine, University of Wisconsin-Madison, Madison, WI, United States

Ferumoxytol-enhanced MRI may enable the assessment of altered immune cell activation and distribution in placental inflammation. In this work, quantitative susceptibility mapping (QSM) is proposed to assess the temporal variation of ferumoxytol concentration in the placenta. Three healthy pregnant rhesus monkeys were imaged at six time points relative to ferumoxytol injection. Longitudinal quantification of placental magnetic susceptibility and R1/R2/R2* relaxometry were performed to provide a preliminary assessment of the ferumoxytol variation in healthy rhesus placenta. This study demonstrated the feasibility of ferumoxytol-enhanced QSM and relaxometry in the rhesus placenta and may provide a method for the evaluation of placental inflammation.

4868 Computer 117

Fatty acid composition with metabolic changes of livers from high fat diet-fed mice using in vivo and in vitro proton magnetic resonance spectroscopy

Kyu-Ho Song[1], Min-Young Lee[1], Chi-Hyeon Yoo[1], Song-I Lim[1], and Bo-Young Choe[1]

[1]Department of Biomedical Engineering, and Research Institute of Biomedical Engineering, The Catholic University of Korea College of Medicine, Seoul, Korea, Republic of

Our animal studies suggest that unsaturated fatty acids may be upregulated or downregulated in a chronic model of non-alcoholic fatty liver disease (NAFLD). Further assessment of the strengths of our analytical parameters, which is essential for research and clinical evaluation of disease, should account for signal decay and bias in sequence selection. This will provide an effective means to quantify lipid content and to characterize NAFLD.

4869 Computer 118

Self resonated clip for in-utero mouse embryonic MRI

Dung Minh Hoang[1], Orlando Aristizabal[1], Daniel Turnbull[1], and Youssef Zaim Wadghiri[1]

[1]Radiology, NYU - School of Medicine, New York, NY, United States

In this study, we introduce a newly designed technique called clipping to help stabilize the imaged embryos. Furthermore, this setup has potential for high-throughput imaging of live embryos using large volume coils in combination with individual inductive coupling loops for each embryo. Our results showed that the clipping technique secure the embryo for an extended imaging time of more than 90 minutes. The combination of volume coil and inductive coupling loop [ref] helps increasing the signal to noise ratio (SNR) for more than 3 folds compare to the volume coil alone and closely reach the level of commercial 4 channel received only surface coil.

4870 Computer 119

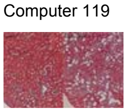

Multi-parametric MRI of Murine Unilateral Ureter Obstruction

Feng Wang[1,2], Keiko Takahashi[3], Hua Li[1], Zhongliang Zu[1,2], Junzhong Xu[1,2], Raymond C. Harris[3], Takamune Takahashi[3], and John C. Gore[1,2]

[1]Institute of Imaging Science, Vanderbilt University, Nashville, TN, United States, [2]Radiology and Radiological Sciences, Vanderbilt University, Nashville, TN, United States, [3]Division of Nephrology and Hypertension, Vanderbilt University, Nashville, TN, United States

Multi-parametric MRI techniques may allow the assessment of renal injury and function in a sensitive and objective manner. This study aimed to evaluate an array of MRI methods that exploit endogenous contrasts for their sensitivity in detecting abnormal features associated with kidney disease in a murine model of unilateral ureter obstruction (UUO). Diffusion weighted imaging (DWI), quantitative magnetization transfer (qMT), chemical exchange saturation transfer (CEST), and nuclear Overhauser enhancement (NOE) provide specific information about the cellular and molecular changes produced by UUO.

4871 Computer 120

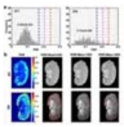

Assessment of Renal Fibrosis in Murine Diabetic Nephropathy Using Quantitative Magnetization Transfer MRI

Feng Wang[1,2], Daisuke Katagiri[3], Ke Li[1], Shinya Nagasaka[3], Hua Li[1], Keiko Takahashi[3], Suwan Wang[3], C. Chad Quarles[1,2], Ming-Zhi Zhang[3], Raymond C. Harris[3], John C. Gore[1,2], and Takamune Takahashi[3]

[1]Institute of Imaging Science, Vanderbilt University, Nashville, TN, United States, [2]Radiology and Radiological Sciences, Vanderbilt University, Nashville, TN, United States, [3]Division of Nephrology and Hypertension, Vanderbilt University, Nashville, TN, United States

Current clinical tests are insufficient for non-invasively assessing renal fibrosis. Here we evaluated the utility of high-resolution quantitative magnetization transfer (qMT) MRI to detect renal fibrosis using a murine model of progressive DN and compared the results with histological analyses. Our results show that high-resolution qMT could provide an index to reveal renal cortical fibrosis.

Electronic Poster

Preclinical CV Imaging

Exhibition Hall — Wednesday 14:45 - 15:45

4872 Computer 1

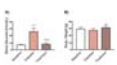

Reversible Changes in Cardiac Function and Metabolism in an Inducible Mouse Model of Type 1 Diabetes

Dragana Savic[1], Maria Rohm, Vicky Ball, Mary Kate Curtis, Lisa Heather, Frances M Ashcroft, and Damian J. Tyler

[1]University of Oxford, Oxford, United Kingdom

Heart disease is the leading cause of death in Type 1 diabetic patients, however the mechanistic link has not been fully established. In this study an inducible and reversible mouse model of Type 1 diabetes was used. Depression of cardiac function and the increase in blood glucose occur in combination with suppression of pyruvate to bicarbonate conversion. By reversing diabetes with Glibenclamide, cardiac function and blood glucose concentration was restored. This study demonstrated changes that occur alongside the development of a reversible model of Type 1 diabetes and how the action of Glibenclamide can affect metabolism and function of the heart.

4873 Computer 2

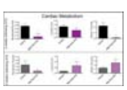

Type 1 Diabetic Hearts show Unexpected Biphasic Metabolic and Functional Progression as Evaluated with Hyperpolarised [1-13C]Pyruvate and CINE MR.

Dragana Savic[1], Vicky Ball, Carolyn Carr, Lisa Heather, and Damian J. Tyler

[1]Department of Physiology, Anatomy & Genetics, University of Oxford, Oxford, United Kingdom

Type 1 diabetes patients are insulin deficient resulting in hyperglycaemia. Diabetic patients have a higher risk of cardiovascular diseases. In this study the progression of cardiac metabolic and functional decline was followed in a streptozotocin (STZ) induced Type 1 diabetic model. Flux through pyruvate dehydrogenase was significantly decreased at 2 and 6 weeks post STZ injection. Interestingly, the incorporation of the ^{13}C-label from pyruvate into lactate and alanine was decreased at 2 weeks, but significantly increased at 6 weeks. Cardiac output was normalized after 6 weeks. Such studies will allow a better understanding of the interactions between metabolism and function in the diabetic heart.

4874 Computer 3

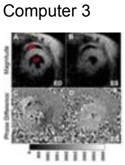

Repeatability and User Variability of Myocardial Tissue Phase Mapping in Mice

Nivedita K. Naresh[1], Cynthia Yang[1], Sol Misener[1], Bradley D. Allen[1], Michael Markl[1,2], James C. Carr[1,3,4], and Daniele Procissi[1]

[1]Radiology, Northwestern University, Chicago, IL, United States, [2]Biomedical Engineering, Northwestern University, Chicago, IL, United States, [3]Medicine, Northwestern University, Chicago, IL, United States, [4]McCormick School of Engineering, Northwestern University, Chicago, IL, United States

Mouse models can help investigate the molecular mechanisms underlying complex cardiovascular diseases. Assessment of myocardial regional wall motion plays a very important role in the diagnosis and management of several cardiovascular diseases and can be linked to many underlying biological processes. In this study, we evaluated the repeatability and inter-user variability of the myocardial tissue phase mapping method in mice. We found that myocardial tissue phase mapping can be performed with good repeatability and little user variability in mice to reliably quantify both global and regional myocardial velocities.

4875 Computer 4

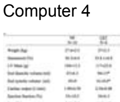

MRI/PET of Myocardial Extracellular Volume in a Canine model of Chemotherapy

Chia-Ying Liu[1], Cynthia Davies-Venn[1], Comfort Elumogo[1], Rolf Symons[1], Victoria Hoffmann[2], Kelly Rice[2], Roberto Maass-Moreno[1], Veit Sandfort[1], Stefan Zimmermann[3], Amir Pourmorteza[1], Mark Ahlman[1], and David Bluemke[1]

[1]Radiology and Imaging Sciences, National Institutes of Health, Bethesda, MD, United States, [2]Division of Veterinary Resources, National Institutes of Health, [3]Department of Radiology, Johns Hopkins Hospital, MD, United States

We used simultaneous MR/FDG PET to measure the myocardial extracellular volume (ECV) and glucose metabolism (estimated by standard uptake value, SUV) in a canine model of chemotherapy (ChT); comparison was made to ECV in relationship to a myocardial infarct (MI) models. MRI ECV in the ChT group was elevated by 16% and 23% compared to the MI group in the remote and adjacent myocardial segments, respectively. PET SUV in the ChT group was reduced by 49% and 41% compared to the MI group in the remote and adjacent myocardial segments, respectively. Difference was also observed in the MRI partition coefficient but not in the native T1.

4876 Computer 5

Evaluation of the impact of strain correction on the secondary eigenvector of diffusion with in vivo and ex vivo porcine hearts

Pedro Ferreira[1], Sonia Nielles-Vallespin[2], Ranil de Silva[1], Andrew Scott[1], Daniel Ennis[3], Daniel Auger[4], Jonathan Suever[5], Xiaodong Zhong[6], Bruce Spottiswoode[7], Dudley Pennell[1], Andrew Arai[2], and David Firmin[1]

[1]Cardiovascular BRU, Royal Brompton Hospital, London, United Kingdom, [2]NHLBI, National Institutes of Health, MD, United States, [3]Department of Radiological Sciences, UCLA, CA, United States, [4]Biomedical Engineering, University of Virginia, VA, United States, [5]Geisinger Medical Center, PA, United States, [6]Siemens Healthcare, GA, United States, [7]Siemens Healthcare, TN, United States

Myocytes have a laminar organization, where sheets of myocytes interleave with collagen-lined shear layers. Cardiac diffusion tensor imaging is capable of probing sheet dynamics with secondary diffusion directions, although questions remain about cardiac strain being a possible confounder. Here we study the validity of strain-correcting cardiac diffusion tensor data by directly comparing in vivo DTI data without and with strain correction, to ex vivo DTI data of the same porcine hearts arrested in a diastolic or systolic conformation. Results show that the current strain correction model exaggerates the contribution of microscopic strain to diffusion resulting in an over-correction.

4877 Computer 6

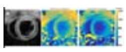

Simultaneous Cardiac and Renal oblique-slice T1-Mapping Differentiates Contrast Agent Activity in Normal and Doxorubicin-treated Rats

Ronald J Beyers[1], Dean Schwartz[2], Tessa Hutchinson[3], Meghan Ward[3], Nouha Salibi[1,4], Christian Goldsmith[3], and Thomas Denney[1]

[1]MRI Research Center, Auburn University, Auburn, AL, United States, [2]Department of Anatomy, Physiology and Pharmacology, Auburn University, Auburn, AL, United States, [3]Department of Chemistry and Biochemistry, Auburn University, Auburn, AL, United States, [4]MR R&D, Siemens Healthcare, Malvern, PA, United States

We developed a cardiac multi-oblique-slice T1-mapping sequence, called ***Tmax***, for simultaneous ***in vivo*** cardiac and multi-region T1-mapping in rats. We validated ***Tmax*** with gadolinium contrast agent (CA) scans then applied it to support our concurrent development of a reactive oxygen species activated T1-shortening agent, called H4qtp2, in doxorubicin-treated (Dox) rats. The new ***Tmax*** sequence performed excellent at simultaneously quantifying gadolinium T1 effects in cardiac and renal regions. However, application of ***Tmax*** with low dose levels of H4qtp2 CA in Dox rats gave marginal results from too low dose of H4qtp2 to sufficiently affect the T1 and quantify Dox-induced pathology

---

4878 Computer 7

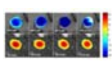

TWO-DIMENSIONAL PHASE-CONRAST MAGNETIC RESONANCE IMAGING AS TOOL TO DETERMINE HEPATIC HEMODYNAMICS IN RATS WITH A HEALTHY, FIBROTIC OR CIRRHOTIC LIVER

Denise Schaffner[1,2,3], Dominik von Elverfeldt[4], Peter Deibert[1,2], Irmgard Merfort[3], Adhara Lazaro[1,2], Lisa Lutz[2,5], Manfred W. Baumstark[1,2], Wolfgang Kreisel[2], and Wilfried Reichardt[4,6,7]

[1]Institute for Exercise- und Occupational Medicine, Center for Medicine, Medical Center - University of Freiburg, Freiburg, Germany, [2]Faculty of Medicine, University of Freiburg, Freiburg, Germany, [3]Department of Pharmaceutical Biology and Biotechnology, University of Freiburg, Freiburg, Germany, [4]Department of Radiology Medical Physics, Medical Center – University of Freiburg, Freiburg, Germany, [5]Institute of Clinical Pathology, Medical Center – University of Freiburg, Freiburg, Germany, [6]German Cancer Consortium (DKTK), Heidelberg, Germany, [7]German Cancer Research Centre (DKFZ), Heidelberg

In this work we wanted to test a Magnetic Resonance (MR) scanning protocol as a non-invasive tool to determine hepatic hemodynamics and to assess the liver fibrosis degree in an animal model of liver fibrosis and cirrhosis. MR rat liver images provided a good discrimination of healthy from diseased liver, but for the assessment of liver fibrosis degree histology is indispensable. The results show that portal and aortal flow patterns for a cardiac cycle could be measured with high reliability in Conclusion, this MR scanning protocol presents a reliable non-invasive tool to determine hepatic hemodynamics in healthy and diseased rats

---

4879 Computer 8

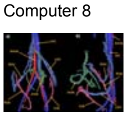

Feasibility of 4D-Flow Imaging of Uterine Blood Flow in the Pregnant Rhesus Macaque

Philip Corrado[1], Jacob Macdonald[1], Sydney Nguyen[2], Kevin Johnson[1], Chris Francois[3], Ronald R. Magness[4], Scott B. Reeder[1,3,5,6,7], Ian Bird[8], Dinesh Shah[8], Thaddeus G. Golos[8,9], and Oliver Wieben[1,3]

[1]Medical Physics, University of Wisconsin Madison, Madison, WI, United States, [2]Endocrinology & Reproductive Physiology, University of Wisconsin Madison, Madison, WI, United States, [3]Radiology, University of Wisconsin Madison, Madison, WI, United States, [4]Obstetrics & Gynecology, University of South Florida, Tampa, FL, United States, [5]Biomedical Engineering, University of Wisconsin Madison, [6]Medicine, University of Wisconsin Madison, [7]Emergency Medicine, University of Wisconsin Madison, [8]Obstetrics & Gynecology, University of Wisconsin Madison, Madison, WI, United States, [9]Comparative Biosciences, University of Wisconsin Madison, Madison, WI, United States

4D-Flow MRI is introduced as an alternative to Doppler velocimetry in monitoring blood flow to the placenta in pregnancy. Our 3D radially undersampled PC-VIPR technique provided volumetric coverage of uterus and relevant vasculature with a 10-minute scan. Uterine arteries and ovarian veins were visualized in a 0.83mm isotropic resolution angiogram and flow rates and vessel sizes were measured retrospectively. Repeated scans of four rhesus macaques on subsequent days showed reproducibility of flow rate and cross sectional area measurements in vessels of interest, demonstrating the potential for 4D-Flow MRI for assessing utero-placental vascular health.

4880 Computer 9

4D flow MRI measurements in ex vivo beating pig hearts as a testing platform for transcathether aortic valve implantation

Eva S Peper[1], Alberto Leopaldi[2], Sjoerd van Tuijl[2], Nicky de Jonge[2], Gustav J Strijkers[3], Arend de Weger[4], Aart J Nederveen[1], Henk A Marquering[3], and Pim van Ooij[1]

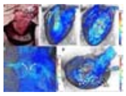

[1]Department of Radiology, Academic Medical Center, Amsterdam, Netherlands, [2]LifeTec Group, Eindhoven, the Netherlands, Netherlands, [3]Department of Biomedical Engineering & Physics, Academic Medical Center, Amsterdam, Netherlands, [4]Department of Cardiothoracic Surgery, Leiden University Medical Center, Leiden, Netherlands

In this 4D flow MRI study, ex vivo beating pig heart models in an MR-compatible setup mimicking human physiological conditions were used to investigate flow alterations after implantation of artificial valves designed for transcathether aortic valve implantations (TAVI). Two pig hearts had implanted TAVI valves (one with and one without attachment to the aortic sinuses) and were compared to five pig hearts without valve implantation. For both pig hearts with implanted valves, substantial aortic backflow, and thus paravalvular leakage, was observed. The ex vivo set-up presented is thus suitable for cardiac flow experiments.

4881 Computer 10

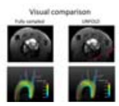

Evaluation of accelerated preclinical 4D-flow imaging with UNFOLD

Moritz Braig[1], Axel J. Krafft[1], Jochen Leupold[1], Juergen Hennig[1], Marius Menza[1], and Dominik von Elverfeldt[1]

[1]Medical Physics, University Medical Center Freiburg, 79106, Germany

There is growing interest in preclinical imaging and analysis of complex flow patterns. For example, 4D flow imaging of mouse models with vascular plaques or aortic constriction could provide insights into the development and pathogenesis of cardiovascular diseases. Unfortunately, 4D-flow MRI is often compromised by a trade-off of reasonable acquisition durations and achievable spatial resolution. Our work evaluates an undersampling strategy, namely UNFOLD, for preclinical 4D flow MRI, which has the potential to decrease measurement time by 50%. Artifacts emerging from the undersampling are removed by unaliasing in the temporal domain using a lowpass filter after fourier transformation.

4882 Computer 11

Quantitative gated and non-gated rat phase contrast MRI: optimized analysis of blood flow and wall shear stress.

Chen-You Huang[1], Chiun-Wei Huang[2], Shao-Chieh Chiu[2], Wu-Chung Shen[1], and Shin-Lei Peng[1]

[1]Department of Biomedical Imaging and Radiological Science, China Medical University, Taichung, Taiwan, [2]Center for Advanced Molecular Imaging and Translation, Chang Gung Memorial Hospital

Goals of this study are to test effects of gated/non-gated, velocity encoding (VENC) and spatial resolution on blood flow, wall shear stress (WSS) and artery area when performing phase-contrast (PC) MRI for rat common carotid artery (CCA). Results show the usage of gated instrument can provide more reproducible results. VENC has insignificant influences on flow, WSS and artery area. To compromise the trade-off between accuracy and time-consuming, the resolution of 0.21 mm is suggested for extracting hemodynamic information about rat CCA.

4883 Computer 12

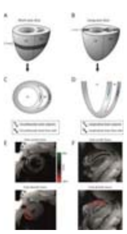

Right ventricular myocardial strain in rats

Emil Espe[1], Jan Magnus Aronsen[1,2], Lili Zhang[1], and Ivar Sjaastad[1]

[1]Institute for Experimental Medical Research, University of Oslo, OSLO, Norway, [2]Bjørknes College, Oslo, Norway

The function of the right ventricle (RV) is closely linked to clinical outcome in many cardiovascular diseases. Experimental heart disease in rodents play an irreplaceable role in modern cardiovascular research, but no in vivo method exists offering robust measurements of RV myocardial function in small animals.

We used phase-contrast MRI to measure RV strain in rats. We found that RV strain and ejection fraction were closely related, and confirmed that high RV afterload is linked to reduced RV strain.

We show, for the first time, that it is possible to accurately measure myocardial function in the RV in rodents.

4884 Computer 13

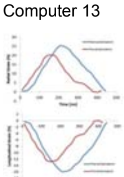

Cardiac MRI measurement of right ventricular strain using feature tracking in a model of embolic pulmonary hypertension.

Zachary Borden[1], Donald Benson[1], Alejandro Roldan[2], Heidi Kellihan[3], Ashley Mulchrone[4], Naomi Chesler[4], and Christopher Francois[1]

[1]Radiology, University of Wisconsin-Madison, Madison, WI, United States, [2]Radiology and Medical Engineering, University of Wisconsin-Madison, Madison, WI, United States, [3]Veterinary Medicine, University of Wisconsin-Madison, Madison, WI, United States, [4]Biomedical Engineering, University of Wisconsin-Madison, Madison, WI, United States

Right ventricular strain was assessed using an MRI tissue tracking algorithm on bSSFP axial sequences in both acute and chronic embolic pulmonary hypertension canine models. Strain values were heterogeneous in the acute population with statistically significant decreases in acute radial and longitudinal strain rate and chronic radial and longitudinal strain and strain rate values. Findings suggest MRI cardiac strain measurement is a promising technique in the clinical evaluation of post embolic pulmonary hypertension patients.

4885 Computer 14

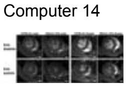

Cardiac Magnetic Resonance for Characterizing a Spontaneous Hypertrophic Cardiomyopathy Mouse Model

Min-Chi Ku[1], Till Huelnhagen[1], Andreas Pohlmann[1], and Thoralf Niendorf[1,2,3]

[1]Berlin Ultrahigh Field Facility, Max Delbrück Center for Molecular Medicine in the Helmholtz Association, Berlin, Germany, [2]Experimental and Clinical Research Center, Charite Medical Faculty and the Max Delbrueck Center for Molecular Medicine in the Helmholtz Association, Berlin, Germany, [3]DZHK (German Centre for Cardiovascular Research), partner site Berlin, Germany

HCM is the most common inherited heart disease. The two most frequently seen mutated genes are MYH7 and MYBPC3 which account for nearly 80% of familiar HCM. In this study we hypothesized that these gene variants will affect both LV and RV function. By *in-vivo* CMR we detected LV hypertrophy in a mouse strain DBA/2J bearing the two gene variants. Interestingly there is no defected LV function found but changes in RV function as both male and female DBA/2J mice had declined RVEF. Our results provide new insights into the correlation of genetic alteration and HCM phenotype.

4886 Computer 15

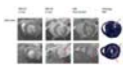

4D Cine Strategy for Assessment of Mouse Cardiac Function and Infarct Size in a Single Acquisition Optimized for a Clinical 3T MR System

Lindsey A Crowe[1], Fabrizo Montecucco[2], Federico Carbone[2], Iris Friedli[1], Anne-Lise Hachulla[1], Vincent Braunersreuther[3], Francois Mach[3], and Jean-Paul Vallée[1]

[1]Department of Radiology, Geneva University Hospitals, Geneva, Switzerland, [2]Department of Internal Medicine, University of Genoa, Italy, [3]Department of Cardiology, Geneva University Hospitals, Geneva, Switzerland

Small cardiac imaging on clinical 3T machines is an important, cost effective translational step for new contrast media and sequence validation. We developed for the first time a new 4D strategy tailored for 3T to simultaneously assess function and infarct in mice, validated against 2D cine, post mortem and histology. Isotropic 3D cardiac cine of mice on a clinical 3T system improved coverage and reduced flow artifacts with higher spatial and temporal resolution for more accurate quantification of cardiac function. Infarct volume enhancement was quantifiable from the same 3D cine acquisition.

4887 Computer 16

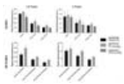

Gadobutrol- vs. gadoterate meglumine-enhanced multi-phase 3D-MRA and 4D-MRA at 1.5T and 3T: an intra-individual quantitative and qualitative comparison of macrocyclic contrast agents in minipigs

Dariusch Reza Hadizadeh[1], Gregor Jost[2], Vera Catharina Keil[1], Christian Marx[1], Maximilian Rauch[1], Frederic Carsten Schmeel[1], Hubertus Pietsch[2], Hans Heinz Schild[1], and Winfried Albert Willinek[3]

[1]Radiology, University of Bonn, Bonn, Germany, [2]MR and CT Contrast Media Research, Bayer Pharma AG, Berlin, Germany, [3]Zentrum für Radiologie, Neuroradiologie, Sonographie und Nuklearmedizin, Krankenhaus der barmherzigen Brüder, Trier, Germany

In an animal model bolus kinetics and image quality of the macrocyclic contrast agents (CA) gadobutrol (standard and half-dose) and gadoterate meglumine (standard-dose) were investigated intra-individually in multi-phase 3D- (MP3D) MRA and in 4D-MRA at 1.5T and 3T. Standard dose gadobutrol provided significantly higher signals in both MP3D- and 4D-MRA at both field strengths. Differences were most prominent in venous imaging phases. At 3T, arterial first pass peaks were truncated in 7/8 minipigs using standard dose CA. Image quality analysis of MP3D confirmed higher image quality in venous phases with standard-dose gadobutrol compared to gadoterate meglumine at both field strengths.

4888 Computer 17

Histological validation of loading lag of heart iron with respect to liver iron in a rabbit model

xiaodong chen[1,2,3], Zipan Chen[4], Heng Lv[5], Ziliang Cheng[6], Qihua Yang[6], Zuoquan Zhang[7], Zebin Luo[1], Jiaji Mao[6], Queenie Chan[8], Yingjie Mei[9], Jingwen Huang[6], Wubiao Chen[1], Biling Liang[6], and Hua Guo[10]

[1]Affiliated hospital of Guangdong Medical College, Zhanjiang, People's Republic of China, [2]Sun Yat-Sen Memorial Hospital, Guangzhou, People's Republic of China, [3]Tsinghua University, Beijing, People's Republic of China, [4]Shiyan People's Hospital, [5]Peking University Shenzhen Hospital, [6]Sun Yat-Sen Memorial Hospital, [7]The Fifth Affiliated Hospital of Sun Yat-Sen University, [8]Philips Healthcare, Hong Kong, [9]Philips Healthcare, Guangzhou, [10]Tsinghua University

Whether there exists a lag in the iron loading between liver and heart in transfusion dependent patients has clinical significance in prevention and treatment of heart iron overload. We performed this study to verify this time lag on a rabbit model. The result shows that the iron loading, measured with pathology, MRI and atomic absorption spectrophotometer, was much faster and heavier in the liver than that in the heart. Therefore, there existed a time lag between heart and liver iron overload on the rabbit model. This may lead to improved clinical guidelines for cardioprotection.

4889 Computer 18

Multiparametric CMR protocol and analysis methods for the detection of early cardiotoxicity remodelling in the mini-swine.

Delphine Perie[1], Clémence Balosetti[1], Hélène Héon[2], Nagib Dahdah[3], Farida Cheriet[1], Matthias Friedrich[4], and Daniel Curnier[5]

[1]Mechanical Engineering, Polytechnique Montreal, Montreal, QC, Canada, [2]Research Center, CHUM, Montreal, QC, Canada, [3]Pediatric cardiology, CHU Sainte-Justine, Montreal, QC, Canada, [4]Health Center, McGill University, Montreal, QC, Canada, [5]Kinesiology, Université de Montréal, Montreal, QC, Canada

Some Cardiovascular magnetic resonance (CMR) studies investigated the long term effects of cancer treatments, but were never applied to the detection of early changes during cardiotoxicity remodelling. The CMR parameters we investigated in the miniature swine therapeutic model with doxorobucin was able discriminate treated animals from controls. Differences were detectible earlier than onset of classical echocardiographic changes. Translating these observations to personalized medicine approach could be the premise for the oncologist to know accurately when the treatment just starts to have deleterious effect on myocardium instead of just observing that the heart was damaged by doxorubicin.

4890 Computer 19

A spontaneous type 2 diabetic rhesus monkey model for cardiac MR study

Yu Zhang[1], Jie Zheng[2], and Fabao Gao[3]

[1]West China Hospital, Sichuan University, Chengdu, People's Republic of China, [2]Mallinckrodt Institute of Radiology, Washington University School of Medicine in St. Louis, [3]West China HospitaL, Sichuan University, Chengdu

The aim of this study was to provide a human-like diabetic monkey model for cardiovascular research. Myocardial function and tissue characterizations were measured by CMR in 14 diabetic and 5 control monkeys. In addition to diastolic dysfunction, minor and moderate diffuse fibrosis was shown in cardiac T1, T1r, ECV, and non-contrast fibrosis index images in all the hearts of all diabetic monkeys, confirmed by histopathology finding in one diabetic monkey.

4891 Computer 20

Early Prediction of Chronic Infarct Size by Acute Strain: A Cardiac MRI Study of Myocardial Infarction in Pigs

Sarayu Parimal[1], Smita Sampath[1], Ibrahim Mazlan[2,3], Grace Croft[2,3], Teresa Totman[2,3], Yvonne Tay Wei Zheng[4], Elaine Manigbas[4], Michael Klimas[5], Jeffrey L. Evelhoch[5], Dominique P.V. Kleijn[2,3], and Chih-Liang Chin[1]

[1]Translational Biomarkers, Merck Sharp & Dohme, Singapore, Singapore, [2]Cardiovascular Research Institute, National University Heart Centre, Singapore, [3]Department of Surgery, Yong Loo Lin School of Medicine, National University of Singapore, Singapore, [4]Comparative Medicine Imaging Facility, Center for Life Sciences, National University of Singapore, Singapore, [5]Translational Biomarkers, Merck & Co., Inc., West Point, PA, United States

We characterized cardiac structure and function longitudinally in myocardial infarcted pigs, induced by permanent ligation of left circumflex artery of left ventricle (LV), to identify early strain biomarkers that are predictive of late stage remodeling. Pigs were imaged pre- and post-surgery at 1-wk and 4-wk. Reduction of percentage of infarct was observed at basal antero-lateral and mid infero-lateral regions at 4-wk post-surgery. Decreased peak circumferential strain was observed at infarcted areas showing compromised contractility. In addition, ROC analyses revealed that acute strain at 1-wk and early strain change from baseline can predict chronic infarct size suggesting that LV strain could potentially serve as early biomarker for novel therapies.

4892 Computer 21

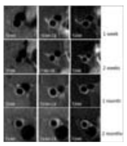

Aortic Wall MR Imaging for Assessing Rosuvastatin Therapy in Atherosclerotic Animal Model

Juan Huang[1], Yan Song , Mingmei Li, Xiaotao Deng, Sheng Jiao, Jingying Yu, Min Chen, and Xiaoqi Wang

[1]Beijing Hospital, Beijing, People's Republic of China

Here we present the high-resolution MRI imaging for assessing therapy of titrated rosuvastatin for atherosclerosis in rabbit models. This study shows that abdominal aorta wall in both control and treated rabbits get thicker with prolonged continuous feeding of cholesterol, aortic plaques grows bigger with this progression. The MRI vascular wall imaging measured atherosclerotic plaques with well correlation of histological classifications. Statical regression showed that the group with rosuvastatin treatment reduced the aortic plaques comparing to the control rabbits.

4893 Computer 22

magna cum laude

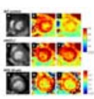

T1 Mapping with Nitric Oxide Synthase (NOS) Inhibition Detects Impaired Coronary Endothelial Function in Mice Fed a High Fat Diet

Sophia Xinyuan Cui[1] and Frederick H. Epstein[1,2]

[1]Biomedical Engineering, University of Virginia, Charlottesville, VA, United States, [2]Radiology, University of Virginia, Charlottesville, VA, United States

Endothelial nitric oxide synthase (eNOS)-mediated production of NO regulates the microvasculature, controlling both vessel diameter and permeability. We hypothesized that T1 mapping of the healthy heart during NOS inhibition would detect increased water content resulting from increased coronary microvascular permeability, while a blunted change in T1 between baseline and NOS inhibition would indicate coronary eNOS dysfunction. Using these methods, we detected an increase in myocardial T1 of 113±15 ms due to NOS inhibition in control mice, but no change in eNOS-/- or HFD mice, demonstrating the eNOS mechanism and detection of coronary endothelial dysfunction in a model of heart disease.

Electronic Poster

Thoracic MRI

Exhibition Hall Wednesday 14:45 - 15:45

4894 Computer 25

Comparison of Differentiation Capability among CEST Imaging, DWI and FDG-PET/CT in Patients with Pulmonary Lesions

Yoshiharu Ohno[1,2], Masao Yui[3], Mitsue Miyazaki[4], Yuji Kishida[5], Sinichiro Seki[1,2], Katsusuke Kyotani[6], and Takeshi Yoshikawa[1,2]

[1]Division of Functional and Diagnostic Imaging Research, Department of Radiology, Kobe University Graduate School of Medicine, Kobe, Japan, [2]Advanced Biomedical Imaging Research Center, Kobe University Graduate School of Medicine, Kobe, Japan, [3]Center for Medical Research and Development, Toshiba Medical Systems Corporation, Otawara, Japan, [4]MR Research, Toshiba Medical Research Institute USA, Vernon Hills, IL, United States, [5]Division of Radiology, Department of Radiology, Kobe University Graduate School of Medicine, Kobe, Japan, [6]Center for Radiology and Radiation Oncology, Kobe University Hospital, Kobe, Japan

Chemical exchange saturation transfer (CEST) imaging is suggested as a new technique for MR-based molecular imaging techniques in vivo and in vitro studies. We hypothesized that newly developed CEST imaging may have a similar potential for differentiating malignant from benign pulmonary nodules and masses, when compared with DWI and FDG-PET/CT. The purpose of this study was to directly and prospectively compare the differentiation capability among CEST imaging, DWI and FDG-PET/CT in patients with pulmonary lesions.

4895 Computer 26

Comparison of the Capability for Quantitative Distinguishing Malignant from Benign Pulmonary Nodules among Dynamic First-Pass CE-Perfusion ADCT and MRI and FDG-PET/CT

Yoshiharu Ohno[1,2], Yuji Kishida[3], Sinichiro Seki[1,2], Shigeharu Ohyu[4], Masao Yui[4], Wakiko Tani[5], Noriyuki Negi[5], Katsusuke Kyotani[5], and Takeshi Yoshikawa[1,2]

[1]Division of Functional and Diagnostic Imaging Research, Department of Radiology, Kobe University Graduate School of Medicine, Kobe, Japan, [2]Advanced Biomedical Imaging Research Center, Kobe University Graduate School of Medicine, Kobe, Japan, [3]Division of Radiology, Department of Radiology, Kobe University Graduate School of Medicine, Kobe, Japan, [4]Center for Medical Research and Development, Toshiba Medical Systems Corporation, Otawara, Japan, [5]Center for Radiology and Radiation Oncology, Kobe University Hospital, Kobe, Japan

Quantification of perfusion parameter from dynamic CE-perfusion MRI at 3T system may be more difficult than that at 1.5T system, and contrast media concentration may have larger influence to measurement error of perfusion parameter on a 3T system. We hypothesized that a bolus injection protocol with appropriately small contrast media volume can provide accurate pulmonary perfusion parameter on dynamic CE-perfusion MRI at a 3T system. The purpose of this study was to determine the appropriate contrast media volume for quantitative assessment of dynamic CE-pulmonary MRI, when compared with dynamic CE-area-detector CT (ADCT) for quantitative evaluation of perfusion within whole lung.

4896 Computer 27

Asthma Ventilation Abnormalities Measured using Fourier-Decomposition Free-breathing Pulmonary [1]H MRI

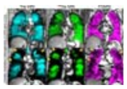

Dante PI Capaldi[1], Khadija Sheikh[1], Rachel L Eddy[1], Sarah Svenningsen[1], Miranda Kirby[2], David G McCormack[3], Grace Parraga[1], and Canadian Respiratory Research Network

[1]Robarts Research Institute, London, ON, Canada, [2]Centre for Heart Lung Innovation, Vancouver, ON, Canada, [3]Division of Respirology, University of Western Ontario, London, ON, Canada

Hyperpolarized noble-gas-MRI provides a way to visualize and regionally measure ventilation-heterogeneity in asthma, which has been shown to be sensitive to treatment response. Fourier-decomposition of free-breathing [1]H MRI (FDMRI) has been proposed as an alternative way to evaluate regional-ventilation without the need for exogenous contrast. We hypothesized that ventilation-abnormalities would be qualitatively and quantitatively similar between the two imaging methods, and hence our objective was to measure ventilation-defects using FDMRI in asthma patients for comparison with inhaled-gas-MRI. Preliminary results in asthma showed that FDMRI ventilation-abnormalities were related to hyperpolarized noble-gas-MRI and clinical measurements of ventilation-heterogeneity in severe-asthmatics.

4897 Computer 28

Multicentre repeatability of ADC estimates from diffusion weighted (DW) MRI in lung cancer: influence of segmentation methodology and statistical descriptor

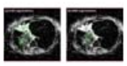

Alexander Weller[1], M-V Papoutsaki[1], JC Waterton[2], Arturo Chiti[3], Matthew Blackledge[1], Matthew Orton[1], David Collins[1], and Nandita de-Souza[1]

[1]Radiotherapy and Imaging, The Institute of Cancer Research, Surrey, United Kingdom, [2]Centre for Imaging Sciences, Division of Informatics Imaging & Data Sciences, University of Manchester, MANCHESTER, United Kingdom, [3]Department of Biomedical Sciences, Humanitas University, Rozzano (Milano), Italy

Using a multi-platform diffusion weighted MRI protocol in lung tumors, apparent diffusion coefficient (ADC) repeatability was well below the change expected for treatment response. ADC coefficients of variation (CoV) varied depending on lesion size and segmentation methodology (range 2.6-10.8%; three times greater for lesions >3cm than lesions<3cm). Performing tumor segmentation on high-b-value images produced lower, more repeatable ADC estimates than if segmenting on low-b-value images. Using median versus mean statistical descriptors for signal averaging prior to ADC calculation did not affect ADC quantitation or repeatability.

4898 Computer 29

Retrospective Image Sorting for Phase REsolved Lung Perfusion Imaging (PRELP)

Andreas Voskrebenzev[1,2], Marcel Gutberlet[1,2], Filip Klimes[1,2], Till Kaireit[1,2], Alexander Rotärmel[1,2], Christian Schönfeld[1,2], Frank Wacker[1,2], and Jens Vogel-Claussen[1,2]

[1]Diagnostic and Interventional Radiology, Medical School Hannover, Hannover, Germany, [2]Biomedical Research in Endstage and Obstructive Lung Disease Hannover (BREATH), German Center for Lung Research (DZL), Hannover, Germany

Currently, only self-gated or ultra-fast sequences allow an adequate temporal resolution to resolve different cardiac phases during lung perfusion. First studies show the benefit of this additional information. Nevertheless such techniques are not widely available. Therefore, in this study a post processing method is assessed, which can increase the temporal resolution by sorting images according to their cardiac phase using a piecewise cosine fit. The feasibility is demonstrated in 6 healthy volunteers and two patients with chronic thromboembolic hypertension (CTEPH). The easy implementation and possibility of retrospective evaluation of existing Fourier Decomposition acquisitions are the advantages of this method.

4899 Computer 30

Free Breathing Regional Alveolar Ventilation Quantification - comparison to Fractional Ventilation derived by Fourier Decomposition Lung MRI

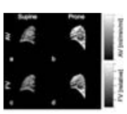

Filip Klimeš[1,2], Andreas Voskrebenzev[1,2], Marcel Gutberlet[1,2], Agilo Kern[1,2], Till Kaireit[1,2], Alexander Rotärmel[1,2], Frank Wacker[1,2], and Jens Vogel-Claussen[1,2]

[1]Institute of Radiology, Hannover Medical School, Hannover, Germany, [2]Biomedical Research in Endstage and Obstructive Lung Disease Hannover (BREATH), Hannover, Germany

Fourier Decomposition (FD) is able to assess lung ventilation and perfusion in one free breathing measurement without any contrast agent. To establish a ventilation-perfusion (VQ) scan robust measurements and absolute quantification is required. Unlike for absolute perfusion quantification, there has been only little success regarding absolute ventilation quantification using FD MRI. Borrowing concepts from oxygen enhanced imaging a regional alveolar ventilation measurement in free breathing is introduced. This method is compared with Fractional Ventilation (FV) and tested for physiological plausibility by assessment of volunteers in supine and prone position. The results show good agreement with available literature and show a similar gravitational behaviour as FV.

4900 Computer 31

Impact of Helium-Oxygen Inhalation on Aerosol Deposition in Asthmatic Rats using UTE-MRI

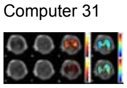

Hongchen Wang[1], Felicia Julea[1], Georges Willoquet[1], Catherine Sebrié[1], Sébastien Judé[2], Anne Maurin[2], Stéphanie Rétif[3], Sharuja Natkunarajah[3], Stéphanie Lerondel[3], Rose-Marie Dubuisson[1], Luc Darrasse[1], Geneviève Guillot[1], Ludovic de Rochefort[1], and Xavier Maître[1]

[1]Imagerie par Résonance Magnétique Médicale et Multi-Modalités (UMR8081) IR4M, CNRS, Univ. Paris-Sud, Université Paris-Saclay, Orsay, France, [2]Centre de Recherches Biologiques, CERB, Baugy, France, [3]Centre d'Imagerie du Petit Animal CIPA, PHENOMIN-TAAM UPS44, CNRS, Orléans, France

Asthma is a worldwide chronic respiratory disease. The common treatment by inhaled therapy needs quantitative imaging approaches to understand the impact of carrier gas on aerosol deposition. 3D UTE-MRI combined with aerosolized Gd-DOTA was applied onto spontaneous breathing and mechanically ventilated asthmatic animals. Here, administration and imaging protocols were developed to ventilate and nebulize control and asthmatic rats in order to compare the resulting aerosol distribution with two carrier gas mixtures: air and helium-oxygen.

4901 Computer 32

Evaluation of Regional Lung Function in Interstitial Lung Disease with Hyperpolarized Xenon-129 Lung 3D SB-CSI

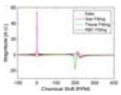

Jaime Mata[1], Kun Qing[1], Nicholas Tustison[1], Tallisa Altes[1,2], John Mugler[1], Michael Shim[1], Lucia Flors[1], Grady Miller[1], and Borna Mehrad[1]

[1]University of Virginia, Charlottesville, VA, United States, [2]University of Missouri, MO, United States

3D Single-Breath Chemical Shift Imaging (3D SB-CSI) is capable of non-invasively assessing regional lung ventilation and gas uptake/exchange within a single breath-hold, typically less than 10 seconds. From this study, we present preliminary clinical results of 3D SB-CSI from healthy and interstitial lungdisease (ILD) subjects. Having novel information on regional changes in ventilation and gas uptake/exchange allows for a better understanding of lung physiology, disease progression, and treatment efficacy.

4902 Computer 33

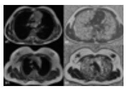

Differentiation of thymic hyperplasia from thymic tumors with MR quantitative fat fraction technique in adulthood

Xiu-Long Feng[1], Yu-Chuan Hu[1], Lin-Feng Yan[1], Shi-jun Duan[1], Gang-Feng Li[1], Xiao-Cheng Wei[2], Guang-Bin Cui[1], and Wen Wang[1]

[1]Department of Radiology, Tangdu Hospital, Fourth Military Medical University, Xi'an, People's Republic of China, [2]MR Research China, GE Healthcare China, Beijing, China

MRI estimated proton density fat fraction (MRI-PDFF) gives quantitative information of fat deposition in soft tissue. This study retrospectively evaluate the effectiveness of MRI-PDFF for distinguishing thymic hyperplasia from thymic tumors. As a conclusion, a significant higher mean fat fraction values were found in thymic hyperplasia compared to thymic tumors. MRI-PDFF technique could be used to differentiate thymic hyperplasia from thymic tumors before treatment.

4903 Computer 34

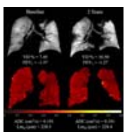

Hyperpolarised 3He Diffusion-Weighted MRI in Mild Cystic Fibrosis Children and Age-matched Healthy Controls

Ho-Fung Chan[1], Guilhem J Collier[1], Laurie Smith[1,2], Helen Marshall[1], Juan Parra-Robles[1], Felix C Horn[1], Graham Norquay[1], Neil J Stewart[1], Chris J Taylor[2], Ina Aldag[2], Alex Horsley[3], and Jim M Wild[1]

[1]Academic Unit of Radiology, University of Sheffield, Sheffield, United Kingdom, [2]Sheffield Children's Hospital, Sheffield, United Kingdom, [3]Manchester Adult CF Centre, Manchester, United Kingdom

Hyperpolarised gas MRI is sensitive to lung ventilation heterogeneity in early cystic fibrosis (CF) disease. However, lung microstructural changes that might accompany early lung disease in CF is less well explored. DW-MRI measurements were compared in mild CF children and age-matched healthy controls, and reassessed after a 2-year interval in the CF group. No significant difference in DW-MRI metrics (in contrast to changes in lung ventilation, VD%) was observed between healthy controls and CF children, and between baseline and 2-year follow-up visits. These results suggest that no acinar microstructural changes occur in early stage CF despite increases in ventilation heterogeneity.

4904 Computer 35

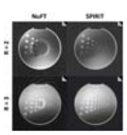

Accelerated Stack-of-Spirals Breath-hold UTE Lung Imaging

John P. Mugler, III[1], Craig H Meyer[2], Josef Pfeuffer[3], Alto Stemmer[3], and Berthold Kiefer[3]

[1]Radiology & Medical Imaging, University of Virginia, Charlottesville, VA, United States, [2]Biomedical Engineering, University of Virginia, Charlottesville, VA, United States, [3]Application Development, Siemens Healthcare, Erlangen, Germany

Stack-of-spirals and cones trajectories have been proposed to permit breath-hold ultrashort-echo-time (UTE) acquisitions of the human lung, although further acceleration would be valuable to permit improvements such as shorter breath-holds for respiratory comprised patients or higher spatial resolution. In this work, an accelerated UTE 3D stack-of-spirals pulse sequence was implemented using undersampled, dual-density spiral waveforms for acquisition and a SPIRiT-based algorithm for image reconstruction. Preliminary testing in healthy volunteers using 2-fold acceleration provided image quality comparable to that achieved with the original, unaccelerated pulse sequence.

4905 Computer 36

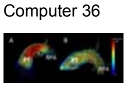

4D and 2D phase-contrast MRI for the evaluation of pulmonary artery hemodynamics in patients with pulmonary hypertension and healthy volunteers

Malte Sieren[1], Clara Berlin[1], Thekla Helene Oechtering[1], Peter Hunold[1], Daniel Droemann[2], Joerg Barkhausen[1], and Alex Frydrychowicz[1]

[1]Clinic for Radiology and Nuclear Medicine, University Hospital Schleswig-Holstein, Lübeck, Germany, [2]Medical Clinic III, Pulmonology, University Hospital Schleswig-Holstein, Lübeck, Germany

2D and 4D phase-contrast MRI (PC MRI) has been subject of recent studies to noninvasively diagnose pulmonary hypertension. The aim of this study was to compare values derived from both imaging techniques in a study collective consisting of healthy volunteers and patients with PH. Although 4D PC MRI generates higher quantitative values in comparison to 2D PC MRI, both sequences were able to distinguish volunteers from patients. In addition, 4D PC MRI visualized blood flow, underlining its additional value to detect secondary flow patterns in patients.

4906 Computer 37

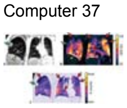

Ultra-fast balanced SSFP signal enhancement ratio mapping of the human lung parenchyma at 1.5T

Orso Pusterla[1,2], Gregor Sommer[3], Mark Wiese[4], Didier Lardinois[4], Michael Tamm[5], Jens Bremerich[3], Francesco Santini[1,2], Grzegorz Bauman[1,2], and Oliver Bieri[1,2]

[1]Department of Radiology, Division of Radiological Physics, University of Basel Hospital, Basel, Switzerland, [2]Department of Biomedical Engineering, University of Basel, Basel, Switzerland, [3]Clinic of Radiology and Nuclear Medicine, Cardiac and Thoracic Imaging, University of Basel Hospital, Basel, Switzerland, [4]Clinic of Thoracic Surgery, University of Basel Hospital, Basel, Switzerland, [5]Clinic of Pneumology, University of Basel Hospital, Basel, Switzerland

In this work, we propose a new conceptual framework for functional pulmonary parenchyma imaging in the clinical setup from two volumetric ultra-fast balanced steady-state free precession (ufSSFP) breath-hold acquisitions before and after contrast agent administration. The resulting signal enhancement ratio (SER) maps of the parenchyma in patients shows similarity to SPECT/CT fusion images. The method requiring only two breath-hold acquisitions is rapid and amenable for clinical use.

4907 Computer 38

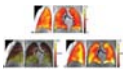

[Free-breathing multi-slice ultra-fast SSFP acquisitions for multi-volumetric morphological and functional lung imaging]

Orso Pusterla[1,2], Grzegorz Bauman[1,2], and Oliver Bieri[1,2]

[1]Department of Radiology, Division of Radiological Physics, University of Basel Hospital, Basel, Switzerland, [2]Department of Biomedical Engineering, University of Basel, Basel, Switzerland

Multi-volumetric breath-hold imaging was recently proposed for respiratory $$$\alpha$$$-mapping, a novel quantitative measure of pulmonary ventilation. In this work, we evaluate the feasibility to derive 3D pulmonary functional maps from morphological lung data which are reconstructed from a time-series of multi-slice 2D ultra-fast SSFP scans acquired in free-breathing (4D-MRI).

4908 Computer 39

High Spatiotemporal Resolution 4D-MRI for Evaluation of Spatially Resolved Pulmonary Function

Hersh Chandarana[1,2], Li Feng[1,2], David Smith[2], Jean Delacoste[3], David Stoffel[2], Priya Bhattacharji[2], Hoi Cheung Zhang[2], Thomas Benkert[1,2], Daniel K Sodickson[1,2], Matthias Stuber[3], Kai Tobias Block[1,2], and Ricardo Otazo[1,2]

[1]Center of Advanced Imaging Innovation and Research (CAI2R), Department of Radiology, New York University School of Medicine, New York, NY, United States, [2]Bernard and Irene Schwartz Center for Biomedical Imaging, Department of Radiology, New York University School of Medicine, New York, NY, United States, [3]Department of Radiology, University Hospital (CHUV) and University of Lausanne (UNIL), Lausanne, Switzerland.

Spirometry provides global measures of lung function, whereas CT provides morphologic information but limited functional information. Current tests are limited in providing spatially resolved function of each lung separately. To address this need, we have developed a 4D ultra-short echo time MRI method where respiratory motion information is extracted directly from the acquired k-space data during normal and deep breathing maneuvers, and motion-resolved reconstruction is performed to extract spatially resolved functional information of each lung. Such a method will improve the ability to diagnose and manage Chronic Obstructive Pulmonary Disease, which is a major cause of death worldwide.

4909 Computer 40

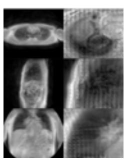

Spatial Tagging to Assess Regional Ventilation of Lung Parenchyma with Endogenous Contrast

Eamon Doyle[1,2], Roberta Kato[3], Jonathan M Chia[4], and John C Wood[1,2]

[1]Biomedical Engineering, University of Southern California, Los Angeles, CA, United States, [2]Cardiology, Children's Hospital of Los Angeles, Los Angeles, CA, United States, [3]Pediatrics, Children's Hospital of Los Angeles, Los Angeles, CA, United States, [4]Philips Healthcare, Gainesville, FL, United States

Tagging techniques such as SPAMM and CSPAMM have been useful for assessment of dynamic cardiac tissue deformation. Recent advances in ultra-short echo time (UTE) imaging have enable imaging of lung parenchyma. In this work, we evaluate the possibility of using spatial tags in conjunction with UTE imaging to assess regional ventilation and tissue stiffness with non-enhanced, endogenous contrast.

4910 Computer 41

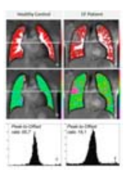

Detection of pulmonary perfusion deficits in patients with cystic fibrosis by means of Self-gated Non–Contrast-Enhanced Functional Lung (SENCEFUL) MRI

Andreas Steven Kunz[1], Andreas Weng[1], Tobias Wech[1], Clemes Wirth[1], Christian Kestler[1], Helge Hebestreit[2], Florian Segerer[2], Thorsten Bley[1], Herbert Köstler[1], and Simon Veldhoen[1]

[1]Institute for Diagnostic and Interventional Radiologiy, University Hospital Wuerzburg, Wuerzburg, Germany, [2]Department of Pediatrics, University Hospital Wuerzburg, Wuerzburg, Germany

The study's purpose was to assess the performance of Self-gated Non–Contrast-Enhanced Functional Lung (SENCEFUL)-MRI in detecting pulmonary perfusion deficits in patients with cystic fibrosis (CF). Nineteen patients with cystic fibrosis and 19 matched healthy controls underwent SENCEFUL-MRI at 1.5T. Four blinded readers rated perfusion and phase (i.e. temporal distribution of pulmonary blood flow) maps separately regarding local deficits followed by simultaneous assessment of both maps. Furthermore, phase data was plotted in histograms for objective comparison to the reader's results. SENCEFUL-MRI revealed statistically significant differences between CF-patients and controls. Furthermore, it demonstrated its potential in detection of pulmonary perfusion deficits.

4911 Computer 42

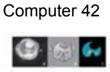

Detecting Differences in Parenchymal and Vascular Oxygenation in the Lungs with Quantitative Susceptibility Mapping

Teckla G Akinyi[1,2], Jinbang Guo[1,3], Jason C Woods[1,3], Chunlei Liu[4], Luke Xie, and Zackary I Cleveland[1,2]

[1]Center for Pulmonary Imaging Research, Cincinnati Children's Hospital Medical Center, Cincinnati, OH, United States, [2]Biomedical Engineering, University of Cincinnati, Cincinnati, OH, United States, [3]Department of Physics, Washington University, Saint Louis, MO, United States, [4]Electrical Engineering and Computer Sciences, University of California -Berkeley, Berkeley, CA, United States

Quantitative susceptibility (QSM) mapping measures the spatial distribution of magnetic susceptibility, and is thus sensitive to the chemical and microstructure properties of tissues. Here we have combined QSM with multi-echo, radial ultra-short echo-time (UTE) MRI to assess regional variations in lung susceptibility in mice. We demonstrate QSM can differentiate between lung parenchyma, which is paramagnetic due to the presence of molecular O2 and pulmonary vasculature which is diamagnetic. Moreover, we demonstrated that the susceptibility differences between these two lung regions increases with increased oxygen partial pressure, demonstrating the approach's sensitivity to regional pulmonary function.

4912 Computer 43

Quantification of regional lung ventilation in COPD patients: Validation of ventilation-weighted Fourier decomposition-MRI with dynamic fluorinated gas MRI and lung function testing.

Till Frederik Kaireit[1,2], Marcel Gutberlet[1,2], Andreas Voskrebenzev[1,2], Julia Freise[3], Tobias Welte[3], Frank Wacker[1,2], and Jens Vogel-Claussen[1,2]

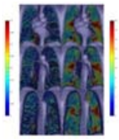

[1]Institute of Diagnostic and Interventional Radiology, Hannover Medical School, Hannover, Germany, [2]Biomedical Research in Endstage and Obstructive Lung Disease Hannover (BREATH), German Center for Lung Research (DZL), Hannover, Germany, [3]Clinic of Pneumology, Hannover Medical School, Hannover, Germany

Quantification of regional lung ventilation is of high relevance for lung diseases like chronic obstructive lung disease (COPD) or asthma. Regional ventilation of the lungs in COPD patients was assessed using ventilation-weighted Fourier decomposition-MRI and validated with real-time dynamic fluorinated MRI and lung function test. Strong correlations were found comparing both techniques with each other and with lung function testing which is used for COPD classification.

4913 Computer 44

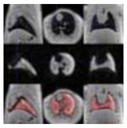

Development and comparison of 19F and hyperpolarized 129Xe lung MRI for preclinical application in mice

Alexandre A Khrapitchev[1], Rohan S Virgincar[1,2], James R Larkin[1], Niloufar Zarghami[1], Sheena Wallington[1], Ana L Gomes[1], Stuart Gilchrist[1], Paul Kinchesh[1], Sean Smart[1], and Nicola R Sibson[1]

[1]CR-UK/MRC Oxford Institute for Radiation Oncology, Department of Oncology, University of Oxford, Oxford, United Kingdom, [2]Biomedical Engineering, Duke University, Durham, NC, United States

The ^{19}F approach is easier and cheaper to implement than the hyperpolarized gas setup and is immediately applicable to a range of pre-clinical work. However, ^{129}Xe MRI provides a unique dynamic tool that may have important applications warranting the additional effort and cost involved. We have compared lung ^{19}F MRI with hyperpolarized ^{129}Xe MRI, in both cases using an Ultra Short Echo (UTE) sequence on a 7.0T preclinical spectrometer.

4914 Computer 45

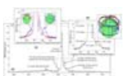

Localized spectroscopy of hyperpolarized xenon-129 dissolved in the human head with a dedicated receiver array

Madhwesha Rao[1], Neil Stewart[1], Graham Norquay[1], Fraser Robb[1,2], and Jim Wild[1]

[1]University Of Sheffield, Sheffield, United Kingdom, [2]GE Healthcare Inc, Aurora, OH, United States

This study investigates the spectral signal of hyperpolarized ^{129}Xe dissolved in the human head in vivo using a dedicated radiofrequency receiver coil array. With a 2.5-fold higher signal to noise ratio of the array compared to a conventional transmit-receive radiofrequency coil, we detected 8 spectral peaks compared to 5 peaks reported in an earlier study. From this, we postulate an individual assignment of spectral peaks for hyperpolarized ^{129}Xe dissolved in white matter and soft cartilaginous tissue, which were previously undistinguishable.

4915 Computer 46

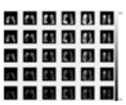

3D mapping of alveolar oxygen partial pressure with hyperpolarized 129Xe.

Iga Muradyan[1], Alan Hrovat[2], Mikayel Dabaghyan[2], and Samuel Patz[1]

[1]Radiology, Brigham and Women's Hospital, Harvard Medical School, Boston, MA, United States, [2]Mirtech, Inc., Brockton, MA, United States

Obtaining regional alveolar pO_2 is a coveted goal in pulmonary medicine, as it reflects both ventilation and perfusion. Hyperpolarized gases, mostly ^{3}He were used to map p_AO_2. For ^{3}He this is straightforward as helium is virtually insoluble in tissue. Xe, however, dissolves into tissue and blood and is carried away from the alveolar space, thus contributes to the loss of the ^{129}Xe MRI signal. To date no attempt has been made to address this issue. Here we report a novel use of SB-XTC to measure p_AO_2 in vivo while simultaneously measuring and taking into account xenon gas exchange on the signal decay.

4916 Computer 47

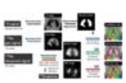

A Pipeline for Quantifying 129Xe Gas Exchange MRI across Pulmonary Disorders

Ziyi Wang[1], Scott Haile Robertson[2], Jennifer Min Wang[3], Mu He[4], and Bastiaan Driehuys[1,2,5]

[1]Biomedical Engineering, Duke University, Durham, NC, United States, [2]Medical Physics Graduate Program, Duke University, Durham, NC, United States, [3]School of Medicine, Duke University, Durham, NC, United States, [4]Electrical and Computer Engineering, Duke University, Durham, NC, United States, [5]Radiology, Duke University Medical Center, Durham, NC, United States

With its solubility and abundant chemical shift in different tissues, hyperpolarized ^{129}Xe is uniquely suited to imaging pulmonary function. Previous efforts have demonstrated the ability to map gas transfer to interstitial barrier tissues and red blood cells (RBCs) using the gas-phase signal as a reference. Here, we extend this analysis by using a healthy reference cohort to establish relevant thresholds for quantitative display. With this methodology we now produce maps of ventilation, barrier uptake, and RBC transfer that demonstrate readily distinguishable patterns in a variety of obstructive, restrictive and vascular disorders.

4917 Computer 48

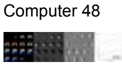

Regional analysis of gas-uptake parameters in the lung using hyperpolarized 129Xe chemical shift saturation recovery spectroscopy and dissolved-phase imaging: a reproducibility study

Agilo Luitger Kern[1,2], Marcel Gutberlet[1,2], Kun Qing[3], Andreas Voskrebenzev[1,2], Filip Klimeš[1,2], Till Kaireit[1,2], Christoph Czerner[1,2], Heike Biller[2,4], Frank Wacker[1,2], Kai Ruppert[5], Jens Hohlfeld[2,4], and Jens Vogel-Claussen[1,2]

[1]Institute of Diagnostic and Interventional Radiology, Hannover Medical School, Hannover, Germany, [2]Biomedical Research in Endstage and Obstructive Lung Disease Hannover (BREATH), German Center for Lung Research (DZL), Hannover, Germany, [3]Department of Radiology and Medical Imaging, University of Virginia, Charlottesville, VA, United States, [4]Clinical Airway Research, Fraunhofer Institute for Toxicology and Experimental Medicine, Hannover, Germany, [5]Department of Radiology, University of Pennsylvania, Philadelphia, PA, United States

We performed a regional analysis of hyperpolarized ^{129}Xe gas-uptake parameters in the lung using localized chemical shift saturation recovery spectroscopy and dissolved-phase imaging with a three-point Dixon method for comparison. Localization of spectroscopic data acquired without spatial encoding was achieved using a 16-channel receive coil and Spectral Localization Achieved by Sensitivity Heterogeneity (SPLASH). The reproducibility of all parameters was studied and coefficients of variation are reported. Localized CSSR data exhibit evidence of gravitational effects in consistency with dissolved-phase imaging. The septal wall thickness derived from evaluation of CSSR data using the Patz model can be determined regionally with high reproducibility.

Electronic Poster

Breast Imaging

Exhibition Hall — Wednesday 14:45 - 15:45

4918 Computer 73

Correlation of dedicated breast PET and dynamic contrast MRI: Appearance of breast background parenchyma and breast cancers

Kanae K. Miyake[1,2,3], Debra M. Ikeda[2], Andrei H. Iagaru[2], Andrew Quon[2], Bruce L. Daniel[2], Jafi A. Lipson[2], Sunita Pal[2], Erik Mittra[2], Haiwei Henry Guo[2], Yuji Nakamoto[3], Shotaro Kanao[3], Masako Kataoka[3], and Kaori Togashi[3]

[1]Radiology, Rakuwakai Otowa Hospital, Kyoto, Japan, [2]Radiology, Stanford University School of Medicine, Stanford, CA, United States, [3]Diagnostic Imaging and Nuclear Medicine, Kyoto University Hospital, Kyoto, Japan

A recently developed ring-shaped PET scanner dedicated for breast (dbPET) provides high-resolution 3D images of a breast. We investigated the correlation between dbPET with ^{18}F-fluorodeoxyglucose and dynamic contrast MRI (DCE-MRI) findings in respect to breast background parenchyma and mass-forming breast cancers. Background parenchymal uptake on dbPET was not associated with background parenchymal enhancement on DCE-MRI. Tumor appearance on dbPET was similar to that on DCE-MRI in majority of cases, suggesting improved spatial resolution of dbPET as well as its feasibility for the use of the combined image analysis with DCE-MRI aiming at functional and structural assessment of primary breast tumors.

4919 Computer 74

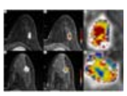

Correlation of Pharmacokinetic Parameters with Prognostic factors of Breast Cancers: a Retrospective Study in Dynamic Contrast-Enhanced MRI with CAIPIRINHA-Dixon-TWIST-VIBE Technique

Yiqi Hu[1], Tao Ai[1], Xu Yan[2], Dominik Nickel[3], and Liming Xia[1]

[1]Radiology, Tongji Hospital, Wuhan, People's Republic of China, [2]Siemens Healthcare, MR Collaboration NE Asia, People's Republic of China, [3]Siemens Healthcare, MR Collaboration

As the use of neoadjuvant chemotherapy is gradually increased in the treatment of breast cancer, evaluating its therapeutic effect is gaining importance. This study investigated the correlation between pharmacokinetic parameters using high spatial and temporal resolution dynamic contrast-enhanced MR imaging (DCE-MRI) and the prognostic factors for breast cancers. The results showed quantitative parameters (Ktrans, kep) were significantly correlated to the prognostic factors (PR, Ki-67) of breast cancers. Quantitative parameters (Ktrans, kep) of high spatial and temporal resolution DCE-MRI may be good indicators of therapeutic effect of patients undergoing neoadjuvant treatment.

4920 Computer 75

Breast Cancer and Body Adiposity by Breast MRI

Wenlian Zhu[1] and Dmitri Artemov[1,2]

[1]Division of Cancer Imaging Research, Department of Radiology, The Johns Hopkins University School of Medicine, BALTIMORE, MD, United States, [2]Department of Oncology, The Sidney Kimmel Comprehensive Cancer Center, The Johns Hopkins University School of Medicine

Using the thickness of the upper abdominal adipose layer measured from breast MRI as a surrogate body adiposity marker, this retrospective investigation validated a positive correlation between breast cancer and body adiposity in a cohort of 1616 breast MRI patients. Additionally, triple negative breast cancer was significantly associated with a younger age and higher body adiposity with respect to the hormone receptor positive breast cancer, while the hormone and HER-2 receptor positive (triple positive) type is only associated with a younger age. A trend of low body adiposity was observed in DCIS patients in the 30 – 49 age range.

4921 Computer 76

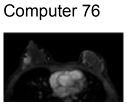

Effect of menstrual cycle on background parenchymal enhancement and the detectability of breast cancer by contrast-enhanced breast MRI: a multicenter study of an Asian population

Takeshi Kamitani[1], Hidetake Yabuuchi[2], Mitsuhiro Tozaki[3], Yoshihide Kanemaki[4], Satoshi Kawanami[5], Koji Sagiyama[1], Yuzo Yamasaki[1], Seitaro Shin[1], and Hiroshi Honda[1]

[1]Department of Clinical Radiology, Kyushu University, Fukuoka, Japan, [2]Department of Health Sciences, Kyushu University, Fukuoka, Japan, [3]Department of Radiology, Sagara Hospital Affiliated Breast Center, Kagoshima, Japan, [4]Breast and Imaging Center, St. Marianna University School of Medicine, Kawasaki, Japan, [5]Department of Molecular Imaging & Diagnosis, Kyushu Universtiy, Fukuoka, Japan

Background parenchymal enhancement (BPE) on breast contrast MRI is known to be associated with the menstrual cycle. We conducted a multicenter study to evaluate the effect of the menstrual cycle on BPE and cancer detectability by contrast-enhanced breast MRI in an Asian population. The Degrees of BPE and cancer detectability were assessed quantitatively and qualitatively. BPE were strongest in the proliferative phase. The detectability of breast cancer was better at the menstrual and proliferative phases than at secretary phase. Not only the proliferative phase but also the menstrual phase is suitable for breast MRI examinations of premenopausal Asian women.

4922 Computer 77

Early enhancement heterogeneity and density on ultrafast bilateral DCE-MRI may differentiate benign and malignant breast lesions

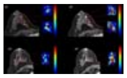

Federico Pineda[1], Naoko Mori[2], Hiroyuki Abe[1], David Schacht[1], and Gregory Karczmar[1]

[1]Radiology, University of Chicago, Chicago, IL, United States, [2]Tohoku University

Heterogeneity of enhancement has been shown to be a marker for malignancy in breast DCE-MRI, however standard dynamic protocols typically have low temporal resolution (60 to 90 seconds). Fast protocols have the advantage of accurately measuring early lesion kinetics. Heterogeneity of lesion enhancement in the first time-point (6 to 9 seconds) after arterial enhancement in the breast differed significantly between malignant and benign lesions; differences were not significant at later time-points.

4923 Computer 78

High Resolution Breast Diffusion Weighted Imaging Using 2-D Navigated Multishot SENSE EPI with Image Reconstruction using Image-Space Sampling Function (IRIS) at 3 T

Habib Rahbar[1], Averi E Kitsch[1], Hans Peeters[2], Adrienne Kim[1], Tyson Nunn[3], and Savannah C Partridge[1]

[1]Radiology, University of Washington, Seattle, WA, United States, [2]Body/Oncology, Philips Healthcare, Best, Netherlands, [3]Radiology, Seattle Cancer Care Alliance, Seattle, WA, United States

Conventional diffusion weighted (DW) MRI relies on a single-shot (SS) echo planar imaging (EPI) acquisition, which suffers from limited spatial resolution and detrimental geometric distortions. Multishot (MS) EPI techniques hold potential to improve the image quality and spatial resolution of DW MRI. We tested the feasibility and performance for breast imaging of a recently developed DW MS-EPI sequence incorporating a novel IRIS image reconstruction approach. Our initial results demonstrate this DW MS-EPI technique to provide robust high resolution breast DW images, with good image quality and reduced geometric distortion compared to conventional DW SS-EPI.

4924 Computer 79

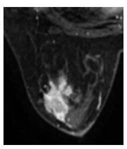

Intravoxel motion diffusion-weighted imaging and dynamic contrast-enhanced MRI of breast: comparison of perfusion-related parameters

Lei Jiang[1], Jiayin Gao[2], Zhujin Xu[2], Xu Lu[2], Dandan Zheng[3], Yiming Zhou[4], and Min Chen[2]

[1]Beijing Hospital, Beijing, People's Republic of China, [2]Beijing Hospital, [3]GE Healthcare, [4]Chaoyang Hospital

IVIM is a research and clinical focus in recent years. Whether its perfusion-related parameters are correlated with those obtained from DCE is still under debate. So the purpose is to investigate their correlation by performing both IVIM and DCE on 31 malignant and 35 benign lesions from 59 patients. Their diagnostic performance and correlation were investigated. No strong correlation was found between them, although their diagnostic performance is similar in terms of perfusion parameters. So IVIM is useful in lesion differentiation and potentially comparable with DCE-derived perfusion-related parameters. IVIM-derived perfusion-related parameters are probably a new entity of microcirculation parameters.

4925 Computer 80

The Clinical Significance of Accompanying NME on Preoperative MR Imaging in Breast Cancer Patients

Hye Mi Gweon[1] and Eun Ju Son[2]

[1]Gangnam Severance Hospital, Yonsei University College of Medicine, Seoul, Korea, Republic of, [2]Gangnam Severance Hospital, Yonsei University College of Medicine

Our study evaluated the significance of accompanying NME in invasive breast cancer on preoperative MR imaging and assess the factors affecting the significance. We found that 24.5 % IDC with mass feature was accompanied by NME on preoperative MR imaging. Among them, 55 % accompanying NME had malignant pathologic results. Especially, HER2 positivity was significantly associated with malignant pathologic results of NME. Our results suggest that the accompanying NME should be carefully investigated on preoperative MR images and individually determined according to molecular subtypes.

4926 Computer 81

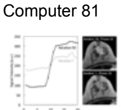

Effect of Compressed Sensing Reconstruction Parameter on Ultrafast Dynamic Contrast Enhanced Breast MRI

Hajime Sagawa[1], Masako Kataoka[1], Shotaro Kanao[2], Natsuko Onishi[2], Maika Urago[3], Marcel Dominik Nickel[4], Masakazu Toi[5], Kyoji Higashimura[1], and Kaori Togashi[2]

[1]Department of Radiology, Kyoto University Hospital, Kyoto, Japan, [2]Department of Diagnostic Imaging and Nuclear Medicine, Kyoto University Graduate School of Medicine, Kyoto, Japan, [3]Kyoto University Hospital, Kyoto, Japan, [4]Siemens Healthcare GmbH, Erlangen, Germany, [5]Department of Breast Surgery, Kyoto University Graduate School of Medicine, Kyoto, Japan

The aim of this study is to assess the impact of the number of iterations of CS reconstruction on kinetic parameters and the image similarity in DCE-MRI of the breast. Breast examinations include ultrafast DCE-MRI using CS were conducted for 21 patients. The images were reconstructed with different numbers of iterations, and the semi-quantitative and quantitative kinetics parameters were compared. The reconstructed images were evaluated by root mean square error (RMSE) and structural similarity (SSIM) as the quantitative image evaluation. In small number of iteration, the all kinetics parameters were underestimated especially in malignant lesion with hypervascularity.

4927 Computer 82

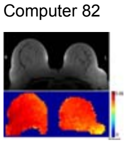

Uniform flip angle 3D tailored excitation for MR breast imaging at 3T

Yi-Cheng Hsu[1,2], Sebastian Littin[2], Ying-Hua Chu[1,2], Fa-Hsuan Lin[1,3], and Maxim Zaitsev[2]

[1]Institute of Biomedical Engineering, National Taiwan University, Taipei, Taiwan, [2]Medical Physics, Department of Radiology, University Medical Center Freiburg, Freiburg, Germany, [3]Department of Neuroscience and Biomedical Engineering, Aalto University, Espoo, Finland

We proposed a two pulses excitation method using the linear gradients to achieve uniform 3D breast excitation. Different to previous studies, we don't need extra hardware and this method is applicable to all MRI systems. Compared to conventional excitation method, our method was able to achieve a more uniform flip angle (8.24% to 5.6%) and the mean flip angle difference between the left and the right breast was improved from 10.2% to 1.5%.

4928 Computer 83

3T full breast diffusion imaging at sub-millimeter resolution with high immunity to artifacts

Eddy Solomon[1], Gilad Liberman[1], Noam Nissan[2], Edna Furman-Haran[3], Miri Sklair-Levy[4], and Lucio Frydman[1]

[1]chemical Physics, Weizmann Institute of Science, Rehovot, Israel, [2]Radiology, Sheba-Medical-Center, [3]Life Sciences Core Facilities, Weizmann Institute of Science, Rehovot, Israel, [4]Sackler School of Medicine,Tel Aviv University

SPatio-temporal ENcoding (SPEN) MRI has been recenlty employed to quantify apparent diffusion coefficients in breast and in other challenging organs, thanks to its high immunity to B_0-inhomogeneities and to chemical shift heterogeneities. In this study a new SPEN protocol is proposed combing multi-band pulses providing full coverage of both breasts with improved signal-noise-ratio, and multi-shot interleaved acquisitions achieving sub-millimeter spatial resolution. This provides a representation of the anatomical features that is similar to TSE, plus diffusion information containing insight into a lesion's nature. Validations and examples are shown at 3T, including healthy female volunteers and patients with breast malignancies.

4929 Computer 84

Comparison of Radial and Cartesian Acquisitions in Breast MRI for Improved Visualization of the Axilla

Ping Ni Wang[1], Roberta M Strigel[1,2,3], Andre Fischer[4,5], Kang Wang[6], Julia V Velikina[1], Frank Korosec[2], Ty A Cashen[6], Kevin M Johnson[1], and James H Holmes[2]

[1]Department of Medical Physics, University of Wisconsin Madison, Madison, WI, United States, [2]Department of Radiology, University of Wisconsin Madison, Madison, WI, United States, [3]Carbone Cancer Center, University of Wisconsin Madison, Madison, WI, United States, [4]Cardiac Center of Excellence, GE Healthcare, Garching bei München, Germany, [5]GE Global Research Europe, Garching bei München, Germany, [6]Global MR Applications & Workflow, GE Healthcare, Madison, WI, United States

Dynamic contrast-enhanced (DCE) MRI is being increasingly used in the detection and diagnosis of breast cancer. Cartesian sampling is routinely used however ghosting artifacts caused by cardiac motion are a well known challenge that in some instances can severely obscure the gland tissue, axilla and even known cancer. Radial sampling has an intrinsic advantage for diminishing motion artifacts by averaging low special frequency signals through oversampling of central k-space data. In this study, we demonstrated the feasibility of using a 3D stack-of-stars radial acquisition to provide motion free images of the entire breast region including the axilla.

4930 Computer 85

Diffusion Kurtosis as an in vivo Imaging Marker for Characterizing Breast Carcinoma: Correlation with Cellular Proliferation

Yao Huang[1], Yan Lin[1], Zhening Wang[1], Jiahao Liang[1], Renhua Wu[1], Weixun Lin[2], and Wei Hu[3]

[1]Department of Radiology, 2nd Affiliated Hospital of Shantou University Medical College, China, Shantou, People's Republic of China, [2]Department of General Surgery, 2nd Affiliated Hospital of Shantou University Medical College, China, Shantou, People's Republic of China, [3]Department of Radiology,1st Affiliated Hospital of Hubei Science and Technology College,Xianning Central Hospital,China, Xianning, People's Republic of China

This study aimed to assess the diagnostic accuracy of DKI technique in breast cancer patients, and to evaluate the potential associations between DKI-derived parameters and cellular proliferation of breast cancer. Mean kurtosis (MK) derived from DKI exhibited the maximal AUCs (0.972) and corresponding optimal sensitivity (90.2%) and specificity (95.2%) for distinguishing malignancy from benign lesions. Furthermore, positive correlation between MK and pathological prognostic factors (Ki-67 expression and histological grade) were found. Preliminary findings highlighted the potential utility of DKI as a sensitive MR sequence for imaging studies and diagnostic improvement of breast masses.

4931 Computer 86

Serial Quantitative BPE measures on MRI: Correlation with 18F-FDG PET SUV measures in Normal Breast Tissue of Patients Undergoing Breast Cancer Therapy

Averi Kitsch[1,2], Habib Rahbar[1,2], Lanell Peterson[3,4], Jennifer Specht[3,4], and Savannah Partridge[1,2]

[1]Radiology, University of Washington, Seattle, WA, United States, [2]Breast Imaging, Seattle Cancer Care Alliance, Seattle, WA, United States, [3]University of Washington, Seattle, WA, United States, [4]Seattle Cancer Care Alliance, Seattle, WA, United States

There is emerging data on the association of background parenchymal enhancement (BPE) on breast MRI with breast cancer risk. However, the underlying mechanism of BPE and its biologic relationship with cancer development remain unknown. Our study investigated the correlation of BPE with FDG PET standardized uptake values (SUV) in normal contralateral breast tissue of 35 women undergoing neoadjuvant chemotherapy. We found quantitative BPE area measures correlated with SUV metrics, and each decreased with therapy. Our findings suggest BPE reflects increased metabolic activity in normal breast tissue, which may provide valuable information for predicting cancer risk and response to therapy.

4932 Computer 87

Restriction Spectrum Imaging in Breast Cancer: Improved Evaluation of Response to Neoadjuvant Chemotherapy

Rebecca Rakow-Penner[1], Nicholas Albino-Kroesing[2], Boya Abudu[2], Nathan White[1], David Karow[1], Hauke Bartsch[1], Joshua Kuperman[1], Dennis Adams[3], Natalie Schenker-Ahmed[1], Anne Wallace[4], Sarah Blair[4], Haydee Ojeda-Fournier[1], and Anders Dale[1]

[1]Radiology, University of California San Diego, La Jolla, CA, United States, [2]University of California San Diego, La Jolla, CA, United States, [3]Pathology, University of California San Diego, La Jolla, CA, United States, [4]Surgery, University of California San Diego, La Jolla, CA, United States

Restriction spectrum imaging (RSI) is an advanced diffusion imaging technique based on a model with increased sensitivity to cancer cells with high nuclear to cytoplasm ratio. This abstract is the initial evaluation comparing RSI to standard diffusion imaging in breast cancer in assessing response to chemotherapy. RSI Z-scores, in comparison to the ADC, demonstrated increased conspicuity and significance in evaluating response to chemotherapy. RSI may be a more reliable diffusion imaging technique in evaluating response to treatment.

4933 Computer 88

Comparison of Breast Pharmacokinetic Parameters in Fat-Water and Water Only Images

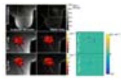

Philip K. Lee[1], Brian A. Hargreaves[2], Bruce L. Daniel[2], and Subashini Srinivasan[2]

[1]Electrical Engineering, Stanford University, Stanford, CA, United States, [2]Radiology, Stanford University, CA, United States

Pharmacokinetic parameters such as K^{trans}, k_{ep} and v_e can be estimated from contrast enhanced breast MRI using Tofts model. Previous simulation has shown that K^{trans} has a maximum bias of 82% at 5s temporal resolutions in the presence of fat. In this work, we have compared the PK parameters estimated from in-phase fat-water, and water-only images in 7 malignant and 4 benign lesions. The presence of fat introduced biases in K^{trans} and k_{ep} respectively of –0.02 min^{-1} and 0.01 min^{-1} in malignant lesions and –0.001 min^{-1} and –0.003 min^{-1} in benign lesions, but did not affect the classification of lesions.

4934 Computer 89

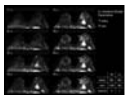

Ultrafast Dynamic Contrast Enhanced MRI of the Breast Using Compressed Sensing: A Novel Technique for Separate Visualization of Breast Arteries and Veins in Very Early Phase

Natsuko Onishi[1], Masako Kataoka[1], Shotaro Kanao[1], Hajime Sagawa[2], Mami Iima[1], Rena Sakaguchi[1], Akane Ohashi[1], Ayami Ohno Kishimoto[1], Marcel Dominik Nickel[3], Masakazu Toi[4], and Kaori Togashi[1]

[1]Department of Diagnostic Imaging and Nuclear Medicine, Kyoto University Graduate School of Medicine, Kyoto, Japan, [2]Division of Clinical Radiology Service, Kyoto University Hospital, Kyoto, Japan, [3]MR Application Predevelopment, Siemens Healthcare GmbH, Erlangen, Germany, [4]Department of Breast Surgery, Kyoto University Graduate School of Medicine, Kyoto, Japan

Ultrafast dynamic contrast enhanced (UF-DCE) MRI using compressed sensing enabled very fast scanning of the breast (every 3.7 sec/frame), and separately visualized breast arteries and veins. Breasts with cancers showed significantly shorter time intervals between arterial and venous visualization than the contralateral breasts without cancers. The time intervals in the breast with cancers tended to be shorter than those in the breasts with benign lesions. Shorter time intervals in breasts with cancers may reflect higher vascularity in malignancy. UF-DCE MRI has a potential to enable the differentiation of breast cancers in very early phase (0-60sec after contrast injection).

4935 Computer 90

Automatic Breast Tumor Segmentation Methods for Mass and Non-mass Lesions for Quantitative Morphology and Texture Analysis

Xinxin Wang[1], Yang Zhang[1], Jeon-Hor Chen[1,2], Siwa Chan[3], and Min-Ying Su[1]

[1]University of California, Irvine, Irvine, CA, United States, [2]E-Da Hospital and I-Shou University, Kaohsiung, Taiwan, [3]Tzu-Chi General Hospital, Taichung, Taiwan

A breast tumor segmentation platform for mass and non-mass tumors on 3D MRI was developed. The segmentation of non-mass lesions is challenging. We developed a new method based on region-growing with the threshold determined by comparison of the intensity histograms in an ROI containing suspicious tumor region vs. outside ROI containing normal fibroglandular tissues. Breast MRI of 122 patients with pathologically-confirmed breast cancer were studied. Of them, 14 had triple negative, 29 had HER2-positive, and 51 had Hormonal-positive, HER2-negative breast cancers. The segmented tumor ROI was analyzed to obtain morphology and texture parameters for differentiation of these 3 molecular subtypes.

4936 Computer 91

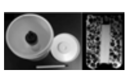

Correction of image distortion and gradient nonlinearity in DTI of breast cancer

Lisa J Wilmes[1], Ek T Tan[2], Evelyn Proctor[1], Jessica Gibbs[1], Nola M Hylton[1], and David C Newitt[1]

[1]Radiology and Biomedical Imaging, University of California San Francisco, San Francisco, CA, United States, [2]GE Global Research, Niskayuna, NY

The individual and combined effects of correction for susceptibility-induced distortion, distortion due to eddy currents, and bias from gradient non-linearity on breast DTI metrics were evaluated. Using an ice-water phantom we found that the correction of gradient nonlinearity resulted in strong bias reduction, while the distortion correction provided further reduction of bias and variance. The effects of these corrections were quantified in 12 subjects with malignant breast tumors and found to parallel the effects measured in the phantom.

4937 Computer 92

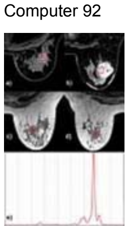

Locally altered lipid profiles: a hallmark of breast cancer metabolism?

Ileana Hancu[1], Christopher Sevinsky[1], Beatrice Andre[2], Fiona Ginty[1], Elizabeth Morris[2], and Sunitha Thakur[2]

[1]GE Global Research Center, Niskayuna, NY, United States, [2]Memorial Sloan Kettering Cancer Center, New York City, NY, United States

Cancer cells are known to produce their own fatty acids (FA's) and co-opt local fat reserves for energy/cell division needs. In this study, single-voxel MRS data were used to assess the spatial/spectral lipid profiles of normal volunteers and subjects with suspicious lesions. Statistically different lipid profiles were found in tumors than in the contralateral breast of cancer patients; the latter were similar to lipid profiles of normal volunteers. Fibrocystic epithelial/breast cancer cell NMR experiments confirmed differential FA composition/uptake for the two cell types. MRI/MRS-based profiling of lipid metabolism may provide a unique tool for better breast cancer tumor detection/characterization.

4938 Computer 93

Enabling high resolution MRE images of the breast

Stefan Heinz Hoelzl[1], Sweta Sethi[2], Jelizaveta Sudakova[1], Ayse Sila Dokumaci[1], Jurgen Henk Runge[1], Tony Ng[3], Arnie Purushotham[4], and Ralph Sinkus[1]

[1]Division of Imaging Sciences and Biomedical Engineering, King's College London, London, United Kingdom, [2]Department of Research Oncology, Guy's and St Thomas' NHS Foundation Trust, London, United Kingdom, [3]Division of Cancer Studies, King's College London, London, United Kingdom, [4]Department of Imaging Chemistry and Biology, King's College London, London, United Kingdom

Achieving high-resolution MR-Elastography images of the breast is a challenge due to shear wave attenuation and shadowing effects in breast tissue resulting in loss of wave energy and hence poor signal to noise ratio. We present a novel breast transducer set-up to ensure complete wave penetration throughout the entire breast. Waves reach even far upwards to enable quantification of axillary lymph nodes. Mechanical vibrations are generated via a novel concept utilizing an eccentric rotor that yields inherently constant amplitude with driving frequency. Volunteer results of wave speed and attenuation at 2mm isotropic resolution are presented including the axilla region.

4939 Computer 94

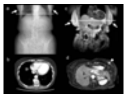

The detectability of mammary lesions dependent on the patients' arm position and breathing style during a liver study

Yasuo Takasu[1,2], Yuko Shimada[1], Tosiaki Miyati[2], and Toshiki Shiozaki[1]

[1]Osaka Red Cross Hospital, Osaka, Japan, [2]Division of Health Sciences, Graduate School of Medical Sciences, Kanazawa University., Kanazawa, Japan

This study aimed to evaluate whether the incidental finding of the mammary lesions was influenced by the patient's arm position and respiration style during liver magnetic resonance imaging (MRI). If the mammary lesion was detected earlier, treatment could be performed earlier. Therefore, the finding of mammary lesion during liver studies was useful information. The incidental detection of mammary lesions was influenced by the patient's arm position and breathing style. Unexpected mammary lesions could be detected when the arms were positioned at the sides of the body and the exhalation style was used during liver MRI.

4940 Computer 95

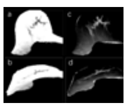

Co-registration of Breast MRI and CT Using Gravity Unloading

Yang Zhang[1], Jeon-Hor Chen[1,2], Siwa Chan[3], and Min-Ying Su[1]

[1]Tu & Yuen Center for Functional Onco-Imaging, University of California, Irvine, Irvine, CA, United States, [2]E-Da Hospital and I-Shou University, Kaohsiung, Taiwan, [3]Tzu-Chi General Hospital, Taichung, Taiwan

A biomechanical simulation method for co-registration of breast MRI and low-dose chest computed tomography (LDCT) images is presented, by aligning the images in a virtually unloaded configuration. The breast tissue was considered as neo-Hookean material, and the finite element method was applied to simulate the deformation from gravity-unloading. The Demon's non-rigid registration algorithm was applied to co-register the gravity-unloaded MRI and LDCT models. Fourteen normal subjects who received both breast MRI and LDCT for breast and lung cancer screening were analyzed. The results show that the pre-processing using gravity unloading can facilitate the co-registration of LDCT and MRI.

4941 Computer 96

Development of Robust Texture Parameters for Characterizing Normal Breast Parenchymal Patterns

Yang Zhang[1], Jeon-Hor Chen[1,2], Siwa Chan[3], Dah-Cherng Yeh[4], and Min-Ying Su[1]

[1]Tu & Yuen Center for Functional Onco-Imaging, University of California, Irvine, Irvine, CA, United States, [2]E-Da Hospital and I-Shou University, [3]Tzu-Chi General Hospital, Taichung, Taiwan, [4]Taichung Veterans General Hospital, Taichung, Taiwan

The non-fat-sat T1-weighted breast MRI of 57 normal healthy women were analyzed. In order to test the robustness of parameters we compared the texture analyzed from the ROI's of different sizes as the largest cuboid that can fit within the breast and cover 30%, 40%, and 50% of fibroglandular tissue slices. 21 texture features were selected as robust features that were not greatly affected by the cuboid ROI size. The concordance correlation coefficient of the percent density between bilateral breasts was very high, 0.98. Of all texture parameters, "Information Measure for Correlation (IMC)" and "Contrast" show the highest ccc, 0.90-0.98.

Electronic Poster

Body: Cancer

Exhibition Hall — Wednesday 14:45 - 15:45

4942 Computer 97

Investigating the role of DCE-MRI, over T2 and DWI, in accurate PIRADS-v2 assessment of clinically significant peripheral zone prostate lesions, as defined at radical prostatectomy

Mehdi Taghipour[1], Elmira Hassanzadeh[1], Francesco Alessandrino[2], Mukesh Harisinghani[3], Clare M.C Tempany[1], and Fiona M Fennessy[1,2]

[1]Radiology, Harvard Medical School, Brigham and Women's Hospital, BOSTON, MA, United States, [2]Imaging, Dana-Farber Cancer Institute, Boston, MA, United States, [3]Radiology, Harvard Medical School, Massachusetts General Hospital, Boston, MA, United States

DCE has a secondary role in detecting peripheral zone lesions using PIRADS v2 and is limited to PZ lesion with DWI score of 3. The goals of this study are to determine the frequency with which DCE plays a role changing the final PI-RADS assessment score for PZ lesions, and 2) determine the accuracy of DCE-MRI in upgrading the assessment score . 271 patients with biopsy proven prostate cancer diagnosis, a mp-MRI, and who underwent curative radical prostatectomy were included in the study. DCE played a role only in 16.6% (45/271) of patients and showed sensitivity of 63.8% in upgrading lesions. In conclusion, the added value of DCE to T2-WI and DWI is very limited in diagnosis of csPC.

4943

Computer 98

Fine-tuned Deep Convolutional Neural Network for Automatic Detection of Clinically Significant Prostate Cancer with Multi-parametric MRI

Xinran Zhong[1,2], Hung Le Minh[3], Holden Wu[1,2], Michael Kuo[1], Steven Raman[1], William Hsu[1], Xin Yang[3], and Kyunghyun Sung[1,2]

[1]Department of Radiological Sciences, University of California, Los Angeles, Los Angeles, CA, United States, [2]Physics and Biology in Medicine IDP, University of California, Los Angeles, Los Angeles, CA, United States, [3]School of Electronics Information and Communications, Huazhong University of Science and Technology, Wuhan, People's Republic of China

A deep convolutional neural network (CNN) based automatic classification system to distinguish between indolent and clinically significant prostate carcinoma using multi-parametric MRI (mp-MRI) is proposed. By applying data augmentation, 138 lesions were used to fine-tune the pre-trained CNN model called Overfeat. Those fine-tuned models were then shown to provide better performance than existing pre-trained CNN method, texture features based system as well as PI-RADS standards on a separate 40 testing cases.

4944 Computer 99

Low-To-High b-Value DWI Ratio Image in Multiparametric MRI of the Prostate: Feasibility, Optimal Combination of b-Values, and Comparison with ADC Maps for the Detection of Prostate Cancer

Franklin Olumba[1], Parker Lawson[1], Alexander Liu[1], Robert E. Lenkinski[1], Qing Yuan[1], Ivan Pedrosa[1], Gaurav Khatri[1], Takeshi Yokoo[1], Daniel Costa[1], and Yin Xi[1]

[1]Radiology, UT Southwestern Medical Center, Dallas, TX, United States

This study demonstrated the feasibility of generating a DWI-based image that compares the signal intensity on low versus high b-values (DWI_{ratio} image) and compared this model-independent approach to the conventional ADC map in terms of quantitative relative contrast (RC) in signal intensity between lesion and normal tissues and subjective assessment of artifacts, lesion conspicuity, and overall image quality by blinded radiologists. The DWI_{ratio} images showed significantly higher RD and lower artifacts and non-inferiority in lesion conspicuity and overall image quality. The model-independent nature of this approach has the potential to improve inter-subject and inter-vendor reproducibility of DWI data for the detection of prostate cancer when compared to ADC maps.

4945 Computer 100

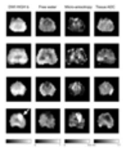

Mapping prostatic microscopic anisotropy using linear and spherical b-tensor encoding: A preliminary study

Markus Nilsson[1], Filip Szczepankiewicz[2], Mikael Skorpil[3,4], Carl-Fredrik Westin[5], Lennart Blomqvist[3,4,6,7], and Fredrik Jäderling[6,7]

[1]Clinical Science, Radiology, Lund University, Lund, Sweden, [2]Clinical Sciences Lund, Medical Radiation Physics, Lund University, Lund, Sweden, [3]Department of Radiology, Uppsala University, Uppsala, Sweden, [4]Department of Radiation Sciences, Umeå University, Umeå, Sweden, [5]Brigham and Women's Hospital, Harvard Medical School, Boston, MA, United States, [6]Department of Molecular Medicine and Surgery, Karolinska Institute, Stockholm, Sweden, [7]Department of Diagnostic Radiology, Karolinska University Hospital, Solna, Sweden

Diffusion tensor imaging (DTI) has the potential to improve prostate cancer detection, since anisotropy is expected to correlate with tumor aggressiveness and differentiation. Differences in fractional anisotropy between cancer and normal tissue have been observed, although data is somewhat contradictory. A problem with DTI is its inability to distinguish low anisotropy from high orientation dispersion. In this study, we map the anisotropy independent of orientation in the prostate, by the use of a novel diffusion-encoding technique that permits encodings with variable b-tensor shapes. The microscopic anisotropy was found to be generally higher in cancer than in normal prostatic tissue.

4946 Computer 101

Preoperative breast MR Imaging in patients with primary breast cancer has the potential to decrease the rate of repeated surgeries

Heike Preibsch[1], Benjamin Wiesinger[1], Claus Claussen[1], Konstantin Nikolaou[1], and Katja C Siegmann-luz[2]

[1]Diagnostic and Interventional Radiology, University Hospital Tuebingen, Tuebingen, Germany, [2]Diagnostic Breast Center and Mammography Screening Brandenburg Ost

In our study cohort the mastectomy rate did not differ (39 % vs. 39 %) between patients with and without preoperative breast MRI, although tumor stages and focality were higher in the group of patients undergoing MRI. Breast MRI was beneficial for 20.3 % (127/626) of the patients as additional foci of cancer in the same or contralateral breast were diagnosed (n=122) or MRI could prove a lesser extent of carcinoma (n=5). Patients receiving preoperative MRI had a lower chance of repeated surgery (p=0.007). Preoperative breast MRI did not delay surgery (20.3 days vs. 19.8 days, p=0.7).

4947 Computer 102

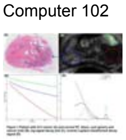

Inverse Laplace transform analysis using a fast multi-echo TSE sequence for prostate cancer diagnosis

Shiyang Wang[1], Harsh Agrawal[2], Milica Medved[1], Tatjana Antic[3], Ambereen Yousuf[1], Gregory Karczmar[1], Roger Bourne[4], and Aytek Oto[1]

[1]Radiology, University of Chicago, Chicago, IL, United States, [2]R&D Institute, Samsung R&D Institute, Bangalore, India, [3]Pathology, University of Chicago, Chicago, IL, United States, [4]Health Science, University of Sydney, Sydney, Australia

To evaluate the inverse Laplace model fitting to multiple TE TSE data for prostate cancer diagnosis. Prostate tissue has glandular structure with luminal volume and epithelial cells forming the walls of gland. The underlying physical phenomenon in prostate cancer can be accurately captured using two-compartment T2 decay modeling. It is impossible to acquire MR images to perform accurate multi-compartment T2 decay model in clinically feasible scan times since multiple T2W MRI images over a wide range of echo times are required. Recently a fast multi-echo TSE (ME-TSE) T2 mapping technique, k-t-T2 MRI was developed to obtain high resolution T2 maps in clinically feasible scan time. In this study, a new implementation of the inverse Laplace transform was applied to the multi-echo TSE T2WI data. We present evidence that multiple slow components can be present in the decaying T2WI signal in the normal tissue in the prostate but were absent in pathology confirmed cancers on k-t-T2 data.

4948 Computer 103

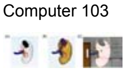

3D Virtual Reality Models Created from MRI data for Pre-operative Evaluation of Renal Cancer

Nicole Wake[1], William C. Huang[2], James F. Borin[2], Daniel K. Sodickson[1], and Hersh Chandarana[1]

[1]Bernard and Irene Schwartz Center for Biomedical Imaging, Center for Advanced Imaging Innovation and Research, Department of Radiology, New York University School of Medicine, New York, NY, United States, [2]Department of Urology, New York University School of Medicine, New York, NY, United States

The objective of this study was to create patient-specific 3D virtual reality kidney cancer models and to evaluate pre-operative planning decisions made using these models. Virtual 3D models were compared to 3D printed models. These models may alter the surgical plan, and could promote both nephron-sparing surgery and preservation of healthy parenchyma, as surgeons gain a better visualization of the size and location of a tumor in relation to normal tissue and vital structures.

4949 Computer 104

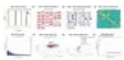

Diagnostic Performance in MR-visible Prostate Cancer: Can a Quantitative Computer-aided Diagnosis System Be Superior to the Qualitative PI-RADS v2 Guideline?

Jing Wang[1], Yang Fan[2], and Yudong Zhang[3]

[1]Center for Medical Device Evaluation, CFDA, Beijing, People's Republic of China, [2]MR Research China, GE Healthcare, Beijing, People's Republic of China, [3]Department of Radiology, the First Affiliated Hospital with Nanjing Medical University, Nanjing, People's Republic of China

A novel CAD system was developed for prostate cancer detection based on multi-parametric MRI, including textured T2w, DKI and Tofts-Ktrans. MR features were evaluated by using machine-assisted classification methods such as PCA and SVM analysis. The validation performed in 54 patients confirmed as PCa, to determine whether the CAD has the ability to correct diagnosis in MR-visible prostate cancer, as comparison with a proposed structured PI-RADS v2. Our results showed that the automatic PCa detection using CAD had significantly higher AUC than PI-RADS v2 in distinguishing cancer from normal prostate tissue.

4950 Computer 105

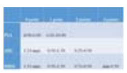

Developing pre-biopsy multiparameteric MRI based risk calculator for predicting prostate cancer in men with PSA 4-10 ng/ml

Durgesh Kumar Dwivedi[1,2], Rajeev Kumar[3], Alok Kumar Dwivedi[4], Girdhar S. Bora[3], Sanjay Thulkar[5], Sanjay Sharma[5], Siddhartha Datta Gupta[6], and Naranamangalam R. Jagannathan[1]

[1]Department of NMR and MRI Facility, All India Institute of Medical Sciences, New Delhi, Delhi, India, [2]Department of Radiodiagnosis, King George's Medical University, Lucknow, India, [3]Department of Urology, All India Institute of Medical Sciences, New Delhi, Delhi, India, [4]Division of Biostatistics and Epidemiology, Department of Biomedical Sciences, Texas Tech University Health Sciences Center, El Paso, Texas, TX, United States, [5]Department of Radiodiagnosis, All India Institute of Medical Sciences, New Delhi, New Delhi, India, [6]Department of Pathology, All India Institute of Medical Sciences, New Delhi, New Delhi, India

Risk calculators have traditionally utilized PSA values in addition to the clinical variables to predict risk assessment of prostate cancer (PCa). For the first time, we aimed to develop pre-biopsy mpMRI based simple risk score (RS) and a predictive model in predicting the risk of PCa in men with clinically challenging value of PSA (4-10 ng/ml) if a TRUS-guided biopsy is performed. The predictive model and developed simplistic 6-point mpMRI score based risk calculator in this study could be routinely used in predicting PCa in clinical management for men with PSA 4-10 ng/ml.

4951 Computer 106

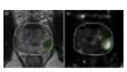

Impact of Temporal Resolution on Quantitative DCE-DISCO Measurements in Prostate Cancer

James A Rioux[1,2,3], Peter M Lakner[1,4], Steve Patterson[1], Mark Parker[1,5], Jennifer Merrimen[6], Cheng Wang[6], Chris V Bowen[1,2,3], and Sharon Clarke[1,2,3]

[1]Biomedical Translational Imaging Centre (BIOTIC), Nova Scotia Health Authority, Halifax, NS, Canada, [2]Diagnostic Radiology, Dalhousie University, Halifax, NS, Canada, [3]Physics and Atmospheric Science, Dalhousie University, Halifax, NS, Canada, [4]Computer Science, Dalhousie University, Halifax, NS, Canada, [5]School of Health Sciences, Dalhousie University, Halifax, NS, Canada, [6]Pathology, Dalhousie University, Halifax, NS, Canada

Depending on the particular application, the temporal resolution of dynamic contrast-enhanced MRI may have an impact on measurements of quantitative parameters related to contrast agent kinetics. In this study we retrospectively altered the temporal resolution of DCE-DISCO acquisitions in patients with prostate cancer, and examined the effect on the rate constant K^{trans} in both normal tissue and cancer (as confirmed by histopathology). The difference in mean K^{trans} values between tissue types was found to vary significantly with temporal resolution between 4 and 10s, suggesting that the uptake dynamics in cancer are more accurately sampled at higher temporal resolution.

4952 Computer 107

Automatic Segmentation and Tracking of Tumor Associated Vasculature Using High-temporal Resolution Dynamic Contrast Enhanced MRI of the Breast: Preliminary Results

Chengyue Wu[1], Federico D. Pineda[2], Gregory S. Karczmar[2], and Thomas E. Yankeelov[1]

[1]Department of Biomedical Engineering, The University of Texas at Austin, Austin, TX, United States, [2]Department of Radiology, The University of Chicago

We present a post-processing analysis of high-temporal resolution dynamic contrast enhanced MRI (DCE-MRI) data to automatically detect, segment, and track tumor associated vasculature within the breast. We hypothesize that such an analysis will be useful in both the diagnostic and prognostic settings.

4953 Computer 108

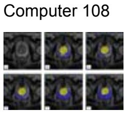

A New Multi-Atlas Selection Strategy for Zone Segmentation of the Prostate

Michela Antonelli[1], Edward W Johnston [2], Manuel Jorge Cardoso[1], Benoit Presles[1], Shonit Punwani*[2], and Sebastien Ourselin*[1,3]

[1]Translational Imaging Group, CMIC, University College London, London, United Kingdom, [2]Academic Radiology, University College London Centre for Medical Imaging, London, UK, [3]Dementia Research Centre, Department of Neurodegenerative Disease, UCL Institute of Neurology, London, UK

Automatic segmentation of the prostate into peripheral and transition zones is paramount in developing computer aided diagnosis systems for prostate cancer diagnosis, as cancer behaves differently in each zone. We propose a multi-atlas based segmentation (MAS) algorithm characterized by a new atlas selection strategy: the performance of a subset of atlases is evaluated considering how well that subset segments the image that is most similar to the target image. Comparison of our method with three other MAS algorithms on fifty-five patients shows a statistically significant improvement on the segmentation accuracy.

4954 Computer 109

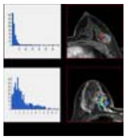

Contribution of Radiomics Features from DCE-MRI and DWI in Differentiating Benign from Malignant Lesions in Suspicious Breast (MRI BI-RADS Category 4) Findings

Bin Hu[1], Lina Zhang[2], Ke Xv[2], Shu Li[2], Songbai Li[2], Ning Huang[3], and Yan Guo[3]

[1]First Affiliated hospital of China Medical University, Shenyang, People's Republic of China, [2]First Affiliated hospital of China Medical University, [3]GE Healthcare， Lifescience， China

We aimed to find a promising tool to improve the diagnostic efficiency of suspious breast lesions classified in BI-RADS Category 4 from malignant lesions in order to avoid unnecessary biopsy,surgery,even psychological pressure. 33 patients (all female, 27y-82y) were included in our retrospective study and all underwent pre-operative breast DCE-MRI and DWI using a 3.0T MRI (SIEMENS Magntom Verio 3.0T).The radiomics features were acquired by Omni-Kinetics software (GE Healthcare).Non-parametric test and ROC curve were used in statistical analysis.The results implied that the radiomics parameters,especially skewness, kurtosis,IDM and inertia in Ktrans and ADC had great potential.

4955 Computer 110

Prostate cancer detection with multiparametric MRI based computer-aided diagnosis: which sequence is the dominant technique

Ge Gao[1], Xiaoying Wang, Chengyan Wang, and Jue Zhang

[1]Radiology, Peking University First Hospital, Beijing, People's Republic of China

Differ from PI-RADS v1, the updated PI-RADS v2 offers a decision process that puts the sequences as different role in scoring process and results in a final five-point score. However, the efficiency of each sequence in prostate cancer (PCa) detection in peripheral zone (PZ) and transition zone (TZ) is investigated by radiologists reading test preliminarily, which is highly depends on reader's expertise and experience. This work applied a previous published machined learning model to investigate the weight of different sequences, including T2WI, DWI/ADC and DCE, in clinical significant PCa detection, and found that DWI/ADC performed the best both in PZ and TZ clinical significant PCa detection among these basic sequences which is recommended by PI-RADS v2

4956 Computer 111

Prostate shapes between prostate cancer patients with and without biochemical recurrence post-treatment are different : Preliminary study

Soumya Ghose[1], Rakesh Shiradkar[1], Jhimli Mitra[1], Rajat Thawani[1], Mirabela Rusu[2], Michael Feldman[3], Amar Gupta[4], Andrei Purysko[5], Lee Ponsky[6], and Anant Madabhushi[1]

[1]Department of Biomedical Engineering, Case Western Reserve University, Cleveland, OH, United States, [2]GE Global Research, [3]Perelman School of Medicine, University of Pennsylvania, [4]Diagnostic Radiology, Cleveland Clinic Foundation, Cleveland, OH, [5]Diagnostic Radiology, Cleveland Clinic Foundation, Cleveland, OH, United States, [6]Urology, Case Western Reserve University School of Medicine

In a single center IRB approved retrospective study, statistically significant differences in the shape of the prostate gland were observed between BCR+ and BCR- populations.

4957 Computer 112

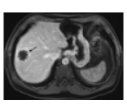

Poor enhancement of colorectal liver metastases on delayed phase gadobutrol enhanced MRI may be related to increased number of APC mutations

Helen Cheung[1], Arun Seth[2], Yutaka Amemiya[2], Eugene Hsieh[3], Paul Karanicolas[3], Natalie Coburn[3], Xiaoyang Liu[3], Vikrum Seth[2], Calvin Law[3], and Laurent Milot[1]

[1]Medical Imaging, Sunnybrook Health Sciences Centre, University of Toronto, Toronto, ON, Canada, [2]Sunnybrook Research Institute, [3]Sunnybrook Health Sciences Centre

We recently demonstrated that delayed enhancement of colorectal liver metastases (CRLM) on gadobutrol-enhanced MRI is associated with long-term survival. We performed a hypothesis-generating pilot study to determine whether delayed enhancement on MRI is related to the number and types of genetic mutations. There were a greater number of somatic APC mutations in hypoenhancing tumors compared to isoenhancing tumors or hyperenhancing tumors (N=15, p=0.013). There was no difference in the number of germline mutations or number of overall somatic mutations among MRI groups. Poor enhancement of CRLM on delayed phase gadobutrol-enhanced MRI may correlate with increasing number of somatic APC mutations.

4958 Computer 113

Rectal perfusion parameters normalized to tumour free rectal wall can predict complete pathological response to neoadjuvant chemoradiotherapy.

Sonal Krishan[1] and Anirudh Kohli[2]

[1]Radiology, Medanta Hospital Gurgaon, Gurgaon, India, [2]Radiology, Medanta Hospital, India

The aim of this study was to evaluate absolute and normalized change in qualitative and semi quantitative perfusion parameters in predicting complete pathological response to CRT. Perfusion parameters of Pre and post treatment imaging of histopathologically proven 10 patients with rectal cancer who had complete response and complete absence of tumour on histopathology following complete treatment (Group 1) were compared with 10 patients with residual tumour on histopathology following treatment (Group 2). The two groups were matched for T stage of tumour. Semiquantittaive perfusion MRI parameters (Ktrans, Kep, Ve, IAUC; Toft model) were quantified by manually delineating a region of interest in the upper, mid and lower third of tumour at least 1cm square, in addition similar parameters were obtained from the normal rectal wall atleast 1cm away from the potential resection margin, absolute as well as values normalized values to the perfusion in the normal rectal wall were evaluated. Qualitative perfusion parameters were also assessed (wash in, wash out, TTP, AT, PEI, iAUC). After CRT, all patients underwent complete surgical resection and the surgical specimen served as the gold standard. Difference in absolute and normalized qualitative parameters were compared within each group using paired t-test and between each group using ANOVA. Washin, Washout, PEI, Ktrans, IAUC in the complete pathological responders when normalized to the adjacent normal rectal wall showed ratio's approaching near 1 suggesting that rectal perfusion returns similar to the adjacent normal rectal wall in complete pathological responders. The difference in the normalized values in the responders and non responders was statistically significant. Within group change in absolute mean values in the responders and non responders was not statistically significant. Perfusion parameters can be used in predicting response to treatment, when normalised to the adjacent normal rectal wall.

4959 Computer 114

Differentiation of low- and high- grade hepatocellular carcinomas with texture features and a machine learning model in arterial phase of contrast-enhanced MR

Wu Zhou[1], Qiyao Wang[1], Guangyi Wang[2], Zaiyi Liu[2], Changhong Liang[2], and Lijuan Zhang[1]

[1]Shenzhen Institutes of Advanced Technology, Chinese Academy of Sciences, Shenzhen, People's Republic of China, [2]Department of Radiology, Guangdong General Hospital, Guangdong Academy of Medical Sciences

Texture has been a recognized feature for biological aggressiveness of hepatocellular carcinomas (HCCs). However, texture feature alone may not be optimal to characterize malignancy of HCC. Computer-aided techniques combined with multi-feature fusion may be a method of choice for the preoperative assessment of the aggressiveness of HCC. To this end, a computer-aided method in the combination with machine learning technique based on texture analysis for malignancy differentiation of HCCs was desmonrated and high classification performance(AUC>0.9) of the classifier was achieved to differentiate low- and high- grade of HCCs.

4960 Computer 115

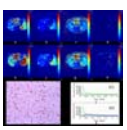

Quantitative dynamic contrast enhanced magnetic resonance imaging of hepatocellular carcinoma: A prospective self-control study between single and dual input arterial function

Meiling Li[1], Jian Lu[1], Hongwei Liang[1], Jifeng Jiang[1], and Peng Cao[2]

[1]Department of Radiology, Nantong Third People's Hospital, Nantong University, Nantong, People's Republic of China, [2]GE healthcare, Shanghai, People's Republic of China

This prospective self-control study was designed to explore if there is difference between single and dual arterial input function (AIF) for analyzing quantitative dynamic contrast enhanced magnetic resonance imaging (DCE-MRI) of hepatocellular carcinoma (HCC). Our result showed that there is no statistical difference of quantitative parameters K^{trans}, V_e, V_p between single and dual AIF groups. The parameter K_{ep} was different between two groups, but it had a parallel relationship with CD34-MVD of HCC, for that, dual AIF didn't have advantage over single AIF.

4961 Computer 116

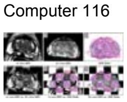

A New System to Spatially Align In Vivo MRI, Ex Vivo MRI, and Whole-Mount Histopathology Slides for Integrated Prostate Cancer Research

Holden H Wu[1,2], Steven Raman[1], Pooria Khoshnoodi[1], Alan Priester[2], Kyunghyun Sung[1,2], Daniel Margolis[1,3], Preeti Ahuja[1], Anthony Sisk[4], Jiaoti Huang[4,5], Robert Reiter[6], and Dieter Enzmann[1]

[1]Radiological Sciences, UCLA, Los Angeles, CA, United States, [2]Bioengineering, UCLA, Los Angeles, CA, United States, [3]Radiology, Cornell University, New York, NY, United States, [4]Pathology, UCLA, Los Angeles, CA, United States, [5]Pathology, Duke University, Durham, NC, United States, [6]Urology, UCLA, Los Angeles, CA, United States

Multi-parametric MRI is an indispensable tool for prostate cancer (CaP) management and spatial alignment of in vivo MRI to histopathology is critical for its development. In addition, ex vivo MRI has distinct advantages for investigating ultrahigh-resolution MRI and quantitative MRI of CaP. In this work, we propose a new system for spatial alignment of in vivo MRI, ex vivo MRI, and whole-mount histopathology slides. Results from a pilot study of CaP patients demonstrate successful integration with the clinical workflow and good spatial alignment of the image sets. This new system may enable novel research of CaP biomarkers and predictive models.

4962 Computer 117

Comparison of Radiologist Perception of Image Quality of Advanced Diffusion vs. RESOLVE Diffusion

Bonnie N. Joe[1], Kimberly Ray[1], Amie Lee[1], Vignesh Arasu[1], Lisa Wilmes[1], Vibhas Deshpande[2], Sinyeob Ahn[2], and Nola Hylton[1]

[1]Radiology and Biomedical Imaging, UCSF, San Francisco, CA, United States, [2]Siemens Medical Solutions

In order to gain acceptance of DWI in the clinical setting, consistent high image quality with minimal breast distortion is required. Although time of acquisition is slightly longer for the RESOLVE compared with the advanced diffusion sequence, the benefits of improved image quality, particularly with respect to image distortion and phase ghosting are preferred by clinical breast imaging radiologists based on this reader study. The theoretical benefits of using readout-segmented diffusion imaging technique in RESOLVE to improve image quality can be realized in a routine clinical practice.

4963 Computer 118

Spatially-sensitive model for detection of prostate cancer on multiparametric MRI

Ethan Leng[1], Jin Jin[2], Lin Zhang[2], Christopher A. Warlick[3], Benjamin Spilseth[4], Joseph S. Koopmeiners[2], and Gregory J. Metzger[1]

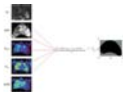

[1]Center for Magnetic Resonance Research, University of Minnesota, Minneapolis, MN, United States, [2]Division of Biostatistics, School of Public Health, University of Minnesota, Minneapolis, MN, [3]Department of Urologic Surgery, Institute of Prostate and Urologic Cancers, University of Minnesota, Minneapolis, MN, United States, [4]Department of Radiology, University of Minnesota, Minneapolis, MN, United States

A novel predictive model of prostate cancer (PCa) on multiparametric MRI was developed that takes into account the spatial distribution of PCa within the prostate and the spatially-autocorrelated nature of mpMRI data. The performance of the proposed model was compared to the LASSO-based model we previously described on 34 PCa cases using both voxel-wise metrics (AUC) and slice-wise metrics ($$$s_s$$$) we recently developed. The proposed model achieved superior predictive performance both in terms of AUC (0.81 vs 0.77) and $$$s_s$$$ (0.45 vs. 0.35) over the 34 cases, with significant improvements for the majority of cases.

4964 Computer 119

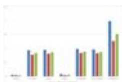

Texture analysis of prostate MRI by using the Gray-Level Co-Occurrence Matrix (GLCM) for the characterization of prostate cancer, normal prostatic peripheral zone, and transition zone

Sung Kyoung Moon[1], Hyug-Gi Kim[2], Kyung Mi Lee[1], and Joo Won Lim[1]

[1]Radiology, Kyung Hee University Hospital, College of Medicine, Kyung Hee University, Seoul, Korea, Republic of, [2]Biomedical Engineering, College of Electronic Information Engineering, Kyung Hee University, Korea, Republic of

GLCM is a mathematical method that extracts the various quantitative parameters representing texture features of the images. Our hypothesis is that the texture analysis of prostate MRI can be an additional problem-solving tool in differentiating cancer and normal prostate tissue. The texture parameters of ROIs in prostate cancer, normal peripheral zone, and normal transitional zone in T2WI were extracted and compared statistically in 20 prostate cancer patients. The correlation, energy, and maximum probability in prostate cancer and peripheral zone are significantly different. The texture analysis can be used for the characterization and differentiation of prostate cancer and normal prostate tissue.

4965 Computer 120

To quantitatively investigate the contrast ratio of prostate cancer of computed high diffusion-weighted imaging (DWI) from DWIs acquired from lower b-values and correlation to tumour aggressiveness

RAYMOND LEE[1], Gladys Lo[1], and Ka Fat John Chan[1]

[1]DEPARTMENT OF DIAGNOSTIC & INTERVENTIONAL RADIOLOGY, HONG KONG SANATORIUM & HOSPITAL, HONG KONG, Hong Kong

Apparent Diffusion Coefficient (ADC) maps obtained diffusion weighted imaging (DWI) have been shown to detect prostate cancer (PCa) and also correlate with tumor aggressiveness. Recent studies showed that improve detection of prostate cancer by high b-value DWI. However, high b-value images have an inherently low signal-to-noise ratio (SNR) and are prone to increased susceptibility artefact. Computed DWI (cDWI) is a method capable of obtaining high b-value images, which avoids the technical challenges of actually measuring them. Previous studies with limited sample size have evaluated the cDWI with high b-value but results were not conclusive. Current study may give an insight whether high b-value cDWI is valuable for differentiation of high risk versus low risk PCa.

Electronic Poster

Gastrointestinal MRI

Exhibition Hall Wednesday 14:45 - 15:45

4966 Computer 49

Metabolic Imaging of β3-adrenoreceptor Activated BAT and its Systemic Effect on Abdominal Fat in Diet Induced Obese Model

Jadegoud Yaligar[1], Sanjay Kumar Verma [1], Venkatesh Gopalan [1], Anantharaj Rengaraj[1], Tian Xianfeng[1], Anna Ulyanova[1], Bhanu Prakash K.N[1], Suresh Anand Sadananthan[2], Navin Michael[2], and S. Sendhil Velan [1]

[1]Laboratory of Metabolic Imaging, Singapore Bioimaging Consortium, A*STAR, Singapore, [2]Singapore Institute for Clinical Sciences, A*STAR, Singapore

Imbalance in dietary intake and energy expenditure are associated with obesity, diabetes and metabolic disorders. Adipocyte size and expansion of adipose tissue plays a critical role towards the progression of diet induced obesity. Brown adipose tissue (BAT) plays a critical role in modulating different fat depots in the body. BAT can be functionally activated by administering the β3-adrenergic agonist. Understanding the mechanisms associated with BAT activation and the possibility of reversing insulin resistance and its impact on whole body metabolism is of current clinical interest for combating diabetes. In the current study, we investigated the fat partitioning in high fat diet induced obese rodent model by β-adrenergic-mediated BAT activation.

4967 Computer 50

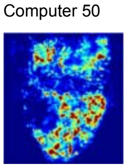

Analysis of motility in apparently normal small bowel – relationship to Crohn's symptoms

Ruaridh M Gollifer[1], Alex Menys[1], Jesica Makanyanga[1], Carl A, J Puylaert[2], Frans M Vos[2,3], Jaap Stoker[2], David Atkinson[1], and Stuart A Taylor[1]

[1]Centre for Medical Imaging, University College London (UCL), London, United Kingdom, [2]Department of Radiology, Academic Medical Center (AMC), Amsterdam, Netherlands, [3]Quantitative Imaging Group, Delft University of Technology, Delft, Netherlands

Crohn's disease (CD) patients often suffer abdominal symptoms even when their disease is apparently in remission with no identifiable active inflammation.[1] Ongoing aberrant gut motility has been postulated as a cause, and this can now be quantified using MRI.[2] This study tested the association between abdominal symptoms based on the Harvey-Bradshaw Index (HBI) and MRI derived motility metrics in morphologically healthy small bowel in CD patients. An inverse association was found between reduced motility spatial variation across the small bowel and symptoms, particularly diarrhoea. This association was strongest when HBI scores were higher.

4968 Computer 51

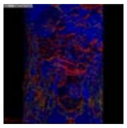

Feasibility of Performing Dynamic and Delayed Enhancement and Magnetization Transfer Ratios in pediatric patients undergoing clinically-indicated MRE: pilot study to assess image quality for quantitative evaluation

Mary-Louise Catherine Greer[1,2], Susan Shelmerdine[3], Kedar Patil[1,2], Claire Cuscaden[4], Debra Drossman[1], and Logi Vidarsson[1]

[1]Department of Diagnostic Imaging, The Hospital for Sick Children, Toronto, ON, Canada, [2]Department of Medical Imaging, University of Toronto, Toronto, ON, Canada, [3]Department of Radiology, Great Ormond Street Hospital, London, United Kingdom, [4]Department of Radiology, The Royal Brisbane and Women's Hospital, Brisbane, Australia

Purpose: Assess feasibility of applying magnetization transfer (MT) and dynamic and delayed enhancement (DCE) sequences during MR Enterography(MRE) in children.

Methods: REB approved, in this prospective study, patients =/< 18 years undergoing MRE for suspected or proven inflammatory bowel disease were consented for application of MT and DCE sequenced in addition to standard clinical sequences. These were assessed and prospectively recruited and imaging sequences applied. Imaging was subjectively analysed by two radiologists or a radiologists and physicist in the first arm by consensus for sequence modification.

Results: Inter and intra-reader analysis was undertaken.

Conclusion: DCE is robust, MTR requires further modification.

4969 Computer 52

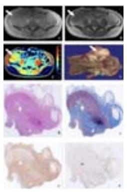

Magnetization transfer MRI for evaluating bowel fibrosis and inflammation in patients with stricturing Crohn’s disease

Xuehua Li[1], Zhuangnian Fang[1], Siyun Huang[1], Li Huang[1], Zhongwei Zhang[2], Xu Yan[3], Xiaolei Zhu[4], Jinjiang Lin[1], Mengchen Zhang[1], Mengjie Jiang[1], Shiting Feng[1], Canhui Sun[1], and Ziping Li[1]

[1]Department of Radiology, The First Affiliated Hospital of Sun Yat-Sen University, Guangzhou, People's Republic of China, [2]Department of Biomedical Engineering, Cancer Biology and Radiology, Wake Forest School of Medicine, NC, United States, [3]MR Collaboration NE Asia, Siemens Healthcare, Shanghai, People's Republic of China, [4]MR Scientific Marketing NE Asia, Siemens Healthcare, Guangzhou, People's Republic of China

This study aimed to assess the efficacy of Magnetization Transfer MRI (MTI) for evaluating bowel fibrosis and inflammation in patients with stricturing Crohn’s Disease (CD). Bowel wall MTR with normalization to skeletal muscle was calculated and correlated to histologic fibrosis and inflammation as well as amount of type I collagen and vessel density. The results showed that normalized MTRs correlated with histologic fibrosis and type I collagen scores, but did not correlate with inflammation scores or vessel densities. Thus, MTI can accurately detect and distinguish varying degrees of bowel fibrosis with or without coexisting inflammation in human CD.

4970 Computer 53

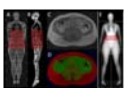

Comparison of Measurement of Abdominal Visceral Adipose Tissue in Men and Women by MRI vs. DXA

Cherie R Shook[1], Bret H Goodpaster[1], and Heather H Cornnell[1]

[1]Translational Research Institute for Metabolism and Diabetes, Florida Hospital, Orlando, FL, United States

Visceral adipose tissue (VAT) has been identified as a significant contributing factor to the metabolic complications of obesity and cardio-metabolic disease, thus its precise measurement is becoming more clinically relevant. Both MRI and DXA were used to measure different components of body composition including VAT, and these results were compared by gender. Both scan acquisitions took similar amounts of time, but DXA results were calculated automatically while MR data processing was completed offline, thus took more time. The results from this study indicate that DXA is a precise measure of only a portion of VAT while MRI can give a more accurate measurement of total VAT across the entire abdomen, potentially avoiding gender bias.

4971 Computer 54

Clinical application of 3D VIBECAIPI-DIXON for enhanced imaging of the small intestine

Yang Yu[1], Lu Liang[1], and Tao Jiang

[1]Beijing Chaoyang Hospital, Beijing，China, People's Republic of China

The abstract discussed the clinical application of a fast 3D VIBE sequence with Dixon fat saturation and CAIPIRINHA acceleration techniques (3D VIBECAIPI-DIXON) by compare to a standard 2D FLASH sequence with spectral fat saturation and conventional GRAPPA acceleration technique (2D FlashGRAPPA-fs) for enhanced imaging of the small intestine

---

4972 Computer 55

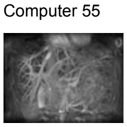

Phase Contrast Magnetic Resonance Imaging using Non-contrast-enhanced Magnetic Resonance Angiography using Balanced Steady-State Free-Precession Sequence and Time-Spatial Labeling Inversion Pulse: Measuring Left Gastric Vein Flow Velocity to Predict Esophageal Varices Development and Rupture

Akihiro Furuta[1], Hiroyoshi Isoda, Shigeshi Kohno, Koji Tokunaga, Ayako Ono, Rinpei Imamine, Rikiya Yamashita, Shigeki Arizono, Aki Kido, Naotaka Sakashita, and Kaori Togashi

[1]Kyoto University, Kyoto, Japan

LGV flow velocity is clinically important to foresee esophageal varices development and rupture. But it is difficult to measure it's velocity exactly by echo or only phase contrast MRI (PC-MRI). To measure LGV flow velocity, 2D PC-MRI were set perpendicularly across vessel segments in the cross-sectional slice position determined from 3D selective visualized LGV using non-contrast-enhanced MRA with balanced steady-state free-precession sequence and time-spatial labeling inversion pulse. LGV flow velocity of all subjects could be measured exactly. This method is useful to measure LGV flow velocity.

4973 Computer 56

Assessment of Histological Differentiation in Gastric Cancers Using Whole-Volume Histogram Analysis of Apparent Diffusion Coefficient Maps

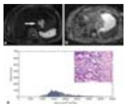

Zhengyang Zhou[1], Song Liu[2], Jian He[2], and Weibo Chen[3]

[1]Department of Radiology, Drum Tower Hospital, School of Medicine, Nanjing University, Nanjing, People's Republic of China, [2]Department of Radiology, Drum Tower Hospital, School of Medicine, Nanjing University, [3]Philips Healthcare, Shanghai, People's Republic of China

Seventy-eight patients with gastric cancer were underwent MRI to investigate whether the histogram analysis of the entire tumor volume in ADC maps could differentiate between histological grades. A series of histogram parameters were calculated and correlated with the histological grade of the surgical specimen. There were significant differences in the 5th, 10th, 25th, and 50th percentiles, skew, and kurtosis between poorly and well-differentiated gastric cancers. There were correlations between the degrees of differentiation and histogram parameters, including the 10th percentile, skew, kurtosis, and max frequency. Histogram analysis of the ADC maps can be useful in differentiating between histological grades.

4974 Computer 57

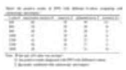

Diffusion-weighted MR Enterography imaging of the ileocecal segment: optimizing b-value for visually differentiating inflammatory and neoplastic lesions

Hao Yu[1], Daoyu Hu[1], Yaqi Shen[1], Zhen Li[1], Jianjun Li[1], Zi Wang[1], and Yanchun Wang[1]

[1]Department of Radiology, Tongji Hospital Tongji Medical College Huazhong University of Science and Technology, Wuhan, People's Republic of China

To evaluate the ability of conventional MR Enterography (MRE) including coronal and axial T1/T2 weighted imaging and Diffusion-weighted imaging with different b-values(b=400,600,800,1000,1200,1500,3000 sec/mm2)to visually illustrate inflammatory lesions and neoplastic lesions in the ileocecal region comparing with colonoscopy or surgical results.As a result,MRE and DWI were capable of revealing the lesions in the ileocecal segment. DWI was superior to detect lesions especially inflammations comparing with conventional MRE, and the optimal b value of DWI for MRE was 800 sec/mm2 at 3T. Hyperintensity of ileocecal lesion on DWI with high b(› 1000 sec/mm2) value wes more favor for tumor-like lesion.

4975 Computer 58

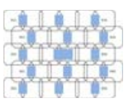

Ultra-fast abdominal imaging with high parallel-imaging factors: Comparative study of a 60-channel receiver coil with the standard coil set-up

Ahmed E Othman[1], Petros Martirosian[2], Wilhelm Horger[3], Jakob Weiss[2], Jana Taron[2], Karsten Jahns[3], Konstantin Nikolaou[2], and Mike Notohamiprodjo[2]

[1]Radiology, University Hospital Tübingen, Tübingen, Germany, [2]Radiology, University Hospital Tübingen, [3]Siemens Healthineers

In this study, we evaluated a novel 60-channel coil setup for ultra-fast abdominal imaging using high PAT factors in a phantom, in healthy volunteers and in patients. We found that the 60-channel coil-setup is superior to a conventional 30-channel coil-setup yielding higher SNR and superior image quality and enabling ultra-fast image acquisition with diagnostic image quality.

4976 Computer 59

Radiomics Model for Preoperative Prediction of Lymph Node Metastasis in Rectal Cancer after Neoadjuvant Chemoradiatherapy Therapy

Haitao Zhu[1], Xiaoyan Zhang[1], Xiaoting Li[1], Yanjie Shi[1], Huici Zhu[1], and Yingshi Sun[1]

[1]Peking University Cancer Hospital and Institute, Beijing, People's Republic of China

Preoperative evaluation of lymph node metastasis in locally advanced rectal cancer remains a problem especially after neoadjuvant chemoradiatherapy treatment (NCT). This study proposed a MRI-based radiomics method to predict lymph node involvement in rectal after NCT. Beside the features from the tumor, features from the lymph nodes were also included for the construction of the radiomics model to increase the accuracy of prediction. 10-fold cross-validation among 300 patients produced ROC with average AUC=0.78. Independent validation with 118 patients produced ROC with AUC=0.81.

4977 Computer 60

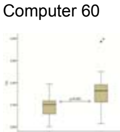

Pretreatment diffusion kurtosis imaging for predicting the response of locally advanced rectal cancer to neoadjuvant chemoradiation therapy

Hongliang Sun[1], Yanyan Xu[1], Kaining Shi[2], and Wu Wang[1]

[1]Radiology, China-Japan Friendship Hospital, Beijing, People's Republic of China, [2]Philips Healthcare China, Beijing, People's Republic of China

Diffusion kurtosis imaging (DKI) is an emerging technique, which could reflect restricted water diffusion within the complex microstructure of most tissues based on non-Gaussian diffusion model. It has been reported that DKI was used in central system diseases, tumor grade, even assessment of treatment response. However, there is limited research reported about the clinical application of DKI in rectal cancer, and the value of DKI in monitoring rectal cancer treatment was still unclear.

4978 Computer 61

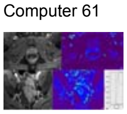

Dynamic Contrast-Enhanced Imaging of the Rectum Using Golden-Angle Radial Sparse Parallel MRI (GRASP): Initial Experience and Comparison to a Conventional Approach Using Time-resolved Angiography With Interleaved Stochastic Trajectories (TWIST).

Daniel Hausmann[1], Jing Liu[2], Philipp Riffel[1], Johannes Budjan[1], Robert Grimm [3], Tobias Block[4], Stefan O Schoenberg[1], and Ulrike I Attenberger[1]

[1]Institute of Clinical Radiology and Nuclear Medicine, University Medicine Mannheim, Mannheim, Germany, [2]Department of Radiology, Peking Universtiy First Hospital, Beijing, China, [3]Siemens Healthcare, Erlangen, Germany, [4]Department of Radiology, New York University, New York City, NY, USA

MR perfusion images to discriminate between normal rectal wall and rectal cancers with less variance of perfusion values and superior image quality compared to conventional TWIST-Angiography can be generated using time-resolved free-breathing MRI with continuous golden-angle radial sampling and iterative reconstruction (GRASP). Additional morphologic assessment (“one-stop-shop”) with high spatial resolution, artifact-insensitive, multiphase, contrast-enhanced imaging may increase accuracy and diagnostic confidence of the examination.

4979 Computer 62

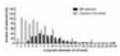

The Limitation in Predicting Lymph Nodes Stage by Using Magnetic Resonance Imaging on the Criterion of Size with Histopathological Analysis as Reference

Caizhen Feng[1], Jin Cheng[1], Jing Wu[1], Gongwei Wang[2], Yingjiang Ye[2], and Yi Wang[1]

[1]Radiology, People's Hospital, Peking University, Beijing, People's Republic of China, [2]People's Hospital, Peking University, Beijing, People's Republic of China

In spite of LN status is critical to the prognosis of patients with gastric cancer, MDCT and MRI cannot accurately assess metastatic LNs prior to surgery.In our study, 802 LNs of 30 patients with gastric carcinoma were harvested.during D2 lymphadenectomy. Only 36.7% (295/802) LNs were detected on preoperative MRI.. 31.5% (217/688) LNs (<8mm) were identified as malignant by pathology, whereas, 44.7% (51/114) LNs (≥8mm) were defined as metastatic. Forty-one metastatic LNs (19%, 41/215) with(≦3mm) were found in 7 patients (23.3%, 7/30) and caused N stage upstaging in 3 patients, which could not be detected by MRI.

4980 Computer 63

Dynamic contrast enhanced MR imaging for therapeutic response assessment after neoadjuvant Chemoradiotherapy in patient with local advanced rectal cancer

Yanfen Cui[1], Xiaotang Yang [1], and Ning Huang[2]

[1]Shanxi Province Tumor Hospital, Taiyuan, People's Republic of China, [2]GE Healthcare China

The pre-CRT Ktrans value and the percentage decrease in the Ktrans after CRT could be helpful to predict good therapeutic response to CRT for LARC. This may allow for personalized treatment-options in rectal cancer patients.

4981 Computer 64

PET/MRI for rectal cancer staging: Longer PET acquisition times result in increased identification of nodal metastatic disease.

Colin Burke[1], Thomas Hope[1], Michael Ohliger[1], Zhen Wang[1], Katherine Van Loon[2], and Madhulika G. Varma[3]

[1]Department of Radiology & Biomedical Imaging, University of California, San Francisco, San Francisco, CA, United States, [2]Gastrointestinal Oncology, The UCSF Helen Diller Family Comprehensive Cancer Center, University of California, San Francisco, San Francisco, CA, [3]Colorectal Surgery, University of California, San Francisco, San Francisco

Rectal cancer nodal staging guides the decision to whether neo-adjuvant chemoradiation is needed prior to surgical resection and is a predictor of survival and recurrence. However, staging based on size and morphologic criteria alone is limited. Our data suggests that increased PET acquisition times with PET/MRI increases the identification of nodal metastatic disease in rectal cancer, particularly in small nodes sized 5 mm or less.

4982 Computer 65

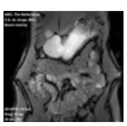

Dynamic MRI For Bowel Motility Imaging – How Fast And How Long?

C.S. de Jonge[1], R.M. Gollifer[2], A.J. Nederveen[1], D. Atkinson[2], S.A. Taylor[2], J. Stoker[1], and A. Menys[2]

[1]Department of Radiology, Academic Medical Center (AMC), Amsterdam, Netherlands, [2]Centre for Medical Imaging, University College London (UCL), London, United Kingdom

Dynamic (cine) MRI of bowel motility is now routinely performed in clinical practice and advances in post-processing have enabled robust quantitation of this data facilitating numerous research applications. Generally, motility sequences are acquired in a 20 second breath hold at a temporal resolution of 1 fps. In this study, we investigate these core assumptions and provide guidance information for future studies. In summary, we show that a temporal resolution of at least 1 fps is necessary for a scan duration of at least 10 seconds. This is consistent with the majority of small bowel motility studies to date.

4983 Computer 66

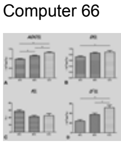

Optimization of high b values for intravoxel incoherent motion imaging of rectal cancer : a pilot study

Yankai Meng[1], Chongda Zhang [1], Hongmei Zhang[1], and Chunwu Zhou [1]

[1]Department of Radiology, National Cancer Center/Cancer Hospital, Chinese Academy of Medical Sciences and Peking Union Medical College, Beijing, People's Republic of China

To optimize the high b values (>200s/mm2) for intravoxel incoherent motion imaging of rectal cancer and to observe the effect of high b values variation on IVIM parameters. Three groups (A group with all 16 b values: 0,10,20,30,40,60,80,100,150,200,400,800,1000,1200,1500,2000, B group with 14 b values: 0,10,20,30,40,60,80,100,150,200,400,800,1000,1200 and C group with 12 b values: 0,10,20,30,40,60,80,100,150,200,400,800) were selected respectively for measurement by a radiologist. The average values of each measurement were used for statistical analysis. One-way analysis of variance (ANOVA) and post-hoc test were performed on the mean values of IVIM parameters in groups A, B, and C, with a significance level of P <0.05. The p values of ANVOA results in ADC、D、D* values were less than 0.05, the differences were statistically significant. The p values of Bonferroni post-hoc test in D、D*、f values were not statistically significant differences in group A and B. With the number of high b values decrease, the values of ADC、D、D* values and standard error were increased, while of f values was not changed significantly. In our study, the reproducibility of the IVIM parameters caused by high b value variation was not significant. The value of selected b > 1500 need to be further studied.

4984 Computer 67

Optimized ROI size on ADC measurements of normal pancreas, pancreatic cancer and mass-forming chronic pancreatitis

Chao Ma[1], Jing Li[1], Mbaiaourer Barak Bouka[1], Panpan Yang[1], Li Wang[1], Luguang Chen[1], Li Su[2], Yong Zhang[3], Jianxun Qu[3], Shiyue Chen[1], Qiang Hao[1], and Jianping Lu[1]

[1]Radiology, Changhai Hospital of Shanghai, Shanghai, People's Republic of China, [2]School of Pharmacy, Second Military Medical University, Shanghai, People's Republic of China, [3]MR Research China, GE Healthcare, Shanghai, People's Republic of China

The effect of ROI size on ADC measurements in normal pancreatic tissue or pancreatic lesions have rarely been studied. This study investigated the influences of ROI size in ADC measurements for the differentiation between normal pancreas (NP), mass-forming chronic pancreatitis (MFCP) and pancreatic ductal adenocarcinoma (PDAC).

4985 Computer 68

Diffusion kurtosis imaging for differentiating tumor KRAS mutation status in rectal cancer

Yanyan Xu[1], Hongliang Sun[1], Kaining Shi[2], and Wu Wang[1]

[1]Radiology, China-Japan Friendship Hospital, Beijing, People's Republic of China, [2]Philips Healthcare, China, Beijing, People's Republic of China

Diffusion kurtosis imaging (DKI), which is a non-Gaussian diffusion-weighted model proposed by Jensen et al [1], has the potential to characterize both normal and pathologic tissue [1-3], meanwhile, providing a new option for tumor garde [4] and assessment of treatment response [5-7]. Previous studies [1-3, 8] found that DKI could better account for restricted water diffusion within the complex microstructure of most tissues. To our knowledge, however, no study has included evaluation of DKI characteristic in rectal cancer, especially in the aspect of KRAS mutant, which associated with clinical treatment and prognosis of colorectal cancers [9].

4986 Computer 69

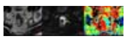

The utilization of DDC value in detecting the status of LVI in rectal cancer patients at 3.0T MRI

Guangwen Zhang[1] and Jinsong Zhang[2]

[1]Xijing Hospital, xi'an, People's Republic of China, [2]Xijing Hospital, People's Republic of China

In this study, we aimed to investigate the value of DDC in assessing the status of lymphovascular invasion in patients with rectal cancer. Ninety-eight patients with rectal adenocarcinoma underwent DWI with 16 b-values at 3.0T MR system. We found there was an significant difference in DDC value between the LVI presence group (DDC=0. 893±0.151×$10^{-3}mm^2/s$, n=46) and the LVI absent group (DDC=0. 825±0.127×$10^{-3}mm^2/s$, n=52), (P=0.018). We speculate that DDC value derived from multi-b value DWI could be a useful functional parameter in detecting the status of LVI in rectal cancer patients.

4987 Computer 70

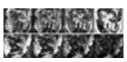

Measuring T1 and T2 of the small bowel wall at 3T

Hannah Grace Williams[1,2], Penny A Gowland[1], Luca Marciani[2], Robert Scott[3], Guruprasad Aithal[2,3], and Caroline L Hoad[1,3]

[1]Sir Peter Mansfield Imaging Centre, School of Physics and Astronomy, University of Nottingham, Nottingham, United Kingdom, [2]Nottingham Digestive Diseases Centre, School of Medicine, University of Nottingham, Nottingham, United Kingdom, [3]NIHR Biomedical Research Unit in Gastrointestinal and Liver Diseases, Nottingham University Hospital, Nottingham, United Kingdom

Available techniques to measure in-vivo bowel permeability are inadequate for stratifying patients to identify those at risk of complications from increased bowel permeability. T_1 and T_2 measurements could potentially be indicators of changes in bowel wall structure and thus permeability. We have measured the T_1 and T_2 of the bowel wall to be 1.68±0.57 s and 0.08 ±0.02 s respectively. We found significant variations between and within subjects. However it is currently unknown whether some of these variations are real and some due to errors in the measurement process.

4988 Computer 71

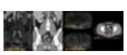

MR versus CT Imaging for Identifying the Etiology of Abdominal Pain in Emergency Department Patients

Michael Dean Repplinger[1], Perry J Pickhardt[2], Rebecca L Bracken[1], Douglas R Kitchin[3], Jessica B Robbins[2], Timothy J Ziemlewicz[2], and Scott B Reeder[2]

[1]Emergency Medicine, University of Wisconsin - Madison, Madison, WI, United States, [2]Radiology, University of Wisconsin - Madison, Madison, WI, United States, [3]Radiology, St. Mary's Hospital, Madison, WI, United States

Our study aimed to evaluate the diagnostic accuracy of MR versus CT for identifying the etiology of abdominal pain in emergency department patients. This is a prospective study that included patients ≥12-years-old who were being evaluated for possible appendicitis. All patients underwent both MR and CT; images were interpreted by three radiologists who were blind to the patient’s outcome. There were 113 instances of acute abdominal processes (15 different diagnoses). The overall accuracy of NC-MR, CE-MR, and CT was 77%, 83%, and 90% for individual reads and 82%, 84%, and 94% for consensus reads.

4989 Computer 72

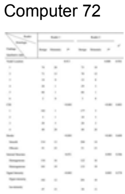

Chemical Shift Effect Predicting Lymph Node Status in Rectal Cancer using High-Resolution MR Imaging with Node-for-node Matched Histopathological Validation

chongda zhang[1], hongmei zhang[1], feng ye[1], yuan liu[1], and chunwu zhou[1]

[1]Department of Diagnostic Radiology, National Cancer Center/Cancer Hospital, Chinese Academy of Medical Sciences and Peking Union Medical College, Beijing, People's Republic of China

To evaluate the value of chemical shift effect (CSE), as well as other criteria for the prediction of lymph node status. Lymph nodes harvested from transversely whole-mount specimens were compared with in vivo and ex vivo images to obtain MR characteristics including CSE, as well as other predictors of 255 benign and 35 metastatic nodes. Our results revealed that CSE is a reliable predictor for differentiating benign from metastatic lymph nodes. Other predictors of nodal location, border, signal intensity and minimum distance to rectal wall were also proved to be useful for the diagnosis.

Electronic Poster

Muscle

Exhibition Hall Wednesday 16:15 - 17:15

4990 Computer 25

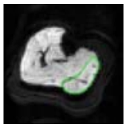

A quantitative relationship between R2* and deoxyhemoglobin levels in calf muscle

Kexin Hao[1], Gwenael Layec[2], Corey R. Hart[3], Christopher C. Conlin[4], Kristi Carlston[4], Vivian S. Lee[4], and Jeff L. Zhang[4]

[1]Department of Electrical and Computer Engineering, University of Utah, Salt Lake City, UT, United States, [2]Department of Internal Medicine, University of Utah School of Medicine, Salt Lake City, UT, United States, [3]Department of Exercise and Sports Science, University of Utah, UT, United States, [4]Department of Radiology and Imaging Sciences, University of Utah, Salt Lake City, UT, United States

This study examined the relationship between R_2* measurements from BOLD MRI and deoxyhemoglobin (HHb) measurements from near-infrared spectroscopy (NIRS) in calf muscle of subjects with varying degrees of peripheral artery disease (PAD). Following plantar-flexion exercise, the time required for R_2* and HHb to recover to resting-state values was recorded. Linear regression was used to relate recovery time between R_2* and HHb. This quantitative relationship enables estimation of HHb from MRI-measured R_2*, which can help to improve the assessment of PAD since MRI can easily be performed for muscle tissue that is too deep for NIRS evaluation.

4991 Computer 26

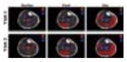

Noninvasive Measurement of Calf Muscle Perfusion Immediately after Plantar Flexion Exercise in Elderly Patients with Heart Failure and Preserved Ejection Fraction

Robert A. Kraft[1], Craig A. Hamilton[1], Peter H. Brubaker[2], W. Scott Hoge[3], M. Constance Linville[4], J. Thomas Becton[5], Richard J. Thompson[6], Mark J. Haykowsky[7], and Dalane W. Kitzman[5]

[1]Biomedical Engineering, Wake Forest University School of Medicine, Winston-Salem, NC, United States, [2]Health and Exercise Science, Wake Forest University, Winston-Salem, NC, United States, [3]Radiology, Brigham and Women's Hospital and Harvard Medical School, Boston, MA, [4]Department of Biomedical Engineering, Wake Forest University School of Medicine, Winston-Salem, NC, United States, [5]Cardiology, Wake Forest University School of Medicine, Winston-Salem, NC, United States, [6]Bioengineering, University of Alberta, Edmonton, Canada, [7]College of Nursing and Health Innovation, University of Texas at Arlington, Arlington, TX

The pathophysiology of Heart Failure Patients with Preserved Ejection Fraction is poorly understood but there is increasing evidence that skeletal muscle blood flow and metabolism play important roles in this disease. Accurately and non-invasively measuring skeletal muscle blood flow with sufficient temporal resolution to measure skeletal muscle blood flow dynamics in individual muscles is challenging. We present a optimized version of pseudo-Continuous ASL capable of measuring blood flow map of the calf every 16 seconds. Data from two healthy adults is presented.

4992 Computer 27

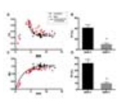

Stimulated Echo DTI in skeletal muscle of patients with Becker Muscular Dystrophy

Celine Baligand[1], Jedrzej Burakiewicz[1], Melissa T. Hooijmans[1], Olivier Scheidegger[2], Matt G. Hall[3], Paola Porcari[4], Erik H. Niks[5], Pierre G. Carlier[2], Christopher Clark[3], Andrew Blamire[4], Jan J.G.M. Verschuuren[5], and Hermien E. Kan[1]

[1]Department of Radiology, Leiden University Medical Center, C.J. Gorter Center for High-field MRI, Leiden, Netherlands, [2]NMR laboratory, Institute of Myology, Paris, France, [3]Institute of Child Health, University College of London, London, United Kingdom, [4]Institute of Cellular Medicine and Newcastle Magnetic Resonance Centre, Newcastle University, Newcastle upon Tyne, United Kingdom, [5]Department of Neurology, Leiden University Medical Center, Leiden, Netherlands

Cellular sizes in skeletal muscle are significantly larger than in the brain. Therefore standard spin-echo (SE)-DTI with inherently short diffusion times may lack sensitivity for the study skeletal muscle of neuromuscular disorders (NMDs). Alternatively, stimulated-echo (STE-)DTI allows for much longer diffusion times, increasing sensitivity to cell size. Due to the challenges presented by fat replacement STE-DTI has not been previously applied in NMDs. Here, we show that STE-DTI is feasible in Becker Muscular Dystrophy patients, and can detect FA differences compared to healthy controls in mildly affected muscles.

4993 Computer 28

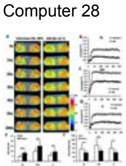

T1ρ and Dynamic BOLD MR imaging to evaluate the change of skeletal muscles of lower extremity in diabetes patients

Xingui Peng[1] and Shenghong Ju[2]

[1]Department of Radiology, Zhongda Hospital, Medical School, Southeast University, Nanjing, People's Republic of China, [2]Department of Radiology, Zhongda Hospital, Medical School, Southeast University

This study aimed to measure the BOLD response in the calf muscle in T2DM patients during post-occlusive reactive hyperemia and to study whether T1ρ MR Imaging of calf muscle could differentiate T2DM patients from normal subjects. Twenty-two T2DM patients and twenty age-matched healthy volunteers were performed MR scanning. T1ρ relaxation time and maximal ΔT2* change (ΔT2*max) and time to peak (TTP) were measured. Our results showed that the lower degree of the increase (ΔT2*max and TTP) in calf muscles of DM patients. In addition, T1ρ relaxation time in TA muscle was significant higher in DM patient than in healthy subjects.

4994 Computer 29

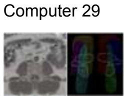

Automated assessment of paraspinal muscles fat composition based on the segmentation of chemical shift encoding-based water/fat-separated images

Friedemann Freitag[1], Thomas Baum[1], Michael Dieckmeyer[1], Jan S. Kirschke[2], Holger Eggers[3], Christian Buerger[3], Cristian Lorenz[3], and Dimitrios C. Karampinos[1]

[1]Department of Diagnostic and Interventional Radiology, Klinikum rechts der Isar, Technical University of Munich, Munich, Germany, [2]Department of Diagnostic and Interventional Neuroradiology, Klinikum rechts der Isar, Technical University of Munich, Munich, Germany, [3]Philips Research Laboratories, Hamburg, Germany

Chemical shift encoding-based water-fat MRI derived proton density fat fraction (PDFF) of the paraspinal muscles has been emerging as important surrogate marker in subjects with intervertebral disc disease, osteoporosis, sarcopenia, and neuromuscular disorders. However, measurements of paraspinal muscle PDFF are currently limited in clinical routine due to the required time-consuming manual segmentation procedure. The present study aimed to develop an automatic segmentation algorithm of the paraspinal muscles at the lumbar spine based on water-fat MRI and compared the performance of this algorithm to ground truth data based on manual segmentation.

4995 Computer 30

Diurnal changes of Acetylcarnitine in human vastus lateralis muscle and response to exercise: a 7T 1H MRS study

Radka Klepochová[1,2,3], Ladislav Valkovič[3,4,5], Martin Gajdošík[1,3,6], Thomas Hochwartner[7], Norbert Bachl [7], Harald Tschan[7], Michael Krebs[6], Siegfried Trattnig[1,3], and Martin Krššák[1,3,6]

[1]High-Field MR Center, Department of Biomedical Imaging and Image-Guided Therapy, Medical University of Vienna, Vienna, Austria, [2]Department of NMR Spectroscopy and Mass Spectrometry, Faculty of Chemical and Food Technology, Slovak University of Technology, Bratislava, Slovakia, [3]Christian Doppler Laboratory for Clinical Molecular MR Imaging, Vienna, Austria, [4]University of Oxford Centre for Clinical Magnetic Resonance Research, University of Oxford, John Radcliffe Hospital, Oxford, United Kingdom, [5]Department of Imaging Methods, Institute of Measurements Science, Slovak Academy of Sciences, Bratislava, Slovakia, [6]Division of Endocrinology and Metabolism, Department of Medicine III, Medical University of Vienna, Vienna, Austria, [7]Center of Sport Science and University Sport, University of Vienna, Vienna, Austria

Carnitine plays an important role in fat metabolism. A long-echo time proton magnetic resonance spectroscopy protocol was implemented for detection of skeletal muscle acetylcarnitine during the day and after exercise on a clinical 7T scanner in the thigh (vastus lateralis) muscle. Our observation point towards diurnal changes of acetylcarnitine concentration which tended to be higher in the morning than after lunch. Moreover, following 10 minutes of high-intensity exercise the concentration significantly increased and again significantly decreased 15 minutes after cessation of the exercise. Our data emphasize the need for strict standardization,physical activity and dietary conditions for the measurement of the acetylcarnitine/carnitine.

4996 Computer 31

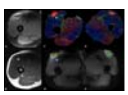

Normalized STEAM-based DTI parameters allow robust assessment of muscle tears in football players.

Chiara Giraudo[1], Stanislav Motyka[1], Michael Weber[2], Manuela Karner[1], Christoph Resinger[3], Siegfried Trattnig[1], and Wolfgang Bogner[1]

[1]Department of Biomedical Imaging and Image-guided Therapy-MR Centre of Excellence, Medical University of Vienna, Vienna, Austria, [2]Department of Biomedical Imaging and Image-guided Therapy, Medical University of Vienna, Vienna, Austria, [3]Orthopedic Department, Evangelisches Krankenhaus Wien, Vienna, Austria

STEAM-based DTI was applied to investigate lower limbs' muscle tears in athletes using the contralateral muscles as reference.To account for possible physiological differences in DTI metrics between right and left limb, a ratio between two ROIs on the injured side (i.e.,one on the tear and one on a healthy area) and two ROIs on the contralateral limb (i.e.,both on healthy areas) was used. The ratio showed that structural changes, expressed by modifications in MD, FA, RD, fibers' number and length, occur in muscle tears and are quantifiable by DTI.These findings are expected to improve the therapeutic management of muscle injuries.

4997 Computer 32

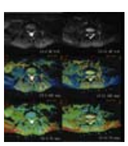

Paraspinal Muscle Changes with Chronic Low Back Pain by Using 3.0T MR Diffusion Tensor Imaging Technology

Li Yiwen[1], Yuan Huishu[1], and Xie Lizhi[2]

[1]Radiology, Peking University Third Hospital, Beijing, People's Republic of China, [2]GE Healthcare, MR Research China, Beijing, People's Republic of China

The purpose of the current study is to assess the potential difference of multifidus muscle between non-specific chronic low back pain patients and the healthy individuals using DTI and to compare the sensitivity of DTI to conventional lumbar MRI in detecting muscle pathological changes. DTI and conventional MRI parameters were obtained including FA, ADC, MD and tCSA, fCSA, fCSA/tCSA ratio. Compared to the healthy individuals, NCLBP patients demonstrated differences in DTI parameters of bilateral multifidus muscles. We conclude that DTI is more sensitive in detecting paraspinal muscle pathological changes in the early stage of lumbar degeneration than conventional lumbar MRI.

4998 Computer 33

Validity of skeletal muscle fiber type distinguished using q-space imaging

Junichi Hata[1,2,3], Kanehiro Fujiyoshi[2], Osahiko Tsuji[2], Yuji Komaki[2,3], Keigo Hikishima[4], Masaya Nakamura[2], and Hideyuki Okano[1,2]

[1]RIKEN Brain Science Institute, Saitama, Japan, [2]Department of Physiology, Keio University School of Medicine, Tokyo, Japan, [3]Central Institute for Experimental Animals, Kanagawa, Japan, [4]Okinawa Institute of Science and Technology, Okinawa, Japan

We developed a technology that the muscle composition ratio can be non-invasively visualize at q-space imaging. And, these MR image confirmed validation by comparison to the skeletal muscle histology. We scanned diffusion data using 7T MRI scanner and performed analysis to calculate QSI index. The mice lower leg was stained by several solutions to enable muscle typing. As a result, the cell size by sections showing the correlation between the QSI indices. Moreover, the visualization in a staining compared, it is possible to obtain the same image. We confirmed validation by comparing the stained image to QSI.

4999 Computer 34

ROI-based Evaluation of Diffusion Tensor Metric of Skeleton Muscles

Sarah Keller[1], Jin Yamamura[2], Shaheen Ahmed[3], Gerhard Adam[2], Nancy Rollins[3], and Zhiyue J. Wang[3]

[1]Diagnostic and Interventional Radiology and Nuclear Medicine, University Medical Center Hamburg Eppendorf, Hamburg, Germany, [2]Diagnostic and Interventional Radiology and Nuclear Medicine, University Medical Center Hamburg Eppendorf, Hamburg, [3]Radiology, University of Texas Southwestern Medical Center, Dallas, TX, United States

This study evaluates and compares a pixel-based and ROI-based quantification of DTI-metrics for skeleton muscles in healthy subjects. Besides SNR, an “intra-ROI diffusion direction dispersion angle" is evaluated as a quantitative metric to assess reliability of ROI-based DTI-metrics

---

5000

Computer 35

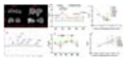

MRI/S Assessment of Skeletal Muscle Morphology and Energetics in Mdx Muscle Injured Mouse as a Model for Duchenne Muscular Dystrophy

HASAN ALSAID[1], Mary Rambo[1], Tinamarie Skedzielewski[1], Alan McDougal[2], Fritz Kramer[2], and Beat Jucker[1]

[1]Bioimaging, IV/IVT, PTS, GlaxoSmithKline, King of Prussia, PA, United States, [2]Muscle Metabolism DPU, MPC TAU, GlaxoSmithKline, King of Prussia, PA, United States

The purpose of this study was to longitudinally and non-invasively assess the effect of eccentric contraction induced muscle damage in the Mdx mouse as a model for Duchenne Muscular Dystrophy using non invasive MRI and MRS. Mdx mice showed a significant increase in absolute T2 value at baseline and a severe increase in the exercised leg at Day 2 following injury compared to the Wild type group. PCr/Pi ratios decreased in the Mdx group acutely upon exercise induced damage and resolved by day 7. The fraction of Undamaged Limb Force is correlated negatively with T2 and positevely with the PCr/Pi ratios.

5001

Computer 36

Development of an MR-Compatible Ergometer for Use in Quantifying Human Skeletal Muscle Bioenergetics During Supine Dynamic Contractions of the Knee Extensors

Rajakumar Nagarajan[1], Youssef Jaber[2], Miles Bartlett[3], Liam F Fitzgerald[3], Julia Miehm[3], Frank C Sup IV[2], and Jane A Kent[1,3]

[1]Human Magnetic Resonance Center, Institute for Applied Life Sciences (IALS), University of Massachusetts, Amherst, MA, United States, [2]Department of Mechanical & Industrial Engineering, University of Massachusetts, Amherst, MA, United States, [3]Kinesiology, University of Massachusetts, Amherst, MA, United States

The goal of this project was to develop an MR-compatible, multi-modal ergometer for the reliable measurement of human skeletal muscle torque, velocity, power and joint angle during 31P MRS studies of knee extensor muscle energetics. Intracellular [PCr], [Pi] and pH were determined in the vastus lateralis with 4-s time resolution during 4 min of maximal voluntary isokinetic contractions at 240 degrees per second, with a 30 degree range of motion. High S/N for both the MRS and power data indicate that this tool will be useful in future studies of in vivo muscle bioenergetics.

5002

Computer 37

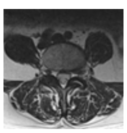

Study of correlation between multifidus muscles atrophy and degenerative diseases of lumbar spine in patients with low back pain using MRI

Jiufa Cui[1], Mingqian Huang[2], and Mark Schweitzer[2]

[1]Affiliated hospital of Qingdao University, Qingdao, People's Republic of China, [2]Department of Radiology, stony brook university hospital, Stony brook, NY, United States

Multifidus muscles (MF) atrophy are common in patients with Low back pain (LBP). Degenerative diseases of the lumbar spine, such as disc herniation, disc degeneration and facet joint osteoarthritis, are leading cause of LBP. Various studies have previously focused on the relationship between MF atrophy and disc degeneration, disc herniation. However, the results are inconsistent. Besides, no study for the correlation between MF atrophy and facet joint osteoarthritis has previously been conducted. This study will investigate the correlation between MF atrophy and disc degeneration, disc herniation, facet joint osteoarthritis using MRI.

5003

Computer 38

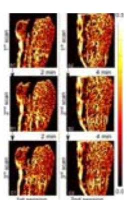

Repeatability of quantitative muscle strain and strain rate measurements by means of synchronous dynamic muscle MRI during electrical muscle stimulation

Xeni Deligianni[1,2], Michele Pansini[3], Meritxell Garcia[4], Anna Hirschmann[4], Arno Schmidt-Trucksäss[5], Oliver Bieri[1,2], and Francesco Santini[1,2]

[1]Radiology, Division of Radiological Physics, University of Basel Hospital, Basel, Switzerland, [2]Biomedical Engineering, University of Basel, Basel, Switzerland, [3]Ricerche Diagnostiche Srl, Bari, Italy, [4]Musculoskeletal Radiology, Clinic of Radiology and Nuclear Medicine, University of Basel Hospital, Basel, Switzerland, [5]Sports Medicine, University of Basel, Switzerland

Stimulation of the quadriceps muscle group of the thigh and synchronous phase contrast imaging at a 3T MRI scanner were applied to six healthy volunteers, to assess repeatability of the dynamic strain and strain rate maps. The repeatability was higher for strain (ICC=0.665-0.751) than for strain rate (ICC=0.242-0.571) and the correlation of the results increased with longer intra-scan rest periods. In conclusion, strain and strain rate measured with synchronous MRI of EMS-controlled muscle contraction are repeatable, though attention should be paid to intra-stimulation rest periods.

5004

Computer 39

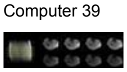

Assessment of Spontaneous Mechanical Activities in Musculature by Simultaneous Multi-Slice Diffusion-Weighted Imaging and Fiber-Tractography Data Validation

Martin Schwartz[1,2], Petros Martirosian[1], Guenter Steidle[1], Michael Erb[3], Bin Yang[2], and Fritz Schick[1]

[1]Section on Experimental Radiology, University of Tuebingen, Tuebingen, Germany, [2]Institute of Signal Processing and System Theory, University of Stuttgart, Stuttgart, Germany, [3]Biomedical Magnetic Resonance, University of Tuebingen, Tuebingen, Germany

Simultaneous multi-slice diffusion-weighted imaging (DWI) was applied on human right calf for imaging Spontaneous Mechanical Activity in Musculature (SMAM) in multiple slices in order to improve assessment of the spatial extension of these spontaneous activities. For data validation, diffusion-tensor images (DTI) were acquired with subsequent fiber tractography to fuse anatomical fiber orientation to spontaneous events in DWI. High accordance between both modalities and reliable application of simultaneous multi-slice diffusion-weighted imaging is demonstrated.

5005 Computer 40

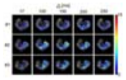

Estimation of the Sensitivity Characteristics and Detection Capability of Diffusion-Weighted MR Sequences in Imaging Spontaneous Mechanical Activity in Musculature

Martin Schwartz[1,2], Guenter Steidle[1], Petros Martirosian[1], Ander Ramos-Murguialday[3,4], Alto Stemmer[5], Bin Yang[2], and Fritz Schick[1]

[1]Section on Experimental Radiology, University of Tuebingen, Tuebingen, Germany, [2]Institute of Signal Processing and System Theory, University of Stuttgart, Stuttgart, Germany, [3]Institute for Medical Psychology and Behavioural Neurobiology, University of Tuebingen, Tuebingen, Germany, [4]Neurotechnology Laboratory, TECNALIA Health Department, San Sebastian, Spain, [5]Siemens Healthcare GmbH, Erlangen, Germany

Spontaneous mechanical activity in musculature (SMAM) can be observed from time to time in diffusion-weighted images (DWI) of the human lower leg. In DWI, motion sensitivity is usually restricted to a time window between diffusion-sensitizing dephasing and rephrasing gradients. Capabilities to detect SMAM occurring outside this time window by DWI are expected to be clearly reduced. The temporal sensitivity of diffusion-weighted sequences to SMAM is evaluated by varying diffusion-sensitizing time. In addition, concurrent surface electromyography (sEMG) measurements were performed in order to reveal the temporal correlation of the events in both modalities.

5006 Computer 41

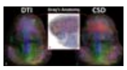

Crossing muscle fibres in the tongue resolved using constrained spherical deconvolution

Luuk Voskuilen[1,2,3], Valentina Mazzoli[2,4,5], Jos Oudeman[2], Ludi E. Smeele[1,6], Alfons J.M. Balm[1,6], Ferdi van der Heijden[1,7], Martijn Froeling[8], Gustav J. Strijkers[9], and Aart J. Nederveen[2]

[1]Department of Head and Neck Oncology and Surgery, Netherlands Cancer Institute, Antoni van Leeuwenhoek Hospital, Amsterdam, Netherlands, [2]Department of Radiology, Academic Medical Center, Amsterdam, Netherlands, [3]Department of Oral and Maxillofacial Surgery, Academic Centre for Dentistry Amsterdam and Academic Medical Center, University of Amsterdam and VU University Amsterdam, Amsterdam, Netherlands, [4]Biomedical NMR, Department of Biomedical Engineering, Eindhoven University of Technology, Eindhoven, Netherlands, [5]Orthopaedic Research Lab, Radboud UMCN, Nijmegen, Netherlands, [6]Department of Oral and Maxillofacial Surgery, Academic Medical Center, Amsterdam, Netherlands, [7]Department of Robotics and Mechatronics, MIRA Institute, University of Twente, Enschede, Netherlands, [8]Department of Radiology, University Medical Center Utrecht, Utrecht, Netherlands, [9]Biomedical Engineering and Physics, Academic Medical Center, Amsterdam, Netherlands

Tongue muscle architecture is suspected to be important in the prediction of speech and swallowing complications after surgery. The tongue contains areas of crossing muscle fibres unable to be resolved by diffusion tensor imaging (DTI). We show that constrained spherical deconvolution (CSD) is able to distinguish these crossing fibres *ex vivo* and *in vivo* using a clinically acceptable scan time of 10 min. Also, we show improved tractography in CSD compared to DTI, allowing segmentation of different tongue muscles which conforms to known anatomy.

5007 Computer 42

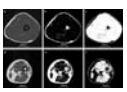

Magnetic Resonance Methods for Quantitative Evaluation of Intramuscular Adipose Tissue

Alexandra Grimm[1,2], Heiko Meyer[2], Mathias Nittka[2], Esther Raithel[2], Oliver Chaudry[1], Andreas Friedberger[1], Michael Uder[3], Wolfgang Kemmler[1], Klaus Engelke[1], and Harald H. Quick[1,4,5]

[1]Institute of Medical Physics, University Erlangen-Nuremberg, Erlangen, Germany, [2]Product Definition & Innovation, Siemens Healthcare GmbH, Diagnostic Imaging, Magnetic Resonance, Erlangen, Germany, [3]Institute of Radiology, University Hospital Erlangen, Erlangen, Germany, [4]Erwin L. Hahn Institute for Magnetic Resonance Imaging, University Duisburg-Essen, Essen, Germany, [5]High Field and Hybrid MR Imaging, University Hospital Essen, Essen, Germany

Intramuscular adipose tissue directly affects physical performance. 56 subjects (80 ± 5 yrs) with sarcopenia and 23 physically well-trained subjects (28 ± 4 yrs), all male, were examined at the thigh on a 3T MR system using quantitative MRI and MRS sequences. The results show that the use of spectroscopy involves challenges with regard to representative assessment of the entire muscle and might overestimate fat in low-fat tissues as muscle tissue. Furthermore, 2pt in comparison to 6pt Dixon sequences should be used with caution for quantitative evaluation, while multi-echo Dixon sequences are capable of quantifying intramuscular adipose tissue.

5008 Computer 43

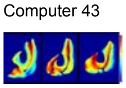

Heterogeneity of Quadriceps Muscle Activation during Isometric Contractions as revealed by Velocity Encoded Phase Contrast (VE-PC) Imaging.

Toshiaki Oda[1], Vadim Malis[2], Taija Juutinen Finni[3], and Shantanu Sinha[4]

[1]Hyogo University of Teacher Education, Katō, Hyōgo, Japan, [2]Physics, UC San Diego, San Diego, CA, United States, [3]The University of Jyväskylä, Jyväskylä, Finland, [4]Radiology, UC San Diego, San Diego, CA, United States

The relative contributions of the four compartments of the quadriceps to force production are clinically very important information. The spatial and temporal heterogeneity of velocity and strain, (surrogate biomarkers of neural activation) was determined, within and between different compartments of normal quadriceps and along the proximo-distal (Z) axis, during isometric contraction using gated VE-PC imaging. Statistically significant differences were determined, within the same muscle compartment, across compartments and between different Z axis positions. Determining how these change in the diseased state e.g. post-ACL tear will be important in tailoring rehabilitative strategies, with particular relevance to preventing early onset of osteoarthritis.

5009 Computer 44

MUSCLE: MUlti SliCe Localized Excitation 31P-MRS

Alexander Gussew[1], Martin Krämer[1], Kevin Moll[1], and Jürgen R. Reichenbach[1]

[1]Medical Physics Group, Institute of Diagnostic and Interventional Radiology, Jena University Hospital - Friedrich Schiller University Jena, Jena, Germany

We present a new ^{31}P-MR spectroscopy pulse sequence, the so called Multi-SliCe-Localized-Excitation approach (MUSCLE), which enables time resolved, interleaved non-spin-echo acquisitions of spectra in multiple muscle slabs. The accuracy of slab selection was successfully verified at 3 T by *in vitro* measurements in a multiple compartment phantom as well as by *in vivo* measurements of moderately loaded human calf muscles.

5010 Computer 45

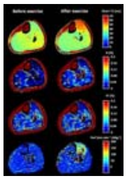

Quantitative NMR imaging of short and long T2 components in the SKM tissue by 1H T2- relaxometry study

Teresa Gerhalter[1,2], Pierre-Yves Baudin[3], Noura Azzabou[1,2], Eriky Caldas[1,2], Harmen Reyngoudt[1,2], Pierre Carlier[1,2], and Benjamin Marty[1,2]

[1]Institute of Myology, NMR Laboratory, Paris, France, [2]CEA, DRF, I²BM, MIRCen, Paris, France, [3]CRIS, Tournai, Belgium

Muscle water T2 is currently being used to assess and monitor the pathology of neuromuscular disorders. The vascular signal of water T2 is close to the one of fat, which might have an impact on the fat fraction quantification using a 2-component fitting approach on MSME data. Here, we examined the impact of long water T2 variations during exercise on fat quantification using the 2-component extended phase graph (EPG) model. Exercise increased the short T2 and the ratio between the amplitudes of short and long T2 signals suggesting an impact of the vascular space on the fat fraction quantification.

5011 Computer 46

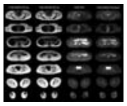

T2-weighted Dixon TSE for accelerated simultaneous grading of whole body skeletal muscle fat infiltration and edema in patients with neuromuscular diseases

Sarah Schlaeger[1], Elisabeth Klupp[1], Dominik Weidlich[2], Barbara Cervantes[2], Marcus Deschauer[3], Benedikt Schoser[4], Sarah Bublitz[3], Federica Montagnese[4], Christoph Katemann[5], Hendrik Kooijman[5], Ernst J. Rummeny[2], Claus Zimmer[1], Jan S. Kirschke[1], and Dimitrios C. Karampinos[2]

[1]Department of Diagnostic and Interventional Neuroradiology, Technical University of Munich, Munich, Germany, [2]Department of Diagnostic and Interventional Radiology, Technical University of Munich, Munich, Germany, [3]Department of Neurology, Technical University of Munich, Munich, Germany, [4]Friedrich-Baur-Institut, Ludwig-Maximilians-University, Munich, Germany, [5]Philips Healthcare, Hamburg, Germany

The assessment of fatty infiltration and edema in the whole body musculature of patients with neuromuscular diseases typically requires the separate performance of a T_1-weighted sequence and a fat suppressed T_2-weighted sequence. T_2-weighted Dixon TSE enables the generation of T_2-weighted fat-separated and water-separated images, which could be used to simultaneously assess fatty infiltration and edema and to reduce total scan time. The present study examines the diagnostic performance of whole body T_2-weigthed Dixon TSE imaging in 10 patients with neuromuscular diseases.

5012 Computer 47

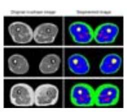

Magnetic resonance imaging estimates of intermuscular fat density in the thigh in sarcopenia population: correlation with physical performances

Yu Xin Yang[1], Wee Shiong Lim[1,2], Mei Sian Chong[1], Laura Tay[1,2], Suzanne Yew[1], Audrey Yeo[1], and Cher Heng Tan[3]

[1]Institute of Geriatrics and Active Ageing, Tan Tock Seng Hospital, Singapore, Singapore, [2]Geriatric Medicine, Tan Tock Seng Hospital, Singapore, Singapore, [3]Diagnostic Radiology, Tan Tock Seng Hospital, Singapore, Singapore

Emerging evidence suggests that intermuscular fat (IMF) accumulation is associated with reduced muscle quality and increased risk of physical limitation. However, the impact and mechanism of IMF in sarcopenia or sarcopenic obesity (SO) are still unclear. MRI is a promising tool for early detection of sarcopenia and SO. This may translate to use in clinical trials and in future clinical practice, where quantitative assessment may become standard of care. . This study aims to study a new index that we term “IMF density”, shows promise as an important quantitative variable that reflects patients’ physical performances.

Electronic Poster

Emerging Technologies & Other Tissues

Exhibition Hall Wednesday 16:15 - 17:15

5013 Computer 49

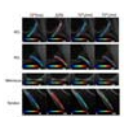

Highly Efficient Bi-Component T2* Mapping of the Knee using Ultra-short Echo Ramped Hybrid Encoding

Hyungseok Jang[1], Fang Liu[1], Richard Kijowski[1], and Alan B McMillan[1]

[1]Department of Radiology, University of Wisconsin, Madison, WI, United States

T2* analysis is used in musculoskeletal imaging to characterize tendon, meniscus, and cartilage in human joints. With the development of high performance gradient systems, ultrashort time echo (UTE) imaging has become more feasible, allowing robust bi-component of short and long T2* tissue components. Many studies have been performed to realize robust and clinically feasible bi-component T2* imaging, but the long acquisition time required to obtain multiple echo images remains challenging. In this study, we propose a novel, rapid imaging scheme for bi-component T2* analysis, based on ramped hybrid encoding (RHE) that allows robust bi-component T2* estimation within a single scan.

5014 Computer 50

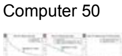

Bi-exponential T2* mapping of peripheral nerve from in-vivo human scans with a 3D UTE cones sequence.

Daehyun Yoon[1] and Brian Hargreaves[1]

[1]Department of Radiology, Stanford university, Palo Alto, CA, United States

Previous studies with nerve samples have demonstrated the existence of multiple signal components with different T2 or T2* relaxation times in peripheral nerves. The short- T2* signal component has received significant research attention, based on its correlation with myelin health of nerve fiber in many neurological diseases. However, little research has been conducted with in vivo human scans to separate the short-T2* component and the long-T2* component in peripheral nerves. Using a 3D ultra-short echo time (UTE) cones sequence, we demonstrate the feasibility of capturing and separating both bi-exponential T2* signal components from in vivo human nerve scans

---

5015 Computer 51

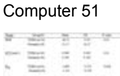

Type 2 diabetes alters bone marrow fat content and marrow blood flow as seen by IDEAL-IQ and DCE MRI

Lin Yuan[1], Zha Yunfei[1], Lin Hui[2], and Wu Bing[2]

[1]Renmin Hospital of Wuhan University, wuhan, People's Republic of China, [2]GE healthcare, wuhan, China

To explore the effect of type 2 diabetes on bone marrow fat contnent(BMF) and marrow blood flow, as well as the association of the bone marrow fat contnent and marrow perfusion in type 2 diabetes mellitus (T2DM) patients. 26 healthy nondiabetic subjects and 24 T2DM patients underwent lumbar IDEAL-IQ and DCE-MRI. The marrow fat content(BMF) and the marrow perfusion parameters (Ktrans, Kep, Ve) of lumbar vertebra all showed significant difference between T2DM patients and the healthy individuals. In addition, transfer constant (Ktrans) was negatively correlated with BMF in T2DM patients.

5016 Computer 52

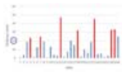

Knee-to-coil automatic distance detection for misalignment alert system during MRI acquisition

Takamasa Sugiura[1], Toshimitsu Kaneko[1], Tomoyuki Takeguchi[1], Kensuke Shinoda[2], Takuya Fujimaki[2], and Hiroshi Takai[2]

[1]Toshiba Corporation, Kawasaki, Japan, [2]Toshiba Medical Systems Corporation, Otawara, Japan

For high quality knee MRI image acquisition, the coil must be centrally aligned with the knee. However, precise alignment can suffer from patient motion and is currently performed by eye. We propose a method to automatically measure the misalignment between coil and knee to alert the clinical operator. This is done by calculating the distance between the coil and the knee joint gap by processing the localizer image with a machine learning technique, which was achieved with a mean accuracy of 3.3 mm. Our experiments further indicated a safe margin for knee-to-coil misalignment within a threshold of 20 mm.

5017 Computer 53

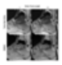

Metal Artifact Reduction MRI around Cobalt-Chromium Arthroplasty Implants: The Negative Effect of Long Echo Trains on Implant-related Artifact

Neil Mithilesh Kumar[1], Cesar Netto, Lew Schon, and Jan Fritz[2]

[1]Radiology, Johns Hopkins Hospital, Baltimore, MD, United States, [2]Radiology, Johns Hopkins Hospital

We demonstrate the negative effects of increasing echo train lengths on total implant-related artifact in a setting of controlled bandwidth, echo spacing and effective echo time. For the practical purpose of metal artifact reduction sequence MR imaging with use of turbo spin echo pulse sequences, high receiver bandwidth can be recommended as the first line means, whereas long echo train length may not be recommended and used cautiously due to the potential of substantial degradation of image quality.

5018 Computer 54

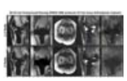

Compressed Sensing SEMAC MRI of Total Knee Arthroplasty Implants: Intra-subject Comparison at 1.5 and 3 Tesla

Jan Fritz[1], Benjamin Fritz[2], Gaurav K Thawait[1], Wesley D Gilson[3], Christoph Forman[4], Esther Raithel[4], Mathias Nittka[4], Robert Sterling[1], and Paul Khanuja[1]

[1]The Johns Hopkins University School of Medicine, Baltimore, MD, United States, [2]Orthopaedic University Hospital Balgrist, [3]Siemens Healthcare USA, [4]Siemens Healthcare GmbH

Because susceptibility artifacts increase with field strength, MRI of knee arthroplasty implants is commonly performed at 1.5T. However, 3T MRI offers substantially higher SNR and may be the only available option. SEMAC can achieve substantial metal artifact reduction at 3T, but requires prolongs scan times. Capitalizing on the inherent sparsity of SEMAC data, compressed sensing-based pseudo-randomized undersampling and iterative reconstruction can substantially accelerate data acquisition. We show the clinical feasibility of highly accelerated 3T MRI of CoCr knee arthroplasty implants using a compressed sensing SEMAC TSE sequence with metal artifact reduction capabilities and acquisition times similar to 1.5T.

5019 Computer 55

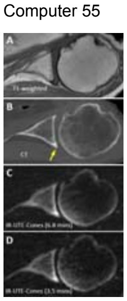

3D IR-UTE-Cones for High Contrast MR Imaging of Lamellar Bone

Anthony S. Tadros[1], Justin W. West[2], Amin Nazaran[1], Ya-Jun Ma[1], Heinz R. Hoenecke[2], Jiang Du[1], and Eric Y. Chang[1,3]

[1]Department of Radiology, University of California, San Diego Medical Center, La Jolla, CA, United States, [2]Orthopedic Surgery, Scripps Clinic, La Jolla, CA, United States, [3]Radiology Service, VA San Diego Healthcare System, San Diego, CA, United States

Lamellar bone is poorly evaluated using conventional magnetic resonance (MR) imaging secondary to its inherently short T2 relaxation time. Rather, the contours of lamellar bone are often inferred based on marrow signal. In the setting of shoulder instability or pre-operative planning for arthroplasty, rotator cuff integrity and glenoid bone defects are frequently assessed using both MRI and computed tomography (CT), respectively. An MR imaging technique to directly image lamellar bone could potentially eliminate the need for a CT scan and be particularly useful for young patients with acute shoulder instability.

5020 Computer 56

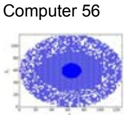

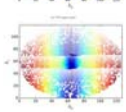

Compressed Sensing 3D GRASE for Faster PD-weighted Knee Imaging

Alexandra Cristobal-Huerta[1], Dirk Poot[1], Mika Vogel[2], and Juan Antonio Hernandez-Tamames[1]

[1]Department of Radiology and Nuclear Medicine, Erasmus MC, Rotterdam, Netherlands, [2]GE Healthcare B.V., Hoevelaken, Netherlands

Accelerated 3D-FSE using Compressed Sensing (CS) with a 30% scanning time reduction has been recently introduced and evaluated for knee MR images. 3D-GRASE is a hybrid FSE-EPI sequence that can achieve higher time-efficiency scans, since it acquires more k-space data per refocusing pulse. The purpose of this work is to present CS 3D-GRASE to achieve even faster musculoskeletal MRI acquisitions.

5021 Computer 57

Feasibility of synthetic MRI in knee in routine practice: image quality and diagnostic accuracy

Bénédicte MA Delattre[1], Maria Isabel Vargas[1], and Sana Boudabbous[1]

[1]*Geneva University Hospitals, Geneva, Switzerland*

Synthetic MRI is a very promising method to generate different contrasts used in clinical practice from quantitative T1, T2 and PD measurements. In this study we confirmed the feasibility of Synthetic MR in knee examinations, allowing generation of T1, PD and STIR images in faster time than conventional imaging with appropriate quality and good diagnosis confidence.

5022 Computer 58

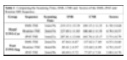

Application of Simultaneous Multi-Slice TSE in High-Resolution Hand and Foot Imaging

Feifei Gao[1], Yinghui Ge[1], Yi Wei[1], Shufang Wei[1], Xiaojing Kan[1], Panli Zuo[2], Dingxin Wang[3], and Tianyi Qian[2]

[1]*Radiology, Zhengzhou University People's Hospital, Zhengzhou, People's Republic of China,* [2]*Siemens Healthcare, MR Collaborations NE Asia, Beijing, People's Republic of China,* [3]*Siemens Medical Solutions USA, Inc., MN, United States*

The turbo spin echo sequence is one of the most frequently used MR sequences in routine musculoskeletal exams. Its short scan time has allowed it to become a popular clinical choice because it reduces the possibility of motion artifact especially in patients with low tolerance for MR exams. In order to further shorten the scan time and increase temporal and/or spatial resolution, simultaneous multi-slice technique has been widely applied during brain image acquisition. In this study we tried to apply a prototypical SMS-TSE sequence to hand and foot imaging. Compared to the standard TSE sequence, the SMS-TSE had the same image quality and a shorter acquisition time.

5023 Computer 59

Model-enhanced ZTE rendering of musculoskeletal structures

Gaspar Delso[1], Michael Carl[2], and Graeme McKinnon[2]

[1]*GE Healthcare, Cambridge, United Kingdom,* [2]*GE Healthcare, United States*

The objective of the present study was to improve three-dimensional visualisation of ZTE-based bone images by incorporating a-priori anatomical information in the rendering process.

5024 Computer 60

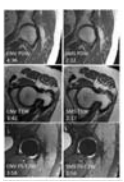

Simultaneous multi-slice TSE imaging of the hip joint: Acquisition time reduction and imaging quality.

Mayuko Haraikawa[1], Masashi Suzuki[1], Yuki Hara[1], Kayu Takezawa[1], Nanami Okano[1], Iichiro Osawa[1], Kaiji Inoue[1], Eito Kozawa[1], Junji Tanaka[1], Keisuke Watarai[2], Taishi Unezawa[1], Atsushi Kondo[1], Hiroshi Imai[3], Thomas Beck[4], Dingxin Wang[5], and Mamoru Niitsu[1]

[1]*radiology, Saitama Medical University Hospital, Saitama, Japan,* [2]*orthopedics, Saitama Medical University Hospital, Saitama, Japan,* [3]*Siemens Healthcare K.K, Tokyo, Japan,* [4]*Siemens Healthcare GmbH, Erlangen, Germany,* [5]*Siemens Healthcare, Minneapolis, United States*

Simultaneous-Multi-Slice Turbo-Spin-Echo (SMS TSE) protocols were added to our conventional (CNV) hip joint MR examination in 21 patients. Image quality of acetabular labrum, articular cartilage, round ligament and bony trabeculae were evaluated by three reviewers and showed comparable image quality, whereas SMS was slightly better for bony trabeculae. If CNV is substituted by SMS, total scan time can be reduced by approximately 40%. Although SMS protocols showed higher specific absorption rate (SAR), it only accounted for 20% of scans which exceeded the first level of SAR limit. SMS could be applied to clinical examination with advantage of acquisition time reduction.

5025 Computer 61

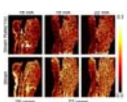

Age-related differences in quantitative muscular contraction parameters measured by synchronous dynamic MRI of electrical muscle stimulation

Xeni Deligianni[1,2], Christopher Klenk[3], Meritxell Garcia[4], Michele Pansini[5], Anna Hirschmann[4], Arno Schmidt-Trucksäss[3], Oliver Bieri[1,2], and Francesco Santini[1,2]

[1]*Radiology, Division of Radiological Physics, University of Basel Hospital, Basel, Switzerland,* [2]*Biomedical Engineering, University of Basel, Basel, Switzerland,* [3]*Sports Medicine, University of Basel, Basel, Switzerland,* [4]*Musculoskeletal Radiology, Clinic of Radiology and Nuclear Medicine, University of Basel Hospital, Basel, Switzerland,* [5]*Ricerche Diagnostiche Srl, Bari, Italy*

Stimulation of the quadriceps muscle group of the thigh and synchronous phase contrast imaging at a 3T MRI scanner were applied to six young and 13 elderly volunteers, to assess age-related differences. Dynamic strain and strain rate maps were reconstructed. Age-related differences both for strain and strain rate were observed and the significance of the difference increased when the vastus intermedius muscle was included.

5026 Computer 62

Utilization of phase data to improve image contrast in UTE MRI at 3T

Aiming Lu[1], Joel P Felmlee[1], and Krzysztof R Gorny[1]

[1]*Mayo Clinical, Rochester, MN, United States*

MR imaging with UTE/ZTE sequences has attracted significant clinical interest in recent years due to their many inherent merits, such as resilience to motion and flow artifacts, capability to achieve high acceleration factors and minimize acoustic noise, as well as capability to capture signal from tissues with ultra-short T2s/T2*s. However, ZTE acquisitions and many UTE acquisitions require the use of low flip angles and, as a consequence, deliver mostly proton density weighted contrast. Magnetization preparation such as fat suppression with UTE/ZTE is time consuming as k-space center data needs to be acquired every TR. Therefore, exploiting the other inherent information such as signal phase is important. In this work, we demonstrate that phase images obtained with UTE can be exploited to enhance the tissue contrast such as fat/water differentiation and enable improved cortical bone visualization, and generate susceptibility map in the volunteer knee on a clinical scanner at 3T.

5027 Computer 63

Improvement of 3D diffusion-prepared MR neurography in the extremities using improved diffusion-sensitized driven-equilibrium (iDSDE) with phase-cycling turbo field echo sequence

Takayuki Sakai[1], Masami Yoneyama[2], Atsuya Watanabe[1], Iain Ball[3], Toshiaki Miyati[4], and Noriyuki Yanagawa[1]

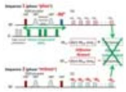

[1]Eastern Chiba Medical Center, Chiba, Japan, [2]Philips Electronics Japan, Tokyo, Japan, [3]Philips Electronics Australia, North Ryde, Australia, [4]Kanazawa University, Ishikawa, Japan

Diffusion-sensitized driven-equilibrium with phase-cycling T1-turbo field-echo (pc-DSDE) enables the visualization of peripheral nerves. However, pc-DSDE has several problems, such as low image stability, poor reproducibility, and partially remaining venous signals. To solve these problems, we improved DSDE pre-pulse module (iDSDE) including B1-insensitive RF pulse and orthogonally combined motion- and diffusion-sensitized gradient scheme. iDSDE showed better visualization of peripheral nerves without contamination of veins.

5028 Computer 64

Lipid Suppression Around Metal Implants Using a B1-Optimized Adiabatic Inversion Pulse

S Sivaram Kaushik[1], Andrew Huettner[2], Peter LaViolette[3], Andrew Nencka[3], and Kevin Koch[3]

[1]MR Applications and Workflow, GE Healthcare, Waukesha, WI, United States, [2]MR Systems Engineering, GE Healthcare, Waukesha, WI, United States, [3]Radiology, Medical College of Wisconsin, Milwaukee, WI, United States

A nonlinear iterative optimization algorithm was used to design an adiabatic inversion pulse with a bandwidth of 3.2 kHz. With a larger bandwidth, the new pulse maintains the same SAR as the original inversion pulse and also has an improved spectral profile. Images obtained on a phantom, and in-vivo, show improved fat suppression, and reduced ripple artifacts in the slice domain. In addition to improving image quality, the optimized RF pulse may improve the diagnostic ability of STIR with 3D multi spectral imaging.

5029 Computer 65

Musculoskeletal imaging of the extremities with a compact 3T MRI with high-performance gradients

Paul T Weavers[1], Matt Frick[1], Erin M Gray[1], David Stanley[2], Joshua D Trzasko[1], Shengzhen Tao[1], Yunhong Shu[1], Derrick Doolittle[1], John Huston III[1], Thomas K.F. Foo[3], and Matt A Bernstein[1]

[1]Radiology, Mayo Clinic, Rochester, MN, United States, [2]GE Healthcare, [3]MRI, GE Global Research, Niskayuna, NY, United States

A compact, low-cryogen 3T MRI system with high-performance gradients has been developed and tested on healthy volunteers. This compact 3T MRI unit has the potential to dramatically impact MRI by offering simplified siting and strong gradient performance at lower cost. In addition to brain and pediatric imaging, the scanner offers an ideal platform for musculoskeletal (MSK) imaging of the extremities.

5030 Computer 66

Initial Experience of MAGiC of the knee at 3T MRI: comparison with conventional T1-weighted image and T2 mapping

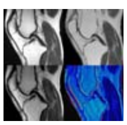

Sunghoon Park[1], Young Ju Lee[2], Sung-Min Gho[2], Seungnam Back[3], and Kyu-Sung Kwack[1]

[1]Radiology, Ajou University School of Medicine, Suwon, Korea, Republic of, [2]MR Applications and Workflow, GE healthcare, Korea, Republic of, [3]MR, GE healthcare, Korea, Republic of

Synthetic MR is able to acquire T1-, T2-, proton density-weighted image and quantitative map simultaneously and has the potential to reduce the overall examination time. Synthetic MR image have comparable image qualities with that of conventional MR images for the knee joint.

5031 Computer 67

Imaging and Quantification of Grafted Mesenchymal Stem Cells in Rat Knee Joint

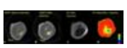

Sergey Magnitsky[1], Jaskanwaljeet Kaur[1], Yu-An Evan Lay[2], Geetha Mohan[2], Jinjin Zhang[3], Djaudat Idiyatullin[3], Michael Garwood[3], and Nancy Lane[2]

[1]Radiology, UCSF, San Francisco, CA, United States, [2]Center for Musculoskeletal Health, UC Davis, [3]Radiology, University of Minnesota

Mesenchymal Stem Cells (MSCs) have high potentials for a treatment of bone diseases. T2*w-MRI in combination with iron labeling of MSCs has shown promising results for the detection of therapeutic cells. However, this method is not applicable for the detection of MSCs in knee joints because both the iron labeled cells and bones produce a hypointense signal. We have shown that the SWIFT sequence overcomes this limitation and generates a distinct and quantifiable signal from iron labeled cells in a knee joint *in vivo*. Proposed protocol opens new opportunities for *in vivo* monitoring of cell therapy of bone disorders.

5032 Computer 68

Chemical Shift Displacement and Recovery-based Simultaneous Water and Lipid Imaging for Quantitative Multiparametric MRI

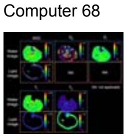

Naoki Ohno[1], Tosiaki Miyati[1], Shuto Suzuki[1], Hirohito Kan[2], Toshitaka Aoki[2], Yoshitaka Nakamura[1], Yuki Hiramatsu[1], and Toshifumi Gabata[3]

[1]Institute of Medical, Pharmaceutical and Health Sciences, Kanazawa University, Kanazawa, Japan, [2]Department of Central Radiology, Nagoya City University Hospital, Nagoya, Japan, [3]Department of Radiology, Kanazawa University Hospital, Kanazawa, Japan

In general, it is difficult to obtain functional information about water and lipid in tissues at the same time. We, therefore, developed a novel method using chemical shift displacement and recovery-based separation of lipid tissue (SPLIT) with different inversion times, echo times, and b-values to simultaneously acquire diffusion, perfusion, T_1, T_2, and lipid fraction in the calf. All parameters obtained with the SPLIT were consistent with previously reported values. This method enables simultaneous acquisition of functional information without special pulse sequence.

5033 Computer 69

Clinical interpretation of asymptomatic medial collateral ligament injury observed on magnetic resonance imaging in adolescent baseball players

Yoshikazu Okamoto[1], Kiyoshi Maehara[1], Kenta Tanaka[1], and Tetsuya Kanahori[1]

[1]University of Tsukuba, Tsukuba, Japan

This presentation clarified the clinical interpretation of 'asymptomatic MCL injury of the elbow observed on MRI among adolescent baseball players' by comparing the findings of MRI with those of standard clinical orthopedic examinations including palpation and US. Our results suggested the finding includes a broad spectrum of injuries; namely, a group of injuries that are characterized by changes associated with 'adaptation' and group of a 'pre-injury' characterized by changes to symptomatic MCL injury.

5034 Computer 70

Utility of Radial Reformation of Three-dimensional Fat-suppressed Multi-echo Gradient-recalled-echo Imaging in the Evaluation of Acetabular Labral Injuries and Femoroacetabular Impingement

Keizo Tanitame[1], Takahiro Sueoka[2], Yukiko Honda[3], Yuji Takahashi[3], Akira Naito[1], and Kazuo Awai[3]

[1]Chugoku Rosai Hospital, Kure, Japan, [2]Hiroshima Prefectural Hospital, Hiroshima, Japan, [3]Hiroshima University Hospital, Hiroshima, Japan

Radial images through the center of the acetabulum in the plane including the entire acetabular rim are useful for evaluating acetabular labral injuries, and those perpendicular to the center of the femoral head through the central axis of the femoral neck enable evaluation of the morphological findings of femoroacetabular impingement. Continuous thin-slice images from optimized 3D fat-suppressed multi-echo gradient-recalled-echo allow 360° radial reformation of hip joints, offering precise evaluation of the range of acetabular labral injury and femoroacetabular impingement morphology.

5035 Computer 71

A feasibility study of MR T2-mapping for evaluating birth-related levator ani muscle injury

yujiao zhao[1], zhizheng zhuo[2], and wen shen[1]

[1]Department of Radiology, Tianjin First Center Hospital, Tianjin, People's Republic of China, [2]Philips Healthcare, Beijing, China, beijing

Currently, the abnormal morphology of LAM is assessed with an unaided subjective diagnosis. But T2 mapping can quantitatively evaluate the injury muscle and indicate the injured degree and region of the LAM. In this study, we investigate whether the quantitative MR T2-mapping can evaluate birth-related levator ani muscle injury. The results showed that T2-mapping can quantitatively assess birth-related levator ani muscle injury and T2-mapping color-coded images show the range and degree of LAM injury visually. Moreover, it is helpful for detecting micro lesions which is difficult for just using PDWI images.

5036 Computer 72

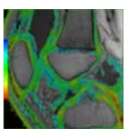

Value of quantitative T2 mapping in detecting early joint changes in children with haemophilia

Shufang Wei[1], yinghui Ge[1,2,3], Xiaojing Kan[1], and Feifei Gao[1]

[1]henan province people hosptial, zhengzhou, People's Republic of China, [2]henan provice people hospital, [3]henan provice people hospital, zhengzhou, People's Republic of China

T2 mapping imaging, as one of the MRI functional imaging, is sensitive to the changes of early cartilage components in the early stage of HA, hinting that T2 mapping imaging may be used as a tool to diagnose the cartilage disease in the early stage of HA.

Electronic Poster

Topics in Acquisition

Exhibition Hall Wednesday 16:15 - 17:15

5037 Computer 73

Echo-planar imaging with the Dynamic Multi-Coil Technique (DYNAMITE-EPI)

Umesh Suryanarayana Rudrapatna[1], Fabian Fluerenbrock[2], Terence W Nixon[1], Robin A de Graaf[1], and Christoph Juchem[1]

[1]Yale School of Medicine, New Haven, CT, United States, [2]RWTH Aachen University, Aachen, Germany

Despite numerous improvements in MRI technology, the fundamental gradient hardware has always been designed to generate linear and orthogonal fields. This mould was broken with the advent of DYNAmic Multi-coilI TEchnique (DYNAMITE), which uses non-linear and non-orthogonal B$$$_{0}$$$ fields for shimming and imaging. Besides vastly expanding the field shaping possibilities, this new technology also promises faster switching and lower eddy currents. For widespread uptake of this technology, proving its suitability for performing widely used contemporary scans like EPI is a must. In this work we share our results from the first successful implementation of DYNAMITE-EPI.

5038 Computer 74

magna cum laude

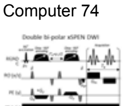

DTI measurements with exceptional resilience to field heterogeneities in challenging brain regions

Eddy Solomon[1], Gilad Liberman[1], Zhiyong Zhang [1], and Lucio Frydman[1]

[1]chemical Physics, Weizmann Institute of Science, Rehovot, Israel

This study presents a new diffusion tool based on a novel single-shot 2D MRI method called xSPEN. xSPEN is characterized with unusual resilience to field heterogeneities, but extending it to DTI requires to overcome the strong intrinsic diffusion weighting of this technique. To achieve this we formulated xSPEN's diffusion weighting using a novel, spatially localized b- matrix analysis, and devised a novel diffusion-weighting scheme that overcomes xSPEN's original limitations. These methods were numerically validated and applied to new DTI xSPEN sequences with which we mapped diffusion in often unreachable human head regions, including optic nerve and olfactory bulb regions.

5039 Computer 75

How to spend your time? Using multi-echo acquisition versus increasing sampling rate in resting-state fMRI

Daniele Mascali[1], Keith Jamison[2], Emily Kittelson[2], Kâmil Uğurbil[2], Essa Yacoub[2], Shalom Michaeli[2], Melissa Terpstra[2], Federico Giove[1], and Silvia Mangia[2]

[1]*Museo Storico della Fisica e Centro Studi e Ricerche "Enrico Fermi", Rome, Italy,* [2]*Center for Magnetic Resonance Research, Dept. of Radiology, University of Minnesota, Minneapolis, MN, United States*

High sampling rate is pivotal for differentiating neuronal-related from spurious correlations in resting-state-fMRI (rsfMRI). Acquiring multi-echoes (ME) during an EPI readout increases contrast-to-noise, but it can compromise temporal resolution even when combined with multiband (MB). Therefore, whether MBME-EPI is ultimately beneficial for rsfMRI remains unclear. To address this, we collected data at 3T with 2-mm resolution using MBME-EPI and the human-connectome-project MB-single-echo-EPI. Data were evaluated for spectral amplitude, consistency and specificity. MBME-EPI showed significant gains in all quantities when physiological noise and sampling rate were matched between time-series. However, there was no clear gain when different sampling rates were considered.

5040

magna cum laude

Computer 76

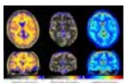

Insights from a combined study: Linking two modalities – total water content distribution and isotropic water fraction.

Zaheer Abbas[1,2], Farida Grinberg[1,2], Ezequiel Farrher[1], Krzysztof Dzieciol[1], Elene Iordanishvili[1], and Nadim Jon Shah[1,2]

[1]*Medical Imaging Physics, Institute of Neuroscience and Medicine, Juelich, Germany,* [2]*Faculty of Medicine, RWTH Aachen, JARA, Aachen, Germany*

Two methods – distributions of total free water (FW) content and unrestricted, isotropic water fraction (IWF) were studied in order to establish a possible link between them. MRI protocols were set in order to obtain quantitative FW maps as well as IWF distributions, based on a free water elimination DTI method. Joint histograms reveal strong correlation and suggest the way FW can complement the information obtained from IWF. Combining both modalities (FW and IWF distributions) in presence of pathologies may help to define the pathophysiological basis of different disorders and identify predictors of clinical symptoms.

5041

Computer 77

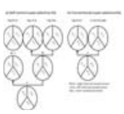

Omitting the control condition using self-control super-selective Arterial Spin Labeling to reduce total scan time for flow territory mapping

Thomas Lindner[1], Naomi Larsen[1], Olav Jansen[1], and Michael Helle[2]

[1]*Clinic for Radiology and Neuroradiology, University Hospital Schleswig-Holstein, Kiel, Germany,* [2]*Tomographic Imaging Department, Philips Research, Hamburg, Germany*

Selective Arterial Spin Labeling (ASL) is established to perform non-contrast enhanced flow territory mapping. In super-selective pCASL only one artery of interest is labeled while the efficiency in contralateral arteries is near zero. To obtain a holistic picture of all brain perfusion territories, the label and control experiments have to be repeated for each artery, prolonging scan time. In this study, it is hypothesized that due to the (almost) negligible signal contribution of non-tagged arteries, selective perfusion images can be calculated from a single scan that is performed without the acquisition of control images.

5042

Computer 78

Imaging inferior alveolar neurovascular bundle using zero echo time magnetic resonance imaging

Chuanchen Zhang[1], Changhu Liang[2], Chuanying Shi[3], Mingzhen Wu[3], and Bin Zhang[4]

[1]*Department of Radiology, Liaocheng People's Hospital, Shandong University, Liaocheng, People's Republic of China,* [2]*Department of Radiology, Shandong Medical imaging research institute,* [3]*Liaocheng People's Hospital, Shandong University,* [4]*Liaocheng People's Hospital, Shandong University*

The goal of the present study was to evaluate ZTE acquisitions for the inferior alveolar neurovascular bundle (IANB) identification. For this purpose, 15 volunteers were scanned using a standard 3D ZTE sequence with a voxel size of 0.8×0.8×0.8 mm on a 3 Tesla MR unit. Both subjective and objective analyses were performed on all acquired IANB images. The results indicate that ZTE-MRI is feasible for the IANB imaging without the use of contrast material.

5043

Computer 79

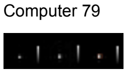

Quantitative Measures of Arteriole Flow in Human Perivascular Spaces

Xiaopeng Zong[1] and Weili Lin[1]

[1]*Department of Radiology and Biomedical Research Imaging Center, University of North Carolina at Chapel Hill, Chapel Hill, NC, United States*

Pulsatility of blood flow in human perivascular spaces may play an important role in clearing metabolic waste from the brain. However, flow measurement within small arterioles using MRI are hampered by the limited spatial resolutions of MRI. We report an approach that can accurately measure flow in sub-voxel tubular structures such as arterioles by combining time of flight and phase contrast MRI. The accuracy of our method were first demonstrated in a flow phantom study. Then, flows of penetrating arterioles were obtained in human subjects. Our results demonstrate the importance of correction of partial volume effects in measuring arteriole flow.

5044

Computer 80

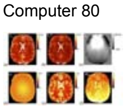

Quantitative MRI method, a multi-pathway multi-echo approach

Cheng-Chieh Cheng[1], William Scott Hoge[1], Tai-Hsin Kuo[2], and Bruno Madore[1]

[1]*Radiology, Brigham and Women's Hospital, Harvard Medical School, Boston, MA, United States,* [2]*Department of Imaging system, Philips Healthcare, Taipei, Taiwan*

A novel quantitative imaging method based on steady-state signals was proposed to simultaneously resolve MR-related parameters. A special, two-flip angle acquisition was implemented to account for the fluctuations in B_1^+ field. Furthermore, we developed a motion-resistant sampling scheme to lessen the impact of motion on steady-state signal for *in vivo* brain scans. A 3D brain imaging that extracts main MR-related parameters such as T_1, T_2, T_2^*, M_0, B_0, and B_1^+ was performed here in less than 12 minutes.

5045 Computer 81

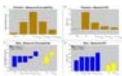

Dynamic Monitoring of Brown Adipose Tissue Activation and White Adipose Tissue Beiging

Gregory Simchick[1,2], Amelia Yin[3], Hang Yin[3], and Qun Zhao[1,2]

[1]Physics and Astronomy, University of Georgia, Athens, GA, United States, [2]Bio-Imaging Research Center, University of Georgia, Athens, GA, United States, [3]Biochemistry and Molecular Biology, University of Georgia, Athens, GA, United States

The treatment of obesity is clinically significant as it is related to many serious heart diseases and diabetes. Therefore, it is very advantageous to be able to non-invasively monitor whether or not a treatment is effective. Presented here is a method using magnetic resonance imaging (MRI) based water-fat separation, quantitative susceptibility mapping (QSM), and transverse relaxation rate (R_{2}^{*}) to dynamically monitor brown adipose tissue (BAT) activation and the white adipose tissue (WAT) beiging process. In a mouse model, increases in susceptibility between 40-164% and increases in R_{2}^{*} between 32-71% were observed in intracapsular BAT and inguinal WAT indicating metabolic changes related to BAT activation and WAT beiging.

5046 Computer 82

Optimal Control Pulse Design for Contrast in MRI: in vivo applications

Eric Van Reeth[1], Hélène Ratiney[1], Sophie Gaillard[1], Michael Tesch[2], Olivier Beuf[1], Steffen Glaser[2], and Dominique Sugny[3,4]

[1]CREATIS - CNRS UMR 5220 - INSERM U1206 - Université Lyon 1 - INSA Lyon - Université Jean Monnet Saint-Etienne, Villeurbanne, France, [2]Department of Chemistry, Technische Universität München, Munich, Germany, [3]Laboratoire Interdisciplinaire Carnot de Bourgogne, Dijon, France, [4]Technische Universität München Institute for Advanced Study, Munich, Germany

Optimal control RF pulse design has recently been proposed to address the optimization of image contrast in MRI - in order to explore the theoretical contrast bound of a given imaged system. Their use has recently been validated on a real MRI scanner to contrast various *in vitro* samples. This abstract extends these results to *in vivo* applications, and shows that contrasts obtained with standard weighting strategies on rat and mouse brains can be improved or inverted. This demonstrates both the interest and flexibility that one can get when using optimal contrast pulses for *in vitro* and *in vivo* applications.

5047 Computer 83

Bloch-Siegert Phase-Encoded MRI with a Single RF Coil and Frequency-Swept Pulses

Christopher J Hasselwander[1] and William A Grissom[1]

[1]Biomedical Engineering, Vanderbilt University, Nashville, TN, United States

RF encoding using the Bloch-Siegert shift has the potential to replace conventional gradient encoding with cheaper RF gradients, and can directly replace gradient pulsing in common MRI sequences. However, current implementations require large frequency offsets to prevent on-resonance excitation, which subsequently requires high RF power for encoding as well as separate imaging and encoding RF coils. Here we show that frequency-swept encoding RF pulses enable the use of a single RF coil for imaging and encoding since the frequency offset can be brought much closer to resonance.

5048 Computer 84

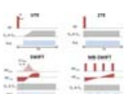

Optimal MRI pulse sequence to quantify iron-oxide nanoparticles at high concentration

Jinjin Zhang[1], Michael Garwood[1], and Djaudat Idiyatullin[1]

[1]Center for Magnetic Resonance Research, Department of Radiology, University of Minnesota, Minneapolis, MN, United States

Recent advances in nanotechnology have allowed for the effective use of iron oxide nanoparticles (IONP) in magnetic nanoparticle hyperthermia for cancer therapy and in cell tracking for immunotherapy. Noninvasive imaging techniques for tracking and quantifying IONPs in-vivo will be necessary for accurate assessment. In this study, we have tested four representative ultra-short T2 sensitive MRI pulse sequences, UTE, ZTE, SWIFT and MB-SWIFT, to compare their performance for measuring IONPs at clinically relevant high concentration range. Multiple performance metrics were evaluated, compared, and summarized.

5049 Computer 85

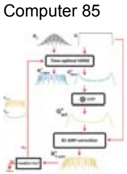

A simple optimization approach to making time efficient VERSE-multiband pulses feasible on non-ideal gradients

Samy Abo Seada[1], Jo Hajnal[1], and Shaihan Malik[1]

[1]Division of Imaging Sciences and Biomedical Engineering, King's College London, London, United Kingdom

Multiband pulses can have long durations, which can be reduced by applying the VERSE approach to optimize the combination of gradient and RF pulse to make full use of available hardware performance. The resulting time-varying gradients are demanding and can lead to excitation errors on non-ideal gradient systems. In this work we incorporated the measured gradient impulse response function (GIRF) into an iterative VERSE design method and validated the result using simulation and experiments.

5050 Computer 86

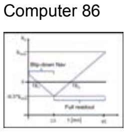

Simultaneous interleaved blip up/down readout for dynamic off-resonance correction in functional EPI

Benjamin Zahneisen[1], Murat Aksoy[1], and Julian Maclaren[1]

[1]Stanford University, Stanford, CA, United States

Motion and geometric distortions of EPI acquisitions remain challenging as motion during an fMRI scan affects the stability of the time series in two ways: Rigid motion displaces voxels by “moving” the spins. A change in head orientation and the complex interplay of external and internal susceptibility differences lead to a change in the off-resonance field. In combination with an EPI readout this change in off-resonance field leads to an “apparent” voxel displacement. Here, we propose the simultaneous acquisition of a blip-down navigator with the original blip-up host-EPI sequence which is used to derive a snapshot of dynamic off-resonance changes.

5051 Computer 87

Using the inflow effect to determine velocity in the carotid artery: comparison with phase contrast velocity mapping

Neville D Gai[1] and John A Butman[1]

[1]*Radiology & Imaging Sciences, NIH Clinical Center, Bethesda, MD, United States*

Phase contrast (PC) imaging is commonly employed for mapping velocities in cerebral arteries. This requires a dedicated sequence along with acquisition of two sets of image data. In addition, PC imaging can be compromised by residual eddy currents, motion, selection of velocity encoding value (VENC) and imaging plane in relation to the vessel. In this work, a magnitude based method exploiting the inflow effect was employed to determine velocity in the carotid arteries. A standard 3D T1w SPGR sequence was used eschewing the need for a dedicated sequence. By measuring signal in ROIs at two locations of the artery and jugular vein, velocity independent of B1 inhomogeneity can be derived. The effect of B1+ field was also taken into account. It was shown that the velocity estimated with this technique shows significant correlation with PC based velocity while showing no significant differences in the right and left CAs in 12 volunteers.

5052 Computer 88

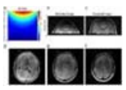

Magnetic Resonance Imaging under Highly Inhomogeneous B0 Fields using Missing-Pulse Steady-State Free Precession (MP-SSFP)

Naoharu Kobayashi[1], Djaudat Idiyatullin[1], Gregor Adriany[1], and Michael Garwood[1]

[1]*Center for Magnetic Resonance Research,Department of Radiology, University of Minnesota, Minneapolis, MN, United States*

In vivo human brain imaging under highly inhomogeneous B_0 field of 250 kHz off-resonance variation over 20 cm is demonstrated. The B_0 field inhomogeneity was generated by mounting a head gradient coil at 36 cm off the isocenter of a 90-cm 4T magnet. Brain imaging was performed with 3D missing-pulse steady-state free precession using the inhomogeneous field gradient for spatial (readout) encoding. Frequency-modulated pulses were employed to excite the widely distributed spin frequencies in the inhomogeneous field with easily achievable RF peak power (~1 kW). By providing combined T_1, T_2, and high diffusion weighting, images with clear delineation of brain anatomy were produced.

5053 Computer 89

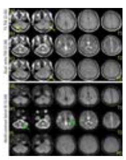

A Rapid Hybrid Spiral Spin-Echo Technique for Simultaneous Multi-Contrast Fat-Water Imaging

Zhiqiang Li[1], Dinghui Wang[1], and James G Pipe[1]

[1]*Imaging Research, Barrow Neurological Institute, Phoenix, AZ, United States*

In the conventional MR setting, each contrast is typically acquired with a different scan/sequence, often resulting in long scan time and inter-scan misregistration. Simultaneous multi-contrast imaging has advantages such as good registration, reduced scan time, etc. In this project we propose a hybrid spiral SE technique for simultaneous T1, T2, and PD imaging, with fast scan speed and improved image quality.

5054 Computer 90

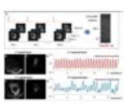

Improved image-based navigators (iNAVs) for free-breathing cine DENSE using principle component analysis to separate the stimulated echo and T1 relaxation signals

Xiaoying Cai[1], Yang Yang[1], Xiaodong Zhong[2,3], Daniel S Weller[4], Michael Salerno[1,5,6], and Frederick H Epstein[1,5]

[1]*Biomedical Engineering, University of Virginia, Charlottesville, VA, United States,* [2]*MR R&D Collaborations, Siemens Healthcare, Atlanta, GA, United States,* [3]*Department of Radiology and Imaging Sciences, Emory University, Atlanta, GA,* [4]*Electrical and Computer Engineering, University of Virginia, Charlottesville, VA, United States,* [5]*Radiology, University of Virginia,* [6]*Medicine, University of Virginia*

Cine displacement encoding with stimulated echoes (DENSE) is an accurate strain imaging technique that generally requires breath-holding. We have recently developed a free-breathing method with image-based navigators (iNAVs) that makes use of the localized signal generation property of stimulated echoes (STE) to facilitate the estimation of heart motion due to respiration. However the non-localized echo due to T1 relaxation presents challenges. We propose to use principle component analysis (PCA) to separate the STE and T1-relaxation echo signals and improve the accuracy of motion estimation with iNAVs for free-breathing cine DENSE.

5055 Computer 91

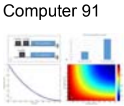

A Method of Fat Saturation with Better Transmit Field Inhomogeneity Immunity

Xiaocheng Wei[1] and Yongchuan Lai[2]

[1]*MR Research China, GE Healthcare, Beijing, People's Republic of China,* [2]*MR Engineering, GE Healthcare, Beijing, People's Republic of China*

Discrimination between signals from fat and water is of great importance in clinical practice. Chemical saturation, the most widely used fat suppression method, has degraded performance in an in-homogeneity transmit field, and may jeopardize the diagnosis effectiveness. In this abstract, we proposed an improved fat saturation method employing multiple chemical saturation segments. Phantom and volunteer evaluation results show that new method has much less residual lipid signal and can achieve more uniform lipid saturation over big field of view under inhomogeneity condition. Which support the conclusion that proposed method has superior transmit field inhomogeneity immunity.

5056 Computer 92

SUPER: a novel acquisition and reconstruction strategy for improved efficiency and resolution in parameter mapping

Chenxi Hu[1] and Dana Peters[1]

[1]*Yale University, New Haven, CT, United States*

Standard parameter mapping methods such as T1 and T2 mapping suffer from long scan time and low resolution due to the need to sample multiple images along the relaxation curve. Here we propose a novel acquisition and reconstruction strategy to improve efficiency by undersampling each k-space frame in the phase-encoding direction. By shifting the undersampling pattern circularly in each time frame, the relaxation signal at spatially distinct voxels is modulated and combined into a single signal, which can be used to reconstruct the parameters by solving a small-size nonlinear equation. This technique is especially suitable for applications where multiple TIs or TEs are needed, and can improve either resolution or acquisition time.

5057 Computer 93

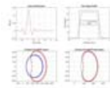

2D acquisition mode for T1 and T2 estimation using an ellipse-fitting approach on phase cycled bSSFP data

Yulia Shcherbakova[1], Cornelis A.T. van den Berg[2], Pim T.S. Borman[1], Chrit T.W. Moonen[1], and Lambertus W. Bartels[3]

[1]Center for Imaging Sciences/Imaging Division, University Medical Center Utrecht, Utrecht, Netherlands, [2]Dept. of Radiotherapy/Imaging Division, University Medical Center Utrecht, Utrecht, Netherlands, [3]Image Sciences Institute/dept. of Radiology, University Medical Center Utrecht, Utrecht, Netherlands

The ellipse fitting approach for simultaneous estimation of the relaxation times T_1 and T_2 from phase-cycled balanced steady-state free precession (PC-bSSFP) has been so far limited to the 3D acquisition mode due to sensitivity to slice profile imperfections. In this work we present the results of a 2D approach which is based on a RF excitation pulse optimization. This minimally affects the ellipse fitting leading to minimal corruption of T_1 and T_2 quantification from 2D PC-bSSFP data.

5058 Computer 94

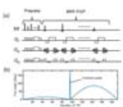

Fast and robust magnetic resonance fingerprinting with Cartesian sampling using random RF and gradient spoilers to reset the longitudinal and transverse magnetization

Daiki Tamada[1], Takashi Watanabe[1], Tomoyuki Takeguchi[1], and Hitoshi Kanazawa[2]

[1]Toshiba Corporation, Kawasaki, Japan, [2]Toshiba Medical Systems Corporation, Otawara, Japan

A prepulse for resetting longitudinal and transverse magnetization is proposed in order to accelerate magnetic resonance fingerprinting (MRF) with Cartesian sampling. A pulse sequence was developed based on a steady-state free precession sequence in which the prepulse consists of a set of radio frequency (RF) pulses and gradient spoilers. Simulation and experimental results demonstrated that the prepulse enables fast MRF in the presence of additional sequence modules, such as respiration triggering.

5059 Computer 95

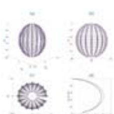

Relaxometry via steady-state ring-locked trajectories

James C Korte[1], Bahman Tahayori[2], Peter M Farrell[1], Stephen M Moore[3], and Leigh A Johnston[1]

[1]Dept. Electrical & Electronic Engineering, University of Melbourne, Melbourne, Australia, [2]Dept. Electrical and Computer Systems Engineering, Monash University, Melbourne, Australia, [3]IBM Research, Melbourne, Australia

It is known that steady-state ring-locked trajectories are formed on an elliptical manifold under a constant amplitude and constant frequency excitation envelope. Here we demonstrate that the excitation envelope can be expressed in terms of the spin-system parameters and a target steady-state trajectory, providing control of the magnetisation on the steady-state ellipsoid when spin-system parameters, such as the relaxation constants, are known. Conversely, we exploit this relationship between excitation parameters and unknown relaxation constants to develop a volume relaxometry technique, which can potentially be extended to relaxation mapping due to the elliptical nature of balanced SSFP.

5060 Computer 96

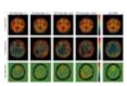

Magnetic Resonance Fingerprinting using phase cycling bSSFP (phc-MRF) in presence of B0 inhomogeneity.

Simone Coppo[1], Bhairav Bipin Mehta[1], Dan Ma[1], Yun Jiang[1], and Mark Alan Griswold[1]

[1]Radiology Department, Case Western Reserve University, Cleveland, OH, United States

Magnetic Resonance Fingerprinting (MRF) is a newly developed approach for accurate and efficient multi parameter mapping. This work proposes a balanced steady state free precession (bSSFP) based MRF framework which introduces different phase cycling (phc-MRF) to compensate for banding artifact induced by B_0 inhomogeneity. The phc-MRF was tested in both phantoms and in vivo. The preliminary results show the robustness of the phc-MRF to banding artifacts while maintaining the precision of parameter estimation and B_0 sensitivity.

Electronic Poster

Reconstruction & Post-Processing

Exhibition Hall — Wednesday 16:15 - 17:15

5061 Computer 97

Semi-automated identification of Substantia Nigra in healthy controls and patients with Parkinson's Disease: a feasibility study using MP2RAGE

Maria Eugenia Caligiuri[1], Gaetano Barbagallo[2], Tobias Kober[3], Umberto Sabatini[4], Aldo Quattrone[1,2], and Andrea Cherubini[1]

[1]Neuroimaging Unit, Institute of Bioimaging and Molecular Physiology (IBFM-CNR), Catanzaro, Italy, [2]Institute of Neurology, University Magna Graecia, Catanzaro, Italy, [3]Healthcare Sector IM&WS S, Siemens Schweiz AG, Renens, Switzerland, [4]Institute of Neuroradiology, University Magna Graecia, Catanzaro, Italy

Reliable in vivo assessment of human substantia nigra (SN) requires highly trained operators and different MRI sequences. Advanced techniques have recently facilitated SN identification, but their acquisition in routine clinical practice may not be feasible. MP2RAGE allows for quantitative T1 mapping with an acceptable acquisition time (< 10 minutes). Moreover, SN can be seen on T1 maps, but not on standard MPRAGE. In this study, we tested the feasibility of semi-automated SN identification on MP2RAGE-derived T1 maps by using a thresholding approach, and compared SN volume and T1 values between healthy controls and patients with Parkinson's disease.

5062 Computer 98

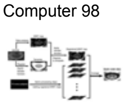

Myelin water atlas for cervical spinal cord: A template for spinal cord pathway myelin microstructure

Hanwen Liu[1,2], Emil Ljungberg[3], Erin MacMillan[3], Laura Barlow[4], Shannon Kolind[3], John Kramer[2,5], and Cornelia Laule[2,6,7]

[1]Physics, University of British Columbia, Vancouver, BC, Canada, [2]International Collaboration on Repair Discoveries, Vancouver, BC, Canada, [3]Medicine, University of British Columbia, Vancouver, BC, Canada, [4]UBC Hospital, University of British Columbia, Vancouver, BC, Canada, [5]Kinesiology, University of British Columbia, Vancouver, BC, Canada, [6]Radiology, University of British Columbia, Vancouver, BC, Canada, [7]Pathology and Laboratory Medicine, University of British Columbia, BC, Canada

In-vivo microstructural information of myelin in the spinal cord is desirable for studying spinal cord injury and neurodegenerative diseases. We used myelin water imaging combine with Spinal Cord Toolbox to create a standard microstructure template specific to myelin content, so-called myelin water atlas, for healthy cervical spinal cord. The resulting atlas is able to distinguish myelin content in 7 different spinal cord pathways and agrees with well-known anatomical characteristics. Our work shows the potential of using a myelin water atlas as a microstructure reference to visualize demyelination in spinal cord injuries or diseases.

5063 Computer 99

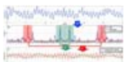

Visualization of Cardiac and Respiratory Pressure Gradient of Cerebrospinal Fluid Based on Asynchronous Two-Dimensional Phase Contrast Imaging

Saeko Sunohara[1], Satoshi Yatsushiro[2], Mitsunori Matsumae[3], and Kagayaki Kuroda[1,2]

[1]Graduate School of Engineering, Tokai University, Hiratshuka, Kanagawa, Japan, [2]Graduate School of Science and Technology, Tokai University, Hiratsuka, Kanagawa, Japan, [3]Department of Neurosurgery, Tokai University School of Medicine, Isehara, Kanagawa, Japan

To visualize the distribution of the pressure gradients of the cardiac- and respiratory-driven cerebrospinal fluid (CSF), asynchronous two-dimensional phase-contrast velocity imaging was performed in 9 healthy subjects. The pressure gradients were calculated by the Navier–Stokes equations after the total CSF motion was classified into either cardiac or the respiratory components in the frequency domain. In the prepontine, the pressure gradients in the caudal-to-cranial direction were 14.9 ± 3.17 Pa/m for cardiac components and 1.28 ± 0.46 Pa/m for respiratory components; the cardiac pressure gradient was also significantly larger than the respiratory pressure gradient in other regions.

5064 Computer 100

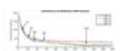

On the profile ordering of Golden Angle radial Simultaneous Multi-Slice imaging

Pim Borman[1], Rob H.N. Tijssen[1], Bas Raaymakers[1], Chrit Moonen[2], and Clemens Bos[2]

[1]Radiotherapy, UMC Utrecht, Utrecht, Netherlands, [2]Imaging Division, UMC Utrecht, Utrecht, Netherlands

Golden angle radial sampling allows for flexible sliding window reconstructions while minimizing motion sensitivity and undersampling artifacts. Simultaneous MultiSlice (SMS) can be used to increase the spatial coverage without decreasing the framerate. Here we show that the golden angle profile ordering is in principle not compatible with the in-plane phase cycling scheme required by SMS. It follows that these are only compatible for a certain number of spokes, namely when the number of spokes is part of the Fibonacci sequence ***and*** the SMS factor is a divisor of this number.

5065 Computer 101

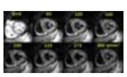

Non-rigid Groupwise Registration for Intravoxel Incoherent Motion Imaging of the Heart

Valery Vishnevskiy[1], Georg Spinner[1], Christian Stoeck[1], Constantin von Deuster[1], and Sebastian Kozerke[1]

[1]Institute for Biomedical Engineering, ETH Zurich, Zurich, Switzerland

Intravoxel Incoherent Motion (IVIM) imaging is an attractive approach for contrast-agent free in vivo perfusion measurement in the heart. Since the data is acquired during free breathing, nonrigid respiratory motion is considerable and needs to be corrected before estimation of IVIM parameters. In order to provide accurate image registration, an approach with parametric total variation regularization of displacements and low-rank structure of aligned images stack is presented. The proposed method allows for robust IVIM parameter estimation and improves mean squared residuals of the IVIM model by 24% on average compared to state-of-the-art non-rigid registration methods.

5066 Computer 102

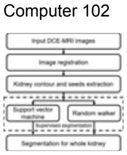

A supervised automated segmentation strategy for renal DCE-MR images

Wenjian Huang[1], Hao Li[1,2], Jue Zhang[1,3], Xiaoying Wang[1,4], and Jing Fang[1,3]

[1]Academy for Advanced Interdisciplinary Studies, Peking University, Beijing, People's Republic of China, [2]Department of Radiology, University of Cambridge, United Kingdom, [3]College of Engineering, Peking University, Beijing, People's Republic of China, [4]Department of Radiology, Peking University First Hospital, Beijing, People's Republic of China

A supervised DCE-MR images classification strategy is proposed in this study. First, the training set was obtained by an automated seeds extraction procedure. Subsequently, support vector machine (SVM) and random walk algorithms were employed as two separate classification approaches to achieve image segmentations, respectively. The automated segmentations and a repeated manual segmentation were compared quantitatively with a reference manual segmentation. The average similarity indexes for SVM, random walker and repeated manual segmentation were 0.78, 0.76 and 0.72, respectively. The results indicate that the proposed strategy yield a satisfied similarity with manual segmentation and is more stable than the manual segmentation.

5067 Computer 103

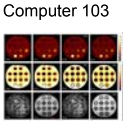

Improving Accuracy in MR Fingerprinting by Off-Resonance Deblurring

Peter Koken[1], Thomas Amthor[1], Mariya Doneva[1], Holger Eggers[1], Karsten Sommer[1], Jakob Meineke[1], and Peter Börnert[1,2]

[1]Philips Research Europe, Hamburg, Germany, [2]Dept. Radiology, LUMC, Leiden, Netherlands

Efficient, highly under-sampled spiral acquisition is preferred in magnetic resonance fingerprinting (MRF). However, although the spiral is very efficient in terms of sampling, it is sensitive to all kinds of off-resonance effects resulting in signal blurring. This effect leads to geometric distortion and matching errors, reducing accuracy significantly. To overcome these limitations, the present work proposes to combine spiral-based MRF with field map-based deblurring, e.g. by conjugate phase reconstruction (CPR). The basic feasibility of this approach for under-sampled MRF is shown in phantom and in-vivo experiments, underlining the effectiveness of this simple correction approach paving the way for even more efficient MRF sampling.

5068 Computer 104

Partial volume effect correction for surface-based cortical mapping

Camille Van Assel[1], Gabriel Mangeat[1,2], Benjamin De Leener[1], Nikola Stikov[1,3], Caterina Mainero[2,4], and Julien Cohen-Adad[1,5]

[1]NeuroPoly Lab, Institute of Biomedical Engineering, Polytechnique Montreal, Montreal, QC, Canada, [2]Athinoula A. Martinos Center for Biomedical Imaging, Charlestown, MA, United States, [3]Montreal Health Institute, Montreal, QC, Canada, [4]Harvard Medical School, Boston, MA, United States, [5]Functional Neuroimaging Unit, CRIUGM, Université de Montréal, Montreal, QC, Canada

Partial Volume Effect (PVE) hampers the accuracy of studies aiming at mapping MRI signal in the cortex due to the close proximity of adjacent white matter (WM) and cerebrospinal fluid (CSF). The proposed framework addresses this issue by disentangling the various sources of MRI signal within each voxel, assuming three classes (WM, gray matter, CSF) within a small neighbourhood. MRI scans of 17 healthy subjects suggest robust estimations of PVE, allowing accurate extraction of MRI metrics using surface-based analysis. This method can be particularly useful for probing pathology in outer or inner cortical layers, which are subject to strong PVE with adjacent CSF or WM.

5069 Computer 105

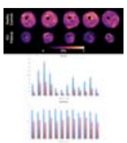

Muscle Change Associated with Time in Intensive Care Unit (ICU)

Michael Perrins[1,2], Lucy V Hiscox[1], Calum Gray[1], Scott Semple[1], Lucy Barclay[3], Rachael Kirkbride[3], Lisa Salisbury[3], Colin Brown[4], Timothy Walsh[3], Edwin J.R van Beek[1], Neil Roberts[1], and David Griffith[3]

[1]Clinical Research Imaging Centre, The University of Edinburgh, Edinburgh, United Kingdom, [2]MRC Centre for Inflammation Research, The University of Edinburgh, Edinburgh, United Kingdom, [3]Anaesthesia, Critical Care and Pain Medicine, The University of Edinburgh, Edinburgh, United Kingdom, [4]The Mentholatum Company Ltd., East Kilbride, United Kingdom

Muscle wasting is common during critical illness. In this study, thigh muscles of previously mobile patients surviving an episode of severe critical illness were imaged by Magnetic Resonance Imaging (MRI) during convalescence and compared to healthy controls. We present preliminary findings of the first clinical study using Magnetic Resonance Elastography (MRE) to measure muscle stiffness (kPa) and muscle cross-sectional area (mm^2) for Intensive Care Unit (ICU) patients. A statistically significant reduction in muscle area and muscle stiffness in patients was found when compared to the healthy control group. There was a significant cross-sectional muscle area increase following ICU patient discharge.

5070 Computer 106

Improved Denoising of Dynamic Arterial Spin Labeling with Infimal Convolution of Total Generalized Variation Functionals (ICTGV)

Matthias Schloegl[1], Stefan Spann[1], Christoph Aigner[1], Martin Holler[2], Kristian Bredies[2], and Rudolf Stollberger[1]

[1]Institute of Medical Engineering, Graz University of Technology, Graz, Austria, [2]Institute of Mathematics and Scientific Computing, University of Graz, Austria

Dynamic arterial spin labeling MRI provides important quantitative information about blood arrival time and perfusion. However, the inherently low signal-to-noise ratio requires repeated measurements to achieve a reasonable image quality. This leads to long acquisition times and hence increases the risk of motion artifacts, which impedes clinical applicability. To overcome this limitation we propose to reconstruct the dynamic ASL data employing ICTGV regularization from a reduced number of averages. The performance of the method is evaluated on synthetic and in-vivo ASL data.

5071 Computer 107

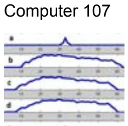

Fast Non-iterative Image Reconstruction for O-space Imaging

Maolin Qiu[1], Yuqing Wan[1], and R. Todd Constable[1]

[1]Yale School of Medicine, New Haven, CT, United States

MRI with non-linear spatial encoding magnetic fields (SEM) can provide high quality MR images, but there images are usually calculated using iterative optimization procedures. Such reconstruction methods can take a long time to converge, and the results may depend on the initial iteration parameters. We propose a fast, non-iterative image reconstruction method for O-space imaging based on the local K-space and local SEMs and demonstrate its effectiveness for image reconstruction of nonlinear O-space imaging data.

5072 Computer 108

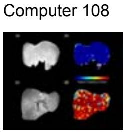

Wavelet based Texture Analysis of Liver Fibrosis in Delayed Phase Gadolinium-Enhanced T1-weighted in vivo Images

Lavanya Umapathy[1], Jonathan Brand[2], Jean-Philippe Galons[3], Lars Furenlid[2,3], Diego Martin[3], Maria Altbach[3], and Ali Bilgin[1,4]

[1]Electrical and Computer Engineering, University of Arizona, Tucson, AZ, United States, [2]College of Optical Sciences, University of Arizona, Tucson, AZ, United States, [3]Medical Imaging, University of Arizona, Tucson, AZ, United States, [4]Biomedical Engineering, University of Arizona, Tucson, AZ, United States

Non-invasive imaging techniques that can identify early structural changes due to fibrosis in vivo are of high clinical importance. In this work, a five-level wavelet decomposition of biopsy confirmed normal and fibrotic ex vivo liver tissues is performed and histogram-based features are extracted from the wavelet subbands. A linear classifier is trained using the top 10 features and applied to classify liver fibrosis in Gadolinium-enhanced delayed phase T1-weighted in vivo images. The results show that normal samples yield low posterior probabilities for fibrosis whereas these values are very high for fibrotic samples.

5073 Computer 109

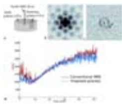

An alternative to phase image-based Magnetic Resonance Elastography (MRE) using k-space data processing

Nadège Corbin[1,2], Elodie breton[1], Michel de Mathelin[1], and Jonathan Vappou[1]

[1]ICube, University of Strasbourg, CNRS, IHU Strasbourg, Strasbourg, France, [2]Wellcome Trust Centre for Neuroimaging, UCL Institute of Neurology, London, United Kingdom

MR Elastography (MRE) requires substantial data processing involving phase image reconstruction, wave enhancement and inverse problem solving. The objective of this study is to propose an alternative reconstruction method based on direct k-space data processing, particularly adapted to applications requiring fast MRE measurements such as the monitoring of elasticity changes. Elastograms are directly reconstructed from raw MR data without prior phase image reconstruction, circumventing thereby the delicate step of phase unwrapping. The k-space MRE method shows promising results by providing elasticity values similar to the ones obtained with conventional MRE in phantoms and in vivo in porcine liver.

5074 Computer 110

Texture Analysis for Evaluating Image Registration

Vikas Kotari[1] and Vasiliki N Ikonomidou[2]

[1]Electrical Engineering, Geroge Mason University, Fairfax, VA, United States, [2]Bioengineering, George Mason University

Accurate image registration is essential for both cross-sectional and longitudinal MR studies. In longitudinal studies aligning same contrast intra-subject images, which are the focus of our work, registration is assumed to be a rigid body problem. This assumption is questionable due to global and local changes in brain volume either due to hydration or atrophy. Consequently, misregistration at the voxel level may occur in these studies, which might lead to subject data being discarded. This misregistration is evident particularly around the cortex. Visual inspection of images is used to determine registration accuracy. While this approach is suitable for assessing alignment of landmark structures, it fails to capture the millimteric or sub-millimetric misregistrations. Automatic metrics can precisely estimate the overall performance of a given registration algorithm by employing an evaluation database. However, to estimate the registration accuracy of a given pair of images, such metrics are unsuitable. In this work we propose texture analysis of a subtraction image to evaluate the registration accuracy of a given pair of same contrast, intra-subject images. Once registered, images are intensity normalized, blurred and subtracted. In the event of registration errors, or violation of the rigid body assumption, the subtraction images have artifacts. The texture features of these artifacts are different from the artifact-free (clean) areas of the subtraction images. Using a texture-based classifier, artifact areas in the subtraction images that indicate failed registration are identified. In addition to determining if the registration has failed, our approach can identify the specific locations of misregistration, which can be corrected, leading to a more inclusive subject data.

5075 Computer 111

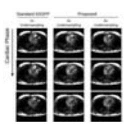

Dynamically Phase-Cycled bSSFP Cardiac Cine in a Single Breathhold with Phase-Cycle Consistency Regularization

Corey Allan Baron[1], Anjali Datta[1], and Dwight G Nishimura[1]

[1]Stanford University, Stanford, CA, United States

At high field strengths, cardiac cine acquisitions acquired with balanced SSFP can suffer from banding artifacts. To mitigate this issue, dynamically phase-cycled cardiac cine was acquired in a single breathhold with undersampling rates of 4 and 6, and images were reconstructed with a phase-cycle banding profile regularization that exploits redundancy between phase-cycles.

5076 Computer 112

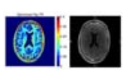

Myelin Water Fraction Estimation from Optimized Steady-State Sequences using Kernel Ridge Regression

Gopal Nataraj[1], Jon-Fredrik Nielsen[2], and Jeffrey A. Fessler[1]

[1]Electrical Engineering and Computer Science, University of Michigan, Ann Arbor, MI, United States, [2]Biomedical Engineering, University of Michigan, Ann Arbor, MI, United States

This work introduces a new framework for myelin water fraction (MWF) estimation. We use a novel scan design approach to construct a sequence a fast steady-state sequences and optimize corresponding flip angles and repetition times for precise MWF estimation. We quantify MWF and five other parameters per voxel using a novel method based on kernel ridge regression. We obtain MWF maps in vivo that are comparable to those reported in literature, with possibly shorter overall scan time.

5077 Computer 113

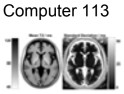

A T2 Template Map from a Healthy Cohort to Identify Localized Anomalies in Single Subjects

Tom Hilbert[1,2,3], Alexis Roche[1,2,3], Cristina Granziera[4,5], Guillaume Bonnier[5], Kieran O'Brien[6,7], Tony Stöcker[8], Pavel Falkovskiy[1,2,3], Reto Meuli[2], Jean-Philippe Thiran[2,3], Gunnar Krueger[2,3,9], and Tobias Kober[1,2,3]

[1]Advanced Clinical Imaging Technology, Siemens Healthcare AG, Lausanne, Switzerland, [2]Department of Radiology, University Hospital (CHUV), Lausanne, Switzerland, [3]LTS5, École Polytechnique Fédérale de Lausanne, Lausanne, Switzerland, [4]Neuroimmunology Unit, Neurology, Department of Clinical Neurosciences, Centre Hospitalier Universitaire Vaudois (CHUV) and University of Lausanne (UNIL), Lausanne, Switzerland, [5]Martinos Center for Biomedical Imaging, Massachusetts General Hospital and Harvard Medical School, Boston, MA, United States, [6]Center for Advanced Imaging, the University of Queensland, Brisbane, Australia, [7]Siemens Healthcare Pty Ltd, Brisbane, Australia, [8]German Center for Neurodegenerative Diseases, Bonn, Germany, [9]Siemens Medical Solutions USA, Inc., Boston, MA, United States

We construct a database of normal T2 values by spatially normalizing quantitative maps from healthy subjects into a common space. A low standard deviation across all subjects demonstrates good reproducibility of the T2 values in white matter and deep grey matter. Additionally we adopt a standard voxel-based procedure that compares the quantitative T2 map of a patient to the database and test it on three multiple sclerosis datasets. The obtained z-score maps show that white matter lesions can be detected in the limits of the available resolution and the applied smoothing.

5078 Computer 114

Temperature Mapping of Fluorinated (19F) Gas in a Cool Down Experiment

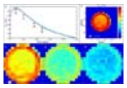

Tobias J. Hoh[1,2], Eduardo Coello[1,2], Jorge Carretero Benignos[2], Axel Haase[1], and Rolf F. Schulte[2]

[1]Technische Universität München, Munich, Germany, [2]GE Global Research, Munich, Germany

Magnetic resonance imaging (MRI) temperature mapping of gases is challenging due to limited sensitivity. In this proof of concept study, proton thermometry methods from tissue temperature monitoring were transferred to ^{19}F gas MRI.

A phase-dependent ^{19}F resonance frequency shift temperature mapping is proposed for fluorinated gas at 3T based on a spiral readout to overcome limitations of ultra-short relaxation times.

This work demonstrates the feasibility of 2D thermometry in a canonical setup with inert fluorinated gases.

5079 Computer 115

Improved 23Na MRI Quantification of the Human Brain at 3T Using Partial Volume Correction Techniques

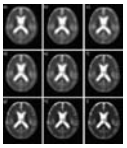

Tie-Qiang Li[1], Elaine Lui[2], and Patricia Desmond[2]

[1]Department of Radiology, University of Melbourne, Melbourne, Australia, [2]Department of Radiology, University of Melbourne

In this study we have focused on the development and application of PVC techniques for improving the quantification accuracy of STC with 23Na MRI at 3T. Although PVEs are known to induce errors in quantification, it has not been widely used in 23Na MRI. While different PVC algorithms have been proposed in the PET literature, each method has its limitations and relies on simplified assumptions. The proposed hybrid methods, such as GTM+RBV, aimed to overcome such limitations are most robust.

5080 Computer 116

Optimization of brain extraction increases global cortical thickness accuracy

Antonio Carlos da Silva Senra Filho[1], Gareth J. Barker[2], Luiz Otávio Murta Junior[1], and Flavio Dell'Acqua[3]

[1]Department of Computing and Mathematics, University of Sao Paulo, Ribeirao Preto, Brazil, [2]Department of Neuroimaging, King's College London, London, United Kingdom, [3]Department of Forensic & Neurodevelopmental Sciences, King's College London, London, United Kingdom

Reconstruction of the cortical surface is of great importance as a biomarker for many brain diseases, and in recent years a number of advances in image processing and analysis have been made in the cortical reconstruction process. However, despite the scientific community employing a range of advanced surface reconstruction algorithms in order to improve quantitative accuracy, cortical thickness measurement is still a challenge. Here, we address the question of whether a better brain extraction procedure can improve the cortical surface reconstruction. Our analyses suggest that a more accurate brain mask directly affects the global cortical thickness estimate, reducing its quantitative uncertainty.

5081 Computer 117

ADRIMO: Anatomy-DRIven MOdelling of spatial correlation to improve analysis of arterial spin labelling data

David Owen[1], Andrew Melbourne[2], David L Thomas[2,3], Joanne Beckmann[4], Jonathan Rohrer[3], Neil Marlow[4], and Sebastien Ourselin[2]

[1]Translational Imaging Group, University College London, London, United Kingdom, [2]Translational Imaging Group, University College London, [3]Dementia Research Centre, University College London, [4]Institute for Women's Health, University College London

Arterial spin labelling (ASL) offers valuable measurements of perfusion in the brain and other organs. However, ASL data have low SNR and are prone to partial volume effects. We present a Bayesian model of anatomically-derived spatial correlation in ASL data (ADRIMO), which improves the accuracy of perfusion estimates and hence improves the analysis of ASL data. The method is assessed experimentally by examining ASL images from a cohort of 130 preterm-born adolescents.

5082 Computer 118

Reduction of ringing artifacts for high resolution 3D RARE imaging at high magnetic field strengths

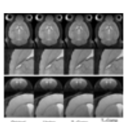

Martin Krämer[1], Karl-Heinz Herrmann[1], Silvio Schmidt[2], Otto W Witte[2], and Jürgen R Reichenbach[1,3,4,5]

[1]Medical Physics Group, Institute of Diagnostic and Interventional Radiology, Jena University Hospital - Friedrich Schiller University Jena, Jena, Germany, [2]Hans Berger Department for Neurology, Jena University Hospital - Friedrich Schiller University Jena, Jena, Germany, [3]Michael Stifel Center for Data-driven and Simulation Science Jena, Friedrich Schiller University Jena, Jena, Germany, [4]Abbe School of Photonics, Friedrich Schiller University Jena, Jena, Germany, [5]Center of Medical Optics and Photonics, Friedrich Schiller University Jena, Jena, Germany

High resolution 3D-RARE imaging at 9.4T can be very challenging due to increased artifacts caused by strong T_2- and Gibbs ringing. In this work, we present the combination of two correction algorithms, local subvoxel-shift unringing and T_2-compensation, to reduce effectively both types of artifacts. For this purpose, the local subvoxel-shift algorithm has been extended to the third spatial dimension and evaluated in healthy mice.

5083 Computer 119

Personalized map to assess diffuse and focal brain damage

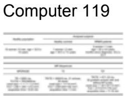

Guillaume Bonnier[1], Alexis Roche[2,3], Tom Hilbert[3,4,5], Gunnar Krueger[6], Cristina Granziera[1,7], and Tobias Kober[4]

[1]MGH/MIT/HMS Athinoula A. Martinos Center for Biomedical Imaging, Massachusetts General Hospital, Harvard Medical School, Charlestown, MA, United States, [2]Advanced Clinical Imaging Technology, Siemens Healthcare AG, Lausanne, Switzerland, [3]Department of Radiology, University Hospital (CHUV), Lausanne, Switzerland, [4]Siemens Healthcare AG, Advanced Clinical Imaging Technology, Lausanne, Switzerland, [5]LTS5, École Polytechnique Fédérale de Lausanne, Lausanne, Switzerland, [6]Siemens Medical Solutions USA, Inc., Malvern, MA, United States, [7]Neuroimmunology Unit, Neurology, Department of Clinical Neurosciences, Centre Hospitalier Universitaire Vaudois (CHUV) and University of Lausanne (UNIL), Lausanne, Switzerland

We propose a new methodology, which is based on the quantification of region-specific brain tissue-properties to provide personalize maps of brain damage in a single patient. To achieve this aim, we used T1, T2, T2* and MTI maps and applied the method to detect brain abnormalities in multiple sclerosis patients.

5084 Computer 120

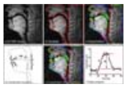

Test-retest repeatability of human speech biomarkers from static and real-time dynamic magnetic resonance imaging

Johannes Toger[1], Tanner Sorensen[1], Krishna Somandepalli[1], Asterios Toutios[1], Sajan Goud Lingala[1], Shrikanth Narayanan[1], and Krishna S Nayak[1]

[1]Ming Hsieh Department of Electrical Engineering, University of Southern California, Los Angeles, CA, United States

This study presents a test-retest repeatability framework for quantitative speech biomarkers from static MRI and real-time MRI (RT-MRI), and applies the framework to healthy volunteers (n=8). Repeatability was quantified using intraclass correlation coefficient (ICC) and mean within-subject standard deviation (σe). Inter-study agreement was strong to very strong for static anatomical biomarkers, (ICC: min/median/max 0.71/0.89/0.98, σe: min/median/max 0.90/2.20/6.72 mm), poor to very strong for dynamic RT-MRI biomarkers of articulator motion range (ICC: 0.26/0.75/0.90, σe: 1.6/2.5/3.6 mm) and poor to very strong for velocity (ICC: 0.26/0.56/0.93, σe: 2.2/4.4/16.7 cm/s). The introduced framework can be used to guide future development of speech biomarkers.

Electronic Poster

Cartilage

Exhibition Hall — Wednesday 16:15 - 17:15

5085 Computer 1

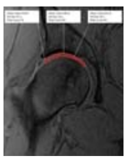

Slipped Capital Femoral Epiphysis Causes Early Cartilage Degeneration in Young Adults – an 11 year follow-up study with dGEMRIC

Jakob Örtegren[1], Pernilla Peterson[2], Jonas Svensson[3], and Carl Johan Tiderius[1]

[1]Dept of Orthopedics, Skane University Hospital, Lund, Sweden, [2]Dept. of Translational Medicine, Lund University, Malmö, Sweden, [3]Dept. of Medical Imaging and Physiology, Skane University Hospital, Lund, Sweden

The longitudinal effects of Slipped Capital Femoral Epiphysis (SCFE) on hip cartilage integrity and hip function are poorly understood. In this study, 44 hips were evaluated with delayed Gadolinium-enhanced MRI of cartilage (dGEMRIC) in average 11 years after SCFE. A low dGEMRIC index was detected in SCFE hips compared to unaffected hips, with gradually lower dGEMRIC index anteriorly in the hip joint. Furthermore, a low dGEMRIC index correlated both with impaired hip function and femuroacetabular impingement (FAI), which further strengthens the theory of FAI as a mediator of osteoarthritis after SCFE.

5086 Computer 2

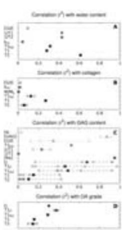

Revisiting the experimental base of compositional biomarkers: A meta-analysis study

Jose G Raya[1], Amparo Ruiz[1], and Uran Ferizi[1]

[1]Department of Radiology, New York University School of Medicine, New York, NY, United States

We aim to perform a meta-analysis of the corpus of experimental results accumulated for compositional MRI biomarkers of articular cartilage used in clinical studies. We summarized the data according to the statistical evidence that is reported. We report the correlation of MRI parameters with composition, the ability of MRI parameters to detect group differences between healthy and degraded cartilage, and the ability of MRI to detect cartilage damage.

5087 Computer 3

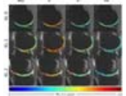

Changes in collagen and proteoglycan in cartilage with OA severity

Jose G Raya[1], Uran Ferizi[1], Amparo Ruiz[1], Steven B Abramson[2], Jenny Bencardino[1], and Svetlana Krasnokutsky Samuels[2]

[1]Department of Radiology, New York University School of Medicine, New York, NY, United States, [2]Department of Medicine, New York University School of Medicine, New York, NY, United States

The objective of this work was to investigate differences in cartilage matrix composition and structure across subjects with different stages of OA severity and test if the changes in the collagen network are concomitant or subsequent to the changes in proteoglycan.

5088 Computer 4

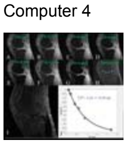

Magnetic resonance imaging of the zone of calcified cartilage (ZCC) in the knee joint using 3D UTE Cones sequences

Yinghua Zhao[1,2], Yajun Ma[1], Michael Carl[3], Xing Lu[1], Yanchun zhu[1], Eric Y Chang[1,4], and Jiang Du[1]

[1]University of California, San Diego, San Diego, CA, United States, [2]Radiology, Third Affiliated Hospital of Southern Medical University (Academy of Orthopedics · Guangdong Province), Guangzhou, People's Republic of China, [3]GE Healthcare, San Diego, CA, United States, [4]Radiology Service, VA San Diego Healthcare System, San Diego, CA, United States

The zone of calcified cartilage (ZCC) is a thin layer between articular cartilage and bone. The ZCC plays an important role in the pathogenesis of osteoarthritis (OA) but has never been imaged in vivo with magnetic resonance (MR) imaging techniques. In this study we aimed to investigate the feasibility of direct imaging of the ZCC in healthy volunteers using a three dimensional (3D) ultrashort echo time (UTE) Cones sequence on a clinical whole body 3T scanner.

5089 Computer 5

Knee cartilage T_2 mapping with T_2-prepared isotropic 3D GRE has equivalent precision and higher accuracy compared to multi-slice TSE in volunteers and patients at 3T

Roberto Colotti[1], Patrick Omoumi[1], Gabriele Bonanno[1,2,3], Jean-Baptiste Ledoux[1], and Ruud B. van Heeswijk[1]

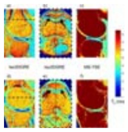

[1]Department of Radiology, University Hospital (CHUV) and University of Lausanne (UNIL), Lausanne, Switzerland, [2]Division of Cardiology, Department of Medicine, Johns Hopkins University, Baltimore, United States, [3]Division of MR Research, Department of Radiology, Johns Hopkins University, Baltimore, United States

The goal of this study was to compare the precision and accuracy of a novel isotropic 3D T_2-prepared gradient-echo T_2 mapping technique (Iso3DGRE) with the clinical standard 2D multi-slice turbo spin-echo (MS-TSE) for T_2 mapping of knee cartilage at 3T. A phantom study was performed to determine the accuracy of both techniques against the reference standard spin echo (SE). T_2 mapping of knee cartilage was then performed in 13 healthy volunteers and 5 patients with late-stage osteoarthritis. Compared to MS-TSE, Iso3DGRE T_2 mapping resulted in T_2 values with equivalent precision and slightly higher accuracy at a higher spatial resolution.

5090 Computer 6

GRAPPATINI put to use: How MSK applications benefit from highly undersampled T2 mapping and synthetic contrasts

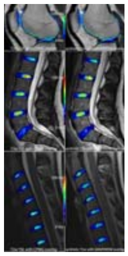

Marcus Raudner[1], Tom Hilbert[2,3,4], Tobias Kober[2,3,4], Vladimir Juras[1], Ewald Moser[5], Claudia Kronnerwetter[1], David Stelzeneder[6], and Siegfried Trattnig[1]

[1]High Field MR Centre, Department of Biomedical Imaging and Image-guided Therapy, Medical University of Vienna, Vienna, Austria, [2]Advanced Clinical Imaging Technology, Siemens Healthcare AG, Lausanne, Switzerland, [3]Department of Radiology, University Hospital (CHUV), Lausanne, Switzerland, [4]LTS5, Ecole Polytechnique Fédérale de Lausanne, Lausanne, Switzerland, [5]Center for Medical Physics and Biomedical Engineering, Medical University of Vienna, Vienna, Austria, [6]Department of Orthopaedics, Medical University of Vienna, Vienna, Austria

The quantitative measurement of the T2 relaxation time has been shown to be a useful tool for radiological diagnosis. However, the use of quantitative MRI (qMRI) in clinical routine is often hindered due to long acquisition times. Here, we assess T2 parameters in the lumbar and cervical spine as well as the knee using GRAPPATINI, a model-based accelerated T2 mapping sequence. Additionally, synthetic T2-weighted (T2w) images are derived from the quantitative maps. The T2 maps and synthetic T2w images are compared to conventional T2w and T2 mapping sequences, yielding an overall 5.8-fold time-saving.

5091 Computer 7

High-resolution In-vivo Mapping of the Proteoglycan-bound Water Fraction in Articular Cartilage of the Human Knee Joint

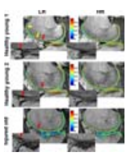

Mustapha Bouhrara[1], David A. Reiter[1], Kyle W. Sexton[1], Christopher M. Bergeron[1], Linda M. Zukley[1], and Richard G. Spencer[1]

[1]National Institute on Aging (NIA), National Institutes of Health (NIH), Baltimore, MD, United States

We demonstrate the clinical feasibility of high-resolution (HR) in-vivo mapping of proteoglycan water fraction (PgWF) in human knee cartilage by combining the mcDESPOT protocol for data acquisition and Bayesian Monte Carlo (BMC) analysis for data analysis. For all subjects, PgWF maps derived from low resolution datasets exhibited partial volume and magnetic susceptibility effects leading, respectively, to an overestimation and an underestimation of PgWF values in several cartilage regions. These issues were absent in HR PgWF maps. Further, BMC-mcDESPOT demonstrates high reproducibility and stability in the estimation of PgWF as compared to the conventional stochastic region contraction (SRC) algorithm.

5092 Computer 8

Effects of Fat Saturation on T2* Quantification

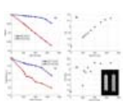

Michael Carl[1], Amin Nazaran[2], Jiang Du[2], and Graeme M Bydder[2]

[1]GE Healthcare, San Diego, CA, United States, [2]UCSD, CA, United States

The T_2 relaxation of MRI signals is an important parameter in assessment of pathology. Here we analyze the effects that Fat Saturation pulses of various bandwidths have on the values of T_2 quantification. We found that Fat Saturation can have a notable effect on the measured T_2 values of multi-component tissues. Since the dispersion is less for smaller FS bandwidths, longer FS pulses can help to minimize the effects.

5093 Computer 9

UTE-MT Imaging Can Reliably Evaluate Macromolecules in MSK Tissues: A Sequential Collagenase Enzymatic Treatment Study

Xin Cheng[1,2], Yajun Ma[1], Eric Y Chang[1,3], and Jiang Du[1]

[1]Department of Radiology, University of California San Diego, San Diego, CA, United States, [2]Department of Histology & Embryology, Jinan University, Guangzhou, People's Republic of China, [3]Radiology Service, VA San Diego Healthcare System, CA, United States

In this study, we aimed to evaluate UTE-MT derived macromolecule fractions in articular cartilage subject to sequential collagenase enzymatic treatment. The preliminary result suggests that UTE-MT imaging and signal modeling allows for quantitative evaluation of macromolecular fractions in articular cartilage. Furthermore, results from UTE-MT imaging and signal modeling are insensitive to the magic angle effect, which is a huge advantage over the conventional T2 and T1rho measures. The water and macromolecular changes in both short and long T2 tissues in the knee joint using UTE-MT provides a “whole-organ” approach, and may be useful in the diagnosis and treatment of OA.

5094 Computer 10

UTE-T2* Profile Analyses Correlate with Walking Mechanics 2 Years After ACL Reconstruction

Ashley A Williams[1], Matthew R Titchenal[1], and Constance R Chu[1]

[1]Department of Orthopaedic Surgery, Stanford University, Stanford, CA, United States

This work examines the use of UTE-T2* profile analysis to assess sub-surface knee cartilage structural changes in 26 ACL-reconstructed subjects and compares UTE-T2* metrics to kinetic and kinematic measures of walking. UTE-T2* profile characteristics detect differences between ACL-reconstructed and uninjured knees. Side-to-side differences in an individual’s UTE-T2* profile metrics correlate with side-to-side differences in their gait metrics. The results suggest that UTE-T2* profile characteristics of cartilage are a useful metric for identifying cartilage subsurface changes early after ACLR and may reflect matrix changes resulting from altered loading.

5095 Computer 11

UTE-T2* Profile Analyses Correlate to Patient Reported Outcomes 2 Years After ACL Reconstruction

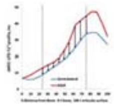

Ashley A Williams[1], Matthew R Titchenal[1], and Constance R Chu[1]

[1]Department of Orthopaedic Surgery, Stanford University, Stanford, CA, United States

Identification of patients with early cartilage degeneration who are at greater risk for poor clinical outcomes is critical for development of interventions to reduce osteoarthritis risk after ACL injury. This study tested the hypothesis that UTE-T2* profile analysis of knee cartilage correlates with patient reported outcomes (PRO) in ACL-reconstructed subjects 2 years after surgery. UTE-T2* mean values and profile characteristics in 27 ACL-reconstructed subjects correlated with patient reported pain and symptoms. Side-to-side differences in UTE-T2* profiles of some high functioning individuals suggest that this UTE metric may provide earlier warning of cartilage at risk for progressive degeneration than PRO.

5096 Computer 12

Predictive value of T2 Mapping for untreated patellar cartilage defects

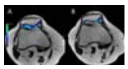

Markus Schreiner[1,2], Sebastian Apprich[1], Vladimir Mlynarik[2], Pavol Szomolanyi[2], Martin Zalaudek[2], Benedikt Hager[2], Vladimir Juras[2], Michael Weber[3], Reinhard Windhager[1], and Siegfried Trattnig[2,4]

[1]Department of Orthopaedics, Medical University of Vienna, Vienna, Austria, [2]High Field MR Center, Department of Biomedical Imaging and Image-Guided Therapy, Medical University of Vienna, Vienna, Austria, [3]Department of Biomedical Imaging and Image-Guided Therapy, Medical University of Vienna, Vienna, Austria, [4]CD Laboratory for Clinical Molecular MR Imaging, Medical University of Vienna, Vienna, Austria

Assessment and adequate treatment of articular cartilage lesions are a common challenge in clinical orthopaedic routine. To allow for better disease prediction and thus evidence-based treatment selection, there is a strong need for objective predictive markers. In this study we demonstrate the predictive potential of T2 mapping in the assessment of untreated patellar cartilage lesions over an average follow up time of four years.

5097 Computer 13

Efficacy of GelrinC in the treatment of chondral and osteochondral lesions: MRI results based on semi-quantitative MOCART scoring and T2 mapping

Markus Schreiner[1,2], Kitty Ohel[3], Livnat Ben-Zur[3], Sebastian Röhrich[2], Martin Zalaudek[2], Pavol Szomolanyi[2], Vladimir Juras[2], Vladimir Mlynarik[2], Reinhard Windhager[1], and Siegfried Trattnig[2,4]

[1]Department of Orthopaedics, Medical University of Vienna, Vienna, Austria, [2]High Field MR Center, Department of Biomedical Imaging and Image-Guided Therapy, Medical University of Vienna, Vienna, Austria, [3]Regentis Biomaterials Ltd, Or Akiva, Israel, [4]CD Laboratory for Clinical Molecular MR Imaging, Vienna, Austria

The treatment of femoral cartilage lesions still remains a challenge. Established cartilage repair techniques include microfracture (MFX), acellular scaffolds and cell based therapies such as ACI and MACI, which differ in associated morbidity and outcome. Therefore, there have been strong research efforts to develop novel treatment alternatives. In this study, we demonstrate that GelrinC, a novel acellular biodegradable implant, allows a successful treatment of both chondral and osteochondral femoral lesions in a minimal invasive one-step procedure. For both lesion types a substantial improvement of MOCART scores as well as T2 values has been demonstrated over a 24-month period.

5098 Computer 14

Feasibility of GRASP DCE-MRI in children with Juvenile Idiopathic Arthritis (JIA)

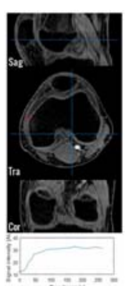

Paul de Heer[1], Robert Hemke[1], Cristina Lavini[1], Jasper Schoormans[2], Bram F. Coolen[2], Anouk M. Barendregt[1], Gustav J. Strijkers[2], Mario Maas[1], Jaap Stoker[1], Aart J. Nederveen[1], and Jurgen H. Runge[1,3]

[1]Radiology, AMC, Amsterdam, Netherlands, [2]Biomedical Engineering & Physics, AMC, Amsterdam, Netherlands, [3]Division of Imaging Sciences and Biomedical Engineering, King's College London, London, United Kingdom

Juvenile Idiopathic Arthritis (JIA) is the most common rheumatic disease in childhood and represents one of the leading causes of pediatric acquired disability. The aim of our study was to evaluate feasibility of high spatiotemporal resolution GRASP DCE-MRI in children with JIA and secondly to compare image quality between GRASP and conventional DCE-MRI in evaluating synovitis. In this pilot study, GRASP DCE-MRI proved to be feasible in a child with JIA. Moreover, for the evaluation of synovitis significantly higher spatial resolution and much cleaner signal-enhancement plots could be obtained using GRASP compared to conventional DCE-MRI.

5099 Computer 15

Cartilage mapping in asymptomatic hips with cam-type FAI: Does the MRI T1ρ profile change over time?

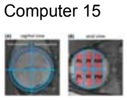

Gerd Melkus[1,2], George Grammatopoulos[3], Kawan S Rakhra[1,2], and Paul E Beaulé[3,4]

[1]Medical Imaging, The Ottawa Hospital, Ottawa, ON, Canada, [2]Radiology, University of Ottawa, Ottawa, ON, Canada, [3]Orthopaedic Surgery, The Ottawa Hospital, Ottawa, ON, Canada, [4]Faculty of Medicine, University of Ottawa, Ottawa, ON, Canada

In this study, we investigated whether the T1ρ profile of the hip cartilage changes over time in a subject group with asymptomatic cam-type femoroacetabular impingement (FAI). After the initial T1ρ data acquisitions, the scans were repeated on the same group in a mean time interval of 3.3 years. For the majority of the subject group there were no significant T1ρ changes in the whole joint and in different hip cartilage regions. However, 1 patient (out of 12) showed significant (>20%) increased T1ρ values (i.e. proteoglycan reduction).

5100 Computer 16

High resolution MRF-FISP with radial acquisition for MSK imaging

Dongyeob Han[1], Taehwa Hong[1], and Dong-Hyun Kim[1]

[1]School of Electrical & Electronic Engineering, Yonsei University, Seoul, Korea, Republic of

Magnetic resonance fingerprinting (MRF) provides rapid quantification of proton density, T1 and T2 mapping using spiral acquisition. However, for high resolution imaging, spiral imaging can be limiting due to its relatively long readout time. In this study, we implemented high resolution ($0.5x0.5mm^2$) MRF-FISP using golden angle random rotating radial acquisition.

5101 Computer 17

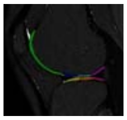

Texture characteristics of articular cartilage of patients with articular cartilage osteoarthritis based on MR T2 mapping images

Shan Wang[1], Cui-Ping Ren[1], Jing-Liang Cheng[1], and Zhi-zheng Zhuo[2]

[1]The First Affiliated Hospital of Zhengzhou University, ZhengZhou, People's Republic of China, [2]Clinical Science, Philips Healthcare, Beijing, People's Republic of China

We tried to evaluat OA by using the T2 mapping and the texture characteristics. Thirty-seven patients and sixteen healthy volunteers were recruited in this study. The results showed that the T2 value is higher in patients than in controls and some texture characteristics in two groups are different. It can be concluded that texture analysis combined with T2 maping are an useful tool for diagnosis of OA patients.

5102 Computer 18

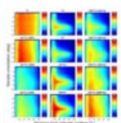

Orientation anisotropy of quantitative MRI relaxation parameters in articular cartilage

Nina Hänninen[1], Jari Rautiainen[1], Lassi Rieppo[2,3], Simo Saarakkala[2,3,4], and Mikko Johannes Nissi[1,5]

[1]Department of Applied Physics, University of Eastern Finland, Kuopio, Finland, [2]Research Unit of Medical Imaging, Physics and Technology, University of Oulu, Oulu, Finland, [3]Medical Research Center Oulu, Oulu University Hospital and University of Oulu, Oulu, Finland, [4]Department of Diagnostic Radiology, Oulu University Hospital, Oulu, Finland, [5]Diagnostic Imaging Center, Kuopio University Hospital, Kuopio, Finland

Classical and several rotating frame quantitative MR relaxation parameters have been used for evaluation of composition and structure of articular cartilage, and demonstrated to have variable sensitivity to orientation of the tissue in magnetic field. The orientation dependence of several relaxation parameters in articular cartilage have been previously investigated and were now further analyzed and compared to polarized light microscopy results. T_1, adiabatic $T_{1\rho}$ with HS1 pulse and CW-$T_{1\rho}$ at 2 kHz spin-lock demonstrated the least orientation dependence. Usefulness of the parameters for osteoarthritis diagnostics, as reported in the literature, was evaluated together with the orientation sensitivity.

5103 Computer 19

Feasibility of Simultaneous Bilateral Knee Imaging with a Dual-Coil Setup

Feliks Kogan[1], Evan Levine[1], Uchechukwuka Monu[1], Akshay Chaudhari[1], Garry Gold[1], and Brian Hargreaves[1]

[1]Radiology, Stanford University, Stanford, CA, United States

Osteoarthritis (OA) is commonly a bilateral disease. While long scan time and costs have precluded separate scanning of both knees in clinical MRI, there is evidence that bilateral examinations are beneficial for evaluation of OA changes, especially for longitudinal studies. In this study, we demonstrate the feasibility of simultaneously imaging both knees with similar scan time, SNR, and quantitative accuracy compared to single knee acquisitions.

5104 Computer 20

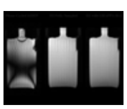

bSSFP Elliptical Signal Model With GRAPPA Parallel Imaging for Musculoskeletal Applications

Grayson Tarbox[1], Joseph Valentine[2], Meredith Taylor[2], and Neal Bangerter[2,3]

[1]Brigham Young University, Provo, UT, United States, [2]Electrical Engineering, Brigham Young University, [3]Radiology, University of Utah

Balanced steady-state free precession imaging using the elliptical signal model geometrical solution can be combined with a GRAPPA parallel imaging reconstruction that preserves phase information to shorten scan times.

5105 Computer 21

Semi-automated Segmentation of Hip Cartilage in Physiological Magnetic Resonance Imaging: A Fast, Accurate, and Clinically Viable Methodology

Daniel J Park[1], Scott Fernquest[1], Antony Palmer[1], Marija Marcan[2], Irina Voiculescu[2], and Siôn Glyn-Jones[1]

[1]Nuffield Department of Orthopaedics, Rheumatology, and Musculoskeletal Sciences, University of Oxford, Oxford, United Kingdom, [2]Department of Computer Science, University of Oxford, Oxford, United Kingdom

Physiological Magnetic Resonance imaging (pMRI) offers the potential of diagnosing osteoarthritis at a stage where patients may benefit from intervention, and acting as an assay of disease to test the efficacy of novel early intervention treatments. pMRI data, however, requires segmentation to allow morphological and biochemical quantitative analysis. Manual segmentation is time consuming and a viable automated segmentation method in the hip remains elusive. We have produced a fast, accurate, and reproducible semi-automated method of segmentation to allow wider implementation of pMRI for use in quantitative analysis of early OA in the hip in both research and clinical settings.

5106 Computer 22

Comparison of T2 and T1rho mapping of ankle cartilage between young healthy females and dancers

Hon J. Yu[1], Alex Luk[1], Jimmy Ton[1], Edward Kuoy[1], Jeff Russell[2], Kelli Sharp[3], and Hiroshi Yoshioka[1]

[1]Radiological Sciences, University of California, Irvine, CA, United States, [2]Science and Health in Artistic Performance, Ohio University, Athens, OH, [3]Arts-Dance, University of California, Irvine, CA, United States

This study demonstrates an angular-dependent T2 and T1ρ profile of talar dome cartilage at 3T using novel angular-segmentation methodology for the potential of quantitative functional assessment of cartilage *in vivo*. The results in this study indicate T2 values over the posterior weight-bearing portion were higher in young dancers than age-matched healthy volunteers even though cartilage thickness and volumes were not significantly different between two cohorts.

5107 Computer 23

Validation study T2 and T1rho mapping of the ankle cartilage using healthy volunteers

Hon J. Yu[1], Alex Luk[1], Jimmy Ton[1], Edward Kuoy[1], Jeff Russell[2], Kelli Sharp[3], and Hiroshi Yoshioka[1]

[1]Radiological Sciences, University of California, Irvine, CA, United States, [2]Science and Health in Artistic Performance, Ohio University, Athens, OH, [3]Arts-Dance, University of California, Irvine, CA, United States

This study demonstrates feasibility in manual segmentation of talar dome using MRI of the ankle and provides a systematic approach in assessment of image-based segmentation utilizing purely geometrical attributes and subsequent validation of angle-dependent analysis of T2 and T1ρ mapping of the cartilage. The results clearly demonstrates the magic angle effect of the talar dome cartilage on T2 mapping and also the important fact that repeatability assessment of segmentation should be made using the geometrical attributes rather than the underlying segmentation-based quantity.

5108 Computer 24

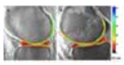

Assessing reliability of 3D Cones UTE-T2* sequence for detecting subsurface changes in cartilage and meniscus

Aditi Guha[1], Ashley A Williams[1], and Constance R Chu[1]

[1]Department of Orthopedic Surgery, Stanford University, Stanford, CA, United States

The purpose of this study is to establish the reliability of the UTE-T2* mapping method using 3DCones sequence shown to detect subsurface changes in knee cartilage and meniscus. Scans were performed on cadaver knee specimen using 3DCones acquisition at 3T with 8 and 12 TEs. Reliability was assessed by the intraclass correlation coefficient (ICC) calculated as 0.77 and 0.91 for the 8 and 12 point techniques. The method is good to excellently reproducible for both techniques. Hence, the 3DCones UTE-T2* mapping technique can reliably evaluate subsurface changes in meniscus and cartilage and help identify at-risk OA patients.

Electronic Poster

Bone & Muscle

Exhibition Hall — Wednesday 17:15 - 18:15

5109 Computer 1

Improved delineation of air-bone interface in in-vivo high-resolution bright bone ZTE MRI at 3T

Aiming Lu[1], Krzysztof R Gorny[2], Mai Lan Ho[2], John III Huston[2], Robert J Witte[2], John I Lane[2], Dan Rettmann[3], Michael Carl[3], and Gaspar Delso[3]

[1]Mayo Clinic, Rochester, MN, United States, [2]Mayo Clinical, Rochester, MN, United States, [3]GE Healthcare

Using MRI for depicting solid cortical bone structures is of increasing clinical interest. Due to its low water content and short transverse relaxation time, cortical bone appears as signal void in conventional gradient echo or spin echo pulse sequences. This allows “black bone” techniques to be used when air does not confuse the visualization of cortical bone. In cases differentiation between bone tissues and ai are desired “bright bone” techniques utilizing Ultrashort echo time (UTE) or Zero TE (ZTE) MRI-have been proposed. Long T2-suppression methods (e.g., echo subtraction, long T2 saturation) are often applied to generate positive cortical bone contrast. However, clinical applications of these methods are still limited due to significant increase in acquisition time and reduced SNR efficiency. Recently a prototype proton density (PD)-weighted, zero TE (ZT) sequence has been demonstrated clinically. This work aims to improve the bright bone MRI using the ZTE sequence by optimizing the bone signal during data acquisition, minimizing partial volume effect with ultra high resolution data acquisition and optimizing the image processing for better bone/air differentiation.

5110 Computer 2

Three-Dimensional Adiabatic Inversion Recovery Prepared Ultrashort Echo Time Cones (3D IR-UTE-Cones) Imaging of Cortical Bone in the Hip

Amin Nazaran[1], Michael Carl[2], Yajun Ma[1], Saeed Jerban[1], Yanchun Zhu[1], Eric Y. Chang[1,3], and Jiang Du[1]

[1]The University California, San Diego, San Diego, CA, United States, [2]GE Healthcare, San Diego, CA, United States, [3]Radiology Service, VA San Diego Healthcare System

Ultra short echo time (UTE) techniques have been used to image cortical bone. However, imaging cortical bone in hip has been challenging due to limited signal-to-noise ratio (SNR), robust long T2 suppression, and long scan time. UTE sequences with TEs down to 32µs are able to acquire signal from both short and long T2* tissue. To suppress long T2* tissue, the combination of inversion recovery (IR) and UTE imaging can be used. In this report, we applied three-dimensional adiabatic inversion recovery prepared UTE with Cones trajectories (3D IR-UTE-Cones) to suppress long T2 tissue and to directly quantify cortical bone in the hip in vivo at 3T.

5111 Computer 3

Does Free Water T1 Differ in Different Regions of Human Cortical Bone? A Clinical Quantification Approach

Atena Akbari[1,2], Shahrokh Abbasi-rad[1,2], Amirali Kazeminejad[1,3], and Hamidreza Saligheh Rad[1,2]

[1]Quantitative Medical Imaging Systems Group, Research Center for Cellular and Molecular Imaging, Tehran University of Medical Sciences, Tehran, Iran, Tehran, Iran, [2]Medical Physics and Biomedical Engineering Department, Tehran University of Medical Sciences, Tehran, Iran, Tehran, Iran, [3]School of Electrical and Computer Engineering, University of Tehran, Tehran, Iran, Tehran, Iran

MR structural imaging is proved to be able of featuring cortical bone hierarchical structure by obtaining enough signal from hydrogen protons of short T_2^* components of bone. Extreme variability of free water quantities found in cortical bone pores during aging or bone disease, furnishes researchers with a great source of information to inspect bone health. In this study, we employed short time of echo MR imaging approach to quantify cortical bone free water T_1 in different regions of tibia to extract the porosity distribution pattern of cortical bone and its alteration with age in eight healthy volunteers.

5112 Computer 4

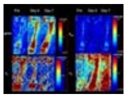

MRI study of the changes of perfusion and fat content in radiation-induced bone marrow injury in rats

kejun wang[1], Yunfei Zha[1], and Xiao Xu[2]

[1]Department Of Radiology, Renmin Hospital Of Wuhan University, wuhan, People's Republic of China, [2]GE Healthcare, Shanghai, People's Republic of China

This study is to investigate whether adipocytes influence bone marrow microcirculation based on DCE-MRI and ex vivo high-resolution MAS 1H NMR spectroscopy. In this animal review committee-approved study, Rat Femurs were evaluated through DCE-MRI, 1H HRMAS NMRS, and histopathologic analysis before irradiation and on days 4 and 7 after irradiation. The results showed Ktrans and adipocytes gradually increased a peak on the 7th day after irradiation. In conclusion, bone marrow microcirculation permeability correlation with fat content after irradiation suggested for the first time that a pathophysiology mechanism based on fat- vascular permeability in the injury of bone marrow microcirculation.

5113 Computer 5

Long-term prognostic value of whole-body MRI fat fraction signal changes following initial Bortezomib treatment of patients with multiple myeloma

Arash Latifoltojar[1], Margaret Hall-Craggs[1], Alan Bainbridge[2], Neil Rabin[2], Rakesh Popat[1], Ali Rismani[2], Kwee Yong[1], and Shonit Punwani[1]

[1]University College London, London, United Kingdom, [2]University College London Hospital, United Kingdom

Quantitative MRI assessment of treatment response using advanced novel imaging techniques have shown promises for monitoring outcome in patients with symptomatic multiple myeloma (MM), undergoing intensive chemotherapy.

In this work we are investiagting the potential of whole-body mDixon MRI's signal fat fraction early changes as a prognostic imaging biomarker for long-term follow-up of MM patients.

5114 Computer 6

Subregional variation in proximal femoral bone marrow fat composition assessed at 3T

Dimitri MARTEL[1], Benjamin LEPORQ[2], Mary BRUNO[1], Sean BOONE[1], and Gregory CHANG[1]

[1]Department of Radiology, New York University School of Medicine, Bernard and Irene Schwartz Center for Biomedical Imaging, New York City, NY, United States, [2]Université de Lyon; CREATIS CNRS UMR 5220, Inserm U1206, INSA-Lyon, UCBL Lyon 1, Villeurbanne, France

Recent studies have shown skeletal variation of bone marrow adipose tissue (bMAT) and its role in bone remodeling. Our aim was to assess the variation in bMAT composition in five regions within the proximal femur in both controls and OP patients using a chemical shift encoded (CSE) imaging technique.

5115 Computer 7

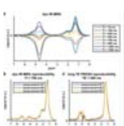

Measuring fat unsaturation and polyunsaturation in vertebral bone marrow using dynamic inversion-recovery single-voxel spectroscopy

Stefan Ruschke[1], Andreas Hock[2], Dominik Weidlich[1], Ernst J. Rummeny[1], Jan S. Kirschke[3], Thomas Baum[1], Roland Krug[4], and Dimitrios C. Karampinos[1]

[1]Department of Diagnostic and Interventional Radiology, Klinikum rechts der Isar, Technical University of Munich, Munich, Germany, [2]Philips Healthcare, Hamburg, Germany, [3]Department of Neuroradiology, Technical University of Munich, Klinikum rechts der Isar, Munich, Germany, [4]Radiology and Biomedical Imaging, University of California, San Francisco, San Francisco, CA, United States

The assessment of vertebral bone marrow fat unsaturation is attracting growing interest for applications in bone metabolism and osteoporosis. Especially in younger subjects, the presence of a strong and broad water peak confounds the extraction of surrounding peaks (olefinic and glycerol peaks), which are used for the determination of fat unsaturation. Inversion-recovery spectroscopy allows the extraction of these peaks by differentiating the signals based on different T1 relaxation times between water and fat. The feasibility of using inversion-recovery spectroscopy was evaluated in a phantom experiment in comparison with gas chromatography and in vivo in four young and healthy volunteers.

5116 Computer 8

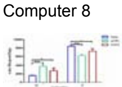

Quantitative Analysis of Avascular Necrosis of the Femoral Head Using the Multi-Echo 3D Dixon MR Sequence

bing xie[1], jingjing li[1], jie wang[1], mingshan du[1], wei chen[1], Xiaoyue zhou[2], Panli zuo[3], and Xiaodong zhong

[1]radiology, Southwest Hospital, Third Military Medical University, chongqing, People's Republic of China, [2]MR Collaboration, Siemens Healthcare Ltd, shanghai, People's Republic of China, [3]MR Collaboration, Siemens Healthcare Ltd, beijing, People's Republic of China

Avascular necrosis of thefemoral head (ANFH) is a pathological process that results from interrupted or impaired blood supply to bone. The multi-echo 3D Dixon technique provides the water/fat ratio quantification for evaluation of the bone marrow edema and the stage of ANFH. Our study demonstrated that femoral head water/fat permillage in ANFH was significantly higher than that of the healthy hips.

5117 Computer 9

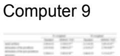

SEMAC-VAT MR Imaging Increases Clinical Detection Rates of Local Lesions in Patients with Titanium Screws at 3T

Xiaona Li[1], Zhigang Peng[1], Panli Zuo[2], Yi Sun[2], Nittka Mathias[3], and Jianling Cui[1]

[1]Radiology, the Third Hospital of Hebei Medical University, Shijiazhuang, People's Republic of China, [2]MR Collaboration NE Asia, Siemens Healthcare, Shanghai, People's Republic of China, [3]Siemens Healthcare, Erlangen, Germany

To compare the clinical detection rates in local lesions using the slice-encoding for metal artifact correction (SEMAC) & view angle tilting (VAT) Turbo Spin Echo (TSE) with the standard TSE sequence in patients with titanium screws. Following surgery, patients with reported discomfort at the operation site were examined with both TSE and SEMAC-VAT TSE imaging. They were also examined by digital radiography (DR) and computed tomography (CT). All images were assessed and scored. Despite the long scan time, SEMAC-VAT TSE reduced metal-induced artifacts and may improve the diagnostic sensitivity compared to standard TSE, DR and CT.

5118 Computer 10

Clinical evaluation of the fat deposition of patients with sacroiliitis by using mDIXON Quant technique

Ying Zhan[1], Xinwei Lei[1], Yingying An[1], Jin Qu[1], and Zhizheng Zhuo[2]

[1]Tian Jin First Central Hospital, Tianjin, People's Republic of China, [2]Philips Healthcare, Beijing, People's Republic of China

The study was using fat fraction (FF) to investigate the fat deposition of sacroiliitis. 3T MRI with mDIXON Quant technique was performed. All patients were divided into three groups: simple edema group, edema-fat deposition group and simple fat deposition group. The FF of both edema and fat deposition areas were obtained on FF image. The FF of edema areas was higher in edema-fat deposition group than simple edema group. The FF of fat deposition areas was higher in simple fat deposition group than edema-fat deposition group. mDIXON Quant technique could be used for assessing the situation of the disease.

5119 Computer 11

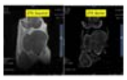

Bone Imaging Using MR: Inversion Recovery Vs Tissue Segmentation

Michael Carl[1], Graeme McKinnon[2], and Gaspar Delso[3]

[1]GE Healthcare, San Diego, CA, United States, [2]GE Healthcare, WI, United States, [3]GE Healthcare, United Kingdom

Many musculoskeletal tissues such as cortical bone have very short transverse relaxation times and require specialized pulse sequences such as UTE or ZTE for optimal signal acquisition. Recently, these sequences have been used to directly visualize cortical bone by suppressing surrounding long T2 tissues such as fat or muscle by either magnetization preparation using inversion recovery, or logarithmic tissue segmentation. In this work, we compare these techniques on a cadaveric bovine knee specimen. Both inversion recovery UTE as well as tissue segmented ZTE imaging proved promising method for direct bone imaging with CT-like image appearance.

5120 Computer 12

Accuracy of Age Estimation based on Undersampled MR Images of the Hand

Bernhard Neumayer[1,2], Matthias Schloegl[3], Christian Payer[4], Thomas Widek[1,2], Thomas Ehammer[1], Rudolf Stollberger[2,3], and Martin Urschler[1,2,4]

[1]Ludwig Boltzmann Institute for Clinical Forensic Imaging, Graz, Austria, [2]BioTechMed-Graz, Graz, Austria, [3]Institute of Medical Engineering, Graz University of Technology, Graz, Austria, [4]Institute for Computer Graphics and Vision, Graz University of Technology, Graz, Austria

The topic of age estimation in living persons is important for sports competitions as well as unaccompanied minors without valid documents and has recently gained interest. Recommended imaging protocols are based on modalities using ionizing radiation and therefore MRI is currently investigated for its eligibility to replace these measurements. This study investigates the accuracy of MRI-based age estimation for retrospectively undersampled data to determine the degree of inaccuracies introduced by an acceleration of the acquisition technique using commercially available undersampling strategies. For this purpose the data is analyzed by a radiologist and using an automatic method.

5121 Computer 13

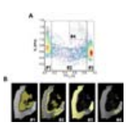

MRE derived stiffness of the gluteus maximus muscle: reproducibility and correlation to T2 and fat-fraction

Jules L. Nelissen[1,2], Dorien Verschuren[1], Larry de Graaf[1], Cees W. J. Oomens[3], Klaas Nicolay[1], Ralph Sinkus[4], Jurgen H. Runge[4,5], Aart J. Nederveen[5], and Gustav J. Strijkers[2]

[1]Biomedical NMR, Eindhoven University of Technology, Eindhoven, Netherlands, [2]Preclinical and Translational MRI, Academic Medical Center, Amsterdam, Netherlands, [3]Biomechanics of Soft Tissues, Eindhoven University of Technology, Eindhoven, Netherlands, [4]Division of Imaging Sciences & Biomedical Engineering, King's College London, London, United Kingdom, [5]Radiology, Academic Medical Center, Amsterdam, Netherlands

Skeletal muscle pathology is often accompanied by abnormal fat deposition, fibrosis, and edema. Altered muscle biomechanical properties associated with these compositional changes can be quantitatively assessed with MRE. We present MRE measurements of the gluteus maximus muscle. In healthy volunteers, we have tested reproducibility and correlated the shear modulus G_d to T_2 and fat-fraction FF_{dix} measured using Dixon. Acceptable intra and inter reproducibility was found. Expected difference in G_d between gluteus maximus and subcutaneous fat was confirmed. Correlation plots of T_2 and FF_{dix} with G_d showed that MRE can derive biomechanical properties that potentially can provide additional information to characterize skeletal muscle pathology.

5122 Computer 14

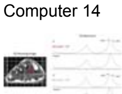

Mapping of Intramyocellular Lipid Content in Foot Muscle

Kenneth Wengler[1,2], Chien-Hung Lin[2], Mingqian Huang[2], Elaine Gould[2], Mark Schweitzer[2], and Xiang He[2]

[1]Biomedical Engineering, Stony Brook University, Stony Brook, NY, United States, [2]Radiology, Stony Brook University, Stony Brook, NY, United States

Diabetic neuropathy is a leading cause of diabetic foot ulcer and has been shown to be induced by insulin resistance. Itramyocellular lipid (IMCL) measured by MRS in large skeletal muscles has been shown to correlate with insulin resistance. In this study a generalized Lorentzian approximation is used to estimate the IMCL and EMCL frequency shift as a function of muscle fiber bundle orientation. DTI is used to measure the fiber bundle orientation and provide prior information for IMCL/EMCL peak fitting. 2D-CSI is used to quantify IMCL contents in foot muscle groups of healthy subjects and diabetic patients.

5123 Computer 15

summa cum laude

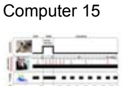

Effects of Load Induced Metabolic Changes of a Single Muscle on Whole Body Physiology

Kevin Moll[1], Alexander Gussew[1], Maria Nisser[2], Steffen Derlien[2], and Jürgen R. Reichenbach[1]

[1]Medical Physics Group, Institute of Diagnostic and Interventional Radiology, Jena University Hospital - Friedrich Schiller University Jena, Jena, Germany, [2]Institute of Physiotherapy, Jena University Hospital - Friedrich Schiller University Jena, Jena, Germany

^{31P} MR spectroscopy enables a non-invasive evaluation of a metabolic response to a given exercise. A combination of this technique with other methods like ^{1}H MRS, spirometry and blood lactate diagnostics improves the application field. Therefore, a broad range of metabolic parameters were acquired during an exercise of a single calf muscle to evaluate the effects of local energy demands on global parameters. We observed high adaptations resulting in good correlations between peripheral and locally measured values.

5124 Computer 16

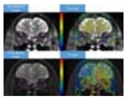

Evaluating the Extraocular Muscle Changes in Thyroid Associated Ophthalmopathy using T1ρ—A Preliminary Study

Tan Guo[1], Bing Wu[2], Dandan Zheng[2], Xiaoxiong Wang[3], Xiaoxia Wang[4], Yan Song[1], and Min Chen[1]

[1]Radiology, Beijing Hospital, Beijing, People's Republic of China, [2]MR Research China, GE Healthcare, Beijing, People's Republic of China, [3]Ophthalmology, Beijing Hospital, [4]Endocrinology, Beijing Hospital

This study is to investigate and compare the changes of extraocular muscles in patients with active thyroid associated ophthalmopathy shown by T1ρ and T2 maps. The superior differential ability of T1ρ comparing to the currently used T2 mapping is encouraging and the flexibility in exploring the different in spin lock frequencies would be promising tool in evaluating the extraocular muscle changes with thyroid associated ophthalmopathy.

5125 Computer 17

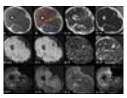

Age-related changes in healthy thigh musculature: Multi-parametric MR imaging analysis

Min A Yoon[1], Suk-Joo Hong[1], Chang Ho Kang[2], Kyung-Sik Ahn[2], Baek Hyun Kim[3], and In Seong Kim[4]

[1]Department of Radiology, Korea University Guro Hospital, Seoul, Korea, Republic of, [2]Department of Radiology, Korea University Anam Hospital, Seoul, Korea, Republic of, [3]Korea University Ansan Hospital, Gyeonggi-do, Korea, Republic of, [4]Siemens Healthcare Korea, Seoul, Korea, Republic of

Purpose: To identify MR parameters that are significantly associated with aging in healthy thigh muscles and investigate age-related characteristics.

Methods: Thirty healthy subjects underwent multi-parametric MRI of the right thigh, including IVIM-DWI, DTI, multi-echo Dixon imaging, DCE-MRI. Parametric maps of the thigh muscles (divided into three compartments) were analyzed. Relationships between parameters and age were assessed with simple and multiple linear regression analyses.

Results: Fractional anisotropy (slope=1.018) and V_e (slope=2.151) in anterior compartment and fat percentage in posterior compartment (slope=2.031) showed significant relationships to age ($p<0.05$).

Conclusion: Several MRI parameters of the thigh muscles were associated with normal aging.

5126 Computer 18

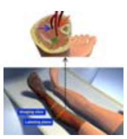

Quantitative Lower Limb Perfusion Territory Imaging with Vessel Encoded Arterial Spin Labeling

Lian Ding[1], Fei Gao[2], Chengyan Wang[1], Wenjian Huang[1], Jue Zhang[1,2], Xiaoying Wang[1,3], and Jing Fang[1,2]

[1]Academy for Advanced Interdisciplinary Studies, Peking University, Beijing, People's Republic of China, [2]College of Engineering, Peking University, Beijing, People's Republic of China, [3]Department of Radiology, Peking University First Hospital, Beijing, People's Republic of China

Critical limb ischemia (CLI) represents the most severe clinical manifestation of peripheral arterial disease (PAD). It has been proved that l lower extremity arterial stenosis and collateral circulation compensatory ability after occlusion play an important role on CLI. This study proposed a strategy for assessment of lower extremity arterial stenosis and collateral circulation compensatory ability by the noninvasive vessel-encoded arterial spin labeling (VEASL) to quantitatively assess perfusion territory of lower extremity arterial. The lower limb perfusion territory image and the angiosome map were obtained in this study, indicating the potential of VEASL for CLI assessment.

5127 Computer 19

Evaluation of T1p time in the quadriceps muscle after an Anterior Cruciate Ligament Reconstruction: Relationship to muscle strength and injury recovery

Brian Noehren[1,2], Richard Lawless[3], Peter Hardy[4], Anders Andersen[3], and Moriel Vandsburger[5,6]

[1]Rehabilitation Sciences, University of Kentucky, Lexington, KY, United States, [2]Orthopaedic Surgery, University of Kentucky, Lexington, KY, United States, [3]University of Kentucky, Lexington, KY, United States, [4]Radiology, University of Kentucky, Lexington, KY, United States, [5]Department of Physiology, University of Kentucky, Lexington, KY, United States, [6]Department of Bioengineering, University of California Berkeley, CA, United States

Anterior Cruciate Ligament Injuries are associated with long term loss of quadriceps muscle strength. Accumulation of greater collagen in the extracellular matrix around muscle fibers could limit recovery. T1p applied to the quadriceps muscle could identify patients at risk for not having a good recovery because of collagen deposition. T1p imagining of the injured and non injured quadriceps of 6 subjects was performed. We found significantly higher T1p times in the injured limb as well as a significant association to greater muscle weakness. These results show the potential application of T1p to identify individuals with muscle dysfunction.

5128 Computer 20

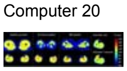

Evaluation of fast radial T1 mapping for skeletal muscle tissue characterization

Benjamin Marty[1,2], Bertrand Coppa[1,2], Pierre-Yves Baudin[3], and Pierre G. Carlier[1,2]

[1]NMR Laboratory, Institute of Myology, Paris, France, [2]NMR Laboratory, CEA, DRF, I²BM, MIRCen, Paris, France, [3]Consultants for Research in Imaging and Spectroscopy, Tournai, Belgium

The development of quantitative NMR outcome measures in order to monitor natural history of neuromuscular disorders or therapeutic interventions is crucial. Global muscle T1 values is strongly affected in chronic disease when healthy muscle is replaced by fat and this parameter can be used for diagnostic purposes. Nevertheless, very little is known about the effects of tissue water compartmentation and distribution on muscle T1 values. Here, we investigated the variations of skeletal muscle T1 values under various physiological conditions using a fast T1 mapping sequence and evaluated the potential of this biomarker in the context of disease monitoring.

5129 Computer 21

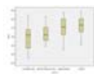

Quantitative evaluation of supraspinatus fatty infiltration and its relationship with tendon tear severity by using mDIXON-Quant technique

Jin Qu[1], Xinwei Lei[1], Ying Zhan[1], Huixia Li[1], Yingying An[1], and Zhizheng Zhuo[2]

[1]Tianjin First Center Hospital, Tianjin, People's Republic of China, [2]Philips Healthcare, Beijin, People's Republic of China

The purpose of this study was to evaluate fatty infiltration of supraspinatus quantitatively using fat fraction measurements and investigate the relationship between fatty infiltration, muscle atrophy and tendon tear severity. Quantitative assessment of fatty infiltration was performed using 3T MRI with a mDIXON-Quant technique in 85 patients. The degree of fatty infiltration and muscle atrophy significantly increase with the extent of rotator cuff tear. The tendon tear severity correlated with fatty infiltration and muscle atrophy, and muscle atrophy correlated with fatty infiltration. mDIXON-Quant can be a reliable and accurate tool to quantify fatty degeneration of the rotator cuff muscles.

5130 Computer 22

Phosphodiester-levels in Muscle Assessed using 31P MRS are an Early Marker for Disease Activity in DMD

Melissa T. Hooijmans[1], Nathalie Doorenweerd[1,2], Jedrzej Burakiewicz[1], Celine A. Baligand[1], Jan J.G.M. Verschuuren[2], Andrew G. Webb[1], Erik H. Niks[2], and Hermien E. Kan[1]

[1]C.J.Gorter Center for High-field MRI, Dept. of Radiology, Leiden University Medical Center, Leiden, Netherlands, [2]Dept. of Neurology, Leiden University Medical Center, Leiden, Netherlands

Quantitative MR of muscle is increasingly important as potential outcome measure for therapy development in DMD. Since therapy is aimed at preserving or improving muscle tissue, an early marker that reflects muscle state with a suitable dynamic range is essential. Unfortunately, water T2 and %fat do not meet this criteria. Therefore, we aimed to assess whether phosphodiester (PDE)-levels detected by 31P MRS could fill this gap. We have shown a two-fold increase in PDE-levels compared to controls and its detection prior to structural changes which confirm the potential of PDE as an early marker for disease activity in DMD patients.

5131 Computer 23

Non-Gaussian diffusion of human skeletal muscle water and metabolites observed using proton diffusion-weighted spectroscopy

David A. Reiter[1], Christopher Bergeron[1], Richard G. Spencer[1], Luigi Ferrucci[1], and Itamar Ronen[2]

[1]National Institute on Aging, NIH, Baltimore, MD, United States, [2]C.J. Gorter Center for High Field MRI, Department of Radiology, Leiden University Medical Center, Leiden, Netherlands

Micro- and ultrastructural properties of skeletal muscle have a direct impact on function and modulate the diffusion of both water and metabolites. Anomalous diffusion models can be used to characterize non-Gaussian diffusion and specifically subdiffusive dynamics, which are expected to reflect ultra-structural tissue properties. Here, we present fits of the single-parameter Mittag-Leffler diffusion model to diffusion weighted spectroscopy data, showing subdiffusive motions of skeletal muscle water and metabolites.

5132 Computer 24

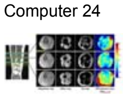

Measurement and Correction for the Magnetic Susceptibility Effects of Fat in Venous Oximetry: Application in the Quantification of Muscle Oxygen Consumption (VO2) with Plantar Flexion Exercise

Esther H Yang[1], Amy A Kirkham[1], and Richard B. Thompson[1]

[1]Biomedical Engineering, University of Alberta, Edmonton, AB, Canada

The magnetic field shift within cylindrical blood vessels can be used to estimate venous oxygen saturation, based on the magnetic susceptibility of deoxyhemoglobin. However, conduit veins in the periphery are often surrounded by fat, which has a larger magnetic susceptibility than water and the venous blood pool. It is shown that the magnetic susceptibility effects of fat can confound estimation of venous oxygen saturation. A new method to correct for these effects is described with application for plantar flexion exercise, for the measurement of muscle oxygen extraction, blood flow and calculation of oxygen consumption (VO_2).

Electronic Poster

Spine, Tumors & Miscellaneous

Exhibition Hall Wednesday 17:15 - 18:15

5133 Computer 25

Correlation Between Bone Marrow Fatty Deposition Under Vertebral Endplates with Lumbar Intervertebral Disc Degeneration

Xiaodong Zhang[1], Yinxia Zhao[1], Yingjie Mei[2], and Shaoyong Hu[1]

[1]Department of medical radiology, The Third Affiliated Hospital of Southern Medical University（Academy of orthopedics •Guangdong Province）, Guangzhou, People's Republic of China, [2]Philips Healthcare, Guangzhou, People's Republic of China

The intervertebral disc without blood supply obtained nutrient substance diffusing from the microcirculation under vertebral endplates. Some studies showed the fat deposition of bone marrow may pressure vessels and blood sinus, which could affect the microcirculation. So the fatty content of bone marrow under vertebral endplates can reflect the degeneration of the vertebral. However, the correlation of fatty content of bone marrow with lumbar intervertebral disc degeneration is not clear. The purpose of our study was to analyze the correlation between bone marrow fatty fraction under vertebral endplates with Pfirrmann Grades and T2* value of lumbar intervertebral disc.

5134 Computer 26

Dynamic Morphometric Changes in Degenerative Lumbar Spondylolisthesis: A Pilot Study of Standing Magnetic Resonance Imaging

Raphaële charest-morin[1], Honglin Zhang[2], Michael Bond[3], Amy Phillips[4], Shannon Patterson[5], David Wilson[3], and John Street[3]

[1]Department of Orthopaedics, Centre Hospitalier Universitaire de Québec, Quebec, QC, Canada, [2]Department of Orthopaedics, University of British Columbia, Vancouver, BC, Canada, [3]Department of Orthopaedics, University of British Columbia, [4]Center for Hip Health and Mobility, University of British Columbia, [5]Department of Radiology, Vancouver General Hospital

The planning of spine surgery for degenerative lumbar spondylolisthesis (DLS) is currently based on supine MR images while patients experience symptoms in the upright posture. This study employed an upright Open MRI to determine whether the MRI-based measurements of the spinal and neural elements used in planning surgery are different in the symptomatic, upright posture than in the supine posture. We found upright MRI scanning detected dynamic morphometric differences in a number of clinically important radiographic parameters in patients with DLS. Upright MRI may help in planning minimally invasive surgeries for DLS.

5135 Computer 27

Changes in tracer kinetics in the endplates of degenerating intervertebral discs

L. Tugan Muftuler[1], Volkan Emre Arpinar[2], and Ali Ersoz[3]

[1]Department of Neurosurgery, Medical College of Wisconsin, Milwaukee, WI, United States, [2]Department of Radiology, Medical College of Wisconsin, Milwaukee, WI, United States, [3]Department of Biophysics, Medical College of Wisconsin, Milwaukee, WI, United States

This study investigated changes in perfusion and diffusion in the cartilaginous endplates and subchondral bones around the degenerating discs. It has been suggested that such abnormalities might indicate inflammatory changes that might lead to chronic low back pain. A high spatial and temporal resolution DCE-MRI technique was implemented and tested on a group of volunteers. Pharmacokinetic model was used to quantify the changes in the regions of interest. Results demonstrated significant changes in contrast agent uptake and washout in the cartilaginous and bony endplate regions as the adjacent disc degenerated.

5136 Computer 28

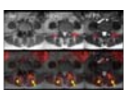

Whole body FDG PET/MRI for assessment of facet joint osteoarthritis: Direct comparison of FDG uptake with MRI and CT features

Munenobu Nogami[1,2], Shinsuke Shimoyama[2], Yuichi Wakabayashi[2], Utaru Tanaka[2], Yoshiaki Watanabe[3], Akihito Ohnishi[2], Tatsuya Nishii[2], Yoshiko Ueno[2], Atsushi K Kono[3], Kazuhiro Kubo[2], Satoru Takahashi[2], and Kazuro Sugimura[2]

[1]Department of Radiology, Hyogo Cancer Center, Akashi, Japan, [2]Department of Radiology, Kobe University Graduate School of Medicine, Kobe, Japan, [3]Department of Radiology, National Cerebral and Cardiovascular Center, Suita, Japan

Hybrid PET/MRI scanner is an emerging modality and utilized not only for oncological or neurological purposes but also for assessment of musculoskeletal disease. Simultaneous acquisition of PET and MRI enables precise anatomical localization of PET tracers and further understanding of mechanism of the tracer uptake by using MRI information. Our hypothesis was that PET/MRI can reveal the pathophysiological mechanism of facet joint osteoarthritis by the simultaneous whole body imaging. The results showed MRI features on PET/MR significantly correlated with FDG uptake in the facet joint osteoarthritis and may be superior to CT based evaluation.

5137 Computer 29

Vertebral strength prediction in diabetic patients: quantification of bone marrow fat content obtained by IDEAL-IQ

Shinpei Yamaguchi[1], Takatoshi Aoki[1], Koichi Nakagami[1], Masami Fujii[1], Yoshiko Hayashida[1], Yosuke Okada[2], Yoshiya Tanaka[2], and Yukunori Korogi[1]

[1]Radiology, University of Occupational and Environmental Health, Kitakyushu, Japan, [2]First department of Internal Medicine, University of Occupational and Environmental Health, Kitakyushu, Japan

Although bone mineral density (BMD) by dual X-ray absorptiometry (DXA) has been used to predict bone strength, diabetes mellitus (DM) patients have an elevated fracture risk despite normal BMD. We evaluated the availability of the fat fraction (FF) using IDEAL-IQ for vertebral strength prediction in DM patients. The correlation between the failure load by CT-based finite-element method and the BMD with age and the FF using IDEAL-IQ was significantly higher than that between the failure load and the BMD alone ($p<.001$). FF using IDEAL-IQ in combination with BMD measurements can potentially be used in predicting bone strength in DM patients.

5138 Computer 30

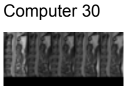

3D variable flip angle fast spin echo imaging of the cervical spine : Improved image quality and decreased scan time with outer volume suppression

Ho-Joon Lee[1], Suchandrima Banerjee[2], Dong Eun Kim[3], Sung-Min Gho[3], and Seung-Koo Lee[1]

[1]Radiology, Yonsei University College of Medicine, Seoul, Korea, Republic of, [2]Global MR Applications & Workflow, GE Healthcare, Menlo Park, CA, [3]GE Healthcare, Seoul, Korea, Republic of

Application of the volumetric fast spin echo (FSE) imaging in MRI is increasing, due to innate capability for multi-planar reconstruction, and potentials for a simplified workflow. However application to the cervical and thoracic area may be challenging because ghosting/phase encoded motion artifacts from swallowing, respiration and pulsations are frequent and severe in these regions, leading to image degradation. 3D FSE with outer volume suppression is a robust method for imaging the cervical spine, which provides improved image quality at a decreased scan time.

5139 Computer 31

Preliminary investigation: Gaussian and non-Gaussian measurements of water diffusion in diagnostic differentiation of focal lesions of malignant spinal bone tumors

Miyuki Takasu[1], Yuji Akiyama[1], Kazushi Yokomachi[1], Yoko Kaichi[1], Chihiro Tani[1], Koichi Oshio[2], and Kazuo Awai[1]

[1]Diagnostic Radiology, Hiroshima University Hospital, Hiroshima, Japan, [2]Diagnostic Radiology, Keio University School of Medicine, Japan

We compared the potential of various diffusion parameters obtained from Gaussian and non-Gaussian diffusion models in differentiating focal lesions of malignant spinal tumors. Mean signal intensity was calculated by placing ROIs within focal lesions for 9 b-values in each subject. ADC, frac<1, frac>3, and PG(D) differed significantly between focal lesions of myeloma and LCA. Frac>3 and PG(D) was significantly different between focal lesions of myeloma and MMK. Non-Gaussian diffusion parameters may provide additional information and improve the differentiation of malignant focal lesions compared with conventional diffusion parameters, which would be helpful in improving therapy strategies.

5140 Computer 32

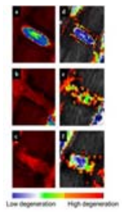

Q-space imaging is a novel technique to evaluate intervertebral disc degeneration.

Daisuke Nakashima[1], Nobuyuki Fujita[1], Junichi Hata[2,3], Takeo Nagura[1], Kanehiro Fujiyoshi[4], Hideyuki Okano[2,3], Masahiro Jinzaki[5], Morio Matsumoto[1], and Masaya Nakamura[1]

[1]Department of Orthopaedic Surgery, Keio University School of Medicine, Tokyo, Japan, [2]Department of Physiology, Keio University School of Medicine, Tokyo, Japan, [3]Central Institute for Experimental Animals, Kawasaki, Japan, [4]Department of Orthopaedic Surgery, Murayama Medical Center, Japan, [5]Department of Radiology, Keio University School of Medicine, Tokyo, Japan

Pfirrmann classification on T2WI has been the qualitative grading of intervertebral disc (IVD) degeneration which is difficult to classify subtle changes of degeneration. A quantitative and more sensitive classification system has been sought.

In this research, probability at zero displacement obtained from Q-space imaging (QSI) which is a quantitative diffusion-weighted MRI procedure made it possible to observe the effect of the regenerative antioxidant drug: N-Acetyl Cystaine on IVD degeneration which could not be observed by using T2 mapping.

Probability at zero displacement obtained from QSI has the possibility to be a novel biomarker of IVD degeneration.

5141 Computer 33

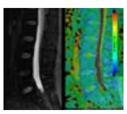

T1rho Imaging Quantification of Early Intervertebral Disc Degeneration in Pilots on 3.0T Magnetic Resonance

Xiulan Zhang[1], Yongmin Bi[2], Wanshi Zhang[2], and Lizhi Xie[3]

[1]Radiology Department, The First People's Hospital of Jingzhou,Jingzhou, China,People's Republic of, Jingzhou, People's Republic of China, [2]Department of CT&MRI, Air Force General Hospital, Beijing, China, People's Republic of, [3]GE Healthcare, MR Research China, Beijing, China, People's Republic of

Degenerative disc disease is an occupational disease of the military pilots, which seriously influcenes their health and normal training. Early disc degeneration begins with changes in biochemical compositions which is mainly characterized by proteoglycan lose and cannot be detected on conventional MRI imaging[1-2]. T1rho is a quantitative imaging technique to reflect changes in the extracellular matrix, such as modifications in the intervertebral disc PG content[3]. In this study，Bivariate correlation analysis was performed to compare T1rho values to the degenerative grade, disc space level, age and flight time of the pilots. T1rho values of Lumbar intervertebral discs in pilots demonstrated significantly negative correlations with degenerative grade, age and flight time, except for disk space levels. T1rho can be potentially used as a valid clinical method in the quantitative diagnosis of early intervertebral disc degeneration in asymptomatic Pilots.

5142 Computer 34

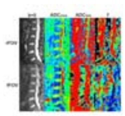

The comparison of full FOV and reduced-FOV IVIM Diffusion-weighted imaging of Spinal bone marrow

Dong Xing[1], Yunfei Zha[1], Fang Liu[1], Liang Li[1], Feifei Zeng[1], Yuan Lin[1], Wei Gong[1], Lei Hu[1], Jiao Wang[1], Bing Wu[2], and Hui Lin[2]

[1]Department of Radiology, Renmin Hospital of Wuhan University, Wuhan, People's Republic of China, [2]GE healthcare China

IVIM (Intravoxel incoherent motion) provides perfusion quantification without the need for intravenous contrast injection, and has been used to the spinal bone marrow lesions[1,2]. However, diffusion weighted imaging is prone to image deformation, especially with a large FOV. Hence the quantitative measurement of IVIM in spinal bone morrow may be affected. Reduced FOV DWI is known to reduce the level of image distortion, and the purpose of this study is to compare the IVIM parameters obtained using full FOV or reduced FOV imaging.

5143 Computer 35

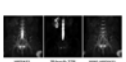

Improved visualization of diffusion-prepared MR neurography (SHINKEI) in the pelvis using high-intensity reduction (HIRE) technique

Hitoshi Tadenuma[1], Kayoko Abe[2], Masami Yoneyama[3], Yasuhiro Goto[1], Makoto Suzuki[1], Mamoru Takeyama[1], and Shuji Sakai[2]

[1]Department of Radiological Service, Tokyo Women's Medical University, Tokyo, Japan, [2]Department of Diagnostic Imaging and Nuclear Medicine, Tokyo Women's Medical University, Tokyo, Japan, [3]Philips Electronics Japan, Ltd, Tokyo, Japan

The role of MRI in the diagnosis of Lumbrosacral plexopathy is in depiction of the anatomical detail of pelvic nerves. This study attempted the improvement of the pelvic nervous depiction using HIRE-SHINKEI. This applies HIRE technique, and requires both SHINKEI and additional 3D heavily T2W scan to subtract the data. HIRE-SHINKEI can improve the depiction of nerves by subtracting signals of the background. This new technique has great potential to help the diagnosis for the peripheral nerve disorders of the lumbosacral region.

5144 Computer 36

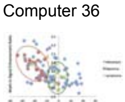

Differential Diagnosis of Myeloma, Lymphoma, and Metastatic Cancer in the Spine Using DCE-MRI Kinetic Parameters

Ning Lang[1], Huishu Yuan[1], and Min-Ying Su[2]

[1]Department of Radiology, Peking University Third Hospital, Beijing, People's Republic of China, [2]Tu and Yuen Center for Functional Onco-Imaging, Department of Radiological Sciences, University of California, Irvine, CA, United States

A retrospective DCE-MRI of 23 patients with confirmed myeloma and 13 patients with spinal lymphoma were found. A group of 76 patients with different metastatic cancers in the spine was used as a comparison group. Three heuristic parameters: the steepest wash-in enhancement ratio, the initial area under the curve (IUAC) enhancement ratio, and the wash-out slope were measured. In the ROC analysis based on the wash-out slope, myeloma can be differentiated from lymphoma with AUC=0.913, and from mets with AUC=0.828. The wash-out slope can also differentiate lung mets from breast mets with AUC=0.812, and from thyroid mets with AUC=0.891.

5145 Computer 37

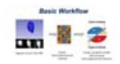

Radiomics of Musculoskeletal Masses Using T2-Weighted Magnetic Resonance Images

Stephen M Fisher[1], Alfonso Rodriguez[2], Jing Wang[2], Michael Folkert[2], and Avneesh Chhabra[1]

[1]Radiology, UT Southwestern, Dallas, TX, United States, [2]Radiation Oncology, UT Southwestern, Dallas, TX, United States

Texture analysis has yet to be exploited in musculoskeletal tumors. In this study we aimed to create a novel predictive model based on features of benign and malignant musculoskeletal masses and test this model against existing methods used in other parts of the body. Our workflow shows promise for creating accurate classifiers of benign and aggressive tumors based on T2-weighted MRI images.

5146 Computer 38

Comparison of whole-body morphologic and functional MRI with automated "bone subtraction" CT-image analysis for monitoring of longitudinal spine involvement in patients with multiple myeloma

Marius Stefan Horger[1], Sebastian Werner[1], Wolfgang Thaiss[2], and Christopher Kloth[1]

[1]Radiology, Eberhard-Karls-University Tuebingen, Tuebingen, Germany, [2]Radiology, Eberhard-Karls-Univesity Tuebingen, Tuebingen, Germany

Imaging diagnosis and therapy monitoring of multiple myeloma (MM) is challenging due to the combined bone and bone marrow involvement and at the same time often imperative due to possible failure of hematological markers (e.g. non-secretory myeloma). MRI is the most powerful MM-imaging technique for visualization of medullar involvement whereas CT optimally detects myeloma bone-disease (BMD). A new CT post-processing software (bone subtraction-BS) is generating subtraction (difference) maps of baseline and follow-up non-enhanced CT exams highlighting the course of BMD. Hence, the purpose of this study was to assess strengths and limitations of these two imaging modalities for longitudinal disease monitoring.

5147 Computer 39

Dynamic susceptibility contrast perfusion MR imaging in distinguishing malignant from benign soft tissue tumors in limbs: A pilot study

Yitong Bian[1], Guohong Jin[2], Yanliang Wang[3], Gang Niu[1], and Jian Yang[1]

[1]Fisrt Affiliated Hospital of Xi'an Jiaotong University, Xian, People's Republic of China, [2]General Affiliated Hospital of Ningxia Medical University, Yinchuan, People's Republic of China, [3]Luoyang Central Hospital Affiliated to Zhengzhou University

Precise differential and qualitative diagnoses for extremities soft tissue tumors(STTs) are of vital importance. Dynamic susceptibility contrast perfusion MRI(DSC-MRI) enables assessment of overall tumor vascularity, allowing indirect evaluation of the biological aggressiveness of tumors. Therefore, this study aims to discuss the feasibility of DSC-MRI to preliminarily assess in the differentiation between benign and malignant extremities STTs. Our results showed that DSC-MRI might be a non-invasive imaging technique that can play a role in identifying malignant and benign STTs in limbs and provide reliably pathological or physiological information for clinic.

5148 Computer 40

Texture analysis based on intra-voxel incoherent motion MR imaging for the differentiation of benign and malignant bone tumors

Ying Li[1], Cuiping Ren[1], Jingliang Cheng[1], and Zhizheng Zhuo[2]

[1]Zhengzhou University First Affiliated Hospital, Zhengzhou,Henan, People's Republic of China, [2]Clinical Science, Philips Healthcare, People's Republic of China

This work investigated and evaluated the role of texture analysis based on intra-voxel incoherent motion(IVIM) MR imaging to characterize the bone tumors,and furtherly evaluate the ability of the texture parameters to differentiate benign and malignant bone tumors by using a couple of classifiers, which might be helpful for clinical diagnosis and studies. The texture parameters have the ability to character the bone tumor and the naïvebayes classifier showed the best performance in the differentiation of benign and malignant bone tumors.

5149 Computer 41

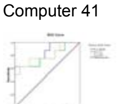

Characterization of benign and malignant soft tissue tumors using dynamic contrast enhanced magnetic resonance imaging

Ying Li[1], Cuiping Ren[1], Jingliang Cheng[1], and Zhizheng Zhuo[2]

[1]Zhengzhou University First Affiliated Hospital, Zhengzhou,Henan, People's Republic of China, [2]Clinical Science, Philips Healthcare, People's Republic of China

This work investigated and evaluated the role of dynamic contrast enhanced magnetic resonance imaging(DCE-MRI) in characterizing the soft tissue tumors, and furtherly evaluate the ability of permeability parameters to differentiate benign and malignant tumors by using random tree and artificial neural network classifiers, which might be helpful for clinical diagnosis and studies.

5150 Computer 42

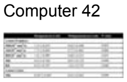

Feasibility study of diffusional kurtosis imaging for the differentiation of musculoskeletal benign and malignant tumors

Ying Li[1], Cuiping Ren[1], Jingliang Cheng[1], and Zhizheng Zhuo[2]

[1]Zhengzhou University First Affiliated Hospital, Zhengzhou,Henan, People's Republic of China, [2]Clinical Science, Philips Healthcare, People's Republic of China

This work investigated and evaluated the role of magnetic resonance (MR) diffusion kurtosis imaging(DKI) in characterizing the musculoskeletal tumors, and furtherly evaluate the ability of DKI parameters to differentiate benign and malignant tumors by using a classifier based on random forest method, which might be helpful for clinical diagnosis and studies.

5151 Computer 43

Feasibility study of intra-voxel incoherent motion MR imaging for the differentiation of benign and malignant bone tumors

Ying Li[1], Cuiping Ren[1], Jingliang Cheng[1], and Zhizheng Zhuo[2]

[1]Zhengzhou University First Affiliated Hospital, Zhengzhou,Henan, People's Republic of China, [2]Clinical Science, Philips Healthcare, People's Republic of China

This work investigated and evaluated the role of intra-voxel incoherent motion(IVIM) MR imaging in characterizing the bone tumors, and furtherly evaluate the ability of IVIM parameters to differentiate benign and malignant tumors by using a support vector machine (SVM) classifier, which might be helpful for clinical diagnosis and studies.

5152 Computer 44

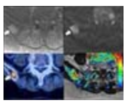

Dynamic Contrast-Enhanced Magnetic Resonance Imaging Parameters in Metastatic Bone Lesions of Non-small Cell Lung Cancer: Comparison between Lesions with and without Epidermal Growth Factor Receptor (EGFR) Mutation in Primary Cancer

Hyun Su Kim[1] and Young Cheol Yoon[1]

[1]Radiology, Samsung medical center, Seoul, Korea, Republic of

The presence of the epidermal growth factor receptor (EGFR) gene mutation is associated with a high rate of distant metastasis and poor prognosis in patients with non-small cell lung cancer (NSCLC). EGFR signaling acts as mediator of bone metastasis by increasing tumor cell proliferation and promotes synthesis and secretion of numerous angiogenic growth factors. We propose that metastatic bone lesions with and without the EGFR mutation in primary NSCLC have different perfusion profiles and dynamic contrast-enhanced magnetic resonance imaging (DCE-MRI) parameters can reveal the differences.

5153 Computer 45

Meniscus T2 Relaxation Time in Patients with Varying Degrees of Knee Joint Degeneration

Richard Kijowski[1], Benjamin Beduhn[1], Michael G Fazio[1], and Fang Liu[1]

[1]Department of Radiology, University of Wisconsin-Madison, Madison, WI, United States

This study was performed to investigate changes in meniscus T2 relaxation time at various stages of knee joint degeneration. T2 mapping was performed on the knees of 121 patients with meniscus tears. T2 of the torn and untorn portions of the medial and lateral meniscus were measured. The severity of radiographic osteoarthritis was assessed using the Kellgren-Lawrence (KL) grading scale. There was a significant difference ($p<0.001$) in meniscus T2 between KL0, KL1, and KL2 subjects in both the torn and untorn portions of the meniscus with KL2 subjects having the highest T2 and KL0 subjects having the lowest T2.

5154 Computer 46

Circumferential and Radial Variations in T2, T2* and T1rho in the Osteoarthritic Meniscus

Marianne Susan Black[1], Garry Evan Gold[2], Marc Elliot Levenston[1], and Brian Andrew Hargreaves[2]

[1]Mechanical Engineering, Stanford University, Stanford, CA, United States, [2]Radiology, Stanford University, Palo Alto, CA, United States

The menisci of the knee are important for distributing load at the knee joint, and meniscal damage has been shown to precede cartilage degeneration in the knee. We examined radial and circumferential meniscal variation in T2, T2* and T1rho relaxation times in osteoarthritic menisci. Menisci were divided into 3 circumferential regions (anterior, body, and posterior) and then further into 3 radial regions (inner, middle, and outer). Significant differences were found between circumferential and radial regions for T2, but only between circumferential regions for T2* and T1rho. Changes in meniscal regional variations could be important in tracking osteoarthritis disease progress.

5155 Computer 47

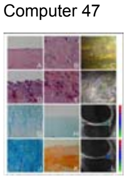

T2-Mapping Relaxation Time Correlates with Histopathological Degree of Degeneration in Meniscal Tissue

Susanne Eijgenraam[1], Frans Bovendeert [1], Yvonne Bastiaansen [2], Duncan Meuffels[2], Jamal Guenoun [1], Stefan Klein[3], Max Reijman[2], and Edwin Oei[1]

[1]Radiology and Nuclear Medicine, Erasmus MC, Rotterdam, Netherlands, [2]Orthopedic Surgery, Erasmus MC, Rotterdam, Netherlands, [3]Medical Informatics, Erasmus MC, Rotterdam, Netherlands

To validate meniscal T2-mapping, which is suggested to detect early meniscal degeneration, T2 relaxation times of ten menisci (five traumatically torn and five degenerative menisci from 10 patients) were compared to histopathology as the gold standard to assess meniscal degeneration. T2 relaxation times were found to correlate well with histopathological degree of degeneration in meniscal tissue ($r_s = 0.64$, $P = 0.001$). Degenerative meniscal tissue was found to exhibit significantly higher T2 relaxation times compared to non-degenerated meniscal tissue (22.7±3.0 ms and 18.2 ±5.1 ms ($P = 0.02$) respectively). Therefore, T2-mapping is a promising quantitative imaging biomarker for meniscal degeneration.

Electronic Poster

Parallel Imaging

Exhibition Hall Wednesday 17:15 - 18:15

5156 Computer 49

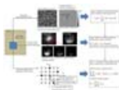

Parallel Imaging Reconstruction from Randomly Undersampled Data with k-space Variant Sparsity Constraints

Yu Y. Li[1,2]

[1]Cardiac Diagnostic Imaging, St. Francis Hospital, Roslyn, NY, United States, [2]Radiology, Cincinnati Children's Hospital Medical Center, Cincinnati, OH, United States

A new parallel imaging reconstruction framework is proposed to accelerate MRI using both coil sensitivity and data sparsity. This framework uses random undersampling and performs parallel imaging reconstruction with a k-space variant constraint. No calibration data are needed. It is demonstrated that this new approach offers a gain over conventional parallel imaging in imaging acceleration.

5157 Computer 50

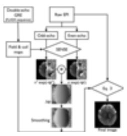

Iterative SENSE with Integrated EPI Nyquist Ghost and Distortion Corrections

Uten Yarach[1,2], Hendrik Mattern[1], and Oliver Speck[1]

[1]Department of Biomedical Magnetic Resonance, Otto-von-Guericke University Magdeburg, Magdeburg, Germany, [2]Department of Radiological Technology, Chiang Mai University, Chaigmai, Thailand

The quality of EPI image is intrinsically hindered by Nyquist ghost and geometric distortion which are commonly handled by a 1D non-phase encoded reference and a field map based corrections, respectively. In some cases, a 2D phase reference is required, but scan time is increased. The geometric-mismatch between EPI and coil sensitivities is another concern. Here, the 2D phase correction (without prolonging scan time) and the distortion correction are integrated into a single forward operator rather than considering them consecutively. The results show that the stable reduction in Nyquist ghosting and distortion can improve the tSNR of EPI time series.

5158 Computer 51

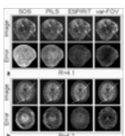

Fast 3D Variable-FOV Reconstruction for Parallel Imaging with Localized Sensitivities

Yigit Baran Can[1], Efe Ilicak[1,2], and Tolga Çukur[1,2,3]

[1]Electrical and Electronics Engineering, Bilkent University, Ankara, Turkey, [2]National Magnetic Resonance Research Center (UMRAM), Bilkent University, Ankara, Turkey, [3]Neuroscience Program, Bilkent University, Ankara, Turkey

Several successful iterative approaches have recently been proposed for parallel-imaging reconstructions of variable-density (VD) acquisitions, but they often induce substantial computational burden for non-Cartesian data. Here we propose a generalized variable-FOV PILS reconstruction 3D VD Cartesian and non-Cartesian data. The proposed method separates k-space into non-intersecting annuli based on sampling density, and sets the 3D reconstruction FOV for each annulus based on the respective sampling density. The variable-FOV method is compared against conventional gridding, PILS, and ESPIRiT reconstructions. Results indicate that the proposed method yields better artifact suppression compared to gridding and PILS, and improves noise conditioning relative to ESPIRiT, enabling fast and high-quality reconstructions of 3D datasets.

5159 Computer 52

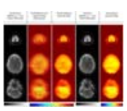

Analytical G-factor Calculation for Slice-GRAPPA with Dual “Even-Odd” Kernels (SG-DK)

Haifeng Wang[1,2], Jonathan R. Polimeni[1,2,3], Berkin Bilgic[1,2], Lawrence L. Wald [1,2,3], and Kawin Setsompop[1,2]

[1]Massachusetts General Hospital, Boston, MA, United States, [2]Harvard Medical School, Boston, MA, United States, [3]Harvard-MIT Division of Health Sciences and Technology, Massachusetts Institute of Technology, Cambridge, MA, United States

Slice-GRAPPA (SG) is often used to reconstruct blipped-CAIPI simultaneous multi-slice EPI data, in particular in conjunction with the dual even-odd kernel approach (SG-DK) to mitigate ghosting related reconstruction artifacts. To achieve good performance in blipped-CAIPI acquisition, the CAIPI shift factor should be optimized in a case by case manner to minimize g-factor penalty. The g-factor is influenced by the reconstruction approach and so far a fast analytical g-factor calculation has been developed only for standard SG reconstruction but not SG-DK, where time-consuming Monte Carlo simulation is still needed. Here we propose an analytical g-factor calculation for SG-DK and demonstrate that the proposed method is fast and accurate. Our simulation and experimental results also highlight the superior performance of SG-DK over SG reconstruction, both in mitigating image artifacts and noise penalty.

5160 Computer 53

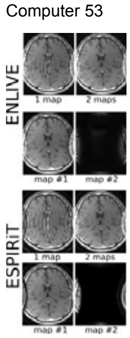

ENLIVE: A Non-Linear Calibrationless Method for Parallel Imaging using a Low-Rank Constraint

H. Christian M. Holme[1,2], Frank Ong[3], Sebastian Rosenzweig[1,2], Robin N. Wilke[1,2], Michael Lustig[3], and Martin Uecker[1,2]

[1]Diagnostic and Interventional Radiology, University Medical Center Göttingen, Göttingen, Germany, [2]partner site Göttingen, DZHK (German Center for Cardiovascular Research), Göttingen, Germany, [3]Electrical Engineering and Computer Sciences, University of California, Berkeley, Berkeley, CA, United States

We propose an extension to Regularized Non-Linear Inversion (NLINV), which simultaneously reconstructs multiple images and sets of coil sensitivity profiles. This method, termed ENLIVE (Extended Non-Linear InVersion inspired by ESPIRiT), can be related to a convex relaxation of the NLINV problem subject to a low-rank constraint. From NLINV, it inherits its suitability for calibrationless and non-Cartesian imaging; from ESPIRiT it inherits robustness to data inconsistencies.

5161 Computer 54

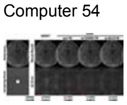

Feature Refinement Scheme for Improved STEP Parallel Imaging Reconstruction

Zechen Zhou[1] and Chun Yuan[2,3]

[1]Philips Research China, Shanghai, People's Republic of China, [2]Vascular Imaging Lab, Department of Radiology, University of Washington, WA, United States, [3]Center for Biomedical Imaging Research, Department of Biomedical Engineering, Tsinghua University, Beijing, People's Republic of China

In this work, we incorporated the Feature Refinement (FR) scheme into the Self-supporting Tailored k-space Estimation for Parallel imaging reconstruction (STEP) image reconstruction framework to enhance its capability for structural representation in image domain, and developed a novel Weber Local Descriptor (WLD) method to improve the extraction of local image boundaries. With the preliminary experiments, it has been demonstrated that the improved STEP with WLD FR scheme can provide more accurate estimation of image details in comparison to original STEP and existing classic method.

5162 Computer 55

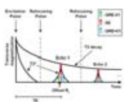

A new pattern for Autocalibrated Parallel Imaging Reconstruction for GRASE: APIR4GRASE

Chaoping Zhang[1], Alexandra Cristobal-Huerta[2], Juan Antonio Hernández-Tamames[2], Stefan Klein[1], and Dirk H.J. Poot[1,2,3]

[1]Departments of Medical Informatics and Radiology, Erasmus MC, Rotterdam, Netherlands, [2]Departments of Radiology and Nuclear Medicine, Erasmus MC, Rotterdam, Netherlands, [3]Imaging Science and Technology, Delft University of Technology, Delft, Netherlands

We propose a subsampled interleaved parallel acquisition pattern for Autocalibrated Parallel Imaging Reconstruction for GRASE (APIR4GRASE) which considers different echoes during each refocusing of the GRASE as if they originated from different coil channels. APIR4GRASE eliminates ghosting artifacts caused by the phase and amplitude modulations in traditional GRASE split sampling pattern and achieves an additional acceleration factor of 1.3 compared to a fully sampled GRASE k-space. In addition, multiple contrast (spin echo and gradient echo) images are reconstructed. Experiments on a phantom demonstrate the effectiveness of our method.

5163 Computer 56

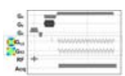

Improved Parallel Imaging with Resilience to Gradient Errors

Gigi Galiana[1] and Nadine Luedicke[2]

[1]Radiology and Biomedical Imaging, Yale University, New Haven, CT, United States, [2]Biomedical Engineering, Yale University, New Haven, CT, United States

FRONSAC encoding, which adds a rapidly oscillating low-amplitude nonlinear gradient to a standard undersampled trajectory based on linear gradients, has been shown to significantly improve k-space coverage and parallel imaging reconstructions. This abstract further shows that a fixed FRONSAC waveform improves image quality for Cartesian trajectories of various FOV and resolution, while avoiding many of the pitfalls of other highly efficient gradient trajectories. Results show that FRONSAC provides better reconstruction than Cartesian encoding alone, while offering better resilience to delays and off-resonance effects than non-Cartesian trajectories, such as spiral.

5164 Computer 57

Accelerated MR cardiac cine using TSPIRiT with generalized data fidelity

Yilong Liu[1,2], Mengye Lyu[1,2], and Ed X. Wu[1,2]

[1]Laboratory of Biomedical Imaging and Signal Processing, The University of Hong Kong, Hong Kong, People's Republic of China, [2]Department of Electrical and Electronic Engineering, The University of Hong Kong, Hong Kong, People's Republic of China

MR cardiac cine plays a key role in quantifying the cardiac function. The measurement accuracy is highly dependent of both spatial and temporal resolution, which can be improved substantially by acceleration with parallel imaging. SPIRiT, a GRAPPA-like parallel imaging reconstruction, can be applied to cardiac cine by incorporating temporal sensitivity estimation (TSPIRiT). In this study, we propose to enhance MR cardiac cine using TSPIRiT with generalized data fidelity (GDF) based on the assumption that k-space signal in cardiac cine changes smoothly. Results show that the proposed method can provide better tradeoff between SNR and temporal resolution when compared with TSPIRiT and k-t SPIRiT.

5165 Computer 58

Improved SPIRiT Operator for Joint Reconstruction of Multiple T2-weighted Images

Toygan Kilic[1,2], Efe Ilicak[1,2], Tolga Çukur[1,2], and Emine Ulku Saritas[1,2]

[1]Electrical and Electronics Engineering, Bilkent University, Ankara, Turkey, [2]National Magnetic Resonance Research Center, Bilkent University, Ankara, Turkey

Recently, compressed-sensing (CS) was proposed to jointly reconstruct undersampled multi-contrast datasets to exploit the common structural features therein. Here, we propose a method to improve joint reconstruction of multi-contrast acquisitions. Inspired by the SPIRiT framework for parallel imaging, our method linearly synthesizes missing data for each contrast from neighboring k-space data for all contrasts. To improve reconstruction quality, the proposed method high-pass filters calibration data to emphasize the weight of intermediate spatial frequencies in the interpolation operator. Phantom and in vivo results at 3T indicate that the proposed method outperforms reconstructions with conventionally estimated interpolators.

5166 Computer 59

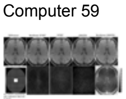

Nonlinear SPIRiT using a second order virtual coil for improved parallel imaging reconstruction

Sen Jia[1], Yanjie Zhu[1], Lei Zhang[1], Yiu-cho Chung[1], Jing Cheng[1], Leslie Ying[2], Xin Liu[1], Hairong Zheng[1], and Dong Liang[1]

[1]Shenzhen Institutes of Advanced Technology, Shenzhen, People's Republic of China, [2]The state University of New York (SUNY) at Buffalo, United States

The nonlinear relationship between missing and acquired data in k-space has been proved in nonlinear GRAPPA. In this work, we propose nonlinear SPIRiT which integrates the polynomial kernel method into SPIRiT via a simple second-order virtual coil approach. The proposed method represents the relationship between missing and acquired data in k-space of SPIRiT using a more accurate nonlinear model. In vivo results demonstrated that nonlinear SPIRiT could suppress aliasing artifact or noise better than SPIRiT, and was applicable to more acceleration scenarios than nonlinear GRAPPA.

5167 Computer 60

Impact of FLASH based autocalibration scans on high-resolution GRAPPA accelerated EPI at 7T

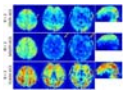

Joelle E Sarlls[1] and S. Lalith Talagala[1]

[1]*NINDS/NMRF, National Institutes of Health, Bethesda, MD, United States*

It has been shown that the temporal SNR (tSNR) of GRAPPA EPI can be improved by using different autocalibration scan (ACS) acquisitions. We evaluated the impact of using FLASH-ACS for high resolution, GRAPPA accelerated EPI at 7T. We compared the tSNR, ghost levels and distortions characteristics of EPI data reconstructed using SSEPI, MSEPI and FLASH based ACS at different acceleration factors and resolutions. Results showed that the tSNR of GRAPPA accelerated EPI improved by 60-100% when using FLASH-ACS data during image reconstruction. FLASH-ACS reconstructions also had less residual EPI ghost and identical image distortions compared to SSEPI-ACS and MSEPI-ACS.

5168 Computer 61

Accelerating T2* Mapping with Maximum Likelihood Estimation (MLE) and Parallel Imaging (PI)

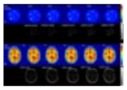

Wajiha Bano[1,2], Arnold Julian Vinoj Benjamin[1,2], Ian Marshall[2], and Mike Davies[1]

[1]*Institute for Digital Communication, University of Edinburgh, Edinburgh, United Kingdom,* [2]*Centre for Clinical Brain Sciences, University of Edinburgh, Edinburgh, United Kingdom*

The utility of MR parametric mapping is limited due to the lengthy acquisition time. A Maximum Likelihood Estimation (MLE) and Parallel Imaging (PI) method is presented for MR parameteric mapping. The approach is based on a high Signal to Noise ratio (SNR) assumption such that the noise can be modelled as Gaussian and estimates the parameters that maximizes the signal from a multichannel coil. The method was tested on a multi-echo gradient-echo T2* mapping experiment in a phantom and a human brain. Accurate T2* maps were reconstructed up to an acceleration factor of 6 with a small error for phantom and human brain.

5169 Computer 62

A Novel Method to Increase SNR of GRAPPA Reconstruction

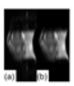

Yu Ding[1], Renjie He[1], Qi Liu[1], Renkuan Zhai[2], Guobin Li[2], Jian Xu[1], and Weiguo Zhang[2]

[1]*UIH America, Inc., Houston, TX, United States,* [2]*Shanghai United Imaging Healthcare Co., Ltd, Shanghai, People's Republic of China*

We propose a novel method to improve GRAPPA reconstruction when blood vessel pulsation artifacts appear. It removes the artifacts in the ACS lines, and boosts the SNR of GRAPPA reconstruction. Volunteer study confirmed that the proposed method improved image quality of GRAPPA reconstruction in 3T FSE knee scan.

5170 Computer 63

SPID Compressed Sensing for Parallel MRI: Flexible Sampling and Rapid Reconstruction

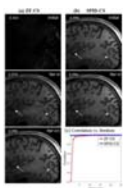

Efrat Shimron[1], Andrew G. Webb[2], and Haim Azhari[1]

[1]*Biomedical Engineering Department, Technion - Israel Institute of Technology, Haifa, Israel,* [2]*C.J. Gorter Center for High Field MRI Research, Department of Radiology, Leiden University, Leiden, TN, Netherlands*

We introduce a new method combining Compressed Sensing (CS) and parallel MRI (pMRI) for fast MRI acquisition. The method, termed SPID-CS, is advantageous over existing methods since it (1) produces a high-quality initial reconstruction, (2) avoids aliasing related to sub-Nyquist sampling by joining information from different coils, (3) enables flexible k-space sampling, (4) converges much faster than conventional CS and (5) enables clinical real-time reconstruction due to its extremely short runtime.

5171 Computer 64

Alias-reduced multicoil single-shot spatial temporally encoded MRI with referenceless sensitivity encoding

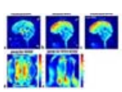

Ying Chen[1], Lisha Yuan[1], Yi Sun[2], and Jianhui Zhong[1]

[1]*Center for Brain Imaging Science and Technology, Zhejiang University, Hangzhou, People's Republic of China,* [2]*MR Collaboration Northeast Asia, Siemens Healthcare, Shanghai, People's Republic of China*

Single-shot spatiotemporally encoded (SPEN) MRI is a novel fast imaging scheme with remarkably reduced geometric distortions at high field compared to conventional single-shot EPI. The k-space along SPEN dimension is undersampled, resulting in aliases at regions of rapid profile variation. The feasibility of utilizing sensitivity profiles of array receiver coils to unravel the undersampling aliases is investigated. High resolution relative sensitivity profiles can be obtained from multicoil 2D polynomial fitting of the SPEN reconstructed images without additional reference scans. The effectiveness of the SPEN SENSE strategy is validated by healthy human brain scans at 3T.

5172 Computer 65

Enhancing resolution in single-shot MRI by SUper-resolved SPEN with SENSE (SUSPENSE)

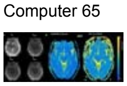

Gilad Liberman[1], Eddy Solomon[1], Michael Lustig[2], and Lucio Frydman[1]

[1]*Chemical Physics, Weizmann Institute of Science, Rehovot, Israel,* [2]*Department of Electrical Engineering and Computer Sciences, Berkeley, CA*

Spatio-temporal encoding (SPEN) delivers single-scan images with increased robustness to shift and susceptibility artifacts. These acquisitions are usually carried out in a “hybrid” mode that prevents a sufficiently dense sampling along the SPEN domain. Alleviating this resolution loss had so far demanded the acquisition of multiple interleaved scans. The present study demonstrates that by relying on multiple sensors, a similar resolution enhancement can be achieved in a single shot. The principles and potential of the ensuing Super-resolved SPEN with SENSE (SUSPENSE) is demonstrated, with sub-mm single-shot 3T image acquisitions on phantoms and humans.

5173 Computer 66

Spiral SENSE MP-RAGE using long readouts and an expanded signal model

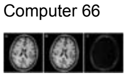

Franciszek Hennel[1], Maria Engel[1], Lars Kasper[1], Bertram Wilm[1], and Klaas P Pruessmann[1]

[1]Institute for Biomedical Engineering, ETH and University of Zurich, Zurich, Switzerland

Spiral readout was used to accelerate the standard T1-weighted 3D head scan based on MPRAGE at 3 Tesla without any compromise on images quality. The encoding model used by the reconstruction included the static magnetic field map as well as the k-space trajectory and a dynamic field correction provided by a field camera. The study demonstrates the utility of state-of-the-art spiral scanning for routine MRI applications.

5174 Computer 67

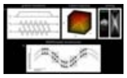

GRAPPA Reconstructed Wave-CAIPI MPRAGE at 7 Tesla

Jolanda Melissa Schwarz[1], Daniel Brenner[1], Eberhard Daniel Pracht[1], and Tony Stoecker[1]

[1]German Center for Neurodegenerative Diseases (DZNE), Bonn, Germany

In this work, a GRAPPA-based reconstruction for wave-CAIPI acquisitions is presented. 16-fold accelerated full brain MPRAGE images with 1 mm isotropic resolution and high image quality are measured in 45 seconds and a clear improvement compared to Cartesian CAIPIRINHA sampling can be observed. It is demonstrated that optimization of the gradient waveforms further improves image quality.

5175 Computer 68

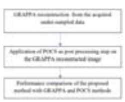

Combined Application of GRAPPA and POCS for Fast MR Image Reconstruction

Hassan Shahzad[1,2] and Hammad Omer[3]

[1]Electrical Engineering, COMSATS Institute Of IT, Rawalpindi, Pakistan, [2]National Center for Physics, Islamabad, Pakistan, [3]COMSATS Institute Of IT, Islamabad, Pakistan

The proposed work presents a combination of GRAPPA and Compressed sensing (POCS) to reconstruct MR images from the highly under-sampled data. Firstly, GRAPPA is applied to the acquired under-sampled data. The output of GRAPPA which contains aliasing artifacts (especially for high acceleration factors) is fed in to POCS which solves for the solution image iteratively and produces a reconstructed image with minimal aliasing artifacts. The reconstruction results are compared with GRAPPA and POCS separately. The results show that the proposed method significantly reduces the aliasing artifacts as compared to GRAPPA or POCS reconstructions.

5176 Computer 69

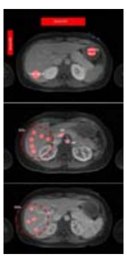

Influence of temporal resolution on liver perfusion using golden-angle radial sparse parallel MRI

Nikolaos S Kallistis[1], Kai Tobias Block[2], Robert Grimm[3], Hersh Chandarana[2], Ian Rowe[1], and Steven P Sourbron[4]

[1]Leeds Institute of Biomedical and Clinical Sciences, University of Leeds, Leeds, United Kingdom, [2]School of Medicine, New York University, New York, NY, United States, [3]Siemens AG Healthcare MR, Erlangen, Germany, [4]Leeds Institute of Cardiovascular and Metabolic Medicine, University of Leeds, Leeds, United Kingdom

Golden-angle radial sparse parallell (GRASP) MRI uses temporal regularization in the reconstruction, which risks distorting temporal profiles and reducing DCE-MRI parameter accuracy and precision. The aim of this study is to investigate this issue for liver DCE-MRI by measuring kinetic parameters on data reconstructed at variable temporal resolution. The results depend on temporal resolution according to well-known patterns also observed in simulations and fully sampled data. A systematic error remains at the highest temporal resolution, but this is more likely due to well-known issues of signal saturation. Image reconstruction at lower temporal resolution risks degrading diagnostic image quality due to the mixing of images with different contrast. We conclude that: (1) temporal regularization in GRASP is unlikely to induce significant error in kinetic parameters; (2) images should be reconstructed at high temporal resolution around 2-4s.

5177 Computer 70

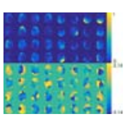

Absolute B1- estimation without a homogeneous receive coil

Olivia W Stanley[1,2], Ravi S Menon[1,2], and L Martyn Klassen[2]

[1]Department of Medical Biophysics, The University of Western Ontario, London, ON, Canada, [2]Centre for Functional and Metabolic Mapping, The University of Western Ontario, London, ON, Canada

Fitting the relative B_1^- maps derived from a B_1^+ shim acquisition to the Helmholtz equations allows for the calculation of absolute B_1^- maps. The sensitivity profiles can then be used to optimally combine coils in subsequent acquisitions. In addition, absolute B_1^- maps allow for the removal of the receive sensitivity from the combined images. This was validated in a GE-EPI sequence and found to produce images with lower phase standard deviation and increased temporal signal-to-noise ratios across the brain. Both of these differences were found to be statistically significant in a Student's t-test.

5178 Computer 71

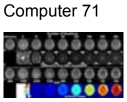

The Signal-to-Noise Behavior of 3D SPIRiT Image Reconstruction

Yulin V Chang[1], Marta Vidorreta[2], and John Detre[2]

[1]National Institutes of Health, Bethesda, MD, United States, [2]Neurology, University of Pennsylvania, Philadelphia, PA, United States

Self-consistent parallel imaging (SPIRiT) is a self-calibrated, iterative parallel imaging technique that is not restricted by a particular k-space sampling pattern. 3D SPIRiT takes advantage of the 3D arrangement of a modern receive array to further improve image quality. Although SPIRiT was shown to yield higher image quality than does GRAPPA, especially at acceleration factors higher than 2, its signal-to-noise behavior has not been rigorously studied. In this study we investigate the image quality behavior of 3D SPIRiT and determine the optimal condition for best image quality.

5179 Computer 72

Intracranial artery vessel wall reconstruction via feature refinement

Jing Cheng[1], Sen Jia[1], Lei Zhang[1], Yanjie Zhu[1], Yuanyuan Liu[1], Leslie Ying[2], Xin Liu[1], Hairong Zheng[1], and Dong Liang[1]

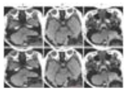

[1]Shenzhen Institutes of Advanced Technology,Chinese Academy of Sciences, Shenzhen, People's Republic of China, [2]Department of Electrical Engineering, The State University of New York (SUNY) at Buffalo, NY, United States

Depicting the vessel wall of intracranial arteries at high resolution and contrast is important to evaluate the intracranial artery disease. This paper propose a feature refinement strategy for improving the reconstruction quality of intracranial artery vessel wall by incorporating the feature descriptor into the reconstruction framework of L1-SPIRiT. Results on in vivo MR data have shown that the feature refinement method is capable of reconstructing the vessel wall with higher contrast than the method without feature refinement, and thus presents great potential for MR vessel wall imaging.

Electronic Poster

Fat+Water Imaging

Exhibition Hall — Wednesday 17:15 - 18:15

5180 — Computer 73

A novel method for Rapid 3D fat and water decomposition using a GlObally Optimal multi-surface Estimation (R-GOOSE)

Chen Cui[1], Abhay Shah[1], Xiaodong Wu[1], Dan Thedens [2], and Mathews Jacob[1]

[1]Electrical and Computer Engineering, University of Iowa, Iowa City, IA, United States, [2]Radiology, University of Iowa, Iowa City, IA, United States

A 3D Rapid, GlObally Optimal Surface Estimation (R-GOOSE) algorithm for fat-water decomposition in MRI is proposed. The fat-water separation is formulated as an optimization problem with data consistency and field-map smoothness penalty. The data consistency only contains exact minimizers from the fully discretized field-map value volume. The proposed method employs a connectivity-reduced graph construction that enables the new formulation to be solved efficiently. The method is validated by the 17 datasets from the 2012 ISMRM Challenge with thirty-fold computational gain compared to our previous method GOOSE while the high quantitative accuracy is maintained. Fat fraction maps obtained from the proposed method also provides a good marker for degenerative muscle diseases in newly collected lower limb datasets.

5181 — Computer 74

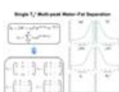

A Generalized Formulation for Parameter Estimation in MR Signals of Multiple Chemical Species

Maximilian Nikolaus Diefenbach[1], Stefan Ruschke[2], and Dimitrios C Karampinos[2]

[1]Department of Diagnostic and Interventional Radiology, TUM Technical University of Munich, Munich, Germany, [2]Department of Diagnostic and Interventional Radiology, Technical University of Munich, Munich, Germany

The purpose of this work is to develop a generalized formulation to study the parameter estimation of complex MR signals and its multi-species components.

5182 — Computer 75

Fat tissue mimics for validation of magnetic resonance thermometry

Slavka Carnicka[1], Kathryn Keenan[1], Elizabeth Mirowski[2], Mark Brown[3], Christopher Suiter[4], Tara Fortin[4], Hannah Erdevig[1], Karl Stupic[1], and Stephen Russek[1]

[1]Physical Measurement Laboratory, National Institute of Standards and Technology, Boulder, CO, United States, [2]High Precision Devices Inc., Boulder, CO, United States, [3]Department of Radiology, University of Colorado School of Medicine, Denver, CO, United States, [4]Applied Chemicals and Materials Division, National Institute of Standards and Technology, Boulder, CO, United States

Phase-based magnetic resonance thermometry is used for monitoring minimally invasive ablation therapies like focused ultrasound therapy. MRT is prone to errors when applied in tissues with high fat content (e.g. breast tissue, fatty liver) due to heat-induced susceptibility changes. Therefore, there is a need for developing well characterized adipose tissue mimics that could serve as standards for validation of MRT techniques. In this study we showed that all measured adipose tissue mimics are representative of human adipose tissue with similar chemical spectra and thermal dependence of susceptibility shift and are reproducible standards for human adipose tissue validation MRI techniques.

5183 — Computer 76

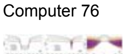

Spectrally selective spin-lock for fat-water imaging and simultaneous T1rho quantification

Weitian Chen[1]

[1]Imaging and Interventional Radiology, The Chinese University of Hong Kong, New Territory, Hong Kong

In conventional T1rho imaging, the fat signal is usually suppressed to avoid image artifacts and quantification errors. It is desirable to acquire both water and fat images for certain diseases. In this work, we present an approach to use spectrally selective spin-lock pulses to achieve T1rho quantification with simultaneous fat-water imaging. The theoretical analysis is provided with proof on numerical phantoms.

5184 — Computer 77

Fat Suppressed Highly Accelerated Dynamic Imaging utilizing View Sharing, Compressed Sensing and Parallel Imaging

Naoyuki Takei[1], Kang Wang[2], Lloyd Estkowski[3], Ken Arai[4], Mitsuhiro Bekku[4], Hiroyuki Kabasawa[1], and Ersin Bayram[5]

[1]Global MR Applications & Workflow, GE Healthcare, Hino, Tokyo, Japan, [2]Global MR Applications & Workflow, GE Healthcare, Madison, WI, United States, [3]Global MR Applications & Workflow, GE Healthcare, Menlo Park, CA, United States, [4]MR Engineering, GE Healthcare, Hino, Tokyo, Japan, [5]Global MR Applications & Workflow, GE Healthcare, Houston, TX, United States

DISCO (Differential Subsampling with Cartesian Ordering) is high spatial-temporal imaging technique with Dixon based fat suppression for 3D volumetric Abdominal imaging. We developed DISCO with frequency selective presaturation pulse for fat suppression (FatSAT) called FatSAT DISCO. The feasibility study explores the computational advantage of FatSAT DISCO in accelerating scan time with compressed sensing technique and demonstrated that it is a promising technique for achieving faster imaging for 4D dynamic MR imaging with robustness to image artifact and light computation demand for clinical use.

5185 Computer 78

Classification of White and Brown Adipose Tissue using a Support Vector Machine

Brandon Campbell[1,2], Gregory Simchick[1,2], Hang Yin[3], and Qun Zhao[1,2]

[1]Physics and Astronomy, University of Georgia, Athens, GA, United States, [2]Bio-Imaging Research Center, University of Georgia, Athens, GA, United States, [3]Biochemistry and Molecular Biology, University of Georgia, Athens, GA, United States

Determining the volume and distribution of white adipose tissue (WAT) and brown adipose tissue (BAT) by magnetic resonance imaging (MRI) is clinically important. Previous WAT and BAT classification has relied on using fat fraction and proton relaxation time via fixed multi-peak spectroscopic models. However, the recently proposed Multi-Varying-Peak MR Spectroscopy (MVP-MRS) model allows for the selection of appropriate classification features for differentiation between WAT and BAT. Furthermore, these multi-peak features allow prediction of a 'browning' or 'beigeing' process of WAT by using a Support Vector Machine (SVM) learning algorithm.

5186 Computer 79

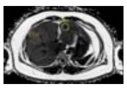

Quantitative Liver Fat Measurements in Obese Adolescents: Comparison between using MR Spectroscopy and Chemical-shift Water-fat Fat-fraction Techniques

Steve Cheuk Ngai Hui[1], David Ka Wai Yeung[1], and Winnie Chiu Wing Chu[1]

[1]Department of Imaging and Interventional Radiology, The Chinese University of Hong Kong, Hong Kong, Hong Kong

Liver fat contents measured by magnetic resonance spectroscopy and chemical-shift water-fat separation imaging were compared in a group of obese adolescents. Distribution of fat in left and right liver lobes was also compared. Results demonstrated that fat contents obtained from both MR modalities were highly correlated and agreed to each other. In obese adolescents with non-alcoholic fatty liver disease, fat distribution was non-uniform between left and right lobes. This study supports the use of fat-fraction map to measure liver fat, which can shorten the scanning time by acquiring information about body adipose tissue and liver fat within a single sequence.

5187 Computer 80

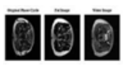

In-Vivo Fat Water Separation with Multiple-Acquisition bSSFP

Michael Anthony Mendoza[1], Joseph Valentine[2], and Neal Bangerter[3]

[1]Electrical Engineering, Brigham Young University, North Ogden, UT, United States, [2]Electrical Engineering, Brigham Young University, provo, UT, United States, [3]Electrical Engineering, Brigham Young University, Provo, UT, United States

In this work, we present a novel technique that combines the advantages of bSSFP with Dixon reconstruction in order to produce robust water fat decomposition with high SNR in a short imaging time, while simultaneously reducing banding artifacts that traditionally degrade image quality.

5188 Computer 81

Water and fat separation using a Gauss-Newton Trust-Region based algorithm

Carlos Sing-Long[1,2], Cristobal Arrieta[3,4], Curtis N Wiens[5], Diego Hernando[5,6], and Sergio Uribe[4,7]

[1]Institute for Biological and Medical Engineering, Schools of Engineering, Medicine and Biological Sciences, Pontificia Universidad Catolica de Chile, Santiago, Chile, [2]Biomedical Imaging Center, Pontificia Universidad Catolica de Chile, [3]Electrical Engeneering Department, Pontificia Universidad Catolica de Chile, Santiago, Chile, [4]Biomedical Imaging Center, Pontificia Universidad Catolica de Chile, Santiago, Chile, [5]Radiology, University of Wisconsin, Madison, WI, United States, [6]Medical Physics, University of Wisconsin, Madison, WI, United States, [7]Radiology Department, School of Medicine, Pontificia Universidad Catolica de Chile, Santiago, Chile

We propose an algorithm based on a Gauss-Newton Trust-Region algorithm that estimates the field map and water and fat concentrations in two steps for all pixels at once. The results are comparable to those obtained with the state-of-art methods.

5189 Computer 82

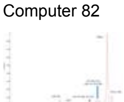

Using a general model or measuring the intramuscular lipid spectrum: impact on the fat infiltration quantification in skeletal muscle

Noura Azzabou[1,2], Harmen Reyngoudt[1,2], and Pierre G. Carlier[1,2]

[1]NMR Laboratory, Institute of Myology, Paris, France, [2]CEA, DRF, I²BM, MIRCen, Paris, France

The purpose of this work was to study the impact of fat model on the quantification of fatty infiltration in skeletal muscle. To this end, we acquired multi-echo 1H-NMRS from 23 subjects affected by an inflammatory myopathy and measured the lipid spectrum of each subject. We also acquired 3D gradient echo volumes at different TEs. Fat and water maps were reconstructed in two cases: (i) with a unique mean fat model (ii) with a fat model specific to each subject. The results of comparison showed a good agreement between both methods and the difference never exceeded 4%.

5190 Computer 83

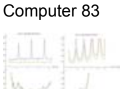

How accurately can fat be quantified? A Bayesian View

Xiaoqi Wang[1], Li Xu[2], and Xiaoguang Cheng[2]

[1]Philips Healthcare, Beijing, People's Republic of China, [2]Department of Radiology, Beijing Jishuitan Hospital

An error analysis was carried, under frame work of Bayesian probability theory, for fat quantification using multiple gradient echo sequences to separate water and fat content in MRI signal. The results confirm that this method is accurate when protocols are carefully designed; this analysis also provides guideline in designing parameter settings to achieve optimal accuracy in fat quantification measurements.

5191 Computer 84

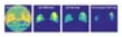

Accurate and reliable fat-water MRI breast density measurements

Jie Ding[1], Patricia A Thompson[2,3], Yi Gao[4,5], Marilyn T Marron[6], Betsy C Wertheim[6], Maria I Altbach[6,7], Jean-Philippe Galons[6,7], Denise J Roe[6,8], Fang Wang[9], Gertraud Maskarinec[10], Cynthia A Thomson[6], Alison Stopeck[3,11], and Chuan Huang[1,5,12,13]

[1]Biomedical Engineering, Stony Brook University, Stony Brook, NY, United States, [2]Pathology, Stony Brook Medicine, Stony Brook, NY, United States, [3]Cancer Center, Stony Brook Medicine, Stony Brook, NY, United States, [4]Biomedical Informatics, Stony Brook Medicine, Stony Brook, NY, United States, [5]Computer Science, Stony Brook University, Stony Brook, NY, United States, [6]Cancer Center, University of Arizona, Tucson, AZ, United States, [7]Medical Imaging, University of Arizona, Tucson, AZ, United States, [8]Epidemiology and Biostatistics, University of Arizona, Tucson, AZ, United States, [9]Stony Brook Medicine, Stony Brook, NY, United States, [10]Cancer Center, University of Hawaii at Manoa, Honolulu, HI, United States, [11]Hematology and Oncology, Stony Brook Medicine, Stony Brook, NY, United States, [12]Radiology, Stony Brook Medicine, Stony Brook, NY, United States, [13]Psychiatry, Stony Brook Medicine, Stony Brook, NY, United States

Breast density (BD) is a risk factor for breast cancer, which makes the accurate measurement of BD a priority. Mammography is most widely used for BD determination (MG-BD) but ionizing radiation prohibits its use. BD derived from fat-water decomposition MRI (FWMRI-BD) has been proposed. Here we developed an optimized FWMRI-BD measurement (FraG+W) and compared it to MG-BD and a previous FWMRI-BD measurement (Fra80/90). Both FWMRI-BD measures were strongly correlated with MG-BD and exhibited superior test-retest reliability. The proposed automated FraG+W, which quantifies the entire fibroglandular and water content of the breast, is more accurate and reliable than the previous Fra80/90.

5192 Computer 85

A new Phase Unwrapping Method Based on Wraps Identification and Local Surface Fitting for Water-Fat Separation

Junying Cheng[1,2], Yingjie Mei[2,3], Biaoshui Liu[2], Xiaoyun Liu[1], Wufan Chen[1,2], and Yanqiu Feng[2]

[1]School of Automation Engineering, University of Electronic Science and Technology of China, Chengdu, People's Republic of China, [2]School of Biomedical Engineering and Guangdong Provincial Key Laboratory of Medical Image Processing, Southern Medical University, Guangzhou, People's Republic of China, [3]Philips Healthcare, Guangzhou, People's Republic of China

The phase information is widely used, for example water-fat separation, susceptibility imaging, etc. The phase-unwrapping methods are generally needed to estimate the underlying true phase from the principal period (-π, π]. While current phase-unwrapping methods are affected by noise, rapid phase change and disconnected regions. This paper presents an algorithm combined a wrapping identification scheme by thresholding the difference map between the local variations between phasor and wrapped phase, with the local polynominal surface fitting to merge the disconnected components and estimate the phase value of residual pixels in quality guidance region-growing way. The results demonstrate the proposed method provides an accurate and reliable unwrapped results and has potential application to phase-related MRI in practice.

5193 Computer 86

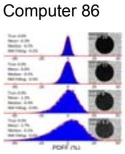

Noise Properties of Proton Density Fat Fraction Estimated using Chemical Shift Encoded MRI

Nathan T Roberts[1,2], Diego Hernando[1,3], James H Holmes[1], Curtis N Wiens[1], and Scott B Reeder[1,3,4,5,6]

[1]Radiology, University of Wisconsin - Madison, Madison, WI, United States, [2]Electrical & Computer Engineering, University of Wisconsin - Madison, Madison, WI, United States, [3]Medical Physics, University of Wisconsin - Madison, Madison, WI, United States, [4]Medicine, University of Wisconsin - Madison, Madison, WI, United States, [5]Emergency Medicine, University of Wisconsin - Madison, Madison, WI, United States, [6]Biomedical Engineering, University of Wisconsin - Madison, Madison, WI, United States

The purpose of this work was to characterize the noise distribution of proton density fat fraction estimation and provide alternatives to averaging for unbiased estimation. Monte-Carlo simulations and phantom experiments were used to validate the theoretically derived noise distribution. Results demonstrated that at low SNR, median and Nelder-Mead fitting algorithm estimators have reduced bias compared to the mean estimator.

5194 Computer 87

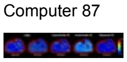

Muscular fat fraction using high-resolution imaging – comparison of three T2-based methods and chemical shift-encoded imaging

Lena Trinh[1], Pernilla Peterson[1], Emelie Lind[1], Lars E Olsson[1], and Sven Månsson[1]

[1]Medical Radiation Physics, Department of Translational Medicine, Lund University, Skåne University Hospital, Malmö, Sweden

The most common method for fat-water separation nowadays is chemical shift-encoded imaging (CSEI). However, when studying fat accumulation in skeletal muscles and high spatial resolution fat fraction (FF) images are desired, CSEI might be challenging due to the increased inter-echo spacing. Here, three alternative methods based on T2-relaxation times, have been explored and compared to CSEI by calculating the muscular fat fraction of ten healthy volunteers. All T2-based methods resulted in qualitatively improved high-resolution FF images compared to CSEI, while a 2-parameter non-linear least square fit showed best quantitative agreement to low resolution CSEI.

5195 Computer 88

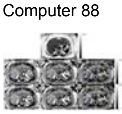

Improving the Noise Propagation Behavior of Different Fatty Acid Quantification Techniques using Spectral Denoising

Manuel Schneider[1], Felix Lugauer[1], Dominik Nickel[2], Brian M Dale[3], Berthold Kiefer[2], Andreas Maier[1], and Mustafa R Bashir[4,5]

[1]Pattern Recognition Lab, Department of Computer Science, Friedrich-Alexander-Universität Erlangen-Nürnberg, Erlangen, Germany, [2]MR Applications Predevelopment, Siemens Healthcare GmbH, Erlangen, Germany, [3]MR R&D Collaborations, Siemens Healthcare, Cary, NC, United States, [4]Radiology, Duke University Medical Center, Durham, NC, United States, [5]Center for Advanced Magnetic Resonance Development, Duke University Medical Center, Durham, NC, United States

MRI is not only capable of quantifying the fat content, but also the fatty acid composition of human adipose tissue. Especially for low fat fractions, fatty acid quantification is sensitive to image noise. Including prior information or additional parameter approximations into the quantification method helped to improve the noise propagation behavior, but also introduced a systematic bias. Performing spectral denoising in between image reconstruction and fatty acid quantification kept the systematic bias as well as the noise in the parameter maps low, and hence allows for more flexible protocol selection and shorter acquisition times.

5196 Computer 89

Hydration imaging of skeletal muscle tissue based on fat referenced water-fat separated MRI

Thobias Romu[1,2], Patrik Tunón[3], Fredrik Uhlin [4,5,6], Micael Gylling[4], Mårten Segelmark[4,6], Anders Fernström[4,6], and Olof Dahlqvist Leinhard[2,6]

[1]Department of Biomedical Engineering, Linköping University, Linköping, Sweden, [2]Center for Medical Image Science and Visualization (CMIV), Linköping University, Linköping, Sweden, [3]Advanced MR Analytics AB, Linköping, Sweden, [4]Department of Nephrology, Region Östergötland, Sweden, [5]Biomedical Engineering, Tallinn University of Technology, Estonia, [6]Department of Medical and Health Sciences, Linköping University, Sweden

This work introduces a signal model for imaging of the local hydration of lean tissue, based on water-fat separated MRI. The signal model is calibrated on a healthy cohort and then evaluated on a cohort of hemodialysis patients.

5197 Computer 90

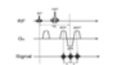

Flexible spin echo triple echo Dixon (flexible STED) for fat suppressed T1-weighted imaging

Jong Bum Son[1], Colleen Costelloe[1], Ken-Pin Hwang[1], Tao Zhang[2], Ersin Bayram[2], John Hazle[1], and Jingfei Ma[1]

[1]The University of Texas MD Anderson Cancer Center, Houston, TX, United States, [2]GE Healthcare, WI, United States

The conventional spin-echo (SE) sequence produces the best available T1-contrast and is often used for imaging of brain, head and neck, and spine. Unfortunately, the inclusion of fat suppression pulses in an SE acquisition substantially reduces the number of slices per TR and therefore the overall scan efficiency. In this work, we developed a flexible spin-echo triple-echo Dixon (flexible STED) technique that enables SE Dixon imaging with high efficiency. The feasibility of the technique is demonstrated with in vivo post-contrast fat-suppressed T1-weighted imaging of spine.

5198 Computer 91

MRI Quantification of Liver Proton Density Fat Fraction during Free Breathing using a Motion-Insensitive Single-Shot 2D Technique

B. Dustin Pooler[1], Jeannine A. Ruby[1], Diego Hernando[1], Ann Shimakawa[2], and Scott B. Reeder[1]

[1]University of Wisconsin, Madison, WI, United States, [2]GE Healthcare, Waukesha, WI, United States

Chemical shift encoded (CSE-MRI) techniques have been previously validated for the measurement of liver proton density fat fraction (PDFF), which serves as a biomarker for liver fat content. However, current CSE-MRI techniques rely upon 3D volumetric or 2D interleaved acquisitions, both of which are sensitive to motion and require the patient to suspend respiration. In this study, we demonstrate the feasibility of a "single shot" 2D sequential CSE-MRI technique to freeze motion. 2D sequential CSE-MRI demonstrates superior performance during free breathing when compared to 3D and 2D interleaved acquisitions.

5199 Computer 92

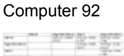

Measurement of spleen fat on MRI-proton density fat fraction arises from reconstruction of noise

Cheng William Hong[1], Gavin Hamilton[1], Catherine Hooker[1], Charlie C Park[1], Calvin Andrew Tran[1], Jeffrey Schwimmer[2], Scott B Reeder[3], and Claude B Sirlin[1]

[1]Liver Imaging Group, Department of Radiology, University of California, San Diego, San Diego, CA, United States, [2]Department of Pediatrics, Division of Pediatric Gastroenterology, Rady Children's Hospital, San Diego, CA, United States, [3]Departments of Radiology, Medical Physics, Biomedical Engineering, Medicine, and Emergency Medicine, University of Wisconsin, Madison, Madison, WI, United States

Non-zero proton density fat fraction (PDFF) is commonly observed in the spleen on chemical-shift-encoded MRI. A prospective assessment in 42 research subjects with no visible fat peaks on MR spectroscopy demonstrated small amounts of splenic fat (PDFF up to 4%) using four different MRI-based fat fraction estimation techniques. These measurements were poorly correlated with each other, implying that fat measurements in spleen are likely artifactual rather than representing true splenic fat.

5200 Computer 93

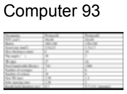

Comparison of MRI techniques for hepatic fat and iron quantification in the UK Biobank study

Chloe Hutton[1], Michael Gyngell[1], Matteo Milanesi[1], and Michael Brady[1]

[1]Perspectum Diagnostics, Oxford, United Kingdom

We compared standard Dixon and T2* relaxometry with “IDEAL” for measuring liver proton density fat fraction (PDFF) and T2*, surrogate metrics for steatosis and iron burden respectively. Results in 118 UK Biobank study participants showed very good correlation between the two methods. Dixon PDFFs were consistently lower than IDEAL PDFFs, explained by the 20° flip angle used for Dixon, introducing a T1 bias and deviation from true PDFF values. Results also showed improved image quality for IDEAL, highlighting the strength of this technique to serve as a reliable and simultaneous biomarker of liver fat and iron overload.

5201 Computer 94

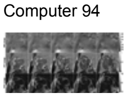

Quantitative Cardiac B0, Fat Fraction, and R2* Mapping using Pre-Channel-Combination Phase Processing

Zahra Hosseini[1,2], Junmin Liu[2], and Maria Drangova[1,2,3]

[1]Biomedical Engineering Graduate Program, University of Western Ontario, London, ON, Canada, [2]Imaging Research Laboratories, Robarts Research Institute, London, ON, Canada, [3]Department of Medical Biophysics, University of Western Ontario, London, ON, Canada

Multi-echo gradient echo MR imaging enables the generation of quantitative B_0, fat fraction and R_2* maps, from which tissue can be characterized. When applied to cardiac imaging these methods face the challenge presented due to the large susceptibility differences between lung and heart. We present a novel post-processing pipeline for multi-echo GRE phase images that processes the phase data prior to channel combination to enable generation of robust quantitative cardiac maps enabling accurate tissue visualization and characterization.

5202 Computer 95

Biased Fuzzy C means based intensity inhomogeneity correction for segmentation of abdominal fat in DIXON MR Images

Krishna Kanth Chitta[1], Bhanu Prakash KN[1], Suresh Sadananthan[2], and Sendhil Velan S[1]

[1]Laboratory of Molecular Imaging, Singapore Bioimaging Consortium, Singapore, Singapore, [2]Singapore Institute for Clinical Sciences, Singapore

Uniform distribution of intensity values for a given tissue type is desirable for accurate segmentation and quantification. Factors like non-uniform static magnetic field, motion artifacts, and inconsistent RF coil sensitivity introduce intensity inhomogeneity during MR image acquisition. Several methods for intensity inhomogeneity correction are proposed in the literature. We explored the suitability of Biased fuzzy C-means (BFCM) correction for quantification of abdominal fat from Dixon images. In our study we formulated a new 2-pass, 2D (intra-slice and inter-slice) BFCM framework for improved segmentation and quantification of abdominal fat.

Electronic Poster

The Many Faces of High Strength

Exhibition Hall Wednesday 17:15 - 18:15

5203 Computer 97

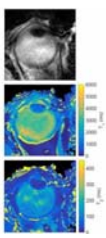

Cartesian MR Fingerprinting at 7T for Rapid Quantification of Relaxation Times in the Eye

Kirsten Koolstra[1], Jan-Willem Beenakker[1], Peter Koken[2], Thomas Amthor[2], Andrew Webb[1], and Peter Börnert[2]

[1]Leiden University Medical Center, Leiden, Netherlands, [2]Philips Research Hamburg, Germany

MR imaging of the eye requires a sequence of scans with different contrast to provide the necessary information on ocular conditions. In this study we apply Cartesian MR fingerprinting in the eye at 7T to add quantitative information to the standard clinical protocol, with the final goal of advancing disease diagnosis.

5204 Computer 98

RF slice shimming at 7T with power control on a commercial 8-channel transmit coil

Christopher J. Mirfin[1], Stephen Bawden[1], Paul Glover[1], Penny A. Gowland[1], and Richard Bowtell[1]

[1]Sir Peter Mansfield Imaging Centre, University of Nottingham, Nottingham, United Kingdom

We investigate the performance that can be achieved by applying volume and slice shimming on the commonly-used Nova 8-channel transmit/32-channel receive head coil, whilst controlling the total transmit power, as a proxy for global SAR. Under this constraint, our results suggest that shimming on individual axial slices can significantly improve the achievable B1 field uniformity (39.0% ± 3.9%) for the same transmit power as normal quadrature mode.

5205 Computer 99

Resolution Enhancement in Ultra-High Field 3D Echo-Planar Imaging Using a Planes-on-a-Paddlewheel with Asymmetric Readout Train (POP-ART) Trajectory

Daniel Stäb[1] and Markus Barth[1]

[1]The Centre for Advanced Imaging, The University of Queensland, Brisbane, Australia

3D planes-on-a-paddlewheel (POP) EPI is a non-Cartesian readout scheme realized by rotating EPI readout planes about the phase encoding axis. We show that the additional use of echo-asymmetry allows for significant improvements in spatial resolution without negative effects on echo-time, dropouts and distortions. The concept called POP-ART was evaluated at 7T. Whole brain images were obtained at a spatial resolution of $0.78 \times 0.78 \times 1.0 mm^3$ within less than 1 minute by using an echo-asymmetry of only 28%. Being faster spoiled gradient-echo and providing resolutions not achievable by corresponding Cartesian EPI techniques, the trajectory is of interest for T2* weighted or quantitative susceptibility imaging.

5206 Computer 100

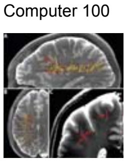

Quantitative measurements of perivascular spaces at 7T, using a semi-automatic tracking method

JM Spijkerman[1], HJ Kuijf[2], WH Bouvy[3], MI Geerlings[4], J Hendrikse[1], PR Luijten[1], and JJM Zwanenburg[1]

[1]Department of Radiology, University Medical Center Utrecht, Utrecht, Netherlands, [2]Image Sciences Institute, University Medical Center Utrecht, Utrecht, Netherlands, [3]Brain Center Rudolf Magnus, Department of Neurology, University Medical Center Utrecht, Utrecht, Netherlands, [4]Julius Center for Health Sciences and Primary Care, University Medical Center Utrecht, Utrecht, Netherlands

Currently, perivascular spaces (PVS) are mostly investigated with qualitative measures. In this work, PVS in the centrum semiovale were tracked using a semi-automatic method, and PVS length and tortuosity were determined. Univariate and multivariate linear regression was performed for age, number of tracked PVS, PVS length, and PVS tortuosity. The results show that quantitative assessment of PVS beyond counting is feasible, and a significant positive association between PVS length and the number of tracked PVS was found. These quantitative measurements may be more suitable than qualitative methods to investigate PVS.

5207 Computer 101

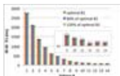

T1 Mapping of NIST Phantom at 7T

Yi-Fen Yen[1], Kathryn E. Keenan[2], Karl F. Stupic[2], Andre van der Kouwe[1], and Jonathan R. Polimeni[1,3,4]

[1]Athinoula A. Martinos Center for Biomedical Imaging, Massachusetts General Hospital, Charlestown, MA, United States, [2]Physical Measurement Laboratory, National Institute of Standards and Technology (NIST), Boulder, CO, United States, [3]Harvard-MIT Division of Health Sciences and Technology, Massachusetts Institute of Technology, Cambridge, MA, United States, [4]Department of Radiology, Harvard Medical School, Boston, MA, United States

We are reporting quantitative T1 values of the NIST T1 phantom at 7T for the first time by using IR-SE method. We also compared the accuracy of T1 mapping by using MP2RAGE and variable flip angle (VFA) methods against the IR-SE T1s at 7T and found MP2RAGE gave more accurate T1 measure than VFA, for T1 of 300 ms to 2000ms (the range of brain T1). Although the accuracy of MP2RAGE at 7T was not as good as that at 3T (also shown), MP2RAGE is a promising technique for accurate brain T1 mapping at 7T within a clinically acceptable scan time.

5208 Computer 102

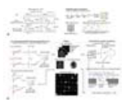

Shuffled Magnetization Prepared Multi-contrast Rapid Gradient Echo Imaging at 7T

Peng Cao[1], Shuyu Tang[1], Xucheng Zhu[1], Andrew Leynes[1], Angela Jakary[1], and Peder Larson[1]

[1]1Department of Radiology and Biomedical Imaging, UCSF, San Francisco, CA, United States

In this study, we aimed to explore accelerated acquisition of multi-contrast 3D images with different magnetization preparation times. We combined shuffled acquisition in k-space, parallel imaging, compressed sensing and pixel-wise low rank Hankel matrix reconstruction, achieving reconstruction of tens of multi-contrast 3D images from three 3-minute scans.

5209 Computer 103

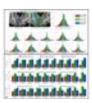

An in vivo analysis of cerebral cortex organization using a new partial volume method applied to 7T MP2RAGE

Guillaume Bonnier[1], Kieran O'Brien[2,3], Pascal Sati[4], Mario Joao Fartaria[5], Jon R Polimeni[1], Alexis Roche[5,6], Daniel S Reich[4], Gunnar Krueger[7], and Cristina Granziera[1,8]

[1]MGH/MIT/HMS Athinoula A. Martinos Center for Biomedical Imaging, Massachusetts General Hospital, Harvard Medical School, Charlestown, MA, United States, [2]Center for Advanced Imaging, University of Queensland, Brisbane, Australia, [3]Siemens Healthcare Pty Ltd, Brisbane, Australia, [4]Translational Neuroradiology Unit, National Institute of Neurological Disorders and Stroke, National Institutes of Health, Bethesda, MD, United States, [5]Advanced Clinical Imaging Technology, Siemens Healthcare AG, Lausanne, Switzerland, [6]Department of Radiology, University Hospital (CHUV), Lausanne, Switzerland, [7]Siemens Medical Solutions USA, Inc., Malvern, MA, United States, [8]Neuroimmunology Unit, Neurology, Department of Clinical Neurosciences, Centre Hospitalier Universitaire Vaudois (CHUV) and University of Lausanne (UNIL), Lausanne, Switzerland

We performed an analysis of the cortex organization of 10 healthy subjects using partial volume information. Tissue concentration were estimated using a novel algorithm applied to 7T MP2RAGE high resolution images (0.75mm), and ultra high resolution (0.35mm). We identified 3 distinct layers characterized by presence of WM-like signal (inner layer), only GM (central layer) and GM/CSF partial volume (outer layer).

5210 Computer 104

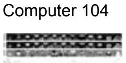

Slice-wise first-order shimming of the human spinal cord at 7T

S. Johanna Vannesjo[1], Yuhang Shi[1], Irene Tracey[1], Karla L. Miller[1], and Stuart Clare[1]

[1]FMRIB centre, Nuffield Department of Clinical Neurosciences, University of Oxford, Oxford, United Kingdom

Spinal cord imaging would benefit from the SNR increase at ultra-high field, to depict small structures inside the cord. However, higher background field strengths also increase susceptibility-induced B_0 field distortions, causing image distortions and signal dropouts. To improve field homogeneity, we here implement slice-wise first-order shimming in the cervical spinal cord at 7T. The slice-wise shim settings were calculated based on a B_0 field map and a semi-automatically generated spinal cord mask. We demonstrate that the slice-wise shims can improve signal levels in a high-resolution anatomical multi-echo GRE sequence.

5211 Computer 105

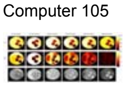

Gradient Moment Dependent T2 Accuracy in FISP Magnetic Resonance Fingerprinting (MRF) at 7T

Christian Anderson[1], Charlie Wang[1], Yuning Gu[1], Yun Jiang[1], Dan Ma[2], Mark Griswold[1,2], Xin Yu[1,2,3], and Chris Flask[1,2,4]

[1]Biomedical Engineering, Case Western Reserve University, Cleveland, OH, United States, [2]Radiology, University Hospitals Cleveland Medical Center, Cleveland, OH, United States, [3]Physiology and Biophysics, Case Western Reserve University, Cleveland, OH, United States, [4]Pediatrics, University Hospitals Cleveland Medical Center, Cleveland, OH, United States

Magnetic Resonance Fingerprinting allows for rapid, simultaneous multi-parametric quantification. The use of a FISP imaging kernel is necessary due to field inhomogeneity in human body and preclinical imaging. We have observed that increases in the applied gradient moment lead to gradient moment size dependent changes in T2 accuracy. By examining different applied gradient moments we illustrate this loss of T2 accuracy while T1 measurement accuracy is maintained. This has implications for FISP MRF design and the implementation of unbalanced gradient moments for quantification.

5212 Computer 106

Test-Retest Evaluation Spontaneous FMRI Signal: HCP 7T Reliability

Xi-Nian Zuo[1], Yin-Shan Wang[1], Dan-Yang Sui[1], and Xiu-Xia Xing[2]

[1]Chinese Academy of Sciences, Beijing, People's Republic of China, [2]Beijing University of Technology, Beijing, People's Republic of China

We employed the test-retest HCP datasets scanned at both 3T and 7T scanners from a same group of 62 healthy adults to compare differences in common functional metrics of the human connectome between 3T and 7T rfMRI settings in terms of their regional variations, individual variability and test-retest reliability. Our findings revealed metric-specific differences in both spatial patterns and reliability between 3T and 7T scanners whereas 7T improves reliability of global metrics but reduces reliability of local metrics of the functional connectomes.

5213 Computer 107

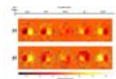

An SNR analysis of DENSE at 7T vs 3T for the measurement of whole brain tissue pulsatility

Ayodeji L Adams[1], Peter R Luijten[1], and Jaco J.M Zwanenburg[1]

[1]Department of Radiology, University Medical Center Utrecht, Utrecht, Netherlands

Cardiac induced brain tissue pulsatility holds potential as a means to study the viscoelastic properties of the aging brain. In this study we measured the brain tissue motion in 8 healthy volunteers with DENSE at both 7T and 3T, and assessed the gain in SNR between field strengths. 4D SNR maps for both field strengths were made and examined with a robust histogram analysis. The mean SNR for all volunteers at 7T and 3T was 21.2 ± 6.3 and 7.1 ± 2.5 respectively. The higher SNR at 7T will likely yield greater accuracy in quantifying brain tissue pulsatility.

5214 Computer 108

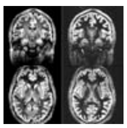

Fluid and white matter suppression (FLAWS) with MP2RAGE sequence at 7T.

Yuta Urushibata[1], Hideto Kuribayashi[1], Junko Inoue[1], Tobias Kober[2,3,4], John Grinstead[5], and Tomohisa Okada[6]

[1]Siemens Healthcare K.K., Tokyo, Japan, [2]Advanced Clinical Imaging Technology, Siemens Healthcare AG, Lausanne, Switzerland, [3]Department of Radiology, University Hospital (CHUV), Lausanne, Switzerland, [4]LTS5, École Polytechnique Fédérale de Lausanne (EPFL), Lausanne, Switzerland, [5]Siemens Medical Solutions, Inc., United States, [6]Kyoto University, Kyoto, Japan

Fluid and white matter suppression (FLAWS) is a technique to suppress cerebrospinal fluid (CSF) and white matter (WM) using the MP2RAGE sequence, which has been introduced for 3T. In this study, FLAWS was applied at 7T and compared to a SPACE double inversion recovery (DIR). Inversion times of the sequences were optimized for volunteer brain images at 7T. FLAWS showed better suppression of CSF and WM, more homogeneous gray matter (GM) delineation, as well as better GM/WM contrast compared with DIR.

5215 Computer 109

High resolution PET insert for high field preclinical MRI: evaluation of single ring system using 7T field strength

Willy Gsell[1], Uwe Himmelreich[1], Cindy Casteels[2], Christophe M. Deroose[2], Antonio J. Gonzalez[3], Albert Aguilar[3], Carlos Correcher[4], Emilio Gimenez[4], Cesar Molinos[4], Ramiro Polo[4], Thorsten Greeb[5], Ralph Wissmann[5], Sven Junge[5], and Jose M. Benlloch[3]

[1]Biomedical MRI, Department of Imaging and Pathology, KU Leuven, Leuven, Belgium, [2]Nuclear Medicine, Department of Imaging and Pathology, KU Leuven, Leuven, Belgium, [3]i3M, Valencia, Spain, [4]Oncovision, Valencia, Spain, [5]Bruker Biospin, Ettlingen, Germany

We designed a novel PET insert based on monolithic LYSO crystals. From our first evaluation, we can conclude that sub-millimeter detector spatial resolution, combined with accurate photon DOI determination, make it possible to acquire high resolution reconstructed images. This enables us now to combine simultaneously high resolution and sensitivity PET with high field preclinical MRI to extract simultaneously complex data from anatomical to molecular information and to dynamically follow non-invasively animal models of different pathologies with no compromise in performance of each imaging modality.

5216 Computer 110

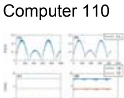

Pseudo-SSFP magnetic resonance fingerprinting (MRF) at 9.4T

Jinhyeok Choi[1] and Hyeonjin Kim[1,2]

[1]Department of Biomedical Sciences, Seoul National University, Seoul, Korea, Republic of, [2]Department of Radiology, Seoul National University Hospital, Seoul, Korea, Republic of

A balanced steady-state-free-precession (bSSFP) sequence may be preferred in magnetic resonance fingerprinting (MRF) for its high SNR. However, as demonstrated recently at 3.0T, the echo formation in bSSFP is hindered by randomly varying flip-angles in a B0-dependent manner, and yet, the destroyed spin-echo-like signal behavior can be restored by tailoring sequence timings according to varying flip-angles such that the spin ensemble is driven into a pseudo-steady-state. Given more severe B0-inhomogeneity at high-field, we explored the efficacy of the pseudo-steady-state-free-precession (pSSFP) sequence in MRF (pSSFP-MRF) at 9.4T. Our results suggest that pSSFP-MRF has great potential for single-scan multiparameter mapping at high-field.

5217 Computer 111

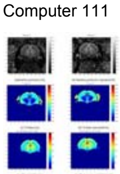

High Resolution Pseudo Continuous Arterial Spin Labeling (pCASL) of mouse brain at 9.4 Tesla

Sankar Seramani[1], Lydiane Hirschler[2], Emmaneul Luc Barbier[2], and Kuan Jin Lee[1]

[1]Laboratory of Molecular Imaging, Singapore Bioimaging Consortium, Singapore, Singapore, [2]Université Grenoble Alpes, Grenoble Institut des Neurosciences, Grenoble, France

The objective of this study was to show the feasibility of performing ASL based high resolution perfusion imaging in the mouse brain at 9.4 Tesla. In this work we applied   pCASL with phase optimization technique at the labeling plane to minimize the effect of B0 inhomogenity . We used fcFLASH based technique to measure the labeling efficiency of pCASL sequence and compared the labeling efficiency with FAIR ASL in mouse brain. Based on our results, with the proposed method of phase optimization, labelling slice can be place away from the iso-center of the magnet. This will allow us to place the imaging slice at the isocenter, which has showed significant improvement in the image quality of the mouse brain at ultra-high field strengths.

5218

Computer 112

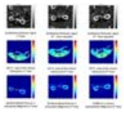

Comparison of pCASL and FAIR for measuring Renal Blood Flow (RBF) of mouse kidney at 9.4T

Sankar Seramani[1], Lydiane Hirschler[2], Boominathan Ramasamy[1], Sakthivel Sekar[1], Kishore Bhakoo[1], Emmanuel Luc Barbier[2], and Kuan Jin Lee[1]

[1]Laboratory of Molecular Imaging, Singapore Bioimaging Consortium, Singapore, Singapore, [2]Université Grenoble Alpes, Grenoble Institut des Neurosciences, Grenoble, France

Arterial Spin Labeling (ASL) is a non-invasive MRI technique which can be used to measure quantitative renal perfusion without the injection of contrast agents. The goal of this study is to compare the performance of pCASL with FAIR in measuring Renal Blood Flow in mouse kidney at Ultra High Field (UHF) MR. Based on our experimental results, pCASL based perfusion measurement shows similar reproducibility when compared to FAIR method. pCASL shows better SNR sensitivity and lower in ROI variation of RBF in the kidney when compared to FAIR based ASL method at 9.4 Tesla.

5219

Computer 113

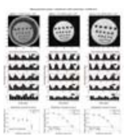

Spatial Resolution Analysis Comparing Density-Adapted and Conventional Projection Reconstruction in Chlorine-35 MRI at 9.4 T

Ruomin Hu[1], Matthias Malzacher[1], Mathias Davids[1], Andreas Neubauer[1], Simon Konstandin[2], and Lothar R. Schad[1]

[1]Computer Assisted Clinical Medicine, Heidelberg University, Mannheim, Germany, [2]MR-Imaging and Spectroscopy, Universty of Bremen, Bremen, Germany

^{35}Cl MRI has been of interest for both human and animal in vivo applications to visualise chloride homeostatic changes. In this study we performed measurements of resolution phantoms at an isotropic resolution of 0.490 and 0.326 mm using scanner-equipped ultrashort echo time 3D (UTE3D) and newly implemented density-adapted 3D projection reconstruction (DA-3DPR) sequences with subsequent spatial resolution analysis. DA-3DPR images with visibly higher SNR are capable of resolving both gross and fine structures with more reliable signal distributions and more consistent rendition of structure shapes. Moreover, penalty-free radial oversampling leads to more extended artefact-free regions, allowing for smaller FOVs and reduced measurement times.

5220

Computer 114

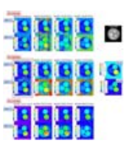

Initial implementation of magnetic resonance fingerprinting on a preclinical 14.1 T scanner

Yasuhiko Terada[1]

[1]University of Tsukuba, Tsukuba, Japan

Magnetic resonance fingerprinting (MRF) is a technique that enables simultaneous quantification of tissue parameters in a single scan. So far, MRF has been realized mostly for clinical 1.5 T and 3 T scanners, and a preclinical 7 T scanner. Application to a higher field scanner is limited and challenging because of the increased sensitivity to system hardware imperfections, such as B0 and B1 inhomogeneities and slice-profile imperfection. In this study, we assessed the feasibility of the MRF approach in a preclinical, wide-bore 14.1 T system.

5221

Computer 115

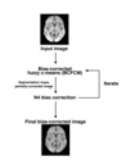

Robust Bias Correction and Segmentation of 7 Tesla Structural Brain Images with an iterative Bias-Corrected Fuzzy C-means and N4 Bias Correction (iBCFCM+N4)

Andrew Palmera Leynes[1], Melanie Morrison[1], Angela Jakary[1], Peder Larson[1], and Janine Lupo[1]

[1]Radiology and Biomedical Imaging, University of California San Francisco, San Francisco, CA, United States

To introduce and evaluate a novel strategy for iterative combination of bias-corrected fuzzy c-means (BCFCM) and N4 bias correction for robust bias correction and segmentation in 7 Tesla brain imaging studies.

5222

Computer 116

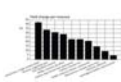

Cost-effectiveness analysis of mascara for eye-blink detection in ultra-high field MRI

Joep Wezel[1] and Jan-Willem M. Beenakker[2]

[1]Radiology, Leiden University Medical Center, Leiden, Netherlands, [2]Ophthalmology, Leiden University Medical Center, Leiden, Netherlands

Mascara has been proposed as a simple approach to correct for eye-motion artefacts via detection of induced B_0 changes when blinking. In this study we measure the B_0 changes from 10 different types of mascara. We can differentiate three different categories of mascara, in which in violation of Murphy's law the cheapest brands result in the strongest B_0 field changes.

5223

Computer 117

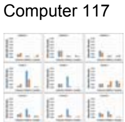

Quantitative Evaluation of Micro-vessel Blood Flow in Subcortical Nuclei with High-resolution TOF-MRA at 7T

Xianchang Zhang[1,2], Qi Yang[3,4], Qingle Kong[1,2], Zhaoyang Fan[3], Jing An[5], Rong Xue[1,2,6], and Zihao Zhang[1]

[1]State Key Laboratory of Brain and Cognitive Science, Beijing MR Center for Brain Research, Institute of Biophysics, Chinese Academy of Sciences, Beijing, People's Republic of China, [2]University of Chinese Academy of Sciences, Beijing, People's Republic of China, [3]Biomedical Imaging Research Institute, Cedars-Sinai Medical Center, Los Angeles, CA, United States, [4]Xuanwu Hospital, Beijing, People's Republic of China, [5]Siemens Shenzhen Magnetic Resonance Ltd., Shenzhen, People's Republic of China, [6]Beijing Institute for Brain Disorders, Beijing, People's Republic of China

TOF-MRA at 7T ultra-high field has been proven to have advantages in imaging the perforating arteries originating from the middle cerebral artery. In this study, a novel method of VOI-based micro-vessel density measurement was developed to quantitatively assess the blood flow in subcortical nuclei. Using this technique, the vascular density (VD) of specific basal ganglia sub-regions can be evaluated. Preliminary results showed that VD values of specific nuclei were different among Cerebral Autosomal Dominant Arteriopathy with Subcortical Infarcts and Leukoencephalophy (CADASIL) patients, stroke patients, and healthy volunteers. VOI-based micro-vessel density measurement may be useful in differentiating the etiology of cerebral small vessel diseases.

5224 Computer 118

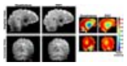

3D FLAIR at 7T using Direct Signal Control

Arian Beqiri[1], Hans Hoogduin[2], Alessandro Sbrizzi[2], Joseph V Hajnal[1,3], and Shaihan J Malik[1]

[1]Biomedical Engineering and imaging Sciences, King's College London, London, United Kingdom, [2]Image Sciences Institute, University Medical Centre Utrecht, Utrecht, Netherlands, [3]Centre for the Developing Brain, King's College London, London, United Kingdom

3D-FLAIR imaging at 7T using a 3D Turbo Spin Echo (TSE) readout is a useful tool for assessment of neurological disorders. The method does however suffer from variation in signal homogeneity due to B_1^+ inhomogeneities making whole-brain coverage difficult.

In this work, image uniformity is improved by using Direct Signal Control (DSC). The DSC method uses predictions of echo amplitudes to compute optimized RF shims that vary on a pulse by pulse basis throughout the echo train with the aim of homogenising signal properties. Low signal in the centre of the brain and cerebellum is effectively recovered in multiple subjects.

5225 Computer 119

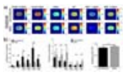

Quantitative CEST MRI using Image Downsampling Expedited Adaptive Least-squares (IDEAL) fitting

Iris Yuwen Zhou[1], Enfeng Wang[2], Jerry S Cheung[1], Xiaoan Zhang[2], Giulia Fulci[3], and Phillip Zhe Sun[1]

[1]Athinoula A. Martinos Center for Biomedical Imaging, Massachusetts General Hospital and Harvard Medical School, Charlestown, MA, United States, [2]Zhengzhou University, [3]Department of Neurosurgery, Massachusetts General Hospital and Harvard Medical School, Charlestown, MA, United States

CEST MRI is sensitive to dilute metabolites with exchangeable protons, allowing tissue characterization in diseases such as acute stroke and tumor. CEST quantification using multi-Lorentzian fitting is challenging due to its strong dependence on image SNR, initial values and boundaries. Here we proposed an Image Downsampling Expedited Adaptive Least-squares (IDEAL) fitting algorithm that quantifies CEST images based on initial values from multi-Lorentzian fitting of iteratively less downsampled images. The IDEAL fitting provides smaller coefficient of variation and higher contrast-to-noise ratio at a faster fitting speed compared to conventional fitting. It revealed pronounced CEST contrasts in tumors which were not found using conventional method. The proposed method can be generalized to quantify MRI data where SNR is suboptimal.

5226 Computer 120

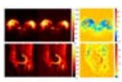

Adaptive combine reconstruction of sodium MRI data of breast and knee at 7 T: optimization and comparison to sum-of-square reconstruction.

Lenka Minarikova[1,2], Stefan Zbyn[1,2,3], Olgica Zaric[1,2], Stephan Gruber[1,2], Armin Nagel[4,5], and Siegfried Trattnig[1,2]

[1]High Field MR Centre, Department of Medical Imaging and Image-guided Therapy, Medical University of Vienna, Vienna, Austria, [2]Christian Doppler Laboratory for Clinical Molecular MR Imaging, Vienna, Austria, [3]Research Unit of Medical Imaging, Physics and Technology, University of Oulu, Oulu, Finland, [4]Institute of Radiology, University Hospital Erlangen, Erlangen, Germany, [5]Division of Medical Physics in Radiology, German Cancer Research Centre (DKFZ), Heidelberg, Germany

In this work, adaptive combine (AC) reconstruction was optimized on breast and knee sodium MRI data, acquired with a 14-channel breast and a 15-channel knee coils. AC reconstruction was compared with the standard sum-of-square (SoS) reconstruction. The optimal reconstruction parameters were: the lowest interpolation factor of two and an overlap of the analysis block of two to eight pixels. Images reconstructed using the AC had lower noise floor when compared to the SoS. However, when a multichannel coil with low noise correlation between elements is used, the advantage of AC reconstruction decreases.

Electronic Poster

Acquisition & Artifacts

Exhibition Hall Thursday 8:15 - 9:15

5227 Computer 1

High-Resolution fMRI of the visual system at 3T using Zoomed Excitation via Tx-SENSE

R. Allen Waggoner[1], Kenichi Ueno[2], Josef Pfeuffer[3], Keiji Tanaka[1], and Kang Cheng[1,2]

[1]Laboratory for Cognitive Brain Mapping, RIKEN - BSI, Wako-shi, Japan, [2]Support Unit for Functional Magnetic Resonance Imaging, RIKEN - BSI, Wako-shi, Japan, [3]Application Development, Siemens Healthcare, Erlangen, Germany

Zoomed EPI with a transmit SENSE excitation was used to perform high-resolution fMRI of the human visual cortex at 3T. Tx acceleration was used to reduce the minimum TE by 6ms. BOLD responses were detected in the visual cortex with sub-millimeter in-plane resolution. A monocular stimulation paradigm was employed, and voxels displaying a left or right eye preference were detected, but ocular dominance columns were not apparent. These results show that using transmit SENSE at 3T with a 2-channel pTx system for high-resolution fMRI is possible, but would benefit from further steps to improve tSNR.

5228 Computer 2

Functional MRI of the auditory cortex: maintaining the steady-state in EPI for silent inter-volume delays with different durations

Manoj Shrestha[1], H. Sean Lee[1,2], Ulrike Nöth[1], and Ralf Deichmann[1]

[1]Brain Imaging Center (BIC), Goethe University Frankfurt, Frankfurt am Main, Germany, [2]Max Planck Institute for Empirical Aesthetics, Frankfurt am Main, Germany

An fMRI sequence for studying the auditory cortex is proposed, allowing for the insertion of silent delays of variable duration between EPI volumes during which auditory stimuli may be presented. Signal steady state conditions are maintained via spin saturation at fixed time points before each EPI volume. The method was successfully tested in vivo, yielding reliable activation of the primary auditory cortex. Results also show that high saturation efficiency is required to avoid erroneous activation patterns in compartments with long T_1 such as cerebrospinal fluid.

5229 Computer 3

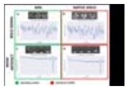

Identification of BOLD and non-BOLD components using Multi-Echo ICA analysis: is native space better than MNI space?

Jed Wingrove[1], Owen O'Daly[1], and Fernando Zelaya[1]

[1]Centre for Neuroimaging Sciences, IoPPN, King's College London, London, United Kingdom

This work looks to see the effects of analysing and de-noising resting state functional data in the native space in comparison to the conventional methodology which utilises the normalistaion, by voxel interpolation and re-sampling, of images to a standard space. We sought to investigate these effects in rs-fMRI data collected in healthy volunteers and analysed with multi-echo ICA de-noising and seed based connectivity.

5230 Computer 4

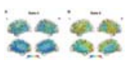

Dynamic functional connectivity using multi-band multi-echo EPI (M2-EPI) imaging for resting-state fMRI

Junjie Wu[1], Shiyang Chen[2], Ganesh Chand[3], Kyle Pate[1], Amit Saindane[1], and Deqiang Qiu[1]

[1]Department of Radiology and Imaging Sciences, Emory University School of Medicine, Atlanta, GA, United States, [2]Department of Biomedical Engineering, Georgia Institute of Technology & Emory University School of Medicine, Atlanta, GA, United States, [3]Department of Medicine, Emory University School of Medicine, Atlanta, GA, United States

In this abstract, we evaluated dynamic functional connectivity (FC) using multi-band multi-echo EPI (M2-EPI) resting-state data, which has higher temporal resolution, less susceptibility related signal dropouts and better signal-to-noise ratio. Dynamic FC and its states can be observed using M2-EPI data. Reduced temporal variation in dynamic FC was found using M2-EPI data acquisition as compared to conventional single-shot EPI imaging. The use of M2-EPI BOLD imaging may help to better delineate the structure of resting-state functional networks.

5231 Computer 5

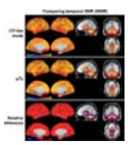

High resolution resting-state functional MRI at 7 Tesla using RF parallel transmission

Xiaoping Wu[1], Edward J. Auerbach[1], An T. Vu[2], Steen Moeller[1], Keith Jamison[1], Sebastian Schmitter[1,3], Pierre-Francois Van de Moortele[1], Essa Yacoub[1], and Kamil Ugurbil[1]

[1]Radiology, University of Minnesota, Minneapolis, MN, United States, [2]Center for Imaging of Neurodegenerative Diseases, VA Healthcare System, San Francisco, CA, United States, [3]Physikalisch-Technische Bundesanstalt, Berlin, Germany

A major component of the Human Connectome Project (HCP) in the WU-Minn consortium is multiband-accelerated whole-brain resting-state functional MRI (rfMRI) at both 3T and 7T. Although providing better contrast and higher spatial resolutions, the 7T acquisition is compromised by RF nonuniformity. Here, we demonstrate the utility of RF parallel transmission (pTx) for 7T HCP-type rfMRI with 1.6-mm isotropic resolutions. Our results show that pTx can significantly enhance temporal SNR across the entire cortical surfaces and in many subcortical voxels relative to a CP-like-mode RF shimming mimicking single-transmit configurations, thereby holding great potential for acquiring high-quality, high-resolution and high-efficiency rfMRI data.

5232 Computer 6

Quantitative assessment of cerebral venous oxygenation in mouse using T2-Relaxation-Under-Spin-Tagging (TRUST) MRI at 11.7T

Zhiliang Wei[1], Jiadi Xu[1], Peiying Liu[1], Lin Chen[1], Wenbo Li[1], Peter van Zijl[1], and Hanzhang Lu[1]

[1]Department of Radiology, The Johns Hopkins University, Baltimore, MD, United States

Venous oxygenation level reflects the cerebral metabolic rate of oxygen and its measurement facilitates studies of animal models of diseases. We developed a non-invasive and non-contrast-agent method based on T2-Relaxation-Under-Spin-Tagging (TRUST) to quantify cerebral venous oxygenation in mice at 11.7T. A series of studies were performed to optimize key imaging parameters. This method may prove useful in studies of brain physiology and pathophysiology in animal models.

5233 Computer 7

Susceptibility Artifact Correction for DBS-fMRI using a PSF Mapping-based Reversed Gradient Approach

Myung-Ho In[1], Shinho Cho[1], Yunhong Shu[2], Hoon-Ki Min[1,2,3], Matthew A. Bernstein[2,3], Oliver Speck[4,5,6,7], Kendall H. Lee[1,3], and Hang Joon Jo[1]

[1]Departments of Neurologic Surgery, Mayo Clinic, Rochester, MN, United States, [2]Departments of Radiology, Mayo Clinic, Rochester, MN, United States, [3]Departments of Physiology and Biomedical Engineering, Mayo Clinic, Rochester, MN, United States, [4]Department of Biomedical Magnetic Resonance, Institute for Experimental Physics, Otto-von-Guericke University Magdeburg, Magdeburg, Germany, [5]German Centre for Neurodegenerative Diseases (DZNE), Magdeburg, Germany, [6]Leibniz Institute for Neurobiology, Magdeburg, Germany, [7]Center for Behavioral Brain Sciences, Magdeburg, Germany

Deep brain stimulation (DBS) fMRI has been considered as an emerging tool in investigating the DBS mechanisms and corresponding clinical outcomes, but suffers from severe susceptibility artifacts near metallic electrodes and tissue/air boundaries. A recent study showed that point spread function (PSF) mapping-based reverse gradient approach has a potential to correct distortions even in gradient-echo echo-planar imaging (GE-EPI) images with opposite phase-encoding polarity using a PSF dataset. To minimize the susceptibility artifacts, in this study, we apply the PSF approach for DBS-fMRI in swine. The results demonstrate that this approach can be beneficial for improving the reliability of DBS-fMRI.

5234 Computer 8

Mouse somatosensory fMRI at 9.4T using a single-shot Variable Refocusing Flip Angle 3D GRASE

Joonsung Lee[1], Hyun-Ji Shim[1,2], Hahnsung Kim[3], Jungryun Lee[1], Sangwoo Kim[1], Jeong Pyo Son[1,2], Won Beum Jung[1,3], and Seong-Gi Kim[1,2,3]

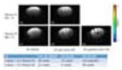

[1]*Center for Neuroscience Imaging Research, Institute for Basic Science, Suwon, Korea, Republic of,* [2]*Department of Health Sciences and Technology, Samsung Advanced Institute for Health Sciences and Technology, Sungkyunkwan University, Suwon, Korea, Republic of,* [3]*Department of Biomedical Engineering, Sungkyunkwan University, Suwon, Korea, Republic of*

A single-shot variable flip angle (VFA) 3D GRASE imaging protocol was proposed for mouse somatosensory spin echo fMRI. Given echo-spacing of 24ms and echo train length of 8, 3D GRASE imaging parameters such as phase-encode schedule in partition direction and variable refocusing flip angles were designed to achieve pseudo-continuous signal modulation and effective TE of 40ms. BOLD fMRI experiments were performed using 9.4T MRI with ketamine anesthetized mice. For eight slice acquisition of electrical forepaw simulation fMRI, the proposed single-shot VFA 3D GRASE protocol achieved higher tSNR, t-values and larger activation areas than conventional 2D SE-EPI.

5235 Computer 9

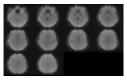

Feasibility study of gradient echo recalled readout segmented EPI with VB-EPI for ultra-silent fMRI

Patrick Liebig[1,2], Robin Martin Heidemann[2], Bernhard Hensel[1], and David Porter[3]

[1]*University of Erlangen-Nuremberg, Erlangen, Germany,* [2]*Siemens Healthcare GmbH,* [3]*Fraunhofer MEVIS*

We present an application of Variable-Blipped-EPI (VB-EPI) with readout-segmented EPI[1], which has possible benefits for functional Magnetic Resonance Imaging (fMRI) experiments. Acoustic noise is reduced by lowering the amplitude of the readout (RO) gradient, which is possible due to the RO segmentation, and by prolonging the duration of the phase encoding (PE) blips simultaneously. Even with standard Cartesian parallel imaging techniques, like Generalized Autocalibrating Partially Parallel Acquisitions (GRAPPA)[2], high resolution images can be obtained with high image quality.

5236 Computer 10

Comparison of Carotid Arterial Signal Automatically Extracted from fMRI Data and Pulse Oximetry

Jeff Gunter[1], Joshua Trzasko[1], Bret Borowski[1], and Clifford Jack,Jr.[1]

[1]*Radiology, Mayo Clinic, Rochester, MN, United States*

Using only imaging data from an fMRI time series carotid cardiac cycle information may be automatically extracted. By merging data across slices "faster than TR" sampling is achieved. The resulting time series agree with pulse oximetry (PO) data. The distribution of relative peak times between PO and fMRI has standard deviation of around 40ms. The fMRI data was quite reliable with cardiac signal observed for all but two of approximately 3000 seconds; PO data was much less reliable.

5237 Computer 11

Motion-Robust Fetal Brain Imaging using Inner Echo Volumar Imaging

Rita G Nunes[1,2,3], Giulio Ferrazzi[3], Anthony N Price[3], Jana Hutter[3], Andreia S Gaspar[2,3], Mary Rutherford[3], and Joseph V Hajnal[3]

[1]*Institute for Systems and Robotics / Department of Bioengineering, Instituto Superior Técnico, Universidade de Lisboa, Lisbon, Portugal,* [2]*Instituto de Biofísica e Engenharia Biomédica, Faculdade de Ciências, Universidade de Lisboa, Lisbon, Portugal,* [3]*Division of Imaging Sciences and Biomedical Engineering, King's College London, London, United Kingdom*

The first fetal functional MRI studies used standard 2D multi-slice Echo Planar Imaging acquisitions, relying on post-processing for addressing motion-related effects. To reduce motion sensitivity, the use of Echo Volumar Imaging (EVI) combined with localized excitation has previously been proposed, but the very heterogeneous maternal environment renders selective excitation extremely challenging. We explored a more robust method combining EVI with inner volume imaging. By obtaining selective excitation from a spin-echo, sensitivity to field inhomogeneity is decreased, and spurious contributions from maternal tissue can be avoided. The method was tested in an adult and demonstrated in fetal imaging in utero.

5238 Computer 12

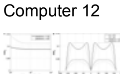

Multi-slice balanced SSFP is an excellent alternative to GE-EPI for rodent fMRI at ultra-high field

Ileana Ozana Jelescu[1], Olivier Reynaud[1], Analina Raquel da Silva[1], and Rolf Gruetter[1]

[1]*Centre d'Imagerie Biomédicale, Ecole Polytechnique Fédérale de Lausanne, Lausanne, Switzerland*

Balanced SSFP (bSSFP) can be used as an alternative to gradient-echo (GE)-EPI for BOLD fMRI when image distortions and signal drop-outs are severe at high field. However, on animal systems, 3D-bSSFP acquisitions have low temporal resolution due to limited acceleration options and single slice offers insufficient coverage. Here, we perform multi-slice bSSFP in a pseudo-steady-state and show that non-distorted BOLD fMRI activation maps can be obtained, with comparable performance to GE-EPI. Future work will focus on resting-state fMRI using bSSFP and on the exploration of bSSFP BOLD contrast mechanisms at 14 Tesla.

5239 Computer 13

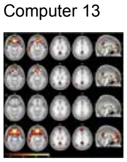

Improved functional connectivity between the ventromedial prefrontal cortex and amygdala with multi-echo EPI: a resting state analysis

Brice Fernandez[1], Laura Leuchs [2], Philipp G. Sämann [2], Michael Czisch[2], and Victor I. Spoormaker[2]

[1]*Applications & Workflow, GE Healthcare, Orsay, France,* [2]*Neuroimaging Unit, Max Planck Institute of Psychiatry, Munich, Germany*

EPI suffers from signal loss in the ventromedial prefrontal cortex (vmPFC), a region of special interest in affective neuroscience. Last year, we showed that Multi-echo EPI (MEPI) was performing better than EPI in the vmPFC using a fear conditioning task. In the present work, we used a seed in the vmPFC, derived from the fear conditioning data, for a seed-based analysis on resting-state data collected from the same subjects. We demonstrate that the additional vmPFC cluster extent detected in the fear conditioning task reflects anatomically/functionally relevant activation as it is connected to bilateral amygdala and to the default mode network.

5240 Computer 14

A more accurate account of the effect of k-space sampling and signal decay on the effective spatial resolution in functional MRI

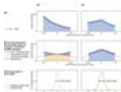

Denis Chaimow[1,2] and Amir Shmuel[3,4]

[1]University of Tübingen, Tübingen, Germany, [2]Center for Magnetic Resonance Research, University of Minnesota, Minneapolis, MN, United States, [3]Montreal Neurological Institute, McGill University, Montreal, QC, Canada, [4]Center for Magnetic Resonance Research, University of Minnesota, MN, United States

We show that the magnitude PSF fails to accurately represent the true effects of k-space sampling and signal decay. As an alternative, we propose to model fMRI with separate MR sampling and signal decay effects. We approximate the latter as a convolution with a Gaussian PSF or, if the effect is that of high-pass filtering, as reversing the effect of a convolution with a Gaussian PSF. At 7T signal decay in SE has a moderate blurring effect (FWHM = 0.89 voxels). Gradient-Echo acts as a high-pass filter, reversing blurring with FWHM = 0.59 voxels.

5241 Computer 15

SCITH Approach Reveals Stable Functional Connectivity

Zhan Xu[1], Guangyu Chen[1], and Shi-Jiang Li[1]

[1]Biophysics, Medical College of Wisconsin, Milwaukee, WI, United States

Current Multi-Echo fMRI approach can only acquire up to three echoes due to the fast T2* decay. We hypothesized that more echo will improve the capability of increasing the BOLD CNR and denoise accuracy, and we managed to acquire up to six echoes using our within TR keyhole based approach: SCITH. Our preliminary data showed increased BOLD CNR and resting-state functional connectivity(FC), less temporal FC fluctuation and more consistent inter-subject FC in the same population.

5242 Computer 16

The clinical relevance of correcting susceptibility-related distortions in presurgical fMRI at 7 T

Pedro Lima Cardoso[1], Barbara Dymerska[1], Beáta Bachratá[1], Florian Ph.S. Fischmeister[1,2], Nina Mahr[1,2], Eva Matt[1,2], Siegfried Trattnig[1], Roland Beisteiner[1,2], and Simon Daniel Robinson[1]

[1]High Field Magnetic Resonance Centre, Department of Biomedical Imaging and Image-guided Therapy, Medical University of Vienna, Vienna, Austria, [2]Study Group Clinical fMRI, Department of Neurology, Medical University of Vienna, Vienna, Austria

The clinical relevance of correcting susceptibility-related distortions using a recently-developed dynamic distortion correction (DDC) approach is assessed. This was applied in fMRI data acquired from a group of 12 patients with a range of neuropathologies at 7 T. Despite the presence of pathologies, time series of artifact-free field maps were generated. If distortion correction was neglected, substantial displacements, both in EPI geometry and activation, were observed. Two cases with potential clinical implications were identified. The DDC was able to accurately correct distortions in all cases and is shown to be effective and clinically relevant in presurgical planning at 7 T.

5243 Computer 17

magna cum laude

Characterization of laminar profiles in human auditory cortex using a dense 24-channel temporal lobe array at 3T

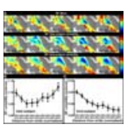

Pu-Yeh Wu[1], Ying-Hua Chu[1], Jo-Fu Lotus Lin[1], Shang-Yueh Tsai[2], Wen-Jui Kuo[3], and Fa-Hsuan Lin[1,4]

[1]Institute of Biomedical Engineering, National Taiwan University, Taipei, Taiwan, [2]Institute of Applied Physics, National Chengchi University, Taipei, Taiwan, [3]Institute of Neuroscience, National Yang Ming University, Taipei, Taiwan, [4]Department of Neuroscience and Biomedical Engineering, Aalto University, Espoo, Finland

By using a dedicated 24-channel temporal lobe array and surface based laminar depth analysis, we revealed the tonotopic representations in the human primary auditory cortex on a 3T MRI system. We found that, compared to deep and superficial layers, the minimal inter-subject variability of the tonotopic representation and frequency tuning width were found at the middle layer. Locations in the auditory cortex with finer frequency tuning had smaller inter-subject variability. Taken together, our findings suggested that middle layer of the auditory cortex has more specific frequency preference and selectivity, consistent with neurophysiological animal studies.

5244 Computer 18

Segmented EPI reconstruction based on physiological information for fMRI studies

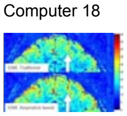

Guoxiang Liu[1] and Takashi Ueguchi[1]

[1]National Institute of Information and Communications Technology, Suita-shi,Osaka, Japan

We proposed a new segmented EPI reconstruction method based on physiological information to reduce influence of physiological noise. A human brain was scanned on a 7T MRI scanner using segmented EPI, while recording cardiac pulse and respiration data. Our results showed that the proposed reconstruction method can reduce the respiratory-related and cardiac-related signal changes in fMRI studies.

5245 Computer 19

Multiband Echo-SHift EPI (MESH-EPI): Applications at 3T

E Daniel Gomez[1], Zahra Fazal[1], José P Marques[1], Thomas Beck[2], Benedikt A Poser[3,4], and David G Norris[1]

[1]Donders Institute for Brain, Cognition and Behaviour, Radboud University Nijmegen, Nijmegen, Netherlands, [2]Application Development, Siemens Healthcare, Erlangen, Germany, [3]Faculty of Psychology and Neuroscience, Maastricht University, Maastricht, Netherlands, [4]Maastricht Brain Imaging Center (MBIC), Maastricht University, Maastricht, Netherlands

In the current abstract we explore the applications of Multiband Echo-SHifted (MESH) EPI as a potential tool for fMRI at 3T. We compare MESH and SMS-EPI in two sets of experiments: the first looking into typical fMRI protocols, and the second with a focus in BOLD contrast and temporal resolution optimization. We conclude that MESH can increase the temporal efficiency of fMRI and be used to reduce distortions without sacrificing BOLD contrast.

5246 Computer 20

Prospective Motion Correction of Multi-Band Multi-Echo fMRI During Overt Speech to Localize the Language Network

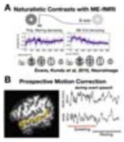

Prantik Kundu[1], Joao Correia[2], Saadi Ghatan[3], Daniel Samber[4], Michael Herbst[5], and Benedikt A Poser[2]

[1]Radiology and Psychiatry, Icahn School of Medicine at Mount Sinai, New York, NY, United States, [2]Cognitive Neuroscience, Maastricht University, [3]Neurosurgery, St. Lukes Roosevelt Hospital Center, New York, NY, [4]Radiology, Icahn School of Medicine at Mount Sinai, New York, NY, United States, [5]University Hospital Freiburg, Freiburg, Germany

The functional localization of language and other clinically relevant brain networks at the subject-level has been limited by fMRI artifacts such as head motion. These artifacts have forced task-based fMRI for functional localization to be designed around strict timing and strong constraints, such as silent reading in 20-second task-rest blocks. Such limits make experiments hard to follow by patients and not ecologically valid. Dealing with these artifacts, especially at patient level, has been challenging with standard fMRI methods. Here we combine the acquisition technologies of multi-echo fMRI, multi-band acceleration, camera-based prospective motion correction, and 7T MRI, to image canonical language and other networks during overt speech with 7T MRI using stimuli with complex language content with naturalistic timing.

5247 Computer 21

Study of the PSF distortion correction for ultra-high field BOLD fMRI

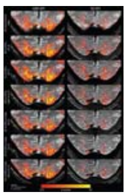

Catarina Rua[1,2], Myung-Ho In[3], Renat Yakupov[4], Hendrik Mattern[4], Mauro Costagli[2], Mark Symms[5], Alberto Del Guerra[1], Michela Tosetti[2,6], and Oliver Speck[4,7,8,9]

[1]Department of Physics, University of Pisa, Pisa, Italy, [2]Imago7 Research Center, Pisa, Italy, [3]Department of Neurologic Surgery, Mayo Clinic, Rochester, MN, United States, [4]Biomedical Magnetic Resonance, Otto-von-Guericke University, Magdeburg, Germany, [5]GE Healthcare, Pisa, Italy, [6]IRCCS Stella Maris, Pisa, Italy, [7]Leibniz Institute for Neurobiology, Magdeburg, Germany, [8]Center for Behavioral Brain Sciences, Magdeburg, Germany, [9]German Center for Neurodegenerative Diseases, Magdeburg, Germany

Distortion correction is an essential step for anatomically faithful analysis of ultra-high-field fMRI data due to strong susceptibility-induced geometric distortions in echo-planar imaging (EPI). Although the point-spread-function (PSF) method allows accurate unwarping and increase in SNR, its effectiveness in modulating the undistorted BOLD signal is still unknown. In this study we applied the PSF-based distortion correction using different types of correction kernels to GRE- and SE-EPI data at different resolutions and directly to the BOLD contrast maps, and evaluated the effectiveness by assessing functional contrast, specificity, and false-positive-rate.

5248 Computer 22

Poloxamer: a new means to recover functional network information in the rodent’s deep brain structures

Georges Hankov[1,2,3,4], Giovanna Diletta Ielacqua[1,4], Basil Künnecke[2], Thomas Mueggler[2], Markus von Kienlin[2], and Markus Rudin[1,3,4]

[1]Institute for Biomedical Engineering, ETH and University Zurich, Zurich, Switzerland, [2]Roche Pharma Research & Early Development, Neuroscience Discovery, Roche Innovation Center Basel, F. Hoffmann-La Roche Ltd, Basel, Switzerland, [3]Neuroscience Center Zurich, Zurich, Switzerland, [4]Institute of Pharmacology and Toxicology, University of Zurich, Zurich, Switzerland

In the past years, functional MRI studies in rodents have become more frequent. The signal losses in gradient-echo EPI due to the increased sensitivity to magnetic susceptibility differences at higher magnetic field, however, make fMRI studies of deep brain structures difficult. Here we propose the use of Poloxamer, a non-toxic amphiphilic triblock copolymer well known for its thermo-reversible properties and pharmaceutical application to fill up the air cavities in the rodent middle and external ear canals. This practical method considerably increases geometric fidelity of the functional images, opening up the possibility to longitudinally investigate rodent’s deep brain networks.

5249 Computer 23

PRESTO: an alternative to EPI for functional-MRI in rodents

Georges Hankov[1,2,3,4], Basil Künnecke[2], Markus Rudin[1,3,4], and Markus von Kienlin[2]

[1]Institute for Biomedical Engineering, ETH and University Zurich, Zurich, Switzerland, [2]Roche Pharma Research & Early Development, Neuroscience Discovery, Roche Innovation Center Basel, F. Hoffmann-La Roche Ltd, Basel, Switzerland, [3]Neuroscience Center Zurich, Zurich, Switzerland, [4]Institute of Pharmacology and Toxicology, University of Zurich, Zurich, Switzerland

With the increasing need for translational readouts, the number of fMRI studies in rodents has grown exponentially in the recent years. Nonetheless, methodological questions regarding fMRI data acquisition in small animals yet have been poorly addressed. In this work, we evaluate the use of the PRESTO sequence for fMRI in rodents: a 3D alternative to EPI using echo-shifting and echo-trains minimizing distortions and artefacts related to the higher magnetic fields, while providing better brain coverage and faster temporal resolution, allowing appropriate physiological noise sampling.

5250 Computer 24

Increased BOLD activation with high degree spherical harmonic shimming at 7T

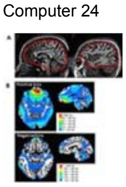

Tae Kim[1], Yoojin Lee[1], Tiejun Zhao[2], Hoby P Hetherington[1], and Jullie W Pan[1]

[1]University of Pittsburgh, Pittsburgh, PA, United States, [2]Siemens, Pittsburgh, PA, United States

B_0 shimming is important for gradient echo functional MRI where T_2^* signal loss and precession occur from both physiological and non-physiological susceptibility effects. We used the high degree shim insert (3rd, 4th and two 5th degree shims) to assess its effect for 2mm isotropic whole brain GE-EPI BOLD (breath-hold induced) signal at 7T. Comparing 1st-2nd with high degree shimming, the $\Delta|B_0|$ changes are spatially varying. For activation, the largest regions of increase are in the inferior frontal region; the largest regions of decrease are in the middle temporal lobe. Overall, there is a 4.3% increase in total activated pixels.

Electronic Poster

fMRI: Contrast Mechanisms

5251 Computer 25

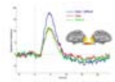

Attentional modulation on the fMRI signal at human visual cortex revealed by fine timing characteristics but not amplitudes

Ying-Hua Chu[1], Jo-Fu Lotus Lin[1], Pu-Yeh Wu[1], Kevin W.-K. Tsai[2], Yi-Tien Li[1], Yi-Cheng Hsu[1], Shang-Yueh Tsai[3,4], Wen-Jui Kuo[5], and Fa-Hsuan Lin[1,6]

[1]Institute of Biomedical Engineering, National Taiwan University, Taipei, Taiwan, [2]Aim for the Top University Project Office, National Taiwan Normal University, Taipei, Taiwan, [3]Institute of Applied Physics, National Chengchi University, Taipei, Taiwan, [4]Research Center for Mind Brain and Learning, National Chengchi University, Taipei, Taiwan, [5]Institute of Neuroscience, National Yang-Ming University, Taipei, Taiwan, [6]Department of Neuroscience and Biomedical Engineering, Aalto University, Espoo, Finland

By asking subjects engaging a decision task of two levels of difficulty based on foveal stimuli, we measured the BOLD dynamics elicited by checkerboard flashing shown at the peripheral visual fields with two levels of attention using high precision simultaneous-multi-slice inverse imaging (SMS-InI TR = 0.1 s; 5 mm isotropic resolution). Results shown insignificant difference in the amplitude of the BOLD response by two tasks, while time characteristics of onset, time-to-half, and width differ significantly between tasks in the range of hundreds of milliseconds.

5252 Computer 26

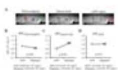

MR microscopy of Aplysia californica at 17.2T suggests that the diffusion fMRI signal originates from neural swelling

Yoshifumi Abe[1], Khieu Van Nguyen[1], Tomokazu Tsurugizawa[1], Luisa Ciobanu[1], and Denis Le Bihan[1]

[1]NeuroSpin, CEA, Gif-sur-Yvette, France

Diffusion fMRI (DfMRI) allows to monitor brain function without BOLD vascular confounding effects. To elucidate the origin of the DfMRI response we performed DfMRI experiments at single neuron and ganglia level upon dopamine stimulation of *Aplysia californica* buccal ganglia using 17.2T MR microscopy. Neural swelling, evidenced from optical microscopy, resulted in an intracellular ADC increase reflecting cytoplasm dilution and an ADC decrease at ganglia level. While the mechanism of this ADC decrease remains putative these results are consistent with the hypothesis that the ADC decrease observed with DfMRI upon neuronal activation at tissue level reflects activation induced cell swelling.

5253 Computer 27

Arterial Spin Labeling fMRI in White Matter at 7 Tesla

Leonardo Greco[1] and Olivier Reynaud[1]

[1]CIBM, EPFL, Lausanne, Switzerland

To date, the White Matter (WM) tracts functionality is never directly assessed using fMRI, but only inferred indirectly via healthy/impaired cortical connectivity. In this study, we use Arterial Spin Labeling (ASL), a non-invasive, quantitative, reproducible fMRI technique, to investigate WM Cerebral Blood Flow (CBF) dynamics at high field. We first show that WM CBF can be measured using standard 2D-EPI-PASL at 7T; and quantify CBF changes in GM and WM during finger-tapping. While the BOLD signal was only found elevated in GM, a net CBF increase was observed in GM and contralateral (but not ipsilateral) WM during the task (+77/25%).

5254 Computer 28

Spin echo and Gradient echo BOLD fMRI at ultrahigh magnetic field of 15.2T

SoHyun Han[1], JinYong Park[1], Woochul Jeong[1], and Seong-Gi Kim[1,2]

[1]Center for Neuroscience Imaging Research, Institute for Basic Science (IBS), Suwon, Korea, Republic of, [2]Department of Biomedical Engineering, Sungkyunkwan University, Suwon, Korea, Republic of

In general, gradient-echo (GE) BOLD contains extravascular (EV) contributions from all sized vessels, while spin-echo (SE) BOLD is sensitive to microvessels. Based on simulation, the EV BOLD signal is dependent linearly on B_0 for macrovessels, and quadratically on B_0 for microvessels. Here, we performed GE and SE BOLD fMRI of α-chloralose anesthetized rats responding to forepaw stimulation on an ultrahigh magnetic field of 15.2T. Stimulation-induced R_2 change was quadratically on B_0, indicating that microvessel contributions are dominant. SE BOLD at ultrahigh fields can detect precise activation sites and can be used for high-resolution fMRI to detect fine functional structures.

5255 Computer 29

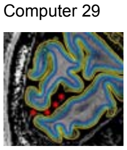

Macrovascular contributions to high-resolution balanced SSFP- and GE-EPI-based fMRI at 9.4T evaluated using surface-based cortical depth analyses in human visual cortex

Jonathan R. Polimeni[1,2,3], Natalia Zaretskaya[4,5,6], Johannes Stelzer[7], Jonas Bause[7], Philipp Ehses[7,8], Lawrence L. Wald[1,2,3], and Klaus Scheffler[7,8]

[1]Athinoula A. Martinos Center for Biomedical Imaging, Massachusetts General Hospital, Charlestown, MA, United States, [2]Department of Radiology, Harvard Medical School, Boston, MA, United States, [3]Harvard-MIT Division of Health Sciences and Technology, Massachusetts Institute of Technology, Cambridge, MA, United States, [4]Centre for Integrative Neuroscience, University of Tübingen, Tübingen, Germany, [5]Department of Psychology, University of Tübingen, Tübingen, Germany, [6]Department of Physiology of Cognitive Processes, Max Planck Institute for Biological Cybernetics, Tübingen, Germany, [7]High-Field MR Center, Max Planck Institute for Biological Cybernetics, Tübingen, Germany, [8]Department for Biomedical Magnetic Resonance, University of Tübingen, Tübingen, Germany

Several strategies have been proposed for maximizing neuronal specificity of fMRI by utilizing pulse sequences that are primarily sensitive to signal changes within microvasculature. Here we compare the microvascular sensitivity of high-resolution balanced SSFP and gradient-echo EPI at 9.4T using cortical depth analyses within human visual cortex. Because of the large draining vessels lying along the pial surface, the behavior of fMRI signals as a function of cortical depth can provide helpful insights into the vascular contributions. Our preliminary analyses suggest that, for the protocols used here, both balanced SSFP and EPI show similar cortical depth profiles of BOLD responses.

5256 Computer 30

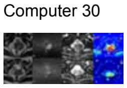

Combined dynamic contrast enhanced MRI and diffusion-weighted imaging to evaluate the neoadjuvant chemotherapy (NACT) effect in patients with cervical cancer

Yusen Feng[1], Yingying Ding[2], Ya Zhang[3], Chengde Liao[3], Yan Jin[2], and Peng Cao[4]

[1]Radiology Department, Third Affiliated Hospital of Kunming Medical University, kunming, People's Republic of China, [2]Radiology Department, Third Affiliated Hospital of Kunming Medical University, [3]Third Affiliated Hospital of Kunming Medical University, [4]GE healthcare

In this article,to prospectively investigate the changes of quantitative parameters in dynamic contrast-enhanced MRI (DCE-MRI) and the apparent diffusion coefficient (ADC) of diffusion weighted imaging (DWI) in cervical cancer patients before and after neoadjuvant chemotherapy (NACT).It showed that quantitative parameters of DCE-MRI and ADC provided a new noninvasive way to reflect the changes of hemodynamics and water molecular diffusion in cervical cancer patients with NACT.

5257 Computer 31

Characterize the Effect of Regional Variations in Venule Vasculature Related to Temporal Variability of Hemodynamic Responses Latency at the Human Primary Visual Cortex

Yi-Tien Li[1,2], Jo-Fu Lotus Lin[1], Pu-Yeh Wu[1], Kevin W.-K. Tsai[3], and Fa-Hsuan Lin[1,4]

[1]Institute of Biomedical Engineering, National Taiwan University, Taipei, Taiwan, [2]Department of Medical Imaging, Taipei Medical University - Shuang Ho Hospital, New Taipei, Taiwan, [3]Aim for the Top University Project Office, National Taiwan Normal University, Taipei, Taiwan, [4]Department of Neuroscience and Biomedical Engineering, Aalto University, Espoo, Finland

We correlated between the temporal chacteristics of the BOLD signals and venule structure at human primary visual cortex (V1). Functional MRI was measured by the high temporal resolution (100ms) simultaneous-multi-slice inverse imaging. Venule probability map was estimated from high spatial resolution (0.85mm) susceptibility-weighted imaging (SWI). Significant correlation was found between venule density and intra-/inter-subject temporal variability of the BOLD signal at V1. This correlation suggests that the temporal instability of BOLD signal is likely attributed to vascular structure or reactivity.

5258 Computer 32

Gadoxetic acid-enhanced MR imaging of the liver: the effect on hepatic fat quantification in hepatobiliary phase using mDXION-Quant

shuangshuang xie[1], qing li[1], zhizheng zhuo[2], yue cheng[1], and wen shen[1]

[1]Tianjin First Center Hospital, Tianjin, People's Republic of China, [2]Philips healthcare, Beijing, People's Republic of China

This study evaluated the effect of Gd-EOB-DTPA on fat quantification using a multiecho reconstruction technique with T2* correction. Forty-six patients with suspected hepatic tumors underwent Gd-EOB-DTPA enhanced MR imaging and single breath hold 3D mDIXON-Quant for hepatic fat quantification before and 20 minutes after the administration of Gd-EOB-DTPA. Fat fraction (FF) and R2* of the liver parenchyma, spleen parenchyma and vertebral body were measured and compared between pre- and post-contrast. FF measurements of liver, spleen, vertebral body and R2* measurements of liver, spleen revealed no significant difference between the two measurements, and R2* increased in liver and vertebral body significantly after 20 minutes of Gd-EOB-DTPA administration. In addition, good agreement of FF measurement was seen in the Bland-Altman plots. We conclude mDXION-Quant can obtain stable fat quantification in the hepatobiliary phase, without the impact of an increased R2* in liver parenchyma. But R2* maps should be obtained prior to Gd-EOB-DTPA administration.

5259 Computer 33

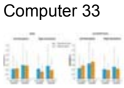

Relative latency and temporal variability of BOLD fMRI signal in the ventral visual pathway

Jo-Fu Lotus Lin[1], Ying-Hua Chu[1], Yi-Cheng Hsu[1], and Fa-Hsuan Lin[1,2]

[1]Institution of Biomedical Engineering, National Taiwan University, Taipei, Taiwan, [2]Department of Neuroscience and Biomedical Engineering, Aalto University, Espoo, Finland

We used simultaneous-multi-slice inverse imaging to characterize the relative latency and temporal variability of BOLD signals in the human ventral visual pathway with 0.1 s precision. The intra-subject and inter-subject variability were 0.39 (s) +/- 0.49 (s) and 0.51 (s) +/- 0.77 (s) when images of faces were presented. When scrambled faces were shown, the intra-subject and inter-subject variability were 0.42 (s) +/- 0.46 (s) and 0.56 (s) +/- 0.74 (s). With higher temporal resolutions, we showed temporal variability of HRF vary across cortical areas. Within the same cortical area, the temporal variability of HRF differ between different visual stimulations.

5260 Computer 34

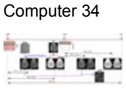

Simultaneous assessment of total CBV, aCBV and BOLD measures at 7 Tesla in motor and somatosensory cortices

Rosa M Sanchez Panchuelo[1], Robert Turner[1,2,3], and Susan Francis[1]

[1]Sir Peter Mansfield Imaging Centre, University of Nottingham, Nottingham, United Kingdom, [2]Max Planck Institute for Human Cognitive and Brain Sciences, Leipzig, Germany, [3]University of Amsterdam, Amsterdam, Netherlands

We combined Arterial Spin Labelling (ASL) and Vascular Space Occupancy (VASO) techniques into a double acquisition FAIR sequence with double echo readout to provide simultaneous measures of arterial Cerebral Blood Volume (aCBV), total CBV and BOLD signals. Using this technique at 7T, we successfully detected aCBV and total CBV (and BOLD) changes induced by both a motor task and a vibrotactile sensory stimulation paradigm, and show that activation maps derived with the independent ASL and VASO techniques largely overlap.

5261 Computer 35

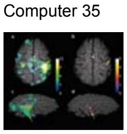

Functional brain imaging with high spectral and spatial resolution MRI at 3T

Sean Foxley[1], Xiaodong Guo[1], and Gregory S Karczmar[1]

[1]Radiology, University of Chicago, Chicago, IL, United States

Functional data were acquired of a finger tapping experiment using a conventional EPI approach as well as using high spectral and spatial resolution water spectra acquired using EPSI at 3T. Activation maps of both acquisition strategies were produced and compared. Expected task dependent areas of activation were seen in both, however, activation volumes were smaller in EPSI data. This could indicate that different Fourier components of the water spectrum are differentially affected by the BOLD effect. If this is the case, detailed analyses of the water spectrum could contribute to our understanding of the relationship between cognitive processes and the hemodynamic response.

5262 Computer 36

A Robust non-balanced SSFP fMRI Technique for High Field: Comparison with SE-EPI and bSSFP Techniques at 7 Tesla

Vahid Malekian[1,2], Abbas Nasiraei Moghaddam[1,3], Mahdi Khajehim[1], and David Norris[2]

[1]Biomedical Engineering, Amirkabir University of Technology (Tehran Polytechnic), Tehran, Iran, [2]Donders Institute for Brain, Cognition and Behaviour, Radboud university Nijmegen, Nijmegen, Netherlands, [3]School of Cognitive Sciences, Institute for Research in Fundamental Sciences (IPM), Tehran, Iran

T2-weighted fMRI methods including Spin-Echo (SE) and balanced SSFP (bSSFP), became of particular interest to reach superior functional specificity in high field application. However, both techniques suffer from a number of practical limitations. SE fMRI may be SAR limited at high fields. On the other hand, bSSFP suffers from dark bands. To eliminate dark bands in bSSFP, non-balanced-SSFP (nbSSFP) fMRI was previously suggested. Here, we developed a robust version of nbSSFP by using a single SSFP-echo sequence to decrease motion effects. The performance of the suggested sequence is evaluated and the results obtained are compared with bSSFP and SE-EPI fMRI.

5263 Computer 37

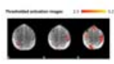

Targeted fMRI using radial acquisition and polar reconstruction

Banafshe Shafiei Zargar[1], Farzaneh Keyvanfard[1,2], and Abbas Nasiraei Moghaddam[1,2]

[1]Biomedical Engineering, Amirkabir University of Technology (Tehran Polytechnic), Tehran, Iran, [2]School of Cognitive Sciences, Institute for Research in Fundamental Sciences (IPM), Tehran, Iran

Recently there has been growing interests in radial fMRI. However, the reconstruction algorithm is also an important issue in K-space radial sampling. In this work, we have investigated the effect of a novel reconstruction method based on polar Fourier transform, for radially acquired fMRI data in polar coordinates. Based on its special features such as central focusing behavior, the obtained results demonstrate the capability of this method in reliable activity detection in targeted regions and also show a higher temporal stability in those areas.

5264 Computer 38

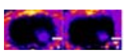

Crossover Intra-individual Comparison Study of Non-ionic and Ionic Gadolinium Based Contrast Agents in the Quantitative Evaluation of C6 Glioma with DCE-MRI

Ying Li[1], Rui Li [1], Wenjia Liu[1], Xin Lou[1], and Lin Ma[1]

[1]PLA General Hospital, Beijing, People's Republic of China

In this crossover intra-individual comparison study, we aimed to compare the non-ionic (godadiamide, Gd-DTPA-BMA) and ionic (gadopentetate dimeglumine, Gd-DTPA) Gadolinium based contrast agents (GBCA) in the quantitative evaluation of C6 glioma with dynamic contrast enhanced MR imaging (DCE-MRI) at 3.0 T MR scanner. K^{trans}, V_e and V_P maps were generated. Three radiologists independently performed tumor segmentation and value calculation. Gd-DTPA-BMA has significant more pixel counts of glioma in K^{trans} map and increased tendency for average K^{trans} and K_{ep} values, indicating that DCE-MRI with Gd-DTPA-BMA may be more suitable and sensitive for the evaluation of glioma.

5265 Computer 39

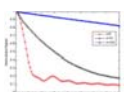

The Role of Microvascular Blood Motion in BOLD fMRI

Kenneth Wengler[1], Andrea He[2], Hoi-Chung Leung[3], Xiang He[4], and Chuan Huang[1,4,5]

[1]Department of Biomedical Engineering, Stony Brook University, Stony Brook, NY, United States, [2]Syosset High School, Syosset, NY, United States, [3]Department of Psychology, Stony Brook University, Stony Brook, NY, United States, [4]Department of Radiology, Stony Brook University, Stony Brook, NY, United States, [5]Department of Psychiatry, Stony Brook University, Stony Brook, NY, United States

While the existing BOLD signal model often use a single-compartmental, empirical relationship among fMRI response, blood flow and neural metabolic demand, some model parameters can only be determined from calibration challenges. In this study, for the first time, the role of intravascular blood motion on BOLD response is evaluated by Monte-Carlo simulation. Combined with an analytical description of extravascular contribution, a unified BOLD signal model without the need for calibration can be established, enabling the quantification of neurovascular coupling efficiency in both goal directed and spontaneous neuronal activations.

5266 Computer 40

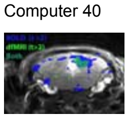

Diffusion functional MRI (dfMRI) yields highly defined tonotopic representation in the in vivo mouse

Cristina Chavarrias[1], Guilherme Blazquez Freches[1], and Noam Shemesh[1]

[1]Champalimaud Neuroscience Programme, Champalimaud Centre for the Unknown, Lisbon, Portugal

Diffusion fMRI (dfMRI) is highly promising for improving the detection of active regions with higher spatial accuracy, as well as for its potential of resolving faster dynamics than its BOLD counterpart. To test this hypothesis, we compared BOLD and dfMRI in the auditory pathway of the mouse, which exhibits clear tonotopy in electrophysiology. Our findings suggest that dfMRI activation maps are more localized and are in agreement with the expected area of activation in the inferior colliculus; dfMRI signals were also ~3s faster than BOLD signals. These results are expected to enable brainwide characterization of auditory reorganization, function, and plasticity.

5267 Computer 41

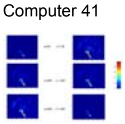

Evaluation of two novel MRI techniques for the assessment of intracranial pulsatility

Bowen Fan[1], Lirong Yan[2], Kay Jann[2], Mayank Jog[2], Ying Kui[3], and Danny JJ Wang[2]

[1]Department of Engineering Physics, Tsinghua University, Beijing, People's Republic of China, [2]Laboratory of FMRI Technology， Mark & Mary Stevens Neuroimaging and Informatics Institute，Keck School of Medicine，University of Southern California, University of Southern California, CA, United States, [3]Key Laboratory of Particle and Radiation Imaging, Ministry of Education, Medical Physics and Engineering Institute, Department of Engineering Physics, Tsinghua University, Beijing, People's Republic of China

The brain pulsatility plays an important role in various cerebral pathology, such as brain tumor and traumatic brain injury. Two MRI methods have been recently developed for assessing brain biomechanical features using a ECG-gated cine sequence with different processing strategies. In this study, we evaluated and compared the two methods. Consistent findings were obtained using both methods that the majority of cardiac-induced brain pulsatile motion occurs in the brain stem and basal ganglia as well as in big arteries.

5268 Computer 42

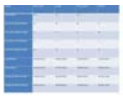

ADCtotal Ratio and D Ratio Derived from Intravoxel Incoherent Motion Early after TACE Were Independent Predictors for Survival in Hepatocellular Carcinoma

Lifang Wu[1]

[1]Radiology, zhongshan hospital, shanghai, People's Republic of China

The purpose of this study was to explore the threshold of IVIM parameters,ADCtotal and ADC(0,500) ratios 24-48 hours after TACE to assess early response in patients with unresectable HCC and to compare the association between diffusion–weighted imaging with the IVIM-DWI and mRECIST with survival. Our study show that the ADCtotal ratio and D ratio 24-48 hours after TACE were independent predictors for response to TACE for HCC, and showed stronger association with PFS than mRECIST.

5269 Computer 43

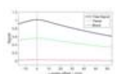

Bayesian Inference of Brain Oxygenation and Deoxygenated Blood Volume in Acute Stroke using Streamlined Quantitative BOLD

Matthew T Cherukara[1], Alan J Stone[2], Davide Carone[3], Radim Licenik[3], George WJ Harston[3], James Kennedy[3], Michael A Chappell[1], and Nicholas P Blockley[2]

[1]Institute of Biomedical Engineering, Department of Engineering Science, University of Oxford, Oxford, United Kingdom, [2]FMRIB Centre, Nuffield Department of Clinical Neuroscience, University of Oxford, Oxford, United Kingdom, [3]Acute Stroke Programme, Radcliffe Department of Medicine, University of Oxford, Oxford, United Kingdom

Streamlined Quantitative-BOLD provides a method for quantifying brain oxygen metabolism, in particular, deoxygenated blood volume and oxygen extraction fraction, based on linear fitting of values obtained from an asymmetric spin-echo sequence. It is possible that a curve-fitting approach may yield more robust values for these parameters. This study investigated the feasibility of estimating brain metabolic and vascular parameters through a Bayesian framework, through simulations, and analysis of patient data. It was found that under the current model, simultaneous estimation of oxygen extraction fraction and blood volume was not reliable, suggesting a limit to the model or acquisition protocol.

5270 Computer 44

A study of identifying patients with Alzheimer's disease based on resting-state fMRI

Shuai Mao[1], Changle Zhang[1], Heather T. Ma[1], Na Gao[1], Yanwu Yang[1], and Yan Wang[1]

[1]Harbin Institute of Technology Shenzhen Graduate School, Shenzhen, People's Republic of China

Based on resting-state fmri (rs-fMRI) data, this study aims to investigate the method of identifying AD and normal controls through the procedure of feature extraction and pattern recognition. We extracted the ALFF and ReHo parameters based on pre-processed resting-state fMRI data, and calculated some key parameters in graph theory through the functional connectivity network. Then the examination of the reliability of those features shows a satisfactory recognition rate of 94.4% to distinguish AD and normal controls.

5271 Computer 45

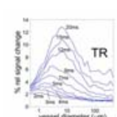

The neurovascular fingerprint of BOLD bSSFP: the impact of vessel size, orientation and intravascular contribution

Klaus Scheffler[1,2], David Kleinfeld[3,4], Philbert Tsai[3], Mario Báez-Yánez[1], and Philipp Ehses[1]

[1]MPI biol Cybernetics, Tübingen, Germany, [2]Department of Biomedical Magnetic Resonance, University of Tübingen, Tübingen, Germany, [3]Department of Physics, University of California at San Diego, San Diego, CA, [4]Section of Neurobiology, University of California, La Jolla, CA

The neurovascular fingerprint of BOLD (blood oxygen level dependent) bSSFP (balanced steady-state free precession) is analyzed by Monte Carlo simulations for different vessel geometries and on a vectorized vessel data set of mouse parietal cortex. The results support that bSSFP yields vascular properties similar to those found with spin echo BOLD, a small intravascular signal contribution except for larger vessels, and a high selectivity to microvessels.

5272 Computer 46

Which fMRI contrast is most specific for high resolution layer-dependent fMRI? Comparison study of GE-BOLD, SE-BOLD, T2-prep BOLD and blood volume fMRI?

Laurentius Huber [1], Jun Hua [2], Valentin G Kemper[3], Sean Marrett[4], Benedikt A Poser[3], and Peter A Bandettini[1]

[1]SFIM, NIMH, Bethesda, MD, United States, [2]FM Kirby Research Center, Johns Hopkins, United States, [3]MBIC, Maastricht University, Netherlands, [4]NIMH, United States

fMRI at ultra-high field strengths (≥7T) allow submillimeter voxels across different cortical layers. A big challenge to infer layer-dependent activity information, however, is to find an fMRI contrast that has the best combination of local specificity to microvascular responses within cortical layers and sensitivity to detect activity changes. Here we compare contrast mechanisms that have been proposed to be applicable to layer-dependent fMRI, including blood volume fMRI with VASO, SE-BOLD, T2/T1ρ-prep-BOLD, diffusion weighted T2-prep-BOLD. We find that CBV-weighted VASO and T2-prep methods have a favorable compromise between sensitivity and specificity. Hence, we believe that these fMRI methods might be better suited for layer-dependent applications than conventionally used GE-BOLD and SE-EPI.

5273 Computer 47

Comparison of BOLD and CBV impulse-response to visual stimulation in humans in the presence of Ferumoxytol

Jacco A de Zwart[1], Peter van Gelderen[1], Matthew Schindler[2], Pascal Sati[2], Jiaen Liu[1], Daniel S Reich[2], and Jeff H Duyn[1]

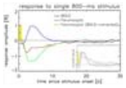

[1]Advanced MRI section, LFMI, NINDS, National Institutes of Health, Bethesda, MD, United States, [2]Translational Neuroradiology section, NINDS, National Institutes of Health, Bethesda, MD, United States

Ferumoxytol is a blood-pool-bound superparamagnetic iron-oxide particle (SPIO) that has been shown to yield CBV-dominated fMRI contrast in humans. Differences in impulse-response (IR) timing were previously demonstrated in animals when comparing SPIO-fMRI to BOLD-fMRI. Since BOLD IR is known to differ between humans and animals, we aimed to repeat this SPIO-fMRI to BOLD-fMRI comparison in humans. SPIO-fMRI was performed in human visual cortex and IR was compared to BOLD data from the same subjects. Shorter stimulus onset time and time-to-peak were found. Stimulus design minimized neuronal interaction effects between stimuli; residual inter-stimulus interaction effects, presumably vascular in origin, were found to be minor in SPIO-fMRI, on the same scale as in BOLD.

5274 Computer 48

THE IMPACT OF THE LOCAL, MESOSCOPIC FREQUENCY DISTRIBUTION AND DIFFUSION IN GRAY AND WHITE MATTER TO THE STATIC bSSFP SIGNAL PROFILE

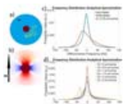

Mario Gilberto Báez-Yánez[1,2], Philipp Ehses[1,3], and Klaus Scheffler[1,3]

[1]Department of High-Field Magnetic Resonance, Max Planck Institute for Biological Cybernetics, Tuebingen, Germany, [2]Graduate Training Centre of Neuroscience, University of Tuebingen, Tuebingen, Germany, [3]Department of Biomedical Magnetic Resonance, University of Tuebingen, Germany

The phase accumulation that spins experience during a MR sequence is closely linked to the microstructure within the voxel, and basically produces changes in T2* or T2. The present abstract demonstrates how the static bSSFP signal profile is modified by the influence of local susceptibility differences produce by the underlying local-frequency distribution and diffusion effects related to white matter and gray matter at 9.4T. We apply an analytical presentation of the diffusion-modified frequency distribution, previously only used for gradient and spin echoes, to bSSFP and we prove the applicability of this theory to bSSFP by Monte Carlo simulations and measurements.

Electronic Poster

fMRI: Basic Neuroscience Applications: Connectivity Based

Exhibition Hall — Thursday 8:15 - 9:15

5275 Computer 49

Dynamic Changes of Functional Connectivity within and between Resting State Networks in Intractable Mesial Temporal Lobe Epilepsy

Chao Zhang[1], Kuncheng Li[1], Nan Chen[1], and Hongyu Yang[1]

[1]Xuanwu Hospital,Capital Medical University, Beijing, People's Republic of China

This study aimed to observe dynamic functional organization changes of large-scale resting state network (RSN) in MTLE and the patient who got seizure free after surgical treatment. Subject specific RSNs of three groups (healthy controls, presurgical group and posttreatment group) were extracted using group-information guided independent component analysis. Then, we calculated and compared the FC results between three groups, and we found FC altered markedly before and after surgical treatment. In addition, there was no statistical difference between posttreatment group and healthy controls. Our results may provide valuable information for further understanding of the pathophysiological mechanisms of intractable MTLE.

5276 Computer 50

Topologically Reorganized Functional Connectivity in Children with Abacus Training

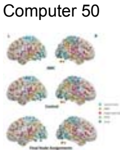

Ye Xie[1], Jian Weng[1], Chunjie Wang[1], and Feiyan Chen[1]

[1]Bio-X Laboratory, Department of Physics, Zhejiang University, Hangzhou, People's Republic of China

Cognitive training is an interesting topic in Neuroscience. Abacus-mental based calculation (AMC) training improves math ability that indicates it might affect functional connectivity architecture. Modularity analysis showed between-group differences in visual network and cingulo-opercular network (CON). Compared to the controls, increased local efficient observed in visual network, while decreased in CON in AMC experts. An alternative reason is that visual-spatial strategy involving in AMC training rather than languish strategy, leading to different trend to networks related to different function. Our findings shed light on topological reorganization of functional connectivity induced by AMC training.

5277 Computer 51

Is Iron Concentration Linked to Structural Connectivity in the Subthalamic Nucleus? Implications for Planning of Deep Brain Stimulation

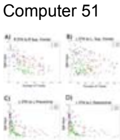

Wahaj Patel[1,2], Alexey Dimov[3], Yi Wang[3], Yihang Yao[3], Brian Kopell[4,5], and Rafael O'Halloran[1,4]

[1]Radiology, Icahn School of Medicine at Mount Sinai, New York, NY, United States, [2]The City College of New York, New York, NY, United States, [3]Weill Cornell Medical College, [4]Psychiatry, Icahn School of Medicine at Mount Sinai, [5]Neurosurgery, Icahn School of Medicine at Mount Sinai

The relationship between iron concentration, evaluated via quantitative susceptibility mapping (QSM) and white matter connectivity, assessed with 3T MRI, was explored. Such a relationship might be useful in deep brain stimulation (DBS) surgical planning, where both QSM and white matter connectivity are gaining interest. For several relevant regions of interest in movement disorders such as the superior frontal, pre central and post central gyrus there was a strong correlation between STN connectivity and QSM intensity. To allow quick assessment of the spatial variation of connectivity in the STN, an RGB image was computed from connectivity in 3 regions of interest.

5278 Computer 52

Shared and Specific Intrinsic Functional Connectivity Patterns in Unmedicated Bipolar Disorder and Major Depressive Disorder

Ying Wang[1], Junjing Wang[2], Yanbin Jia[3], Tao Liu[3], Yao Sun[1], Shuming Zhong[3], Zhongping Zhang[4], Li Huang[1], and Ruiwang Huang[2]

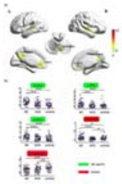

[1]Medical Imaging Center, First Affiliated Hospital of Jinan University, Guangzhou, People's Republic of China, [2]Center for the Study of Applied Psychology & MRI Center,Center, Key Laboratory of Mental Health and Cognitive Science of Guangdong Province, School of Psychology, South China Normal University, Guangzhou, [3]Department of Psychiatry, First Affiliated Hospital of Jinan University, Guangzhou, People's Republic of China, [4]MR Research China, GE Healthcare, Beijing

Our findings suggest that bipolar disorder (BD) and major depressive disorder (MDD) may have some shared and morespecific impairments of functional connectivity patterns during the depressiveperiod, providing new evidence for pathophysiology of BD and MDD at thelarge-scale whole brain connectivity level.

5279 Computer 53

Increased resting-state functional connectivity within subgenual anterior cingulate cortex network reveals the neural substrate of emotion regulation following mindfulness-based stress reduction (MBSR) training

Yao-Chia Shih[1,2], Chang-Le Chen[2,3], Shih-Chin Fang[4], Tzung-Kuen Wen[5], Da-Lun Tang[6], Si-Chen Lee[7], and Wen-Yih Isaac Tseng[2,3,8]

[1]Institute of Biomedical Engineering, National Taiwan University, Taipei, Taiwan, [2]Institute of Medical Device and Imaging, National Taiwan University College of Medicine, Taipei, Taiwan, [3]Graduate Institute of Brain and Mind Sciences, National Taiwan University College of Medicine, Taipei, Taiwan, [4]Department of Neurology, Cardinal Tien Hospital Yonghe Branch, New Taipei City, Taiwan, [5]Department of Buddhist Studies, Dharma Drum Institute of Liberal Arts, New Taipei City, Taiwan, [6]Department of Mass Communication, Tamkang University, Taipei, Taiwan, [7]Department of Electrical Engineering, National Taiwan University, Taipei, Taiwan, [8]Molecular Imaging Center, National Taiwan University, Taipei, Taiwan

Mindfulness-based stress reduction (MBSR) has been known to improve emotion regulation and cure mood disorders. The present longitudinal study aimed to clarify the effects of MBSR training and practice on the neural substrates of emotion regulation. Resting-state functional MRI (rsfMRI) exams were performed at three time points to investigate changes of functional connectivity (FC) within the subgenual anterior cingulate cortex (sgACC) network. MBSR training and practice strengthened the FC of sgACC with the inferior frontal gyrus and with the insula, and reduced the level of anxiety and depression. The findings reveal the neural substrates of emotion regulation process following MBSR.

5280 Computer 54

Tinnitus distress is linked to enhanced resting-state functional connectivity from the limbic system to the auditory cortex

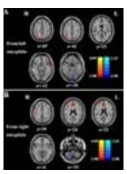

Yu-Chen Chen[1], Wenqing Xia[2], and Xindao Yin[1]

[1]Department of Radiology, Nanjing First Hospital, Nanjing Medical University, Nanjing, China, Nanjing, People's Republic of China, [2]Nanjing First Hospital, Nanjing Medical University, Nanjing, China, Nanjing, People's Republic of China

Our results identified disrupted effective connectivity networks in the limbic regions of tinnitus patients. Tinnitus severity was positively correlated with a bilateral increase in effective connectivity from the amygdala to the auditory cortex on the same side. In addition, tinnitus duration was positively correlated with enhanced effective connectivity from the right hippocampus to the left auditory cortex. These findings mainly emphasized the crucial role of limbic system and limbic-auditory interaction in tinnitus patients, which could help enhance our understanding of the neuropathological mechanisms underlying tinnitus.

5281 Computer 55

The GABA Level in DMN Modulate the Brain Network Centrality

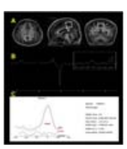

Tun-Wei Hsu[1,2], Jy-Kang Adrian Liou[1,2], Chien-Yuan Eddy Lin[3,4], Ralph Noeske[5], and Jiing-Feng Liring[1,6]

[1]Department of Radiology, Taipei Veterans General Hospistal, Taipei, Taiwan, [2]Department of Biomedical Imaging and Radiological Sciences, National Yang-Ming University, Taipei, Taiwan, [3]GE Healthcare, Taipei, Taiwan, [4]GE Healthcare MR Research China, Beijing, People's Republic of China, [5]GE Healthcare, Berlin, Germany, [6]Faculty of Medicine, School of Medicine, National Yang-Ming University, Taipei, Taiwan

In this study, we combined resting-state functional magnetic resonance imaging (rsfMRI) and advanced magnetic resonance spectroscopy technique to demonstrate a positive relationship between levels of inhibitory neurotransmitter gamma-aminobutyric acid (GABA) within posterior cingulate cortex/precuneus (PCC/PCu) and high network centrality of primary network. High network centrality propagates and contributes to efficient information flow in brain network. The PCC/PCu is a key component of default mode network (DMN) and high regional GABA levels expressing in the PCC/PCu area deactivate DMN activities related to internal thoughts for reallocating attention resources from internal processes to goal directed external stimuli with high network centrality.

5282 Computer 56

Accelerated intermittent theta burst stimulation, applied to the left DLPFC, influences dynamics in depression related networks

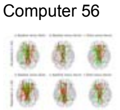

Debby Klooster[1,2,3], Rene Besseling[1,2,3], Suzanne Franklin[1], Antoine Bernas[1], Romain Duprat[2], Albert Aldenkamp[1,2,3], and Chris Baeken[2]

[1]Eindhoven University of Technology, Eindhoven, Netherlands, [2]University Hospital Ghent, Ghent, Belgium, [3]Academic Center for epileptology Kempenhaeghe, Heeze, Netherlands

The effect of accelerated intermittent theta burst stimulation (aiTBS) is investigated in three resting-state networks involved in depression: default mode network (DMN), central executive network (CEN), and salience network (SN). Multivariate Granger causality analysis was performed between time-series representing each network and between time-series of nodes belonging to these networks. The effects of the latter analysis were quantified by the in- and out-degree. No between-network effects were found but specific connections showed increased or decreased Granger causality after stimulation. Clinical responders showed changes in the in- and out-degree of the anterior cingulate, known to be important in depression pathology.

5283 Computer 57

Abnormal Heschl's gyrus resting-state functional connectivity in patients with presbycusis

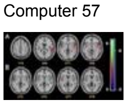

Fei Gao[1], Guangbin Wang[1], Bin Zhao[1], Fuxin Ren[1], and Weibo Chen[2]

[1]Shandong Medical Imaging Research Institute, Shandong University, Jinan, People's Republic of China, [2]Philips Healthcare, Shanghai, People's Republic of China

This study revealed abnormal resting-state functional connectivity between the Heschl's gyrus and distributed regions located in the hearing-related and language-related areas in patients with presbycusis. Our findings could be important for exploring imaging evidence of central component of presbycusis.

5284 Computer 58

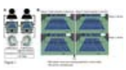

The Synchronization of Brain Activity in Real-Time Human Interaction Revealed by fMRI Hyperscanning

Jacky Tai-Yu Lu[1], Claire Hui-Chuan Chang[2], Shu-Yu Huang[1], Wen-Jui Kuo[3], and Fa-Hsuan Lin[4,5]

[1]Graduate Institute of Biomedical Electronics and Bioinformatics, National Taiwan University, Taipei, Taiwan, [2]College of Humanities and Social Sciences, Taipei Medical University, Taipei, Taiwan, [3]Institute of Neuroscience, National Yang-Ming University, Taipei, Taiwan, [4]Institute of Biomedical Engineering, National Taiwan University, Taipei, Taiwan, [5]Department of Neuroscience and Biomedical Engineering, Aalto University, Espoo, Finland

This study used functional magnetic resonance imaging (fMRI) hyperscanning to estimate the synchronization of human brain activations in interpersonal interaction by inter-subject correlation (ISC) analysis. Brain activations of pairs of subjects were recorded simultaneously during real-time video tennis game under cooperation, competition, and a control condition involving no interaction. Compared to control condition, higher ISC was found in premotor area (BA6) and right precuneus in the two game conditions. The finding of premotor area suggests that mutual action understanding was supported by the mirror neuron system during interpersonal interaction.

5285 Computer 59

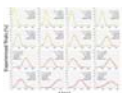

Sense of agency is a biological function sustained by a somatosensory-premotor network

Tommaso Gili[1,2], Valentina Ciullo[2,3], Daniela Vecchio[2,3], Gianfranco Spalletta[2,4], and Federica Piras[2]

[1]Enrico Fermi Center, Rome, Italy, [2]Neuropsychiatry Laboratory, IRCCS Santa Lucia Foundation, Rome, Italy, [3]Psychology Department, Sapienza University, Rome, Italy, [4]Menninger Department of Psychiatry and Behavioral Sciences, Baylor College of Medicine, Houston, TX, United States

Sense of agency (SoA) refers to the experience of controlling one's own actions. Temporal distortions between the action and the effect mislead agency attribution. We investigated the covariance between the amount of functional interactions among brain regions at rest and SoA. We found that the functional network involved in self-agency attribution included the premotor and somatosensory cortices bilaterally, and the right superior parietal lobule. This provides the first evidence that functional connectivity at rest in healthy subjects varies along with experienced SoA, implying that self-agency is processed within an intrinsic brain functional module.

5286 Computer 60

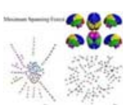

Organization and hierarchy of the human brain functional network at rest lead to a chain-like core.

Tommaso Gili[1,2], Rossana Mastrandrea[3], Andrea Gabrielli[4], Fabrizio Piras[1,2], Gianfranco Spalletta[2,5], and Guido Caldarelli[3,4]

[1]Enrico Fermi Center, Rome, Italy, [2]Neuropsychiatry Laboratory, IRCCS Santa Lucia Foundation, Rome, Italy, [3]Networks Unit, IMT School for Advanced Studies, Lucca, Italy, [4]Institute for Complex Systems, CNR, Rome, Italy, [5]Menninger Department of Psychiatry and Behavioral Sciences, Baylor College of Medicine, Houston, TX, United States

The intrinsic functional architecture of the brain and its alterations due to cognitive engagement, ageing and diseases are nodal topics in neuroscience, attracting considerable attention from many disciplines of scientific investigation. Complex network theory offers powerful tools to investigate brain connectivity disclosing the structure of the human brain functional network. Here we put forward a number of methods to investigate the network of brain areas coupled by their functional coordination without introducing exogenous thresholds. In this way we overcame the problem of having a fully connected network and found the intrinsic structure of the functional architecture of the brain.

5287 Computer 61

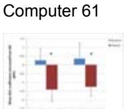

Oxytocin influences the directed connectivity between the precuneus and the dorsolateral prefrontal cortex

Jyothika Kumar[1], Sarina J Iwabuchi[2], Birgit A Völlm[1], and Lena Palaniyappan[3]

[1]Division of Psychiatry and Applied Psychology, University of Nottingham, Nottingham, United Kingdom, [2]Radiological Sciences, Division of Clinical Neuroscience, University of Nottingham, Nottingham, United Kingdom, [3]Department of Psychiatry & Robarts Research Institute, University of Western Ontario, London, ON, Canada

The default mode network (DMN) is now known to play an important role in social cognition. Thus, we hypothesized that the social neuropeptide oxytocin (OXT) will modulate the connectivity of the DMN. We used Granger Causality Analysis and found that intranasal OXT modulates the effective or 'causal' connectivity between the precuneus: a key DMN node and the dorsolateral prefrontal cortex, a key region in the central executive network. Thus, OXT has the potential to enhance the cooperative role of the DMN, which could explain the mechanistic action by which OXT improves social cognition in disorders such as autism and schizophrenia.

5288 Computer 62

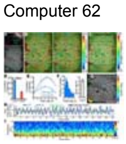

Identify the neural basis of vascular dynamic network connectivity with high-field fMRI

Yi He[1,2], Maosen Wang[1,2], Xuming Chen[1,2], and Xin Yu[1]

[1]High-field Magnetic Resonance, Max Planck Institute for Biological Cybernetics, Tuebingen, Germany, [2]Graduate Training Centre of Neuroscience, International Max Planck Research School, University of Tuebingen, Tuebingen, Germany

The vascular dynamic network connectivity was detected with the resting-state fMRI in rodent and human brains (abstract: 3115). However, the basis of vascular dynamic connectivity is unclear. Here, the GCaMP6-mediated calcium signal simultaneously detected by fiber optics with fMRI showed slow-freuqncy fluctuation (0.01-0.04Hz) correlated to the single-vessel fMRI signal fluctuation with lead times from 1 to 5 seconds. In addition, the correlation was observed on the slow-frequency oscillation of the power profile of the spontaneous calcium burst spikes with frequency bandwidth of 1-10Hz. Thus, the vascular dynamic network connectivity demonstrates the hemodynamic state changes coupled to the brain state fluctuation.

5289 Computer 63

Individualized Functional Parcellation of Human Amygdala using a Semi-Supervised Clustering Method based on 7T Resting State fMRI Data

Xianchang Zhang[1,2], Hewei Cheng[3], Zhentao Zuo[1], Ke Zhou[1], Bo Wang[1], Lin Chen[1,2], Yong Fan[4], and Rong Xue[1,2,5]

[1]State Key Laboratory of Brain and Cognitive Science, Beijing MR Center for Brain Research, Institute of Biophysics, Chinese Academy of Sciences, Beijing, People's Republic of China, [2]University of Chinese Academy of Sciences, Beijing, People's Republic of China, [3]Department of Biomedical Engineering, School of Bioinformatics, Chongqing University of Posts and Telecommunications, Chongqing, People's Republic of China, [4]Department of Radiology, Perelman School of Medicine, University of Pennsylvania, Philadelphia, United States, [5]Beijing Institute for Brain Disorders, Beijing, People's Republic of China

Functional subspecialization of human amygdala has been revealed in a variety of studies based on histological, in-vivo imaging, and meta-data. However, most of the existing studies identified functional subregions of amygdala at a group level. In this study, we investigated individualized functional neuroanatomy of amygdala based on 7T resting-state fMRI data with high spatiotemporal resolution. Our results have demonstrated that an improved semi-supervised clustering algorithm successfully parcellated individual subjects' amygdala into 3 subregions, each of them having distinctive functional connectivity patterns. The individualized functional subregions of amygdala may better capture individual variability in functional neuroanatomy than their group level counterparts.

5290 Computer 64

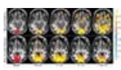

Contrary Effect of Stressful vs. Non-stressful Striped Patterns on Human Visual Cortical Functional Connectivity

Jie Huang[1] and David C. Zhu[1,2]

[1]Department of Radiology, Michigan State University, East Lansing, MI, United States, [2]Department of Psychology, Michigan State University, East Lansing, MI

Areas across the visual cortex are functionally connected. A stressful striped pattern induces perceptual illusions/distortions and visual discomfort in most people, headaches in patients with migraine, and seizures in patients with photosensitive epilepsy. In contrary, a non-stressful striped pattern does not induce such effects. This study found that a 25-min visual stimulation showed a significantly contrary effect of the stressful vs. non-stressful striped patterns on human visual cortical functional connectivity (FC). To the contrary of the strengthening effect of the stressful striped pattern on the FC, the non-stressful striped pattern showed a weakening effect on the FC.

5291 Computer 65

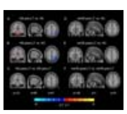

Impact of previous episodes of hepatic encephalopathy on post-transplantation brain function recovery

Yue Cheng[1] and Wen Shen[2]

[1]Tianjin First Central Hospital, Tianjin, People's Republic of China, [2]Tianjin First Central Hospital, People's Republic of China

Purpose: To investigate the impact of prior episodes of hepatic encephalopathy (HE) on post-transplantation brain function recovery. Method: Thirty-three cirrhotic patients (HE, n=15 and noHE, n=18) and 30 healthy controls were included. Functional connectivity strength (FCS) were compared between the pre-LT data and the post-LT data, respectively. Results: For the noHE group, the altered FCS found pre-LT largely returned to nearly normal levels soon after LT. The abnormal FCS prior to LT was largely preserved in the HE group, including high-level cognition-related and vision-related areas. Conclusion: Pre-LT episode of HE may have adverse effects on post-LT brain function recovery.

5292 Computer 66

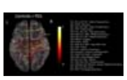

Effects of motor dysfunction on functional connectivity and network topology in Parkinson's disease

Karthik Sreenivasan[1], Virendra Mishra[1], Zhengshi Yang[1], Xiaowei Zhuang[1], Sarah Banks[1], Dietmar Cordes[1,2], and Ryan R Walsh[1]

[1]Cleveland Clinic Lou Ruvo Center for Brain Health, Las Vegas, NV, United States, [2]University of Colorado Boulder, Boulder, CO, United States

The objective of this study was to use resting-state functional connectivity and graph theory to determine how the topology of the network is altered in PD with respect to severity of motor dysfunction. The current study revealed altered functional connectivity and topological properties of networks in PD with respect to severity of motor dysfunction. Our results point to a shift towards a less efficient network topology with altered integration and segregation in more motorically affected patients.

5293 Computer 67

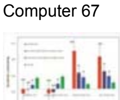

Differential changes in functional connectivity of fronto-striatal and motor-striatal circuits in early and premanifest Huntington's Disease measured by ultra-high field (7T) resting state BOLD fMRI

Jun Hua[1,2], Martin Kronenberger[3,4], Xinyuan Miao[1,2], James Pekar[1,2], Peter van Zijl[1,2], and Christopher Ross[3,4,5]

[1]Dept. of Radiology, Johns Hopkins University School of Medicine, Baltimore, MD, United States, [2]F.M. Kirby Research Center for Functional Brain Imaging, Kennedy Krieger Institute, Baltimore, MD, United States, [3]Department of Neurology, Johns Hopkins University School of Medicine, Baltimore, MD, United States, [4]Department of Psychiatry and Behavioral Sciences, Johns Hopkins University School of Medicine, Baltimore, MD, United States, [5]Department of Neuroscience and Pharmacology, Johns Hopkins University School of Medicine, Baltimore, MD, United States

Huntington’s disease (HD) is a neurodegenerative disorder characterized by motor, cognitive and behavioral deficits. The striatum is one of the first brain regions that show detectable atrophy in HD. Reduced functional connectivity between striatum and motor cortex has been reported. Here, we report decreased motor-striatal connectivity but increased fronto-striatal connectivity in early/premanifest HD patients. We speculate that this may imply a compensatory mechanism, where additional cortical regions are recruited to subserve functions that have been impaired due to HD pathology. We also found strong correlations between functional connectivity and genetic measures, suggesting its potential value as a biomarker for HD.

5294 Computer 68

Subthalamic nucleus activation under audio-motor transformation in lateralized Parkinson’s disease

Oleksii Omelchenko[1], Zinayida Rozhkova[2], Irina Karaban[3], and Mykola Makarchuk[4]

[1]Human and Animal Physiology, Taras Shevchenko National University of Kyiv, Kyiv, Ukraine, [2]Medical Clinic BORIS, Kyiv, Ukraine, [3]Department of extrapyramidal disorders, D. F. Chebotarev Institute of Herontology, Kyiv, Ukraine, [4]Taras Shevchenko National University of Kyiv, Kyiv, Ukraine

We hypothesized that audio-motor transformation (AMT) play an important role in voice-guided movement initiation with STN involvement. We propose AMT-related subthalamic nucleus activation analysis in lateralized PD for tremor asymmetry influence study. We identified PD symptoms laterality dependent STN activation peculiarities. Obligatory left STN activation in AMT supposes its role in motor command switching. Bilateral STN activation during the movement execution supports its proposed role as a motor error correction node.

5295 Computer 69

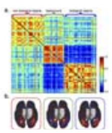

Distributed and overlapping cortical networks represent visual categories

Haiguang Wen[1], Junxing Shi[1], Kuan Han[1], and Zhongming Liu[2]

[1]Electrical and Computer Engineering, Purdue University, West Lafayette, IN, United States, [2]Electrical and Computer Engineering and Biomedical Engineering, Purdue University, West Lafayette, IN, United States

The principle of cortical representations when thousands of real-life objects and categories are involved remains unclear. Here, we built a computational model of the human visual system by using a deep neural network and predicted the cortical responses to natural visual stimuli. In particular, we trained the model by using fMRI data obtained while subjects watched very long (>10 hours) natural movie stimuli that contained thousands of visual object categories. Based on the model, we systematically analyzed the activation patterns in the brain induced by different kinds of object categories. We found that the categorical information was represented by distributed and overlapping cortical networks, as opposed to discrete and distinct areas. Three cortical networks represented such broad categories as biological objects, non-biological objects, and background scenes. More fine-grained categorical representations in the brain suggest that visual objects share more (spatially) similar cortical representations if they share more similar semantic meanings.

5296 Computer 70

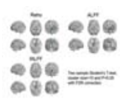

An fMRI-based neurologic signature of lower back pain

Jing Liu[1], Zhizheng Zhuo[2], Juan Wei[3], Queenie Chan[4], and Xiaoying Wang[1]

[1]Peking University First Hospital, Beijing, People's Republic of China, [2]Philips Healthcare, Beijing China, [3]Philips Research China, Shanghai, China, [4]Philips Healthcare, Hongkong China

Brain function MRI (fMRI) could successfully demonstrate that differences in the pattern of brain activity to lower back pain (LBP) can be used as a neurological marker to distinguish between individuals with and without LBP. Medical, legal and business professionals have recognized the importance of this research topic and of developing objective measures of LBP and other chronic pain.

5297 Computer 71

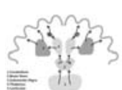

Morphological And Functional Research In Parkinson Disease By Magnetic Resonance Imaging

Shuaiwen Wang[1], Junqiang Lei[1], and Shunlin Guo[1]

[1]Department of Radiology, the First Hospital of Lanzhou University, Lanzhou, People's Republic of China

Parkinson's disease (PD) is the second most common neurodegenerative disease after AD, and the most frequent subcortical degenerative disease.We hope to found morphological and functional characteristic change in PD

5298 Computer 72

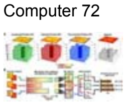

Modulation of Expectation on Sound-to-Meaning Mapping during Speech Processing: An fMRI Study

Bingjiang Lyu[1,2,3], Jianqiao Ge[1,2,3], Zhendong Niu[4], Li Hai Tan[5], Tianyi Qian[6], and Jia-Hong Gao[1,2,3]

[1]Center for MRI Research, Peking University, Beijing, People's Republic of China, [2]McGovern Institute for Brain Research, Peking University, Beijing, People's Republic of China, [3]Beijing City Key Lab for Medical Physics and Engineering, Peking University, Beijing, People's Republic of China, [4]School of Computer Science and Technology, Beijing Institute of Technology, Beijing, People's Republic of China, [5]Center for Language and Brain, Shenzhen Institute of Neuroscience, Shenzhen, People's Republic of China, [6]MR Collaborations NE Asia, Siemens Healthcare, Beijing, People's Republic of China

Spoken language comprehension relies on both the identification of individual words and the expectations arising from contextual information. A distributed fronto-temporal network is known to facilitate the mapping of speech sounds onto corresponding meanings. However, how prior expectations influence this efficient mapping at the neuroanatomical level, especially for individual words, remains unclear. Using functional magnetic resonance imaging, we addressed this question in the framework of the dual-stream model by investigating both the neural substrates and their mutual functional and effective connectivity. Our results revealed how this ubiquitous sound-to-meaning mapping in daily communication is achieved in a predictive manner.

Electronic Poster

fMRI: Physiology

Exhibition Hall Thursday 8:15 - 9:15

5299 Computer 73

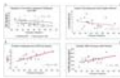

Lower Resting Cerebral Blood Flow but Greater Cerebrovascular Reactivity in Young Adults with Higher Aerobic Fitness

Catherine Foster[1], Jessica J Steventon[1,2], Daniel Helme[1], Valentina Tomassini[3], and Richard G Wise[1]

[1]School of Psychology, Cardiff University Brain Research Imaging Centre, Cardiff, United Kingdom, [2]School of Medicine, National Mental Health Research Institute, Cardiff, United Kingdom, [3]School of Medicine, Institute of Psychological Medicine and Clinical Neurosciences, Cardiff, United Kingdom

We measured the association between aerobic fitness and cerebral blood flow (CBF) and cerebrovascular reactivity (CVR) in young, healthy adults using multiple inversion time (MTI) arterial spin labelling (ASL), with a hypercapnic challenge to assess CVR. The results show that higher fitness is associated with lower baseline CBF and greater CVR. Although studies with a larger sample size are required to clarify the relationship between fitness and cerebrovascular function in early adulthood, the current results suggest that aerobic fitness may promote vascular efficiency and reserve.

5300 Computer 74

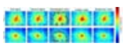

Where is Physiological Noise Lurking in $$$k$$$-Space?

Toni Karvonen[1,2], Arno Solin[3], Ángel F. García-Fernández[1], Filip Tronarp[1], Simo Särkkä[1], and Fa-Hsuan Lin[4,5]

[1]Department of Electrical Engineering and Automation, Aalto University, Espoo, Finland, [2]Aalto NeuroImaging, Aalto University, Espoo, Finland, [3]IndoorAtlas Ltd., Helsinki, Finland, [4]Institute of Biomedical Engineering, National Taiwan University, Taipei, Taiwan, [5]Department of Neuroscience and Biomedical Engineering, Aalto University, Espoo, Finland

We analyze the structure of physiological noise in the $$$k$$$-space of BOLD fMRI. We use DRIFTER which is an algorithm based on optimal Bayesian smoothing techniques for separation of the fMRI signal to a BOLD signal component and physiological noises. DRIFTER is run independently for each spatial frequency and it is shown that the physiological noise lies in the $$$k$$$-space points with low spatial frequency and that its amplitude is proportional to the BOLD signal. This result suggests that we can lower the computational burden without losing estimation accuracy by running DRIFTER only on a subset of $$$k$$$-space points.

5301 Computer 75

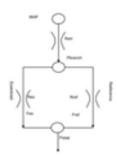

Measuring cerebrovascular reactivity in terms of resistance

James Duffin[1], Olivia Sobczyk, Adrian Crawley, Julien Poublanc, Kevin Sam, Lashmi Venkatrahavan, David Mikulis, and Joseph Fisher

[1]Anaesthesia, University of Toronto, Toronto, ON, Canada

Conventional measurements of cerebrovascular reactivity (CVR) are often based on the BOLD changes in response to a ramp CO_2 stimulus ranging from hypo- to hypercapnia. Using a simple model of two vascular beds, one with a healthy standard reference resistance, competing for the same limited blood supply, we derive the sigmoidal relative resistance changes in the other branch of the model from measured BOLD responses. Maps displaying the spatial pattern of the relative resistance sigmoid parameters describe the physiology and pathophysiology of the vessels themselves and thus may provide more clinically useful insight.

5302 Computer 76

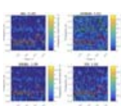

Retrospective Independent Component Estimation of Respiratory and Cardiac Artefact Residuals (RICERCAR) in BOLD-fMRI.

Michael Hütel[1], Andrew Melbourne[1], Dave Thomas[1], Jonathan Rohrer[1], and Sebastien Ourselin[1]

[1]UCL, London, United Kingdom

Variations in the heart and respiration rate have an impact on BOLD-fMRI signal variations. The cardiac cycle causes a pulsatile arterial blood flow which causes slice-specific signal changes resulting in artificial correlations between voxels within the same slice. The introduction of multi-band (MB) EPI acquisitions such as in the Human Connectome Project (HCP) increase such artificial correlations because many slices are acquired at the same slice time. We find physiological-related spatial Independent Components (ICs) and remove their corresponding time courses from BOLD-fMRI scans. Our method RICERCAR outperforms RETROICOR as well as FIX.

5303 Computer 77

The effect of low-level carbon monoxide exposure on BOLD FMRI

Caroline R Bendell[1], Shakeeb H Moosavi[1], and Mari Herigstad[1,2]

[1]Biological and Medical Sciences, Oxford Brookes University, Oxford, United Kingdom, [2]Academic Unit of Radiology, University of Sheffield, Sheffield, United Kingdom

Carbon monoxide (CO) is a cerebral vasodilator, yet effects of low-level CO exposure (from e.g. smoking) on BOLD FMRI remain unknown. We scanned 12 never-smokers at 3T before and after inhaling low-level CO (or air as a control). CO significantly reduced BOLD response to carbon dioxide during breath holds and attenuated visual cortex activation during visual stimulation and fingertapping, but also increased premotor cortex activation during fingertapping. This indicates that CO generally dampens BOLD signal (possibly through elevated baseline CBF), but that the effect may be task- and/or region-dependent. Caution should be exercised when comparing populations with different CO levels.

5304 Computer 78

Effects of anesthesia on BOLD, electrophysiology, and PO2 signals in the whisker barrel cortex

Daniil P Aksenov[1], Limin Li[1], Michael Miller[1], Robert Linsenmeier[2], and Alice M Wyrwicz[1]

[1]NorthShore University HealthSystem, Evanston, IL, United States, [2]Northwestern University, Evanston, IL, United States

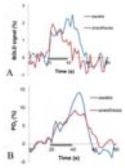

A comprehensive understanding of the relationship between neuronal activity and oxygen dynamics in the brain is vital for the accurate interpretation of fMRI results. This study investigates the relationship between changes in blood and tissue oxygen as well as neuronal activity in the awake and anesthetized states. We compare BOLD, PO_2 and electrophysiological signals in the barrel cortex during whisker stimulation in awake and isoflurane-anesthetized rabbits. Our findings suggest that the relationship between BOLD, PO_2 and electrophysiological responses is considerably different in the awake and anesthetized states.

5305 Computer 79

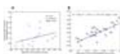

Quantitative Mapping of Cerebrovascular Reactivity using Resting-state BOLD fMRI: A Validation in Healthy Adults

Ali Golestani[1], Luxi Wei[2], and Jean Chen[2,3]

[1]Department of Psychology, University of Toronto, Toronto, ON, Canada, [2]Department of Medical Biophysics, University of Toronto, Toronto, ON, Canada, [3]Rotman Research Institute at Baycrest, Toronto, ON, Canada

Cerebrovascular reactivity (CVR) is commonly mapped as the response of the blood oxygenation level dependent (BOLD) signal to a hyper/hypocapnic breathing challenge, which might be intolerable for some patients. We proposed a method to estimate quantitative CVR using intrinsic fluctuations of end-tidal CO_2 ($PETCO_2$) during resting-state fMRI data acquisition (rs-qCVR). We validated our rs-qCVR method against the “gold-standard” hyper/hypocapnic CVR method, demonstrating significantly association between the two in the majority of the healthy subjects.

5306 Computer 80

Comparison of Quantitative Specific Ventilation Imaging in the Lung with Oxygen Enhanced 1H and 3He Multibreath MRI

Tatsuya J Arai[1,2,3], Felix C Horn[2], Rui Carlos Sá[3], Madhwesha R Rao[2], Guilhem Collier[2], Rebecca J Theilmann[3], G. Kim Prisk[3], and Jim M Wild[2]

[1]UT Southwestern Medical Center, Dallas, TX, United States, [2]Academic Unit of Radiology, The University of Sheffield, Sheffield, United Kingdom, [3]Pulmonary Imaging Laboratory, University of California, San Diego, San Diego, CA, United States

Two multi-breath imaging techniques for quantifying specific ventilation based on oxygen enhanced ^{1}H and hyperpolarized 3He gas MRI were cross-validated with spatially matched data from the same subjects. With a custom RF torso ^{1}H array configured with ^{3}He T-R coil in situ we were able to separately acquire ^{1}H and hyperpolarized ^{3}He MRI during a single scanning session without repositioning the subject. The preliminary study demonstrated qualitative as well as quantitative similarities between the two techniques.

5307 Computer 81

Quantification of Neural Energetic Changes during Visuomotor Learning using Arterial Spin Labelling FMRI

Catherine Foster[1], Jessica Steventon[1,2], Ian Driver[1], Daniel Helme[1], Valentina Tomassini[3], and Richard G Wise[1]

[1]School of Psychology, Cardiff University Brain Research Imaging Centre, Cardiff, United Kingdom, [2]School of Medicine, Neuroscience and Mental Health Research Institute, Cardiff, United Kingdom, [3]School of Medicine, Institute of Psychological Medicine and Clinical Neurosciences, Cardiff, United Kingdom

Recovery of motor function following neurological damage is dependent on functional neuroplasticity. Mechanisms of adaptive plasticity are not well understood, thus limiting the ability to predict recovery following rehabilitation. This study examined the suitability of calibrated fMRI to study cerebrovascular changes during motor learning, as cerebrovascular function plays an important role in neuroplasticity. Results showed cerebral blood flow, BOLD and oxygen metabolism increases from rest with task but decreases with task-learning. However, high inter-subject response variability was observed. Calibrated fMRI shows promise for studying cerebrovascular changes during learning but the repeatability and stability of measurements requires further investigation.

5308 Computer 82

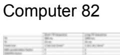

Impact of Physiological Noise on Serial Correlations in Fast Simultaneous Multislice (SMS) EPI at 7T

Saskia Bollmann[1], Alexander Puckett[2], Ross Cunnington[2], and Markus Barth[1]

[1]Centre for Advanced Imaging, The University of Queensland, Brisbane, Australia, [2]Queensland Brain Institute, The University of Queensland, Brisbane, Australia

We investigated the influence of physiological noise on statistical inference in fMRI at the single-subject level. By comparing two SMS sequences with a short and a long TR, we explored the interaction between repetition time, physiological noise modelling and the autoregressive model used to characterize serial correlations in fMRI data. Using variational Bayesian inference, we found that fMRI acquisitions with a short TR require accurate modelling of cardiac and respiratory processes to successfully remove serial correlations from the fMRI time series. For the SMS sequence with a longer TR, the standard AR model of order 1 proved sufficient.

5309 Computer 83

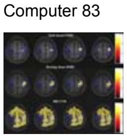

Comparison of BH CVR and resting state fMRI to “gold standard” task-based fMRI for assessment of brain tumor-induced neurovascular uncoupling

Shruti Agarwal[1], Haris I. Sair[1], Sachin Gujar[1], Arvind P. Pathak [1,2], and Jay J. Pillai[1]

[1]Russell H. Morgan Department of Radiology and Radiological Science, Johns Hopkins University School of Medicine, Baltimore, MD, United States, [2]Dept. of Biomedical Engineering, Johns Hopkins University School of Medicine, Baltimore, MD, United States

Neurovascular Uncoupling (NVU) can critically limit presurgical mapping using blood oxygen level dependent functional magnetic resonance imaging (BOLD fMRI). False-negative activations caused by NVU can lead to erroneous interpretation of clinical fMRI examinations. Brain tumor-related NVU has been previously demonstrated on task-based BOLD fMRI (tbfMRI) and resting state BOLD fMRI (rsfMRI). The purpose of this study is to demonstrate that NVU in the sensorimotor network can be similarly detected on rsfMRI and BH CVR maps as evident in the criterion standard tbfMRI.

5310 Computer 84

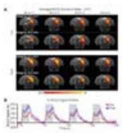

Pharmacological inactivation of dorsal hippocampus enhances responses and induces adaptation to sound in midbrain

Celia M. Dong[1,2], Russell W. Chan[1,2], Leon C. Ho[1,2], Alex T.L. Leong[1,2], Eddie Wong[1,2], Lei Wang[1,2,3], Felix F. Chen[3], Condon Lau[4], and Ed X. Wu[1,2]

[1]Laboratory of Biomedical Imaging and Signal Processing, The University of Hong Kong, Hong Kong, Hong Kong, [2]Department of Electrical and Electronic Engineering, The University of Hong Kong, Hong Kong, Hong Kong, [3]Department of Electrical and Electronic Engineering, Southern University of Science and Technology, Shenzhen, People's Republic of China, [4]Department of Physics and Materials Science, City University of Hong Kong, Hong Kong, Hong Kong

The hippocampus is associated with the memory and learning, meanwhile, receives signal from all sensory system indirectly. However, whether and how the hippocampus influences sound processing in the auditory system remains unclear. Our recent study showed that optogenetic stimulation of hippocampus enhances the brain bilateral auditory cortex connectivity. This fMRI study investigated the influence of hippocampus on auditory processing in the inferior colliculus (IC) by using tetrodotoxin (TTX) to pharmacologically deactivate the dorsal hippocampus. For the first time, our results revealed that the dorsal hippocampus plays a dynamic role in shaping the IC auditory response.

5311 Computer 85

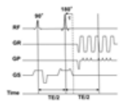

Cerebral oxygen extraction fraction measurement using an asymmetric spin echo EPI approach

Yong Zhang[1], Zhongping Zhang[1], Kang Wang[2], and Zhenyu Zhou[1]

[1]MR Research China, GE Healthcare, Shanghai, People's Republic of China, [2]GE Healthcare, Milwaukee, WI, United States

Quantitative measurement of oxygen delivery and consumption in the brain can provide insight into neurovascular and metabolic coupling. A single shot asymmetric spin echo (ASE) EPI sequence was implemented for quantitative oxygen extraction fraction (OEF) measurement in healthy volunteers for the feasibility study. OEF results were in good agreement with the normal range of 30%-40% reported in the previous literature. ASE EPI shows the potential to provide quantitative OEF maps with good brain coverage and without the need of gas challenges. Further investigation is required to evaluate the sensitivity of OEF measurement in the disease situation, such as stroke.

5312 Computer 86

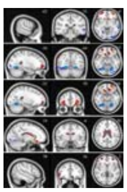

Eigenvector Centrality Mapping in Detecting Parkinson's Disease

Zhengshi Yang[1], Ryan Walsh[1], Virendra Mishra[1], Karthik Sreenivasan[1], Xiaowei Zhuang[1], Sarah Banks[1], and Dietmar Cordes[1,2]

[1]Cleveland Clinic Lou Ruvo Center for Brain Health, LAS VEGAS, NV, United States, [2]University of Colorado Boulder, CO, United States

Eigenvector centrality (EC) is a parameter-free method to measure the centrality of complex brain network structures without a priori assumption. It is here applied to resting state fMRI data acquired from normal controls (NC) and Parkinson's disease (PD) subjects for the purpose of detecting centrality abnormality in PD, a disease known to impact neural networks diffusely. The features extracted from EC were able to accurately classify subjects when used with linear discriminant analysis and support vector machine.

5313 Computer 87

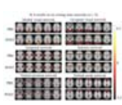

Modulation of resting state networks after slow and periodic visual stimulation in humans

Lei Wang[1,2,3], Celia M. Dong[1,2], Alex T. L. Leong[1,2], Xunda Wang[1,2], Leon C. Ho[1,2], Russell W. Chan[1,2], Felix F. Chen[3], and Ed X. Wu[1,2]

[1]Laboratory of Biomedical Imaging and Signal Processing, The University of Hong Kong, Hong Kong, Hong Kong, [2]Department of Electrical and Electronic Engineering, The University of Hong Kong, Hong Kong, Hong Kong, [3]Department of Electrical and Electronic Engineering, Southern University of Science and Technology, Shenzhen, People's Republic of China

Periodicity is inherent in numerous external sensory stimuli. However, its effect on large-scale resting state brain networks has not been fully understood. This study investigated brain networks before and after periodic visual stimulation in low frequency (1Hz) using resting state functional MRI. Enhanced connectivity in visual, temporal, salience and ventral attention networks were detected after 1Hz visual stimulation. Furthermore, power spectrum analysis showed increase in infra-slow (<0.1Hz) rsfMRI activity. These findings suggest that slow and periodic visual stimulation initiates and/or facilitates certain neuromodulatory mechanisms such as neural oscillations, leading to increased rsfMRI connectivity.

5314 Computer 88

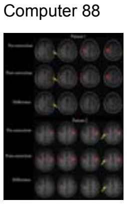

fMRI activation optimization in the setting of brain tumor-induced neurovascular uncoupling using resting state BOLD ALFF

Shruti Agarwal[1], Hanzhang Lu[1], and Jay J. Pillai[1]

[1]Russell H. Morgan Department of Radiology and Radiological Science, Johns Hopkins University School of Medicine, Baltimore, MD, United States

The phenomenon of neurovascular uncoupling (NVU) is an under-recognized but very important limitation of clinical BOLD fMRI because it can lead to non-visualization of eloquent cortex and resultant inadvertent surgical resection of vital brain tissue leading to permanent postoperative disability. In this study we demonstrate a novel method for correcting for the spuriously decreased ipsilesional motor activation associated with NVU through use of a novel resting state fMRI (rsfMRI) frequency domain metric-- ALFF (amplitude of low-frequency fluctuation)-- in patients with perirolandic low grade gliomas.

5315 Computer 89

Functional MRI of Brain's White Matter in Alzheimer's Disease

Xiaowei Song[1,2], Hui Guo[1,3], Sujoy Ghosh-Hajra[2], Careesa Liu[2], Yunting Zhang[3], and Ryan CN D'Arcy[1,2]

[1]Health Sciences and Innovation, Fraser Health Authority, Surry, BC, Canada, [2]Simon Fraser University, Burnaby, BC, Canada, [3]Medical Imaging, Tianjin Medical University General Hospital, Tianjin, People's Republic of China

Impaired white matter (WM) integrity is common in Alzheimer's disease (AD), in addition to gray matter degeneration. While fMRI has been widely used in understanding the disease-associated changes, results so far have omitted the WM even though WM activation has repeatedly been reported in healthy younger adults in recent fMRI studies. Here we applied three tasks targeting interhemispheric transfer at 3.0T to extend the WM fMRI research to clinical applications in AD-dementia. The study detected fMRI activation in the corpus callosal WM in 87% individuals with early AD and normal cognitive aging (NC), and a difference between AD and NC.

5316 Computer 90

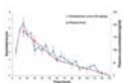

Etomidate anaesthesia for fMRI in mice revisited: Subcutaneous administration facilitates experimental procedures

Rebecca Klee[1], Thomas Mueggler[1], Andreas Bruns[1], Nicole Wyttenbach[1], Antonio Ricci[1], Rodolfo Gasser[1], Markus von Kienlin[1], and Basil Künnecke[1]

[1]Pharma Research and Early Development, Roche Innovation Center Basel, F. Hoffmann-La Roche Ltd, Basel, Switzerland

Etomidate has recently been proposed as a hypnotic for high-fidelity fMRI in mice. It largely preserves cerebrovascular autoregulation and basal perfusion, thus providing a large window for hemodynamic-based fMRI readouts. However, commercially available formulations of etomidate come at low concentration and are suitable only for intravenous infusion, hence resulting in large infusion volumes and difficult procedures in small rodents. Here, we demonstrate that fMRI-compatible anaesthesia can be readily achieved upon subcutaneous administration of etomidate formulated as aqueous solution. We further propose to substitute etomidate with its short-acting analogue cyclopropyl-methoxycarbonyl metomidate to avert long recovery times due to subcutaneous depot formation.

5317 Computer 91

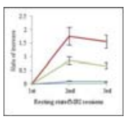

Resting state connectivity analysis for normal and abnormal physiology conditions during fMRI data acquisition

Sun Young Chae[1,2], Geun Ho Im[3,4], Jisu Hong[1,5], Moon-Sun Jang[3,4], Hyunjin Park[1,5], and Jung Hee Lee[1,2,4]

[1]Center for Neuroscience Imaging Research, Institute for Basic Science (IBS), Suwon, Korea, Republic of, [2]Department of Health Sciences and Technology, SAIHST, Sungkyunkwan University, Seoul, Korea, Republic of, [3]Center for Molecular and Cellular Imaging, Samsung Biomedical Research Institute, Seoul, Korea, Republic of, [4]Department of Radiology, Samsung Medical Center, Sungkyunkwan University School of Medicine, Seoul, Korea, Republic of, [5]Department of Electronic, Electrical and Computer Engineering, Sungkyunkwan University, Suwon, Korea, Republic of

Unlike blood oxygen level dependent (BOLD)-fMRI, accurate physiologic adjustment for subjects during rs-fMRI data acquisition does not seem to be critical for the quality of the final data. In this study, we performed rs-fMRI measurements during normal and abnormal physiological conditions and analyzed betweenness centrality (BC), degree centrality (DC) and eigenvector centrality (EC). In this study, we demonstrate that physiologic conditions seem to have a direct effect on the rs-fMRI result. Thus, the results of our current study suggest that normal physiologic condition should be maintained for rs-fMRI data acquisition.

5318 Computer 92

The Gut-Brain-Axis: from gut feelings to gut memory

Deepika Bagga[1,2], Karl Koschutnig[2], Bhageshwar Mohan[3], Christoph Stefan Aigner[4], Johanna Reichert[1,2], Peter Holzer[2,5], and Veronika Schöpf[1,2]

[1]Institute of Psychology, University of Graz, Graz, Austria, [2]BioTechMed, Graz, Austria, [3]Institute of Chemical Engineering, Graz University of Technology, Graz, Austria, [4]Institute of Medical Engineering, Graz University of Technology, Graz, Austria, [5]Institute of Experimental and Clinical Pharmacology, Medical University of Graz, Graz, Austria

The present study investigated the effect of probiotic administration on emotional memory in healthy volunteers using fMRI. The preliminary results showed that probiotic intake for 4-5 weeks improved the response accuracy significantly and this was accompanied by a decrease in the neural activity in the brain areas associated with emotions and memory formations. This decrease was more prominent for unpleasant stimuli as compared to neutral stimuli. Considering the scarce literature on gut microbiota and brain interactions in humans, our findings might provide a gateway for further understanding of mechanisms of gut-brain interactions and their effect on emotions and memory.

5319 Computer 93

summa cum laude

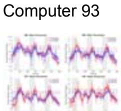

BOLD Signal Changes in Spinal Cord with Hypercapnia

Benjamin N Conrad[1,2], Satoshi Maki[1], Jennifer M Watchmaker[3], Bailey A Box[1], Robert L Barry[4,5], Seth A Smith[1,3], and John C Gore[1,3]

[1]Institute of Imaging Science, Vanderbilt University, Nashville, TN, United States, [2]Neuroscience, Vanderbilt University, Nashville, TN, United States, [3]Radiology and Radiological Sciences, Vanderbilt University Medical Center, Nashville, TN, United States, [4]Radiology, Athinoula A. Martinos Center for Biomedical Imaging, Massachusetts General Hospital, Charlestown, MA, United States, [5]Radiology, Harvard Medical School, Boston, MA, United States

A hypercapnic gas challenge was used to demonstrate blood oxygenation level dependent (BOLD) signal changes in the cervical spinal cord, and the sensitivities of two functional acquisition sequences (standard single shot (GE-EPI) and 3D multishot (3D-EPI) gradient echo EPI) were compared. Results indicated that both acquisitions were able to detect signal changes of about 1% in gray matter and higher values in white matter confirming that BOLD effects in the cord are reliable. The 3D multishot sequence exhibited higher temporal SNR and reduced susceptibility distortions, making it an attractive option for BOLD fMRI in the spinal cord.

5320 Computer 94

fMRI-based brain responses to bitter and sucrose gustatory stimulation for nutrition research in the minipig model

Nicolas Coquery[1], Paul Meurice[1], Régis Janvier[1], Eric Bobillier[1], Stéphane Quellec[2], Hervé Saint-Jalmes[3], and David Val-Laillet[1]

[1]UR1341 ADNC, INRA, Saint-Gilles, France, [2]UR TERE, IRSTEA, Rennes, France, [3]UMR1099, INSERM, Rennes, France

The minipig model is of high interest for brain research in nutrition and associated pathologies considering the similarities to human nutritional physiology, brain structures and functions[1,2] . In the context of a gustatory stimulation paradigm, fMRI can provide crucial information about the sensory, cognitive and hedonic integration of exteroceptive stimuli in healthy and pathological nutritional conditions. To date, this is the first intent to describe gustatory stimulation in minipigs using fMRI.

5321 Computer 95

Deciphering the functional projections of the lateral hypothalamus with optogenetic fMRI

Jan Kevin Schluesener[1] and Xin Yu[1]

[1]Translational Neuroimaging and Neural Control Group, High-Field Magnetic Resonance Department, Max-Planck Institute for Biological Cybernetics, Tuebingen, Germany

The lateral hypothalamus (LH) is a central node of the brain to mediate brain states. It is comprised of highly heterogeneous neuronal populations and diverse projections. It remains elusive how different neuronal LH subdivisions mediate the brain state. Here, we developed an optogenetic method to map LH functional projections and investigate functional connectivity upon LH activation. Optical stimulation of the LH can directly activate the preoptic area, central thalamus and the subiculum area, and increase the cortical resting-state correlation. This work makes it possible to further target different LH neuronal populations and decipher cell-type specific functional projections.

Electronic Poster

fMRI Analysis

Exhibition Hall — Thursday 9:15 - 10:15

5322 Computer 1

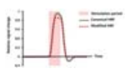

Modeling the hemodynamic response function in rat fMRI study

Chen-You Huang[1], Chiun-Wei Huang[2], Shao-Chieh Chiu[2], Wu-Chung Shen[1], and Shin-Lei Peng[1]

[1]Department of Biomedical Imaging and Radiological Science, China Medical University, Taichung, Taiwan, [2]Center for Advanced Molecular Imaging and Translation, Chang Gung Memorial Hospital

Previous rat fMRI studies have been analyzed by statistical parametric mapping (SPM) but the SPM is designed for human fMRI studies. In this study, we examine whether the default settings including delay time, statistic methods and hemodynamic response function (HRF) shape in SPM can directly transform to rat fMRI studies. Results show statistic methods do not affect the mapping of brain activation. However, the delay time and HRF shapes have significant impacts on extracting brain activation, especially in primary somatosensory cortex and striatum. We therefore suggest the HRF should be optimized to approach better sensitivity in other rat fMRI studies.

5323 Computer 2

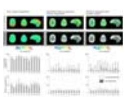

Accounting for serial correlation in GLM residuals during resting state fMRI nuisance regression

Molly G Bright[1,2], Christopher R Tench[2], and Kevin Murphy[3]

[1]Sir Peter Mansfield Imaging Centre, School of Medicine, University of Nottingham, Nottingham, United Kingdom, [2]Division of Clinical Neurosciences, School of Medicine, University of Nottingham, United Kingdom, [3]CUBRIC, School of Physics and Astronomy, Cardiff University, United Kingdom

In resting-state fMRI nuisance regression, a General Linear Model (GLM) is employed to fit and remove the variance associated with a noise model. Without "ground-truth" knowledge, the noise models must be tested and improved to obtain accurately cleaned datasets without "throwing the baby out with the bath-water." Valid statistical inference on a GLM fit requires normally-distributed residuals, which is not the case when intrinsic brain fluctuations are present. We demonstrate that existing pre-whitening tools can be appropriately applied to account for serial autocorrelation in resting-state fluctuations during nuisance regression, allowing statistical differentiation of true and simulated noise models.

5324 Computer 3

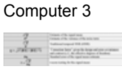

Evaluating the impact of SNR, sampling interval and number of samples on functional sensitivity using the General Linear Model framework

Nadège Corbin[1], Guillaume Flandin[1], Oliver Josephs[1], Nick Todd[2], Karl J Friston[1], and Martina F Callaghan[1]

[1]Wellcome Trust Centre for Neuroimaging, UCL Institute of Neurology, London, United Kingdom, [2]Department of Radiology, Brigham and Women's Hospital, Harvard Medical School, Boston, MA, United States

In fMRI, functional sensitivity is dictated by many factors related to the data acquisition scheme, most notably image SNR, temporal resolution and the number of samples acquired. Advanced acquisition techniques, such as 2D multiband imaging, are popular for fMRI studies because they afford the possibility of greatly increasing temporal resolution allowing more samples to be acquired per unit time, but at the cost of image SNR and increased temporal auto-correlations. This study uses the General Linear Model framework to disentangle these effects and determine the net impact on functional sensitivity, as parameterised via temporal SNR and t-scores.

5325 Computer 4

Spatial Adaptive Kernel Canonical Correlation Analysis

Zhengshi Yang[1], Xiaowei Zhuang[1], Tim Curran[2], Richard Byrd[2], Virendra Mishra[1], Karthik Sreenivasan[1], and Dietmar Cordes[1,2]

[1]Cleveland Clinic Lou Ruvo Center for Brain Health, LAS VEGAS, NV, United States, [2]University of Colorado Boulder, CO, United States

Spatially adaptive multivariate methods were applied in fMRI activation analysis to alleviate low sensitivity in commonly used Gaussian smoothing single voxel analysis. Usually these methods require constraint to avoid the curse of high degrees of freedom. We have developed a novel spatially adaptive kernel canonical correlation analysis method, which does not require constraint and has superior performance compared to other methods.

5326 Computer 5

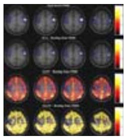

Value of frequency domain resting state fMRI metrics ALFF & fALFF in the assessment of brain tumor induced neurovascular uncoupling

Shruti Agarwal[1], Hanzhang Lu[1], and Jay J. Pillai[1]

[1]Russell H. Morgan Department of Radiology and Radiological Science, Johns Hopkins University School of Medicine, Baltimore, MD, United States

In brain tumor patients, coupling between neuronal activity and BOLD response is often disrupted (known as neurovascular uncoupling (NVU)), resulting in dangerous underestimation of true extent of eloquent cortex in pre-surgical planning. With increasing popularity of resting state fMRI (rsfMRI) for presurgical mapping, it becomes critical to investigate effects of NVU in rsfMRI. A recent study demonstrated that tumor-related NVU can impact resting state functional connectivity within the sensorimotor network as assessed using a seed-based correlation analysis (SCA).2 We now explore whether NVU may also affect the rsfMRI frequency domain metrics ALFF (amplitude of low-frequency fluctuation) & fALFF (fractional ALFF).

5327 Computer 6

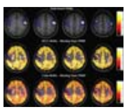

The resting state fMRI regional homogeneity (ReHo) metrics KCC-ReHo & Cohe-ReHo are valid indicators of tumor-related neurovascular uncoupling

Shruti Agarwal[1], Haris I. Sair[1], and Jay J. Pillai[1]

[1]Russell H. Morgan Department of Radiology and Radiological Science, Johns Hopkins University School of Medicine, Baltimore, MD, United States

The validity of BOLD fMRI in pre-surgical planning may be severely compromised due to disruption of the normal coupling between neural activity and the consequent microvascular blood flow response (neurovascular uncoupling, or NVU). The effects of brain tumor-induced NVU on resting state BOLD fMRI (rsfMRI) have been previously described through seed-based correlation analysis (SCA). In this study, we evaluated regional homogeneity of resting state fMRI data using Kendall's coefficient of concordance (KCC-ReHo) & Coherence (Cohe-ReHo) metrics and compared these results with those of “gold standard”motor task-based (tbfMRI) activation to determine their effectiveness in detecting NVU in the sensorimotor network.

5328 Computer 7

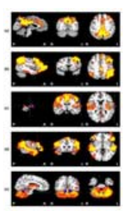

Reproducibility of Functional Connectivity Measures acquired at different times of day

Jia Fan[1], Ernesta Meintjes[1,2], and A Alhamud[1,2]

[1]MRC/UCT Medical Imaging Research Unit, Department of Human Biology, University of Cape Town, Cape Town, South Africa, [2]Cape Universities Body Imaging Centre (CUBIC-UCT), Cape Town, South Africa

Resting state fMRI (rs-fMRI) used to detect and evaluate resting state functional connectivity (RSFC) in both healthy subjects and patients. However, the reproducibility of rs-fMRI may be influenced by the time of day when the scan is performed. In this work, we investigated the reproducibility of resting state networks by comparing scans performed in the morning (immediately after the scanner was switched on) and again in the late afternoon (after all daily scans were done) on six different days. Our results showed higher RSFC in afternoon scans in 5 regions within 5 networks .

5329 Computer 8

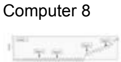

Investigating the feasibility of classifying independent components in resting state BOLD fMRI with sparse paradigm free mapping

Cesar Caballero-Gaudes[1], Oihane Ezama[1], Manuel Delgado-Alvarado[2,3], and Maria Cruz Rodriguez-Oroz[1,4,5,6]

[1]Basque Center of Cognition, Brain and Language, Donostia - San Sebastian, Spain, [2]Biodonostia Health Research Institute, Donostia-San Sebastian, Spain, [3]Neurology Department, University Hospital Marqués de Valdecilla, Santander, Spain, [4]Neuroscience Area, Biodonostia Health Research Institute, Donostia-San Sebastian, Spain, [5]Centro de Investigacion Biomedicas en Red Enfermedades Neurodegenerativas (CIBERNED), Institute Carlos III, Spain, [6]Ikerbasque. Basque Foundation for Science, Bilbao, Spain

This work proposes a novel method for the classification of ICs in resting-state fMRI data based on sparse paradigm free mapping (PFM), a deconvolution approach that enables detecting BOLD events without prior information of their timing. This approach uses a single temporal feature, the significance of the deconvolution model estimated with PFM. Our results demonstrate that despite its simplicity this approach achieves similar sensitivity in classifying the neuronal-related BOLD components to the more complex classification method of ICA-AROMA, but with less specificity in classifying noise components. In addition, it can improve the identification of physiological noise components.

5330 Computer 9

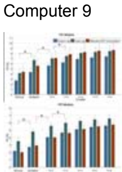

Region-specific modeling of heart rate and respiratory volume signal contributions in whole-brain high-spatial resolution resting-state fMRI at 7 Tesla

Joana Pinto[1], Sandro Nunes[1], Marta Bianciardi[2], Afonso Dias[1], Luis Miguel Silveira[3], Lawrence Wald[2], and Patricia Figueiredo[1]

[1]Institute for Systems and Robotics - Lisbon and Department of Bioengineering, Instituto Superior Tecnico, Universidade de Lisboa, Lisbon, Portugal, [2]Department of Radiology, A.A. Martinos Center for Biomedical Imaging, MGH and Harvard Medical School, Boston, MA, United States, [3]INESC-ID and Department of Electrical and Computer Engineering, Instituto Superior Tecnico, Universidade de Lisboa, Lisbon, Portugal

Several strategies have been proposed for correcting physiological noise in rs-fMRI, including different models of respiratory volume (RV) and heart rate (HR) effects. Although group-level model optimization has often been employed, it has been reported that these effects are highly variable across subjects and brain regions. Here, we investigated the impact of optimizing the time-lags of RV and HR physiological noise contributions at different levels of specificity in 7 Tesla rs-fMRI. We found that a regional optimization based on a clustering approach taking into account the time-lags' individual spatial variability explained more fMRI signal variance than group or subject-based optimizations.

5331 Computer 10

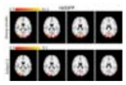

A Group level analysis to compare characteristics of balanced SSFP fMRI with non-balanced techniques

Arash Foroudi Ghasemabadi[1], Mahdi Khajehim[1], Vahid Malekian[1], and Abbas Nasiraei Moghaddam[1,2]

[1]Biomedical Engineering, Amirkabir University of Technology (Tehran Polytechnic), Tehran, Iran, [2]School of Cognitive Sciences, Institute for Research in Fundamental Sciences (IPM), Tehran, Iran

Non-balanced SSFP has been recently suggested as a viable approach for T2-weighted SSFP fMRI. Compared to bSSFP, it entirely eliminates the problematic banding artifacts. However, its sensitivity has not yet been systematically investigated. In this study, fixed effects group analysis was performed on balanced and non-balanced SSFP data from seven healthy subjects in 7 T. We found that, group activation maps are generally similar, besides, mean z-values for the two methods are not significantly different. The obtained results suggest that the newly developed nbSSFP method is a viable approach to substitute bSSFP in high resolution fMRI studies.

5332 Computer 11

Relationship of seed-based connectivity and amplitude of low-frequency fluctuations in resting-state functional MRI

Parul Chachra[1], Suresh Emmanuel Joel[1], Rakesh Mullick[1], and Radhika Madhavan[1]

[1]GE Global Research, Bangalore, India

Resting-state functional magnetic resonance imaging (rs-fMRI) has been suggested to provide key understanding of large-scale network organization in human brain. Harnessing rs-fMRI, we have examined the relationship of seed-based connectivity (SBC) with amplitude of low-frequency fluctuations (ALFF) and fractional ALFF (fALFF). We recorded rs-fMRI from healthy volunteers and measured regional ALFF, fALFF and SBC. We demonstrate that ALFF and fALFF were weakly correlated to SBC and the correlation was specifically stronger for selected networks. Our results suggest that ALFF/fALFF and SBC may be driven by the same underlying factors and thus co-vary in a similar manner.

5333 Computer 12

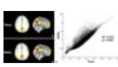

Group level property of functional correlation tensor can reveal default mode network

Yang Fan[1], Jing Wang[2], Bingjiang Lyu[3], Bing Wu[1], and Zhenyu Zhou[1]

[1]MR Research China, GE Healthcare, Beijing, People's Republic of China, [2]Center for Medical Device Evaluation, CFDA, Beijing, People's Republic of China, [3]Center for MRI Reserch, Peking University, Beijing, People's Republic of China

Recently, a novel technique was proposed directly integrated resting-state fMRI and DTI to construct a local spatio-temporal correlation tensor from resting state fMRI data. In individual level, the functional correlation tensor can be used to tract white matter fibers. However, there is no knowledge of group level property of functional correlation tensor. In the present study, group averaged tensorial properties (e.g. FA and trace) of functional correlation tensor were investigated. It is shown that the group averaged trace map of functional tensor can reveal default mode network. And our results are consistent across different datasets.

5334 Computer 13

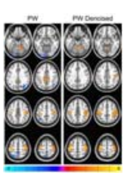

A Novel Multiband Multi-Echo Simultaneous ASL/BOLD Sequence for Task-Based fMRI

Alexander D. Cohen[1], Andrew S. Nencka[1], and Yang Wang[1]

[1]Radiology, Medical College of Wisconsin, Milwaukee, WI, United States

A novel multiband multi-echo ASL sequence was employed to collect high-resolution, whole-brain simultaneous ASL/BOLD fMRI data. Four echoes were collected allowing multi-echo independent component analysis (ME-ICA) denoising to be applied to both the BOLD and ASL data. Subjects performed a finger-tapping task, and activation was compared between datasets with and without denoising. The multi-echo denoised BOLD dataset detected the most activation compared to activation calculated using the combined echoes and only the second echo. Additional activation was observed for the denoised perfusion-weighted data compared to the original perfusion-weighted data. There was also less spurious negative activation for the PWDN data.

5335 Computer 14

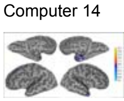

Quantitative data-driven analysis for resting-state fMRI data reveals functional connectivity differences in epilepsy patients

Yanlu Wang[1,2], Ivanka Savic Berglund[3], Martin Uppman[2], and Tie-Qiang Li[1,2]

[1]Medical Radiation and Nuclear Medicine, Karolinska University Hospital, Stockholm, Sweden, [2]Department of Clinical Sciences, Intervention and Technology, Karolinska Institute, Stockholm, Sweden, [3]Department of Women's and Children's Health, Karolinska University Hospital, Stockholm, Sweden

Quantitative data-driven analysis (QDA) has shown to be robust and intuitive method to extract functional connectivity information from resting-state fMRI data for group-level comparison. In this study, the QDA method is applied to patients suffering from epileptic seizures. Multiple brain regions of significant (p<0.01) differences were detected. The results are consistent with published works in temporal lobe epilepsy and frontal lobe epilepsy in literature using invasive methods. All brain regions experience down-regulation in functional connectivity in epilepsy patients compared to healthy control subjects.

Computer 15

A New Method of HRF Estimation Containing High Frequency Content

Xiaowei Zhuang[1], Zhengshi Yang[1], Virendra Mishra[1], Karthik Sreenivasan[1], and Dietmar Cordes[1,2]

5336

[1]Cleveland Clinic Lou Ruvo Center for Brain Health, Las Vegas, NV, United States, [2]University of Colorado Boulder, Boulder, CO, United States

A new HRF estimation method was introduced to improve the accuracy in recovering HRFs with wider frequency range. This non-smooth optimization problem was solved via BFGS technique. Results from simulated data demonstrate the accuracy and reliability of this new method in recovering HRF. Results from an event-related fMRI dataset further demonstrate the ability of the proposed method in capturing the variation of HRFs across different brain regions and subject populations.

5337 Computer 16

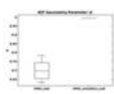

Solution for Cluster Failure: Simple Method to Obtain Spatially Smooth Residuals with nearly Gaussian Auto-Correlation Functions

Kaundinya Gopinath[1], Simon Lacey[2], Randall Stilla[2], Venkatagiri Krishnamurthy[1], and Krish Sathian[2]

[1]Department of Radiology & Imaging Sciences, Emory University, Atlanta, GA, United States, [2]Department of Neurology, Emory University

Recent studies have shown that cluster-wise family-wise error rate (FWE) corrected inferences made in parametric statistical methods based fMRI studies over the past couple of decades were invalid due to incorrect these methods incorrectly specifying that spatial auto-correlation functions (sACF) of fMRI data had a gaussian shape. In this study we proposed a method to obtain fMRI inferential statistic residuals with gaussian sACF. Results show that this method substantially increases the detection power of group-level inference tests while not significantly changing the voxelwise statistic maps. Additionally it makes inferences based on assumption of gaussian sACF valid again.

5338 Computer 17

Non-linear Realignment Using Minimum Deformation Averaging for Single-subject fMRI at Ultra-high Field

Saskia Bollmann[1], Steffen Bollmann[1], Alexander Puckett[2], Andrew Janke[1], and Markus Barth[1]

[1]Centre for Advanced Imaging, The University of Queensland, Brisbane, Australia, [2]Queensland Brain Institute, The University of Queensland, Brisbane, Australia

Motion dominates the contribution to variance in fMRI time series and it is therefore important to account for this variability correctly. Currently, most correction schemes use a rigid body realignment procedure, but interactions with magnetic field inhomogeneities and physiological fluctuations lead to non-linear deformations. Non-linear realignment increased spatial resolution by harvesting sub-voxel shift information with little impact on tSNR. Activated regions showed a better delineation with a clear match to anatomical features. Importantly, our proposed method can be applied to already acquired fMRI data sets to improve spatial conspicuity.

5339 Computer 18

Prior Knowledge Oriented Independent Component Analysis (pICA) for Component Identification in Functional MRI

Gengyan Zhao[1], Vivek Prabhakaran[1,2], Elizabeth M. Meyerand[1,3], and Rasmus Birn[1,4]

[1]Medical Physics, University of Wisconsin - Madison, Madison, WI, United States, [2]Radiology, University of Wisconsin - Madison, WI, United States, [3]Biomedical Engineering, University of Wisconsin - Madison, WI, United States, [4]Psychiatry, University of Wisconsin - Madison, WI, United States

Independent component analysis (ICA), as a data-driven signal decomposition method, has been widely used in fMRI. Sources of the measurement can be separated according to the rule of maximum independency, but it usually cannot naturally generate a source which is highly correlated with the signal we are interested in. To solve this problem, we propose a new method, prior knowledge oriented ICA (pICA), to drive ICA to a set of sources with the SOI among them. Experiments of simulation and fMRI show this new method has higher specificity and accuracy in identifying the SOI and its corresponding spatial map.

5340 Computer 19

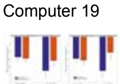

Power law exponent analysis of the resting state BOLD signal as a potential measure of excitatory-inhibitory balance in Alzheimer's disease

Niharika Gajawelli[1,2], Bradley Voytek[3], Danny JJ Wang[1], Berislav Zlokovic[4], Arthur W Toga[1], Meng Law[1], John Morris[5], Tammie Benzinger[6], and Judy Pa[1]

[1]Stevens Neuroimaging and Informatics Institute, University of Southern California, Los Angeles, CA, Los Angeles, CA, United States, [2]Biomedical Engineering, University of Southern California, Los Angeles, CA, [3]Department of Computational Cognitive Science and Neuroscience, University of California, San Diego, CA, [4]Zilkha Neurogenetic Institute, University of Southern California, Los Angeles, CA, [5]Knight Alzheimer Disease Research Center, Washington University, St. Louis, MO, [6]Department of Radiology and Neurological Surgery, Washington University, St. Louis, MO

The power spectrum of the functional MRI (fMRI) signal is 1/f-distributed: the power (P) is proportional to inverse frequency (1/f) with scaling factor (B), the power law exponent (PLE). The PLE, in electrophysiology, may reflect the relative balance of excitation and inhibition. Here, we examine the PLE of fMRI power spectrums in the default mode network in older adults with a clinical dementia rating score of 0, 0.5, or 1. PLE analysis may help us understand the potential regional inhibitory/excitatory balance of underlying architecture, given that the BOLD signal is a surrogate marker of local field potentials and post-synaptic processes.

5341 Computer 20

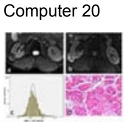

Subtypes Differentiation of Renal Cell Carcinoma (<4cm) Using Whole-volume Histogram Analysis of Apparent Diffusion Coefficient Maps

Haojie Li[1], Yonghong Hao[1], Daoyu Hu[1], and Zhen Li[1]

[1]Radiology, Tongji Hospital, Tongji Medical College, Huazhong University of Science and Technology, Wu Han, People's Republic of China

Because of different subtypes of RCC have different prognoses and respond differently to targeted therapies, accurate identification of the specific diagnosis prior to treatment is important. In this study, our results demonstrate that the combination of r-FOV DWI and the whole-lesion histogram analysis method may help in the interpretation of DWI of small renal masses and determine the optimal ADC parameter for quantitative assessment. The 75th percentile ADC value was more reliable than other histogram parameter values in distinguishing clear cell from non-clear cell RCCs with high sensitivity and specificity, potentially improving the accuracy of pretreatment diagnosis and selection of clinical therapy.

5342 Computer 21

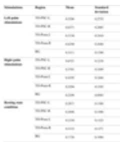

Detection of Functional Activity in Somatosensory Pathways Using Tactile Stimulations

Xi Wu[1,2], Zhipeng Yang[1,2], Stephen K. Bailey[3], Jiliu Zhou[1], Laurie C. Cutting[4,5], John C. Gore[2,5,6], and Zhaohua Ding[2,6,7]

[1]Department of Computer Science, Chengdu University of Information Technology, Chengdu, People's Republic of China, [2]Vanderbilt University Institute of Imaging Science, Nashville, TN, United States, [3]Brain Institute, Vanderbilt University, Nashville, TN, United States, [4]Vanderbilt Kennedy Center, Vanderbilt University, Nashville, TN, United States, [5]Department of Radiology and Radiological Science, Vanderbilt University Medical School, Nashville, TN, United States, [6]Department of Biomedical Engineering, Vanderbilt University, Nashville, TN, United States, [7]Department of Electrical Engineering and Computer Science, Vanderbilt University, Nashville, TN, United States

Functional magnetic resonance imaging has been widely used in measuring functional connectivity between cortical regions, but it has not been well-established in white matter to date. While we have previously demonstrated that resting state BOLD signals exhibit structure-specific correlations, suggesting that neural activities may be encoded in white matter BOLD signals as well, in this study we further confirm that functional stimulations can induce activities in relevant white matter pathways.

5343 Computer 22

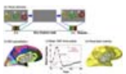

Characterization of the Gray Matter Hemodynamic Response Function with High-Resolution Functional MRI

Amanda J. Taylor[1], Jung Hwan Kim[1], and David Ress[1]

[1]Neuroscience, Baylor College of Medicine, Houston, TX, United States

Functional magnetic resonance imaging (fMRI) measures the hemodynamic response to neural activation. Brief periods (2 s) of multisensory neural stimulation evoke the hemodynamic response function (HRF) across the majority of cerebral cortex. High (2 mm) spatial resolution enables the characterization of the HRF restricted to the gray matter, avoiding partial volume effects into nearby white matter and vascular tissue. HRF amplitude and timing measurements from eight healthy subjects showed temporal stability and stereotypical spatial amplitude patterns, suggesting that this method could be adapted to diagnose pathologies associated with abnormal neurovascular coupling.

5344 Computer 23

Confound Suppression in Resting State fMRI using Sliding Windows and Running Mean

Cameron Trapp[1], Kishore Vakamudi[1], and Stefan Posse[1,2,3]

[1]Neurology, University of New Mexico, Albuquerque, NM, United States, [2]Physics and Astronomy, University of New Mexico, [3]Electrical Engineering, University of New Mexico

We analytically investigate the characteristics of a recently developed sliding window methodology designed for real time analysis of resting state connectivity. The suppression of various types of confounds is investigated both in this analytical framework and numerically. It is shown that this methodology not only acts as a high pass filter and denoiser, but behaves as a model free despiking and confound suppression tool.

5345 Computer 24

Inflated false positive rates in fMRI depend on the voxel size of normalized images

Karsten Mueller[1], Jöran Lepsien[1], Harald E. Möller[1], and Gabriele Lohmann[2,3]

[1]Max Planck Institute for Human Cognitive and Brain Sciences, Leipzig, Germany, [2]Department of Biomedical Magnetic Resonance, University Hospital Tübingen, Tübingen, Germany, [3]Magnetic Resonance Center, Max Planck Institute for Biological Cybernetics, Tübingen, Germany

Recently, Eklund et al published a manuscript discussing the issue of false positive results in functional MRI (fMRI) using the most common software packages. In their analysis, image upscaling was performed in fMRI preprocessing after registering images into a standard space (normalization). We show that the degree of image upscaling used for normalization impacts the statistical results when using the Gaussian Random field approach. A higher upscaling generally leads to smaller p-values increasing the number of false positive clusters. This result is quite troubling because statistical inference should not depend on a preprocessing parameter which can be chosen ad libitum.

Electronic Poster

fMRI: Basic Neuroscience Applications: Non-Connectivity Based

Exhibition Hall — Thursday 9:15 - 10:15

5346 Computer 25

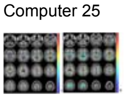

Voxel-level comparison of regional neural activity in patients with type 2 diabetes mellitus

Dong Zhang[1], Changzheng Shi[1], Rong Ma[1], Zhongping Zhang[2], and Liangping Luo[1]

[1]Medical Imaging Center, The First Affiliated Hospital of Jinan University, Guangzhou, People's Republic of China, [2]MR Research China, GE Healthcare, Beijing

People with high risk of diabetes exhibited decreased ReHo in right temporal lobes, left pallidum/ lenticular nucleus/insula/Heschl gyrus and left cingulate cortex and declined fALFF in left Heschl gyrus, left supramarginal gyrus and left cingulate cortex, which is consistent with type 2 diabetes mellitus (T2DM) patients. These abnormal regions may be regarded as the endophenotype of T2DM in resting-state BOLD-fMRI.

5347 Computer 26

Dyslexia therapy customization based on dorsal-ventral pathway representation

Sunita Gudwani[1], Senthil Kumaran[1], Rajesh Sagar[2], SN Dwivedi[3], and Naranamangalam R Jagannathan[1]

[1]Department of NMR and MRI Facility, All India Institute of Medical Sciences, New Delhi, India, [2]Department of Psychiatry, All India Institute of Medical Sciences, New Delhi, India, [3]Department of Biostatistics, All India Institute of Medical Sciences, New Delhi, India

Reading necessitates skill mastering of phonological (sound to letter), orthographic (knowledge of letter identities, position), and semantic (words meaning) processing requiring optimal interface of ventral-dorsal routes. Dyslexia, a developmental reading disorder, is an umbrella term with heterogeneity of behavioral deficits constrains the management efficiency. Persistent deficits lead to emotional, academic, social consequences necessitating evidence-based interventions. The study was planned on neurobiological-model to customize the therapeutic management. Dorsal pathway (BOLD activation) reorganization associated with improvement in reading rate, accuracy, spelling and writing flow suggest neurobiological normalization in dyslexics observed post-remediation on comparing therapy group with non-therapy and age-matched typical readers.

5348 Computer 27

Altered hemodynamic response in visual cortex observed in high-school American football players

Trey Edward Shenk[1], Meghan Robinson[2], and Thomas Talavage[3]

[1]Electrical and Computer Engineering, Purdue University, West Lafayette, IN, United States, [2]The Translational Research Center for TBI and Stress Disorders, VA Boston Healthcare System, Boston, MA, United States, [3]Purdue University, West Lafayette, IN, United States

There is growing concern that subconcussion could have an effect on the neural health of contact sports athletes. The hemodynamic response was measured and changes were observed in high school football athletes after exposure to impacts.

5349 Computer 28

Dexmedetomidine-induced CBF changes measured with Arterial Spin Labeling

Marta Vidorreta[1,2], Sihua Xu[3], Fan N Yang[3], Andrew McKinstry-Wu[4], Alexander Proekt[4], Brenna Shortal[4], Hengyi Rao[3], Max B Kelz[4], and John A Detre[1,2]

[1]Neurology, University of Pennsylvania, Philadelphia, PA, United States, [2]Radiology, University of Pennsylvania, Philadelphia, PA, United States, [3]Neurology, University of Pennsylvania, PA, United States, [4]Anesthesiology, University of Pennsylvania, PA, United States

Dexmedetomidine infusion was used to induce pharmacological unconsciousness akin to natural non-REM sleep, and brain resting-state activity changes were monitored using Arterial Spin Labeling and EEG recordings.

Our results confirm that functional changes associated with non-REM sleep in both centrencephalic and cortical structures can be monitored with ASL, revealing that selective regional CBF decreases are associated with the loss of consciousness, most significantly in the reticular activating system. The thalamic/cortical GM CBF ratio was also found to be a reliable marker of conscious state.

5350 Computer 29

Linear and non-linear BOLD effects in grip force execution are reproduced in observation

Letizia Casiraghi[1,2], Adnan AS Alahmadi [3,4], Karl J Friston [5], Claudia AM Gandini Wheeler-Kingshott[6,7,8], and Egidio D'Angelo [1,2]

[1]Department of Brain and Behavioral Sciences, University of Pavia, Pavia, Italy, [2]Brain Connectivity Center, C. Mondino National Neurological Institute, Pavia, Italy, [3]Department of Diagnostic Radiology, Faculty of Applied Medical Science, KAU, Jeddah, Saudi Arabia, [4]UCL Institute of Neurology, Queen Square MS center, University College London, London, United Kingdom, [5]UCL Institute of Neurology, Wellcome Trust Centre for Neuroimaging, University College London, United Kingdom, [6]Department of Brain and Behavioral Sciences, University of Pavia, Italy, [7]UCL Institute of Neurology, Queen Square MS Centre, University College London, London, United Kingdom, [8]Brain MRI 3T Mondino Research Center, C. Mondino National Neurological Institute, Pavia, Italy

In this pilot study, we investigated whether the non-linear BOLD response to varying grip force (GF) is reproduced when observing others performing the task. We used an fMRI squeezeball paradigm with two conditions: action execution (AE - subjects performed the task) and action observation (AO - subjects watched a video of the task). In both conditions, activations were detected in areas constituting the action execution-observation network and both areas evidenced linear and non-linear relations with the GF. These results indicate that action observation calls on the same context sensitive and high level processing necessary for execution.

5351 Computer 30

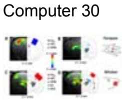

Modality specific thalamic activations in rat brain by fMRI

Basavaraju G Sanganahalli[1,2,3], Peter Herman[1,2,3], Garth J Thompson[1,3], and Fahmeed Hyder[1,2,3,4]

[1]Radiology and Biomedical Imaging, Yale University, New Haven, CT, United States, [2]Quantitative Neuroscience with Magnetic Resonance, Yale University, New Haven, CT, United States, [3]Magnetic Resonance Research Center, Yale University, New Haven, CT, United States, [4]Biomedical Engineering, Yale University, New Haven, CT, United States

The thalamus is a crucial node in cortical-subcortical circuits important for human emotion, cognition, and memory. While invasive studies in animals have revealed rich anatomical and functional separation of various thalamic nuclei, we sought to parse the different portions of the rat thalamus in relation to tactile (forepaw, whisker) and non-tactile (visual, olfactory) stimuli by high field fMRI (11.7T). We reproducibly detected BOLD activations of VPL, VPM, POM, dLGN, and MDT, where MDT activation is a novel indication of this structure's involvement during olfactory processing. These results have significance in understanding the role of both cortical-subcortical circuits during sensory integration.

5352 Computer 31

Acute effects of alcohol on brain perfusion monitored with 3D pseudo continuous arterial spin labeling(3D PCASL)

liang zhang[1] and jun chen[2]

[1]radiology, Renmin Hospital of Wuhan University, Wu Han, People's Republic of China, [2]Radiology, Renmin Hospital of Wuhan University, Wu Han, People's Re

Despite the fact that alcohol have impact on human brain function, the mechanism is not yet well understood. In order to detect the changes of blood perfusion i

---

5353 Computer 32

Potential changes of cerebral perfusion alterations in sensorineural hearing loss

Xiaomin Xu[1] and Gaojun Teng[2]

[1]Jiangsu Key Laboratory of Molecular Imaging and Functional Imaging Department of Radiology, Nanjing, People's Republic of China, [2]Jiangsu Key Laboratory of Molecular Imaging and Functional Imaging Department of Radiology

To explore the effect of hearing loss on cerebral perfusion, by using a whole brain arterial spin-labeling (ASL) MRI technique. We recruited 8 hearing loss patients and 6 healthy controls, and identified the cuneus with hypoperfusion in SHL patients which may provide new insights into SHL-associated psychological abnormalities.

5354 Computer 33

Alteration of intrinsic brain activity in children with obstructive sleep apnea syndrome revealed by resting-state functional magnetic resonance imaging

Shuangfeng Yang[1], Shengpei Wang[2,3,4,5], Yue Liu[1], Wenfeng Li[1], Hongbin Li[6], Jishui Zhang[7], Yang Fan[8], Hua Cheng[1], Huiguang He[2,3,4,5], and Yun Peng[1]

[1]Imaging Center, Beijing Children's Hospital, Capital Medical University, Beijing, People's Republic of China, [2]The State Key Laboratory of Management and Control for Complex Systems, Institute of Automation, Chinese Academy of Sciences, Beijing, People's Republic of China, [3]Research Center for Brain-inspired Intelligence, Institute of Automation, Chinese Academy of Sciences, Beijing, People's Republic of China, [4]Center for Excellence in Brain Science and Intelligence Technology, Chinese Academy of Sciences, Beijing, People's Republic of China, [5]Department of pattern recognition and intelligent system, University of Chinese Academy of Sciences, Beijing, People's Republic of China, [6]Otolaryngology, Beijing Children's Hospital, Capital Medical University, Beijing, People's Republic of China, [7]Neurology department, Beijing Children's Hospital, Capital Medical University, Beijing, People's Republic of China, [8]MR Research China, GE Healthcare, Beijing, People's Republic of China

Obstructive sleep apnea syndrome (OSAS) in adults has been demonstrated tobe associated with brain functional and structural changes. However, little is known about the changes in regional synchronization of spontaneous brain activity and spontaneous fluctuations in children with OSAS. In the present study, regional homogeneity (ReHo) analysis and amplitude of low-frequency fluctuation (ALFF) based on resting-state functional magnetic resonance imaging (MRI) were used to investigate spontaneous brain activity in children with OSAS compared with controls (CN). As a result, children with OSAS showed significant functional alterations of the cerebellum and temporal gyrus in children with OSAS.

5355 Computer 34

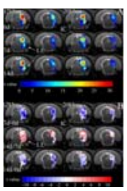

Transient reduction in auditory midbrain responses following acute noise exposure

Condon Lau[1], Eddie Wong[2], Woody Ho[1], Bin Yang[3], and Ed Wu[2,4]

[1]Department of Physics and Materials Science, City University of Hong Kong, Kowloon, Hong Kong, [2]Department of Electrical and Electronic Engineering, The University of Hong Kong, Hong Kong, [3]Department of Radiology, Children's Hospital of Fudan University, Shanghai, People's Republic of China, [4]Laboratory of Biomedical Imaging and Signal Processing, The University of Hong Kong, Hong Kong

Noise pollution can significantly affect sound processing, even without causing hearing loss. In this study, adult rat subjects are exposed to 100 dB sound level noise for 15 minutes. Functional magnetic resonance imaging (fMRI) and auditory brainstem response (ABR) testing with sound stimulation are performed before, 7 days after, and 14 days after exposure. ABR results show no significant threshold elevation, indicating no significant abnormalities in and near the ear. fMRI results show significant response reductions in the auditory midbrain 7 days after exposure. This suggests transient changes in central auditory gain following acute noise exposure.

5356 Computer 35

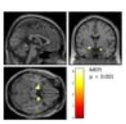

Multi-Echo EPI improves olfaction-related brain activation

Sonja Blankenagel[1,2], Ana Beatriz Solana[3], Brice Fernandez[4], Christoph Hofstetter[5], Andreas Dunkel[5], Thomas Hofmann[5], Hans Hauner[6,7], and Jessica Freiherr[1,2]

[1]Fraunhofer Institute for Process Engineering and Packaging (IVV), Freising, Germany, [2]Diagnostic and Interventional Neuroradiology, RWTH Aachen University, Aachen, Germany, [3]GE Global Research, Munich, Germany, [4]GE Healthcare, Orsay, France, [5]Food Chemistry and Molecular Sensory Science, Technical University of Munich, Freising, Germany, [6]ZIEL Institute for Food and Health, Clinical Nutritional Medicine, Technical University of Munich, Munich, Germany, [7]Institute of Nutritional Medicine, Klinikum rechts der Isar, Technical University of Munich, Munich, Germany

Multi−echo planar imaging (MEPI) was explored regarding its ability to overcome the limitations of conventional EPI imaging in studies related to olfaction. MEPI offers great sensibility even in brain regions, which are affected by susceptibility artifacts in EPI imaging. Five subjects were scanned using an event-related olfactory task with both sequences. The subsequent comparison shows that three echoes MEPI has advantages regarding olfaction-related brain activation compared to single echo EPI.

5357 Computer 36

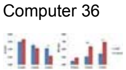

Working memory improved by abacus training in Chinese children: an fMRI study utilizing a spatial n-back task

Chunjie Wang[1], Jian Weng[1], Yuqiu Liu[2], Hui Zhou[1], and Feiyan Chen[1]

[1]Department of Physics, Zhejiang University, Hangzhou, People's Republic of China, [2]Department of Psychology, Zhejiang University, Hangzhou, People's Republic of China

To examine whether abacus training improves working memory (WM), sixty-four children were randomly assigned into two groups, matched for intelligence. One group received abacus training for five years while the other group had no any abacus experience. WM was measured by a n-back task. The results showed that children with training were more accurate and faster than their peers. They also had greater activation and functional connectivity in the frontoparietal regions. The findings suggest that AMC training may be an effective method to improve WM in school children, which may have implications to help individuals with cognitive deficits.

5358 Computer 37

Audio-motor interactions during musical playing with an external timing reference

Shu-Chi Pai[1], Ying-Hua Chu[1], Hui-Chuan Chang[2], and Jo-Fu Lin[1]

[1]Institute of Biomedical Engineering, National Taiwan University, Taipei, Taiwan, Taipei, Taiwan, [2]College of Humanities and Social Sciences, Taipei Medical University, Taipei, Taiwan

Previous studies have demonstrated brain activation patterns during musical playing. However, while musical playing with multiple sources of auditory inputs is essential for musical practices and group performance, it is less understood. By using an MR-compatible piano keyboard, the present study compared musical playing with or without acoustic feedback or external timing reference. Functional MRI contrasts showed BOLD signal increase in bilateral Superior Temporal Gyrus and BA 42 during musical playing with an external timing reference, which indicates a neuronal processing pattern relating to the coordination of multiple auditory inputs.

5359 Computer 38

Characteristics of brain spontaneous neuronal activity in chronic alcoholics using different resting-state fMRI algorithm

Yilin Zhao[1], Jun Chen[1], and Hui Lin[2]

[1]Radiology, Renmin Hospital of Wuhan University, Wuhan, People's Republic of China, [2]GE Healthcare, GE MR Research China, People's Republic of China

Resting-state fMRI reflected spontaneous baseline neuronal activity.The fractional amplitude of low frequency fluctuation (fALFF) and regional homogeneity(ReHo) method had been developed to analyze the blood oxygenation level-dependent signal fluctuations in voxelwise analysis across the whole brain.In this study, we combined two resting-state fMRI algorithm to explore the features of brain spontaneous activities in chronic alcoholics.The results indicated the abnormality activities of some nodes in the default mode network and reward circuit. It is our hope that in future studies this technique may provide the opportunity to examine the integrity of networks involving the above loops in chronic alcoholics.

5360 Computer 39

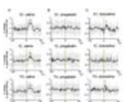

BOLD-fMRI evaluation of analgesic effects on allodynia-specific pain using fibromyalgia model rats

Sosuke Yoshinaga[1], Naoya Yuzuriha[1], Yuri Kitamoto[1], Mitsuhiro Takeda[1], Hiroshi Sato[2], and Hiroaki Terasawa[1]

[1]Department of Structural BioImaging, Faculty of Life Sciences, Kumamoto University, Kumamoto, Japan, [2]Bruker BioSpin K.K., Yokohama, Japan

The aim of this study is to evaluate the effects of analgesic agents on the allodynia-specific response in an animal model of fibromyalgia. Before and after the treatment with analgesic agents, BOLD experiments using green laser stimulation were performed. Before the treatments with analgesic agents, S1, IC, and TH exhibited BOLD responses (S1: 1.1%, IC: 0.8%, TH: 0.7%). These responses were inhibited by pregabalin treatment and to a lesser extent by duloxetine treatment (S1: 0.4%, IC: not detected, TH: 0.4%). Our experimental system provides a robust preclinical and clinical evaluation system for new analgesic agents.

5361 Computer 40

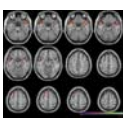

Preliminary study of hypoxic exposure effect on pilots using the Resting-State Functional Magnetic Resonance Imaging

liu jie[1], zhang wan shi, cheng jing liang, zhang yong, xu xian rong, and qian long

[1]first affiliated hospital of zhengzhou university, zhengzhou, People's Republic of China

The study was about the Resting-State fMRI of pilots before and after hypoxic exposure. It proved that the feasibility of monitor the real-time cerebral functional activity change by using MRI. Otherwise, it confirmed that hypoxic exposure inhibited the cognitive functions of pilots to some extent.

5362 Computer 41

Representation of Taxonomic and Thematic Knowledge of the Human Brain

Yangwen Xu[1], Weiwei Men[2], Tianyi Qian[3], Thomas Beck[4], Jiahong Gao[2], and Yanchao Bi[1]

[1]National Key Laboratory of Cognitive Neuroscience and Learning & IDG/McGovern Institute for Brain Research, Beijing Normal University, Beijing, People's Republic of China, [2]Center for MRI research, Peking University, Beijing, People's Republic of China, [3]MR Collaboration NE Asia, Siemens Healthcare, Beijing, People's Republic of China, [4]Siemens Healthcare, Erlangen, Germany

Decades of studies have identified a list of brain areas specific to a certain taxonomic category. However, neural representations incorporating both taxonomic and thematic knowledge are not well understood. In this study, we applied representational similarity analyses to investigate the underlying organizing principles of high-resolution neural activation patterns induced by different categories and themes at different cortical levels. In contrast to taxonomic representation, we did not find specific neural substrates representing thematic knowledge. Instead, neural activation patterns specific to thematic information emerged only when taxonomic differences were controlled for. These results suggest that the brain is dominated by taxonomic knowledge and then modified by thematic knowledge.

5363 Computer 42

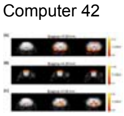

A BOLD analysis of the olfactory perception system in the mouse whole brain, using independent component analysis

Hirotsugu Funatsu[1], Fuyu Hayashi[1], Sosuke Yoshinaga[1], Mitsuhiro Takeda[1], Naoya Yuzuriha[1], Shunsuke Kusanagi[1], and Hiroaki Terasawa[1]

[1]Department of Structural BioImaging, Faculty of Life Sciences, Kumamoto University, Kumamoto, Japan

A BOLD analysis can trace real-time odor responses at high spatial resolution. Rodents have well-developed olfactory systems, and thus BOLD studies have mainly been performed in rodents. However, mice have smaller brains and are more susceptible to peripheral hemodynamic changes than rats, which make it harder to obtain sufficient BOLD signals. This study revealed the real-time odor response in the mouse whole brain by the BOLD experiment with periodical odor stimulations using a high-sensitivity cryogenic probe and the high-detectability analytical method, Independent Component Analysis (ICA). The signal changes of the activation sites corresponded to the human canonical hemodynamic response function.

5364 Computer 43

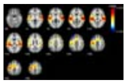

Repetition effects in early blind adults revealed by fMRI adaptation

Laureline Arnaud[1], Lucie Ménard[2], and Vincent L. Gracco[3,4]

[1]Integrated Program in Neuroscience, McGill University, Montreal, QC, Canada, [2]Linguistics Department, Université du Québec à Montréal, Montréal, QC, [3]School of Communication Sciences and Disorders, McGill University, Montréal, QC, Canada, [4]Haskins Laboratories, New Haven, CT, United States

Behavioural and fMRI studies have revealed enhanced auditory abilities and differences in the brain organization of early blind individuals compared to sighted. We used fMRI to assess cortical interactions associated with speech processing of repeated and novel stimuli. Although the in-scanner behavior for the blind and sighted groups were comparable, there were a number of cortical activation and deactivation differences. Additionally, the blind participants were better at a post-scan recall task. Cross-modal recruitment of occipital areas was found in the blind participants. They also showed widespread repetition-enhancement effects, suggesting that additional attention mechanisms contribute to their enhanced auditory word encoding abilities.

5365 Computer 44

Mouse BOLD fMRI imaging during operant learning at ultra-high field (14 T)

Naohiro Jomura[1], Teppei Shintani[1], Keisuke Sakurai[1], Jun Kaneko[1], and Tatsuhiro Hisatsune[1]

[1]Department of Integrated Biosciences, The University of Tokyo, Tokyo, Japan

A setup for operant learning fMRI was developed and inserted in a horizontal bore 14 T MRI. After the habituation of head-fixed mice, visual stimulation was delivered as CS and a water as reward was supplied automatically in response to licking behavior, for an operant learning task. We analyzed fMRI data between the correct and the error trials and found the BOLD elevation of brain areas including the visual cortex and the hippocampal formation when mice performed the correct trial. Mouse BOLD fMRI in operant learning task will offer unexperienced data to basic as well as clinical research fields.

5366 Computer 45

fMRI detection of neuromodulation induced neuroplasticity after spinal cord injury

Vijai Krishnan[1,2], Anna Schwartz[1], William Stokes[1], Jeff W.M. Bulte[2], Jineta Banerjee[2], Aline Thomas[2], Pablo Celnik[3], and Galit Pelled[1,2]

[1]F.M. Kirby Center, Kennedy Krieger Institute, Baltimore, MD, United States, [2]Department of Radiology, Johns Hopkins University School of Medicine, Baltimore, MD, United States, [3]Physical Medicine and Rehabilitation, Johns Hopkins University School of Medicine, MD, United States

Spinal cord injury (SCI) leads to severe motor and sensory deficits. New advances in non-invasive neuromodulation technologies such as transcranial magnetic stimulation (TMS) have shown promise in facilitating recovery following brain injuries. Here we tested whether TMS therapy can be developed as a rehabilitative approach in a rat model of SCI. High-resolution functional MRI (fMRI) at 11.7 T was used to detect cortical activity associated with post-injury neuroplasticity. A battery of behavioral tests was used to monitor gross changes in motor behavior. Our results demonstrate that TMS therapy is beneficial in improving post-SCI functional outcomes.

5367 Computer 46

Evidence of modulation of laminar profiles by contextual modulation in V1 using high-resolution fMRI

Kimberly B Weldon[1], Michael-Paul Schallmo[2], Philip C Burton[3], Andrea N Grant[4], and Cheryl A Olman[1]

[1]Department of Psychology, University of Minnesota, Minneapolis, MN, United States, [2]Department of Psychology, University of Washington, Seattle, WA, United States, [3]Office of the Associate Dean for Research, University of Minnesota, Minneapolis, MN, United States, [4]Department of Neuroscience, University of Minnesota, Minneapolis, MN, United States

We characterized depth-dependent laminar profiles of surround suppression in human early visual cortex with high-resolution 7T fMRI. In a block-design participants viewed circular target stimuli (gratings defined by sinusoidal luminance modulation) surrounded by an annulus with a grating either parallel or orthogonal to the target grating. The surround was placed either adjacent to the target grating (Near) or separated from the target by 2° of visual angle (Far). Results show a similar activation profile for Parallel and Orthogonal conditions in the Far condition across depth. For the Near condition, contextual modulation occurred more in deep, rather than superficial layers.

5368 Computer 47

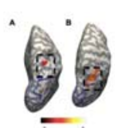

Top-down modulation in a directed sensory attention task

Kevin M. Aquino[1], Rodika Sokoliuk[2], Rosa Sanchez-Panchuelo[1], Simon Hanslmayr[2], Stephen Mayhew[2], Karen Mullinger[1,2], and Susan Francis[1]

[1]Sir Peter Mansfield Imaging Centre, School of Physics and Astronomy, University of Nottingham, Nottingham, United Kingdom, [2]Centre for Human Brain Health (CHBH), University of Birmingham, Birmingham, United Kingdom

Attentional top-down effects are known to modulate responses when spatially directing attention within sensory modality. The directing of attention between sensory modality is less well understood. Here we present fMRI data using a Posner type attention paradigm between sensory areas (visual and somatosensory). We show that the visual, somatosensory and IPS regions are recruited during attention periods, with some of these areas modulated by degree of attention. Additional IPS regions were modulated strongly with attention recruitment. This paradigm presents top-down influence on cortical regions, allowing the study of the top-down influences of attention switching between sensory modalities.

5369 Computer 48

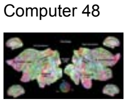

Encoding and decoding semantic information of natural movies from 7T human brain activity provided by the Human Connectome Project

Nehemia Mekete[1] and An Thanh Vu[2]

[1]UC Berkeley, Berkeley, CA, United States, [2]Center for Imaging of Neurodegenerative Diseases, Veteran Affairs Health Care System, San Francisco, CA, United States

We demonstrate the utility of the new 7T fMRI movie dataset made publicly available by the WashU-UMinn Human Connectome Project (HCP, www.humanconnectome.org) by reconstructing the movies participants watched, based on their fMRI brain activity and two general models of the human brain: a structural model and a semantic model. Although we were only marginally successful when using the structural model (most likely because participants were allowed to freely view the movie without a fixation task), we were able to successfully decode the semantic content of the held out movie data, with surprisingly high accuracy (r~0.8, and p<10^-10).

Electronic Poster

fMRI: Connectivity Methods

Exhibition Hall — Thursday 9:15 - 10:15

5370 — Computer 49

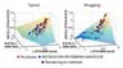

Physiological noise correction improves sensitivity, specificity, and reproducibility of resting-state functional connectivity in a reading model

Venkatagiri Krishnamurthy[1,2,3], Lisa C. Krishnamurthy[2,3,4], Dina M. Schwam[5], Daphne Greenberg[5], and Robin D. Morris[3,6]

[1]Dept. of Neurology, Emory University, Atlanta, GA, United States, [2]Center for Visual and Neurocognitive Rehabilitation, Atlanta VAMC, Decatur, GA, United States, [3]Center for Advanced Brain Imaging, GSU/GT, Atlanta, GA, United States, [4]Dept. of Physics & Astronomy, Georgia State University, Atlanta, GA, United States, [5]Dept. of Educational Psychology, Special Education, and Communication Disorders, Georgia State University, Atlanta, GA, United States, [6]Dept. of Psychology, Georgia State University, Atlanta, GA, United States

Amongst several sources of noise, physiological noise (PN) from cardiac and respiratory cycles affects reliable quantification of rsFC measures such as correlation coefficient (CC). The purpose of this study is to determine the effects of PN on specificity, sensitivity and reproducibility of rsFC maps in a 'reading' model. We show that a combination of multiple methodologies to correct for such noise leads to improved signal fluctuations (tSNR) that culminates in higher specificity and sensitivity to neuronal fluctuations that are closer to actual ground truth. Applying our methodologies to a 'reading' model, we show that, irrespective of session, correction for PN results in meaningful discrimination of reading networks between typical and struggling readers.

5371 — Computer 50

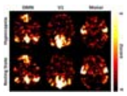

On the feasibility of estimating functional connectivity from hypercapnia BOLD MRI data

Xirui Hou[1,2], Peiying Liu[1], Micaela Chan[3], Gagan Wig[3,4], Denise Park[3], and Hanzhang Lu[1]

[1]The Russell H. Morgan Department of Radiology, Johns Hopkins School of Medicine, Baltimore, MD, United States, [2]Department of Biomedical Engineering, Johns Hopkins School of Medicine, Baltimore, MD, United States, [3]Center for Vital Longevity and School of Behavioral and Brain Sciences, University of Texas at Dallas, Dallas, Texas, Dallas, TX, United States, [4]Department of Psychiatry, University of Texas Southwestern Medical Center, Dallas, TX, United States

Resting-state fMRI, particular based on Blood-Oxygenation-Level-Dependent (BOLD) signal, has been extensively used to measure functional connectivity (FC) in the brain. A recent report proposed that FC can also be evaluated from hypercapnia BOLD image. In this work, we aim to systematically compare FC derived from hypercapnia BOLD data with those obtained from traditional resting-state BOLD data in a large cohort (170 healthy participants). Our results suggest that the hypercapnia and resting-state FC maps are spatially correlated across voxels, amplitude-wise correlated across subjects.

5372 — Computer 51

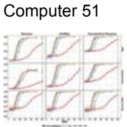

Community detection in resting state functional connectivity networks beyond the resolution limit

Carlo Nicolini[1], Cecile Bordier[1], and Angelo Bifone[1]

[1]Center for Neuroscience and Cognitive Systems, Istituto Italiano di Tecnologia, Rovereto (TN), Italy

Graph-theoretical analysis has been widely applied to study the modular organization of brain functional connectivity networks. However, existing methods suffer from a fundamental resolution limit. Here, we propose and validate a novel, resolution-limit-free approach dubbed Asymptotical Surprise. Application of this method to human resting state networks reveals the presence of heterogeneously distributed modules, corresponding to neuroanatomically and functionally plausible networks. The finer partition afforded by Asymptotical Surprise enables a more accurate identification of connector hubs, the brain regions that are thought to be responsible for the integration of functionally segregated modules into a cohesive structure.

5373 — Computer 52

Structural basis of functional networks: A fMRI/DTI fusion approach in network level

Farzaneh Keyvanfard[1,2] and Abbas Nasiraei Moghaddam[1,2]

[1]Biomedical Engineering, Amirkabir University of Technology (Tehran Polytechnic), Tehran, Iran, [2]School of Cognitive Sciences, Institute for Research in Fundamental Sciences (IPM), Tehran, Iran

MRI provides the capability of obtaining different information from various aspects of the brain. More comprehensive understanding of the brain can be achieved by combining multimodal brain imaging data. Using Diffusion Tensor Imaging (DTI) in addition to resting state fMRI (rs-fMRI), we have proposed a novel multivariate fusion approach to find supportive structural basis of brain functional networks. Two known functional networks and their counterpart structural networks were extracted through this method.

5374 — Computer 53

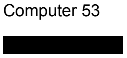

Bayesian Spatio-temporal Model for Brain Resting State Connectivity

Hakmook Kang[1], Hernando Ombao[2], Chris Fonnesbeck[3], Zhaohua Ding[3], and Victoria L Morgan[3]

[1]Vanderbilt University, Nashville, TN, United States, [2]University of California, Irvine, [3]Vanderbilt University

Current approaches separately analyze concurrently acquired diffusion tensor imaging (DTI) and functional magnetic resonance imaging (fMRI) data. The primary limitation of these approaches is not to use all available information in estimation of resting state functional connectivity (FC). To overcome this limitation, we developed a Bayesian hierarchical spatio-temporal model that incorporated structural connectivity (SC) into estimating FC, where SC based on DTI was used to construct a prior for FC based on resting state fMRI (rs-fMRI) data. Simulations and data analysis concluded that our model achieved smaller false positive rates and was robust to data decimation compared to the conventional approach.

5375 Computer 54

Influence of temporal filtering and global signal regression on resting state networks in the rat brain

Robert Becker[1], Claudia Falfan-Melgoza[1], Jonathan Reinwald[1], and Wolfgang Weber-Fahr[1]

[1]RG Translatioanl Imaging, Department Neuroimaging, Central Institute of Mental Health, Medical Faculty Mannheim / Heidelberg University, Mannheim, Germany

In a test-retest fMRI experiment we examined the influence of temporal filtering and global signal regression (GSR) on resting state networks in rats. Connectivity and topological properties as well as their test-retest reliability were assessed for eight filtering variants (with and without GSR, four frequency bands). We found GSR to strongly impair the expected structure of networks. The choice of temporal filtering frequencies whereas did not have a significant effect. Test-retest-reliability was low for all filtering variants. Based on our results we recommend to use less restrictive bandpass filters but no GSR.

5376 Computer 55

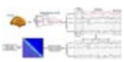

The Early Global Function Connectivity Stability in Infants during the Neonatal Period

Yue Cai[1,2], Yuan Shi[3], Yang Fan[4], Wei Gao[5,6], and Jiahong Gao[2]

[1]Department of Biomedical Engineering, Peking University, beijing, People's Republic of China, [2]Center for MRI Research, Academy for Advanced Interdisciplinary Studies, Peking University, Beijing, People's Republic of China, [3]Daping Hospital, Third Military Medical University, Daping Hospital, Third Military Medical University, Chongqing, People's Republic of China, [4]MR Research China, GE Healthcare, Beijing, People's Republic of China, [5]Biomedical Imaging Research Institute (BIRI), Department of Biomedical Sciences and Imaging, Cedars-Sinai Medical Center, los angeles, CA, United States, [6]Department of Radiology and Biomedical Research Imaging Center, University of North Carolina Chapel Hill, United States

This study proposes an improved method named global functional connectivity stability (GFCS) to quantify the brain dynamic functional connectivity at a voxel-wise level. The GFCS was applied to investigate the overall functional connectivity stability and its correlation with time in infants during the period from late preterm to the term equivalent age (TEA). It is shown that infants presented high functional stability predominantly in the sensorimotor areas, temporal lobe, posterior cingulate cortex (PCC) and medial prefrontal cortex. With time, the frontal areas appeared more variable while the sensorimotor cortex appeared more stable in infants during the neonatal period.

5377 Computer 56

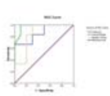

A computer aid diagnosis of diabetic nephropathy based on the combination of IVIM and BOLD imaging

Lihua Chen[1], Zhizheng Zhuo[2], Tao Ren[1], Shuangshuang Xie[1], Yu Zhang[2], and Wen Shen[1]

[1]Radiology, Tianjin First Center Hospital, Tianjin, People's Republic of China, [2]Philips healthcare, Beijing, People's Republic of China

To detect the changes of kidney diseases, magnetic resonance imaging(MRI) as a noninvasive approach has been proved to be more suitable for detecting and monitoring diabetic nephropathy(DN). Intravoxel incoherent motion (IVIM) and blood oxygenation level dependent (BOLD) MR imaging have been confirmed their high potential in detecting changes of renal function in patients with chronic renal diseases and transplanted kidneys.

5378 Computer 57

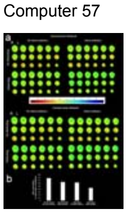

Resting State Network Dynamics using Sliding-Window Detrending and Meta-Statistics: A New Approach for Real-time fMRI

Kishore Vakamudi[1], Kunxiu Gao[2], Cameron W Trapp[3], Greg Scantlen[4], and Stefan Posse[5,6]

[1]Neurology, Physics and Astronomy, University of New Mexico, Albuquerque, NM, United States, [2]NeurInsight LLC, Albuquerque, [3]Neurology, Physics and Astronomy, University of New Mexico, [4]CreativeC LLC, Albuquerque, [5]Neurology, Physics and Astronomy, Electrical and Computer Engineering, University of New Mexico, Albuquerque, NM, United States, [6]NeurInsight LLC, Albuquerque, NM, United States

This study introduces a real-time confound-tolerant approach for mapping resting-state network (RSN) dynamics that is compatible with ultra-high-speed fMRI and integrates the following processing steps: (a) iterative optimization of seed selection, (b) sliding-window online detrending of confounding signals, and (c) seed-based sliding-window correlation analysis using hierarchical running averages (meta-statistics) for mapping connectivity dynamics. The method maximizes sensitivity and specificity of mapping RSNs with enhanced suppression of spurious connectivity in WM and GM. This methodology is suitable for online monitoring of data quality, for clinical applications and basic neuroscience research of resting-state connectivity, for which there are no currently available tools.

5379 Computer 58

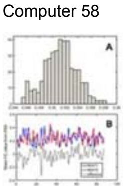

Pseudo-bootstrap network analysis - an application in functional connectivity fingerprinting

Hu Cheng[1], Ao Li[1], Andrea Avena-Koenigsberger[1], Chunfeng Huang[1], and Sharlene Newman[1]

[1]Indiana University, Bloomington, IN, United States

As an alternative to template based brain parcellation in functional connectivity analysis, nearly equal-sized random parcellations are applied to individual subjects multiple times to obtain a pseudo-bootstrap sample of the functional network. As one application, the method was applied on the HCP resting state dataset to identify individuals across scan sessions based on the mean functional connectivity. With a parcellation number of 278 and bootstrap sample size of 400, an accuracy rate of ~90% was achieved by simply finding the maximum correlation of mean functional connectivity of pseudo-bootstrap samples between two scan sessions.

5380 Computer 59

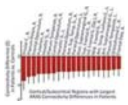

Functional connectivity disturbances of the ascending reticular activating system in temporal lobe epilepsy

Dario J. Englot[1], Peter E. Konrad[1], Monica L. Jacobs[1], John C. Gore[1], Bassel W. Abou-Khalil[1], and Victoria L. Morgan[1]

[1]*Vanderbilt University, Nashville, TN, United States*

Seizures in temporal lobe epilepsy (TLE) disturb brain network physiology and lead to brain connectivity disturbances. We used resting-state functional MRI (fMRI) recordings in TLE patients and controls to examine functional connectivity between brainstem ARAS structures and cortical/subcortical regions. ARAS connectivity was significantly lower in TLE patients than controls, with largest connectivity decreases noted in neocortical regions ipsilateral to the epileptogenic zone. Diminished ARAS connectivity was related to seizure frequency and neuropsychological impairments. Functional connectivity analysis of small brainstem structures using fMRI is feasible and may provide important information regarding mechanisms of disease in neurological disorders.

5381 Computer 60

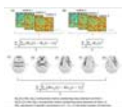

Reproducibility of graphical measures and dynamic network features in resting state fMRI

Sue-Jin Lin[1,2], Tobias R. Baumeister[2,3], Alex MacKay[4,5], Irene Vavasour[5], David K.B. Li[5,6], and Martin J McKeown[1,2,6]

[1]*Graduate Program in Neuroscience, University of British Columbia, Vancouver, BC, Canada,* [2]*Pacific Parkinson's Research Centre, UBC Hospital, Vancouver, BC, Canada,* [3]*Department of Biomedical Engineering Program, University of British Columbia,* [4]*Department of Physics and Astronomy, University of British Columbia,* [5]*Department of Radiology, UBC Hospital,* [6]*Neurology, Faculty of Medicine, University of British Columbia*

Resting state fMRI (rsfMRI) has been widely used to study brain function. Numerous informative features derived from rsfMRI data have been proposed, such as graphical metrics and dynamic connectivity, but their robustness is uncertain. In order to verify their reproducibility, we acquired rsfMRI three times for 11 subjects and calculated 7 graphical measures and 7 dynamic network features. None of the measures showed significant differences among the three rsfMRI sessions. Therefore, we concluded that graphical measures and dynamic network features in rsfMRI are at least robust to inter-trial variability, which should ameliorate uncertainties when applying them to clinical research.

5382 Computer 61

Cue-Induced reactivity of brain in abstinence and methadone maintenance treatment for heroin addiction: an event-related functional magnetic resonance imaging study

Xuan Wei[1], Jiajie Chen[1], Qiang Li[2], and Wei Wang[2]

[1]*Radiology department of Tangdu hospital, The Fourth Military Medical University, Xi'an, People's Republic of China,* [2]*Radiology department of Tangdu hospital, The Fourth Military Medical University, People's Republic of China*

Purpose Our research aims to research abstinence and methadone maintenance treatment, to reveal which abstinence way is better and to compare their cue-reactivity in heroin-dependent individuals.

Materials and Methods 24 heroin-dependent patients under abstinence,19 heroin-dependent patients under MMT and 20 healthy volunteers were recruited. The functional images were acquired by using a spin-echo EPI.

Results MMT group brain regions which had differences in cue-reactivity intensity were significantly positive correlation with craving changes, and abstinence group did not exist. **Discussion and Conclusion** This study showed that abstinence is more advantageous than MMT to reduce heroin addiction in drug cue-reactivity.

5383 Computer 62

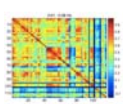

Frequency characteristics of resting-state fMRI functional networks

Nicole Yuen[1] and Jean Chen[1,2]

[1]*Roman Research Institute, Toronto, ON, Canada,* [2]*Medical Biophysics, University of Toronto, Toronto, ON*

This study examines the frequency dependence of functional connectivity patterns as measured using resting-state fMRI (rs-fMRI). We decompose the rs-fMRI signal into its intrinsic mode functions (IMFs) using the recently proposed variational mode decomposition (VMD) technique, which provides increased frequency precision and reduced modal mixing than previous methods. We show that many functional connectivity patterns can only be seen in a certain frequency range, contrasting previous findings. We concluded that the correlation patterns are frequency dependent and are more prominent and consistent in the lower frequency range.

5384 Computer 63

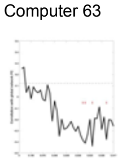

Dynamic Functional Connectivity within the Default Mode Network is associated with the Complexity of its Network Nodes

Kay Jann[1] and Danny JJ Wang[1]

[1]*Laboratory of FMRI Technology (LOFT), USC Stevens Neuroimaging and Informatics Institute, Keck School of Medicine of USC, University of Southern California, Los Angeles, CA, United States*

While dynamic functional connectivity (dynFC) provides an estimate of the information transfer between brain network nodes, the signal dynamics at each node represents the local information processing. Here we assessed the relation between dynFC within the default mode network and the complexity/regularity of fMRI signal of network nodes. We found that a more complex and thus less predictable signal in a node allows for a more dynamic connectivity and hence a richer repertoire of different FC states.

5385 Computer 64

Effects of tCDS to vmPFC functional connectivity after 36 hours total sleep deprivation: a resting-state fMRI study

Li Jiyuan[1], Song Yunlong[1], Shao Yongcong[2], Pan Zhibin[1], Wu Yao[1], and Zhou Lu[2]

[1]CT and MRI, The General Hospital of The Air Force People's Liberation Army, Beijing, People's Republic of China, [2]Cognitive and Mental Health Research Center, Beijing Institute of Basic Medical Sciences, Beijing, People's Republic of China

There are fifteen health indibiduals recruited in order To explore the changes of functional connectivity in vmPFC with tDCS stimuli after 36 hours sleep deprivation. Colleceting resting-state fMRI data under the tDCS stimuli and sham stimuli conditions. Using the vmPFC as the seed region,and then the time courses of all brain voxels were correlated separately with the mean time course generated from the ROI by Pearson cross-correlation. Finally, we found that tDCS can effectively mediate the dysfunction of brain connectivity.

5386 Computer 65

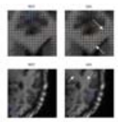

White Matter Resting-State fMRI with Hypercapnic Respiratory Challenge

Tung-Lin Wu[1,2], Jennifer Watchmaker[1], Li Min Chen[1,3], Adam W Anderson[1,2,3], Zhaohua Ding[1,2,3], and John C Gore[1,2,3]

[1]Vanderbilt University Institute of Imaging Science, Nashville, TN, United States, [2]Biomedical Engineering, Vanderbilt University, Nashville, TN, United States, [3]Radiology and Radiological Sciences, Vanderbilt University, Nashville, TN, United States

In order to further elucidate the biophysical origins of spatio-temporal correlation tensors and validate the possibility of detecting BOLD signals in white matter, we acquired resting-state fMRI in volunteers breathing alternately room air and CO_2 enriched air to induce a hypercapnic-normoxic change in CBF and CBV. Our hypercapnic respiratory challenge experiments suggest that spatio-temporal correlations in white matter may be driven by local hemodynamic effects, consistent with BOLD effects instead of other potential mechanisms. Our results also imply and support our previous observation that BOLD signals in white matter can be reliably detected, and resting-state correlations between voxels are anisotropic.

5387 Computer 66

Temporal evolution of effective connectivity analysis in anaesthetised mice

Qasim Bukhari[1], Aileen Schroeter[1], and Markus Rudin[1,2]

[1]Institute of Biomedical Engineering, ETH and University of Zurich, Zurich, Switzerland, [2]Institute of Pharmacology and Taxicology, University of Zurich, Zurich, Switzerland

Dynamic functional connectivity (dFC) analysis has gained considerable interest in the past years. The goal of this technique is to estimate the temporal changes of resting state functional connectivity networks and get insights into brain pathologies by analyzing these dynamic patterns. dFC uses functional connectivity correlations as a means to understand the brain functional principle. Dynamic Causal Modeling (DCM) has been widely used in the neuroimaging community to estimate the effective connectivity by fitting a neuronal model to the observed fMRI data. Stochastic DCM together with Bayesian Model Comparison applied to resting state fMRI data results in the selection of the most plausible neuronal model explaining the observed data. The input to these model estimation methods are the full length time series extracted from the regions of interest of mouse resting state fMRI data, neglecting the temporal evolution of the model parameters. In this work we combine the two approaches by estimating the temporal changes in the effective connectivity as derived from DCM.

5388 Computer 67

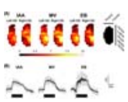

Stimulus-evoked fMRI activations are a subset of resting-state fMRI networks in the rat olfactory bulb

Garth J Thompson[1,2], Basavaraju G Sanganahalli[1,2,3], Keeley Baker[4,5], Justus V Verhagen[4,5], Gordon M Shepherd[5], and Fahmeed Hyder[1,2,3,6]

[1]Radiology and Biomedical Imaging, Yale University, New Haven, CT, United States, [2]Magnetic Resonance Research Center (MRRC), Yale University, New Haven, CT, United States, [3]Quantitative Neuroscience with Magnetic Resonance (QNMR) Core Center, Yale University, New Haven, CT, United States, [4]The John B. Pierce Laboratory, New Haven, CT, United States, [5]Neurobiology, Yale University, New Haven, CT, United States, [6]Biomedical Engineering, Yale University, New Haven, CT, United States

Are coordinated activations of the brain during sensory stimulation linked to the synchronized activations or “functional connectivity” observed with resting state fMRI? We recorded odor-stimulation fMRI and resting state fMRI in the rat olfactory bulb’s glomerular sheet. Glomerular activations due to three odors were compared to spontaneous fluctuations organized as twenty-two independent component networks. Networks correlated with activation in an odor-specific manner. We reconstructed approximations of activation which retained odor specificity for two of three odors, despite being constructed from resting state data. Our results suggest a function for synchronized resting oscillations in reinforcing stimulation-specific responses.

5389 Computer 68

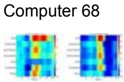

Dynamic Functional Connectivity in Event-Related fMRI and its implications in Epilepsy

Ashish Kaul Sahib[1,2], Michael Erb[1], Klaus Scheffler[1,3], Thomas Ethofer[1,4], and Niels Focke[2]

[1]Department of Biomedical Magnetic Resonance, University Hospital tuebingen, Tuebingen, Germany, [2]Department of Neurology/Epileptology, University Hospital tuebingen, Tuebingen, Germany, [3]Max-Planck-Institute for Biological Cybernetics, Tuebingen, Germany, [4]Department of General Psychiatry, University Hospital tuebingen, Tuebingen, Germany

To assess the impact of repetition time (TR) and window size on the temporal features of BOLD functional connectivity (FC) using a sliding window approach in event-related fMRI. in addition, test the feasibility of this approach in epilepsy. We calculated the functional connectivity degree (FCD) by counting the total number of connections of a given voxel above a predefined threshold based on Pearson correlation. In summary, we showed that dynamic FCD transients are better detectable with sub-second TR than conventional TR, indicating a potential to study the temporal characteristics of interictal epileptiform discharges and seizures in epilepsy patients.

5390 Computer 69

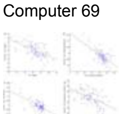

Topological Networks reorganization in two profile of High Potential Children: a resting state fMRI study.

Ilaria Suprano[1], Chantal Delon-Martin, Gabriel Kocevar, Claudio Stamile, Salem Hannoun , Pierre Fourneret, Olivier Revol, Fanny Nusbaum, and Dominique Sappey-Marinier

[1]Université Claude Bernard - Lyon 1, Lyon, France

High Potential Children diagnosis remains unclear. We proposed to examine 56 children with a resting state fMRI study. The profile of network topology was explored in two different groups of HP estimating the hub disruption index (k). A disruption of the order of importance of specific nodes in both the HP groups was found with a stronger reorganization in heterogeneous group. This results may offer a confirm of the different psychiatric characteristics that exist between the HP profiles. The sensitivity of graph metrics based on rs-fMRI was demonstrated to be very helpful to provide a better characterization of HP children.

5391 Computer 70

Diffusion kurtosis imaging with tract-based spatial statistics reveals white matter alterations in children with obstructive sleep apnea syndrome

Wenfeng Li[1], Hongwei Wen[2], Yun Peng[1], Hongbin Li[1], Yang Wen[1], Hua Cheng[1], Yang Fan[3], Huiguang He[2], and Yue Liu[1]

[1]Beijing Children's Hospital,Capital Medical University, Beijing, People's Republic of China, [2]Chinese Academy of Sciences, Beijing, People's Republic of China, [3]GE Healthcare, Beijing, People's Republic of China

It is reported that OSAS may cause cognitive function disorder of children due to chronic hypoxia for a long time [1] . However, it is not clear whether there are any structural changes of cerebral regions, e.g. white matter (WM). Diffusion kurtosis imaging is now widely used in the detection of cortical structural changes across kinds of diseases. In the present study, DKI is used to investigate microstructural changes of WM in OSAS children compared with normal healthy controls.

5392 Computer 71

Graph theoretical analysis of the modular organization of resting state functional connectivity in the rat

Stefano Tambalo[1], Giulia Scuppa[1], Carlo Nicolini[1], Cecile Bordier[1], and Angelo Bifone[1]

[1]Center for Neuroscience and Cognitive Systems, Istituto Italiano di Tecnologia, Rovereto (TN), Italy

Modular organization of resting state functional connectivity has been demonstrated in human studies using graph theoretical approaches. Various methods, characterized by different resolutions, have enabled the investigation of the functional connectivity structure of the human brain at different scales. Here, we extend these approaches to the study of resting state connectivity in the rat, and demonstrate for the first time the existence of multi-scale, functionally segregated modules in this species.

Electronic Poster

fMRI: Multimodal

Exhibition Hall Thursday 9:15 - 10:15

5393 Computer 73

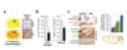

How does chronic neuroinflammation affect resting state functional connectivity?

Esteban Adrian Oyarzabal[1,2,3], SungHo Lee[1,4,5], Manasmita Das[1,2], Sheng Song[6,7], and Yen-Yu Ian Shih[1,2]

[1]Neurology, University of North Carolina at Chapel Hill, Chapel Hill, NC, United States, [2]Biomedical Research Imaging Center, University of North Carolina at Chapel Hill, Chapel Hill, NC, United States, [3]Neurobiology Laboratory, National Institute of Environmental Health Sciences, RTP, NC, United States, [4]University of North Carolina at Chapel Hill, Chapel Hill, NC, United States, [5]Biomedical Research Imaging Center, University of North Carolina at Chapel Hill, [6]Neurobiology Laboratory, National Institute of Environmental Health Sciences, [7]National Institute of Environmental Health Sciences, RTP, NC, United States

Chronic neuroinflammation, present in most neuropathologies, has long-term consequences on neurocircuit connectivity synchrony and strength. By implementing multi-modal techniques to quantify neuroinflammation, we found a strong association linking the intensity of neuroinflammation with depressed functional connectivity. We partly attribute these changes to neurodegeneration and the loss of central NE.

5394 Computer 74

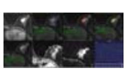

The Combine Analysis of improved Multi-parametric MR for identifying the different subtypes and immunohistochemical expression of Breast cancer

Weixiong Fan[1], Xiaofeng Chen[1], Fengyan Cheng[1], Yabao Cheng[2], Tai Xu[3], Guijin Li[4], Xiaolei Zhu[5], and Shuai Li[6]

[1]Department of Radiology(MRI), Meizhou City People's Hospital, Meizhou,Guangdong, People's Republic of China, [2]Department of Radiology (MRI), Meizhou City People's Hospital, People's Republic of China, [3]Department of breast surgery, Meizhou City People's Hospital, Meizhou,Guangdong, People's Republic of China, [4]Departmen of Siemens Healthcare application, Siemens Healthcare, Guangdong, People's Republic of China, [5]MR scientific marketing NE Asia, Siemens Healthcare, Guangdong, People's Republic of China, [6]MR scientific marketing NE Asia, Siemens Healthcare, Beijing, People's Republic of China

The aim of this study was to explore the different subtypes and immunohistochemical expression of breast cancer in improved multi-parametric MR imaging. By introducing the free breathing of ultrafast temporal resolution dynamic VIBE (TWIST-VIBE) and readout segmentation of long variable echo-trains (RESOLVE) techniques, quantitative pharmacokinetic (PK), semi-quantitative DCE-MRI based on curve of time concentration and diffusion parameters were extracted to analyze it. The results show that significant differences in multi parametric parameters Kep and rADC among the different subtypes of Breast cancer. Those parameters were hopeful to be a non-invasive measurement for assessing the subtypes and the biology, histological features of breast cancer.

5395 Computer 75

Fluctuations of the EEG-fMRI correlation reflect intrinsic strength of functional connectivity in default mode network

Tuija Keinänen[1,2], Seppo Rytky[2], Vesa Korhonen[1], Juha Nikkinen[3], Osmo Tervonen[1], Matias Palva[4], and Vesa Kiviniemi[1]

[1]Diagnostic Radiology, Oulu University Hospital, Oulu, Finland, [2]Clinical Neurophysiology, Oulu University Hospital, Oulu, Finland, [3]Oncology and Radiotherapy, Oulu University Hospital, [4]Neuroscience Center, University of Helsinki

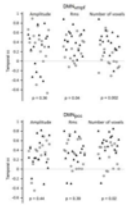

Resting-state networks (RSN) functional connectivity has shown to be temporally dynamic in the brain. Also the correlations between infra slow fluctuations in electroencephalography (EEG) and blood oxygen level-dependent signal have shown dynamic variability over time. Here, we used simultaneous EEG-fMRI with ultra-fast magnetic resonance encephalography to study the link between the variations of these correlations and variations in RSN functional connectivity. The results suggest that the correlation strength is markedly linked to the strength of underlying functional connectivity. This leads to low correlations when averaged over a long period, high momentary synchrony can be reached due to intrinsic RSN dynamics.

5396 Computer 76

Neurochemical Basis of the BOLD Change in Attention Control - a combined task-based fMRI and 1H-MRS

Pui Wai Chiu[1,2], Hui Zhang[1], Issac Ip[3], Savio Wai Ho Wong[3], Tianyin Liu[4], Gloria Hoi Yan Wong[5], Queenie Chan[6], Kelvin Kai Wing Yau[7], Leung Wing Chu[8,9], and Henry Ka Fung Mak[1,2,9]

[1]Department of Diagnostic Radiology, The University of Hong Kong, Hong Kong, Hong Kong, [2]State Key Laboratory of Brain and Cognitive Sciences, The University of Hong Kong, Hong Kong, Hong Kong, [3]Department of Special Education and Counselling, The Education University of Hong Kong, Hong Kong, Hong Kong, [4]Sau Po Centre on Ageing, The University of Hong Kong, Hong Kong, Hong Kong, [5]Department of Social Work and Administration, The University of Hong Kong, Hong Kong, Hong Kong, [6]Philips Healthcare, Hong Kong, Hong Kong, Hong Kong, [7]Department of Management Sciences, City University of Hong Kong, Hong Kong, Hong Kong, [8]Department of Medicine, Queen Mary Hospital, Hong Kong, Hong Kong, [9]Alzheimer's Disease Research Network, The University of Hong Kong, Hong Kong, Hong Kong

fMRI can indirectly measure brain activity, but the biochemical underpinnings of the BOLD changes are still unknown. Nevertheless, ^{1}H-MRS can bridge such gap by measuring Glx [summation of glutamate (Glu) and glutamine (Gln)], where Glu is one of the mediators of neurovascular coupling. In this study, we aim to elucidate the complex relationship between attention control (numerical Stroop) and its associated neurochemical changes by combining the biochemical information from task-based fMRI and ^{1}H-MRS. Our result showed that the anterior cingulate cortex was positively correlated with Glx. This is the first study providing neurochemical explanation of the BOLD change during attention control task.

5397 Computer 77

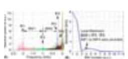

Empirical Model Decomposition Removes Non-stationary EEG Noise in Simultaneous fMRI-EEG Acquisition

Kevin Wen-Kai Tsai[1], Hsin-Ju Lee[2], Wen-Jui Kuo[2], Jo-Fu Lotus Lin[3], and Fa-Hsuan Lin[3,4]

[1]Aim for the Top University Project Office, National Taiwan Normal University, Taipei, Taiwan, [2]Institute of Neuroscience, National Yang-Ming University, Taipei, Taiwan, [3]Institute of Biomedical Engineering, National Taiwan University, Taipei, Taiwan, [4]Department of Neuroscience and Biomedical Engineering, Aalto University, Espoo, Finland

Non-stationary EEG noise from simultaneous fMRI-EEG acquisition could be conventionally removed by optimal basis selection and followed by a low-pass filtering. An empirical model decomposition (EMD) method was applied to partially remove non-stationary EEG noise from simultaneous fMRI-EEG acquisition. Our results suggested that EMD method could reveal similar auditory evoked potential with optimal basis selection and low-pass filtering without prior knowledge or cut-off frequency, thus preserving high frequency signal not empirically related to the non-stationary noise. This EMD method allows us to investigate human brain high frequency EEG oscillation in the simultaneous fMRI-EEG measurement.

5398 Computer 78

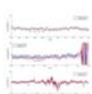

Correcting motion-affected gradient artifacts in EEG-fMRI: a modeling approach

Shuoyue Zhang[1], Bruno Riemenschneider[1], Maxim Zaitsev[1], Jürgen Hennig[1], and Pierre LeVan[1]

[1]Department of Radiology, Medical Physics, University Medical Center Freiburg, Freiburg, Germany

Simultaneous acquisition of electroencephalography (EEG) and functional magnetic resonance imaging (fMRI) is extensively applied for brain mapping due to the high temporal resolution of EEG and high spatial resolution of fMRI. But gradient artifacts on the EEG cannot be optimally corrected in the presence of abrupt head movements. In this work, we demonstrate a method to model motion-related gradient artifacts. Thus we obtain not only an improvement in gradient artifact correction, but also infer motion information directly from the EEG.

5399 Computer 79

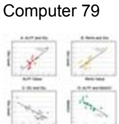

Investigation of the relationship between metabolic basis of thalamus and brain spontaneous activity revealed by a study combined fMRI and MRS

Zhengge Wang[1], Bing Zhang[1], and Bin Zhu[1]

[1]Radiology, Nanjing Drum Tower Hospital, The Affiliated Hospital of Nanjing University Medical School, Nanjing, People's Republic of China

Several recent studies have reported a correlation between regional glutamate concentration and BOLD activation. In this study, we combined resting-state fMRI and MRS to investigate whether this association maintain in spontaneous brain activity in the thalamus. Significant positive correlation was found between glutamate concentration and the ALFF and ReHo in left thalamus; negative correlation between glutamate and DC in left thalamus. Furthermore, the ALFF of left primary motor cortex and bilateral auditory cortex were affected by left thalamus glutamate. This provides insight into better understanding the neuronal and biochemical mechanisms of thalamus function.

5400 Computer 80

Comparison of fMRI and MEG language localization tasks—a prospective study of noninvasive presurgical functional mapping

Li Zheng[1], Jingwei Sheng[1], Tianyi Qian[2], Thomas Beck[3], and Jia-hong Gao[1]

[1]Center for MRI Research, Peking University, Beijing, People's Republic of China, [2]Siemens Healthcare, MR Collaborations NE Asia, Beijing, People's Republic of China, [3]Siemens Healthcare, Application Development, Erlangen, Germany

In patients with intractable epilepsy, anomalous cortical organization could be observed and pre-surgical planning involving the localization of cortical language areas is critical. As a prospective study, we compared language localization using functional magnetic resonance imaging (fMRI) and magnetoencephalography (MEG) with advanced source estimate method in 18 volunteers. Group analysis results showed something similar or discordant between fMRI and MEG activation. It is consider that fMRI technique combined MEG can used for the preoperative localization and postoperative functional evaluation in the future.

5401 Computer 81

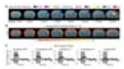

Low frequency activity from somatosensory thalamus propagates brain-wide and modulates top-down visual processing

Alex T. L. Leong[1,2], Russell W. Chan[1,2], Xunda Wang[1,2], Celia M. Dong[1,2], Leon C. Ho[1,2], and Ed X. Wu[1,2]

[1]Laboratory of Biomedical Imaging and Signal Processing, The University of Hong Kong, Hong Kong, Hong Kong, [2]Department of Electrical and Electronic Engineering, The University of Hong Kong, Hong Kong, Hong Kong

Top-down/descending control is a critical stage in sensory processing that underlies numerous cognitive processes. Recent studies uncovered the prevalence of converging long-range networks across multiple sensory modalities as anatomical substrates that likely mediate sensory top-down control. Using an optogenetic fMRI technique that we recently developed to examine patterns of large-scale brain-wide interactions mediated by the somatosensory thalamo-cortical network, we demonstrated that propagating low frequency activity (~1Hz) underlying such interactions enhanced visual responses in the superior colliculus. This work presents a new approach to investigate the functional roles of top-down control and their underlying brain mechanisms.

5402 Computer 82

Correction of Gradient Artefacts in Simultaneous EEG-FMRI from Rotating Gradient Trajectories

Mark Chiew[1], Jostein Holmgren[2], Nadine N Graedel[1], Dean Fido[1], Catherine E Warnaby[1], and Karla L Miller[1]

[1]FMRIB Centre, University of Oxford, Oxford, United Kingdom, [2]Institute of Psychology, University of Oslo

We propose a method for correcting gradient artefacts in simultaneous EEG-FMRI that are variable from shot-to-shot, where artefacts cannot be identified via averaging. The artefact model is extracted from a data-driven decomposition that identifies the signal contributions which show geometric variation matching that of the trajectory rotation model. We show that this correction, applied to a rotating EPI trajectory, works just as well as standard approaches applied to conventionally sampled (non-rotating) EPI data. This will allow the use of more flexible sampling approaches in simultaneous EEG/FMRI that facilitate highly accelerated dynamic image reconstruction.

5403 Computer 83

Simultaneous trimodal MR-flumazenil-PET-EEG imaging in a rest-task-rest design in humans

Irene Neuner[1,2,3,4], Ravichandran Rajkumar[1,2,3,4], Praveen Sripad[1], Christine Wyss[1,4,5], Jörg Mauler[1], Lutz Tellmann[1], Elena Rota Kops[1], Jürgen Scheins[1], Markus Lang[6], Frank Boers[1], Christoph Lerche[1,4], Johannes Ermert[6], Bernd Neumaier[6], Jürgen Dammers[1], Karl-Josef Langen[1,7], Hans Herzog[1], Wolfram Kawohl[4,5], and N Jon Shah[1,3,4,8,9]

[1]Institute of Neuroscience and Medicine 4 (INM4), Forschungszentrum Juelich GmbH, Juelich, Germany, [2]Department of Psychiatry, Psychotherapy and Psychosomatics, RWTH Aachen University, Aachen, Germany, [3]JARA – BRAIN – Translational Medicine, Juelich, Germany, [4]TRIMAGE-consortium, Juelich, Germany, [5]Department of Psychiatry, Psychotherapy and Psychosomatics, University Hospital of Psychiatry, Zurich, Switzerland, [6]Institute of Neuroscience and Medicine 5 (INM5), Forschungszentrum Juelich GmbH, Juelich, Germany, [7]Department of Nuclear Medicine, RWTH Aachen University, Aachen, Germany, [8]Department of Neurology, RWTH Aachen University, Aachen, Germany, [9]Department of Electrical and Computer Systems Engineering, and Monash Biomedical Imaging, School of Psychological Sciences, Monash University, Melbourne, Australia

How quickly does the human brain switch back from a task mode to the resting state condition? This question is addressed in a small sample of healthy volunteers employing a simultaneous trimodal MR-flumazenil-PET-EEG approach at 3T. Based on the fMRI results, we observe an increase in ReHo - a measure of local connectivity - coupled with a slight decrease in the binding potential of [^{11}C] Flumazenil in the PCC which is a major hub of the default mode network; this indicates a change of the GABA-ergic driven inhibitory tonus. This is accompanied with changes in the alpha band over parietal electrodes.

5404 Computer 84

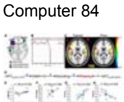

GABA MRS combined with resting state functional connectivity to explore decoding and fluency skills of typical and struggling readers

Lisa C. Krishnamurthy[1,2,3], Venkatagiri Krishnamurthy[2,3,4], Dina M. Schwam[5], Daphne Greenberg[5], and Robin D. Morris[3,6]

[1]Dept. of Physics & Astronomy, Georgia State University, Atlanta, GA, United States, [2]Center for Visual and Neurocognitive Rehabilitation, Atlanta VAMC, Decatur, GA, United States, [3]Center for Advanced Brain Imaging, GSU/GT, Atlanta, GA, United States, [4]Dept. of Neurology, Emory University, Atlanta, GA, United States, [5]Dept. of Educational Psychology, Special Education, and Communication Disorders, Georgia State University, Atlanta, GA, United States, [6]Dept. of Psychology, Georgia State University, Atlanta, GA, United States

Previous reports have shown that resting concentrations of gamma-amino butyric acid (GABA) will predict resting state Functional Connectivity (rsFC) measures as well as amplitude of task activation. The goal of this study is to model how the neurochemical profile interplays with the connectivity underlying the decoding and fluency components of the reading circuit. Our model is in support of recent task-based fMRI observations, but goes beyond by interrogating the underlying networks that support the behavior, and combining that information with the neurochemistry that characterize the trait. These preliminary results of combining MRS and rsFC with neuropsychological measures are promising, and will help identify the underlying dysfunction in struggling adult readers' brain circuitry.

5405 Computer 85

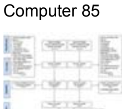

Multimodal meta-analysis of neural correlates in first-episode drug-naïve major depressive disorder

Weina Wang[1], Youjin Zhao[2], Xinyu Hu[2], and Qiyong Gong[2]

[1]West China Hospital of Sichuan University, Chengdu, People's Republic of China, [2]West China Hospital of Sichuan University, People's Republic of China

Evidence of structural and resting-state functional brain abnormalities in MDD has been inconsistent. We conducted the first multimodal meta-analysis of voxel-based morphometry (VBM) and amplitude of low-frequency fluctuation (ALFF) studies in first-episode drug-naïve MDD patients. 15 VBM data setsand 11 ALFF data sets were included. A multimodal meta-analysis was used to highlight brain regions with both structural and functional abnormalities. The multimodal meta-analysis identified conjoint structural and functional differences in the left lateral orbitofrontal cortex and right supplementary motor area. Dissociated anatomical and functional brain abnormalities in MDD were also observed. Meta-analysis revealed in MDD a complex pattern of conjoint and dissociated structural and functional brain abnormalities in brain regions involved in cognition and emotional processing.

5406 Computer 86

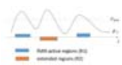

Multimodal functional imaging using modified fMRI-weighted minimum-norm estimation

Jing Xu[1], Tianyi Qian[2], Thomas Beck[3], and Jia-Hong Gao[1]

[1]Center for MRI Research, Peking University, Beijing, People's Republic of China, [2]MR Collaborations NE Asia, Siemens Healthcare, Beijing, People's Republic of China, [3]Application Development, Siemens Healthcare, Erlangen, Germany

Multimodal functional neuroimaging by combining fMRI and EEG has been studied to achieve high-resolution reconstruction of the spatiotemporal cortical current density (CCD) distribution. Although fMRI-constrained EEG/MEG source imaging can enhance spatiotemporal resolution of functional neuroimaging, it has been reported that hard fMRI constraint can result in misidentification of neuronal sources if mismatches exist between fMRI activations and EEG/MEG sources. In this study, we propose a new method modified fMRI-weighted minimum-norm estimation (mfMNE) to solve the problem of fMRI–EEG integrated source imaging. This method may be a promising option for solving the mismatches between fMRI and EEG/MEG in the fMRI-constrained EEG/MEG source imaging.

5407 Computer 87

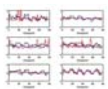

A Comparison of BOLD Signal Amplitude and Electrical Activity During Task Performance in MS and Healthy Control Subjects: Evidence of Neurovascular Decoupling

Mark J Lowe[1], Wanyong Shin[1], Balu Krishnan[2], and Lael Stone[2]

[1]Imaging Institute, Cleveland Clinic, Cleveland, OH, United States, [2]Neurlogic Institute, Cleveland Clinic, Cleveland, OH, United States

Recent reports indicate that cerebrovascular reactivity (CR) may be impaired in multiple sclerosis (MS). Here we report initial studies to use simultaneous measurements of electroencephalography (EEG) and BOLD during performance of a motor task. Using EEG-derived predictors of BOLD response, we show that, while EEG robustly predicts the amplitude of the BOLD signal in healthy control subjects, the estimation is very poor in MS patients. This could be direct evidence of cerebrovascular decoupling of the BOLD signal in MS.

5408 Computer 88

Investigation of neural mechanism underlying ipsi- and contra-lateral acupuncture analgesia in the capsaicin-induced pain model

Xuan Niu[1], Yuchen Zhang[1], Qiuli Zhang[1], Haining Li[1], Zhuonan Wang[1], Yingxiang Sun[1], Lijun Bai[2], and Ming Zhang[1]

[1]The First Affiliated Hospital of Xi'An Jiaotong University, Xi'an, People's Republic of China, [2]The Key Laboratory of Biomedical Information Engineering,Ministry of Education, Department of Biomedical Engineering, School of Life Science and Technology, Xi'an Jiaotong University, Xi'an, People's Republic of China

This paper presents an original research to investigate the underlying neural mechanism on analgesia at ipsi- or contra-lateral acupuncture with capsaicin-induced allodynia on human body. Our findings further suggested that DMN participants in the modulation of spatial-oriented attention on placebo analgesia as a mechanism underlying the degree to which treatment side corresponding to the pain. Notably, disruptions of the DMN may account for the cognitive and behavioral impairments in chronic pain patients. In addition, it may possibly reflect individual variation in placebo response, thus, as a valuable neural biomarker to predict clinical curative effect in acupuncture treatment.

5409 Computer 89

Altered structure and function reflect chronic pain in patients with idiopathic trigeminal neuralgia

Yuan Wang[1,2], Dongyuan Cao[3], Bethany Remeniuk[2,4], David Seminowicz[2], and Ming Zhang[1]

[1]Department of Medical Imaging, The First Affiliated Hospital of Xi'an Jiaotong University, Xi'an, People's Republic of China, [2]Department of Neural and Pain Sciences, School of Dentistry, University of Maryland Baltimore, Baltimore, MD, United States, [3]Key Laboratory of Shaanxi Province for Craniofacial Precision Medicine Research, Stomatological Hospital, Xi'an Jiaotong University Health Science Center, Xi'an, People's Republic of China, [4]Department of Psychiatry and Behavioral Sciences, Johns Hopkins University School of Medicine, Baltimore, MD, United States

To testify the hypothesis of morphometric and functional alterations of patients with idiopathic trigeminal neuralgia (ITN), we displayed gray matter volume (GMV) reductions in the anterior and middle cingulate cortex (ACC and MCC), insula, and several regions of temporal lobe. Additionally, enhanced functional connectivity was revealed between right insula and ACC, medial prefrontal cortex, posterior cingulate cortex (PCC), and dorsal lateral prefrontal cortex in ITN patients. Furthermore, GMV of left inferior temporal gyrus negatively correlated with pain intensity and disease duration in patients, and connectivity of right insula-ACC was negatively associated with pain scores, depression, and anxiety ratings, respectively.

5410 Computer 90

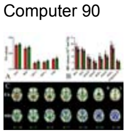

Alterations of white matter integrity and hippocampal functional connectivity in type 2 diabetes without cognitive impairment

Qian Sun[1], Guan-Qun Chen[2], Yu Ying[3], Yu-Chuan Hu[3], Lin-Feng Yan[3], Xin Zhang[3], Yang Yang[3], Wen Wang[3], Ying Han[2], and Guang-Bin Cui[3]

[1]Department of Radiology, Tangdu Hospital, Fourth Military Medical University, Xi'an, People's Republic of China, [2]Department of neurology, Xuan Wu Hospital, Capital Medical University, People's Republic of China, [3]Department of Radiology, Tangdu Hospital, Fourth Military Medical University, People's Republic of China

Researchers and clinicians interested in neuroimaging and type 2 diabetes mellitus without cognitive impairment, with a particular interest in diffusion tensor imaging (DTI) and resting state functional magnetic resonance imaging (rs-fMRI)

5411 Computer 91

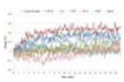

Detecting gamma frequency neural activity using simultaneous multiband EEG-fMRI

Makoto Uji[1], Ross Wilson[1], Susan T. Francis[2], Stephen D. Mayhew[1], and Karen J. Mullinger[1,2]

[1]Centre for Human Brain Health (CHBH), University of Birmingham, Birmingham, United Kingdom, [2]SPMIC, School of Physics and Astronomy, University of Nottingham, Nottingham, United Kingdom

We establish a methodology for optimal combination of simultaneous EEG recording with sparse multiband fMRI that preserves high resolution, whole brain fMRI coverage with broad-band EEG signal measurement uncorrupted by MR gradient artefacts. We demonstrate the ability of this approach to record gamma frequency (>50Hz) EEG signals, that are usually obscured during continuous fMRI data acquisition. In a novel application to a motor task we observe a positive correlation between gamma and BOLD responses, supporting and extending previous findings concerning the coupling between neural and haemodynamic measures of brain activity.

5412 Computer 92

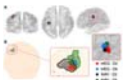

SomatoMotor Mapping in MEG

Eleanor Barratt[1], George O'Neill[1], Rosa Sanchez-Panchuelo[1], Matthew Brookes[1], and Susan Francis[1]

[1]School of Physics, University of Nottingham, Nottingham, United Kingdom

Sensorimotor mapping allows separation of the brain's representation of individual digits. This is possible using functional magnetic resonance imaging (fMRI), but is more challenging in magnetoencephalography (MEG) where it has been demonstrated by mapping evoked responses. Here, we use ultra-high field (7T) fMRI to map digits in a finger-tapping experiment, and contrast our findings to equivalent results showing the spatial signatures of beta band oscillatory responses measured in MEG. We show that the MEG beta rebound can be mapped topographically.

5413 Computer 93

Toward real-time head motion corrections in simultaneous EEG-fMRI: Convolutional neural network classification of EEG-derived motion independent components.

Chung-Ki Wong[1], Vadim Zotev[1], Raquel Phillips[1], Masaya Misaki[1], and Jerzy Bodurka[1,2,3]

[1]Laureate Institute for Brain Research, Tulsa, OK, United States, [2]Stephenson School of Biomedical Engineering, University of Oklahoma, Norman, OK, United States, [3]Center for Biomedical Engineering, University of Oklahoma, Norman, OK, United States

In EEG-fMRI, EEG electrodes record head motions with a high temporal resolution (EEG-motion-sensor), which can be utilized for retrospective slice-by-slice fMRI motion correction. EEG motion components derived from independent component (IC) analysis were automatically identified by the common features observed in the IC mean power spectral density, spatial projection topographic map, and signal contribution. For real-time application of the EEG-motion-sensor, pre-trained models are desirable for faster classification. We used convolutional neural network to evaluate performance of motion-IC classification model. High speed and classification accuracy were achieved on a large EEG-fMRI dataset, suggesting the possibility of real-time EEG-motion-sensor applications for fMRI.

5414 Computer 94

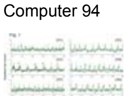

Multi-scale peak detection method for an automatic cardioballistic artifact period determination directly from EEG-fMRI data

Chung-Ki Wong[1], Qingfei Luo[1], Vadim Zotev[1], Raquel Phillips[1], and Jerzy Bodurka[1,2,3]

[1]Laureate Institute for Brain Research, Tulsa, OK, United States, [2]Stephenson School of Biomedical Engineering, University of Oklahoma, Norman, OK, United States, [3]Center for Biomedical Engineering, University of Oklahoma, Norman, OK, United States

In simultaneous EEG-fMRI, the period of cardioballistic artifact (BCG) in EEG is required for the artifact removal. Recording the electrocardiogram (ECG) waveform during fMRI is difficult, often causing inaccurate period detection. Since the BCG artifact waveform in EEG-fMRI is relatively invariable compared to the ECG waveform, we propose a multiple-scale peak-detection algorithm to determine directly the BCG period from EEG-fMRI data. The algorithm achieves a high detection accuracy of the BCG artifact occurrence on a large EEG-fMRI dataset without using the ECG waveforms, virtually eliminating the need for ECG for BCG artifact removal.

5415 Computer 95

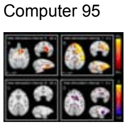

Effect of DBS stimulation intervals on brain activity and dopamine release

Christin Y. Sander[1], John Arsenault[1,2], Bruce R Rosen[1], Wim Vanduffel[1,2], and Joseph B Mandeville[1]

[1]Athinoula A. Martinos Center for Biomedical Imaging, Department of Radiology, Massachusetts General Hospital, Harvard Medical School, Charlestown, MA, United States, [2]Laboratory of Neuro- and Psychophysiology, Katholieke Universiteit, Leuven, Belgium

In this study, deep brain stimulation with chronically implanted electrodes in the unilateral ventral tegmental area of a monkey was performed. The purpose was to determine stimulation paradigms for a range of inter-stimulation intervals that would enable the simultaneous observation of brain activity using fMRI and endogenous dopamine release using [^{11}C]raclopride-PET. While long inter-stimulation intervals produced a unilateral focal CBV response in the striatum but no change in [^{11}C]raclopride binding, short intervals produced a more widespread CBV response and displacement of [^{11}C]raclopride. This study shows the effect of stimulation parameters on brain activity, neurotransmitter release and its limits of detectability.

5416 Computer 96

Mapping TMS immediate effects by concurrent TMS/fMRI using a dedicated high-sensitivity coil array

Martin Tik[1], Michael Woletz[1], Lucia Navarro de Lara[1], Ronald Sladky[1], André Hoffmann[1], Allan Hummer[1], Nicole Geissberger[1], and Christian Windischberger[1]

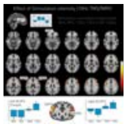

[1]Division MR Physics, Center for Medical Physics and Biomedical Engineering, Medical University of Vienna, Wien, Austria

In this work we show the feasibility of a novel concurrent TMS/fMRI setup based on two multi-channel receive arrays that allows for **whole brain fMRI data acquisition during brain stimulation**. We show that stimulation at frequencies of 1 and 10Hz, respectively, leads to distinct changes in BOLD signal. We also report increased TMS-related network effects with higher stimulation. This validity check sets the frame for efficacy studies investigating the TMS stimulation of cortical areas for modulating complex brain networks.

Electronic Poster

Thermal/HIFU

Exhibition Hall | Thursday 13:00 - 14:00

5417 Computer 1

In-Bore MRI-Guided and Monitored Laser Ablation for Renal Malignancy: Outcome Data from 46 Treated Tumors with 24-Month Median Follow-up

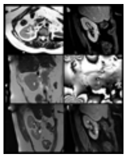

Sherif G. Nour[1,2], Kareem K Elfatairy[3], Debra O Weber[3], Melinda M. Lewis[4], and Viraj A Master[5]

[1]Radiology and Imaging Sciences, Emory University Hospitals and School of Medicine, Atlanta, GA, United States, [2]Interventional MRI Program, Emory University Hospitals and School of Medicine, Atlanta, GA, United States, [3]Radiology and Imaging Sciences, Interventional MRI Program, Emory University Hospitals, Atlanta, GA, United States, [4]Pathology, Emory University Hospitals and School of Medicine, Atlanta, GA, United States, [5]Urology, Emory University Hospitals and School of Medicine, Atlanta, GA, United States

Interventional MRI technology has been used to guide and monitor renal ablation procedures because of its ability to provide online feedback on ablation progress and determine treatment endpoints based of individual tumor responses. The field of Interventional MRI lacks the abundance of outcome data that provide the evidence for the added value of using MRI technology to guide interventions. We report the long-term efficacy data for interactive guidance and real-time monitoring of 46 renal ablation procedures performed entirely within an interventional MRI suite using a short introducing needle and a flexible laser fiber.

5418 Computer 2

Quantitative Evaluation of Thermochemical Ablation Injections in Bovine Liver Phantoms using ^{23}Na MRI

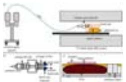

Tobias Theis[1], Nicolas G. R. Behl[1], Erik N. K. Cressman[2], Armin M. Nagel[1,3], Sebastian Flassbeck[1], Aaron Kujawa[1], Peter Bachert[1], Mark E. Ladd[1], and Florian Maier[1]

[1]Medical Physics in Radiology, German Cancer Research Center (DKFZ), Heidelberg, Germany, [2]Interventional Radiology, The University of Texas MD Anderson Cancer Center, Houston, TX, United States, [3]Institute of Radiology, University Hospital Erlangen, Erlangen, Germany

Thermochemical ablation (TCA), a novel minimally invasive ablation therapy, was quantitatively evaluated using ^{23}Na MRI at 7T. In this study, eight TCA injection experiments were performed using eight *ex vivo* bovine liver phantoms. Normalization on the reference tubes and B_1-correction of the ^{23}Na images were performed to get quantitative values. This improved the maximum relative error of the estimated amount of substance by a factor of 3.6. The total injected amount was accurately determined. This study shows that quantitative ^{23}Na MRI provides detailed information about TCA injections, which is important for computational modelling of the method and cell damage prediction.

5419 Computer 3

Monitoring Cryoablation using Short Inversion Recovery Ultrashort Echo Time (STIR-UTE) MRI

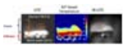

Junichi Tokuda[1], Kemal Tuncali[1], Ravi T Seethamraju [2], Clare M Tempany[1], and Ehud J Schmidt[1]

[1]Radiology, Brigham and Women's Hospital and Harvard Medical School, Boston, MA, United States, [2]Siemens Healthcare, Boston, MA, United States

We propose a new technique to delineate the area below the critical temperature in the frozen tissue during cryoablation using STIR UTE MRI. It relies on the temperature-dependency of the T1 in the frozen tissue. We demonstrated the technique in an ex vivo swine kidney sample using a 3T MRI scanner with a STIR PETRA sequence. To create a uniform temperature gradient, the sample was placed between dry-ice and warm bath, while UTE and STIR UTE images were being acquired. The STIR UTE image demonstrated hyper-intensity in the frozen area, relative to hypo-intensity in the UTE image.

5420 Computer 4

Field drift-correction of PRFS temperature mapping using interleaved non selective free induction decay (FID) readouts

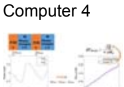

Cyril J Ferrer[1], Lambertus W Bartels[1], Tijl van der Velden[1], Charles Mougenot[1], Chrit T.W Moonen[1], and Clemens Bos[1]

[1]UMC Utrecht, Utrecht, Netherlands

During long hyperthermia procedures guided by MR thermometry, drift of the main magnetic field leads to systematic errors in PRFS measurements, compromising the required temperature monitoring. In this study we evaluated if interleaving acquisition of PRFS MRT with non-selective FID readouts using conventional receive coil elements allows for correcting the drift effects in PRFS thermometry. Automated field drift correction using interleaved non-selective FIDs allowed maintaining a precision and accuracy better than 1°C. This temperature precision would typically be required for controlling a hyperthermia procedure.

5421 Computer 5

MR Relaxation Properties in MR Coagulation for Vascular Repair

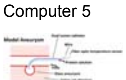

Ming Zhao [1,2], Ouri Cohen[2], Erez Nevo[3], R.Gilberto Gonzalez[2], and Jerome L. Ackerman[2]

[1]Department of Physics, University of Massachusetts Lowell, Lowell, MA, United States, [2]Martinos Center, Department of Radiology, Massachusetts General Hospital, Charlestown, MA, United States, [3]Robin Medical, Inc., Baltimore, MD, United States

As part of a project to develop MR-induced RF heating of a coagulable biomaterial for minimally invasive repair of vascular lesions, we investigate the relationship between the heat coagulation behavior and MR relaxation properties of egg white. This protein solution is a good model for the analogous behavior of human serum albumin solution, an optimal (but expensive) biomaterial for MR coagulation. We find that large changes in both T_2 and the width of the magnetization transfer spectrum clearly indicate the temperature at which the coagulation process occurs. T_2 and MT weighted MR images identify coagulated material in an aneurysm phantom.

5422 Computer 6

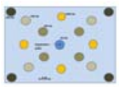

Effect of the transceive phase on MR thermometry in aqueous mediums

G. Salim[1], P. Baron[1], D.H.J. Poot[1], J.A. Hernandez Tamames[1], T. Drizdal[2], M.M. Paulides[2], S. Klein[3], and G. Salim[1]

[1]Radiology dept., Erasmus Medical Center, Rotterdam, Netherlands, [2]Radiation Oncology dept., Erasmus Medical Center, Rotterdam, Netherlands, [3]Biomedical Imaging Group Rotterdam (BIGR), Erasmus Medical Center, Rotterdam, Netherlands

In this work we illustrate the effect of changes in the transceive phase on the quality of MR thermometry in acqueous medium.

5423 Computer 7

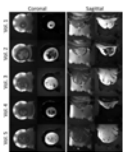

In Vivo Evaluation of a Multi-echo Pseudo-Golden Angle Stack of Stars Thermometry Method

Bryant T. Svedin[1], Allison Payne[1], and Dennis L. Parker[1]

[1]Radiology and Imaging Sciences, University of Utah, Salt Lake City, UT, United States

A multi-echo pseudo-golden angle stack of stars sequence for use in free-breathing interventional procedures is evaluated in vivo with 5 healthy volunteers for use in MR thermometry in the breast. High spatial and temporal resolution (1.3 mm^3, 1.43 s) is achieved through k-space filtering. PRF temperature, T2*, ρ (signal magnitude at TE = 0), respiration correction and fat/water separation are simultaneously measured. Use of a pseudo-golden angle increment allows for the removal of phase (and therefore PRF temperature) artifacts due to changing k-space sampling between reconstructed time points. k-Space sampling based phase reference library greatly improves temperature standard deviation compared to a single baseline reference.

5424 Computer 8

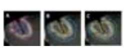

A Methodology for Deriving Thermal Dose Model Parameters from Perioperative MR Data

Christopher MacLellan[1,2], David Fuentes[1,2], Sujit Prabhu[3], Ganesh Rao[3], Jeffrey S. Weinberg[3], John D. Hazle[1,2], and R. Jason Stafford[1,2]

[1]Imaging Physics, MD Anderson Cancer Center, Houston, TX, United States, [2]The University of Texas Graduate School of Biomedical Sciences at Houston, Houston, TX, United States, [3]Neurosurgery, MD Anderson Cancer Center, Houston, TX, United States

Real-time damage estimates provided by Magnetic Resonance Temperature Imaging (MRTI) and appropriate thermal dose models can provide crucial feedback during of thermal ablation procedures. However, these models are not tailored to the post-treatment radiological endpoints that are used to verify the extent of the thermal lesion after therapy. A technique is developed to allow estimation of thermal dose model parameters through retrospective analysis of MRTI and post-treatment imaging. The feasibility of this technique is investigated in a protein coagulation phantom and clinical ablation data.

5425 Computer 9

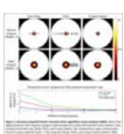

Highly accelerated Cartesian MR thermometry without parallel imaging using undersampled partial Fourier acquisition and k-space hybrid reconstruction

Rebecca E Weires[1,2] and Will Grissom[1,2]

[1]Department of Biomedical Engineering, Vanderbilt University, Nashville, TN, United States, [2]Institute of Imaging Science, Vanderbilt University, Nashville, TN, United States

Partial Fourier temperature mapping using the k-space hybrid algorithm is shown to be more accurate than conventional partial Fourier reconstruction, and the use of partial Fourier acquisition patterns improves the performance of the k-space hybrid algorithm. Undersampled partial Fourier acquisition with k-space hybrid reconstruction can be used to achieve highly accelerated, artifact-free temperature mapping with a robust Cartesian acquisition. Reconstruction is parallelized in the slice dimension and frequency-encoded dimension to achieve real-time volumetric EPI temperature mapping, without parallel imaging.

5426 Computer 10

Visualization of the VIM Thalamic Nucleus using Synthesized MPRAGE Images

Jiachen Zhuo[1], Steven Roys[1], John Hebel[1], Erma Owens[1], Prashant Raghavan[1], Dheeraj Gandhi[1], and Rao P Gullapalli[1]

[1]Diagnostic Radiology and Nuclear Medicine, University of Maryland School of Medicine, Baltimore, MD, United States

The ventral intermediate nucleus (VIM) of the thalamus is a highly effective target for treatment of essential tremor (ET). Visualization of VIM is however challenging due to the lack of T1 or T2 MRI contrast between the various thalamic nuclei. In this study, we used synthesized MPRAGE images with varied inversion time (TI) (SynTI images) to visualize the VIM for pre-surgical planning in MRgFUS treatment of ET. Verification based on 24hr post-treatment lesion location on four patients showed good agreement from the identified VIM with lesion center.

5427 Computer 11

MR-HIFU mild hyperthermia for recurrent rectal cancer: updated results from a phase I clinical trial

William Chu[1], Robert M Staruch[2], Samuel Pichardo[3,4], Yuexi Huang[5], Merrylee McGuffin[1], Ruby Endre[5], Gregory Czarnota[6], and Kullervo Hynynen[5]

[1]Radiation Oncology, Sunnybrook Health Sciences Centre, University of Toronto, Toronto, ON, Canada, [2]Clinical Sites Research Program, Philips Research, Cambridge, MA, United States, [3]Thunder Bay Regional Research Institute, Thunder Bay, ON, Canada, [4]Electrical Engineering, Lakehead University, Thunder Bay, ON, Canada, [5]Physical Sciences Platform, Sunnybrook Research Institute, Toronto, ON, Canada, [6]Radiation Oncology, Sunnybrook Health Sciences Centre, Toronto, ON, Canada

We present the updated results of our phase I trial that delivers mild hyperthermia using magnetic resonance-guided high intensity focused ultrasound (MR-HIFU) combined with radiation and chemotherapy in the treatment of locally recurrent rectal cancer. Participation in the study is based on careful consideration of patient and tumor factors. MR-HIFU mild hyperthermia was delivered in three sessions during a 17-day regimen. MR-HIFU mild hyperthermia was successfully delivered and the procedure was well tolerated. No adverse effects have been reported following the combined treatment to date.

5428 Computer 12

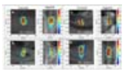

In Vivo Targeting Accuracy Assessment of a MR-guided Focused Ultrasound Device (MRgFUS) Equipped with Tracking Coils

Sara Johnson[1], Bryant T Svedin[2], and Allison Payne[3]

[1]Bioengineering, University of Utah, Salt Lake City, UT, United States, [2]Physics, University of Utah, Salt Lake City, UT, United States, [3]Radiology, University of Utah, Salt Lake City, UT

MR-guided focused ultrasound (MRgFUS) ablation treatments can be improved with more accurate and faster treatment planning. In this study, a fast, automatic tracking coil system is employed to predict the ultrasound transducer focus for treatment planning purposes. The accuracy of the geometric focus predictions was assessed in vivo with a breast-specific MRgFUS device. This study reports a targeting accuracy of 3.1 ± 1.4mm, measured as the average Euclidean distance between the volumetric center of mass of thermal sonications and their predicted focal locations.

5429 Computer 13

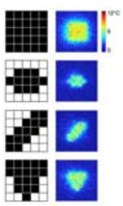

MR Thermometry-guided Ultrasound Hyperthermia of User-Defined Regions Using the ExAblate Prostate Ablation Array

Eugene Ozhinsky[1], Vasant A. Salgaonkar[2], Chris J. Diederich[2], and Viola Rieke[1]

[1]Radiology and Biomedical Imaging, University of California San Francisco, San Francisco, CA, United States, [2]Radiation Oncology, University of California San Francisco

We have implemented a real-time MR thermometry-guided system for ultrasound hyperthermia delivery within user-defined regions and validated it in phantom experiments. It was based on the commercial ExAblate prostate transducer, RTHawk real-time MRI system and featured accelerated PRFS MR thermometry and automated steering of the ultrasound focus to ensure uniform heating of the entire region of treatment.

5430 Computer 14

Active catheter tracking for cardiac MR thermometry during radiofrequency ablation

Solenn Toupin[1,2], Valéry Ozenne[1], Pierre Bour[1,3], Rainer Schneider[4], Matthieu Lepetit-Coiffé[2], Baudouin Denis de Senneville[5], Erik Dumont[3], Pierre Jaïs[6], and Bruno Quesson[1]

[1]Imaging, IHU Liryc (Electrophysiology and heart modeling institute), Bordeaux, France, [2]Siemens Healthineers France, Saint-Denis, France, [3]IGT (Image Guided Therapy), Pessac, France, [4]Siemens Healthineers, Germany, [5]IMB (Mathematics Institute of Bordeaux), Bordeaux, France, [6]Electrophysiology and Ablation Unit, IHU Liryc (Electrophysiology and heart modeling institute), Bordeaux, France

Cardiac MR thermometry provides a real-time monitoring of temperature distribution in myocardium during catheter-based radiofrequency ablation. One major challenge of this technique is the compensation of motion induced by the heart contraction and respiration. In this study, we propose to perform fast multi-slice proton resonance frequency (PRF) shift MR thermometry combined with a real-time slice following technique, based on active catheter tracking. Performance of this approach was evaluated in vitro on a moving agar gel phantom.

5431 Computer 15

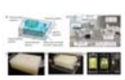

Detailing radio frequency heating induced release of a fluorescent model drug attached to a thermoresponsive polymer carrier: A 7.0 T thermal MR study

Yiyi Ji[1], Alexander E. Dunn[2], Michal Pham[1], Werner Hoffmann[3], Min-Chi Ku[1], Helmar Waiczies[4], Sonia Waiczies[1], Cyrille Boyer[2], May Lim[2], Thoralf Niendorf[1,4,5], and Lukas Winter[1]

[1]Berlin Ultrahigh Field Facility (B.U.F.F.), Max Delbrück Center for Molecular Medicine in the Helmholtz Association (MDC), Berlin, Germany, [2]School of Chemical Engineering, University of New South Wales, Sydney, Australia, [3]Physikalisch-Technische Bundesanstalt (PTB), Berlin, Germany, [4]MRI.TOOLS GmbH, Berlin, Germany, [5]Experimental and Clinical Research Center (ECRC), a joint cooperation between the Charité Medical Faculty and the Max Delbrück Center for Molecular Medicine in the Helmholtz association, Berlin, Germany

Utilizing the RF pulses of the MR system for MR imaging, controlled RF heating and temperature monitoring with MRTh in an integrated system is appealing for MR guided thermal interventions. In this work, we demonstrate for the first time the applicability of our integrated system for targeted drug delivery using a pH- and thermoresponsive polymer. Upon RF heating to T>LCST, the polymers released 50% of its load in 30min, and 89% in 120min. Temperature monitoring with MRTh and external fiber optic temperature sensors were well correlated, with a deviation of 0.2-0.9°C.

5432 Computer 16

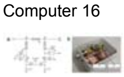

Higher is better: High peak and high average RF power transmit/receive switch for an integrated RF heating applicator operating at 297 MHz (7.0 Tesla)

Yiyi Ji[1], Werner Hoffmann[2], Michal Pham[1], Celal Oezerdem[1], Helmar Waiczies[3], Thoralf Niendorf[1,3,4], and Lukas Winter[1]

[1]Berlin Ultrahigh Field Facility (B.U.F.F.), Max Delbrück Center for Molecular Medicine in the Helmholtz Association (MDC), Berlin, Germany, [2]Physikalisch-Technische Bundesanstalt (PTB), Berlin, Germany, [3]MRI.TOOLS GmbH, Berlin, Germany, [4]Experimental and Clinical Research Center (ECRC), a joint cooperation between the Charité Medical Faculty and the Max Delbrück Center for Molecular Medicine in the Helmholtz association

An integrated RF heating system utilizes the MR spin excitation frequency together with dedicated RF antennas for controlled RF heating and MR imaging in an integrated system. Operating the MR power amplifier for both RF heating and MR imaging applications simultaneously requires customized transmit/receive (Tx/Rx) switches that can handle both high peak powers and high average powers. In this work we designed, built and evaluated a high power Tx/Rx switch for handle MRI and RF heating requirements.

5433 Computer 17

PRF temperature and velocity mapping of complex fluid flow inside a pin fin array heat exchanger

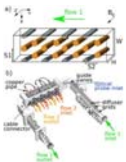

Waltraud B. Buchenberg[1], Florian Wassermann[2], Martin Bruschewski[3], Sven Grundmann[3], Axel J. Krafft[1], Jürgen Hennig[1], and Bernd Jung[4]

[1]Department of Radiology, University Medical Center Freiburg, Medical Physics, Freiburg, Germany, [2]Department of Fluid Mechanics and Aerodynamics, Technische Universität Darmstadt, Darmstadt, Germany, [3]Institute of Fluid Mechanics, University of Rostock, Rostock, Germany, [4]Interventional and Pediatric Radiology, University Hospital, Institute of Diagnostic, Bern, Switzerland

MR thermometry (MRT) and MR velocimetry (MRV) allow to non-invasively measure temperature and velocity fields. Therefore, they are well-suited to address medical questions; however, they can also be a valuable tool to study fluid flow and heat transfer phenomena in technical devices. Here, PRF temperature and velocity measurements were performed in a complex flow setup: a pin fin array consisting of multiple copper tubes which is frequently used in industrial processes for cooling purposes. MRV and MRT are excellent techniques to gain new insights into fundamental heat transfer phenomena and they greatly extend conventional tools for temperature and velocity measurements.

5434 Computer 18

Dynamically Modified BHT Model Enhanced PRF Shift Thermometry for Monitoring Microwave Ablation

Jinchao Wu[1], Xing Wei[2], Jiafei Yang[2], Bingyao Chen[2], Zijing Dong[3], Shuo Chen[1], and Kui Ying[1]

[1]Key Laboratory of Particle and Radiation Imaging, Ministry of Education, Department of Engineering Physics, Tsinghua University, Beijing, People's Republic of China, [2]Department of Orthopedics, First Affiliated Hospital of PLA General Hospital, Beijing, People's Republic of China, [3]Department of Biomedical Engineering, Tsinghua University, Beijing, People's Republic of China

A Bio-Heat Transfer (BHT) model enhanced PRF method was introduced to improve the temporal resolution and to recover the lost signal caused by the susceptibility of probe in microwave ablation. Simulation results of MR-guided microwave ablation performed in an agar phantom show that the proposed method can recover the temperature map with the largest error less than 2°C and increase the temporal resolution to 1s or 0.5s with adequate computing capacity.

5435 Computer 19

A fully electronically steered phased array with 4096 elements for ultrasound treatments under MRI guidance

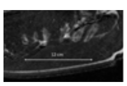

Yuexi Huang[1], Ben Lucht[1], Rohan Ramdoyal[1], Samuel Guneseelan[1], Tyler Portelli[1], Ping Wu[1], and Kullervo Hynynen[1,2,3]

[1]Physical Sciences Platform, Sunnybrook Research Institute, Toronto, ON, Canada, [2]Department of Medical Biophysics, University of Toronto, Toronto, ON, Canada, [3]Institute of Biomaterials and Biomedical Engineering, University of Toronto, Toronto, ON, Canada

A flat focused ultrasound array of 13 cm in diameter with 4096 elements was manufactured in house with center-to-center element spacing of half-wavelength at the centre frequency of approximately 500 kHz. The design allows for a much wider steering range. Feasibility for thermal ablation and hyperthermia over large target volumes was demonstrated in animal studies.

5436 Computer 20

A Three-dimensional Target Tracking Technique for MRgHIFU using an Image Matching Method with Liver Deformation Volumes Obtained via Time-Resolved Volume Acquisitions

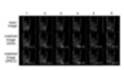

Etsuko Kumamoto[1,2], Daisuke Kokuryo[2], and Kagayaki Kuroda[3,4]

[1]Information Science and Technology Center, Kobe University, Kobe, Japan, [2]Graduate School of System Informatics, Kobe University, Kobe, Japan, [3]Graduate School of Engineering, Tokai University, Hiratsuka, Japan, [4]Center for Frontier Medical Engineering, Chiba University, Chiba, Japan

MRgHIFU treatment for liver requires a tracking technique to “lock on” to the focal spot at the target tissue region during respiratory-induced motion for targeting and temperature imaging. Here, we proposed a target tracking technique using template matching methods. A pre-operative, multi-slice sagittal image series under natural slow breathing was acquired, and a database, including a three-dimensional translation and deformation behavior of the liver and the target, was constructed. Intra-operative target tracking was performed by acquiring a single sagittal slice. The experimental results were demonstrated the feasibility of the three-dimensional target tracking technique using a template matching methods.

5437 Computer 21

Variation of B1+ Homogeneity and SNR Efficiency in Select Water Bolus Designs for Transcranial MR-Guided Focused Ultrasound

Matthew R. Tarasek[1], Benny Assif[2], Eyal Zadicario[2], and Desmond T.B. Yeo[1]

[1]MRI, GE Global Research, Niskayuna, NY, United States, [2]Insightec Ltd., Tirat Carmel, Israel

Transcranial magnetic resonance (MR)-guided focused ultrasound (tcMRgFUS) has gained prominence as a technology for treating several brain pathologies. A typical FUS applicator has a large water bolus in direct contact with the patient’s head to provide (i) acoustic coupling to the patient, and (ii) a means to remove heat generated from acoustic absorption in the skull. These water bolus structures can lead to significant image artefacts. Here we use electromagnetic simulations to assess water bolus compartment designs that have different electrical properties. The goal is to downselect a design that produces improved B1+ homogeneity and SNR in a region of interest.

5438 Computer 22

Monitoring of Microbubbles Stable Cavitation in a Flowing Phantom by Using MRI

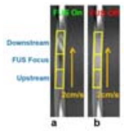

Cheng-Tao Ho[1], Chen-Hua Wu[1], Shih-Tsung Kang[1], Wen-Shiang Chen[2], Po-Hung Hsu[3], Hao-Li Liu[3], Chih-Kuang Yeh[1], and Hsu-Hsia Peng[1]

[1]Department of Biomedical Engineering and Environmental Sciences, National Tsing Hua University, Hsinchu, Taiwan, [2]Department of Physical Medicine and Rehabilitation, National Taiwan University Hospital, Taipei, Taiwan, [3]Department of Electrical Engineering, Chang-Gung University, Taoyuan, Taiwan

We aim to real-time monitor the signal intensity (SI) change of microbubbles in the presence of stable cavitation (SC) effect in a flowing phantom to comprehend the combining effects of SC and flow. Distinct reduced SI was observed, particularly in the focused ultrasound (FUS) focus and downstream regions, during transmitting FUS pulses. More substantial SI changes can be observed with increase of acoustic pressure. In this study, we verified the feasibility of using HASTE sequence to real-time monitor SI changes at the presence of SC effect of MBs in a flowing phantom.

5439 Computer 23

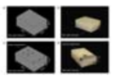

PRF thermometry accuracy at 7.0T for thermal MR applications with and without the presence of fat

Michal Pham[1], Yiyi Ji[1], Hendrik Paysen[1], Eva Oberacker[1], Till Huelnhagen[1], Thoralf Niendorf[1,2,3], and Lukas Winter[1]

[1]Berlin Ultrahigh Field Facility (B.U.F.F.), Max Delbrück Center for Molecular Medicine in the Helmholtz Association, Berlin, Germany, [2]Experimental and Clinical Research Center (ECRC), a joint cooperation between the Charité Medical Faculty and the Max Delbrück Center for Molecular Medicine, Berlin, Germany, [3]MRI.TOOLS GmbH, Berlin, Germany

Proton resonance frequency (PRF) shift temperature mapping is influenced by B_0 field drift, temperature dependent electromagnetic property changes that alter phase velocity, alpha calibration and temperature dependent magnetic susceptibility changes. This work details PRF thermometry at 7.0T of a thermal MR setup. In a homogeneous agarose phantom PRF reading accuracy is within the accuracy of fiber optic sensor readings (0.29±0.21)°C. Temperature dependent magnetic susceptibility changes in pure fat lead to significant temperature reading errors. However, for more realistic thermal MR applications in the human brain (ΔT<10°C, volume fat fractions< 10-20%), temperature reading accuracy is comparable to water-based samples.

5440 Computer 24

Percutaneous MRI-guided focal cryoablation of recurrent prostate cancer: how we do it

Christiaan G. Overduin[1], Joyce G.R. Bomers[1], Michiel J.P.M. Sedelaar[2], Sjoerd F.M. Jenniskens[1], and Jurgen J. Fütterer[1,3]

[1]Radiology and Nuclear Medicine, Radboud University Medical Centre, Nijmegen, Netherlands, [2]Urology, Radboud University Medical Centre, Nijmegen, Netherlands, [3]MIRA Institute for Biomedical Engineering and Technical Medicine, University of Twente, Enschede, Netherlands

We present a feasible and safe approach to perform transperineal MRI-guided focal cryoablation in patients with recurrent PCa after radiotherapy, with encouraging initial results.

Electronic Poster

MR Safety

Exhibition Hall — Thursday 13:00 - 14:00

5441 Computer 97

Real-time measuring of active medical devices malfunction, rectification and induced gradient voltages during MRI exam: low-frequency voltage sensor for MRI safety test.

Thérèse Barbier[1,2], Sarra Aissani[1], Nicolas Weber[1], Julie Kabile[1], Cédric Pasquier[1], and Jacques Felblinger[1,3]

[1]IADI, U947, INSERM, Université de Lorraine, Nancy, France, [2]Axon' Cable, Montmirail, France, [3]CIC 1433 Innovation Technologique, INSERM, CHRU Nancy, Nancy, France

An MR compatible low-frequency voltage probe design will be presented. This tool is used to monitor active implanted medical devices during MRI exam as well as measuring the gradients switching induced voltage or RF rectification thus allowing MRI safety assessment and combined field tests.

5442 Computer 98

Quasi MR-imaging Artefact Free ECoG and Intracortical Electrodes

Johannes B. Erhardt[1], Maria Vomero[1,2], Jochen Leupold[3], Calogero Gueli[1,2], Sam Kassegne[2], and Thomas Stieglitz[1]

[1]Dep. of Microsystems Engineering, University of Freiburg, Freiburg, Germany, [2]Dep. of Mechanical Engieneering, San Diego State University, United States, [3]Dep. of Radiology, University Medical Center Freiburg, Germany

The combination of implantable neural electrodes and fMRI holds great potential for better understanding the human brain. However, the image acquisition - especially in the vicinity of the implants - is compromised by artifacts caused by metal components. In this work we address this issue by studying different types of devices in terms of designs and materials, and by quantifying their MRI artifacts. Doing so we demonstrate the quasi artifact-free behavior of a hybrid probe combining surface and penetrating carbon electrodes into a single sheet of polyimide, after comparing it with conventional implants in high field MRI and clinical fMRI.

5443 Computer 99

Adaptive SAR mass-averaging compared against thermal simulations in the presence of a titanium hip prosthesis in 7T pTx MRI

Aurelien Destruel[1,2], Kieran O'Brien[2,3], Markus Barth[2], Jin Jin[1], Feng Liu[1], and Stuart Crozier[1]

[1]School of Information Technology and Electrical Engineering, The University of Queensland, Brisbane, Australia, [2]Centre for Advanced Imaging, The University of Queensland, St Lucia, Australia, [3]Siemens Healthcare Pty Ltd, Brisbane, Australia

The lack of study and guidelines means there is currently no imaging of orthopaedic metal implants at 7T MRI. Local RF heating should preferably be monitored to ensure that no heating occurs close to the implant. SAR_{10g} is the current preferred method to monitor the patients' local radiofrequency exposure. This study shows that keeping SAR_{10g} under recommended values does not ensure that heating remains under safe values close to a hip prosthesis when compared with the more relevant thermal simulations. A new adaptive SAR mass-averaging approach is introduced and gives more reliable prediction of the location and magnitude of heating.

5444 Computer 100

Neurological MRI protocols for patients with DBS equipment in situ consistent with new B1+RMS -limited MR Conditional product label

Annie Papadaki[1,2], M. Jorge Cardoso[3], Stephen J. Wastling[1,2], Tarek Yousry[1,2], Ludvic Zrinzo[4], Indran Davagnanam[1,2], and John S, Thornton[1,2]

[1]Lysholm Department of Neuroradiology, National Hospital for Neurology and Neurosurgery, University College London Hospital, London, United Kingdom, [2]Department of Brain Repair and Rehabilitation, Institute of Neurology, University College London, London, United Kingdom, [3]Translational Imaging Group, Centre for Medical Image Computing (CMIC), Department of Medical Physics and Bioengineering, University College London, [4]Unit of Functional Neurosurgery, Institute of Neurology, University College London

We modified routine clinical head MRI protocols to be compliant with a new MR conditional product label for deep brain stimulation (DBS) devices limiting B_{1+RMS} to ≤2.0μT. 12 healthy volunteers were scanned using the routine and modified protocols. Quantitative signal to noise (SNR) and contrast to noise ratio (CNR) analysis was performed, as well as blinded rating of images by a neuroradiologist. Routine and B_{1+RMS} -limited sequences yielded very similar SNR and grey vs. white matter CNR values, indicating that the B_{1+RMS} condition had been achieved with minimum impact on image quality, consistent with the neuroradiologist's qualitative assessment.

5445 Computer 101

Analysis of MRI gradient induced voltage on Deep Brain Stimulator lead using high resolution anatomical models

Xi Lin Chen[1], Shiloh Sison[1], Xin Huang[1], Shi Feng[1], and Richard Williamson[1]

[1]St Jude Medical, Sylmar, CA, United States

When a patient with implantable device such as deep brain stimulator undergoes MR scan, the exposure to gradient fields can induce strong voltage across the lead and cause unintended stimulation to the patient or damage the device. In this study, three tiers of voltage determination approach recommended by ISO/TS 10974 ED2 were executed. The analysis results indicate that the tier 3 approach which utilizes realistic gradient coil designs, anatomical models and numerical simulations may arrive at predicted voltage value five times lower than tier 1 approach because of the avoidance of over-conservative assumptions.

5446 Computer 102

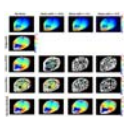

Potential for Estimation of Perfusion from MR Thermometry – A Simulation Study

Giuseppe Carluccio[1,2] and Christopher Michael Collins[1,2]

[1]Radiology, Center for Advanced Imaging Innovation and Research (CAI2R), New York University, New York, NY, United States, [2]Radiology, Bernard and Irene Schwartz Center for Biomedical Imaging, New York University, New York, NY, United States

Among the several parameters that affect temperature computation, blood perfusion is one of the most relevant. According to some studies, perfusion may change significantly with local temperature changes: therefore, it is relevant to characterize both the baseline value of perfusion and its dependence on local temperature for a correct temperature estimation with numerical simulations. In this work, we compare the efficiency and the robustness to noise levels of three different methods to estimate blood perfusion based on the analysis of temperature images which can be acquired, for example, with MR thermometry sequences.

5447 Computer 103

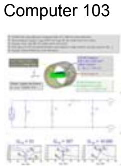

Coil losses significantly alter the electromagnetic fields of a 64 MHz quadrature driven birdcage coil

Mikhail Kozlov[1,2], Leonardo M Angelone[3], and Wolfgang Kainz[3]

[1]MR:comp GmbH, Gelsenkirchen, Germany, [2]Max Planck Institute for Human Cognitive and Brain Sciences, Leipzig, Germany, [3]Division of Biomedical Physics, U.S. FDA, CDRH, Office of Science and Engineering Laboratories, Silver Spring, MD, United States

We investigated the dependence of the incident electric field (***E***) generated in the ASTM phantom on the coil losses. The results showed that magnetic field (***H***) normalized to √wbSAR, depends on capacitor ***Q*** factors. To avoid systematic errors in predicting the induced electric fields inside a human body the coil model should include realistic coil losses. Our results indicate that the use of ratio ***E*** to ||***H***|| at the coil iso-center normalization to predict ***E*** inside a human body located in a commercial birdcage coil based on a numerical coil model with arbitrary coil losses can result in high errors.

5448 Computer 104

Sensitivity of the transfer function on the dielectric properties of the surrounding media: a case study

Mikhail Kozlov[1,2] and Wolfgang Kainz[3]

[1]MR:comp GmbH, Gelsenkirchen, Germany, [2]Max Planck Institute for Human Cognitive and Brain Sciences, Leipzig, Germany, [3]Division of Biomedical Physics, U.S. FDA, CDRH, Office of Science and Engineering Laboratories, Silver Spring, MD, United States

In this case study we show the dependence of the lead transfer function and the RF-induced power deposition (***P***) on the presence of heterogeneous tissues around of the lead tip. Depending on the lead length, our results shows a dramatic non-linear dependence of ***P*** on a small volume of a different tissue surrounding the lead tip, i.e., a fatty pocket, when using a TF derived in a homogeneous media. Thus, using TFs derived in a homogeneous media can result in large systematic errors in predicting ***P***, and consequently the lead tip heating, of AIMDs inside a human body.

5449 Computer 105

Study of RF coupling and heating in multi-wire SEEG Electrodes.

Tanvir Baig[1], Bhumi Bhusal[1], Pallab Bhattacharyya[2], Stephen Jones[2], and Michael Martens[1]

[1]Physics, Case Western Reserve University, Cleveland, OH, United States, [2]Cleveland Clinic Foundation, Cleveland, OH, United States

A SEEG electrode contains a number of contact points and as many number of insulated wires each following a contact. Here, we studied the coupling among the contact wires of SEEG electrode inserted into phantom, by using temperature measurements at different contact points, and varying the lengths of contact wires. From the experiment, we saw that, changing the length of one contact wire will result in change in temperature rise to other contacts also, even if wire lengths corresponding to those contacts are unchanged. This shows significant coupling among the wires at the RF frequency of 3T MRI system.

5450 Computer 106

Analytical Solution for Electric Field Induced Inside Ellipsoidal Conductor by Time-Varying Magnetic Fields in MRI

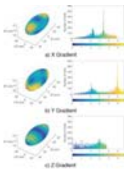

Peter J Shin[1] and Daniel B Vigneron[1]

[1]University of California, San Francisco, San Francisco, CA, United States

An analytical, closed-form solution for the electric field induced inside an ellipsoidal conductor by time-varying gradients in MRI was developed. We applied the method to calculate the electric field for an ellipsoid centered on the isocenter having the semi-axis lengths 20 cm, 15 cm, and 40 cm in LR, AP, and SI directions. We observed that, due to the geometry, ramping up on the Y-axis resulted in the highest electric field intensity. Furthermore, we found that, when the ellipsoid is shifted in the SI direction, the electric field intensity increases approximately 100%.

5451 Computer 107

High Resolution Volume Of Interest Acquisition With 3D Gradient Echo Sequence Using Reduced FOV 2D-RF Excitation Pulse.

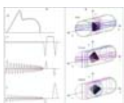

Malek I MAKKI[1,2]

[1]MRI Research, University Children Hospital, Zurich, Switzerland, [2]BioFlow, University Picardie Jules Verne, Amiens, France

We designed high spatio-temporal resolution imaging sequence by reducing the excited 3D volume to the object of interest in the slab. A fast spoiled gradient recalled echo acquisition sequence was modified by incorporating spiral selective 2DRF excitation in 2 perpendicular gradients. Three different combinations of slice-select gradient axis (XY, YZ, and XZ) were tested simultaneously in axial, coronal and sagittal prescription planes and different imaging parameters to define the best scheme that provides extremely high resolution spatial imaging, with low SAR and minimum artefact on clinically available scanner.

5452 Computer 108

RF safety of an implanted port catheter in direct vicinity of a 7T transmit head coil

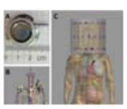

Oliver Kraff[1], Yacine Noureddine[1,2], Eileen Frerk[1,3], Andreas K Bitz[4], Mark E Ladd[1,4], and Harald H Quick[1,5]

[1]Erwin L. Hahn Institute for MRI, University Duisburg-Essen, Essen, Germany, [2]MR Safety Testing Laboratory, MR:comp GmbH, Gelsenkirchen, Germany, [3]Hamm-Lippstadt University of Applied Sciences, Hamm, Germany, [4]Medical Physics in Radiology, German Cancer Research Center (DKFZ), Heidelberg, Germany, [5]High Field and Hybrid MR Imaging, University Hospital Essen, Essen, Germany

Potential RF-induced heating from an implanted port catheter in direct vicinity of a local transmit head coil at 7T was investigated. The assessment included direct measurements of E-field and temperature in a rectangular head/shoulder phantom filled with tissue simulating liquid as well as numerical SAR and thermal simulations in two human body models. Two different RF coils were used for the evaluation, a custom-made 8-channel head coil and the widely-available Nova Medical head coil. No evidence of RF-induced heating was found. Identical transmit power restrictions apply with or without port for both investigated RF coil types.

5453 Computer 109

Assessment of specific absorption rate and temperature increase induced by artificial hip joints during MRI scans

Youngseob Seo[1,2]

[1]Korea Research Institute of Standards & Science, Daejeon, Korea, Republic of, [2]Medical Physics, University of Science & Technology, Daejeon, Korea, Republic of

Heating of patients or burning of biological tissues by RF power induced by medical implants during MRI scan is a significant patient safety concern. The poor reliability and repeatability of the manufacturer-reported SAR values on clinical MRI systems have been acknowledged. High SAR and temperature change occur on both head and tail of artificial hip joints. It is essential to assess the safety of MRI system for patient with medical implant by measuring not only accurate SAR deposited in the body, but also temperature elevation due to the deposited SAR during clinical MRI.

5454 Computer 110

Predictive modelling for Sacral Nerve Stimulation Lead heating - Pathway factors and their effect on MRI RF-induced stimulation lead heating

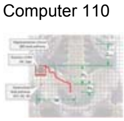

Scott Kalpin[1], Norbert Kaula[2], and Ramez Shehada[3]

[1]Systems Engineering, Nuvectra Medical, Broomfield, CO, United States, [2]R&D, Nuvectra Medical, Broomfield, CO, United States, [3]R&D, Medical Technology Labs, La Mirada, CA, United States

A formula based methodology for predicting Sacral Nerve Stimulation lead temperatures when undergoing MRI exposures is presented. A generalized lead pathway model having 4 primary factors is used to represent the clinical placement. Twelve experimental configurations are selected based on variation of these generalized factors. Heating data measured in an MRI phantom is used to formulate an analytical model. Predictions from the model are compared against the actual data measured in MRI testing. The mean squared error for the model against the 12 test cases is 0.112 °C.

5455 Computer 111

Suitability of right angle pathway for testing RF-induced Spinal Cord Stimulation lead heating in an MRI

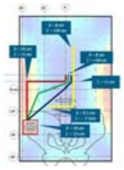

Scott Kalpin[1], Norbert Kaula[2], and Ramez Shehada[3]

[1]Systems Engineering, Nuvectra Medical, Broomfield, CO, United States, [2]R&D, Nuvectra Medical, Broomfield, CO, United States, [3]R&D, Medical Technology Labs, La Mirada, CA, United States

This work evaluates the suitability of various pathway models to represent the worst-case heating for a Spinal Cord Stimulation lead when subjected to MRI RF-intensive exposure. The ideal model represents relevant pathways that a lead can take between any two points with the fewest variable factors. One model, used for evaluation of safety for Spinal Cord Stimulation (SCS) devices, describes a path with 4 variable factors – IPG starting position (Z), vertical rise of the proximal end of the lead (H1), lateral span width (W), and rise of the distal end of the lead within the central axis (H2). The "right angle" model is evaluated direct diagonal, half-way diagonal, and one in which all vertical rise is confined to the central axis of the MRI.

5456 Computer 112

Safety of MRI on patients with abandoned/retained cardiac leads: Patient-derived simulation studies at 64MHz and 127MHz

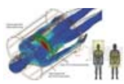

Laleh Golestanirad[1], Amir Ali Rahsepar[2], Jeremy C Collins[2], Rod S Passman[3], Giorgio Bonmassar[4], Boris Keil[5], James C Carr[2], and Lawrence L Wald[1]

[1]Massachusetts General Hospital, Charlestown, MA, United States, [2]Radiology, Northwestern University, Chicago, IL, United States, [3]Medicine, Northwestern University, [4]Radiology, Massachusetts General Hospital, Charlestown, MA, United States, [5]Life Science Engineering, Mittelhessen University of Applied Sciences (THM), Giessen, Germany

Despite the tremendous effort to develop MRI safety protocols to reduce complications in patients with cardiac implantable electronic devices with intact leads, almost nothing is known about the variation and extent of RF heating in patients with fractured or abandoned leads. Here we report the preliminary results of the first systematic simulation study of RF-induced SAR amplification at and around abandoned cardiac leads in patients undergoing MRI at 1.5 T and 3.0 T with different imaging landmarks.

5457 Computer 113

Spatial analysis of acoustic noise transfer function: is the noise level increased by the presence of a patient inside the imager bore during MRI?

Takashi Hamaguchi[1], Tosiaki Miyati[2], Naoki Ohno[2], Tatsuhiko Matsushita[3], Masanori Ozaki[4], Tetsuya Minami[5], Wataru Kouda[5], and Toshifumi Gabata[5]

[1]Department of Radiology, Kanazawa University Hospital, Kanazawa, Japan, [2]Faculty of Health Sciences, Institute of Medical, Pharmaceutical and Health Sciences, Kanazawa University, Kanazawa, Japan, [3]Department of Radiology, Kyoto University Hospital, Kyoto, Japan, [4]MR Engineering, GE Healthcare Japan, Hino, Japan, [5]Faculty of Medicine, Institute of Medical, Pharmaceutical and Health Sciences, Kanazawa University, Kanazawa, Japan

The purpose of our study was to evaluate the spatial distribution of a gradient-pulse-to-acoustic-noise transfer function (GPAN-TF) with and without a phantom inside the bore. This study showed that the spatial distribution of GPAN-TFs with a phantom in the bore was significantly larger than that with an empty imager. The GPAN-TF spectrum for high frequency range were increased by the phantom. Therefore, the patient would be exposed to a more unpleasant sound than conventional evaluation in an empty scanner. The multipoint analysis using GPAN-TFs revealed structural differences in respective gradient coils under a situation similar to actual MR examination.

5458 Computer 114

The ultimate local SAR in realistic body models: Preliminary convergence results

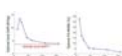

Bastien Guerin[1,2], Stephen F Cauley[1,2], Jorge F Villena[3], Athanasios G Polimeridis[4], Elfar Adalsteinsson[5,6,7], Luca Daniel[7], Jacob K White[7], and Lawrence L Wald[1,2,5]

[1]Radiology, Massachusetts General Hospital, Charlestown, MA, United States, [2]Harvard Medical School, Boston, MA, United States, [3]Cadence Design Systems, Feldkirchen, Germany, [4]Skolkovo Institute of Science and Technology, Moscow, Russian Federation, [5]Harvard-MIT Division of Health Sciences Technology, Cambridge, MA, United States, [6]Institute for Medical Engineering and Science, Massachusetts Institute of Technology, Cambridge, MA, United States, [7]Dept of Electrical Engineering and Computer Science, Massachusetts Institute of Technology, Cambridge, MA, United States

We extend our previously reported methodology for computation of the ultimate signal-to-noise ratio in realistic body models to the computation of the ultimate specific absorption rate (SAR) in the head of the Duke body model at 3 Tesla. We optimize 90° magnitude least-squares RF pulses subject to hundreds of thousands of SAR constraint for increasing numbers of electromagnetic fields in the basis set. As the size of the basis set increases, we show that the local SAR decreases toward a value that we call the "ultimate local SAR".

5459 Computer 115

B1+ maps in adults and children heads at 7.0T: selection of the generic human head model and maximum local SAR evaluation

Gianluigi Tiberi[1,2], Mauro Costagli[1,2], Laura Biagi[2], Nunzia Fontana[3], Riccardo Stara[4], Mark R Symms[5], Mirco Cosottini[6], Renzo Guerrini[7], and Michela Tosetti[1,2]

[1]Imago7, Pisa, Italy, [2]IRCCS Stella Maris Foundation, Pisa, Italy, [3]Dipartimento di Ingegneria dell'Informazione, Pisa, Italy, [4]Dipartimento di Fisica, Pisa, Italy, [5]General Electric ASL Scientist (EMEA), Pisa, Italy, [6]Dipartimento di Ricerca Traslazionale e delle Nuove Tecnologie in Medicina e Chirurgia, Pisa, Italy, [7]Meyer Children's Hospital, Firenze, Italy

In this study we compare B1+ simulations performed on generic anatomic models with subject-specific measured B1+ maps, performed on both adults and children. We introduce a cost function, based on the normalized standard deviations (the ratio between standard deviation and average) of B1+ maps (magnitude), to guide the selection of generic human model to be used for subject-specific maximum local SAR evaluation. Maximum local SAR does not show a significant variation with subject weight and with subject cranial circumference. Limits on maximum SAR are always met for the sequence here considered (SILENT), in all adults and children.

5460 Computer 116

fMRI in Parkinson's Disease: Post STN-DBS implant.

Mohit Saxena[1], Cameron McIntyre[1], and Benjamin Lee Walter[2]

[1]*Neuromodulation Center, Case Western Reserve University, Cleveland, OH, United States,* [2]*Neurology, University Hospitals, Cleveland Medical Center, Cleveland, OH, United States*

We present a method to conduct fMRI in Parkinson's disease patients with fully implanted bilateral STN Medtronic Activa DBS. This allows for fMRI evaluation of clinically optimized settings or other settings that may reveal anatomical correlations with benefits and side effects.

5461 Computer 117

Analytic Validation of a Computational Model of Magnetic Force in Linear Magnetic Materials

Spencer B Parent[1], William Handler[2], John Drozd[2], and Blaine A Chronik[1,2]

[1]*Medical Biophysics, Western University, London, ON, Canada,* [2]*Physics and Astronomy, Western University, London, ON, Canada*

The current procedures and guidelines for testing forces on medical devices require that testing be performed in a MR setting, which is both timely and costly. To reduce test time and cost, a computational model of magnetic force was developed. Using a test case where an analytic solution of magnetic force can be applied, it is shown that for materials with magnetic susceptibility (chi)<10^{5} ppm, a computational model of magnetic force was correct within 10% error and this error decreases to less than 1% for chi<10^{4} ppm. Size of object is shown to have little effect on error.

5462 Computer 118

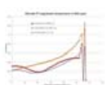

Comparing Transfer Functions in Different Tissues with a Spinal Cord Stimulation System for Estimation of RF Heating during MRI Scans

Xiaoyi Min[1] and Shiloh Sison[2]

[1]*St. Jude Medical, Inc, Sylmar, CA, United States,* [2]*St. Jude Medical, Inc, Sunnyvale, CA, United States*

The objective of this study is to compare transfer functions (TFs) of a Spinal Cord Stimulation (SCS) system in high permittivity media (HPM), low permittivity media (LPM) and in spinal cord by using computer simulations. For a SC model, we modeled the anatomical and conductive properties of the lower thoracic (T7-T10) spinal cord. The TF curves in HPM and in SCS follow each other closely. With a SC model, the compound tissue effect around the lead was seen. Lowering HPM conductivity would shift the curve slightly up that with the SC model for in-vivo.

5463 Computer 119

Loopoles vs. conventional MR loops under safety considerations

Jörg Felder[1], Chang-Hoon Choi[1], and N. Jon Shah[1,2]

[1]*Institute of Neuroscience and Medicine (INM-4), Forschungszentrum Jülich, Jülich, Germany,* [2]*Faculty of Medicine, Department of Neurology, JARA, RWTH Aachen University, Aachen, Germany*

While the application of loopole configurations may be beneficial to improve B_1 distribution at high fields it comes with the drawback of reduced voltage withstanding capability during transmission. This either implies use with lower transmit power or the addition of more capacitors which in turn degrades the quality factor of the coil and thus efficiency and sensitivity of the antenna element.

5464 Computer 120

A web-based searchable system to confirm MRI compatibility for medical implants in Japan

Yasuhiro Fujiwara[1], Hitoshi Fujioka[2], Tomoko Watanabe[2], Maiko Sekiguchi[2], and Ryuji Murakami[1]

[1]*Department of Medical Imaging, Faculty of Life Sciences, Kumamoto University, Kumamoto, Japan,* [2]*Medie Corporation, Tokyo, Japan*

The purpose of this study was to develop a web-based searchable MRI safety information system for confirming medical implant compatibility and to evaluate the usefulness of the system. The system allows MRI compatibility confirmation to be performed over internet. This system facilitates obtaining MRI safety information for medical implants easily and rapidly, thereby improving the safety of MRI examination.

Electronic Poster

MRS Processing

Exhibition Hall — Thursday 13:00 - 14:00

5465 Computer 25

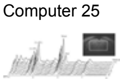

Estimating acetate extracellular fraction in the rat brain using diffusion-weighted MRS and modeling of tissue microstructure

Marco Palombo[1], Masoumeh Dehghani[2], Nicolas Kunz[3], Bernard Lanz[2], Rolf Gruetter[2,3], and Julien Valette[1]

[1]*Molecular Imaging Research Center (MIRCen), Commissariat à l'Energie Atomique, Fontenay-aux-Roses, France,* [2]*Laboratory of Functional and Metabolic Imaging (LIFMET), Ecole Polytechnique Fédérale de Lausanne, Lausanne, Switzerland,* [3]*Center for Biomedical Imaging (CIBM), Ecole Polytechnique Fédérale de Lausanne, Lausanne, Switzerland*

While most brain metabolites detected by *in vivo* MRS are intracellular, some of them, in particular energy metabolism substrates such as glucose, lactate and acetate, are also known to be significantly present in the extracellular space. Although of high metabolic significance and of practical importance for metabolic flux quantification in labeling studies, the accurate determination of the extracellular fraction remains challenging. Here we propose to use diffusion-weighted MRS combined with modeling of tissue microstructure to estimate acetate's extracellular fraction in the rat brain, which we find to be ~45%.

5466 Computer 26

Magnetization exchange between water and downfield metabolites in human brain at 9.4T

Nicole D Fichtner[1,2], Ioannis-Angelos Giapitzakis[3], Nikolai Avdievich[3], Ralf Mekle[4], Daniel Zaldivar[3], Anke Henning[2,3], and Roland Kreis[1]

[1]Depts. Radiology and Clinical Research, University Bern, Bern, Switzerland, [2]Institute for Biomedical Engineering, UZH and ETH Zurich, Zurich, Switzerland, [3]Max Planck Institute for Biological Cybernetics, Tuebingen, Germany, [4]Center for Stroke Research Berlin (CSB), Charité Universitätsmedizin Berlin, Berlin, Germany

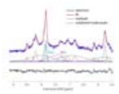

Ultra-high field strengths provide higher signal to noise ratio and improved separation of metabolites in spectroscopy, allowing for more precise characterization of peaks. In particular, this improved peak resolution may be of benefit for characterization of the downfield (5-10ppm) spectrum, which is not yet well characterized; this experiment aims to improve knowledge of downfield peaks by investigating their exchange rates and T_1 values at 9.4T, using inversion transfer experiments and metabolite cycling to allow for non-water suppressed acquisition.

5467 Computer 27

A Subspace Approach to Spectral Quantification

Yudu Li[1,2], Fan Lam[2], Bryan Clifford[1,2], and Zhi-Pei Liang[1,2]

[1]Department of Electrical and Computer Engineering, University of Illinois at Urbana-Champaign, Urbana, IL, United States, [2]Beckman Institute for Advanced Science and Technology, University of Illinois at Urbana-Champaign, Urbana, IL, United States

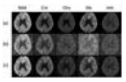

This work presents a novel spectral model for spectral quantification, which represents each spectral component using a subspace instead of a parametric basis function with unknown parameters. The proposed model enables efficient and effective incorporation of both spectral and spatial prior information to improve the quantification performance. The proposed method is validated using both simulation and experimental data, demonstrating superior performance to existing methods using parametric spectral bases. This method is expected to be useful for processing noisy MRSI data.

5468 Computer 28

Quantitative analysis of in vivo MEGA-PRESS spectra in mice at 9.4T

Jia Guo[1], Yanping Sun[2], Zhu Gang[3], Scott A. Small[4], and Douglas L. Rothman[5]

[1]Department of Biomedical Engineering, Columbia University, New York, NY, United States, [2]Department of Medicine, Columbia University, New York, NY, [3]Bruker BioSpin, Billerica, MA, [4]Departments of Neurology, Radiology or Psychiatry, Columbia University, New York, NY, [5]Departments of Biomedical Engineering or Radiology and Biomedical Imaging, Yale University, New Haven, CT

As of yet J-difference editing methods such as MEGA-PRESS have not been applied to in vivo mouse studies due to low sensitivity and the lack of an automated program to analyze the data. To overcome the obstacles, a fully automated software toolkit MRSMouse was developed for the quantitative analysis of MEGA-PRESS data of the mouse brain. With MRSMouse, we demonstrated the feasibility and reproducibility of MEGA-PRESS for detection of GABA in the mouse brain using a Bruker BioSpec 94/20 9.4T system. During anesthesia, significant decreases of mouse thalamic GABA levels caused by isoflurane were noticed in vivo for the first time.

5469 Computer 29

Association of NAA Resonance Frequency with Axonal Orientation

Andrew A Maudsley[1], Mohammed Z. Goryawala[1], and Sulaiman Sheriff[1]

[1]Radiology, University of Miami, Miami, FL, United States

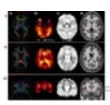

The resonance frequencies of tissue metabolite are affected by cellular-level variations in magnetic susceptibility and the compartmentation of each metabolite. One prominent finding for 1H MRS studies of the brain is differences of the N-Acetylaspartate (NAA) resonance frequency in white matter, which is hypothesized to reflect the inter-axonal localization of this metabolite and susceptibility variations that are dependent on the orientation of the major axonal bundles relative to the applied magnetic field. In this study, the dependence of the NAA frequency on axonal orientation was evaluated using voxel-based analysis of a whole-brain MRSI and diffusion-tensor imaging.

5470 Computer 30

Quantitative MRI of In Vivo Water and Lipid Concentrations with the ERETIC Method

Eric Baetscher[1], Thomas M Barbara[1], Manoj Sammi[1], Krista Vandenborne[2], Glenn Walter[2], and William D Rooney[1]

[1]Advanced Imaging Research Center, Oregon Health & Science University, Portland, OR, United States, [2]Department of Physical Therapy, University of Florida, Gainesville, FL, United States

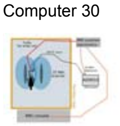

A synthetic radio-frequency (RF) signal, which is received along with the ^{1}H magnetic resonance (MR) signal in magnetic resonance imaging (MRI), is used to determine absolute tissue water and lipid quantities. We show application of this ERETIC method (electronic reference to access *in vivo* concentration) to musculoskeletal imaging, with the potential to better track disease progression in Duchenne Muscular Dystrophy (DMD), and other muscle pathologies.

5471 Computer 31

MR Spectroscopy shows that high fat diet changes composition and distribution of mammary gland fat in a transgenic mouse model of breast cancer

Dianning He[1], Devkumar Mustafi[1], Xiaobing Fan[1], Sully Fernandez[2], Erica Markiewicz[1], Marta Zamora[1], Jeffrey Mueller[3], Joseph Sachleben[4], Matthew J Brady[2], Suzanne D Conzen[5], and Gregory S Karczmar[1]

[1]Radiology, The University of Chicago, Chicago, IL, United States, [2]Medicine, Adult and Pediatric Endocrinology, Diabetes, and Metabolism, The University of Chicago, Chicago, IL, United States, [3]Pathology, The University of Chicago, Chicago, IL, United States, [4]Biochemistry & Molecular Biology, The University of Chicago, Chicago, IL, United States, [5]Medicine, Hematology and Oncology, The University of Chicago, Chicago, IL, United States

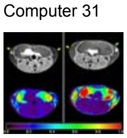

Epidemiological studies show increased risk of breast cancer associated with Western diets containing high animal fat. The aim of this study was to evaluate changes in mammary fat composition due to a high animal fat diet (HAFD), compared to a low fat diet (LFD), in a mouse model of breast cancer. Localized MR spectroscopy and high spectral and spatial resolution (HiSS) MRI data were acquired at 9.4T. The saturated fat fractions **increased** and the polyunsaturated bond component **decreased** significantly in HAFD mice compared to LFD mice. Fat images obtained from HiSS demonstrated increased mammary fat concentration in HAFD mice than LED mice.

5472 Computer 32

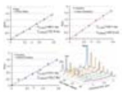

Probing In Vivo Metabolite Relaxation by Linear Quantification of RF Driven Steady States

Linqing Li[1], Ningzhi Li[1], Li An[1], and Jun Shen[1]

[1]National Institute of Mental Health, National Institute of Health, Bethesda, MD, United States

A driven steady states technique for brain metabolite relaxation measurement is proposed. Multiple steady states driven by long pulse train were used to quantify T2 of brain metabolites in vivo. The proposed technique does not need to vary echo time of the measuring sequence such as PRESS. A simple linear equation for quantification of driven steady state spectra was derived using Bloch equations. The derived equation was verified by Bloch simulations, phantom and in-vivo experiments.

5473 Computer 33

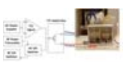

Novel Approach for Simultaneous In Vivo 31P MRS Measurements in Frontal and Occipital Lobes of Human Brain with Dynamic Shimming

Byeong-Yeul Lee[1], Xiao-Hong Zhu[1], Myung Kyun Woo[1], and Wei Chen[1]

[1]Center for Magnetic Resonance Research, Department of Radiology, University of Minnesota Medical School, Minneapolis, MN, United States

Functional/metabolic changes in different brain regions of interest are of importance for better understanding of the pathophysiological mechanism underlying the human brain diseases. In this work, we present a novel design of the dual-channel ^{31}P MRS system for simultaneous measurements of cerebral high-energy phosphate metabolism from two brain regions of interest by incorporating a new pulse sequence and two separated RF surface coils with a transistor-transistor logic (TTL) controller. By successfully implementing this method, we are able to obtain high quality *in vivo* ^{31}P MR spectra from both frontal and occipital lobes within the same amount of time as the traditional method covering one brain region. From an engineering perspective, this new approach provides a cost-effective solution for *in vivo* ^{31}P MRS study of multiple brain regions with a conventional single-channel transmitter-receiver configuration. Therefore, this valuable MR tool can be used in examining the cerebral energy metabolism across different brain regions, and the same approach could be employed to other spin applications.

5474 Computer 34

Prior-Knowledge Quantitation of Glutamate, Glutamine, GABA, and Glutathione using Covariance J-resolved spectroscopy

Zohaib Iqbal[1] and M. Albert Thomas[1]

[1]Radiological Sciences, University of California - Los Angeles, Los Angeles, CA, United States

The two dimensional J-resolved spectroscopy technique is capable of resolving many metabolites in vivo from a volume of interest. However, the spectral resolution along the indirect dimension is generally very poor in these acquisitions. One solution is to apply a covariance transformation along the indirect dimension to yield a resulting Covariance J-resolved (CovJ) spectrum with high spectral resolution. While spectral resolution is enhanced, currently there are no methods available to fit the non-linear aspects of the covariance reconstruction. Here, we have developed a non-linear fitting algorithm capable of yielding Glutamate, Glutamine, GABA, and Glutathione concentrations in vivo using CovJ spectra.

5475 Computer 35

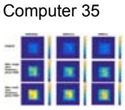

Spectral-Dephasing based Non-Local Means for Spatially Adaptive Denoising in 3D-MRSI

Dhritiman Das[1,2], Eduardo Coello[1,2], Axel Haase[1], Rolf F. Schulte[2], and Bjoern H. Menze[1]

[1]Technical University of Munich, Garching, Germany, [2]GE Global Research, Munich, Germany

We present a data-driven technique for denoising 3D Magnetic Resonance Spectroscopic Imaging (MRSI) data. Our proposed method involves a novel spectral de-phasing and re-phasing approach which increases the phase dimension of the spectra to deal with the arbitrary complex phase in the data. This is coupled with an anisotropic non local means (NLM) filter-based pattern-recognition across the multi-slice data to select similar spectra patches having a similar phase for denoising. We show that our method leads to a mean SNR improvement by an average factor of 4.5 while preserving the spectral resolution of the metabolites.

5476 Computer 36

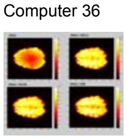

Absolute quantification of brain metabolites by 1H-MRSI using gradient echo imaging of ~2s as a concentration reference: initial findings

Eva Heckova[1], Bernhard Strasser[1], Michal Považan[1,2], Gilbert Hangel[1], Siegfried Trattnig[1,2], and Wolfgang Bogner[1,2]

[1]High Field MR Centre, Medical University of Vienna, Vienna, Austria, [2]Christian Doppler Laboratory for Clinical Molecular MR Imaging, Vienna, Austria

The unsuppressed internal water signal is a standard reference method used for quantification of brain metabolites in 1H-MRSI, however it requires additional water unsuppressed acquisition, which is in case of MRSI time demanding. Therefore we compared the performance of water signal reference acquired with unsuppressed MRSI and with ~2s long gradient echo imaging integrated into MRSI sequence. Our findings indicates that gradient echo imaging can be used as a concentration reference for 1H-MRSI.

5477 Computer 37

Simple and general automatic quality control of 3D 1H MRSI data of the prostate using intrinsic spectral properties

Nassim Tayari[1], Jiri Obels[1], Thiele Kobus[1], Tom W.J. Scheenen[1], and Arend Heerschap[1]

[1]Department of Radiology and Nuclear Medicine, Radboud university medical center, Nijmegen, Netherlands

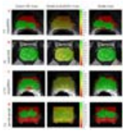

Proton 3D MR spectroscopic imaging (MRSI) provides spatial metabolic information of the prostate for improved cancer detection, localization, and staging. Clinical application of MRSI of prostate requires automatic quality control of spectra. We propose Qratio, a ratio balancing constructive spectral components of choline and citrate signals with destructive elements of lipid signals, water residuals and noise. We demonstrate that Qratio can serve as a general, fast and automated tool for quality control of prostate MRSI data, independent of field strength (1.5-7T) and acquisition protocol. The Qratio can be displayed as maps and performs with an accuracy of 88±3% and AUC=0.93.

5478 Computer 38

Quality Control of MRSI data using efficient data labelling

Nuno Pedrosa de Barros[1], Richard Iain McKinley[1], Roland Wiest[1], and Johannes Slotboom[1]

[1]SCAN / Neuroradiology, University Hospital Bern (Inselspital), Bern, Switzerland

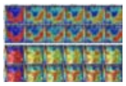

MRSI-data frequently contains bad-quality spectra, what can prevent proper quantification and consequently lead to data misinterpretation. Machine-learning based methods have been proposed for automatic quality control of MRSI-data with performance levels identical to expert's-manual-checking and that can classify thousands of spectra in a matter of a few seconds. Besides this, a considerable amount of time needs to be spent labelling data required to train these algorithms. Here we present a method that allows to actively select those spectra that carry the most information for the classification, allowing to reduce drastically the amount of time needed for labelling.

5479 Computer 39

Ghostbusters for MRS: Automatic Detection of Ghosting Artifacts using Deep Learning

Sreenath P Kyathanahally[1], Andre Doering[1], and Roland Kreis[1]

[1]Depts. Radiology and Clinical Research, University of Bern, Bern, Switzerland

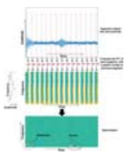

Ghosting artifacts in spectroscopy are problematic since they superimpose with metabolites and lead to inaccurate quantification. Detection of ghosting artifacts using traditional machine learning approaches with feature extraction/selection is difficult since ghosts appear at different frequencies. Here, we used a "Deep Learning" approach, that was trained on a huge database of simulated spectra with and without ghosting artifacts that represent the complex variations of ghost-ridden spectra. The trained model was tested on simulated and in-vivo spectra. The preliminary results are very promising, reaching almost 100% accuracy and further testing on in-vivo spectra will hopefully confirm its ghost busting capacity

---

5480 Computer 40

Spectral quality: rosette spectroscopic imaging in human brain at 3T

Claudiu Schirda[1], Tiejun Zhao[2], Yoojin Lee[1], Hoby P Hetherington[1], and Jullie W Pan[3]

[1]Radiology, University of Pittsburgh, Pittsburgh, PA, United States, [2]Siemens Medical Systems, [3]MRRC, University of Pittsburgh, Pittsburgh, PA

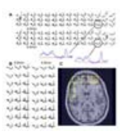

Highly efficient sampling strategies based on gradient trajectories can accelerate MRSI studies by 1-2 orders of magnitude compared to conventional acquisitions. However, increasing acceleration and gradient slew rates commonly result in a predictable decline in spectral quality. This report uses rosette trajectory spectroscopic imaging studies to assess how spectral quality and Cramer Rao lower bounds influence how sensitive the MRSI and metabolite ratios are to the expected variation of tissue gray matter.

5481 Computer 41

Factors influencing Data Quality in a Multi-Center Breast MR Spectroscopy Trial (ACRIN 6657 Extension)

Patrick J Bolan[1], Benjamin A Herman[2], Gregory J Metzger[1], Eunhee Kim[3], David C Newitt[4], Savannah Partridge[5], Michael Garwood[1], Mark A Rosen[6], and Nola M Hylton[4]

[1]Radiology, University of Minnesota, Minneapolis, MN, United States, [2]Center for Statistical Sciences, Brown University, Providence, RI, United States, [3]National Institute of Neurological Disorders and Stroke, NIH, Bethesda, MD, United States, [4]Radiology, University of California, San Francisco, CA, United States, [5]Radiology, University of Washington, Seattle, WA, United States, [6]Radiology, Hospital of the University of Pennsylvania, Philadelphia, PA, United States

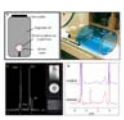

The **ACRIN 6657-extension** trial, the first multi-center trial using magnetic resonance spectroscopy (MRS) in breast cancer, has completed and its initial results have been recently published. This study reports on the quality of the MRS data and identifies technical and logistic factors that contributed to a lower-than-anticipated data yield.

5482 Computer 42

Phase-rotation acquisition to study imperfections of PRESS

Sophie M. Peereboom[1], Maximilian Fuetterer[1], and Sebastian Kozerke[1]

[1]Institute for Biomedical Engineering, University and ETH Zurich, Zurich, Switzerland

A phase-rotation acquisition scheme is able to separate different signals in PRESS. In this work phase-rotation PRESS measurements were complemented by simulations to assess origins of spectral distortions in cardiac spectroscopy. Simulations show that, when using a phase-rotation acquisition scheme for PRESS without spoilers, more motion is acceptable when pulses are better calibrated. However, because of non-ideal pulse profiles, spoilers cannot be fully omitted if moving tissue is studied. It is shown that phase-rotation acqusition can, by combining simulations and measurements, be used as an elegant tool to investigate spectral distortions and optimize sequence parameters in PRESS of moving tissue.

5483 Computer 43

Impact of time sample selection and model function design on the quantification of fatty acid composition: in vitro and in vivo studies.

Angeline Nemeth[1], Hélène Ratiney[1], Benjamin Leporq[1], Amandine Coum[2,3], Giulio Gambarota[2,3], Kevin Seyssel[4], Bérénice Segrestin[5], Pierre-Jean Valette[6], Martine Laville[5], and Olivier Beuf[1]

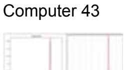

[1]Univ. Lyon, INSA-Lyon, Université Claude Bernard Lyon 1, UJM-Saint Etienne, CNRS, Inserm, CREATIS UMR 5220, U1206, F69621, Lyon, France, [2]INSERM, UMR 1099, Rennes, France, [3]Univ Rennes 1, LTSI, Rennes, France, [4]Department of Physiology, Faculty of Biology and Medicine, University of Lausanne, Lausanne, Switzerland, [5]Centre de Recherche en Nutrition Humaine Rhône-Alpes (CRNH-RA), Centre Hospitalier Lyon Sud, Pierre-Bénite, Lyon, France, [6]Hospices Civils de Lyon, Département d'imagerie digestive, CHU Edouard Herriot, Lyon, France

Interest in the follow-up of fatty acid composition(saturated, polyunsaturated and monounsaturated fatty acid) in the body is growing. Quantitative MR spectroscopy can give access to this fat composition. Today, several quantification methods are used (e.g LCModel, AMARES). However the statistical outcome issued from a quantitative analysis of the lipid signal can be greatly influenced by the used quantification method. We analyze 1) the impact of the time sample selection and design of the model function on the parameter identifiability 2) the quantification results obtained with different quantification models on acquisitions performed in vitro (oils) and in vivo (subcutaneous adipose tissue).

5484 Computer 44

A Novel Method for Absolute Metabolite Quantification of 1H Spectroscopic Imaging in the Human Brain Based on Water Measurement with Ultrashort TE

Michal Bittšanský[1], Milada Kováčová[2], Oliver Štrbák[1], Petra Hnilicová[1], and Dušan Dobrota[3]

[1]Biomedical Center Martin, Jessenius Faculty of Medicine, Comenius University, Martin, Slovakia, [2]Faculty of Mathematics, Physics and Informatics, Comenius University, Bratislava, Slovakia, [3]Jessenius Faculty of Medicine, Comenius University, Martin, Slovakia

We introduce an easily implementable quantification method *in vivo* based on unsuppressed water measurement (pulse-acquire FID sequence with low flip-angle, short TE and TR and geometry identical to metabolite MRSI). Our quantification is practically independent on water relaxation times, requires only short extra measurement time and is robust enough in pathologies like tumors. We tested its results in a homogeneous phantom, healthy volunteers and tumor patients using a head resonator and an 8-channel array coil for acquisition.

5485 Computer 45

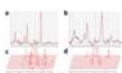

Water lineshape fitting method to overcome B0 field inhomogeneity for NMR spectroscopy

Donghyun Hong[1], Seyedmorteza Rohani Rankouhi[1], Jan-Willem Thielen[1], and David G. Norris[1,2]

[1]Erwin L. Hahn Institute for Magnetic Resonance Imaging, University of Duisburg-Essen, Essen, Germany, [2]Donders Institute for Brain, Cognition and Behavior, Radboud University, Nijmegen, Netherlands

Good B0 field homogeneity is an essential requirement for NMR single voxel spectroscopy. Previously proposed spectral fitting method assumes that all metabolite signals have a Lorentzian shape. However, B0 inhomogeneity may both broaden the linewidth, and modify the lineshape into an asymmetric form. This study has demonstrated a water lineshape fitting method to overcome B0 inhomogeneity using corresponding metabolite fitting models by water lineshape. We obtained similar relative metabolite signal intensities and improved spectral fitting quality regardless of the field homogeneity condition.

5486 Computer 46

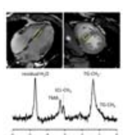

Repeatability of myocardial creatine and triglyceride concentration measurements with ^{1}H-MRS

Adrianus J. Bakermans[1], Paul de Heer[1,2], Gustav J. Strijkers[3], S. Matthijs Boekholdt[4], Aart J. Nederveen[1], and Jeroen A.L. Jeneson[1,5]

[1]Department of Radiology, Academic Medical Center, Amsterdam, Netherlands, [2]C.J. Gorter Center for High Field MRI, Department of Radiology, Leiden University Medical Center, Leiden, Netherlands, [3]Department of Biomedical Engineering and Physics, Academic Medical Center, Amsterdam, Netherlands, [4]Department of Cardiology, Academic Medical Center, Amsterdam, Netherlands, [5]Neuroimaging Center, University Medical Center Groningen, Groningen, Netherlands

Changes in myocardial total creatine (tCr) and triglyceride (TG) content have been linked to the pathogenesis of cardiomyopathy. An assessment of repeatability for absolute quantification of myocardial [tCr] and [TG] is required for ^{1}H-MRS to be employed for longitudinal monitoring of therapeutic efficacy. This work reports intra- and inter-exam repeatability of [tCr] and [TG] measurements with ^{1}H-MRS at 3 Tesla. Our results indicate that the repeatability of the ^{1}H-MRS assay will be sufficient to detect a >50% depletion of the tCr pool, and >50% changes in myocardial TG levels with 95% confidence in a single subject.

5487 Computer 47

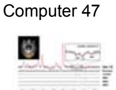

Accurate determination of cerebral lactate and glutamate concentration changes during a long visual stimulus

Carolina Fernandes[1], Bernard Lanz[1], Chen Chen[1], and Peter Morris[1]

[1]Sir Peter Mansfield Imaging Centre, University of Nottingham, Nottingham, United Kingdom

Estimation of metabolic changes during neuronal activation represents a challenge for *in vivo* MRS, particularly in the case of lactate, whose dissociation from other resonances is not straightforward. To reliably quantify lactate, the lipid and macromolecular signals were significantly reduced by using a long TE (144 ms) and the remaining macromolecular signals in the vicinity of the lactate peak were individually fitted with lorentzian peaks. Statistically significant changes in lactate and glutamate levels during 15 min of visual stimulation were detected in the visual cortex, unveiling a distinctive metabolic response pattern, which can provide further insight into brain activation mechanisms.

5488 Computer 48

Full Density Matrix Simulation of Spatially Localized Magnetic Resonance Spectroscopy

Yan Zhang[1], Li An[1], and Jun Shen[1]

[1]National Institute of Mental Health, Bethesda, MD, United States

Numerical simulations of three-dimensionally localized MRS spectra have been very time-consuming for multi-spin systems because the current state-of-the-art requires computation of a large ensemble of spins pixel-by-pixel in three dimensional space. In this abstract it was found that spatial coordinates of the full set of spin density operators labeled by slice selection gradients can be projected onto one dimension after slice selection as long as the crusher gradients are refocused. Therefore, the conventional three-dimensional simulation can be converted to a one-dimensional problem in cases such as the commonly used PRESS or STEAM. The proposed method was implemented using a computer program written in Java language.

Electronic Poster

MRS Acquisition Methods

Exhibition Hall Thursday 13:00 - 14:00

5489 Computer 49

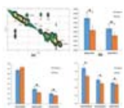

Correlation of Diffusion Weighted Imaging and Echo Planar Correlated Spectroscopic Imaging of Breast Cancer in 3T

Rajakumar Nagarajan[1,2], Maithili Gopalakrishnan[2], Amir Huda[3], Melissa Joines[2], Nanette Debruhl[2], and Michael A Thomas[2]

[1]Human Magnetic Resonance Center, Institute for Applied Life Sciences (IALS), University of Massachusetts, Amherst, MA, United States, [2]Radiological Sciences, University of Califonia Los Angeles, Los Angeles, CA, United States, [3]Physics, California State University, Fresno, CA, United States

In vivo magnetic resonance spectroscopy (MRS) of the breast can be used to measure the level of choline-containing compounds, which is a biomarker of malignancy. The advantage of four dimensional (4D) echo-planar correlated spectroscopic imaging (EP-COSI) enables full slice coverage of the breast facilitating recording of multi-voxel based two-dimensional (2D) MRS than the single-voxel based localized correlated spectroscopy (L-COSY). Also in addition to differentiate malignant from benign, EP-COSI can differentiate the healthy fatty from glandular. Decreased ADC values derived from diffusion weighted imaging (DWI) can be correlated with increased choline and decreased lipids quantified by the EP-COSI technique.

5490 Computer 50

Improving the quality of DW spectra in the supraclavicular fossa with a navigator-gated and cardiac-triggered flow-compensated diffusion-weighted STEAM MRS acquisition

Dominik J. Weidlich[1], Andreas Hock[2], Stefan Ruschke[1], Daniela Franz[1], Hans Hauner[3], Ernst J. Rummeny[1], and Dimitrios C. Karampinos[1]

[1]Department of Diagnostic and Interventional Radiology, Technical University Munich, Munich, Germany, [2]Philips Healthcare, Hamburg, Germany, [3]Else Kröner Fresenius Center for Nutritional Medicine, Technical University Munich, Munich, Germany

Measuring in vivo blood perfusion within the brown adipose tissue depot of the human supraclavicular fossa is highly relevant in metabolic and obesity research. DW-MRS can probe perfusion properties by measuring the IVIM signal of the water peak. However, DW-MRS of the supraclavicular fossa remains a challenging task due the high sensitivity of the region to motion and the associated poor spectral quality. The present work proposes a DW-MRS methodology with a flow compensated acquisition combining cardiac and respiratory tracking to improve spectral quality. IVIM results for the water peak are shown for the first time in the supraclavicular fossa.

5491 Computer 51

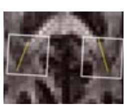

Dual Voxel Diffusion Weighted MR-Spectroscopy

Vincent Oltman Boer[1], Henrik Lundell[1], Tim Bjørn Dyrby[1,2], Itamar Ronen[3], and Esben Thade Petersen[1,4]

[1]Danish Research Centre for Magnetic Resonance, Centre for Functional and Diagnostic Imaging and Research, Copenhagen University Hospital Hvidovre, Hvidovre, Denmark, [2]Department of Applied Mathematics and Computer Science, Technical University of Denmark, Lyngby, Denmark, [3]C. J. Gorter Center for High Field MRI, Department of Radiology, Leiden University Medical Centre, [4]Electrical Engineering, Technical University of Denmark, Lyngby, Denmark

Diffusion weighted spectroscopy is a technique with inherent long scan times. Here it was implemented in a simultaneous multi-voxel technique. This allows simultaneous assessment of multiple brain locations, and gives possibilities to extend the diffusion schemes with more directions and b-values.

5492 Computer 52

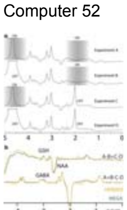

Simultaneous Hadamard Editing of GABA and glutathione

Muhammad Gulamabbas Saleh[1,2], Georg Oeltzschner[1,2], Kimberly L. Chan[1,2,3], Nicolaas A.J. Puts[1,2], Mark Mikkelsen[1,2], Michael Schär[1,2], Ashley D. Harris[4,5], and Richard A.E. Edden[1,2]

[1]Russell H. Morgan Department of Radiology and Radiological Science, The Johns Hopkins University School of Medicine, Baltimore, MD, United States, [2]F. M. Kirby Center for Functional Brain Imaging, Kennedy Krieger Institute, Baltimore, MD, United States, [3]Department of Biomedical Engineering, The Johns Hopkins University School of Medicine, Baltimore, MD, United States, [4]Department of Radiology, University of Calgary, Calgary, AB, Canada, [5]Child and Adolescent Imaging Research Program, Alberta Children's Hospital Research Institute, Hotchkiss Brain Institute, University of Calgary, Calgary, AB, Canada

Hadamard Encoding and Reconstruction of MEGA-Edited Spectroscopy (HERMES) allows the simultaneous, separable editing of GABA and GSH, the two most frequently edited metabolites. Rather than a two-step ON/OFF encoding of MEGA editing, HERMES uses a four-step Hadamard encoding matrix to orthogonally edit multiple metabolites. We demonstrate the method through simulations, phantom and in vivo experiments. HERMES provides excellent separation of GABA and GSH with a two-fold reduction in scan time, while maintaining spectral quality and SNR, compared to sequentially acquired measurements of GABA and GSH using MEGA-PRESS.

5493 Computer 53

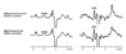

Real-time frequency and motion corrected Hadamard encoded spectral editing (CHASE)

Anouk Marsman[1], Vincent Oltman Boer[1], Mads Andersen[2], and Esben Thade Petersen[1,3]

[1]Danish Research Centre for Magnetic Resonance, Centre for Functional and Diagnostic Imaging and Research, Copenhagen University Hospital Hvidovre, Hvidovre, Denmark, [2]Philips Healthcare, Copenhagen, Denmark, [3]Dept. Electrical Engineering, Technical University of Denmark, Denmark

Inhibitory neurotransmitter GABA and antioxidant GSH are suggested to be implicated in psychiatric and neurological disorders. These metabolites can be measured in the human brain in vivo using edited ^{1}H-MRS. However, traditional MEGA editing can only be performed for one metabolite at a time, whereas Hadamard encoded spectral editing assesses both metabolites in one sequence, thereby reducing total scan time twofold. As the relatively small GABA and GSH signals as well as the Hadamard paradigm are highly susceptible to frequency drift and motion, real-time frequency and motion correction was added to the sequence.

5494 Computer 54

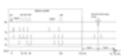

The use of MEGA-sLASER with J-refocusing echo time extension to measure the proton T2 of lactate in healthy human brain at 7 T

Chen Chen[1], Bernard Lanz [1], Carolina Fernandes[1], Susan Francis[1], Penny Gowland[1], and Peter Morris[1]

[1]Sir Peter Mansfield Imaging Centre, University of Nottingham, Nottingham, United Kingdom

The challenges in T_2 measurement of lactate (Lac) in healthy brain tissue include J-modulation, signal overlaps and low concentration. To overcome these and characterize Lac T_2 relaxation in normal brain tissue at 7T (for the first time), this study used a MEGA-sLASER sequence with J-refocusing echo time extension. The measured T_2 value of Lac was 182±10 ms in healthy human brain (occipital lobe), which can be used for absolute quantification of Lac. The measured T_2 of NAA (169±8 ms) agrees with previous 7T reports. With high sensitivity, this approach showed its potential in detecting changes in Lac T_2 in pathology.

5495 Computer 55

Inter and intra-subject repeatability study of GABA Editing using MEGA-PRESS and ImSpecial Sequence

Meng Gu[1], Ralph Hurd[2], Laima Baltusis[3], and Daniel Spielman[1]

[1]Radiology, Stanford University, Stanford, CA, United States, [2]GE Healthcare, Menlo Park, CA, United States, [3]Center for Cognitive and Neurobiological Imaging, Stanford University, Stanford, CA, United States

GABA editing with frequency-insensitive macromolecule suppression using improved MEGA-SPECIAL sequence (ImSpecial) has been developed. By using a very frequency-selective editing pulse with a pulse width of 30 ms, macromolecule was suppressed without applying a lysine-symmetric editing. An inter and intra-subject repeatability studies were conducted to evaluate GABA editing with MEGA-PRESS and ImSpecial. Compared with GABA+/Cre levels using MEGA-PRESS, GABA/Cre levels using ImSpecial is about 40% less with lower variations for both inter and intra-subject repeatability studies, demonstrating significant MM suppression achieved using ImSpecial.

5496 Computer 56

Regional GABA concentration comparison in the human brain with the interleaved short TE sLASER and MEGA-sLASER sequence at 7T

Donghyun Hong[1], Seyedmorteza Rohani Rankouhi[1], Jan-Willem Thielen[1], and David G. Norris[1,2]

[1]Erwin L. Hahn Institute for Magnetic Resonance Imaging, University of Duisburg-Essen, Essen, Germany, [2]Donders Institute for Brain, Cognition and Behavior, Radboud University, Nijmegen, Netherlands

GABA is challenging to resolve due to j-couplings and overlapping signals. Previously proposed GABA editing ans short TE approach at UHF make it possible to measure relative GABA concentration. We measured GABA concentration with the interleaved sequence at various brain regions, and found an optimal method to estimate GABA in terms of spectral fitting quality. Occiptal cortex showed a high GABA concentration, and GABA editing approach gave a reliable spectral fitting quality.

5497 Computer 57

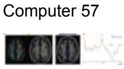

J-difference editing of Creatine in the human brain

Kimberly Chan[1,2,3], Richard Edden[2,3], and Peter Barker[2,3]

[1]Biomedical Engineering, Johns Hopkins School of Medicine, Baltimore, MD, United States, [2]Russell H. Morgan Department of Radiology and Radiological Science, Johns Hopkins School of Medicine, Baltimore, MD, United States, [3]F. M. Kirby Research Center for Functional Brain Imaging, Kennedy Krieger Institute, Baltimore, MD, United States

In in vivo proton spectra, Creatine (Cr) and phosphocreatine are usually regarded as non-coupled spin systems (1). This abstract reports on the observation of a small coupling between the creatine CH2 (3.91 ppm) and CH3 (3.02 ppm) groups. A series of J-difference edited experiments were performed both in a phantom and in the human brain to demonstrate that a coupling exists. This coupling was found to have a coupling constant of 0.28 Hz in an isotropic phantom and an even greater coupling in a white matter region.

5498 Computer 58

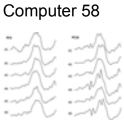

Investigating the effect of phase cycling schemes on GABA-edited spectroscopy using MEGA-PRESS

Jia-Ren Lin[1], Jhih-Ling Liang[1], Yi-Ru Lin[1], Cheng-Wen Ko[2], and Shang-Yueh Tsai[3]

[1]Department of Electronic and Computer Engineering, National Taiwan University of Science and Technology, Taipei, Taiwan, [2]Department of Computer Science and Engineering, National Sun Yat-sen University, Kaohsiung, Taiwan, [3]Research Center for Mind, Brain and Learning, National Chengchi University, Taipei, Taiwan

The application of phase cycling scheme in combination with interleaved off-odd switch has been suggested for MEGA-PRESS method in many previous reports but the effect of phase cycling schemes on the spectral shape of GABA peak and on the GABA quantification has not been studied yet. Here, performance of phase cycling by different number of steps were and by modified interleaved scheme were compared. The results show that phase cycling is necessary to be applied prior interleaved on-off switch and minimum shape cycling steps are suggested to minimize subtraction artifacts possibly resulting from on-off frequency drift and motion.

5499 Computer 59

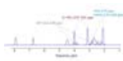

MEGA-PRESS for simultaneous aspartate and glutamate quantification at 3T.

Petr Menshchikov[1,2], Tolibjon Akhadov[2], Il'ya Melnikov[2], and Natalia Semenova[1,2]

[1]Semenov Institute of Chemical Physics, Russian Academy of Sciences, Moscow, Russian Federation, [2]Clinical and Research Institute of Urgent Pediatric Surgery and Trauma, Moscow, Russian Federation

Direct Asp observation using PRESS, STEAM etc. in the human brain is strongly complicated by J-evolution and overlapping with other metabolites. In this work we have adjusted MEGA-PRESS for simultaneous Asp and Glu estimation. According to Vespa simulation as well as phantoms and in vivo studies TE=115ms was chosen as the best for Asp (2.65 and 2.80 ppm) and Glu (2.13 ppm) quantification without overlapping. Asp is the main precursor of neuronal marker NAA. NAA have been shown to be reduced in many disorders. Using this method allows accurate investigation of this important metabolic pathway.

5500 Computer 60

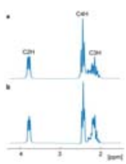

Highly resolved ^{1}H decoupled spectroscopy with a shorter constant time delay using the 2D CT-PRESS with J refocusing

Hidehiro Watanabe[1] and Nobuhiro Takaya[1]

[1]Center for Environmental Measurement and Analysis, National Institute for Environmental Studies, Tsukuba, Japan

The 2D constant time localized sequence of CT-PRESS with J refocusing was proposed, having features of good peak resolution via ^{1}H decoupling along F_1 and of J refocusing by a 90-degree pulse at the first echo time. By controlling the time point of J refocusing, shorter constant time delay of T_{ct} can be achieved. This method was developed on a 4.7 T whole-body MR system. Phantom experiments were demonstrated using brain mixture solutions. Three resonances at 2.28 ppm of GABA C2H, 2.35 ppm of glutamate C4H and 2.44 ppm of glutamine C4H were resolved on the phantom spectra.

5501 Computer 61

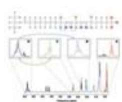

Homonuclear spectral editing to measure ectopic lipid composition in vivo with 1H-MRS

Lucas Lindeboom[1,2] and Robin de Graaf[3]

[1]Dept. of Human Biology/Human Movement Sciences, NUTRIM school for Nutrition and Translational Research in Maastricht, Maastricht University Medical Center, Maastricht, Netherlands, [2]Dept. of Radiology, NUTRIM school for Nutrition and Translational Research in Maastricht, Maastricht University Medical Center, Maastricht, Netherlands, [3]Dept. of Radiology and Biomedical Imaging, Magnetic Resonance Research Center, Yale University School of Medicine, New Haven, CT, United States

1H-MRS has been used extensively to measure the total amount of lipids stored in organs like skeletal muscle and liver and it has been found that these so called ectopic fat stores are associated with insulin resistance. The role of the composition of these lipid stores (e.g. saturated vs. unsaturated fatty acids) in metabolic disturbances is unclear. Here we show the feasibility of spectral editing techniques to characterize lipid composition in adipose tissue and skeletal muscle in vivo. Estimations of lipid composition with our approach are in line with invasive biopsy studies.

5502 Computer 62

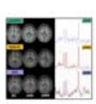

Local metabolites of healthy human brain measured with whole brain spectroscopic imaging and with single voxel spectroscopy - a study to compare different 1H-MRS data acquisitions and data analyses

Birte Schmitz[1], Andrew A Maudsley[2], Sulaimann Sheriff[2], Heinrich Lanfermann[1], and Xiao-Qi Ding[1]

[1]Institute of Diagnostic and Interventional Neuroradiology, Hannover Medical School, Hannover, Germany, [2]Department of Radiology, University of Miami School of Medicine, FL, United States

Local metabolite concentrations in 60 healthy volunteers were estimated from EPSI data that were analyzed from individual voxel measurements and using spectral integration over a ROI and compared to results from single-voxel acquisitions. Linear regression analysis was used to estimate age-dependence of metabolite concentrations obtained with each of the three different methods. The results were compared with each other for quantitative evaluation of EPSI acquisition at short TE for detection of brain metabolites.

5503 Computer 63

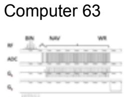

Integration of Water Referencing with Water Suppression for Absolute Quantification of High-Speed MR Spectroscopic Imaging

Akram Etemadi Amin[1], Elena Ackley[2], Kevin Fotso[2], Stephen R Dager[3], and Stefan Posse[2,4,5]

[1]Physisc and Astronomy, U New Mexico, Albuquerque, NM, United States, [2]Neurology, U New Mexico, Albuquerque, NM, United States, [3]Radiology, U Washington, Seattle, WA, United States, [4]Physics and Astronomy, U New Mexico, Albuquerque, NM, United States, [5]Electrical and Computer Engineering, U New Mexico, Albqueruque, NM, United States

We present a new approach with negligible impact on overall scan time that integrates a short water reference acquisition and navigators into the water suppression module, to spatially and spectrally encode the water signal before suppression. We show that this approach enables quantitative 2D and 3D high-speed MR spectroscopic imaging (MRSI) of brain metabolites, for range of pre-localization techniques (slice-selective, slab-selective or PRESS), at short and long TE, and at different slice locations. This method significantly reduces the acquisition time of volumetric MR spectroscopic imaging and is compatible with a wide range of spectroscopic acquisition methods.

5504 Computer 64

Simultaneous water and lipid suppression for brain 1H MR spectroscopy at 7T using multiple RF pulses with spoiling phases

Linqing Li[1], Li An[1], Ningzhi Li[1], and Jun Shen[1]

[1]National Institute of Mental Health, National Institute of Health, Bethesda, MD, United States

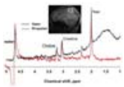

The variation of RF phases may effectively suppress water and lipid coherent signals, as similar effect has been previously demonstrated in GRE MR imaging sequences. We demonstrate a new suppression sequence capable of simultaneous water and lipid suppression with short inter-pulse delay and RF phase spoiling. Monte Carlo analysis showed that the proposed technique can significantly improve both accuracy and precision of metabolite quantification by suppressing lipid contamination.

5505 Computer 65

Overdiscrete Reconstruction for Signal Enhancement in Single Voxel Spectroscopy

Eduardo Coello[1,2], Ralph Noeske[3], Bjoern Menze[1], Axel Haase[1], and Rolf Schulte[2]

[1]Technische Universität München, Munich, Germany, [2]GE Global Research, Munich, Germany, [3]GE Healthcare, Potsdam, Germany

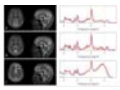

This work proposes an overdiscrete reconstruction for Single Voxel Spectroscopy (SVS). It is demonstrated that in single voxel acquisitions benefit from the SNR and linewidth improvement obtained by correcting for of B_0 inhomogeneities and the optimization of the Spatial Response Function (SRF), as compared to regular signal averaging. This method, enables SV acquisitions in challenging brain areas, i.e. where B_0 shimming is sub-optimal, and corrects for spectral artifacts such as peak aliasing.

5506 Computer 66

Ultra-short echo STEAM with TE of 3 ms improves 1H-MRS based lipid quantification and allows fast localization of 31P metabolite signals in the liver at 7T

Martin Gajdošík[1,2], Marek Chmelík[3,4], Lorenz Pfleger[1,2], Anton Luger[2], Siegfried Trattnig[1,4], and Martin Krššák[1,2]

[1]High-field MR Centre, Department of Biomedical Imaging and Image-guided Therapy, Medical University of Vienna, Vienna, Austria, [2]Division of Endocrinology and Metabolism, Department of Internal Medicine III, Medical University of Vienna, Vienna, Austria, [3]Clinical Molecular Imaging, Karl Landsteiner Institute, Vienna, Austria, [4]Christian Doppler Laboratory for Clinical Molecular MR Imaging, Vienna, Austria

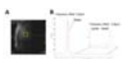

Liver fat quantification with *in vivo* ^{1}H-MR spectroscopy is challenging at ultra-high fields also due to very short T_2 times. Ultra-short TE localized sequence using Gaussian pulses with TE of 3ms was developed and its advantages could be utilized also with ^{31}P-MR spectroscopy. Our data showed, that localization was feasible in large homogeneous tissues such as liver providing liver fat measurement with unprecedented precision. The detection of ^{31}P signals was feasible and resulted in high spectral resolution in acceptable time.

5507 Computer 67

T_2 relaxation times of metabolites measured with LASER and PRESS at 3 T

Dinesh K Deelchand[1], Edward J Auerbach[1], and Małgorzata Marjańska[1]

[1]CMRR, University of Minnesota, Minneapolis, MN, United States

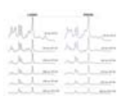

The goal of this study was to compare the apparent transverse relaxation time (T_2) constants of metabolites obtained using LASER and PRESS sequences in the human brain at 3 T. A 25% higher apparent T_2s of total N-acetyl aspartate, total creatine and total choline were measured with LASER sequence as compared to PRESS while comparable apparent T_2s were measured for strongly coupled metabolites, e.g., glutamate and *myo*-inositol, with both sequences.

5508 Computer 68

J-difference semi-LASER for GABA editing

Ralph Noeske[1]

[1]GE Healthcare, Berlin, Germany

The performance of a *J*-difference spectral editing technique based on the across vendor implementation of semi-LASER with high bandwidth GOIA-WURST adiabatic gradient modulated refocusing pulses for a GABA+ and macromolecule-suppressed GABA protocol was investigated. Phantom measurements show a T_E dependence of the edited 3ppm GABA signal that allows using the longer T_E of 80ms to implement a macromolecular-suppressed protocol with higher signal compared to a PRESS based implementation.

5509 Computer 69

Voxel Based Transmit Gain Calibration using Bloch-Siegert semi-LASER at 7T

Ralph Noeske[1], Alessandra Toncelli[2], Hana Hlavata[3], and Michela Tosetti[3,4]

[1]GE Healthcare, Berlin, Germany, [2]INFN and Department of Physics, University of Pisa, Pisa, Italy, [3]IMAGO7 Foundation, Pisa, Italy, [4]IRCCS Stella Maris, Pisa, Italy

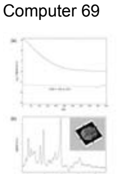

A voxel-based implementation of the Bloch-Siegert phase shift method within a semi-LASER based localization sequence that shows a high robustness to determine transmit gain (TG) for the same volume that is excited for the spectroscopy experiment is demonstrated at 7T. Phantom and in-vivo measurements show higher robustness over a large range of initial TG settings and voxel locations resulting in a faster and more reliable calibration procedure to achieve good voxel selection and spectrum quality and avoid additional calibration steps.

5510 Computer 70

Optimal Echo Time for In-Vivo Glutamate Detection at 7T Using semi-LASER 1H-MRS

Dickson Wong[1,2], Amy Schranz[1,2], and Robert Bartha[1,2]

[1]Medical Biophysics, The University of Western Ontario, London, ON, Canada, [2]Centre for Functional and Metabolic Mapping, Robarts Research Institute, London, ON, Canada

At ultra-high field (7T), the quantification of glutamate by ¹H-MRS is more accurate and precise than at lower field strengths. The semi-LASER ¹H-MRS pulse sequence has advantages at high field but requires the use of relatively long radio frequency pulses to reduce power deposition. Typically, the shortest achievable echo times (TE) are sub-optimal for glutamate detection. In this study, the optimal TE for glutamate detection was estimated by time-domain simulation and verified against in-vivo measurements. Using simulations, the optimal TE was found to be 125 ms. In-vivo measurements in one subject produced a result of ~102 ms. Both results suggest that the glutamate signal is greater at longer TEs (100-125 ms) when using semi-LASER at 7T compared to the shortest achievable TEs (40-60 ms).

5511 Computer 71

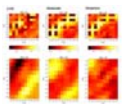

Robust detection of 2-hydroxyglutarate at 7T high field with a fully adiabatic LASER sequence

Morteza Esmaeili[1,2] and Ovidiu Cristian Andronesi[1]

[1]Athinoula A. Martinos Center for Biomedical Imaging, Department of Radiology, Massachusetts General Hospital, Harvard Medical School, Boston, MA, United States, [2]Department of Circulation and Medical Imaging, Norwegian University of Science and Technology, NTNU, Trondheim, Norway

With increasing number of high field 7T MR systems in clinical setting, the potential of using advanced MR modalities such as MR spectroscopy is increasing. Imaging 2-hydroxyglutarate (2-HG) can genotype IDH mutations in gliomas. However, the MR signal of this metabolite is overlapped with other resonances, hampering robust quantification of 2-HG. Here we optimized the timing of LASER sequence for robust detection of 2-HG at high field 7T in the presence of B1 inhomogeneity.

5512 Computer 72

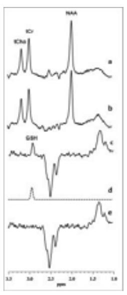

Effects of Iron Content on J-edited 1H MRS Measures of Cortical Glutathione Investigated In Vivo with Quantitative Susceptibility Mapping (QSM)

Kofi M. Deh [1], Xiangling Mao[1], Yize Zhao[2], Guoxin Kang[1], Pascal Spincemaille[1], Yi Wang[1], and Dikoma C. Shungu[1]

[1]Radiology, Weill Cornell Medicine, New York, NY, United States, [2]Healthcare Policy and Research, Weill Cornell Medicine, New York, NY, United States

As the primary intracellular antioxidant, glutathione (GSH) is involved in free radical reactions *in vivo* involving paramagnetic iron II/III as catalysts or cofactors, suggesting that findings low tissue GSH by MRS could reflect T_2 signal loss due to differences in iron content, rather than a genuine antioxidant deficit. This study estimated brain iron content using QSM to assess whether GSH deficits previously reported in patients with chronic fatigue syndrome (CFS) were genuine or simply a T_2 signal loss. No iron content differences were found between patients and controls, supporting a genuine GSH deficit in CFS.

Electronic Poster

MRSI Methods

Exhibition Hall Thursday 13:00 - 14:00

5513 Computer 73

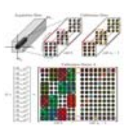

S-ESPIRiT: Estimation of Coil Sensitivity Maps from MR Spectroscopic Imaging Data Using ESPIRiT

Namgyun Lee[1,2], Vincent Oltman Boer[3], Esben Thade Petersen[3], and Gyunggoo Cho[1]

[1]Korea Basic Science Institute, Daejeon, Korea, Republic of, [2]University of Southern California, Los Angeles, CA, United States, [3]Danish Research Centre for Magnetic Resonance (DRCMR)

Estimating a set of coil sensitivity maps that is consistent with the low-resolution SENSE model is challenging in SENSE spectroscopic imaging. Recently, ESPIRiT, an autocalibrating approach to estimate sensitivity maps for MR imaging, that combines both advantages of SENSE and GRAPPA has been developed. In this work, we propose a spectroscopic extension of ESPIRiT, referred to as S-ESPIRiT, to estimate sensitivity maps from Cartesian 2D spectroscopic k-space data. The proposed method was demonstrated using 2D spectroscopic imaging data of a brain metabolite phantom acquired with a semi-LASER pulse sequence and a 32-channel receive head coil on a 7T MRI scanner.

5514 Computer 74

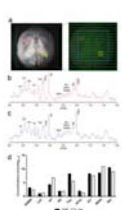

semi-adiabatic SPECIAL-based ¹H MRSI at 9.4T: Implementation and preliminary validation in a rat brain

Hyeong-Hun Lee[1] and Hyeonjin Kim[1,2,3]

[1]Department of Biomedical Sciences, Seoul National University, Seoul, Korea, Republic of, [2]Department of Radiology, Seoul National University Hospital, Seoul, Korea, Republic of, [3]Department of Transdisciplinary Studies, Graduate School of Convergence Science and Technology, Seoul National University, Suwon, Korea, Republic of

Given the issues of chemical shift displacement error, B_1 inhomogeneity and short T_2 at high field, a semi-adiabatic SPECIAL-based MRSI sequence was implemented at 9.4T, which is equipped with a pair of broad-band hyperbolic secant adiabatic full passage pulses for refocusing, and yet, allows a minimum TE of as short as 4.98 ms. In phantom, the effect of the prolonged minimum TE on the J-evolution of coupled spins is negligible. In a rat brain, preliminary quantitative results are in close agreement with the previous results obtained by using single-voxel MRS.

5515 Computer 75

High resolution MRSI using compartmental low rank algorithm: demonstration using undersampled EPSI

Ipshita Bhattacharya[1], Ralph Noeske[2], Baolin Yang[3], Rolf F Schulte[4], and Mathews Jacob[1]

[1]Department of Electrical and Computer Engineering, The University of Iowa, Iowa City, IA, United States, [2]GE Healthcare, Postdam, Germany, [3]GE Healthcare, Waukesha, WI, United States, [4]GE Global Research, Munich, Germany

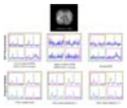

Improved spatial resolution is the need of the hour for MRSI. In this work we propose an algorithm which provides a comprehensive and automatic approach to recover high resolution metabolite maps from highly undersampled acquisitions; the improved spatial resolution translates to improved spectral quality and reduced leakage artifacts. The proposed algorithm is also quite flexible and can be readily used in a variety of sequences, including EPSI, CSI, and spirals acquisition schemes.

5516 Computer 76

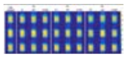

Evaluation of Compressed Sensing reconstructions of 3D Echo Planar Spectroscopic Imaging using TV, Wavelet-$$$\ell_{1}$$$, and TV+Wavelet-$$$\ell_{1}$$$ based regularization.

Andres Saucedo[1], Zohaib Iqbal[1], Manoj K. Sarma[1], and M. Albert Thomas[1]

[1]Radiological Sciences, University of California, Los Angeles, Los Angeles, CA, United States

Magnetic Resonance Spectroscopic Imaging (MRSI) is a valuable tool to characterize metabolic concentrations and changes in several spatial locations in a single recording. However, the long acquisition time of conventional three-dimensional (3D) MRSI limits its practical application. Non-uniformly sampled 3D echo planar spectroscopic imaging (EPSI) has been proposed to accelerate the scan time, combined with compressed sensing (CS) to retain reconstruction fidelity. We apply the novel approach of reconstructing 3D EPSI data by applying TV, Wavelet-$$$\ell_{1}$$$, and TV + Wavelet-$$$\ell_{1}$$$ CS-based regularization on both the combined spectral and two undersampled spatial dimensions. These three reconstruction methods were evaluated in both simulated and in retrospectively undersampled data of a brain phantom.

5517 Computer 77

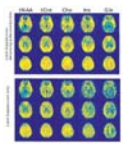

Low-Rank TGV Reconstruction of High-Resolution 1H-FID-MRSI of whole brain slices

Antoine Klauser[1], Dimitri Van De Ville[1,2], and François Lazeyras[1]

[1]Department of Radiology and Medical Informatics, University of Geneva, Geneva, Switzerland, [2]Institute of Bioengineering, École Polytechnique Fédérale de Lausanne, Lausanne, Switzerland

High resolution MRSI data were acquired with 2D FID-MRSI at 3T and a post-processing including lipid suppression, low-rank approximation and TGV-reconstruction is proposed. The resulting metabolic images of tNAA, tCre, Cho, Ins and Glx showed a substantial gain in quality, CRLB values associated and the SNR. This effect was particularly marked for lower signal metabolite: Ins and Glx. In addition, the proposed post-processing reconstructed efficiently under-sampled data allowing a 2- or 4-fold acquisition acceleration.

5518 Computer 78

magna cum laude

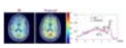

Macromolecule Mapping with Ultrashort-TE Acquisition and Metabolite Spectral Prior

Fan Lam[1], Yudu Li[1,2], Bryan Clifford[1,2], and Zhi-Pei Liang[1,2]

[1]Beckman Institute for Advanced Science and Technology, University of Illinois at Urbana-Champaign, Urbana, IL, United States, [2]Department of Electrical and Computer Engineering, University of Illinois at Urbana-Champaign, Urbana, IL, United States

This work presents a novel method for macromolecule mapping and quantification. The proposed method integrates an FID-based MRSI acquisition with a generalized series (GS) model based extrapolation scheme. The FID acquisition allows for the use of ultrashort echoes and short repetition times for fast imaging with improved SNR efficiency. The GS model effectively makes use of the spectral priors from single voxel spectroscopy and allows for reformulating the back-extrapolation of metabolite signals as a linear problem (in contrast to conventional nonlinear methods). Results from in vivo experiments demonstrate that MM signals estimated by the proposed method are consistent with an inversion recovery based method and lead to better metabolite quantification.

5519 Computer 79

magna cum laude

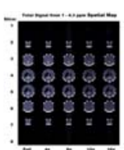

Covariance Five Dimensional Echo Planar J-resolved Spectroscopic Imaging

Zohaib Iqbal[1] and M. Albert Thomas[1]

[1]Radiological Sciences, University of California - Los Angeles, Los Angeles, CA, United States

Chemical shift imaging is a very important method used to investigate several pathologies in vivo. A recent technological development incorporating an echo planar readout, a non-uniform sampling scheme, and an iterative, non-linear reconstruction is the five dimensional echo planar J-resolved spectroscopic imaging (5D EP-JRESI) method. While this technique is capable of obtaining 3 spatial and 2 spectral dimensions in vivo, the indirect spectral dimension has a low spectral resolution, which may hinder accurate metabolite quantitation. In this study, a novel approach using a covariance transformation after reconstruction is assessed and compared to the 5D EP-JRESI method.

5520 Computer 80

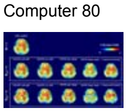

Comparison of different acceleration methods for high-resolution metabolite mapping using 1H FID MRSI at 9.4T

Sahar Nassirpour[1,2], Paul Chang[1,2], and Anke Henning[1,3]

[1]MPI for Biological Cybernetics, Tuebingen, Germany, [2]IMPRS for Cognitive and Systems Neuroscience, Eberhard Karls University of Tübingen, Tuebingen, Germany, [3]Institute of Physics, Ernst-Moritz-Arndt University Greifswald, Greifswald, Germany

Reliable metabolite mapping of the human brain using ultra-short TE and TR ^{1}H FID-MRSI is possible at ultra-high fields. However, MRSI studies with high spatial resolutions and brain coverage suffer from long scan times. To make these studies clinically relevant, different acceleration methods are used at the price of losing SNR. The aim of this study is to implement and compare different in-plane acceleration methods: SENSE, GRAPPA and compressed sensing for high-resolution metabolite mapping of the human brain at 9.4T without lipid suppression.

5521 Computer 81

Density Weighted Concentric Circle Trajectories for Brain MRSI at 7T

Lukas Hingerl[1], Bernhard Strasser[1], Philipp Moser[1], Gilbert Hangel[1], Siegfried Trattnig[1,2], and Wolfgang Bogner[1]

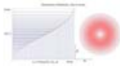

[1]High Field MR Centre, Medical University of Vienna, Vienna, Austria, [2]Christian Doppler Laboratory for Clinical Molecular MR Imaging, Medical University of Vienna, Vienna, Austria

A density weighted concentrically circular echo-planar trajectories readout scheme is presented for brain MRSI at 7 T. We give an analytic solution for the variable radii distribution in order to intrinsically measure a Hamming weighted k-space. A comparison with post acquisition filtered equidistant concentric circles is done. Invivo metabolic maps and spectra are shown.

5522 Computer 82

Metabolite-Cycling Short-Echo Time Magnetic Resonance Spectroscopic Imaging using a Concentric Ring k-space Trajectory

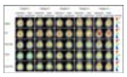

Uzay E Emir[1], Brian Burns[2], Mark Chiew[1], Peter Jezzard[1], and Albert Thomas[3]

[1]Oxford Centre for Functional MRI of the Brain (FMRIB), University of Oxford, Oxford, United Kingdom, [2]Department of Oncology, University of Oxford, Oxford, United Kingdom, [3]Department of Radiological Sciences, University of California, Los Angeles, CA, United States

In this study, the feasibility of acquiring and quantifying short-echo (TE = 14 ms), two-dimensional (2D) STEAM MRSI spectra from the motor cortex was demonstrated by utilizing a non-water-suppressed metabolite-cycling technique. The increase in measurement time by the metabolite-cycling is counterbalanced by a time-efficient concentric ring k-space trajectory. High quality spectra were acquired from 36 localized 2mL voxels in 8 minutes. The metabolite spectra and estimated concentrations were in agreement between non-water-suppressed and water-suppressed MRSI techniques. Findings of this study demonstrate that a non-water-suppressed metabolite-cycling MRSI technique can perform robustly on clinical MRI scanners and within a clinically feasible acquisition time.

5523 Computer 83

Full-field of view GM and WM spectroscopy in vivo using spatial lipid pattern estimation and BASE-SLIM localization

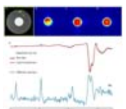

Peter Adany[1], In-Young Choi[1,2,3], and Phil Lee[1,2]

[1]Hoglund Brain Imaging Center, University of Kansas Medical Center, Kansas City, KS, United States, [2]Department of Molecular & Integrative Physiology, University of Kansas Medical Center, [3]Department of Neurology, University of Kansas Medical Center

The presence lipids of several orders of magnitude higher concentrations than metabolites in the extracranial tissues present significant challenges for the reliable acquisition and quantification of 1H MRSI, especially in the outer perimeter areas of the brain. We developed a novel spatial lipid reconstruction technique to remove nuisance lipid signals in 1H MRS. We applied lipid reconstruction to MRSI data and performed BASE-SLIM localization on the lipid-subtracted signal. Using this method, high quality compartment spectra of GM and WM could be obtained.

5524 Computer 84

Multi-region Semi-Adiabatic Spectral-Spatial Spectroscopic Imaging (SASSI) sequence for accelerated MRSI at 7T

Rebecca Emily Feldman[1] and Priti Balchandani[1]

[1]Translational and Molecular Imaging Institute, Icahn School of Medicine at Mount Sinai, New York, NY, United States

High field MRI permits us to leverage increased signal-to-noise ratio (SNR) and spectral separation between metabolite peaks for more sensitive metabolite detection at higher spatial resolutions. However, the acquisition of high-resolution spectral grids can be prohibitively time intensive. Accelerated MRSI acquisitions are challenged by the limitations at 7T. We develop a multi-region SPSP excitation pulse and use it to create a novel low power, B_1 insensitive multi-region SASSI sequence with minimal chemical shift to enable accelerated MRSI.

5525 Computer 85

IRREGULAR SPIRAL ACQUISITION FOR COMPRESSIVE SENSING IN MRSI

Jabrane Karkouri[1,2], Fabien Millioz[1], Magalie Viallon[1], Rémy Prost[1], and Hélène Ratiney[1]

[1]Université de Lyon, INSA‐Lyon, Université Claude Bernard Lyon 1, UJM-Saint Etienne, CNRS, Inserm, CREATIS UMR 5220, U1206, F‐69621, LYON, France, Lyon, France, [2]Siemens Healthineers, Saint-Denis, France

Magnetic resonance spectroscopic imaging (MRSI) has multiple interests in clinical practice but it faces quite long acquisition time in practice which limits their use in a clinical environment. In this work, a new fast Magnetic Resonance Spectroscopic image acquisition method, based on Compressed Sensing and the a priori known support of the metabolites chemical shift, is introduced and evaluated based on a k-t space spiral sampling. In the real-world noisy scenario the error in the recovered spectrum highly depends on the acquired samples. We reduce this error to an acceptable level by selecting irregularly the samples using the Sequential Backward Selection algorithm. Our method has been applied on an in vivo 31P acquisition, to prove the feasibility of the proposed approach.

5526 Computer 86

Prospective frequency correction using outer volume suppression-localized navigator for MR Spectroscopic Imaging

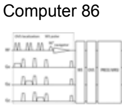

Chu-Yu Lee[1], In-Young Choi[1,2,3], and Phil Lee[1,3]

[1]Hoglund Brain Imaging Center, University of Kansas Medical Center, Kansas City, KS, United States, [2]Department of Neurology, University of Kansas Medical Center, Kansas City, KS, United States, [3]Department of Molecular & Integrative Physiology, University of Kansas Medical Center, Kansas City, KS, United States

Data acquisitions for magnetic resonance spectroscopic imaging (MRSI) require a long scan time to increase SNR and for spatial encoding. During the prolonged scan time, maintaining a constant static magnetic field (B0) is important for a robust MRSI measurement. However, frequency drifts occur over time even in advanced MR systems and become larger when high shim currents or rapidly switched gradients are applied. The frequency drift causes broad and distorted spectral lineshapes, reduced SNR, and quantification errors. These effects can be mitigated retrospectively and prospectively. However, in MRSI measurements, these effects can only be mitigated using the prospective frequency correction, because each spectrum is phase-encoded. The prospective frequency correction is typically achieved by incorporating a PRESS-based interleaved reference scan (PRESS-IRS) as a navigator, termed as PRESS-IRS navigator. A small excitation flip angle (10-20°) is used for the PRESS-IRS navigator to reduce the saturation-induced SNR loss on metabolite signals. Nonetheless, the SNR loss remains unavoidable and becomes notable when the imperfect refocusing pulses or a short repetition time (TR) are used in MRSI. In this study, a new prospective frequency correction method is introduced. The new method utilizes the outer volume suppression-localized navigator, termed OVS-localized navigator, resulting in no perturbations of metabolite signals and thus no saturation-induced SNR losses. Meanwhile, a precise measurement of the frequency drift and the effective correction is achieved. The presented method was demonstrated in two-dimensional (2-D) MRSI measurements under the large frequency drift induced by a fMRI experiment.

5527 Computer 87

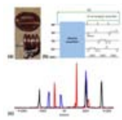

Rigid Motion Correction in MRSI Using Wireless Active Markers

Yibo Zhao[1], Chao Ma[2], Chang Gao[1], Kui Ying[1], Jinsong Ouyang[2], and Georges El Fakhri[2]

[1]Engineering Physics, Tsinghua University, Beijing, People's Republic of China, [2]Gordon Center for Medical Imaging, Radiology, Massachusetts General Hospital, Harvard Medical School, Boston, MA, United States

For brain imaging, even with head restraints, maximum translations in the range of 5-10 mm and rotations of 1-4 degrees are sometimes observed. The rigid body motion of the subject during MRSI acquisition can degrade both the spatial resolution and spectral quality. In this work, we developed a wireless active marker based method to track and correct motion in MRSI.

5528 Computer 88

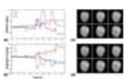

Motion Correction for 1H-MRSI of the Brain Using Unsuppressed Water Signals

Bryan Clifford[1,2], Xi Peng[2,3], Yudu Li[1,2], Zhi-Pei Liang[1,2], and Fan Lam[2]

[1]Electrical and Computer Engineering, University of Illinois at Urbana-Champaign, Urbana, IL, United States, [2]Beckman Institute for Advanced Science and Technology, Urbana, IL, United States, [3]Paul C Lauterbur Research Center for Biomedical Imaging, Shenzhen Institutes of Advanced Technology, Shenzhen, People's Republic of China

Head motion poses a significant problem in MRSI experiments, especially for 1H-MRSI of the brain performed without water or lipid suppression. In this work we propose a practical method specifically designed to track head motion and correct for its effects on 1H-MRSI data acquired without water suppression. By using the companion spectroscopic water signals, we are able to track head motion with navigators collected in circular and linear trajectories. A specialized data processing scheme is also proposed for processing the navigator data along with the unsuppressed spectroscopic water signals to determine the motion parameters.

5529 Computer 89

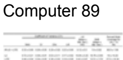

Lipid Suppression in 3D Magnetic Resonance Spectroscopic Imaging

Mohammed Goryawala[1], Andrew A Maudsley[1], and Sulaiman Sheriff[1]

[1]University of Miami, Miami, FL, United States

Proton MR spectroscopic imaging (MRSI) is complicated by the presence of subcutaneous lipids, which, if not suppressed before Fourier reconstruction, cause ringing in metabolite maps due to limited k-space sampling. In this study inversion recovery (IR) based lipid suppressed acquisition was compared to non-lipid suppressed acquisition combined with two methods for reducing lipid ringing in whole brain MRS imaging. Results indicate non-lipid suppressed acquisition using the ℓ2-regularization or Papoulis-Gerchberg algorithm for reconstruction is possible without significant ringing artifacts, however, can have a detrimental effect on spectral linewidth and baseline, resulting in smaller spatial coverage than IR based lipid-suppressed acquisition.

5530 Computer 90

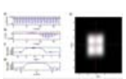

A Minimum-Phase Shinnar-Le Roux Spectral-Spatial Excitation RF Pulse for Water and Lipid Suppression in 1H MRSI of Body Extremities

Kexin Deng[1], Chao Ma[2], Kui Ying[3], and Georges El Fakhri[2]

[1]Biomedical Engineering, Tsinghua University, Beijing, People's Republic of China, [2]Gordon Center for Medical Imaging, Radiology, Massachusetts General Hospital, Harvard Medical School, Boston, MA, United States, [3]Engineering Physics, Tsinghua University, Beijing, People's Republic of China

It is challenging to remove nuisance water and lipid signals in ^{1}H-MRSI of body extremities. Strong lipid signals exist both in the subcutaneous layer and bone marrow but also in the muscle, i.e., intramyocellular and extramyocellular lipids. This work presents a novel minimum-phase Shinnar-Le Roux (SLR) spectral-spatial excitation RF pulse for both water and lipid suppression in 1H-MRSI of body extremities. We have validated the proposed method using Bloch equation simulation, phantom, and in vivo studies.

5531 Computer 91

High resolution cortical spectroscopy at 7T using lipid signal crushing and a high density receive array.

Alex Bhogal[1], Carrie Wismans[1], Christiaan Vinckers[2], Peter R Luijten[1], Dennis WJ Klomp[1], and Jannie P Wijnen[1]

[1]Radiology, University Medical Center Utrecht, Utrecht, Netherlands, [2]Psychiatry, University Medical Center Utrecht, Utrecht, Netherlands

In this work we attempt to overcome MRSI limitations associated with extra-cranial lipid signal leakage and low SNR at high resolution. We use a dedicated crusher coil for lipid signal removal, in combination with a high density receive array and an 7T MR scanner for boosted SNR.

5532 Computer 92

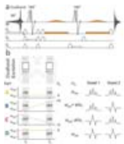

Spatial Hadamard encoding of J-edited spectroscopy using slice-selective editing pulses

Kimberly Chan[1,2,3], Georg Oeltzschner[2,3], Michael Schär[3], Peter Barker[2,3], and Richard Edden[2,3]

[1]Biomedical Engineering, Johns Hopkins School of Medicine, Baltimore, MD, United States, [2]F. M. Kirby Research Center for Functional Brain Imaging, Kennedy Krieger Institute, Baltimore, MD, United States, [3]Russell H. Morgan Department of Radiology and Radiological Science, Johns Hopkins School of Medicine, Baltimore, MD, United States

A new approach for simultaneous dual-voxel J-difference spectral editing is described, that uses spatially selective spectral-editing pulses and Hadamard encoding. The theoretical framework for Spatial Hadamard Editing and Reconstruction for Parallel Acquisition (SHERPA) was developed, applying gradient pulses during the frequency selective editing pulses. SHERPA was simulated for GABA, tested in a two-compartment GABA phantom, and applied to the left and right hemispheres of ten normal subjects. SHERPA was successfully implemented with results in close agreement with conventional MEGA-PRESS scans. Compared to conventional single-voxel single-metabolite J-difference editing, two-fold acceleration is possible without significant loss of SNR using the SHERPA method.

5533 Computer 93

A Vendor-Agnostic MRSI Acquisition and Reconstruction XML Descriptor Format

Marram P Olson[1], Jason C Crane[1], Peder Larson[1], and Sarah J Nelson[1]

[1]Radiology and Biomedical Imaging, UCSF, San Francisco, CA, United States

The evaluation of MRSI data is complex because data files are encoded with vendor specific file formats and there is a lack of standardized tools for reconstruction. A standard way to describe raw MRSI data is necessary for the reconstruction of sequences utilizing parallel and non-Cartesian sampling strategies. In this work we are developing a vendor neutral data format to define MRSI sequences with arbitrary k-space trajectories that can be used by reconstruction software to understand the data acquisition scheme. This file format is XML-based and uses the ISMRMRD header as a basis for its scheme.

5534 Computer 94

Using 3D MEGA-LASER MRSI to study the role of basal ganglia GABA and Glx in response selection in Manganese neurotoxicology

Ruoyun Ma[1,2], Sandy Snyder[1,3], Ann-Kathrin Stock[4], Wolfgang Bogner[5], Ovidiu C. Andronesi[6], Christian Beste[4], and Ulrike Dydak[1,2]

[1]School of Health Sciences, Purdue University, West Lafayette, IN, United States, [2]Department of Radiology and Imaging Sciences, Indidana University School of Medicine, Indianapolis, IN, United States, [3]Department of Speech, Language, and Hearing Sciences, Purdue University, West Lafayette, IN, United States, [4]Cognitive Neurophysiology, Department of Child and Adolescent Psychiatry, Faculty of Medicine of the Technische Universität Dresden, Germany, [5]Department of Biomedical Imaging and Image-guided Therapy, High Field MR Center, Medical University of Vienna, Vienna, Austria, [6]Martinos Center for Biomedical Imaging, Massachusetts General Hospital, Harvard Medical School, Boston, MA, United States

This pilot study on manganese (Mn) neurotoxicity investigates the association between deficits in response selection and GABA and Glx levels in basal ganglia structures using MEGA-LASER 3D MRSI. Using a novel automated brain-structure-specific quantification approach for GABA+ and Glx, we studied three basal ganglia structures and the thalamus in Mn-exposed welders and controls. A modified Simon task was used to measure selection inhibition. GABA+ and Glx in putamen and globus pallidus were associated with response times in the most complicated experimental scenario in Mn-exposed subjects; whereas thalamic Glx levels were associated with response time for all subjects.

5535 Computer 95

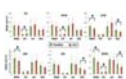

Assessment of Neurochemical changes in HIV adults Using Accelerated MR Spectroscopic Imaging and Compressed Sensing Reconstruction

Rajakumar Nagarajan[1,2], Eric S Daar[3], Ebrahim Haroon[4], Zohaib Iqbal[2], Neil Wilson[2], Sathya Arumugam[2], Mario Guerrero[3], and Michael A Thomas[2]

[1]Human Magnetic Resonance Center, Institute for Applied Life Sciences (IALS), University of Massachusetts, Amherst, MA, United States, [2]Radiological Sciences, University of California Los Angeles, Los Angeles, Los Angeles, CA, United States, [3]Medicine, Harbor-UCLA Medical Center, Torrance, CA, United States, [4]Psychiatry and Behavioral Sciences, Emory School of Medicine, GA, United States

In this work, we have successfully evaluated the accelerated 5D EP-JRESI sequence in 16 adult HIV-infected patients and 15 healthy subjects. Compared to healthy subjects, significant neurochemical changes were observed in HIV+ patients on ART: elevated Ch/Cr ratios in frontal gray, right frontal white and right basal ganglia locations, decreased Glx ratios in the left frontal white, right basal ganglia, occipital gray and white and right insular cortical regions. There was also decreased NAA/Cr in the left basal ganglia and right occipital white regions. In the HIV+ patients, a positive correlation was recorded between the left basal ganglia NAA/Cr and the number of years of ART treatment ($r=0.58$, $p<0.02$).

5536 Computer 96

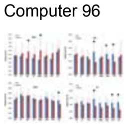

Accelerated 3D Echo Planar Spectroscopic Imaging of HIV: Metabolite Changes Correlation with CD4 count and Number of Years of Treatment

Rajakumar Nagarajan[1,2], Eric S Daar[3], Zohaib Iqbal[2], Manoj K Sarma[2], Mario Guerrero[3], and Michael A Thomas[2]

[1]Human Magnetic Resonance Center, Institute for Applied Life Sciences (IALS), University of Massachusetts, Amherst, MA, United States, [2]Radiological Sciences, University of California Los Angeles, Los Angeles, Los Angeles, CA, United States, [3]Medicine, Harbor-UCLA Medical Center, Torrance, CA, United States

In vivo proton magnetic resonance spectroscopy studies of HIV-infected humans have demonstrated region-specific changes in brain metabolites including N-acetylaspartate, creatine, choline, glutamate/ glutamine, and myo-inositol. Using a 3D EPSI technique, we examined metabolite ratios with respect to creatine in several regions of brain in 18 HIV adults (mean age 46.2 years) and 15 healthy controls (mean age 43.4 years). We have demonstrated for the first time the feasibility of a novel accelerated 3D EPSI method in HIV-infected adults compared to age matched healthy controls and correlated with CD4 counts and number of years of treatment.

Electronic Poster

5537 Computer 1

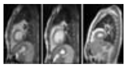

Low-field cardiac MRI for cardiac radiosurgery using an integrated MRI-guided radiotherapy system

H Michael Gach[1], Roger Nana[2], Clifford G Robinson[3], Philip S Cuculich[4], Rojano Kashani[3], Jeffrey D Bradley[3], Michael C Roach[3], James F Dempsey[5], Sasa Mutic[3], and Olga Green[3]

[1]Radiation Oncology and Radiology, Washington University in St Louis, St Louis, MO, United States, [2]ViewRay, Oakwood Village, OH, United States, [3]Radiation Oncology, Washington University in St Louis, St Louis, MO, United States, [4]Cardiovascular, Washington University in St Louis, St Louis, MO, United States, [5]ViewRay, Mountain View, CA, United States

Integrated MRI-guided radiotherapy (MRIgRT) systems perform simultaneous MRI acquisitions during radiation therapy to optimize the accuracy of dose delivery. Cardiac radiosurgery using stereotactic body radiation therapy (SBRT) is a promising new treatment option for cardiac arrhythmias. We imaged the heart with a novel ungated radial TrueFISP sequence on a 0.35 T MRIgRT system. The sequence is being developed for next generation SBRT. Image artifacts associated with the sequence were measured using a Medtronic implantable cardiac defibrillator (ICD) in hydrogel and extended 13 cm from its center. Thus, artifacts should not preclude MRIgRT for most patients with ICDs.

5538 Computer 2

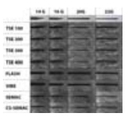

Interventional MRI at 3T: Compressed Sensing SEMAC for Improved Needle Visualization

Jan Fritz[1], Wesley D Gilson[2], Christoph Forman[3], Esther Ratihel[3], Mathias Nittka[3], and Allan Belzberg[1]

[1]The Johns Hopkins University School of Medicine, Baltimore, MD, United States, [2]Siemens Healthcare USA, [3]Siemens Healthcare GmbH

Interventional MR imaging at 3 Tesla benefits from high signal and affords visualization and subsequent targeting of submillimeter structures, but needle artifacts may be exaggerated. Optimized fast gradient echo- and turbo spin echo-based pulse sequences minimize in-plane signal displacement, but through-plane artifacts remain. Compressed Sensing Slice-Encoding Metal Artifact Correction (SEMAC) MRI has the ability to minimize through-plane displacement, and thus holds promise to improve the accuracy of device localization. We demonstrate the clinical feasibility of Compressed Sensing SEMAC TSE for interventional MR imaging at 3 Tesla and visualization of the needle artifact with high accuracy.

5539 Computer 3

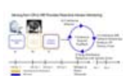

Controlling Brain Infusion Distributions: Moving from Surgical Planning to Real-Time MR Guidance

Martin Brady[1], Raghu Raghavan[1], Andrew L Alexander[2,3], and Walter F Block[2,3,4]

[1]Therataxis, Baltimore, MD, United States, [2]TherVoyant, Madison, WI, United States, [3]Medical Physics, University of Wisconsin- Madison, Madison, WI, United States, [4]Biomedical Engineering, University of Wisconsin- Madison, Madison, WI, United States

The hetergeneity of the brain makes designing a desired end drug distribution through pressurized catheters difficult. We present a method to utilize real-time MR monitoring of a co-infused Gd tracer during initial stages of the infusion to derive a real-time 3D estimate of the velocity front. We also describe a new algorithm that uses the velocity front to provide surgical feedback on the likely final infusion distribution.

5540 Computer 4

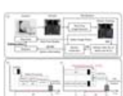

Real-Time Motion Prediction for Feedback Control of MRI-Guided Interventions

Xinzhou Li[1,2], Samantha Mikaiel[1,3], James Simonelli[4], Yu-Hsiu Lee[4], Tsu-Chin Tsao[4], and Holden H. Wu[1,2,3]

[1]Radiological Sciences, University of California, Los Angeles, Los Angeles, CA, United States, [2]Bioengineering, University of California, Los Angeles, Los Angeles, CA, United States, [3]Physics and Biology in Medicine, University of California, Los Angeles, CA, United States, [4]Mechanical and Aerospace Engineering, University of California, Los Angeles, Los Angeles, CA, United States

MRI is capable of providing flexible soft tissue contrast and real-time guidance of interventions. Real-time information about the motion of tissues and devices is essential to provide feedback for physician and robotic control of MRI-guided interventions. In this work, a new motion prediction algorithm using MRI-based motion tracking and multi-rate Kalman filtering is proposed to provide accurate and real-time motion information. Experiments and simulations show that Kalman filtering with expectation maximization training and multi-rate data fusion is able to achieve low motion prediction error. This new algorithm has potential in providing real-time feedback information for MRI-guided interventions.

5541 Computer 5

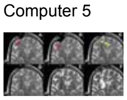

Hemorrhage Events during MR Guided DBS Implantations

Alastair Martin[1], Philip Starr[2], Jill Ostrem[3], and Paul Larson[2]

[1]Radiology and Biomedical Imaging, UCSF, San Francisco, CA, United States, [2]Neurological Surgery, UCSF, [3]Neurology, UCSF

MR guidance is increasingly being used to implant DBS electrodes. The technique is extremely accurate and permits patients to be under general anesthesia during the procedure. The incidence of complications during these procedures, however, has not been established. We report on the incidence of hemorrhagic events during 231 surgical procedures (374 electrodes implanted). The ability to detect hemorrhage intra-operatively is demonstrated and factors contributing to hemorrhage incidence are identified. Total hemorrhage rates and symptomatic hemorrhage rates were found to be 2.4%/electrode implanted and 1.1%/electrode implanted respectively, which is comparable to conventional surgical approaches for DBS implantation.

5542 Computer 6

Unseen Clinically Significant Prostate Cancer on 3T Multiparametric MRI Challenging Screening and Focal Therapy: An In-bore MRI-Guided Biopsy Study of MRI Negative Areas

Kareem K Elfatairy[1], Christopher P Filson[2], Omer G Kucuk[3], Peter J Rossi[4], Viraj A Master[2], and Sherif G Nour[1]

[1]Radiology, Emory University-School of Medicine, Atlanta, GA, United States, [2]Urology, Emory University-School of Medicine, Atlanta, GA, United States, [3]Hematology-Oncology and Urology, Emory University-School of Medicine, Atlanta, GA, United States, [4]Radiation Oncology, Emory University-School of Medicine, Atlanta, GA, United States

The use of multiparametric MRI for prostate cancer screening is challenged by the potential missing of clinically significant cancer in areas with no visible abnormalities. We randomly biopsied areas with no visible targets under direct MRI guidance. Out of 43 biopsied areas, negative predictive value for clinically significant cancers was 90.7% suggesting a very low potential for harboring clinically significant cancers and supporting the use of mpMRI in cancer screening and active surveillance. An extended biopsy approach including sampling of areas without visible MRI abnormalities may still need to be considered prior to focal therapy.

5543 Computer 7

The role of in-bore MR-guided prostate biopsies in patients With discrepancy between MRI findings and TRUS biopsies

Sverre Langørgen[1], Brage Krüger-Stokke[1], Øystein Størkersen[2], May-Britt Tessem[3], Helena Bertilsson[4], Tone Frost Bathen[3], and Kirsten Margrethe Selnæs[3]

[1]Departement of Radiology and Nuclear Medicine, St Olavs Hospital, Trondheim, Norway, [2]Department of Pathology and Genetics, St Olavs Hospital, Trondheim, Norway, [3]Department of Circulation and Medical Imaging, Norwegian University of Science and Technology, Trondheim, [4]Departement of Urology, St Olavs Hospital, Trondheim, Norway

A retrospecive review of 34 patients who had been to former TRUS guided prostate biopsies, where there was a discrepancy between MRI reported tumor suspicious findings and histology. They were re-biopsied with MRGB. We could verify cancer in 14 of 24 patients with former negative or benign histology. We also upgraded 7 out of 10 patients from low-grade to intermidiate or high-grade cancer. In addition to finding former unknown cancers, we also found that the urologists settled with benign diagnoses from MRGB. They then decided to end investigations in these patients.

5544 Computer 8

Inline Adaptive Spiral Off-Resonance Correction for MRI-guided interventions

Matthew Restivo[1], Michael Hansen[1], Hui Xue[1], and Adrienne Campbell-Washburn[1]

[1]Biochemistry and Biophysics Center, Division of Intramural Research, National Heart, Lung, and Blood Institute, National Institutes of Health, Bethesda, MD, United States

Spiral imaging is appealing for MRI-guided interventions due to the need for high frame rate dynamic imaging and low RF power sequences to reduce RF-induced heating in metallic guidewires. Unfortunately, spiral images are susceptible to image distortions due to off-resonance which must be corrected. In this work, we implement a real-time interactive spiral sequence and a fast reconstruction in the Gadgetron that performs inline off-resonance correction that adapts to slice position and orientation changes. We show the effectiveness of our correction in both phantom and in-vivo volunteer images with reconstruction times that are approaching real-time.

5545 Computer 9

magna cum laude

MR-Guided Mixed-Reality For Surgical Planning: Set-Up and Perceptual Accuracy

Subashini Srinivasan[1], Amanda Wheeler[2], Brian Hargreaves[1], and Bruce Daniel[1]

[1]Department of Radiological Sciences, Stanford University, Palo Alto, CA, United States, [2]Department of Surgery, Stanford University, Palo Alto, CA, United States

Microsoft HoloLens provides the ability to visualize 3D holograms of preoperative MRI in addition to the physical environment. In this work we have developed a HoloLens application that aligns these preoperative holograms to the patient. The accuracy of perceiving these holograms was evaluated by presenting different shapes of holograms in random locations and comparing their positions to ground truth. The current set-up enables visualization and perception of holograms with a margin tolerance of < 6 mm.

5546 Computer 10

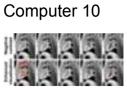

Advanced Passive Tracking and Visualization of MR-Compatible Diagnostic Electrophysiology Catheter

Sébastien Roujol[1], Radhouene Neji[1,2], Henry Chubb[1], John Silberbauer[1], Tom Lloyd[3], Thomas Pohl[4], Rainer Schneider[4], Nick Kampa[3], James Harrison[1], Steven Williams[1], Rahul Mukherjee[1], Louisa O'Neill[1], John Whitaker[1], Matthew Wright[1], Tobias Schaeffter[1], Mark O'Neill[1], and Reza Razavi[1]

[1]Division of Imaging Sciences and Biomedical Engineering, King's College London, London, United Kingdom, [2]MR Research Collaborations, Siemens Healthcare Limited, Frimley, United Kingdom, [3]Imricor Medical Systems, Burnsville, MN, United States, [4]Siemens Healthcare GmbH, Erlangen, Germany

MRI shows promise for the guidance of electrophysiology (EP) procedures. MR-guided EP procedures require reliable catheter tracking capabilities. Passive catheter tracking enable positive or negative contrast visualization of the catheter in the MR-images using for example integrated ferromagnetic/paramagnetic materials or contrast agent. Positive contrast visualization remains challenging and often sensitive to imaging/post-processing parameters. Negative contrast techniques remain associated with confounding factors (i.e. any other signal void) which complicate visual catheter tracking. In this study, we sought to develop and evaluate a novel framework for passive catheter tracking with negative contrast combined with automatic tracking and enhanced visualization of the catheter.

5547 Computer 11

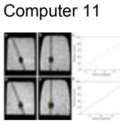

Simultaneous MR imaging and control of an MR compatible afterloader: feasibility of real-time HDR brachytherapy source tracking

Ellis Beld[1], Marinus A. Moerland[1], Jeroen Schuurman [2], Frank Zijlstra[3], Max A. Viergever[3], Jan .J.W. Lagendijk[1], and Peter R. Seevinck[3]

[1]Department of Radiotherapy, UMC Utrecht, Utrecht, Netherlands, [2]Elekta NL, Veenendaal, Netherlands, [3]Image Sciences Institute, UMC Utrecht, Utrecht, Netherlands

For MR-guided high-dose-rate (HDR) brachytherapy, an MR-compatible afterloader was developed, required for real-time HDR brachytherapy source tracking. This afterloader should be able to function well close to the MRI scanner. The functioning of both the MR-compatible afterloader and the MRI scanner, while operating simultaneously, was investigated. Source localization was performed by a phase-only cross correlation localization method. The results demonstrate that the afterloader was able to send the source to predefined source positions, while simultaneously performing MR imaging. Combined with high-temporal resolution imaging and fast reconstruction/post-processing, this study shows the feasibility of real-time source tracking for MR-guided HDR brachytherapy.

5548 Computer 12

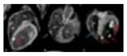

Non-contrast-enhanced imaging of RF ablation lesions in the heart

Michael A. Guttman[1], Susumu Tao[1], Aravindan Kolandaivelu[1], Sarah Fink[1], Henry Halperin[1], and Daniel A. Herzka[2]

[1]Division of Cardiology, Johns Hopkins University, School of Medicine, Baltimore, MD, United States, [2]Department of Biomedical Engineering, Johns Hopkins University, School of Medicine, Baltimore, MD, United States

Non-contrast-enhanced T1-weighted imaging has been demonstrated to be an effective technique for visualization of acute RF ablation lesions in the heart. Current practice does not include any soft tissue visualization, which could lead to gaps or incomplete ablations and possible recurrence of symptoms. We propose a T1-weighted sequence with long TI to increase contrast between normal and ablated myocardium. Images are presented demonstrating the technique after ablations in the ventricles, left atrium and pulmonary vein.

5549 Computer 13

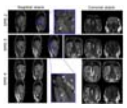

Using multi-stack simultaneous multi-slice bSSFP for improved motion characterization during MR-guided radiotherapy

Pim Borman[1], Clemens Bos[2], Sjoerd Crijns[1], Chrit Moonen[2], Bas Raaymakers[1], and Rob H.N. Tijssen[1]

[1]Radiotherapy, UMC Utrecht, Utrecht, Netherlands, [2]Imaging Division, UMC Utrecht, Utrecht, Netherlands

Integrated MR-guided radiotherapy systems make it possible to monitor intra-fraction anatomy changes due to motion. A Simultaneous Multi-Slice (SMS) balanced SSFP sequence with interleaved stacks is used for dynamic imaging, where SMS is used to increase the spatial coverage without decreasing the frame rate. It is shown that SMS factors up to 4 are feasible without significant artifacts, for both orthogonal and parallel stacks.

5550 Computer 14

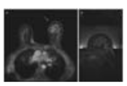

Improved planning of MR-HIFU therapy for breast cancer using image registration of pre- and per- treatment mDixon MRI

Ieva Braškutė[1], Clemens Bos[1], Roel Deckers[1], and Lambertus W. Bartels[1]

[1]UMC Utrecht, Utrecht, Netherlands

During Magnetic Resonance Imaging-guided High Intensity Focused Ultrasound (MR-HIFU) ablation of breast tumors, localization of the tumor during the treatment procedure is important for proper treatment planning. However, the use of a contrast agent during thermal ablation is preferably avoided for reasons of safety and practicality. We propose an image registration approach using pre-treatment eligibility CE and per-treatment non-CE breast MR scans, acquired with a dedicated mDixon-based tumor localization scan. We demonstrate the feasibility of our method in a volunteer study.

5551 Computer 15

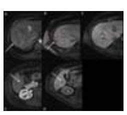

An Approach for Accurate Quantification of Hepatic Metastatic Burden during MRI-Guided Laser Ablation: Impact on Management Decisions in 41 Patients

Danial I Mir[1], Kareem K Elfatairy[1,2], Debra Overby Weber[1], and Sherif G Nour[1,3]

[1]Radiology and Imaging Sciences, Emory University Hospital, Atlanta, GA, United States, [2]Interventional MRI Program, Emory University Hospital, Atlanta, GA, United States, [3]School of Medicine, Emory University, Atlanta, GA, United States

Treatment of patients with metastatic liver disease requires accurate quantification of hepatic tumor burden and precise three dimensional localization. We demonstrate that intraprocedural MRI utilizing IV gadoxetate disodium (Eovist®) administration with controlled breath suspension under general anesthesia results in the detection additional hepatic metastatic deposits in 25% of cases, not appreciated on prior diagnostic imaging. In 88% of these cases this discovery led to a change in clinical management strategy that may have influenced patient outcomes.

5552 Computer 16

MRI-compatible Voltage Device Tracking (VDT) navigation: Simultaneous Tracking and imaging with high-gradient-duty-cycle sequences via complete removal of Gradient Induced Voltages. Initial results.

Mikayel Dabaghyan[1], Jose de Arcos[2], Raymond Kwong[3], William Stevenson[3], Jeff Schweitzer[4], Greg Olson[4], and Ehud Schmidt[2]

[1]Mirtech, Inc, Brockton, MA, United States, [2]Radiology, Brigham and Women's Hospital, Boston, MA, United States, [3]Cardiology, Brigham and Women's Hospital, Boston, MA, United States, [4]St. Jude Medical, Minnetonka, MI, United States

Voltage Device Tracking (VDT), a method for catheter navigation, during MRI is explored. VDT utilizes multiple catheter electrodes that measure both the spatial location of the electrode and the ECG on the vessel wall (EGM) at that location. Electrode spatial-localization is performed by driving intermittent sinusoidal signals at kHz frequencies between surface electrodes, and measuring the signals received by the catheter. Large (>1V) signals (GIV), generated within the body by the MR gradients during a scan interfere with the much smaller (~10mV) tracking signals. We applied two approaches to remove GIVs, which allowed VDT visualization with <5% GIV contamination.

5553 Computer 17

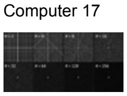

Investigation of Phase-only Cross Correlation (POCC) for Passive Marker Tracking with a limited Number of Projections

Andreas Reichert[1], Axel Joachim Krafft[1], and Michael Bock[1]

[1]Dept. of Radiology, Medical Physics, Medical Center – University of Freiburg, Freiburg, Germany

In MR-guided interventions passive markers serve as needle guides for percutaneous biopsies and can be followed automatically to visualize the planned needle trajectory. This is achieved by tracking techniques which acquire two cross-sectional Cartesian tracking images of a cylindrical marker to determine the position information. We show that the implementation of radially undersampled tracking images might be used to reduce the duration of percutaneous needle procedures by about 80%.

5554 Computer 18

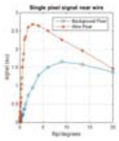

'Pulse-acquire' method for obtaining the guidewire coupling modes of a PTx transmit array

Felipe Godinez[1], Joseph Hajnal[1], Greig Scott[2], Ronald Mooiweer[1], and Shaihan Malik[1]

[1]Imaging and Biomedical Engineering, King's College London, London, United Kingdom, [2]Electrical Engineering, Stanford University, United States

A method for measuring relative coupling between elements of a parallel transmit (PTx) array and conductive structures such as guidewires or braided catheters. The method relies on strong local enhancement of B1 fields close to conductors due to induced currents. Data acquired from single pulse-acquire measurements using very low flip angles is hence dominated by these induced current contributions. Coupling matrices for N-channel arrays can therefore be estimated using only N pulses; it is demonstrated that these are similar to those obtained from dedicated current sensors.

5555 Computer 19

Clinical evaluation of automatic localization of prostate gold Fiducial Markers for MR-only Radiotherapy

Matteo Maspero[1], Cornelis AT van den Berg[1], Frank Zijlstra[1], Hans C de Boer[1,2], Gert J Meijer[1,2], Max A Viergever[1], Jan JW Lagendijk[1,2], Linda GW Kerkmeijer[1,2], and Peter R Seevinck[1]

[1]Center for Image Sciences, UMC Utrecht, Utrecht, Netherlands, [2]Cancer Center, UMC Utrecht, Utrecht, Netherlands

A novel approach aiming at automatic localization of gold Fiducial Markers (FMs) used in prostate radiotherapy to accurately perform patient positioning is presented and evaluated. The proposed method correctly detected 49/51 FMs in 17 patients when compared to FMs locations manually detected on MR. The spatial accuracy (median) and precision (STD) achieved were 0.2 mm, and 1.2 mm, respectively, when compared to relative FMs locations obtained with CT. When combined with a manual check, this approach could be a safe way to eliminate CT during radiotherapy planning, facilitating an MR-only workflow.

5556 Computer 20

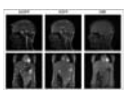

Quantitative Image Analysis of Real-Time Golden Angle Radial iSSFP for Interventional MRI

Samantha Mikaiel[1,2], Thomas Martin[1,2], Kyunghyun Sung[1,2,3], and Holden H Wu[1,2,3]

[1]Radiological Sciences, University of California Los Angeles, Los Angeles, CA, United States, [2]Biomedical Physics, University of California Los Angeles, Los Angeles, CA, United States, [3]Bioengineering, University of California Los Angeles, Los Angeles, CA, United States

Real-time visualization is crucial to the success of MRI-guided minimally invasive cancer interventions. We have developed golden-angle (GA) ordered radial integrated-SSFP (iSSFP), which can suppress banding artifacts associated with bSSFP while maintaining similar T_2/T_1 contrast. In this work, we further analyze the tissue contrast as well as passive visualization of interventional needles using GA radial iSSFP. In volunteer scans, we verify that GA radial iSSFP achieves T_2/T_1 tissue contrast similar to bSSFP while suppressing banding artifacts. With phantom scans we show that iSSFP reduced the size of the needle-induced signal void, versus that seen on bSSFP. These advantages of GA Radial iSSFP show its potential for improving real-time MRI-guided interventions.

5557 Computer 21

Hydrostatically Actuated MRI-Compatible Motion Platform for Dynamic MRI Research

Samantha Mikaiel[1,2], James Simonelli[3], Yu-Hsiu Lee[3], Xinzhou Li[1,4], Kyunghyun Sung[1,2,4], Tsu-Chin Tsao[3], and Holden H Wu[1,2,4]

[1]Radiological Sciences, University of California Los Angeles, Los Angeles, CA, United States, [2]Biomedical Physics, University of California Los Angeles, Los Angeles, CA, United States, [3]Mechanical and Aerospace Engineering, University of California Los Angeles, Los Angeles, CA, United States, [4]Bioengineering, University of California Los Angeles, Los Angeles, CA, United States

Motion is one of the main challenges in MRI, including interventional MRI. While many dynamic imaging and motion compensation techniques have been created, comparisons and validation are difficult, since it is difficult to reproduce in vivo motion for multiple experiments. This work proposes the design and development of a 1 Degree-of-Freedom hydrostatically actuated MRI-compatible motion platform, which can reliably reproduce programmed motion for dynamic MRI experiments.

5558 Computer 22

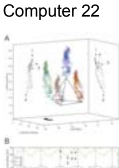

Motion-corrected high-resolution intra-cardiac imaging using MR-Tracking coils: reducing the effect of noise on motion estimation

Jose de Arcos[1], Mikayel Dabaghyan[1], William G Stevenson[2], Junichi Tokuda[1], Raymond Y Kwong[2], Ravi T Seethmaraju[3], Jeff Schweitzer[4], and Ehud J Schmidt[1]

[1]Radiology, Brigham and Women's Hospital, Boston, MA, United States, [2]Cardiology, Brigham and Women's Hospital, Boston, MA, United States, [3]Siemens Healthcare, Boston, MA, United States, [4]St. Jude Medical, Minnesota, MN, United States

We developed an intra-cardiac MRI (ICMRI) catheter to monitor heating during MRI-guided electro-physiological ablative procedures. ICMRI includes an imaging coil that expands within the cardiac chambers and a tetrahedral-shaped array of MR-tracking coils, intended to compensate for cardiac motion during the imaging process. In this study, we used real swine cardiac MR-tracking data, which may contain varying levels of positional uncertainty (noise), to develop algorithms that filter this noise, and thus do not distort the motional (translational/rotational) estimates, required for delivering non-blurred high-resolution intra-cardiac images. Our results show that submillimiter-error motion reconstruction is feasible under realistic levels of noise.

5559 Computer 23

Feasibility study for implementing low-field MRI with SPIO nanoparticles for endovascular interventions – An alternative to X-ray guided techniques

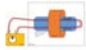

Jordy K. van Zandwijk[1,2], Frank F.J. Simonis[1], Robert H. Geelkerken[1,2], Robert Meerwaldt[2], Friso G. Heslinga[1], and Bennie ten Haken[1]

[1]Faculty of Science and Technology, University of Twente, Enschede, Netherlands, [2]Vascular Surgery, Medisch Spectrum Twente, Enschede, Netherlands

Low-field magnetic resonance imaging (lf-MRI) using super-paramagnetic iron-oxide (SPIO) nanoparticles as contrast agent seems to be a promising radiation free alternative to guide endovascular interventions in patients with critical limb ischemia (CLI). We propose an innovative workflow on how to deploy lf-MRI during such an intervention and investigate in phantoms the achievable contrast and resolution levels. The results showed that this combination of lf-MRI with SPIO contrast has potential to guide endovascular interventions, but that high quality pre-operative imaging might be required in deployment of this technique.

5560 Computer 24

Of Active Catheters and Guidewires: How do Guidewires affect the Tracking Signal Intensity?

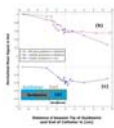

Thomas Lottner[1], Ali Caglar Özen[1], Simon Reiss[1], Timo Heidt[2], Axel J. Krafft[1], Lisa C. Besch[2], Klaus Düring[3], Constantin von zur Mühlen[2], and Michael Bock[1]

[1]Dept. of Radiology, Medical Physics, Medical Center - University of Freiburg, Freiburg, Germany, [2]Department of Cardiology and Angiology I, University Heart Center, Freiburg, Germany, [3]MaRVis, Frechen, Germany

Active tracking or profiling coils mounted on catheters provide high signal. Other devices in the vicinity can alter the signal acquired by the catheters. The effects of guidewires on the signal from actively tracked catheters were investigated in phantom and in vivo. A standard metallic guidewire and a MR safe guidewire with a passive marker were introduced through the catheter and tested for different positions at the tip. The signal loss was substantial for both guidewires. When the metallic guidewire passed through the catheter tip, the signal was unstable, whereas the MR safe guidewire did not cause any distortions.

Electronic Poster

MR Contrast & EM Safety

Exhibition Hall — Thursday 14:00 - 15:00

5561 Computer 97

summa cum laude

Contrast Deposition Within the Dentate Nucleus After Repetitive Administration: Comparison of Linear versus Macrocyclic Gadolinium Contrast Agents

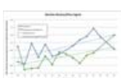

Eugene Huo[1], Bing Tian[1], David Saloner[1], Michael Hope[1], Christopher Hess[1], William Dillon[1], and Thomas Hope[1]

[1]Department of Radiology & Biomedical Imaging, University of California, San Francisco, San Francisco, CA, United States

Although gadolinium deposition in nephrogenic systemic fibrosis is limited to patients with abnormal renal function, more recent rat and human studies have demonstrated gadolinium deposition in specific brain structures in subjects without renal failure. We report here one of the largest studies evaluating gadolinium deposition in terms of both number of patients and number of doses, verifying the impact of the structural differences between the two most commonly used classes of agents (linear vs macrocyclic) and demonstrating a previously undescribed plateau in signal intensity ratio increase in patients who have received more than 25 administrations of gadolinium.

5562 Computer 98

Gadolinium Containing Metabolites in Brain Tissue. A Study in Rats

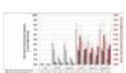

Thomas Frenzel[1], Gregor Jost[1], Chirag Apte[2], and Hubertus Pietsch[1]

[1]Bayer AG, Berlin, Germany, [2]University of British Columbia, Vancouver, BC, Canada

After the repeated dosing of linear or macrocyclic GBCAs in rats, the brain was fractionated 3 and 24d p.i. Cerebrum, cerebellum and pons were separated, homogenized and divided into an insoluble and soluble fraction, which was separated into low and high molecular weight molecules. The gadolinium concentration in the brain was very low. A large portion of the Gd in the linear GBCA groups was found in the insoluble fraction and a smaller portion in large macromolecules. The Gd in the macrocyclic GBCA groups was only found in the soluble fraction and in small molecules. Gd excretion was still ongoing.

5563 Computer 99

In vivo measurements of gadolinium accumulation in bone of healthy individuals following administration of gadolinium-based contrast agents: a pilot study

Michelle L. Lord[1], Fiona E. McNeill[2], James L. Gräfe[3], Michael D. Noseworthy[4,5], and David R. Chettle[2]

[1]Radiation Sciences Graduate Program, McMaster University, Hamilton, ON, Canada, [2]Department of Physics and Astronomy, McMaster University, Hamilton, ON, Canada, [3]Department of Physics, Ryerson University, Toronto, ON, Canada, [4]McMaster School of Biomedical Engineering, McMaster University, Hamilton, ON, Canada, [5]Department of Electrical and Computer Engineering, McMaster University, Hamilton, ON, Canada

The use of gadolinium (Gd) based contrast agents is being questioned due to its recently discovered retention in healthy individuals following administration. Our newest generation x-ray fluorescence system has been used in a small pilot study for in vivo Gd measurements in bones of healthy individuals, who have previously received these contrast agents. Preliminary results show a significant difference between the Gd-exposed and control groups, suggesting Gd accumulation in healthy individuals. Our system has performed the first human in vivo measurement of Gd in bone and has the potential to be used in further studies of accumulation in the body.

5564 Computer 100

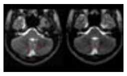

Characterization of Gadolinium Deposition in the Brain Manifest as T2-hypointensity and T1-hyperintensity Associated with Repeat Monthly Triple-Dose Gadopentetate Dimeglumine Administration for 2 years in the BECOME Trial

Paul Allen DiCamillo[1,2], Michael Benjamin Shvarts[1,2], Ravi Bhasker Patel[2,3,4], Jhimli Mitra[3], Pallavi Tiwari[3], Stuart D Cook[5], Diego Cadavid[5], Robert T Naismith[6], Samantha Lancia[6], and Leo J Wolansky[1,2]

[1]Radiology, University Hospitals Cleveland Medical Center, Cleveland, OH, United States, [2]Case Western Reserve University School of Medicine, Cleveland, OH, United States, [3]Department of Biomedical Engineering, Case Western Reserve University School of Medicine, Cleveland, OH, United States, [4]Radiation Oncology, University Hospitals Cleveland Medical Center, Cleveland, OH, United States, [5]Department of Neurology, Rutgers-New Jersey Medical School, Newark, NJ, United States, [6]Neurology, Washington University School of Medicine, St. Louis, MO, United States

We characterize the brain parenchymal deposition of Gadolinium (Gd) in the dentate nucleus (DN) and globus pallidus (GP) in a cohort of 16 subjects with multiple sclerosis (MS), each of whom had systematically received one year of serial monthly triple dose Gd (3-dose Gd) and optional additional monthly exposure for a second year. Progressive increase in T1 signal and decrease in T2 signal is found in both the dentate nucleus and globus pallidus.

5565 Computer 101

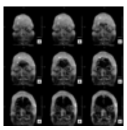

SKIN ENHANCEMENT WITH GADOLINIUM BASED CONTRAST AGENTS

Akira YAMAMOTO[1], Tsutomu OKADA[1], Yasutaka FUSHIMI[1], Tomohisa OKADA[2], and Kaori TOGASHI[1]

[1]Department of Diagnostic Imaging and Nuclear Medicine, Kyoto University Graduate School of Medicine, Kyoto, Japan, [2]Human Brain Research Center, Graduate School of Medicine, Kyoto University, Kyoto, Japan

Skin tissue showed enhancement after GBCA administration. This phenomenon was confirmed by profile curve analysis. Subtraction image between pre-post contrast was calculated after image registration. This subtraction image showed distinct contrast effect of the skin tissue and may be helpful for the clinical diagnosis.

5566 Computer 102

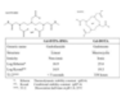

Comparison of Gd-DTPA-BMA versus Gd-DOTA of Gadolinium retention in human bone tissue with renal function

Takaki Maeda[1], Hitomi Hara[2], Toshihiro Akisue[2], Yuki Iwama[3], Ryosuke Kuroda[2], Masahiko Fujii[4], and Kazuro Sugimura[5]

[1]Radiology, Kobe University Hospital, Kobe, Japan, [2]Orthopedic Surgery, Kobe University Graduate School of Medicine, [3]Radiology, Hyogo Prefectural Nishinomiya Hospital, [4]Kobe Minimally Invasive Cancer Center, [5]Kobe University Graduate School of Medicine

The purpose of this study was to determine the gadolinium (Gd) retention in human bone tissue after administration of Gd contrast agent such as macrocyclic (Gd-DOTA) or linear (Gd-DTPA-BMA) chelate at a standard single clinical dose and to evaluate its correlation with renal function.

5567 Computer 103

Gadolinium presence in the brain: Detection and quantification of gadolinium based contrast agents in the cerebrospinal fluid in rats

Gregor Jost[1], Thomas Frenzel[1], Jessica Lohrke[1], Diana Lenhard[2], Shinji Naganawa[3], and Hubertus Pietsch[1]

[1]MR & CT Contrast Media Research, Bayer Pharma AG, Berlin, Germany, [2]Institute of Vegetative Physiology, Charité, Berlin, Germany, [3]Department of Radiology, Nagoya University Graduate School of Medicine, Nagoya, Japan

The infiltration of six marketed and one experimental gadolinium based contrast agents (GBCA) from blood into the cerebrospinal fluid (CSF) was evaluated in rats by repeated fluid attenuated (FLAIR) MRI up to 4h. Quantitative gadolinium measurements in CSF samples (4.5 and 24h) were performed by ICP-MS. No differences in penetration and distribution into the CSF were observed for the marketed GBCAs. FLAIR imaging demonstrates a kinetic from the inner CSF cavities to the subarachnoid space, suggesting an infiltration via the choroid plexus and a passive distribution with CSF flow. After 24h an almost complete GBCA clearance from CSF was observed.

5568 Computer 104

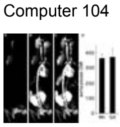

A Manganese-Based Alternative to Gadolinium: Contrast Enhanced MR Angiography at 3T and In Vivo Stability

Eric M Gale[1], Hsiao-Ying Wey[1], Ian Ramsay[1], David E Sosnovik[1], and Peter Caravan[1]

[1]A. A. Martinos Center for Biomedical Imaging, MGH/ Harvard Medical School, Charlestown, MA, United States

We evaluated the efficacy of a new manganese-based contrast agent, Mn-PyC3A, in contrast-enhanced MR angiography by comparison to Gd-DTPA in a baboon model at 3T. Mn-PyC3A clearance was assessed by dynamically scanning the excretory organs and performing serial blood draws out to 60 min. Mn-PyC3A plasma clearance and metabolism were quantified from the drawn blood. Mn-PyC3A generates equivalent vessel-to-muscle contrast-to-noise ratios as Gd-DTPA at 3T, clears via a mixed renal and hepatobiliary pathway, and is excreted unchanged. Mn-PyC3A is a functionally equivalent gadolinium-free alternative for contrast-enhanced MRI angiography.

5569 Computer 105

Ferumoxytol as an Alternative to Gadolinium-based MRI Applications in Patients With and Without Renal Impairment: Acute and Short-term Safety Experience

Kim-Lien Nguyen[1,2], Takegawa Yoshida[1,3], Isidro B Salusky[4], Peng Hu[1,3], and J. Paul Finn[1,3]

[1]Diagnostic Cardiovascular Imaging Laboratory, David Geffen School of Medicine at UCLA, Los Angeles, CA, United States, [2]Division of Cardiology, David Geffen School of Medicine at UCLA and VA Greater Los Angeles Healthcare System, Los Angeles, CA, United States, [3]Department of Radiological Sciences, David Geffen School of Medicine at UCLA, [4]Department of Pediatric Nephrology, David Geffen School of Medicine at UCLA

Recent concerns about gadolinium deposition in biologic tissues and discontinuation of gadofosveset trisodium have created increased interest in the off-label use of ferumoxytol as an MRI contrast agent. Limited safety data relating to the diagnostic use of ferumoxytol are available. We summarize our safety experience with ferumoxytol as an alternative MRI contrast agent in 285 unique patients (314 injections) with all levels of renal function.

5570 Computer 106

Immediate Reactions to Gadolinium Based Contrast Agents: a Meta-Analysis

Ashkan Heshmatzadeh Behzadi[1], Yize Zhao[2], Zerwa Farooq[3], and Martin R. Prince[4]

[1]Radiology, Weill Cornell Medical College, New York, NY, United States, [2]Department of Healthcare Policy and Research, Weill Cornell Medical College, New York, [3]Radiology, Weill Cornell Medical Center, [4]Department of Radiology, Cornell and Columbia Universities, New York, NY, United States

Recently there has been increased attention focused on GBCA safety and data on the numbers of reactions have begun to be reported in large Studies. Here we combine data from multiple papers in a meta-analysis to determine if certain GBCA or classes of GBCA may have different immediate reaction profiles.

5571 Computer 107

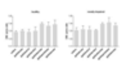

Impact of renal impairment on T1-weighted signal increase and gadolinium presence in the rat brain after multiple administrations of gadolinium based contrast agents

Hubertus Pietsch[1], Thomas Frenzel[1], Jessica Lohrke[1], and Gregor Jost[1]

[1]MR & CT Contrast Media Research, Bayer Pharma AG, Berlin, Germany

The impact of renal insufficiency on the T1-weighted signal intensity (SI) increase in the cerebellar nuclei (CN) and on the brain gadolinium concentration was evaluated by comparing 5/6-nephrectomized to healthy control rats. Eight weeks after repeated high-dose GBCA administrations a significantly higher CN/pons SI ratio compared to a saline control group was found for linear GBCAs. This was independent of the renal status. No altered SI ratios compared to the saline group were observed after administration of macrocyclic GBCAs. Inductive coupled plasma mass spectrometry revealed higher gadolinium concentrations for all GBCAs in the cerebellum of renally impaired rats.

5572 Computer 108

T1-signal increases as a marker of Gd-deposition in pediatric brain: findings after multiple exposures to gadobenate dimeglumine

Guenther Schneider[1], Paul Raczeck[1], Arno Buecker[1], and Jonas Stroeder[1]

[1]Saarland University Medical Center, Homburg, Germany

The possibility of Gd deposition in the pediatric brain following exposure to GBCAs is a potentially serious issue. Our study of 34 pediatric patients that received between 5 and 15 administrations of low dose (0.05 mmol/kg bodyweight) gadobenate dimeglumine (MultiHance; Bracco) revealed no differences in T1-signal in the DN, GP, pons and thalamus relative to measurements made in 24 age- and weight-matched control subjects that had never been exposed to any GBCA. Likewise no meaningful differences were seen in DN–pons and GP–thalamus SI ratios. We consider low dose gadobenate to be safe and effective for diagnosis and routine follow-up of pediatric oncologic patients.

5573 Computer 109

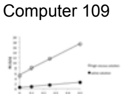

Strong enhancement of relaxivity of gadolinium contrast agent in solution with intracellular viscosity: Quantitative estimation of the deposited contrast agent in the brain

Ken Masuyama[1,2], Masayuki Taguchi[1], and Toru Yamamoto[3]

[1]Graduate School of Health Sciences, Hokkaido University, Sapporo, Japan, [2]Department of Medical Radiation Technology, Teine Keijinkai Hospital, Sapporo, Japan, [3]Faculty of Health Sciences, Hokkaido University, Sapporo, Japan

High T1-weighted signal appears in brain of patients who have experienced MRI examinations using gadolinium contrast agent several times. The relaxation effect of gadolinium contrast agent strongly depends on the viscosity of the solution, and the average viscosity in the cell is higher than that of the free water. However, the relaxation effect of the gadolinium contrast agent in the cell has been unknown. In this study, we investigated the longitudinal relaxivity of it – concentration dependence of longitudinal relaxation rate in solution with intracellular viscosity. The intracellular viscosity strongly enhances the longitudinal relaxivity of the gadolinium contrast agent.

5574 Computer 110

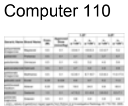

Gadolinium Calculator for Safe Dosing of Gadolinium Based Contrast Agents

Scott B Reeder[1,2], Elizabeth A Simcock[1], Bryan E Ramirez[1], Joseph H Rowley[3], and Howard A Rowley[1]

[1]Radiology, University of Wisconsin, Madison, WI, United States, [2]Medical Physics, University of Wisconsin, Madison, WI, [3]Department of Computer Science, University of California, Santa Cruz

In this work, we describe the design, implementation, and utilization of an online and smartphone gadolinium calculator used to calculate gadolinium-based contrast agent (GBCA) dose. By providing a readily available, reliable, and rapid means of calculating the volume of a GBCA, we aim to ensure accurate dosing so as to avoid accidental over- or under-dosing. Utilization tracking demonstrated progressively increasing use of the online gadolinium calculator with a total of 22,074 page visits from 68 countries, logged during a 9-month tracking period.

5575 Computer 111

Impact of Abdominal Magnetic Resonance Imaging on DNA Double Strand-Breaks in Human Blood Lymphocytes

Saravanabavaan Suntharalingam[1], Emil Mladenov[2], Georg Iliakis[2], Michael Forsting[1], Oliver Kraff[3,4], Harald H. Quick[3,4], and Kai Nassenstein[1]

[1]Department of Diagnostic and Interventional Radiology and Neuroradiology, University Hospital Essen, Essen, Germany, [2]Institute of Medical Radiation Biology, University Hospital Essen, Essen, Germany, [3]Erwin L. Hahn Institute for Magnetic Resonance Imaging, University Hospital Essen, Essen, Germany, [4]High Field and Hybrid MR Imaging, University Hospital Essen, Essen, Germany

Magnetic resonance imaging is considered to be a safe alternative to other imaging techniques that use ionizing radiation, such as computed tomography. Initially driven by X-ray and CT imaging studies, within the recent years different in vitro and in vivo studies analyzed the impact of MR imaging on DNA integrity in human lymphocytes but reported contradictory results. In this study on patients referred to clinical abdominal MRI, γ-H2AX immunofluorescence microscopy was used to determine DNA integrity. No evidence of DNA damage induced by abdominal MRI in a clinical setting was found.

5576 Computer 112

RF Heating Studies on Anesthetized Swine Using Fractionated Dipole Antennas at 10.5 T

Yigitcan Eryaman[1], Russell L. Lagore[1], Arcan Erturk[1], Lynn Utecht[1], Patrick Zhang[1], Angel Torrado-Carvajal[2,3], Esra Abaci Turk[4], Lance DelaBarre[1], Gregory J Metzger[1], Gregor Adriany[1], Kamil Ugurbil[1], and J. Thomas Vaughan[1]

[1]University of Minnesota-Center for Magnetic Resonance Research, Minneapolis, MN, United States, [2]Athinoula A. Martinos Center for Biomedical Imaging, Department of Radiology, Massachusetts General Hospital and Harvard Medical School, MA, United States, [3]Medical Image Analysis and Biometry Laboratory, Universidad Rey Juan Carlos, Madrid, Spain, [4]Boston Children's Hospital, Harvard Medical School, MA, United States

We measured temperature increase (ΔT) in anesthetized swine using fluoroscopic probes and compared our results to the simulated solutions obtained from digital models of the same swine. For our studies, we used a 4 channel fractionated dipole array that is placed on the neck/upper back region. Electromagnetic and thermal simulations were performed along with in vivo experiments with different RF excitation patterns at 10.5 T.

5577 Computer 113

RF safety assessment of a 32-channel integrated body coil for 7 Tesla: Thermal dose evaluation at high SAR level

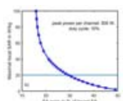

Thomas M. Fiedler[1], Stephan Orzada[2], Martina Flöser[1], Harald H. Quick[2,3], Mark E. Ladd[1,2], and Andreas K. Bitz[1]

[1]Medical Physics in Radiology, German Cancer Research Center (DKFZ), Heidelberg, Germany, [2]Erwin L. Hahn Institute for MRI, University Duisburg-Essen, Essen, Germany, [3]High Field and Hybrid MR Imaging, University Hospital Essen, Essen, Germany

RF safety assessment for a 32-ch body coil for 7T was performed based on SAR, tissue temperature, and a thermal dose model (CEM43°C). Temperature simulations considered a temperature-dependent thermoregulation. The tissue temperature limit is exceeded when SAR limits are adhered to. However, based on the thermal dose limit, the maximum input power determined from SAR limits can be exceeded by up to a factor of 5 without noticeable limitations in permissible exposure time in MR examinations. This increased input power allows for improved B_1^+ homogeneity with 50% reduced flip angle error compared to the input power determined from SAR limits.

5578 Computer 114

The effect of variable amniotic fluid conductivity and fetal tissues properties on B1+ and local SAR for fetal imaging at 3T

Shaihan J Malik[1], Jeffrey W Hand[1], and Joseph V Hajnal[1]

[1]Division of Imaging Sciences & Biomedical Engineering, King's College London, London, United Kingdom

Effects on B_1^+ and local specific absorption rate of varying the conductivity of fetal tissues and amniotic fluid (σ_{AF}) in a model of a 7 month pregnant woman within a 3T birdcage coil are investigated numerically. Results indicate that a realistic value of σ_{AF} is required to estimate power to produce a chosen B_1^+ in the fetus and fetal SAR_{10g}. Fetal properties adjusted for gestational age impact on B_1^+ and result in increased fetal SAR_{10g} compared to adult value based simulations. Smaller changes in SAR_{10g} are predicted between detailed fetal models and homogeneous ones with volume weighted average dielectric properties.

5579 Computer 115

Assessment of specific absorption rate and energy deposition in over 14,000 clinical MRI examination at 1.5 and 3 Tesla scanners

Amir Ali Rahsepar[1], Laleh Golestanirad[2], Hassan Haji-Valizadeh[3], Haris Saybasili [1], Julie A Blaisdell [1], Michael Markl[3], John Kirsch[4], James C Carr[1], and Jeremy D Collins[1]

[1]Department of Radiology, Northwestern University, Chicago, IL, United States, [2]Athinoula A. Martinos Center for Biomedical Imaging, Boston, MA, United States, [3]Department of Biomedical Engineering, McCormick School of Engineering, Chicago, IL, United States, [4]Siemens Medical Solutions, Boston, MA, United States

Although SAR value is an important factor in device heating, but this study also provides information about the other factors like the total amount of delivered RF energy, time period of RF delivery and most importantly the pause between pulse sequences should be considered

---

5580 Computer 116

Optimization of the order and spacing of the sequences to reduce the maximum SAR-induced temperature reached during an MRI examination

Giuseppe Carluccio[1,2] and Christopher Michael Collins[1,2]

[1]Radiology, Center for Advanced Imaging Innovation and Research (CAI2R), New York University, New York, NY, United States, [2]Radiology, Bernard and Irene Schwartz Center for Biomedical Imaging, New York University, New York, NY, United States

We demonstrate that the maximum SAR-induced temperature in an examination can be lowered with strategic ordering of the sequences in the exam. Using numerical simulations, here we optimize the order of and time between sequences in a spine exam to minimize the maximum temperature reached in a human body model without increasing the duration of the exam. The optimized sequence has a maximum temperature 0.63 C lower than the original.

5581 Computer 117

Peripheral Nerve Stimulation in MRI: Insights from a three level analysis and coupled EM-electrophysiological simulations in neuro-functionalized human models

Antonino Mario Cassara'[1], Esra Neufeld[1], Gisela Hagberg[2], Manuel Guidon[3], Klaus Scheffler[4], and Niels Kuster[1,5]

[1]IT'IS Foundation, Zurich, Switzerland, [2]Max Plank Institute - Tuebingen, [3]Zurich MedTech, [4]Max Plank Institute - Tuebingen, Germany, [5]ETH, Zurich, CH

The mechanisms of peripheral nerve stimulation (PNS) induced by the fast switching of MRI gradient coils are only partially understood, stimulation sites and E-field (or dB/dt) thresholds show large inter-subject variability and neurostimulation models based on the amphibian SENN axon model are not ideal. We propose a 3 level computational investigation that combines analysis of E-field exposure, of activation functions, and of multi-parametric EM-electrophysiological simulations in neuro-functionalized human models for different axon models and gradient waveforms. Results concerning E-field/dB/dt thresholds values and sites of neurostimulation are compared with published experimental data. A functional uncertainty analysis is also provided.

5582 Computer 118

Evaluation of SMS sequence on the AIMD MRI model validation

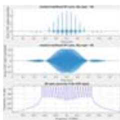

Yuliang Du[1], Xi Lin Chen[2], Will Lui[2], Shi Feng[2], and Shiloh Sison[2]

[1]CRMD-Hardware Development, St Jude Medical, Sylmar, CA, United States, [2]St. Jude Medical

Impacts of SMS imaging technique on the AIMD design, transfer function measurement, model calculation and system validation were thoroughly analyzed. The RF frequency broadening from the SMS imaging sequence has minimal impacts to the existing device design and test methodology.

5583 Computer 119

Graphene for MRI Applications at 7T: Opportunities for SAR reduction

Gianluigi Tiberi[1,2], Guo Liu[3], Raj Mittra[4], and Michela Tosetti[1,2]

[1]Imago7, Pisa, Italy, [2]IRCCS Stella Maris Foundation, Pisa, Italy, [3]Xidian University, Xidian, People's Republic of China, [4]University of Central Florida in Orlando, Orlando, FL

SAR management is critical at ultra-high field (UHF) strength where RF field energy deposition in the subject increases and its distribution becomes very inhomogeneous. Here we illustrate simulation results for a test example in order to show how a graphene sheet can be used to obtain a SAR reduction without sacrificing the coil efficiency significantly. Specifically, the presence of the graphene sheet leads a maximum local SAR reduction up to 47%. Thus, from the simulation here shown, it follows that graphene sheets can be successfully used in MRI applications at 7T for enhancing the safety with respect to SAR issue

5584 Computer 120

Safety and Function of Programmable Ventriculo-Peritoneal Shunt Valves: An in vitro 7 Tesla Magnetic Resonance Imaging Study

Karsten H Wrede[1,2], Bixia Chen[1,2], Ulrich Sure[2], Harald H Quick[1,3], and Oliver Kraff[1]

[1]Erwin L. Hahn Institute for MRI, University of Duisburg-Essen, Essen, Germany, [2]Department of Neurosurgery, University Hospital Essen, University of Duisburg-Essen, Essen, Germany, [3]High Field and Hybrid MR Imaging, University Hospital Essen, University of Duisburg-Essen, Essen, Germany

This in vitro study tests function, safety and image artifacts of the two worldwide most frequently implanted programmable VP-shunt valves in a 7 Tesla whole body MRI system. Both tested programmable VP-shunt valves lost their ability to be reprogramed after exposure to the static magnetic field and are therefore unsafe for use in 7 Tesla whole body scanners in their current design. Magnetic coercivity of the permanent magnets in the programming mechanisms was insufficient. Image artifacts adjacent to the valves, however, were tolerable.

Electronic Poster

NMR & ESR & Education

Exhibition Hall — Thursday 14:00 - 15:00

5585 Computer 25

Properties of Localization by Adiabatic SElective Refocusing (LASER) sequence

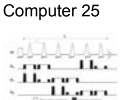

Dinesh K Deelchand[1], Edward J Auerbach[1], and Małgorzata Marjańska[1]

[1]CMRR, University of Minnesota, Minneapolis, MN, United States

This abstract reviews and highlights the various properties and advantages of the LASER pulse sequence

5586 Computer 26

A MatLab-based simulation program (tcaSIM$_2$) for predicting NMR spectra and MS data for ^{13}C tracer experiments

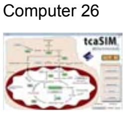

A. Dean Sherry[1,2], Qiang Li[3], Mark Jeffrey[3], Shawn Burgess[1], and Craig R. Malloy[1]

[1]Advanced Imaging Research Center, University of Texas Southwestern Medical Center, Dallas, TX, United States, [2]Chemistry, University of Texas at Dallas, Richardson, TX, United States, [3]Advanced Imaging Research Center, UT Southwestern Medical Center

A MatLab-based program is presented for predicting ^{13}C NMR spectra and mass ^{13}C isotopomer data of various tissue metabolites in a ^{13}C tracer experiments. The program is useful for predicting changes in ^{13}C multiplet patterns in NMR spectra and changes in mass isotopomer ratios in mass spectral data as a tissue responds to changes in flux of various substrates through completing pathways involving mitochondrial metabolism.   The program tcaSIM$_2$ (copies available free of charge) is also valuable for teaching metabolism and analysis of ^{13}C NMR data and mass spec data in metabolic tracer experiments.

5587 Computer 27

Use of MR Spectroscopy in Clinical Trials

Alexander Peter Lin[1], Benjamin Rowland[1], and John R Griffiths[2]

[1]Center for Clinical Spectroscopy, Brigham and Women's Hospital, Boston, MA, United States, [2]Cancer Research UK Cambridge Institute, University of Cambridge, Cambridge, United Kingdom

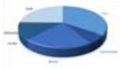

Magnetic resonance spectroscopy (MRS) is an ideal tool for therapeutic monitoring in clinical trials although its role has not been formally examined. An initial search in a clinical trials database showed 488 studies; however the results were cross-referenced with the scientific literature to yield 61 studies demonstrating the use of MRS in clinical trials. It is most frequently used to study hepatic lipid content, followed by studies of skeletal muscle, and finally the brain, which surprisingly was only 15% of the MRS studies. A review is provided to assess its importance as a non-invasive and quantitative biomarker for disease.

5588 Computer 28

Effect of liver transplantation on muscle metabolism and the abdomen adipose tissue volume in diabetic and non-diabetic patients

Petr Sedivy[1], Miloslav Drobny[1], Monika Dezortova[1], Irena Hejlova[2], Monika Cahova[3], Pavel Trunecka[2], and Milan Hajek[1]

[1]MR-unit, Institute for Clinical and Experimental Medicine, Prague, Czech Republic, [2]Hepatogastroenterology Department, Institute for Clinical and Experimental Medicine, Prague, Czech Republic, [3]Centre of Experimental Medicine, Institute for Clinical and Experimental Medicine, Prague, Czech Republic

Liver transplantation (TxL) is a treatment that rapidly improves the clinical status of patients. However, side effects due to long-term immunosuppressive therapy may negatively influence the function of certain organs and metabolism. ^{31}P MRS and MRI are suitable methods for the clinical examination of muscles and abdomen fat volume in transplanted patients. Our pilot results show that TxL leads to an improvement of resting muscle metabolism in especially in diabetic patients and an increase of volume visceral fat in a short term (six months) after transplantation.

5589 Computer 29

Relationship Between BOLD fMRI and Functional MRS the Medial Temporal Lobe

Simona Nikolova[1], Shauna Stark[1], and Craig E.L. Stark[1,2]

[1]Department of Neurobiology and Behavior, University of California, UCI, Irvine, CA, United States, [2]Center for the Neurobiology of Learning and Memory, University of California, Irvine, CA, United States

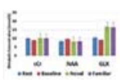

Structures in the medial temporal lobe (MTL) like the hippocampus play a critical role in memory. Functional disruptions of the MTL (typically studied with BOLD fMRI) are present in a range of disorders and diseases. The relative and indirect nature of BOLD makes it difficult to interpret findings such as the hippocampal “hyperactivity” that has been tied to age-related cognitive decline and the progression to Alzheimer’s Disease. In this work, “functional” MR spectroscopy is combined with simultaneous BOLD during memory tasks to investigate the relationship between the two. While task-related activity is observed in both, there are points of departure.

5590 Computer 30

Online quantification of lactate concentration in microdialysate during cerebral activation using 1H-MRS and sensitive NMR microcoil

Leslie Mazuel[1], Ursule Dumont[2], Noël Pinaud[2], Vanessa Zhendre[2], Silvia Rizzitelli[2], Jordy Blanc[1], Hélène Roumes[1], Anne-Karine Bouzier-Sore[1], and Yannick Crémillieux[2]

[1]CRMSB, Université de Bordeaux, Bordeaux, France, [2]Institut des Sciences Moléculaires, Université de Bordeaux, Bordeaux, France

The role of lactate in neuronal activation is central in the hypothesis of the astrocyte-to-neurons lactate shuttle. In this work, we implement highly sensitive 1H-MRS on brain microdialysate in order to monitor online the lactate fluctuations during neuronal activation in the S1BF area. The custom-made microcoil used in this study was shown to be sensitive enough for measuring a 40% increase in lactate concentration during brain stimulation.

5591 Computer 31

1H and 13C NMR evaluation of pH-dependent structural characteristics of lonidamine

Kavindra Nath[1], Jeffrey Roman[1], David S Nelson[1], Andrew Butterworth[1], Stephen Pickup[1], Dennis B Leeper[2], and Jerry D Glickson[1]

[1]University of Pennsylvania, Philadelphia, PA, United States, [2]Thomas Jefferson University, Philadelphia, PA, United States

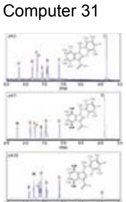

We seek to understand the pH-dependent physicochemical changes of lonidamine (LND), an antineoplastic drug, particularly to locate the sites of ionization. LND samples at pH 2, 7, and 13 were analyzed using ^{1}H and ^{13}C NMR. The results indicate that there is a noticeable change in the chemical shifts for a few atoms in LND from neutral to alkaline pH. These changes demonstrate that LND is ionized at its imidazole α-nitrogen. In addition, the expected ionization of the carboxyl group of LND at acid pH is not directly observed, and this may be due to a rapid-exchange phenomenon.

5592 Computer 32

Characterization of Water Compartment Exchange in Ex-Vivo Human Cartilage Using Two-Dimensional Relaxometry

Kyle William Sexton[1], David A. Reiter[1], Hasan Celik[2], Kenneth Fishbein[1], Tariq Nayfeh[3], and Richard G. Spencer[1]

[1]Magnetic Resonance Imaging and Spectroscopy Section, National Institute on Aging, Baltimore, MD, United States, [2]University of California, Berkeley, CA, United States, [3]Medstar Harbor Hospital, Baltimore, MD, United States

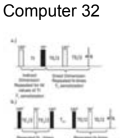

One-dimensional transverse relaxometry has proven to be an effective method for characterizing macromolecular compartments in cartilage. Two-dimensional studies extend the capabilities of these types of experiments, providing characterization of tissue compartments in terms of correlated relaxation times and providing a means of probing intercompartmental exchange. We provide results of T_2-T_2 and T_1-T_2 relaxometry experiments on human articular cartilage, indicating that exchange between tissue compartments may be augmented in degraded tissue.

5593 Computer 33

Full Digital Cancellation-based NMR with Concurrent Excitation and Acquisition using a Lock-in Amplifier

Ali Caglar Özen[1], Mazin Jouda[2], Jan Korvink[2], and Michael Bock[1]

[1]Deptartment of Radiology, Medical Physics, Medical Center – University of Freiburg, Freiburg, Germany, [2]Institute of Microstructure Technology, Karlsruhe Institute of Technology, Karlsruhe, Germany

Concurrent Excitation and Acquisition (CEA) offers fundamental advantages for NMR such as 100% signal acquisition efficiency, true zero echo time, reduction of acoustic noise, and decreased peak RF power. Bandwidth of the excitation in CEA is independent of the RF power, allowing detection very broad resonances. In this work, a CEA system is introduced with a full digital cancellation. The system uses a lock-in amplifier combined with an arbitrary signal generator. Preliminary results for NMR of various samples are represented and discussed.

5594 Computer 34

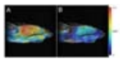

In vivo brain redox status and blood-brain barrier function in diethylmaleate-treated mice by EPR imaging and ME-MRI

Hirotada G Fujii[1], Miho C Emoto[1], Yuta Matsuoka[2], and Ken-ichi Yamada[2]

[1]Sapporo Medical University, Sapporo, Japan, [2]Kyushu University, Fukuoka, Japan

EPR imaging has been used to visualize redox status in oxidative brain diseases, but the role of cerebral glutathione (GSH) is not clear. In this study, using the mouse model of GSH depletion with diethylmaleate (DEM), the role of GSH in brain redox status was examined. The remarkable change in redox status in DEM-treated mouse brain was visualized with EPR imaging, and in vitro assay showed decrease in the level of GSH. ME-MRI clearly visualized blood-brain barrier dysfunction in DEM-treated mice. Results indicate that GSH plays an important role in the maintenance of both brain redox status and BBB integrity.

5595 Computer 35

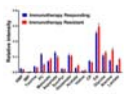

Unique molecular signatures to distinguish immunotherapy responding and resistant cell lines in melanoma by NMR spectroscopy and MR hyperpolarization

Shivanand Pudakalakatti[1], Ashvin Jaiswal[2], Prasanta Dutta[1], Michael Curran[2], and Pratip Bhattacharya[1]

[1]Department of cancer systems imaging, University of Texas M D Anderson Cancer Center, Houston, TX, United States, [2]Department of Immunology, University of Texas M D Anderson Cancer Center, Houston, TX, United States

The cancer immunotherapy has brought new ray of hope in cancer patients with its capability of curing cancer with less side effects. However not all patients responds to therapy. In this study we have employed Nuclear Magnetic Spectroscopy (NMR) and in vivo hyperpolarized 1-13C pyruvate magnetic resonance spectroscopy (MRS) to differentiate immunotherapy responding from immunotherapy resisting melanoma.

5596 Computer 36

Lactate and lipid provide identifying biomarkers for good quality sperm by ^{1}H MRS

Sarah J Calvert[1], Steven Reynolds[2], Martyn N Paley[2], and Allan A Pacey[1]

[1]Academic Unit of Reproductive & Developmental Medicine, University of Sheffield, Sheffield, United Kingdom, [2]Academic Unit of Radiology, University of Sheffield, Sheffield, United Kingdom

^{1}H MRS was used to examine good and poor sperm populations to identify biomarker differences between them. Spectra were binned to 0.02ppm and two-way ANOVA with Bonferroni correction, Wilcoxon match rank test and ROC curve analyses were used to find bins with significant differences between good and poor sperm. All three statistical methods identified the bins at 1.24-1.32ppm which correlates with overlapping lipid and lactate peaks. Differences in these peaks may result from metabolic differences between the two sperm populations and this may give a useful insight into the pathology of sperm dysfunction.

5597 Computer 37

Metabolic differences in patients with Overt and Potential Celiac disease Studied by in-vitro Proton NMR

Uma Sharma[1], Deepti Upadhyay[1], Prasenjit Das [2], Siddhartha Datta Gupta [2], Govind K Makharia[3], and Naranamangalam R Jagannathan[1]

[1]Nuclear Magnetic Resonance and MRI Facility, All India Institute of Medical Sciences, New Delhi, India, [2]Pathology, All India Institute of Medical Sciences, New Delhi, India, [3]Gastroenterology & Human Nutrition, All India Institute of Medical Sciences, New Delhi, India

Potential celiac disease (CeD) patients have immunological abnormalities similar to CeD but unlike CeD, their duodenum displays normal histology. In-vitro proton NMR study of small intestinal mucosa of these patients demonstrated metabolic abnormalities associated with the intestinal inflammation. Both potential CeD and CeD patients had lower concentration of histidine compared to controls while lower glycine was seen only in CeD. Since, both amino acids exert anti-inflammatory effects; their reduced levels suggested compromised cytoprotective mechanism. Significantly higher level of glycerophosphocholine seen in potential CeD compared to CeD might have contributed for renewal of enterocytes and thus to normal small intestine histology.

5598 Computer 38

High-resolution MRS characterization of malignant ascites in two different models of ovarian cancer

Santosh K Bharti[1], Flonné Wildes[1], Chien-Fu Hung[2], TC Wu[2], Zaver M Bhujwalla[1,3], and Marie-France Penet[1,3]

[1]JHU ICMIC Program, Division of Cancer Imaging Research, The Russell H. Morgan Department of Radiology and Radiological Science, The Johns Hopkins University School of Medicine, Baltimore, MD, United States, [2]Pathology, The Johns Hopkins University School of Medicine, [3]Sidney Kimmel Comprehensive Cancer Center, The Johns Hopkins University School of Medicine

Malignant ascites occurs in approximately 37% of terminal ovarian cancer patients. It significantly contributes to poor quality of life and mortality. Advances in understanding malignant ascites formation and finding new therapeutic options are urgently needed. High-resolution proton magnetic resonance spectroscopy provides opportunities to characterize biofluid metabolites and can be easily translated to the clinic. Here, we are investigating the metabolic profile of ascites obtained in two different experimental models of ovarian cancer. To further understand the differences observed between both models, we completed our study by analyzing the metabolic profiles of those cells in culture and their corresponding conditioned media.

5599 Computer 39

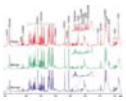

High-resolution 1H MRS human plasma profiling of pancreatic ductal adenocarcinoma

Santosh K Bharti[1], Michael Goggins[2,3], and Zaver M Bhujwalla[1,3]

[1]JHU ICMIC Program, Division of Cancer Imaging Research, The Russell H. Morgan Department of Radiology and Radiological Science, The Johns Hopkins University School of Medicine, Baltimore, MD, United States, [2]Departments of Pathology and Medicine, The Sol Goldman Pancreatic Cancer Research Center, The Johns Hopkins University School of Medicine, Baltimore, MD, United States, [3]Sidney Kimmel Comprehensive Cancer Center, The Johns Hopkins University School of Medicine, Baltimore, MD, United States

The dismally poor 5 year survival rate of less than 6% in pancreatic ductal adenocarcinoma (PDAC) increases to ~50% with early stage PDAC making early detection critically important. Metabolic characterization of patient plasma samples provides a unique opportunity to identify biomarkers to assist in routine screening to detect of PDAC. Here, in a preliminary study, we have characterized the metabolic profiles of plasma samples from normal, benign, and PDAC patients. Even with a limited sample we identified a significant increase in β-hydroxybutyrate, acetate, acetoacetate, lactate and pyruvate in PDAC compared to normal plasma.

5600 Computer 40

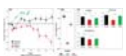

Interrogating Liver Metabolic Stress due to Cancer-Induced Cachexia

Santosh K Bharti[1], Paul T Winnard Jr.[1], Yelena Mironchik[1], Anirban Maitra[2], and Zaver M Bhujwalla[1,3]

[1]JHU ICMIC Program, Division of Cancer Imaging Research, The Russell H. Morgan Department of Radiology and Radiological Science, The Johns Hopkins University School of Medicine, Baltimore, MD, United States, [2]MD Anderson Cancer Center, The University of Texas, Houston, TX, United States, [3]Sidney Kimmel Comprehensive Cancer Center, The Johns Hopkins University School of Medicine, Baltimore, United States

Cachexia is a poorly understood metabolic syndrome characterized by cancer-induced tissue wasting and weight loss. Cachexia occurs with the highest frequency and severity in pancreatic ductal adenocarcinoma (PDAC). To further understand this syndrome, here we used ^{1}H MRS to analyze liver metabolites in mice with and without cachexia-inducing PDAC. We detected profound liver weight loss in cachectic mice. ^{1}H MR spectra identified significant depletion of lactate, glucose and glutathione in cachectic mice that provide new insights into the syndrome and may present novel strategies to prevent or reduce cachexia-induced weight loss and the morbidity and mortality associated with the syndrome.

5601 Computer 41

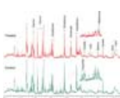

Phenformin Induces Profound Metabolic Changes in Lung Cancer Cells

Santosh Kumar Bharti[1], Ellen Tully[2], Edward Gabrielson[2], and Zaver M Bhujwalla[3,4]

[1]Radiology, JOHNS HOPKINS UNIVERSITY, BALTIMORE, MD, United States, [2]Department of Pathology, The Johns Hopkins University School of Medicine, Baltimore, MD, United States, [3]JHU ICMIC Program, Division of Cancer Imaging Research, The Russell H. Morgan Department of Radiology and Radiological Science, The Johns Hopkins University School of Medicine, Baltimore, MD, United States, [4]Sidney Kimmel Comprehensive Cancer Center, The Johns Hopkins University School of Medicine, Baltimore, United States

Lung cancer is a leading cause of cancer associated death in United States and worldwide. Non-small cell lung cancer (NSCLC) accounts for 85% of all lung cancer cases in the United States. Use of metformin is associated with improved cancer treatment outcomes, reduction in cancer incidence and decreased mortality, and because of a higher potency, phenformin may be a more promising anti-cancer agent. Here, we have used 1H MRS of cell extracts to investigate the effect of phenformin on A549 cells. Significant metabolic changes were observed following phenformin treatment

---

5602 Computer 42

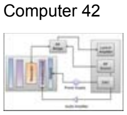

A Very Low-cost EPR Spectrometer Using 3D Design and Manufacturing

Bahareh Behzadnezhad[1,2], Jian Dong[1], Nader Behdad[1], and Alan McMillan[2]

[1]Dept of Electrical and Computer Engineering, University of Wisconsin-Madison, Madison, WI, United States, [2]Dept of Radiology, University of Wisconsin-Madison, Madison, WI, United States

This study describes a very low-cost EPR spectrometer that can be feasibly constructed using general purpose laboratory equipment combined with the use of 3D electromagnetic design and additive manufacturing. We demonstrate a functioning, homebuilt, low-cost continuous wave EPR spectrometer operating at 115 MHz. The development of a low-cost spectrometer has applications in education and for other general laboratory purposes.

5603 Computer 43

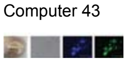

Detection of Tumor Spheroid Metabolism Using Hyperpolarized Magnetic Resonance Spectroscopy

Sui-Seng Tee[1], Izabela Suster[1], Sangmoo Jeong[1], Roozbeh Eskandari[1], Valentina Di Gialleonardo[1], Kristin L Granlund[1], Vesselin Miloushev[1], Steven Truong[2], and Kayvan Keshari[1]

[1]Memorial Sloan Kettering Cancer Center, New York, NY, United States, [2]Hunter College, New York

Cell-line tumor spheroids or patient-derived organoids are 3D structures that self-organize when grown in a suitable extracellular matrix. As they mirror in vivo physiology and biology well, these structures have been used as surrogates for clinical trials. This study describes the ability to grow spheroids in NMR-compatible scaffolds that metabolize hyperpolarized [1-13C] pyruvate. These spheroids are also sensitive to AKT inhibition that manifest in significantly decreased lactate production. Histological analysis confirms on-target inhibition, demonstrating that hyperpolarized magnetic resonance spectroscopy can be used to probe treatment response in spheroids that can mimic human disease.

5604 Computer 44

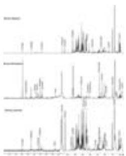

Comprehensive Metabolic Profiling of Urosepsis with positive and negative controls

Suruchi Singh[1], Tanushri Chatterji[2], Manodeep Sen[2], Ishwar Ram Dhayal[3], and Raja Roy[1]

[1]Centre of Biomedical Research, Lucknow, India, [2]Department of Microbiology, Dr. Ram Manohar Lohia Institute of Medical Sciences, Lucknow, India, [3]Department of Urology, Dr. Ram Manohar Lohia Institute of Medical Sciences, Lucknow, India

This study presents the metabolic perturbation in serum and urine samples while comparing Urosepsis with negative and positive controls. It explores the metabolic differentiation of serum samples with sepsis and urine samples with urinary tract infection (UTI) (considered as positive controls), and healthy controls (considered as negative controls) respectively. The serum and urine metabolic profile mainly depicted changes occurring due to severity and spread of infection. The statistical Partial Least Square Discriminant Analysis (PLS-DA) model was robust enough to differentiate the three groups distinctively in both serum and urine samples.

5605 Computer 45

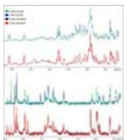

Metabolomical NMR measurements of cell cultures: Increasing the metabolic stability of lysed cells by additional heating due to enzymatic inactivation.

Gaelle Diserens[1], Damian Hertig[2,3], Martina Vermathen[2], Balazs Legeza[4], Christa E. Flueck[4], Jean-Marc Nuoffer[3], and Peter Vermathen[1]

[1]Depts. Radiology and Clinical Research, University Bern, Bern, Switzerland, [2]Dept. Chemistry and Biochemistry, University Bern, Bern, Switzerland, [3]University Institute of Clinical Chemistry, Bern University Hospital, Bern, Switzerland, [4]Pediatric Endocrinology and Diabetology of the Dept. Pediatrics & Dept. Clinical Research, University Bern, Bern, Switzerland

Advanced NMR measurements of biological samples may take several hours. Preanalytical issues may impact the metabolite content, potentially leading to misinterpretation. Our aim was to investigate by ^{1}H HR-MAS NMR the impact of different cell handling preparation protocols (lysis with and without heating) on the stability of the cell metabolome over the measurement time. In lysed fibroblasts and adrenal-cells, metabolism was ongoing over-time, contrary to a stable metabolite content of the lysed-heated cells. Therefore, to minimize metabolome modifications over the measurement time, it is suggested to use cell lysis in combination with heat inactivation for extended HR-MAS NMR measurements.

5606 Computer 46

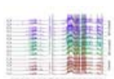

Metabolomic Analysis of Dendritic Cell Vaccination

Ram Bahadur Khattri[1], Farhad Dastmalchi[2], James R. Rocca[3], Maryam Rahman[2], and Matthew Merritt[4]

[1]Department of Biochemistry & Molecular Biology, University of Florida, Gainesville, FL, United States, [2]Department of Neurosurgery, University of Florida, Gainesville, FL, United States, [3]Mcknight Brain Institute, University of Florida, Gainesville, FL, United States, [4]Department of Biochemistry and Molecular Biology, University of Florida, Gainesville, FL, United States

We use ^{1}H NMR metabolomics to measure the impact of immunotherapy intended to target glioblastoma multiforme in a murine model. Cellular immunotherapy is a promising new platform for cancer treatment. Analysis of the urine of C57Bl6 mice revealed a set of metabolites associated with changes in glycolysis after immunotherapy treatment.

5607 Computer 47

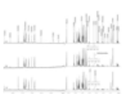

NMR Based Metabolomics of Human Filtered-Serum: An Appraisal of Chronic Stable Angina and Myocardial Infarction

Ashish Gupta[1], Sudeep Kumar[2], Shiridhar kashyap[2], Deepak Kumar[3], and Aditya Kapoor[2]

[1]metabolomics, Centre of Biomedical Research, Lucknow, India, [2]Cardiology, SGPGIMS, Lucknow, India, [3]Metabolomics, Centre of Biomedical Research, Lucknow, India

To address the shortcomings of the conventional biochemical approach for the precise identification of myocardial infarction (MI), and differentiation from chronic stable angina (CSA), and normal coronary (NC) subjects, we applied filtered serum based metabolomics using 1H NMR spectroscopy. The study comprises filtered sera from CAD [CSA (n=88, MI (n=90)], and NC (n=55) subjects. NMR-measured metabolites and clinical evaluation data were examined separately using chemometric approach to probe the signature descriptors for each cohort. This approach reveals that filtered serum based metabolic profiling can differentiate not only NC from CSA and MI but also CSA from MI.

5608 Computer 48

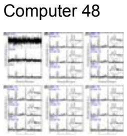

Effect of Coil Proximity on Parallel Spectroscopic Data Collection with Phased Array Coils

Candace C Fleischer[1], Xiaodong Zhong[1,2], and Hui Mao[1]

[1]Department of Radiology and Imaging Sciences, Emory University, Atlanta, GA, United States, [2]MR R&D Collaborations, Siemens Healthcare, Atlanta, GA, United States

Parallel imaging and spectroscopy are facilitated by multi-channel phased array coils. An important step is the combination of individual data from each channel, yet the effect of the non-uniformity of array coils on signal-to-noise ratio (SNR) is poorly characterized. Here, we present a systematic framework for identifying vulnerabilities in phased array coils for MRS. We demonstrate the importance of voxel position and coil proximity on overall SNR in a phantom and human subject, with significant SNR improvements after selectively filtering individual spectra based on pre-determined SNR thresholds which must be optimized for each phased array coil and volume of interest.

Electronic Poster

Non-Proton MRI & MRS

Exhibition Hall Thursday 14:00 - 15:00

5609 Computer 49

The feasibility of absolute quantification for 31P MRS at 7T

Lucian A. B. Purvis[1], Ladislav Valkovic[1], Matthew D. Robson[1], and Christopher T. Rodgers[1]

[1]OCMR, Department of Cardiovascular Medicine, University of Oxford, Oxford, United Kingdom

Calculation of in vivo concentrations requires knowledge of the B_1 field. A common solution to this problem has been to use field maps measured in phantoms, but this becomes increasingly difficult at high field. The size of the effect of material and B_0 field strength determining B_1 in the liver using phosphorus (^{31}P) phantoms was investigated at 1.5, 3, and 7T using CST simulations. The effect of concentration differences at 7T was demonstrated using 15 and 30mM phosphate phantoms. At 1.5T, using phosphate phantoms with concentrations between 5-40mM give an error of less than 3%. This increases to 10% at 3T, and 20-114% at 7T.

5610 Computer 50

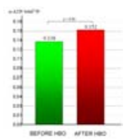

Effect of hyperbaric oxygenation on human brain phosphate metabolites at 3 Tesla. In vivo 31P MRS study

Andrei Valerievich Manzhurtsev[1,2], Olga Vasyukova[3], Victoria Victorovna Sergeeva[4], Tolibjon Abdullaevich Akhadov[2], Ilia Andreevich Mel'nikov[2], Olga Vasil'evna Bozhko[2], and Natalia Alexandrovna Semenova[1,2,5]

[1]N.M.Emanuel Institute of Biochemical Physics of RAS, Moscow, Russian Federation, [2]Radiology, Research Institute for Childen Emergency Surgery and Traumatology, Moscow, Russian Federation, [3]National Research Nuclear University "MEPhI", Moscow, Russian Federation, [4]Hyperbaric Oxygenation Dept., Research Institute for Childen Emergency Surgery and Traumatology, Moscow, Russian Federation, [5]N.N. Semenov Institute of Chemical Physics of RAS, Moscow, Russian Federation

This study is aimed to reveal the effects of hyperbaric oxygenation on human brain phosphate metabolites using ^{31}P MRS. At first, ^{31}P MRS study was conducted, after that the subjects took a session in hyperbaric chamber (1.2 atmosphere, 100% O_2) and then ^{31}P MRS study was repeated. The increase of α-ATP peak intensity was revealed after hyperbaric oxygenation, while other peak intensities and pH remained unchanged. This phenomenon is likely to happen because of [NAD(H)] increase, that might confirm the positive effect of hyperbaric oxygenation on human brain metabolism.

5611 Computer 51

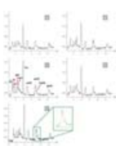

31P spectroscopic imaging of the human brain at 3T: effect of NOE and 1H-decoupling

Mark J. van Uden[1], Tom H. Peeters[1], Tom W.J. Scheenen[1], and Arend Heerschap[1]

[1]Radiology and Nuclear Medicine, Radboud university medical center, Nijmegen, Netherlands

^{31}P MRS of the brain can reveal changes in energy and lipid metabolism in healthy and diseased brain. In this abstract we compare ^{31}P MRS measurements with and without NOE and/or ^{1}H-decoupling. Adding nuclear Overhauser enhancement (NOE) and ^{1}H-decoupling to a ^{31}P MRS measurement at 3T increases spectral resolution to that at 7T and improves sensitivity so that the theoretical difference with 7T is partly compensated for. At relatively short repetition times both ^{1}H-decoupling and NOE have to be taken into account for proper quantification.

5612 Computer 52

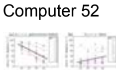

Different activated calf muscle groups measured simultaneously during plantar flexion exercise with multiple knee angles using multivoxel 31P-MRS.

Fabian Niess[1], Georg Bernd Fiedler[1], Albrecht Ingo Schmid[1], Sigrun Goluch[1], Roberta Frass-Kriegl[1], Michael Wolzt[2], Ewald Moser[1], and Martin Meyerspeer[1]

[1]Center for Medical Physics and Biomedical Engineering, Medical University Vienna, Vienna, Austria, [2]Department of Clinical Pharmacology, Medical University Vienna, Vienna, Austria

The distribution of workload between GM and SOL during plantar flexion exercise is strongly linked to the knee angle. This work investigates the differences in muscle activation of GM and SOL during plantar flexion with multiple knee angles. Time series spectra of both muscle groups were acquired simultaneously with high time resolution using dynamic multi-voxel 31P MRS. A linear correlation was found between knee angle and 31P MRS parameters related to muscle activation (PCr depletion, pH, PCr recovery time), confirming predominant involvement of GM with a straight knee, and increasing contributions of SOL with a bent knee.

5613 Computer 53

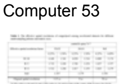

Optimization of Regularization Parameters of Compressed Sensing Reconstruction for Fast Phosphorus MR Spectroscopic Imaging of Human Brain.

Gokce Hale Hatay[1], Muhammed Yildirim[1,2], and Esin Ozturk-Isik[1]

[1]Institute of Biomedical Engineering, Bogazici University, Istanbul, Turkey, [2]Advanced Diagnostic Imaging, Philips Healthcare, Best, Netherlands

This study aims at investigating the effects of compressed sensing data acquisition and reconstruction factors for accelerated phosphorus MR spectroscopic imaging (^{31}P-MRSI). Simulated ^{31}P MRSI datasets containing healthy and tumor regions were created based on the metabolite information of brain tumor patient ^{31}P-MRSI acquired at 3T. k-space data were randomly undersampled with three different reduction factors while preserving the central portion for different noise levels, reduced datasets were reconstructed using compressed sensing by combining eleven different total variation and L1-norm penalties. Findings showed that data acquisition pattern and reconstruction parameters have a significant effect on the resultant ^{31}P-MRSI spectral quality.

5614 Computer 54

Dynamic 31P MR spectroscopy of fatigue in triceps surae muscles on post-poliomyelitis patients versus healthy age-matched volunteers at 3T

Xeni Deligianni[1,2], Tanja Haas[3], Patricia Hafner[4], Simone Schmidt[4], Vanya Gocheva[4], Francesco Santini[1,2], Oliver Bieri[1,2], and Dirk Fischer[4]

[1]Radiology, Division of Radiological Physics, University of Basel Hospital, Basel, Switzerland, [2]Biomedical Engineering, University of Basel, Basel, Switzerland, [3]Radiology, Clinic for Radiology and Nuclear Medicine, University of Basel Hospital, Basel, Switzerland, [4]Pediatric Neurology, Universitäts-Kinderspital beider Basel (UKBB), Basel, Switzerland

This study was focused on comparing the metabolism of triceps surae muscles on postpoliomyelitis patients and age-matched healthy volunteers through dynamic 31P spectra acquisition at 3T magnetic field. It has been suggested previously that in postpolio patients, metabolic changes are secondary to neurogenic pathways, but may influence Pi/PCr ratios. Here, it was shown that baseline PDE/PCr ratios were higher in patients. During exercise, controls performed significantly higher work and the change of Pi/PCr ratios was lower than in patients. Investigation of the correlation of Pi/PCr with the degree of the disease could be a promising clinical direction.

5615 Computer 55

Improvement in 31P CSI voxel tissue segmentation

Xian-Feng Shi[1], Young-Hoon Sung[1], Douglas Kondo[1], Colin Andrew Riley[2], and Perry Renshaw[1]

[1]Psychiatry, University of Utah, Salt Lake City, UT, United States, [2]The Brain Institute, University of Utah, Salt Lake City, UT, United States

The aim of the present study was to test a novel method for improving the subcortical tissue segmentation results, of the anatomical brain images acquired using a 31P/1H dual-tuned coil. When a dual-tuned 31P/1H coil is utilized to perform phosphorus-31 magnetic resonance spectroscopy studies of subcortical brain regions, the resulting anatomical images suffer from both low signal-to-noise ratio, and from reduced image contrast. By registering this volume image on a second anatomical image acquired using a single-tuned, 12 channel 1H head coil, we found that the subcortical tissue segmentation accuracy was significantly improved.

5616 Computer 56

Short TE PRESS-based proton observed carbon edited (POCE) 13C Magnetic Resonance Spectroscopy with a volumetric 1H transmitter for in vivo rat brain imaging at 7T

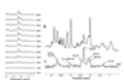

Chathura Kumaragamage[1,2], Dan Madularu[2,3], Axel Mathieu[2,3], Henk De Feyter[4], Natasha Rajah[2,3], and Jamie Near[1,2,3]

[1]Biomedical Engineering, McGill University, Montreal, QC, Canada, [2]Brain Imaging Centre, Douglas Mental Health University Institute, Montreal, QC, Canada, [3]Department of Psychiatry, McGill University, Montreal, QC, Canada, [4]Radiology and Biomedical Imaging, Yale University, New Haven, CT, United States

Carbon-13 (13C) magnetic resonance spectroscopy (MRS) remains to be the only noninvasive method capable of measuring neuroenergetics and neurotransmitter cycling in the brain in vivo [1]. However, 13C MRS is a challenging technique to implement, and suffers from low sensitivity. In this study we investigated a short TE (12.6 ms) PRESS localized proton observed carbon edited 13C MRS utilizing a volumetric resonator for proton excitation. The designed platform demonstrates high sensitivity to 1H signals, provides excellent localization, and high resolution 1H and 1H-[13C] spectra for in vivo rat brain imaging.

5617 Computer 57

Quantitative analysis of hyperpolarized [1-13C]pyruvate metabolic kinetics using Bayesian Inference algorithms

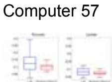

Nikolaos Dikaios[1], Charlie J. Daniels[2], Ferdia A. Gallagher[2], James O'Callaghan[3], David Atkinson[3], and Shonit Punwani[3]

[1]Electrical Engineering, University of Surrey, Guildford, United Kingdom, [2]Radiology, University of Cambridge, [3]Centre for Medical Imaging, University College London

Metabolic processes monitored by MRS precede the micro-structural changes visualised by MRI. It is well-recognised that cancer cells reprogram their metabolic pathways to meet their energy demands for abnormal proliferation. Pyruvate is produced through the breakdown of glucose in glycolysis, and is essential for providing cellular energy. Histological studies have shown increased exchange of pyruvate to lactate in prostate cancer, demonstrating a positive correlation with more aggressive disease. In regions of up-regulation of glucose metabolism, [1-13C] pyruvate is more readily converted to [1-13C]lactate, providing added value for diagnostic imaging. This work aims to robustly quantify the exchange rates between pyruvate and lactate using Bayesian Inference algorithms.

5618 Computer 58

Comparison of direct 13C and indirect 1H-[13C] MR detection methods for the study of dynamic metabolic turnover in the human brain

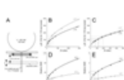

Hao Chen[1], Henk M De Feyter[1], Peter B Brown[1], Douglas L Rothman[1], and Robin A de Graaf[1]

[1]MRRC, Yale University, New Haven, CT, United States

A wide range a direct ^{13}C and indirect ^{1}H-[^{13}C] MR detection methods exist to probe dynamic metabolic pathways in the human brain. Choosing an optimal detection method is difficult as sequence-specific features regarding spectral resolution, power requirements and sensitivity complicate a straightforward comparison. Here we combine density matrix simulations with experimentally determined values for intrinsic ^{1}H and ^{13}C sensitivity, T_1 and T_2 relaxation and transmit efficiency to allow selection of an optimal ^{13}C MR detection method for a given application and magnetic field.

5619 Computer 59

The effect of malonate, succinate, oxaloacetate and 2-deoxy-D-glucose on boar sperm metabolism using ^{13}C MRS

Nurul Fadhlina Ismail[1], Steven Reynolds[1], Sarah Calvert[2], Allan Pacey[2], and Martyn Paley[1]

[1]Academic Unit of Radiology, University of Sheffield, Sheffield, United Kingdom, [2]Academic Unit of Reproductive & Developmental Medicine, University of Sheffield, Sheffield, United Kingdom

One in five young men has poor semen quality, including low motility. Studying energy metabolism may provide better understanding of sperm motility. We acquired ^{13}C Magnetic Resonance spectra of sperm incubated with ^{13}C-glucose with different concentrations of inhibitors: malonate, oxaloacetate, succinate, and 2-deoxy-D-glucose. This study examined the effect of these inhibitors on sperm lactate production and vitality, with a secondary aim to observe Krebs cycle intermediates in the MR spectrum. Glucose signal significantly decreased with increasing oxaloacetate concentration. Malonate and oxaloacetate and 2DG significantly decreased in lactate production. These inhibitors did not lead to observable ^{13}C labelled Krebs cycle intermediates.

5620 Computer 60

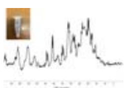

NMR and MRS studies of the neurotoxic oligomer of α-Synuclein toward investigating its *in vivo* structure

Keika Saito[1], Mitsuhiro Takeda[1], Sosuke Yoshinaga[1], and Hiroaki Terasawa[1]

[1]Department of Structural BioImaging, Faculty of Life Sciences, Kumamoto University, Kumamoto, Japan

α-Synuclein (α-Syn) is an abundant protein in neurons, and changes to a neurotoxic α-helical oligomer *in vitro*. The goal of our study is to investigate the structure of the α-Syn oligomer *in vivo*, by delivering ^{13}C-labeled α-Syn into mouse brains and performing a ^{13}C CEST experiment. We report the MRS detection of the ^{13}C signals of the α-Syn monomer in an agarose gel phantom, mimicking a physiological environment. We also report that the *in vitro* oligomerization rate of α-Syn varies, depending on buffer conditions. We envisage that the CEST effect will be detected by adjusting the oligomerization kinetics of α-Syn.

5621 Computer 61

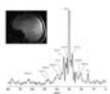

Feasibility of localized, 1H decoupled natural abundance 13C-MRS of human brain at 7T using double tuned array coils and polarization transfer

Guillaume Donati[1] and Rolf Gruetter[1,2]

[1]Laboratory for Functional and Metabolic Imaging, CIBM, EPFL, Lausanne, Switzerland, [2]Department of Radiology, Universities of Lausanne and Geneva, Lausanne, Geneva, Switzerland

The inherent low sensitivity of ^{13}C-MRS makes detection of natural abundance metabolites in human brain challenging. We aimed to demonstrate that double-tuned array coils are particularly well-suited for ^{13}C-MRS studies *in vivo*, as they provide high sensitivity and high transmit efficiency over a large FOV. To further enhance the SNR, DEPT sequence was used to transfer polarization from ^{1}H to ^{13}C, as well as WALTZ-16 ^{1}H-decoupling, all within FDA guidelines. Natural abundance metabolites such as glutamate, glutamine, NAA and creatine were successfully detected and decoupled in 30 minutes acquisition time, showing strong efficiency and sensitivity of our measurement setup.

5622 Computer 62

A 35Cl ToRo Resonator System for Preclinical MRI/MRS at 9.4T

Matthias Malzacher[1], Ruomin Hu[1], Jorge Chacon-Caldera[1], Andreas Neubauer[1], and Lothar R Schad[1]

[1]Computer Assisted Clinical Medicine,Medical Faculty Mannheim, Heidelberg University, Mannheim, Germany

Chloride (Cl^-) is next to the cations Na^+ and K^+ the most abundant non-organic anion in the mammals. Assessment of chlorine's (^{35}Cl) concentration in tissue could provide further insights into tissue viability in addition to tissue sodium concentration. Yet, low Signal-to-Noise ratio (SNR) is challenging for the RF hardware components. To overcome these challenges, a Transmit-only-Receive-only (ToRo) system for ^{35}Cl MRI/MRS at 9.4T was developed comprised of an actively-decoupled linearly-driven 16 leg low-pass Birdcage transmitter coil combined with two different receiver coils. Substantial SNR gain was reached using receive-only elements compared to the Birdcage coil in TxRx mode.

5623 Computer 63

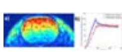

Simultaneous measurement of metabolic rates of oxygen via ^{17}O NMR imaging in brain and muscle tissue of rat at 16.4T

Hannes Michel Wiesner[1,2], Dávid Zsolt Balla[3], Klaus Scheffler[2,4], Kamil Ugurbil[1], Xiao-Hong Zhu[1], Wei Chen[1], Kamil Uludag[5], and Rolf Pohmann[2]

[1]CMRR, Radiology, University of Minnesota Medical School, Minneapolis, MN, United States, [2]MRC Department, MPI for Biological Cybernetics, Tübingen, Germany, [3]Department of Physiology of Cognitive Processes, MPI for Biological Cybernetics, Tübingen, Germany, [4]Radiology, University of Tübingen, Tübingen, Germany, [5]MBIC, Faculty of Psychology and Neuroscience, Maastricht University, Maastricht, Netherlands

In this study, we exploit the feasibility of the ^{17}O MRSI technique for simultaneous measurement of the metabolic rates of oxygen in brain and surrounding muscle based on ROI analysis of dynamics of tissue $H_2{}^{17}O$ time courses acquired at 16.4T with 3D ^{17}O MRSI. An established three-phase model originally developed for brain application was extended with certain assumptions applied to the resting temporalis muscle of rats.

5624 Computer 64

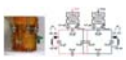

Design and construction of a novel double-tuned 1H/19F coil using PIN-diode switches at 9.4T

Chang-Hoon Choi[1], Suk-Min Hong[1], YongHyun Ha[1], and N. Jon Shah[1,2]

[1]Institute of Neuroscience and Medicine-4, Forschungszentrum Juelich, Juelich, Germany, [2]Faculty of Medicine, Department of Neurology, JARA, RWTH Aachen University, Aachen, Germany

A double-tuned ^{1}H/^{19}F coil using PIN-diode switches was developed and evaluated its performance on a 9.4T preclinical MRI scanner. This proposed design uses an inductor rather than a capacitor in series with the PIN-diode so that the resonance frequency is shifted in the opposite direction compared to the conventional method. This is a key difference from the previous developments and in this way we can maintain the SNR or image quality of the X-nuclei (therefore ^{19}F); the SNR is nearly as good as a single-tuned ^{19}F coil.

5625 Computer 65

Study of MR characteristics of anti-psychotic drugs using fluorine (19F) MR spectroscopy at 9.4 T

Chu-Yu Lee[1], In-Young Choi[1,2,3], Jean C Dinh[4], William M Brooks[1,2], J. Steven Leeder[4,5], and Phil Lee[1,3]

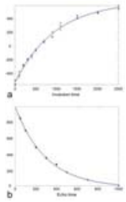

[1]Hoglund Brain Imaging Center, University of Kansas Medical Center, Kansas City, KS, United States, [2]Department of Neurology, University of Kansas Medical Center, Kansas City, KS, United States, [3]Department of Molecular & Integrative Physiology, University of Kansas Medical Center, Kansas City, KS, United States, [4]Division of Clinical Pharmacology, Toxicology, and Therapeutic Innovation, Children's Mercy Hospital, Kansas City, MO, United States, [5]Department of Pediatrics, Children's Mercy Hospital, Kansas City, MO, United States

19F MRS allows assessment of fluorine containing anti-psychotic drugs in the brain. However, the reliable quantification remains challenging due to low drug concentrations and MR characteristics of the drugs are not well understood. This study aimed to characterize MR properties of four anti-psychotic drugs: pimozide, paliperidone, risperidone, and racemic fluoxetine, in phantoms at 9.4 T. Our results demonstrated that pimozide, paliperidone and risperidone showed over 50 ppm differences in chemical shifts and over 200 ms differences in T1 and T2 relaxation times compared with racemic fluoxetine. These different MR characteristics may have important implications for the 19F MRS technique development.

5626 Computer 66

Monitoring of cell proliferation by 19F-MRS via quantitation of 3'-deoxy-3'-fluorothymidine (FLT) and its monophosphate metabolite (FLT-MP) in invivo

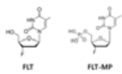

Inok Ko[1], Ki-Hye Jung[1], Kyung Jun Kang[1], Kyo Chul Lee[1], Yong Jin Lee[1], Jung-Young Kim[1], Sang Moo Lim[2], and Ji-Ae Park[1]

[1]Division of RI-Convergence Research, Korea Institute Radiological and Medical Sciences, Seoul, Korea, Republic of, [2]Department of Nuclear Medicine, Korea Institute Radiological and Medical Sciences, Seoul, Korea, Republic of

Distinguishing between FLT(fluorothymidine) and FLT-MP(flruorothymidine - monophosphate) by imaging methods is important for evaluating the tumor cell proliferation rate. The aim of this study is to develop and validate a suitable ^{19}F MR Spectroscopy for measuring TK1 activity via quantitation of FLT and FLT-MP in vivo. We observed the good correlations between SNR and FLT concentration (r2= 0.94). In phantom study, the locations of FLT and FLT-MP was -175.99, -175.24 ppm, respectively. *In vivo* study, FLT spectrum in mouse tumor was observed in 25 min after injection, whereas FLT-MP spectrum occurred in 90 min after injection. This result shows that ^{19}F MR Spectroscopy is suitable for monitoring of FLT-MP generation in *in vivo*.

5627 Computer 67

Simultaneous multi-parametric and quantitative estimation of 23Na physical properties at 7 Tesla using QuICS

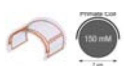

Lisa Leroi[1], Arthur Coste[1], Ludovic de Rochefort[2], Mathieu Santin[3], Romain Valabrègue[3], Franck Mauconduit[4], Marie-France Hang[1], Edouard Chazel[1], Jérémy Bernard[1], Michel Luong[5], Eric Giacomini[1], Denis Le Bihan[1], Cyril Poupon[1], Fawzi Boumezbeur[1], Cécile Rabrait-Lerman[1], and Alexandre Vignaud[1]

[1]Neurospin, CEA, Pais-Saclay University, Saclay, France, [2]CRMBM, UMR 7339, Aix-Marseille University, Marseille, France, [3]Institut Cerveau Moelle - ICM, CENIR, UPMC-Inserm U1127, CNRS 7225, Paris, France, [4]Siemens Healthineers, Saint-Denis, France, [5]IRFU, CEA, Paris-Saclay University, Saclay, France

Quantifying physical properties of sodium could be of benefit to assess more specifically changes in cellular homeostasis accompanying neuroinflammatory or neurodegenerative diseases. This work aimed at adapting for ^{23}Na MRI at 7 Tesla the Quantitative Imaging using Configuration States (QuICS) method, primarily developped for ^{1}H MRI. We demonstrate the possibility to not only estimate accurately the T_1, T_2, FA, M_0 and ADC simultaneously for ^{23}Na at physiological concentration at UHF, but to acquire 3D maps for all of them.

5628 Computer 68

Realistic simulation of 23Na brain data: Understanding the influence of acquisition parameters on the accuracy of 23Na concentration measurement

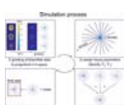

Jonathan M. Lommen[1], Nicolas G.R. Behl[1], Peter Bachert[1], Mark E. Ladd[1], and Armin M. Nagel[1,2]

[1]Medical Physics in Radiology, German Cancer Research Center (DKFZ), Heidelberg, Germany, [2]Institute of Radiology, University Hospital Erlangen, Erlangen, Germany

Sodium (^{23}Na) is connected to tissue physiology and can be spatially resolved by MRI. Low in-vivo concentrations and short relaxation times render a quantitative determination challenging. We present a simulation method which allows synthesizing realistic ^{23}Na MRI raw data. Thereby, most effects in typical quantification experiments on the basis of an external concentration reference can be studied. To establish a reference accuracy level, we investigate the influence of T_2^* decay, undersampling, TE, and TR on ^{23}Na quantification. The presented simulations can be used for the testing and evaluation of quantitative reconstruction methods as well as to test significance in clinical studies.

5629 Computer 69

Improving Sodium Concentration Measurements using sub-sampled Non-Cartesian Trajectories and Non-Linear Iterative Reconstruction algorithm

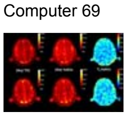

Arthur Coste[1], Nicolas Chauffert[1], Fawzi Boumezbeur[1], Alexandre Vignaud[1], Philippe Ciuciu[1], Guillaume Madelin[2], Kathrin Reetz[3], Denis Le Bihan[1], Cécile Rabrait-Lerman[1], and Sandro Romanzetti[3]

[1]NeuroSpin, CEA, Paris Saclay University, Paris, France, [2]Center for Biomedical Imaging, Department of Radiology, New York University Langone Medical Center, New York, USA, [3]Neurology Department, Aachen University Clinic, Germany

In this work we explored different aspects that could benefit to in vivo Sodium concentration measurements in order to reduce Acquisition Time to improve patient comfort and an reduce risk of motion artifacts. We studied two Non Cartesian image reconstruction methods and explored subsampling.

5630 Computer 70

Investigation of Strophanthin Induced Na-/K-ATPase Blockage by Means of 23Na Multi Quantum Spectroscopy in a High Density Cell Culture on Chip

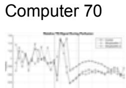

Andreas Neubauer[1], Matthias Malzacher[1], Victor Schepkin[2], Jorge Chacon-Caldera[1], Ruomin Hu[1], Eric Gottwald[3], Cordula Nies[3], David Thiele[3], and Lothar Schad[1]

[1]Computer Assisted Clinical Medicine/CBTM, Heidelberg University, Mannheim, Germany, [2]CIMAR, National High Magnetic Field Laboratory/FSU, Tallahassee, FL, United States, [3]Institute for Biological Interfaces-5, Karlsruhe Institute of Technology, Eggenstein-Leopoldshafen, Germany

Sodium multi quantum (MQ) spectroscopy was used to record single (SQ) and triple quantum (TQ) resonances from a 3D cell culture implanted in a MRI compatible bioreactor under the strophanthin induced inhibition of the sodium-potassium pump (Na-/K-ATPase) at 9.4T. The results show a clear alteration in the ratio TQ/SQ under strophanthin influence. Due to the high control of physiological parameters the bioreactor provides, this alteration can be directly linked to the inhibition of the Na-/K-ATPase.

5631 Computer 71

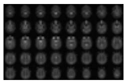

Sodium short and long T2* components in the normal human brain: a multi-TE 23Na MRI study at 7T

Mark Bydder[1], Armin Nagel[2], Adil Maarouf[1,3], Jeremy Verneuil[1], Patrick Viout[1], Maxime Guye[1,3], Jean-Philippe Ranjeva[1], and Wafaa Zaaraoui[1]

[1]Aix-Marseille Univ, CNRS, CRMBM, Marseille, France, [2]University Hospital Erlangen, Institute of Radiology, Erlangen, Germany, [3]Aix-Marseille Univ, APHM, Hopital de la Timone, CEMEREM, Marseille, France

The study aimed to provide values of the short and long T2* sodium components of the human brain at 7T using a multi-echoes 23Na MRI approach (n=24 TE). These results may help improving sodium quantification at 7T.

5632 Computer 72

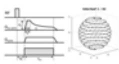

Validation and Initial Results from Dynamic 23Na fMRI

Mark Bydder[1], Wafaa Zaaraoui[1], Lothar Schad[2], Maxime Guye[1], and Jean-Philippe Ranjeva[1]

[1]Aix-Marseille Université, Marseille, France, [2]Heidelberg University

In this abstract we develop and validate an MRI acquisition/reconstruction method to derive the temporal dynamics of 23Na within a 20 min scan.

Electronic Poster

MRS Applications

Exhibition Hall Thursday 14:00 - 15:00

5633 Computer 73

summa cum laude

Interregional associations between GABA+, Glx and BOLD contrast changes during acute pain perception in the human brain – A combined 1H fMRS and fMRI study

Marianne Cleve[1], Alexander Gussew[1], Gerd Wagner[2], and Jürgen R. Reichenbach[1]

[1]Medical Physics Group, Institute of Diagnostic and Interventional Radiology, Jena University Hospital - Friedrich Schiller University Jena, Jena, Germany, [2]Psychiatric Brain & Body Research Group Jena, Department of Psychiatry and Psychotherapy, Jena University Hospital, Jena, Germany

Possible associations between BOLD and left insular GABA+/tCr and Glx/tCr levels were investigated by conducting whole brain fMRI measurements and ^{1}H MEGA-PRESS MRS at 3 T in healthy subjects prior to and during acute pain stimulation. A significant negative correlation between insular resting state GABA+/tCr levels and BOLD response was obtained in the supplementary motor area with transition to the mid-cingulate cortex. Furthermore, insular ΔGlx revealed a significant positive association with BOLD signal in the left anterior and right posterior insula. These findings suggest interregional interrelations between metabolite levels and stimulus induced BOLD response in the pain processing network.

5634 Computer 74

Abnormal developmental trajectories of brain metabolites contributed to abnormal muscle tone development in infants with prenatal methamphetamine and tobacco-exposure

Linda Chang[1], Sara Hayama[1], Steven Buchthal[1], Chathura Siriwardhana[1], Daniel Alicata[1], Zachary Pang[1], Tricia Wright[1], Jon Skranes[2], and Thomas Ernst[1]

[1]University of Hawaii at Manoa, Honolulu, HI, United States, [2]Pediatrics, Sorlandet Hospital, Arendal, Norway

In prior studies, children with prenatal methamphetamine-(PME) or tobacco-exposure (PTE) showed elevated brain metabolites levels. The current study evaluated infants with PME and PTE during the first 5 months of life and found abnormal developmental trajectories of metabolites in the frontal white matter, with abnormally lower levels of total creatine [tCr], N-acetylaspartate [NAA], and glumate+glutamine [Glx] at baseline, and steeper developmental trajectories that resulted in normal or elevated levels after 2-months old. Furthermore, the trajectories of basal ganglia-[NAA] and corticospinal tract-[tCr] further contributed to the slower muscle tone development in PME infants, especially the males.

5635 Computer 75

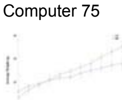

Neurochemical alterations in the hippocampus induced by high-fat diet: In vivo magnetic resonance spectroscopy

Song-I Lim[1,2], Kyu-Ho Song[1], Chi-Hyeon Yoo[1], Dong-Choel Woo[2], and Bo-Young Choe[1]

[1]Department of Biomedical Engineering, and Research Institute of Biomedical Engineering. The Catholic University of Korea College of Medicine, Seoul, Korea, Republic of, [2]Asan Institute for Life Sciences, Asan Medical Center, Seoul, Korea, Republic of

In this study, we investigated the neurochemical alterations in mouse hippocampus using *in vivo* proton magnetic resonance spectroscopy. We also examine the effect of high-fat diet on the levels of abdominal fat, plasma leptin, and corticosterone. The decrease in mIns concentration seen in HF diet mice without corresponding Gln-Glu alternation may reflect changes in glial function. In addition, the observed total choline levels indicate attenuated membrane turnover in HF diet mice. We therefore suggest that diets rich in saturated fats induce a stress-related response through metabolic disturbance and HPA axis dysfunction, which may indicate a relationship between obesity and depression.

5636 Computer 76

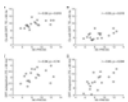

Reliability of in vivo Glx measurements from GABA-edited MRS at 3T

Elodie Boudes[1,2], Rachelle S Loo[1,2], Kari AL Parsons[1,2], Gareth J Barker[3], David Lythgoe[3], Richard AE Edden[4,5], R Marc Lebel[6], Martin P Wilson[7], and Ashley D Harris[1,2]

[1]Radiology, University of Calgary, Calgary, AB, Canada, [2]CAIR Program, Alberta Children's Hospital Research Institute and Hotchkiss Brain Institute, University of Calgary, [3]Department of Neuroimaging, Institute of Psychiatry, Psychology & Neuroscience, King's College London, [4]Radiology, The Johns Hopkins School of Medicine, [5]F. M. Kirby Research Center for Functional Brain Imaging, Kennedy Krieger Institute, [6]General Electric Healthcare, [7]School of Psychology, University of Birmingham

Mixed glutamate/glutamine (GLX) signal contributes to spectra acquired for GABA editing, both as a co-edited peak in the difference spectrum and in the OFF subspectrum. GLX results are often included in GABA studies, but the reliability of these metrics has received little attention. In this study, we examine the relationship between GLX measures, using a short-TE PRESS as a “gold standard”, and comparing GLX measured from the co-edited peak and the OFF subspectrum from typical GABA+ and macromolecule-suppressed GABA acquisitions.

5637 Computer 77

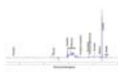

Prognostic utility of cervicovaginal fluid acetate-glutamate ratio for risk of preterm delivery within two weeks of presentation with symptoms of threatened preterm labour

Emmanuel Amabebe[1], Steven Reynolds[2], Victoria Stern[1], Graham Stafford[3], Martyn Paley[2], and Dilly Anumba[1]

[1]Academic unit of Reproductive and Developmental Medicine, University of Sheffield, Sheffiled, United Kingdom, [2]Academic unit of Radiology, University of Sheffield, Sheffiled, United Kingdom, [3]School of Clinical Dentistry, University of Sheffield, Sheffield, United Kingdom

Accurate identification of pregnant women with symptoms of preterm labor (PTL) most likely to deliver prematurely soon after presentation/assessment is crucial for prompt clinical decision making and allocation of scarce resources by minimizing unnecessary hospitalizations and treatments, as well as by triaging patients to the centers with optimal care facilities. We determined the predictive capacity of cervicovaginal fluid (CVF) acetate/glutamate ratio in pregnant women presenting with symptoms of threatened PTL using ^{1}H-NMR. The ratio of CVF acetate to glutamate demonstrated better prediction of delivery within 2 weeks of symptomatic presentation, compared to either acetate or glutamate alone.

5638 Computer 78

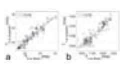

Reproducibility for MRS-Based Relaxometry and Identification of Influential Parameters

Bernhard Neumayer[1,2], Thomas Widek[1,2], Chris Boesch[3], and Eva Scheurer[4]

[1]Ludwig Boltzmann Institute for Clinical Forensic Imaging, Graz, Austria, [2]BioTechMed-Graz, Graz, Austria, [3]Department of Clinical Research (AMSM), University of Bern, Bern, Switzerland, [4]Department of Forensic Medicine, University of Basel, Basel, Switzerland

The different relaxation times of the water and the fat compartment in human lumbar vertebrae make it necessary to determine these values for a correct calculation of the fat fraction, which is used as a biomarker for various applications. This study investigates the reproducibility of relaxometry in human lumbar vertebrae to serve as a basis for future studies. Furthermore, factors like age, sex, and physique are investigated for their influence on the derived T_1 and T_2 values to investigate whether relaxation times of the fat and water compartments can serve as biomarkers in addition to the fat fraction.

5639 Computer 79

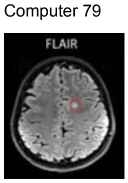

Mapping brain macromolecules in patients with multiple sclerosis using 1H-MRSI at 7T

Michal Považan[1,2], Eva Heckova[1], Gilbert Hangel[1], Bernhard Strasser[1], Stephan Gruber[1], Assunta Dal-Bianco[3], Fritz Leutmezer[3], Siegfried Trattnig[1,2], and Wolfgang Bogner[1,2]

[1]Department of Biomedical Imaging and Image-guided Therapy, High Field MR Centre, Medical University Vienna, Vienna, Austria, [2]Christian Doppler Laboratory for Clinical Molecular MR Imaging, Vienna, Austria, [3]Department of Neurology, Medical University Vienna, Vienna, Austria

Multiple sclerosis (MS) is a disease of the central nervous system associated with demyelination and glial activation affecting large areas of white matter. ^{1}H-MRSI may detect the metabolic changes induced by MS and facilitate the differentiation between MS lesions. Our study aimed to detect and map the signal of macromolecules in healthy controls and MS patients. 2D FID-based ^{1}H-MRSI was used with measurement time under 6 minutes. We found increased macromolecules in the perilesional region and decreased macromolecules in most of the lesions. However, in some lesions, macromolecules were increased, which may be possibly related to pathological activation of lesion.

5640 Computer 80

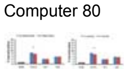

Decreased tNAA concentration in female college basketball players with mild depression/anxiety symptoms

Xian-Feng Shi[1], Perry Renshaw[1], and Deborah Yurgelun-Todd[1]

[1]Psychiatry, University of Utah, Salt Lake City, UT, United States

The aim of the present study was to examine possible gender differences in 1H brain metabolite concentrations in male and female college basketball players. Decreased total N-acetylaspartate/N- acetylaspartylglutamate (tNAA) levels within white matter tissue were observed in female basketball players with symptoms of depression or anxiety (p = 0.0256 /p = 0.0112).

5641 Computer 81

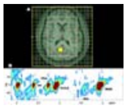

Cerebral Metabolite Changes and Cognitive Clinical Correlates in Perinatally HIV-infected Young Adults

Manoj K Sarma[1], Margaret A Keller[2], Tamara Welikson[3], Sathya Arumugam [1], David E Michalik[4], Irwin Walot[5], Karin Nielsen-Saines[6], Jaime Deville[6], Andrea Kovacs[7], Eva Operskalski[7], Joseph Ventura[8], and M. Albert Thomas[1]

[1]Radiological Sciences, UCLA School of Medicine, Los Angeles, CA, United States, [2]Pediatrics, Harbor-UCLA Medical Center, Torrance, CA, United States, [3]Semel Institute for Neuroscience and Human Behavior, UCLA School of Medicine, Los Angeles, CA, United States, [4]Infectious disease-Pediatrics, Miller Children's Hospital, Long Beach, CA, United States, [5]Radiology, Harbor-UCLA Medical Center, Torrance, CA, United States, [6]Pediatrics, UCLA School of Medicine, Los Angeles, CA, United States, [7]Pediatrics, Keck School of Medicine of USC, Los Angeles, CA, United States, [8]Psychiatry and Biobehavioral Sciences, UCLA School of Medicine, Los Angeles, CA, United States

A recently implemented 5D echo-planar J-resolved spectroscopic sequence using 8x acceleration and compressed sensing reconstruction was evaluated in 7 perinatally infected and 8 healthy youths. Selected metabolite ratios with respect to Cr were detected bilaterally in the basal ganglia, anterior insular cortex, posterior insular cortex, frontal white and occipital/frontal gray regions of the two groups. Statistically significant differences were found between metabolite ratios (/Cr) of HIV-infected youing adults and healthy control subjects in the occipital gray N-acetylaspartate, right basal ganglia glutamine/glutamate, left anterior insular cortex choline, and left posterior insular cortex. Also, our pilot findings suggest a possible difference in energy metabolism between perinatally HIV-infected young adults and controls without HIV. The metabolite ratios correlated with neuropsychological test scores showing cognitive impairment as result of HIV-infection and/or long term ART.

5642 Computer 82

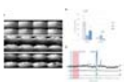

In vivo measurement of metabolic changes associated with chick embryo development using 1H-NMR spectroscopy at 14.1 Tesla

Antoine Cherix[1], Brodier Laurent[2,3], Jean-Marc Matter[2,3], and Rolf Gruetter[1,4,5]

[1]Laboratory for Functional and Metabolic Imaging (LIFMET), Ecole Polytechnique Fédérale de Lausanne, Lausanne, Switzerland, [2]Department of Biochemistry, University of Geneva, Geneva, Switzerland, [3]Department of molecular biology, University of Geneva, Geneva, Switzerland, [4]Department of Radiology, University of Geneva, Geneva, Switzerland, [5]Department of Radiology, University of Lausanne, Lausanne, Switzerland

^{1}H-MRS was used to study the metabolic changes associated with development of the neural tissue ***in vivo*** longitudinally. Different tissues (yolk, eye and vitreous body) of developing chickembryos were scanned at three different stages (E3, E6 and E8) for metabolic quantification. As expected, results indicate that a critical juncture appears between stages E3 and E6 in terms of energetic status of the embryo.

5643 Computer 83

Can we predict the chemotherapy outcomes and efficacy - metabolomics approach for predicting response to anticancer drugs: in vitro 1H MRS of living human melanoma and bladder carcinoma at 9.4T

Katarzyna Pierzchala[1], Nicolas Kunz[1], and Rolf Gruetter [1]

[1]Center for Biomedical Imaging, EPFL / CIBM, Lausanne, Switzerland

The number of patients diagnosed with cancer is increasing. Therefore the ability to predict tumor response to therapeutic agents remains a major challenge. Tumor cell metabolism is currently examined by 1H MRS with the aim of getting more insight into the differences between normal and neoplastic tissues, characterize their metastatic potential/finding prognostic markers, and monitoring the effect of therapies. In this study we demonstrate the feasibility of characterizing in-vitro living cells and present changes in the metabolic profile of WM793 and T24 cells lines subjected to chemotherapy. These results show promise for more personalized treatment protocols for cancer patients.

5644 Computer 84

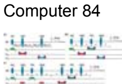

Improving the detection of scalar-coupled resonances at short and moderate echo times for in vivo rat MRS at 9.4 T

Liangjie Lin[1,2,3], Yanqin Lin[1], Dan Tian[1], Hongyi Yang[4], Zhiliang Wei[2,3], Peter B. Barker[2,3], Kai Zhong[4], and Zhong Chen[1]

[1]Department of Electronic Sciense, Xiamen University, Xiamen, People's Republic of China, [2]Russell H. Morgan Department of Radiology and Radiological Science, Johns Hopkins University, Baltimore, MD, United States, [3]F. M. Kirby Center for Functional Brain Imaging, Kennedy Krieger Institute, Baltimore, MD, United States, [4]High Magnetic Field Laboratory, CAS Center for Excellence in Brain Science, Chinese Academy of Sciences, Hefei, People's Republic of China

Conventional localized ^{1}H MRS pulse sequences, such as PRESS and STEAM, generally suffer from ***J*** coupling modulations which can aggravate attenuation of multiplet resonances during echo times. Here, the “perfect echo” module combined with an optimized localization scheme is utilized for in-phase single-voxel in vivo MRS at 9.4 T. The relative signal intensities of multiplet to singlet resonances acquired at short and moderate echo times increase substantially in comparison with those at PRESS spectra. Therefore, direct MRS quantification of many important metabolites, such as glutamine, glutamate, γ-aminobutyrate, aspartate, and myo-inositol, may be improved.

5645 Computer 85

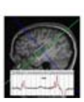

The subjective intensity of pain in healthy subjects is inversely correlate with posterior insular GABA levels

Margot Thiaucourt[1], Polina Shabes[2], Natalie Schloss[3], Markus Sack[1], Ulf Baumgaertner[2], Christian Schmahl[3], and Gabriele Ende[1]

[1]Neuroimaging, Central Institute of Mental Health, Mannheim, Germany, [2]Center for Biomedicine and Medical Technology Mannheim, Medical Faculty Mannheim, Mannheim, Germany, [3]Psychosomatic Medicine and Psychotherapy, Central Institute of Mental Health, Mannheim, Germany

We present single voxel MEGA-PRESS MRS data from the posterior insula of 20 healthy women demonstrating a significant association of GABA and the subjective pain thresholds. These findings are in good agreement with the postulated role of the posterior insula for pain information processing. In this region pain is first processed and the sensory aspects of pain perception is elaborated and then conveyed to the anterior insula where it is related to emotional and cognitive aspects of pain perception. The data corroborate that GABA levels seem to be an important mediator for pain perception.

5646 Computer 86

Altered intrinsic neuronal activity correlates with GABA levels in the auditory region of patients with presbycusis

Fei Gao[1], Guangbin Wang[1], Bin Zhao[1], Fuxin Ren[1], and Weibo Chen[2]

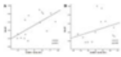

[1]Shandong Medical Imaging Research Institute, Shandong University, JINAN, People's Republic of China, [2]Philips Healthcare, Shanghai, People's Republic of China

In this study, we used J-difference edited MRS and resting-state fMRI to investigate correlation between intrinsic neuronal activity and GABA levels in the auditory cortex of patients with presbycusis. Our results indicated that abnormalities in GABAergic neurotransmission may underlie resting-state functional deficits in presbycusis.

5647 Computer 87

Investigation of metabolic changes during watching movie using fMRS at 3T system

Jia-Ren Lin[1], Yi-Ru Lin[1], and Shang-Yueh Tsai[2,3]

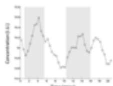

[1]Department of Electronic and Computer Engineering, National Taiwan University of Science and Technology, Taipei, Taiwan, [2]Graduate Institute of Applied Physics, National Chengchi University, Taipei, Taiwan, [3]Research Center for Mind, Brain and Learning, National Chengchi University, Taipei, Taiwan

Recent studies have reported metabolic change during visual and motor stimulation using MRS at 7T MRI system. We think there is potential to perform fMRS experiments at 3T system. Visual stimuli were given with block design consisting of 2 black-white movie clips and 3 rest sections. Our preliminary results showed that Glu concentrations in visual cortex increases by 1.39% during watching movie, while NAA and Cre have no significant change. The observed Glu change was comparable to previous study performed at 7T.

5648 Computer 88

Identification of Prostate Cancer with MR Spectroscopic Imaging and Diffusion-weighted Imaging at 3 Tesla

Yousef Mazaheri[1], Amita Shukla-Dave[2], Debra A Goldman[3], Chaya S Moskowitz[3], Victor E Reuter[4], Oguz Akin[5], and Hedvig Hricak[5]

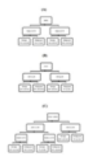

[1]Medical Physics, Memorial Sloan Kettering Cancer Center, New York, NY, United States, [2]Medical Physics, Memorial Sloan Kettering Cancer Center, [3]Epidemiology and Biostatistics, Memorial Sloan Kettering Cancer Center, [4]Pathology, Memorial Sloan Kettering Cancer Center, [5]Radiology, Memorial Sloan Kettering Cancer Center

The aims of our study were to retrospectively measure metabolite ratios and apparent diffusion coefficient values for benign and malignant PZ tissue at 3T, develop statistically-based rules for classifying benign and malignant PZ tissue, and assess the rules' performance, using whole-mount step-section pathology as the reference standard.

5649 Computer 89

Using broadband refocusing pulses for increased sensitivity for 2HG detection to determine glioma IDH mutation status

Sunitha B Thakur[1], Robert J Young[1], Robin Fatovic[1], Ralph Noeske[2], Martin Janich[3], Andrei Holodny[1], and Ingo K Mellinghoff[1]

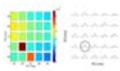

[1]Memorial Sloan Kettering Cancer Center, New York, NY, United States, [2]GE HealthCare, Berlin, Germany, [3]GE Global Research, Munich, Germany

2-hydroxyglutarate in IDH1/2 mutated tumors is of clinical interest and can be measured in-vivo by magnetic resonance spectroscopy. Goal of this work was to compare results obtained using the standard reduced flip angle refocusing pulses with results using broadband refocusing pulses. Sensitivity improvement was observed in phantoms and demonstrated in vivo.

5650 Computer 90

1H NMR based metabolomics study of serum in Parkinson's patients

Sadhana Kumari[1], Senthil Kumaran[1], Vinay Goyal[2], SN Dwivedi[3], Achal Srivastava[2], and Naranamangalam R Jagannathan[1]

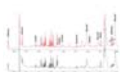

[1]Department of NMR and MRI Facility, All India Institute of Medical Sciences, New Delhi, India, [2]Department of Neurology, All India Institute of Medical Sciences, New Delhi, India, [3]Department of Biostatistics, All India Institute of Medical Sciences, New Delhi, India

Proton metabolic profile of serum samples in 20 patients with Parkinson's disease (PD) and 10 healthy controls (HC) was studied using 700 MHz NMR spectrometer. Data were processed using MestReNova software (version: 10.0) and integral values were evaluated. PLS-DA multivariate analysis was performed to compare the metabolic differences between PD patients and HC using MetaboAnalyst (version: 3.0) software. We found elevated levels of glucose, fatty acid, glutamine, lactate, choline, creatine and acetate in PD patients in comparison with HC (on t-test, $p<0.05$), indicating disturbances in lipid metabolism, fatty acid oxidation and mitochondrial damage leading to dopaminergic deficiency in Parkinson's disease.

5651 Computer 91

NEURO 2D CORRELATED SPECTROSCOPY IDENTIFIES NEURO DEREGULATION IN SOLDIERS EXPOSED TO BLAST PRIOR TO DISCERNIBLE CHANGES BY CONVENTIONAL IMAGING

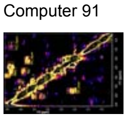

Graham J Galloway[1,2], Scott G Quadrelli[1,3,4], Aaron J Urquhart[1], Katie Trickey[1], Peter Malycha[1], Theresa Keane[5], and Carolyn E Mountford[1]

[1]Translational Research Institute, Woolloongabba, Australia, [2]Centre for Advanced Imaging, The University of Queensland, Brisbane, Australia, [3]University of Newcastle, Australia, [4]Institute for Health and Biomedical Innovation, Brisbane, Australia, [5]Department of Defence, Australian Government, Sydney, Australia

This pilot study reports clear deregulation in the neurochemistry of defense personnel exposed to repeated blast. The changes recorded are different to those reported for mTBI, PTSD and chronic pain. No differences between blast exposed and healthy were recorded by MRI sequences T1WI, FLAIR or SWI. In vivo neuro 2D spectroscopy recorded deregulation with PC and GPC, NAA and GABA all decreased compared to the healthy non exposed brain. We we did not observe any changes in the fucosolated glycans, which are reflective of pain, repetitive brain injury and/or cognitive deficit.

5652 Computer 92

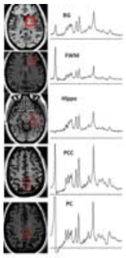

7T Brain MRS in HIV Infection: Effects of Cognitive Impairment

Mona A Mohamed[1], Peter B Barker[1], Richard Skolasky[2], and Ned C Sacktor[3]

[1]Radiology, Johns Hopkins Medical Institutions, Baltimore, MD, United States, [2]Orthopedic, Johns Hopkins Medical Institutions, Baltimore, MD, United States, [3]Neurology, Johns Hopkins Medical Institutions, Baltimore, MD, United States

Higher magnetic field such as 7T provides increased sensitivity, better signal to noise ratio and more reliable measure of the metabolite concentrations. In this study, 7T MRS was used to measure brain metabolites in HIV+ patients in 5 brain regions. Our study showed impaired neuronal integrity across the white and gray matter as well as possible impaired astrocyte osmoregulation in patients with symptomatic cognitive impairment. In conclusion, 7T MRS brain metabolites measurement can be used as reliable biomarkers for the assessment of cognitive status in HIV+ patients.

5653 Computer 93

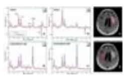

Microstructural dynamic changes in ischemic stroke in humans measured with diffusion-weighted magnetic resonance spectroscopy at 3 T

Francesca Branzoli[1,2], Bélen Díaz-Fernández [3], Malgorzata Marjanska[4], Edward Auerbach[4], Romain Valabrègue[1,2], Itamar Ronen[5], Stéphane Lehéricy[1,2], and Charlotte Rosso[1,2,3]

[1]Brain and Spine Institute (ICM), Center for Neuroimaging Research (CENIR), Paris, France, [2]UPMC Paris 6, INSERM, U1127; CNRS, UMR 7225, Paris, France, [3]Service des Urgences Cérébrovasculaires, Hòpital Pitié-Salpétrière, Paris, France, [4]Center for Magnetic Resonance Research and Department of Radiology, University of Minnesota, Minneapolis, MN, United States, [5]C. J. Gorter Center for High Field MRI, Department of Radiology, Leiden University Medical Center, Leiden, Netherlands

Diffusion-weighted ^{1}H magnetic resonance spectroscopy (DW-MRS) probes the diffusion properties of metabolites, which are differentially compartmentalized in brain tissue and are thus more specific than water molecules to the intra-cellular environment. The aim of this study was to measure water and metabolite diffusion in the human brain in the acute, sub-acute and choronic stage of ischemic stroke, in order to better characterize the microstructural dynamic changes ongoing at different stages of the disease, in both infarcted and periferal regions, by disentangling neuronal, glial and extra-cellular pathological processes.

5654 Computer 94

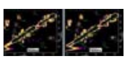

Enhanced detection of weak metabolites with short initial echo time 2D L-COSY

Jameen ARM[1], Karen Ribbons[2], Jeannette Lechner-Scott[3], Kate Skehan[4], Shiami Luchow[3], M. Albert Thomas[5], and Saadallah Ramadan[6]

[1]University of Newcastle, Newcastle, Australia, [2]John Hunter Hospital, Australia, [3]Hunter Medical Research Institute, Australia, [4]HMRI Imaging centre, Hunter Medical Research Institute, Australia, [5]University of California Los Angeles, CA, United States, [6]University of Newcastle, Australia

The detection of weak neurometabolites such as g-aminobutyric acid (GABA), glutathione (GSH), glycerophosphocholine (GPC), phosphorylethanolamine (PE) with 2D L-COSY can be challenging due to lower concentrations. Moreover, the standard initial echo time ($TE_{initial}$) of 30ms yields suboptimal SNR due to shorter T2*. In this study, we compared short $TE_{initial}$ of 20ms vs 30ms to evaluate improved detection of low concentration metabolites. Our results show a significant increase in SNR with $TE_{initial}$ of 20ms compared to 30ms. Short $TE_{initial}$ of 20ms has increased potential in the detection of peaks from weak neurometabolites.

5655 Computer 95

Investigation of long-term effect of a high-fat diet using quantitative MRI and 1H MRS for assessing body and liver fat, and muscle mass

Jong-Hee Hwang[1], In-Young Lee[2], Jung-Hyun Kim[2], and Jae Seung Kim[2]

[1]Institute for Clinical Diabetology, German Diabetes Center, Leibniz Institute for Diabetes Research, Heinrich Heine University, Düsseldorf, Germany, [2]Lee Gil Ya Cancer and Diabetes Institute, Gachon University, Incheon, Korea, Republic of

Repetitive and noninvasive MR examinations of fat content can provide indispensable information for longitudinal metabolic studies. It is of great interest to understand how obesity in youth affects the fat metabolism later in life. Thus we longitudinally examined mice with/without a high-fat diet [HFD] for 8 weeks from 13 to 67 weeks old using MRI and 1H MRS. As a result, visceral fat restored normalcy in 10 weeks after the termination of HFD, subcutaneous and liver fat returned to normalcy in ~ 16 - 20 weeks as compared to controls.
